University of Alberta

Protaspides of Ptychopariida and taxonomy of Hystricuridae, with discussion of ancestry
of Proetida

By

Dong-Chan Lee   ©

A thesis submitted to the Faculty of Graduate Studies and Research in partial fulfillment
of the requirements for the degree of Doctor of Philosophy

Department of Earth and Atmospheric Sciences

Edmonton, Alberta

Fall 2002

The author has granted a non-exclusive licence allowing the National Library of Canada to reproduce, loan, distribute or sell copies of this thesis in microform, paper or electronic formats.

L'auteur a accordé une licence non exclusive permettant à la Bibliothèque nationale du Canada de reproduire, prêter, distribuer ou vendre des copies de cette thèse sous la forme de microfiche/film, de reproduction sur papier ou sur format électronique.

The author retains ownership of the copyright in this thesis. Neither the thesis nor substantial extracts from it may be printed or otherwise reproduced without the author's permission.

L'auteur conserve la propriété du droit d'auteur qui protège cette thèse. Ni la thèse ni des extraits substantiels de celle-ci ne doivent être imprimés ou autrement reproduits sans son autorisation.

0-612-81218-9

Canadä

University of Alberta

Library Release Form

Name of Author: Dong-Chan Lee

Title of Thesis: Protaspides of Ptychopariida and taxonomy of Hystricuridae, with discussion of ancestry of Proetida

Degree: Doctor of Philosophy

Year this Degree Granted: 2002

Permission is hereby granted to the University of Alberta Library to reproduce single copies of this thesis and to lend or sell such copies for private, scholarly or scientific research purposes only.

The author reserves all other publication and other rights in association with the copyright in the thesis, and except as herein before provided, neither the thesis nor any substantial portion thereof may be printed or otherwise reproduced in any material form whatever without the author's prior written permission.

Dong-Chan Lee

10840-67 Ave.
Edmonton Alberta T6H 2A3

Date: *Sep. 25, 2002*

University of Alberta
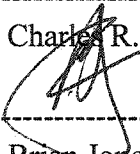
Faculty of Graduate Studies and Research

The undersigned certify that they have read, and recommend to the Faculty of Graduate Studies and Research for acceptance, a thesis entitled "Protaspides of Ptychopariida and taxonomy of Hystricuridae, with discussion of ancestry of Proetida" submitted by Dong-Chan Lee in partial fulfillment of the requirements for the degree of Doctor of Philosophy

----
Dr. Brian D. E. Chatterton

Dr. Charles R. Stelck

Dr. Brian Jones

Dr. Mark V. H. Wilson

Dr. Nigel Hughes

Aug 23 / 2002

Supervisor writes the date that the thesis is approved by committee

ABSTRACT

Species within the order Ptychopariida are considered to have given rise to the family Hystricuridae, the primitive family of the order Proetida. The family is considered to contain ancestors to various younger groups of the Proetida. This evolutionary speculation is investigated by revising taxonomy of the Ptychopariida and the Hystricuridae.

Protaspides of 34 Cambrian ptychopariid species are re-described. All the protaspid specimens are compared with one another and with post-protaspid specimens of all the species. The 34 species are classified into 28 genera, 17 families, and nine groups of superfamilial rank. Each of these nine groups is characterized by a distinctive protaspid form; five of them are assigned to the suborder Ptychopariina and the remaining four to the suborder Olenina.

The taxonomy of the Hystricuridae is revised upon the basis of 173 species that have been referred to the family and newly discovered materials from the Great Basin in the western United States. The revision concludes that the family includes 12 genera and 52 species. Seven genera are newly erected: *Carinahystricurus*, *Glabellosulcatus*, *Parahillyardina*, *Paramblycranium*, *Politohystricurus*, *Pseudoplethopeltis*, and *Spinohystricurus*. Pygidia are associated for 10 genera of the Hystricuridae and for 15 genera that have been and are considered to be related to the family.

The revised taxonomies and new information, in particular on protaspid and pygidial morphologies, give a new insight into the origin of the Proetida. Comparison of the pygidia leads to division of the hystricurid pygidia into two morphotypes, one with a pygidial fulcral ridge and the other without the structure. The first morphotype, present in

Hystricurus, the primitive genus of the Hystricuridae, appears to have transformed from the ptychopariid form and been retained in some younger proetide groups. The second morphotype, present in non-*Hystricurus* hystricurid genera, is considered to have derived from the first and to have gone extinct.

Protaspid morphologies of the Hystricuridae are considered to have transformed from those of ptychopariid protaspid morphotype B that represents a group consisting of the Cedariidae, Anomocaridae, Crepicephalidae, Marjumiidae, and Llanoaspididae. This suggests that the origin of the Hystricuridae, and subsequently the Proetida, may lie in the taxa possessing morphotype B.

ACKNOWLEDGEMENT

I would like to express my sincere thanks to Dr. B. D. E. Chatterton who has given me a full support. I also like to thank to all my committee members, Dr. Brian Jones, Dr. Mark Wilson, Dr. Charles Stelck, and Dr. Nigel Hughes.

I am very grateful for George Braybrook who has been extremely generous about SEM photography and my being as a part-time technician.

Finally, I like to thank for my family's support. My wife, Heekyoung and my two beautiful daughters, Somee and Soyeon have been encouraging me for many difficult times. All the other family members back in Korea, they cannot be omitted.

TABLE OF CONTENTS

CHAPTER I. INTRODUCTION

CHAPTER II. PROTASPIDES OF PTYCHOPARIIDE TRILOBITES AND THEIR TAXONOMIC IMPLICATIONS

CHAPTER III. TAXONOMY OF HYSTRICURIDAE (PROETIDA) AND RELATED TAXA

CHAPTER IV. PROBLEMS OF ESTABLISHING RELATIONSHIPS ON THE BASIS OF ONTOGENETIC DATA

CHAPTER V. CONCLUSIONS AND DISCUSSIONS

CHAPTER VI. BIBLIOGRAPHY

LIST OF TEXT-FIGURES

LIST OF PLATES

LIST OF APPENDICES

CHAPTER I

INTRODUCTION

PTYCHOPARIID PROBLEM

The "ptychopariid problem" is one of the most intractable problems in trilobite systematics. It entails classification and phylogenetic relationships of important trilobite higher taxa. The problem is two-fold, the unstable taxonomy of the Ptychopariida itself, and the unsolved evolutionary relationships of the Ptychopariida with such post-Cambrian groups as Olenina, Harpina, Asaphida, Proetida, and Phacopida.

The Ptychopariida appeared during the Early Cambrian and was considered to disappear during the Early Ordovician. The post-Cambrian trilobite groups, until recently, were considered to have appeared shortly after the close of the Cambrian, and many of them flourished soon after they appeared. It was believed that the post-Cambrian groups appeared as or shortly after most Cambrian groups including the Ptychopariida became extinct. This has been translated into taxonomic schemes where the groups below and above the Cambro-Ordovician boundary were taxonomically separated with reference to the stratigraphic boundary. This stratophenetic approach has prevailed, in particular, in the taxonomy of the Cambrian ptychopariide species. This taxonomic contention appears to have trilobite workers confine their interests to the groups below or above the Cambrian-Ordovician boundary—they have called themselves or been called, a "Cambrian trilobite worker," or "Ordovician specialist." Needless to say, this separation of interests did not encourage the workers to extensively study the trilobite groups across the boundary. Interpretations of macroevolutionary patterns that the trilobites displayed have also been affected by this contention. For example, the 'biomere' concept advocated by Palmer (1965a) and Stitt (1975) corresponds with the stratigraphic boundaries of evolutionary events such as extinctions and adaptive radiations. There was even a speculation by some that post-Cambrian trilobite groups were cryptogenetically derived from uncalcified, soft-bodied trilobites during a short period of time spanning from the Upper Cambrian to the Lower Ordovician (e.g., Whittington, 1981).

It is well recognized by many authors (e.g., Whittington, 1981; Fortey, 1990; Foote, 1990) that the ptychopariid problem mainly stems from the morphology of the ptychopariide trilobites. Fortey (*in* Whittington *et al.*, 1997, p. 296) described them as having, "a tapering glabella, a preglabellar field, opisthoparian sutures, rimlike cephalic borders extending into genal spines, natant hypostome, usually more than 12 thoracic segments, and a small transverse, well-furrowed pygidium without remarkable features." The minor variations of this basic morphologic theme are too inseparable among the ptychopariide species to make widely acceptable groupings possible. Due to such a continuous range of morphologies, the geographic and stratigraphic occurrences have often played a role in defining species, resulting in excessive splitting into taxa that are difficult to discriminate. Even with these secondary criteria, the taxonomic scheme of the Ptychopariida at every hierarchical level—in particular, at the family and superfamily level—is far from stable. The problem also stems from the unresolved evolutionary relationships of the ptychopariides with major post-Cambrian trilobite groups mentioned above. To resolve the evolutionar relationships by removing the taxa ancestral to the

1

post-Cambrian groups from the Ptychopariida will contribute to the solution of the ptychopariid problem.

In comparison to the general ptychopariide morphology, the morphologies of post-Cambrian groups are much more distinctive; for example, Fortey (1990) listed diagnostic features of many post-Cambrian orders that are distinguishable from the ptychopariide morphology. However, the earliest and most primitive members of these post-Cambrian groups approximate the typical ptychopariide morphology. For instance, many authors claimed similarities between Hystricuridae, the primitive family of the Proetida, and such Cambrian ptychopariide groups as the Solenopleuridae (Fortey, 1990), *Onchopeltis* (Fortey, 1983), and Catillicephalidae (Shergold, 1991a). Although the order Phacopida is defined by many 'good' synapomorphies, its primitive members such as *Bavarilla* and *Pharostoma* appear to have the ptychopariid morphology (Fortey, 1990).

Because of the ptychopariide similarities of the primitive members, the ancestry or the sistergroup of these post-Cambrian groups is believed to lie within the Ptychopariida. Fortey and Chatterton (1988) suggested that the ancestry of the Asaphida lies in the Anomocaracea that was previously classified under the Ptychopariida. Not only are the relationships among the ptychopariides problematic, but the relationships of the ptychopariides to the other groups are problematic. This contention that the ancestors to many post-Cambrian groups are ptychopariides makes it even more intractable to find the solution for the ptychopariid problem. At the analytical level, the number of taxa to be incorporated would be astronomical; the major trilobite groups except Agnostida, Redlichiida, and perhaps Corynexochida need to be included in the analysis.

Applying methodologies of cladistics or phylogenetic systematics to the study on the hypothetical extinction and appearance of trilobite groups at the Cambro-Ordovician boundary reveal that many paraphyletic groups are involved in this evolutionary event (Fortey, 1989). The magnitude of the extinction or taxonomic turnover rate across the boundary has been assessed to be much lower than previously speculated (e.g., Westrop, 1989; Edgecombe, 1992). Therefore it is necessary to remove paraphyletic groups and establish more natural classification schemes. Some comparative taxonomic studies on the groups across the boundary that mainly deal with parts of the ptychopariid problem have been carried out (e.g., Fortey and Chatterton, 1988; Fortey, 1990; Edgecombe, 1992; Lee and Chatterton, 2001).

The previous approaches to the problem were to focus on discovering reliable characters to diagnose each post-Cambrian group with the appropriate ptychopariide ancestor. For instance, Fortey and Chatterton (1988) claimed that the presence of a median suture and an 'asaphoid' protaspis define the Asaphida which includes many ptychopariide taxa in the concept. Fortey (1990) argued that a natant hypostomal condition is a derived state, and used it to define his Libristoma which is a taxon nearly equivalent to the Ptychopariida in terms of its content. As mentioned above, he listed diagnostic features of members of his Libristoma such as the Proetida and Asaphida. Fortey ended his discussion of the concept of the Ptychopariida by stating, "... there will probably remain a core of ptychopariids sharing only the primitive grade of libristomae organization, and differing only in characters of the most trivial kind .... These will likely remain classified together, as perhaps they should." This epitomizes the current status of our understanding—perhaps, our frustration thereby—of the ptychopariid problem. Edgecombe (1992) tested parts of the ptychopariid problem with cladistic methodologies

2

such as the ghost lineage concept and taxonomic congruence. He revealed that many components of the Asaphida sensu Fortey and Chatterton (1988) possess undisclosed stratigraphic extensions well into the Middle Cambrian, and the Proetida would have originated before late Middle Cambrian.

OBJECTIVES

This study deals with two groups involved in the ptychopariid problem, the Ptychopariida itself and the Hystricuridae of the Proetida. As shown in Text-fig. I-1, the currently accepted taxonomic schemes of the two groups appear to accord with the stratigraphic boundary between the Cambrian and Ordovician. The Ptychopariida is mostly Cambrian in age and the Hystricuridae is restricted to the Early Ordovician; non-hystricurid proetides have been considered to be derived from the Hystricuridae and thus are younger than the Early Ordovician in age.

The ancestry of the Proetida is believed to be in the Hystricuridae (Fortey and Owens, 1975) and ultimately within the Ptychopariida, as mentioned above. However, detailed ancestor-descendant relationships between these groups have not been established. It is partly because few attempts have been made to analyze morphologies comparatively, of all these groups across the stratigraphic boundaries. Proetide workers tend to focus on the trilobites from the Middle Ordovician and upwards, and ptychopariide workers on the trilobites from the Upper Cambrian and downwards. The hystricurids have been mostly documented as a minor element in many regional trilobite studies.

The first step towards determining how members of these groups are related is to create taxonomic schemes for the Ptychopariida and the Hystricuridae that are reliable enough for detailed analytical studies such as cladistic analysis. Taxonomies of non-hystricurid proetides appears to be reliable to the extent that they have been utilized for many analytical approaches based on taxonomic diversities (e.g., Adrain *et al.*, 1998). Since the ptychopariides and hystricurids are evolutionarily related to each other (e.g., Fortey, 1983), the ultimate taxonomic scheme for each group, of course, will be established by analyzing all the groups together, which requires an analysis with a much wider scope. Conducting a taxonomic revision of the Ptychopariida and Hystricuridae separately will form a foundation for resolving part of the ptychopariid problem.

Taxonomy is "the practice of recognizing, naming, and ordering taxa into a system of words consistent with any kind of relationships among taxa that the investigator has discovered in nature." (Christoffersen, 1995). The taxonomy in this study is practiced upon the basis of comparing morphologies of the taxa and detecting similarities and differences of the morphologies. The morphologic similarities shared by the taxa are taken to indicate a membership of a higher ranked taxon. The similarities may be homologous or homoplasious, and this status of the similarities ultimately informs the nature of the taxa. It will reveal how these taxa are phylogenetically related, which will give a clear insight to the ultimate solution for the ptychopariid problem. The determination of the status of the similarities cannot be easily achieved without character analysis using a computer in the case where many taxa are involved, as in this study. However, the number of taxa involved in this study is likely to overpower the computational abilities currently available to us. The taxonomy, as established in this study, will provide a fundamental data base for framing a workable hypothesis of

3

phylogenetic relationships of relevant taxa. For example, a reliable taxonomic scheme helps in the selection of the taxa and characters to be analyzed, in cases where it is simply impossible to include all related taxa in an analysis.

The taxonomy of the Ptychopariida is revised in particular at the superfamily level mainly upon the basis of the protaspid features (Chapter II) and that of the Hystricuridae upon the basis of comparing their morphologies with those of both derived proetide members and plesiomorphic ptychopariides (Chapter III). The comparisons are attempted to be exhaustive geographically and stratigraphically.

PTYCHOPARIIDA (CHAPTER II)

The Lower Cambrian witnessed the appearance of a trilobite group called the Ptychopariida which existed into the Lower Ordovician. According to the most recent classification scheme (Fortey *in* Whittington *et al.*, 1997), the order consists of 31 families. The superfamilial groupings of these families are yet to be determined; for example, more than 60% of the families have been classified into "Superfamily Uncertain" of the Ptychopariida (e.g., see Westrop, 1995).

Chapter II aims to provide a taxonomic scheme by examining ptychopariide protaspides. Earlier ontogenetic stages of members of a higher taxonomic group are generally known to bear a greater morphologic resemblance than later stages. The resemblance is usually taken to indicate a community of descents (Darwin, 1860; Chatterton and Speyer *in* Whittinton *et al.*, 1997). This assumption makes it very attractive to investigate protaspid features of the ptychopariides for classifying them at a familial or superfamilial rank. Protaspides have been described for more than 50 ptychopariide species by a Taiwanese paleontologist, Chung-Hung Hu. In Chapter II, ontogenies of 34 ptychopariide species are re-illustrated with scanning electron microphotographic techniques that enable us to see more detail and thus collect more accurate morphologic data, and to examine whether the protaspid specimens are correctly associated with more mature stages that have been named. Upon the basis of morphologic similarities of these protaspides, including putative synapomorphies and symplesiomorphies, the taxonomy of these species at higher ranks is revised. The similarities at protaspid and holaspid stages are incorporated to make new suggestions for evolutionary relationships of these species and evaluate previous hypotheses.

HYSTRICURIDAE OF PROETIDA (CHAPTER III)

Througout the text, "hystricurids" or "hystricurid" refer to the concept of the Hystricuridae before the taxonomic revision made in Chapter III. The Lower Ordovician family, Hystricuridae Hupé, 1953, which is the stratigraphically earliest family of the Proetida, is known to have derived within the ptychopariides (Fortey, 1983) and to have given rise to several younger families of the Proetida such as the Dimeropygidae and Bathyuridae (Fortey, 1990). The Hystricuridae is considered to lie evolutionarily and stratigraphically between the ptychopariides and proetides (Text-fig. I-1). In Chapter III, the taxonomy of the Hystricuridae is revised mainly on the basis of post-protaspid morphologic information. 86 formally named species and 87 species in open nomenclature have been referred to the family. All these species are morphologically compared on the basis of their illustrations in publications and re-examination of specimens that were loaned from institutions all around the world. Not only are the taxa

4

compared within the "hystricurids," but they are also compared with ptychopariides and non-"hystricurid" proetides. This comparative analysis contributes to sorting out the "hystricurids" and thus providing a fundamental data base for discovering a natural concept of the Hystricuridae. This will ultimately help to solve the origin of the Proetida, which is a part of the ptychopariid problem.

PROBLEMS OF ESTABLISHING RELATIONSHIPS ON THE BASIS OF ONTOGENETIC DATA (CHAPTER IV)

The morphologic information that will be incorporated into building the taxonomic scheme for the Ptychopariida and Hystricuridae is supplied by two growth stages, holaspides and protaspides. These two different stages often lead to different classification schemes. The morphologic information employed by this study shows a great bias towards the holaspides, in terms of quantity; the protaspides have been described for a much smaller number of species. This bias will not be corrected altogether because the preservation potential of the protaspides is much lower. This reality leads me to consider assumptions and methodologies used to incoporate morphologic information from both ontogenetic stages in an evolutionarily meaningful manner. The outcome of the classification will be affected by which assumptions and methodologies are employed. For the taxonomic revision of the Ptychopariida and Hystricuridae, morphologic features from both growth stages are considered to be of equal value; which is only one of several options that systematists may employ when dealing with characters from different ontogenetic stages. Theoretical and operational issues about how to use the morphologic characters from different ontogenetic stages are discussed from various standpoints, including cladistics. This will facilitate the formulation of pending systematic analyses of the Ptychopariida and Hystricuridae that will most likely utilize the cladistic paradigm.

LOCALITIES OF SPECIMENS AND SAMPLES

Protaspides described in the Chapter II were loaned from the University of Cincinnati (UCGM; all specimens were recently transferred into the Cincinnati Museum Center), National Museum of Natural History of Smithsonian Institution (USNM), and Geological Survey of Canada (GSC; all the specimens were affixed by TNUM in the literatures, but they were transferred into the Geological Survey of Canada and given a new GSC specimen number). The geographic localities where these protaspid specimens were collected by Chung-Hung Hu are shown in Text-fig. I-2. Additional silicified materials are collected by the author from the Upper Cambrian Dunderberg Formation of McGill section ('F' in Text-fig. I-3) and the Middle Cambrian Marjum Formation ('C' in Text-fig. I-3). Only four horizons (MJ-1, MJ-2, MJ-3, and MJ-4) were sampled from the Marjum Formation. Of them, MJ-3 yielded abundant silicified specimens: GPS reading for the horizon is 39°21'25.5" & 113°16'59.2".

Silicified materials for the "hystricurids" were collected from the Garden City Formation and Fillmore Formation ('A', 'B', 'D', and 'E' in Text-fig. I-3). All the materials were obtained from five sections, Locality 5 and 6 in Hillyard Canyon (Text-fig. I-5 and I-6), Locality 11 in Green Canyon (Text-fig. I-7), Section E in Willden Hills or Middle Mountains (Text-fig. I-8), and Section H in Heckothorn Hills. Specimens that were previously described by several authors are housed in the following institutions:

5

Museum Victoria in Australia (NMVP), Geologisk Museum in Denmark (MGUH), University of Cincinnati in USA (UCGM: all specimens have recently been transferred to Cincinnati Museum Center (CMC-P)), Seoul National University in South Korea (SNU), New York State Museum in USA (NYSM), University of Tasmania in Australia (UTGD), Smithsonian Institution in USA (USNM), Geological Survey of Canada (GSC), Nanjing Institute in China (NI), and Yale Peabody Museum of Natural History in USA (YPM).
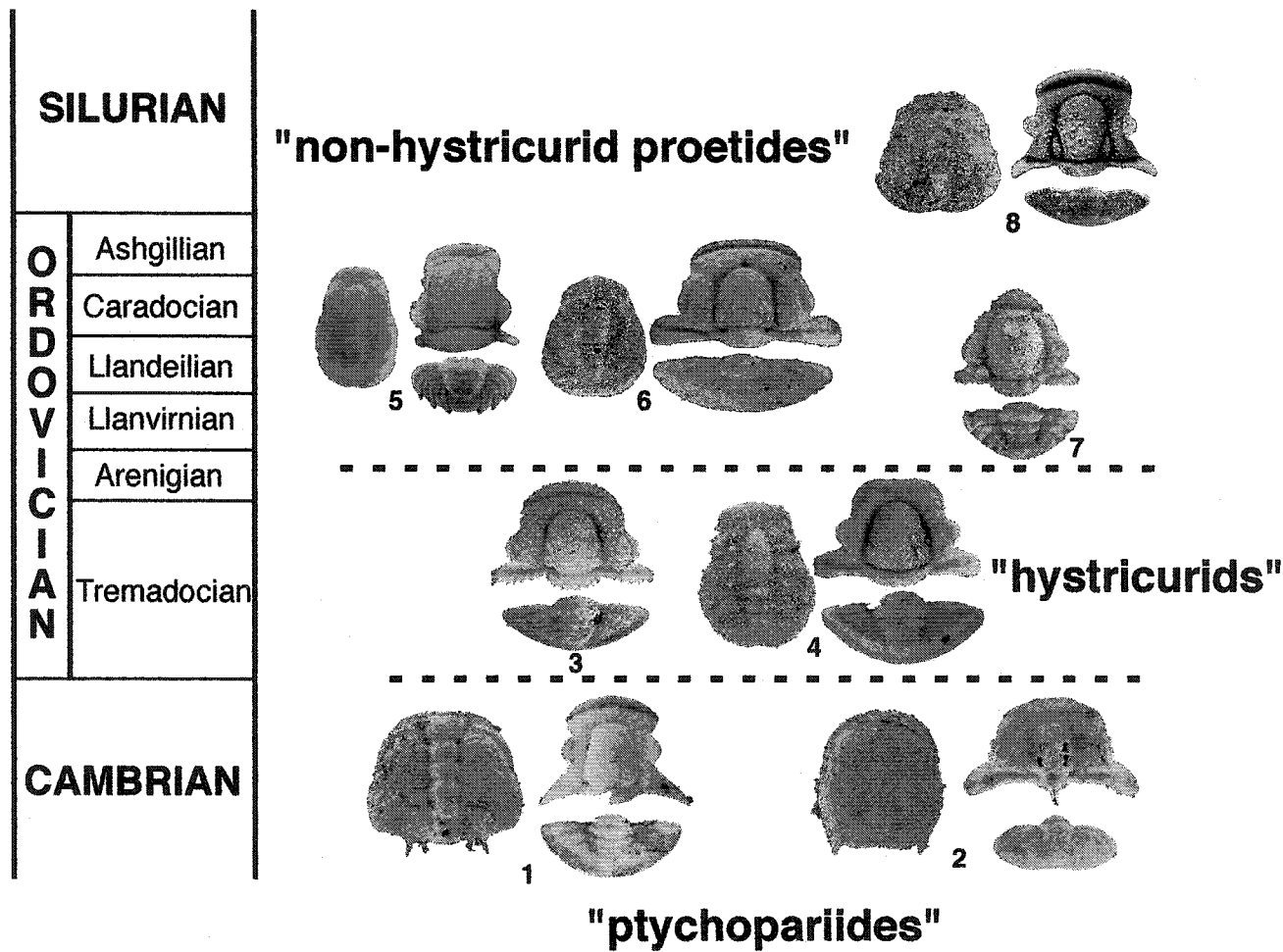
TEXT-FIGURE I-1. Stratigraphic occurrence of proetides, "hystricurids" and ptychopariides, which have played a role in diagnosing each taxon and/or spearating one from another. The vertical thickness of the Ordovician series is not to scale. 1. Upper Cambrian *Aphelaspis*, 2. Middle Cambrian *Bolaspidella*, 3. Lower Ordovician *Hystricurus*, 4. Lower Ordovician *Spinohystricurus* n. sp., 5. Upper Ordovician *Stenoblepharum*, 6. Middle Ordovician *Paratoernquistia*, 7. Middle Ordovician *Dimeropygiella*, 8. Silurian aulacopleurid, *Maurotarion* and*Otarion*.

TEXT-FIGURE I-2. Localities where Hu collected specimens in North America.

Locality 1. Lower Cambrian Buelina Formation, near Caborca, northwestern Sonora, Mexico (*Olenellus truemani*)

Locality 2. Middle Cambrian Langston Formation (?), northeast side of road in Santaquin Canyon, Wasatch Mountains, Utah (*Pagetia resseri*; *Ptarmigania aurita*)

Locality 3. A: Lower Ordovician Garden City Formation, Hillyard Canyon, southern Idaho (*Leiostegium formosa*). B: Upper Cambrian St. Charles Formation, north of Mink Creek, southern Idaho (*Ptychaspis bullasa*)

Locality 4. A: Lower Ordovician of Deadwood Formation, south side of Sheep Mountains, Sundance, Crook County, northeastern Wyoming (*Missisquoia cyclochila*; *Apoplanias rejectus*). B: Lower Ordovician of Deadwood Formation, Reutes Canyon, Bearlodge Ranch, northeast Wyoming (*Paranumia triangularia*). C: Upper Cambrian of Deadwood Formation, south slope of Sheep Mountain, near Bearlodge Ranch, east-central Wyoming (*Arapahoia arbucklensis*).

Locality 5. Upper Cambrian of Deadwood Formation A: Bear Butte section, southeastern Deadwood City, South Dakota (*Blountia bristolensis*; *Glaphyraspis parva*). B: Lead, northern Black Hills, Lawrence County, South Dakota (*Crepicephalus deadwoodiensis*). C: Galena section, southeast of Deadwood City, South Dakota (*Housia ovata*; *Pulchricapitus davisi*). D: Boxelder section, near Nemo, northwest of Rapid City, South Dakota (*Drabia typica*). E: south side of Dark Canyon, west of Rapid City, South Dakota (*Aphelotoxon triangularia*). F: White Canyon, northeast of Deadwood City, South Dakota (*Orygmaspis (Parabolinoides) contractus*). G: Brownsill Junction, south of Deadwood City, South Dakota (*Taenicephalus shumardi*). H: Moll section, southeast of Deadwood City, South Dakota (*Aphelaspis haguei*; *Irvingella major*). I: Little Elk Creek and Dark Canyon, Black Hills, South Dakota (*Elvinia roemeri*)

Locality 6. Upper Cambrian Bonneterre Dolomite A: Little Sauk Creek and Stout Creek, Iron County, Missouri (*Komaspidella laevis*; *Welleraspis lochmanae*). B: St. Francois County, Missouri (*Norwoodella halli*)

Locality 7. Upper Cambrian Dunderberg Formation, McGill section, east-central Nevada (*Glaphyraspis parva*; *Aphelaspis brachyphasis*)

Locality 8. Middle Cambrian Marjum Formation, near Swasey Peak, House Range, western Utah (*Bolaspidella housensis*; *Modocia laevinucha*)

Locality 9. Upper Cambrian (formation unknown, but most probably Langston Formation), near Wasatch Mountains, Utah (*Cedarina cordillerae*; *Apomodocia conica*)

Locality 10. A: Middle Cambrian Meagher Formation, west side of south Boulder Creek, west Madison County, Montana (*Glyphaspis paucisulcata*). B: Upper Cambrian Pilgrim Formation, south Boulder Creek, Madison County, Montana (*Syspacheilus dunoirensis*; *Nixonella montanensis*)

Locality 11. Upper Cambrian Dry Creek Shale, Big Horn Mountains, north-central Wyoming (*Housia vacuna*; *Ponumia obscura*)

Locality 12. Middle Cambrian Porter Road Formation, St. John, New Brunswick, Canada (*Solenopleura acadica*)

Locality 13. Upper Cambrian Hamburg Limestone, Cherry Creek, east-central Nevada (*Aphelaspis subditus*)

Locality 14. Upper Cambrian Nolichucky Formation, Tennesse (*Aphelaspis tarda*)

Locality 15. Upper Cambrian Notch Peak Formation, Lawson Cove, Wah Wah Range, southwestern Utah (*Aphelaspis? anyta*; *Dytremacephalus granulosus*)
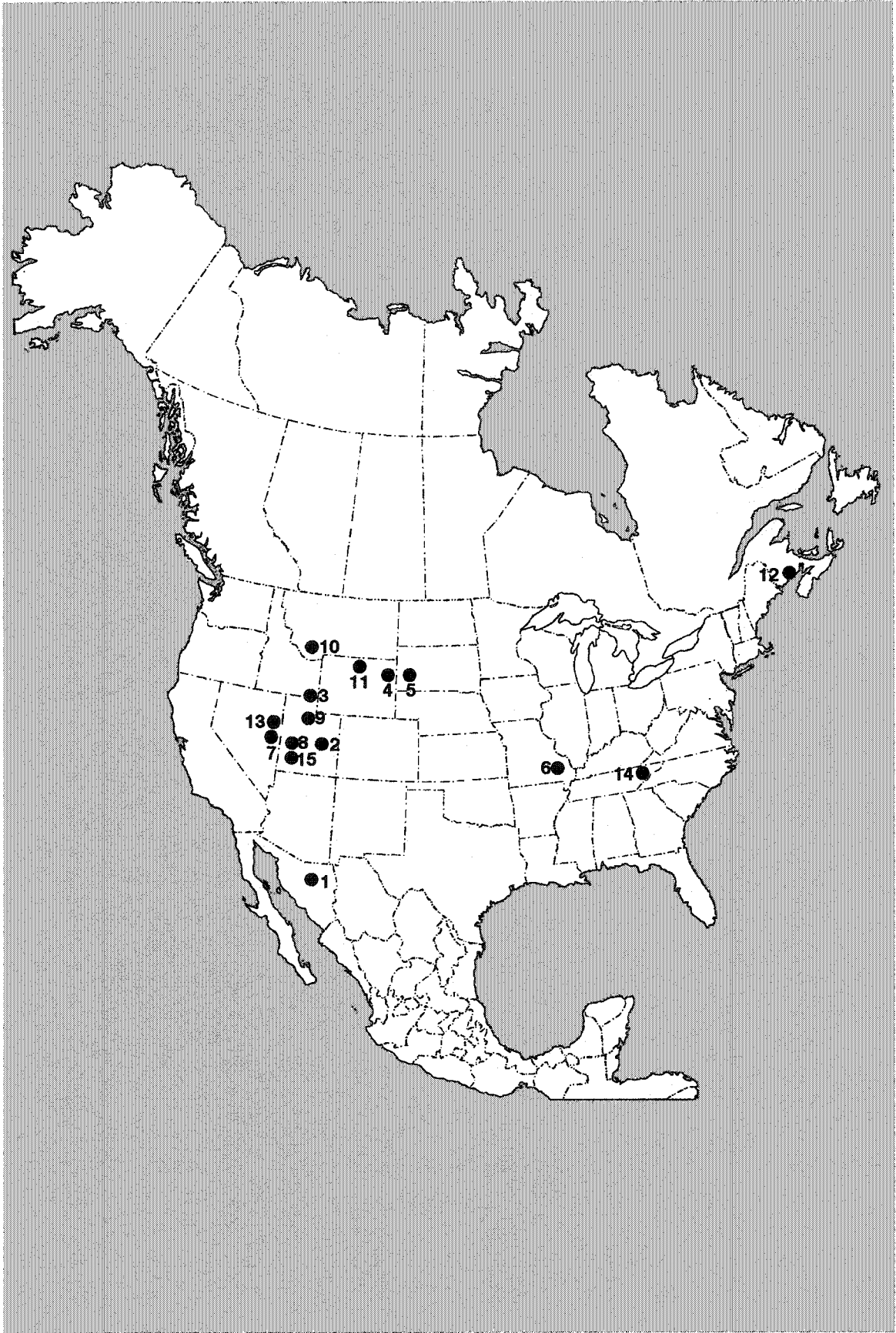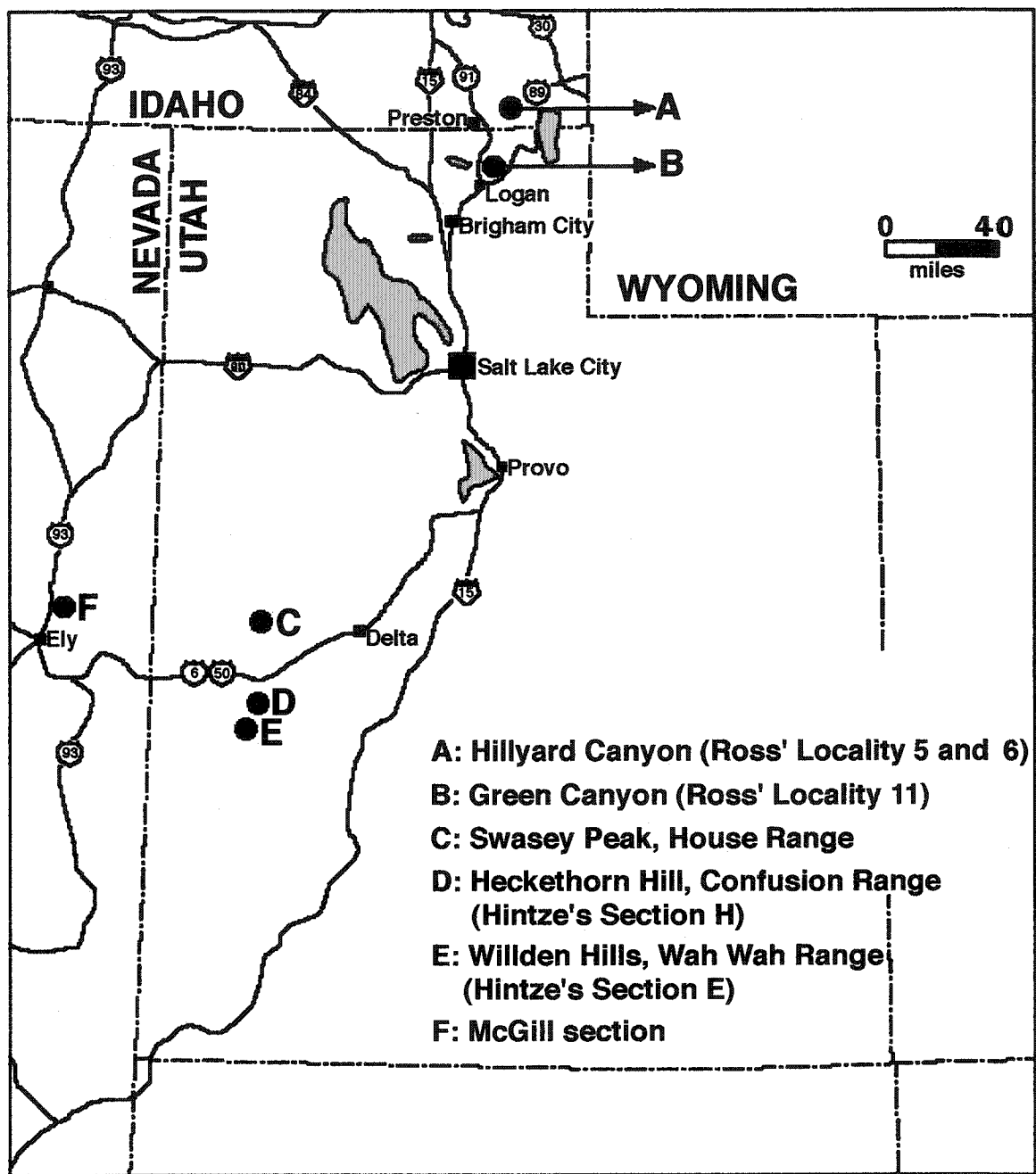
TEXT-FIGURE I-3. Sampling localities where silicified materials were collected for ptychopariide protaspides (Chapter II) and "hystricurids" (Chapter III).

11
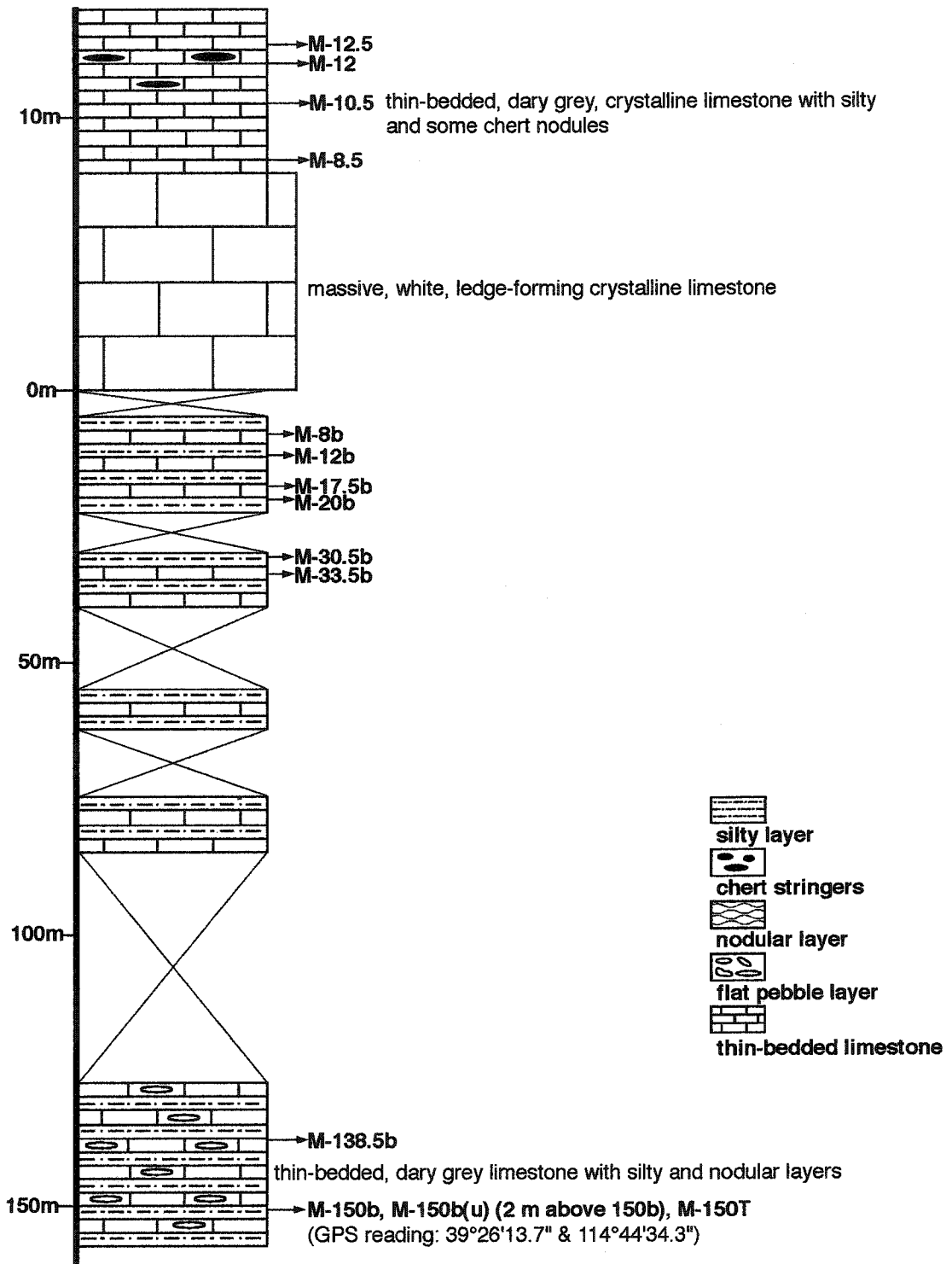
TEXT-FIGURE I-4. Lithologic column of Dunderberg Formation exposed at McGill section, east-central Nevada ('F' in Text-fig. I-3) and sampling horizons.

12
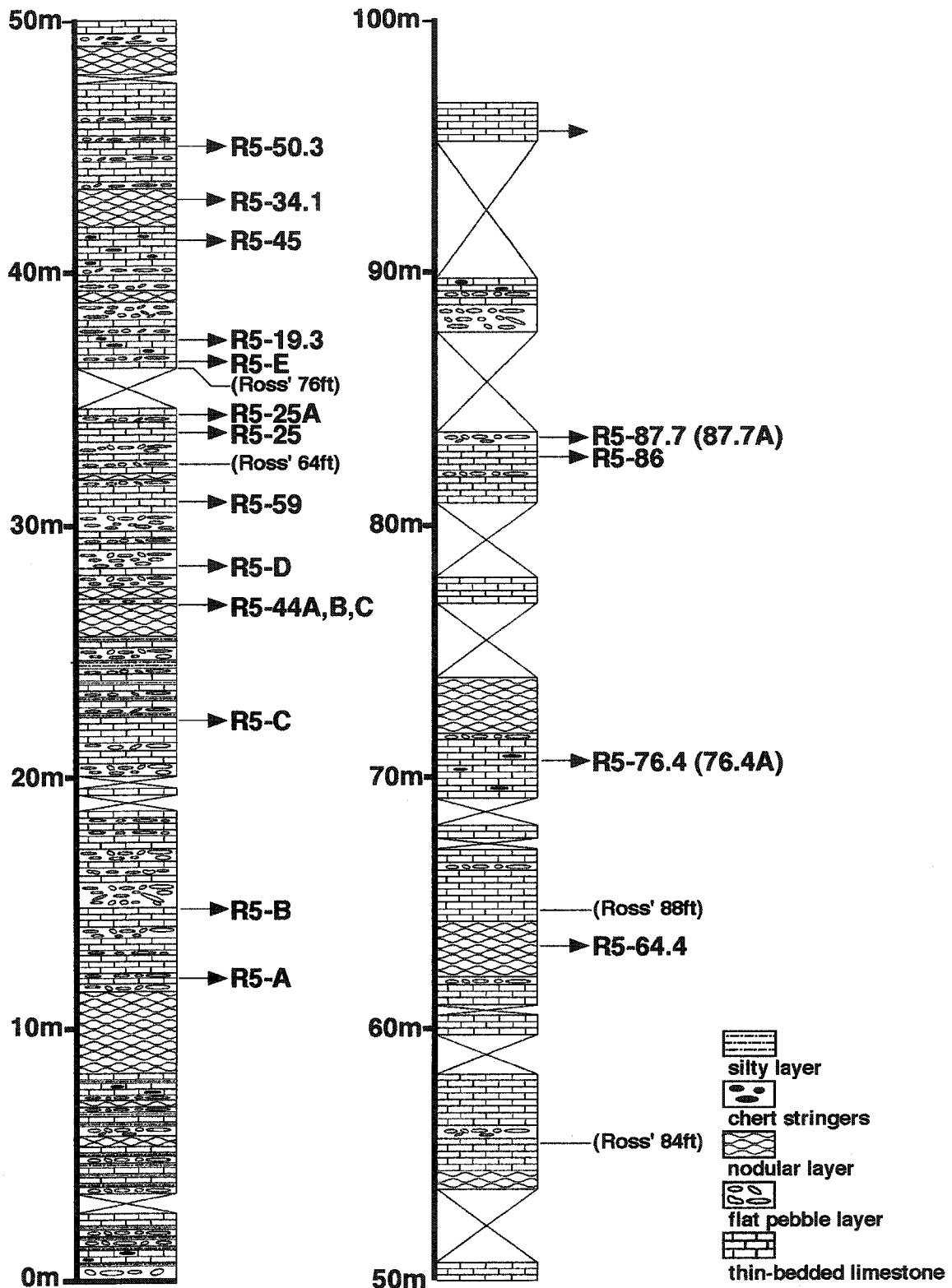
TEXT-FIGURE I-5. Lithologic column of Garden City Formation exposed at west side of Hillyard Canyon (Ross (1951)'s Locality 5; 'A' in Text-fig. I-3) and position of sampling horizons.

13
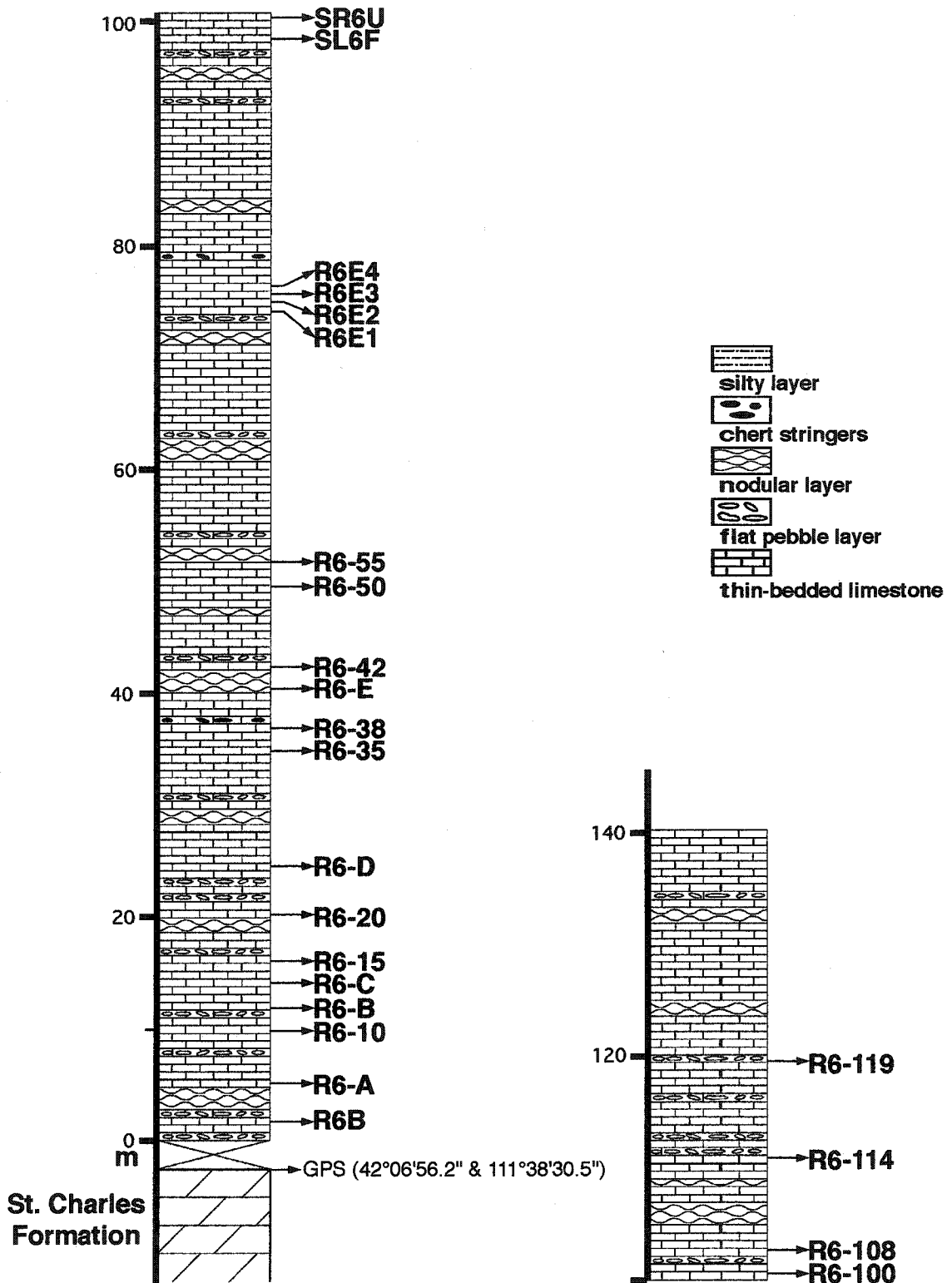
TEXT-FIGURE I-6. Lithologic column of Garden City Formation exposed along the ridge, east side of Hillyard Canyon (Ross (1951)'s Locality 6; 'A' in Text-fig. I-3) and position of sampling horizons.

14
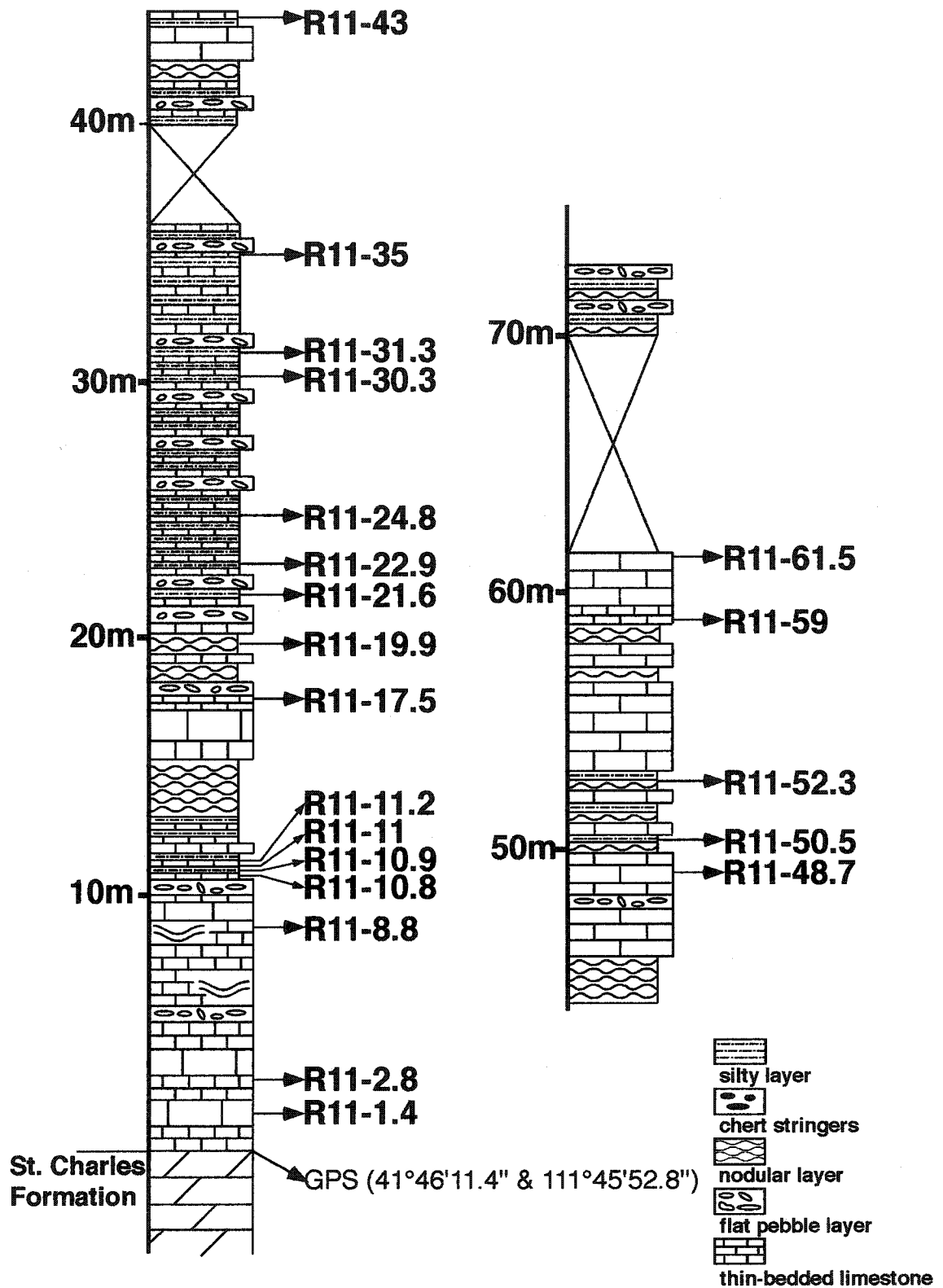
TEXT-FIGURE I-7. Lithologic column of Garden City Formation exposed at Green Canyon (Ross (1951)'s Locality 11; 'B' in Text-fig. I-3) and position of sampling horizons.

15
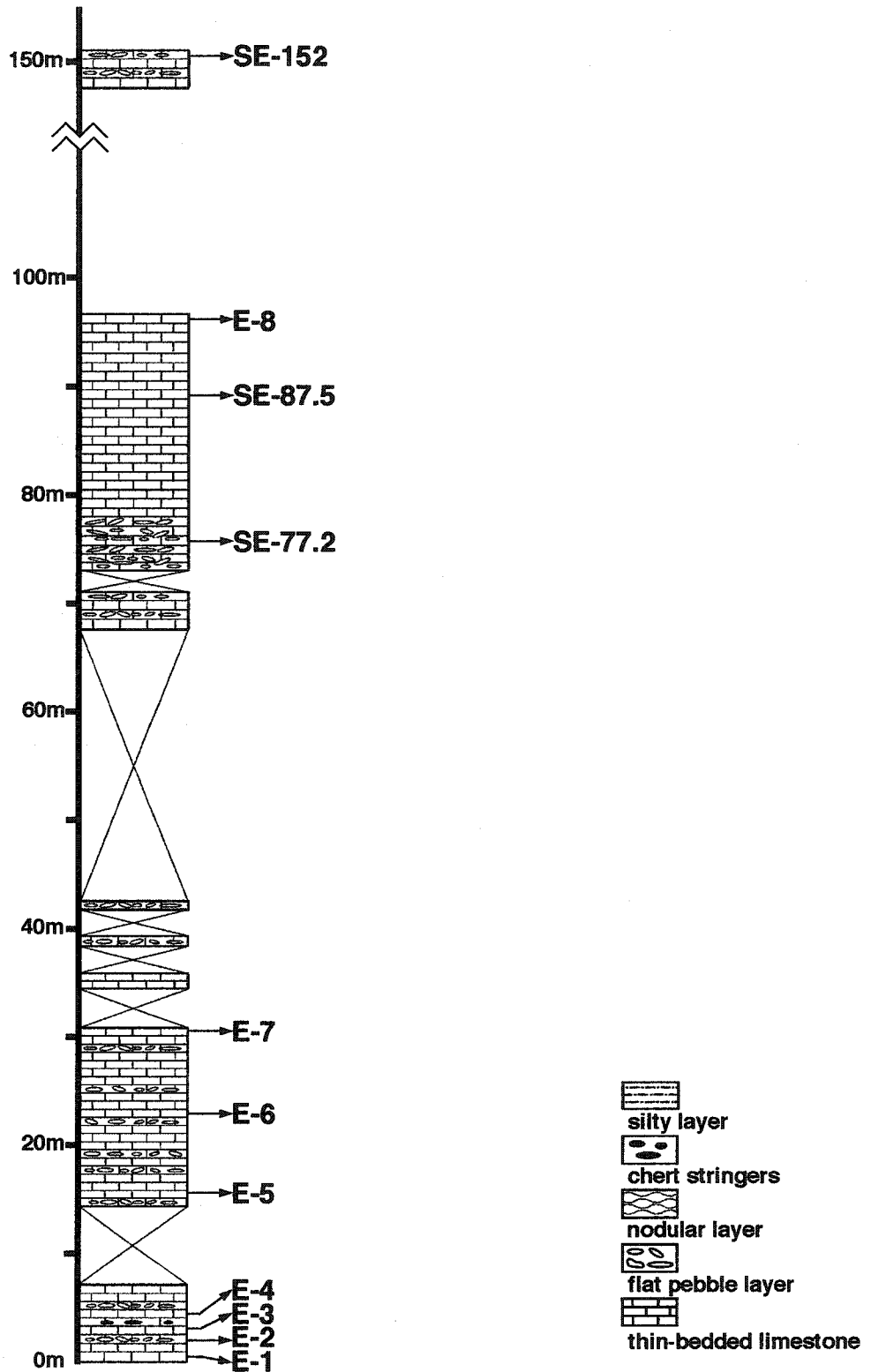
TEXT-FIGURE I-8. Lithologic column of Fillmore Formation exposed at Willden Hills (or Middle Mountain) of Wah Wah Range (Hintze (1953)'s Section E; 'E' in Text-fig. I-3) and position of sampling horizons.

16

CHAPTER II

PROTASPIDES OF PTYCHOPARIID TRILOBITES AND THEIR TAXONOMIC IMPLICATIONS

INTRODUCTION

Relationships between members of the order Ptychopariida have not been firmly established, in particular, at the superfamily level; more than 60 percent of families have been left to "superfamily uncertain" (e.g., see Westrop, 1995). Fortey (*in* Whittington *et al.*, 1997) discussed the three sources from which this taxonomic difficulty stems. The ptychopariide species exhibit a wide and continuous range of morphologic variations within the generally termed "ptychopariid morphology." This has made it difficult to establish acceptible clusterings at the superfamily level and even at the lower taxonomic ranks. Secondly, many taxa have been known only from cranidia. Without any critical evalutations of morphologies, stratigraphic and geographical criteria have come into play in the taxonomy, resulting in an excessive splitting. Furthermore, the well-accepted paraphyly of the Ptychopariida, indicating that the group contains ancestors of several post-Cambrian orders such as the Proetida, has made the taxonomic exercise for the ptychopariides further complicated.

Recently, protaspides of the trilobites have provided significant morphologic information for defining higher taxa of the trilobites. Fortey and Chatterton (1988) reviewed the concept of the Asaphida and argued that the "asaphoid-type" protaspis serves as a synapomorphy of the group. These taxonomic studies assume that the protaspides, as an earlier developmental stage of the trilobites, are morphologically more conservative towards the higher taxonomic ranks, and thus are considered evolutionarily more important at the higher taxonomic ranks. This follows from von Baer's laws. The protaspides of the Ptychopariida have been simply called the "ptychopariid-type" and there have been few attempts to comparatively analyze their morphologies. Chatterton and Speyer (*in* Whittington *et al.*, 1997), in the most recent review of the ptychopariid protaspides, listed their "diagnostic" features and supported the paraphyly of the Ptychopariida.

During 1960s to 1980s, Chung-Hung Hu, a Taiwanese trilobite worker, described ontogenies of many Cambrian trilobites which are mostly from Laurentia. He described ontogenies of over 100 species, many of which belong to the Ptychopariida, in about 40 publications (see Chatterton and Speyer *in* Whittington *et al.*, 1997, for a list of publications). Chatterton and Speyer (*in* Whittington *et al.*, 1997) reviewed the ptychopariid protaspides only based on the illustrations in each publication. However, since the protaspid specimens in Hu's publications all were illustrated by light photography and only in dorsal view, the morphological information available appears to be poor for a comparative morphologic study. This relatively poor illustration is one of the main reasons why Hu's numerous ontogenetic works have rarely been employed for any kind of comparative studies.

This study aims to provide much more detailed morphologic information on the protaspid specimens by re-illustrating them using scanning electron microphotography (SEM). SEM technique reveals the features that could not be detected by conventional

light photographic techniques. The protaspid specimens were photographed in various angles (dorsal, lateral, anterior, and posterior, and ventral if available) to provide a much complete information as possible on their morphologic features.

In addition to the ptychopariide protaspides, those of other higher taxa such as redlichiids, agnostids, and corynexochids available to the author are redescribed and examined. These groups will serve as the outgroup in a cladistic analysis of the Ptychopariida.

ASSUMPTIONS FOR ASSOCIATING PROTASPIDES

One of the fundamental tasks in trilobite ontogenetic studies is to correctly associate protaspid specimens with holaspid specimens of a particular species. One of the reasons that Hu's published ontogenetic data have rarely been used is because there are incorrect associations. It is the initial task in this work to investigate whether the protaspid specimens are correctly associated with a particular species.

The firstly-employed criterion for associating protaspid specimens is "co-occurrence." Protaspid specimens are likely to be associated with a species which is represented by co-occurring holaspid specimens. For example, when silicified protaspid specimens are secured from one block of limestone, their association with one of the species represented by co-occurring holaspid materials is accepted with the highest confidence. Likewise, the specimens from one slab of shale or limestone allow one to confidently associate the protaspides with a co-occuring species. The confidence of the association is much higher if only a single species is present. This "co-occurrence" criterion asssumes that co-occurring individuals lived in the same place and probably at the same time. If ontogeny entails the change in mode of life in association with metamorphosis, usually planktonic to benthic, (Chatterton and Speyer *in* Whittington *et al.*, 1997) the planktonic protaspides could have drifted away and then been deposited in different places from the benthic protaspides. It is expected that the planktonic protaspides would have a greater geographic distribution than the benthic mode of the same species.

It is unfortunate that Hu did not provide detailed sampling information such as a lithologic column with sampling horizons in his publications. It has been informed to the author that he acquired the samples from the late Lochman-Balk who collected the samples. Therefore the "co-occurrence" criterion cannot be employed in its full strength to investigate the association of protaspides. Only the lithology of the samples containing protaspid and holaspid specimens allows the author to investigate whether the protaspid specimens co-occur with the holaspid specimens. However, the same lithology can be repeated within a few meters with alternations of different lithologies or a section of tens of meters in thickness may be lithologically monotonous. Thus, even the same lithology provides few useful tools for examining the association of protaspid specimens described by Hu. All the samples containing the protaspid and holaspid specimens of one species described by Hu happen to be lithologically identical.

The second criterion for the association of protaspides is to examine whether morphologies of the protaspid specimens are carried into smaller meraspid cranidia of a particular species. When morphologies of the protaspides transform into those of the smallest post-protaspid specimen within a "reasonable" or "acceptable" range, the protaspid specimens are assigned to a species represented by the post-protaspid

18

specimens. However, metamorphosis, which is considered to usually occur across protaspid and meraspid periods during ontogenies of many trilobite species (e.g., *Isotelus*, Tripp and Evitt, 1986), poses a problem in applying this criterion. The "co-occurrence" criterion allows one to associate protaspides that morphologically greatly deviate from post-protaspides; the association of *Isotelus* protaspides by Evitt (1961) is the best example. This association still needs to satisify the assumption that both protaspides and post-protaspides lived where they are found, as stated above.

It is not uncommon to find several protaspid specimens together with holaspid specimens representing several different species. As a result, it is very difficult to determine whether a metamorphosis took place across the protaspid and meraspid periods for cases where protaspid and meraspid specimens exhibit great morphologic dissimilarities. Where metamorphosis is found in all known ontogenies of a particular higher taxon, it may be expected that the metamorphosis occcurs in all the member of that taxon. In this case, the metamorphosis is a significant developmental event of the ontogenies of that taxon. However, no such data are available for ontogenies of the Ptychopariida. As a matter of fact, comparative developmental studies on trilobite ontogenies, which allow one to predict taxonomic frequencies of the metamorphosis, are yet to be carried out. In this study, it is therefore assumed that the metamorphosis did not take place across the protaspid and meraspid periods of the ptychopariide species.

Of the disarticulated body parts of a meraspid individual, the cranidium serves as the most reliable criterion for the association. The transitory pygidium of the meraspides and protopygidium of the protaspides are usually too small and featureless to be used for investigating the association. Once the association of a certain species is examined by the morphologic continuity criterion, the corrected association provides a supplementary criterion. It can be used to investigate the association of other species which have been considered to belong to the same higher taxon. For this case, it is necessary to assume that the protaspid morphologies are more similar towards the higher taxonomic ranks.

TERMINOLOGIES
Chatterton and Speyer (*in* Whittington *et al*. 1997) objected the usage of anaprotaspid and metaprotaspid stages to subdivide the protaspid period of all trilobite ontogenies. It is because two separate developmental events are required for trilobite protaspides to develop from anaprotaspis to metaprotaspis, and each event occurs simultaneously in some taxa and separately in others. The two events are the appearance of recognizable protopygidial region with respect to its volume and the impression of a furrow to separate the protopygidial from cephalic regions. The examination of the protaspides of the Ptychopariida indicates that the two events occur simultaneously during the ptychopariide ontogenies. The differentiation of the protopygidium from the cephalon is the first transverse segmentation event in the trilobite ontogeny. Therefore, the protaspid stage when the protopygidium is yet to be differentiated is referred to as an anaprotaspid stage, and the stage when the protopygidium is differentiated and recognized by the posterior cranidial marginal furrow is referred to as a metaprotaspid stage.

19

SYSTEMATIC PALEONTOLOGY

Order **REDLICHIIDA** Richter, 1932
Suborder **OLENELLINA** Walcott, 1890
Family **OLENELLIDAE** Walcott, 1890
Olenellidae sp. A
Pl. II-1, Figs. 10-13

1971, *Olenellus truemani*, Hu [part], p. 76-78, pl. 8, figs. 1, 4, 7, 9 [only].
Remarks. Meraspid cranidia of this species differ from *Olenellus truemani* in having a less distinctively defined proximal portion of ocular ridge and less well-developed anterior border furrow.

Genus **OLENELLUS** Hall, 1861
Olenellus truemani Walcott, 1913
Pl. II-1, Figs. 1-9

1913, *Olenellus truemani* Walcott, p. 316, pl. 54, figs. 2-10.
1952, *Olenellus* (*Olenellus*) *truemani* Lochman *in* Cooper *et al.*, p. 89, pl. 18, figs. 6-12.
1971, *Olenellus truemani*, Hu [part], p. 76-78, pl. 8, figs. 2-3, 5, 8, 10-26 [only].
Occurrence of Illustrated Materials. Buelina Formation, Lower Cambrian, near Caborca, northwestern Sonora, Mexico (locality 1 in Text-fig. I-2)
Association. None of these specimens shows a sign of the presence of the protopygidial region (e.g., see Pl. II-1, Fig. 7), indicating that all belongs to the meraspid period. CMC-P 38724a, d, f, and i (Pl. II-1, Figs. 10-13) differ from meraspid cranidia of *Olenellus truemani* (Pl. II-1, Figs. 1-7) in having less distinct ocular ridge and anterior border. They are assigned to Olenellidae sp. A.

Order **AGNOSTIDA** Salter, 1864
Suborder **EODISCINA** Kobayashi, 1939

Remarks. Fortey (*in* Whittington *et al.*, 1997) summarized arguments for assigning the suborder Eodiscina either to the Agnostida or to the Ptychopariida, and favored its placement within the Agnostida, which is accepted herein.

Superfamily **EODISCOIDEA** Raymond, 1913a
Family **EODISCIDAE** Raymond, 1913a
Genus **PAGETIA** Walcott, 1916b
Pagetia resseri Kobayashi, 1944
Pl. II-2, Figs. 1-12

1939 *Pagetia clytia* Resser, p. 25-26, pl. 2, figs. 6-8.
1943 *Pagetia resseri* Kobayashi, p. 40, nomina nudum.
1944 *Pagetia resseri* Kobayashi, p. 64.
1944 *Pagetia* (*Eopagetia*) *resseri* Kobayashi, p. 37
1966 *Pagetia resseri*, Rasetti, p. 509-510, pl. 60, figs. 19-25.
1971 *Pagetia clytia*, Hu, p. 74-76, pl. 7, figs. 15-32, text-fig. 35.
Daignosis. See Rasetti (1966, P. 509) for holaspid diagnosis. **Anaprotaspis.** Shield subpentagonal shield. Axis spindle-shaped and lower than pleural region. Three pairs of

20

fixigenal lobes present.

Stratigraphic and Geographic Distributions. This species occurs in Middle Cambrian strata of *Bathyuriscus-Elrathina* Zone and *Albertella* Zone. It has been reported from Langston Formation in Idaho and Utah.

Occurrence of Materials Described Herein. *Bathyuriscus-Elrathina* (Middle Cambrian) Zone of most probably Langston Formation (see Rasetti, 1966, p. 510) exposed at northeast side of road in Santaquin Canyon, Wasatch Mountains, Utah (locality 2 in Text-fig. I-2).

Description of Protaspides

Anaprotaspid stage (CMC-P 38723i; Pl. II-2, Figs. 1-4). Shield elongated hexagonal in outline; 0.256 mm long and 0.258 mm; anterior margin incurved and depressed. Axis spindle-shaped, with maximum width being 26% of shield width; its anterior half continuous down-slopes anteriorly and posterior half dorsally swollen; three transglabellar furrows faintly impressed. Pair of large lobes present in anterior half of fixigenae with highest independent convexity, and gently slopes adaxially; a small tubercle developed immediately behind the lobe; less convex lobe developed behind the tubercle

Remarks. Rasetti (1966) pointed out that Resser (1939) mistakenly identified *Pagetia resseri* from Ptarmigania strata of Langston Formation as *Pagetia clytia* which occurs in Spence Shale. *P. clytia* can be easily discriminated from *P. resseri* by its weakly impressed pygidial pleural furrows (compare Rasetti, 1966, pl. 59, fig. 34 and pl. 60, fig. 19). The specimens re-described herein are transferred into *P. resseri*.

Hu (1971) assigned the protaspid specimen of *Pagetia resseri* (Pl. II-2, Figs. 1-4) to "paraprotaspid" stage which was considered to develop an articulatory boundary, or at least a furrow, between cephalon and pygidium. However, the SEM picture reveals that no demarcated protopygidial portion of the specimen is developed. The longest lobe on the axis represents "Lp" which includes a proliferative zone probably at its posteromost end. Other eodiscid protaspides (*Shizhudiscus longquanensis*, Zhang and Clarkson, 1993, text-fig. 3; *Neocobboldia chinlinica*, Zhang, 1989, fig. 3; *Pagetia ocellata*, Shergold, 1991b, figs. 3A-3G) are characterized by a depressed or concave frontal glabella, a large anterior fixigenal lobe, a tubercle pair immediately behind the lobe, and a much less convex posterior fixigenal area, and elongated and convex "Lp." All these features are found in *P. resseri*.

Order CORYNEXOCHIDA Kobayashi, 1935

Remarks. This order is considered to include three suborders Corynexochina, Leiostegiina, and Illaenina (Fortey *in* Whittington *et al.*, 1997). The family Kingstoniidae represented by *Blountia* in this work has anaprotaspides (Pl. II-6, Figs. 1-8) similar to those of the Corynexochida, so that the family is questionably placed in this order (see below).

Suborder CORYNEXOCHINA (Kobayashi, 1935)
Family DOLICHOMETOPIDAE Walcott, 1916a
Genus PTARMIGANIA Raymond, 1928
Ptarmigania aurita Resser, 1939
Pl. II-3, Figs. 1-16, Text-fig. V-1.1, 1.2

21

1939 *Ptarmigania aurita* Resser, p. 37-38, pl. 3, figs. 35, 36.

?1939 *Ptarmigania* sp. undetermined Resser, p. 42, pl. 3, fig. 34.

1971 *Ptarmigania aurita*, Hu [part], p. 80-82, pl. 10, figs 2-4, 14, 16-23 [only].

Diagnosis. See Hu (1971, p. 80) for holaspid diagnosis. **Anaprotaspis.** Shield with deeply indented posterior margin. Sagittal furrow present. Anterior pits pinhole-like. **Metaprotaspis.** Shield hexagonal. Glabella strongly forward-expanding. Eye ridge present. Three pairs of fixigenal tubercles.

Remarks. A small cranidium, to which no species name was given by Resser (1939, pl. 3, fig. 34), is provisionally considered to represent a meraspid cranidium of *Ptarmigania aurita*. It bears a great resemblance to the cranidium of *P. aurita* (Pl. II-3, Fig. 12).

Stratigraphic and Geographic Distributions. This species occurs in *Elrathina-Bathyuriscus* Zone of Langston Limestone in Idaho and Utah.

Occurrence of Materials Described Herein. *Elrathina-Bathyuriscus* Zone (Middle Cambrian). Santaquin Canyon, Utah (locality 2 in Text-fig. I-2). The locality from which the specimens of *Ptarmigania aurita* were collected is very close to the one (of Langston Formation) from which Resser (1939) described nine *Ptarmigania* species.

Association of Protaspides. Specimen CMC-P 38727e (Pl. II-3, Figs. 17-20) shows a glabellar front which is more convex dorsally and anteriorly than any other anaprotaspid specimens of *Ptarmigania aurita*, suggesting the possibility that the specimen could belong to another *Ptarmigania* species; Resser (1939, p. 38-42) reported eight other *Ptarmigania* species from the same locality. The morphologic deviation from protaspides of *P. aurita* (Pl. II-3, Figs. 1-9) does not seem to be great enough to assign the specimen CMC-P 38727e to a different genus; it is assigned to *Ptarmigania* sp. A.

Specimen CMC-P 38727a (Pl. II-3, Figs. 21-23) does not have the indented posterior margin observed in other anaprotaspides of comparable size (e.g., CMC-P 38727c, Pl. II-3, Figs. 1-3). Furthermore, the specimen has axial furrows which, although weakly developed, are parallel-sided. The presence of widely-spaced anterior pits, sagittal furrow, and probably fixigenal spine pairs (see Pl. II-3, Fig. 21) indicate that it could belong to the Corynexochida. However, the greater similarities are found with protaspides of Middle Cambrian ptychopariids, *Ptychoparella* sp. A (Blaker and Peel, 1997, figs. 74.1, 74.2) in sharing a narrow (tr.) axis whose L3/L2/L1 slightly tapers forwards but L4 rapidly expands forwards, widely-spaced anterior pits, an entire posterior shield margin, and a rectangular shield outline. This specimen is assigned to Ptychopariina sp. A.

Hu (1971, pl. 10, figs. 6-18) described several early meraspid cranidia of *Ptarmigania aurita*. One of them, CMC-P 38727n (Pl. II-3, Figs. 13-16), was identified as an early meraspis. However, the specimen does not have the articulation between its cephalon and pygidium but it has the posterior cranidial marginal furrow instead. Thus, the specimen is considered herein as a metaprotaspis. In doing so, the cranidia which are smaller than this specimen (e.g., Pl. II-3, Figs. 24-27) cannot be meraspides of *Ptarmigania aurita*. They are assigned to Corynexochida sp. A; but it cannot be ruled out that they are meraspid cranidia of CMC-P 38727a.

Description of Protaspides

Anaprotaspid stage (CMC-P 38727b, c, d; Pl. II-3, Figs. 1-9). Shield circular in outline; 0.341 mm (avg.) long (the measurement is made between anterior end and indented posterior end) and 0.427 mm (avg.) wide. Axial furrows not incised; sagittal furrow

22

present; anteriormost glabella lobe triangular. Anterior pits distinct and widely-spaced. Posterior margin indented concave in dorsal view, and gently arched in posterior view. Two short pairs of fixigenal spine pairs present; anterior pair located at anterior one-third of shield length (see Pl. II-3, Fig. 1, the left spine is preserved); posterior fixigenal spine broadly based. Differentiation of protopygidium recognized by presence of occipital ring as a small node.

Metaprotaspid stage (CMC-P 38727n; Pl. II-3, Figs. 13-16). Shield hexagonal in outline; 0.708 mm in sagittal length and 0.840 mm in transverse width. Glabella forward-expanding; L4 trapezoidal and L3/L2/L1 posteriorly tapering; glabellar furrows shallower than axial furrows. Anterior pits pinhole-shaped. Palpebro-ocular ridge developed; its adaxial end located immediately next to anterior pits. Anterior fixigenal area flat and lower-leveled. Three pairs of tubercles on fixigenal area (comparable to circumocular tubercles in phacopids; for example, see Chatterton and Speyer, 1997, fig. 176); anteriormost pair opposite to S3 glabellar furrows; mid-pair opposite to S1; posteriormost pair located about mid-pleural length and immediately anterior to posterior cranidial border furrow. Posterior cranidial marginal furrow obtusely diagonal. Protopygidium with two axial rings, occupies 25% of sagittal shield length.

Protaspides of *Ptarmigania aurita* and their taxonomic implications. The metaprotaspis of *Ptarmigania aurita* (Pl. II-3, Figs. 13-16) shares many features with Ibexian leiostegiid metaprotaspides (Pl. II-4, Figs. 7, 8). The most noticeable difference is that the latter has two pairs of pygidial marginal spines. The leiostegiid protaspides in turn share a great similarity with scutelluids and illaenids. This strongly supports the evolutionary connection between corynexochids and illaenids through the leiostegiids, as suggested by Fortey (*in* Whittington *et al.*, 1997). Anaprotaspides (Pl. II-3, Figs. 1-9) of *P. aurita* are similar to kingstoniid anaprotaspides described below (*Blountia nixonensis*, Pl. II-6, Figs. 1-3), suggesting a possible taxonomic affinity of kingstoniids with corynexochiids.

Robison (1967) described protaspides of *Bathyuriscus fimbriatus* (pl. 24, figs. 1-5). The late anaprotaspis of *B. fimbriatus* mainly differs from the anaprotaspides of *Ptarmigania aurita* (Pl. II-3, Figs. 1-9) in apparently lacking a sagittal furrow in the axis. The latter feature probably could not be observed in *B. fimbriatus* due to a poorer resolution of light photography used in Robison's work than SEM technique used in this work. Chatterton and Speyer (*in* Whittington *et al.*, 1997, fig. 170.10) illustrated anaprotaspis of *Bathyuriscus* sp. using SEM photography, which clearly reveals the presence of the sagittal furrow. Apart from that the anaprotaspides of *P. aurita* have a more widely-spaced posterior fixigenal spine pair, anaprotaspides of *P. aurita* and *B. fimbriatus* are greatly similar to each other.

Robison (1967) mentioned that the holaspid differences between the corynexochids and ptychopariids are due to differential growth rates and suggested that both groups are closely related. Blaker and Peel (1997) described protaspides of *Ptychoparella* sp. (figs. 74.1, 74.2). They have an axis which has a rapidly forward-expanding L4 that appears to be confluent with palpebro-ocular ridge and slightly forward-tapering L3/L2/L1/L0. The same axial configuration is found in the metaprotaspis and early meraspid cranidia of *Bathyuriscus fimbriatus* (Robison, 1967, pl. 24, figs. 5, 6, 7) and *Ptarmigania aurita* (Pl. II-3, Fig. 12). The anaprotaspis assigned to Ptychopariina sp. A (Pl. II-3, Figs. 21-23) apparently is an intermediate between *Ptychoparella* sp. and *B. fimbriatus*. The meraspid

23

cranidia tentatively assigned to Corynexochida sp. A (Pl. II-3, Figs. 24-27) appears to be indistinguishable from those of *Ptychoparella* sp. A (Blaker and Peel, 1997, fig. 74.4) and *B. fimbriatus* (Robison, 1967, pl. 24, figs. 6, 7) This leads to a possibility that the most recent ancestry of the Corynexochida and Ptychopariida was in a primitive group of either taxon, not in the paraphyletic Redlichiida as commonly inferred (e.g., Fortey, 1990, text-fig. 19).

Suborder LEIOSTEGIINA Bradley, 1925
Family LEIOSTEGIIDAE Bradley, 1925
Genus LEIOSTEGIUM Raymond, 1913a
Leiostegium formosa Hintze, 1953
Pl. II-4, Figs. 1-19, Text-figs. II-1.3, 1.4

1953 *Leiostegium formosa* Hintze, p. 189-190, pl. 8, figs. 8-10.

Diagnosis. A species of *Leiostegium* with forward-expanding glabella and pair of pygidial marginal spines. **Anaprotaspis**. Shield hexagonal. Axis forward-expanding. Posterior fixigenal spines present. **Metaprotaspis**. Shield hexagonal. Glabella forward-expanding. Anterior pits distinct. Three pairs of fixigenal tubercles. Two pairs of protopygidial marginal spines.

Occurrence of Illustrated Materials. *Tesselacauda* Zone (Ibexian, Lower Ordovician) of Garden City Formation, southern Idaho (locality 3A in Text-fig. I-2).

Remarks. *Leiostegium formosa* (Pl. II-4, Fig. 16-18) is unique among other *Leiostegium* species in having a forward-expanding glabella; other species have a forward-tapering or parallel-sided glabella (e.g., see Shergold, 1975, pl. 45, fig. 7). The forward-expanding glabella is certainly reminiscent of the corynexochids. The corynexochid affinity of *L. formosa* based on protaspid similarities lead to suggest that *L. formosa* evolutionarily connect the Corynexochida and the Leiostegiidae which is considered to be ancestral to Styginidae which in turn is considered to be ancestral to the suborder Illaenina (see below).

Overall cranidial architecture of *Leiostegium formosa*, except for the large palpebral lobe, is similar to *Harydia* cf. *metion* (Westrop, 1986, pl. 9, figs. 20-23) which is questionably assigned to the Missisquoiidae. Likewise, the holaspid cranidial features of the Leiostegiidae and Missisquoiidae are so similar that their close evolutionary relationships have been proposed by several workers (e.g., Fortey and Shergold, 1984, p. 322). However, their protaspides greatly differ from each other and lend no support to the close relationship (see below).

Description of Protaspides.

Anaprotaspid stage (UA 12758-12760, Pl. II-4, Figs. 1-5). Shield hexagonal in outline; 0.551 mm (avg.) in sagittal length and 0.730 mm (avg.) in transverse width. Axis forward-expanding with distinct anterior pits. Pair of spines, which is homologous with posterior fixigenal spines or protopygidial marginal spines, present. Doublure inturned.

Metaprotaspid stage (UA 12761-12763, Pl. II-4, Figs. 6-9). Shield hexagonal in outline; 0.726 mm (avg.) in sagittal length and 0.880 mm (avg.) in width. Three pairs of fixigenal spines develop. Posterior cranidial marginal furrow and border turns forwards at their distal ends. Protopygidium elongated semi-circular in outline, occupying 68 % of the sagittal entire shield length. Two pairs of marginal spines; anterior pair relatively long and stout and posterior pair very small.

24

Protaspides of *Leiostegium formosa* and Their Taxonomic Implications. The remarkable similarities of metaprotaspides of *Leiostegium formosa* (Pl. II-4, Figs. 6-9) with those of *Ptarmigania aurita* (Pl. II-3, Figs. 13-16) strongly indicate a corynexochid affinity of the former species. They share a hexagonal shield, a forward-expanding glabella, pinhole-like anterior pits, a distally widening and forward-curving posterior cranidial border furrow, and three pairs of fixigenal tubercles. Anaprotaspides of *L. formosa* (Pl. II-4, Figs. 1-5) have a hexagonal shield and a parallel-sided L3/L2/L1/Lp and only posterior fixigenal spines and lack a sagittal furrow, which allow me to readily distinguish them from anaprotaspides of *P. aurita* (Pl. II-3, Figs. 1-9).

There are only two species assigned to the Leiostegiina and whose protaspides have been described; *Missisquoia cyclochila* (Hu, 1971) which was assigned to the Missisquoiidae and *Komaspidella laevis* (Hu, 1970a) which was previously assigned to the Leiostegiidae. Protaspides of these two species (Pl. II-5, Figs. 1-9 and Pl. II-8, Figs. 1-7) are not similar to protaspides of *Leiostegium formosa* (Pl. II-4, Figs. 1-9). This supports the taxonomic assignment made in this work; *Komaspidella* is assigned to the Kingstoniidae and Missisquoiidae is questionably retained in the Corynexochida.

The metaprotaspides of *Leiostegium formosa* are remarkably similar to those of the Styginidae and Illaenidae (see the reference list in Chatterton and Speyer *in* Whittington *et al.*, 1997, p. 222). The most distinctive features shared by *L. formosa* and illaenines are a forward-expanding glabella reaching the anterior margin, a protopygidial spine pair(s), and fixigenal tubercle pairs. More similarities are found with the styginid protaspides (e.g., *Failleana*, Chatterton, 1980). Considering that the earliest appearance of the styginids is early Arenigian (Lane and Thomas, 1983, text-Fig. 7), the Tremadoc *L. formosa* could be ancestral to the styginids which are the primitive group of the Illaenina.

?Order **CORYNEXOCHIDA** Kobayashi, 1935
?Suborder **LEIOSTEGIINA** Bradley, 1925
Family **MISSISQUOIIDAE** Hupé, 1953

Remarks. Various opinions on the suprafamilial position of this family have been proposed. Shergold (1975, p. 195) noted cranidial similarities to the Leiostegiidae and assigned the Missisquoiidae to the superfamily Leiostegiacea. Ludvigsen (1982, p. 119) suggested that the family would be the ancestor to the Styginidae which in turn appears to be the ancestor to the Illaenidae and Scutelluidae. He presented the similarities between *Missisquoia depressa* and *Perischoclonus capitalis* (Whittington, 1963, pl. 22, figs. 4, 13) as evidence. Later, Lane and Thomas (1983, p. 155) contradicted Ludvigsen's view and claimed that the cephalic morphologies of the Missisquoiidae are much more similar to Cambrian Corynexochida than post-Cambrian Scutelluina (=Illaenina of Fortey *in* Whittington *et al.*, 1997). In particular, they claimed that the morphologies of the rostral plate and pygidium are readily distinguished from those of the styginids. In any case, the relationships of the Missisquoiidae within the Corynexochida have been suggested.

The characteristic features shared by Corynexochida and post-Cambrian Scutelluina are a forward-expanding glabella and a large, wide rostral plate (Lane and Thomas, 1983, p. 154). However, most missisquoiids have a subrectangular or forward-tapering glabella and a small, triangular rostral Pl.. The lack of a preglabellar field appears to be the only feature shared by Corynexochida and Scutelluina. Protaspid features also lend no support to the inclusion of the Missisquoiidae in the Corynexochida (see below).

25

The Missisquoiidae clearly shares several cranidial features with the Ordovician Leiostegiidae (excluding the Pagodiidae, see Fortey *in* Whittington *et al.*, 1997). They are a trapezoidal cranidial outline, a subrectangular or slightly forward-tapering glabella, an inflated palpebral area of fixigenae, and most importantly the lack of a preglabellar field. In contrast, their pygidia show some differences, including the lack of a broad marginal border in the missisquoiids. Nonetheless, holaspid morphologies are obviously indicative of the inclusion of the Leiostegiidae and Missisquoiidae within the same suprafamilial taxon. However, protaspid features do not support a close relationship (see below).

Genus **MISSISQUOIA** Shaw, 1951

Remarks. Fortey (1983, p. 197) regarded *Missisquoia* as a junior subjective synonym of *Parakoldinioidia* Endo, 1937. Westrop (1986, p. 66-67) recognized differences in palpebral lobe morphologies between the two genera and claimed that *Missisquoia* is a valid genus. He claimed that *Parakoldinioidia* has "a larger palpebral lobe that is set some distance from the glabella on a well inflated fixed cheek and is defined by a firmly impressed palpebral furrow." *Parakoldinioidia* additionally differs from *Missisquoia* in having sparsely-distributed larger tubercles on the cranidial surface (compare Shergold, 1980, pl. 30, figs. 1-4 and Taylor and Halley, 1974, pl. 3, figs. 1-4). However, it is questionable whether these differences can be considered taxonomically sufficient for separating the two genera. In addition, most illustrated cranidia of these two genera have incompletely preserved palpebral lobes, so that the size of palpebral lobe does not seem to be a useful character to discriminate one genus from the other. As a matter of fact, the size of the palpebral lobe is not conspicuously larger in proportion to cranidial size in *Parakoldinioidia*, when comparing *P.* sp. aff. *P. bigranulosa* (Shergold, 1980, pl. 30, fig. 2) with *M. typicalis* (Westrop, 1986, pl. 1, fig. 36). The distance between the glabella and palpebral lobe appears to be nearly identical in the two genera and the depth of palpebral furrow does not seem to be useful for discriminating these taxa as suggested by Westrop (see Lu *et al.*, 1965, pl. 131, fig. 22, and Taylor and Halley, 1974, pl. 3, fig. 1). The type species of both genera, *P. typicalis* (Lu *et al.*, 1965, pl. 130, figs. 20-22) and *M. typicalis* (Taylor and Halley, 1974, pl. 3, figs. 1-4) further share a medial pit at the glabellar front. As Fortey (1983) expressed, the generic name *Missisquoia* is very familiar to biostratigraphers as well as trilobite workers, as a zonal index for the Lower Ordovician. Westrop (1986) also expressed some reservations in regard to his argument favoring the separation of *Missisquoia* from *Parakoldinioidia*. In this work, the author retains *Missisquoia* as a valid genus because the name has been used such a long time by many workers as a biostratigraphic index, although it is concluded that this genus may well be a junior synonym of *Parakoldinioidia*.

Missisquoia cyclochila Hu, 1971
Pl. II-5, Figs. 1-19, Text-fig. V-1.7
1971 *Missisquoia cyclochila* Hu [part], p. 107-109, pl. 20, figs. 7, 8, 10-28 [only].
1971 *Highgatella facila* Hu [part], p. 103-105, pl. 21, figs. 1, 4, 5 [only].
Diagnosis. See Hu (1971, p. 107) for holaspid diagnosis. **Metaprotaspis.** Shield circular and flattened. Axis less convex. Glabella slightly forward-expanding.
Remarks. Westrop (1986, p. 67) synonymized *Missisquoia cyclochila* with *Missisquoia typicalis*. When comparing the cranidium (Pl. II-5, Figs. 15, 16) with 1.87 mm in sagittal

26

length of *M. cyclochila* with that of *M. typicalis* (Westrop, 1986, pl. 1, figs 36, 37; Taylor and Halley, 1974, pl. 3, figs 1-4) with about 2 mm in sagittal length, the most noticeable difference is that *M. typicalis* has a medial pit at the glabellar front as clearly shown in *Missisquoia depressa* (Stitt, 1971, pl. 8, fig. 5) whereas *M. cyclochila* lacks the medial pit. Furthermore, the pygidium (Pl. II-5, Figs. 17, 18; 1.47 mm in sagittal length) of *M. cyclochila* differs from that of *M. typicalis* (Westrop, 1986, pl. 1, fig. 35; 2.1 mm in sagittal length) in lacking a spinose margin. Therefore, *M. cyclochila* is considered here a separate species from *M. typicalis*.

Occurrence of Materials Described Herein. *Missisquoia* Zone (Ibexian) of Deadwood Formation exposed south side of Sheep Mountains, Sundance, Crook County, northeastern Wyoming (locality 4A in Text-fig. I-2).

Association of Protaspides with *Missisquoia cyclochila*, *Apoplanias rejectus* and *Paranumia triangularia*. Hu (1971, 1973) reported protaspides of *Missisquoia cyclochila*, *Highgatella facila* (synonymized under *Apoplanias rejectus* in this study; see below) and *Paranumia triangularia* from the Lower Ordovician strata of Deadwood Formation exposed at Sheep Mountain, northeastern Wyoming. The protaspid specimens associated with each species by Hu (1971, 1973) are very similar to one another, so that a detailed morphologic analysis was carried out to investigate whether they are correctly associated. Eight different protaspid morphologic groupings are recognized in Hu's collection. The association with holaspid materials which have provided criteria for species identification, was mainly based upon morphologic transformation into the early meraspid cranidium of each species.

The first morphologic group includes specimens CMC-P 38740a, 38740d, and 38740e (Pl. II-5, Figs. 1-9), which are associated with *Missisquoia cyclochila*. The second group comprises specimens CMC-P 38749d, 38749e, 41556l, and 41556k (Pl. II-30, Figs. 1-13), which are assigned to *Apoplanias rejectus*. The third consists of CMC-P 38749f (Pl. II-22, Figs. 1-4) which is assigned to *Paranumia triangularia*. The fourth consists of CMC-P 38740c (Pl. II-5, Figs. 20, 21), the fifth of CMC-P 38749c (Pl. II-5, Figs. 22-24), the sixth of CMC-P 41556m (Pl. II-22, Figs. 16-19), the seventh of CMC-P 38749a and 38749b (Pl. II-5, Figs. 25-28), and the eighth of CMC-P 38740b (Pl. II-30, Figs. 23-27). Specific assignment of these last four groups is yet to be determined.

The first two groups of protaspides are similar to each other. The first group differs from the second in possessing a less convex shield and axis, less distinct axial furrows, a more rectangular shield outline (more circular in the second), and a parallel-sided axis whose L4 gently expands forwards (spindle-shaped axis in the second). Comparing an early meraspid cranidium of *Missisquoia cyclochila* (Pl. II-5, Fig. 11; 0.4 mm in sagittal length) with that of *Apoplanias rejectus* (Pl. II-30, Fig. 17; 0.364 mm in sagittal length) helps to associate the protaspides with each species. In particular, their glabellar shapes provide crucial evidence for the associations. The cranidium of *M. cyclochila* has a forward-expanding L4 and parallel-sided L3/L2/L1, whereas that of *A. rejectus* has a forward-tapering glabella. A forward-expanding L4 and parallel-sided L3/L2/L1 are present in the first protaspid group and the early meraspid cranidium of *M. cyclochila*. A forward-tapering glabella occurs in the second protaspid group and in the cranidium of *A. rejectus*. The holaspid cranidium of *M. cyclochila* (Pl. II-5, Fig. 15, 16) has a subrectangular glabella which is slightly waisted at mid-glabellar length, and that of *A. rejectus* (Pl. II-30, Figs. 18-19) has a forward-tapering glabella. As a result, each of the

27

two glabellar architectures is consistent throughout their ontogenies. The other distinguishing feature is development of an eye ridge in the meraspid stage in *A. rejectus* (Pl. II-30, Fig. 17). Since both protaspid groups lack an eye ridge, its development is considered unique to the *A. rejectus* ontogeny.

Specimens CMC-P 38749f (Pl. II-22, Figs. 1-4) has a relatively long, straight anterior margin and a narrow (tr.) axis with weakly developed glabellar furrows. The available early meraspid cranidium of *Paranumia triangularia* (Pl. II-22, Fig. 5) has the same glabellar configuration as this protaspid specimen.

Specimens CMC-P 38740c (Pl. II-5, Figs. 20, 21) have a narrow parallel-sided axis with distinct anterior pits which are similar to the protaspis of *Paranumia triangularia* (CMC-P 38749f). However, the specimen has a more elongated shield outline and distinct transglabellar furrows. It could belong to the species which is closely related to *P. triangularia*, a questionable phylacterid; it is assigned to species undertermined A.

Specimen CMC-P 38749c (Pl. II-5, Figs. 22-24) has a spindle-shaped axis which however is strongly annulated by adaxial indentations of glabellar furrows. it is assigned to species undetermined B. Its lateral profile is similar to CMC-P 38740c.

Specimen CMC-P 41556m (Pl. II-22, Figs. 16-19) has a strongly tapering spindle-shaped bilobed axis and at least two pairs of fixigenal spines. It is not unlikely that this specimen represents an earlier ontogenetic stage of one of the three above-mentioned species. Its sagittal length of 0.314 mm is greater than the protaspis of *Paranumia triangularia* (Pl. II-22, Figs. 1-4) which is 0.304 mm long, that of *Missisquoia cyclochila* (Pl. II-5, Figs. 1-3), and that of *Apoplanias rejectus* (Pl. II-30, Figs. 1-7) which are 0.304 mm long.

Specimens 38749a and 38729b (Pl. II-5, Figs. 25-28), although incompletely preserved, are certainly smaller than the metaprotaspides of the three species, suggesting that they may represent an earlier ontogenetic stage of one of these species. Alternatively, these smaller specimens could belong to the ontogeny of a species together with CMC-P 41556m, when considering that all three share the bilobed axis. The specimen CMC-P 41556m is named species undetermined Q and the specimens 38749a and 38749b are named species undetermined C.

Specimen CMC-P 38740b (Pl. II-30, Figs. 23-27) is 0.316 mm long, which is smaller than metaprotaspides of *Missisquoia cyclochila* (Pl. II-5, Figs. 4-9), but larger than the anaprotaspis of *M. cyclochila* (Pl. II-5, Figs. 1-3). It has a much more convex occipital ring and pygidial axial ring than metaprotaspides of *M. cyclochila*. Compared to metaprotaspides of *Apoplanias rejectus* (Pl. II-30, Figs. 1-7), it lacks a bilobation of the spindle-shaped axis. The specimen is named species undetermined T.

Description of Protaspides

Anaprotaspid stage (CMC-P 38740a, Pl. II-5, Figs. 1-3). Shield circular in outline with anterior and posterior margins being rather straight. 0.276 mm long and 0.273 mm wide. Axis parallel-sided. Transglabellar furrows weakly developed

Metaprotaspid stage (CMC-P 38740d, e). Shield sub-circular in outline with rather straight anterior margin. 0.325 mm (avg.) wide and 0.324 mm (avg.) wide. Axis parallel-sided with forward-expanding L4 and reaches anterior and posterior shield margin; maximum width 28% (avg.) of shield width; glabellar furrows very weakly developed. Differentiation of protopygidium only recognized by presence of distinct occipital ring; one axial ring present; sagittal length of protopygidium 15% (avg.) of entire shield

28

length.

Protaspides of *Missisquoia cyclochila* **and their taxonomic implications.** *Missisquoia cyclochila* and *Komaspidella laevis* are the only two species which were considered to belong to the Leiostegiina of Corynexochida and for which protaspid information is available (Chatterton and Speyer *in* Whittington *et al.*, 1997, p. 222-223). Protaspides of *M. cyclochila* differ from those of *K. laevis* (Pl. II-8, Figs. 1-8) in having a less strongly expanding L4, a more forwardly-tapering shield, and a less convex shield and axis. Leiostegiid protaspides from Ibexian Garden City Formation (Pl. II-4, Figs. 1-9), which are of corynexochid type, share few similarities with the protaspides of both species, suggesting that both genera are not members of the suborder Leiostegiina. The genus *Komaspidella* is a member of the Kingstoniidae (Westrop, 1992, p. 246; see *Komaspidella laevis* below).

Corynexochid affinity of the Missisquoiidae is not corroborated by protaspid morphologies. The missisquoiid protaspides are not comparable to any protaspides of the corynexochid such as *Ptarmigania aurita* (Pl. II-3, Figs. 1-16). The latter is readily discriminated from the former by its forward-expanding glabella and pinhole-like anterior pits in metaprotaspides, and its indented posterior margin and sagittal furrow in anaprotaspides. Thus, protaspid and holaspid features (see above) do not agree with the inclusion of the Missisquoiidae within the Corynexochida. At the present, the Missisquoiidae is questionably placed in the Leiostegiina.

?Order **CORYNEXOCHIDA** Kobayashi, 1935
?Family **KINGSTONIIDAE** Kobayashi, 1935

Remarks. The family Kingstoniidae is known to include, in its minimally accepted context, *Kingstonia* Walcott, 1924, *Ankoura* Resser, 1938a, and *Ithycephalus* Resser 1938a. The following genera have been regarded as members of the Kingstoniidae by various workers; *Bynumia* Walcott, 1924, *Bynumina* Resser, 1942, *Acheilus* Clark, 1924, *Larifugula* Ludvigsen, 1982, *Calvipelta* Westrop, 1986, *Pugionicauda* Westrop, 1986, *Clelandia* Cossman, 1902, *Blountia* Walcott, 1916b, *Maryvillia* Walcott, 1916b, and *Komaspidella* Kobayashi, 1938. In the most recent attempt, Westrop (1992, p. 244) identified a narrow (sag. and exsag.) transverse band-like occipital ring as a putative synapomorphy of the Kingstoniidae. He included only *Kingstonia, Ankoura, Ithycephalus, Bynumia, Bynumina, Komaspidella,* and provisionally *Blountia* in the concept of the Kingstoniidae.

Morphologies of *Bynumia* and *Bynumina* are comparable to those of *Kingstonia* species which show a wide range of morphologic variations. For example, *Kingstonia spicata* and *Kingstonia montanensis* (Lochman and Hu, 1962, pl. 4, figs. 1, 12) have a rather acutely triangular cranidial outline which is readily comparable to *Bynumia* species (e.g., *Bynumia lata*, Lochman and Hu, 1962, pl. 3, fig. 19). Cranidia of *Kingstonia walcotti* (Pratt, 1992, pl. 25, fig. 1) are very similar to *Bynumina missouriensis* (Resser, 1942, pl. 10, figs. 24, 25) except for very shallow axial furrows. Thus, the inclusion of *Bynumia* and *Bynumina* within the Kingstoniidae is very plausible. The genus *Pugionicauda* (Westrop, 1986, pl. 41, figs. 37-39) is unique among the kingstoniids in having a relatively large and more arcuate palpebral lobe. Since its pygidium is very similar to *Kingstonia spicata* (Lochman and Hu, 1962, pl. 4, fig. 21) and its glabellar outline is also similar to *Kingstonia, Pugionicauda* is regarded as a member of the

29

Kingstoniidae.

Ludvigsen (1982, p. 75) erected *Larifugula* as a new genus and questionably assigned it to the Kingstoniidae. He mentioned cranidial similarities with *Bynumia* and *Bynumiella*. However, *Larifugula* has a forward-expanding glabella with two or three pairs of glabellar furrows which are situated well inside the glabella (Ludvigsen, 1982, figs. 56A; Ludvigsen *et al.*, 1989, pl. 37, fig. 13). Further, it has a relatively distinct anterior cranidial border furrow and eye ridge and a long occipital spine. These features are not found in any other kingstoniids, but are in better agreement with a euptychaspidine, *Kathleenella* (see Westrop, 1986, pl. 10, figs. 19-21). Thus, *Larifugula* is excluded from the Kingstoniidae. The genus *Calvipelta* has glabellar features more similar to ptychaspidids in having a nearly imperceptible preglabellar furrow and relatively deep axial furrows in posterior half of glabella. It resembles *Larifugula*, so that *Calvipelta* is also excluded from the Kingstoniidae.

It has been a recurring opinion that *Clelandia* is related to kingstoniids (e.g., Westrop, 1986). Its overall cranidial morphologies are certainly similar to the kingstoniids. However, the genus is unique in having yoked free cheeks which is not known in any kingstoniids. Further, its small pygidium has marginal spines that are short and directed inwards (see Pl. III-39, Figs. 12, 18, 19). Thus, the taxonomic inclusion of *Clelandia* in the Kingstoniidae is considered questionable as argued by Westrop (1992).

Ludvigsen (1986) discussed the nomenclatural history of *Acheilus* in great details. He assigned it to the Kingstoniidae mainly because of its cranidial similarities with *Bynumia* and *Bynumina* (see Resser, 1942, pl. 9, figs. 5, 8, 19, 43, pl. 10, figs. 20, 25) which are considered as definite kingstoniid member. Cranidium of *Acheilus* has a subrectangular glabella which is constricted between the eyes, a laterally-tapering occipital ring, and a preoccipital furrow which shallows and becomes narrow adaxially. The morphology of occipital ring ascertains that *Acheilus* is not a kingstoniid.

Genus BLOUNTIA Walcott, 1916b

Remarks. The genus *Blountia* had been regarded as a member of the family Asaphiscidae until Westrop (1992) suggested that it could belong to the Kingstoniidae. Westrop (1992, p. 244) recognized the presence of an occipital ring as a short (tr.) transverse band as a putative synapomorphy and included *Blountia* within the Kingstoniidae. The cranidia of *Blountia* and definite kingstoniid genera such as *Kingstonia* and *Ankoura* (see Lochman and Hu, 1962, pl. 4, figs. 1, 47) are similar in all having a triangular outline, a slightly forward-tapering or subrectangular glabella, and a palpebral lobe that is small and located well anterior to the mid-glabellar length. Thus, cranidial features suggest their close taxonomic affinity. However, the pygidia of *Blountia* (Westrop, 1992, figs. 18.1, 18.2, 18.5) are distinct from those of *Kingstonia* (Lochman and Hu, 1962) with respect to the semi-circular outline and the wide flat border that is distinctively separated from a flat pleural field by an abrupt change of relief, which is typical of Middle Cambrian *Asaphiscus*, a definite member of the Asaphiscidae (see Palmer, 1954a, pl. 16, fig. 7). The pygidia of *Blountia* and *Kingstonia* are similar to one another in having numerous axial rings that usually outnumber the countable pleural segments and the anteriormost pleural furrow that is much deeper than the pleural and interpleural furrows behind it. Westrop (1992) added the absence of the thoracic pleural furrows observed in *Blountia* as further evidence to support the exclusion

30

of this genus from the Asaphiscidae.

Protaspides of *Blountia bristolensis* strongly suggest a close evolutionary relationship between *Blountia* and Corynexochida (see below). They have a triangular glabellar frontal lobe and deep anterior pits in the anaprotaspid stages, and a forward-expanding glabella and relatively discrete eye ridges in the metaprotaspid stages (see Pls. II-6, II-7). All these features accord with those of the corynexochid protaspides (see Pl. II-3). Although it is still open to question whether or not *Blountia* belongs to the Kingstoniidae or the Asaphiscidae, the protaspid morphologies strongly suggest that *Blountia* is closely related to the Corynexochida.

Blountia bristolensis Resser, 1938a
Pl. II-6, Figs. 1-22, Pl. II-7, Figs. 1-16, Text-figs. II-1.5, 1.6

1938a *Blountia bristolensis* Resser, p. 65, pl. 12, fig. 24.
1938a *Maryvillia bristolensis* Resser, p. 87, pl. 12, fig. 38.
1942 *Maryvillia hydrida*, Resser [part], p. 71-72, pl. 13, figs. 14, 15 [only].
1944 *Blountia nixonensis* Lochman *in* Lochman and Duncan [part], p. 43, pl. 4, figs. 7-9, 12 [only].
1954b *Blountia nixonensis*, Palmer, p. 722, pl. 79, fig. 4.
1962b *Blountia bristolensis*, Palmer, p. 22, pl. 3, figs. 33-34.
1975 *Blountia nixonensis*, Hu, [part], p. 257-262, pl. 2, figs. 1-3, 5, 7-35, text-fig. 2A-J, [only].

Diagnosis. see Palmer (1962b, p. 22) for holaspid diagnosis. **Anaprotaspis.** Shield subcircular. Anterior pits widely-spaced and distinct. Sagittal furrows present. Three pairs of fixigenal spines present; anterior pair at anterior one-third of shield length. **Metaprotaspis.** Shield subrectangular. Glabella forward-expanding. Axis narrow. Axial furrows diverges with gently curving outline. Anterior pits deeper than axial furrows and broad.

Stratigraphic and Geographic Distributions. This species occurs in *Crepicephalus* and *Aphelaspis* Zones (upper Marjuman to lower Steptoean of Upper Cambrian) and has been reported from Nolichucky Formation in Virginia, Cap Mountain Formation and Riley Formation in Texas, Pilgrim Formation in Montana, and Conasuaga Formation in Alabama.

Occurrence of Materials Described Herein. *Aphelaspis* Zone (Lower Steptoean) of Deadwood Formation. Bear Butte section, about 6 miles southeastern Deadwood City, South Dakota (locality 5A in Text-fig. I-2).

Remarks. A cranidium assigned to this species by Lochman (*in* Lochman and Duncan, 1944, pl. 4, figs. 10, 11) has a short frontal area and lacks a distinct anterior border furrow and a preglabellar field. It may be identified as a leiostegiid which has a similar cranidial configuration.

Association of Protaspides. Specimen CMC-P 42617d (Pl. II-7, Figs. 17-19) is more circular and has more narrowly-spaced anterior pits than early anaprotaspides of *Blountia bristolensis* (Pl. II-6, Figs. 1-5). Specimen CMC-P 42617f (Pl. II-7, Figs. 20-23) has a spindle-shaped L3/L2/L1 with a sagittal furrow and L4 whose posterior end is depressed and strongly converges posteriorly, resulting in a nearly triangular outline. Late anaprotaspis (Pl. II-6, Figs. 6-8) of *B. bristolensis* of comparable size, possesses a subtrapezoidal L4 which is consistently convex sagittally, and a parallel-sided L3/L2/L1

31

without the sagittal furrow. The spacing of the anterior pits indicates that these two specimens could belong to the same species. The possession of a sagittal furrow in CMC-P 42617d and 42617f suggests a corynexochid affinity; both specimens are assigned to species undertermined D.

Description of Protaspides.

Early anaprotaspid stage (CMC-P 42617b, e, Pl. II-6, Figs. 1-5). Shield subquadrate in outline with its posterior half slightly tapering; 0.414 mm (avg.) wide and 0.381 mm (avg.) long. Anterior pits distinct and widely-spaced. Sagittal furrow weakly developed. At least two pairs of fixigenal spines developed (see CMC-P 42617b); anterior pair located at posterior one-seventh sagittal shield length. Posterior margin broadly and shallowly indented. Surface covered with fingerprint-like microsculpture.

Late anaprotaspid stage (CMC-P 42617g, Pl. II-6, Figs. 6-8). Shield 0.482 mm wide and 0.458 mm long. L3/L2/L1 parallel-sided; L4 subtrapezoidal.

Early metaprotaspid stage (CMC-P 42617h, i, j, k, l, Pl. II-6, Figs. 9-22). Shield subrectangular in outline; 0.557 mm (avg.) wide and 0.529 mm (avg.) long. L3/L2/L1 gently tapers posteriorly; in some specimens (e.g., CMC-P 42617i), L3 bilobed; width of L3 takes about 20% (avg.) of shield width; transglabellar furrows as deep as axial furrows. Palpebro-ocular ridge moderately convex. Posterior fixigenal spines broadly based and widely spaced. Occipital ring convex wider (tr.) than L1. Posterior cranidial marginal furrow very weakly developed (see lateral view of CMC-P 42617i). Lateral shield margin surrounded by narrow and flat border. Protopygidium with one axial ring; protopygidial sagittal length occupies 17% (avg.) of shield length.

Late metaprotaspid stage (CMC-P 42617m, n, o, Pl. II-7, Figs. 1-6). Shield 0.653 mm (avg.) wide and 0.632 mm (avg.) long. Width of L3 takes 20% (avg.) of shield width. L4 separated from anterior shield margin by narrow (sag.) flat border. Posterior cranidial marginal furrow and cranidial border furrow more distinct. Sagittal length of protopygidium occupies 18% (avg.) of shield length.

Protaspides of *Blountia bristolensis* and Their Taxonomic Implications. A close taxonomic affinity of *Blountia* with the Kingstoniidae has been suggested by several workers (Shergold and Szudy, 1984; Westrop, 1992; Pratt, 1992). Protaspides have been described for two *Kingstonia* species; *Kingstonia montanensis* (Hu, 1986, pl. 15, figs. 1-7) and *Kingstonia ara* (Hu, 1968, pl. 3, figs. 1-6). The association of protaspid materials with *K. ara* needs to be re-examined, because some of these protaspides (Hu, 1968, pl. 3, figs. 1, 2, 6) are very similar to those of *Welleraspis swartzi* (Hu, 1968, pl. 1, figs. 1-4; Rasetti, 1954, pl. 62, figs. 1-4), which co-occurs with *K. ara*. The protaspid materials assigned to *K. ara* could belong to *W. swartzi*. Compared to these materials, the other protaspid specimens (Hu, 1968, pl. 3, figs. 3-5) have a narrower (tr.) and less rapidly posteriorly tapering axis. Such axial configuration is found in metaprotaspides of *K. montanensis* (Hu, 1986, pl. 15, figs. 3-7).

Anaprotaspides of *Kingstonia montanensis* (Hu, 1986, pl. 15, figs. 1, 2) have a circular shield with a pair of distinct anterior pits; although other features are not observable in his illustrations, the anaprotaspides are similar to those of *Blountia bristolensis* (Pl. II-6, Figs. 1-8) and those of species undetermined I (Pl. II-12, Figs. 22-27). Anaprotaspides of *Kingstonia ara* (Hu, 1968, pl. 3, figs. 1, 2) seem to belong to *Welleraspis swartzi*, as stated above. The anaprotaspis of *Komaspidella laevis* (a Kingstoniidae, Pl. II-8, Figs. 1-4) exhibits another morphotype such as a rectangular and

32

convex shield and very weakly-developed axial furrows; its association with *K. laevis* is questionable. As a result, anaprotaspides of the kingstoniid species cannot be used for comparative studies.

Metaprotaspides of the two *Kingstonia* species, *K. montanensis* and *K. ara* exhibit some differences. For example, the axis of *K. montanensis* metaprotaspides (Hu, 1986, pl. 15, figs. 3-7) is narrower, which seems to be reasonable as a specific variation. Metaprotaspides of *Blountia bristolensis* (Pl. II-6, Figs. 9-22, Pl. II-7, Figs. 1-6) differ from these *Kingstonia* metaprotaspides in having a much more rapidly forward-expanding L4, a less distinct posterior cranidial border, and much less deeply-impressed posterior cranidial border furrow. Thus, protaspid morphologic information does not support the kingstoniid affinity of *Blountia*. However, the meraspid cranidia of the *Kingstonia* species (e.g., Hu, 1986, pl. 15, fig. 9) are greatly similar to those of *B. bristolensis* (Pl. II-7, Figs. 7-9), suggesting the kingstoniid affinity of *Blountia*.

Strikingly, anaprotaspides of *Blountia bristolensis* (Pl. II-6, Figs. 1-5) resemble those of the Middle Cambrian *Ptarmigania aurita* of the Corynexochina (Pl. II-3, Figs. 1-9). They share a sagittal furrow, widely distributed anterior pits, and an indented posterior margin. Anaprotaspides of *Bathyuriscus fimbriatus* (a corynexochine, Robison, 1967, pl. 24, figs. 1-5) has fixigenal spine pairs whose positions are similar to those of *B. bristolensis*. Their size ranges from 0.27 to 0.43 mm in sagittal length and 0.29 to 0.48 mm in width. The anaprotaspides of *B. bristolensis* fit into the ontogenetic trajectory of *Bathyuriscus fimbriatus* (Robison, 1967, text-fig. 2). *B. bristolensis* retains a forward-expanding glabella until meraspid stages (e.g., Pl. II-7, Figs. 8, 9) as *P. aurita* (Pl. II-3, Fig. 12) and *Bathyuriscus fimbriatus* (Robison, 1967, pl. 24, figs. 6-7) do. The meraspid cranidium of *B. bristolensis* is only distinguished from those of the corynexochids in developing a narrow anterior border and a distinct eye ridge separated from the anterior border. Thus, the corynexochid affinity of *Blountia* is clear.

<center>

Order **PTYCHOPARIIDA** Swinnerton, 1915
Suborder **PTYCHOPARIINA** Ritcher, 1932

</center>

TAXA POSSESSING PROTASPID MORPHOTYPE A

Protaspides of *Komaspidella laevis* of the Kingstoniidae, *Glaphyraspis parva* of the Lonchocephalidae, and *Bolaspidella housensis* of the Menomoniidae are characterized by a subrectangular to subcircular, flattened shield, a forward-expanding axis with more strongly forward-expanding glabellar front and a small protopygidium.

<center>

Family **KINGSTONIIDAE** Kobayashi, 1935

</center>

Remarks. see above (under *Blountia*) for the discussion of the concept of this family.

<center>

Genus **KOMASPIDELLA** Kobayashi, 1938

</center>

1944 *Akataspis* Lochman *in* Lochman and Duncan, p. 102

Remarks. Westrop (1992) assigned *Komaspidella*, which had been classified under the Leiostegiidae, to the Kingstoniidae. Its morphologies such as a triangular overall cranidial outline, a subrectangular glabella, a narrow (sag. and exsag.) occipital ring, a shallow furrow delimiting the back of the palpebro-ocular ridge, a triangular pygidium

<center>33</center>

with numerous segments, a deeply incised anteromost pleural furrow, and no discernible pygidial marginal border, are all in agreement with the Kingstoniidae such as *Kingstonia*. A long post-axial pygidial spine is also found in both *Kingstonia* (*K. spicata*, Lochman and Hu, 1962, pl. 4, figs. 3, 13, 14, 18, 21) and *Komaspidella* (*K. modesta*, Lochman and Duncan, 1944, pl. 13, figs. 23, 25). The differences lies in that *Komaspidella* has a posterior facial suture that runs transversely, a shorter frontal area, and deep pygidial axial furrows. These are considered to be generic variations.

Komaspidella laevis Rasetti, 1961
Pl. II-8, Figs. 1-15, Text-fig. V-2.2
1961 *Komaspidella laevis* Rasetti, p. 115, pl. 21, figs. 6, 7, 9-11.
1968 *Komaspidella laevis*, Lochman, p. 1161, pl. 150, figs. 12-17, 19, 20, 22-25, 27.
1970a *Komaspidella laevis*, Hu [part], p. 144-149, pl. 1, figs. 2, 5, 7-25 [only].

Diagnosis. A species of *Komaspidella* with downsloping palpebral area, narrower frontal area, and parallel-sided pygidial axis. **Metaprotaspis**. Shield subrectangular. L4 strongly forward-expanding and L3/L2/L1 slightly forward-expanding. Palpebro-ocular ridge present.

Stratigraphic and Geographic Distributions. This species occurs in *Crepicephalus* Zone (upper Marjuman of Upper Cambrian), and has been reported from Conococheague Formation in Virginia and Bonneterre Dolomite in Missouri.

Occurrence of Materials Described Herein. *Crepicephalus* Zone of Bonneterre Dolomite. Little Sauk Creek and Stout Creek, Iron County, Missouri (locality 6A in Text-fig. I-2).

Association of Protaspides. Two different protaspid ontogenetic sequences are recognized upon the basis of the outline. The first consists of CMC-P 40274b and 40274e (Pl. II-8, Figs. 1-8) which have a somewhat rectangular shield. The second, consisting of CMC-P 40274c and 40274d (Pl. II-9, Figs. 28-33), have a rather rounded shield. The eye ridge, which is observed in CMC-P 40274e (Pl. II-8, Figs. 5-8) and early meraspid cranidia, is not distinct in the metaprotaspis, CMC-P 40274d (Pl. II-9, Figs. 31-33). The first sequence is assigned to *Komaspidella laevis* and the second to other co-occurring species. The association of CMC-P 40274b is not as confident as that of CMC-P 40274e, since the former specimen has no visible features comparable to the latter except for the rectangular shield outline and the forward-expanding axis defined by very weakly-developed axial furrows. It seems most probable that the two protaspid specimens of the second ontogenetic sequence represent protaspides of *Glaphyraspis* species co-occurring with *K. laevis* (see "Association of Protaspides" under *Glaphyraspis parva*). Specimen CMC-P 40274f (Hu, 1970a, pl. 1, fig. 6), the early meraspid cranidium, is also assigned to *Glaphyraspis parva*, since it does not show the characteristic features of *K. laevis* such as a rectangular outline and an eye ridge. These features are evident in specimen CMC-P 40274g (Pl. II-8, Fig. 9), the second smallest meraspid cranidium, and the metaprotaspid specimen (CMC-P 40274e, Pl. II-8, Figs. 5-8).

Because the anterior portion is covered by matrix, it is difficult to decide which species CMC-P 40274a (Pl. II-8, Figs. 16-19) belongs to; it is assigned to species undetermined E.

Description of Protaspides
Anaprotaspid stage (CMC-P 40274b, Pl. II-8, Figs. 1-4). Shield subrectangular in

34

outline and very slightly tapers posteriorly; 0.259 mm long and 0.228 mm wide. Axis forward-expanding; axial furrows very weakly impressed.

Metaprotaspid stage (CMC-P 40274e, Pl. II-8, Figs. 5-8). Shield 0.411 mm long, 0.371 mm wide. Axis forward-expanding; width of L3 34% of shield width; axial furrows moderately incised; transglabellar furrows shallower than axial furrows; occipital furrow deepest and broadest. Palpebro-ocular ridge delimited posteriorly by shallow furrows. Posterior cranidial marginal furrows diagonally directed and moderately impressed. Protopygidium with at least two axial rings; pleural and interpleural furrows indistinct; sagittal length of protopygidium occupies 12% of shield length.

Protaspides of *Komaspidella laevis* and Their Taxonomic Implications. Anaprotaspis of *Komaspidella laevis* (Pl. II-8, Figs. 1-4) is not comparable to that of any corynexochid species and any kingstoniid species. Anaprotaspis of *Cedarina cordillerae* (Pl. II-11, Figs. 1-4) displays the most similar morphology to that of *K. laevis* ; both species share a rectangular shield and a forward-expanding axis posteriorly ending with a small node. But *K. laevis* anaprotaspis lacks anterior pits and an indented posterior margin.

The metaprotaspis of *Komaspidella laevis* (Pl. II-8, Figs. 5-7) is similar to metaprotaspides of two *Kingstonia* species (Hu, 1968, pl. 3, figs. 3-5; Hu, 1986, pl. 15, figs. 3-7) in having a parallel-sided axis with a forward-expanding L4 and a large palpebro-ocular ridge. Compared to metaprotaspides of *Blountia bristolensis*, which is questionably assigned to the Kingstoniidae (Pl. II-6, Figs. 9-22, Pl. II-7, Figs. 1-6), this metaprotaspis of *K. laevis* differs in possessing a wider (tr.) axis, a less rapidly forward-expanding L4, a deeper posterior cranidial border furrow, and a larger palpebro-ocular ridge, and lacking anterior pits.

The condition of glabella exhibited by the *Komaspidella laevis* metaprotaspis (Pl. II-8, Figs. 5-7) is similar to those of metaprotaspides of *Welleraspis* species (Hu, 1964, pl. 24, figs. 24, 25; Hu, 1968, pl. 1, fig. 3; Rasetti, 1954, pl. 62, figs. 1-4). All of them have a relatively wide (tr.) axis with a rapidly forward-expanding straight-sided L4. However, in the metaprotaspides of *Welleraspis* species, L3/L2/L1 also expands forwards. The additional differences include much deeper axial furrows and transglabellar furrows and a more convex axis in *Welleraspis* metaprotaspides. The relationship between *Komaspidella* and *Welleraspis*, thus Kingstoniidae with Catillicephalidae, seems plausible. This suggestion is further supported by similarities between metaprotaspides of *Kingstonia ara* (Hu, 1968, pl. 3, figs. 3-5) and *Welleraspis swartzi* (Hu, 1968, pl. 1, figs. 1-3).

A forward-expanding glabella and eye ridge in the metaprotaspis of *Komaspidella laevis* are also found in several species possessing the protaspid morphotype B. Hu (1970a, p. 149) noted that it is similar to that of *Nixonella montanensis* (Llanoaspididae, Pl. II-16). In metaprotaspis of *Komaspidella laevis* (Pl. II-8, Fig. 5), the L4 has a trapezoidal outline and is defined by straight-sided axial furrows; metaprotaspides of *Blountia bristolensis* show the same condition (Pl. II-6, Figs. 9-22). In contrast, the protaspides of the superfamily B (e.g., Pl. II-15, Fig. 9) show that the expansion occurs from the mid-length of L4 and it is not as rapid as in *K. laevis*. In addition, the furrow defining the eye ridge in the metaprotaspis of *K. laevis* is much broader than that in protaspides of superfamily B.

Of most interest is the morphologic differences displayed by the protaspides of *K. laevis* and *Blountia bristolensis*. If the Kingstoniidae includes *Blountia* and *Komaspidella*

35

as suggested by Westrop (1992), morphologic differences of their protaspides (in particular the anaprotaspides) suggest that the family is not a natural group.

Family **LONCHOCEPHALIDAE** Hupé, 1955

Remarks. Rasetti (1954) reviewed several genera which were considered to belong to Lonchocephalidae and Catilicephalidae in recent classification schemes (e.g., Pratt, 1992). Rasetti (1954, p. 600) "decided to place this dividing line between *Welleraspis* and *Distazeris*, where at present there seems to be a somewhat wider morphological gap than between any other two of the genera in question." This implies that the taxonomically separating of these two families is at best arbitrary. Pratt (1992), the most recent discussion on the status of the two families, even mentioned a possibility that the two families could be united. The morphologic continuities between members of these two families are obvious and their similarities are certainly plesiomorphic.

Genus **GLAPHYRASPIS** Resser, 1937
Glaphyraspis parva (Walcott, 1899)
Pl. II-9, Figs. 1-26, Pl. II-46, Figs. 10-16, Text-fig. V-2.3

1899 *Liostractus parva* Walcott, p. 463, pl. 65, fig. 6.
1937 *Glaphyraspis parva*, Resser, p. 12.
1938 *Raaschella ornata* Lochman, p. 82, pl. 18, figs. 6-10.
1944 *Raaschella occidentalis* Lochman and Duncan, p. 43, pl. 4, figs. 1-5
1954b *Raaschella ornata*, Palmer, p. 764, pl. 89, figs. 7-9.
1956 *Raaschella occidentalis*, Shaw, p. 51, pl. 12, figs. 1, 5.
1960 *Glaphyraspis occidentalis*, Lochman and Hu, p. 815, pl. 97, figs. 1-8.
1961 *Glaphyraspis parva*, Rasetti, p. 112, pl. 22, figs. 14-17.
1962a *Glaphyraspis ornata*, Palmer, p. 93, pl. 19, figs. 15-19, 26, 27.
1962 Glaphyraspis parva, Lochman and Hu, p. 438, pl. 68, figs. 7-52.
1965 *Glaphyraspis parva*, Rasetti, p. 40, pl. 10, figs. 9-17.
1965 *Glaphyraspis ornata*, Rasetti, p. 41, pl. 10, fig. 8, pl. 11, figs. 13, 14.
1965b *Glaphyraspis ornata*, Palmer, p. 51, figs. 15-17, 20-22.
1968 [non] *Glaphyraspis ornata*, Lochman, p. 1157, pl. 149, figs. 12-19, 22.
1971 *Glaphyraspis parva*, Hu and Tan [part], p. 66-71, pl. 9, figs. 2-33 [only].
1980 [?] *Glaphyraspis occidentalis*, Ergaliev, p. 139, pl. 8, figs. 15, 16.
1992 *Glaphyraspis parva*, Pratt, p. 71, pl. 26, figs 13-22.

Diagnosis. see Pratt (1992, p. 71) for holaspid diagnosis. **Metaprotaspis.** Shield subcircular. Axial furrows very shallow and slightly forward-expanding. Pair of posterior fixigenal spines short and stout. Protopygidim tiny and transverse.

Stratigraphic and Geographic Distributions. This species occurs in the *Crepicephalus* (uppermost Marjuman) to *Aphelaspis* or equivalent zones such as the *Glyptagnostus reticulatus* Zone (lowermost Steptoean Stage of Upper Cambrian). It has been reported from Deadwood Formation in South Dakota, DuNoir Limestone and Dry Creek Shale in Wyoming, Pilgrim Formation in Montana, Dunderberg Formation in Nevada, Nolichucky Formation in Tennessee, Conococheague Formation in Virginia, Riley Formation in Texas, and Rabbitkettle Formation in Northwestern Territory.

Occurrence of Materials Described Herein. *Aphelaspis* Zone (lowermost Steptoean) of Deadwood Formation. Moll Section, Bear Butte, south-eastern Deadwood City, northern

36

Black Hills, South Dakota (locality 5A in Text-fig. I-2). Silicified materials illustated in Pl. II-46 are from the *Aphelaspis* Zone of Dunderberg Formation, McGill section, east-central Nevada (locality 7 in Text-fig. I-2 and see also Text-figs. I-3, 4).

Association of Protaspides. Specimen CMC-P 40310 (Pl. II-9, Fig. 34) is too poorly preserved to determine whether they are correctly associated; it is identified as species undetermined G. Specimen CMC-P 40274c (Pl. II-9, Figs. 28-30), which was assigned to *Komaspidella laevis* by Hu (1970a), is very similar to CMC-P 40310a and 40310b (Pl. II-9, Figs. 1-7). Its morphologies are continuous into specimen CMC-P 40274d (Pl. II-9, Figs. 31-33) which was also assigned to *K. laevis* by Hu (1970a). These two specimens are most probably referable to a *Glaphyraspis* species, so are named in open nomenclature, *Glaphyraspis* sp. A. There is an unnamed new species, which was previously referred to as *Glaphyraspis ornata* by Hu (1968), co-occurs with *K. laevis* (see Pratt, 1992, p. 71)

A meraspid cranidial specimen 40310j (Pl. II-9, Fig. 27) has a forward-expanding glabella. Since the glabella of *Glaphyraspis parva* changes from slightly forward-expanding to forward-tapering, the specimen cannot belong to the ontogeny of *G. parva*. It shows similarities to meraspid cranidia of co-occurring *Blountia bristolensis* (see Pl. II-7, Figs. 7-9). The meraspid cranidium is assigned to species undetermined F.

Description of Protaspides

Anaprotaspid stage (CMC-P 40310a, Pl. II-9, Figs. 1-4). Shield subrectangular in outline; 0.218 mm long and wide. Axis parallel-sided, occupying 30% of shield width.

Metaprotaspid stage (CMC-P 40310b, d, c, e, Pl. II-9, Figs. 5-16). Shield subrectangular in outline with rounded anterior margin; 0.314 mm (avg.) long and 0.325 mm (avg.) wide. Glabella relatively wide (32% (avg.) of shield width), consistently slightly forward-expanding, and reaches anterior margin; three transglabellar furrows faintly-developed. Posterior fixigenal spine short and blunt. Fixigenal area slopes steeply distally. Posterior fixigenal spine short and stout. Posterior cranidial border furrow shallow and relatively broad. Posterior cranidial marginal furrow shallow and narrow. Protopygidium small (sag.; 12% (avg.) of sagittal shield length) but wide (tr.), with one axial ring (Lp).

Protaspides of *Glaphyraspis parva* and Their Taxonomic Implications.
Metaprotaspides of *Glaphyraspis parva* (Pl. II-9, Figs. 8-16) are characterized by possessing a very small (sag. and exsag.) and transversely wide protopygidium. Palmer (1962a, pl. 19, figs. 16-17) described the silicified materials of *G. parva* from Upper Cambrian strata of Nevada which well fit within the size range of the materials from Deadwood Formation described above.

Metaprotaspides of *Welleraspis* (Hu, 1964, pl. 24, figs. 19-25; Rasetti, 1954, pl. 62, figs. 1-4), a catillicephalid which has been considered to be closely related to the lonchocephalids, have a forward-expanding glabella and a steeply-sloping distal portion of fixigenal area as do *Glaphyraspis* protaspides. The difference lies in that all the furrows in the catillicephalid protaspides are much more deeply incised than in the lonchocephalids, and the catillicephalid protaspides have a prominent eye ridge and more convex axis. A close taxonomic affinity of these two genera, thus between the two families seems more reasonable. Protaspides of *Pemphigaspis* (a catillicephalid, Hu, 1968, pl. 2, figs. 1-2) resemble closely those of *Welleraspis*. If the two families should remain separate, the depth of the furrows in their protaspides provides a character for distinguishing one from the other.

37

Of other Cambrian ptychopariid families, the Middle Cambrian Menomoniidae has protaspides that are comparable to those of *Glaphyraspis* (e.g., *Bolaspidella*, Robison, 1964). The anaprotaspides of *Bolaspidella housensis* (Pl. II-40, Figs. 1-15) are greatly similar to the metaprotaspides of *Glaphyraspis parva* (Pl. II-9, Figs. 8-16) in having a subrectangular shield with a rounded anterior margin, a forward-expanding glabella, and a posterior fixigenal spine. Their meraspid cranidia (Pl. II-9, Figs. 17-19 for *Glaphyraspis*; Pl. II-40, Figs. 5, 10 for *Bolaspidella*) are very similar. Shaw (1966, p. 856) mentioned a taxonomic affinity between the Menomoniidae and Onchonotopsididae which was synonymized under the Catillicephalidae by Pratt (1992, p. 70).

<center>Family MENOMONIIDAE Walcott, 1916a</center>

Remarks. Pratt (1992) provided the most recent account for the concept of the family.

<center>Genus BOLASPIDELLA Resser, 1937</center>
<center>*Bolaspidella housensis* (Walcott, 1886)</center>
<center>Pl. II-40, Figs. 1-15, Pl. II-41, Figs. 1-10, Pl. II-42, Figs. 1-13, Pl. II-43, Figs. 1-21, Text-
fig. V-2.4</center>

1886 *Ptychoparia housensis* Walcott, p. 201, pl. 25, fig. 5
1937 *Bolaspidella housensis*, Resser, p. 4.
1954a *Bolaspidella housensis*, Palmer, p. 57, pl. 16, fig. 3.
1964 *Bolaspidella housensis*, Robison, p. 555, pl. 88, figs. 16-21, pl. 89, figs. 1-11.

Diagnosis. see Robison (1964, p. 555) for holaspid diagnosis. **Anaprotaspis.** Shield subrectangular. Posterior margin broadly indented forwards. Posterior fixigenal area with pair of short and stout posterior fixigenal spines, and strongly protruded ventrally. Hypostome shield-shaped and with nine marginal spines. **Metaprotaspis.** Protopygidium transverse and small. Axis slightly forward-expanding with more strongly expanding glabellar front.

Stratigraphic and Geographic Distributions. This species occurs in *Bolaspidella* (late Middle Cambrian) Zone. It has been reported from Wheeler Shale and Marjum Formations in western Utah.

Occurrence of Materials Described Herein. *Bolaspidella* Zone (late Middle Cambrian) of Marjum Formation. near Swasey Peak, House Range, western Utah (locality 8 in Text-fig. I-2 and see also Text-fig. I-3).

Description of Protaspides

Early Anaprotaspid Stage (UA 12772, UA 12796, UA 12797, UA 12798; Pl. II-40, Figs. 1-5, Pl. II-43, Figs. 14-21). Shield subquadrate in outline and smooth; sagittal length ranges from 0.27 to 0.34 mm and transverse width from from 0.3 to 0.35 mm. Pair of posterior fixigenal spine short and spaced narrowly. Posterior margin indented forwards and arched dorsally.

Late Anaprotaspid Stage (UA 12773-12775; Pl. II-40, Figs. 6-12). Shield subrectangular in outline and smooth; 0.39-0.45 mm wide and 0.38-0.48 mm long. Posterior fixigenal spines widely spaced and protruded ventral to posterior shield margin. Posterior margin between posterior fixigenal spines widely bilobed. Hypostome shield-shaped; median body elongated; four pairs of lateral marginal spines short and with blunted end.

Metaprotaspid Stage (UA 12776, 12777; Pl. II-40, Figs. 13-15, Pl. II-41, Figs. 1, 2).

<center>38</center>

Shield subrectangular in outline; 0.46-0.49 mm wide and 0.47-0.49 mm long. Posterior cephalic border weakly developed.

Development of Tubercles on Meraspid Cranidia. Of interest is the development of small regularly-distributed tubercles on glabella, fixigena, and thoracic segments (see Pl. II-42, Figs. 11, 13). Compared to hystricurid species (e.g., Pl. III-16, Figs. 4, 9, 12), the tubercles are much smaller and less prominent. However, their distributions as paired three or four tubercles alongside the glabella, and a row of tubercles that seem to continuous from fixigena to thoracic segments are comparable to the "hystricurids." Another interesting feature comparable to the "hystricurids" is the development of thoracic axial spines. The first three thoracic segments of *Bolaspidella housensis* lack the axial spine, and five segments posterior to them possess axial spines, and the remaining posterior segments do not have the spine (see Pl. II-42, Fig. 13, Pl. II-43, Figs. 8, 13). A similar arrangement of thoracic axial spines is seen in such hystricurids as *Spinohystricurus* (see Pl. III-16, Figs. 1, 4). A variation lies in the number of thoracic axial spines and which segment from the anterior possesses the spine.

Comparison of Protaspides and Taxonomy. It is *Glaphyraspis* that have the morphologically closest protaspides (see Pl. II-9, Fig. 14, Pl. II-46, Figs. 10-12), suggesting the close affinity of the Memononiidae and Lonchocephalidae.

Family **CATILLICEPHALIDAE** Raymond, 1938

Remarks. Pratt (1992, p. 70, 72) synonymized the family Onchonotopsididae Shaw, 1966 under the Catellicephalidae.

Genus **WELLERASPIS** Kobayashi, 1935

Remarks. Rasetti (1954) questionably placed *Lonchocephalus* and *Welleraspis* within the Solenopleuridae and suggested that the Catillicephalidae was derived from these two Middle Cambrian genera with *Lonchocephalus* as the least specialized genus.

Pratt (1992, p. 72) regarded *Welleraspis* as a member of the Catillicephalidae, which is accepted herein, and considered it to be more closely related to *Pemphigaspis*. However, the glabellar outline of *Welleraspis* is similar to both catillicephalid genera and to *Lonchocephalus* of the Lonchocephalidae. As mentioned above (see "Remarks" under Lonchocephalidae), the similarities between these two families and the difficulty in finding a distinct morphologic gap between them could result in their fusion into a single family (e.g., compare CMC-P 397411 and 39741t of *Welleraspis lochmanae* (Pl. II-10, Figs. 9-11) and 40310o and 40310c' of *Glaphyraspis parva* (Pl. II-9, Figs. 20, 24-26).

In contrast, protaspid morphologies of *Welleraspis* (Hu, 1964, 1968) differ from those of *Glaphyraspis* (see Pl. II-9) in having a much strongly forward-expanding glabella and glabellar lobes bilobed by a deep sagittal furrow. This contradicts the suggestion that the two families, Lonchocephalidae and Catillicephalidae, should be united upon the basis of their inseparable holaspid morphologies.

Welleraspis lochmanae Hu, 1969
Pl. II-10, Figs. 1-14

1968 *Lonchocephalus chippewaensis australis*, Lochman, p. 1157, pl. 149, figs 1, 3-11.
1968 *Welleraspis jerseyensis* (Weller), Lochman, 1968, p. 1160, pl. 149, fig. 2, pl. 150, figs. 1-11.

39

1969 *Welleraspis lochmanae*, Hu [part], p. 440-445, pl. 1, figs. 4-35 [only].

Diagnosis. see Hu (1969, p. 440) for holaspid diagnosis.

Stratigraphic and Geographic Distributions. This species occurs in the *Crepicephalus* Zone (upper Marjuman of Upper Cambrian) and has been reported from the Bonneterre Dolomite in Missouri.

Occurrence of Materials Described Herein. *Crepicephalus* Zone of Bonneterre Dolomite; Little Sauk Creek and Stout Creek, Iron County, Missouri (locality 6A in Text-fig. I-2).

Association of Protaspides. Metaprotaspides of other *Welleraspis* species (*W. lata*, Hu, 1964, pl. 24, figs. 19-25; *W. swartzi*, Rasetti, 1954, pl. 62, figs. 1-4) are characterized by a forward-expanding, strongly annulated axis with a rapidly expanding L4. Specimen CMC-P 39741c (Pl. II-10, Figs. 15-18) has a forward-expanding axis that does not have distinct transglabellar furrows and the rapidly-expanding L4. Further its shield is not as convex as those of other *Welleraspis* species. The specimen exhibits some similarities with metaprotaspides of *Glaphyraspis parva* (Pl. II-9, Figs. 8-16) such as a consistently forward-expanding axis. However, its lateral profile is more flattened than the metaprotaspides and early meraspid cranidia of *G. parva* (Pl. II-9, Figs. 17-18). The specimen most probably represents a protaspid stage of *Madarocephalus laetus* (a catillicephalid, Rasetti, 1965, pl. 8, fig. 20) which has a forward-expanding glabella without distinct glabellar furrows. Specimen CMC-P 40280n (Pl. II-16, Figs. 23-25), which was assigned to *Nixonella montanensis*, probably represents an earlier stage of CMC-P 39741c; both specimens are named in open nomenclature, Catillicephalidae sp. A. *M. laetus* occurs in the Nolichucky Formation of northeastern Tennessee and specimen CMC-P 39741c in the Bonneterre Dolomite of Missouri, but both occur in the *Crepicephalus* Zone.

Specimen CMC-P 39741b (Pl. II-10, Figs. 19-22) with 0.306 mm of sagittal length and CMC-P 39741d (an early meraspid cranidium, Pl. II-10, Fig. 23) show faintly-developed axial furrows and an elongated shield outline, which are not typically observed in *Welleraspis* protaspides. Both specimens are assigned to Catillicephalidae sp. B. Due to poor preservation, it is also difficult to determine whether or not specimen 39741a (Pl. II-10, Figs. 24-25) is correctly associated; it is named species undetermined H.

Protaspides of *Welleraspis* Species and Their Taxonomic Implications. Protaspides of *Pemphigaspis bullata* (Hu, 1968, pl. 2, figs. 12-16, 21-25, 27, text-fig. 3) are greatly similar to those of *Welleraspis* (Rasetti, 1954; Hu, 1964) lending additional morphologic support to the close relationship between the two genera based on holaspides. This supports the placement of *Welleraspis* within the Catillicephalidae. The axis of anaprotaspides of *Welleraspis lata* (Hu, 1964, pl. 24, figs. 19-21) is forward-expanding and differentiated into four lobes, the middle two of which are bilobed. Such an axial configuration continues into its metaprotaspides.

The metaprotaspis of *Komaspidella laevis* (Pl. II-8, Figs. 5-7) has a wide (tr.) axis with a rapidly forward-expanding L4 and a distinct eye ridge, features which are also evident in the *Welleraspis* metaprotaspides. This suggests that the Catillicephalidae is closely related to the Kingstoniidae.

TAXA POSSESSING PROTASPID MORPHOTYPE B

Cedarina cordillerae of the Cedariidae, *Apomodocia conica* of the ?Cedariidae,

40

Glyphaspis paucisulcata of the Anomocaridae, *Crepicephalus deadwoodiensis* of the Crepicephalidae, *Syspacheilus dunoirensis* and *Modocia laevinucha* of the Marjumidae and *Nixonella montanensis* of the Llanoaspididae share a similar protaspid morphology. It is characterized by a oval to subrectangular and relatively convex shield, a forward-expanding L4 (except for *Cedarina*), shallow axial furrows, parallel-sided L3/L2/L1, shallow anterior pits, and a distinct anterior border.

Remarks. In the Treatise (Moore, 1959), each of the above families belongs to a different superfamily; the Cedariidae and Llanoaspididae to the Raymondinacea, the Crepicephalidae to the Crepicephalacea, and the Anomocaridae to the Anomocaracea. These superfamilies are not defined by shared derived characters and not regarded as a natural group. Since then, most workers (e.g., Westrop, 1986; Pratt, 1992) classified these families under 'superfamily uncertain.' Fortey (*in* Whittington *et al.*, 1997), in the most recent classification mainly based on his earlier works (Fortey and Chatterton, 1988; Fortey, 1990), retained Cedariidae and Crepicephalidae within the Superfamily Ptychoparioidea (which certainly includes several other superfamilial groupings) and assigned Anomocaridae to the superfamily Anomocaroidea of the Asaphida (see also Fortey and Chatterton, 1988). Fortey (*in* Whittington *et al.*, 1997) did not list the Llanoaspididae; it is apparent that he synonymized it with one of the listed families under Ptychopariida, most probably, with the Cedariidae or Raymondinidae.

Holaspid cranidial and pygidial features of the species described below are apparently similar to one another. These similarities are also found in many other families outside this apparent new superfamilial grouping, so they are clearly symplesiomorphic and have little value to diagnose the superfamily.

Protaspides of *Sao hirsuta* (Solenopleuropsinae, Whittington, 1957, pl. 116, figs. 14-21) exhibit some similarities with protaspides of this superfamily. The forward-expanding glabella and slender eye ridge are comparable to *Glyphaspis paucisulcata* (Pl. II-13), *Syspacheilus dunoirensis* (Pl. II-15) and *Apomodocia*? sp. (Pl. II-12, Figs. 13-15). The solenopleuropsinae could belong to this superfamilial groupiing, not to the Solenopleuracea which includes *Solenopleura*. Protaspides of *Solenopleura* (Pl. II-28) are much different from those of *Sao*.

This group of superfamilial rank appears to be paraphyletic, because *Glyphaspis paucisulcata*, *Syspacheilus dunoirensis*, *Nixonella montanensis*, and *Crepicephalus deadwoodiensis* are regarded as subsequently branching off from the ancestry of the Proetida.

Family CEDARIIDAE Raymond, 1937

Remarks. Lochman (*in* Moore, 1959) placed the Cedariidae as a subfamily within the family Raymondinidae. Later Palmer (1962b, p. 23) argued that cranidia of *Cedaria* have dissimilarities from those of *Llanoaspis* (type genus of Lochman's Llanoaspidinae) and *Raymondina* (type genus of Lochman's Raymondininae) and the dissimilarities are adequate for maintaining the Cedariidae as a separate family as originally designated by Raymond (1937). This opinion was followed by Pratt (1992, p. 79) and this work. Nonetheless, morphologic similarities indicate that the Cedariidae is related to the Llanoaspididae and Raymondinidae, as stated by Pratt (1992).

Genus CEDARINA Lochman, 1940

41

Cedarina cordillerae (Howell and Duncan, 1939)
Pl. II-11, Figs. 1-16, Text-fig. V-2.5
1939 *Piemontia cordillerae*, Howell and Duncan, p. 9, pl. 1, fig. 4.
1944 *Cedarina cordillerae*, Lochman and Duncan, p. 89-91, pl. 17, figs. 1-10.
1950 *Cedarina cordillerae*, Lochman, p. 347, pl. 50, figs. 20, 21.
1971 *Cedarina cordillerae*, Hu and Li, p. 171-172, pl. 2, figs. 1-37, fig. 2.
1971 *Cedarina cordillerae*, Hu [part], p. 90-92, pl. 13, figs. 2, 4, 8-29 [only].
1992 *Cedarina cordillerae*, Pratt, p. 82, pl. 31, figs. 17-21.

Diagnosis. see Hu (1971, p. 87-88) for holaspid diagnosis. **Early metaprotaspis.** Shield subrectangular. Axis straight-sided and forward-expanding. Occipital ring present as node. Pair of anterior pits distinctly impressed. **Late metaprotaspis.** Shield subrectangular. Axis spindle-shaped with strongly forward-expanding L4. Anterior pits shallowly impressed. Protopygidium small and with two axial rings.

Stratigraphic and Geographic Distributions. This species occurs in the *Cedaria* Zone (lower Marjuman of Upper Cambrian). It has been reported from the Pilgrim Formation of Montana, Utah, and the Rabbitkettle Formation of Northwestern Territories of Canada. **Occurrence of Materials Described Herein.** *Cedaria* zone (lower Marjuman), Wasatch Mountains, Utah (locality 9 in Text-fig. I-2).

Association of Protaspides. Two specimens, CMC-P 38731b and 38731d (Pl. II-11, Figs. 1-8), are considered to represent metaprotaspid stages of *Cedarina cordillerae*. Morphologic transition from the metaprotaspis into the smallest meraspid cranidium (CMC-P 38731h, Pl. II-11, Fig. 9) is fairly reasonable.

Specimen CMC-P 38731a (Pl. II-12, Figs. 22-24) has a circular outline which is not comparable to the metaprotaspides of *Cedarina cordillerae*. Since the specimen is small (0.295 mm in sagittal length), it could be an earlier anaprotaspid stage of *C. cordillerae* which radically metamorphosed into CMC-P 38731b (Pl. II-11, Figs. 1-4). However, morphologies of the specimen are much more reasonably carried into CMC-P 38725a (Pl. II-12, Figs. 25-27) which was incorrectly assigned to *Apomodocia conica*, indicating that both specimens belong to the same species—it is identified as species undetermiined I— which is not formally named due to the absence of the holaspid specimen. Hu (1971) described these two specimens from a single locality in the Wasatch Mountains, Utah, supporting their incorporation into a single ontogeny. Furthermore, CMC-P 38731b of *C. cordillerae* is larger than CMC-P 38731a and smaller than CMC-P 38725a, indicating that the latter two specimens cannot be incorporated into the ontogeny of *C. cordillerae*.

Specimen CMC-P 38731e (Pl. II-11, Figs. 17-19, 0.448 mm in sagittal length) differs from the metaprotaspis of *Cedarina cordillerae* (CMC-P 38731d, Pl. II-11, Figs. 5-8; 0.445 mm in sagittal length) with a similar size in having a proportionately narrower (tr.) axis and a convex forward anterior margin. With respect to other features, both specimens are very similar to one other. Specimen CMC-P 38731f (Pl. II-11, Figs. 20-22) has a forward-expanding axis, a broadly-indented posterior margin with rounded posterior fixigenal spine, and a moderately convex shield. The same features are found in the small metaprotaspis of *C. cordillerae* (CMC-P 38731b, Pl. II-11, Figs. 1-3), which differs from CMC-P 38731f in having a sagittally longer shield. Since the difference in sagittal length between CMC-P 38731b and 39831f is only 0.006 mm, CMC-P 38731f must belong to another species. Likewise, specimen CMC-P 38731e is almost in the same size range as the metaprotaspis of *C. cordillerae*, CMC-P 38731d. The two specimens,

42

CMC-P 38731e and 38731f, are believed to be a cedariid protaspis, and most probably belong to other cedariid genera; they are temporarily described in open nomenclature as Cedariidae sp. A.

Description of Protaspides

Early metaprotaspid stage (CMC-P 38731b, Pl. II-11, Figs. 1-4). Shield elongated rectangle in outline; 0.287 mm wide and 0.340 mm long. Axis straight-sided and slightly forward-expanding up to anterior pits and forward-tapering thereafter; axis reaches anterior and posterior margins. Anterior pits distinctly-impressed and do not reach anterior margin. Anterior margin straight (tr.); posterior margin gently indented, and appears to be dorsally arched. Occipital ring small but prominent node, and demarcates anterior margin of protopygidium; posterior cranidial marginal furrow inconspicuous.

Late metaprotaspid stage (CMC-P 38731d, Pl. II-11, Figs. 5-8). Shield elongated trapezoidal in outline; 0.415 mm wide and 0.445 mm long. Glabella spindle-shaped, with its maximum width being 33% of shield width; its anteriormost end abruptly expands forwards; no anterior border differentiated. Posterior cranidial marginal border distinctly developed and runs at 45° diagonal posteriorly. Occipital ring highly convex, marking highest point in lateral profile. Protopygidium sagittally short, occupying 17% of shield length. One protopygidial axial ring recognizable; interpleural furrow moderately deep.

Protaspides of *Cedarina cordillerae* and Their Taxonomic Implications. Hu and Li (1971) described the ontogeny of *Cedarina cordillerae* from the Pilgrim Formation in Montana. The illustrated metaprotaspid specimens from Montana (pl. 2, figs. 5-10) differ from the Utah specimens described herein in having an elliptical shield, a trapezoidal L4, and distinct glabellar furrows. These differences are not expected in the ontogeny of a single species. However, the Montana specimens, which range from 0.475 to 0.687 mm in sagittal length, are larger than the Utah specimens, thus the Montana specimens are considered to represent a later metaprotaspid stage. A Montana specimen CMC-P 40282b (Hu and Li, 1971, pl. 2, fig. 3) is identical to an early metaprotaspid stage represented by CMC-P 38731b (Pl. II-11, Figs. 1-4) in Utah specimens. Specimen CMC-P 40282 (Hu and Li, 1971, pl. 2, fig. 1) appears to be similar to CMC-P 38731a (Pl. II-12, Figs. 22-24) which is incorrectly associated to *C. cordillerae*. Specimen CMC-P 40282a (Hu and Li, 1971, pl. 2, fig. 2) from Montana is very similar to CMC-P 38731f (Pl. II-11, Figs. 20-22) which is identified here as Cedariidae sp. A.

Protaspides of *Cedarina cordillerae*, *Cedaria milleri*, and *Paracedaria viriosa* were described by Hu and Li (1971), all from the Pilgrim Formation of Montana. Although these ontogenies possibly include incorrect associations, it is certain that the protaspides of the three genera share many similarities. In particular, the discernible early metaprotaspis of *C. cordillerae* (Pl. II-11, Figs. 1-4) is shared by the other two genera; for *C. milleri*, see Hu and Li, 1971, pl. 1, fig. 3 and for *P. viriosa*, see Hu and Li, 1971, pl. 4, fig. 3. Later in ontogeny, *C. milleri* develops a deeper posterior cranidial border furrow and a brim-like posterior cranidial border, and *P. viriosa* develops a relatively wider (tr.) axis.

Metaprotaspides of *Nixonella montanensis* (Llanoaspididae, Pl. II-16, Figs. 5-13) differ from those of *Cedarina cordillerae* in having a parallel-sided, narrower (tr.) axis with a slightly forward-expanding glabellar front and a distinct flat anterior border. *N. montanensis* has a discernible anaprotaspis with a square-shaped shield (Pl. II-16, Figs. 1-3). However, the convexity of the metaprotaspid shield, the relative convexity of its axis,

43

and the overall elliptical shield outline are comparable between the two species. Protaspid morphologies support the close taxonomic affinity of Cedariidae with Llanoaspididae.

Specimen CMC-P 38728d (Pl. II-13, Figs. 28-29), which was incorrectly assigned to Middle Cambrian *Glyphaspis paucisulcata* from the Meagher Formation in Montana, shows a similar overall morphology to that of the early metaprotaspis of *Cedarina cordillerae* (Pl. II-11, Figs. 1-4). However, the former is much larger (0.458 mm in sagittal length; 0.340 mm for the latter), and has a rounded anterior margin and a more rapidly forward-expanding axis. At the instar of similar size, *C. cordillerae* (see Pl. II-11, Figs. 5-8) shows a distinct posterior cranidial marginal border, an entire posterior margin, and an axis whose L3/L2/L1 is spindle-shaped and L4 expands rapidly in front of the anterior pits. Nonetheless, their apparent similarities suggest that Upper Cambrian Cedariidae could have been derived from a Middle Cambrian taxon which has a protaspis similar to CMC-P 38728d (Pl. II-11, Figs. 5-8); it is worthwhile investigating trilobites co-occurring with *Glyphaspis paucisulcata* in the Meagher Formation to search the ancestry of the Cedariidae.

<div align="center">

?Family CEDARIIDAE Raymond, 1937
Genus APOMODOCIA Hu, 1971

</div>

Remarks. Hu (1971, p.85-86) assigned *Apomodocia* to the Parabolinoididae by noting the holaspid similarities with *Orygmaspis* (*Parabolinoides*) and *Taenicephalus* (synonymizing *Maustonia*, see Westrop, 1986, p. 50). However, many of the holaspid similarities of *Apomodocia* are shared with the Cedariidae. *Cedarina cordillerae* (see Pl. II-11, Figs. 13, 14) and *Apomodocia conica* (see Pl. II-12, Figs. 28, 29) share an elongated strongly forward-tapering glabella and a more adaxially located palpebral lobe, which are not evident in the parabolinoidids (see Pl. II-32, Figs. 23, 24). The posterior facial suture of *A. conica* is not of the typical proparian-type which characterizes the Cedariidae, but the suture is directed posteriorly at a much lower angle than it is in the parabolinoidids. The proparian-type suture is evident in an earlier holaspid cranidium of *A. conica* (Hu, 1971, pl. 9, fig. 13). The anterior facial suture of *A. conica* is similar to that of *C. cordillerae* in being parallel-sided or slightly convergent. Species of *Orygmaspis* (*Parabolinoides*) show distinct combinations of anterior facial suture and glabellar shape (Westrop, 1986, text-fig. 34); a parallel-sided anterior facial suture occurs with a subrectangular glabella, and a divergent suture with a forward-tapering glabella. *A. conica* exhibits a parallel-sided anterior facial suture and a forward-tapering glabella, which is not one of the variations known for *Orygmaspis* (*Parabolinoides*). The pygidium of *A. conica* (Pl. II-12, Figs. 30, 31) has as many as six axial rings and a convex pleural field and axis, which is closer to pattern found in the Cedariidae (e.g., Pl. II-11, Figs. 15, 16) than that of the Parabolinoididae; the latter has three to four pygidial axial rings (see Westrop, 1986, text-fig. 34). As a result, *Apomodocia* is considered to be more closely related to the Cedariidae than to the Parabolinoididae, a relationship strongly supported by protaspid features (see below). On the other hand, comparison of the protaspid features prevents me from placing *Apomodocia* within the Cedariidae with confidence (see below).

<div align="center">

Apomodocia conica Hu, 1971
Pl. II-12, Figs. 1-12, 28-31, Text-fig. V-2.6

</div>

<div align="center">

44

</div>

1971 *Apomodocia conica* Hu [part], p. 88-90, pl. 9, figs. 3, 5-19 [only].

Diagnosis. See Hu (1971, p. 88) for holaspid diagnosis. **Metaprotaspis.** Shield subrectangular. L4 forward-expanding. L3/L2/L1 parallel-sided. Posterior fixigenal spine stout, short, broadly-based, and ventrally protruding beyond protopygidium. Posterior cranidial marginal furrow transverse and then directed in 45° at mid-length.

Occurrence of Materials Described Herein. *Cedaria* zone, Wasatch Mountain, Utah (locality 9 in Text-fig. I-2).

Association of Protaspides. Of the protaspid specimens assigned to *Apomodocia conica* by Hu (1971), only three specimens, CMC-P 38725c, e, and g (Pl. II-12, Figs. 4-12) are considered to be protaspides of *Apomodocia conica*. This association is assured by the presence of ventrally-extending posterior fixigenal spines and strongly ventrally-curved fixigenae. However, there is some doubt about this association, when considering that the morphological transition from the largest metaprotaspid specimen (CMC-P 38725g, Pl. II-12, Figs. 10-12) into the smallest cranidium (CMC-P 38725i, Hu, 1971, pl. 9, fig. 9) does not seem to be as continuous as expected. The parallel-sided axis with a forward-expanding L4 changes into a forward-tapering glabella; the anterior margin changes from straight to rounded; and the strongly curved posterior cranidial margin changes into a transversely straight one. Due to the absence of an appropriate meraspid cranidium which would have a parallel-sided glabella, the association of the protaspid specimens cannot be assured with confidence. In effect, the meraspid cranidia of *A. conica* (CMC-P 38725i, j, and k, Hu, 1971, pl. 9, figs. 9-11) are indistinguishable from those of *Cedarina cordillerae*. Either the meraspid cranidia should be re-assigned to *C. cordillerae* or such a great similarity of the meraspides is due to a close evolutionary relationship. Thus, the association of the protaspid specimens of *A. conica* is not as confident as in *C. cordillerae*.

Specimen CMC-P 38731c (Pl. II-12, Figs. 1-3), which was originally assigned to *Cedarina cordillerae*, is incorporated into the ontogeny of *Apomodocia conica*. It has a posterior fixigenal spine pair which has a similar orientation to CMC-P 38725c of *A. conica* (compare Pl. II-12, Figs. 2 and 5), and a straight lateral and posterior shield margin.

Specimen CMC-P 38725b (Pl. II-12, Figs. 13-15) is morphologically similar to CMC-P 38731c (Pl. II-12, Figs. 1-3). The specimen could be an earlier ontogenetic stage of the latter specimen of *Apomodocia conica*. It has a tiny spine pair which is comparable to the posterior fixigenal spine in the larger specimens (e.g., Pl. II-12, Figs. 5, 8, 11). However, the presence of a narrow anterior border and distinct occipital ring prevents me from assigning it to *A. conica*; it is assigned to *Apomodocia*? sp. A. The anterior border, the lateral portion of which could represent a palpebro-ocular ridge, the location of anterior pits which are behind the anterior border, and a nearly straight posterior margin are reminiscent of early protaspis of *Sao hirsuta* (see Whittington, 1957, pl. 116, fig. 14).

Specimen CMC-P 38731g (Pl. II-12, Figs. 19-21), which was incorrectly identified as *Cedarina cordillerae*, has a ventrally-extending posterior fixigenal spines and strongly ventrally-curved fixigenae, which leads me to assign it to *Apomodocia*. However, compared with CMC-P 38725g (Pl. II-12, Figs. 11, 12), it differs in having a more rectangular shield and a less distinct posterior cranidial marginal border furrow. The specimen most probably belongs to a new *Apomodocia* species; it is described herein as *Apomodocia* sp. A. A metaprotaspid specimen CMC-P 38725d (Pl. II-12, Figs. 16-18)

45

does not have ventrally-curved fixigenae and a short genal spine, which characterize *Apomodocia conica*. However, it is very similar to CMC-P 38731g and is considered as an earlier ontogenetic stage of *Apomodocia* sp. A.

Description of Protaspides.

Anaprotaspid stage (CMC-P 38725c, 38731c; Pl. II-12, Figs. 1-6). Shield rectangular outline; 0.405 mm long and 0.375 mm wide. Axis parallel-sided with its frontal part expanding forwards; axial furrows weakly-impressed. Posterior margin slightly indented anteriorly and upturned dorsally. Posterior fixigenal spine short and directed ventrally and posteriorly.

Metaprotaspid stage (CMC-P 38725e, 38725g; Pl. II-12, Figs. 7-12). Shield sub-rectangular in outline; 0.531 mm (avg.) wide and 0.557 mm (avg.) long. Axis parallel-sided with rapidly forward-expanding frontal lobe, occupying 25% of shield width; no anterior border differentiated. Posterior margin slightly indented. Posterior fixigenae strongly curved downwards, its distal portion extends beyond protopygidium in posterior view. Posterior fixigenal spine short and stout. Protopygidium with two or three axial rings and occupies 22% of shield length.

Protaspides of *Apomodocia conica* and Taxonomic Implications. Protaspides of *Apomodocia conica* obviously differ from those of parabolinoidids (see Pl. II-32, Figs. 1-18, 40-42) in having a parallel-sided axis without annulated lobes, an elongated rectangular outline and a distinct posterior fixigenal spine. These features suggest that *Apomodocia* is not a member of the Parabolinoididae. From the cedariid protaspides (Pl. II-11, Figs. 5, 20; see also Hu and Li, 1971, pls. 1, 2, 4), they are distinguished by having a narrower (tr.) axis, and most prominently having a posterior fixigenal area which strongly curved ventrally and a short posterior fixigenal spine. Although the association of the protaspides of *A. conica* is not as confident as those of *Cedarina*, these differences do not allow me to confidently assign *Apomodocia* to the Cedariidae.

Family **ANOMOCARIDAE** Poulsen, 1927

Remarks. Fortey and Chatterton (1988) placed the Anomocaridae in the superfamily Anomocaracea of the Asaphida. The Middle Cambrian Anomocaridae is considered to include ancestors to some families of the Asaphida (Fortey and Chatterton, 1988, text-fig. 27). In their phylogenetic analysis (text-figs. 2, 3), the character that is possessed by the Anomocaridae and allowed them to place the family within the Asaphida is the presence of a median suture. Possession of bacculae is another distinctive synapomorphy that places the Anomocaridae as an immediate sistergroup to two asaphid superfamilies, Asaphacea and Cyclopygacea. An asaphoid protaspis, which has a spherical to ovoid exoskeleton with an enrolled doublure, is another important synapomorphy to cluster the Anomocaridae within the Asaphida.

Genus **GLYPHASPIS** Poulsen, 1927

Remarks. *Glyphaspis* is distinguished from other anomocarids such as *Anomocaroides* (Fortey and Chatterton, 1988, text-fig. 21) and *Anomocarina* (Babcock, 1994, Fig. 6.1-6.5) by possessing a forward-tapering glabella, relatively shorter, less curved, and more distally located palpebral lobes, and a much larger (exsag. and tr.) posterior fixigenal area, and in lacking the bacculae. Its pygidial features are greatly similar to those of *Anomocaroides*.

46

The Auritamidae Öpik, 1967, which is another consistent member of the Anomocaracea, in its cranidial features (e.g., *Auritama aurita*, Öpik, 1967, pl. 13, figs. 9-12) is much more similar to *Anomocaroides* and *Anomocarina* than to *Glyphaspis*. They share larger, highly curved palpebral lobes, a parallel-sided glabella, a much narrower posterior fixigenal area, and bacculae. A spinose pygidial margin (Öpik, 1967, pl. 14, fig. 1) is a unique derived feature of the Auritamidae.

Glyphaspis paucisulcata Deiss, 1939
Pl. II-13, Figs. 1-19, Text-fig. V-2.9

1939 *Glyphaspis paucisulcata* Deiss, p. 96, pl. 16, figs. 15-17.
1939 *Glyphaspis storeyi* Deiss, p. 97, pl. 16, figs. 35-37.
1971 *Glyphaspis* cf. *parkensis*, Hu [part], p. 83-87, pl. 11, figs. 1-3, 5-30 [only]

Diagnosis. A species of *Glyphaspis* with long (sag.) anterior cranidial border, two pairs of glabellar furrows, less distinct palpebral furrows and eye ridge, a sharply-angled antero-lateral corner of pygiidum, and straight anterior pygidial margin. **Early metaprotaspis.** Shield oval with deeply indented posterior margin. L4 forward-expanding. L3/L2/L1 parallel-sided. Palpebro-ocular ridge slender and differentiated from anterior border. Occipital ring as small node. **Late metaprotaspis.** Protopygidium moderate-sized and with entire posterior margin. Anterior pits relatively broad and shallow.

Stratigraphic and Geographic Distributions. This species occurs in *Bathyuriscus-Elrathina* Zone (Middle Cambrian). It has been reported from Pagoda Limestone and Meagher Formation in Montana.

Remarks. *Glyphaspis paucisulcata* was erected only based on pygidial specimens (Deiss, 1939, pl. 16, figs. 15-17) which are indistinguishable from the specimens illustrated herein (CMC-P 38728w, Pl. II-13, Figs. 18-19). The cranidial and pygidial specimens from Montana, originally identified as *Glyphaspis storeyi* (Deiss, 1939, pl. 16, fig. 35), are also indistinguishable from the specimens illustrated herein. Since *G. paucisulcata* was listed earlier, *G. storeyi* is synonymized under *G. paucisulcata*.

Hu (1971, p. 83-87) identified these specimens as *Glyphaspis* cf. *parkensis*. Compared to *Glyphaspis parkensis* from the Canadian Rockies (Rasetti, 1951, pl. 34, figs. 5-7), this species lacks a distinct eye ridge, distinct pleural furrows on the pygidium, distinct glabellar furrows, and diverticulae on the preglabellar field and anterior fixigenal area.

The features distinguishing *Glyphaspis paucisulcata* from other *Glyphaspis* species from Montana (Walcott, 1916b (refer to Resser, 1935 for taxonomic revision); Deiss, 1939) include a long (sag.) anterior border (longer than preglabellar field), two pairs of weakly-impressed glabellar furrows, less distinct palpebral furrows and eye ridge, a sharply angled antero-lateral corner of the pygidium, and a straight anterior pygidial margin.

Occurrence of Materials Described Herein. *Bathyuriscus-Elrathina* Zone (Middle Cambrian) of Meagher Formation, west side of south Boulder Creek, west Madison County, Montana (locality 10A in Text-fig. I-2).

Association of Protaspides. Specimen CMC-P 38728a (Pl. II-13, Figs. 20-21) is similar to CMC-P 38727a (Pl. II-3, Figs. 21-23), which is assigned to Ptychopariina sp. A herein, in having a narrow axis and a rapidly forward-expanding L4. This specimen is named

47

Ptychopariina sp. B.

Specimens CMC-P 38728b and 38728c resemble corynexochid protaspides (e.g., *Ptarmigania aurita*, Pl. II-3, Figs. 1, 4, 7, 17) in possessing distinct widely-spaced anterior pits, an indented posterior margin, and a narrow lateral shield border. Although they do not have a sagittal furrow, the resemblance is so great that they most probably represent protaspides of a corynexochid species with which *Glyphaspis paucisulcata* occurs. Deiss (1939) reported such corynexochids as *Bathyuriscus* along with several *Glyphaspis* species from a locality in Montana which is adjacent to the sampling locality where the protaspid specimens described herein were collected. If these specimens are incorporated into the ontogeny of *G. paucisulcata*, such drastic morphologic transformations as the development of an eye ridge, the shallowing of anterior pits, and the development of forward-expanding axial furrows need to be incorporated. Both specimens are named Corynexochida sp. B.

For the association of specimen CMC-P 38728d of species undetermined J (Pl. II-13, Figs. 28-29), see "Association of Protaspides" under *Cedarina cordillerae*.

Description of Protaspides.

Early metaprotaspid stage (CMC-P 38728e, Pl. II-13, Figs. 1-3). Shield ovate in outline with rounded anterior margin and indented posterior margin; 0.458 mm wide and 0.440 mm long. Axis parallel-sided with frontal lobe forward-expanding. Eye ridge slender; its adaxial ends immediately behind shallow anterior pits. Posterior cranidial marginal border furrow weakly-impressed, diagonally directed posteriorly and does not cross the shield. Protopygidium steeply inclined; posterior margin arched.

Late metaprotaspid stage (CMC-P 38728f, g, Pl. II-13, Figs. 4-10). Shield oval in outline; sagittal length ranges from 0.566 to 0.604 mm and transverse width from 0.511 to 0.592 mm. Axis occupies 27% of shield width. Posterior cranidial border weakly developed, and directed at low angle to transverse. Posterior cranidial marginal furrow distinct. Protopygidium with two axial rings and occupies 18 to 26% of shield length; posterior margin entire.

Protaspides of *Glyphaspis paucisulcata* and Their Taxonomic Implications. Fortey and Chatterton (1988) in their systematic revision of the Asaphina suggested that only derived asaphine groups have the asaphoid-type protaspis and the primitive group including the anomocarids does not have the asaphoid protaspis. Re-illustration clearly demonstrates that the protaspides of *Glyphaspis paucisulcata* (Pl. II-13, Figs. 1-10) are not an asaphoid-type The protaspides of *Glyphaspis paucisulcata* are similar to those *Apomodocia conica* and *Syspacheilus dunoirensis*, suggesting that these species are closely related to one another.

Family CREPICEPHALIDAE Kobayashi, 1935

Remarks. The Crepicephalidae includes *Crepicephalus*, *Coosia*, *Coosella*, *Coosina*, and *Syspacheilus* (Palmer, 1954b; Rasetti, 1956; Pratt, 1992). The latter two workers implied a close relationship between the Crepicephalidae and Blountiinae including *Blountia*; Rasetti (1956, p. 1269) even suggested that both groups would have been derived from such ptychopariids as *Ehmania*, *Ehmaniella*, and *Armonia*.

Genus CREPICEPHALUS Owen, 1852
Crepicephalus deadwoodiensis Hu, 1971

48

Pl. II-14, Figs. 1-31, Text-fig. V-2.10
1971 *Crepicephalus deadwoodiensis* Hu [part], p. 89-92, pl. 14, figs. 2-29, text-fig. 43 [only].

Diagnosis. See Hu (1971, p. 89-90) for holaspid diagnosis. **Anaprotaspis.** Shield subcircular with indented posterior margin. Anterior pits present. **Early metaprotaspis.** Shield subhexagonal. Axis narrow. L4 forward-tapering. Area behind occipital ring relatively long (sag.). Anterior pits deeper than axial furrows. **Late metaprotaspis.** Shield subhexagonal. L4 forward-tapering. Anterior border present. Palpebro-ocular ridge slender. Three pairs of tubercles alongside glabella. Paired tubercles on glabella. Protopygidium large.

Occurrence of Materials Described Herein. *Crepicephalus* Zone (upper Marjuman) of Deadwood Formation. Lead, northern Black Hills, Lawrence Co. South Dakota (locality 5B in Text-fig. I-2).

Association of Protaspides. All specimens illustrated by Hu (1971, pl. 14), except for CMC-P 38732h (Pl. II-14, Figs. 32, 33), are considered to be correctly associated with *Crepicephalus deadwoodiensis.* With respect to the sagittal length, the specimen CMC-P 38732h is intermediate between CMC-P 38732j and 38732k of *C. deadwoodiensis* (Pl. II-14, Figs. 20, 22). Since the specimen CMC-P 38732h lacks the tubercles on fixigenae and glabella which are found in the latter two metaprotaspid specimens, it should not belong to the ontogeny of *C. deadwoodiensis.* However, its indented posterior margin, spindle-shaped axis, and concave and broad lateral and posterior shield border indicate that it is a metaprotaspis of a species of Crepicephalidae, Crepicephalidae sp. A.

The anaprotaspis of *Crepicephalus deadwoodiensis,* CMC-P 38728a (Pl. II-14, Figs. 1, 2) is similar to anaprotaspis of *Nixonella montanensis* (CMC-P 40280m, Pl. II-16, Fig. 1-3) in having a somewhat square-shaped shield and distinct anterior pits. However, the L4 of *C. deadwoodiensis* extends beyond the anterior fixigenal area in lateral profile (Pl. II-14, Fig. 2) whereas that of *N. montanensis* does not. This character which occurs in all the early metaprotaspides of *C. deadwoodiensis* (see Pl. II-14, Figs. 4, 8, 12) guarantees its association with *C. deadwoodiensis.*

Description of Protaspides

Anaprotaspid stage (CMC-P 38732a, b, Pl. II-14, Figs. 1-5). Shield sub-circular in outline, 0.281 mm long and from 0.287 mm wide; posterior margin indented. Anterior pits distinct; frontal glabellar lobe swells dorsally and anteriorly beyond the anterior pits. **Early metaprotaspid stage** (CMC-P 38732c, d, e, f, g, Pl. II-14, Figs. 6-16). Shield subhexagonal in outline, ranges from 0.305 to 0.432 mm in sagittal length and from 0.315-0.437 mm in width; lateral profile sigmoidal. Axis relatively narrow (22% of shield width in average) and parallel-sided with only its anteriormost and posteriormost ends tapering. Anterior pits distinct and becoming shallower towards anterior. Posterior margin moderately indented. Occipital ring as a small node. Protopygidial area behind occipital ring unusually long (sag.), occupying 16 to 25% of shield length; no posterior cranidial marginal furrows impressed. In later stages (CMC-P 38732g, Pl. II-14, Figs. 12-14) posterior lateral flat border developed and slender eye ridge developed.

Late metaprotaspid stage (CMC-P 38732i, j, k, Pl. II-14, Figs. 17, 20-23). Shield elliptical in outline, ranges from 0.653 to 0.821 mm in length and from 0. 558 to 0.740 mm in width. Protopygidium occupies 40% of entire shield length with at least two axial rings. Three pairs of regularly-spaced tubercles develop alongside glabella; this row of

49

tubercles present on pygidial pleural field. Three paired tubercles on glabella; paired tubercles also on pygidial axial rings. Anterior border distinctly differentiated from eye ridge and glabellar front.

Protaspides of *Crepicephalus deadwoodiensis* and Their Taxonomic Implications. *Crepicephalus deadwoodiensis* retains the slightly forward-tapering glabella throughout its ontogeny, which is unique among the members of this superfamily. All the other species changes from a forward-expanding glabella into a forward-tapering glabella mostly during the meraspid period. This species also uniquely possesses the tubercles on the fixigenae in its metaprotaspid stages (Pl. II-14, Figs. 20-23). This tuberculation pattern is identical to that shown in post-Cambrian trilobite groups such as hystricurids (e.g., Lee and Chatterton, 1997b, fig. 3), and lichids and odontopleurids (e.g., Chatterton and Speyer *in* Whittington *et al.*, 1997, figs. 183, 185).

Protaspides of *Crepicephalus deadwoodiensis* and *Blountia bristolensis* (Pl. II-6, Pl. II-7, Figs. 1-6) allow us to test the close relationship between the Crepicephalidae and Blountiinae suggested by Rasetti (1954). The protaspides of *B. bristolensis* possess a sagittal furrow and three pairs of fixigenal spines in anaprotaspid stages and a forward-expanding axis in metaprotaspid stages, and widely-spaced anterior pits and a more broadly-indented posterior margin in both stages, which are not found in the protaspides of *C. deadwoodiensis*. Thus, the close relationship suggested by Rasetti (1954, p. 1269) based on holaspid features is not corroborated by the protaspid morphologies.

Family **MARJUMIIDAE** Kobayashi, 1935

Remarks. Various taxonomic accounts for the concept of this family are found in Robison (1964, 1988) and Pratt (1992).

Genus **SYSPACHEILUS** Resser, 1938a

Remarks. The genus *Syspacheilus* was assigned to the Crepicephalidae (Palmer, 1954b, p. 727-728) mainly based on the observation that the pygidium has "three deep pleural furrows and two or three shallow interpleural grooves about equally spaced." Later, Lochman and Hu (1961, p. 133) claimed that the pygidium assigned to *Syspacheilus* by Palmer (1954b, pl. 78, fig. 10) is a pygidium of *Coosella*, and the correctly associated pygidium of *Syspacheilus* has a narrower border, a wider axis and fewer pleural furrows (Lochman and Hu, 1961, pl. 26, fig. 1). They further argued that the pygidium of *Syspacheilus* is the most primitive of the Crepicephalidae. Based on these pygidial features, Robison (1964, p. 521, 547; 1988, p. 71) assigned *Syspacheilus* to the Marjumiidae along with such genera as *Marjumia* and *Modocia*. Pratt (1992, p. 60) questioned the placement of *Syspacheilus* in the Marjumiidae since species assigned to *Syspacheilus* show a wider variation of pygidial morphologies. Comparing the pygidium of *S. dunoirensis* (Lochman and Hu, 1961, pl. 26, fig. 1) with that of *S. catatate* (Robison, 1988, fig. 21.12) demonstrates how great variations are in the pygidial features of *Syspacheilus*. The former is greatly similar to a *Modocia* pygidium (e.g., *M. planata*, Robison, 1988, figs. 21.7-21.9) in having a narrower border and paired knobs on the terminal piece, whereas the latter is similar to a *Coosella* pygidium (e.g., *C. beltensis*, Palmer, 1954b, pl. 78, fig. 5) in having a wider border and terminal axial ridge. It is evident that *Syspacheilus* has an equal degree of affinity to the Marjumiidae and Crepicephalidae. The opposite ends of these continuous variations in the pygidium are

50

represented by *Marjumia typa* with the pygidial spines that are extensions of the pygidial pleurae (Robison, 1964, pl. 87, fig. 4) and by *Crepicephalus* with the spines that are extensions of the marginal borders (Palmer, 1954b, fig. 4). The pygidia of *Syspacheilus*, *Modocia*, and *Coosella* well fill the gap between these two extremes. Cranidial features also vary without a considerable distinction between the two groups. For example, compare *Coosella prolifica* (Lochman, 1936, pl. 9, figs. 4, 8) and *Marjumia typa* (Robison, 1964, pl. 87, fig. 2).

Protaspides of *Modocia laevinucha* (Pl. II-47) are greatly similar to those of *Syspacheilus dunoirensis* in having an elliptical, less convex, and smooth shield, a L4 that expands forwards at anterior two-thirds of its length, and parallel-sided L3/L2/L1. This supports that *Syspacheilus* is a member of the Marjumiidae.

<center>

Syspacheilus dunoirensis (Miller, 1936)
Pl. II-15, Figs. 1-23, Text-fig. V-2.8

</center>

1936 *Blountia dunoirensis* Miller, p. 27, pl. 8, figs. 25-27.
1944 *Syspacheilus dunoirensis*, Lochman *in* Lochman and Duncan, p. 131-132, pl. 11, figs. 44, 45.
1950 *Syspacheilus occidens*, Lochman, p. 342, pl. 50, figs. 25, 26.
1954b *Syspacheilus dunoirensis*, Palmer, p. 734-735, pl. 78, fig. 9.
1961 *Syspacheilus dunoirensis*, Lochman and Hu, p. 134-135, pl. 26, figs. 1-25, 27-36, 40-48.
1961 *Syspacheilus dunoirensis* var., Lochman and Hu, p. 135, pl. 26, figs. 26, 37-39.
1961 *Syspacheilus praecedens* var. *elongatus*, Lochman and Hu, p. 135, pl. 27, figs. 19-28, 30.
1961 *Coosella vagrans*, Lochman and Hu, p. 132-133, pl. 26, figs. 49-54.
1972 *Syspacheilus dunoirensis*, Hu [part] p. 246-250, pl. 29, figs. 3-11, 13-34 [only].

Diagnosis. See Hu (1972, p. 246) for holaspid diagnosis. **Early metaprotaspis**. Shield hexagonal. Axis narrow. Axial furrows shallow. Anterior pits broad and shallow. **Late metaprotaspis**. Shield subrectangular. Transglabellar furrows weakly-developed. L4 slightly forward-expanding. L3/L2/L1 parallel-sided. Anterior border narrow (sag. and exsag.). Eye ridge slender. Protopygidium relatively large.

Stratigraphic and Geographic Distributions. This species occur in the *Cedaria* Zone (lower Marjuman of Upper Cambrian). It has been recorded from Riley Formation in Texas, Maurice Formation and DuNoir Limestone in Wyoming, and Pilgrim Formation in Montana.

Occurrence of Materials Described Herein. *Cedaria* Zone (Lower Marjuman) of Pilgrim Formation. west-side, South Boulder Creek, Madison County, Montana; light gray colored, medium crystalline limestone (locality 10B in Text-fig. I-2).

Association of Protaspides. Specimen CMC-P 40279 (Pl. II-15, Fig. 24) is very small (0.279 mm in sagittal length) and has a highly convex, circular shield. This specimen could be an earliest anaprotaspid stage. However, the absence of transitional forms in terms of size and morphology into the later ontogenetic stages of *Syspacheilus dunoirensis* seems to make the association highly speculative. A radical metamorphosis in association with a drastic size increase could be possible, which however is usually inferred for specimens occurring in the same bed or the same blocks of limestone for silicified specimens. Of the trilobites from the *Cedaria* Zone, *Norwoodella halli* has an

<center>51</center>

anaprotaspis that has a highly convex shield without any features on the dorsal surface (USNM 143466o, Pl. II-24, Figs. 1-2). It seems possible that CMC-P 40279 could be an earliest ontogenetic stage of *N. halli*; Lochman and Duncan (1944, p. 137) reported a *Norwoodella* species, *N. simplex* from the Pilgrim Formation in Montana. This anaprotaspid specimen is named species undetermined K.

Specimen CMC-P 40279a (Pl. II-15, Fig. 25) is poorly preserved in its anterior part and it has a spindle-shaped axis with a sagittal furrow and strongly convex lateral margin. The ontogenetic transformation from this specimen into the early metaprotaspides of *Syspacheilus dunoirensis* (CMC-P 40279b, d, Pl. II-15, Figs. 1-5) is not reasonable. This specimen is assigned to species undetermined L.

Meraspid cranidium (Pl. II-15, Fig. 16) apparently develop tubercles on fixigena and glabella, but the tuberculation is absent in the metaprotaspides. Thus, the meraspid cranidium is assigned to ontogeny of a *Crepicephalus* species whose metaprotaspides exhibit the tuberculation (see Pl. II-14, Figs. 20, 22).

Description of Protaspides

Early metaprotaspid stage (CMC-P 40279b, d, Pl. II-15, Figs. 1-5). Shield sub-hexagonal in outline; 0.435 mm (avg.) wide and 0.434 mm (avg.) long. Axis parallel-sided and narrow (25% of maximum shield width in average); axial furrows weakly-impressed. Anterior pits shallow and broad. Posterior margin slightly indented and slightly curved upwards. Occipital ring as small node. Protopygidium triangular in outline, anteriorly defined by very weakly incised posterior cranidial marginal furrow, occupying 14% (avg.) of shield length; no axial rings and interpleural furrows developed. **Late metaprotaspid stage** (CMC-P 40279c, e, and f, Pl. II-15, Figs. 6-15). Shield elongated sub-hexagonal to elliptical in outline, ranges from 0.533 to 0.636 mm in sagittal length and from 0.487 to 0.544 mm in width. Axis occupies 25% of shield width. Anterior border flat, narrow, low-leveled and slightly arched forwards. Eye ridge slender. Posterior marginal cranidial border runs horizontally into mid-shield width and curved posteriorly at about 45 degrees; posterior cranidial marginal furrow shallow. Protopygidium, occupying 25% to 36% of shield length, with at least two pygidial axial rings; pleural and interpleural furrows weakly-developed; pygidial axis falls short of posterior margin. In lateral profile, anterior one-fourth steeply inclined and rest of the shield gently inclined.

Protaspides of *Crepicephalus deadwoodiensis* and *Syspacheilus dunoirensis* and Their Taxonomic Implications. Comparison of the protaspides of *Crepicephalus deadwoodiensis* and *Syspacheilus dunoirensis* suggests a close relatiohsip between *Crepicephalus* and *Syspacheilus*. Protaspides of both species share an indented posterior margin, a narrow (tr.) axis, indistinct glabellar furrows, a relatively long (sag.) protopygidial area behind the occipital ring, and development of an anterior border in late metaprotaspid stages. The families represented by these two genera are considered to be classified together under the same superfamily. The late metaprotaspides of *C. deadwoodiensis* differ from those of *S. dunoirensis* in developing tubercles alongside and on the glabella, and having a forward-tapering glabella, and a less steeply inclined frontal area (compare CMC-P 40279f (Pl. II-15, Figs. 9-12) with CMC-P 38732j and 38732k (Pl. II-14, Figs. 20-23)). The early metaprotaspides of *C. deadwoodiensis* differ from those of *S. dunoirensis* in having a more deeply and narrowly indented posterior margin, more distinct anterior pits, and a narrower (tr.) axis (compare CMC-P 40279d (Pl. II-15, Figs.

52

1,2) with CMC-P 38732e (Pl. II-14, Figs. 10-11).

Genus MODOCIA Walcott, 1924
Modocia laevinucha Robison, 1964
Pl. II-47, Figs. 1-14, Text-fig. V-2.11

1964 *Modocia laevinucha* Robison, p. 551, pl. 87, figs. 11-19.

Diagnosis. see (Robison, 1964, p. 551) for holaspid diagnosis. **Anaprotaspis.**
Subquadrate shield with slightly forward-expanding L4. **Metaprotaspis.** Elliptical shield
with slender ocular ridge and flat anterior border.

Stratigraphic and Geographic Distributions. This species occur in the *Bolaspidella*
Zone (late Middle Cambrian) of Marjum Formation, western Utah; the illustrated
materials were recovered in Marjum Formation, near Swasey Peak, House Range, Utah
(locality 8 in Text-fig. I-2 and see also Text-fig. I-3).

Description of Protaspides

Anaprotaspid Stage (UA 12825; Pl. II-47, Figs. 1-5). Shield subquadrate in outline; 0.43
mm in width and 0.42 mm in length. L4 slightly forward-expanding and L3-L0 parallel-
sided. Axial furrow shallow.

Metaprotaspid Stage (UA 12826; Pl. II-47, Figs. 6-10). Shield elliptical in outline; 0.52
mm in width and 0.63 in length. Ocular ridge weakly developed. Posterior cephalic
border almost imperceptible. Anterior border flat. Ocular ridge slender.

Protaspides and Taxonomy. Ana- and metaprotaspides of this species are very similar
to those of *Syspacheilus dunoirensis* (see Pl. II-15, Figs. 1, 9) than to those of
Crepicephalus deadwoodiensis (see Pl. II-14, Figs. 14, 22). This suggests that
Syspacheilus belongs to the Marjumiidae along with *Modocia*, not to the Crepicephalidae
with *Crepicephalus*.

Family LLANOASPIDIDAE Lochman, *in* Lochman and Duncan, 1944
Remarks. Lochman (*in* Lochman and Duncan, 1944, p. 66) erected the family
Llanoaspididae and included *Llanoaspis*, *Pilgrimia*, and questionably *Genevievella*; she
originally named it as Llanoaspidae, but later in the Treatise she corrected it into
Llanoaspididae. Lochman noted an evolutionary relationship between Llanoaspididae and
Leiostegiidae based on similarities of *Genevievella* to the leiostegiids with respect to the
cephalic structure. Lochman in the same work (p. 103-105) placed *Genevievella* in the
Leiostegiidae. Lochman (*in* Moore, 1959) renamed *Pilgrimia* as *Paracedaria* and
assigned it to the Raymondininae, and assigned *Genevievella* to the Llanoaspidinae; both
subfamilies were assigned to the Raymondinidae along with the Cedariinae.

Palmer (1962b, p. 23) suggested that *Llanoaspis* and *Raymondina* have adequate
cranidial differences so that the groups represented by this genus must be regarded as a
separate family. Pratt (1992, p. 83) followed Palmer's opinion and elevated the
Llanoaspidinae into the family Llanoaspididae. Nonetheless, the Llanoaspididae is
considered to be closely related to the Cedariidae.

Genus NIXONELLA Lochman *in* Lochman and Duncan, 1944
1962 *Torridella* Lochman and Hu, p. 16.
Remarks. Lochman (*in* Lochman and Duncan, 1944, p. 105) placed *Nixonella* in the
Leiostegiidae and noted its similarities with *Genevievella* and *Brassicicephalus*. Later,

53

Lochman (*in* Moore, 1959) assigned it to the Pagodiidae which was later regarded as a subfamily of the Leiostegiidae (Shergold, 1975, p. 169). *Nixonella montanensis* shares, with the pagodiines (e.g., *Pagodia* (*Lotosoides*) *turbinata*, Shergold, 1975, pl. 36, fig. 7), deep axial and anterior border furrows, the absence of a preglabellar field, a forward-tapering glabella, and a broad (tr.) palpebral fixigenal area. However, these features are also found in several llanoaspidid species (e.g., *Genevievella simon*, Pratt, 1992, pl. 32, fig. 13). The pagodiine cranidium has a much shorter (sag. and exsag.) anterior border and a strongly inflated fixigenal area and its pygidium (e.g., Shergold, 1975, pl. 36, fig. 3) has a smaller number of segments and deeper and broader pleural furrows. This indicates a somewhat distant affinity of *Nixonella* with the pagodiine species. Protaspid features provide more evidence that *Nixonella* is not a member of the Leiostegiidae (see below).

Later, Robison (1988, p. 67) assigned *Nixonella* to the Llanoaspididae (he misspelled it as Llanoaspidae) mainly based on the pygidial similarities of a new Greenland species, *Nixonella furta* (Robison, 1988, figs. 18.12-18.13) to *Llanoaspis* and *Genevievella*. It seems that the illustrated pygidia of *N. furta* are associated with an undescribed species of *Genevievella*. Such cranidial features of *N. furta* (Robison, 1988, figs. 18.14-18.16) as a divergent anterior facial suture, a diagonally straight posterior facial suture, and a rather slender posterior fixigenal area are not consistent with *Nixonella montanensis* (Pl. II-16) or even species of *Genevievella*. The cranidia seem to have been incorrectly associated with *Nixonella*.

Pratt (1992, p. 83) questioned the separate generic status of *Nixonella* and suggested that *Nixonella* could be adequately embraced by *Genevievella*. From *Genevievella* (see Pratt, 1992, text-fig. 32), however, *Nixonella montanensis* differs in having a longer (sag. and exsag.) anterior border, a longer glabella, and a transverse (not forward-curving) posterior fixigenal area. Furthermore, the pygidium showing weakly-developed pleural furrows (CMC-P 40280r, Pl. II-16, Figs. 18, 19; see also *Nixonella migranta*, Lochman and Hu, 1962, pl. 6, figs. 12, 14, 15) is unique to *Nixonella*; the association of both cranidial and pygidial materials of Greenland *Nixonella furta* is questionable (see above). It is certain that *Nixonella* is a separate genus from *Genevievella*. Nevertheless, cranidial similarities to other llanoaspidid genera such as *Llanoaspis* (Lochman and Duncan, 1944, pl. 7, figs. 14) indicate that *Nixonella* is a llanoaspidid genus. Hu (1972, p. 250-251) synonymized *Torridella* Lochman and Hu, 1962 with *Nixonella*, which is accepted herein.

Nixonella montanensis Lochman *in* Lochman and Duncan, 1944
Pl. II-16, Figs. 1-22, Text-fig. V-2.7

1944 *Nixonella montanensis* Lochman and Duncan [part], p. 105-106, pl. 13, figs. 27, 29-31, [only].

1944 *Nixonella* cf. *montanensis*, Lochman and Duncan, p. 106, pl. 16, figs. 27-29.

1944 *Nixonella*? *wolfensis*, Lochman and Duncan, p. 106, pl. 13, figs. 13, 14.

1962 *Nixonella montanensis*, Lochman and Hu [part], p. 16, pl. 5, figs. 48, 50-52 [only].

1972 *Nixonella montanensis*, Hu [part], p. 251-254, pl. 30, figs. 1-14, 16-21 [only].

Diagnosis. see Hu (1972, p. 251) for holaspid diagnosis. **Anaprotaspis**. Shield square-shaped. Anterior pits deeply-impressed. **Metaprotaspis**. Shield oval. Anterior border

54

narrow (sag. and exsag.). Anterior pits shallow. Axis consistently forward-expanding. Protopygidium medium-sized.

Stratigraphic and Geographic Distributions. This species occurs in the *Cedaria* Zone (lower Marjuman of Upper Cambrian). It has been reported from the Pilgrim Formation in Montana and the DuNoir Limestone in Wyoming.

Occurrence of Materials Described Herein. *Cedaria* Zone of the Pilgrim Formation, South-Boulder Creek, Madison County, Montana (locality 10B in Text-fig. I-2).

Remarks. Lochman (*in* Lochman and Duncan, 1944) described two additional species (*Nixonella* cf. *montanensis* and *Nixonella*? *wolfensis*) which are questionably assigned to *Nixonella*. However, the features that led to a tentative identification such as presence of three pairs of glabellar furrows and deep preglabellar furrows, are evident in the specimens illustrated herein. Thus, they are synonymized with *N. montanensis*. Identification of two pygidia as *Nixonella montanensis* (Lochman *in* Lochman and Duncan, 1944, pl. 13, fig. 28; Lochman and Hu, 1962, pl. 5, fig. 49) are incorrect (see also Hu, 1972, p. 251) since both have distinctly impressed pleural furrows. *Nixonella*? *ovicula* (Lochman and Hu, 1962, pl. 5, figs. 53-58) differs from *N. montanensis* in having a rather oblong shaped glabella.

Nixonella migranta (Lochman and Hu, 1962, pl. 6, figs. 7-18) differs from *Nixonella montanensis* in having a proportionately larger glabella and a rather short (tr.) anterior border. The association of some pygidia with *N. migranta* (Lochman and Hu, 1962, pl. 6, figs. 7, 11, 15, 18) is questionable since the pygidia show a distinctly impressed marginal border furrow and a distinctively defined terminal piece.

Association of Protaspides. Specimen CMC-P 40280n (Pl. II-16, Figs. 23-25) has a strongly forward-expanding axis, less distinct anterior pits, a widely indented posterior margin, and a forwardly-arched anterior margin. These features do not seem consistent with those of metaprotaspides of *Nixonella montanensis* (CMC-P 40280k, j, l, Pl. II-16, Figs. 4-13). The strongly forward-expanding axis and overall shield outline leads one to associate this specimen with CMC-P 39741c (Pl. II-10, Figs. 15-18) which was incorrectly identified as *Welleraspis lochmanae*. These two specimens may represent protaspides of *Madarocephalus laetus* (a catillicephalid, Rasetti, 1965, pl. 8, fig. 20) which also has the straight-sided, forward-expanding glabella in post-protaspid stages; both are tentatively assigned to Catillicephalidae sp. A.

Description of Protaspides.

Anaprotaspid stage (40280m, Pl. II-16, Figs. 1-3). Shield rounded square-shaped in outline; 0.392 mm wide and 0.341 mm long; anterior margin slightly convex forwards and posteriorly margin slightly indented; shield profile more steeply inclined towards posterior and gently inclined towards anterior. Anterior pits strongly developed. Axis slightly forward-expanding; axial furrows very weakly-impressed

Metaprotaspid stage (40280j-l, Pl. II-16, Figs. 4-13). Shield elliptical in outline, ranges from 0.396 to 0.486 mm in width and from 0.428 to 0.540 mm in length. Axis parallel-sided with frontal lobe being slightly forward-expanding, occupying 26% (avg.) of shield width; axial furrows moderately deep. Anterior pits moderately-impressed. Anterior border flat and narrow. Posterior cranidial border narrow; posterior cranidial marginal furrow shallow and convex forwards its mid-length. Protopygidium, occupying 24% (avg.) of shield length, semi-circular in outline; two or three axial rings present; no pleural and interpleural furrows developed

Protaspides of *Nixonella montanensis* and Their Taxonomic Implications. The metaprotaspides of *Nixonella montanensis* are more similar to those of the Crepicephalidae such as *Syspacheilus dunoirensis* (Pl. II-15, Figs. 1-23) than to those of the Cedariidae such as *Cedarina cordillerae* (Pl. II-11, Figs. 1-16). This contradicts the closer relationships suggested between Cedariidae and Llanoaspididae based on holaspid features (see above). As a result, protaspides and holaspides each are likely to produce two different groupings among the Marjumiidae, Cedariidae, and Llanoaspididae.

Protaspides of *Nixonella montanensis* greatly differ from those of *Leiostegium formosa* which are of corynexochid-type (Pl. II-4, Figs. 1-9) in having a more elongated shield, a less strongly forward-expanding glabella, and a narrow anterior cranidial border, and lacking fixigenal tubercles and pygidial marginal spines. This indicates a remote affinity of the Llanoaspididae with the Leiostegiidae which includes the Pagodiinae.

TAXA POSSESSING PROTASPID MORPHOTYPE C

Protaspides of *Housia vacuna* and *Housia ovata* of the Housiinae, *Pulchricapitus davisi* of the ?Pterocephaliinae, *Ponumia obscura*, *Drabia typica*, *Aphelotoxon triangularia*, and *Paranumia triangulata* of the Phylacteridae, *Arapahoia arbucklensis* of the Plethopeltidae, and *Norwoodella halli* of the Norwoodiidae share a similar protaspid morphology. Their anaprotaspides are characterized by a circular to oval, highly convex shield, and anterior pits and axial furrows present in some species. Their early metaprotaspides are characterized by a subquadrate to oval shield, shallow axial furrows, an occipital ring as node in some species. Their late protaspides are characterized by a suboval to oval shield, a slightly forward-tapering axis with a parallel-sided or slightly forward-tapering L4, axial furrows that shallow anteriorly, shallow glabellar furrows (absent in some species), and a relatively small protopygidium with two to four axial rings.

Family PTEROCEPHALIIDAE Kobayashi, 1935

Remarks. This family has been known to include four subfamilies, Aphelaspidinae Palmer, 1960, Housiinae Hupé, 1953, Pterocephaliinae Kobayashi, 1935, and Erixaniinae Öpik, 1963 (Palmer, 1965b; Shergold *in* Shergold and Cooper, 1985). Although the holaspid features of these groups certainly allow for stratophenetic clustering of these subfamilies, the protaspid features of species of each subfamily described herein lend no support to this clustering. In particular, the evolutionary relationship between Housiinae and Aphelaspidinae (Palmer, 1965b) is least supported by protaspid similarities. Since the aphelaspidine protaspides share few similarities with the Housiinae and Pterocephaliinae, the Aphelaspidinae is excluded from the family Pterocephaliidae.

Based on presence of rostral plates, Shergold (*in* Shergold and Cooper, 1985) separated the Aphelaspidinae and Erixaniinae from the Pterocephaliinae and Housiinae, and incorporated the first two subfamilies into the family Elviniidae. Their suggestion that the Aphelaspidinae is not a subfamily of the Pterocephaliidae is in agreement with Fortey and Chatterton (1988) who also questioned the close evolutionary connection between the Aphelaspidinae and Housiinae and suggested the exclusion of the Aphelaspidinae from the Pterocephaliidae.

56

Subfamily **HOUSIINAE** Hupé, 1953

Remarks. This pterocephaliid subfamily is known to include three genera, *Housia* (Walcott, 1916b), *Parahousia* Palmer, 1960, and *Prehousia* Palmer, 1960. This taxon was placed in the Asaphida by Fortey and Chatterton (1988) because it has a median ventral suture which was a synapomorphy of their concept of the Asaphida.

Genus **HOUSIA** Walcott, 1916b
Housia ovata Palmer, 1965b
Pl. II-17, Figs. 1-29, Text-fig. V-3.8

1960 *Housia ovata* Palmer, p. 75-76, pl. 7, figs. 1-7, 9.
1965b *Housia ovata*, Palmer, p. 65-66, pl. 12, figs. 8-11.
1975 *Housia ovata*, Kurtz, p. 1033-1034, pl. 4, figs. 19-20.
1980 *Housia ovata*, Hu [part], p. 381-386, pl. 45, figs. 3, 4, 6, 7, 9-19, 21-34 [only].

Diagnosis. see Palmer (1965b, p. 65-66) for holaspid diagnosis. **Anaprotaspis.** Shield circular. Axis spindle-shaped. Anterior pits shallower than axial furrows. **Metaprotaspis.** Shield suboval in outline. Axis forward-tapering; L4 parallel-sided. Glabellar furrows weakly-impressed. Protopygidium small-sized, strongly projected ventrally, with three axial rings. Pits in axial furrows and posterior cranidial border furrow.

Stratigraphic and Geographic Distributions. This species occurs in the *Dunderbergia* to *Elvinia* Zones (upper Steptoean Stage of Upper Cambrian) and has been reported from the Dunderberg Formation in Nevada and Davis Formation in Missouri.

Occurrence of Materials Described Herein. *Elvinia* Zone of the Deadwood Formation, Galena section, about 5 miles southeast of Deadwood, South Dakota (locality 5C in Text-fig. I-2).

Association of Protaspides. The smallest specimen CMC-P 43418 (Pl. II-17, Figs. 30-33) has a subtrapezoidal L4, spindle-shaped bilobed L3/L2/L1, deeply impressed anterior pits, an indented posterior margin, and three pairs of fixigenal spines. If it is correctly associated, the transformation into the smallest anaprotaspis of *Housia ovata* (CMC-P 43418b, Pl. II-17, Figs. 1-4) requires a drastic metamorphosis. For the present, the specimen CMC-P 43418 (named species undetermined M) is not considered to be incorporated into ontogeny of *Housia ovata*. The specimen is similar to the anaprotaspides that are questionably assigned to *Aphelaspis*? *anyta* (see Pl. II-36, Figs. 1, 6, 8, 10).

Specimen CMC-P 43418d (Pl. II-19, Figs. 20-22) has a posterior cranidial border which strongly curves ventrally and extends further beyond the protopygidium in the posterior view. This feature better agrees with features of *Drabia typica* (Pl. II-19) which also occurs in the *Elvinia* Zone of the Deadwood Formation in South Dakota.

Specimen CMC-P 43418g (Pl. II-18, Figs. 20-22) has its maximum width of axis farther forwards than the metaprotaspides of *Housia ovata* (Pl. II-17, Figs. 9-19), and a more rectangular shield. These features seem to be best carried over from specimen CMC-P 43418a (Pl. II-18, Figs. 17-19). Both are assigned to the ontogeny of *Housia* sp. A, since each is otherwise greatly similar to the equivalent protaspid stages of *Housia ovata*.

A transitory pygidium (CMC-P 43418t, Hu, 1980, pl. 45, fig. 20) is incorrectly associated because it has pleural furrows that reach the margin and the axis does not reach the posterior margin.

57

Description of Protaspides.

Anaprotaspid stage (CMC-P 43418b, c, Pl. II-17, Figs. 1-8). Shield subovoid in outline with straight anterior margin; 0.313 mm (avg.) long and 0.352 mm (avg.) wide. Axis spindle-shaped and with low convexity, with its maximum width being 35% of shield width; anterior and posterior ends relatively rapidly taper; axial furrows shallow anteriorly without distinct anterior pits. Lp with independent convexity.

Metaprotaspid stage (CMC-P 43418e, f, g, h, Pl. II-17, Figs. 9-19). Shield elliptical in outline; sagittal length ranges from 0.538 to 0.638 mm; maximum transverse width from 0.464 to 0.570 mm. Maximum width of axis lies at S1 occupying 37% (avg.) of shield width. Three pairs of glabellar furrows much shallower than axial furrows and shallow adaxially. Row of pits develop on axial furrows and posterior cranidial marginal border furrows. Posterior cranidial border brim-like and straight; its distal portion ventrally extends beyond protopygidium in larger specimens (e.g., CMC-P 43418f, Pl. II-17, Figs. 17-19). Protopygidium with two to three axial rings; pleural furrows distinctly impressed only in anteriormost pygidial pleurae, occupying from 16% to 30% of sagittal shield length. Surface covered with fingerprint-like microsculpture.

Housia vacuna (Walcott, 1890)
Pl. II-18, Figs. 1-16

1890 *Ptychoparia vacuna* Walcott, p. 275, pl. 21, figs. 8, 12.
1951 *Housia vacuna*, Wilson, p. 643-644, pl. 93, figs. 5-13.
1952 *Housia varro* (Walcott), Bell *et al.*, p. 183-184, pl. 30, figs. 3a-d.
1956 *Housia vacuna*, Deland and Shaw, p. 555, pl. 66, fig. 14.
1964 *Housia canadensis*, Lochman, p. 46, pl. 12, figs 16-29.
1965 *Housia vacuna*, Grant, p. 117, pl. 10, figs. 2, 5.
1970b *Housia canadensis*, Hu, p. 254-258, pl. 27, figs. 1-33, pl. 28, figs. 24, 26, 28-31, text-fig. 1, 2.
1986 *Housia vacuna*, Westrop, p. 58-59, pl. 26, figs. 1-11.
1987 *Housia vacuna*, Hart et al., fig. 3-C.
1989 *Housia vacuna* Hohensee and Stitt, p. 873, figs. 5.16-5.20.

Diagnosis. A species of *Housia* with narrower (tr.) pygidium and smooth frontal area. **Anaprotaspis.** Shield circular. Axis spindle-shaped. **Metaprotaspis.** Shield subrectangular. Axis narrow and forward-tapering and with slightly forward-expanding L4.

Stratigraphic and Geographic Distributions. This species occurs in the *Elvinia* Zone (upper Steptoean of Upper Cambrian) and has been reported from the Orr Formation in Utah, Gatesburg Formation in Pennsylvania, Open Door Limestone, Snow Range Formation, and Dry Creek Shale in Wyoming, Deadwood Formation in Montana, Bison Creek Formation in Alberta, and Collier Shale in Arkansas.

Occurrence of Materials Described Herein. *Elvinia* zone of Dry Creek Shale (not Flathead Formation, see Hohensee and Stitt, 1989, p. 866). Big Horn Mountains, north-central Wyoming (locality 11 in Text-fig. I-2).

Association of Protaspides. All the specimens, including the larval ones, are preserved as flattened moulds in greenish shale, so that the features of the protaspid specimens (CMC-P 39744j and k, Pl. II-18, Figs. 1-6) are not sufficiently detailed for comparative study. However, the overall outline and axial width of specimen CMC-P 39744j (Pl. II-

58

18, Figs. 1-4) are similar to those of an anaprotaspis of *Housia ovata* (CMC-P 43418b, c, Pl. II-17, Figs. 1-8), even though the former with 0.242 mm in sagittal length is smaller. The specimen CMC-P 39744k (Pl. II-18, Figs. 5, 6), although more poorly preserved, has a narrower axis with bilobed L3/L2/L1 (see Hu, 1970b, pl. 27, fig, 12) compared to metaprotaspides of *H. ovata* (Pl. II-17, Figs. 9-19). These differences are attributed to ontogenetic deviation of morphologies between the two species. The deviation is even greater in early meraspid stages; meraspid cranidium (CMC-P 39744h, Pl. II-18, Fig. 7) differs from those of *H. ovata* (CMC-P 43418j and 1, Pl. II-17, Figs. 20, 21) in having less distinct axial furrows and a more semi-circular outline.

Description of Protaspides

Anaprotaspid stage (CMC-P 39744j, Pl. II-18, Figs. 1-4). Shield circular in outline; 0.242 mm in transverse width and sagittal length. Axis spindle-shaped. Anterior pits very shallow.

Metaprotaspid stage (CMC-P 39744k, Pl. II-18, Figs. 5, 6). Shield elliptical in outline; 0.458 mm wide and 0.483 mm long. Axial furrows weakly developed and nearly parallel-sided.

Protaspides of *Housia* species and Their Taxonomic Implications. Protaspid morphologies of *Housia* and *Aphelaspis* species strongly support that the Aphelaspidinae cannot be placed in the same family together with the Housiinae. The *Housia* protaspides are easily distinguished by the possession of a spindle-shaped wide axis (e.g., Pl. II-17, Figs. 9, 13, 16) from the *Aphelaspis* protaspides which have a narrower axis with a strongly forward-expanding L4 and slightly forward-expanding L3/L2/L1 (e.g., Pl. II-34, Figs. 1, 4, 8, 11).

<center>?Subfamily PTEROCEPHALIINAE Kobayashi, 1935</center>

Remarks. This taxon comprises *Pterocephalia* Roemer, 1849, *Cernuolimbus* Palmer, 1960, *Sigmocheilus* Palmer, 1960, and *Strigambitus* Palmer, 1965b, *Camaraspis* Ulrich and Resser *in* Walcott, 1924, and questionably *Pulchricapitus* Kurtz, 1975.

<center>Genus PULCHRICAPITUS Kurtz, 1975</center>

Remarks. The suprageneric position of *Pulchricapitus* has not been clarified yet. Westrop (1986, p. 58) noted cranidial similarities with such elviniines as *Elvinia* and *Elburgia*, *Drabia* (a phylacterid), and *Camaraspis* (a unquestionable Pterocephaliinae, Westrop, 1986, p. 58, Hohensee and Stitt, 1989, p. 874). A closer affinity to the Pterocephaliinae than to the Elviniidae was suggested by Hohensee and Stitt (1989, p. 874) who described a pygidium associated with *Pulchricapitus fetosus* (fig. 5.11) and noticed its similarities with the pygidium of *Camaraspis convexa* (Hu, 1979, pl. 9, figs. 30-33). So far, three species of *Pulchricapitus* have been reported. *P. davisi*, *P. parva*, and *P. fetosus*.

Cranidia of these three species are similar to those of *Phylacterus* (see, Westrop, 1986, pl. 43, figs. 1, 4, 5, 7-12) and *Elyaspis* (Kurtz, 1975, pl. 1, fig, 2) in all having, amongst others, a triangular anterior border. The inclusion of *Pulchricapitus* in the Phylacteridae, however, seems implausible since the axial furrows of *Pulchricapitus* shallow out forwards, and its pygidium does not have a steeply down-sloping pleural field. Nonetheless the close taxonomic affinity of *Pulchricapitus* to the Phylacteridae seems plausible.

<center>59</center>

Hu (1980, p. 376) suggested that *Pulchricapitus* might have been derived from a crepicephalid such as *Coosina* or a blountiid such as *Wilsonella*. The smaller cranidia and pygidia of *Pulchricapitus* (e.g., CMC-P 43416b and k, Pl. II-18, Figs. 27, 29; Hohensee and Stitt, 1989, figs. 5.10, 5.11) are similar to those of *Wilsonella pennsylvanica* (Hu, 1968, pl. 5, figs. 2). Holaspid cranidia of *Coosina* (Lochman *in* Moore, 1959, fig. 230.1a) and *Wilsonella* (Hu, 1968, pl. 5, figs. 7, 8) are too different to make it plausible to relate them to *Pulchricapitus*.

<div align="center">

***Pulchricapitus davisi* Kurtz, 1975**
Pl. II-18, Figs. 23-30, Text-fig. V-3.5
</div>

1975 *Pulchricapitus davisi*, Kurtz, p. 1038, pl. 2, figs. 24-26.
1977 *Reaganaspis parva*, Stitt, p. 48, pl. 1, figs. 8, 9.
1980 *Pulchricapitus davisi*, Hu [part], p. 374-376, pl. 43, figs. 15-27, 29-32 [only].
1986 *Pulchricapitus davisi*, Westrop, p. 58, pl. 27, fig. 15.

Diagnosis. see Westrop (1986, p. 58)'s generic diagnosis for holaspid diagnosis.

Metaprotaspis. Shield oval in outline. Axis forward-expanding with more strongly expanding L4. Glabellar furrows shallower than axial furrows. Protopygidium smaller-sized, with two axial rings.

Remarks. Hohensee and Stitt (1989, p. 874) correctly pointed out that the assignment of a pygidium to this species by Hu (1980, pl. 43, fig. 28) was wrong. A transitory pygidium (Pl. II-18, Fig. 29) found in the sample which contains a meraspid cranidium CMC-P 43416k (Hu, 1980, pl. 43, fig. 25) is very similar to the transitory pygidium of *Pulchricapitus fetosus* (Hohensee and Stitt, 1989, figs. 5.10, 5.11). These pygidia are similar to those of *Housia* (e.g., Pl. II-17, Fig. 24), indicating the taxonomic affinity of *Pulchricapitus* to the Housiinae.

Stratigraphic and Geographic Distributions. This species occurs in the *Elvinia* Zone (upper Steptoean of Upper Cambrian) and has been described from the Davis Formation in Missouri, Reagan Sandstone in Oklahoma, Deadwood Formation in South Dakota, and Lyell Formation in Alberta.

Occurrence of Materials Described Herein. *Elvinia* Zone of Deadwood Formation; Galena section, about 4 miles southeast of Deadwood city, along the Black Hills, South Dakota (locality 5C in Text-fig. I-2).

Association of Protaspides. Hu (1980) inadvertently mislabeled the figures of plate 43. He incorrectly labeled from figure 21 thereafter, because he did not include CMC-P 43416g which is illustrated in figure 21 and was mislabeled as CMC-P 43416i. There is no specimen labeled as CMC-P 43416s.

Figure 21 should have been labeled as CMC-P 43416g (Pl. II-18, Fig. 30), figure 28 as CMC-P 43416o, and figure 30 as CMC-P 43416p.

The association of specimen CMC-P 43416 (Pl. II-18, Figs. 31-33) is questionable, since it has very shallow (nearly imperceptible) axial furrows and an elliptical outline. The specimen is slightly shorter than specimen CMC-P 43416a (Pl. II-18, Figs. 23-26) in a sagittal length by 0.036 mm. Such size difference is considered to fall within a single instar, so that the morphologic difference from CMC-P 43416a must be regarded as being taxonomic rather than ontogenetic. Specimen CMC-P 39741b (Pl. II-10, Figs. 19-21), which was incorrectly assigned to *Welleraspis lochmanae*, is indistinguishable from CMC-P 43416. The former is assigned to Catillicephalidae sp. B, which seems to be

<div align="center">60</div>

applied to the latter specimen although the former specimen occurs in the *Crepicephalus* Zone.

Description of Protaspides

Metaprotaspis (CMC-P 43416a, Pl. II-18, Figs. 23-26). Shield oval in outline. 0.361 mm wide and 0.395 mm long. Axis forward-expanding; glabellar furrows shallow sagittally; width of L3 31% of shield width. No distinct anterior pits at antero-lateral corner of L4. Posterior cranidial marginal border directed diagonally posteriorly. Protopygidium with two axial rings and occupies 15% of shield length.

Protaspides of *Pulchricapitus davisi* and Their Taxonomic Implications. The metaprotaspis of *Pulchricapitus davisi* (Pl. II-18, Figs. 23-26) most conspicuously differs from those of *Housia* in possessing a forward-expanding axis; the protaspid morphotype C has a forward-tapering spindle-shaped axis. Compared to aphelaspidine and housiine protaspides, however, the *Pulchricapitus* metaprotaspis is much more similar to the latter group, except for the forward-expanding glabella. The metaprotaspis of *P. davisi* differs from those of *Aphelaspis* in lacking, among others, an eye ridge, a pitted prosopon, tubercle pairs on fixigenae, and a distinct posterior cranidial border that turns forwards distally. Thus, it seems more reasonable that *Pulchricapitus* belongs to a family that includes the housiine trilobites. If *Pulchricapitus* is really a member of the Pterocephaliinae, the protaspid comparison supports the separation of the Aphelaspidinae from the Housiinae and Pterocephaliinae, suggested by Fortey and Chatterton (1988, p. 206-209).

Hu (1980, p. 376) mentioned protaspid similarities among *Pulchricapitus*, *Aphelaspis*, *Parabolinoides* and *Glyphaspis*. SEM photographs of the protaspid specimens, however, reveal that the similarities appear to be shared by many other taxa re-described in this study.

Hu (1980, p. 371) suggested derivation of *Pulchricapitus* from *Wilsonella* of the Blountiinae, which cannot be proved using protaspid morphologies, since no protaspid materials are available for the latter genus. Protaspides of *Blountia bristolensis* (Pl. II-6, II-7), which was previously considered a member of the Blountiinae, but now belongs to the Kingstoniidae, share little similarities with those of *Pulchricapitus*.

Family **PHYLACTERIDAE** Ludvigsen and Westrop *in* Ludvigsen *et al.*, 1989

Remarks. Ludvigsen and Westrop (*in* Ludvigsen *et al.*, 1989, p. 55) included four genera in this family, *Phylacterus* Raymond, 1924, *Westonaspis* Rasetti, 1945, *Cliffia* Wilson, 1951, and *Drabia* Wilson, 1951. Pratt (1992, p. 88) added *Aphelotoxon* to this family. Hohensee and Stitt (1989, p. 864) erected Cliffiidae as a new family to accommodate the same genera. The Cliffiidae is an objective synonym of the Phylacteridae by reason of the priority of timing of publication.

Hohensee and Stitt (1989) noted a probable inclusion of monotypic *Elyaspis* in this family. The most characteristic features of *Elyaspis* (Kurtz, 1975, p. 1038, pl. 1, fig. 2, pl. 4, figs. 10-12) are a divergent anterior facial suture and a straight diagonal posterior facial suture; most other phylacterid genera have a convergent anterior suture and a gently curved posterior suture. *Elyaspis* is similar to *Phylacterus* (e.g., Ludvigsen *et al.*, 1989, pl. 43, fig. 10) in having a triangular anterior border with a distinct straight border furrow and a wide (tr.) anterior fixigenal area. However, *Phylacterus* has a quadrate glabella whereas *Elyaspis* has a forward-tapering glabella. The forward-tapering glabella is

61

similar to that of *Cliffia* (Westrop, 1986, pl. 27, fig. 1) and *Drabia* (Westrop, 1986, pl. 27, fig. 7) which however have a truncated, not rounded as seen in *Elyaspis*, anterior margin. The overall trapezoidal cranidial outline and smaller glabella along with above-mentioned similarities with other phylacterid genera indicate that *Elyaspis* is a valid genus of the Phylacteridae.

Hu (1980, p. 377) assigned these genera to the Acrocephalitinae of the Solenopleuridae. The acrocephalitine cranidia have a trapezoidal outline, a forward-tapering glabella, an acute anterior border, an eye ridge, a small palpebral lobe situated at mid-cranidial length (see *Acrocephalites*, Moore, 1959, fig. 204.11). These features suggest a certain degree of evolutionary connection with the Phylacteridae, even though all the acrocephalitines occur outside the Laurentia. The morphologic similarities shared by *Acrocephalites* and *Cliffia* were also noticed by Wilson (1951, p. 632); in fact, *Cliffia* had been previously identified as *Acrocephalites*. The cranidia of another two relatively well-known acrocephalitine genera, *Pesaia* and *Paracrocephalites* (Moore, 1959, figs. 204.7, 204.15) bear some resemblance with phylacterid genera in sharing a trapezoidal outline, a forward-tapering glabella with a straight lateral margin. In spite of absence of information on pygidia of the acrocephalitines, a close relationship with the phylacterids seem plausible.

Genus **DRABIA** Wilson, 1951

Remarks. *Drabia* is morphologically separated from *Cliffia* by having a wider (tr.) anterior fixigenal area and a more abaxially located palpebral lobe (compare Westrop, 1986, pl. 27, figs. 1 and 7). Ludvigsen and Westrop (1983, p. 21-22) assigned *Drabia* to the subfamily Elviniinae mainly upon the basis of cranidial similarities with *Dytremacephalus* (Palmer, 1965b, pl. 18, figs. 14, 18); the elviniid membership of *Dytremacephalus* is questioned by its protaspid morphologies which suggest a closer relationship with the Aphelaspidinae. Westrop (1986, p. 86) placed more emphasis on pygidial similarities with such phylacterid genera as *Aphelotoxon* and *Cliffia*, thus suggesting that *Drabia* belongs to the same suprageneric taxon with *Aphelotoxon* and *Cliffia*.

Drabia typica (Hu, 1979)
Pl. II-19, Figs. 1-36, Text-fig. V-3.3
1979 *Cliffia typica* Hu [part], p. 57-61, pl. 9, figs. 1, 3-29 [only].
1980 *Housia ovata*, Hu [part], p. 381-386, pl. 45, fig. 5 [only].
1989 *Drabia typica* Hohensee and Stitt, p. 866-867, figs 3.24-3.26.

Diagnosis. A species of *Drabia* with a relatively straight anterior border furrow, shallower glabellar furrows, and narrower (tr.) anterior fixigenal area. **Anaprotaspis.** Shield subcircular and highly convex. **Early metaprotaspis.** Shield subquadrate. Axial furrows very shallow. Occipital ring as transverse node and delimited by posterior cranidial marginal furrow. **Late metaprotaspis.** Shield suboval to oval in outline. Axis forward-tapering. Posterior fixigenal spines extend ventrally beyond protopygidium. Protopygidium medium-sized with three to four axial rings.

Stratigraphic and Geographic Distributions. This species occurs in the *Elvinia* Zone (uppermost Steptoean of Upper Cambrian) and has been reported from the Deadwood Formation in South Dakota and Collier Shale in Arkansas.

62

Occurrence of Materials Described Herein. *Elvinia* Zone of Deadwood Formation; Boxelder section, near Nemo, about 8 miles northwest of Rapid City, South Dakota (locality 5D in Text-fig. I-2).

Remarks. This species was assigned to *Cliffia* by Hu (1979). However, it has a wider (tr.) anterior fixigenal area and a shorter (sag.) glabella, which is in more agreement with the concept of *Drabia*. Thus, I agree with Hohensee and Stitt (1989) who re-assigned it to *Drabia*.

Association of Protaspides. Due to poor preservation, it is very difficult to judge whether the small protaspid specimen CMC-P 43373b (Pl. II-19, Fig. 37) is correctly associated; it is named species undetermined N. Specimen CMC-P 43418d (Pl. II-19, Figs. 20-22), which was previously assigned to *Housia ovata*, has a strongly ventrally curved posterior fixigenal area which extends beyond the protopygidium in posterior view and a posterior cranidial border which directed more posteriorly. These features distinguish this specimen from metaprotaspides of *Housia ovata* (Pl. II-17, Figs. 9-19), which otherwise are very similar to those of *Drabia typica*.

Description of Protaspides.

Anaprotaspid stage (CMC-P 43373a, Pl. II-19, Figs. 1-4). Shield rounded in outline and highly convex; 0.237 mm long sagittally and 0. 252 mm wide; posterior margin broadly and slightly indented forwards or nearly straight; shield gently slopes forwards and posterior portion very steeply slopes ventrally. Axial furrows imperceptible. Fingerprint-like microsculpture covers exoskeletal surface.

Early metaprotaspid stage (CMC-P 43373c, d, Pl. II-19, Figs. 5-10). Shield 0.318 (avg.) mm in maximum width and 0.325 (avg.) mm in sagittal length; posterior margin entire. Axis spindle-shaped and slightly convex; axial furrows weakly impressed and shallow anteriorly to disappear; maximum width at mid-shield length 38% (avg.) of shield width. Occipital ring more distinctly defined by posterior cranidial marginal furrow. Protopygidial area behind occipital ring steeply slopes; sagittal length of protopygidium 11% (avg.) of shield length. Fixigenal area steeply inclined ventrally.

Late metaprotaspid stage (CMC-P 43373e, f, g, h, i, j, and 43418d, Pl. II-19, Figs. 11-31). Shield oval in outline; 0.465 (avg.) mm long sagittally and 0.416 (avg.) mm wide. Maximum axial width at about mid-shield length takes 39% (avg.) of shield width; axial furrows moderately deep. Posterior cranidial marginal furrows distinctly impressed, and diagonal in dorsal view and strongly curved ventrally in posterior view. Posterior fixigenal area strongly curved ventrally and extends beyond protopygidium in posterior view. Protopygidium subtriangular, occupying 20 % (avg.) of sagittal shield length; two to three segments recognized; anteriormost segment with distinct pleural furrow; deep pit develops at antero-lateral corner of first axial ring.

Protaspides of *Drabia typica* and Their Taxonomic Implications. Protaspides of *Drabia typica* (Pl. II-19, Figs. 1-31) are similar to those of *Housia ovata* (Pl. II-17, Figs. 1-19) in having a highly convex shield, absence of anterior pits (or axial furrows shallowing anteriorly), comparatively shallow and narrow axial furrows, an elliptical (or oval) shield, and a spindle-shaped axis. Anaprotaspides of *D. typica* (Pl. II-19, Figs. 1-4) differ from those of *H. ovata* (Pl. II-17, Figs. 1-8) in having a more quadrate shield, much less distinct axial furrows and a wider axis. The metaprotaspides (Pl. II-19, Figs. 5-31) differ in having a posteriorly curved posterior cranidial marginal border (rather straight in *H. ovata*), and lacking glabellar furrows, pits along axial furrows, and fingerprint-like

63

microsculpture on the exoskeletal surface. The protaspid morphologies suggest that *Drabia* and *Housia* have a close taxonomic affinity. Similarities of meraspid cranidia (see Pl. II-17, Fig. 20 and Pl. II-19, Fig. 35) further support the inclusion of *Drabia* and *Housia* within the same group.

The elviniid affinity of *Drabia* is denied by dissimilarities of protaspid morphologies of *Drabia* from those of *Elvinia roemeri*. Compared to *E. roemeri* (Pl. II-38, Figs. 1-15), protaspides of *Drabia typica* (Pl. II-19, Figs. 1-31) lack an eye ridge, a narrow concave border, and a sagittally long area behind the occipital ring, and have a much more convex shield, and a wider forward-tapering axis.

Genus APHELOTOXON Palmer, 1965b

Remarks. When erecting *Aphelotoxon*, Palmer (1965b, p. 79) mentioned morphologic similarities with Marjumian genera such as *Dresbachia*, and *Menomonia* which includes *Densonella* as a junior synonym (see Pratt, 1992, p. 77) and with Lower Ordovician *Clelandia*. The cranidium of *Menomonia semele* (Pratt, 1992, pl. 29, fig. 1) is best compared with that of *Cliffia latagenae* (Westrop, 1986, pl. 27, fig. 1); both have an elongated (tr.) posterior fixigenal area which is much longer (tr.) than the anterior fixigenal area and a forward-tapering glabella with a truncated anterior and a straight lateral margin. The former differs in having a posteriorly incurved anterior border furrow and a shorter (sag.) preglabellar field. Except for these similarities, the menomoniids greatly differ from the phylacterids with respect to cranidial and pygidial features.

Hu (1980, p. 377) questioned the similarities with the Marjuman genera mentioned by Palmer, and assigned *Aphelotoxon* to the subfamily Acrocephalitinae of the Solenopleuridae along with *Cliffia*, *Ponumia*, *Elyaspis*, and *Clelandia* (see discussion above for the possible relationship between Acrocephalitinae and Phylacteridae based on holaspid cranidial features)

Aphelotoxon triangulata Hu, 1980
Pl. II-20, Figs. 1-10, Text-fig. V-3.1

1980 *Aphelotoxon triangulata* Hu [part], p. 377-381, pl. 44, figs. 6, 11-31 [only].
Diagnosis. see Hu (1980, p. 377) for holaspid diagnosis. **Metaprotaspis.** Shield suboval in outline. Axis narrower and slightly forward-tapering; axial furrows very shallow. Protopygidium small-sized with three axial rings.
Occurrence of Materials Described Herein. *Elvinia* Zone (upper Steptoean) of the Deadwood Formation. South side of Dark Canyon, about 4 miles west of Rapid City, South Dakota (locality 5E in Text-fig. I-2).
Association of Protaspides. Specimen CMC-P 43417e (Pl. II-20, Figs. 1-4) is the only protaspis associated with *Aphelotoxon triangulata*. Its cranidial features are continuous into the early meraspid cranidia (e.g., CMC-P 43417k, Pl. II-20, Fig. 5).

Specimens CMC-P 43417c and 43417f (Pl. II-20, Figs. 11-18) comprise a single ontogeny. They differ from the metaprotaspis of *Aphelotoxon triangulata* in having a subrectangular shield and a narrower (tr.) fixigenal area. Apart from these differences, the two specimens exhibit the features of the *A. triangulata* metaprotaspis. They are identified as Phylacteridae sp. A

Specimens 43417, 43417b, d, h, i, and g constitute another ontogenetic sequence, which is described as Phylacteridae sp. B (see below).

64

Specimen CMC-P 43417a (Pl. II-20, Figs. 44-46) shows few features on its dorsal surface. Nevertheless, the low convexity of its shield prevents me from associating it with any phylacterid species; it is named species undetermined O.

Description of Protaspides

Metaprotaspid stage (CMC-P 43417e, Pl. II-20, Figs. 1-4). Shield oval in outline; 0.492 mm long and 0.493 mm wide. Axis spindle-shaped; maximum width of axis 36% of shield width; axial furrows shallow anteriorly. Fixigenal area wide (tr.) and strongly ventrally oriented. Protopygidium occupies 20% of sagittal shield length. Two or three protopygidial axial rings present; anteriormost one with corresponding pleura with moderately-impressed pleural furrow.

Protaspides of _Aphelotoxon triangulata_ and Their Taxonomic Implications. Palmer (1965b, p. 79) mentioned morphologic similarities of _Aphelotoxon_ with some menomoniids such as _Dresbachia, Menomonia_, and _Densonella_. Protaspides of _Bolaspidella housensis_ (a menomoniid, Robison, 1964, pl. 89, figs. 6, 7) differ from metaprotaspis of _Aphelotoxon triangulata_ (Pl. II-20, Figs. 1-4) in having a narrower (tr.) axis, a very narrow (sag. and exsag.) protopygidium, an indented posterior shield margin, and a pair of posterior fixigenal spines. These features are not evident in the metaprotaspis of _A. triangulata_ nor in the protaspides of any phylacterid species described herein. The relationship of the Phylacteridae including _Aphelotoxon_ with the Menomoniidae is not supported by the protaspid morphologies.

Genus PONUMIA Hu, 1970b

Remarks. When erecting _Ponumia_ as a new genus, Hu (1970b) noted similarities with _Aphelotoxon_ and _Cliffia_. The latter genera have a transversely shorter cranidial outline and glabella, two or three pairs of distinct glabellar furrows, and a rather straight lateral glabellar margin.

Hohensee and Stitt (1989, p. 866) synonymized _Ponumia_ under _Aphelotoxon_ based on their cranidial similarities. However, the cranidia of _Aphelotoxon_ (e.g., _A. lumaleasa_, Hohensee and Stitt, 1989, fig. 3.12) have a forward-tapering glabella with a truncated anterior and straight lateral margin with two or three pairs of glabellar furrows and a distinctly-impressed anterior border furrow. These features are not evident in the cranidia of _Ponumia obscura_ (e.g., Pl. II-21, Figs. 25, 26). In addition, the re-illustrated pygidium of _P. obscura_ (Pl. II-21, Figs. 27, 28) reveals that it has an indented posterior margin which is also arched dorsally, and a straight lateral margin which meets the anterior margin at a sharp angle. This pygidial architecture does not agree with that of _Aphelotoxon_ which has a rounded entire pygidial margin (Hohensee and Stitt, 1989, fig. 3.14). Cranidial features discernible from _Aphelotoxon_ include a less distinct anterior border furrow and the lack of glabellar furrows, and a parabolic glabellar outline. Thus, _Ponumia_ is considered as a valid separate genus of the Phylacteridae. The inclusion of _Ponumia_ in the Phylacteridae is supported by its rather triangular cranidial outline and an anteriorly-located palpebral lobe. A laterally-widening posterior cranidial border seems to be shared by all these phylacterid taxa, including _Ponumia_.

The cranidial architecture of _Ponumia_ (see Pl. II-21, Figs. 25, 26) is readily comparable to that of Lower Ordovician _Clelandia_ (Ross, 1951, pl. 29, fig. 1; Westrop, 1986, pl. 41, figs. 20-30) in both having a conical glabella, no distinct anterior cranidial border furrow, and a triangular outline. _Clelandia_ differs from _Ponumia_ in having yoked

65

free cheeks, which have not been described in any phylacterids, two pairs of glabellar furrows, and a narrower (tr.) posterior fixigenal area. The pygidia of *Clelandia* (see Pl. III-39, Fig. 12) are similar to that of *Ponumia obscura* (Pl. II-21, Figs. 27, 28) except for the former developing short marginal spines. The features displayed by these two taxa are not common to the phylacterids.

<div align="center">

Ponumia obscura (Lochman, 1964)

Pl. II-21, Figs. 1-28, Text-fig. V-3.6

</div>

1964 *Bynumiella*? *obscura*, Lochman, p. 46, pl. 9, figs. 21-24.

1970b *Ponumia obscura* (Lochman), Hu [part], p. 259-263, pl. 28, figs. 6-25, 27, 32-35 [only].

1989 *Aphelotoxon lumaleasa* Hohensee and Stitt [part], pl. 3, fig. 11 [only].

Diagnosis. see (Hu, 1970b, p. 258)'s generic diagnosis for holaspid diagnosis.

Anaprotaspis. Shield circular. Axis spindle-shaped, reaching anterior and posterior margins. **Metaprotaspis.** Shield oval in outline. Axis forward-tapering with parallel-sided L4. Protopygidium small-sized with two axial rings.

Stratigraphic and Geographic Distributions. This species occurs in the *Elvinia* Zone (upper Steptoean of Upper Cambrian) and has been described from Deadwood Formation in Montana, Dry Creek Shale in Wyoming, and Collier Shale in Arkansas.

Occurrence of Materials Described Herein. *Elvinia* Zone of Dry Creek Shale. Big Horn Mountains in north-central Wyoming (locality 11 in Text-fig. I-2).

Remarks. One of the cranidia identified as *Aphelotoxon lumaleasa* by Hohensee and Stitt (1989, pl. 3, fig. 11) is indistinguishable from the cranidium illustrated herein (Pl. II-21, Figs. 25, 26). Both cranidia are distinguishable from the cranidia of *A. lumaleasa* (Hohensee and Stitt, pl. 3, figs. 12, 13) by having a less triangular glabella, curved axial furrows (rather straight or even concave axial furrows in *Aphelotoxon*) and a less distinct anterior border furrow, and lacking glabellar furrows.

Association of Protaspides. All the protaspid specimens are preserved as flattened moulds in greenish shale. Since the small anaprotaspid specimens (CMC-P 39745 and 39745a, Pl. II-21, Figs. 29, 30) reveal few morphologic features due to poor preservation, it is difficult to judge whether they are correctly assigned to this species; both are named species undetermined P. Specimen CMC-P 39745a has a broad crescentic ridge developed along the anterior margin. If it is not due to preservation, the ridge is similar to that of the *Olenellus* meraspid cranidia (Pl. II-1, Figs. 1-3).

The other smaller specimens (CMC-P 39745b, c, d, Pl. II-21, Figs. 31-36) have an indented posterior margin, and a spindle-shaped axis with bilobed L3/L2/L1 and a subtrapezoidal L4. These features are also found in CMC-P 43418 (Pl. II-17, Figs. 30-33) which was previously assigned to *Housia ovata*. The association of these small specimens is considered questionable, unless a metamorphosis into the larger anaprotaspides is generalized for ptychopariid trilobites. These three specimens are assigned ?Phylacteridae sp. A, because of their similarities to some phylacterid protaspides. Other specimens are considered to be assigned correctly to this species, since their morphologies gradually transform as their size increases.

Description of Protaspides

Anaprotaspid stage (CMC-P 39745i, j, k, e, g, Pl. II-21, Figs. 1-10). Shield slightly elongated (tr.) circular in outline; sagittal length ranges from 0.315 to 0. 362 mm (0.337

<div align="center">66</div>

in average) and transverse width from 0.295 to 0.358 mm (0.324 in average). Axis spindle-shaped; axial furrows shallow anteriorly; maximum width of axis at mid-shield length 38% of shield width.

Metaprotaspid stage (CMC-P 39745f, m, o, 1, p, Pl. II-21, Figs. 11-20). Shield oval in outline; sagittal length ranges from 0.399 to 0.486 mm (0.440 in average) and transverse width from 0.344 to 0.420 mm (0.386 in average). Maximum width of axis takes 37% of shield width. Posterior cranidial border transversely straight. Protopygidium with one or two axial rings; sagittal length of protopygidium ranges from 10% to 25% of shield length.

Protaspides of *Ponumia obscura* and Their Taxonomic Implications. Protaspides of *Ponumia obscura* (Pl. II-21, Figs. 1-20) strongly suggest that *Ponumia* is a member of the Phylacteridae. They, although flattened, exhibit such phylacterid protaspid features as an oval-shaped shield, a spindle-shaped axis, axial furrows that shallow anteriorly, and a relatively straight posterior cranidial border furrow.

Phylacteridae sp. B
Pl. II-20, Figs. 19-43

Description of Protaspides
Anaprotaspid stage (CMC-P 43417, CMC-P 43417e*, Pl. II-20, Figs. 19-23). Shield rounded rectangular in outline; 0.228 mm long and 0.231 mm wide. Axis spindle-shaped, occupying 36% of shield width at its maximum. Axial furrows end with shallow anterior pits.

Early metaprotaspid stage (CMC-P 43417b, d, Pl. II-20, Figs. 24-31). Shield 0.309 (avg.) long and 0.314 (avg.) wide. Axis 18% of shield width at mid-shield length. Protopygidial area recognized by presence of posterior cranidial marginal furrow defining posterior margin of occipital ring; posterior cranidial marginal furrow not impressed in pleural region; one axial ring recognizable; sagittal length of protopygidium from 32 to 39% of shield length. Glabellar furrows impressed only along axial furrows as short indentations; three pairs present.

Late metaprotaspid stage (CMC-P 43417g, h, i, Pl. II-20, Figs. 32-43). Shield 0.408 (avg.) mm in sagittal length and 0.374 (avg.) mm in width. Maximum axial width 19% (avg.) of shield width. Posterior cranidial border directed diagonally posteriorly. Protopygidium with at least two axial rings; anteromost ring with corresponding interpleural furrow; sagittal length of protopygidium takes 40% (avg.) of shield length. Exoskeletal surface covered with fine granules.

Protaspides of Phylacterid sp. B and Their Taxonomic Implications. Protaspides of Phylacteridae sp. B is characterized by a rounded rectangular shield covered with fine granules, a wider axis, and glabellar furrows. They are more similar to *Ponumia obscura* and *Aphelotoxon triangulata* than to *Drabia typica* in lacking a posterior fixigenal area which curves strongly ventrally and extends beyond the protopygidium. It is not completely unreasonable that this species could be another species of *Aphelotoxon*. Due to absence of holaspid materials referable to a species other than *Aphelotoxon triangularia* from the sampling locality, this species is left in open nomenclature.

Protaspides of the Phylacterid species and Their Taxonomic Implications.
Protaspides of *Ponumia obscura* (Pl. II-21, Figs. 1-20) *Drabia typica* (Pl. II-19, Figs. 1-31), *Aphelotoxon triangulata* (Pl. II-20, Figs. 1-4) and Phylacteridae sp. B (Pl. II-20,

Figs. 19-43) are so similar with one another that without any doubt, these species, thus the genera, belong to the same family. They share a spindle-shaped broad axis defined by shallow axial furrows which shallow out anteriorly, a convex shield, and a strongly ventrally curved posterior fixigenal area. The great resemblance with protaspides of *Housia* (see Pl. II-17, Figs. 1-19) and the phylacterids suggest a close evolutionary relationship between Housiinae and Phylacteridae.

?Family **PHYLACTERIDAE** Ludvigsen and Westrop *in* Ludvigsen *et al.*, 1989
Genus **PARANUMIA** Hu, 1973

Remarks. This monotypic genus was erected by Hu (1973). The type species, *Paranumia triangularia* (Hu, 1973, pl. 1, figs. 1-23), has a triangular cranidial outline, an elongated glabella with a truncated anterior and straight lateral margin and three pairs of glabellar furrows, a very short (sag.) anterior cranidial border, an imperceptible palpebral lobe, an anterior and posterior facial suture that are continuous with each other without any major curvature, and a subtriangular pygidium with a steep pleural field and a wider (tr.) axis. Each feature is shared with different phylacterid genus. The cranidial outline is very similar to *Ponumia* (Pl. II-21, Figs. 25, 26), the glabella to *Phylacterus* (Ludvigsen *et al.*, 1989, pl. 43, fig. 7), and the pygidium to *Cliffia* (Westrop, 1986, pl. 27, fig. 5). *Paranumia* exhibits combinations of features characteristic to each phylacterid genus. The most characteristic feature of this genus, not shared with any of the phylacterid genera, is the absence of a preglabellar field. This combination of similarities and dissimilarities prevents the assignment of *Paranumia* to the Phylacteridae with confidence.

Ludvigsen (1982, p. 120-121) claimed that *Paranumia* is a junior synonym of *Missisquoia* and *Paranumia triangularia* is probably a junior synonym of *Missisquoia enigmata*. However, the cranidium of *Paranumia* (Pl. II-22, Fig. 8) lacks a relatively long (sag.) triangular anterior border, deeply incised glabellar furrows, and a waisted glabella with forward-expanding L4 which are typical of *Missisquoia* (see Dean, 1977, pl. 1, figs. 9, 12, 14). The holaspid pygidium of *P. triangularia* (Pl. II-22, Figs. 12, 13) differs from that of *Missisquoia* (see Dean, 1977, pl. 1, fig. 5) in having a steeply sloping pleural field, a wider axis, a subtriangular outline, and axial furrows that shallow out posteriorly. It is certain that *Paranumia* is not a synonym of *Missisquoia*. The smaller pygidium of *P. triangularia* (Pl. II-22, Figs. 14, 15) is very similar to smaller pygidia of *Missisquoia typicalis* illustrated by Dean (1977, pl. 1, figs. 4, 7) in having a wider (tr.) convex axis, a rather flat post-axial area behind the axis, and a relatively narrow marginal border. Morphologic transformation from these pygidia into the larger pygidium typical of *Missisquoia* is more drastic than into the pygidium of *P. triangularia* (Pl. II-22, Figs. 12, 13). Thus the pygidia assigned to *Missisquoia* species by Dean (1977, pl. 1, figs. 3, 4, 7) is most probably referable to a *Paranumia* species.

Fortey (1983, p. 194-196) treated *Paranumia* as a junior synonym of *Lunacrania* Kobayashi, 1955. However, the glabella of *Paranumia* (Pl. II-22, Fig. 8) is clearly forward-tapering whereas that of *Lunacrania spicata* (Fortey, 1983, pl. 25, figs. 7, 8) is forward-expanding. Most, if not all, missisquoiid species have a parallel-sided or slightly forward-expanding glabella defined by deep axial furrows. As a result, *Paranumia* is not a synonym of *Lunacrania*, but a valid separate genus whose most probable taxonomic affinity lies in the Phylacteridae.

68

Paranumia triangularia Hu, 1973
Pl. II-22, Figs. 1-15, Text-fig. V-3.4
1971 *Missisquoia cyclochila* Hu [part], p. 107-109, pl. 20, fig. 6 [only].
1973 *Paranumia triangularia* Hu [part], p. 86-90, pl. 1, figs. 1-10, 14-23 [only].
? 1977 *Missisquoia typicalis* Shaw, Dean, pl. 1, figs. 4, 7.
? 1977 *Missisquoia enigmata* (Kobayashi), Dean, pl. 1, fig. 3.

Diagnosis. see Hu (1973, p. 86)'s generic diagnosis for holaspid diagnosis.
Metaprotaspis. Shield subquadrate. Axis narrow and spindle-shaped. Anterior pits deeper than axial furrows. Posterior cranidial marginal furrow impressed only behind occipital ring. Protopygidium with one axial ring.
Occurrence of Materials Described Herein. Ibexian Series of the Deadwood Formation, Reutes Canyon, Bearlodge Ranch, northeast Wyoming (locality 4B in Text-fig. I-2). Other materials referable to *Paranumia triangularia* have been reported from Survey Peak Formation in Alberta and Mckay Group in British Columbia.
Association of Protaspides. Specimens of *Paranumia triangularia* occur in Lower Ordovician strata (probably *Missisquoia* Zone) of Deadwood Formation in northeast Wyoming. From the same locality, Hu (1971) described an ontogeny of *Missisquoia cyclochila* and *Apoplanias rejectus*. All the specimens assigned to these three species fall within a relatively narrow morphologic variation and occur in red to buff-colored limestone.

All the protaspid specimens of these three species are classified into eight morphologic groupings (see "Association of Protaspides" under *Missisquoia cyclochila* for discussion on the association). Specimen CMC-P 38749f (Pl. II-22, Figs. 1-4), which was assigned to *Missisquoia cyclochila* by Hu (1971), is considered to be a metaprotaspis of *Paranumia triangularia*. It shows the most narrow and distinctively forward-tapering axis and smooth prosopon. An early meraspid cranidium of *P. triangularia* (CMC-P 41556f, Pl. II-22, Fig. 5) shows the same cranidial feature.
Description of Protaspides
Metaprotaspid stage (38749f, Pl. II-22, Figs. 1-4). Shield subrectangular in outline. 0.304 mm long and wide. Axis narrow (tr.) and spindle-shaped; maximum width 33% of shield width; anterior pits moderately deep. Glabellar furrows very shallow and transglabellar. Occipital ring clearly delimited by posterior cranidial marginal furrow which is absent in pleural region. Protopygidium with one axial ring and occupies 15% of shield length. Exoskeletal surface covered with fingerprint-like microsculpture.
Protaspides of *Paranumia triangularia* and Their Taxonomic Implications. The metaprotaspis of *Paranumia triangularia* (Pl. II-22, Figs. 1-4) is most similar to early metaprotaspides of Phylacterid sp. B (Pl. II-20, Figs. 24-31). Both bear a subrectangular shield outline and moderately deep anterior pits. The metaprotaspis of *P. triangularia* differs in having a narrower (tr.) axis and fingerprint-like microsculpture on the surface (granules on the surface of Phylacteridae sp. B). This further supports the taxonomic relationship of *Paranumia* with the Phylacteridae.

Family **PLETHOPELTIDAE** Raymond, 1925
Genus **ARAPAHOIA** Miller, 1936
Remarks. The genus *Arapahoia* has been included in the family Plethopeltidae (e.g.,

69

Palmer and Peel, 1981, p. 33), ever since Miller (1936) erected it as a new genus and noted similarities with *Plethopeltis* Raymond, 1913a. Recently, Westrop (1992, p. 215) questioned this taxonomic assignment because of the pygidial differences displayed by *Arapahoia* and suggested that Arapahoia may be a plesiomorphic norwoodid. The cranidium of *Plethopeltis* (see Ludvigsen *et al.*, 1989, pl. 45, figs. 1, 3, 4) differs from that of *Arapahoia* in having a more steeply directed posterior facial suture without any conspicuous change of curvature which results in a transversely narrow posterior fixigena—the suture of *Arapahoia* runs transversely and then rapidly curves posteriorly, resulting in a transversely wider posterior fixigena (see Stitt, 1998, figs. 8.2-8.4)—, a transversely wider anterior fixigenal area, and a proportionately larger and usually subrectangular glabella—*Arapahoia* has a forward-tapering glabella. The pygidium of *Arapahoia* (Stitt, 1998, figs. 8.7, 8.8) is wider than longer in outline and has a narrower (tr.) axis, compared to that of *Plethopeltis* (Westrop, 1986, pl. 36, figs. 7, 10). The pygidium (Pl. II-23, Fig. 18) found together with protaspid and cranidial materials of *Arapahoia arbucklensis* seems intermediate between these two morphologic end-members. Several *Arapahoia* species from the *Cedaria* Zone of the Marjuman Stage described by Lochman and Duncan (1944, pl. 10, figs. 10, 25, 33) have pygidia that nicely fill the gap between the two end-members. Westrop (1992, p. 215) recognized the presence of distinct pleural furrows on the anteriormost pygidial segment as a distinguishing feature of *Plethopeltis* from *Arapahoia*. The pygidia of most, if not all, *Arapahoia* species have distinctly-impressed pleural furrows (see Lochman and Duncan, 1944, pl. 10, figs. 10, 25, 33). Of more conspicuous significance appears to be the fact that the pygidia of *Plethopeltis* carry the posterior band of pleura as a ridge well into the border, whereas those of *Arapahoia* have a flat band which does not reach the border. Furthermore, the pygidia of *Arapahoia* do not have a distinctly-impressed interpleural furrow (see Resser, 1942, pl. 7, figs. 3, 5, 22). A thoracic segment of *Arapahoia snowensis* (Hu, 1986, pl. 16, fig. 24) appears to have a square-tipped distal end; the line drawing (Hu, 1986, text-fig. 18.L) apparently differs from the photographic illustration with respect to this feature. This thoracic feature was considered to be informative in resolving the taxonomic position of *Arapahoia* by Westrop (1992, p. 251). As a result, the closer taxonomic affinity of *Arapahoia* with *Plethopeltis* is not as unreasonable as Westrop (1992) suggested.

Arapahoia arbucklensis (Stitt, 1971)
Pl. II-23, Figs. 1-23, Text-fig. V-3.2
1971 *Plethopeltis arbucklensis* Stitt, p. 35, pl. 8, figs. 10-15.
1975 *Plethopeltis arbucklensis* Hu, [part], p. 263-268, pl. 3, figs. 3, 4, 6-35, text-figs. 3B-O, [only].

Diagnosis. A species of *Arapahoia* with shorter (sag.) cranidium and no anterior border furrow. Pygidium narrow (tr.); marginal border furrow concave and broad; three axial rings and terminal piece. **Metaprotaspis.** Shield oval in outline and less convex. Glabella spindle-shaped with L4 forward-expanding. Posterior cranidial marginal furrow very shallow. Protopygidium medium-sized with two axial rings.

Remarks. The holaspid cranidium associated with this species (Pl. II-23, Figs. 22, 23) has a forward-tapering glabella with a straight lateral and rather truncated anterior margin, an indistinct anterior border furrow, an anteriorly located—in front of mid-

70

glabellar length—palpebral lobe, a posterior facial suture that stretches transversely and then rapidly curves backwards, a gently inflated preglabellar field, and a laterally-tapering occipital ring with a short medial spine. These features are similar to those of most *Arapahoia* species (see Westrop, 1992, fig. 17.4, Stitt, 1998, fig. 8.3). The most noticeable difference from other *Arapahoia* species is an indistinct anterior border furrow and a relatively shorter (sag.) cranidium and glabella. As a result, this species is transferred to *Arapahoia*. The cranidium has a resemblance with the *Acheilus* species (a questionable kingstoniid, see Ludvigsen, 1986, fig. 1.5) with respect to, among others, the course of the anterior facial suture. However, *Acheilus* has a subrectangular glabella that is constricted between the eyes, more distinct palpebral furrows, and a occipital furrow that shallows sagittally.

Occurrence of Materials Described Herein. This species occurs in *Missisquoia* Zone of Deadwood Formation (lower Ibexian zone of the Lower Ordovician); South slope of Sheep Mountain, near Bearlodge Ranch, east-central Wyoming (locality 4C in Text-fig. I-2).

Association of Protaspides. Two ontogenetic sequences are recognized among the protaspid specimens. The first consists of CMC-P 42618b and e (Pl. II-23, Figs. 25-31) which are characterized by distinct transglabellar furrows and a shield that is more strongly tapering posteriorly; this sequence is assigned to Plethopletidae sp. A. The second sequence, consisting of CMC-P 42618c, d, and f, (Pl. II-23, Figs. 1-12) is distinguished from the first by the lack of transglabellar furrows, a moderately depressed L4, and more deeply incised axial furrows. Morphologic transition into an early meraspid cranidium (CMC-P 42618h, Pl. II-23, Fig. 13) from the second series is more reasonable because in particular the cranidium lacks transglabellar furrows. Nonetheless, the species represented by the first sequence is not considered to be a taxon distantly related to *Arapahoia arbucklensis*.

CMC-P 42618a (Pl. II-23, Figs. 32, 33) has a spindle-shaped axis with its own independent convexity and bilobed L3/L2/L1, which must have experienced a radical metamorphosis if it represents an ontogenetic stage earlier than metaprotaspides of both sequences. It is named species undetermined R.

Description of Protaspides.

Metaprotaspid stage (CMC-P 42618c, d, f, Pl. II-23, Figs. 1-12). Shield oval in outline, 0.435 mm (avg.) in transverse width and 0.467 mm (avg.) in sagittal length. Axis spindle-shaped; axial furrows defining L4 forwardly diverge and end with broad anterior pits; three pairs of glabellar furrows; maximum width of axis 34% (avg.) of shield width. Posterior cranidial marginal furrow nearly imperceptible. Fixigenal area moderately convex and in posterior view, steeply-sloping close to axial furrows. Protopygidium recognized only by prominent occipital ring. Protopygidium with two axial rings; no pleural and interpleural furrows developed; sagittal length of protopygidium ranges from 17% to 26% of shield length.

Protaspides of *Arapahoia arbucklensis* and Their Taxonomic Implications. The metaprotaspides of *Arapahoia arbucklensis* (Pl. II-23, Figs. 1-12) are comparable to those of *Arapahoia snowensis* (Hu, 1986, pl. 16, figs. 4-7). They share an oval shield and a spindle-shaped axis with forward-expanding L4, supporting the assignment of this species to *Arapahoia*.

The subelliptical to oval shield outline and spindle-shaped axis of the metaprotaspides

71

of *Arapahoia arbucklensis* are shared with the phylacterid and housiine protaspides. The features distinguishing the *Arapahoia* protaspides are a forward-expanding L4 that is well-defined by the axial furrows and depressed below the level of adjacent pleural regions, and a less convex shield (Pl. II-23, Figs. 1-12). Nonetheless, the protaspid similarities suggest that *Arapahoia* be is a member of the superfamily comprising Housiinae and Phylacteridae.

The early meraspid cranidia of these trilobites (Pl. II-23, Figs. 13-15 for *Arapahoia*, see Pl. II-17, Fig. 20 for the Housiinae, and see Pl. II-19, Fig. 35 for Phylacteridae) all have a semicircular outline and a forward-tapering glabella. The forward-tapering glabella of the meraspid cranidium has a slightly constricted at anterior one-third of the glabellar length, which is observed in all of these trilobites.

The holaspid cranidium of *Housia ovata* (Pl. II-17, Fig. 28) is similar to that of *Arapahoia* (see Stitt, 1998, figs. 8.2-8.4; Resser, 1942, pl. 7, figs. 2, 10, 15, 24) in terms of their overall outline and convexity, and the location of palpebral lobe. The *Housia* cranidium differs in having a divergent anterior facial suture and an acutely-pointing anterior border. The pygidium of *Housia* is similar to that of *Arapahoia* (Pl. II-23, Fig. 18) in having a post-axial ridge, a semi-elliptical outline, a broadly concave marginal border furrow, and a posterior band of pleura reaching the border. This supports the inclusion of Araphaoia within the superfamily which includes the Housiinae, suggesting a possibility that the Plethopletidae could belong to the superfamily.

The metaprotaspides of *Kingstonia* (Kingstoniidae, Hu, 1986, pl. 15, figs. 3-7; Hu, 1968, pl. 3, figs. 4-6) apparently have a forward-expanding L4 and parallel-sided L3/L2/L1, thus lending little support to a close evolutionary relationship between *Arapahoia* and the Kingstoniidae such as *Acheilus*.

Family NORWOODIIDAE Walcott, 1916a

Remarks. This family is considered to include *Norwoodia* Walcott, 1916a, *Norwoodella* Resser, 1938a, *Hardyoides* Kobayashi, 1938, *Levisaspis* Rasetti, 1943, *Holcacephalus* Resser, 1938a, and *Paranorwoodia* Rasetti, 1943 (Pratt, 1992, p. 75).

Genus NORWOODELLA Resser, 1938a

Remarks. Compared to other norwoodiid genera, *Norwoodella* has a larger glabella lacking glabellar furrows (Pl. II-24, Figs. 24, 25). Apart from a proparian facial suture and a long posterior fixigenal spine pair, the overall cranidial architecture, including an indistinct anterior border and axial furrows and palpebral lobes located next to axial furrows, is somewhat similar to *Arapahoia* (Pl. II-23, Figs. 22, 23; see also Stitt, 1998, figs. 8.2-8.4). These shared features are also found in the Housiinae. The pygidium of *Norwoodella* is comparable to that of *Arapahoia* (e.g., Stitt, 1998, figs. 8.7, 8.8) in both having an elongated semi-elliptical outline and a relatively broad marginal border furrow. All of these characters suggest a close relationship between *Norwoodella* and *Arapahoia*, and probably between Norwoodiidae and Plethopeltidae. Westrop (1992, p. 251) considered *Arapahoia* as a opisthoparian norwoodiid.

Norwoodella halli Resser, 1938a
Pl. II-24, Figs. 1-25, Pl. II-25, Figs. 1-8, Text-fig. V-3.7
1938a *Norwoodella halli* Resser, p. 90, pl. 10, figs. 45, 46.

72

1940 *Norwoodella halli*, Lochman, p. 47, pl. 5, figs. 31-36.

1963 *Norwoodella halli*, Hu [part], p. 129-132, pl. 19, figs. 1-8, 10-16, 22-36 [only].

1965 *Norwoodella halli*, Rasetti, p. 67-68, pl. 4, figs. 8-15.

Diagnosis. see Hu (1963, p. 129-130) for holaspid diagnosis. **Anaprotaspis.** Shield oval in outline and highly convex, without any distinctive features. **Early metaprotaspis.** Shield oval, with posterior margin being straight. Glabella spindle-shaped; axial furrows very shallow. Posterior fixigenal spines short, projecting ventrally and inwards. Occipital ring transverse node. Posterior cranidial marginal furrow impressed only behind occipital ring. **Late metaprotaspis.** Shield oval in outline. Glabella wide (tr.) and forward-tapering. Frontal area flat and lower-leveled. Posterior cranidial marginal furrow imperceptible. Protopygidium large with four axial rings.

Stratigraphic and Geographic Distributions. This species occurs in the *Cedaria* Zone (lower Marjuman of Upper Cambrian). It has been reported from the Nolichucky Formation in Tennessee and the Bonneterre Dolomite in Missouri.

Occurrence of Materials Described Herein. Upper *Cedaria* Zone of the Bonneterre Dolomite, St. Francois County, Missouri (locality 6B in Text-fig. I-2). Materials from light colored fine to medium grained dolomitic limestone.

Association of Protaspides. Specimens USNM 143466l and 143466n (Pl. II-26, Figs. 1-4, 8-11) have a straight anterior margin and an indented posterior margin. USNM 143466n is smaller than the early anaprotaspis of *Norwoodella halli* (USNM 143466o, Pl. II-24, Figs. 1, 2) by 0.015 mm in sagittal length. It has relatively distinct anterior pits and an elongated hexagonal shield with a straight anterior margin and an indented posterior margin. The early anaprotaspis of *N. halli* (USNM 143466o) has an oval shield and imperceptible axial furrows. The features of USNM 143466n are undoubtedly continuous into USNM 143466l which is 0.435 mm in sagittal length. Specimen USNM 143466f (Pl. II-26, Figs. 12-15) has an elongated shield and a narrower axis, compared to early metaprotaspides of *N. halli* (Pl. II-24, Figs. 9-11, 14, 15). It seems more reasonable that these features are carried over from USNM 143466l, so that USNM 143466f is incorporated into the ontogeny containing USNM 143466n and 143466l. These three specimens is assigned to a norwoodiid species, Norwoodiidae sp. A.

Specimen USNM 143466m (Pl. II-26, Figs. 16-18) is 0.562 mm in sagittal length, which falls within the size range of the late anaprotaspid stage of *Norwoodella halli*. However, this specimen lacks the posterior fixigenal spine pair which is evident in the late anaprotaspis of USNM 143466j (Pl. II-24, Figs. 6-8). The featureless specimen is indistinguishable from the early anaprotaspis of *Norwoodella halli* (USNM 143466o, Pl. II-24, Figs. 1, 2), apart from its larger size. It could belong to another norwoodiid species, Norwoodiidae sp. B, which experienced a paedomorphic development.

Description of Protaspides

Early anaprotaspid stage (USNM 143466o, Pl. II-24, Figs. 1, 2). Shield oval in outline and highly convex; 0.347 mm in transverse width and 0.401 mm in sagittal length. No other features recognizable.

Late anaprotaspid stage (USNM 143466k, j, Pl. II-24, Figs. 3-8). Shield with rounded anterior margin and relatively straight and arched posterior margin; 0.486 mm in width and 0.549 mm in sagittal length. Axis wide (tr.) occupying 40 % of maximum shield width and spindle-shaped. Posterior fixigenal spine short, blunt and broadly based.

Early metaprotaspid stage (USNM 143466i, h, g, Pl. II-24, Figs. 9-11, 14, 15, 17, 18).

73

Shield length ranges from 0.574 to 0. 702 mm and width from 0.521 to 0.649 mm. Axis stands well above fixigenal area with its own convexity and club-shaped (more rapidly tapering posteriorly); maximum width at about mid-shield length 41% (avg.) of shield width. Cranidium occupies 82 % (avg.) of shield sagittal length. Protopygidial area recognized only in axial region by distinct occipital ring. Short and blunt spine present at posterolateral end of protopygidium.

Late metaprotaspid stage (USNM 143466d, e, Pl. II-25, Figs. 1-8). Shield 1.056 mm in length and 0.817 mm in width. Axis club-shaped and wide (tr.) occupying 47% (avg.) of shield width. Protopygidium semi-circular, with 38% (avg.) of shield length; at least four axial rings present; no pleural and interpleural furrows developed; posterior pygidial margin broadly arched.

Protaspides of *Norwoodella halli* and Their Taxonomic Implications. Palmer (1962a, pl. 19, figs. 20-25, text-fig. 2B) illustrated protaspides of a norwoodiid, *Hardyoides minor* from the *Aphelaspis* zone of the Deadwood Formation (lower Steptoean). Lochman and Hu (1960, pl. 98) and Hu and Li (1971, pl. 3, figs 1-32, fig. 4) reported protaspides of *Holcacephalus* (= *Hardyoides*) *tenerus* from the *Cedaria* Zone of the DuNoir Limestone in Wyoming and the Pilgrim Formation in Montana. Although *H. tenerus* protaspides are smaller than those of *H. minor*, both are very similar, including palpebral lobe swellings and a forward-expanding glabella.

The *Hardyoides* protaspides are much smaller than the early anaprotaspis of *Norwoodella halli* (Pl. II-24, Figs. 1, 2); the protaspides of *Hardyoides* range from 0.288 to 0.414 mm in sagittal length, whereas the early anaprotaspis of *N. halli* is 0.401mm. *Hardyoides* protaspides differ in having a rather circular and less convex shield, three pairs of fixigenal spines (in *H. minor*), a forward-expanding axis defined by distinct axial furrows, and transglabellar furrows. It is certain that the protaspides do not suggest a strong evolutionary relationship between the two norwoodiid genera, as suggested by Hu and Li (1971, p. 181).

Protaspides of *Norwoodia occidentalis* and *N. chattertoni* (Pratt, 1992, pl. 28, figs. 4, 5, 15) are comparable to late metaprotaspides of *Norwoodella halli* (Pl. II-25) in sharing an oval shield, a spindle-shaped axis and a protopygidium with at least three axial rings. The late metaprotaspides of *N. halli* have a much wider (tr.) axis and an imperceptible posterior cranidial marginal border; these differences continue to exist in meraspid and holaspid stages.

Protaspid and holaspid morphologic data available for norwoodiid genera suggest their disparate groupings within the family. Protaspid morphologies suggest a close affinity between *Norwoodia* and *Norwoodella*, whereas holaspid morphologies do so between *Norwoodia* and *Hardyoides*; *Hardyoides* and *Norwoodella* do not share any evolutionarily significant similarities, neither at protaspid nor holaspid stages.

Of the taxa whose ontogeny is described herein, protaspides of *Norwoodella* are most similar to phylacterids (e.g., *Aphelotoxon* and *Cliffia*), housiines, and *Arapahoia*, thus suggesting the superfamilial clustering of these trilobites. They share an oval and convex shield and a spindle-shaped axis. Post-protaspid morphologies of *Norwoodella* are also similar to these two groups, in particular to *Arapahoia*. One of the remarkable features of the protaspides of *Norwoodella* is the posterior fixigenae which strongly curve downwards and then inwards; it is conspicuous in early metaprotaspides and late anaprotaspides (Pl. II-24, Figs. 8, 11). The metaprotaspides of *Drabia typica* (Pl. II-19,

74

Figs. 13, 15, 21, 30) have the fixigenae which strongly curve downwards, but do not curve inwards. Another noticeable feature unique to *Norwoodella* protaspides is the width of the axis that is widest among the trilobites possessing the protaspid morphotype C.

Superfamily **DIKELOCEPHALACEA** Miller, 1889

Remarks. Ludvigsen and Westrop (1983) revised the superfamily Dikelocephalacea to include only three families, Dikelocephalidae, Saukiidae, and Ptychaspididae. Fortey and Chatterton (1988), in their cladistic analysis, placed the superfamily as a sistergroup to Remopleuridacea. In the cladograms (text-figs. 1-4), an inflated palpebral lobe with deep palpebral furrow and a posterior glabellar bulge define the clade of the two superfamilies. Westrop (1995, p. 23) recently questioned the validity of these features as synapomorphies by observing their occurrence in other taxa such as a bathyurid, loganellid, and idahoiid.

Family **PTYCHASPIDIDAE** Raymond, 1924
Subfamily **PTYCHASPIDINAE** Raymond, 1924
Ptychaspis bullasa Lochman and Hu, 1959
Pl. II-27, Figs. 1-14, Text-fig. V-4.3

1959 *Ptychaspis bullasa*, Lochman and Hu, p. 422-424, pl. 58, figs. 21-42.
1962 *Ptychaspis bullasa*, Bell and Ellinwood, p. 405, pl. 58, figs. 14-17.
1970 *Ptychaspis bullasa*, Longacre, p. 44, pl. 2, figs. 4, 5.
1971 *Ptychaspis bullasus*, Hu [part], p. 97-99, pl. 17, figs. 2, 4, 5-34 [only].
1977 *Ptychaspis bullasa*, Stitt, p. 43, pl. 2, fig. 4.

Diagnosis. see Hu (1971, p. 97) for holaspid diagnosis. **Metaprotaspis.** Shield circular. Axis narrow and parallel-sided. Palpebro-ocular ridge wide. Anterior pits broad. Protopygidium very small. Exoskeletal surface covered with fingerprint-like ornaments.
Stratigraphic and Geographic Distributions. This species occurs in the *Ptychaspis-Saukia* faunule and time-equivalents such as the *Saratogia* Zone (upper Sunwaptan of Upper Cambrian) and has been reported from the St. Charles Dolomite in Idaho, the Honey Creek Formation in Oklahoma, and the Wilberns Formation in Texas.
Occurrence of Materials Described Herein. *Ptychaspis-Prosaukia* Zone (upper Sunwaptan) of St. Charles Formation. north of Mink Creek, Preston Quadrangle, Idaho (locality 3B in Text-fig. I-2).
Association of Protaspides. Association of CMC-P 38735a (Pl. II-27, Fig. 15) is questionable unless a relatively radical metamorphosis is inferred. The specimen has a subquadrate shield and a slightly forward-expanding, wide (tr.) axis with bilobed L3/L2. It is more comparable to CMC-P 39743a and 39743b of *Orygmaspis* (*Parabolinoides*) *contracta* (Pl. II-32, Figs. 1-6) but differs in the wider axis with bilobed L3/L2. This specimen is named species undetermined S. Specimen CMC-P 38735c (Pl. II-27, Figs. 16-19) differs from CMC-P 38735b of the same size (Pl. II-27, Figs. 1-3) by possessing a more circular shield, a narrower (tr.) axis, a narrow (sag. and exsag.) frontal area and anterior border, a slender eye ridge, and a shorter (sag.) L4. Nonetheless, its possession of the expanding L4, fingerprint-like microsculpture, and posteriorly-extending eye ridge, and convexity of shield similar to metaprotaspides of *Ptychaspis bullasa*, suggests that the specimen belongs to *Ptychaspis*; it may be referable to *Ptychaspis granulosa* which

75

co-occurs with *P. bullasa*. The specimen is identified as Ptychaspidinae sp. A.

Description of Protaspides

Metaprotaspid stage (CMC-P 38735b, d, Pl. II-27, Figs. 1-7). Shield circular to elliptical in outline with straight anterior margin; sagittal length ranges from 0.440 to 0.485 mm and transverse width from 0.464 to 0.501 mm. Glabella cylindrical; L4 trapezoidal and rapidly expands forwards from level of anterior pits; L3/L2/L1 parallel-sided, with their width taking 28% (avg.) of shield width. Eye ridge fairly large, with low independent convexity, and extends posteriorly up to mid-shield length. Frontal area including anterior border and anterior fixigenal area flat and narrow, and differentiated from eye ridge and L4. Posterior cranidial marginal furrows nearly straight except being slightly convex forwards at mid-length. Protopygidium with one to two axial rings and fairly broad (tr.) pleural region without pleural or interpleural furrows; sagittal length of protopygidium 13% (avg.) of entire shield length. Surface covered with fingerprint-like microsculpture.

Protaspides of *Ptychaspis bullasa* and Their Taxonomic Implications. Protaspides of *Ptychaspis bullasa* (Pl. II-27, Figs. 1-7) considerably differ from those of *Remopleurides*, a typical remopleuridacean, that are definitely of asaphoid-type (Fortey and Chatterton, 1988, text-fig. 11.4-11.7). Thus, their sistergroup relationship is doubtful. The protaspides are different from any ptychopariide protaspides in having, amongst others, a large palpebro-ocular ridge that posteriorly extends into mid-shield length, thus supporting the separate taxonomic status of the Dikelocephalacea.

Superfamily SOLENOPLEURACEA Angelin, 1854

Remarks. Geyer (1998) treated the superfamily Conocoryphacea Angelin, 1854 as a synonym of the Solenopleuracea.

Family SOLENOPLEURIDAE Angelin, 1854

Remarks. The family Conocoryphidae Angelin, 1854 was synonymized under the Solenopleuridae (Geyer, 1998).

Subfamily SOLENOPLEURINAE Angelin, 1854
Genus SOLENOPLEURA Angelin, 1854
Solenopleura acadica Whiteaves *in* Matthew, 1885
Pl. II-28, Figs. 1-7

1885 *Solenopleura acadica* Whiteaves *in* Matthew, p. 76-77, pl. 7, fig. 15
1887 *Solenopleura acadica*, Matthew, p. 157-160, pl. 2, figs. 5, 6.

Diagnosis. A species of *Solenopleura* with semicircular cephalon and fourteen thoracic segments. **Anaprotaspis**. Shield circular. L4 forward-expanding. L3/L2/L1 spindle-shaped. Anterior pits distinct and located well inside from anterior shield margin.

Occurrence of Materials Described Herein. Middle Cambrian Porter Road Formation, St. John, New Brunswick, Canada (locality 12 in Text-fig. I-2).

Description of Protaspides

Anaprotaspid stage (UA 11934, Pl. II-28, Fig. 1). Shield circular, 0.373 mm long. L4 forward-expanding; L3/L2/L1/Lp spindle-shaped. Anterior pits distinct.

Metaprotaspid stage (UA 11936, Pl. II-28, Fig. 3). Shield circular, 0.436 mm long and

76

0.505 mm wide. L4 forward-expanding; L3/L2/L1 spindle-shaped. Anterior pits distinct. **Protaspides of** *Solenopleura* **and Their Taxonomic Implications**. Protaspides of *Solenopleura acadica* are characterized by having a circular shield, a forward-expanding L4, a spindle-shaped L3/L2/L1, and a pair of distinct anterior pits that are located well inside of the shield. They differ from Lower Cambrian *Crassifimbra walcotti* (an Antagminae, Palmer, 1958, pl. 26, figs. 1, 2) in lacking posterior marginal spines and lateral border, and having a broader (tr.) axis with spindle-shaped L3/L2/L1. From *Sao hirsuta* (a Solenopleuropsinae [=Saoinae], Whittington, 1957, pl. 116, figs. 14-21), the *Solenopleura* protaspides differ in lacking an eye ridge, and in having anterior pits that are located well inside the anterior shield margin. The L4 of *S. hirsuta* is much more strongly forward-expanding than that of *S. acadica*.

In effect, the protaspides of *Sao* are more similar to the protaspid morphotype B, suggesting that *Sao* and *Solenopleura* both may not belong to the same family, the Solenopleuridae. The anaprotaspides of Lower Cambrian *Ptychoparella* sp. A (Ptychopariidae, Blaker and Peel, 1997, figs. 74.1, 74.2) have a trapezoidal shield, a narrow axis, and less distinct anterior pits which allow one to easily distinguish them from that of *S. acadica*.

Suborder OLENINA Burmeister, 1843

Diagnosis of Protaspides. Shield circular to subquadrate in outline. Axis forward-expanding to parallel-sided; L4 usually more strongly forward-expanding. Glabellar furrows distinct. Eye ridge present in some species. Protopygidium relatively small and projecting strongly ventrally.

Remarks. Fortey (1990, p. 561-562) strongly argued that the suborder embraces only the family Olenidae whose monophyly has long been accepted by most trilobite workers. He conceived that many other groups assigned to the Olenina or the superfamily Olenacea, together with the Olenidae became morphologically adapted to the dysaerobic environment that the olenid trilobites inhabited. Further he claimed that there is no synapomorphic characters to phylogenetically connect those groups with the Olenidae. The groups that have been united with the Olenidae within the superfamily Olenacea are Pterocephaliidae (as including Aphelaspidinae), Elviniidae, Parabolinoididae, and Idahoiidae (Ludvigsen and Westrop, 1983; Westrop, 1986; Shergold, 1980; Pratt, 1992).

Ludvigsen and Westrop (1983, p. 16) mentioned a probability that there would be several subordinate groups within their context of the Olenacea. Fortey (1990) also mentioned that the Olenidae would be included within a major libristomate group. A conceivable classification scheme is to erect a new superfamily of the Olenina which includes appropriate groups out of the families listed above and serves as a sistergroup to the Olenidae. Protaspides of Olenidae, Aphelaspidinae, Parabolinoididae, and Elviniidae allow us to explore this possibility (see below).

Based on protaspid morphologic data, the suborder Olenina consists of four subordinate groups, the Olenacea which only includes Olenidae, a group characterized by the protaspid morphotype D which only includes Parabolinoididae, a group possessing the protaspid morphotype E which only includes the Aphelaspidinae, and the Elviniidae which is characterized by the protaspid morphotype F.

77

Superfamily OLENACEA Burmeister, 1843

Diagnosis of Protaspides. Shield circular to oval in outline. Axis forward-expanding to forward-tapering. Glabellar furrows distinct but shallower than axial furrows. Anterior border absent. Anterior pits usually deeper than axial furrows. Eye ridge slender, if present. Posterior fixigenal marginal spines long and slender, if present. Protopygidium strongly projecting ventrally, with long slender marginal spines.

Remarks. This superfamily includes only one family, Olenidae. The strong monophyly of this group has been accepted (see Fortey, 1990), mainly because of its exceptionally continuous stratigraphic record in Scandinavia (e.g., Henningsmoen, 1957). However, protaspid features described below and from other literatures strongly contradict its monophyly.

Family OLENIDAE Burmeister, 1843
Subfamily OLENINAE Burmeister, 1843
Genus OLENUS Dalman, 1827
Olenus gibbosus (Wahlenberg, 1821)
Pl. II-29, Figs. 1-27, Text-fig. V-4.11

1821 *Entomostracites gibbosus* Wahlenberg [part], p. 39, pl. 1, fig. 4 [only].
1878 *Olenus gibbosus* Angelin, p. 55, pl. 25, fig. 5
1927 *Olenus gibbosus*, Strand, p. 320-329, pl. pl. 2, figs. 1-14
1942 *Olenus gibbosus*, Størmer, pl. 81, figs. 9a-e, 10a-e.
1957 *Olenus gibbosus*, Henningsmoen, 1957, p. 105, pl. 1, fig. 1, pl. 3, pl. 9, fig. 7.
1971 *Olenus gibbosus*, Hu, p. 99-101, pl. 18, figs. 1-32, text-fig. 47.

Diagnosis. See Hu (1971, p. 99) for holaspid diagnosis. **Anaprotaspis.** Shield circular. Axis slightly forward-expanding with strongly expanding L4. Palpebro-ocular ridge slender and differentiated from anterior border. Lateral shield border narrow and delimited by concave border furrow. Three pairs of fixigenal spines; anterior pair located opposite L2. **Metaprotaspis.** Shield subcircular. Posterior fixigenal spine long and slender. Protopygidium medium-sized and strongly ventrally projecting. Protopygidial marginal spine long and slender. Exoskeletal surface pitted.

Occurrence of Materials Described Herein . Alum Shales (Upper Cambrian), Ringsaker Station, Norway.

Description of Protaspides
Anaprotaspid stage (CMC-P 38736a, b, c, Pl. II-29, Figs. 1-8). Shield circular in outline; 0.353 mm (avg.) wide and 0.322 mm (avg.) long. Axis convex, forward-expanding, and reaches anterior and posterior shield margins; L4 trapezoidal; L3/L2/L1/Lp parallel-sided or slightly tapering posteriorly and bilobed; maximum width of axis at L2 takes 25% (avg.) of shield width. Three pairs of fixigenal spines; anterior pair located opposite to L2 and middle pair opposite to S0; spines short and broadly-based; Flat, narrow lateral border connecting all three fixigenal spines. Eye ridge distinctly developed.

Metaprotaspid stage (CMC-P 38736d, e, f, Pl. II-29, Figs. 9-19). Shield ranges 0.318 to 0.418 mm in sagittal length and 0.422 mm (avg.) wide. Glabella forward-expanding; L4 trapezoidal; L3/L2/L1 spindle-shaped but more strongly tapering posteriorly, with L2 being widest (27% of shield width); bilobation disappears. Protopygidium steeply tilted ventrally, bearing two to three axial rings and pair of marginal spines; sagittal length of

78

protopygidium ranges 7 to 20% of entire shield length.

<div align="center">

Genus APOPLANIAS Lochman, 1964
Apoplanias rejectus Lochman, 1964
Pl. II-30, Figs. 1-22, Text-fig. V-4.10

</div>

1964 *Apoplanias rejectus* Lochman [part], p. 57, pl. 14, figs. 26-31 [only].
1971 *Apoplanias rejectus*, Stitt, p. 46-47, pl. 8, fig. 16.
1971 *Missisquoia cyclochila* Hu [part], p. 107-109, pl. 20, figs. 4, 5, 9 [only].
1971 *Highgatella facilia* Hu [part], p. 103-105, pl. 21, figs. 6-26 [only].
1973 *Highgatella facilia*, Hu, p. 90, pl. 1, figs 25-28, 30-32.
1973 *Paranumia triangularia* Hu [part], p. 86-90, pl. 1, figs. 12, 13 [only].
1982 *Apoplanias rejectus*, Ludvigsen, p. 66, figs 51M-T, 69K-Q.
1986 *Apoplanias rejectus*, Westrop, p. 40-41, pl. 19, figs 6-8.
1989 *Apoplanias rejectus*, Dean, p. 20, pl. 8, figs. 4-9, 12, 14.
1995 *Apoplanias rejectus*, Westrop, p. 23, pl. 5, fig. 5.

Diagnosis. See Ludvigsen (1982, p. 65)'s generic diagnosis for holaspid diagnosis.
Metaprotaspis. Shield oval in outline. Axis slightly spindle-shaped. Glabellar furrows shallower than axial furrows. Occipital ring transverse node. Posterior cranidial marginal furrow only impressed behind occipital ring. One protopygidial axial ring present.
Stratigraphic and Geographic Distributions. This species occurs in Ibexian Zones such as the *Missisquoia* Zone, *Symphysurina* Zone, and *Apoplanias rejectus* fauna. It has been reported from the Deadwood Formation in Montana and Wyoming, the Signal Mountain Limestone in Oklahoma, the Rabittkettle Formation in Northwestern Territories, and the Survey Peak Formation in Alberta.
Remarks. Ludvigsen (1982, p. 66) synonymized *Highgatella facilia* with *Apoplanias rejectus*, which is accepted herein. The yoked free cheeks and general cephalic similarities to *Parabolinella* were cited as evidence to support the inclusion of *Apoplanias* in the Oleninae. A spinose pygidium, which is similar to the pygidium of *Orygmaspis* (*Parabolinoides*) *contractus* (CMC-P 43344r, Pl. II-32, Fig. 25), is associated with this species by Ludvigsen (1982, figs. 69M-O). A spinose pygidium is not uncommon to the Olenidae (see Henningsmoen, 1957, pls. 1-8)
Occurrence of Materials Described Herein. *Missisquoia* Zone (Lower Ordovician) of Deadwood Formation. Sheep Mountain, Sundance, Crook County, northeast Wyoming (locality 4A in Text-fig. I-2).
Association of Protaspides. For detailed account of the association of protaspides with *Apoplanias rejectus*, *Missisquoia cyclochila*, and *Paranumia triangularia* all of which occur in the same locality, refer to "Association of Protaspides" under *Missisquoia cyclochila*.

Meraspid cranidium CMC-P 38740f (Pl. II-30, Fig. 28) has distinct transglabellar furrows which are reminiscent of parabolinoidids (e.g., Pl. II-32, Figs. 19, 38); it is named Parabolinoididae sp. A.
Description of Protaspides
Metaprotaspid stage (CMC-P 38749d, 38749e, 41556l, 41556k, Pl. II-30, Figs. 1-13). Shield elliptical in outline; 0.299 mm (avg.) wide and 0.317 mm (avg.) long. Axis moderately convex, wide (tr.), spindle-shaped, with its anterior less tapering than the posterior, and maximum width at L2 being 36% of shield width; L3/L2/L1 bilobed;

<div align="center">79</div>

transglabellar furrows shallower than axial furrows. Differentiation of protopygidium recognized only by presence of occipital ring which is the most convex axial lobe; sagittal length of protopygidium ranges from 14 to 21% of entire shield length.

Subfamily PELTURINAE Hawle and Corda, 1847
Genus ACEROCARE Angelin, 1854
Acerocare ecorne Angelin, 1878
Pl. II-31, Figs. 1-25, Text-fig. V-4.9

1878 *Acerocare ecorne* Angelin, p. 46-47, pl. 25, fig. 10.
1898 *Acerocare ecorne*, Moberg and Möller, p. 231, pl. 10, figs. 1-10.
1957 *Acerocare ecorne*, Henningsmoen, p. 243, pl. 2, fig. 3, pl. 7, pl. 30, figs. 1-8.
1971 *Acerocare ecorne*, Hu, p. 101-103, pl. 19, figs. 1-34.

Diagnosis. see Hu (1971, p. 101) for holaspid diagnosis. **Anaprotaspis.** Shield suboval. Axis spindle-shaped. Anterior pits deeper than axial furrows. Glabellar furrows shallower than axial furrows. **Metaprotaspis.** Shield subcircular. Glabella wide (tr.), highly convex dorsally, and strongly convex laterally. Anterior pits pinhole-like. Posterior fixigenal spine long and slender. Protopygidium small and strongly projecting ventrally, with long marginal spines.

Occurrence of Materials Described Herein. *Acerocare* Zone (2da) of Upper Cambrian, Nye, Joukoping, Sweden.

Description of Protaspides.

Anaprotaspid stage (CMC-P 38738a, Pl. II-31, Figs. 1-4). Shield suboval in outline, with straight anterior and posterior indented margin; 0.268 mm long and 0.285 mm wide; posterior shield end oriented ventrally. Axis convex and spindle-shaped, with its posterior more strongly tapering; maximum width of axis at L3 37% of shield width; transglabellar furrows much shallower than axial furrows; L3/L2/L1 bilobed. Anterior pits deep and broad.

Metaprotaspid stage (CMC-P 38738b, c, d, e, f, Pl. II-31, Figs. 5-15). Shield ranges from 0.374 to 0.401 mm in transverse width and from 0.340 to 0.380 mm in sagittal length. Axis very wide and strongly convex dorsally, occupying 38% (avg.) of shield width. Posterior fixigenal spine slender and long. Presence of distinct occipital ring delimits protopygidium. Protopygidium tilted ventrally, with one axial ring; marginal spine slender and long; sagittal length 12% (avg.) of entire shield length. Shield surrounded by narrow flat border.

Olenid Protaspides and Their Taxonomic Implications. Protaspides have been described for the following olenid species other than *Olenus gibbosus* (Oleninae), *Apoplanias rejectus* (Oleninae), and *Acerocare ecorne* (Pelturinae) described herein; *Olenus wahlenbergi* (Oleninae, Clarkson and Taylor, 1995), *Parabolinella panosa* (Oleninae, Ludvigsen, 1982, Chatterton and Speyer *in* Whittington *et al.*, 1997), *Parabolina spinulosa* (Olenidae, Clarkson *et al*, 1997), *Triarthrus latissimus* (Triarthrinae, Månsson, 1998), *Triarthrus eatoni* (Triarthrinae, Beecher, 1893, 1895), *Triarthrus thor* (Triarthrinae, Fortey, 1974), *Leptoplastides salteri* (Leptoplastinae, Raw, 1925, 1927), *Leptoplastus crassicornis* (Leptoplastinae, Whitworth, 1970), and *Peltura scarabaeoides* (Pelturinae, Whittington, 1958).

Clarkson and Taylor (1995) described the ontogeny of *Olenus wahlenbergi* from the Alum Shales of Sweden, which appears to be the same locality where *Olenus gibbosus*

80

occurs. The anaprotaspides of *O. gibbosus* (Pl. II-29, Figs. 1, 4) have three fixigenal spines which are not present in the anaprotaspides of *O. wahlenbergi* (Clarkson and Taylor, 1995, figs. 1a, c). The palpebro-ocular ridge present in the anaprotaspides of *O. gibbosus* (Pl. II-29, Fig. 4) appears in the metaprotaspides of *O. wahlenbergi* (Clarkson and Taylor, 1995, figs. 1b, d-f). The protaspides of *Parabolinella panosa* (Chatterton and Speyer *in* Whittington *et al.*, 1997, fig. 172.1) are greatly similar to those of *Olenus*. The most distinguishing feature of the olenine protaspides is that L3/L2/L1 is slightly convex laterally, L3 is constricted at its anterior end and L4 is straight-sided and forward-expanding; protaspides of other olenid subfamilies have a spindle-shaped axis. The triarthrine protaspides (e.g., *Triarthrus latissimus*, Månsson, 1998, figs. 11.a-11.e) appear to have the most similar shape of the axis (see below).

The metaprotaspides of *Apoplanias rejectus* (Pl. II-30, Figs. 1-13) are not readily comparable to any particular olenid species. They are characterized by possessing a more elongated (sag.) shield and a spindle-shaped axis. The bilobed L3/L2/L1 is comparable to *Olenus gibbosus* (Pl. II-29, Figs. 1-8) and the absence of lateral border and elongated shield to the anaprotaspides of *Triarthrus latissimus* (Månsson, 1998, figs. 11a-c). The metaprotaspides of *A. rejectus* lack a palpebro-ocular ridge and a posterior fixigenal spine which are common to the olenid protaspides. Neither does the axis stand above the fixigenae as prominently as in other olenid species, nor does it have the strong independent convexity. Thus, the protaspid features do not clarify the taxonomic affinity of *Apoplanias* with other olenid genera.

Månsson (1998) described the anaprotaspides of *Triarthrus latissimus* which have three pairs of fixigenal spines, a pair of swellings in front of the glabella, weakly-developed glabellar furrows, three pairs of tubercles on the fixed cheeks, and a pitted exoskeletal surface (figs. 11a-c). Their spindle-shaped, wide (tr.) axis and ventrally-oriented protopygidium confirm that they are of the olenid-type. The metaprotaspis of *T. latissimus* (Månsson, 1998, figs. 11d, e) differ from the olenine metaprotaspides in having a more rectangular shield outline, a club-shaped glabella, and lacking a protopygidial marginal spine pair. A metaprotaspis of *Triarthrus thor* from Spitsbergen (Fortey, 1974, pl. 23, fig. 23) differs from that of *T. latissimus* in having deeper glabellar furrows and posterior cranidial border furrow, and distinct protopygidial pleural furrows, and lacking fixigenal spines and tubercles. Nonetheless, their rectangular shield and forward-expanding axis support both belonging to the same subfamily. The position of the three fixigenal spine pairs in the *T. latissimus* anaprotaspides (Månsson, 1998, figs. 11.a, 11.b) is quite different from that of *Olenus gibbosus* (Pl. II-29, Figs. 1, 4, 8). The anterior pair is located at the antero-lateral corner of the shield in *T. latissimus*, whereas the anterior pair in *O. gibbosus* is at mid-shield length (Pl. II-29, Figs. 1, 4). The spine pairs of *T. latissimus* are not based along the shield margin, but slightly inside the margin. The lateral profile of the metaprotaspid shield and club-shaped glabella (Månsson, 1998, fig. 11e) are almost indistinguishable from that of *Acerocare ecorne* (Pl. II-31, Figs. 6, 12, 15).

Protaspides of *Peltura scarabaeoides* (Whittington, 1958, pl. 38, figs. 1-6) are similar to those of *Acerocare ecorne* (Pl. II-31, Figs. 1-15) in having a flat narrow lateral border, a highly convex and a wide axis, and a long posterior fixigenal spine pair. The leptoplastine protaspides (e.g., *Leptoplastus crassicornis*, Whitworth, 1970, pl. 22, figs. 1-9) are most similar to the pelturine protaspides.

81

Fortey (1974, p. 40) stated, "What is striking, however, are the morphological differences between early ontogenetic stages even within the single family Olenidae. This suggests that ontogenies are useful only in confirming relationships between closely related genera, for example within a single subfamily." That the axis is convex and stands well above the fixigenae and the axial furrows are very shallow seems to be shared by all olenid protaspides. Other characters vary from species to species; the shield outline varies from circular (e.g., *O. wahlenbergi*, Clarkson and Taylor, 1995, fig. 1a) to elliptical (*A. rejectus*, Pl. II-30, Figs. 1, 5, 9, 12), and the axis varies from forward-expanding (*O. gibbosus*, Pl. II-29, Figs. 10, 13) to forward-tapering (*A. ecorne*, Pl. II-31, Figs. 1, 5, 7, 9, 11, 13). Such characters as the bilobation of axial lobes, fixigenal spines, pygidial marginal spines, narrow lateral border, and palpebro-ocular ridge are present in some species and absent in the others.

Holaspid morphologies of the olenids are generalized as 'olenimorph' which includes numerous short (sag. and exsag.) thoracic segments with wide pleurae, long genal spines, and a caecate dorsal surface (see Fortey and Owens, 1990, figs. 5.4G and H). The olenimorph is considered to have been evolutionarily invented through adaptation to dysaerobic environments. However, the diagnosis of the Olenidae, or a synapomorphy of the group has not been satisfactorily defined, because within the olenimorph the members explored a wide variety of morphologies (Henningsmoen, 1957). Protaspides seem to have explored as great a variety of morphologies as the adults did.

TAXA POSSESSING PROTASPID MORPHOTYPE D
Protaspides of *Orygmaspis* (*Parabolinoides*) *contractus* and *Taenicephalus shumardi* of the family Parabolinoididae are characterized by a circular to subquadrate shield, a narrow and parallel-sided axis, distinct anterior pits, a small protopygidium with one axial ring.

Family PARABOLINOIDIDAE Lochman, 1956
Remarks. The Parabolinoididae has been regarded as a family of Olenacea until Fortey (1990, p. 560) assigned it to Anomocaroidea of Asaphida because its members have a ventral median suture which is a synapomorphy for the Asaphida. The olenid affinity of the Parabolinoididae has been proposed by several workers. Hu (1981, 1983) depicted an evolutionary tree in which *Parabolinoides* is connected with the olenids through such genera as *Aphelaspis*, *Dytremacephalus*, and *Elvinia*. It is certain that these groups share holaspid (or meraspid in some taxa) similarities, but a problem is whether the similarities are apomorphic or plesiomorphic. Most similarities are considered plesiomorphic, so that they are not useful to define a higher taxon embracing these groups.

The Elviniidae and Aphelaspidinae have also been included within the Olenacea along with the Olenidae (Westrop, 1986; Pratt, 1992). Westrop (1986) claimed a closer relationship between the Olenidae (in particular Oleninae) and Parabolinoididae upon the basis of cephalic morphologies and meraspid cranidial similarities.

Genus ORYGMASPIS Resser, 1937
Subgenus ORYGMASPIS (PARABOLINOIDES) Frederickson, 1949
Remarks. Westrop (1986, p. 46) regarded *Parabolinoides* as a subgenus of *Orygmaspis*

82

by observing the obvious morphologic continuities between the two genera (for a contrary view, see Stitt and Straatmann, 1997, p. 98).

Orygmaspis (*Parabolinoides*) *contractus* (Frederickson, 1949)
Pl. II-32, Figs. 1-25, Text-fig. V-4.1

1949 *Parabolinoides contractus* Frederickson, p. 361, pl. 71, figs. 4-10.
1949 *Parabolinoides hebe* Frederickson, p. 361-362, pl. 70, figs. 7, 8, pl. 71, figs. 1-3.
1953 *Parabolinoides contractus*, Berg, p. 564, pl. 59, fig. 3.
1953 *Parabolinoides hebe*, Berg, p. 564-565, pl. 59, figs. 2, 4.
1962 *Parabolinoides contractus*, Bell and Ellinwood, p. 399, pl. 56, fig. 12.
1962 *Parabolinoides hebe*, Bell and Ellinwood, p. 400-401, pl. 56, figs. 6-11.
1964 *Parabolinoides contractus*, Lochman, p. 49-50, pl. 12, figs. 1-14.
1969 *Parabolinoides contractus*, Hu [part], p. 449-454, pl. 3, figs. 2-15, 18-38 [only].
1970 *Parabolinoides contractus*, Longacre, p. 27, pl. 1, figs. 2-6.
1971 *Parabolinoides contractus*, Stitt, p. 29-30, pl. 2, figs. 11-13.
1975 *Parabolinoides hebe*, Kurtz, p. 1040, pl. 4, figs. 38, 39.
1981 *Parabolinoides contractus*, Hu, p. 160-162, pl. 20, figs. 1-35, text-fig. 1.
1986 *Orygmaspis* (*Parabolinoides*) *contracta*, Westrop, p. 47-48, pl. 17, figs 1-15, pl. 19, figs 9-11, text-fig. 34C.
1997 *Parabolinoides contractus*, Stitt and Straatmann, p. 98-99, figs. 6.6-6.15.

Diagnosis. see Westrop (1986, p. 47) for holaspid diagnosis. **Anaprotaspis.** Shield subquadrate. Axis parallel-sided with forward-expanding L4. Posterior fixigenal spine broadly-based and short. **Metaprotaspis.** Shield circular. Axis narrow and parallel-sided. Glabellar furrows distinct as axial furrows. Protopygidium small with one axial ring.

Stratigraphic and Geographic Distributions. This species occurs in the *Taenicephalus* or *Conaspis* Zone (lower Sunwaptan of Upper Cambrian). It has been reported from the Honey Creek Formation in Oklahoma, the Davis Formation in Missouri, the Franconia Formation in Minnesota and Wisconsin, the Wilberns Formation in Texas, the Deadwood Formation in Montana and South Dakota, the Bison Creek Formation in Alberta

Occurrence of Materials Described Herein. *Conaspis* Zone (lower Sunwaptan) of Deadwood Formation exposed at Bear Butte, Lead, south-eastern Deadwood City and White Canyon, about 5 miles, north-east of Deadwood City, South Dakota (locality 5F in Text-fig. I-2).

Association of Protaspides. Hu (1969, 1980) described protaspides of *Orygmaspis* (*Parabolinoides*) *contractus* from two different localities close to Deadwood City, South Dakota. The specimens occurring in the White Canyon (CMC-P 43344, 43344a, b, Pl. II-32, Figs. 7-15) show some dissimilarities from those (CMC-P 39743a, b, c, Pl. II-32, Figs. 1-6, 16-18) occurring in the Bear butte. They have a comparatively narrower (tr.) and a dorsally more convex axis, and more deeply impressed axial furrows. In considering that the White Canyon specimens (Pl. II-32, Figs. 7-15) all are larger than the two Bear Butte specimens (CMC-P 39743a, b, Pl. II-32, Figs. 1-6), however, the differences are highly likely to be attributed to ontogenetic transformation. As a result, the Bear Butte specimens are considered to represent anaprotaspid stages of *O.* (*P.*) *contractus*.

Specimen CMC-P 39743 of Parabolinoididae sp. B (Pl. II-32, Figs. 28-30) has a relatively narrower (tr.) and parallel-sided axis than other anaprotaspides and it has a pair

of fixigenal spines which is distinct among other specimens. It is rather similar to anaprotaspides of *Olenus gibbosus* (CMC-P 38736a, b, c, Pl. II-29, Figs. 1-8)

Two holaspid pygidial specimens, CMC-P 39743o and 39743p (Pl. II-32, Figs. 26, 27), are excluded from *Orygmaspis (Parabolinoides) contractus*, because both have a much wider (tr.) axis and lack marginal spine pairs, and assigned to *Orygmaspis (Parabolinoides)* sp. A.

Description of Protaspides

Anaprotaspid stage (CMC-P 39743a, b, Pl. II-32, Figs. 1-6). Shield subquadrate in outline; 0.293 mm (avg.) in sagittal length and 0. 343 mm (avg.) in transverse width. Axis slightly forward-expanding and reaches anterior and posterior margin; L4 longest (sag.) and trapezoidal; L3/L2/L1/Lp parallel-sided, with maximum width 28% (avg.) of shield width; transglabellar furrows as deep as axial furrows. Anterior pits broad and distinct. Posterior fixigenal spines short, broadly-based, and blunt. Lateral margin slightly concave.

Metaprotaspid stage (CMC-P 39743c, 43344, 43344a, b, Pl. II-32, Figs. 8-18). Shield circular in outline; 0.384 mm (avg.) wide and 0.371 mm (avg.) long. Glabella parallel-sided, occupying 25% (avg.) of shield width. Differentiation of protopygidium recognized only by presence of occipital ring; one pygidial axial ring present; sagittal length 14% (avg.) of entire shield length.

Genus TAENICEPHALUS Ulrich and Resser *in* Walcott, 1924
Taenicephalus shumardi (Hall, 1863)
Pl. II-32, Figs. 31-42, Text-fig. V-4.2
1863 *Conocephalites shumardi* Hall [part], p. 154, pl. 7, figs. 1, pl. 8, fig. 32 [only].
1924 *Taenicephalus shumardi*, Walcott, p. 59, pl. 13, fig. 1
1925 *Taenicephalus shumardi*, Walcott, p. 117, pl. 17, figs. 15-17.
1942 *Taenicephalus pearli* Resser [part], p. 99, pl. 19, figs. 17-23 [only].
1942 *Taenicephalus holmesi* Resser, p. 100, pl. 19, figs. 24-27.
1942 *Taenicephalus speciosus* Resser, p. 100, pl. 20, fig. 19.
1942 *Taenicephalus castlensis* Resser, p. 106, pl. 21, figs. 24-25.
1942 *Taenicephalus wyomingensis* Resser, p. 106-107, pl. 21, fig. 32.
1944 *Taenicephalus shumardi*, Shimer and Shrock, p. 633, pl. 266, fig. 17.
1951 *Taenicephalus shumardi*, Wilson, p. 652-653, pl. 95, figs. 21-23, 25.
1953 *Taenicephalus shumardi*, Berg, p. 565-566, pl. 59, figs. 11-14.
1959 *Taenicephalus shumardi*, Lochman *in* Moore, p. O274, fig. 202.10.
1951 *Taenicephalus shumardi*, Wilson, p. 652-653, pl. 95, figs. 21-23, 25.
1956 *Taenicephalus cordillerensis* Miller, Deland and Shaw, p. 559, pl. 67, fig. 3
1960 *Taenicephalus shumardi*, Lochman and Hu, p. 811-812, pl. 95, figs. 12-23, 31.
1962 *Taenicephalus shumardi*, Bell and Ellinwood, p. 402, pl. 57, figs. 10-21.
1965 *Taenicephalus shumardi*, Grant, p. 137-138, pl. 12, figs. 21, 22, 25, 26.
1970 *Taenicephalus shumardi*, Longacre, p. 31.
1971 *Taenicephalus shumardi*, Stitt, p. 32, pl. 2, fig. 17.
1975 *Taenicephalus shumardi*, Kurtz, pl. 4, figs. 44-45.
1981 *Taenicephalus shumardi*, Hu, p. 162-165, pl. 21, figs. 1-28, text-fig. 2.
1986 *Taenicephalus shumardi*, Westrop, p. 50-51, pl. 20, figs. 13-15, pl. 21, figs. 5-17.
Diagnosis. see Westrop (1986, p. 50-51) for holaspid diagnosis. **Metaprotaspis.** Shield

84

subquadrate. Axis narrow and parallel-sided. Anterior pits deeper than axial furrows. Protopygidium small with one axial ring.

Stratigraphic and Geographic Distributions. This species occurs in the *Conaspis* or *Taenicephalus* Zone (lower Sunwaptan of Upper Cambrian). It has been reported from the Franconia Formation in Wisconsin and Minnesota, the Gatesburg Formation in Pennsylvania, the Dry Creek Shale in Montana and Wyoming, the Open Door Limestone and the Snowy Range Formation in Wyoming, the Deadwood Formation in South Dakota, the Honey Creek Limestone in Oklahoma, the Wilberns Formation in Texas, the Davis Formation and the Derby-Doerun Dolomite in Missouri, and the Bison Creek Formation in Alberta.

Occurrence of Materials Described Herein. *Conaspis* Zone (lower Sunwaptan) of the Deadwood Formation. east side of road cut, Brownsill Junction, about 6 miles south of Deadwood City, South Dakota (locality 5G in Text-fig. I-2).

Description of Protaspides

Metaprotaspid stage (CMC-P 43343x, Pl. II-32, Figs. 40-42). Shield subquadrate in outline; 0.381 mm wide and 0.347 mm long. Axis parallel-sided with distinct transglabellar furrows; maximum width occupies 27% of shield width. Anterior pits distinctly impressed. Protopygidium mainly represented only by at least one axial ring; pleural region very small; sagittal length of protopygidium 16% of entire shield length.

Comparison with Protaspides of *Orygmaspis* (*Parabolinoides*) *contractus*. The protaspides of *Taenicephalus shumardi* (Pl. II-32, Figs. 40-42) only differ from those of *Orygmaspis* (*Parabolinoides*) *contractus* (Pl. II-32, Figs. 1-18) in having a more quadrate shield and convex fixigenae.

Comparison of Parabolinoidid and Olenid Protaspides and Their Taxonomic Implications. The parabolinoidid anaprotaspides (Pl. II-32, Figs. 1-18, 40-42) have a subquadrate shield, a slightly forward-expanding axis with five axial lobes, a bilobed L3/L2/L1, broad and distinct anterior pits, and a blunt posterior fixigenal spine. The metaprotaspides (Pl. II-32, Figs. 7-15, 40-42) have a circular shield, a cylindrical and narrow axis, and a protopygidium with a very small pleural region. Each of these features is shared with different olenid species. The subquadrate shield of the parabolinoidid anaprotaspides (Pl. II-32, Figs. 1-6) is unique to the family, not shared with any olenid species. The circular shield of the metaprotaspides (Pl. II-32, Figs. 7-18, 40-42) is comparable to that of *Olenus gibbosus* (Pl. II-29, Figs. 9-19). The slightly forward-expanding axis of the parabolinoidid anaprotaspides (Pl. II-32, Figs. 1-6) is comparable to that of *Olenus* species (Pl. II-29, Figs. 1, 4, 8, 9, 13, 17), but the axis of the parabolinoidids expands forwardly without any radical change of the course of axial furrows, whereas the axial furrows of *Olenus* anaprotaspides diverge relatively rapidly at the base of L4. The conditions of the anterior pits such as the depth and width in the parabolinoidids are comparable to those of *Acerocare* (Pl. II-31, Figs. 1-15) as well as *Olenus* (Pl. II-29, Figs. 1-19). The bilobation of L3/L2/L1 is found in the metaprotaspides of *Apoplanias rejectus* (Pl. II-30, Figs. 1-13). The posterior fixigenal spines of the parabolinoidid protaspides are shorter and more broadly-based than those of the olenids, and do not become longer and slender with growth as such olenid protaspides as *Olenus* and *Acerocare* (Pl. II-29, II-31) do. The axis of the parabolinoidid protaspides stands above the fixigenae with its own independent convexity and the axial furrows are relatively shallow. All the olenid species have such a profile of the axis, but have much

85

shallower axial furrows than the parabolinoidid protaspides.

Nonetheless, the best similarities are found with the Oleninae, which includes *Olenus gibbosus* and *Apoplanias rejectus*. The similarities of the early meraspid cranidia between *O. gibbosus* (Pl. II-29, Fig. 20) and the parabolinoidids (Pl. II-32, Figs. 19, 38) have been recognized (e.g., Westrop, 1986). All of them have a strongly annulated glabella, a slender eye ridge, and a pitted fixigenal surface. Some of these features are also found in the early meraspid cranidium of *Apoplanias rejectus* (Pl. II-30, Fig. 20). These similarities, however, can be easily extended into the early meraspid cranidia of *Aphelaspis* (see Pl. II-45, fig. 5), suggesting that those are generalized.

TAXA POSSESSING PROTASPID MORPHOTYPE E

A similar protaspid morphotype is present in *Aphelaspis subditus*, *Aphelaspis haguei*, *Aphelaspis tarda*, and *Aphelaspis*? *anyta* of the Aphelaspidinae, *Dytremacephalus granulosus* of the ?Aphelaspidinae. The protaspides are characterized by a subrectangular to subquadrate to elliptical shield, a slightly forward-expanding axis with strongly forward-expanding L4, glabellar furrows that shallower than axial furrows, anterior pits that are not distinguishable from the axial furrows, and a small protopygidium that is strongly directed ventrally.

Remarks. Protaspid similarities observed in this work and holaspid similarities suggested by several workers indicate that these species are a member of the Olenina.

Family UNCERTAIN
Subfamily APHELASPIDINAE Palmer, 1960

Remarks. The Aphelaspidinae has been placed within the family Pterocephaliidae along with Housiinae and Pterocephalinae (e.g., Pratt, 1992), ever since it was erected by Palmer (1960). Fortey and Chatterton (1988) questioned the membership of the Pterocephaliidae and excluded the Aphelaspidinae because the subfamily lacks a median ventral suture which is a synapomorphy of the Asaphida to which the Housiinae and Pterocephalinae are assigned. The protaspid features of the subfamily described below support the exclusion.

Robison (1964, p. 520) speculated an immediate evolutionary connection between *Aphelaspis* and *Elrathia* by recognizing narrowing of rostral Pl.s as an evolutionary trend for the lineage.

Genus APHELASPIS Resser, 1935
Aphelaspis subditus Palmer, 1962b
Pl. II-33, Figs. 1-22

1962b *Aphelaspis subditus* Palmer [part], p. 35, pl. 4, figs. 20-22 [only].
1965b *Aphelaspis subditus*, Palmer [part], p. 60, pl. 8, figs. 22, 24-26 [only].
1965 *Aphelaspis haguei*, Palmer [part], pl. 9, fig. 19 [left specimen only]
1969 *Aphelaspis subditus*, Hu, p. 445-449, pl. 2, figs. 1-40.
1984 *Aphelaspis subditus*, Palmer, fig. 2B.
1992 *Aphelaspis subditus*, Pratt, p. 53-54. pl. 13, figs. 14-21.

Diagnosis. see Pratt (1992, p. 53-54) for holaspid diagnosis. **Anaprotaspis**. Shield suboval. Axis forward-expanding with more strongly expanding L4. **Metaprotaspis**.

86

Shield subrectangular. Axis slightly forward-expanding with more strongly expanding L4. Axial furrows moderately deep. Glabellar furrows shallower than axial furrows. Posterior cranidial border furrow shallow and turns forwards distally. Protopygidium small and strongly projecting ventrally.

Stratigraphic and Geographic Distributions. This species occurs in the *Aphelaspis* Zone of the Steptoean Stage of Upper Cambrian. It has been reported from the Dunderberg Formation and Hamburg Formation in Nevada, and the Rabittkettle Formation in northwestern Canada.

Occurrence of Materials Described Herein. *Aphelaspis* Zone of the Hamburg Limestone (but more probably from lowermost part of Dunderberg Formation), Cherry Creek, Nevada (locality 13 in Text-fig. I-2).

Description of Protaspides

Anaprotaspid stage (CMC-P 39742, 39742a, Pl. II-33, Figs. 1-6). Shield elliptical in outline; 0.303 mm wide and 0.304 mm long. Axis with five lobes defined by transglabellar furrows, reaches anterior and posterior margins, and its anterior and posterior ends extend beyond fixigenae in lateral profile; L1/L2/L3 parallel-sided and 25% of shield width; L4 forward-expanding (or subtrapezoidal) with its lateral margin being straight-sided, and longest (sag.); Lp with greatest convexity and overhangs posterior margin.

Metaprotaspid stage (CMC-P 39742b, c, Pl. II-33, Figs. 7-13). Shield sub-pentagonal in outline; 0.502 mm (avg.) long and 0.488 mm (avg.) wide. Axis occupying 25% (avg.) of shield width. Posterior cranidial border furrow moderately deep and broad, and runs transversely up to mid-fixigenal width and turns forwards thereafter. Protopygidium oriented strongly ventrally, with 17% (avg.) of the shield length; two axial rings recognized, and no pleural and interpleural furrows developed. Circumocular tubercle pair present immediately in front of posterior cranidial border furrow and at mid-fixigenal width.

Aphelaspis haguei (Hall and Whitfield, 1877)
Pl. II-34, Figs. 1-24, Text-fig. V-4.5

1877 *Crepicephalus* (*Longanellus*) *haguei* Hall and Whitfield, p. 210, pl. 2, figs. 14, 15.
1938a *Aphelaspis simulans* Resser, p. 59, pl. 13, figs. 19-21.
1962b *Aphelaspis subditus* Palmer [part], p. 35-36, pl. 4, fig. 25 [only].
1965b *Aphelaspis haguei*, Palmer, p. 59-60, pl. 9, figs. 19-26.
1965b [?] *Aphelaspis subditus*, Palmer, p. 60, pl. 8, fig. 23 [only].
1965 *Aphelaspis walcotti*, Rasetti, p. 76, pl. 18, figs. 10-20.
1965 *Aphelaspis transversa*, Rasetti, p. 88, pl. 16, figs. 21-27.
1971 *Aphelaspis walcotti*, Hu and Tan [part], p. 62-66, pl. 8, figs. 4, 6-36, pl. 9, figs. 34-36 [only].
1987 *Aphelaspis*, Robison, fig. 13.21B.
1992 *Aphelaspis haguei*, Pratt, p. 53, pl. 13, figs. 1-13.

Diagnosis. see Pratt (1992, p. 53) for holaspid diagnosis. **Metaprotaspis**. Shield subquadrate. Axis forward-expanding with more strongly expanding L4. Axial furrows moderately deep. Glabellar furrows shallower than axial furrows. Palpebro-ocular ridge slender and separated from anterior border. Two pairs of fixigenal tubercles present. Posterior cranidial border furrow shallow and turns forwards distally. Protopygidium

small with two axial rings.

Stratigraphic and Geographic Distributions. This species occurs in the *Aphelaspis* Zone or correlatable zones (e.g., *Glyptagnostus reticulatus* and *Olenaspella regularis* Zones) of lowermost Steptoean Stage of Upper Cambrian. It has been reported from the Dunderberg Formation in Nevada, the Nolichucky Formation in Tennessee, the Deadwood Formation in South Dakota, and the Rabbitkettle Formation, Northwestern Territories, Canada.

Occurrence of Materials Described Herein. *Aphelaspis* Zone of Deadwood Formation; Moll section, Bear Butte, south-eastern Deadwood City, northern Black Hills, South Dakota (locality 5H in Text-fig. I-2); light grey colored, fine to medium crystalline limestone with a few intraformational pebbles.

Association of Protaspides. Specimens CMC-P 40309, 40309a, b, d (Pl. II-34, Figs. 25-36) have a circular shield, a less convex fixigenal area, less distinct glabellar furrows, and lack an eye ridge, so that they constitute a single ontogenetic sequence. These features are not continuous into CMC-P 40309c of *Aphelaspis haguei* (Pl. II-34, Figs. 1-3) which is the smallest metaprotaspis. Since the specimen CMC-P 40309c is smaller than CMC-P 40309d, the four specimens including CMC-P 40309d cannot be a part of the ontogeny of *A. haguei* incorporating CMC-P 40309c. These specimens are assigned to Aphelaspidinae sp. A.

Description of Protaspides

Early metaprotaspid stage (CMC-P 40309c, e, Pl. II-34, Figs. 1-7). Shield subquadrate; sagittal length ranges from 0.330 to 0.361 mm and width from 0.400 to 0.448 mm. Axis convex and stands moderately above fixigenal area, reaches anterior and posterior shield margins, and its anterior and posterior ends extend beyond pleural region in lateral profile; L3/L2/L1 parallel-sided and occupies 22% (avg.) of shield width; L4 forward-expanding with its lateral margin being straight-sided; transglabellar furrows as deep as axial furrows. Eye ridge slender and broadens distally. Anterior border in pleural region narrow and flat; the border in axial region not differentiated. Fixigenal area steeply slopes both abaxially and adaxially, forming moderate ridge in posterior view. Prosopon granulate and pitted. Posterior fixigenal spine short and stout. Anterior pits as deep as axial furrows. Distal margin of shield slightly concave. Protopygidium with one axial ring and 19% (avg.) of shield length.

Late metaprotaspid stage (CMC-P 40309f, g, Pl. II-34, Figs. 8-13). Shield subhexagonal, and from 0.404 to 0.441 mm in sagittal length, and from 0.453 to 0.477 mm in width. L3/L2/L1 25% of shield width. Two pairs of tubercles present in fixigenal area; posterior pair more conspicuous and located immediately in front of posterior cranidial border furrow and at adaxial two-thirds of transverse length of fixigenal area; anterior pair located opposite L3, and larger and indistinct. Posterior cranidial marginal border runs transversely and then turns forwards at two-thirds of fixigenal width; border furrow shallows and widens distally. Protopygidium oriented steeply ventrally and 12% of sagittal length; two axial rings present.

Aphelaspis tarda Rasetti, 1965
Pl. II-35, Figs. 1-29
1965 *Aphelaspis tarda* Rasetti, p. 79-80, pl. 20, figs. 1-18.
1983 *Aphelaspis tarda*, Hu [part], p. 26-29, pl. 10, figs. 1, 3-42 [only].

88

Diagnosis. A species of *Aphelaspis* with a relatively long preglabellar field, upsloping palpebral lobe, and rounded anterolateral corner of pygidium. **Anaprotaspis.** Shield circular. Axis forward-tapering; L4 strongly forward-tapering and convex; L3/L2/L1 bilobed. **Early metaprotaspis.** Shield circular. Axis forward-expanding with strongly expanding L4. Glabellar furrows shallower than axial furrows. Exoskeletal surface covered with fingerprint-like ornaments. Posterior fixigenal spines broadly-based and defined by shallow furrow. Occipital ring as small node. **Late metaprotaspis.** Shield subrectangular. Axis forward-expanding. Posterior cranidial border furrow turns forwards distally. Protopygidium small and strongly projecting ventrally. Cranidial exoskeletal surface covered with pits.

Stratigraphic and Geographic Distributions. This species occurs in the *Aphelaspis* Zone (lowermost Steptoean Stage of Upper Cambrian and in the Nolichucky Formation of Tennessee (locality 14 in Text-fig. I-2). the illustrated materials in this work also occur in the same locality. Many holaspid specimens of several *Aphelaspis* species including *A. tarda* from the Nolichucky Formation are described in Rasetti (1965) where more detailed locality information is available.

Association of Protaspides. Specimens CMC-P 43345 with 0.256 mm in sagittal length (Pl. II-35, Figs. 1-4) and CMC-P 43345a with 0.249 mm in sagittal length (Pl. II-35, Figs. 30-33) are within a similar size range, thus indicating that both could belong to the same ontogenetic instar. However, the former differs from the latter in having a more convex axis with a more convex L4 and lacking a posterior fixigenal spine pair. The morphologic transformation into CMC-P 43345b (Pl. II-35, Figs. 5-7), the smallest late anaprotaspis of *Aphelaspis tarda*, is more continuous from CMC-P 43345. In particular the posterior fixigenal spine of CMC-P 43345a is relatively sharp, whereas that of CMC-P 43345, although incompletely preserved, appears to be broadly-based and blunted. The latter condition is much more continuous into CMC-P 43345b. The L4 of CMC-P 43345 (Pl. II-35, Figs. 1-4) is more convex than that of CMC-P 43345a (Pl. II-35, Figs. 30-33). The convexity of L4 of CMC-P 43345b (Pl. II-35, Figs. 5-7) is more similar to CMC-P 43345. Thus, the specimen CMC-P 43345 is considered to represent an early anaprotaspis of *A. tarda*. The specimen CMC-P 43345a is considered to belong to another *Aphelaspis* species (*Aphelaspis* sp. A) co-occurring with *A. tarda* in the Nolichucky Formation, since the differences are not too great to assign it to a different genus; Rasetti (1965) described 17 *Aphelaspis* species from the Nolichucky Formation.

Description of Protaspides

Early anaprotaspid stage (CMC-P 43345, Pl. II-35, Figs. 1-4). Shield circular in outline; 0.256 mm long and 0.292 mm wide. Axis forward-expanding; L4 most convex and longest with its lateral margin being straight-sided; L3/L2/L1/Lp spindle-shaped but more strongly tapering posteriorly; L3/L2 bilobed, with 28% of shield width; transglabellar furrows shallower than axial furrows. Anterior pits deeper than axial furrows. Posterior fixigenal spine broadly-based.

Late anaprotaspid stage (CMC-P 43345b, c, Pl. II-35, Figs. 5-11). Shield 0.318 mm (avg.) wide and 0.304 mm (avg.) long. Axis parallel-sided with strongly forward-expanding L4; L3/L2/L1 with 25% (avg.) of shield width; sagittal furrow shallower. Posterior fixigenal spine broadly-based and delimited from rest of shield by shallow furrow. Surface with fingerprint-like microsculpture.

Early metaprotaspid stage (CMC-P 43345d, e, f, Pl. II-35, Figs. 12-19). Shield

89

subrectangular with anterior margin being rounded; 0.376 mm (avg.) wide and 0.363 mm (avg.) long. L3/L2/L1/L0 slightly tapers posteriorly, with their maximum with being 25% (avg.) of shield width; transglabellar furrows as deep as axial furrows. Fixigenal tubercle small and exsagittally located opposite to L0 and transversely one-third of fixigenal width from axial furrows. Protopygidium very small and separated from cephalon by shallow posterior cranidial marginal furrow which is confluent with furrow delineating posterior fixigenal spine.

Late metaprotaspid stage (CMC-P 43345g, Pl. II-35, Figs. 20-22). Shield 0.446 mm wide and 0.429 mm long. Axis parallel-sided; L4 less strongly forward-expanding; width of L3 25% of shield width. Fixigenal area ornamented with pits; small pits develop within axial furrows. Posterior cranidial marginal border furrows run diagonally posteriorly and then turn anteriorly at their distal portions. Protopygidium oriented steeply ventrally, 11% of shield sagittal length, and develops two axial rings and no pleural and interpleural furrows.

<center>*Aphelaspis brachyphasis* Palmer, 1962b</center>
<center>Pl. II-44, Figs. 1-12, Pl. II-45, Figs. 1-8, Pl. II-46, Figs. 1-9, Text-fig. V-4.7</center>
<center>1962a *Aphelaspis* sp. Palmer, p. 92-93, pl. 19, figs. 1-14.</center>
<center>1962b *Aphelaspis brachyphasis* Palmer, p. 33-35, pl. 4, figs. 1-19</center>
<center>1965b *Aphelaspis brachyphasis* Palmer, p. 58-59, pl. 8, figs. 13, 17-21.</center>

Diagnosis. See Palmer (1965b, p. 58) for diagnosis for holaspis. **Anaprotaspis**. Three pairs of marginal spines; anterior pair mid-shield length. **Metaprotaspis**. Two pairs of protopygidial marginal spines. L4 forward-expanding and L3/L2/L1 parallel-sided. Five pairs of hypostomal marginal spines with shallowly bifurcated ends.

Stratigraphic and Geographic Distributions. This species occurs in the *Aphelaspis* Zone (lowermost Steptoean Stage) of Upper Cambrian and in the Dunderbug Formation, eastern Nevada (locality 7 in Text-fig. I-2 and see also Text-fig. I-3). the illustrated materials in this work were recovered in sampling horizon M-150 in Dunderburg Formation, McGill Section, eastern Nevada.

Description of Protaspides

Anaprotaspid stage (UA 12799, 12801; Pl. II-44, Figs. 1, 2, 7). Shield circular in outline; 0.35 mm long and 0.43 mm wide. Three pairs of marginal spines; anterior pair located mid-shield length. Four glabellar lobe and Lp present (see Palmer, 1962a, pl. 19, fig. 1).

Early metaprotaspid stage (UA 12800, 12802, 12804, 12805; Pl. II-44, Figs. 3-6, 8-12). Shield subquadrate in outline; 0.49-0.52 mm wide and 0.41-0.43 mm long. Protopygidium strongly directed ventrally. Two pairs of protopygidial marginal spines. L4 forward-expanding and L3-L0 parallel-sided. Posterior cephalid border weakly developed. Posterior cephalic border furrow curved forwards distally. Eye ridge slender; proximal end opposite mid-L4 length. Fixigena covered with tubercles. Hypostome with five pairs of marginal spines with wide and shallowly bifurcated ends.

Late metaprotaspid stage (UA 12803, 12806, 12807; Pl. II-44, Fig. 9, Pl. II-45, Figs. 1-4). Shield trapezoidal in outline; 0.57-0.63 mm in width and 0.51-0.56 mm in length. Protopygidial axial rings differentiated. Protopygidial posterior margin indented dorsally.

Homology of Three Pairs of Marginal Spines in Anaprotaspides of *Aphelaspis* *brachyphasis*. Many ptychopariide anaprotaspides develop three pairs of marginal spines.

<center>90</center>

In most cases, anterior two pairs disappear at a subsequent metaprotaspid stage, and the posterior pair becomes a posterior fixigenal spine. The protaspid ontogeny of *Aphelaspis brachyphasis* allows for different conjecture of the homology of the posterior pair. The metaprotaspides have two pairs of spines along the posterior shield margin. The late metaprotaspides demonstrate that these two pairs are protopygidial (see Pl. II-45, Figs. 2, 4). No development of a fixigenal spine pair in small meraspid cranidia supports this argument (see Pl. II-45, Figs. 5, 6). The distal pair of the spines in these metaprotaspides appear to correspond to the posterior marginal spine pair of the anaprotaspides (compared Pl. II-44, Fig. 1 and Fig. 3). If this correspondence is indicative of homology, the posterior marginal spine pair of the anaprotaspides should be protopygidial. In that case, these protaspid specimens of *A. brachyphasis* cannot belong to the anaprotaspid stage because they develop the protopygidium. However, it cannot be ruled out that they lost the posterior fixigenal spines and then the early metaprotaspides gained two protopygidial spines. It is also possible that the late metaprotaspides lost the posterior fixigenal spines, the distal pair of spines, when they enter the meraspid period.

The protaspides of *Acerocare ecorne* have two pairs of marginal spines (see Pl. II-31, Figs. 9, 13), as this species does. However, the distal pair is fixigenal and the proximal pair is protopygidial. This is evidenced by the fact that the smallest meraspid cranidium (see Pl. II-31, Fig. 17) has the posterior fixigenal spine. *Olenus gibbosus* develops three pairs of marginal spines in its anaprotaspid stage (see Pl. II-29, Figs. 1, 4). Ontogenies of other *Olenus* species (e.g., *O. wahlenbergi*, Clarkson and Taylor, 1995) clearly demonstrate that the posterior pair is fixigenal, not protopygidial. Therefore, the homology of the posterior marginal spine of anaprotaspides is not universal to all the ptychopariide taxa.

Protaspides of *Aphelaspis* species and Their Taxonomic Implications. The protaspides of *Aphelaspis subditus* (Pl. II-33, Figs. 1-12) and *Aphelaspis tarda* (Pl. II-35, Figs. 1-22) are more similar to each other than to those of *Aphelaspis haguei* (Pl. II-34, Figs. 1-13). Protaspides of *A. haguei* are distinguished by possessing a distinct palpebro-ocular ridge, a shorter (sag.) L4, relatively distinct fixigenal tubercles, a shield margin surrounded by a concave border, and a very convex fixigenal area in late metaprotaspid stage. The absence of the anterior and mid-fixigenal spine pairs in these species, which is preserved in silicified specimens (e.g., Pl. II-44, Fig. 1), could be attributed to a preservational effect. However, in *Aphelaspis* species where all the three fixigenal spine pairs occur, they are all slender. Since the posterior fixigenal spines of the above three *Aphelaspis* species are relatively short and stout, the absence of the other two fixigenal spine pairs is most probably real. *Aphelaspis brachyphasis* shows very similar morphologies at the metaprotaspid stages to *Aphelaspis haguei*, but the anaprotaspides of the former differ in having a more square-shaped shield, three pairs of fixigenal spine pairs, and deeper axial furrows. The *Aphelaspis* protaspides are characterized by, among others, a distally forward-curved posterior cranidial border.

The olenid affinity of the Aphelaspidinae has been mentioned by several workers (e.g., Pratt, 1992). Of the olenid species, *Olenus gibbosus* (Pl. II-29) has the protaspides that are most comparable to the *Aphelaspis* protaspides. The anaprotaspides of *O. gibbosus* (Pl. II-29, Figs. 1-8) share with those of *Aphelaspis tarda* (Pl. II-35, Figs. 1-11) a circular shield and a forward-expanding axis with a more strongly expanding L4. The metaprotaspides of *O. gibbosus* (Pl. II-29, Figs. 9-19) are similar to those of *Aphelaspis*

species (Pl. II-33, Figs. 7-13, Pl. II-34, Figs. 8-13, Pl. II-35, Figs. 20-22) in having an eye ridge, a steeply-oriented protopygidium, and a pitted exoskeletal surface. The protaspides of *O. gibbosus* are distinguished by possessing three pairs of fixigenal spines in an anaprotaspid stage (Pl. II-29, Figs. 1, 4) and a long pygidial marginal spine pair in a metaprotaspid stage (Pl. II-29, Fig. 21). The last feature is evident in the silicified specimens of *Aphelaspis brachyphasis* (Pl. II-45, Figs. 1-4). Additional differences include less distinct axial furrows and transglabellar furrows, the absence of fixigenal tubercles (or lobes), and a transversely straight posterior cranidial marginal furrow in the olenid protaspides. The olenid affinity is considered plausible, such that the the Aphelaspidinae is placed in the Olenina together with the superfamily Olenacea including the Olenidae. With other olenid protaspides (e.g., *Acerocare* (Pl. II-31) and *Apoplanias* (Pl. II-30)), *Aphelaspis* shares fewer similarities. There seems to no single protaspid feature that is shared by *Aphelaspis* and all the olenid species, thus suggesting a possible paraphyly of the Olenidae; in effect, the olenid protaspides show considerable variability (see above).

<p style="text-align:center;">*Aphelaspis*? *anyta* (Hall and Whitfield, 1877)
Pl. II-36, Figs. 1-38, Pl. II-37, Figs. 35-38, Text-fig. V-4.4</p>

1877 *Crepicephalus* (*Loganellus*) *anytus* Hall and Whitfield, p. 219, pl. 2, figs. 19-21.
1886 *Liostracus anytus* Brögger, p. 212.
1937 *Dunderbergia anyta* (Hall and Whitfield), Resser, p. 9.
1965b *Dunderbergia*? *anyta*, Palmer, p. 39-40, pl. 4, figs. 8, 10, 14-16.
1971 *Dunderbergia*? *anyta*, Hu, p. 92-94, pl. 15, figs. 1-40, text-fig. 44.
1971 *Dytremacephalus granulosus*, Hu [part], p. 94-97, pl. 16, figs. 6, 7 [only].
Diagnosis. see Hu (1971, p. 92) for holaspid diagnosis. **Metaprotaspis.** Shield circular to subrectangular. Axis parallel-sided with slightly forward-expanding L4. Glabellar furrows shallower than axial furrows. Eye ridge less distinct. Protopygidium medium-sized, with two pairs of marginal spines. Cranidial exoskeletal surface covered with pits.
Stratigraphic and Geographic Distributions. This species occurs in the *Dunderbergia* Zone (upper Steptoean Stage of Upper Cambrian). It has been reported from the Notch Peak Formation in Utah, the Dunderberg Formation in Nevada, and Norway.
Remarks. Palmer (1965b, p. 39-40) assigned this species to the genus *Dunderbergia* in open nomenclature because it has a low convex cranidium, a long genal spine, and a narrower fixigenal area, and a narrower pygidial axis, which do not fall within the concept of *Dunderbergia*. The cranidial and pygidial features of this species strongly resemble those of many *Aphelaspis* species. Among other features, a smoothly curved anterior cranidial border, a more divergent anterior facial suture, and a shorter (sag.) pygidium with narrow (tr.) axis are shared with *Aphelaspis* species, but not with *Dunderbergia* species (see Palmer, 1965b for morphologies of *Aphelaspis* and *Dunderbergia* species). The pygidial border of *Dunderbergia* species is confluent with a post-axial ridge or terminal piece, which is not seen in this species and *Aphelaspis* species. In particular, early meraspid cranidia of this species (Pl. II-36, Fig. 29) are indistinguishable from those of *Aphelaspis* species (Pl. II-35, Fig. 23; see also Palmer, 1962a, pl. 19, figs 11-13). These similarities suggest that this species has a closer affinity with *Aphelaspis* than with *Dunderbergia*. Although no other aphelaspidine genera can better accommodate this species than *Aphelaspis*, the protaspid morphologies of this

<p style="text-align:center;">92</p>

species are dissimilar from those of *Aphelaspis* species, so that this species is questionably assigned to *Aphelaspis*.

A stratophenetic approach seems to have dictated the taxonomy of this species which co-occurs with several *Dunderbergia* species in the *Dunderbergia* Zone; *Aphelaspis* species generally occur in the *Aphelaspis* Zone, which is lower than the *Dunderbergia* Zone.

Occurrence of Materials Described Herein. *Dunderbergia* Zone of the Notch Peak Formation; Lawson Cove, Utah (UGSG collection number is 5503-CO) (locality 15 in Text-fig. I-2).

Assocation of Protaspides. A radical metamorphosis must be inferred between anaprotaspides and metaprotaspides; the accompanying changes include the disappearance of anterior an mid-fixigenal spines, hypostomal spines becoming short and blunted, and the disappearance of bilobation of the axis. The association of the anaprotaspid specimens is provisional.

Description of Protaspides

Anaprotaspid stage (CMC-P 38733a, b, c, d, e, 38734e, Pl. II-36, Figs. 1-13, Pl. II-37, Figs. 35, 36). Shield circular in outline, with straight anterior and indented posterior margins; sagittal length ranges from 0.320 to 0.342 mm and width from 0.338 to 0.376 mm. Axis reaches anterior and posterior margin; Lp/L1/L2/L3 spindle-shaped and bilobed, with its width taking 27% of shield width; L4 subtrapezoidal and forward-expanding. Anterior pits deeper than axial furrows. Three pairs of fixigenal spines; anterior pair located at mid-shield length; posterior pair directed ventrally. Hypostome shield-shaped, with 9 slender marginal spines. Doublure inturned and narrow.

Early metaprotaspid stage (CMC-P 38733f, h, g, 38734f, Pl. II-36, Figs. 14-21, Pl. II-37, Figs. 37, 38). Shield elliptical in outline and ranges from 0.418 to 0.481 mm in width and from 0.412 to 0.472 mm in sagittal length. Anterior and mid-fixigenal spines disappear. Lp/L0/L1/L2/L3 parallel-sided, occupying 14% (avg.) of shield width; sagittal furrow to bilobed L1/L2/L3 disappears. Fixigenal area pitted. Hypostomal spines short and blunt. Eye ridge slender. Anterior pits shallow, but still deeper than axial furrows. Posterior fixigenal spine blunted, short, and pointing ventrally and adaxially. Narrow, flat border surrounds posterior half of shield. Posterior cranidial marginal furrow directed posteriorly. Protopygidium with two axial rings; 24% (avg.) of shield sagittal length; posterior margin indented.

Late metaprotaspid stage (CMC-P 38733i, j, Pl. II-36, Figs. 22-27). Shield from 0.500 to 0.540 mm in width and 0.548 to 0.554 mm in sagittal length. L3/L2/L1/L0 parallel-sided, occupying 26% of shield width. Eye ridge distinct. Protopygidium oriented ventrally; sagittal length 20% of shield length; two pairs of short protopygidial marginal spines. Surface covered with pits.

Protaspides of *Aphelaspis*? *anyta* and Their Taxonomic Implications. The protaspid similarities of *Aphelaspis*? *anyta* with *Aphelaspis subditus* were mentioned by Hu (1971, p. 66). The questionable anaprotaspides of *Aphelaspis*? *anyta* (Pl. II-36, Figs. 1-13, Pl. II-37, Figs. 35-36) are most similar to early anaprotaspides of *Aphelaspis* sp. A (Pl. II-35, Figs. 30-33), but differ in their larger size and in having three pairs of slender fixigenal spines and a spindle-shaped L3/L2/L1. The posterior cranidial border of the *A.*? *anyta* metaprotaspides (Pl. II-36, Figs. 14-27) does not turn forwards at its distal end, which suggests a generic level separation of this species from *Aphelaspis*. Nonetheless, other

93

similarities of the metaprotaspides, such as a parallel-sided L3/L2/L1, a forward-expanding L4 and a ventrally oriented protopygidium, support the placement of this species in the Aphelaspidinae.

The elviniid protaspides (*Elvinia roemeri*, Pl. II-38, Figs. 1-15) are not comparable to the protaspides of *Aphelaspis*? *anyta*, in having a circular, flattened shield surrounded by a narrow marginal border and a slightly forward-tapering narrow axis, supporting that *A.*? *anyta* is not a member of the Elviniinae to which *Dunderbergia* belongs.

Previvous Taxonomic and Evolutionary Suggestions for the Aphelaspidinae. The Aphelaspidinae has been generally considered to be a subfamily of the Pterocephaliidae, along with Housiinae and Pterocephaliinae (Palmer, 1960, 1962b, 1965b; Pratt, 1992). The evolutionary connection of the Aphelaspidinae with the Housiinae was supported by their morphologic continuities through *Prehousia* (Palmer, 1965b, p. 57-58). The stratigraphic occurrences of these trilobites (Palmer, 1965b, fig. 10) correspond with this assumed anagenetic evolutionary lineage in which *Aphelaspis* in the *Aphelaspis* Zone gave rise to *Prehousia* in the *Prehousia* Zone, which in turn gave rise to *Housia* in the *Elvinia* Zone. The stratophenetic changes include the sagittal elongation of the cranidium and glabella, narrowing of the anterior fixigenae, transverse elongation of the posterior fixigenae, inward migration of the palpebral lobes, shallowing of the glabellar furrows, sagittal elongation of the pygidium while maintaining its width, resulting in a more circular outline, and broadening of the pygidial marginal border. Robison (1964, p. 520) proposed the same evolutionary relationship, but he presented narrowing of the rostral plate as evidence (text-fig. 4).

Robison (1964, p. 520) made an evolutionary connection between *Aphelaspis* and *Elrathia* based on the ventral axial structures such as the presence of rostral plate. The cranidial and pygidial architectures of *Aphelaspis* can be readily considered as evolutionary modifications from those of *Elrathia* such as broadening of the anterior fixigenal area, exsagittal shortening of the posterior fixigenal area, and reduction in the number of pygidial segments. Hu (1983, text-fig. 5) suggested that *Aphelaspis* descended from olenids outside the Laurentia, and then it migrated into the continent and gave rise to *Dunderbergia* and *Dytremacephalus*.

Fortey and Chatterton (1988, p. 206-209) reviewed this evolutionary relationship and excluded the Aphelaspidinae from the Pterocephaliidae, and assigned the other two pterocephaliid subfamilies to the Asaphida. The Aphelaspidinae was considered to share only plesiomorphic features with the other two pterocephaliid subfamilies. This was mainly based on the fact that the Aphelaspidinae has a rostral plate and the other two have a median ventral suture, which is regarded as a synapomorphy of the Asaphida.

Aphelaspidine Protaspides and Their Taxonomic Implications. The protaspides of *Aphelaspis* species differ from those of *Housia* (Housiinae, Pl. II-17) in having a parallel-sided axis with a forward-expanding L4, distinct transglabellar furrows, a posterior cranidial marginal border which turns anteriorly at two-thirds length, a palpebro-ocular ridge, and a more rectangular outline. The protaspides of *Pulchricapitus* (?Pterocephaliinae, Pl. II-18, Figs. 23-26) appear to be intermediate between those of the Housiinae and Aphelaspidinae. With the housiine protaspides, they share a wider axis and a convex shield, and both lack a posterior fixigenal spine pair and pygidial marginal spines, which are present in the aphelaspidine protaspides. The *Pulchricapitus* protaspides share with the aphelaspidine protaspides a forward-expanding L4 and a

94

parallel-sided L3/L2/L1. It is certain that the Aphelaspidinae does not have a close enough relationship with the Housiinae to place both subfamilies within the same family, supporting Fortey and Chatterton (1988)'s suggestion.

Since protaspides of *Elrathia* have not been described, and its familial assignment is uncertain (Robison, 1988), the evolutionary connection between *Elrathia* and *Aphelaspis* suggested by Robison (1964, p. 520) is not readily evaluated by using protaspid morphologies. *Elrathia* was considered a member of the family Alokistocaridae along with *Elrathina* (Moore, 1959). Blaker and Peel (1997, p. 124) considered *Elrathina* and *Eoptychoparia* as a junior synonym of *Ptychoparella* of the Ptychopariidae. Of interest is that the anaprotaspides of Lower Cambrian *Ptychoparella* sp. A (Blaker and Peel, 1997, fig. 74.1, 2) are similar to the early metaprotaspides of *Aphelaspis haguei* (Pl. II-34, Figs. 1-7) in their having a subtrapezoidal shield outline, a forward-expanding L4, and a posterior fixigenal spine pair. The former differs in having a narrower (tr.) axis with forward-tapering L3/L2/L1, a smooth exoskeletal surface, and less distinct transglabellar furrows. Other ptychopariid protaspides such as those of *Crassifimbra* (Palmer, 1958, pl. 26, figs. 1, 2), *Ehmaniella* (Kopaska-Merkel, 1981, figs. 1A-D), and *Solenopleura* (Pl. II-28, Figs. 1, 3) mainly differ from the *Ptychoparella* protaspides in having a circular shield. Their protaspid morphologies are indicative of close evolutionary relationships between the Aphelaspidinae and the Ptychopariidae including *Ptychoparella* and probably *Elrathia*. Differences of holaspid morphologies include the lack of a plectrum, and less distinctly-impressed glabellar furrows in Upper Cambrian aphelaspidines. Middle Cambrian *Elrathia* would fit well into this evolutionary sequence.

Comparison of these Lower and Middle Cambrian ptychopariide protaspides with those belonging the Redlichiida and Corynexochida leads to an evolutionarily very interesting point. Zhang and Pratt (1999) described the protaspides of an Early Cambrian redlichiid, *Ichangia*. The protaspides (Zhang and Pratt, 1999, figs. 5.1-5.10) have a circular shield, a strongly forward-expanding L4, a parallel-sided L3/L2/L1, a lateral border, two pairs of fixigenal spines, and a pair of indistinct fixigenal tubercles opposite to Lp; the presence of the last feature in other Cambrian taxa and even in *Ichangia* is not obvious. The first five features are present in the protaspides of a Middle Cambrian corynexochid, *Bathyuriscus* (Robison, 1967, pl. 24, figs. 3-5) and a Lower Cambrian ptychopariid, *Crassifimbra* (Palmer, 1958, pl. 26, fig. 2). The corynexochid protaspides have three pairs of fixigenal spines and the ptychopariid protaspides have one pair of spines. The protaspides of these older trilobite taxa are greatly similar, as noted by Robison (1967). However, the relatively younger trilobites of the Ptychopariida and Corynexochida morphologically deviate from these primitive forms. This suggests that the protaspid morphologies were more evolutionarily constrained than the holaspid morphologies during early part of the Cambrian period. The constraints became loose as they evolved. Such an increase of morphologic disparity at the earlier developmental stages through time could be closely related to the great diversification of the trilobites towards the later part of Cambrian period.

Hu (1983, p. 32-33) claimed that the olenid derivation of *Aphelaspis* is supported by their similar protaspid morphologies. The similarities found between the anaprotaspides of *Olenus gibbosus* (Pl. II-29, Figs. 1-19) and *Aphelaspis* species (see above) are in agreement with Hu's suggestion. This further supports the recurring opinion that the Olenidae is evolutionarily related to many other families, thus incorporating the family

95

within the Olenina along with such groups as the Aphelaspidinae and Elviniidae.

In order to test whether the Aphelaspidinae has a sistergroup relationship with the Olenidae or some Middle Cambrian ptychopariid trilobites, the ontogeny of the trilobites of the latter group, such as *Elrathia*, needs to be described upon the basis of much better specimens.

<div align="center">

?Subfamily APHELASPIDINAE Palmer, 1960
Genus DYTREMACEPHALUS Palmer, 1954b

</div>

Remarks. The genus *Dytremacephalus*, when erected, was considered to be related to *Aphelaspis* (Palmer, 1954b). Later, it was considered more probable that this genus has an elviniid affinity since it shares similarities with *Dunderbergia* and *Elburgia* (Palmer, 1954b, p. 84-85; Pratt, 1992, p. 50). These elviniine genera and *Dytremacephalus* have an angulated anterior border and a much wider (tr.) and shorter (sag.) pygidial axis. Hu (1971, p. 94) assigned this genus to the Pterocephaliidae, without any reasonable explanations.

Hu (1983, text-Fig. 5) suggested that *Aphelaspis* gave rise to *Dunderbergia* and *Dytremacephalus* which in turn gave rise to such elviniine genera as *Elvinia* and *Irvingella*. The cranidial and pygidial architectures of *Aphelaspis* are certainly similar to those of *Dunderbergia* and *Dytremacephalus*. The morphologic differences of *Dunderbergia* and *Dytremacephalus* from *Aphelaspis* include an angulated (vs. smooth) anterior border, a larger glabella, a wider (tr.) pygidial axis, and a pygidial marginal border confluent with a terminal piece. These differences are considered to be within the range of morphologic variation of an evolutionary lineage. The taxonomic separation of *Dunderbergia* and *Dytremacephalus* from *Aphelaspis* was strongly influenced by stratophenetic approaches (e.g., Palmer, 1965b).

Based on holaspid morphologies, the most plausible taxonomy is that *Dytremacephalus*, *Elburgia* and *Dunderbergia* constitute one higher taxon and *Elvinia*, *Irvingella*, and *Elviniella* form another. The latter taxon is characterized by an angulated anterior cranidial border and the latter, which seems to be an evolutionary derivative from the former, by a transglabellar S1 furrow and relatively flat pygidial pleural field. The former seems to be more closely related to the Aphelaspidinae than to the latter taxon.

<div align="center">

Dytremacephalus granulosus Palmer, 1954b
Pl. II-37, Figs. 1-34, Text-fig. V-4.8

</div>

1954b *Dytremacephalus granulosus* Palmer, p. 750, pl. 85, figs. 5, 6.
1965b *Dytremacephalus granulosus*, Palmer, p. 85, pl. 18, figs. 14, 16-19, 21.
1971 *Dytremacephalus granulosus*, Hu [part], p. 94-97, pl. 16, figs. 1-5, 8-36 [only].

Diagnosis. see Hu (1971, p. 94-95) for holaspid diagnosis. **Anaprotaspis.** Shield circular. Axis parallel-sided with forward-expanding L4; L3/L2/L1 bilobed. Posterior fixigenal spines short and slender. **Metaprotaspis.** Shield elliptical. Axis parallel-sided with forward-expanding L4. Axial furrows moderately deep. Glabellar furrows shallower than axial furrows. Posterolateral end of fixigenae projecting ventrally. Posterior fixigenal spines short and slender. Protopygidium small and strongly projecting ventrally, with three axial rings.

Stratigraphic and Geographic Distributions. This species occurs in the *Dunderbergia* Zone of upper Steptoean Stage of Upper Cambrian, and has been reported from the Riley

<div align="center">

96

</div>

Formation in Texas, the Lincoln Peak Formation in Nevada, and the Notch Peak Formation in Utah.

Occurrence of Materials Described Herein. *Dunderbergia* Zone of the Notch Peak Formation (USGS collection no. 5503-CO), Lawson Cove Section (personal communication, Palmer, 1998), Wah Wah Range, Utah (locality 15 in Text-fig. I-2).

Association of Protaspides. Specimen CMC-P 38734e (Pl. II-37, Figs. 35, 36, see also Hu, 1971, pl. 16, fig. 6) has three pairs of fixigenal spines which are typical of *Aphelaspis*? *anyta* (38733). It also has a spindle-shaped L1/L2/L3 which characterizes anaprotaspides of *Aphelaspis*? *anyta* (CMC-P 38733a-d, Pl. II-36, Figs. 1-12). Specimen CMC-P 38734f (Pl. II-37, Figs. 37, 38) has posterior fixigenal spines which are blunt, as seen in *Aphelaspis*? *anyta* (CMC-P 38733f, g, and h, Pl. II-36, Figs. 14-21). Both specimens are re-assigned to *Aphelaspis*? *anyta*.

Description of Protaspides

Anaprotaspid stage (CMC-P 38734a, b, c, d, Pl. II-37, Figs. 1-11). Shield circular in outline; sagittal length ranges from 0.278 to 0.305 mm and width from 0.274 to 0.342 mm; in posterior view, fixigenal area runs horizontally and then rapidly slopes ventrally. Axis reaches anterior and posterior margins; L3/L2/L1 bilobed and parallel-sided, occupying 27% of shield width; L4 strongly forward-expanding, with its lateral margin straight-sided. Posterior fixigenal spine slender and short. Posterior shield margin between posterior fixigenal spines upturned. Doublure inturned and narrow. Hypostome rectangular and 0.113 mm in sagittal length; median lobe triangular; pair of short marginal spines at mid-hypostomal length.

Early metaprotaspid stage (CMC-P 38734g, h, Pl. II-37, Figs. 12-17). Shield ranges from 0.365 to 0.390 mm in width and from 0.356 to 0.374 mm in length. Axis with five lobes; width of L3 26% of shield width; L0 delineated by shallow furrow posteriorly. Protopygidia not delimited by distinct posterior cranidial marginal furrow in pleural region. Base of posterior fixigenal spines broadly spaced.

Late metaprotaspid stage (CMC-P 38734i, j, Pl. II-37, Figs. 18-24). Shield elliptical in outline and ranges 0.400 to 0.460 mm in width and 0.405 to 0.469 mm in length. L3 occupies 27% (avg.) of shield width. Postero-lateral end of fixigenae anterior to posterior fixigenal spines extend beyond posterior fixigenal spines in posterior view. Posterior cranidial border furrow distinctly impressed. Protopygidium occupies 22% (avg.) of shield length and oriented ventrally; pair of short marginal spines; posterior margin slightly arched dorsally.

Protaspides of *Dytremacephalus granulosus* and Their Taxonomic Implications. The protaspides of *Dytremacephalus granulosus* allow us to test the affinity of *Dytremacephalus* to the elviniines. The early metaprotaspides of *Dytremacephalus granulosus* (Pl. II-37, Figs. 12-24) are greatly dissimilar from those of *Elvinia roemeri* (Pl. II-38, Figs. 1-12). The former has a forward-expanding axis, a convex shield, and a pair of posterior fixigenal spines, whereas the latter has a spindle-shaped axis, a flattened shield, concave posterior and lateral shield borders, and a distinct eye ridge. The late metaprotaspides of both species also are very different from each other (see Pl. II-37, Figs. 18-22 and Pl. II-38, Figs. 13-15). The protaspid morphologies do not corroborate the taxonomic placement of *Dytremacephalus* in the Elviniinae together with *Elvinia*. The protaspides of *D. granulosus* are more similar to those of *Aphelaspis*? *anyta* (Pl. II-36, Figs. 14-27) in having a ventrally-oriented protopygidium with marginal spines. The

97

ventrally-extending postero-lateral ends of the fixigenae in the late metaprotaspides (Pl. II-37, Fig. 22) and the short posterior fixigenal spines in the anaprotaspides and early metaprotaspides (Pl. II-37, Figs. 9, 14) readily distinguish *D. granulosus* from *A.? anyta*. Nonetheless, *Dytremacephalus* seems to be more closely related to the Aphelaspidinae than to the Elviniidae.

TAXA POSSESSING PROTASPID MORPHOTYPE F

Protaspides of *Elvinia roemeri* of the Elviniidae differ from those of aphelaspidines in having a circular shield, a spindle-shaped axis with a L4 that is waisted at its mid-length, a distinct eye ridge, and a long post-axial region.

Family **ELVINIIDAE** Kobayashi, 1935
Subfamily **ELVINIINAE** Kobayashi, 1935

Remarks. The Elviniinae was believed to contain *Dunderbergia* Walcott, 1924, *Elburgia* Palmer, 1960, *Elvinia* Walcott, 1924, *Elviniella* Palmer, 1960, *Irvingella* Ulrich and Resser *in* Walcott, 1924 and *Dytremacephalus* Palmer, 1954b (Palmer, 1965b; Pratt, 1992). *Dunderbergia, Elburgia,* and *Dytremacephalus* are considered here to be more closely related to each other and to the Aphelaspidinae (see above); at least it is unlikely that *Dytremacephalus* is a member of the Elviniinae (see above).

Genus **ELVINIA** Walcott, 1924
Elvinia roemeri (Shumard, 1861)
Pl. II-38, Figs. 1-19, Text-fig. V-4.6

1965b *Elvinia roemeri*, Palmer, p. 44, pl. 3, figs. 9, 11, 14, 16 (see for synonymy to date)
1965 *Elvinia roemeri*, Grant, p. 115, pl. 9, fig. 22.
1971 *Elvinia roemeri*, Stitt, p. 21, pl. 1, fig. 11.
1975 *Elvinia roemeri*, Kurtz, p. 1031, pl. 1, fig. 12,
1979 *Elvinia roemeri*, Hu [part], p. 50, pl. 8, figs. 5, 7-28 [only].
1982 *Elvinia roemeri*, Palmer, p. 6, pl. 1, figs., 1, 4, 5.
1986 *Elvinia roemeri*, Westrop, p. 62, pl. 30, figs. 14-16.
1989 *Elvinia roemeri*, Hohensee and Stitt, p. 871, fig. 6.1.
1992 *Elvinia roemeri*; Pratt, p. 48, pl. 11, figs. 1, 2.

Diagnosis. see Palmer (1965b, p. 44) for holaspid diagnosis. **Early metaprotaspis.** Shield circular. Axis spindle-shaped; L4 waisted at mid-length. Eye ridge distinct. Axial furrows shallow. Lateral and posterior shield border flat. Area behind occipital ring relatively long (sag.). **Late metaprotaspis.** Shield elliptical. Axis parallel-sided. Anterior border narrow. Eye ridge separated from anterior border. Protopygidium large with at least three axial rings.

Stratigraphic and Geographic Distributions. This species occurs in the *Elvinia* Zone (uppermost Steptoean of Upper Cambrian). It has been reported from the Dry Creek Shale, Gallatin Formation, and Snowy Range Formation in Wyoming, the Deadwood Formation in South Dakota and Montana, the Notch Peak Formation and St. Charles Dolomite in Utah, the Dunderberg Formation in Nevada, the Honey Creek Formation and Reagan Sandstone in Oklahoma, the Cap Mountain Formation and Wilberns Formation in

98

Texas, the Gatesburg Formation in Pennsylvania, the Davis Formation in Indiana and Missouri, the Collier Shale in Arkansas, the Goodsir Formation in British Columbia, the Bison Creek Formation in Alberta, the Rabbitkettle Formation in Northwest Territories and from Argentina.

Occurrence of Materials Described Herein. *Elvinia* Zone (uppermost Steptoean) of the Deadwood Formation; Galina, Brownsville Junction, Little Elk Creek, Boxelder, Nemo, and Dark Canyon, along the east side of the Black Hills, between Deadwood and Rapid City, South Dakota (locality 5I in Text-fig. I-2).

Association of Protaspides. Of 12 protaspid specimens assigned to *Elvinia roemeri* by Hu (1979), four morphologically separable groupings are recognized by the shape of their axis and the condition of palpebro-ocular ridge. The first protaspid group consists of specimens CMC-P 43372d, f, g, h, i, j, and k (Pl. II-38, Figs. 1-15), which represent the protaspid stages of *Elvinia roemeri*. The glabellar shape that L4 is slightly waisted at its mid-length and L3/L2/L1 is slightly convex laterally is shown in the meraspid cranidia (Pl. II-38, Fig. 16; Hu, 1979, pl. 8, figs. 13-16) as well as these protaspid specimens. Along with the presence of distinct palpebro-ocular ridge, the glabellar shape confirms this association.

The specimens CMC-P 43372 and 43372a (Pl. II-38, Figs. 24, 25) have an axis with spindle-shaped L3/L2/L1 and a subtrapezoidal L4, two pairs of fixigenal spines, which are located well anterior to mid-shield length and project from a flat border. The distinct palpebro-ocular ridge is indicative of being related to *Elvinia roemeri*. Since both are small, it is not entirely implausible that they represent an anaprotaspid stage of *E. roemeri*. However, a metamorphosis must be introduced in order to incorporate them into the ontogeny of *E. roemeri*. Both specimens are assigned to species undetermined W.

Specimen CMC-P 43372b (Pl. II-38, Fig. 20) has an axis similar to that of the early metaprotaspides of *Elvinia roemeri* (Pl. II-38, Figs. 1-12). Due to poor preservation, its association with *E. roemeri* is not confirmed; it is questionably assigned to *Elvinia* sp. A.

Specimen CMC-P 43372e (Pl. II-38, Fig. 21) has a parallel-sided or slightly forward-expanding axis, a less distinct eye ridge, and a slightly indented posterior margin which is also moderately upturned. These features are not comparable to early metaprotaspides of *Elvinia roemeri* (Pl. II-38, Figs. 1-12). This specimen is named species undetermined U.

Specimen CMC-P 43372c (Pl. II-38, Figs. 22, 23) has a forward-expanding axis, which is similar to the anaprotaspis of *Aphelaspis tarda* (Pl. II-35, Figs. 1-4). However, this specimen is much larger than the latter one. This specimen is named species undetermined V.

Description of Protaspides.

Early metaprotaspid stage (CMC-P 43372d, f, g, h, i, j, Pl. II-38, Figs. 1-12). Shield circular in outline and surrounded by concave border; sagittal length ranges from 0.387 to 0.513 mm and width from 0.408 to 0. 522 mm. Axis narrow (occupying 22 % of the shield width) and spindle-shaped; L4 slightly waisted at mid-length. Eye ridge distinct, runs along anterior shield margin and separated from anterior margin by anterior fixigenal area. Occipital ring present as small node. Behind occipital ring, relatively long (sag.) protopygidial region differentiated.

Late metaprotaspid stage (CMC-P 43372k, Pl. II-38, Figs. 13-15). Shield elliptical, with anterior margin straight; 0.625 mm wide and 0.716 mm long. Glabella parallel-sided, occupying 24% of shield width; L4 slightly forward-expanding in its anterior half.

99

Anterior border narrow, and incurved and depressed sagittally. Eye ridge distinct and separated from anterior border by narrow anterior fixigenal area. Posterior cranidial border furrow broad. Protopygidium with 40% of shield length, triangular in outline; anteriormost segment carries distinct pleural furrow.

Protaspides of *Elvinia roemeri* and Their Taxonomic Implications. The metaprotaspides of *Elvinia roemeri* exhibit a unique combination of several features (Pl. II-38, Figs. 1-15), so that it is impossible to determine whether it is closely related to any one of the species described in this work. The palpebro-ocular ridge runs along the anterior shield margin and is located well inside the anterior margin. Of many species which have the palpebro-ocular ridge, the closest condition is found in *Olenus gibbosus* (Pl. II-29, Figs. 1, 4, 8, 9, 13, 17), *Ptychaspis bullasa* (Pl. II-27, Figs. 1, 5) and *Crepicephalus deadwoodiensis* (Pl. II-14, Fig. 22). The concave border surrounds the shield from the mid-shield length and posteriorly thereafter. *Olenus gibbosus* (Pl. II-29, Figs. 1, 4, 8, 9, 13, 17) have the most similar condition of the border. The flattened shield of *E. roemeri* protaspides is also similar to that of the olenid protaspides. The narrow axis with a waisted long L4 and spindle-shaped L3/L2/L1 is unique to *E. roemeri*. Behind the occipital ring, the early protaspides have a sagittally long and flat post-axial region which most probably represents a protopygidial region; although the early metaprotaspides of *Crepicephalus deadwoodiensis* bear the same condition (Pl. II-14, Figs. 10, 15), the region is not as flat as in *E. roemeri*. The circular shield of the early metaprotaspides of *E. roemeri* is similar to that of *O. gibbosus*, some *Aphelaspis* species (e.g., Pl. II-34, Figs. 25, 31), *Dytremacephalus granulosus* (Pl. II-37, Figs. 10, 13). It appears to be *Olenus gibbosus* that shares the most protaspid similarities, so *Elvinia* is assigned to the Olenina together with the Olenidae.

?Subfamily **ELVINIINAE** Kobayashi, 1935
Genus **IRVINGELLA** Ulrich and Resser *in* Walcott, 1924
Irvingella major Ulrich and Resser *in* Walcott, 1924
Pl. II-39, Figs. 1-12

1965b *Irvingella major*, Palmer [part], p. 48, pl. 6, figs. 9-12, 14, 15 [only] (see for synonymy to date).
1965 *Irvingella major*, Grant, p. 126-127, pl. 10, figs. 8, 9, 11.
1971 *Irvingella major*, Stitt, p. 21, pl. 1, fig. 12.
1975 *Irvingella major*, Kurtz, p. 1031, p. 4, fig. 37.
1979 *Irvingella major*, Hu, p. 53, pl. 8, figs. 29-36, text-fig. 2.
1986 *Irvingella major* Westrop, p. 63, pl. 30, figs. 8-13.
1989 *Irvingella major*, Hohensee and Stitt, p. 871, figs. 6.2, 6.3.
1992 *Irvingella major*, Pratt, p. 48-49, pl. 11, figs. 3-6.

Diagnosis. see Palmer (1965b, p. 48) for holaspid diagnosis. **Early metaprotaspis.** Shield circular and strongly convex. Axis parallel-sided. Glabellar furrows shallower than axial furrows. Occipital ring small node. Area behind the occipital ring relatively long. Exoskeletal surface covered with fingerprint-like ornaments. **Late metaprotaspis.** Shield subrectangular and convex. Axis parallel-sided with strongly forward-expanding L4. Protopygidium medium-sized with three axial rings. Two pairs of protopygidial marginal spines present. Posterior protopygidial margin straight.

Stratigraphic and Geographic Distributions. This species occurs in the *Elvinia* and

100

Irvingella major Zones (uppermost Steptoean of Upper Cambrian). It has been reported from the Franconia Formation in Wisconsin, the Gatesburg Formation in Pennsylvania, the Collier Shale in Arkansas, the Reagan Sandstone and Honey Creek Formation in Oklahoma, the Davis Formation in Missouri, the Wilberns Formation in Texas, the Secret Canyon Shale and Dunderberg Formation in Nevada, the Deadwood Formation in South Dakota, the Snowy Range Formation and Gallatin Formation in Wyoming, the Lyell Formation and Bison Creek Formation in Alberta, the Rabbitkettle Formation in Northwest Territories, and from Argentina and Novaya Zemlya of Russia.

Occurrence of Materials Described Herein. *Elvinia* Zone (uppermost Steptoean) of the Deadwood Formation; Moll section, near Bear Butte, about 6 miles southeast of Deadwood, South Dakota (locality 5H in Text-fig. I-2).

Association of Protaspides. Only two protaspid specimens (CMC-P 43375f and g, Pl. II-39, Figs. 1-7) are available. With respect to the shape of the axis and convexity of the shield, both are considered to belong to a single ontogenetic sequence. The parallel-sided glabella of both protaspid specimens is present in a meraspid cranidium (CMC-P 43375e, Pl. II-39, Fig. 8). The late metaprotaspid specimen (CMC-P 43375f, Pl. II-39, Fig. 5) has a protopygidium with short marginal spines which is also observed in a transitory pygidium (CMC-P 43375d, Pl. II-39, Fig. 9). With this regard, the two protaspid specimens are considered correctly associated with *Irvingella major*. However, since the morphologic transition from the transitory pygidia into the holaspid pygidium (e.g., Palmer, 1965b, pl. 6, figs. 9, 11) has not been filled with ontogenetically intermediate forms, the association is not confident.

Palmer (1965b, pl. 6, fig. 13) illustrated a metaprotaspis from the Dunderberg Formation in Nevada, and assigned it to *Irvingella major*. It has a forward-tapering glabella and a non-spinose protopygidial margin. Since the specimen with 0.867 mm in sagittal length is longer than CMC-P 43375f with 0.589 mm in sagittal length, it may represent a later ontogenetic stage of the CMC-P 43375f. However, its forward-tapering glabella cannot be an intermediate between CMC-P 43375f and the smallest meraspid cranidium (Pl. II-39, Fig. 8). Nonetheless, the possibility that Palmer's association is correct cannot be ruled out, since the association of CMC-P 43375f is not confident.

Description of Protaspides

Early metaprotaspid stage (CMC-P 43375g, Pl. II-39, Figs. 1-4). Shield circular and very convex; 0.450 mm wide and 0.424 mm long. Axis parallel-sided with its anteriormost end slightly forward-expanding, with 28% of shield width; transglabellar furrows much shallower than axial furrows. Differentiation of protopygidium recognized by presence of occipital ring; posterior cranidial marginal furrow not impressed. Surface covered with fingerprint-like microsculpture.

Late metaprotaspid stage (CMC-P 43375f, Pl. II-39, Figs. 5-7). Shield elliptical; 0.589 mm long. Posterior cranidial marginal furrow as deep as axial furrows. Protopygidium semicircular in outline and occupies 31% of sagittal shield length; at least two axial rings present; pleural furrows shallow; two pairs of marginal spines developed.

Protaspides of *Irvingella major* and Their Taxonomic Implications. The early metaprotaspis of *Irvingella major* (Pl. II-39, Figs. 1-4) differs from those of *Elvinia roemeri* (Pl. II-38, Figs. 1-15). The two species of the Elviniidae do not seem to have similar protaspides that are expected from two species of the same subfamily. That of *I. major* has a much more convex shield covered with fingerprint-like microsculpture and a

101

parallel-sided, wide axis with a forward-expanding L4, and lacks the eye ridge and flat shield marginal border which are present in protaspides of *E. roemeri* (Pl. II-38, Figs. 1-12).

A possible metaprotaspis of *Irvingella major* (Pl. II-39, Figs. 5-7) differs from that of *Elvinia roemeri* (Pl. II-38, Figs. 13-15) in having a more convex shield, a spinose protopygidial margin and lacking an anterior border. These features are found in metaprotaspides of *Dytremacephalus* (Pl. II-37, Figs. 10, 13). The other possible metaprotaspis of *I. major* (Palmer, 1965b, pl. 6, fig. 13) differs from that of *E. roemeri* in having a forward-tapering glabella and a forward-turning posterior cranidial border. Any metaprotaspides of *I. major* does not show the morphologies similar to those of *E. roemeri*, even though both are strongly believed to belong to the same subfamily. Better-preserved and more specimens are needed to incorporate protaspid morphologies into the taxonomic scheme. For the present, *Irvingella* is placed in the Elvininae with question.

PLATE II-1. *Olenellus truemani* Walcott, 1913. and **Olenellidae** sp. A. All specimens are from the Buelina Formation, Mexico. Figures 1-6 and 10-13 are x 75.

1-9. *Olenellus truemani* Walcott, 1913.
    1. CMC-P 38724c, meraspid cranidium, dorsal view.
    2. CMC-P 38724e, meraspid cranidium, dorsal view.
    3, 4. CMC-P 38724g, meraspid cranidium; 3. Dorsal view, 4. Lateral view.
    5-7. CMC-P 38724h, meraspid cranidium; 5. Dorsal view, 6. Posterior view, 7. Magnified posterior view, x 160: note that there is no protopygidial region developed behind the occipital ring.
    8. CMC-P 38724m, meraspid cranidium, dorsal view, x 20.
    9. CMC-P 38724p, holaspid cranidium, dorsal view, x 10.3.
10-13. **Olenellidae** sp. A.
    10. CMC-P 38724a, meraspid cranidium, dorsal view.
    11. CMC-P 38724d, meraspid cranidium, dorsal view.
    12. CMC-P 38724f, meraspid cranidium, dorsal view.
    13. CMC-P 38724i, meraspid cranidium, dorsal view.
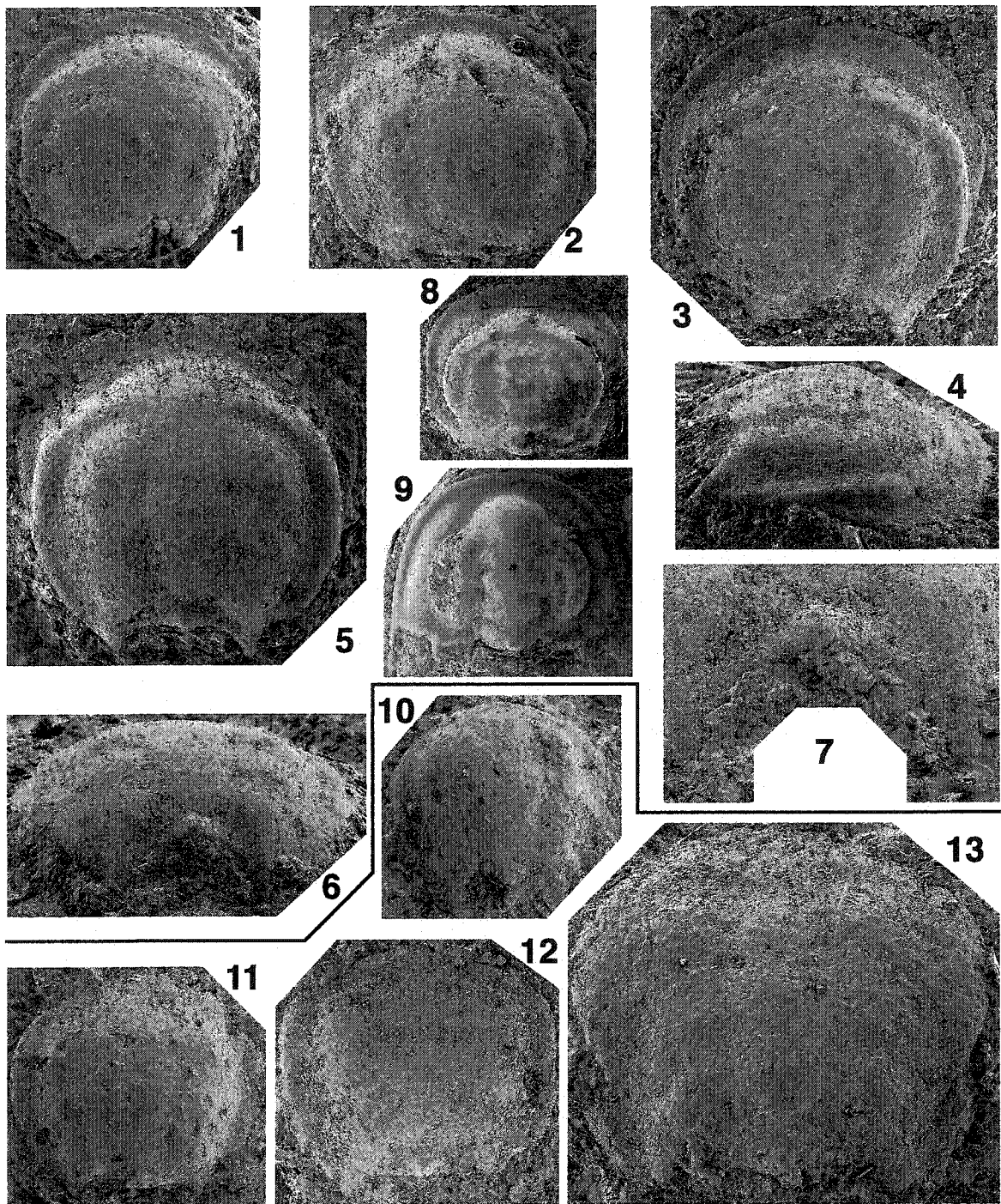
PLATE II-2. *Pagetia resseri* Kobayashi, 1944. All specimens are from the *Bathyuriscus-Elrathina* (Middle Cambrian) Zone of the Langston Formation, Utah. All protaspid specimens (Figs. 1-4) are x 75.

1-12. *Pagetia resseri* Kobayashi, 1944.
    1-4. CMC-P 38723i, anaprotaspis; 1. Dorsal view, 2. Anterior view, 3. Posterior view, 4. Lateral view.
    5. CMC-P 38723b, transitory pygidium, dorsal view, x 51.
    6. CMC-P 38723a, transitory pygidium, dorsal view, x 42.
    7. CMC-P 38723e, transitory pygidium, dorsal view, x 45.
    8. CMC-P 38723l, early meraspid cranidium, dorsal view, x 46.
    9. CMC-P 38723j, early meraspid cranidium, dorsal view, x 43.
    10, 11. CMC-P 38723q, holaspid cranidium, x 19.3; 10. Oblique lateral view, 11. Dorsal view.
    12. CMC-P 38723g, holaspid pygidium, dorsal view, x 22.5.
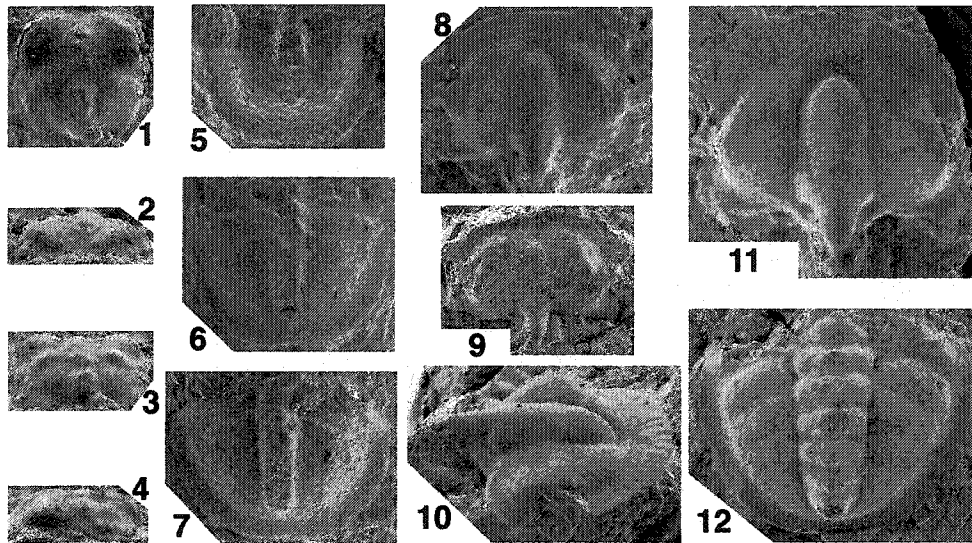
PLATE II-3. *Ptarmigania aurita* Resser, 1939, *Ptarmigania* sp. A, **Ptychopariina** sp. A, and **Corynexochina** sp. A. All the specimens are from the *Elrathina-Bathyuriscus* Zone (Middle Cambrian) of the Langston Formation, Utah. All protaspid specimens (Figs. 1-9, 13-23) are x 75.

1-16. *Ptarmigania aurita* Resser, 1939
    1-3. CMC-P 38727c, anaprotaspis; 1. Dorsal view: note the presence of anterior and mid-fixigenal spine in the left of the shield, 2. Anterior view, 3. Posterior view: note the presence of sagittal furrow.
    4-6. CMC-P 38727b, anaprotaspis; 4. Dorsal view, 5. Lateral view, 6. Anterior view.
    7-9. CMC-P 38727d, anaprotaspis; 7. Dorsal view, 8. Posterior view, 9. Lateral view.
    10-11. CMC-P 38727u, holaspid cranidium, x 24; 10. Dorsal view, 11. Lateral view.
    12. CMC-P 38727q, meraspid cranidium, dorsal view, x 31.
    13-16. CMC-P 38727n, metaprotaspis; 13. Dorsal view: note the development of two pairs of tubercles on fixigenae and distinct palpebrocular ridge, 14. Lateral view, 15. Anterior view, 16. Posterior view.
17-20. *Ptarmigania* sp. A (not described in the text)
    17-20. CMC-P 38727e, anaprotaspis; 17. Dorsal view, 18. Anterior view, 19. Lateral view, 20. Posterior view.
21-23. **Ptychopariina** sp. A (not described in the text)
    21-23. CMC-P 38727a, anaprotaspis; 21. Lateral view, 22. Dorsal view: note that the right of the shield appears to preserve a pair of fixigenal spines, 23. Anterior view.
24-27. **Corynexochina** sp. A. (not described in the text)
    24. CMC-P 38727k, meraspid cranidium, dorsal view, x 40.
    25. CMC-P 38727f, meraspid cranidium, dorsal view, x 47.
    26. CMC-P 38727h, meraspid cranidium, dorsal view, x 48.
    27. CMC-P 38727g, meraspid cranidium, dorsal view, x 52.

108
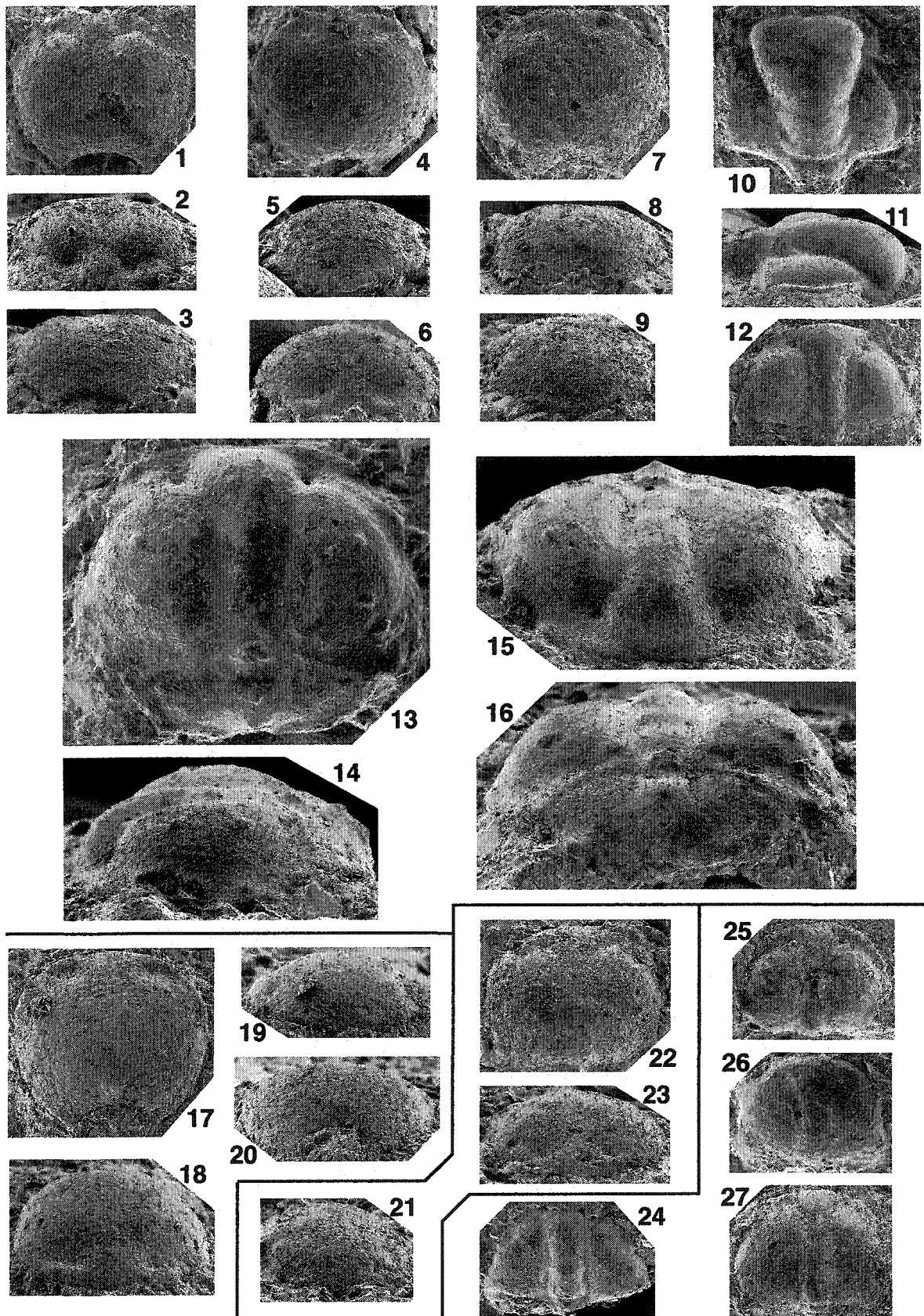
PLATE II-4. *Leiostegium formosa* Hintze, 1953. All specimens are from R5-76.4
  (*Tesselacauda* Zone) of the Garden City Formation, southern Idaho. All protaspid
  specimens (1-9) are x 75.

1-19. *Leiostegium formosa* Hintze, 1953.
  1, 2. UA 12758, anaprotaspis; 1. Dorsal view, 2. Ventral view.
  3. UA 12759, anaprotaspis, dorsal view.
  4, 5. UA 12760, anaprotaspis; 4. Anterior view, 5. Posterior view.
  6, 8. UA 12762, metaprotaspis; 6. Lateral view, 8. Dorsal view.
  7. UA 12761, metaprotaspis, dorsal view: note the presence of three pairs of fixigenal
      tubercles and one pair of pygidial marginal spines.
  9. UA 12763, metaprotaspis, ventral view.
  10. UA 12764, early meraspid cranidium, dorsal view, x 25.
  11. UA 12765, early meraspid cranidium, dorsal view, x 21.
  12. UA 12766, meraspid cranidium, dorsal view, x 19.
  13. UA 12767, transitory pygidium, dorsal view, x 25.
  14. UA 12768, meraspid cranidium, dorsal view, x 19.
  15. UA 12769, transitory pygidium, dorsal view, x 32.
  16-18. UA 12770, early holaspid cranidium; 16. Dorsal view, x 17.5, 17. Anterior view,
      x 17.5, 18. Lateral view, x 22.6.
  19. UA 12771, early holaspid pygidium, dorsal view, x 15.4.

110
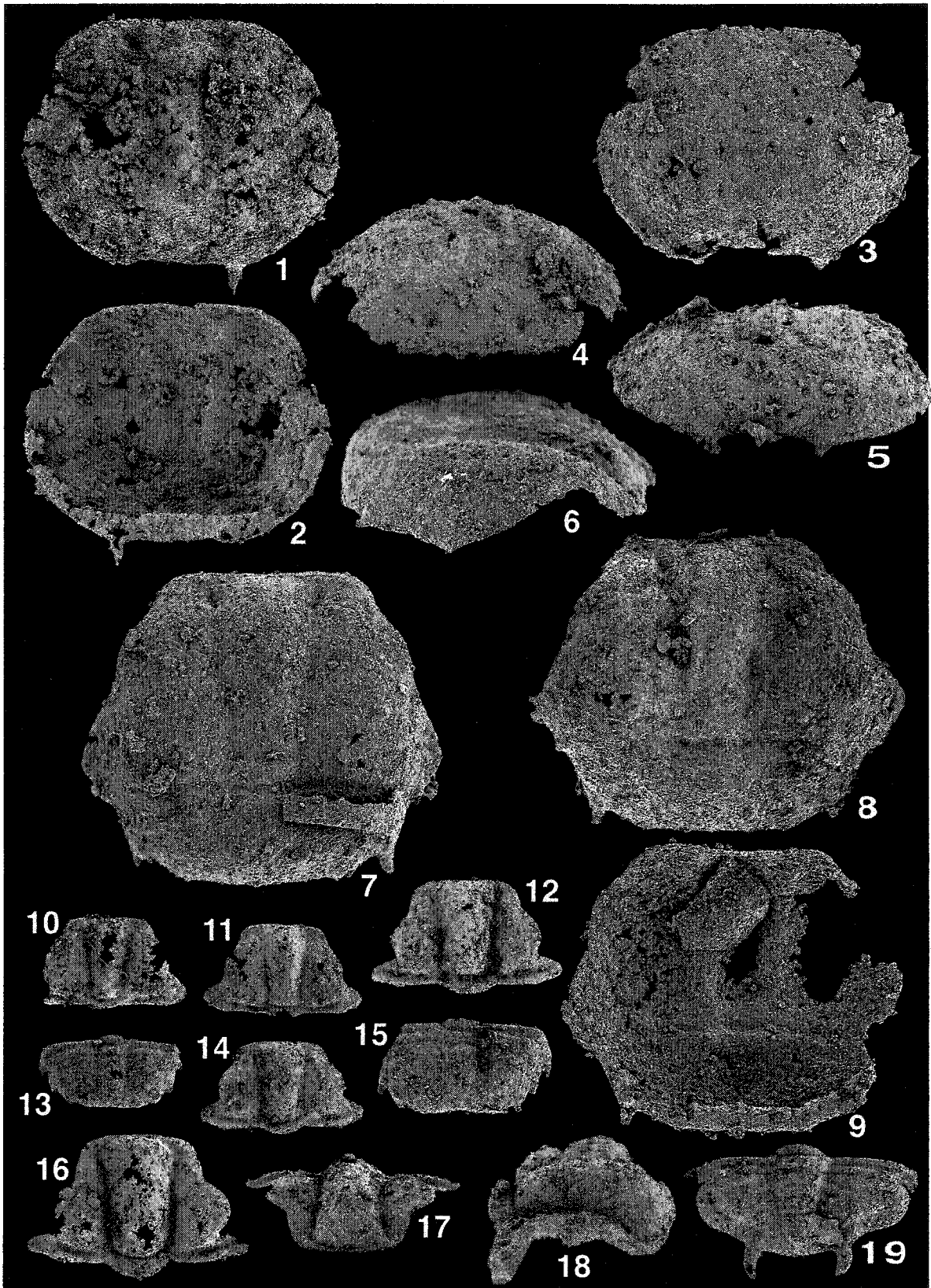
PLATE II-5. *Missisquoia cyclochila* Hu, 1971, **Species undetermined** A and **Species undetermined** B. All the specimens occur in the *Missisquoia* Zone (Ibexian) of the Deadwood Formation, northeastern Wyoming. All protaspid specimens (1-19, 20-28) are x 75.

1-19 *Missisquoia cyclochila* Hu, 1971

    1-3. CMC-P 38740a, anaprotaspis; 1. Dorsal view, 2. Posterior view, 3. Lateral view.

    4-6. CMC-P 38740d, metaprotaspis; 4. Dorsal view, 5. Posterior view, 6. Anterior view.

    7-9. CMC-P 38740e, metaprotaspis; 7. Dorsal view, 8. Posterior view, 9. Lateral view.

    10. CMC-P 38749h, early meraspid cranidium, dorsal view, x 65.

    11. CMC-P 38749o, early meraspid cranidium, dorsal view, x 45.

    12. CMC-P 38749j, early meraspid cranidium, dorsal view, x 57.

    13. CMC-P 38749p, meraspid cranidium, dorsal view, x 47.

    14. CMC-P 38749r, early meraspid cranidium, dorsal view, x 18.

    15, 16. CMC-P 38749, holaspid cranidium; 15. Dorsal view, x 13.3, 16. Anterior lateral view, x 14.4.

    17, 18. CMC-P 38749y, holaspid pygidium; 17. Posterior view, x 16, 18. Dorsal view, x 16.

    19. CMC-P 38749v, transitory pygidium, dorsal view, x 28.

20, 21. **Species undetermined** A (not described in the text)

    20, 21. CMC-P 38740c, metaprotaspis; 20. Dorsal view, 21. Oblique lateral view.

22-24. **Species undetermined** B (not described in the text)

    22-24. CMC-P 38749c, metaprotaspis; 22. Dorsal view: note that the axis is strongly annulated and has bilobed L3/L2/L1, 23. Posterior view, 24. Lateral view.

25-28. **Species undetermined** C (not described in the text)

    25, 26. CMC-P 38749a, anaprotaspis; 25. Dorsal view, 26. Anterior view.

    27, 28. CMC-P 38749b, anaprotaspis; 27. Dorsal view, 28. Posterior view.

112
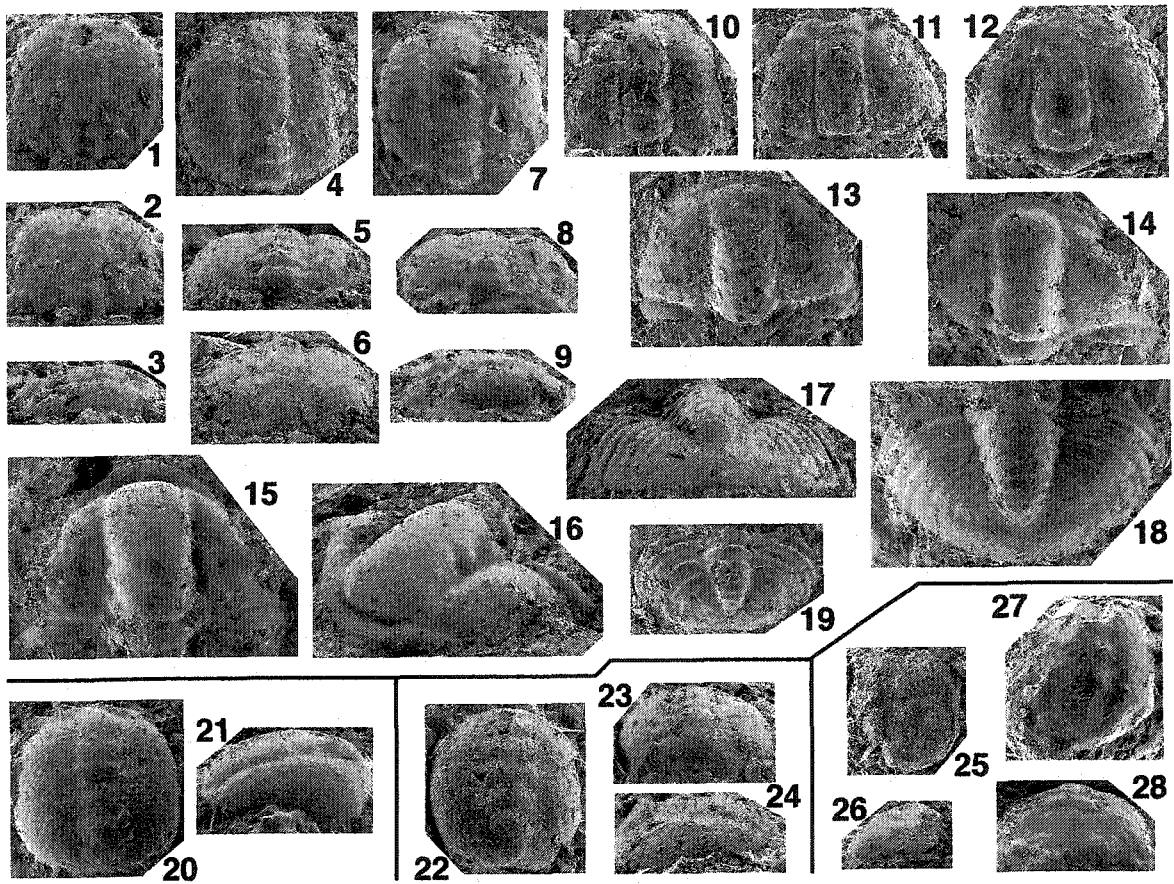
PLATE II-6. *Blountia bristolensis* Resser, 1938. All specimens are from the *Aphelaspis* zone (Lower Steptoean) of the Deadwood Formation, South Dakota, and x 75.

1-22. *Blountia bristolensis* Resser, 1938.
   1-3. CMC-P 42617b, early anaprotaspis; 1. Dorsal view, 2. Lateral view: note the development of sagittal furrow, 3. Anterior view.
   4, 5. CMC-P 42617e, early anaprotaspis; 4. Dorsal view, 5. Lateral view.
   6-8. CMC-P 42617g, late anaprotaspis; 6. Dorsal view, 7. Lateral view: note that the sagittal furrow disappears and parallel-sided axial furrows develop, 8. Anterior view.
   9-11. CMC-P 42617h, early metaprotaspis; 9. Dorsal view, 10. Lateral view, 11. Posterior view: note the presence of occipital ring.
   12-14. CMC-P 42617i, early metaprotaspis; 12. dorsal view, 13. Lateral view, 14. Posterior view.
   15-17.CMC-P 42617k, early metaprotaspis; 15. Posterior view: note that the posterior cranidial border is weakly-developed, 16. Dorsal view, 17. Lateral view.
   18, 19. CMC-P 42617j, early metaprotaspis; 18. Dorsal view, 19. Anterior view.
   20-22. CMC-P 42617l, early metaprotaspis; 20. Dorsal view, 21. Posterior view: note the development of slender posterior cranidial border, 22. Anterior view.

114
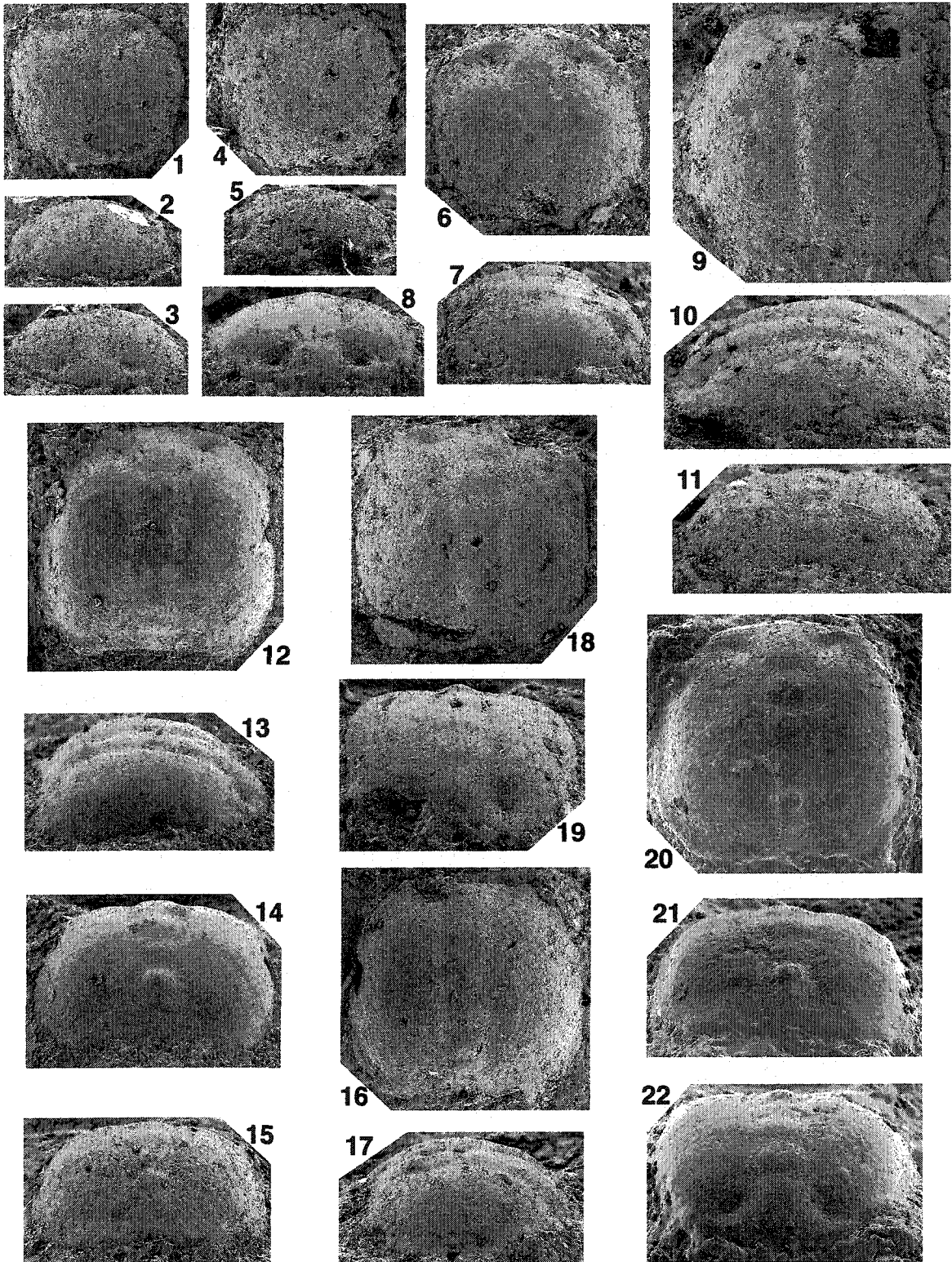
PLATE II-7. *Blountia bristolensis* Resser, 1938 and **Species undetermined** D. All the specimens are from the *Aphelaspis* zone (Lower Steptoean) of the Deadwood Formation, South Dakota. All protaspid specimens (1-6, 17-23) are x 75.

1-16. *Blountia bristolensis* Resser, 1938
   1. CMC-P 42617m, late metaprotaspis, dorsal view.
   2-4. CMC-P 42617n, late metaprotaspis; 2. Anterior view, 3. Dorsal view, 4. Lateral view.
   5, 6. CMC-P 42617o, late metaprotaspis; 5. Dorsal view, 6. Posterior view.
   7. CMC-P 42617u, early meraspid cranidium, dorsal view, x 32.
   8, 9. CMC-P 42617s, early meraspid cranidium; 8. Dorsal view, x 26, 9. Anterior right lateral view, x 23.
   10-11. CMC-P 42617, holaspid cranidium; 10. Dorsal view, x 10.4, 11. Anterior left lateral view, x 8.5.
   12. CMC-P 42617v, early holaspid cranidium, dorsal view, x 14.
   13. CMC-P 42617b', transitory pygidium, dorsal view, x 24.
   14. CMC-P 42617a', transitory pygidium, dorsal view, x 19.
   15, 16. CMC-P 42617h', holaspid pygidium, 15. Dorsal view, x 9, 16. Posterior right lateral view, x 8.8.
17-23. **Species undetermined** D (not described in the text)
   17-19. CMC-P 42617d, anaprotaspis; 17. Lateral view, 18. Dorsal view, 19. Anterior view.
   20-23. CMC-P 42617f, metaprotaspis; 20. Dorsal view, 21. Lateral view: note that L3/L2 is spindle-shaped and bilobed, 22. Anterior view, 23. Posterior view.

116
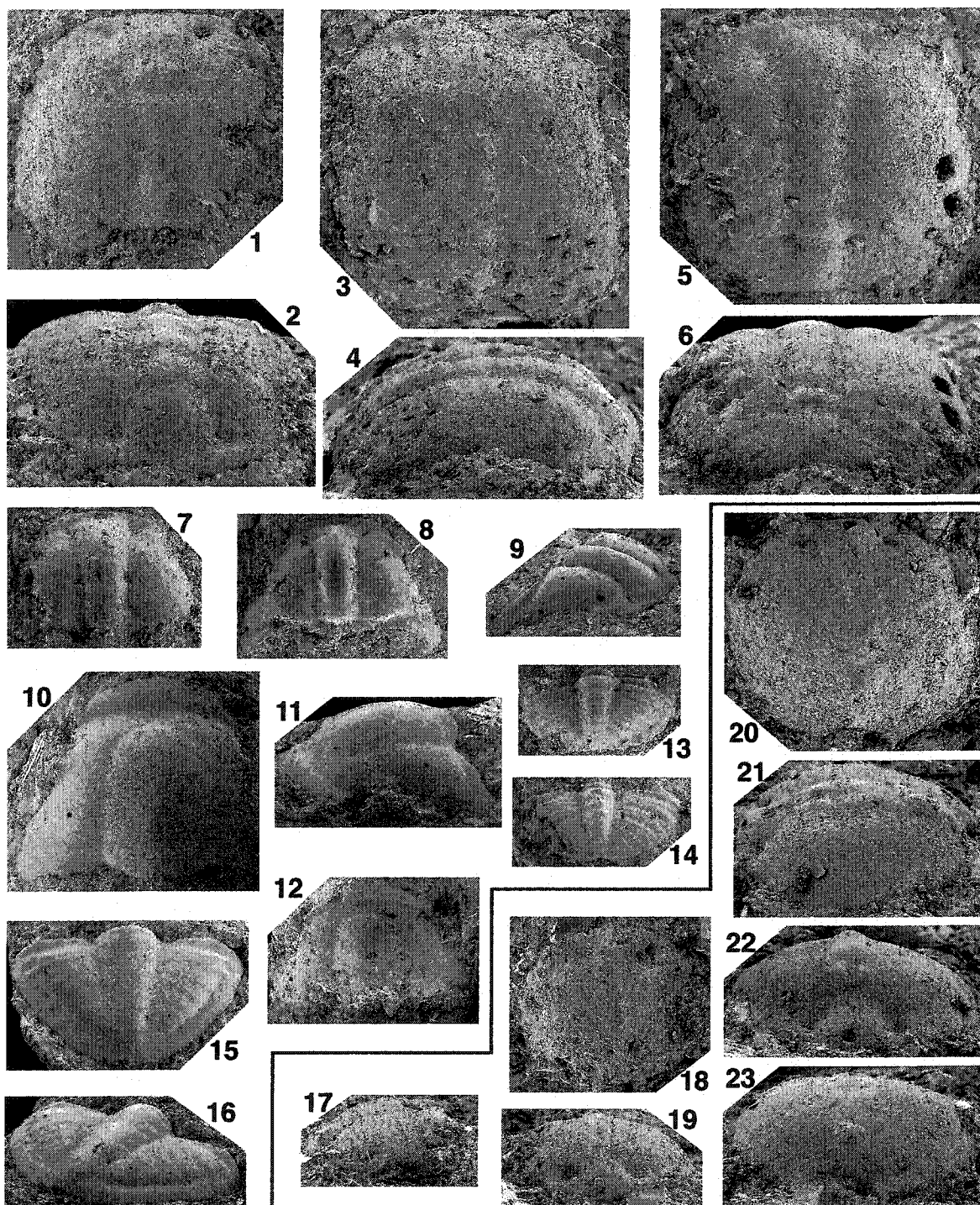
PLATE II-8. *Komaspidella laevis* Rasetti, 1961 and **Species undetermined** E. All the specimens are from the *Crepicephalus* Zone of the Bonneterre Dolomite, Missouri. All protaspid specimens (1-8, 16-19) are x 75.

1-15. *Komaspidella laevis* Rasetti, 1961
    1-4. CMC-P 40274b, anaprotaspis; 1. Dorsal view, 2. Lateral view, 3. Anterior view, 4. Posterior view.
    5-8. CMC-P 40274e, metaprotaspis; 5. Dorsal view, 6. Lateral view, 7. Posterior view, 8. Anterior view.
    9. CMC-P 40274g, early meraspid cranidium, dorsal view, x 59.
    10. CMC-P 40274k, early meraspid cranidium, dorsal view, x 45.
    11-12. CMC-P 40274o, holaspid cranidium; 11. Dorsal view, x 6, 12. Lateral view.
    13. CMC-P 40274m, transitory pygidium, dorsal view, x 28.
    14, 15. CMC-P 40274p, holaspid pygidium, x 8; 14. Dorsal view, 15. Posterior right lateral view.
16-19. **Species undetermined** E (not described in the text).
    16-19. CMC-P 40274a, anaprotaspis; 16. Lateral view, 17. Anterior view, 18. Posterior view, 19. Dorsal view.

118
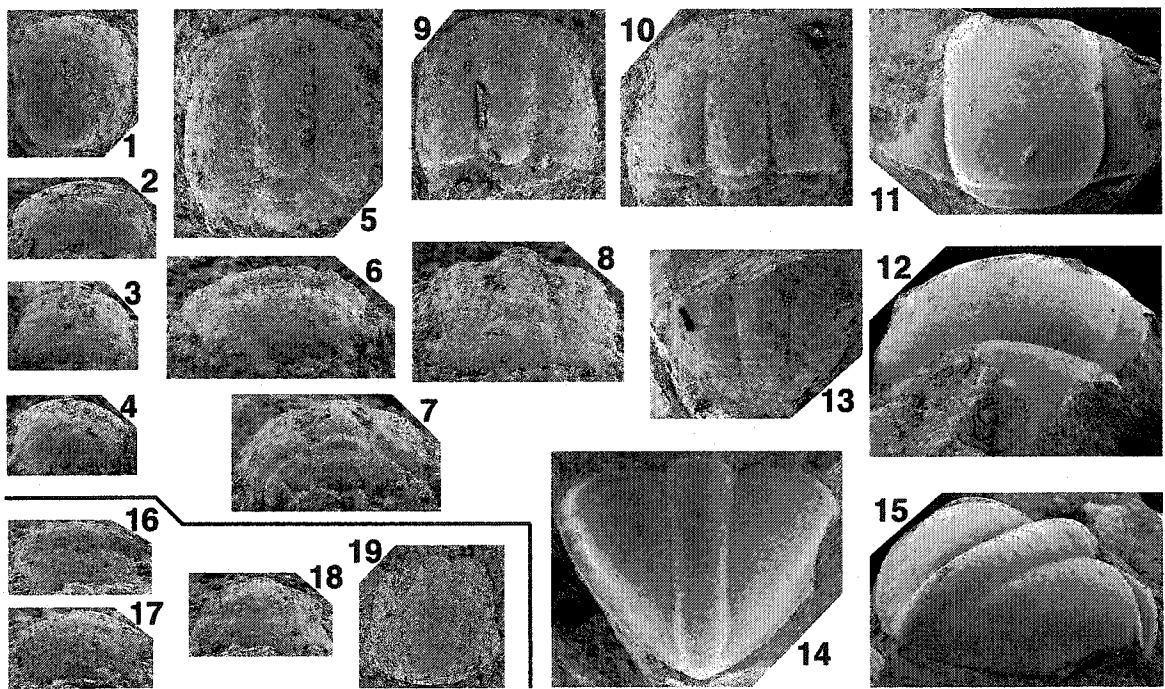
PLATE II-9. *Glaphyraspis parva* (Walcott, 1899), **Species undetermined F,** *Glaphyraspis* sp. A and **Species undetermined** G. All protaspid specimens (Figs. 1-16, 28-33, 34) are x 75.

1-26 *Glaphyraspis parva* (Walcott, 1899) from the *Aphelaspis* Zone (lowermost Steptoean) of the Deadwood Formation, South Dakota;

1-4. CMC-P 40310a, anaprotaspis; 1. Dorsal view, 2. Lateral view, 3. Posterior view, 4. Anterior view.

5-7. CMC-P 40310b, anaprotaspis; 5. Dorsal view, 6. Anterior view, 7. Oblique posterior view.

8-11. CMC-P 40310d, metaprotaspis; 8. Dorsal view, 9. Posterior view: note the presence of transverse, narrow protopygidium, 10. Lateral view, 11. Anterior view.

12, 13. CMC-P 40310c, metaprotaspis; 12. Dorsal view, 13. Oblique posterior view.

14-16. CMC-P 40310e, metaprotaspis; 14. Dorsal view, 15. Oblique posterior view, 16. Lateral view.

17. CMC-P 40310g, early meraspid cranidium, dorsal view, x 59.

18. CMC-P 40310h, transitory pygidium, dorsal view, x 31.

19. CMC-P 40310i, early meraspid cranidium, dorsal view, x 50.

20. CMC-P 40310o, early holaspid cranidium, dorsal view, x 23.

21-23. CMC-P 40310b', holaspid cranidium, x 14.4; 21. Dorsal view, 22. Anterior view, 23. Lateral view.

24-26. CMC-P 40310c', holaspid pygidium, x 22.5; 24. Dorsal view, 25. Posterior view, 26. Lateral view.

27. **Species undetermined** F (not described in the text).

27. CMC-P 40310j, meraspid cranidium, from the *Aphelaspis* Zone (lowermost Steptoean) of the Deadwood Formation, South Dakota, dorsal view, x 26.4.

28-33. *Glaphyraspis* sp. A from the *Crepicephalus* Zone of the Bonneterre Dolomite, Missouri (not described in the text).

28-30. CMC-P 40274c, anaprotaspis; 28. Dorsal view, 29. Posterior view, 30. Lateral view.

31-33. CMC-P 40274d, metaprotaspis; 31. Posterior view, 32. Lateral view, 33. Dorsal view.

34. **Species undetermined** G from the *Aphelaspis* Zone (lowermost Steptoean) of the Deadwood Formation, South Dakota (not described in the text).

34. CMC-P 40310, anaprotaspis, oblique dorsal view.

120
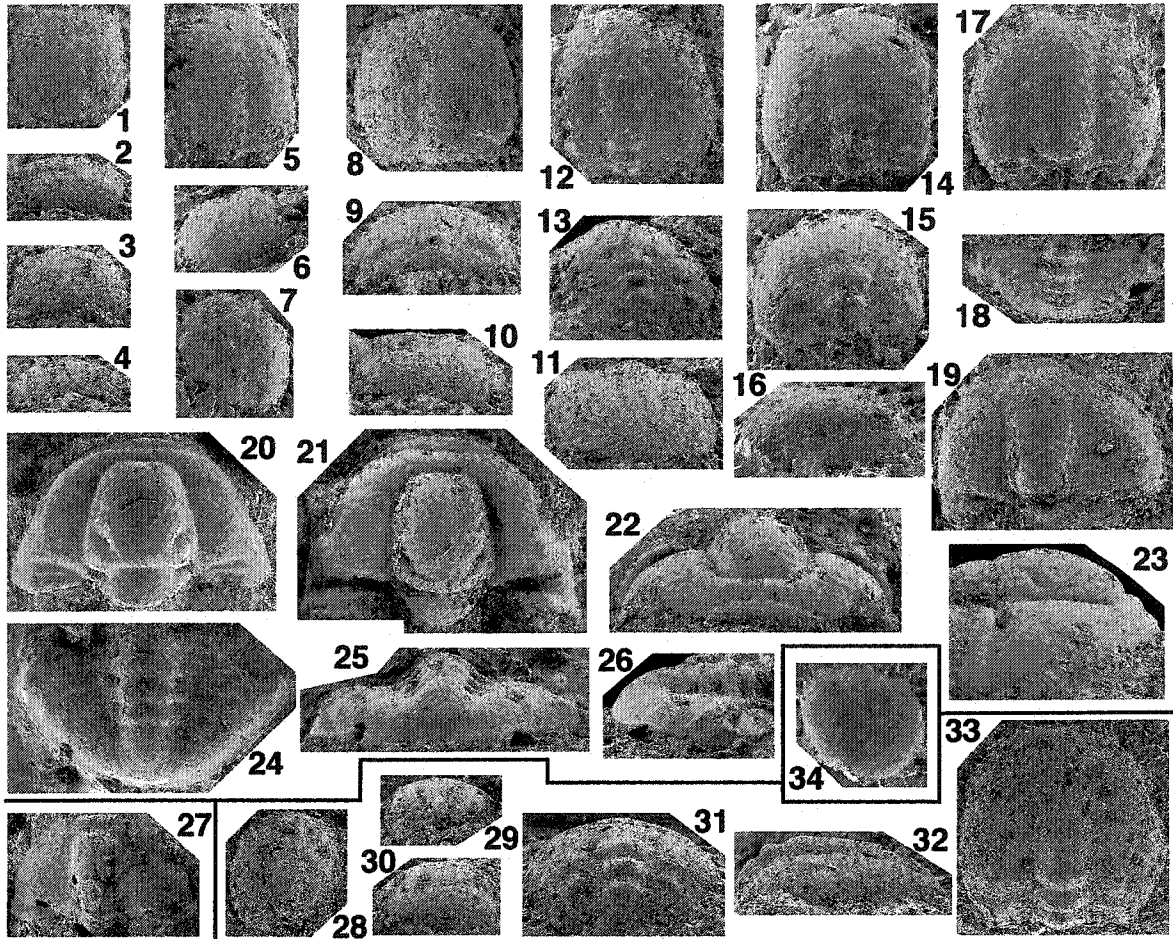
PLATE II-10. *Welleraspis lochmanae* Hu, 1969, **Catillicephalidae** sp. A, **Catillicephalidae** sp. B and **Species undetermined** H. All the specimens are from the *Crepicephalus* Zone of the Bonneterre Dolomite, Missouri. All protaspid specimens (15-25) are x 75.

1-14 *Welleraspis lochmanae* Hu, 1969
  1. CMC-P 39741e, meraspid cranidium, dorsal view, x 35.
  2. CMC-P 39741f, meraspid cranidium, dorsal view, x 32.
  3. CMC-P 39741j, early holaspid cranidium, dorsal view, x 17.
  4. CMC-P 39741r, transitory pygidium, dorsal view, x 55.
  5. CMC-P 39741s, transitory pygidium, dorsal view, x 58.
  6, 7. CMC-P 39741p, holaspid cranidium, x 16.6; 6. Dorsal view, 7. Lateral view: note that the eye is located at ventral side.
  8-10. CMC-P 397411, holaspid cranidium, x 14.9; 8. Lateral view, 9. Dorsal view, 10. Anterior view.
  11. CMC-P 39741t, late meraspid pygidium, dorsal view, x 23.
  12-14. CMC-P 39741x, holaspid pygidium, x 17.7; 12. Lateral view, 13. Dorsal view, 14. Posterior view.
15-18. **Catillicephalidae** sp. A (probably *Madarocephalus*; not described in the text)
  15-18. CMC-P 39741c, metaprotaspis; 15. Dorsal view, 16. Posterior view, 17. Anterior view, 18. Lateral view.
19-23. **Catillicephalidae** sp. B (not described in the text).
  19-22. CMC-P 39741b, metaprotaspis; 19. Dorsal view, 20. Anterior view, 21. Posterior view, 22. Lateral view.
  23. CMC-P 39741d, early meraspid cranidium, dorsal view, x 80.
24, 25. **Species undetermined** H (not described in the text).
  24, 25. CMC-P 39741a, anaprotaspis; 24. Dorsal view, 25. Anterior view.

122
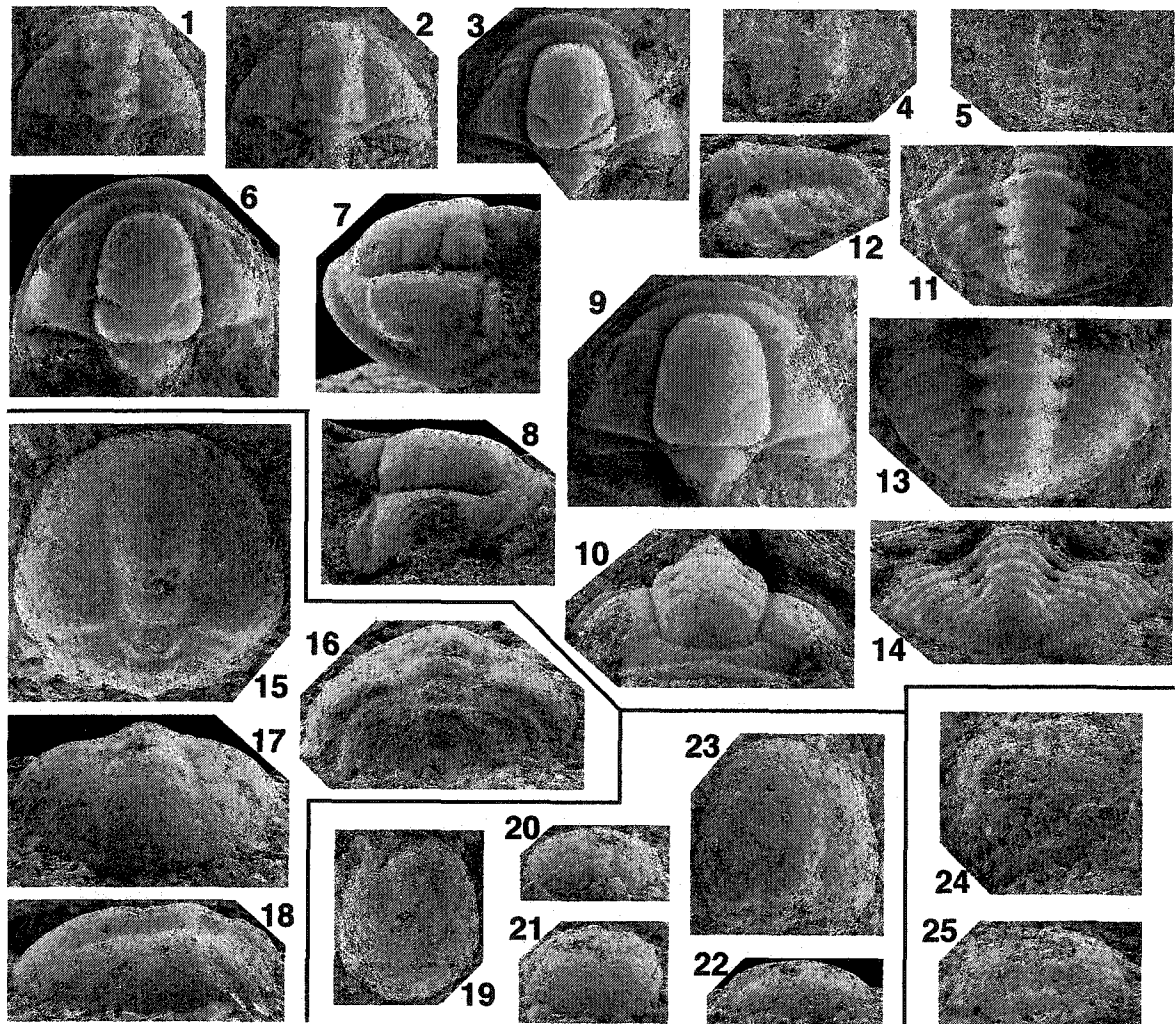
PLATE II-11. *Cedarina cordillerae* (Howell and Duncan, 1939) and **Cedariidae** sp. A. All the specimens are from the *Cedaria* zone (lower Marjuman stage), Utah. All protaspid specimens (Figs. 1-8, 17-22) are x 75.

1-16. *Cedarina cordillerae* (Howell and Duncan, 1939)

  1-4. CMC-P 38731b, early metaprotaspis; 1. Dorsal view, 2. Posterior view: note the presence of occipital ring behind which a very short (sag.) protopygidum is developed, 3. Lateral view, 4. Oblique lateral view.

  5-8. CMC-P 38731d, late metaprotaspis; 5. Dorsal view, 6. Posterior view, 7. Lateral view, 8. Oblique lateral view. note that glabellar front.rapidly expands forwards and no anterior border is differentiated.

  9. CMC-P 38731h, meraspid cranidium, dorsal view, x 49.

  10. CMC-P 38731j, meraspid cranidium, dorsal view, x 23.

  11. CMC-P 38731l, meraspid cranidium, lateral view, x 20.

  12. CMC-P 38731y, transitory pygidium, anterior view, x 21.

  13, 14. CMC-P 38731q, holaspid cranidium, 13. Lateral view, x 4.5, 14. Dorsal view, x 6.3.

  15, 16. CMC-P 38731z, holaspid pygidium; 15. Dorsal view, x 18, 16. Lateral view, x 15.

17-22. **Cedariidae** sp. A (not described in the text).

  17-19. CMC-P 38731e, late metaprotaspis; 17. Dorsal view, 18. Posterior view, 19. Lateral view.

  20-22. CMC-P 38731f, early metaprotaspis; 20. Posterior view, 21. Oblique lateral view, 22. Dorsal view.
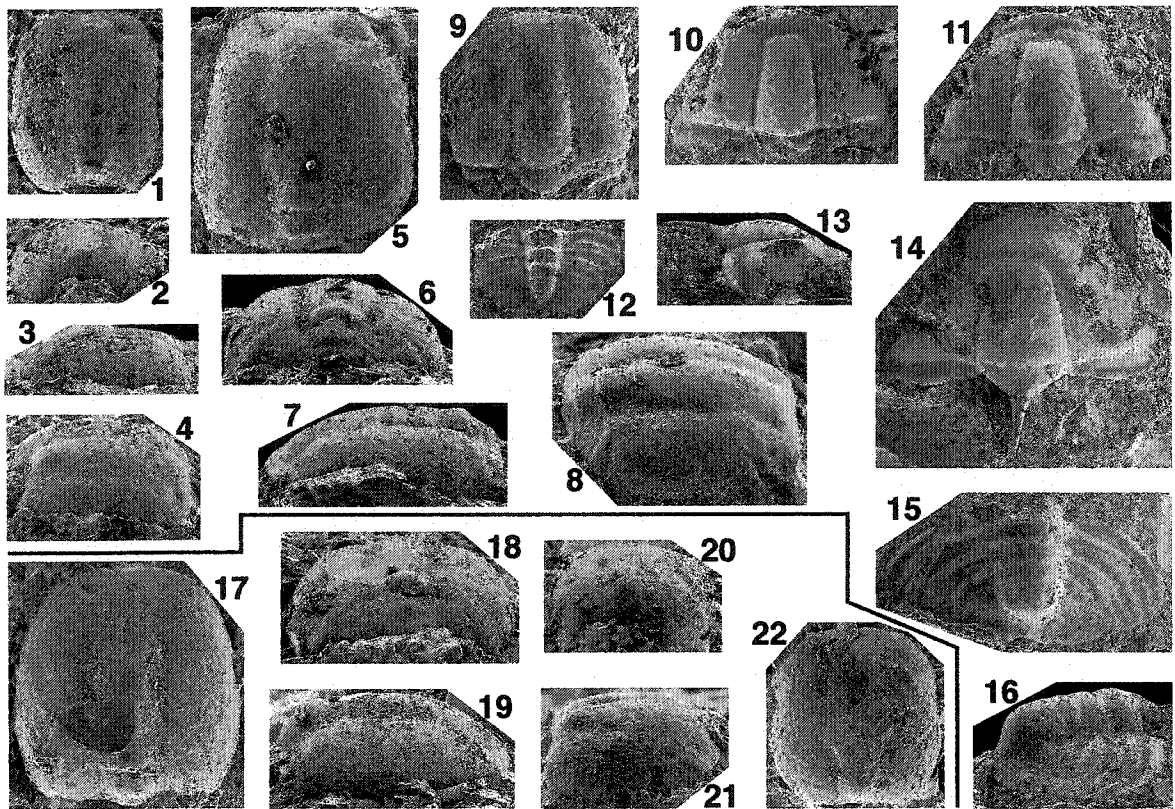
PLATE II-12. *Apomodocia conica* Hu, 1971, *Apomodocia*? sp. A, *Apomodocia* sp. A and **Species undetermined** I. All the specimens are from the *Cedaria* zone, Utah. All protaspid specimens (Figs. 1-27) are x 75.

1-12, 28-31. *Apomodocia conica* Hu, 1971
    1-3. CMC-P 38731c, anaprotaspis; 1. Dorsal view, 2. Oblique posterior view, 3. Lateral view.
    4-6. CMC-P 38725c, anaprotaspis; 4. Dorsal view, 5. Posterior view, 6. Lateral view: note development of posterior fixigenal spine.
    7-9. CMC-P 38725e, metaprotaspis; 7. Dorsal view, 8. Posterior view: note posterior fixigenal spine which is continuous from anaprotaspides, 9. Lateral view.
    10-12. CMC-P 38725g, metaprotaspis; 10. Dorsal view, 11. Lateral view, 12. Anterior view.
    28, 29. CMC-P 38725, holaspid cranidium, x 5; 28. Dorsal view, 29. Anterior view.
    30, 31. CMC-P 38725p, holaspid pygidium; 30. Lateral view, x 4, 31. Dorsal view, x 5.
13-15. *Apomodocia*? sp. A (not described in the text).
    13-15. CMC-P 38725b, anaprotaspis; 13. Dorsal view: note development of distinct anterior border, 14. Posterior view, 15. Lateral view.
16-21. *Apomodocia* sp. A (not described in the text).
    16-18. CMC-P 38725d, metaprotaspis; 16. Dorsal view, 17. Lateral view, 18. Posterior view.
    19-21. CMC-P 38731g, metaprotaspis; 19. Dorsal view, 20. Lateral view, 21. Posterior view; note posterior fixigenal spine which is shorter than in protaspides of *Apomodocia conica*.
22-27. **Species undetermined** I (not described in the text).
    22-24. CMC-P 38731a, anaprotaspis; 22. Dorsal view, 23. Lateral view, 24. Anterior view.
    25-27. CMC-P 38725a, anaprotaspis; 25. Dorsal view, 26. Lateral view, 27. Anterior view.

126
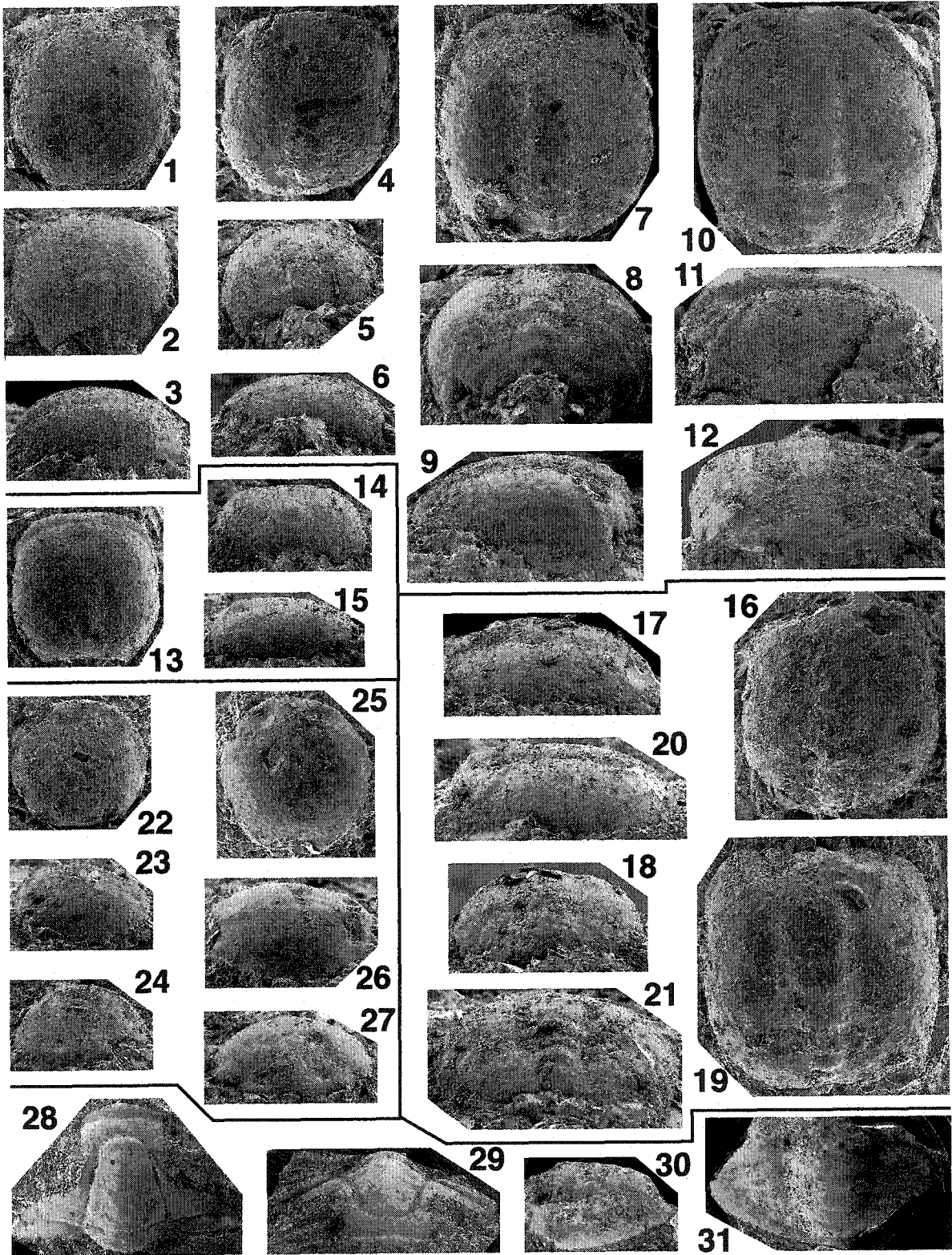
PLATE II-13. *Glyphaspis paucisulcata* Deiss, 1939, **Ptychopariina** sp. B,
Corynexochida sp. B and **Species undetermined** J. All the specimens are from the
Bathyuriscus-Elrathina Zone (Middle Cambrian) of the Meagher Formation,
Montana. All protaspid specimens (Figs. 1-10, 20-29) are x 75.

1-19. *Glyphaspis paucisulcata* Deiss, 1939
   1-3. CMC-P 38728e, early metaprotaspis; 1. Dorsal view: note development of slender
      eye ridge, 2. Posterior view: note that posterior cranidial marginal furrow is
      impressed weakly and does not cross the shield transversely, and occipital ring is
      present as a distinct node, 3. Lateral view.
   4-7. CMC-P 38728f, late metaprotaspis; 4. Dorsal view: note that glabellar front rapidly
      expands forwards from anterior pits, 5. Lateral view, 6. Anterior view, 7. Posterior
      right lateral view.
   8-10. CMC-P 38728g, late metaprotaspis; 8. Dorsal view, 9. Posterior view, 10.
      Oblique lateral view.
   11. CMC-P 38728j, meraspid cranidium, dorsal view, x 24.
   12. CMC-P 38728h, meraspid cranidium, dorsal view, x 31.
   13. CMC-P 38728t, transitory pygidium, dorsal view, x 24.
   14. CMC-P 38728v, holaspid pygidium, dorsal view, x 10.
   15. CMC-P 38728i, meraspid cranidium, dorsal view, x 29.
   16, 17. CMC-P 38728o, holaspid cranidium; 16. Lateral view, x 12, 17. Dorsal view, x
      11.
   18-19. CMC-P 38728w, holaspid pygidium; 18. Dorsal view, x 5, 19. Lateral view, x 8.
20, 21. **Ptychopariina** sp. B (not described in the text).
   20, 21. CMC-P 38728a, anaprotaspis; 20. Dorsal view, 21. Anterior view.
22-27. **Corynexochida** sp. B (not described in the text).
   22-24. CMC-P 38728c, anaprotaspis, 22. Dorsal view, 23. Oblique lateral view, 24.
      Posterior view.
   25-27. CMC-P 38728b, anaprotaspis; 25. Dorsal view, 26. Lateral view, 27. Anterior
      view.
28, 29. **Species undetermined** J (not described in the text).
   28, 29. CMC-P 38728d, metaprotaspis; 28. Dorsal view, 29. Oblique lateral view.

128
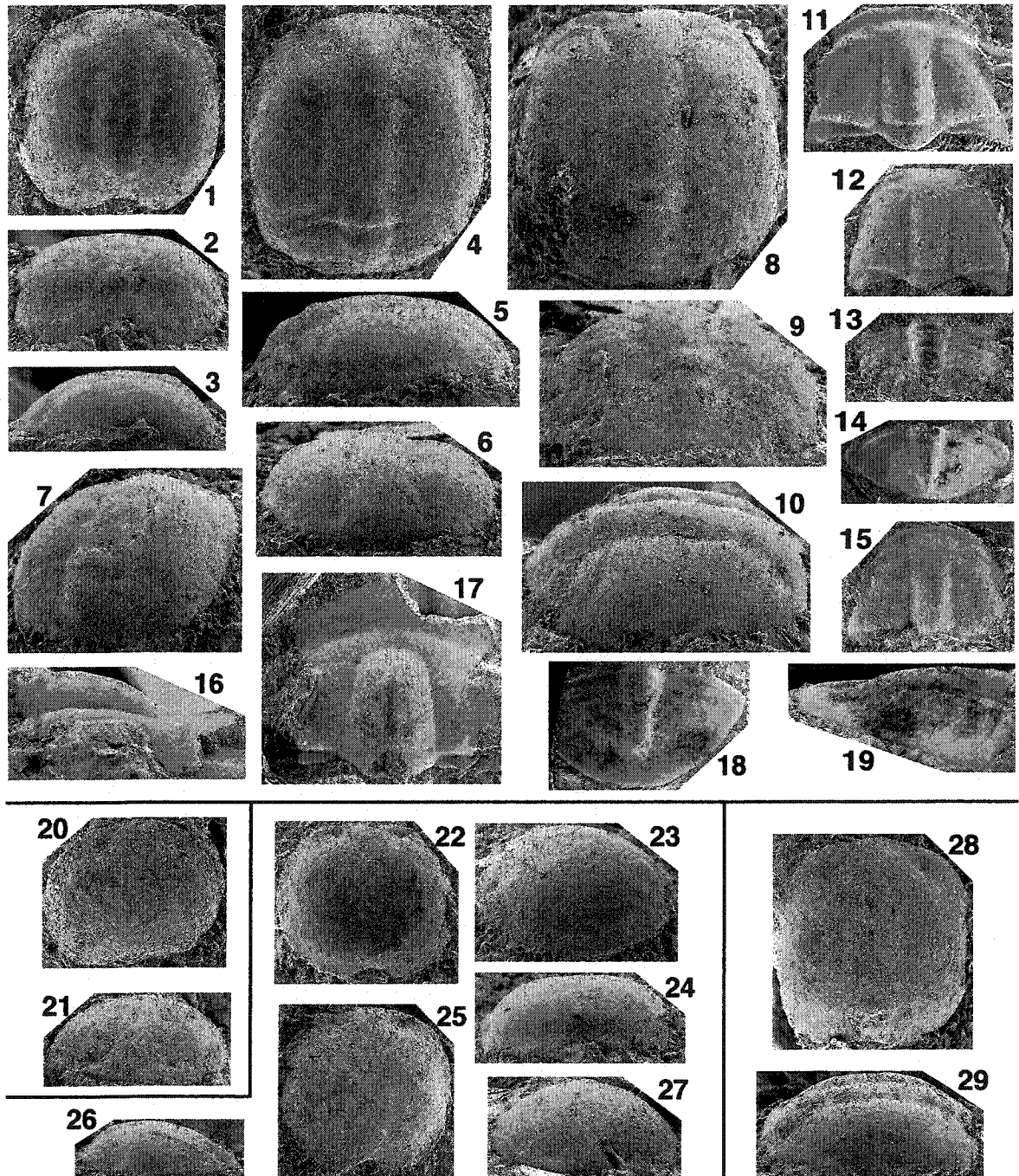
PLATE II-14. *Crepicephalus deadwoodiensis* Hu, 1971 and **Crepicephalidae** sp. A. All the specimens are from the *Crepicephalus* Zone (upper Marjuman) of the Deadwood Formation, South Dakota. All protaspid specimens (Figs. 1-23, 32-33) are x 75. There are some inadvertent mistakes of labeling the specimens made by Hu (1971). In his Pl. 14, Fig. 3 is not CMC-P 38732c, but CMC-P 38732f; Fig. 4 is not CMC-P 38732d, but CMC-P 38732c; Fig. 7 is not CMC-P 38732g, but CMC-P 38732d; the rest of Figs. should have been labeled as an alphabet before the one labeled (e.g., Fig. 8 should have been labeled as CMC-P 38732g, not 38732h).

1-31. *Crepicephalus deadwoodiensis* Hu, 1971
  1, 2. CMC-P 38732a, anaprotaspis; 1. Dorsal view, 2. Lateral view.
  3-5. CMC-P 38732b, anaprotaspis; 3. Dorsal view, 4. Lateral view, 5. Anterior view.
  6-8. CMC-P 38732c, early metaprotaspis; 6. Dorsal view, 7. Anterior view, 8. Lateral view: note occipital ring as a small node.
  9. CMC-P 38732f, early metaprotaspis, dorsal view.
  10, 11. CMC-P 38732e, early metaprotaspis; 10. Dorsal view, 11. Posterior view: note development of occipital ring.
  12-14. CMC-P 38732g, early metaprotaspis; 12. Lateral view: note sigmoidal profile of lateral margin, 13. Posterior view, 14. Dorsal view.
  15, 16. CMC-P 38732d, early metaprotaspis; 15. Dorsal view, 16. Anterior view.
  17. CMC-P 38732i, late metaprotaspis, dorsal view: note development of tubercles on fixigenae.
  18. CMC-P 38732l, meraspid cranidium, dorsal view, x 26: note development of tubercles on fixigenal area which is continuous from metaprotaspides.
  19. CMC-P 38732r, transitory pygidium, dorsal view, x 24.
  20. CMC-P 38732j, late metaprotaspis, dorsal view.
  21-23. CMC-P 38732k, late metaprotaspis, lateral view: note sigmoidal profile of lateral margin which is continuous from early metaprotaspides, 22. Dorsal view, 23. Posterior view: note development of tubercles.
  24. CMC-P 38732o, meraspid cranidium, dorsal view, x 17.
  25. CMC-P 38732u, transitory pygidium, dorsal view, x 13.
  26, 30, 31. CMC-P 38732, holaspid cranidium, 26. Dorsal view, x 10, 30. Oblique antero-lateral view, x 6.7, 31. Anterior view, x 6.7.
  27-29. CMC-P 38732, holaspid pygidium; 27. Dorsal view, x 10, 28. Lateral view, x 6.7, 29. Dorsal view, x 7.5.
32, 33. **Crepicephalidae** sp. A (not described in the text).
  32, 33. CMC-P 38732h, late metaprotaspis; 32. Dorsal view. 33. Posterior view.

130
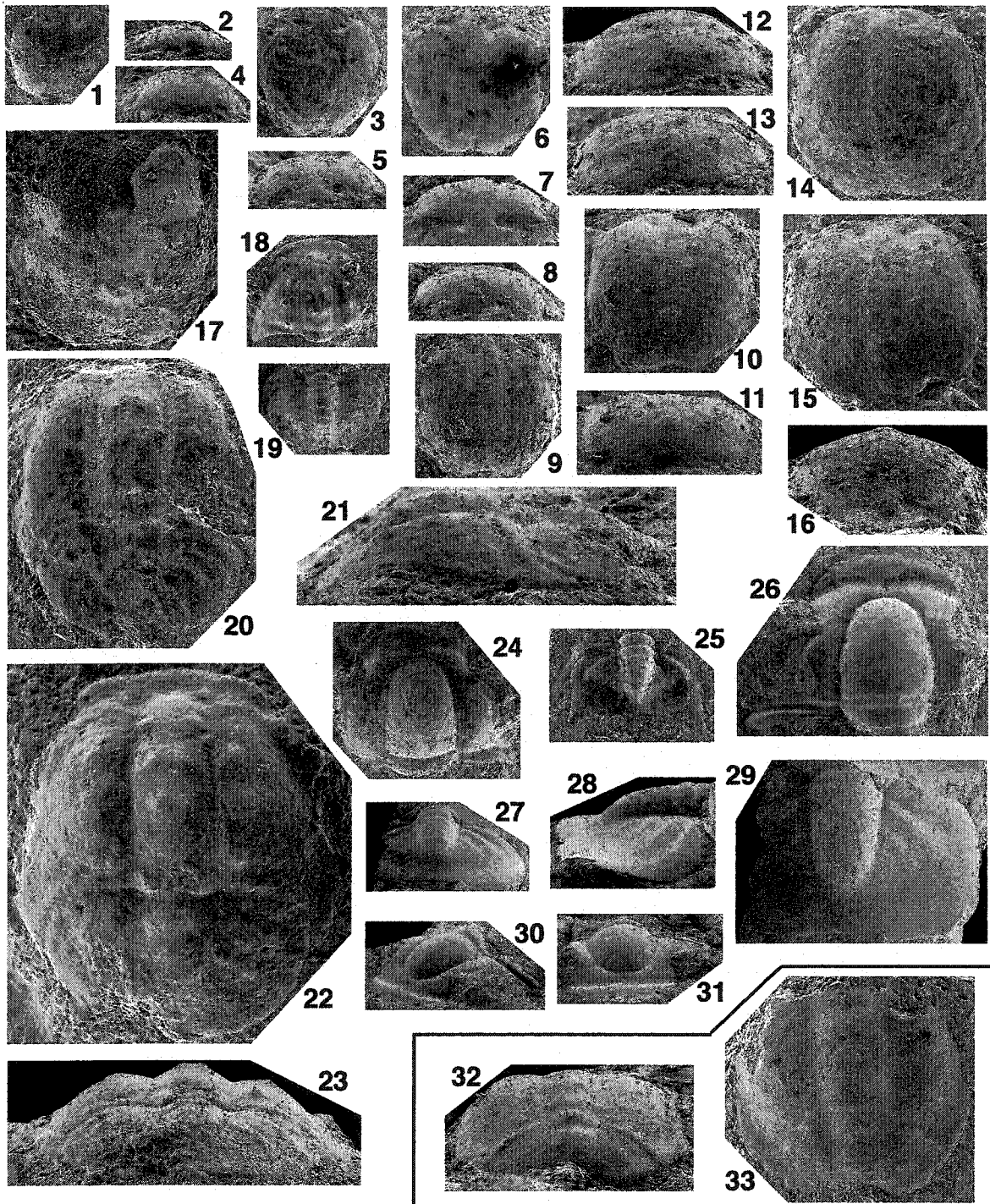
PLATE II-15. *Syspacheilus dunoirensis* (Miller, 1936), *Crepicephalus* sp. A, **Species undetermined** K and **Species undetermined** L. All the specimens are from the *Cedaria* Zone (Lower Marjuman) of the Pilgrim Formation, Montana. All protaspid specimens (Figs. 1-15, 24, 25) are x 75.

1-23. *Syspacheilus dunoirensis* (Miller, 1936)

1, 2. CMC-P 40279d, early metaprotaspis; 1. Dorsal view, 2. Posterior view: note the presence of occipital ring and shallow posterior cranidial marginal furrow.

3-5. CMC-P 40279b, early metaprotaspis; 3. Dorsal view, 4. Lateral view, 5. Anterior view.

6-8. CMC-P 40279c, late metaprotaspis; 6. Dorsal view: note development of slender eye ridge, 7. Lateral view: note that steeply-sloping anterior part of the shield, 8. Posterior view.

9-12. CMC-P 40279f, late metaprotaspis; 9. Dorsal view: note development of narrow flat anterior border and forward-expanding glabellar front, 10. Posterior view, 11. Oblique lateral view, 12. Lateral view: note steeply-sloping anterior part and gently-sloping posterior part of the shield.

13-15. CMC-P 40279e, late metaprotaspis; 13. Dorsal view, 14. Posterior view, 15. Lateral view.

17. CMC-P 40279g, early meraspid cranidium, dorsal view, x 33.

18. CMC-P 40279z, early holaspid pygidium, dorsal view, x 12.

19, 20. CMC-P 40279q, holaspid pygidium; 19. Dorsal view, x 16, 20. Posterior view, x 14.5.

21-23. CMC-P 40279w, holaspid cranidium; 21. Dorsal view, x 11.6, 22. Lateral view, x 8.7, 23. Anterior view, x 8.8.

16. *Crepicephalus* sp. A

16. CMC-P 40279k, meraspid cranidium, dorsal view, x 30.

24. **Species undetermined** K (not described in the text).

24. CMC-P 40279, anaprotaspis, dorsal view; it seems probable that this specimen could belong to a Norwoodella species.

25. **Species undetermined** L (not described in the text).

25. CMC-P 40279a, anaprotaspis, dorsal view: note the development of sagittal furrow.
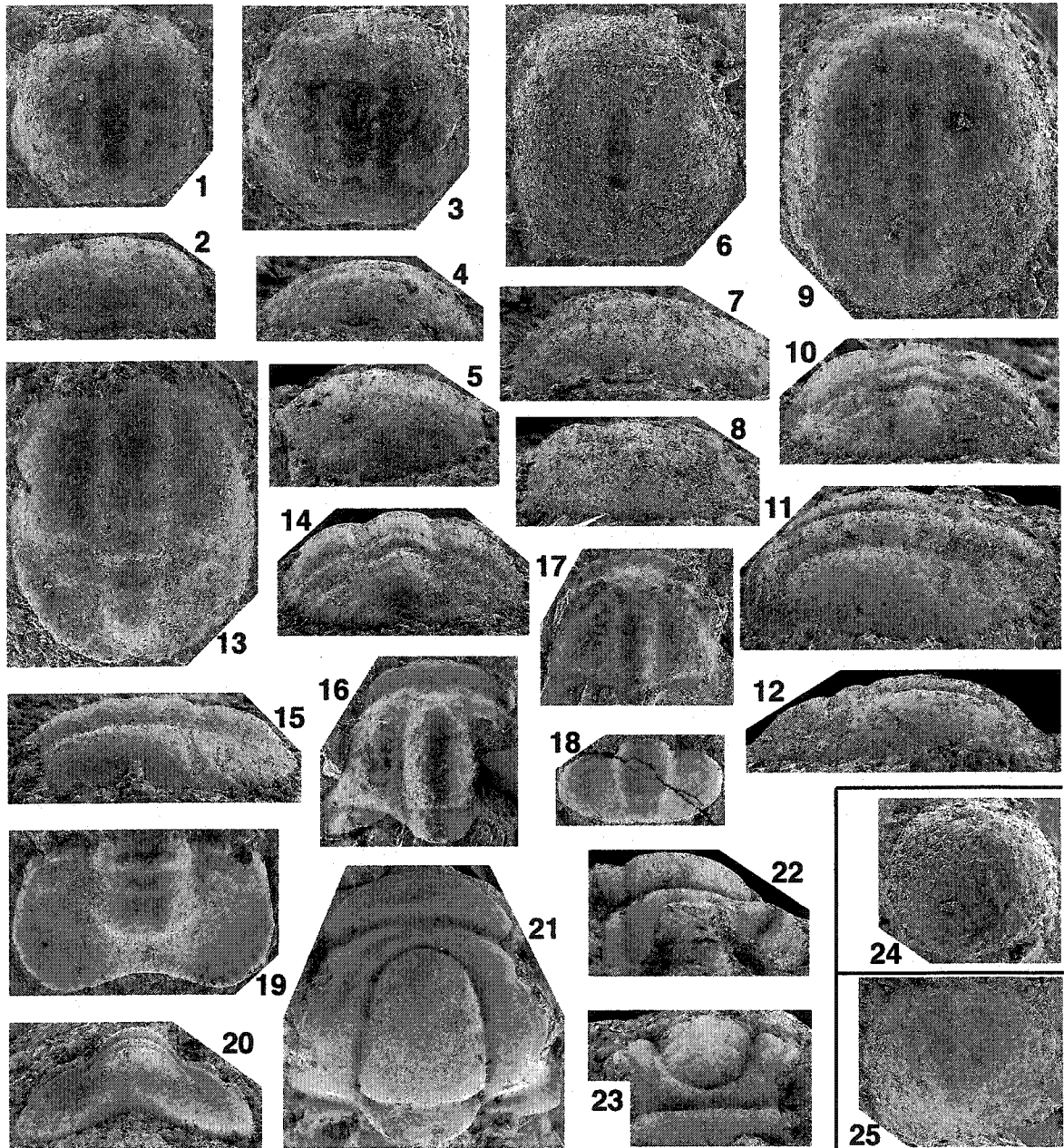
PLATE II-16. *Nixonella montanensis* Lochman *in* Lochman and Duncan, 1944 and **Catillicephalidae** sp. A. All the specimens are from the *Cedaria* Zone of the Pilgrim Formation, Montana. All protaspid specimens (Figs. 1-13, 23-25) are x 75. "*" indicates that the specimen is found in the same limestone sample along with the specimen alphabetically labelled by Hu (1972), but was not illustrated by Hu (1972).

1-22. *Nixonella montanensis* Lochman *in* Lochman and Duncan, 1944
    1-3. CMC-P 40280m, anaprotaspis; 1. Dorsal view, 2. Anterior view, 3. Oblique lateral view.
    4-7. CMC-P 40280k, metaprotaspis; 4. Dorsal view, 5. Anterior view: note distinct development of anterior border, 6. Posterior view, 7. Lateral view.
    8-10. CMC-P 40280j, metaprotaspis; 8. Dorsal view: note that glabellar front rapidly expands forwards, 9. Oblique lateral view, 10. Posterior view.
    11-13. CMC-P 40280l, metaprotaspis; 11. Dorsal view, 12. Oblique lateral view, 13. Posterior view.
    14. CMC-P 40280j*, early meraspid cranidium, dorsal view, x 33.
    15. CMC-P 40280f, early meraspid cranidium, dorsal view, x 27.
    16. CMC-P 40280d, meraspid cranidium, dorsal view, x 17.
    17. CMC-P 40280s, transitory pygidium, dorsal view, x 28.
    18, 19. CMC-P 40280r, holaspid pygidium; 18. Dorsal view, x 15, 19. Lateral view, x 21.
    20-22. CMC-P 40280, holaspid cranidium; 20. Lateral view, x 5.6, 21. Anterior view, x 7.7, 22. Dorsal view, x 8.1.
23-25. **Catillicephalidae** sp. A (not described in the text).
    23-25. CMC-P 40280n, metaprotaspis; 23. Dorsal view, 24. Anterior view, 25. Posterior view: note the presence of occipital ring as a small node.

134
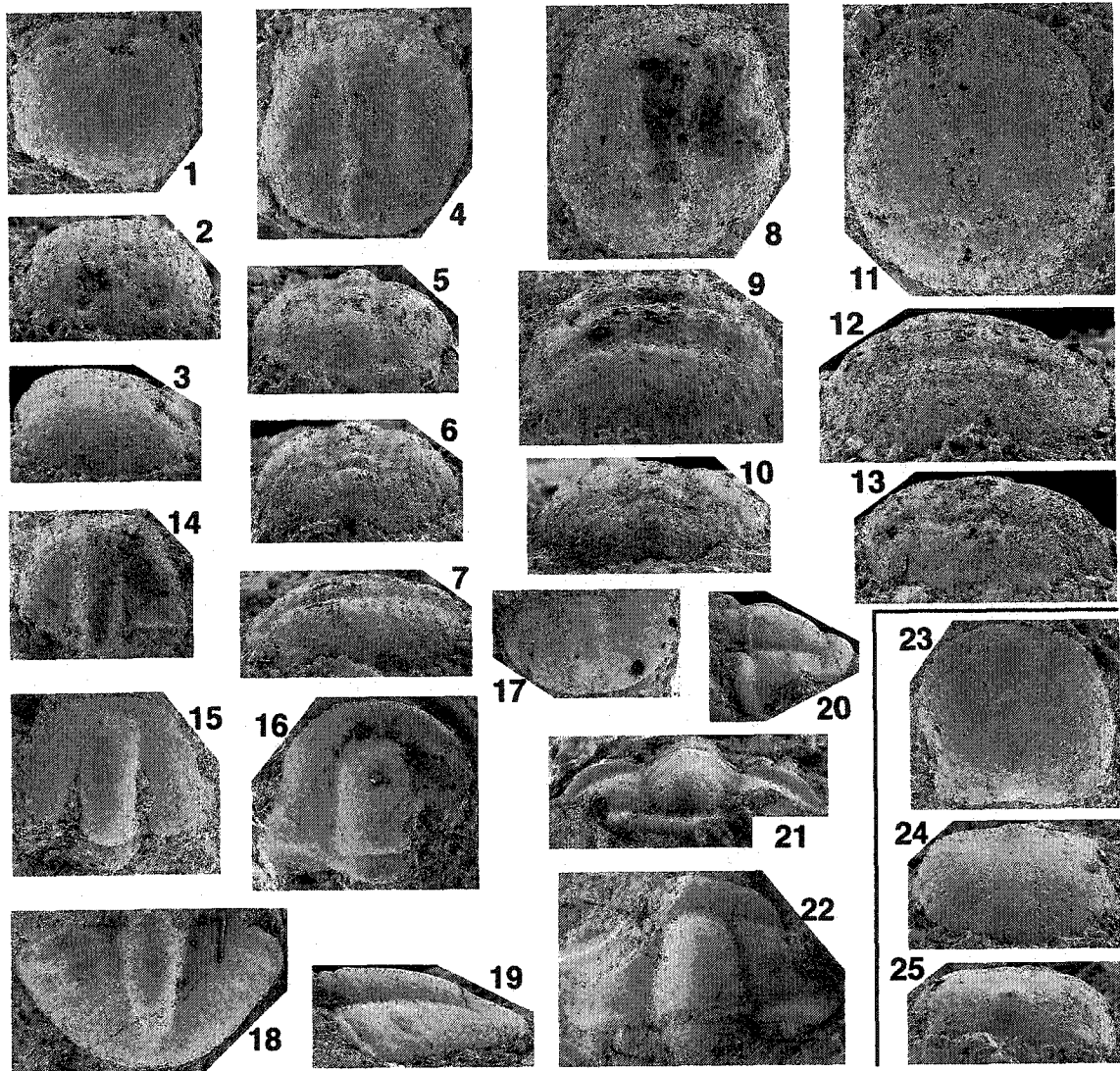
PLATE II-17. *Housia ovata* Palmer, 1965 and **Species undetermined** M. All the specimens are from the *Elvinia* Zone of the Deadwood Formation, South Dakota. All protaspid specimens (Figs. 1-19, 30-33) are x 75.

1-29. *Housia ovata* Palmer, 1965

    1-4. CMC-P 43418b, anaprotaspis; 1. Dorsal view, 2. Anterior view, 3. Posterior view, 4. Lateral view.

    5-8. CMC-P 43418c, anaprotaspis; 5. Dorsal view, 6. Lateral view, 7. Anterior view, 8. Posterior view.

    9-12. CMC-P 43418e, metaprotaspis; 9. Dorsal view, 10. Lateral view, 11. Anterior view, 12. Posterior view.

    13-15. CMC-P 43418h, metaprotaspis; 13. Dorsal view, 14. Lateral view, 15. Anterior view.

    16-19. CMC-P 43418f, metaprotaspis; 16. Dorsal view: note that pits develop in the axial furrows, posterior cranidial marginal furrows, and pygidial pleural furrows, 17. Lateral view, 18. Posterior view, 19. Anterior view.

    20. CMC-P 43418j, early meraspid cranidium, dorsal view, x 43.

    21. CMC-P 43418l, early meraspid cranidium, dorsal view, x 27.

    22. CMC-P 43418n, meraspid cranidium, dorsal view, x 21.

    23. CMC-P 43418u, transitory pygidium, dorsal view, x 25.

    24. CMC-P 43418x, transitory pygidium, dorsal view, x 18: note that six thoracic segments are present and the posteromost one develops long marginal spine..

    25. CMC-P 43418e', holaspid pygidium, dorsal view, x 9.3.

    26. CMC-P 43418y, transitory pygidium, dorsal view, x 17: note the presence of unreleased two thoracic segments.

    27. CMC-P 43418a', early holaspid cranidium, dorsal view, x 14.7.

    28. CMC-P 43418i', holaspid cranidium, dorsal view, x 6.2.

    29. CMC-P 43418d', holaspid cranidium, dorsal view, x 22.

30-33. **Species undetermined** M (not described in the text).

    30-33. CMC-P 43418, anaprotaspis; 30. Dorsal view, 31. Anterior view, 32. Posterior view, 33. Lateral view.

136
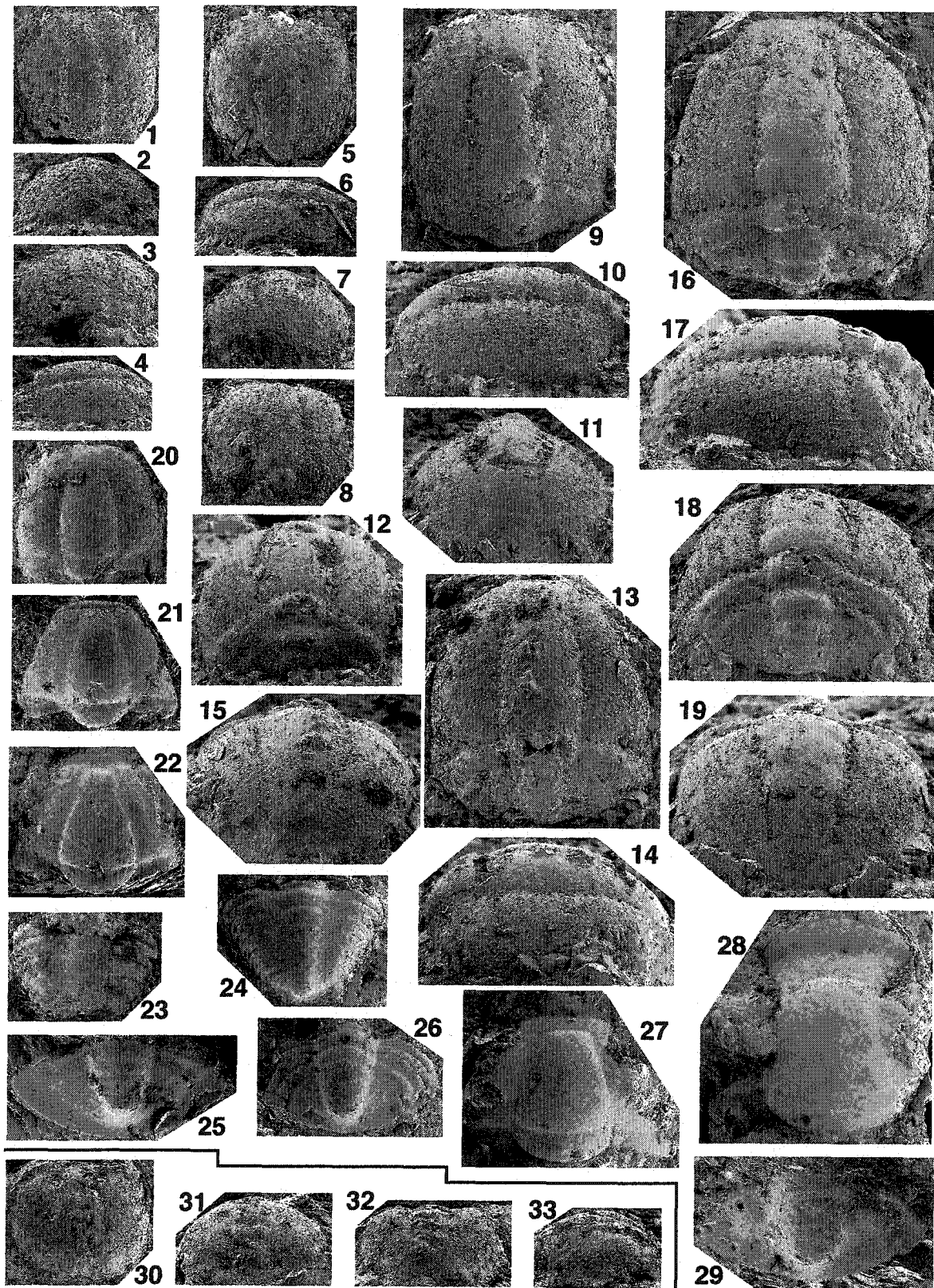
PLATE II-18. *Housia vacuna* (Walcott, 1890), *Housia* sp. A, *Pulchricapitus davisi* Kurtz, 1975, and **Catillicephalidae** sp. B. All protaspid specimens (Figs. 1-6, 17-26, 31-33) are x 75. "*" denotes that the specimen is found in the same limestone sample along with the specimen alphabetically labelled by Hu (1980), but was not described by Hu (1980).

1-16. *Housia vacuna* (Walcott, 1890) from the *Elvinia* zone of the Dry Creek Shale, north-central Wyoming.
  1-4. CMC-P 39744j, anaprotaspis; 1. Dorsal view, 2. Posterior view, 3. Anterior view, 4. Lateral view.
  5, 6. CMC-P 39744k, metaprotaspis; 5. Dorsal view, 6. Oblique lateral view.
  7. CMC-P 39744h, early meraspid cranidium, dorsal view, x 32.
  8. CMC-P 39744e, meraspid cranidium, dorsal view, x 22.
  9. CMC-P 39744g, meraspid cranidium, dorsal view, x 21.
  10. CMC-P 39744s, transitory pygidium, dorsal view, x 32.
  11. CMC-P 39744c', transitory pygidium, dorsal view, x 13.
  12. CMC-P 39744w, transitory pygidium, dorsal view, x 18.
  13. CMC-P 39744z, transitory pygidium, dorsal view, x 16.
  14. CMC-P 39744b', transitory pygidium, dorsal view, x 14.
  15. CMC-P 39744e', holaspid pygidium, dorsal view, x 8.4.
  16. CMC-P 39744a, holaspid cranidium, dorsal view, x 16.
17-22. *Housia* sp. A from the *Elvinia* Zone of the Deadwood Formation, South Dakota (not described in the text).
  17-19. CMC-P 43418a, anaprotaspis; 17. Dorsal view, 18. Posterior view, 19. Oblique lateral view.
  20-22. CMC-P 43418g, metaprotaspis; 20. Dorsal view, 21. Posterior view, 22. Lateral view.
23-30. *Pulchricapitus davisi* Kurtz, 1975 from the *Elvinia* Zone of the Deadwood Formation, South Dakota.
  23-26. CMC-P 43416a, metaprotaspis; 23. Dorsal view, 24. Lateral view, 25. Posterior view, 26. Oblique anterior view.
  27. CMC-P 43416b, early meraspid cranidium, dorsal view, x 31.
  28. CMC-P 43416e, meraspid cranidium, dorsal view, x 33.
  29. CMC-P 43416k*, transitory pygidium, dorsal view, x 21: note that five thoracic segments are yet to be released and pits develop in the pleural furrows.
  30. CMC-P 43416g, holaspid cranidium, dorsal view, x 15.
31-33. **Catillicephalidae** sp. B from the *Elvinia* Zone of the Deadwood Formation, South Dakota (not described in the text).
  31-33. CMC-P 43416, protaspis; 31. Anterior view, 32. Posterior view, 33. Dorsal view.

138
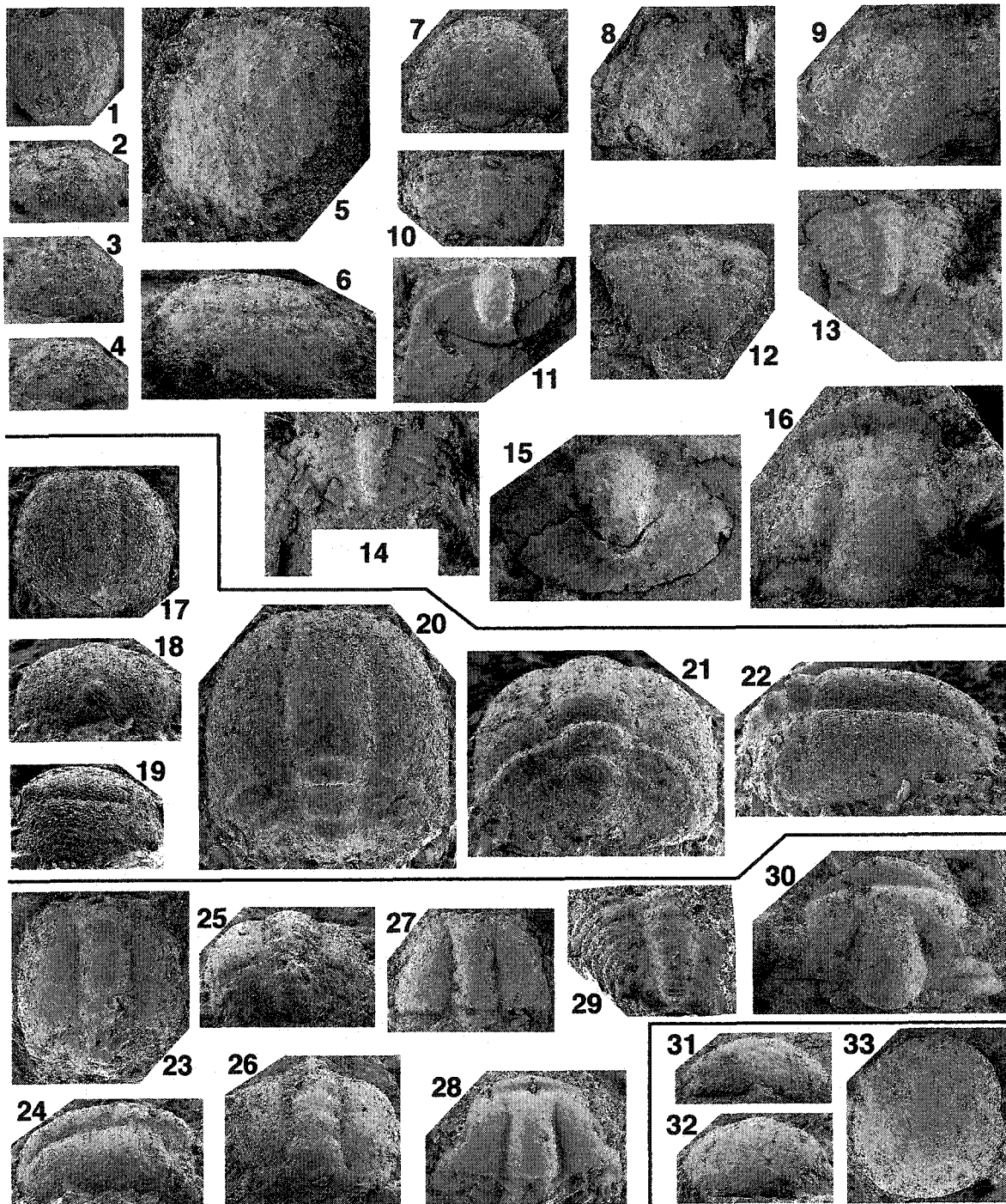
PLATE II-19. *Drabia typica* (Hu, 1979) and **Species undetermined** N. All the specimens are from the *Elvinia* Zone of the Deadwood Formation, South Dakota. All protaspid specimens (Figs. 1-31) are x 75.

1-36. *Drabia typica* (Hu, 1979)
   1-4. CMC-P 43373a, anaprotaspis; 1. Dorsal view, 2. Lateral view, 3. Anterior view, 4. Posterior view.
   5-7. CMC-P 43373c, early metaprotaspis; 5. Dorsal view, 6. Lateral view, 7. Posterior view: note the slit-like impression of posterior cranidial marginal furrow behind the occipital ring as
   8-10. CMC-P 43373d, early metaprotaspis; 8. Dorsal view, 9. Posterior view, 10. Oblique lateral view.
   11-13. CMC-P 43373e, late metaprotaspis; 11. Dorsal view, 12. Lateral view, 13. Posterior view.
   14-16. CMC-P 43373g, late metaprotaspis; 14. Dorsal view, 15. Posterior view, 16. Lateral view.
   17-19. CMC-P 43373h, late metaprotaspis; 17. Dorsal view, 18. Posterior view, 19. Oblique lateral view.
   20-22. CMC-P 43418d, late metaprotaspis; 20. Dorsal view, 21. Posterior view: note that the postero-lateral ends of the fixigenae extends beyond the protopygidium, 22. Oblique lateral view.
   23, 24. CMC-P 43373j, late metaprotaspis; 23. Dorsal view, 24. Oblique posterior view.
   25-27. CMC-P 43373f, late metaprotaspis; 25. Dorsal view, 26. Lateral view, 27. Posterior view: note the ventrally-extended fixigenae.
   28-31. CMC-P 43373j, late metaprotaspis; 28. Dorsal view, 29. Lateral view, 30. Posterior view, 31. Anterior view.
   32. CMC-P 43373, holaspid cranidium, dorsal view, x 15.6.
   33. CMC-P 43373m, early meraspid cranidium, dorsal view, x 43.
   34. CMC-P 43373q, meraspid cranidium, dorsal view, x 33.
   35. CMC-P 43373l, early meraspid cranidium, dorsal view, x 51.
   36. CMC-P 43373k, early meraspid cranidium, dorsal view, x 52.
37. **Species undetermined** N (not described in the text).
   37. CMC-P 43373b, protaspis, x 43.

140
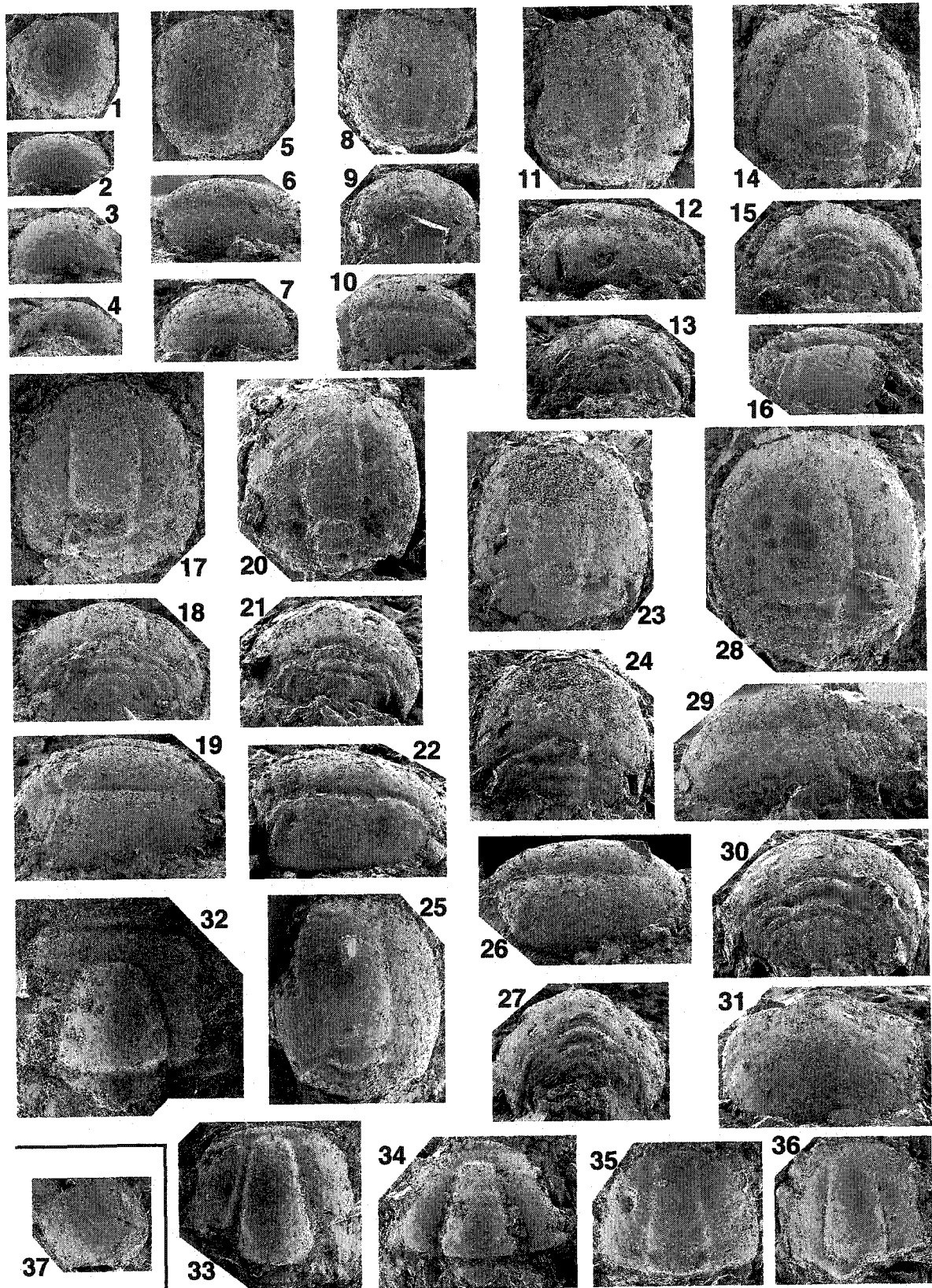
PLATE II-20. *Aphelotoxon triangularia* Hu, 1980, **Phylacteridae** sp. A, **Phylacteridae** sp. B and **Species undetermined** O. All the specimens are from the *Elvinia* Zone (upper Steptoean) of the Deadwood Formation, South Dakota. All protaspid specimens (Figs. 1-4, 11-46) are x 75. "*" denotes the specimen that is found in the same limestone sample along with the specimen alphabetically labelled by Hu (1980), but not described by Hu (1980).

1-10. *Aphelotoxon triangularia* Hu, 1980
    1-4. CMC-P 43417e, metaprotaspis; 1. Dorsal view, 2. Posterior view, 3. Lateral view, 4. Oblique anterior view.
    5. CMC-P 43417k, early meraspid cranidium, dorsal view, x 41.
    6. CMC-P 43417a*, early meraspid cranidium, dorsal view, x 40.
    7. CMC-P 43417o, meraspid cranidium, dorsal view, x 31.
    8. CMC-P 43417y, holaspid cranidium, dorsal view, x 26.
    9. CMC-P 43417c*, meraspid cranidium, dorsal view, x 29.
    10. CMC-P 43417b, transitory pygidium, dorsal view, x 25.
11-18. **Phylacteridae** sp. A (not described in the text).
    11-14. CMC-P 43417c, early metaprotaspis; 11. Dorsal view, 12. Anterior view, 13. Lateral view, 14. Posterior view: note that posterior cranidial marginal furrow is impressed behind the occipital ring.
    15-18. CMC-P 43417f, late metaprotaspis; 15. Dorsal view, 16. Lateral view, 17. Anterior view, 18. Posterior view.
19-43. **Phylacteridae** sp. B
    19-21. CMC-P 43417e*, anaprotaspis; 19. Dorsal view, 20. Posterior view, 21. Lateral view.
    22, 23. CMC-P 43417, anaprotaspis; 22. Dorsal view, 23. Anterior view.
    24-27. CMC-P 43417b, early metaprotaspis; 24. Dorsal view, 25. Posterior view: note the development of weakly-impressed posterior cranidial marginal furrow behind the occipital ring, 26. Lateral view, 27. Anterior view.
    28-31. CMC-P 43417d, early metaprotaspis; 28. Dorsal view: note the development of glabellar furrows, 29. Lateral view, 30. Posterior view, 31. Anterior view.
    32-35. CMC-P 43417h, late metaprotaspis; 32. Dorsal view, 33. Lateral view, 34. Posterior view, 35. Anterior view.
    36-39. CMC-P 43417i, late metaprotaspis; 36. Dorsal view, 37. Lateral view, 38. Posterior view, 39. Anterior view.
    40-43. CMC-P 43417g, late metaprotaspis; 40. Dorsal view, 41. Posterior view, 42. Anterior view, 43. Lateral view.
44-46. **Species undetermined** O (not described in the text).
    44-46. CMC-P 43417a, anaprotaspis; 44. Anterior view, 45. Lateral view, 46. Dorsal view.

142
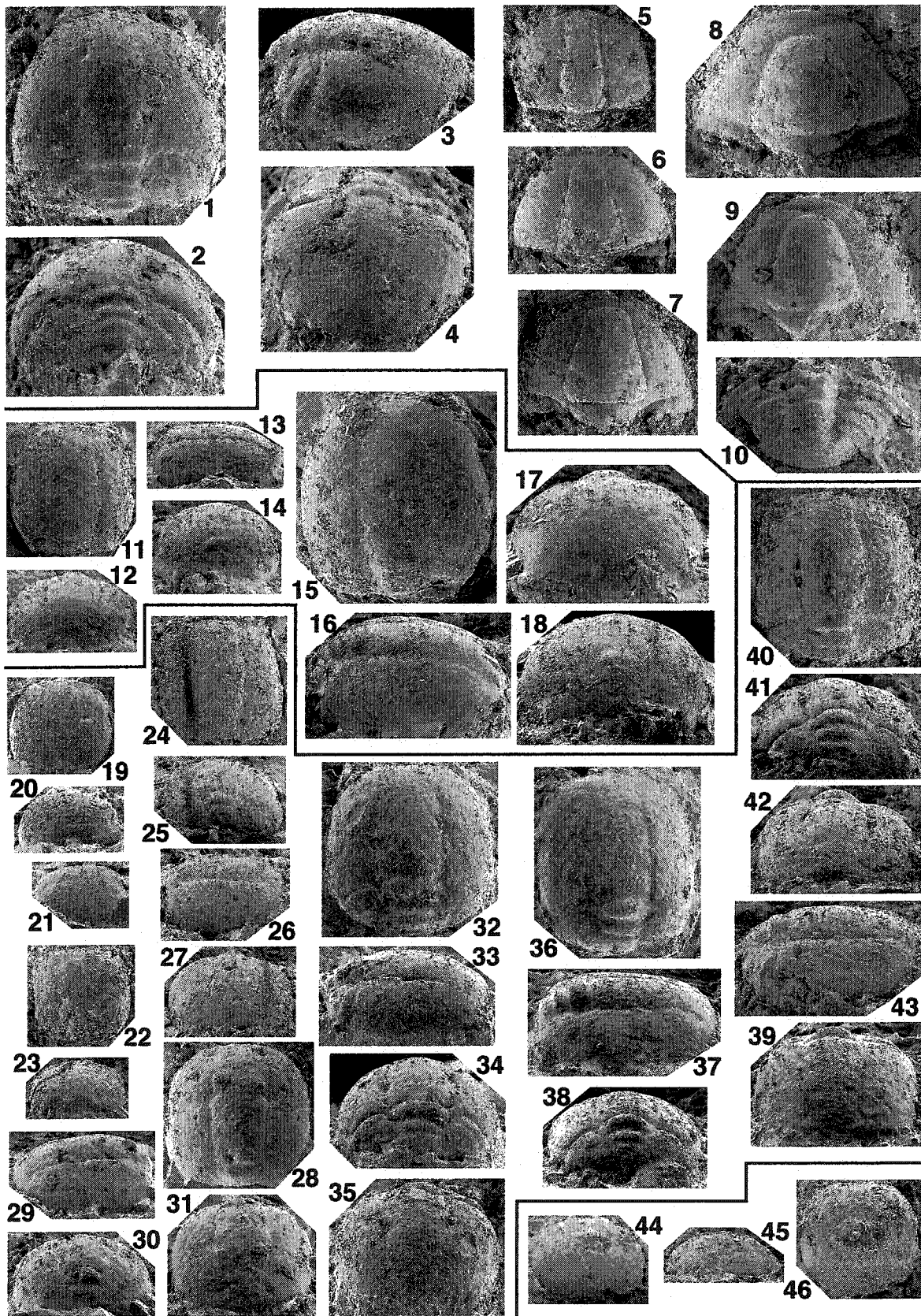
PLATE II-21. *Ponumia obscura* (Lochman, 1964), **Species undetermined** P and ?**Phylacteridae** sp. A. All the specimens are from the *Elvinia* Zone of the Dry Creek Shale, north-central Wyoming. All protaspid specimens (Figs. 1-20, 29-36) are x 75.

1-28. *Ponumia obscura* (Lochman, 1964)
    1, 2. CMC-P 39745i, anaprotaspis; 1. Dorsal view, 2. Lateral view.
    3, 4. CMC-P 39745j, anaprotaspis; 3. Dorsal view, 4. Lateral view.
    5, 6. CMC-P 39745k, anaprotaspis; 5. Dorsal view, 6. Lateral view.
    7, 8. CMC-P 39745e, anaprotaspis; 7. Dorsal view, 8. Lateral view.
    9, 10. CMC-P 39745g, anaprotaspis; 9. Dorsal view, 10. Lateral view.
    11, 12. CMC-P 39745f, metaprotaspis, 11. Dorsal view, 12. Lateral view.
    13, 14. CMC-P 39745m, metaprotaspis; 13. Dorsal view, 14. Lateral view.
    15, 16. CMC-P 39745o, metaprotaspis; 15. Dorsal view, 16. Lateral view.
    17, 18. CMC-P 39745l, metaprotaspis; 17. Dorsal view, 18. Lateral view.
    19, 20. CMC-P 39745p, metaprotaspis; 19. Dorsal view, 20. Lateral view.
    21. CMC-P 39745v, early meraspid cranidium, dorsal view, x 43.
    22. CMC-P 39745r, early meraspid cranidium, dorsal view, x 36.
    23. CMC-P 39745z, transitory pygidium, dorsal view, x 30.
    24. CMC-P 39745q, meraspid cranidium, dorsal view, x 37.
    25, 26. CMC-P 39745t, holaspid cranidium; 25. Dorsal view, x 14, 26. Oblique lateral view, x 18.
    27, 28. CMC-P 39745y, holaspid pygidium; 27. Oblique lateral view, x 21, 28. Dorsal view, x 19.
29, 30. **Species undetermined** P (not described in the text).
    29. CMC-P 39745, anaprotaspis, dorsal view.
    30. CMC-P 39745a, anaprotaspis, dorsal view.
31-36. ?**Phylacteridae** sp. A (not described in the text).
    31, 32. CMC-P 39745b, anaprotaspis; 31. Dorsal view, 32. Lateral view.
    33, 34. CMC-P 39745c, anaprotaspis; 33. Dorsal view, 34. Lateral view.
    35, 36. CMC-P 39745d, anaprotaspis; 35. Dorsal view, 36. Lateral view.

144
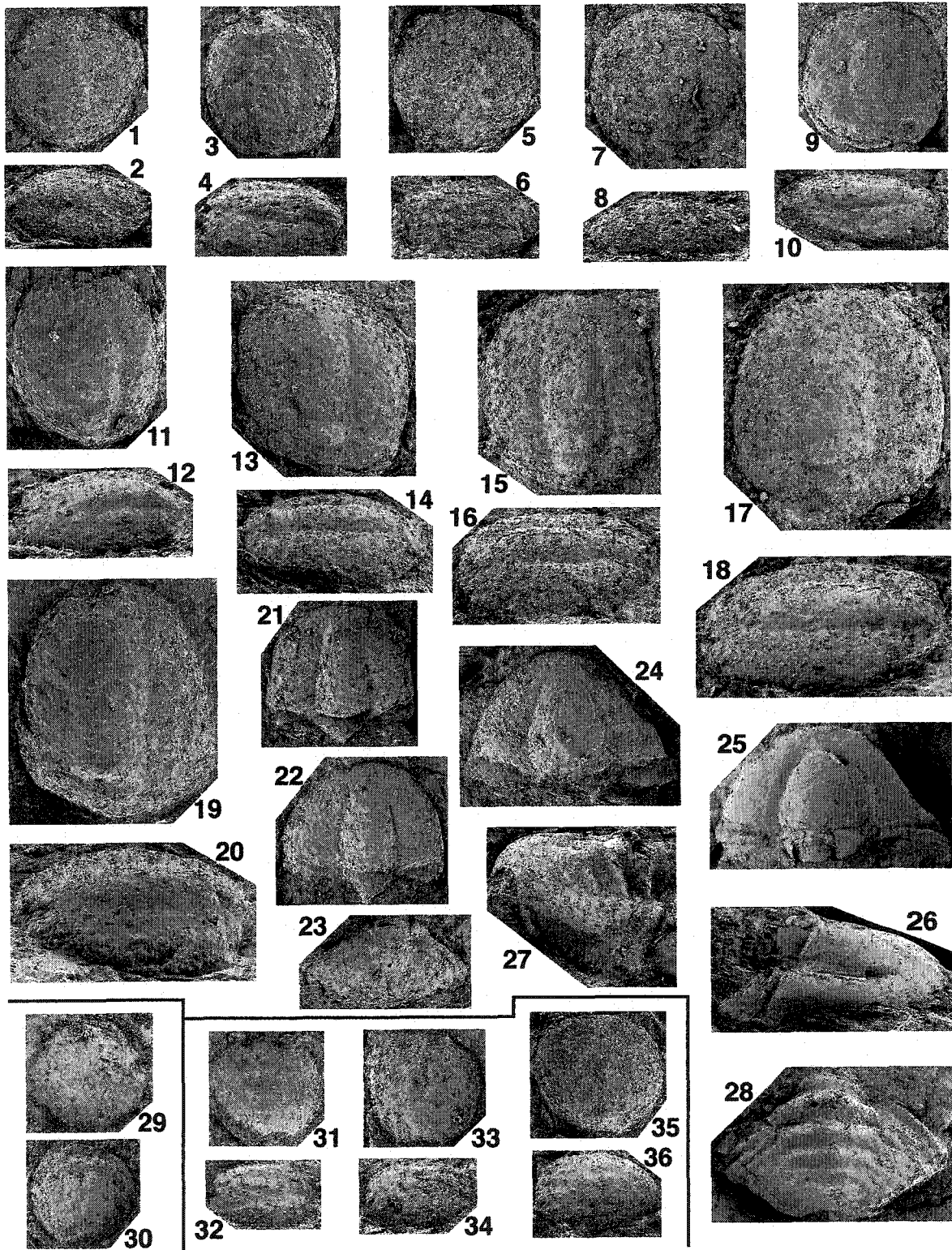
PLATE II-22. *Paranumia triangularia* Hu, 1973 and **Species undetermined** Q. All the specimens are from the Ibexian Deadwood Formation, northeast Wyoming. All protaspid specimens (Figs. 1-4, 16-19) are x 75.

1-15. *Paranumia triangularia* Hu, 1973
   1-4. CMC-P 38749f, metaprotaspis; 1. Dorsal view, 2. Lateral view, 3. Posterior view, 4. Anterior view.
   5. CMC-P 41556f, early meraspid cranidium, dorsal view, x 74.
   6. CMC-P 41556b, early meraspid cranidium, dorsal view, x 34.
   7. CMC-P 41556e, meraspid cranidium, dorsal view, x 31.
   8. CMC-P 41556, holaspid cranidium, dorsal view, x 30.
   9. CMC-P 41556n, transitory pygidium, dorsal view, x 71.
   10. CMC-P 41556p, transitory pygidium, dorsal view, x 63.
   11. CMC-P 41556o, transitory pygidium, dorsal view, x 64.
   12, 13. CMC-P 41556u, holaspid pygidium; 12. Dorsal view, x 23, 13. Lateral view, x 27.
   14, 15. CMC-P 41556r, meraspid pygidium; 14. Dorsal view, x 52, 15. Lateral view, x 50.
16-19. **Species undetermined** Q (not described in the text).
   16-19. CMC-P 41556m, anaprotaspis; 16. Dorsal view: note the development of fixigenal spines, 17. Posterior view, 18. Anterior view, 19. Lateral view.

146
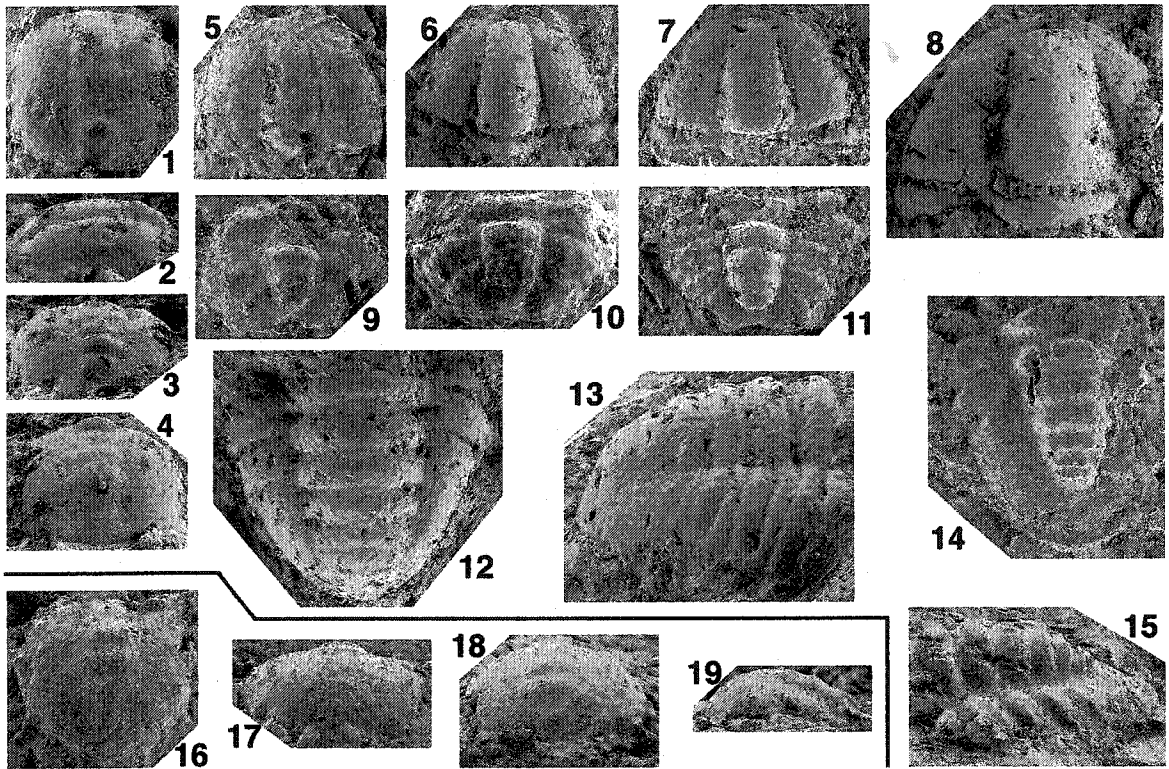
PLATE II-23. *Arapahoia arbucklensis* (Stitt, 1971), **Plethopeltidae** sp. A and **Species undetermined** R. All specimens are from possibly *Missisquoia* Zone of Deadwood Formation, exposed at south slope of Sheep Mountain, near Bearlodge Ranch, east-central Wyoming. All protaspid specimens (Figs. 1-12, 24-33) are x 75.

1-23. *Arapahoia arbucklensis* (Stitt, 1971)

1-4. CMC-P 42618c, metaprotaspis; 1. Dorsal view, 2. Lateral view: note that the glabellar front is lower-leveled than adjacent pleural regions, 3. Oblique posterior view, 4. Anterior view.

5-8. CMC-P 42618d, metaprotaspis; 5. Dorsal view, 6. Lateral view, 7. Posterior view, 8. Anterior view.

9-12. CMC-P 42618f, metaprotaspis; 9. Dorsal view, 10. Lateral view, 11. Posterior view, 12. Anterior view.

13. CMC-P 42618h, early meraspid cranidium, dorsal view, x 41.

14. CMC-P 42618m, early meraspid cranidium, dorsal view, x 33.

15. CMC-P 42618j, meraspid cranidium, dorsal view, x 31.

16. CMC-P 42618p, meraspid cranidium, dorsal view, x 23.

17. CMC-P 42618a', meraspid cranidium, dorsal view, x 17.

18. CMC-P 42618f', holaspid pygidium, dorsal view, x 8.1.

19, 20. CMC-P 42618z, early holaspid pygidium; 19. Dorsal view, x 18, 20. Lateral view, x 26.

21. CMC-P 42618u, transitory pygidium of <u>Arapahoia</u> sp. nov., dorsal view, x 36.

22, 23. CMC-P 42618d', holaspid cranidium, x 11; 22. Oblique lateral view, 23. Dorsal view.

24-31. **Plethopeltidae** sp. A (not described in the text).

24-27. CMC-P 42618b, metaprotaspis; 24. Dorsal view: note that transglabellar furrows are well-developed, 25. Lateral view, 26. Posterior view, 27. Anterior view.

28-31. CMC-P 42618e, metaprotaspis; 28. Dorsal view, 29. Lateral view, 30. Posterior view, 31. Anterior view.

32, 33. **Species undetermined** R (not described in the text).

32, 33. CMC-P 42618a, anaprotaspis; 32. Dorsal view, 33. Oblique posterior view.

148
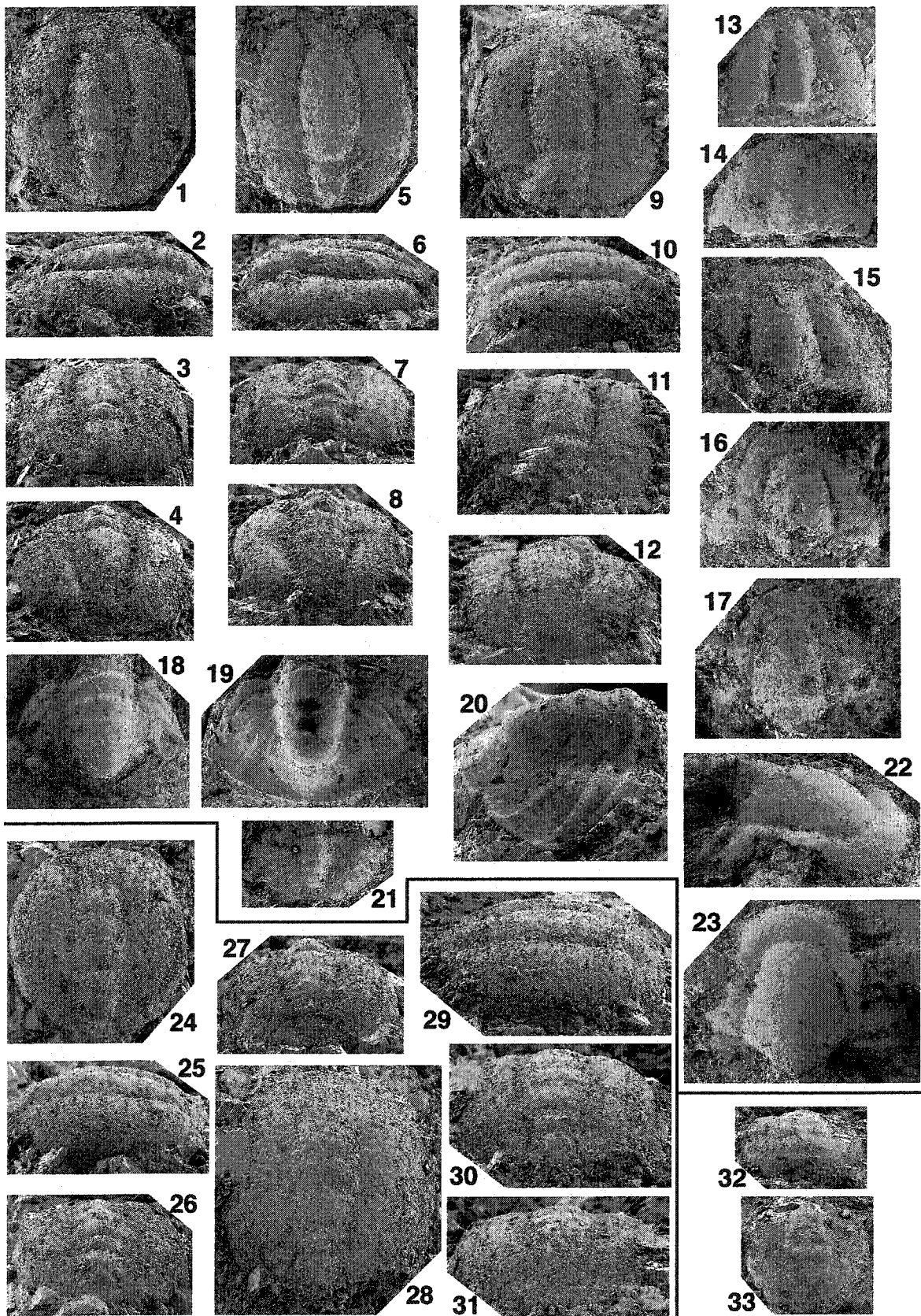
PLATE II-24. *Norwoodella halli* Resser, 1938. All specimens are from the upper *Cedaria* Zone of the Bonneterre Dolomite, Missouri. All protaspid specimens (Figs. 1-11, 14, 15, 17, 18) are x 75.

1-25. *Norwoodella halli* Resser, 1938
    1, 2. USNM 143466o, early anaprotaspis; 1. Dorsal view, 2. Anterior or Posterior view.
    3-5. USNM 143466k, late anaprotaspis; 3. Dorsal view, 4. Posterior view: note the presence of short posterior fixigenal spines that are strongly directed ventrally, 5. Lateral view.
    6-8. USNM 143466j, late anaprotaspis; 6. Dorsal view, 7. Lateral view: note the presence of posterior fixigenal spines, 8. Posterior view.
    9-11. USNM 143466i, early metaprotaspis; 9. Dorsal view, 10. Lateral view, 11. Posterior view.
    12. USNM 143466c, early meraspid cranidium, dorsal view, x 24
    13. USNM 143466x, transitory pygidium, dorsal view, x 31.
    14, 15. USNM 143466h, early metaprotaspis; 14. Dorsal view, 15. Posterior lateral view.
    16. USNM 143466r, early holaspid pygidium, dorsal view, x 12.
    17, 18. USNM 143466g, early metaprotaspis; 17. Dorsal view, 18. Posterior view: note that distal ends of fixigenal area strongly curve inwards.
    19. USNM 143466b, meraspid cranidium, dorsal view, x 23.
    20. USNM 143466w, transitory pygidium, dorsal view, x 27.
    21-23. USNM 143466v, holaspid pygidium; 21. Dorsal view, x 10.3, 22. Posterior view, x 10.3, 23. Lateral view, x 10.
    24, 25. USNM 143466a, holaspid cranidium; 24. Obllique lateral view, x 11.5, 25. Dorsal view, x 12.

150
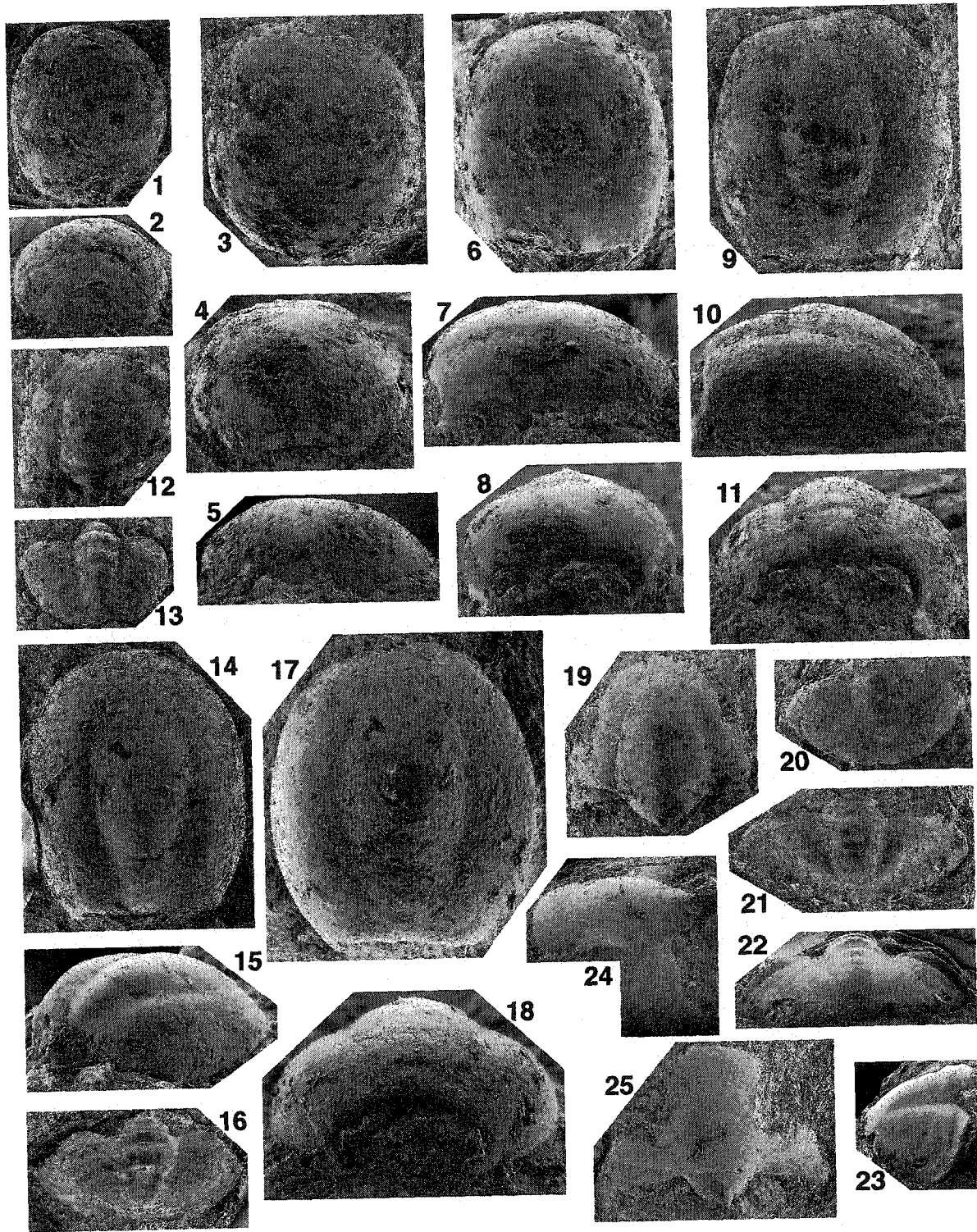
PLATE II-25. *Norwoodella halli* Resser, 1938. All specimens are from the upper *Cedaria* Zone of the Bonneterre Dolomite, Missouri. All protaspid specimens (Figs. 1-8) are x 75.

1-8. *Norwoodella halli* Resser, 1938
    1-4. USNM 143466d, late metaprotaspis; 1. Dorsal view, 2. Posterior lateral view, 3. Posterior view, 4. Lateral view.
    5-8. USNM 143466e, late metaprotaspis; 5. Dorsal view, 6. Lateral view, 7. Posterior view, 8. Posterior lateral view.

152
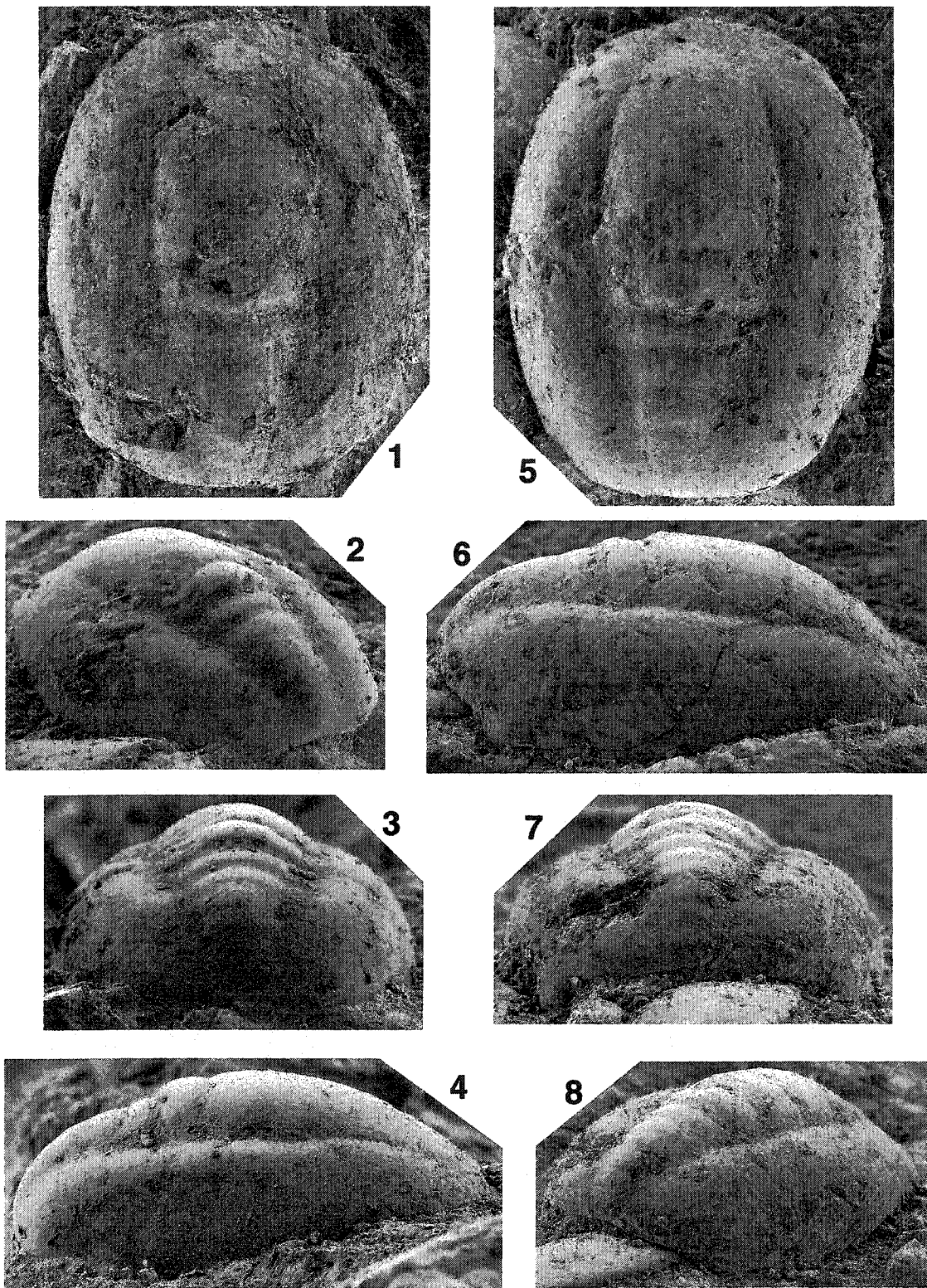
PLATE II-26. Norwoodiidae sp. A and **Norwoodiidae** sp. B. All the specimens are from the upper *Cedaria* Zone of Bonneterre Dolomite, Missouri. "*" denotes the specimen that is found together with the specimen alphabetically labelled, but was not described by Hu (1963). All protaspid specimens (Figs. 1-15) are x 75.

1-15. **Norwoodiidae** sp. A (not described in the text).
  1-4. USNM 143466n, anaprotaspis; 1. Dorsal view, 2. Lateral view, 3. Posterior view, 4. Anterior view.
  5-7. USNM 143466l*, anaprotaspis; 5. Dorsal view, 6. Posterior view, 7. Lateral view.
  8-11. USNM 143466l, anaprotaspis; 8. Dorsal view, 9. Posterior view, 10. Lateral view, 11. Anterior view.
  12-15. USNM 143466f, anaprotaspis; 12. Dorsal view, 13. Posterior view: note that posterior fixigenal spines strongly direct inwards, 14. Posterior lateral view, 15. Lateral view.
16-18. **Norwoodiidae** sp. B (not described in the text).
  16-18. USNM 143466m, anaprotaspis; 16. Dorsal view, 17. Posterior or anterior view, 18. Lateral view.

154
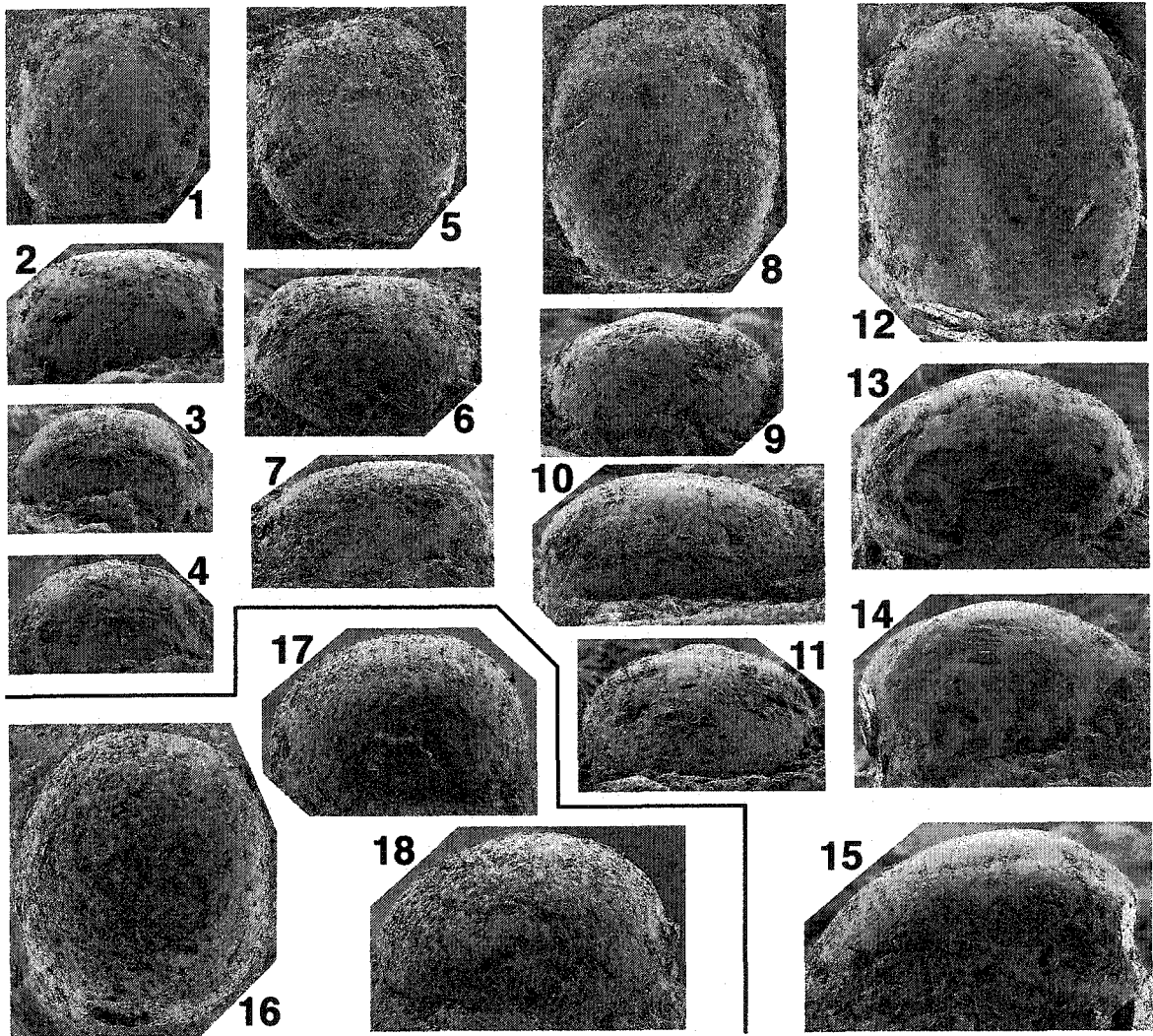
PLATE II-27. *Ptychaspis bullasa* Lochman and Hu, 1959, **Species undetermined** S and **Ptychaspidinae** sp. A. All the specimens are from the *Ptychaspis-Prosuakia* Zone (upper Sunwaptan) of the St. Charles Formation, Idaho. All protaspid specimens (Figs. 1-7, 15-18) are x 75.

1-14. *Ptychaspis bullasa* Lochman and Hu, 1959
    1-3. CMC-P 38735b, metaprotaspis; 1. Dorsal view: note that the eye ridge is large and extends into the mid-shield length, 2. Anterior view: note the development of brim-like anterior border, 3. Lateral view: note the fingerprint-like ornaments on the surface.
    4-7. CMC-P 38735d, metaprotaspis; 4. Anterior view, 5. Dorsal view, 6. Oblique posterior view, 7. Lateral view.
    8. CMC-P 38735e, early meraspid cranidium, dorsal view, x 25.
    9. CMC-P 38735h, late meraspid cranidium, dorsal view, x 18.7.
    10, 11. CMC-P 38735o, holaspid cranidium, x 11.5; 10. Dorsal view, 11. Lateral view.
    12. CMC-P 38735w, transitory pygidium, dorsal view, x 30.
    13. CMC-P 38735x, transitory pygidium, dorsal view, x 24.
    14. CMC-P 38735y, holaspid pygidium, dorsal view, x 9.3.
15. **Species undetermined** S (not described in the text).
    15. CMC-P 38735a, anaprotaspis, dorsal view: note the bilobed L3/L2.
16-19. **Ptychaspidinae** sp. A (not described in the text).
    16-19. CMC-P 38735c, metaprotaspis; 16. Posterior view, 17. Anterior view, 18. Dorsal view, 19. Lateral view.

156
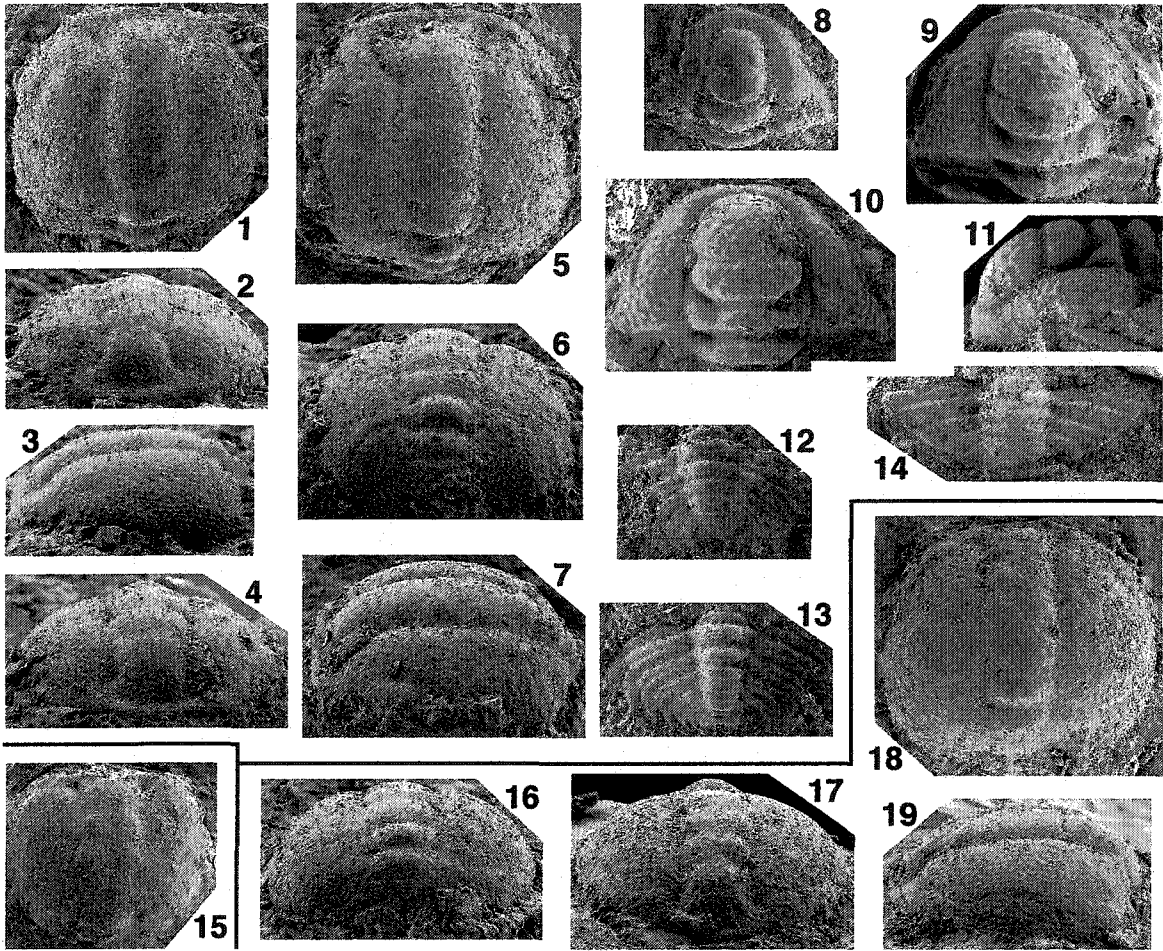
PLATE II-28. *Solenopleura acadica* Whiteaves, 1885. All specimens are from the Middle Cambrian Porter Road Formation, St. John, New Brunswick, and x 75.

1-7. *Solenopleura acadica* Whiteaves, 1885
  1. UA 12833, anaprotaspis, dorsal view.
  2. UA 12834, early meraspid cranidium, dorsal view.
  3. UA 12835, questionable metaprotaspis, dorsal view: note that posterior part of the specimen is covered with matrix.
  4. UA 12836, early meraspid cranidium, dorsal view.
  5. UA 12837, late meraspid cranidium, dorsal view
  6. UA 12838, early meraspid cranidium, dorsal view.
  7. UA 12839, transitory pygidium, dorsal view.

158
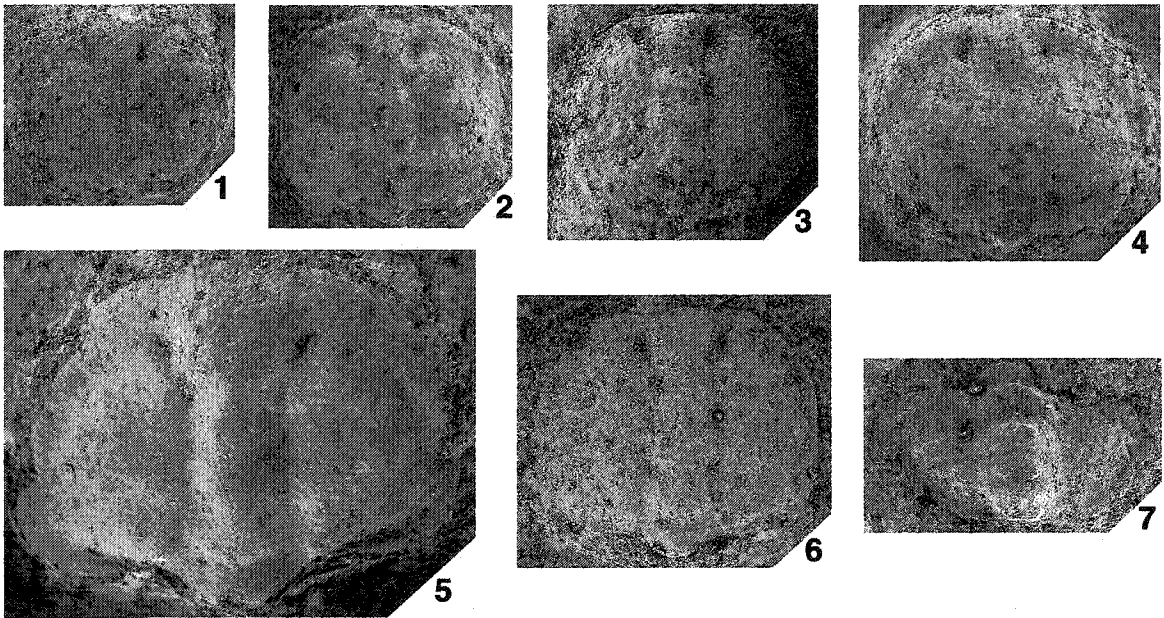
PLATE II-29. *Olenus gibbosus* (Wahlenberg, 1821). All specimens are from the Alum Shales (Upper Cambrian), Norway. All protaspid specimens (Figs. 1-19) are x 75.

1-27. *Olenus gibbosus* (Wahlenberg, 1821)

 1-3. CMC-P 38736a, anaprotaspis; 1. Dorsal view: note the development of two pairs of fixigenal spines in right posterior part of the shield, 2. Posterior view: note the axis with independent convexity, 3. Lateral view: note that anterior and mid-fixigenal spine pairs are preserved in left part of the shield.

 4-7. CMC-P 38736b, anaprotaspis; 4. Dorsal view, 5. Posterior view, 6. Anterior view, 7. Oblique lateral view.

 8. CMC-P 38736c, anaprotaspis, dorsal view.

 9-12. CMC-P 38736d, metaprotaspis; 9. Dorsal view, 10. Anterior view, 11. Oblique lateral view, 12. Posterior view: note that protopygidium is differentiated and oriented ventrally, and the presence of long posterior fixigenal spine (black arrow)

 13-16, 19. CMC-P 38736e, metaprotaspis; 13. Dorsal view, 14. Posterior view, 15. Oblique lateral view, 16. Anterior view, 19. Oblique lateral view: note that the protopygidium is strongly ventrally oriented.

 17, 18. CMC-P 38736f, metaprotaspis; 17. Dorsal view, 18. Posterior view: note a long fixigenal spine (black arrow)

 20. CMC-P 38736i, meraspid cranidium, dorsal view, x 32.

 21. CMC-P 38736n, meraspid cranidium, dorsal view, x 21.

 22. CMC-P 38736z, transitory pygidium, dorsal view, x 49.

 23. CMC-P 38736a', transitory cranidium, dorsal view, x 35.

 24, 25. CMC-P 38736q, holaspid cranidium; 24. Dorsal view, x 22, 25. Oblique anterior view, x 18.

 26, 27. CMC-P 38736b', holaspid pygidium; 26. Oblique posterior view, x 15, 27. Dorsal view, x 13.
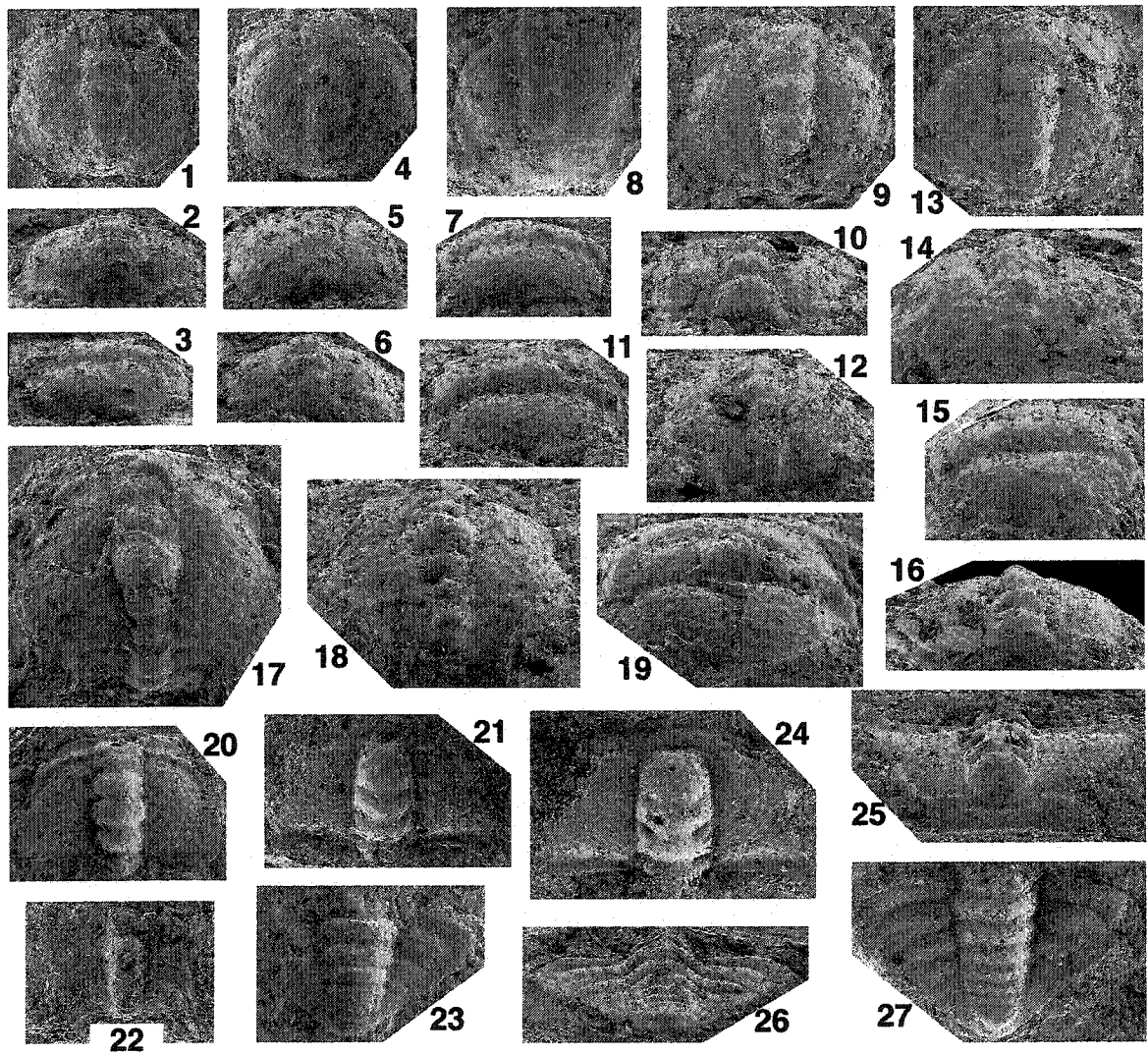
PLATE II-30. *Apoplanias rejectus* Lochman, 1964, **Species undetermined** T and **Parabolinoididae** sp. A. All the specimens are from the *Missisquoia* Zone (Lower Ordovician) of the Deadwood Formation, northeast Wyoming. All protaspid specimens (Figs. 1-13) are x 75.

1-22. *Apoplanias rejectus* Lochman, 1964
  1-3. CMC-P 38749d, anaprotaspis; 1. Dorsal view, 2. Posterior view, 3. Lateral view.
  4-7. CMC-P 38749e, anaprotaspis; 4. Anterior view, 5. Dorsal view, 6. Posterior view, 7. Lateral view.
  8-10. CMC-P 41556l, metaprotaspis; 8. Lateral view, 9. Dorsal view, 10. Posterior view.
  11-13. CMC-P 41556k, metaprotaspis; 11. Anterior view, 12. Dorsal view, 13. Posterior view.
  14. CMC-P 38749i, early meraspid cranidium, dorsal view, x 72.
  15. CMC-P 38740j, early meraspid cranidium, dorsal view, x 29.
  16. CMC-P 38740k, meraspid cranidium, dorsal view, x 25.
  17. CMC-P 38740g, early meraspid cranidium, dorsal view, x 41.
  18, 19. CMC-P 38740q, holaspid cranidium, x 11; 18. Dorsal view, 19. Oblique anterior view.
  20-22. CMC-P 38740u, holaspid pygidium; 20. Lateral view, x 31, 21. Posterior view, x 28, 22. Dorsal view, x 30: note the development of marginal spines.
23-27 **Species undetermined** T (not described in the text).
  23-27. CMC-P 38740b, anaprotaspis; 23. Dorsal view, 24. Anterior view, 25. Posterior view, 26. Lateral view, 27. Oblique lateral view.
28. **Parabolinoididae** sp. A (not described in the text).
  28. CMC-P 38740f, early meraspid cranidium, dorsal view, x 56.
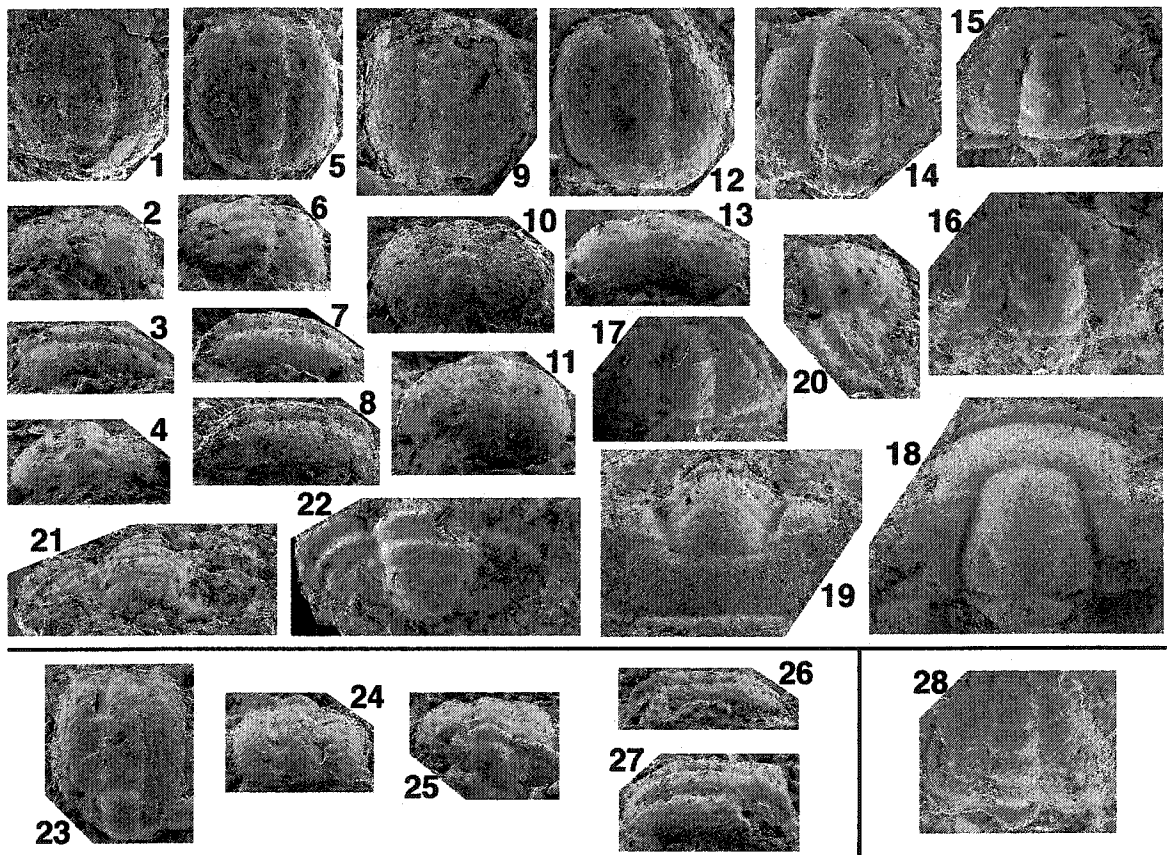
PLATE II-31. *Acerocare ecorne* Angelin, 1878. All specimens from the *Acerocare* Zone (2da) of the Upper Cambrian, Sweden. All protaspid specimens (Figs. 1-15) are x 75.

1-25. *Acerocare ecorne* Angelin, 1878
    1-4. CMC-P 38738a, anaprotaspis; 1. Dorsal view, 2. Oblique posterior view: note the development of posterior fixigenal spine which is short and blunted, 3. Anterior view, 4. Lateral view.
    5, 6. CMC-P 38738c, metaprotaspis; 5. Dorsal view, 6. Lateral view.
    7, 8. CMC-P 38738d, metaprotaspis; 7. Dorsal view, 8. Anterior view.
    9, 10. CMC-P 38738e, metaprotaspis; 9. Dorsal view: note the presence of long posterior fixigenal spine and protopygidial marginal furrow (black arrows), 10. Posterior view.
    11, 12. CMC-P 38738b, metaprotaspis; 11. Anterior view, 12. Lateral view.
    13-15. CMC-P 38738f, metaprotaspis; 13. Anterior view: note the long posterior fixigenal spine indicated by a black arrow, 14. Posterior view, 15. Lateral view.
    16. CMC-P 38738h, early meraspid cranidium, dorsal view, x 45.
    17. CMC-P 38738g, early meraspid cranidium, dorsal view, x 54.
    18. CMC-P 38738k, meraspid cranidium, dorsal view, x 30.
    19-21. CMC-P 38738o, holaspid cranidium; 19. Dorsal view, x 12, 20. Anterior view, x 12, 21. Lateral view, x 11.
    22. CMC-P 38738z, transitory pygidium, dorsal view, x 26.
    23-25. CMC-P 38738c', holaspid pygidium; 23. Oblique posterior view, x 9.6, 24. Lateral view, x 11, 25. Dorsal view, x 9.2.

164
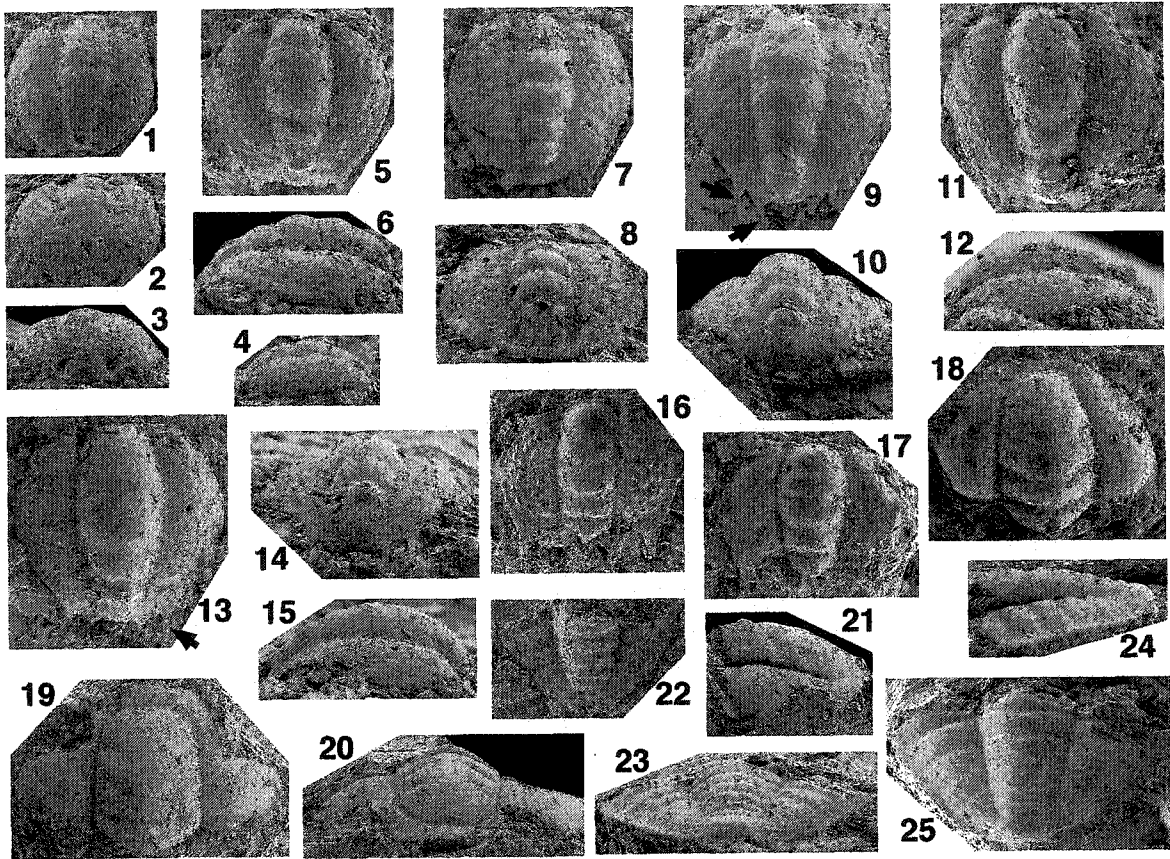
PLATE II-32. *Orygmaspis (Parabolinoides) contractus* (Frederickson, 1949), *Orygmaspis (Parabolinoides)* sp. A, **Parabolinoididae** sp. B and *Taenicephalus shumardi* (Hall, 1863). All the specimens are from the *Conaspis* Zone (lower Sunwaptan) of the Deadwood Formation, South Dakota. All protaspid specimens (Figs. 1-18, 28-30, 40-42) are x 75.

1-25. *Orygmaspis (Parabolinoides) contractus* (Frederickson, 1949)

   1-3. CMC-P 39743a, anaprotaspis; 1. Dorsal view: note the development of short and stout posterior fixigenal spine, 2. Anterior view, 3. Lateral view.

   4-6. CMC-P 39743b, anaprotaspis; 4. Dorsal view, 5. Oblique posterior view, 6. Lateral view.

   7-9. CMC-P 43344, metaprotaspis; 7. Dorsal view, 8. Oblique posterior view, 9. Lateral view.

   10-12. CMC-P 43344a, metaprotaspis; 10. Dorsal view, 11. Anterior view, 12. Oblique posterior view.

   13-15. CMC-P 43344b, metaprotaspis; 13. Dorsal view, 14. Posterior view, 15. Lateral view.

   16-18. CMC-P 39743c, tentatively assigned metaprotaspis; 16. Dorsal view, 17. Oblique lateral view, 18. Posterior view.

   19. CMC-P 43344d, early meraspid cranidium, dorsal view, x 49.

   20. CMC-P 39743f, meraspid cranidium, dorsal view, x 26.

   21. CMC-P 39743i, meraspid cranidium, dorsal view, x 14.

   22. CMC-P 39743n, transitory pygidium, dorsal view, x 14.3.

   23, 24. CMC-P 39743g', holaspid cranidium; 23. Dorsal view, x 8.7, 24. Lateral view, x 10.

   25. CMC-P 43344r, holaspid pygidium, dorsal view, x 10.6.

26, 27. *Orygmaspis (Parabolinoides)* sp. A (not described in the text).

   26. CMC-P 39743o, holaspid pygidium, dorsal view, x 14.5.

   27. CMC-P 39743p, holaspid pygidium, dorsal view, x 9.3.

28-30. **Parabolinoididae** sp. B (not described in the text).

   28-30. CMC-P 39743, anaprotaspis; 28. Dorsal view, 29. Lateral view, 30. Posterior view.

31-42. *Taenicephalus shumardi* (Hall, 1863).

   31. CMC-P 43343l, holaspid cranidium, dorsal view, x 6.1.

   32, 33. CMC-P 43343c, holaspid pygidium; 32. Dorsal view, x 15.2, 33. Lateral view, x 15.4.

   34. CMC-P 43343o, meraspid cranidium, dorsal view, x 26.

   35, 36. CMC-P 43343w, early meraspid cranidium, x 54; 35. Dorsal view, 36. Posterior view.

   37. CMC-P 43343u, early meraspid cranidium, dorsal view, x 52.

   38. CMC-P 43343v, early meraspid cranidium, dorsal view, x 54.

   40-42. CMC-P 43343x, metaprotaspis; 40. Dorsal view, 41. Oblique posterior view, 42. Oblique lateral view.

166
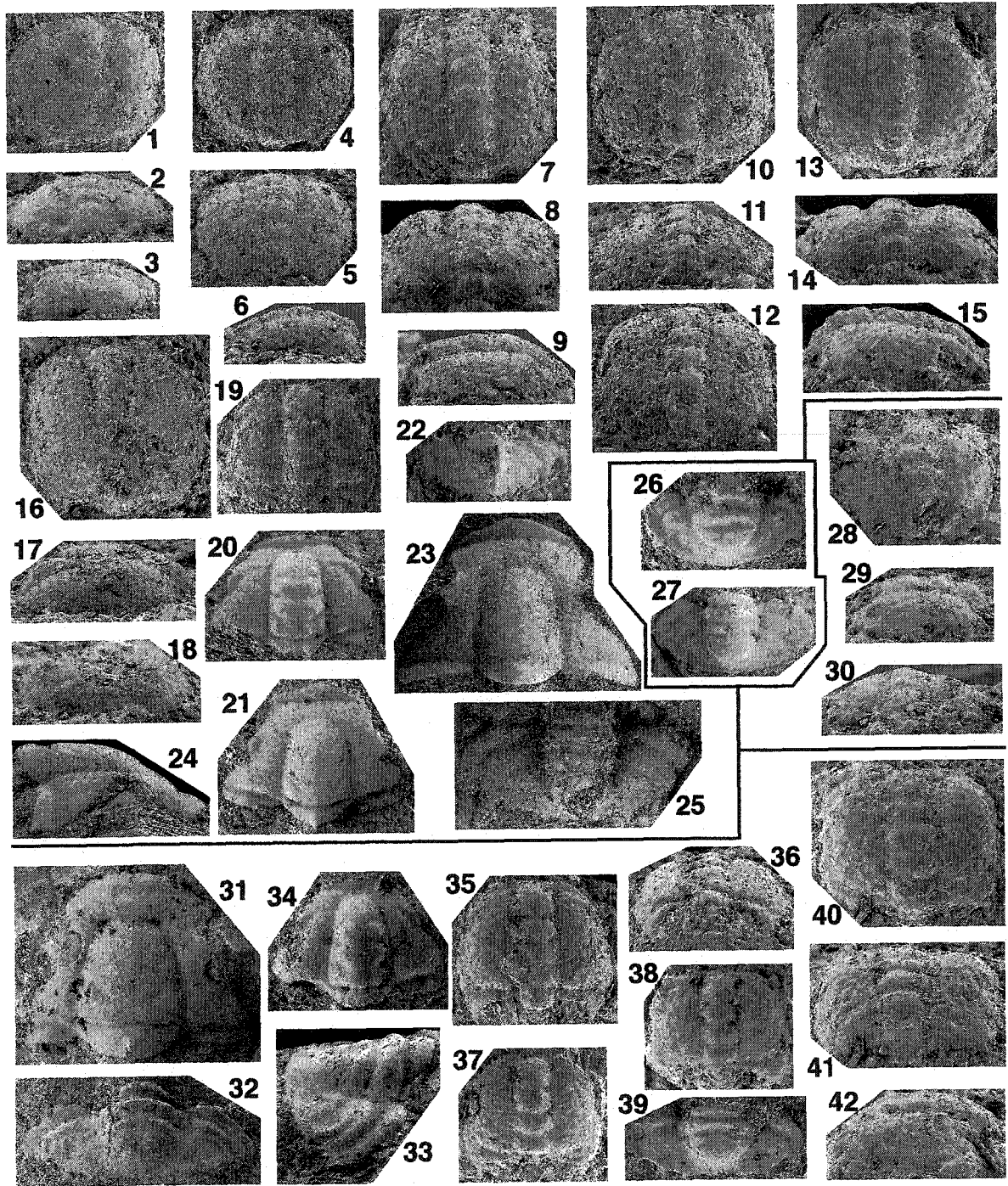
PLATE II-33. *Aphelaspis subditus* Palmer, 1962. All specimens from the *Aphelaspis* zone of the Hamburg Limestone, Nevada. All protaspid specimens (Figs. 1-13) are x 75.

1-22. *Aphelaspis subditus* Palmer, 1962

    1-3. CMC-P 39742, anaprotaspis; 1. dorsal view, 2. Lateral view, 3. Posterior view.

    4-6. CMC-P 39742a, anaprotaspis; 4. Dorsal view, 5. Posterior view, 6. Lateral view.

    7-10. CMC-P 39742b, metaprotaspis; 7. Dorsal view: note that posterior cranidial border turns forwards at its distal end, 8. Posterior view, 9. Anterior view, 10. Lateral view: note that the anterior and posterior ends of the axis extend beyond the pleural regions.

    11-13. CMC-P 39742c, metaprotaspis; 11. Dorsal view, 12. Posterior view, 13. Lateral view.

    14-16. CMC-P 39742n, holaspid cranidium; 14. Dorsal view, x 8.1, 15. Anterior view, x 9, 16. Oblique lateral view, x 9.4.

    17. CMC-P 39742d, early meraspid cranidium, dorsal view, x 21.

    18. CMC-P 39742h, early meraspid cranidium, dorsal view, x 29.

    19. CMC-P 39742j, meraspid cranidium, dorsal view, x 20.

    20. CMC-P 39742k, early holaspid cranidium, dorsal view, x 14.

    21, 22. CMC-P 39742w, holaspid pygidium; 21. Dorsal view, x 4, 22. Lateral view, x 4.8.

168
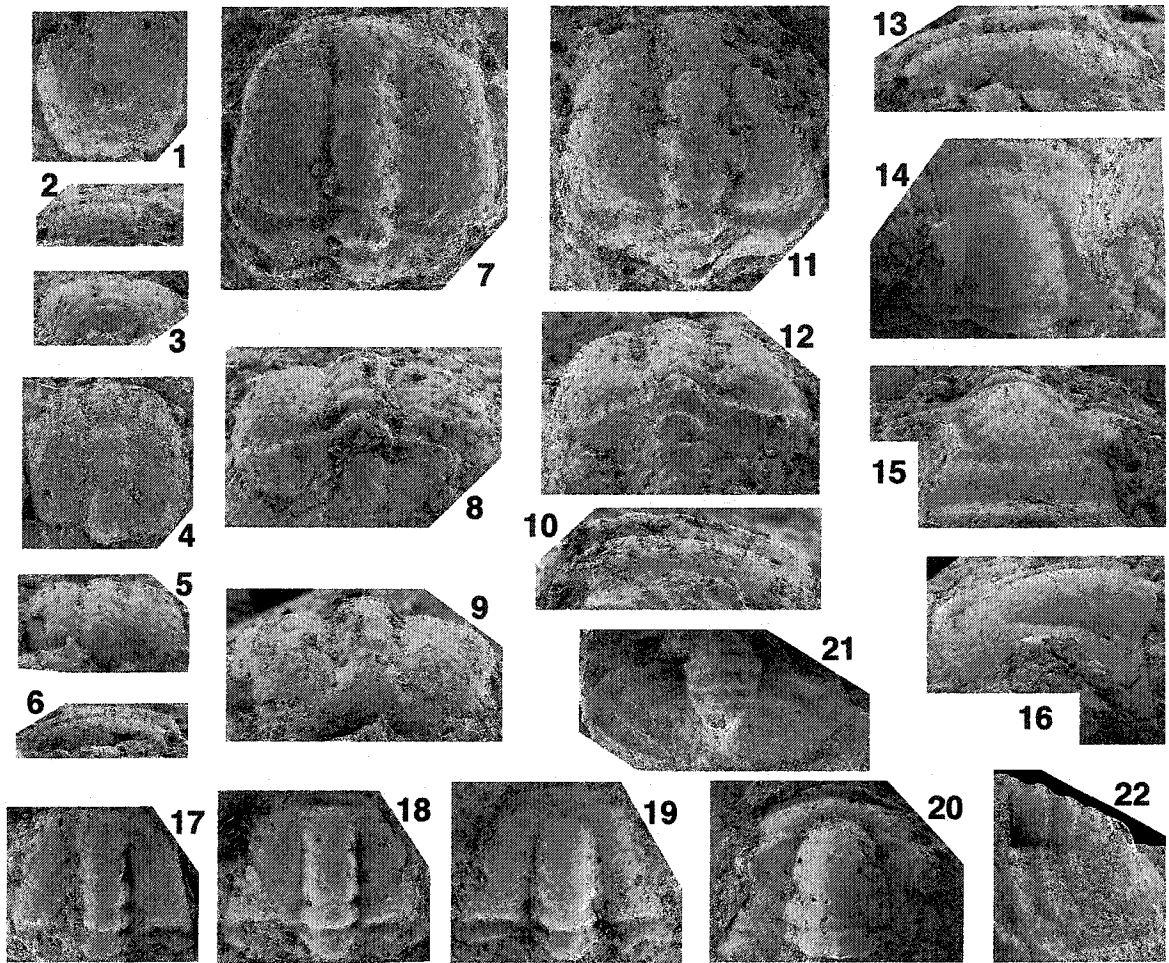
PLATE II-34. *Aphelaspis haguei* (Hall and Whitfield, 1877) and **Aphelaspidinae** sp. A. All the specimens are from the *Aphelaspis* Zone of the Deadwood Formation, South Dakota. All protaspid specimens (1-13, 25-36) are x 75.

1-24. *Aphelaspis haguei* (Hall and Whitfield, 1877)

 1-3. CMC-P 40309c, early metaprotaspis; 1. Dorsal view, 2. Posterior view, 3. Lateral view.

 4-7. CMC-P 40309e, early metaprotaspis; 4. Dorsal view: note that the fixigenal area is pitted, 5. Posterior view, 6. Lateral view, 7. Oblique anterior view.

 8-10. CMC-P 40309g, late metaprotaspis; 8. Dorsal view: note the presence of tubercle pair immediately anterior to posterior cranidial border furrow which turns forwards at its distal end, 9. Posterior view: note that the fixigenal area is strongly convex, 10. Lateral view: note that the axis extends beyond the pleural region.

 11-13. CMC-P 40309f, late metaprotaspis; 11. Dorsal view, 12. Posterior view, 13. Lateral view.

 14. CMC-P 40309h, early meraspid cranidium, dorsal view, x 45.

 15. CMC-P 40309j, early meraspid cranidium, dorsal view, x 43.

 16. CMC-P 40309k, meraspid cranidium, dorsal view, x 32.

 17. CMC-P 40309q, meraspid cranidium, dorsal view, x 16.

 18. CMC-P 40309u, transitory pygidium, dorsal view, x 36.

 19-21. CMC-P 40309w, holaspid pygidium; 19. Lateral view, x 17, 20. Dorsal view, x 13.2, 21. Posterior view, x 13.2.

 22-24. CMC-P 40309c', holaspid cranidium; 22. Lateral view, x 6.5, 23. Dorsal view, x 5.5, 24. Oblique anterior view, x 5.4.

25-36. **Aphelaspidinae** sp. A (not described in the text).

 25-27. CMC-P 40309, anaprotaspis; 25. Dorsal view, 26. Lateral view, 27. Posterior view.

 28, 29. CMC-P 40309b, anaprotaspis; 28. Dorsal view, 29. Lateral view.

 30-32. CMC-P 40309a, anaprotaspis; 30. Lateral view, 31. Dorsal view, 32. Posterior view.

 33-36. CMC-P 40309d, metaprotaspis; 33. Dorsal view, 34. Lateral view, 35. Posterior view, 36. Anterior view.

170
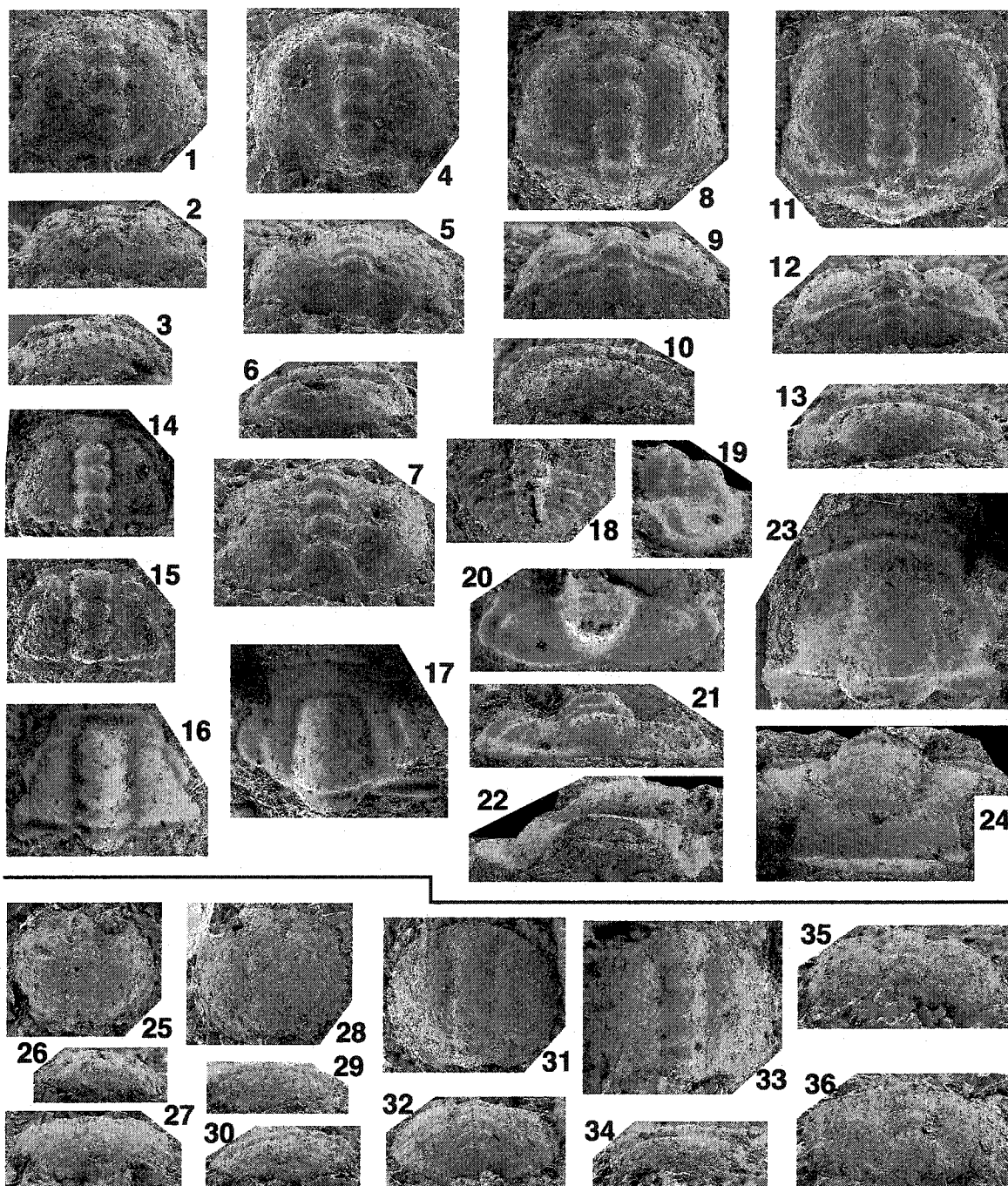
PLATE II-35. *Aphelaspis tarda* Rasetti, 1965 and *Aphelaspis* sp. A. All the specimens are from the *Aphelaspis* Zone (lowermost Steptoean Stage of Upper Cambrian) of the Nolichucky Formation, Tennessee. All protaspid specimens (Figs. 1-13, 25-36) are x 75.

1-29. *Aphelaspis tarda* Rasetti, 1965
    1-4. CMC-P 43345, early anaprotaspis; 1. Dorsal view, 2. Posterior view, 3. Anterior view, 4. Lateral view.
    5-7. CMC-P 43345b, late anaprotaspis; 5. Dorsal view: note that L4 expands forwards rapidly, 6. Lateral view, 7. Anterior view.
    8-11. CMC-P 43345c, late anaprotaspis; 8. Lateral view, 9. Dorsal view, 10. Posterior view, 11. Anterior view.
    12-14. CMC-P 43345f, early metaprotaspis; 12. Dorsal view, 13. Lateral view, 14. Posterior view: note the development of fixigenal tubercles immediately anterior to posterior cranidial marginal furrow which is weakly impressed and does not cross the shield transversely.
    15. CMC-P 43345d, early metaprotaspis, dorsal view.
    16-19. CMC-P 43345e, early metaprotaspis; 16. Dorsal view, 17. Posterior view, 18. Oblique anterior view, 19. Lateral view.
    20-22. CMC-P 43345g, late metaprotaspis; 20. Dorsal view: note the development of pits on the fixigenal area and even in the axial furrows, 21. Lateral view, 22. Posterior view: note that no pits develop on the protopygidium which is oriented strongly ventrally.
    23. CMC-P 43345j, early meraspid cranidium, dorsal view, x 30.
    24. CMC-P 43345q, early meraspid cranidium, dorsal view, x 21.
    25. CMC-P 43345w, transitory pygidium, dorsal view, x 30.
    26. CMC-P 43345h, holaspid cranidium, dorsal view, x 7.
    27. CMC-P 43345x, early holaspid pygidium, dorsal view, x 16.
    28. CMC-P 43345b', holaspid cranidium, dorsal view, x 6.9.
    29. CMC-P 43345r, early holaspid cranidium, dorsal view, x 19.
30-33. *Aphelaspis* sp. A (not described in the text).
    30-33. CMC-P 43345a, anaprotaspis; 30. Dorsal view: note the presence of posterior fixigenal spine which is relatively sharp, 31. Oblique anterior view, 32. Posterior view, 33. Lateral view.

172
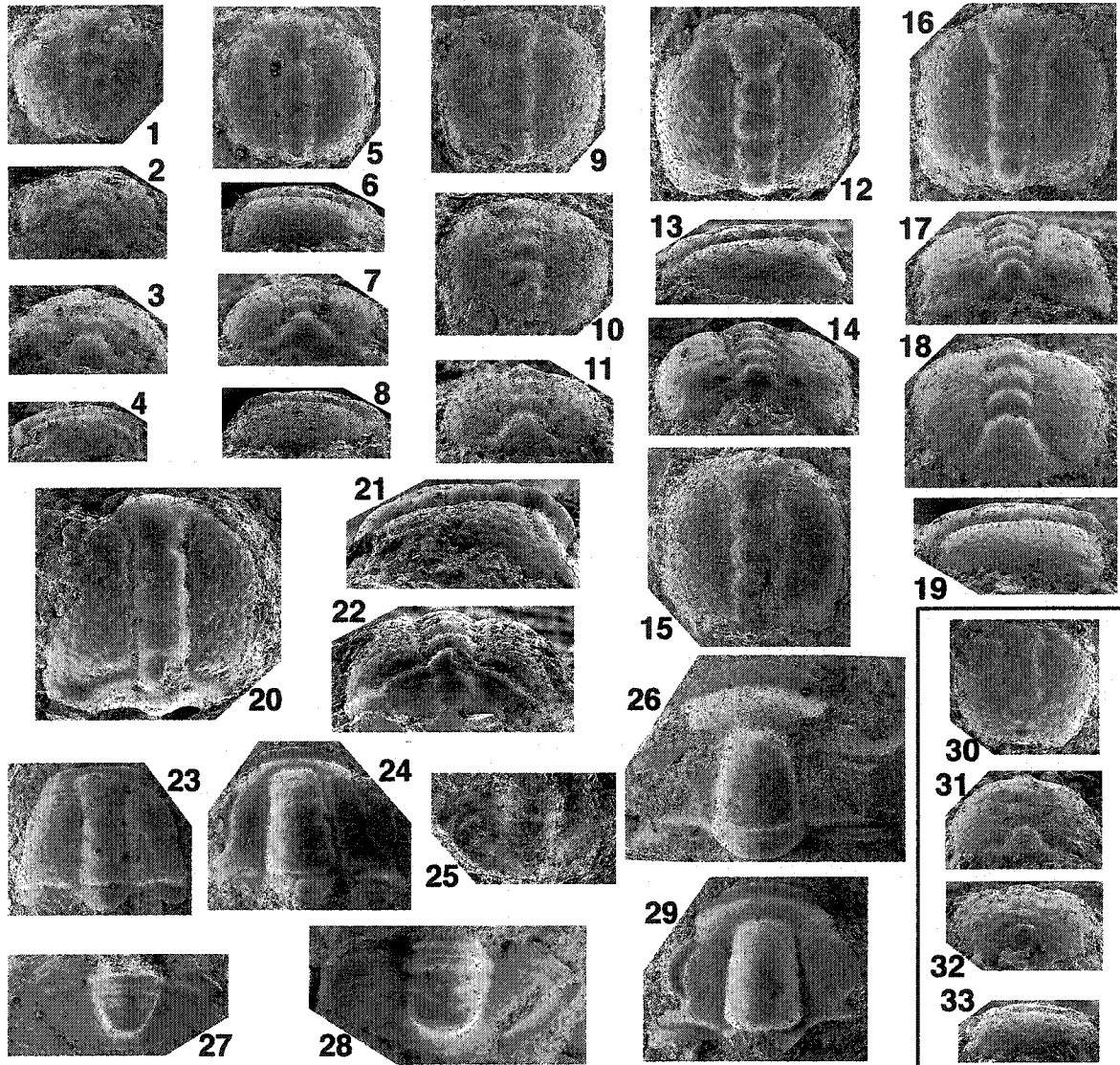
PLATE II-36. *Aphelaspis*? *anyta* (Hall and Whitfield, 1877). All specimens are from the *Dunderbergia* Zone of the Notch Peak Formation, Utah. All protaspid specimens (Figs. 1-27) are x 75.

1-38. *Aphelaspis*? *anyta* (Hall and Whitfield, 1877)

1-5. CMC-P 38733a, anaprotaspis; 1. Dorsal view, 2. Lateral view, 3. Posterior view, 4. Anterior view, 5. Ventral view.

6, 7, 13. CMC-P 38733b, anaprotaspis; 6. Dorsal view, 7. Anterior view, 12. ventral view: note the presence of slender free cheeks and inturned doublure.

8, 9. CMC-P 38733c, anaprotaspis; 8. Dorsal view, 9. Lateral view.

10, 11. CMC-P 38733d, anaprotaspis; 10. Dorsal view, 11. Posterior view.

12. CMC-P 38733e, anaprotaspis, ventral view: note the presence of hypostome with marginal spines.

14-17. CMC-P 38733f, early metaprotaspis; 14. Dorsal view, 15. Anterior view, 16. Lateral view, 17. Posterior view: note that the protopygidium is differentiated between the two posterior fixigenal spines.

18, 19. CMC-P 38733g, early metaprotaspis; 18. Dorsal view, 19. Ventral view: note the hypostome with nine marginal spines, some of which are bifurcated at their ends.

20, 21. CMC-P 38733h, early metaprotaspis; 20. Dorsal view, 21. Posterior view.

22. CMC-P 38733i, late metaprotaspis, dorsal view: the specimen was accidentally broken in half.

23-27. CMC-P 38733j, late metaprotaspis; 23. Dorsal view, 24. Posterior view, 25. Anterior view, 26. Ventral view, 27. Lateral view.

28. CMC-P 38733k, early meraspid cranidium, dorsal view, x 29.

29. CMC-P 38733l, early meraspid cranidium, dorsal view, x 24.

30, 31. CMC-P 38733p, holaspid cranidium; 30. Dorsal view, x 7.2, 31. Lateral view, x 9.6.

32. CMC-P 38733n, meraspid cranidium, dorsal view, x 15.5.

33. CMC-P 38733e', transitory pygidium, dorsal view, x 31.

34. CMC-P 38733f', transitory pygidium, dorsal view, x 32.

35. CMC-P 38733i', transitory pygidium, dorsal view, x 27.

36, 37. CMC-P 38733l', holaspid pygidium; 36. Dorsal view, x 4.6, 37. Oblique lateral view, x 8.

38. CMC-P 38733u, rostral plate, ventral view, x 10.4.

174
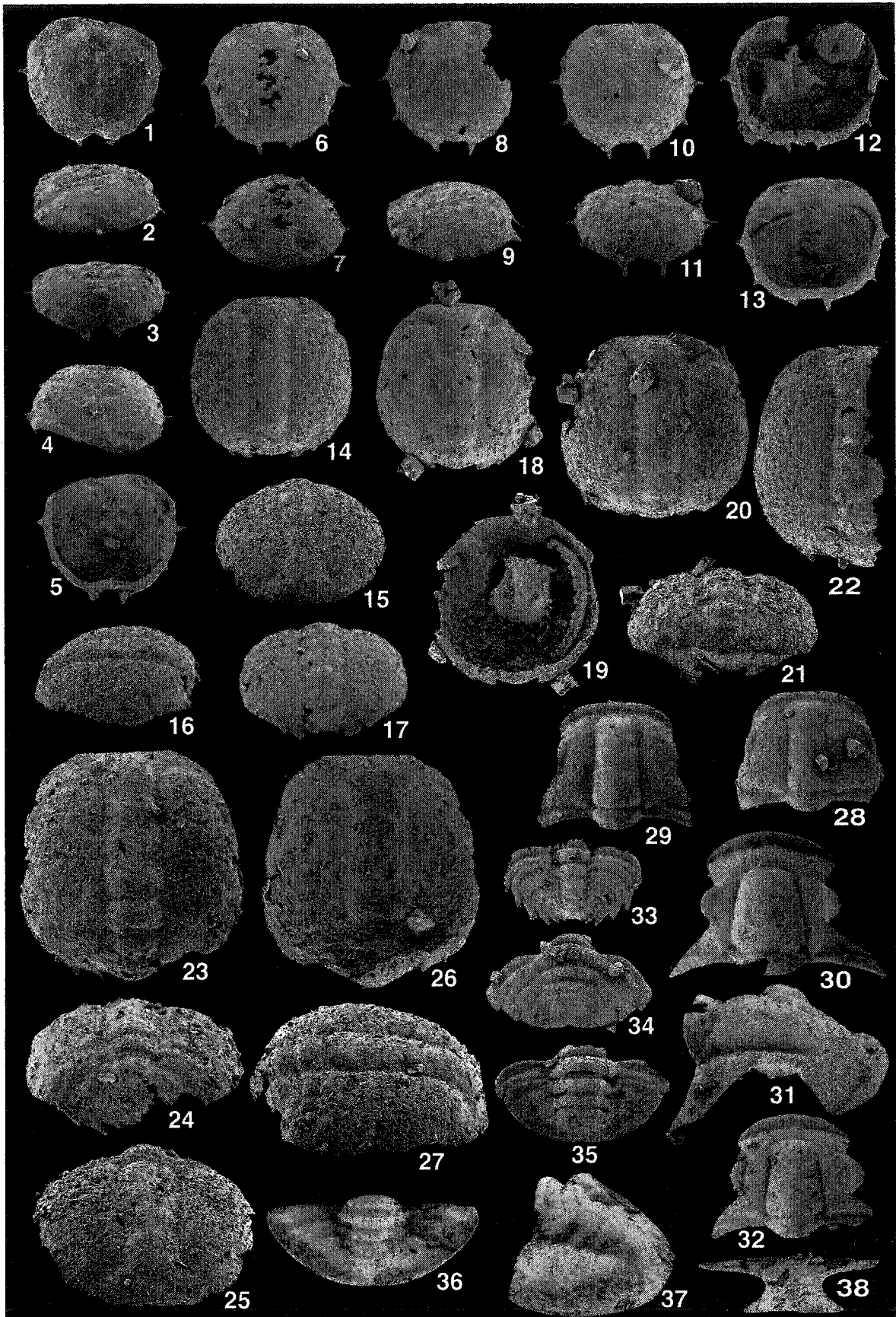
PLATE II-37. *Dytremacephalus granulosus* Palmer, 1954 and *Aphelaspis*? *anyta* (Hall and Whitfield, 1877). All the specimens are from the *Dunderbergia* Zone of the Notch Peak Formation; Lawson Cove, Utah. All protaspid specimens (Figs. 1-23, 35-38) are x 75.

1-34. *Dytremacephalus granulosus* Palmer, 1954

1, 2. CMC-P 38734a, anaprotaspis; 1. Dorsal view, 2. Anterior view.

3-6. CMC-P 38734b, anaprotaspis; 3. Ventral view: note inturned doublure and shield-shaped hypostome with several marginal spines, 4. Dorsal view, 5. Posterior view, 6. Anterior view.

7. CMC-P 38734c, anaprotaspis, dorsal view.

8-11. CMC-P 38734d, anaprotaspis; 8. Lateral view, 9. Posterior view: note the narrowly-spaced posterior fixigenal spines, 10. Dorsal view, 11. Anterior view.

12-15. CMC-P 38734g, early metaprotaspis; 12. Lateral view, 13. Dorsal view, 14. Posterior view: note that posterior fixigenal spines become widely-spaced due to the differentiation of protopygidium, 15. Anterior view.

16, 17. CMC-P 38734h, early metaprotaspis; 16. Dorsal view, 17. Ventral view.

18-20. CMC-P 38734i, late metaprotaspis; 18. Dorsal view, 19. Posterior view, 20. Lateral view.

21-24. CMC-P 38734j, late metaprotaspis; 21. Dorsal view, 22. Posterior view: note that postero-lateral end of fixigenal area ventrally protrudes and posterior fixigenal spine lies inside the postero-lateral end of fixigenal area, 23. Ventral view, 24. Lateral view.

25. CMC-P 38734k, early meraspid cranidium, dorsal view, x 41.

26. CMC-P 38734m, early meraspid cranidium, dorsal view, x 34.

27. CMC-P 38734n, early meraspid cranidium, dorsal view, x 27.

28, 29. CMC-P 38734t, holaspid cranidium; 28. Oblique lateral view, x 13.6, 29. Dorsal view, x 10.8.

30. CMC-P 38734p, holaspid cranidium, dorsal view, x 19.

31, 32. CMC-P 38734h', holaspid pygidium; 31. Dorsal view, x 21, 32. Dorsal view, x 20.

33. CMC-P 38734b', transitory pygidium, dorsal view, x 40.

34. CMC-P 38734e', transitory pygidium, dorsal view, x 30.

35-38. *Aphelaspis*? *anyta* (Hall and Whitfield, 1877)

35, 36. CMC-P 38734e, anaprotaspis; 35. Dorsal view, 36. Posterior view.

37, 38. CMC-P 38734f, early metaprotaspis; 37. Dorsal view, 38. Posterior view: note the presence of short blunted posterior fixigenal spines.

176
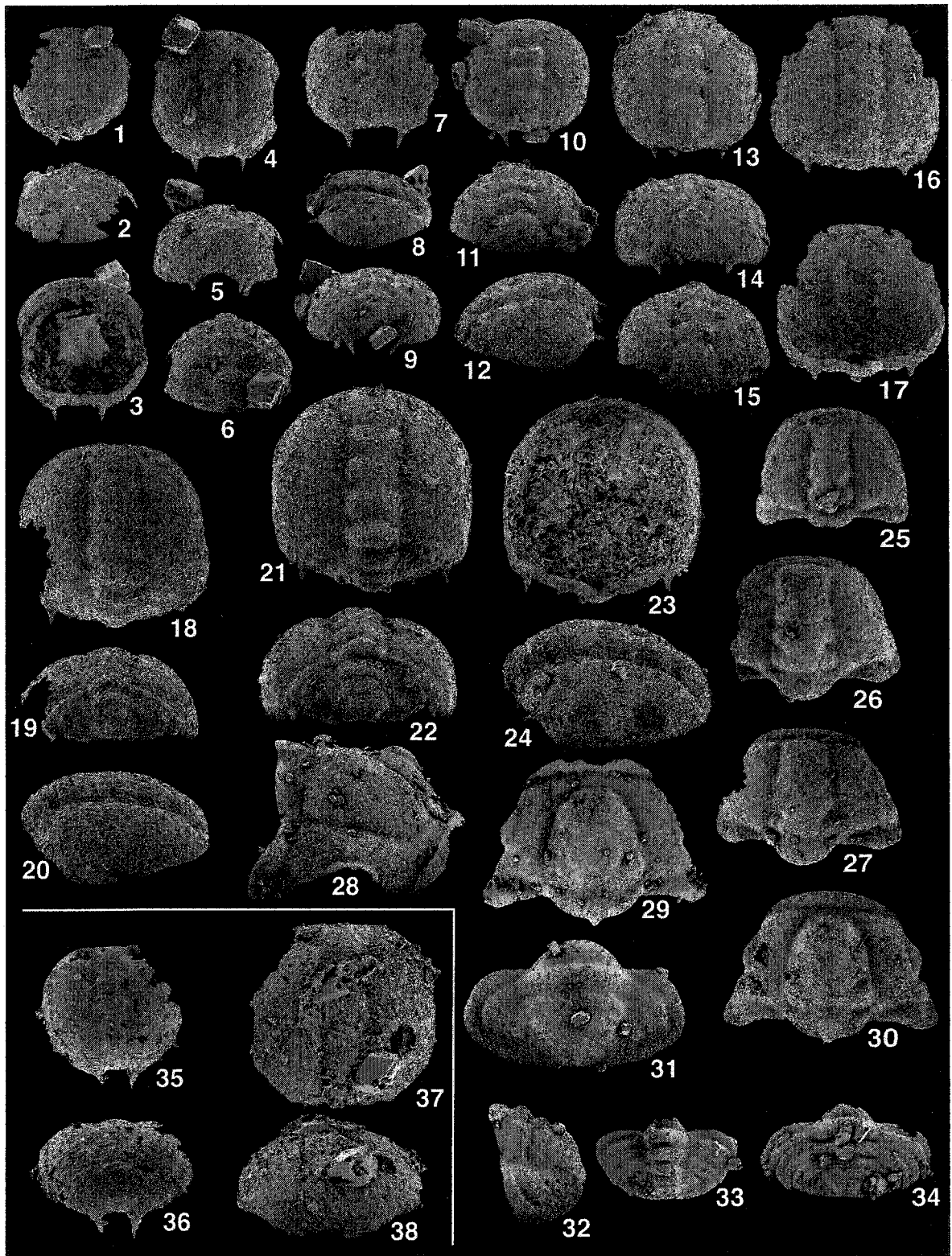
PLATE II-38. *Elvinia roemeri* (Shumard, 1861), *Elvinia* sp. A, **Species undetermined U, Species undetermined** V and **Species undetermined** W. All the specimens are from the *Elvinia* Zone (uppermost Steptoean) of the Deadwood Formation, South Dakota. All protaspid specimens (Figs. 1-15, 20-25) are x 75.

1-19. *Elvinia roemeri* (Shumard, 1861)
    1, 2. CMC-P 43372d, early metaprotaspis; 1. Dorsal view, 2. Anterior view.
    3, 4. CMC-P 43372f, early metaprotaspis; 3. Dorsal view, 4. Lateral view.
    5, 6. CMC-P 43372g, early metaprotaspis; 5. Dorsal view, 6. Posterior view.
    7, 8. CMC-P 43372h, early metaprotaspis; 7. Dorsal view, 8. Posterior view.
    9, 10. CMC-P 43372i, early metaprotaspis; 9. Dorsal view, 10. Anterior view.
    11, 12. CMC-P 43372j, early metaprotaspis; 11. Dorsal view, 12. Lateral view.
    13-15. CMC-P 43372k, late metaprotaspis; 13. Dorsal view, 14. Oblique anterior view, 15. Lateral view.
    16. CMC-P 433721, early meraspid cranidium, dorsal view, x 31.
    17. CMC-P 43372p, meraspid cranidium, dorsal view, x 13.
    18. CMC-P 43372r, holaspid cranidium, dorsal view, x 8.7.
    19. CMC-P 43372z, holaspid pygidium, dorsal view, x 6.1.
20. *Elvinia* sp. A (not described in the text).
    20. CMC-P 43372b, anaprotaspis, dorsal view.
21. **Species undetermined** U (not described in the text).
    21. CMC-P 43372e, metaprotaspis, dorsal view.
22, 23. **Species undetermined** V (not described in the text).
    22, 23. CMC-P 43372c, protaspis; 22. Anterior view, 23. Dorsal view.
24, 25. **Species undetermined** W (not described in the text).
    24. CMC-P 43372, anaprotaspis, dorsal view: note that anterior fixigenal spine located opposite L3 and mid-fixigenal spines are located at mid-shield length.
    25. CMC-P 43372a, metaprotaspis, dorsal view.

178
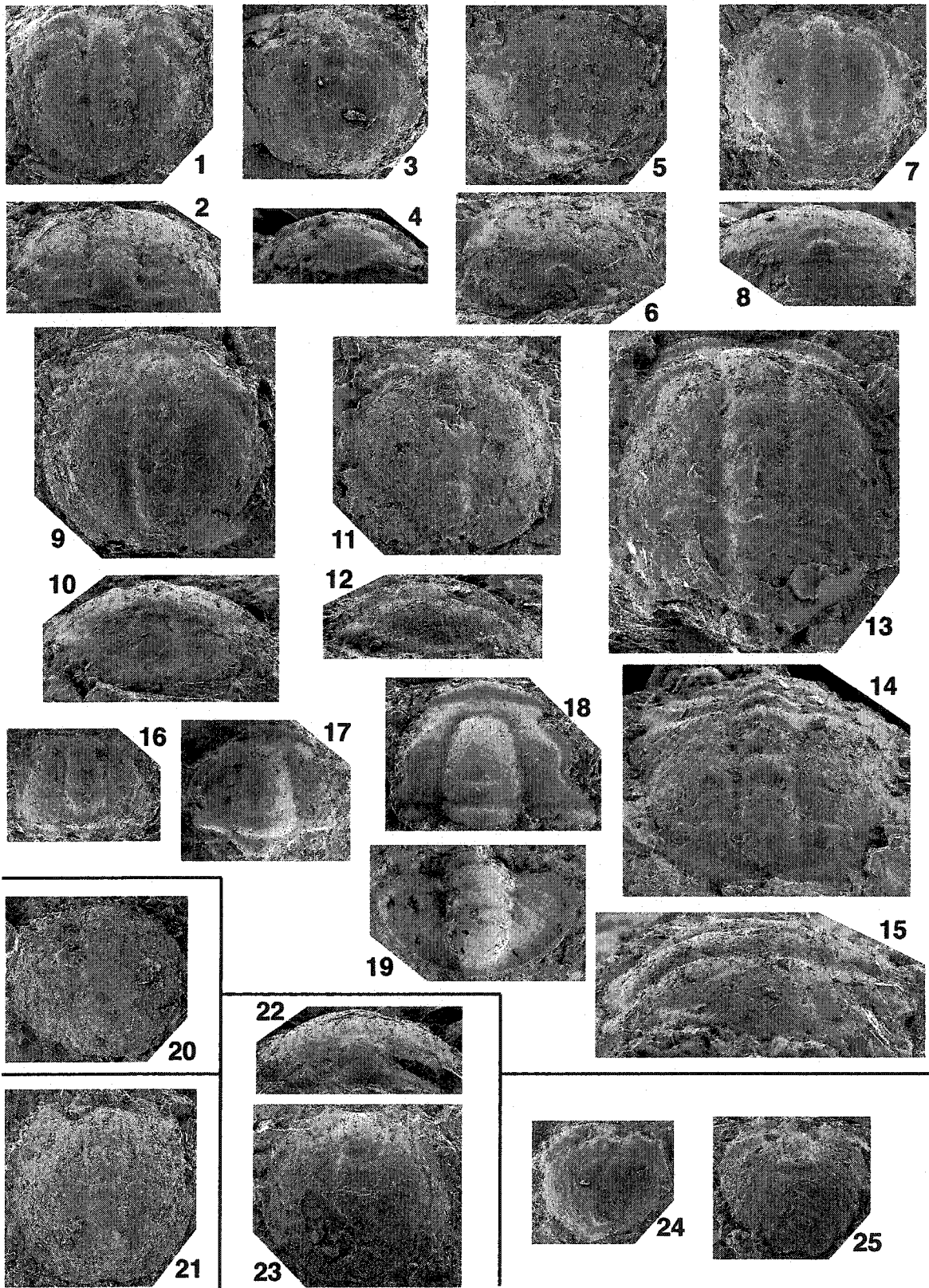
PLATE II-39. *Irvingella major* Ulrich and Resser *in* Walcott, 1924. All specimens are from the *Elvinia* Zone (uppermost Steptoean) of the Deadwood Formation, South Dakota. All protaspid specimens (Figs. 1-7) are x 75.

1-12. *Irvingella major* Ulrich and Resser *in* Walcott, 1924

   1-4. CMC-P 43375g, early metaprotaspis; 1. Dorsal view, 2. Anterior view, 3. Posterior view: note the presence of sagittally long area behind the occipital ring, 4. Lateral view.

   5-7. CMC-P 43375f, late metaprotaspis; 5. Dorsal view: note that the posterior margin of the protopygidium is broadly (tr.) and narrowly (sag. and exsag.) indented and bounded by marginal spines, which is also observed in transitory pygidia, 6. Lateral view, 7. Anterior view.

   8. CMC-P 43375e, meraspid cranidium, dorsal view, x 20.

   9. CMC-P 43375d, transitory pygidium, dorsal view, x 35.

   10. CMC-P 43375a, holaspid cranidium, dorsal view, x 10.3.

   11, 12. CMC-P 43375b, transitory pygidium; 11. Lateral view, x 64, 12. Dorsal view, x 55: note the indented posterior margin and the presence of marginal spines.

180
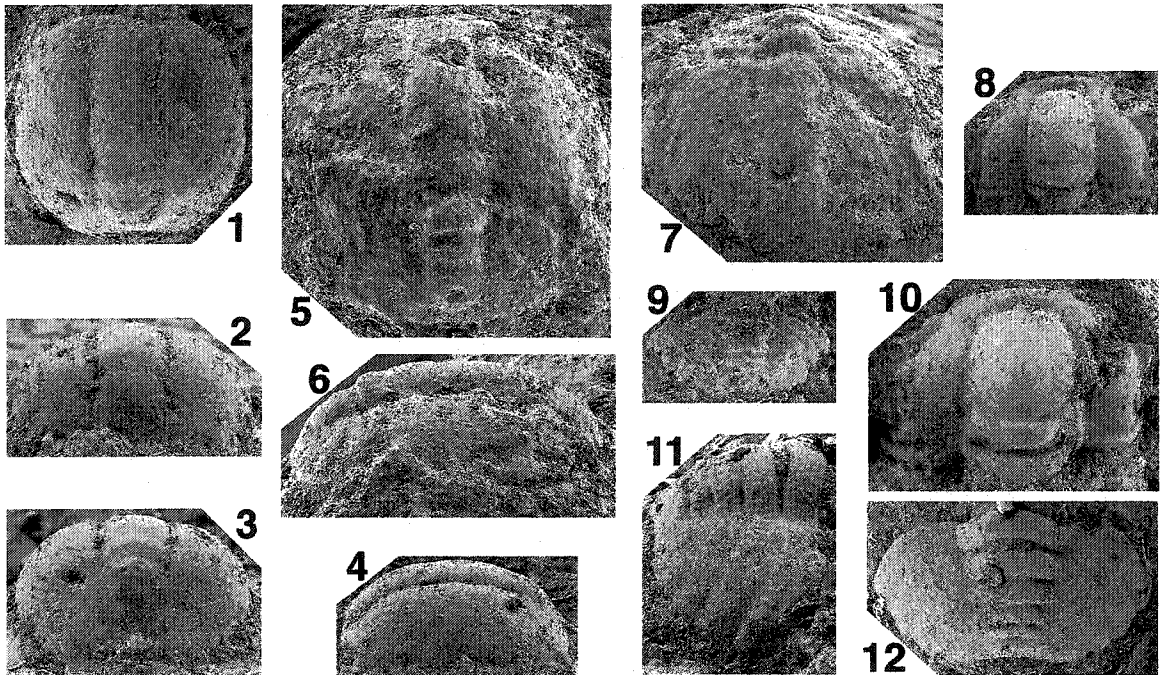
PLATE II-40. *Bolaspidella housensis* (Walcott, 1886). All specimens are from the
Bolaspidella Zone (late Middle Cambrian) of the Marjum Formation, western Utah.
All protaspid specimens (Figs. 1-15) are x 100.

1-15. *Bolaspidella housensis* (Walcott, 1886)
  1-5. UA 12772, early anaprotaspis; 1. Dorsal view, 2. Ventral view, 3. Posterior view,
     4. Lateral view, 5. Anterior view.
  6, 7. UA 12773, late anaprotaspis; 6. Dorsal view, 7. Ventral view; note the presence of
     free cheek and hypostome.
  8-10. UA 12774, late anaprotaspis; 8. Dorsal view, 9. Ventral view, 10. Posterior view.
  11, 12. UA 12775, late anaprotaspis; 11. Dorsal view, 12. Ventral view.
  13-15. UA 12776, metaprotaspis; 13. Dorsal view, 14. Posterior view. 15. Ventral view.

182
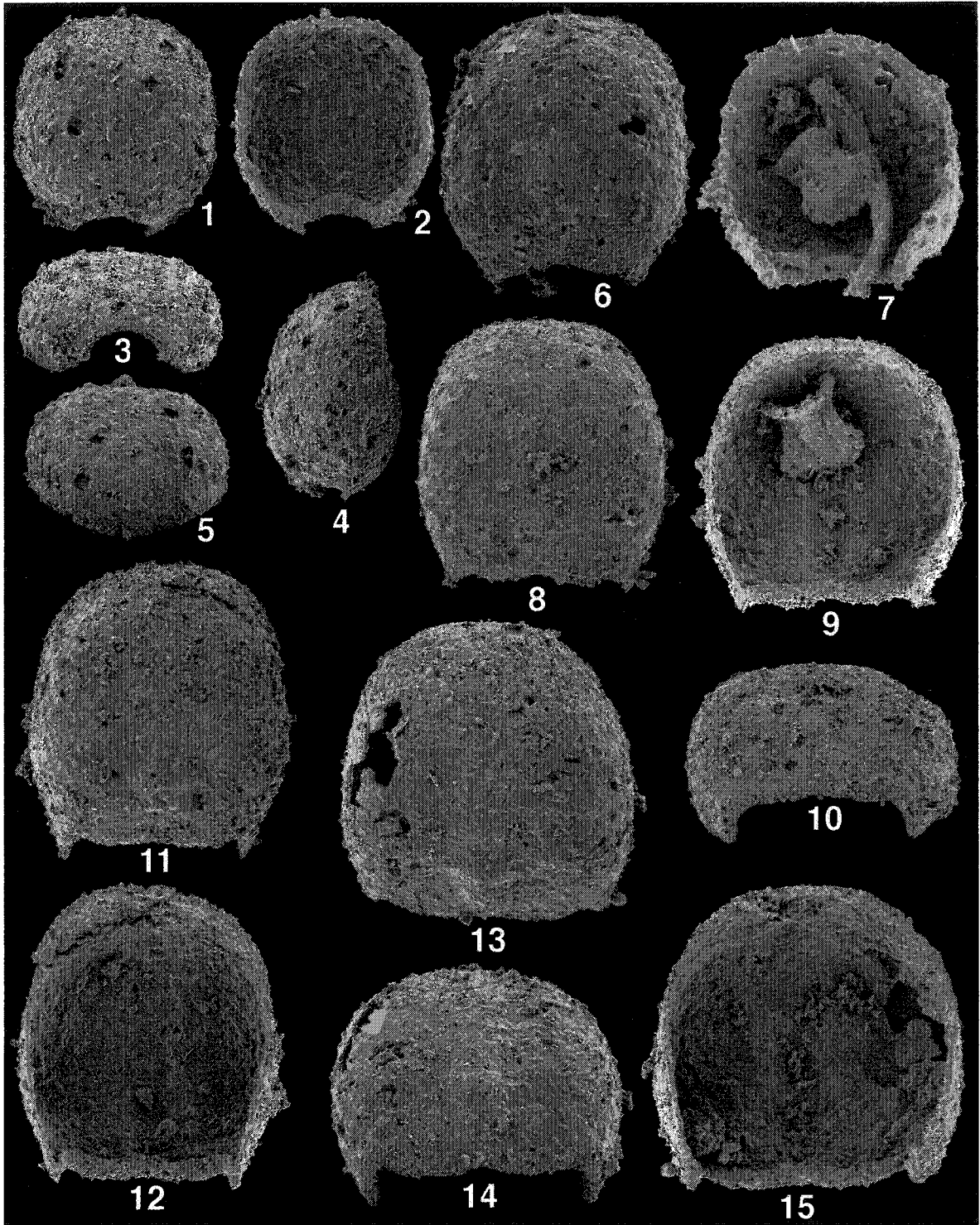
PLATE II-41. *Bolaspidella housensis* (Walcott, 1886). All specimens are from the
Bolaspidella Zone (late Middle Cambrian) of the Marjum Formation, western Utah.
All protaspid specimens (Figs. 1-4, 7-10) are x 100.

1-10. *Bolaspidella housensis* (Walcott, 1886)
    1, 2. UA 12777, metaprotaspis; 1. Dorsal view, 2. Ventral view.
    3, 4, 7, 8. UA 12778, degree 0 meraspis; 3. Dorsal view, 4. Posterior view, 7. Lateral
        view, 8. Ventral view.
    5, 6. UA 12779, meraspid cranidium, x 80; 5. Dorsal view, 6. Lateral view.
    9, 10. UA 12780, degree 1 meraspis; 9. Ventral view, 10. Dorsal view.

184
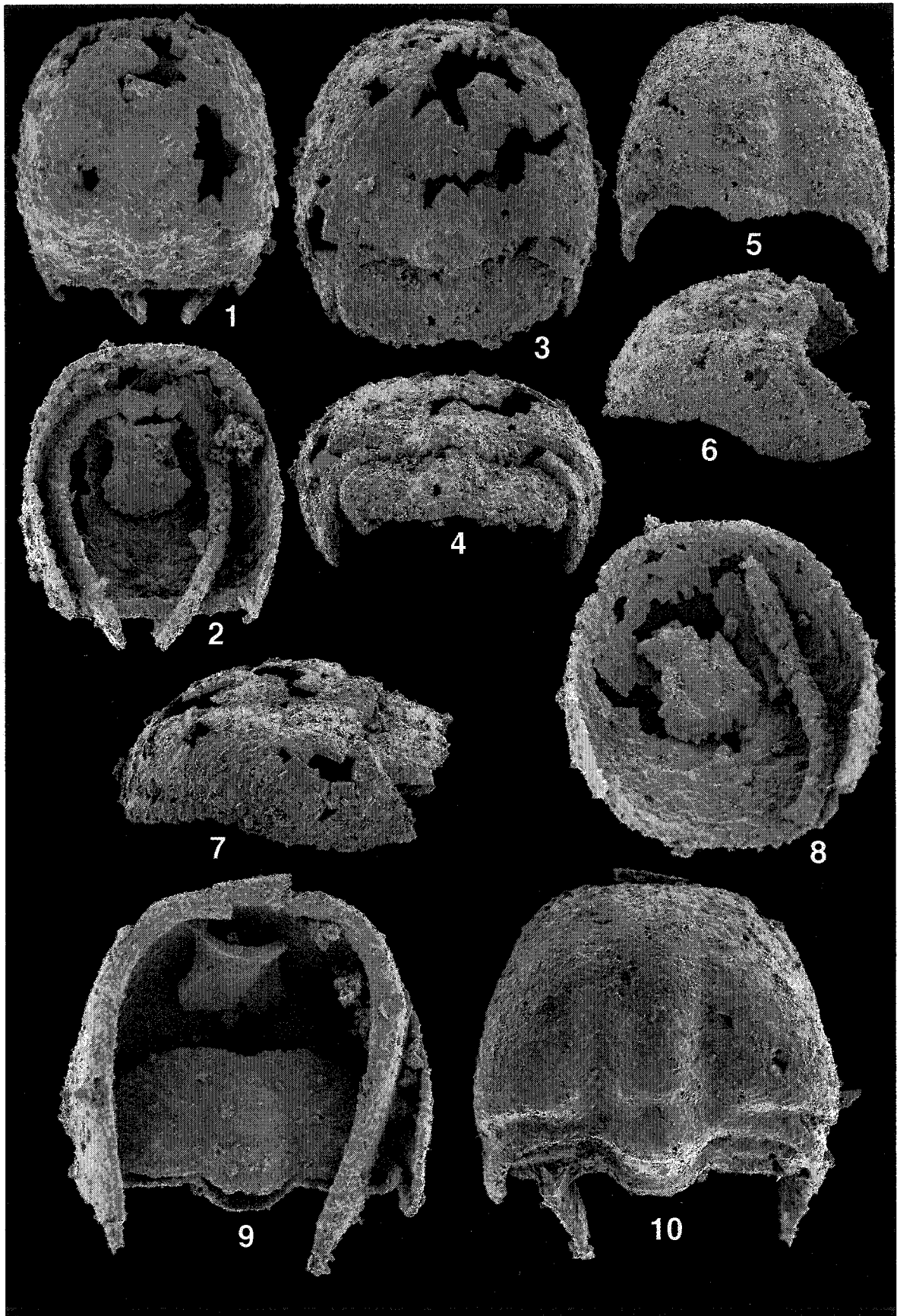
PLATE II-42. *Bolaspidella housensis* (Walcott, 1886). All specimens are from the *Bolaspidella* Zone (late Middle Cambrian) of the Marjum Formation, western Utah.

1-13. *Bolaspidella housensis* (Walcott, 1886)

1, 2. UA 12781, cephalon with one thoracic segment, x 50; 1. Dorsal view, 2. Ventral view.

3, 4. UA 12782, enrolled degree 7 meraspis with posterior four segments possessing axial spines and anterior three without axial spines, x 30; 3. Dorsal view, 4. Ventral view.

5-7. UA 12783, degree 6 meraspis, x 30; 5. Dorsal view, 6. Ventral view; 7. Posterior view.

8-10. UA 12784, enrolled degree 8 meraspis, x 30; 8. Dorsal view, 9. Ventral view, 10. Lateral view.

11, 12. UA 12785, degree 7 meraspis, x 30; 11. Dorsal view, 12. Ventral view; note the development of paired small tubercles on glabella, fixigena, and thoracic segments.

13. UA 12786, degree 8 meraspis, dorsal view, x 30.

186
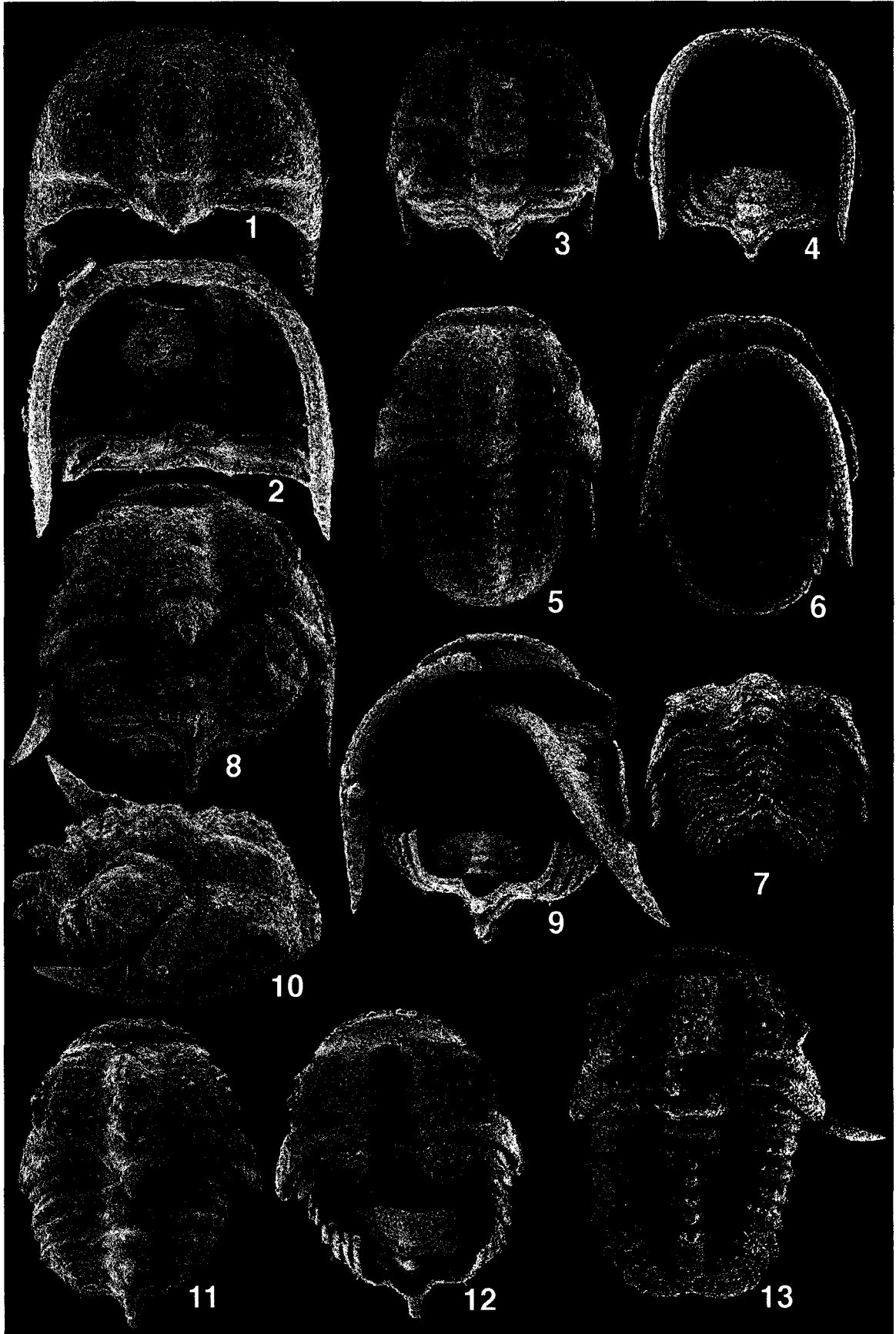
PLATE II-43. *Bolaspidella housensis* (Walcott, 1886). All specimens are from the
Bolaspidella Zone (late Middle Cambrian) of the Marjum Formation, western Utah.

1-21. *Bolaspidella housensis* (Walcott, 1886)
  1. UA 12787, meraspid cranidium, dorsal view, x 50.
  2, 3. UA 12788, cranidium, x 20; 2. Dorsal view, 3. Anterior view.
  4. UA 12789. cranidium, dorsal view, x 20.
  5. UA 12790, free cheek, dorsal view, x 20.
  6, 13. UA 12791, cephalothoracic specimen with 10 thoracic segments, x 20; 6. Dorsal
      view, 13. Lateral view; note that anterior three segments lack axial spines and next
      four segments possess short axial spines and posterior three segments lack axial
      spines.
  7, 8. UA 12792, thorax with 10 segments, x20; 7. Dorsal view, 8. Lateral view; note
      that anterior two segments lack axial spines, the next five segments possess axial
      spines, and the posterior two segments lack axial spines.
  9, 10. UA 12793, pygidium, x 20; 9. Dorsal view, 10. Posterior view.
  11. UA 12794, pygidium, dorsal view, x 30.
  12. UA 12795, pygidium, dorsal view, x 30.
  14, 15. UA 12796, early anaprotaspis, x 100; 14. Dorsal view, 15. Ventral view.
  16, 19-21. UA 12797, early anaprotaspis, x 100; 16. Dorsal view, 19. Lateral view, 20.
      Anterior view, 21. Posterior view.
  17, 18. UA 12798, early anaprotaspis, x 100; 17. Dorsal view, 18. Ventral view.

188
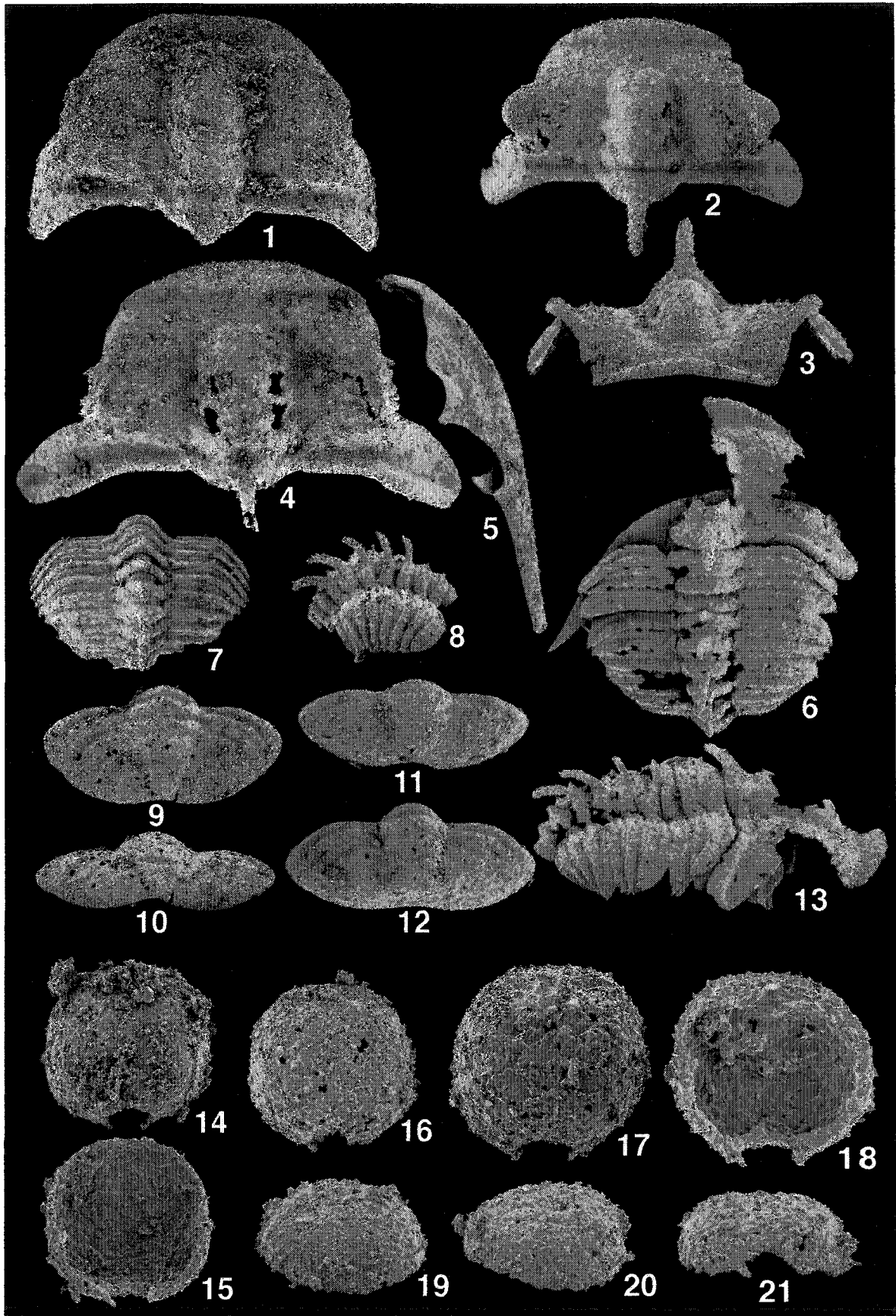
PLATE II-44. *Aphelaspis brachyphasis* Palmer, 1962. All specimens are from the *Aphelaspis* Zone (lower Steptoean Series) of the Dunderberg Formation, eastern Nevada. All protaspid specimens (Figs. 1-12) are x 100.

1-12. *Aphelaspis brachyphasis* Palmer, 1962
    1, 2. UA 12799, anaprotaspis; 1. Dorsal view, 2. Posterior view.
    3-6. UA 12800, early metaprotaspis; 3. Dorsal view, 4. Anterior view, 5. Posterior
        view, 6. Lateral view.
    7. UA 12801, anaprotaspis, ventral view.
    8. UA 12802, early metaprotaspis, ventral view.
    9. UA 12803, late metaprotaspis, ventral view.
    10, 11. UA 12804, early metaprotaspis; 10. Dorsal view, 11. Ventral view.
    12. UA 12805, early metaprotaspis, ventral view.
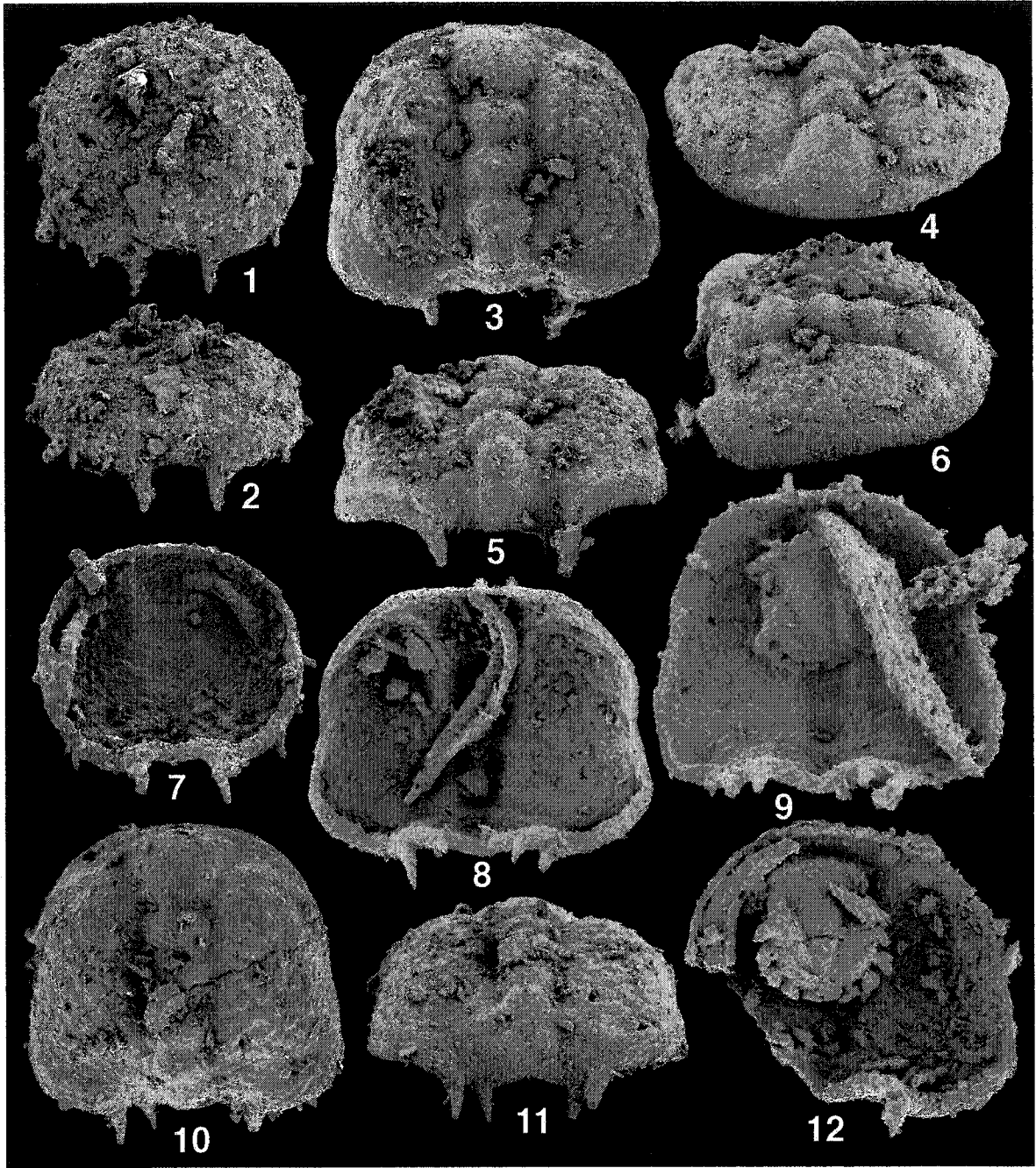
PLATE II-45. *Aphelaspis brachyphasis* Palmer, 1962. All specimens are from the *Aphelaspis* Zone (lower Steptoean Series) of the Dunderberg Formation, eastern Nevada. All specimens are x 100.

1-8. *Aphelaspis brachyphasis* Palmer, 1962
    1, 2. UA 12806, late metaprotaspis; 1. Dorsal view, 2. Posterior view.
    3, 4. UA 12807, late metaprotaspis; 3. Dorsal view, 4. Posterior view.
    5. UA 12808, meraspid cranidium, dorsal view.
    6. UA 12809, meraspid cranidium, dorsal view.
    7. UA 12810, transitory pygidium, dorsal view.
    8. UA 12811, transitory pygidium, dorsal view.

192
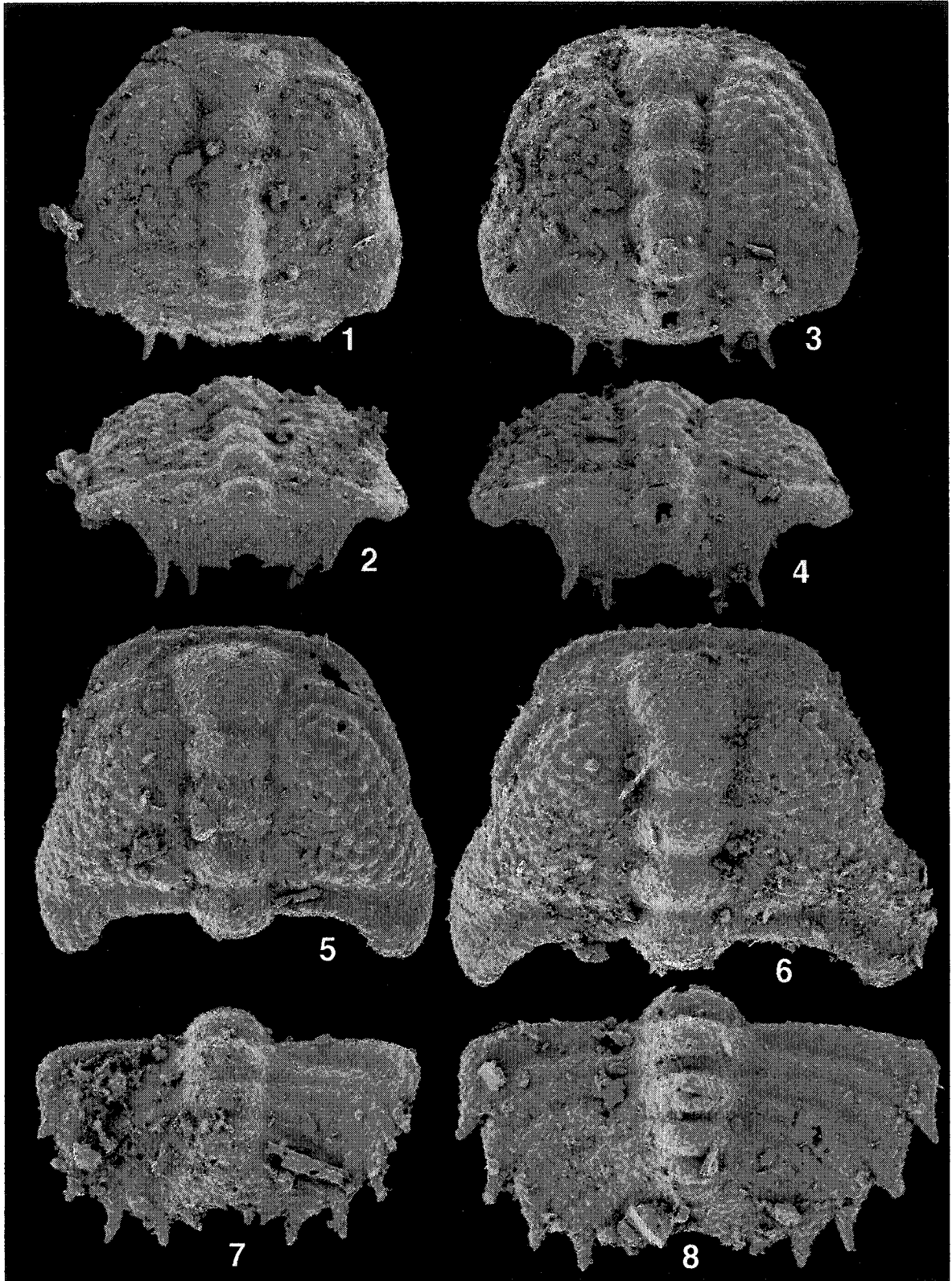
PLATE II-46. *Aphelaspis brachyphasis* Palmer, 1962, *Glaphyraspis parva* (Walcott, 1899) and *Aphelaspis* sp. B. All specimens are from the *Aphelaspis* Zone (lower Steptoean Series) of the Dunderberg Formation, eastern Nevada.

1-9. *Aphelaspis brachyphasis* Palmer, 1962
   1. UA 12812, meraspid cranidium, dorsal view, x 30.
   2, 3. UA 12813, transitory pygidium, x 50; 2. Dorsal view, 3. Posterior view.
   4. UA 12814, pygidium, dorsal view, x 30.
   5. UA 12815, incompletely articulated cephalon, dorsal view, x 30.
   6. UA 12816, incompletely articulated cephalon, dorsal view, x 30.
   7. UA 12817, pygidium, dorsal view, x 20.
   8. UA 12818, hypostome, ventral view, x 75.
   9. UA 12819, cranidium, dorsal view, x 30.
10-16. *Glaphyraspis parva* (Walcott, 1899). All specimens are x 100.
   10-12. UA 12820, anaprotaspis; 10. Dorsal view, 11. Lateral view, 12. Posterior view.
   13, 14. UA 12821, meraspid cranidium; 13. Dorsal view, 14. Lateral view.
   15. UA 12822, meraspid cranidium, dorsal view.
   16. UA 12823, meraspid cranidium, dorsal view.
17, 18. *Aphelaspis* sp. B (not described in the text).
   17, 18. UA 12824, anaprotaspis, x 100; 17. Dorsal view, 18. Posterior view.

194
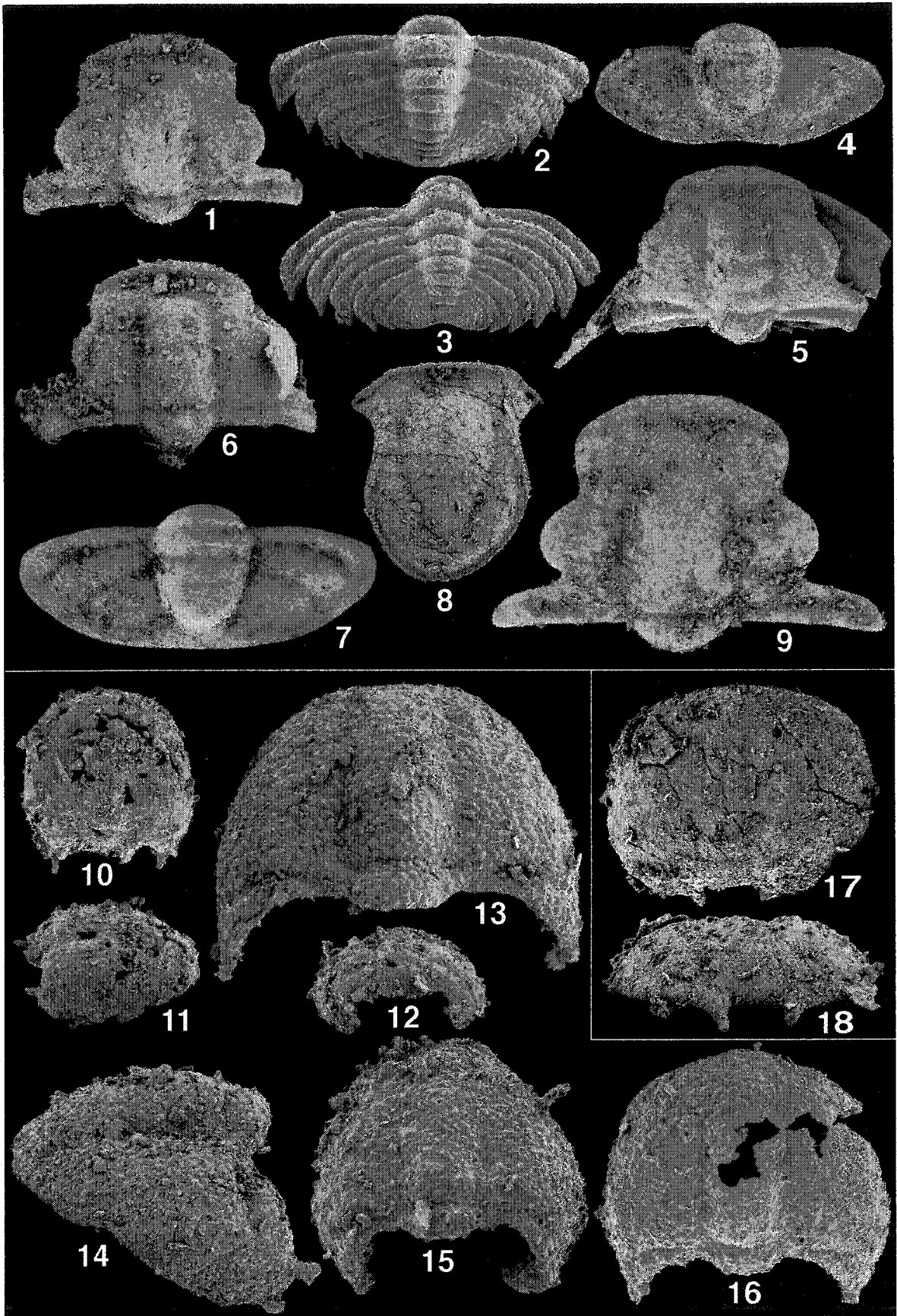
PLATE II-47. *Modocia laevinucha* Robison, 1964. All specimens are from the
  Bolaspidella Zone (late Middle Cambrian) of the Marjum Formation, western Utah.

1-14. *Modocia laevinucha* Robison, 1964.
  1-5. UA 12825, anaprotaspis, x 100; 1. Dorsal view, 2. Ventral view, 3. Anterior view,
    4. Lateral view, 5. Posterior view.
  6-10. UA 12826, metaprotaspis, x 100; 6. Ventral view, 7. Lateral view, 8. Dorsal view,
    9. Posterior view, 10. Anterior view.
  11, 12. UA 12827, degree 2 meraspis, x 50; 11. Dorsal view, 12. Lateral view.
  13. UA 12828, cranidium, dorsal view, x 30.
  14. UA 12829, pygidium, dorsal view, x 20: the association of this pygidium with this
    species is questionable.

196
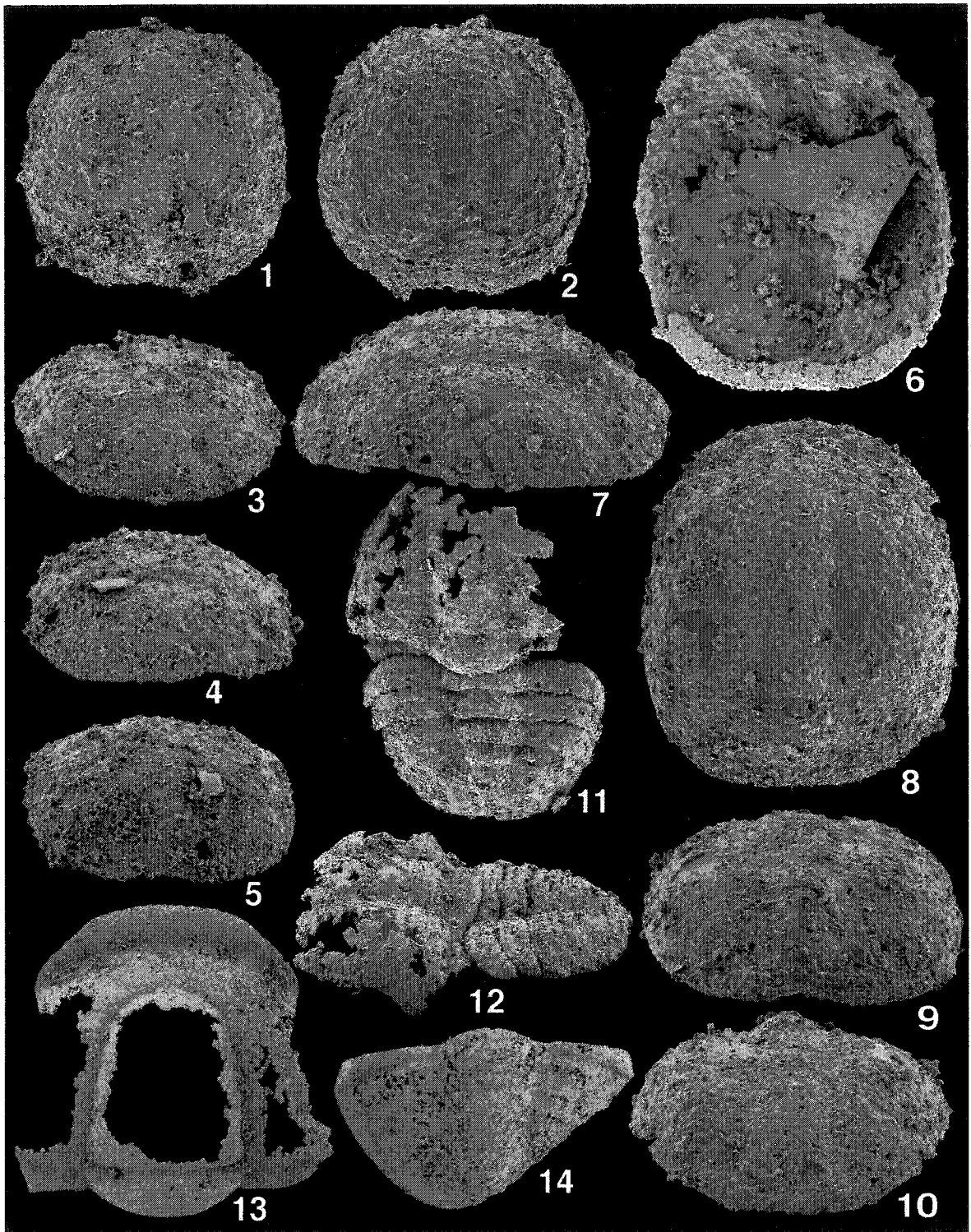
PLATE II-48. Ptychopariina sp. C and **Ptychopariina** sp. D. All specimens are from the *Bolaspidella* Zone (late Middle Cambrian) of the Marjum Formation, western Utah. All protaspid specimens (Figs. 1-11) are x 100.

1-5. **Ptychopariina** sp. C
    1-5. UA 12830, anaprotaspis; 1. Dorsal view, 2. Ventral view, 3. Posterior view, 4. Anterior view, 5. Lateral view.
6-11. **Ptychopariina** sp. D
    6-8. UA 12831, anaprotaspis; 6. Dorsal view, 7. Ventral view, 8. Posterior view.
    9-11. UA 12832, anaprotaspis; 9. Dorsal view, 10. Posterior view, 11. Ventral view.

198
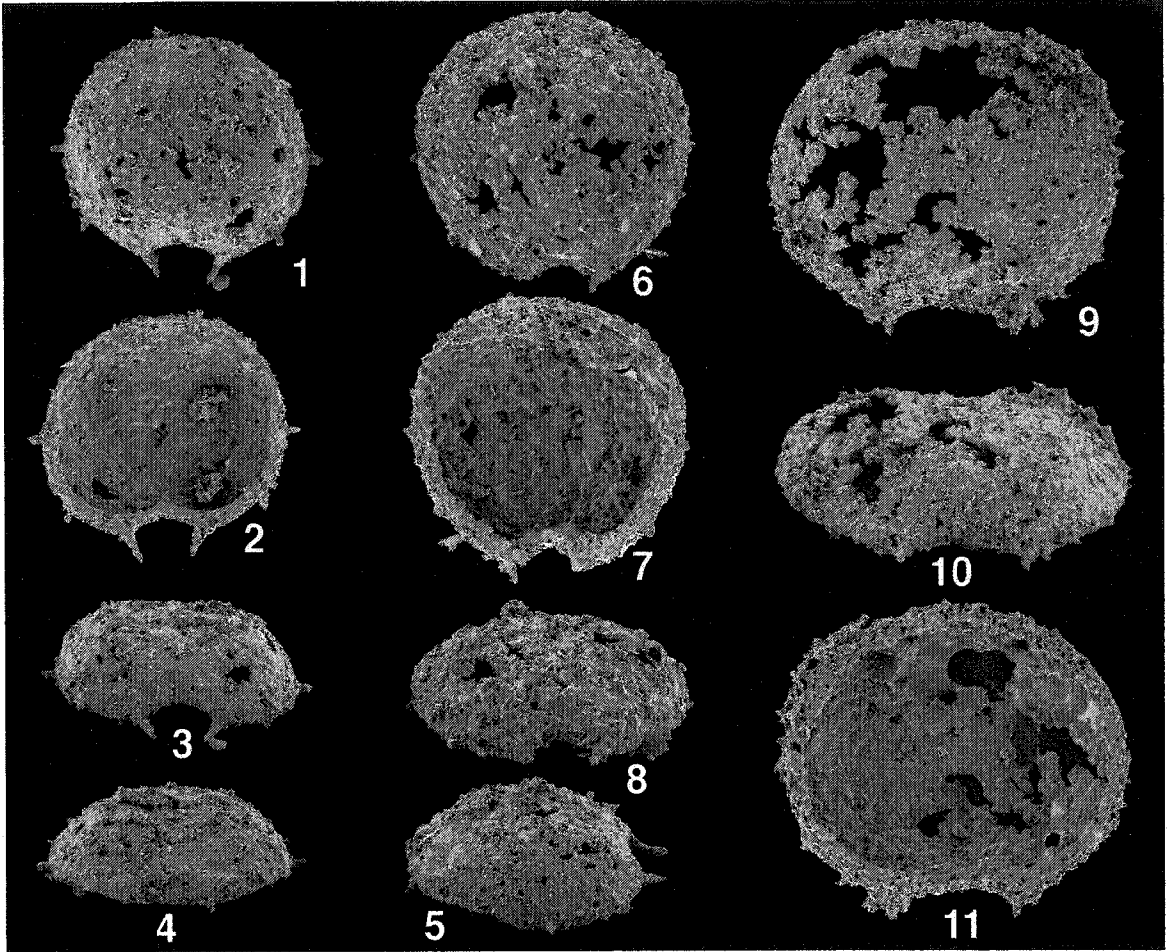
CHAPTER III

TAXONOMY OF HYSTRICURIDAE (PROETIDA) AND RELATED TAXA

Hystorical Accounts of Taxonomy of Hystricuridae

Raymond (1913b) erected a new genus *Hystricurus* on the basis of a single fragmentary cranidium (Pl. III-1, Figs. 1-4). A few species of *Hystricurus* had been occasionally described until Ross (1951) and Hintze (1953) described many species of *Hystricurus* and allies from the Great Basin area. Ross (1951) erected 9 new genera and described 24 new species from the Garden City Formation around the border between Utah and Idaho. Hintze (1953) and his colleagues (Demeter, 1973, Terrell, 1973, Young, 1973) described 10 new species from the Fillmore Formation in central Utah. The number of species described from the Great Basin occupies about 40 percent of all the formally named "hystricurid" species. These studies broadened the concept of the Hystricuridae. The two formations were targeted for sampling the "hystricurids" for this research. A tremendous amount of silicified specimens were secured from the limestone blocks collected from many productive sampling horizons in both formations (Text-figs. I-5 to I-9).

Hupé (1953) erected a new family Hystricuridae with *Hystricurus* as the type genus; he included two genera, *Weeksina* and *Jeffersonia* which were transferred into another family by later workers. He placed the family within the superfamily Solenopleuracea. Poulsen (1954) ranked the group as a subfamily of the Solenopleuridae, which is followed by the Treatise (Moore, 1959) where the group was still placed in the Solenopleuracea of the Ptychopariida. In the Treatise (Moore, 1959) the "hystricurids" included 8 genera, *Hystricurus*, *Amblycranium*, *Hillyardina*, *Pachycranium*, *Parahystricurus*, *Psalikilopsis*, *Psalikilus*, and *Rollia*, and questionably included *Apachia*. The last genus, an Upper Cambrian group, was later transferred into the Dokimocephalidae by Palmer (1965). Later, Öpik (1967) excluded the "hystricurids" from the Solenopleuridae because of the large age discrepancy between the Solenopleurinae and the "hystricurids."

It is Fortey and Owens (1975) who suggested that the "hystricurids" are ancestral to many of the post-Cambrian trilobites which they classified under a newly-erected order Proetida. They placed the "hystricurids" in the Proetida and regarded as the primitive group of the order. Fortey (1983) firstly noted cranidial similarities between Upper Cambrian ptychopariids such as *Onchopeltis* of the Dokimocephalidae and *Hystricurus*, implying a possible affinity between the ptychopariids and "hystricurids" (see also Fortey, 1990). Since then, two different opinions on the higher level classification of the "hystricurids" have been put forward. Ludvigsen and Westrop (*in* Ludvigsen *et al.*, 1989) resurrected the previous opinion, the inclusion of the "hystricurids" within the Solenopleuracea. They argued that the cranidial morphologies of *Hystricurus* and several dokimocephalids are similar enough to support their inclusion within the Solenopleuracea and the pygidial differences warrant their separate familial status. Later, Shergold (1991a) suggested the inclusion of the "hystricurids" within the superfamily Catillicephalacea, by noting the cranidial similarities with lonchocephalines. The superfamilial positions of the "hystricurids" and other families that are considered to be related to the "hystricurids" had not been in agreement.

199

It is the discovery of protaspides of *Hystricurus* (Lee and Chatterton, 1997a) that confirms the inclusion of the "hystricurids" within the Proetida as argued by Fortey and Owens (1975). This confirmation needs the assumption that protaspid similarities are of more important taxonomic value than holaspid similarities, so that the holaspid similarities to the aforementioned ptychopariides are taken to indicate a case of convergence. In the most recent classification (Fortey *in* Whittington *et al.*, 1997), the Hystricuridae is not recognized as a family and it is not clear to which taxon the family belongs.

Before this research, 89 formally named species in 18 genera were definitely or questionably assigned to the Hystricuridae (Appendix III-1). Of these, 35 species, occupying nearly 40 percent, were assigned to *Hystricurus*. 87 species in open nomenclature were referred to the Hystricuridae; of these, 48 species were referred to *Hystricurus*. The taxonomic revision suggests that the Hystricuridae contains 59 species of 12 genera (Appendix III-2); 7 new genera are erected by the author and 7 species are in open nomenclature. 19 genera that have been referred to the Hystricuridae are excluded from the Hystricuridae or questionably assigned to the family (Appendix III-3). Six new genera are erected on the basis of the materials collected by the author, which bear morphologies that can be accommodated within the old concept of the Hystricuridae. These genera are also excluded from the Hystricuridae (Appendix III-3). Throughout the text, the Hystricuridae refers to the concept established by the author and "hystricurids" or "hystricurid" to the previous concepts of the family.

PALEOGEOGRAPHIC DISTRIBUTIONS

89 formally named species that have been referred to as a "hystricurid" have been documented in such Ordovician paleocontinents as Laurentia, Greenland, Siberia, Kazakhstan, and Gondwana (Text-fig. III-1); no "hystricurids" were reported from the Baltic region. Localities of Laurentia are grouped into two paleogeographic regions with reference to the Transcontinental Arch (Text-fig. III-2) that is believed to have played an important role as a geographic barrier during the Lower Ordovician (Lee and Chatterton, 1999). The north of Transcontinental Arch region includes the Great Basin (throughout Utah, Nevada, and Idaho), Williston Basin (in Montana and Wyoming), Colorado Sag, Canadian Rockies (in British Columbia and Alberta) and Alaska. The south of Transcontinental Arch region includes three subordinate regions; south-central United States extending from Missouri to Oklahoma and Texas, eastern North America including New York, Vermont, and Quebec, and western Newfoundland. The Greenland region includes Greenland itself, Ellesmere Island, and Spitsbergen (Text-fig. III-2). In Gondwana, the "hystricurids" have been reported mainly along the western margin of the continent from Australia, the Sino-Korean Platform including Korea and northeast China, South China, and Bohemia (Text-fig. III-1). Detailed information on the geographic localities is compiled in Appendix III-5.

Taoyuania from South China and *Holubaspis* from Bohemia are the only taxa that have been documented outside the temperate zone between 30°N and 30°S latitude where all the other "hystricurid" species inhabited (Text-fig. III-1). These two taxa are excluded from the Hystricuridae *sensu* herein. After the taxonomic revision, only one species, *Glabellosulcatus sanduensis* from South China occurs outside the temperate zone (Text-fig. III-3). The "hystricurids" are mostly associated with shallow water carbonate

200

sequences (Lee and Chatterton, 1999).

39 species (about 66 percent) out of 59 species occur in the north of Transcontinental Arch region (Appendix III-4); 17 species (about 29 percent) occur in the south of Transcontinental Arch region. Five genera—*Pachycranium, Parahystricurus, Parahillyardina, Politohystricurus,* and *Pseudoplethopeltis*—are endemic to Laurentia. *Tanybregma* is restricted to the Sino-Korean Platform and Australia. 44 species are endemic to one of the seven paleogeographic regions.

STRATIGRAPHIC DISTRIBUTIONS

Different biostratigraphic schemes have been developed for each paleogeographic region and their correlation is far from complete. The biostratigraphic scheme of the Ibexian Series developed for the north of Transcontinental Arch region, in particular, the Great Basin of western United States (Ross *et al.,* 1997, fig. 10) is employed as a reference. Conodont and/or graptolite biostratigraphies are used for correlating stratigraphic schemes of regions where trilobite zonation has not been established or the Ibexian trilobite zonation is not well applied. The boundary between the Cambrian and Ordovician is presumed to be contemporaneous in all paleogeographic regions. The boundary between the Tremadocian and Arenigian is generally correlated with the boundary between the *Hintzeia celsaora* and *Protopliomerella contracta* Zone, which is accepted in the correlations.

North of Transcontinental Arch Region. 39 species of the Hystricuridae occurring in the North of Transcontinental Arch region, range from the *Symphysurina* Zone to the *Hintzeia celsaora* Zone (Text-fig. III-4). Of 12 genera of the Hystricuridae, only *Tanybregma* is not associated with Laurentia, which occurs in the Sino-Korean Platform and Australia (Appendix III-4). "Hystricurid" species that are removed from the Hystricuridae range from the Upper Cambrian to the *Trigonocerca typica* Zone of the Ibexian Series (Text-fig. III-4). Two new species, *Parahillyardina sulcata* and *Amblycranium transversus,* are found in the interval from *Paraplethopeltis* to *Leiostegium-Kainella* Zone which was previously considered to be a low diversity interval in Laurentia (Ross *et al.,* 1997).

South of Transcontinental Arch Region. The Ibexian trilobite zonation can be applied to south-central United States (e.g., Stitt, 1983) and eastern North America (e.g., Westrop *et al.,* 1993), whereas a different zonation of the Canadian Series (Flower, 1964, 1978) has been developed for western Newfoundland (e.g., Boyce, 1997). The correlation of "hystricurid" occurrences in western Newfoundland into the Ibexian Series is well established by Boyce (1989, fig. 8), Boyce and Stouge (1997, fig. 4) and Boyce (personal communication, 1997), and is accepted in this study (Text-fig. III-5). The occurrences of "hystricurids" from Missouri cannot be directly correlated into the Ibexian zonation. Boyce (1989, fig. 8) correlated the lithostratigraphic schemes of Missouri with the biozonation of western Newfoundland, which is adapted in this study (Text-fig. III-5). 17 species of the Hystricuridae occur in the south of Transcontinental Arch (Appendix III-4).

In western Newfoundland, the "hystricurids" have been known from the *Hystricurus millardensis* Zone (correlatable to the lower part of the *Symphysurina* Zone) to the *Randaynia saundersi* Zone (equivalent to the interval ranging from the upper part of the *Tesselacauda* Zone to the *Rossaspis superciliosa* Zone) (Text-fig. III-5). The *Hystricurus*

201

millardensis Zone is characterized by the eponymous species (personal communication with Boyce, 1997). Since the species is excluded from the Hystricuridae, the inclusion of the zone within the stratigraphic occurrence of the Hystricuridae is considered questionable. As a result, the stratigraphic occurrence of the Hystricuridae in western Newfoundland is considered to range from the *Hystricurus ellipticus* Zone (correlatable with the interval ranging from the upper part of the *Symphysurina* Zone to the lower part of the *Bellofontia-Xenostegium* Zone) to the *Randaynia saundersi* Zone (Text-fig. III-5).

In Missouri, "hystricurids" have been documented from the Gasconade Formation, the Roubidoux Formation, and the Rich Fountain Formation (Text-fig. III-5). The two species from the Rich Fountain Formation, *Hystricurus abruptus* (=*Chattertonella abrupta* herein) and *Rollia goodwini*—both described by Cullison (1944)—are excluded from the Hystricuridae in this study. The Jefferson City Group consisting of the Rich Fountain Formation and Theodosia Formation corresponds to the Jeffersonian Stage (Flower, 1978; Boyce, 1989, fig. 8) which is correlated into the *Hintzeia celsaora* Zone to *Protopliomerella contracta* Zone (Boyce and Stouge, 1997, fig. 4). Therefore, the Rich Fountain Formation is best correlated with the *Hintzeia celsaora* Zone (Text-fig. III-5).

Many of the species from the Roubidoux Formation and Gasconade Formation described by Heller (1954) and Ulrich (*in* Bridge, 1930) remain in the Hystricuridae *sensu* herein (see Appendix III-5). The correlation of the two formations into the Ibexian zonation is far from accurate. The Roubidoux Formation is considered to be assigned to the Demingian Stage (Boyce, 1989, fig. 8) which is correlated with the *Leiostegium-Kainella* Zone to the *Rossaspis superciliosa* Zone (Boyce and Stouge, 1997, fig. 4). However, the lowermost boundary of the formation was not accurately correlated within the Ibexian zonation. This subsequently poses a problem with correlating the Gasconade Formation. Nonetheless, the Gasconade Formation is most probably correlated with the Gasconadian Stage which is correlated with the interval including the *Symphysurina* Zone to the *Paraplethopeltis* Zone (Boyce and Stouge, 1997, fig. 4). As a result, the Hystricuridae is considered to occur from the *Symphysurina* Zone to the *Rossaspis superciliosa* Zone in Missouri (Text-fig. III-5). It is not known whether the lowermost limit of the Gasconadian stage corresponds to the boundary between the Cambrian and Ordovician.

Greenland Region. A biostratigraphic scheme correlatable to the Ibexian trilobite zonation is yet to be established for the Greenland region. Conodont biostratigraphy and regional lithostratigraphies are used to correlate the "hystricurid" occurrences into the Ibexian zonation (Text-fig. III-5).

The "hystricurids" have been documented from the Cass Fjord Formation, Cape Clay Formation, and Christian Elv Formation of northwest and north Greenland (Poulsen, 1927; Fortey and Peel, 1989), from the Cape Weber Formation and Antiblinbugt Formation of east Greenland (Poulsen, 1937), and from the Cape Clay Formation and Cape Weber Formation of Ellesmere Island (Poulsen, 1946). In Spitsbergen, one "hystricurid" species was reported from the Lower Oslobreen Limestone (Gobbett, 1960). All these "hystricurids" were referred to *Hystricurus*. Only three species remain in the Hystricuridae *sensu* herein (Appendix III-4), which occur in the Cass Fjord Formation (*Hystricurus* (*Triangulocaudatus*) *ravni*), Christian Elv Formation (*Hystricurus* (*Aequituberculatus*) *scrofulosus*), and Eleanor River Formation of Ellesmere and Cape Weber Formation of East Greenland (*Glabellosulcatus*? *crassilimbatus*).

202

The trilobite fauna from the Cass Fjord Formation in Northwest Greenland ranges from Dresbachian (Late Cambrian) to Early Ordovician in age (Palmer and Peel, 1981, fig. 4). Landing and Barnes (1981) reported the *Rossodus manitouensis* conodont fauna from the overlying Cape Clay Formation. The *Rossodus manitouensis* conodont zone is correlated with the *Bellofontia-Xenostegium* and *Paraplethopeltis* Zone (Landing and Barnes, 1981, fig. 2; see also, Ross *et al.*, 1997, fig. 10). Thus, the occurrence of *Hystricurus* (*Triangulocaudatus*) *ravni* is considered to be assignable to the *Symphysurina* Zone at its youngest, but it could also be correlated with the *Missisquoia* or *Eurekia apopsis* Zone.

Fortey and Peel (1989) questionably assigned the occurrence of *Hystricurus* (*Aequituberculatus*) *scrofulosus* from the Christian Elv Formation to the *Rossodus manitouensis* conodont Zone. The overlying Poulsen Cliff Formation yields trilobites which are assignable to the *Rossaspis superciliosa* to *Protopliomerella contracta* Zone (Fortey and Peel, 1982). The age of *H.* (*A.*) *scrofulosus* can be considered to be as young as the *Tesselacauda* Zone. The oldest occurrence of this species, which is in the Cass Fjord Formation (Poulsen, 1927), is considered to be correlated with the *Symphysurina* Zone and/or *Missisquoia* Zone where *Hystricurus* (*Triangulocaudatus*) *ravni* occurs.

Conodont faunas from the Cape Weber Formation of East Greenland where Poulsen (1937) reported *Glabellosulcatus*? *crassilimbatus* are referrable to the interval ranging from the *Bellefontia-Xenostegium* Zone of the Ibexian Series to the *Paralenorthis-Orthidiella* Zone of the Whiterockian Series (Smith, 1991). For the present, the occurrence of *G.*? *crassilimbatus* in East Greenland cannot be assigned with confidence to any of the Ibexian trilobite biozones.

The occurrence of *Glabellosulcatus*? *crassilimbatus* in Ellesmere Island (Poulsen, 1946) is more accurately assignable by correlating the lithostratigraphic schemes. Poulsen (1946) stated that the species was collected from the Cape Weber Formation. Peel and Cowie (1979) renamed the Cape Weber Formation in northwest Greenland as the Canyon Elv Formation, which Peel and Christie (1982, fig. 5) correlated with the lower half of the Eleanor River Formation in Ellesmere Island. Thus, the occurrence of *G.*? *crassilimbatus* is considered to be from same stratigraphic unit as the Eleanor River Formation in Ellesmere Island; the locality '6' of Poulsen (1946, fig. 2) corresponds to the geologic unit '29' of Peel and Christie (1982, fig. 3). The age of the Eleanor River Formation ranges from late Early to early Middle Ordovician (Packard and Mayr, 1982). However, occurrences of trilobites in the underlying and overlying formations allow me to more accurately assign the occurrence of *G.*? *crassilimbatus* to the Ibexian trilobite zones. Fortey (1986) described trilobites from the Wandel Valley Formation and assigned them to the *Trigonocerca typica* Zone; this formation is stratigraphically equivalent to the upper part of the Nunatami Formation and the Cape Webster Formation in Northwest Greenland (Text-fig. III-5). Fortey and Peel (1982) assigned the trilobite fauna from Poulsen Cliff Formation to an interval ranging from the *Rossaspis superciliosa* to *Protopliomerella contracta* Zone. The Eleanor River Formation corresponds to the stratigraphic interval that is overlain by the Cape Webster Formation and underlain by Poulsen Cliff Formation. This suggests that the occurrence of *G.*? *crassilimbatus* in the Eleanor River Formation is assignable to such a long interval as from the *Rossaspis superciliosa* to *Trigonocerca typica* Zone, or to the *Protopliomerella contracta* Zone in the shortest interpretation of the range; the latter option is accepted herein. The

203

occurrence of *G.*? *crassilimbatus* in the Cape Weber Formation of East Greenland is correlated accordingly (Text-fig. III-5).

Hystricurus? *sulcatus* and *Hystricurus*? *armatus* (Poulsen, 1937), which are removed from the concept of the Hystricuridae, occur in the Antilinbugt Formation which is a new name for the Cass Fjord Formation of East Greenland (Peel and Cowie, 1979). Kurtz and Miller (1981) reported the existence of the *Cordylodus lindstromi* and *Rossodus manitouensis* conodont zones in the formation. The first conodont zone is correlated with a part of the *Symphysurina* Zone and the second with the interval spanning two Ibexian zones such as the *Bellofontia-Xenostegium* and *Paraplethopeltis* Zone (Ross *et al.*, 1997, fig. 10). The base of the overlying Cape Weber Formation is considered to be located within the *Rossodus manitouensis* Zone (Smith, 1991). Thus, the occurrences of the two species are assigned to the *Symphysurina* Zone.

Hystricurus wilsoni (=*Flectihystricurus*? *wilsoni* herein) occurs in Lower Oslobreen Limestone in Ny Friesland of Spitsbergen; it is the only record of the "hystricurids" in Spitsbergen. The Lower Oslobreen Limestone is considered to be contemporaneous with the Spora Member of Kirtonryggen Formation which yields such trilobites as *Leiostegium*, *Hystricurus*, and *Symphysurina* indicative of the *Symphysurina* to *Leiostegium-Kainella* Zone (Fortey and Bruton, 1973).

Sino-Korean Platform. A detailed correlation of biostratigraphic zones in Sino-Korean Platform, Australia, and South China has recently been provided by Kim and Choi (1997, fig. 4). Five *Hystricurus* species—*H. megalops* (Kobayashi, 1934), *H. eurycephalus* (Kobayashi, 1934), *H. granosus* (Endo, 1935), *H. truncatus* (Park, 1993) and *H. penchiensis* (Lu *et al.*, 1976)—were reported from the Sino-Korean Platform. After taxonomic revision, six species of the Hystricuridae, *Hystricurus*? *megalops*, *Hystricurus*? *eurycephalus*, *Hystricurus*? *granosus*, *Hystricurus*? *penchiensis*, *Tanybregma paratimsheansis*, and *Glabellosulcatus koreanicus* are known to occur in the region (Appendix III-4).

Hystricurus? *megalops* and *Hystricurus*? *eurycephalus* occur in the *Kayseraspis* Zone which is early Arenigian in age (Text-fig. III-6). The occurrence of *Hystricurus*? *granosus*, *Hystricurus*? *penchiensis* and *Tanybregma paratimsheansis* is assigned to the *Adelograptus-Clonograptus* and *Callograptus taitzehoensis* graptolite Zone (Zhou and Fortey, 1986) which is equivalent to the *Protopliomerops* Zone (late Tremadocian in age; Kuo *et al.*, 1982). *Glabellosulcatus koreanicus* occurs in the *Protopliomerops* Zone (Kim and Choi, 1997). The accurate correlation of the *Protopliomerops* Zone and *Kayseraspis* Zone with the Ibexian trilobite zones is yet to be accomplished. Nonetheless, the *Protopliomerops* Zone most probably ranges from the *Tesselacauda* Zone to *Hintzeia celsaora* Zone, and the *Kayseraspis* Zone ranges from the *Protopliomerella contracta* Zone to the *Trigonocerca typica* Zone, since the boundary between the Tremadocian and Arenigian is considered to correspond to the one between the *Hintzeia celsaora* and *Protopliomerella contracta* Zone

Hystricurus truncatus (=*Tersella truncatus* herein) from South Korea, which is removed from the Hystricuridae, is restricted to the *Protopliomerops* Zone (Park, 1993). **Australia.** The "hystricurids" have been documented from the Florentine Valley Formation (Jell and Stait, 1985b) and the Caroline Creek Sandstone of Tasmania (Jell and Stait, 1985a), the Digger Island Formation of Victoria (Jell, 1985), the Emanuel Formation of Western Australia (Leggs, 1976; Laurie and Shergold, 1996), and the

Pacoota Sandstone of Northern Territory (Shergold, 1991a) (see Appendix III-5).

Species from Tasmania were identified as *Hystricurus penchiensis*, *Hystricurus lewisi*, *Tanybregma tasmaniensis* and *Hystricurus* sp. cf. *H. robustus* by Jell and Stait (1985b) and *Etheridgaspis carolinensis* by Jell and Stait (1985a). *H. penchiensis* and *T. timsheansis* occur in the lower sampling horizon of Florentine Valley Formation in Tasmania (Jell and Stait, 1985b). The horizon is correlated with the La1.5 zone of the Victorian graptolite zones. The upper sampling horizon yielding *H. lewisi* is correlated with OT4 to OT7 of informal assemblages proposed by Banks and Burrett (1980). These assemblages are considered to be correlated with the La2 and La3 zones of the Victorian graptolite zones (Webby *et al.*, 1991, table 1). These Tasmanian species ranges from La1.5 to La3 Zone of the Victorian graptolite zones. The base of the La1.5 Zone is defined by the appearance of a graptolite genus *Adelograptus* which occurs in the *Protopliomerops* Zone in the Sino-Korean Platform (Zhou and Fortey, 1986, table 3). The base of the Arenigian is placed at the top or the base of the La3 graptolite zone which is the youngest of the Lancefieldian stages (Webby *et al.*, 1991, table 1). Therefore, the *H. lewisi* from the upper horizon are considered to be latest Tremadocian in age. *H. penchiensis* and *T. timsheansis* from the lower horizon are considered to be late Tremadocian in age (Text-fig. III-6). *E. carolinensis* is considered to be early Bendigonian in age (Jell and Stait, 1985a). Since the base of the Bendigonian is considered to be equal to or higher than the base of the Arenigian (Webby *et al.*, 1991, table 1), the age of *Etheridgaspis* is early Aregnigian (Text-fig. III-6).

The specimens of all these Tasmanian species are transferred into *Carinahystricurus tasmanacarinatus*, *Etheridgaspis carolinensis*, *Hystricurus*? *megalops*, *Hystricurus*? sp. aff. *H.*? *missouriensis*, *Hillyardina tubularis*, *Tanybregma tasmaniensis*, *Tanybregma timsheansis*, *Tanybregma paratimsheansis*, and *Tasmanaspis lewisi* (see Appendix III-5). Of these, *E. carolinensis* and *T. lewisi* are not regarded as a member of the Hystricuridae *sensu* herein. In Tasmania, the hystricurid occurrence is restricted to the Lancefieldian stages, from the La1.5 to La3 graptolite zone.

From the Digger Island Formation of Victoria, three "hystricurid" species were documented by Jell (1985), of which only one species remains in the Hystricuridae *sensu* herein; *Parahystricurus* sp. cf. *P. fraudator* (=*Glabellosulcatus sanduensis* herein). The age of the Digger Island fauna is considered to be contemporaneous with the *Kainella meridionalis* Zone of Argentina, which is correlatable with the La1 zone of the Lancefieldian Series. The *Kainella meridionalis* Zone is correlated with the upper part of the *Pseudokainella* Zone (Kim and Choi, 1997, fig. 4). Thus, the age of *G. sanduensis* is considered to be early Tremadocian.

Three species in open nomenclature were described from Western Australia by Leggs (1976) and Laurie and Shergold (1996); *Hystricurus* sp. and *Hystricurus* (?*Guizhouhystricurus*) sp. indet. from the Be2 of the Bendigonian Series and *Hystricurus* (*Hystricurus*) sp. cf. *H.* (*H.*) *lewisi* from the Be1 of the Bendigonian Series. Specimens of the first species are transferred into *Hystricurus*? *megalops* and *Hystricurus*? *eurycephalus* which are considered to be included in the Hystricuridae (see Appendix III-5). Specimens of the second species are re-classified into *Hystricurus*? *clavus*, and a bathyurid in this study. The last species is transferred into *Hystricurus*? *eurycephalus*. The age of *H.*? *megalops* and *H.*? *eurycephalus* from Western Australia is considered early Arenigian, following Laurie and Shergold (1996, text-fig. 6).

205

Hystricurus sp. cf. *H. eurycephalus* (*=Hystricurus*? *amadeus* herein; Shergold, 1991a) occurs in sequence 3 of the Pacoota Sandstone (Shergold *et al.*, 1991) which is correlated with the lower part of Emanuel Formation and underlying Kudata Dolomite. This stratigraphic interval is correlated with La3 Zone (Laurie and Shergold, 1996, text-fig. 5) which is considered to be included in the *Protopliomerops* Zone (Kim and Choi, 1997, fig. 4) Thus, *H.*? *amadeus* is considered to be latest Tremadocian in age, like the Tasmanian species.

As a result, the Hystricuridae ranges from the La1 zone of the Lancefieldian Series to the Be2 zone of the Bendigonian Series in Australia. The correlation of the Bendigonian Series with the Ibexian trilobite zones is well established by Laurie and Shergold (1996, text-fig. 6). The La1.5 to La3 zones are most likely to be correlated with the *Protopliomerops* Zone of the Sino-Korean Platform and La1 with the *Pseudokainella* Zone. However, their correlation with the Ibexian trilobite zonation is still open to question, even if they are most likely to range from the *Symphysurina* Zone to the *Rossaspis superciliosa* Zone (Text-fig. III-6).

Siberia and Kazakhstan. Of 16 "hystricurid" species from Siberia and Kazakhstan, only one species from Kazakhstan, *Hystricurus antiquus* (*=Spinohystricurus antiquus* herein; Lisogor, 1961) remains in the Hystricuridae after the taxonomic revision. The poorly preserved cranidia of pygidia from Siberia are questionably assigned to *Hystricurus*? *conicus*. The age of this species is late Tremadocian. Although the accurate correlation of its stratigraphic occurrence is not attempted, the occurrence appears to be correlated with the *Ijacephalus-Nyaya* Zone of Siberia. Other species from Siberia and Kazakhstan occur from earliest Tremadocian (e.g., the *Euloma limitaris-Taoyuania* Zone of *Batyraspis inceptoris* [*=Taoyuania xenisma* herein] from Kazakhstan; Apollonov *et. al.*, 1988, fig. 2) to late Arenigian (e.g., the *Pseudomera-Biolgina* Zone of *Tersella sulcata* from Siberia; Ogienko, 1992, fig. 7) (Text-fig. III-6).

South China. After the taxonomic revision, only a single species, *Glabellosulcatus sanduensis* is known to occur in South China that was previously assigned to *Pharostomina* (Zhou, 1981). The species is reported from an early Tremadocian horizon of the Guotang Formation.

ASSOCIATION OF PYGIDIUM

51 of the 89 formally named "hystricurid" species were erected on the basis of cranidia. It is not surprising that most suggestions on evolutionary relationship and taxonomic affinity of the "hystricurids" (see above) are based on cranidial morphologies. In order to incorporate the pygidial information into the taxonomic revision, this study aims to associate correctly the pygidium and cranidium for the species of the "hystricurids."

An articulated specimen was described for *Hystricurus ravni*, (*=Hystricurus (Triangulocaudatus) ravni* herein, Poulsen, 1927, fig. 5), *Pseudohystricurus obesus* (Demeter, 1973, pl. 6, figs. 13, 14), *Hystricurus penchiensis* (*=Tanybregma timsheansis* herein, Jell and Stait, 1985b, pl. 1, fig. 4), *Hillyardina levis* (*=Parahillyardina newfoundlandia* herein, Boyce, 1989, pl. 6, fig. 6). A few silicified articulated specimens were recovered from the collections made by the author. The pygidial morphology of these articulated specimens allows for associating a pygidium with the cranidium of a species whose morphology is similar to that of each of the species. It is assumed that forms with similar cranidia had similar pygidia. This is employed as the most useful

206

criterion for the association of pygidium.

Secondly, the pygidium is associated based on "co-occurrence." Pygidial and cranidial materials occurring in the same sampling horizon are assumed to belong to the same species. However, it is not uncommon that more than one pygidial and cranidial morphotypes occur together in a single sampling horizon. In such cases, the co-occurrence data for other sampling horizons are cross-examined to find the most probable association and rule out the incorrect association.

Thirdly, the association of pygidia was made possible by using the assumption that morphologic similarities are equally observed in both pygidia and cranidia. If the cranidium of a species is similar to that of a second species, it is assumed that the pygidia of both species are also similar to each other. This criterion applies to the case that disarticulated cranidia of a species were associated with disarticulated pygidia in previous literature. Such matching features as size (particularly, large or small), shell thickness, sculpture (spines, graules, tubercles or absence of sculpture) often occur throughout the exoskeleton, and may be expected to match in the cranidium and pygidium of the same species.

SYSTEMATIC PALEONTOLOGY

Order **PROETIDA** Fortey and Owens, 1975
Family **HYSTRICURIDAE** Hupé, 1953

Diagnosis. Pygidium with fulcral ridge developed between flat inner pleural field and steeply down-sloping outer pleural field or developing a relatively conspicuous slope change between two fields.

Included Genera. *Hystricurus sensu lato*, *Carinahystricurus*, *Glabellolsulcatus*, *Hillyardina*, *Pachycranium*, *Parahillyardina*, *Parahystricurus*, *Paramblycranium*, *Politohystricurus*, *Pseudoplethopeltis*, *Spinohystricurus*, *Tanybregma*.

Pygidial Morphologies of *Hystricurus* and Other Genera. Two pygidial morphotypes are considered to be representative of the Hystricuridae. The first morphotype is associated with *Hystricurus sensu lato* and the second with the remaining hystricurid genera (Text-fig. III-7).

The pygidia of *Hystricurus* are subdivided into four morphotypes, each diagnosing each of the four *Hystricurus* subgenera. The pygidia of *Hystricurus* (*Hystricurus*) are characterized by the most conspicuous fusion of adjacent pleural bands, a large tubercle on the crest of the axial rings and a prominently bilobed terminal piece; the best example is seen in *H.* (*H.*) *crotalifrons* (Boyce, 1989, pl. 10, figs. 7-10). The pygidia of *Hystricurus* (*Butuberculatus*) are differentiated by the development of a prominent tubercle on the distal edge of the posterior pleural bands; *H.* (*B.*) *hillyardensis* (Stitt, 1983, pl. 4, fig. 6) best displays the condition. Those of *Hystricurus* (*Aequituberuclatus*) are distinguished by the development of equal-sized smaller tubercles on the surface; the pygidium of *H.* (*A.*) *ellipticus* (Westrop *et al.*, 1993, pl. 3, fig. 8) represents the best example. *Hystricurus* (*Triangulocaudatus*) has a pygidium that is subtriangular in outline and is smooth in the surface; see Pl. III-11, Figs. 9-13 for *H.* (*T.*) *paragenalatus*.

Two different types of furrows are present in the pleural field of the *Hystricurus* pygidia, which is most prominent in *Hystricurus* (*Hystricurus*). One type is much more

207

deeply-impressed and reaches the margin, whereas the other is weakly-impressed and falls short of the margin. The first is interpreted as the pleural furrow and the second as the interpleural furrow. The band defined by the two pleural furrows represents a pleural rib. The pleural rib of the *Hystricurus* pygidia may be due to the fusion of the adjacent pleural bands. It is this fusion of the adjacent pleural bands that distinguishes the pygidia of *Hystricurus* from those of other hystricurid genera such as *Spinohystricurus*, *Carinahystricurus*, *Hillyardina* and *Parahillyardina*.

Another feature that distinguishes the two pygidial morphotypes of the Hystricuridae is the development of a structure called "pygidial fulcral ridge" between the inner and outer pleural fields of the pygidia of other hystricurid genera; the ridge is usually interrupted by the interpleural furrows. The pygidia of the hystricurid genera other than *Hystricurus* have a tall and steeply down-sloping outer pleural field and relatively flat and narrow inner pleural field.

Genus **HYSTRICURUS** Raymond, 1913b

1955 *Vermilionites* Kobayashi, p. 452-453.
1965 *Glabretina* Lochman, p. 475-476.

Type Species. *Bathyurus conicus* (Billings, 1859). GSC 516, cranidium; Beekmantown Group, near Beauharnois, Quebec; Lower Ordovician.

Diagnosis. Exoskeletal surfaces covered with tubercles; cranidial surfaces covered coarser tubercles than pygidial and librigenal surfaces. Glabella forward-tapering. Pygidia with the pleural ribs delimited by deeply impressed pleural furrows. Prominent tubercles on distal edge of inner pleural field or equal-sized tubercles on pygidial surface.

Remarks. Kobayashi (1955) erected a new genus *Vermilionites* upon the basis of a relatively poorly-preserved cranidium (pl. 6, fig. 4) from the Lower Ordovician McKay Group of British Columbia. Later Boyce (1989) synonymized *Vermilionites* under *Hystricurus*, which is accepted herein (see *Hystricurus exilis* for detailed account of synonymy). *Glabretina*, as a new genus of the Hystricuridae, was named by Lochman (1965). However, the generic diagnosis is considered to be well accommodated within the concept of *Hystricurus* (see *Hystricurus* (*Butuberculatus*) *andrewsi* n. subgen. for detailed account of synonymy)

Fortey and Peel (1989) erected two subgenera of *Hystricurus*. Their major aim appears to have been to solve the taxonomic status of *Paraplethopeltis*. Their new species from Greenland, *Hystricurus* (*Paraplethopeltis*) sp. nov. A was considered to morphologically bridge *Hystricurus* and *Paraplethopeltis*. Thus, they erected two subgenera, *Hystricurus* (*Hystricurus*) and *Hystricurus* (*Paraplethopeltis*). They included all the species that had been referred to *Hystricurus* by that time within *Hystricurus* (*Hystricurus*), and those referred to *Paraplethopeltis* to *Hystricurus* (*Paraplethopeltis*). Their new species, *Hystricurus* (*Paraplethopeltis*) sp. nov. A is considered morphologically closer to some ptychopariides (see *Hystricurus? parascrofulosus* for detailed accounts). Other species referred to *Paraplethopeltis* (e.g., *P. obesa*) are transferred into the family Plethopeltidae because of their pygidial morphologies that are distinguishable from those of the Hystricuridae. The concept of *Hystricurus* (*Paraplethopeltis*) is suppressed in this study.

Taxonomic Conclusion. The concept of *Hystricurus* is still *sensu lato*, because it is suspected that some species assigned to *Hystricurus* herein may be more closely related

208

to some Cambrian ptychopariide taxa. In particular, the stratigraphically younger species of *H. (Aequituberculatus)* and *H. (Triangulocaudatus)* are possible candidates that could be eliminated from *Hystricurus*.

Subgenus HYSTRICURUS (HYSTRICURUS) Raymond, 1913b

Diagnosis. Bands of adjacent pygidial pleurae fused together distally, forming pleural rib that ends in tubercle. Single row of tubercles on both pleural bands. Prominently bilobed terminal piece. Palpebral lobe large and moderately arched. Glabella relatively large and short sagittally, and strongly forward-tapering. Preglabellar field present. Anterior cranidial border furrow distinctively impressed.

Included Species. *H. (H.) conicus* Raymond, 1913b, *H. (H.) oculilunatus* Ross, 1951, *H. (H.) exilis* n. sp., *H. (H.) crotalifrons* (Dwight, 1884), *H. (H.?) sainsburyi* (Ross, 1965).

Remarks. Raymond (1913b) differentiated *Hystricurus* (=*Hystricurus (Hystricurus)* herein) from *Bathyurus* (see Whittington, 1953a, pl. 65, fig. 7) by the former having a short forward-tapering glabella and convex palpebral fixigena. In addition, the cranidia of *Hystricurus (Hystricurus)* differ in having a distinctively-impressed anterior cranidial border furrow, a preglabellar field, a posterior facial suture that is transverse and long, and distally terminated with a blunted end, and a deep occipital furrow throughout its entire stretch.

The pygidia of *Hystricurus (Hystricurus)* differ from those of *Bathyurus* in having pleural furrows that reach the margin, interpleural furrows that are confined to the pleural rib, a bilobed terminal piece, tubercles on the axial rings and pleural bands, and a distinct tubular border.

Hystricurus (Hystricurus) conicus (Billings, 1859)
Pl. III-1, Figs. 1-4

1859 *Bathyurus conicus* Billings, fig. 12c.
1913b *Hystricurus conicus* (Billings), Raymond, p. 60, pl. 7, fig. 9.
1951 *Hystricurus* sp. A Ross, p. 53, pl. 9, figs. 31, 34, 37.
? 1989 *Hystricurus* cf. *H.* sp. A Dean [part], p. 23, pl. 14, fig. 10 [only].
? 1996 *Hystricurus conicus*, Desbiens *et* al., [part], p. 1146, pl. 3, figs. 8, 12 [only].

Holotype. GSC 516, cranidium; Raymond, 1913b, pl. 7, fig. 9 (re-illustrated in Pl. III-1, Figs. 1-4); Lower Ordovician; Beekmantown Group, Quebec.

Diagnosis. Anterior cranidial border narrow (sag. and exsag.), tubular, moderately convex forwards, and gently arched dorsally. Anterior border furrow wide and shallow. No other skeletal parts known.

Description. Anterior cranidial border narrow (sag. and exsag.), tubular, moderately convex forwards, and gently arched dorsally. Anterior border furrow wide and shallow. Preglabellar field slightly convex dorsally. Glabella strongly forward-tapering with rounded anterior margin and nearly straight lateral margin, and slightly convex dorsally with nearly flat crest. Palpebral lobe medium-size (about one-third of cranidial length) and moderately arched laterally. Palpebral furrow distinctly impressed. Tubercles on surface except for preglabellar field.

Remarks. The holotype cranidium was illustrated with a line drawing (Billings, 1859, fig. 12c) and a photograph (Raymond, 1913b, pl. 7, fig. 9). Re-examination and re-illustration of the holotype (Pl. III-1, Figs. 1-4) reveals the following morphologic

features which were not apparent in previous illustrations of this specimen. The anterior border is narrow, tubular and slightly arched dorsally; anterior border furrow is broad and moderately deep (Raymond's photograph misleadingly shows a wider anterior border and a very narrow border furrow); preglabellar field is moderately convex and bears few tubercles; glabella is forward-tapering, its anterior margin is rounded and its lateral margin is nearly straight (Raymond's photograph misleadingly shows a less distinctly forward-tapering glabella, with a relatively truncated anterior margin). Due to poor preservation, the nature of the palpebral lobe and posterior fixigena cannot be accurately determined. On the right side of the specimen, however, half of the palpebral furrow is preserved which allows me to approximately estimate the nature of the palpebral lobe. The palpebral lobe appears to be of moderate size (close to half of glabellar length or one-third of cranidial length), moderately arched laterally, and located posteriorly (its anterior end appears to be slightly anterior to mid-cranidial length).

A cranidium of *Hystricurus* sp. A from the Garden City Formation (Ross, 1951, pl. 9, figs. 31, 34, 37) is greatly similar to the holotype cranidium, and only differs in having a less coarsely-tuberculated surface. A poorly-preserved cranidium from Alberta (Dean, 1989, pl. 14, fig. 10) is similar to the cranidium from the Garden City Formation, but differs in having a relatively straight anterior border, smooth exoskeletal surface and deeper axial furrows. This Albertan cranidium is tentatively assigned to this species.

Four cranidia from the Beauharnois Formation were identified as *Hystricurus conicus* by Desbiens *et* al. (1996). Two of them (pl. 3, figs. 8, 12) have a strongly forward-tapering glabella identical to the holotype cranidium. However, one of them (fig. 8) does not preserve the frontal area so that it cannot be determined whether it has the wide and shallow anterior border furrow and slender border. The cranidium appears to have a longer preglabellar field. The other (fig. 12) appears to have a smaller and weakly arched palpebral lobe and longer preglabellar field. Both of them are questionably referred to *H. (H.) conicus*.

Hystricurus (*Hystricurus*) *oculilunatus* Ross, 1951
Pl. III-1, Figs. 8-11

1951 *Hystricurus oculilunatus* Ross, [part], p. 47-48, pl. 10, figs. 1-3, 5, [only].
1954 *Hystricurus deflectus* Heller, p. 43, pl. 18, fig. 6.
1954 *Hystricurus* sp. Heller, [part], p. 44-45, pl. 18, figs. 7, 8, [only].
1967 *Hystricurus millardensis*, Winston and Nicholls, [part], p. 76, pl. 12, fig. 18, [only].
? 1970 *Hystricurus* aff. *H. genalatus* Ross, [part], p. 72, pl. 10, figs. 22-25, [only].
1973 *Hystricurus acumenis* [= *acumennasus*] Ross, Terrell [part], p. 73, pl. 1, fig. 8, [only].
1973 *Hystricurus oculilunatus*, Terrell, [part], p. 73, pl. 1, figs. 12, 14, [only].
1982 *Pseudohystricurus* sp. aff. *P. rotundus*, Fortey *et al.*, [part], pl. 2, figs. 17, 24, [only].
1983 *Hystricurus* sp. nov. Boyce *in* Stouge and Boyce, pl. 12, figs. 7, 8.
1983 *Hystricurus pseudoculilunatus* Boyce, p. 111-115, pl. 8, figs. 4-8.
1989 *Hystricurus deflectus*, Boyce, p. 40-41, pl. 12, figs. 1-10, pl. 13, figs. 1-10.
Holotype. Y.P.M. 17960, cranidium; Ross, 1951, pl. 10, figs. 2, 3, 5 (re-illustrated in Pl. III-1, Figs. 8-11); *Rossaspis superciliosa* Zone; Garden City Formation, southern Idaho.

210

Diagnosis. Anterior cranidial border wide (sag. and exsag.) and ornamented with fine terrace lines. Anterior cranidial border furrow narrowly impressed. Posterior fixigena transversely elongated and distally terminated with rounded end. Preglabellar median furrow weakly developed. Free cheek with short (one third of exsagittal length of ocular platform) and stout genal spine. Librigenal lateral border and genal spine covered with fine terrace lines. Inner pygidial pleural fields gently convex dorsally. Pygidial marginal border very narrow.

Remarks. Cranidia and free cheeks of *Hystricurus deflectus* from Missouri (Heller, 1954, pl. 18, fig. 6) and Newfoundland (Boyce, 1989, pl. 12, figs. 1-7) are indistinguishable from the holotype cranidium from Idaho. As a result, *H. deflectus* is synonymized under this species.

Two free cheeks of *Hystricurus* sp. from Missouri (Heller, 1954, pl. 18, figs. 7, 8), although relatively poorly preserved, bear all the diagnostic features of this species.

A cranidium of *Hystricurus millardensis* (=*Hystricurus?* *millardensis* herein) from Texas (Winston and Nicholls, 1967, pl. 12, fig. 18) is remarkably similar to the cranidium from Newfoundland (Boyce, 1989, pl. 12, figs. 1-3). It does not develop three pairs of glabellar furrows which is diagnostic to *H.?* *millardensis*.

A cranidium from Nevada (Ross, 1970, pl. 10, figs. 22-25) exhibits a weakly-tapering glabella and narrower anterior border, which cannot be accomodated within the concept of this species. However, overall cranidial architecture is very similar to this species. A co-occurring free cheek (pl. 10, fig. 25) has narrower lateral border and lateral border furrow that shallows out towards postero-lateral corner of ocular platform. These differences do not agree with the free cheeks from Idaho. These cranidia and free cheeks are temporarily retained in this species.

A pygidium from Utah (Terrell, 1973, pl. 1, fig. 8) is indistinguishable from those from Newfoundland. In particular, its weakly tapering axis allows me to differentiate it from the pygidium of *Hystricurus* (*Hystricurus*) *exilis* (Ross, 1951, pl. 17, figs. 23, 28, 29, pl. 19, figs. 13, 14, 17). Pygidia of *Hystricurus acummennasus* (=*Flectihystricurus acummennasus* herein; see Pl. III-49, Figs. 11-13), although their association is not confident, differ in lacking tubercles on pleurae and having fewer segments.

An incomplete cranidium of *Pseudohystricurus* sp. aff. *P. rotundus* from Newfoundland only differs in having a slightly narrower (tr.) frontal area and a proportionately larger glabella; these differences are considered ontogenetic. Compared to *Pseudohystricurus*, it bears a larger, strongly arched palpebral lobe and deeper anterior cranidial border furrow.

Hystricurus (*Hystricurus*) *exilis* n. sp.

? 1948 *Hystricurus binodosus* Weber, [part], p. 7-9, pl. 1, figs. 11, 12, [only].
1951 *Hystricurus oculilunatus* Ross, [part], p. 47-48, pl. 10, figs. 8, 9, 12, [only].
1951 Unassigned pygidium, Ross, pl. 17, figs. 23, 28, 29, pl. 19, figs. 13, 14, 17.
1955 *Vermilionites bisulcatus* Kobayashi, p. 453-454, pl. 6, fig. 4, pl. 9, fig. 2 (re-
    illustrated by Dean, 1989, pl. 15, figs. 1, 2))
1989 *Hystricurus oculilunatus*, Boyce, [part], p. 38-40, pl. 8, figs. 1-4, [only].
1989 *Hystricurus oculilunatus*, Dean, [part], p. 23, pl. 15, figs. 1, 2, [only].
Holotype. Y.P.M. 18299, cranidium; Ross, 1951, pl. 10, figs. 8, 9, 12; *Rossaspis superciliosa* Zone; Garden City Formation, southern Idaho.

211

Diagnosis. Palpebral lobe slender and weakly arched laterally. Palpebral furrow narrow, and shallows and narrows out towards mid-palpebral point. Posterior facial suture runs straight and diagonally. Pygidial marginal border wider and ornamented with fine terrace lines. Axis more rapidly tapering posteriorly. Post-axial ridge well defined by axial furrows. Free cheeks unknown.

Etymology. "exilis" from Latin describes that the palpebral lobe is slender.

Association of Pygidium. Two unassigned pygidia were described by Ross (1951, pl. 17, figs. 23, 28, 29, pl. 19, figs. 13, 14, 17). They are similar to pygidia of *Hystricurus* (*Hystricurus*) *oculilunatus*, and only differ in having a relatively wider marginal border and more rapidly tapering axis. Considering cranidial similarities of this species with *H.* (*H.*) *oculilunatus*, the pygidia are associated with this species.

Remarks. Two poorly-preserved cranidia of *Hystricurus binodosus* (Weber, 1948, pl. 1, figs. 11, 12) have a glabellar architecture similar to the holotype specimen. Since their palpebral lobes and furrows, the most diagnostic feature of this species, are not preserved, they are questionably assigned to this species. Since all materials of *H. binodosus* are poorly preserved and transferred to many other species in this study (see below), the concept of *H. binodosus* is suppressed.

A cranidium from British Columbia, which was identified as *Vermilionites bisulcatus* by Kobayashi (1955, pl. 6, fig. 4; re-illustrated and assigned to *Hystricurus* (*Hystricurus*) *oculilunatus* by Dean (1989, pl. 15, figs. 1, 2)) is smaller than the holotype from Idaho. It bears the weakly-arched palpebral lobe and wider (tr.) frontal area. Such differences as narrower preglabellar field and less strongly tuberculated surface are ontogenetic and due to preservation, respectively.

<div align="center">

***Hystricurus* (*Hystricurus*) *crotalifrons* (Dwight, 1884)**

</div>

1884 *Bathyurus*? *crotalifrons* Dwight, p. 253-254, figs. 4-6.
1889 *Bathyurus conicus* Billings, Whitfield, p. 61-62; pl. 13, figs. 15-21 (figs. 15-17 re-illustrated by Boyce, 1989, pl. 9, figs. 1-6).
1954 *Hystricurus* sp. Heller, [part], p. 44-45, pl. 18, fig. 18, [only].
1959 *Hystricurus oculilunatus*, Berg and Ross, p. 112, pl. 21, fig. 2.
1959 *Hystricurus conicus* (Billings), Poulsen *in* Moore, figs. 204-4a, b.
1962 *Hystricurus conicus* (Billings), Welby, pl. 13, fig. 10.
1983 *Hystricurus oculilunatus*, Boyce *in* Stouge and Boyce, pl. 12, figs. 5, 6.
1983 *Hystricurus oculilunatus*, Boyce, p. 104-110, pl. 6, figs. 7, 8, pl. 7, figs. 1-8, pl. 8, figs. 1-3.
1989 *Hystricurus oculilunatus*, Boyce, [part], p. 38-40, pl. 8, figs. 5-8, pl. 9, figs. 1-10, pl. 10, figs. 1-10, pl. 11, figs. 1-11, [only].
? 1989 *Hystricurus* cf. *H.* sp. A Ross, Dean [part], p. 23, pl. 14, fig. 14 [only].
? 1996 *Hystricurus conicus*, Desbiens *et al.*, [part], p. 1146, pl. 3, figs. 4, 10, 15, [only].
1996 *Hystricurus conicus*, Desbiens *et al.*, [part], p. 1146, pl. 2, fig. 15, pl. 3, figs. 1-3, 5-7, 11, [only].

Holotype. Cranidium, illustrated in Dwight (1884, pl. 7, fig. 4); Wappinger Valley, New York; specimen cannot be located.

Neotype. AMNH 41335, cranidium; Calcifereous Sandrock, Lake Champlain (re-illustrated by Boyce, 1989, pl. 9, figs. 1, 2).

Diagnosis. Glabella short (sag.) and wide (tr.) with relatively truncated anterior margin.

<div align="center">

212

</div>

Anterior cranidial border furrow deep and wide. Cephalic border tubular and wide. Pygidium with most conspicuously bilobed terminal piece. Prominent node on crest of pygidial axial rings. Pygidial pleural furrows reach marginal border with consistent depth. Outer pygidial pleural field nearly absent.

Remarks. In the Treatise (Moore, 1959), the specimens illustrated and identified as *Bathyurus conicus* by Whitfield (1889, pl. 13, figs. 15, 20) were illustrated as the holotype of *Hystricurus conicus*, the type species of *Hystricurus*. Later, Boyce (1989, pl. 9, figs. 1-6) re-illustrated some of Whitfield's materials and assigned all the specimens illustrated by Whitfield to *Hystricurus oculilunatus*.

Boyce (1989) illustrated and assigned several cranidia from west Newfoundland to *Hystricurus oculilunatus*. However, the holotype of *H. oculilunatus* (=*Hystricurus* (*Hystricurus*) *oculilunatus* herein; see Pl. III-1, Figs. 8-11) has a more elongated glabella, and deeper and narrower anterior border that is rather pointed forwards. These differences are considered to be interspecific. The Newfoundland cranidia are assigned to *Hystricurus* (*Hystricurus*) *crotalifrons*, because *Bathyurus*? *crotalifrons* described by Dwight (1884), although poorly preserved and illustrated only by line-drawings, shows a large glabella with incurved lateral margin, wide anterior cranidial border furrow, and rounded anterior cranidial margin.

Dwight (1884) did not designate the holotype of this species. The cranidium first illustrated (pl. 7, fig. 4) is treated as the holotype. Unfortunately, the specimen is illustrated as a line-drawing and Dwight (1884) did not provide any information on the specimen number and attempts to locate the specimen have failed. For these reasons, a cranidium described by Whitfield (1889, pl. 13, fig. 17) is selected as a neotype; Whitfield (1889) illustrated it with a line-drawing and did not give any specimen number, but later Boyce (1989) located and re-illustrated the specimen (pl. 9, figs. 3-6).

A very poorly-preserved cranidium from Alberta (Dean, 1989, pl. 14, fig. 14) bears a glabella similar to this species. The poor preservation of the Albertan specimen prevents me from further taxonomically assessing the specimen.

Two cranidia from the Beauharnois Formation were assigned to *Hystricurus conicus* by Desbiens *et al.* (1996). The cranidia (pl. 3, figs. 4, 10, 15) have a much wider anterior border and narrower border furrow, and smaller palpebral lobes than the holotype cranidium of *H.* (*H.*) *conicus*. They are more similar to those of *Hystricurus* (*Hystricurus*) *crotalifrons*, but differ in having smaller palpebral lobes. Desbiens *et al.* (1996) associated four pygidia for *H. conicus* (pl. 2, fig. 15, pl. 3, figs. 1-3, 6, 7). They are indistinguishable from those of *H.* (*H.*) *crotalifrons* (see Boyce, 1989, pl. 11, figs. 1-13).

Comparison. The concept of *Hystricurus* (*Hystricurus*) *crotalifrons* has been confused with *Hystricurus* (*Hystricurus*) *conicus* because of the poor preservation and illustration of the holotype of the latter species (see detailed accounts of *H.* (*H.*) *conicus*). *H.* (*H.*) *crotalifrons* differs from *H.* (*H.*) *conicus* in having a wider anterior cranidial border and anterior cranidial border furrow, and shorter (sag.) and wider (tr.) glabella whose anterior two-thirds are defined by incurved axial furrows. From *Hystricurus* (*Hystricurus*) *oculilunatus* and *Hystricurus* (*Hystricurus*) *exilis*, this species differs in having a shorter (sag.) glabella, a larger and more strongly arched palpebral lobe, and much more prominent tubercles along the distal edge of pygidium.

213

Hystricurus (Hystricurus?) sainsburyi (Ross, 1965)

? 1961 *Hystricurus conicus* (Billings), [part] Balashova, pl. 1, figs. 12, 13 [only; not fig. 14].

1965 *Hystricurus? sainsburyi* Ross, p. 18, pl. 8, figs. 1-3, 5-7. 10, 11.

Holotype. USNM 144233, cranidium; Ross, 1965, pl. 8, figs. 1-3; Lower Ordovician; Lost River area, Alaska.

Diagnosis. Preoccipital furrow curves forwards medially. Preglabellar furrow deeply impressed. Glabella with relatively truncated anterior margin and straight lateral margin. Anterior cranidial border wide and strongly arched dorsally. Anterior cranidial border furrow narrow. Posterior fixigena long (tr.) and curves posteriorly distally.

Pygidial axis narrow. Posterior margin slightly arched dorsally sagittally. Pleural field gently down-sloping, without any distinct separation between inner and outer pleural fields. Posterior band of anterior pleura and anterior band of posterior pleura fused distally, but without developing tubercles. Marginal border furrow well-impressed.

Librigenal field wide. Lateral librigenal border narrow. Posterior and lateral librigenal border furrows shallow out towards postero-lateral corner of librigenal field. No tubercles on exoskeletal surfaces.

Remarks. Ross (1965) questionably assigned this species to *Hystricurus* because of its large cranidium, *Bathyurus*-like pygidium, and smooth exoskeletal surface. *Hystricurus* (*Hystricurus*) species such as *H.* (*H.*) *crotalifrons* and *H.* (*H.*) *exilis* have pygidia similar to the pygidium of this species. From *Bathyurus* (see Whittington, 1953a, pl. 65, figs. 7, 12), these pygidia differ in having wider pleural furrows, a more discernible and wider border, more deeply impressed axial ring furrows, and a wider inner pleural field and narrower and more steeply sloping outer pleural field. The most conspicuous pygidial feature is that the posterior band of the anterior pleura and the anterior band of the posterior pleura are fused together distally. In other *Hystricurus* species (see Boyce, 1989, pl. 10, fig. 7), the fused bands end with prominent tubercles, whereas this species lacks the tubercles. The smooth cranidial exoskeleton may be a result of its being preserved as an internal mold. The medially curved forward occipital furrow is unique to this species and not seen in any other *Hystricurus* species, but is found in *Bathyurus* (see Whittington, 1953a, pl. 65, fig. 7).

A poorly-preserved cranidium from Kazakhstan identified as *Hystricurus conicus* (Balashova, 1961, pl. 1, fig. 12) displays the truncated anterior and straight lateral glabellar margin, and sagittally forward-curved occipital furrow of this species. However, it shows a wider anterior cranidial border furrow and narrower anterior cranidial border. These features are more comparable to those of *Hystricurus* (*Hystricurus*) *conicus*. This species is questionably referred to *Hystricurus* (*Hystricurus*) because it lacks the bilobed pygidial terminal piece, and has a strongly arched anterior cranidial border and forward-convex preoccipital furrow.

ASSOCIATION OF PYGIDIUM WITH *HYSTRICURUS (AEQUITUBERCULATUS) GENALATUS*, *HYSTRICURUS (TRIANGULOCAUDATUS) PARAGENALATUS* AND *POLITOHYSTRICURUS* AND THEIR ALLIED SPECIES.

Ross (1951) and Hintze (1953) described three *Hystricurus* species, *genalatus*, *paragenalatus*, and *politus* (the last species is transferred into a new genus *Politohystricurus*) from the *Symphysurina* Zone. Each author figured several co-

214

occurring pygidia, but did not associate the pygidia with each of the three species. No articulated specimen has been discovered for any of these species.

In addition to the three species, the following species are newly described from the Great Basin in this study; *Hystricurus* (*Aequituberculatus*) *occipitospinosus*, *Hystricurus* (*Aequituberculatus*) *minutuberculatus*, (these species and subspecies are allied with *Hystricurus* (*Aequituberculatus*) *genalatus*) *Hystricurus* (*Triangulocaudatus*) *convexomarginalis* (this species allied with *Hystricurus* (*Triangulocaudatus*) *paragenalatus*), *Politohystricurus brevispinosus*, *Politohystricurus concavofrontalis*, *Politohystricurus pseudopsalikilus* (these species are allied with *Politohystricurus politus*).

Poulsen (1927) illustrated a complete specimen of *Hystricurus ravni* (=*Hystricurus* (*Triangulocaudatus*) *ravni* herein) from Northwest Greenland (pl. 18, fig. 5; see also, Pl. III-21, Fig. 8). Its cranidium, although deformed, resembles *Hystricurus* (*Triangulocaudatus*) *paragenalatus* (see Pl. III-11, Figs. 2, 15) with respect to the cranidial outline and course of the anterior facial suture. From the sampling horizons where cranidial materials of *H.* (*T.*) *paragenalatus* are recovered, pygidia (see Pl. III-11, Figs. 9-13, 18-22) are recovered that are similar to the pygidium of *H.* (*T.*) *ravni*. The pygidia are characterized by their subtriangular outline, and narrow marginal border. These pygidia from the Great Basin are associated with *H.* (*T.*) *paragenalatus*.

Of the Laurentian *Hystricurus* species from the *Symphysurina* Zone for which pygidia are associated, *H.* (*Aequituberculatus*) *ellipticus* (Westrop *et al.*, 1993, pl. 3, figs. 8, 9), *H.* (*Butuberculatus*) *hillyardensis* (Stitt, 1983, pl. 4, fig. 6), *H.?* *millardensis* (Hintze, 1953, pl. 6, figs. 20, 21) and *H.?* *paramillardensis* (Taylor and Halley, 1974, pl. 3, fig. 10) share similar pygidial shape. All these pygidia have a semi-elliptical outline, deep axial and pleural furrows, small tubercles on the pleural bands and axial rings, and four axial rings and a transversely elongated terminal piece. Pygidium of *Hystricurus* (*Butuberculatus*) *globosus* (Stitt, 1983, pl. 5, figs. 5, 6) is differentiated by its steeply-downsloping outer pleural field whose proximal edge is ornamented by small tubercles, and a narrower axis.

The cranidia of *Hystricurus?* *millardensis* and *Hystricurus?* *paramillardensis* are easily distinguished from those of other species by the presence of fossulae and three pairs of glabellar furrows. The other three *Hystricurus* species, *H.* (*Aequituberculatus*) *ellipticus*, *H.* (*Butuberculatus*) *globosus*, and *H.* (*Butuberculatus*) *hillyardensis* share an oval and convex glabella and deep axial furrows. *H.* (*A.*) *ellipticus* is differentiated from the latter two species by having a divergent anterior facial suture, larger palpebral lobe, shorter preglabellar field, and bluntly terminated distal end of the posterior fixigena. Of the *Hystricurus* species from the Great Basin, *H.* (*Aequituberculatus*) *lepidus* (Pl. III-8, Figs. 2, 7-12) shows the closest cranidial architecture to *H.* (*A.*) *ellipticus* (see Westrop *et al.*, 1993, pl. 3, figs. 1-7). Smaller cranidia of these two species show more similarities, supporting their close taxonomic affinity. This allows me to postulate that *H.* (*A.*) *lepidus* would have a pygidium similar to that of *H.* (*A.*) *ellipticus*.

Most cranidial materials of *H.* (*Aequituberculatus*) *lepidus* are recovered from a sampling horizon, SE-87.5. From this horizon occur cranidia of two other species, *Politohystricurus politus* and *Hystricurus* (*Triangulocaudatus*) *convexomarginalis*. Pygidial materials from this horizon are grouped into three morphotypes. The first is characterized by a longer and subtriangular outline with more axial rings (Pl. III-14, Figs.

215

12-16), the second by an elongated semi-elliptical outline (see Pl. III-8, Figs. 13-19), and the third by a narrow and flat inner pleural field, wide and steeply down-sloping outer pleural field, and strongly upturned posterior margin (Pl. III-24, Figs. 7-11, 13).

The first morphotype is very similar to that of *Hystricurus (Triangulocaudatus) paragenalatus* (see Pl. III-11, Figs. 9-13). Cranidial features of *H. (T.) paragenalatus* are greatly similar to those of *Hystricurus (Triangulocaudatus) convexomarginalis* from SE-87.5. Thus, the first pygidial morphotype is associated with *H. (T.) convexomarginalis*.

The second pygidial morphotype is most similar to the pygidium of *Hystricurus ellipticus* (Pl. III-3, Figs. 15-17). They share a semi-elliptical outline, longer pleural furrows, and convex axis that is as wide as the pleural field. In considering the cranidial similarities, this morphotype is associated with *Hystricurus lepidus*. The pygidia of *H. lepidus* differ from those of *H. ellipticus* in having shallower pleural furrows, less distinctly demarcated terminal piece, less deep axial furrows, and finer tubercles. The association of pygidia with other species allied with *H. lepidus* is mainly based on co-occurrence of the cranidial materials and degree of cranidial similarities with *H. lepidus* (see below)

The third morphotype is associated with *Politohystricurus convergia* because the strongly upturned posterior pygidial margin conforms to the highly uparched anterior cranidial border, and the pygidial materials are as abundant as the cranidial materials of the species. Pygidia are associated with subspecies and species allied with *Politohystricurus politus* based on cranidia which occur with them and the degree of similarity of those cranidia with *P. convergia* (see below).

From slightly lower sampling horizons (E2, E3, E4, and E5 from the Fillmore Formation, R5-34.1 and R6-15 from the Garden City Formation; see Fig. I-5, 6, 8), cranidial materials of such *Hystricurus* species as *H. minutuberculatus* and *H. genalatus* occur. From these horizons, pygidia similar to that of *Hystricurus lepidus* (Pl. III-7, Figs. 12-21) occur. Based on the cranidial similarities of *H. lepidus* and *H. minutuberculatus*, these pygidia are associated with *H. minutuberculatus*.

Subgenus **HYSTRICURUS (AEQUITUBERCULATUS)** n. subgen.
Etymology. "Aequituberculatus" depicts the development of equal-sized small tubercles on pygidial surfaces.
Diagnosis. Pygidial surfaces sparsely covered with equal-sized small tubercles.
Included Species. *H. (A.) genalatus* Ross, 1951, *H. (A.) lepidus* Hintze, 1953, *H. (A.) occipitospinosus* n. sp., *H. (A.) minutuberculatus* n. sp. and *H. (A.) ellipticus* Westrop *et al.*, 1993.
Remarks. Pygidia of the species belonging to this subgenus bear small, but equal-sized tubercles on axial rings and pleural bands. In this regard, they are similar to those of *Hystricurus (Butuberculatus)*, but differ in lacking the prominent tubercle(s) along the distal edge of the inner pleural field. They differ from *Hystricurus (Hystricurus)* in lacking the fusion of adjacent pleurae, and from *Hystricurus (Triangulocaudatus)* in having more transversely elongated outline.

Hystricurus (Aequituberculatus) genalatus Ross, 1951
Pl. III-5, Figs. 1-13, Pl. III-6, Figs. 1-10
1951 *Hystricurus genalatus* Ross, [part], p. 40-42, pl. 8, figs. 1-6, [only].

216

Holotype. Y.P.M. 17926, cranidium; Ross, 1951, pl. 8, figs. 1, 2, 5; *Symphysurina* Zone; Garden City Formation, southern Idaho.

Diagnosis. Frontal area relatively long (sag.) and subequally divided into anterior border and preglabellar field. Anterior cranidial border furrow straight. Anterior cranidial border straight, gently tapers distally, morderately arched dorsally. Anterior facial sutures parallel-sided or slightly divergent before anterior cranidial border furrow. Palpebral fixigena of equal width to half of maximum glabellar width, slightly convex and mostly down-sloping. Palpebral lobe cresentic and tapers towards anterior and posterior ends, and located posterior to mid-cranidial length. Posterior fixigena transverse and slightly curved forwards distally.

Lateral and posterior librigenal border relatively straight. Lateral and posterior librigenal border furrows shallow out posteriorly and laterally respectively, thus both not being confluent with each other. Genal spine slightly shorter than librigenal field and inner margin meets librigenal posterior border at right angle. Eye socle distinctively present.

Pygidium semi-elliptical in outline with discernible anterior two axial rings and triangular terminal piece. Pygidial axis short and strongly tapered posteriorly. Posterior margin slightly upturned and indented forwards. Axial furrows confluent with border furrow. Exoskeletal surface covered with relatively fine tubercles.

Remarks. Ross (1951) and Hintze (1953) assigned several other cranidia to this species (Ross, 1951, pl. 8, figs. 8, 9, 11, 13; Hintze, 1953, pl. 6, figs. 1, 2, 3, 4, 6). These cranidia differ in having a convergent anterior facial suture, shorter (sag.) frontal area, and convex forward-anterior border, and they are assigned to *Hystricurus* (*Aequituberculatus*) *lepidus*, and newly erected species such as *Hystricurus* (*Aequituberculatus*) *minutuberculatus*, and *Hystricurus* (*Aequituberculatus*) *occipitospinosus* (see below).

Hystricurus (*Aequituberculatus*) *lepidus* Hintze 1953
Pl. III-8, Figs. 1-19, Pl. III-9, Figs. 1-16

1951 *Hystricurus genalatus* Ross, [part], p. 40-42, pl. 8, figs. 7-10, 12, 13, [only].
1951 indefinitely assigned pygidia, Ross, [part], pl. 9, figs. 2-5, 7-10, 12, 18.
1953 *Hystricurus genalatus*, Hintze, [part], p. 164-165, pl. 6, figs. 1-4, 6, [only].
1953 *Hystricurus* sp. Hintze, pl. 6, figs. 25, 26.
1953 *Hystricurus lepidus* Hintze, [part], p. 166-167, pl. 7, figs. 12a-12c, [only].

Holotype. 26183 (no acronym provided, but the specimens were said to be deposited in Columbia University, New York), cranidium; Hintze, 1953, pl. 7, figs. 12a-12c; *Symphysurina* Zone; Fillmore Formation, Utah.

Diagnosis. Anterior facial suture turns inwards before anterior cranidial border furrow. Anterior cranidial border convex forwards and narrows laterally. Posterior fixigena steeply down-sloping. Palpebral fixigena greater (tr.) than half of maximum glabellar width, and moderately convex dorsally. Palpebral lobe with its anterior end located anterior to mid-cranidial length.

Rostral suture slightly curved forwards; rostral plate inverted trapezoidal in outline. Librigenal lateral border gently curved laterally.

Pygidium with three axial rings and rounded terminal piece. Pygidial marginal border tubular. Anteriormost pygidial pleural furrow confluent with pygidial marginal border furrow. Anterior two pleural and interpleural furrows well-impressed; posterior ones

217

imperceptible. Cranidial and librigenal surface covered with coarse tubercles, and pygidial pleural segments ornamented with a row of fine tubercles.

Remarks. Pygidia from the *Symphysurina* Zone illustrated by Ross (1951) and Hintze (1953) are indistinguishable from those figured in this study. The materials recovered in this study are larger than the holotype cranidium. The differences such as curvature of anterior cranidial border are considered intraspecific or ontogenetic. Compared with the holotype cranidium, the extreme morphologic end member is figured by Ross (1951, pl. 8, fig. 13). The materials figured in this study fairly well fill the gap between the holotype and the extreme. The free cheeks associated with this species by Hintze (1953, pl. 7, figs. 10, 11) are transferred into *Politohystricurus brevispinosus*.

Hystricurus (Aequituberculatus) occipitospinosus n. sp.
Pl. III-10, Figs. 1-15

1953 *Hystricurus genalatus*, Hintze, [part], p. 164-165, pl. 6, fig. 5, [only].
Etymology. "occipitospinosus" depicts the presence of conspicuous spines on occipital ring.
Holotype. UA 11925, cranidium; Pl. III-10, Figs. 2, 4, 5, 8; *Symphysurina* Zone; Fillmore Formation, Utah.
Diagnosis. Four to eight short and stout spines present on posterior margin of occipital ring. Anterior border furrow shallow. Anterior border flat and wide (tr.). Palpebral lobe strongly arched laterally and defined by discrete palpebral furrow whose curvature is less than that of margin of palpebral lobe. Anterior cranidial border and frontal area, and lateral librigenal border covered with tubercles much finer than on rest of cranidial and librigenal surfaces.

Pygidium with shallower border furrow and relatively strongly medially arched posterior margin.
Remarks. Although illustrated in ventral view, a cranidium assigned to *Hystricurus genalatus* (Hintze, 1953, pl. 6, fig. 5) clearly shows the presence of short spines on occipital ring. This species most similar to *Hystricurus (Aequituberculatus) lepidus*, but is distinguished by the presence of short and stout spines on the occipital ring.

Hystricurus (Aequituberculatus) sp. aff. *H. (A.) occipitospinosus*
Pl. III-15, Figs. 10, 11

Remarks. This pygidium is similar to those of *Hystricurus (Aequituberculatus) occipitospinosus* in having a similar overall outline, and a posterior margin that is dorsally arched and indented forwards. However, it develops prominent short spines on pleural region and fine tubercles on discernible border.

Hystricurus (Aequituberculatus) minutuberculatus n. sp.
Pl. III-6, Figs. 10-20, Pl. III-7, Figs. 1, 2, 7, 10-21

1951 *Hystricurus genalatus* Ross, p. 40-42, [part], pl. 8, fig. 11, [only].
1951 indefinitely assigned pygidia, Ross, p. 40-42, pl. 9, figs. 6, 11, 17.
Etymology. "minutuberculatus" depicts that the exoskeletal surfaces are covered with tubercles smaller than those of other species occurring in stratigraphically higher horizons.
Holotype. UA 11863, cranidium; Pl. III-6, Figs. 10, 11, 14, 18; *Symphysurina* Zone;

218

Fillmore Formation, Utah.

Diagnosis. Exoskeletal surfaces covered with fine tubercles. Anterior cranidial border ornamented with small tubercles and moderately convex forwards. Palpebral lobe of small size. Anterior cranidial border furrow narrow and deeply impressed.

Lateral librigenal border furrow shallows out posteriorly and does not meet posterior librigenal border furrow. Librigenal lateral border and genal spine covered with short spines. Genal spine curved and slightly longer than rest of free cheek. Posterior margin of posterior librigenal border meets genal spine base at slightly greater than right angle.

Pygidium transversely elongated in outline, with entire posterior margin in dorsal view. Four axial rings present on narrow axis. Inner pleural field flat and outer pleural fields rather steeply down-sloping. Fine tubercles on pleural field.

Remarks. Two different cranidial morphotypes are recognized, and each is considered to be a subspecies of this species. The proportional glabellar size is a major difference between the two subspecies.

The associated pygidia (see Pl. III-7, Figs. 12-21) are strikingly similar to those of Silurian *Otarion* (see Adrain and Chatterton, 1994, figs. 7.8). The pygidia of both taxa have a transversely elongated outline, small tubercles on pleural bands, and slightly dorsally arched posterior margin. Larger pygidia of *Otarion* (see Adrain and Chatterton, 1994, fig. 6.24) are remarkably similar to those of *Hystricurus* (*Aequituberculatus*) *lepidus* and *Hystricurus* (*Aequituberculatus*) *occipitospinosus*, in lacking tubercles on pleural regions, and they only differ in having a more transversely elongated outline.

Hystricurus (*Aequituberculatus*) n. sp. A aff. *H*. (*A.*) *minutuberculatus*
Pl. III-7, Figs. 3-6

Remarks. Cranidium of this species differs from *Hystricurus* (*Aequituberculatus*) *minutuberculatus* in having a smaller glabella and wider (tr.) frontal area. Free cheek associated with this species is nearly indistinguishable from that of *Hystricurus* (*Aequituberculatus*) *minutuberculatus*. More materials are needed for further assessing taxonomy of this species.

Hystricurus (*Aequituberculatus*) n. sp. B aff. *H*. (*A.*) *minutuberculatus*
Pl. III-7, Figs. 8, 9

Remarks. This new species resembles *Onchonotellus* (e.g., see Westrop, 1995, pl. 15, fig. 13) with respect to architecture of frontal area and glabellar shape. It differs in having a larger palpebral lobe that is located more posteriorly, and longer preglabellar field. It differs from *Hystricurus* (*Aequituberculatus*) *minutuberculatus* in having a wider frontal area and more posteriorly-located palpebral lobe.

Hystricurus (*Aequituberculatus*) sp. C aff. *H*. (*A.*) *minutuberculatus*
Pl. III-15, Fig. 1

Remarks. This cranidium bears an obliquely posteriorly directed posterior fixigena with truncated end and longer anterior margin.

Hystricurus (*Aequituberculatus*) *ellipticus* (Cleland, 1900)
Pl. III-3, Figs. 15-17
1900 *Bathyurus ellipticus* Cleland, p. 17, pl. 16, figs. 5, 6.

219

1954 *Hystricurus ellipticus* (Cleland), Fisher, pl. 4, figs. 12, 13.

1983 *Hystricurus globosus* Stitt, [part], p. 23-24, pl. 5, fig. 2, [only].

1983 *Hystricurus missouriensis* Ulrich *in* Bridge, Stitt, [part], p. 26-27, pl. 5, fig. 7, [only; not figs. 9, 10].

? 1983 *Hystricurus missouriensis* Ulrich *in* Bridge, Stitt, [part], p. 26-27, pl. 5, fig. 8, [only].

1993 *Hystricurus ellipticus* (Cleland), Westrop *et al.*, p. 1631, pl. 3, figs. 1-9.

Holotype. PRI 5073, cranidium; Fisher, 1954, pl. 4, fig. 12; *Symphysurina* Zone; Tribes Hill Formation, New York State.

Diagnosis. Glabella elongated, ovoid, and convex. Anterior facial suture moderately divergent and turns inwards at anterior cranidial border furrow. Preglabellar field short; anterior border wider (sag.) than preglabellar field. Posterior facial suture transverse or slightly directed forwards and then turns abruptly posteriorly.

Pygidium with wide and longe (tr.) axis. Postaxial ridge triangular and weakly defined by axial furrows. Pleural furrows well impressed and deeper than interpleural furrows.

Remarks. A poorly-preserved small cranidium was assigned to *Hystricurus* (*Aequituberculatus*) *globosus* (Stitt, 1983, pl. 5, fig. 2). It differs from the holotype cranidium of *H.* (*A.*) *globosus* (Stitt, 1983, pl. 5, fig. 1) in having a shallow and straight anterior border furrow. These features are in better agreement with cranidia of *Hystricurus* (*Aequituberculatus*) *ellipticus*.

Stitt (1983) assigned a cranidium to *Hystricurus missouriensis* (pl. 5, fig. 7). The concept of *H.?* *missouriensis*, which is revised herein, cannot accommodate the cranidial morphology of this specimen. Cranidia of *H.?* *missouriensis* (see Ross, 1951, pl. 10, fig. 7) are characterized by a convergent anterior facial suture (thus, transversely narrower frontal area, and transversely shorter anterior margin), longer preglabellar field, and more strongly forward-tapering glabella. This cranidium is remarkably similar to those of *Hystricurus* (*Aequituberculatus*) *ellipticus*.

A free cheek from Oklahoma was assigned to *Hystricurus missouriensis* (Stitt, 1983, pl. 5, fig. 8). Since the cranidium (pl. 5, fig. 7) is transferred to *Hystricurus* (*Aequituberculatus*) *ellipticus*, the free cheek is most likely to belong to this species. However, the poor preservation (in particular, course of facial suture) prevents me from confidently assigning it to this species.

Two poorly-preserved pygidia were also assigned to *Hystricurus missouriensis* (Stitt, 1983, pl. 5, figs. 9, 10). They differ from the pygidium of this species (Pl. III-3, Figs. 15-17) in having a more sagittally elongated outline, and narrower (tr.) inner pleural field. These two specimens cannot be assigned to any species with confidence.

Comparison with Other *Hystricurus* Species. Cranidia of this species are certainly similar to those of *Hystricurus* (*Aequituberculatus*) *lepidus*, but differ in having an oval-shaped, elongated glabella, and a narrower preglabellar field. From *Hystricurus* (*Butuberculatus*) *hillyardensis* and *Hystricurus* (*Butuberculatus*) *globosus*, this species differs in having a wider palpebral lobe and narrower preglabellar field. Pygidia of this species are greatly similar to those of *H.* (*A.*) *lepidus*, *Hystricurus* (*Butuberculatus*) *scrofulosus*, *Hystricurus?* *armatus*, *Hystricurus?* *longicephalus*, *H.* (*T.*) *hillyardensis*, and *Hystricurus?* *millardensis*. These pygidia are characterized by a flat inner pleural field, a gently down-sloping outer pleural field, but lacking the distinct fulcral ridge of tubercles

220

along the distal edge of inner pleural field, and having a weakly-developed post-axial ridge.

Subgenus HYSTRICURUS (TRIANGULOCAUDATUS) n. subgen.

Etymology. "Triangulocaudatus" describes the subtriangular-shaped pygidium.

Diagnosis. Pygidium subtriangular or semielliptical in outline. Axis proportionately wide (tr.) and sagittally long. Marginal border narrow and flat. Anterior facial suture divergent. Pleural and interpleural furrows reach pygidial marginal border furrow. Genal spine twice as long as librigenal field, and inner margin smoothly curved. Lateral and posterior librigenal border furrows meet at postero-lateral corner of librigenal field, and continue into genal spine as single furrow.

Included Species. *H. (T.) paragenalatus* Ross, 1951, *H. (T.) convexomarginalis* n. sp., *H. (T.) ravni* Poulsen 1927.

Remarks. Subtriangular to semielliptical pygidia of these species resemble those of many olenids such as *Olenus* (see Pl. II-29, Fig. 27) and *Acerocare* (see Pl. II-31, Fig. 25).

Hystricurus (Triangulocaudatus) paragenalatus Ross, 1951
Pl. III-11, Figs. 1-22, Pl. III-12, Figs. 1-15

1951 *Hystricurus paragenalatus* Ross, p. 42-45, pl. 8, figs. 14-26.
1951 indefinitely assinged pygidia, [part], Ross, pl. 9, fig. 1.
? 1951 *Hystricurus*? sp. H Ross [part], p. 56, pl. 14, figs. 11, 14, 15 [only].
? 1951 *Parahystricurus*? sp. B Ross, p. 61-62, pl. 14, figs. 4, 6, 7.
1953 *Hystricurus paragenalatus*, Hintze, p. 165, pl. 6, figs. 12-14.
1997a *Hystricurus paragenalatus*, Lee and Chatterton, figs. 2.1-2.8, 3.1.

Holotype. Y.P.M. 17934, cranidium; Ross, 1951, pl. 8, figs. 14, 17, 18; *Symphysurina* Zone; Garden City Formation, southern Idaho.

Diagnosis. Anterior cranidial margin moderately convex forward.

Intraspecific Variations. Cranidia and pygidia of this species show variations with respect to anterior facial suture and curvature of anterior cranidial margin, and ratio of length versus width of pygidium. These variations could represent subspecific variation.

Remarks. Smaller cranidia of *Hystricurus*? sp. H and *Parahystricurus* ? sp. B, which co-occur with *Hystricurus (Triangulocaudatus) paragenalatus*, would represent an earlier ontogenetic stage. They have a divergent anterior facial suture.

Protaspides of this species are described by Lee and Chatterton (1997a, figs. 2.1-2.4). They are characterized by having three distinct tubercles alongside the glabella and lacking any distinct tuberculation on the protopygidial region.

Hystricurus (Triangulocaudatus) sp. A aff. *H. (T.) paragenalatus*
Pl. III-15, Fig. 16

Remarks. This cranidium differs in having a relatively straight anterior margin and narrower (tr.) frontal area. It appears to be a morphologic intermediate between *Hystricurus (Aequituberculatus) genalatus* and *Hystricurus (Triangulocaudatus) paragenalatus*.

221

Hystricurus (*Triangulocaudatus*) sp. B aff. *H.* (*T.*) *paragenalatus*
Pl. III-15, Fig. 2

Remarks. This cranidium differs in having a smaller, more parallel-sided glabella and shorter sagittal length.

Hystricurus (*Triangulocaudatus*) sp. C aff. *H.* (*T.*) *paragenalatus*
Pl. III-15, Figs. 5, 6

Remarks. This pygidium differs in having obliquely directed anterior margin of pleural regions, and obliquely-directed pleural and interpleural furrows. Olenid affinity of this specimen cannot be ruled out; compare with pygidium of *Bienvillia* (Henningsmoen, 1957, pl. 11, figs. 5, 6, 8). It is also similar to *Hystricurus*? *clavus* (Pl. III-4, Figs. 2, 3).

Hystricurus (*Triangulocaudatus*) sp. D aff. *H.* (*T.*) *paragenalatus*
Pl. III-15, Fig. 15

Remarks. This cranidium is different from *Hystricurus* (*Triangulocaudatus*) *paragenalatus* in having a straight anterior margin and longer palpebral lobe.

Hystricurus (*Triangulocaudatus*) *convexomarginalis* n. sp.
Pl. III-13, Figs. 1-11, Pl. III-14, Figs. 1-16

Etymology. "convexomarginalis" describes the anterior cranidial margin that is convex forwards.

Holotype. UA 12111, cranidium; Pl. III-13, Figs. 2, 6; *Symphysurina* Zone; Garden City Formation, southern Idaho.

Diagnosis. Anterior cranidial margin strongly convex forward. Pygidial posterior margin relatively pointed.

Remarks. This species contains two cranidial morphotypes, each of which could be of subspecific value. The subspecific distinction is based on the curvature of anterior cranidial margin, relative size of glabella, and course of anterior facial suture. This species differs from *Hystricurus* (*Triangulocaudatus*) *paragenalatus* in having a strongly forward convex anterior margin and relatively pointed pygidial posterior margin.

Hystricurus (*Triangulocaudatus*) sp. aff. *H.* (*T.*) *convexomarginalis*
Pl. III-15, Figs. 3, 4

Remarks. This cranidium differs in having a longer (tr.) posterior fixigena.

Hystricurus (*Triangulocaudatus*) *ravni* Poulsen, 1927
Pl. III-21, Fig. 8

1927 *Hystricurus ravni* Poulsen [part], p. 283-284, pl. 18, figs. 5, 9 [only]..

Holotype. MGUH 2342, complete exoskeleton; Poulsen, 1927, pl. 18, fig. 5 (re-illustrated in Pl. III-21, Fig. 8); Lower Ordovician (possibly *Missisquoia* to *Symphysurina* Zone); Cass Fjord Formation, northwest Greenland.

Diagnosis. Palpebral lobe small. Anterior facial suture strongly divergent. Glabella forward-tapering with inwardly-curved lateral margin. Posterior facial suture diagonal. Pygidial marginal border narrow. Terminal piece reaches marginal border. 11 thoracic segments.

Remarks. It could be due to deformation that the glabella exhibits a incurved lateral

222

margin. A cranidium assigned to this species by Poulsen (1927, pl. 18, fig. 7) has a strongly arched palpebral lobe and a rather straight lateral glabellar margin which are not observed in the complete specimen (Poulsen, 1927, pl. 18, fig. 5) which has a curved lateral glabellar margin and a slightly arched palpebral lobe. The glabellar shape of the cranidium is more consistent with *Hystricurus? longicephalus* (Poulsen, 1927, pl. 18, fig. 11).

The pygidium illustrated (Poulsen, 1927, pl. 18, fig. 10) differs from that of the articulated specimen (Poulsen, 1927, pl. 18, fig. 5) in having a wider (tr.) and shorter (sag.) outline and a narrower (tr.) axis. A pygidium co-occurring with the cranidium of *Hystricurus? longicephalus* (Poulsen, 1927, pl. 18, fig. 7), which was not described by Poulsen, is indistinguishable from the specimen illustrated by Poulsen (1927, pl. 18, fig. 10). Since the cranidium (Poulsen, 1927, pl. 18, fig. 7) is transferred to *H.? longicephalus* (see below), the co-occurring pygidium and the pygidium illustrated in figure 10 of Poulsen (1927) may well belong to *H.? longicephalus*.

Comparison. The illustration of the holotype by Poulsen (1927, pl. 18, fig. 5) was re-touched to manifest the outline of thoracic segments. The seventh (from the anterior) segment appears to have a long pleural spine on its right side. However, the presence of the spine is not obvious in the left side. If present, the same configuration of the pleural spine development is found in *Flectihystricurus flectimembrus* (see Ross, 1951, pl. 11, fig. 33).

Cranidial morphology of this species is greatly similar to that of *Hystricurus* (*Triangulocaudatus*) *paragenalatus*, in having, amongst others, a divergent anterior facial suture and moderately convex anterior border.

Subgenus HYSTRICURUS (BUTUBERCULATUS) n. subgen.

Etymology. "Butuberculatus" depicts the presence of relatively large tubercles along the distal edge of inner pleural field of the pygidium.

Diagnosis. Pygidium with relatively prominent tubercle(s) along distal edge of inner pleural field and posterior pleural band(s). Relatively smaller tubercles on pleural bands on inner pleural field. Glabella elongated and moderate-sized.

Included Species. *H.* (*B.*) *hillyardensis* Stitt, 1983, *H.* (*B.*) *globosus* Stitt, 1983, *H.* (*B.*) *scrofulosus* Fortey and Peel (1989).

Remarks. Pygidia of these species differ from those of *Hystricurus* (*Hystricurus*) in lacking the fusion of bands of adjacent pleurae, and from those of *Hystricurus* (*Triangulocaudatus*) in developing prominent tubercle(s) along the distal edge of the inner pleural field, and a more transversely elongated outline. *H.* (*B.*) *globosus* develops tubercles on all the pleurae, whereas *H.* (*B.*) *hillyardensis* and *H.* (*B.*) *scrofulosus* develop them only on the most anterior pleura.

These pygidia appear to be gradational into those of ptychopariid-like questionable *Hystricurus* species such as *H.? millardensis* and *H.? armatus*. The latter lack the tubercles altogether, but display an indistinguishable slope change between inner and outer pleural fields.

Hystricurus (*Butuberculatus*) *globosus* Stitt, 1983
1983 *Hystricurus globosus* Stitt, [part], p. 23-24, pl. 5, figs. 1, 5, 6, [only].
? 1983 *Hystricurus globosus* Stitt, [part], p. 23-24, pl. 5, fig. 3, [only].

223

Holotype. OU 10107, cranidium; Stitt, 1983, pl. 5, fig. 1; *Bellefontia-Xenostegium* Zone; McKenzie Hill Limestone, Oklahoma.

Diagnosis. Glabella ovoid and convex. Palpebral lobe small, slender, and very weakly arched laterally, and located at mid-cranidial length. Palpebral furrow well impressed. Anterior border and border furrow gently convex forwards; border furrow narrowly impressed. Two pairs of glabellar furrows short and impressed along lateral side of glabella; anterior pair directed anteriorly and posterior pair posteriorly. Anterior facial suture slightly divergent. Posterior facial suture diagonal.

Pygidium with steeply down-sloping smooth outer pleural field. Smaller tubercles on pleural bands and axial rings. Interpleural furrows distinctly impressed, but shallower than pleural furrows, and reach border. Border narrow.

Remarks. Stitt (1983) associated two free cheeks with this species. One of them (pl. 5, fig. 3) develops terrace lines and fine tubercles on its lateral border, whereas the other (pl. 5, fig. 4) develops only fine tubercles. This difference is considered interspecific. *Hystricurus* (*Butuberculatus*) *hillyardensis*, which develops only fine tubercles on lateral librigenal and anterior cranidial border (see Stitt, 1983, pl. 4, figs. 4, 5), occurs in a slightly lower horizon. The free cheek with only fine tubercles, associated with this species, is transferred to *H.* (*T.*) *hillyardensis*. The other, with tubercles and terrace lines, is questionably associated with this species, because the anterior border of the holotype cranidium is not well preserved so that its ornamentation pattern is not observed.

Two pygidia (Stitt, pl. 5, figs. 5, 6) are associated with this species. They differ from those of *Hystricurus* (*Hystricurus*) *crotalifrons* and *Hystricurus* (*Hystricurus*) *oculilunatus* in having interpleural furrows reaching the border and in lacking fusion of bands of adjacent pleurae. With respect to these features, they are similar to *Hystricurus* (*Butuberculatus*) *hillyardensis* and *Hystricurus* (*Butuberculatus*) *scrofulosus*. In particular, the steeply down-sloping outer pleural field of this species is very similar to that of *Hystricurus* (*Butuberculatus*) *scrofulosus*.

Hystricurus (*Butuberculatus*) *hillyardensis* Stitt, 1983

1951 *Hystricurus* sp. D Ross, p. 54, pl. 9, figs. 35, 36, 38-41.
? 1951 *Hystricurus*? sp. H, [part], Ross, p. 56, pl. 14, figs. 9, 10, 13, [only].
? 1967 *Hystricurus* cf. *H.* sp. D, Winston and Nicholls, p. 76, pl. 12, figs. 12, 22, 25.
1983 *Hystricurus globosus* Stitt, [part], p. 23-24, pl. 5, fig. 4, [only].
1983 *Hystricurus hillyardensis* Stitt, p. 24-25, pl. 4, figs. 3-6.

Holotype. OU 10100A, cranidium; Stitt, 1983, pl. 4, fig. 3; *Symphysurina* Zone; McKenzie Hill Limeston, Oklahoma.

Diagnosis. Presence of eye ridge identifiable by shallow furrow anteriorly defining the ridge. Anterior facial suture divergent.

Pygidium with four axial rings, and short and rounded terminal piece; posteriormost axial ring and terminal piece separated by ring furrow that shallows sagittally. Postaxial region very narrow and apparently separated from border furrow. Tubercles of two different sizes present on pleural bands and axial rings. Axis wide (tr.). Pleural fields gently convex, without distinct separation between inner and outer pleural fields. Pleural furrows much deeper than interpleural furrows and reach border furrow.

Free cheeks with short genal spine. Posterior facial suture directed outwards, resulting in extremely short (tr.) posterior librigenal border furrow. Cranidial and librigenal

224

surface, including cephalic border, covered with densely-distributed, fine tubercles.

Remarks. Two cranidia of *Hystricurus*? sp. H (Ross, 1951, pl. 14, figs. 9-11, 13-15) show similar overall cranidial architecture to this species. Since they are smaller, they could represent earlier ontogenetic stages of other *Hystricurus* species.

Three cranidia from Texas are referred to *Hystricurus* cf. *H.* sp. D (Winston and Nicholls, 1967, pl. 12, figs. 12, 22, 25). Their poor preservation prevents detailed taxonomic assessment. However, the two of them (figs. 22, 25) appear to have a parallel-sided or slightly convergent anterior facial sutures, a narrower frontal area, and a more strongly tapering glabella.

Pygidium of this species (Stitt, 1983, pl. 4, fig. 6) is similar to those of such *Hystricurus* species as *H.* (*Aequituberculatus*) *ellipticus* (see Westrop *et* al., pl. 3, fig. 8), *H.*? *paramillardensis* (see Taylor and Halley, 1974, pl. 3, fig. 10), and *H.* (*Butuberculatus*) *scrofulosus* (Pl. III-3, Figs. 1, 2, 4). With the last species, it shares with the development of small tubercles on posterior bands along the distal edge of the pleural field; the first two species lack it. The pygidium (along with that of *H.* (*A.*) *ellipticus*, *H.*? *paramillardensis*, and *H.* (*B.*) *scrofulosus*) differs from pygidia of *Hystricurus*? *armatus* and *Hystricurus*? *longicephalus* in developing fine tubercles in both pleural bands. Unlike pygidia of *Hystricurus* (*Hystricurus*), the fusion of bands of adjacent pleurae is not complete in these species.

Hystricurus (*Butuberculatus*) *scrofulosus* Fortey and Peel, 1989
Pl. III-3, Figs. 1-8

1927 *Hystricurus ravni*   Poulsen; Poulsen [part], p. 283-284, pl. 18, fig. 8, [only].
? 1948 *Hystricurus* aff. *H. missouriensis*, [part], Cloud and Barnes, pl. 38, fig. 20, [only].
1989 *Hystricurus* (*Hystricurus*) *scrofulosus* Fortey and Peel, p. 10-12, fig. 6A-6M.

Holotype. MGUH 18.993, pygidium; Fortey and Peel, 1989, figs. 6F-6I (re-illustrated in Pl. III-3, Figs. 1, 2, 4); possibly *Tesselacauda* Zone; Christian Elv Formation, North Greenland.

Diagnosis. Cranidium highly convex. Glabella with rounded anterior margin and straight lateral margin. Two pairs of glabellar furrows weakly developed; S1 located opposite posterior end of palpebral lobe and S2 opposite anterior end of palpebral lobe. Preglabellar field relatively short. Anterior cranidial border weakly arched dorsally. Anterior cranidial border furrow deeply impressed. Posterior fixigena with rounded distal end.

Pygidium with subelliptical terminal piece with weakly-developed paired knobs. Outer pleural field steeply down-sloping and covered with fine tubercles; inner pleural field flat; two fields separated by slope change.

Remarks. Fortey and Peel (1989) listed the development of bimodal-sized tubercles as the most diagnostic feature of this species. However, such a development is seen in many other *Hystricurus* species.

A cranidium of *Hystricurus* (*Triangulocaudatus*) *ravni* (Poulsen, 1927, pl. 18, fig. 6) bears a similar course of facial suture and proportion of conical glabella. Such differences as the sagittal width of the preglabellar field and the anterior cranidial border are readily attributable to intraspecific or ontogenetic variation. This cranidium is 5.5 mm in sagittal length and the paratype cranidium of this species (Pl. III-3, Figs. 5-7) is 9 mm in length.

The free cheek described by Poulsen (1927, pl. 18, fig. 8) together with this cranidium shows a larger palpebral lobe that is in accord with this cranidium than it is with the cranidium of *H. (T.) ravni* (Pl. III-21, fig. 8).

Cloud and Barnes (1948) illustrated one cranidium and pygidium, and noted their affinity with *Hystricurus? missouriensis*. The poorly-preserved cranidium (pl. 38, fig. 20) has a longer and more rapidly forward-tapering glabella with a straight lateral margin, and a relatively narrower anterior border and preglabellar field. These discernible features of the cranidium are most comparable to this species. Since the nature of the anterior facial suture and the posterior fixigena cannot be accurately determined, the cranidium is tentatively assigned to this species.

Pygidial morphologies of this species differ from those of *Hystricurus (Hystricurus)* in that bands of adjacent pleurae are not fused together, and a postaxial ridge is not distintively developed. The pygidia are more similar to those of other species of *Hystricurus (Butuberculatus)*, sharing a steeply down-sloping outer pleural field with the former subgenus, and development of prominent tubercles on posterior pleural bands along the distal edge of the inner pleural field with both subgenera, but they are easily discriminated by the development of fine tubercles on outer pleural field. Cranidially, this species differs from *Hystricurus (Butuberculatus) globosus* and *Hystricurus (Butuberculatus) hillyardensis*, in having a straight occipital furrow and relatively truncated glabellar front.

Pygidia of *Hystricurus? armatus*, *Hystricurus? longicephalus*, *Hystricurus? paramillardensis*, and *Hystricurus ellipticus* differ from those of *Hystricurus (Butuberculatus)* species in lacking small tubercles on the posterior pleural bands along the distal edge of the inner pleural field. The development of fine tubercles on the pleural bands and a relatively steeply down-sloping outer pleural field are observed in *H. ellipticus*. Cranidial morphologies of these species can be considered to be tranformed from those of *H.? armatus* and *H.? longicephalus* to those of *H.? paramillardensis* to those of *H. ellipticus*, and finally to those of *Hystricurus (Butuberculatus) globosus* and *Hystricurus (Butuberculatus) hillyardensis*, which would constitute an evolutionary grade. The assignment of such species as *H. (B.) scrofulosus*, *H. (B.) globosus*, *H. (B.) hillyardensis*, and *H. (A.) ellipticus* to *Hystricurus* is confirmed by their pygidial features (presence of small tubercles on the posterior pleural bands along the distal edge of the inner pleural field and/or relatively steeply down-sloping outer pleural field) which appear to have been derived from those of *H.? armatus*, *H.? longicephalus*, and *H.? paramillardensis*.

Hystricurus (Butuberculatus) andrewsi (Lochman, 1965)

1957 *Hystricurus* sp. Ross, [part], p. 488, pl. 43, fig. 21 [only].
1965 *Glabretina andrewsi* Lochman [part], p. 476-477, pl. 62, figs. 1-8, 10-18 [only. not fig. 9].
? 1966 cf. *Glabretina* sp. Lochman, p. 545, pl. 62, fig. 33.

Holotype. USNM 140746, cranidium; Lochman, 1965, pl. 62, figs. 1, 4; *Leiostegium-Kainella* Zone; Deadwood Formation, Montana.

Diagnosis. Posterior fixigena wide exsagittally. Lateral glabellar margin moderately convex laterally. Anterior border furrow curved backwards sagittally. Preglabellar median furrow present. Pygidium with four axial rings and terminal piece.

226

Remarks. Lochman (1965, p. 475-476) erected a new hystricurid genus, *Glabretina*. She listed several differences from *Hystricurus* including the presence of an eye ridge, a preglabellar median furrow, a slightly anteriorly-situated palpebral lobe, and a less rapidly tapering pygidial axis. However, all these features are found in species of *Hystricurus* described after Lochman (1965) erected *Glabretina*. The genus *Glabretina* is considered a junior objective synonym of *Hystricurus*.

Pygidia of this species have small but prominent tubercles along the distal edge of the inner pleural field. In addition to this feature, other pygidial architecture is greatly similar to *Hystricurus* (*Butuberculatus*) *globosus* (see Stitt, 1983, pl. 5, figs. 5, 6). From the other species of *Hystricurus* (*Butuberculatus*), cranidia of this species differ in having much finer tubercles, and less strongly arched palpebral lobes.

Cranidial morphologies of this species are similar to *Spinohystricurus* species (see Pl. III-19, Figs. 2, 10) in having a posteriorly curved anterior cranidial border furrow, but differ in having a wider (tr.) glabella, finer tubercles on the exoskeletal surface, and less strongly arched palpebral lobes. Lochman (1965) assigned a metaprotaspid or early meraspid specimen to this species (pl. 62, fig. 9). However, it does not have a forward-tapering glabellar front and preglabellar field which are seen in hystricurid metaprotaspides (Lee and Chatterton, 1997a). It seems probable that it belongs to an Ordovician ptychopariid. Lochman (1966) assigned a very poorly-preserved cranidium to cf. *Glabretina* sp. (pl. 62, fig. 33). Based on information currently available, the cranidium cannot be assessed taxonomically.

HYSTRICURUS SPECIES FOR WHICH NO PYGIDIUM IS ASSOCIATED

Three species listed below were erected only on the basis of their cranidia. No pygidium is associated for the species even after the taxonomic revision. Although their cranidial morphologies are comparable to other *Hystricurus* species, the absence of pygidial information makes it impossible to assign them to one of four *Hystricurus* subgenera which are separated by pygidial features.

Hystricurus elevatus Heller, 1954

? 1935 *Hystricurus oneotensis* Powell, p. 75-77, pl. 13, figs. 6-8.

1954 *Hystricurus elevatus* Heller, p. 42-43, pl. 18, figs. 1-3, 10-12.

1954 *Hystricurus* sp. Heller, pl. 18, fig. 9.

? 1969 *Hystricurus* cf. *conicus* Flower, p. 33, pl. 7, fig. 4.

1969 *Hystricurus* sp. Flower, pl. 2, fig. 5.

Holotype. U. MO. 10328, cranidium; Heller, 1954, pl. 18, figs. 1-3; Demingian Stage; Roubidoux Formation, Missouri

Differential Diagnosis. Preglabellar field very short (sag.). Anterior cranidial border narrow and moderately arched dorsally. Preglabellar median furrow discretely impressed. Glabella large. Other cranidial features similar to *Hystricurus* (*Butuberculatus*) *scrofulosus*. No other skeletal parts known.

Remarks. The line drawing of the cranidium of *Hystricurus oneotensis* (Powell, 1935, pl. 13, figs. 6-8) does not accurately exhibit the cranidial features. However, its larger glabella and narrow preglabellar field are reminiscent of this species.

The available information indicates that a co-occurring cranidium from Missouri (Heller, 1954, pl. 18, fig. 9) bears all the diagnostic features, except for its smaller size

227

than the holotype cranidium of this species.

Two poorly preserved cranidia from New York (Flower, 1969, pl. 2, fig. 5, pl. 7, fig. 4) are much larger than the Missouri specimens, but they show a similar glabellar shape and appear to have a preglabellar median furrow.

All cranidial specimens assigned to this species do not preserve posterior fixigenal area. Nonetheless, the glabellar shape and form of the frontal area and anterior border are similar to those of *Hystricurus* (*Butuberculatus*) *scrofulosus*.

Hystricurus rotundus (Ross, 1951)
Pl. III-4, Figs. 8-10

1951 *Pseudohystricurus rotundus* Ross, p. 75, pl. 16, figs. 32, 33, 35-37.

1970 *Pseudohystricurus* sp., Ross, p. 72, pl. 10, figs. 29-31.

Holotype. Y.P.M. 18305, cranidium; Ross, 1951, pl. 16, figs. 32, 33, 37 (re-illustrated in Pl. III-4, Figs. 8-10); *Symphysurina* Zone; Garden City Formation, southern Idaho.

Differential Diagnosis. S1 long and weakly developed. Palpebral lobe relatively long and very weakly arched. Preglabellar field short. Occipital furrow less strongly curved posteriorly. Other cranidial features similar to *Hystricurus* (*Butuberculatus*) *hillyardensis*. No pygidium and free cheeks known.

Remarks. Ross (1951, p. 75) assigned this species to *Pseudohystricurus*. However, this species has a divergent anterior facial suture, an elongated slender palpebral lobe which is located posteriorly, and a narrow (exsag.) and transverse posterior fixigenal area. These features are not shown in *Pseudohystricurus*, which is characterized by having small (exsag.) palpebral lobes defined by a straight palpebral furrow, a convergent anterior facial suture, and a wider (exsag.) posterior fixigenal area (see Ross, 1951, pl. 25, 30, 34). The features of this species are found in such *Hystricurus* species as *H.* (*Butuberculatus*) *hillyardensis* and *H.* (*Butuberculatus*) *globosus* (see Stitt, 1983, pl. 4, fig. 3, pl. 5, fig. 1). In particular, the oval-shaped glabella is shared by all these *Hystricurus* species. A paratype cranidium (Ross, 1951, pl. 16, fig. 35) is greatly similar to one of *H.* (*Butuberculatus*) *hillyardensis* (see Ross, 1951, pl. 9, fig. 41), except for the presence of S1 glabellar furrows and weakly arched palpebral lobe.

A cranidium from Nevada (Ross, 1970, pl. 10, figs. 29-31) is almost indistinguishable from the holotype, only differing in having more coarsely tuberculated surfaces. This difference is considered ontogenetic because the Nevada cranidium is much larger (7 mm) than the holotype (2.3 mm).

SPECIES THAT ARE QUESTIONABLY ASSIGNED TO *HYSTRICURUS*

Species discussed below are questionably referred to *Hystricurus*. Although no pygidium is associated with these species even after the taxonomic revision, their cranidial features strongly suggest that the species must be within the Hystricuridae. *Hystricurus*? *megalops*, *Hystricurus*? *eurycephalus*, and *Hystricurus*? *granosus* would be hystricurids with a large palpebral lobe and a straight palpebral furrow. *Hystricurus*? *penchiensis* and *Hystricurus*? *amadeusus* appear to be closely related to *Tanybregma*, a definite hystricurid genus. *Hystricurus*? *missouriensis* apparently belongs to *Hystricurus* (*Hystricurus*).

228

Hystricurus? *megalops* Kobayashi, 1934
Pl. III-37, Figs. 13-15

1934 *Hystricurus megalops* Kobayashi, p. 541, pl. 6, figs. 8, 9.
? 1960 *Hystricurus megalops*, Kobayashi, p. 235, pl. 13, fig. 20.
1976 *Hystricurus* sp. Leggs, [part], p. 5, pl. 1, fig. 1, [only].
1985b *Hystricurus lewisi*, Jell and Stait, [part], p. 5-8, pl. 2, figs. 5A, 5B, [only].
1993 *Hystricurus* sp. Park, p. 93-94, pl. 4, fig. 11.

Holotype. no specimen number designated, cranidium; Kobayashi (1934), pl. 6, figs. 8-9; *Kayseraspis* Zone; Mungok Formation, South Korea.

Neotype. UTGD 122519, cranidium; Jell and Stait, 1985b, pl. 2, figs. 5A, 5B (Pl. III-37, Figs. 13-15 in this study)

Diagnosis. Palpebral lobe large and semi-circular in outline. Palpebral furrows slightly curved outwards at mid-palpebral point or straight. Glabella with straight lateral margin and rounded anterior margin. Anterior facial suture divergent. Anterior cranidial border furrow shallow and wide. Fine tubercles on cranidial surface. No pygidium or free cheek known.

Remarks. The cranidial specimens from South Korea including the holotype (Kobayashi, 1934, pl. 6, figs. 8, 9) are poorly preserved and/or poorly illustrated. Kobayashi (1960, p. 541) described the palpebral lobe and furrow, "eye large, semi-circular, little posterior to middle of cephalon; eye ridge rather distinct, inside of palpebral lobe well defined from fixed cheek by longitutinal groove." The nearly straight palpebral furrow and semi-circular palpebral lobe are evident in the illustration. The same condition of the palpebral lobe and furrow is found in a cranidium from Tasmania (Jell and Stait, 1985b, pl. 2, figs. 5A, 5B). This Tasmanian cranidium shares the same glabellar shape as the holotype cranidium. A large cranidium from Western Australia (Leggs, 1976, pl. 1, fig. 1) has a rapidly tapering glabella and a semi-circular palpebral lobe. Another poorly preserved cranidium (Kobayashi, 1960, pl. 13, fig. 20) appears to have a lateral glabellar margin that is convex laterally, not straight as in the holotype. A smaller cranidium from South Korea (Park, 1993, pl. 4, fig. 11), although its palpebral lobes are not preserved, displays an indistinguishable glabellar shape and frontal area from the neotype.

The semi-circular inflated palpebral lobe defined by a nearly straight palpebral furrow of this species is reminiscent of *Pseudoetheridgaspis* (see Pl. III-75, Figs. 9, 13) and *Etheridgaspis* (see Pl. III-37, Figs. 1. 3). However, the palpebral lobe of this species is much larger than those of *Pseudoetheridgaspis* and *Etheridgaspis*.

Zhou and Fortey (1986, p. 197) suggested that this species may belong to *Omuliovia* mainly because it has a large palpebral lobe. Unlike *Omuliovia* species (e.g., *O. mira*, Chugaeva, 1973, pl. 6, figs. 1, 3, 5), however, the palpebral lobe is not strongly arched and the palpebral furrow does not follow the outline of palpebral lobe.

Hystricurus? *eurycephalus* Kobayashi, 1934

1934 *Hystricurus eurycephalus* Kobayashi, p. 542, pl. 6, fig. 10 (re-illustrated by Shergold, 1991a, pl. 6, fig. 22).
? 1976 *Hystricurus* sp. Leggs, [part], p. 5, pl. 1, fig. 2, [only].
1996 *Hystricurus* (*Hystricurus*) sp. cf. *H* (*H.*) *lewisi* (Kobayashi, 1940), Laurie and Shergold, p. 88-89, pl. 5, figs. 9-12.

Holotype. PA 827, cranidium; Kobayashi, 1934, pl. 6, fig. 10; *Kayseraspis* Zone;

229

Mungok Formation, South Korea.

Differential Diagnosis. Anterior cranidial margin long (tr.). Glabella less forward-tapering and subrectangular in outline. Anterior facial suture strongly divergent. Frontal area wide (tr.). Other cranidial features similar to *Hystricurus*? *megalops*. Free cheeks with long genal spine. Genal spine based at posterior one-third of exsagittal length of librigenal field; inner margin of free cheek strongly curved forwards.

Remarks. Re-illustration of the holotype by Shergold (1991a, pl. 6, fig. 22) makes it possible to readily differentiate this species from *Hystricurus*? *megalops*. This species has a much wider frontal area, a more strongly divergent anterior facial suture, and a shorter (sag.) and less tapering glabella.

Three smaller cranidia from Western Australia (Laurie and Shergold, 1996, pl. 5, figs. 9-11) have a large inflated palpebral lobe defined by a nearly straight palpebral furrow and a wider (tr.) frontal area which are diagnostic to this species. Leggs (1976) described a cranidium (pl. 1, fig. 2) from the Emanuel Formation. This cranidium, although illustrated at an oblique angle, bears a palpebral lobe and furrow indistinguishable from Laurie and Shergold's cranidial specimens.

Hystricurus? *granosus* Endo, 1935

1932 *Bathyurus* sp. (?) indetermined, Endo, p. 110, pl. 26, fig. 1.
1935 *Hystricurus granosus* Endo [part], p. 218, pl. 13, figs. 10, 11 (re-illustrated in Lu *et al.*, 1965, pl. 34, fig. 8) [only].

Syntype. No. 55559, cranidium; Endo, 1935, pl. 13, figs. 10, 11; *Protopliomerops* Zone; Wuting Formation, Manchoukuo, northeast China.

Differential Diagnosis. Glabella elongated. Anterior margin long. Preglabellar field short. Other available cranidial features similar to *Hystricurus*? *megalops*.

Remarks. Zhou and Fortey (1986, p. 198-199) assigned some cranidia that were assigned to this species by Endo (1935, pl. 13, figs. 10-15; see also Lu *et al.*, 1965, pl. 34, fig. 8) to a bathyurid genus *Omuliovia*; other cranidia (pl. 13, figs. 15-20) were transferred to *Annamitella*, a leiostegiid. They illustrated additional cranidia (Zhou and Fortey, 1986, pl. 11, figs. 1, 3, 4) from northeast China. One of the distinguishing characters of *Omuliovia* is the palpebral lobes that are large, strongly arcuate, and distinctively delineated by palpebral furrows (see *O. mira*, Chugaeva, 1973, pl. 6, figs. 1, 3, 5). The cranidial specimens illustrated by Zhou and Fortey (1986, pl. 11, figs. 1, 3, 4) show such a large palpebral lobe, but lack a distinct palpebral furrow. The cranidia illustrated by Endo (1935) do not have the palpebral lobe preserved. As a result, these specimens cannot be assigned to *Omuliovia*.

Other characteristic features of *Omuliovia* include an elongated glabella with a parallel-sided lateral margin and a pointed anterior margin, and relatively distinct and elongated S1 glabellar furrows, and the absence of a preglabellar field. None of these features are found in the syntype cranidia illustrated by Endo (1935, pl. 13, figs. 10, 11; see also Lu *et al.*, 1965, pl. 34, fig. 8). This indicates that these specimens cannot be assigned to *Omuliovia*.

Other remaining cranidia figured by Endo (1935, figs. 12-15), which are smaller than the syntype, appear to have a preglabellar field, a long glabella, a preglabellar median furrow, and S1 glabellar furrows. These features seem to be intermediate between *Omuliovia* and this species.

230

It is concluded that this species is a valid species, but it cannot be placed in *Hystricurus* with confidence.

Comparison and Taxonomy. The anterior border and glabella of this species are very similar to those of *Hystricurus*? *megalops* (Kobayashi, 1934, pl. 6, figs. 8-10).

<center>

Hystricurus? *missouriensis* Ulrich *in* Bridge, 1930

</center>

1930 *Hystricurus missouriensis* Ulrich *in* Bridge, p. 216, pl. 21, figs. 1, 2.
? 1948 *Hystricurus* sp., Cloud and Barnes, pl. 38, fig. 15.
1951 *Hystricurus contractus* Ross, p. 48, pl. 10, figs. 4, 6, 7, 10.

Holotype. U.S.N.M. No. 83538, cranidium; Ulrich *in* Bridge, 1930, pl. 21, figs. 1, 2; Gasconadian Stage; Gasconade Formation, Missouri.

Differential Diagnosis. Anterior facial suture strongly convergent. Palpebral lobe large. Frontal area narrow (tr.). Posterior fixigena triangular in outline. Glabella elongated and parabolic in outline. Other cranidial features similar to *Hystricurus* (*Hystricurus*) *crotalifrons*.

Remarks. Stitt (1983) re-examined the holotype cranidium (Ulrich *in* Bridge, 1930, pl. 21, figs. 1, 2) and claimed that it appears to have a palpebral lobe which is half of the glabellar length, and it has a posterior fixigena similar to *Hystricurus contractus*. The two cranidia of *H. contractus* described by Ross (1951, pl. 10, figs. 4, 6, 7, 10) from the Garden City Formation display the same condition as Stitt (1983) claimed. In addition, the holotype cranidium and the two cranidia from the Garden City Formation, both have a convergent anterior facial suture. *H. contractus* is synonymized with this species. Since the convergent anterior facial suture is not observed in other *Hystricurus* species, this species is questionably referred to *Hystricurus* although other features are similar to *Hystricurus* (*Hystricurus*) *crotalifrons*.

Cloud and Barnes (1948) illustrated an incomplete cranidium from Texas (pl. 38, fig. 15) which shows the same glabellar outline. Due to the poor preservation of, in particular, the frontal area and anterior fixigena, the cranidium is quesitionably assigned to this species.

<center>

Hystricurus*? aff. *H.*? *missouriensis
Pl. III-21, Figs. 1-7

</center>

1985b *Hystricurus lewisi* (Kobayashi), Jell and Stait, [part], p. 5-8, pl. 2, figs. 6, 7, 10, [only].

Remarks. The cranidium from E-4 (Pl. III-21, Fig. 3) is tentatively assigned to this species because it has a straight palpebral furrow. The cranidium from R11-48.7 (Pl. III-21, Figs. 4-7) differs from the holotype in having a rounded distal end of posterior fixigena. This difference is considered ontogenetic.

Cranidia of this species are similar to those of *H.*? *missouriensis* in the course of the anterior facial sutures and glabellar morphology. However, the curvature of the palpebral lobe of the Great Basin specimens is less strong.

<center>

Hystricurus*? *penchiensis Lu *in* Lu *et al.*, 1976
Pl. III-4, Fig. 6

</center>

1976 *Hystricurus penchiensis* Lu *in* Lu *et al.*, [part], p. 54, pl. 7, figs. 10, 12, [only].
Holotype. 23898, cranidium; Lu *in* Lu *et al.* 1976, pl. 7, fig. 10; *Callograptus*?

<center>

231

</center>

taitzehoensis (graptolite) Zone (late Tremadocian); Upper Yehi Formation, northeast China.

Diagnosis. Palpebral lobe large (one-third of cranidial length) and strongly convex laterally, and located far posteriorly (resulting in very short posterior fixigena). Palpebral furrow distinctly impressed and follows outline of palpebral lobe. Anterior cranidial border narrow and slightly convex forwards. Glabellar forward-tapering with rounded anterior margin and straight-sided lateral margin. Anterior facial suture straight and slightly divergent. Lateral librigenal furrow shallows out towards postero-lateral corner of librigenal field. Genal spine short and with narrow base. No other skeletal parts known.

Association of Free Cheeks. The material illustrated in this study (Pl. III-4, Fig. 6) occurs in the Tremadocian strata of South Korea. The free cheek with the identical morphology is also found together with this Korean cranidium (see Son, 2001, pl. 4, fig. 8). This supports the association of the free cheeks with this species.

Remarks. The nature of the palpebral lobes such as the curvature, thickness, and location is undoubtedly similar to that of *Tanybregma timsheansis* (Pl. III-85, Figs. 11-13). However, this species has a shorter palpebral lobe and glabella. Another difference is that the lateral librigenal border furrow shallows out towards the postero-lateral corner of the librigenal field; in *T. timsheansis*, the lateral and posterior librigenal border furrows both continue into the genal spine, developing a longitudinal median ridge and without merging into a single furrow.

This comparison indicates that this *Hystricurus* species is related to *Tanybregma* as well as to *Hystricurus*. Since the single pygidium associated with this species (Lu *et al.*, 1976, pl. 7, fig. 13) is transferred into *Hystricurus*? *clavus*, information on the pygidium is needed to further assess the taxonomic status of this species.

Hystricurus? *amadeusus* n. sp.

1991a *Hystricurus* sp. cf. *H. eurycephalus*, Shergold, [part], p. 33-34, pl. 6, figs. 10-15, 18, [only].

Etymology. "amadeusus" depicts that this species occurs in Amadeus Basin, Australia.

Holotype. CPC 26924, cranidium; Shergold, 1991a, pl. 6, fig. 11; Warendian Stage; Assemblage 2 of Pacoota Sandstone, Amadeus Basin.

Differential Diagnosis. Palpebral lobe small, strongly arched laterally, and located slightly posterior to mid-cranidial length. Glabella short with relatively truncated anterior margin and moderately convex lateral margin. Anterior cranidial border furrow deeply and narrowly impressed. Anterior cranidial margin slightly pointed sagittally. Other cranidial features similar to *Hystricurus*? *penchiensis*.

Remarks. Shergold (1991a) noted affinity of this new species to *Hystricurus*? *eurycephalus*. However, cranidia of this species are different from the holotype of *H.*? *eurycephalus* (Shergold, 1991a, pl. 6, fig. 22) in having a narrower (tr.) frontal area, shorter preglabellar field, and less divergent anterior facial suture, and smaller glabella. The palpebral lobe of this species, although smaller, displays the same curvature as that of *Hystricurus*? *penchiensis*. The natures of the posterior fixigenae and anterior borders are similar in both species. The associated free cheeks (Shergold, 1991a, pl. 6, figs. 16, 17) are transferred into *Paramblycranium populum* (see Pl. III-62, Figs. 4, 11). The pygidium (pl. 6, fig. 18) is too poorly-preserved to assess its association and help the

232

subgeneric position of this species.

Hystricurus? n. sp. aff. *H. (H.) conicus*
Pl. III-1, Figs. 5-7

Differential Diagnosis. Anterior cranidial border wide (sag. and exsag.). Anterior facial suture parallel-sided and turns inwards rapidly after anterior cranidial border furrow (resulting in transversely elongated trapezoidal anterior border). Glabella weakly forward-tapering and moderately crested. Palpebral lobe small (less than one-fourth of cranidial length). Preglabellar field long. Posterior facial suture diagonal. Other cranidial features similar to Hystricurus (*Hystricurus*) *conicus*. No pygidium or free cheeks known.

Remarks. It is the longer preglabellar field and narrower (tr.) frontal area that mainly differentiate this species from Hystricurus (*Hystricurus*) *conicus*. In addition, this species is characterized by its shorter and less strongly-tapering glabella and parallel-sided anterior facial suture.

Such cranidial architecture as a longer frontal area, the course of the anterior facial suture, and the shape of the glabella are comparable to Middle Cambrian *Derikaspis toluni* from Turkey (Dean, 1982, fig. 53a). Pygidia of *D. toluni* (e.g., Dean, 1982, fig. 48) are similar to those of Hystricurus? *longicephalus* (Pl. III-2, Figs. 7, 8).

Genus CARINAHYSTRICURUS n. gen.

Etymology. "Carina-" denotes carinated anterior cranidial and librigenal border.

Type Species. *Parahystricurus carinatus* Ross, 1951; *Tesselacauda* Zone; Garden City Formation, southern Idaho, USA.

Included Species. *C. carinatus* (Ross, 1951), *C. triangularus* n. sp., *C. minuocularis* n. sp., *C. tasmanacarinatus* n. sp.

Diagnosis. Palpebral lobe small, located at mid-cranidial length, and defined by straight but weakly-impressed palpebral furrow. Anterior cranidial border and lateral librigenal border carinated, tightly folded, and ornamented with terrace lines. Librigenal border wide in vertical thickness and considerably thickens at genal spine base. Posterior librigenal border relatively long (tr.). Anterior cranidial border gently arched dorsally. Eye socle absent. Pygidium subtriangular in outline, with three axial rings and terminal piece; pygidial pleural ridge distinctively developed and interrupted by interpleural furrows; pleural furrows only reach the ridge; inner pleural field depressed; outer pleural field steeply inclined.

Association of Pygidium. A partially articulated specimen, UA 12305 (Pl. III-34, Figs. 1, 2, 4-6) from R5-87.7 consists of an incomplete cranidium, complete pygidium, identifiable free cheek, and nine thoracic segments. Another articulated specimen, UA 12301 (Pl. III-33, Figs. 14-16) from R5-76.4 bears a cranidium, left free cheek, and two thoracic segments. The free cheeks bear a relatively shallow border furrow, a relatively sharply turned distal end of posterior facial suture, and no eye socle. The overall outline of the free cheeks is very similar to those of *Spinohystricurus terescurvus* (see Pl. III-18, Figs. 3, 10, 11) and *Carinahystricurus minuocularis* (see Pl. III-35, Fig. 1). From the free cheek of *S. robustus*, they obviously differ in lacking the eye socle and conspicuous tubercles on the librigenal field. The absence of these features well accords with the free

233

cheek of *C. minuocularis*. The association of the free cheeks with *C. minuocularis* is supported by the course of the facial suture and carinated lateral librigenal border which correspond with those of the cranidium. However, the course of the posterior facial suture of the free cheeks of the two articulated specimens (UA 12305 and UA 12301) is more steeply inclined, the eye is larger, and the lateral border is shallower, than those of *C. minuocularis*. Since these librigenal features correspond with the cranidial features of *Carinahystricurus triangularus*, the articulated specimens, thus the pygidium of one articulated specimen (Pl. III-34, Figs. 1, 2, 4-6), are assigned to *C. triangularus*. The associations of pygidia with other *Carinahystricurus* species are based on co-occurrences with the cranidial materials and degree of cranidial similarities with *C. triangularus*.

Pygidia of *Carinahystricurus* are similar to those of *Plethometopus glaber* (Westrop, 1986, pl. 38, figs. 1-3). Pygidia of *P. glaber* have a depressed inner pleural field and a distinct ridge along the distal edge of inner pleural field, but they differ in having a narrower (tr.) inner pleural field, a flat outer pleural field ornamented with terrace lines, and a wider axis.

Comparison with Other "Hystricurids". The carinated anterior cranidial and lateral librigenal border of *Carinahystricurus* are found in *Spinohystricurus terescurvus* (see Pl. III-18, Figs. 2-4, 8). The pygidium of *Carinahystricurus triangularus* is also very similar to those of the latter taxon (see Pl. III-20, Fig. 1). *S. robustus* is distinguished by its strongly arched palpebral lobe and furrow, and coarsely tuberculated cranidial exoskeleton. The pygidium of *Carinahystricurus minuocularis* is similar to those that are provisionally associated with *Paramblycranium cornutum* (see Pl. III-61, Figs. 18, 19) in having an inwardly depressed outer pleural field. Cranidia of *Carinahystricurus* resembles those of *Paramblycranium populum* (see Pl. III-62, Figs. 5, 8), in particular, smaller cranidia of both taxa (compare Pl. III-35, Fig. 15 with Pl. III-62, Fig. 1) are greatly similar to each other. It is the librigenal features that readily distinguish *Carinahystricurus* from *Paramblycranium* (compare Pl. III-35, Fig. 1 with Pl. III-62, Figs. 4, 9); the former is characterized by a carinated border while the latter by a ventrally developed ridge at the genal spine base.

Ross (1951) assigned *Carinahystricurus carinatus* to *Parahystricurus* which however is easily distinguished by its semi-circular palpebral lobe and straight and diagonal posterior facial suture.

Carinahystricurus carinatus (Ross, 1951)
Pl. III-33, Fig. 19
1951 *Parahystricurus carinatus* Ross, p. 60-61, pl. 13, 23-26, 27, 30-32, 35-37.
1951 *Pachycranium* ? sp. Ross, [part], p. 73, pl. 17, figs. 6, 14 [only].
1973 *Parahystricurus carinatus*, Terrell, p. 80, pl. 4, figs. 11, 14.
1973 unassigned pygidium, Terrell, pl. 5, figs. 12, 13.
1973 unassigned pygidium, Terrell, pl. 6, fig. 5.
Holotype. Y.P.M. 18011, cranidium; Ross, 1951, pl. 13, figs. 26, 27, 32.
Diagnosis. Palpebral furrows deeply impressed and straight. Posterior librigenal border furrow deeply impressed and continues into genal spine. Cranidial exoskeleton coarsely tuberculated. Posterior fixigena short (tr.). Posterior facial suture relatively steeply inclined. Axial furrows deeply impressed.
Remarks. It is one of the diagnostic features of this species that the posterior librigenal

234

border furrow continues into the genal spine. The free cheek from Idaho (Ross, 1951, pl. 13, fig. 37) has matrix covering the base of the genal spine, whereas the specimen from Utah (Terrell, 1973, pl. 4, figs. 11, 14) clearly demonstrates this feature. A small free cheek assigned to *Pachycranium*? sp. shows the same configuration of librigenal border furrows.

Two pygidia illustrated by Terrell (1973, pl. 5, figs. 12, 13, pl. 6, fig. 5) show a continuous fulcral ridge and a narrow inner pleural field, which are very similar to the pygidia of *Carinahystricurus triangularus*. The dorsally arched marginal border, which differentiates it from other species, leads to assign it to this species.

Carinahystricurus triangularus n. gen. n. sp.
Pl. III-33, Figs. 1-18, Pl. III-34, Figs. 1-9

Holotype. UA 12292, partially articulated specimen; Pl. III-33, Figs. 1-3; *Tesselacauda* Zone; Garden City Formation, southern Idaho.

Etymology. "triangularus" describes the subtriangular shaped glabella.

Diagnosis. Anterior cranidial border slightly incurved sagittally. Pygidium elongated triangular in outline, with slender fulcral ridge which continues into at least sixth thoracic segment from posterior. Axial furrows shallow out at glabellar base. At least nine thoracic segments present, without axial spine. Posterior fixigena relatively long (tr.) and posterior facial suture moderately steeply inclined.

Remarks. Two thoracopygidial specimens (Pl. III-33, Figs. 17, 18) are assigned to this species because of its subtriangular pygidial outline. Although their strongly developed pleural ridge on the pygidium suggests a possible association with *Spinohystricurus terescurvus*, the feature could be represent that of the earlier ontogenetic stages of *Carinahystricurus*.

Carinahystricurus minuocularis n. gen. n. sp.
Pl. III-35, Figs. 1-22

Holotype. UA 12309, cranidium; Pl. III-35, Fig. 2; *Tesselacauda* Zone; Fillmore Formation, Utah.

Etymology. "minuocularis" denotes that this species has the smallest eye and palpebral lobe among *Carinahystricurus* species

Diagnosis. Palpebral lobe very small. Librigenal doublure considerably widens inwards and backwards, and moderately depressed at postero-lateral corner of librigenal field; the ventral doublural depression continues into genal spine for a short distance. Posterior fixigena wide (tr. and exsag.). Outer pygidial pleural field moderately depressed inwards. Pygidial pleural ridge very strongly raised.

Remarks. The pygidia are associated with this species because they are similar to those of *Carinahystricurus triangularus* and co-occur with the cranidial materials in a sampling horizon, SE-152.

Carinahystricurus tasmanacarinatus n. gen. n. sp.
Pl. III-36, Figs. 1-9

1974 *Hystricurus* sp., Corbett and Bank, pl. 1, fig. 21.
1985b *Hystricurus lewisi* (Kobayashi, 1940), Jell and Stait, [part], p. 5-8, pl. 2, figs. 11, 13-15, pl. 3, figs. 9, 10, 13, [only].

235

Holotype. UTGD 81049, cranidium; Jell and Stait, 1985b, pl. 2, fig. 13 (re-illustrated in Pl. III-36, Figs. 1, 2, 4; La3 Zone of Lancefieldian Series; Florentine Valley Formation, Tasmania, Australia.

Etymology. "tasmanacarinatus" is a composite word from Tasmania (its geographic occurrence) and carinatus (its carinated anterior cranidial and lateral librigenal border).

Diagnosis. Palpebral lobe moderately down-sloping. Palpebral furrow slightly arched laterally and shallows towards mid-palpebral point. Posterior fixigena sharply terminated distally. Pygidium with wide (tr.) axis. Genal spine short. Preoccipital furrow straight.

Remarks. The carinated anterior cranidial border and lateral librigenal border of the specimens lead one to assign the specimens to *Carinahystricurus*. These specimens, along with several other specimens, were assigned to *Hystricurus lewisi* (Kobayashi, 1940) by Jell and Stait (1985b). They synonymized *Tasmanaspis* into *Hystricurus* because they thought the specimens of two *Tasmanaspis* species (*T. lewisi* and *T. longus*) originally described by Kobayashi (1940) are flattened. The discovery of silicified materials showing morphology identical to *Tasmanaspis* species in this study (see Pl. III-82, Fig. 1) allows me to resurrect the genus as a valid taxon. Thus, four cranidia (Jell and Stait, 1985b, pl. 2, figs. 1-4) are re-transferred into *T. lewisi*. These cranidial specimens are characterized by a flat and wide anterior border, shallow and narrow border furrow, and slender posterior fixigena.

Another specimen (Jell and Stait, 1985b, pl. 2, fig. 5) is referred to *Hystricurus megalops* which has a larger inlated palpebral lobe and shallower anterior cranidial border. Cranidia and free cheeks (pl. 2, figs. 6, 7, 10) are referred to *Spinohystricurus obscurus* which is characterized by a strongly arched palpebral furrow and convergent anterior facial suture. A cranidium (pl. 2, fig. 8) is assigned to *Hillyardina tubularis* which has a tubular (not carinated) anterior cranidial border. A free cheek (pl. 2, fig. 12) is assigned to *Tanybregma timsheansis* (pl. 2, fig. 12) which is characterized by a large eye and distinct eye socle.

Comparison with Other "Hystricurids". This Australian species differs from three *Carinahystricurus* species from Laurentia in having a larger strongly arched palpebral lobe, a medially shallowing palpebral furrow, a distally sharply-terminated posterior fixigena, a straight preoccipital furrow, and a wider pygidial axis. These features are seen in *Hillyardina tubularis* (Pl. III-48, Fig. 1) from the same sampling locality. *Carinahystricurus tasmanacarinatus* differs from *H. tubularis* in having a carinated cephalic border, a cephalic surface ornamented with finer and denser tubercles, and a wide pygidial axis that tapers less rapidly posteriorly and lacks distinct bilobation on its terminal piece.

Morphologic similarities and dissimilarities of these Tasmanian hystricurid species from Laurentian species are considered to be geographic variation of *Carinahystricurus* and *Hillyardina*, which otherwise are restricted to Laurentia (see also *Hillyardina tubularis*)

Genus GLABELLOSULCATUS n. gen.

Etymology. "Glabellosulcatus" depicts the presence of discretely impressed S1 glabellar furrows.

Type Species. *Glabellosulcatus koreanicus* n. sp; *Protopliomerops* Zone; Mungok Formation, South Korea.

236

Diagnosis. Glabella subtriangular in outline. S1 glabellar furrow deeply incised. Anterior facial suture convergent. Anterior cranidial border furrow curved backwards sagittally.
Included Species. *G. sanduensis* (Zhou, 1981), *G. smithiae* (Boyce, 1989), *G.?*
crassilimbatus (Poulsen, 1937).
Comparison with "Hystricurids". The condition of the frontal area of *Glabellosulcatus* such as the convergent anterior facial suture and the backwardly-curved anterior border furrow is very similar to that of *Spinohystricurus* (see Pl. III-18, Fig. 6). The latter taxon is distinguished by a much less steep posterior facial suture and a larger palpebral lobe with deeper and laterally convex palpebral furrow. Most *Parahystricurus* species have the triangular posterior fixigena and convergent anterior facial suture, like *Glabellosulcatus*. However, *Parahystricurus* is easily differentiated by its semicircular palpebal lobe. From *Pseudohystricurus*, this genus differs in having a subtriangular glabella and deeply impressed glabellar furrows.

The pygidium of a complete specimen of *Glabellosulcatus koreanicus* (Pl. III-79, Figs. 5-9) is not completely preserved; in particular, the lateral sides are not complete. Nonetheless, the pygidium resembles those of *Hillyardina* (see Pl. III-47, Figs. 14-25). They share a semi-elliptical outline, a wide axis, and a narrow inner pleural field. Judging from the posterior thoracic segments, it appears to have a steeply down-sloping outer pleural field as seen in *Hillyardina*.
Comparison with Ptychopariides. *Onchonotellus privus* from Siberia (Rozova, 1968, pl. 1, figs. 5-9) is similar to *Glabellosulcatus sanduensis* from Australia in having a forward-tapering glabella and a relatively larger palpebral lobe.
Taxonomic Conclusion. The pygidial similarities with *Hillyardina* and cranidial similarities with such hystricurids as *Spinohystricurus* indicate that *Glabellosulcatus* belongs to the Hystricuridae.

Glabellosulcatus koreanicus n. gen. n. sp.
Pl. III-79, Figs. 5-9
Etymology. "koreanicus" depicts its occurrence in South Korea.
Holotype. SNUP 573, articulated specimen; Pl. III-79, Figs. 5-9; *Protopliomerops* Zone; Mungok Formation, South Korea.
Diagnosis. S1 glabellar furrow bifurcated in its end; S2 indistinct. Posterior fixigena transversely elongated, narrow (exsag.), and sharply terminated distally. Posterior and lateral librigenal border furrow separated by swelling developed at postero-lateral corner of ocular platform. Nine thoracic segments, pleural band of each ornamented with a row of fine tubercles. Pygidium with wide axis, two convex axial rings and posteriorly protruded terminal piece. Hypostome small and with triangular median body.
Comparison. The pygidium, although incompletely preserved, is similar to those of *Hillyardina semicylindrica* (Pl. III-47, Figs. 14-21) in many aspects. They share a wide axis with two axial rings and a strongly bilobed terminal piece. A pair of spines comparable to the bilobed terminal piece is observed in some *Pseudohystricurus* species (see Pl. III-77, Figs. 8-11) and *Dimeropygiella* species (see Pl. III-51, Figs. 4, 5, 9).

Glabellosulcatus sanduensis (Zhou, 1981)
Pl. III-79, Figs. 1-4
1981 *Pharostomina sanduensis* Zhou, pl. 1, figs. 10, 11.

237

? 1984 *Pharostomina* cf. *sanduensis* Zhou, Peng, p. 387-388, pl. 9, figs. 9a, b.

1985 *Parahystricurus* sp. cf. *P. fraudator* Ross, Jell, p. 60, pl. 20, figs. 1-3B (re-illustrated in Pl. III-79, Figs. 1-4).

? 1990b *Pharostomina panjiazuiensis* Peng, p. 117-118, pl. 22, figs. 9a, 9b.

Holotype. SD 173, cranidium; Zhou, 1981, pl. 1, fig. 10; early Tremadocian; Guotang Formation, southeast China.

Diagnosis. S1 glabellar furrow long, slit-like, and obliquely directed posteriorly. S2 and S3 short, shallow and directed transversely. Glabella strongly forward-tapering. Posterior fixigena triangular and wide (exsag.). No other skeletal parts are known.

Remarks. Cranidia from South China which were assigned to *Pharostomina* of the Calymenidae (Zhou, 1981, pl. 1, figs. 10, 11; Peng, 1984, pl. 9, figs. 9a, b; Peng, 1990b, pl. 22, figs. 9a, b) exhibit a subtriangular glabella (much larger and more strongly forward-tapering than typical *Pharostomina*) with deep S1 glabellar furrows, a strongly convergent anterior facial suture, a transversely narrower frontal area and a triangular posterior fixigena. *Pharostomina*, as a calymenid typically has deep S1 and S2 glabellar furrows, a very short (or absent) preglabellar field, and a posterior cranidial border that rims the postero-lateral part of the posterior fixigena (see Sduzy, 1955, pl. 6, figs. 62-64). *Pharostomina* from Argentina (Harrington and Leanza, 1957, figs. 123.1-6) is also readily differentiated from these Chinese cranidia with respect to the same morphologic features. All these *Pharostomina* features are not observed in these Chinese specimens. The cranidial features are much more similar to *Glabellosulcatus koreanicus*. The Chinese cranidia are transferred into *Glabellosulcatus*.

Two cranidia described by Peng (1984, 1990b) only differ in having a short spine on the occipital ring. They are questionably assigned to this species. Cranidia from Australia figured by Jell (1985) are indistinguishable from the holotype cranidium from China. Jell (1985) referred these cranidia to *Parahystricurus*. However, they differ from *Parahystricurus* (see Pl. III-63, Figs. 2, 12) in having a larger and rapidly forward-tapering glabella, a transversly narrower frontal area, and a less strongly laterally arched palpebral lobe.

Glabellosulcatus smithiae (Boyce, 1989)

1983 *Parahystricurus* sp. nov., Boyce *in* Stouge and Boyce, pl. 13, figs. 5, 6.

1989 *Parahystricurus smithiae* Boyce, [part], p. 41-43, pl. 14, figs. 1-8, pl. 15, figs. 1-8, pl. 16, figs. 1-6, [only].

Holotype. NFM F-88, cranidium; Boyce, 1989, pl. 14, figs. 1-4; *Randaynia saundersi* Zone of Canadian Series; Boat Harbour Formation, western Newfoundland.

Diagnosis. S1 and S2 glabellar furrows distinctly impressed. Glabella subtriangular with laterally convex lateral margin. Anterior cranidial margin moderately forward convex. Anterior cranidial border furrow distinctively sagittally curved posteriorly. Posterior fixigena transversely long and sharply terminated distally. Posterior and lateral librigenal border furrow separated by swelling developed at postero-lateral corner of librigenal field.

Remarks. No palpebral lobe of all the cranidial specimens illustrated by Boyce (1989, pl. 14, figs. 1-8, pl. 15, figs. 1-4) is preserved, which is the diagnostic feature of *Parahystricurus*. The cranidia have a glabella that is large, short sagittally, and triangular in outline. This cannot be accommodated within the concept of *Parahystricurus* which

238

usually has an elongated glabella with parallel-sided lateral margins. The glabellar condition is similar to such *Glabellosulcatus* species as *G. sanduensis* and *G. koreanicus*. The presence of the slit-like, long glabellar furrows is not known to *Parahystricurus*, whereas these two *Glabellosulcatus* species and the Newfoundland cranidia have the glabellar furrows. The free cheeks associated with the Newfoundland cranidia (Boyce, 1989, pl. 15, figs. 5-8, pl. 16, figs. 1-6) have the posterior and lateral border furrows that do not meet each other at the postero-lateral corner of the librigenal field and lack a longitudinal median furrow on the genal spine which, in *Parahystricurus*, is extended from the posterior librigenal border furrow. This librigenal condition is seen in *G. koreanicus*. The associated pygidium (Boyce, 1989, pl. 16, figs. 7-10) is assigned to co-occurring *Parahillyardina minuspustulata*. It has the pygidial fulcral ridge which is however not as strongly raised as inferred in the articulated specimen of *G. koreanicus*.

Glabellosulcatus? *crassilimbatus* (Poulsen, 1937)
Pl. III-78, Figs. 1-17

1937 *Hystricurus crassilimbatus* Poulsen, [part], p. 47-48, pl. 5, figs. 6-8, [only, not fig. 5].
1946 *Hystricurus crassilimbatus*, Poulsen, p. 327, pl. 22, fig. 18.
1951 *Pseudohystricurus* sp., Ross, p. 75, pl. 16, figs. 26, 27, 31.
? 1957 *Hystricurus* sp., Ross, [part], p. 488, pl. 43, figs. 25, 26.
1966 cf. *Parahystricurus*, Lochman, p. 533, pl. 65, fig. 34.
? 1966 *Hystricurus crassilimbatus*, Lochman, p. 533, pl. 65, fig. 41.
1973 *Pseudohystricurus* sp., Terrell, p. 89, pl. 2, figs. 2, 4.

Holotype. MGUH 3685, cranidium; Poulsen, 1937, pl. 5, fig. 7 (re-illustrated in Pl. III-78, Figs. 12-14); possibly *Protopliomerella contracta* Zone; Cape Weber Formation, East Greenland.

Diagnosis. Glabella elongated. Anterior cranidial border upturned dorsally. Glabellar furrows not discretely impressed. Anterior cranidial border furrow strongly incurved sagittally.

Remarks. The absence of any glabellar furrows prevents me from confidently assigning this species to *Glabellosulcatus*, even though its cranidial architecture is fairly similar to that of other *Glabellosulcatus* species such as *G. sanduensis* and *G. koreanicus*.

Two cranidia from the Cape Weber Formation of East Greenland assigned to *Hystricurus crassilimbatus* (Poulsen, 1937, pl. 5, figs. 6, 7) exhibit a convergent anterior facial suture (a transversely narrow frontal area, accordingly), an anterior border furrow that sagittaly curves backwards, and an elongated glabella. These features better agree with *Pseudohystricurus* than with *Hystricurus*, as speculated by Ross (1951, p. 74). The poorly-preserved thoracopygidial specimen (Poulsen, 1937, pl. 5, fig. 5) appears to have an elongated pygidium without any distinct separation of inner and outer pleural fields. Since the pygidium of *Glabellosulcatus koreanicus* apparently exhibits that distinction (see Pl. III-79, Figs. 7-9), the thoracopygidial specimen must belong to a taxon other than *Glabellosulcatus*.

Ross (1951) illustrated a cranidium (pl. 16, figs. 26, 27, 31) and did not formally name the species. Many specimens collected from the *Tesselacauda* Zone of the Garden City Formation in this study appear to be a morphologic intermediate between the cranidia from Greenland and the cranidium figured by Ross (1951). The illustration of the

239

cranidium in plan view (Ross, 1951, pl. 16, fig. 31) seems to be tilted forwards, so that it looks as if the cranidium has a very strongly convergent anterior facial suture and a very narrow (or almost absent) preglabellar field (compare with Pl. III-78, Fig. 3). The anterior view illustration (pl. 16, fig. 26) is indistinguishable from that of the cranidia from this study (see Pl. III-78, Fig. 5).

A cranidium from Williston Basin (Lochman, 1966, pl. 65, fig. 34), although fragmentary, has a convergent anterior facial suture and a preglabellar median furrow. Its relatively shorter glabella is considered to be ontogenetic, since it is larger than any other materials from Garden City Formation.

Lochman (1966) figured a cranidium (pl. 65, fig. 41) of this species. It is the largest specimen ever described that is referred to this species. The cranidium lacks tubercles and is much less convex than other cranidia. With respect to the overall cranidial architecture, it is reminiscent of some Lower Ordovician *Corbinia* species (e.g., Westrop, 1986, pl. 5, figs. 10, 11, 13). In particular, the cranidium appears to have a parallel-sided anterior facial suture, like the *Corbinia* species. The posterior fixigena which is triangular in *Glabellosulcatus*, but transversely elongated in *Corbinia*, is poorly preserved in this cranidial specimen. The cranidium is questionably assigned to this species.

Two cranidia from the Deadwood Formation (Ross, 1957, pl. 43, figs. 25, 26) have a convergent anterior facial suture and a preglabellar median furrow, which is reminescent of this species. However, they have a glabella with slightly arched lateral margins and a longer palpebral lobe.

<div align="center">Genus HILLYARDINA Ross, 1951</div>

Type Species. *Hillyardina semicylindrica* Ross, 1951; *Rossaspis superciliosa* Zone; Garden City Formation, southern Idaho.

Included Species. *H. tubularis* n. sp.

Diagnosis. Posterior facial suture straight and diagonal; posterior fixigena sharply terminated distally. Axial furrows shallow out at posterior one-third of glabella. Anterior facial suture moderately divergent. Palpebral lobe small, located slightly posterior to mid-cranidial length, and defined by slightly inwardly curved or straight palpebral furrow. Preglabellar median furrow weakly impressed. Doublure of posterior cranidial border distally cut by posterior facial suture at the same angle as posterior cranidial border. Posterior librigenal border continues into genal spine as ridge which is delineated by median furrow on genal spine. Cranidial exoskeleton and librigenal field ornameted by medium-sized tubercules.

Comparison with "Hystricurids". Cranidial similarities of adults strongly suggest that *Hillyardina* is closely related to *Hyperbolochilus* (Boyce, 1989) and *Parahillyardina*. From *Hyperbolochilus*, *Hillyardina* differs in having a tuberculated cephalic exoskeleton, a narrow (sag.) anterior cranidial border and doublure, and a doublure that does not distally protrude beyond the posterior cranidial border. The pygidia associated with *Hillyardina semicylindrica* differ from those of *Parahillyardina* in having fewer axial and pleural segments, a more strongly raised fulcral ridge, and a wider (tr.) axis. The cranidia of *Hillyardina* differ from those of *Parahillyardina* in having a less divergent anterior facial suture, less discretely developed glabellar furrows, a narrower (tr.) glabella, and coarsely tuberculated cranidial and librigenal surfaces.

Comparison with Proetides. The cranidial similarities of *Hyperbolochilus* with some

<div align="center">240</div>

Silurian aulacopleurids are easily extended into *Hillyardina* (see "Comparison with Proetides" under *Hyperbolochilus*). However, the pygidia of *Hillyardina* much differ from those of aulacopleurids in having, amongst others, a strongly-raised fulcral ridge which separates the flat or concave inner pleural field and the steeply down-sloping outer pleural field (for example, compare with Adrain and Chatterton, 1994, figs. 6.25). The aulacopleurid pygidia are much more similar to those of *Hystricurus* species (e.g., *H. (Aequituberculatus) minutuberuclatus*, see Pl. III-7, Figs. 12-21) occurring in the *Symphysurina* Zone.

Taxonomic Conclusion. The tuberculated exoskeletal surface and the presence of the fulcral ridge on the pygidia indicate that *Hillyardina* belongs to the Hystricuridae.

<center>

Hillyardina semicylindrica Ross, 1951

Pl. III-47, Figs. 1-25.

</center>

1951 *Hillyardina semicylindrica* Ross, [part], p. 71-72, pl. 16, figs. 1, 3-7, 9, [only].
1951 unassigned pygidia, Ross, p. 19, figs. 34, 38.
1973 *Hillyardina* sp. A Hintze, Terrell, [part], p. 71-73, pl. 3, fig. 2, [only].

Holotype. Y.P.M. 18035, cranidium; Ross, 1951, pl. 16, figs. 3, 4, 9; *Rossaspis superciliosa* Zone; Garden City Formation, southern Idaho.

Diagnosis. Anterior cranidial border and lateral librigenal border flat and wide. Anterior cranidial border furrow shallow. Lateral and posterior librigenal border furrows meet at postero-lateral corner of librigenal field and continues into genal spine as longitudinal median furrow. Two pairs of glabellar furrows weakly developed as non-pustulose patches or weak adaxial indentations from axial furrows. Pygidium with strongly raised fulcral ridge which is interrupted by three interpleural furrows reaching tubular border.

Association of Pygidium. The pygidial association for this species is based on the cranidial similarities with *Parahillyardina* to which two articulated specimens possessing the pygidium are assigned. The pygidial specimens (Pl. III-47, Figs. 14-25) co-occur in R6E2 and R6-114 (97) with the cranidia of this species.

Remarks. A free cheek assigned to this species by Ross (1951, pl. 16, figs. 2, 8) is re-assigned to *Hyperbolochilus marginauctum* (see "Remarks" under *Hyperbolochilus marginauctum marginauctum*).

Boyce (1989) assigned a pygidium illustrated by Ross (1951, pl. 19, figs. 32, 35) to this species. The pygidium, however, has a much narrow axis and border, a fulcral ridge which is not interrupted by interpleural furrows, and an inwardly depressed outer pleural field. This pygidial morphotype (Pl. III-61, Figs. 18-22, 25, 26) is tentatively assigned to *Paramblycranium cornutum*.

Terrell (1973) identified a cranidium from the Fillmore Formation as *Hillyardina* sp. A. The cranidium shows the same course of anterior and posterior facial sutures and the same size of palpebral lobe as the specimens of *Hillyardina semicylindrica* from the Garden City Formation do. It slightly differs in having a more posteriorly convex occipital furrow and occipital ring. Since it is much larger than the cranidial specimens from the Garden City Formation, the differences are considered to be ontogenetic. Two free cheeks assigned to *Hillyardina* sp. A by Terrell (1973, pl. 3, figs. 1, 4) display too a strongly divergent anterior facial suture which does not match with the course of the anterior facial suture of the cranidium. The course conforms to that of cranidia of *Hyperbolochilus marginauctum marginauctum*.

<center>241</center>

Several smaller cranidia (e.g., Pl. III-47, Fig. 8) are found with the larger cranidia in the same sampling horizons, R6E2 and R6-114(97). Several taxa such as *Hillyardina*, *Pachycranium* (Pl. III-57, Figs. 14-17), *Parahillyardina* (Pl. III-57, Fig. 6, Pl. III-56, Fig. 4), and *Parahystricurus* (Pl. III-63, Figs. 3, 4, 15), all of which co-occur in several sampling horizons of the *Rossaspis superciliosa* Zone, appear to share very similar smaller cranidia. They develop three or four rows of paired tubercles on the glabella ("rachial" series), four or five tubercles alongside the glabella ("outer" series), a row of tubercles (usually two to four) on the anterior border, and tubercles on the distal part of the anterior fixigena and palpebral lobe. This tuberculation pattern is found in protaspides and smaller cranidia of aulacopleurids (e.g., see Adrain and Chatterton, 1994, figs. 1.1-1.3, 7.1-7.4) and *Hystricurus* (e.g., see Lee and Chatterton, 1997a, figs. 5.3, 5.4). This suggests the close evolutionary relationships of these taxa. The assignment of these smaller cranidia to *Hillyardina semicylindrica* is simply based on the co-occurrence data.

<div align="center">

***Hillyardina tubularis* n. sp.**
Pl. III-48, Figs. 1-10
</div>

1985b *Hystricurus lewisi* (Kobayashi, 1940), Jell and Stait, [part], p. 5-8, pl. 2, fig. 8, [only].

1985b *Hystricurus* sp. cf. *H. robustus* Ross, Jell and Stait, [part], p. 8, pl. 3, figs. 8, 11, 12, pl. 4, figs. 1, 3, 4, 6, [only; not pl. 3, fig. 14].

? 1985b *Hystricurus* sp. cf. *H. robustus* Ross, Jell and Stait, [part], p. 8, pl. 4, figs. 2, 5, 7, [only].

Etymology. "tubularis" describes the tubular anterior cranidial border.

Holotype. UTGD 96708, cranidium; Jell and Stait (1985b), pl. 4, fig. 6 (re-illustrated in Pl. III-48, Figs. 1-3); La3 Zone of Lancefieldian Series; Florentine Valley Formation, Tasmania, Australia.

Diagnosis. Anterior cranidial border tubular. Anterior cranidial border furrow deeply impressed and posteriorly curved sagittally. Palpebral furrow shallows towards mid-palpebral point. Preglabellar field narrow. Pygidial fulcral ridge less strongly raised. Pygidium with four axial rings and bilobed terminal piece. 11 thoracic segments present. Row of small tubercles developed on both thoracic pleural bands (larger tubercules on posterior bands and smaller ones on anterior bands), and diminish towards the posterior and disappear in at least the most posterior segment. Palpebral lobe downsloping towards mid-palpebral point.

Remarks. A pygidium assigned to *Hystricurus* sp. cf. *H. robustus* by Jell and Stait (1985b, pl. 3, fig. 14) is longer relative to the width and lacks the distinct fulcral ridge along the distal edge of the inner pleural field. The pygidium is likely to belong to a species close to *Tanybregma timsheansis* (Pl. III-85, Figs. 11, 15).

A cranidium assigned to *Hystricurus lewisi* by Jell and Stait (1985b, pl. 2, fig. 8) bears, amongst others, the tubular anterior border, so that it is assigned to this species (see *Carinahystricurus tasmanacarinatus* for taxonomic assessment of all the specimens assigned to *H. lewisi*).

Free cheeks associated with the cranidia by Jell and Stait (1985b, pl. 4, figs. 2, 5, 7) have terrace lines on their lateral border, whereas the anterior cranidial border is ornamented with fine tubercles. The free cheeks could be associated with a species close to *Tanybregma timsheansis* which has a lateral librigenal border ornamented with the

<div align="center">242</div>

terrace lines (Jell and Stait, 1985b, pl. 1, fig. 6). Their discrete eye socle appears to support this taxonomic assessment. However, the size and pattern of tuberculation on the librigenal field appear to be in agreement with those of cranidial surface of *Hillyardina tubularis*. The free cheeks are questionably retained in this species.

Jell and Stait (1985b) questionably assigned the specimens to *Hystricurus robustus* (=*Spinohystricurus robustus* herein). They differ from *S. robustus* (see Pl. III-19, Figs. 1, 2, 6) in having a tubular anterior border (carinated anterior border in *S. robustus*), a straight palpebral furrow (strongly arched furrow in *S. robustus*), a down-sloping palpebral lobe (inflated palpebral lobe in *S. robustus*), and a sharply terminated posterior fixigena (blunted fixigena in *S. robustus*).

Comparison with Other "Hystricurids". Cranidial morphologies of *Hillyardina tubularis* are similar to those of *Carinahystricurus tasmanacarinatus* (Pl. III-36, Figs. 1, 2, 4; see also Jell and Stait, 1985b, pl. 2, figs. 11, 15). Amongst others, both species have a palpebral lobe which down-slopes towards the mid-palpebral point, and the palpebral furrow which shallows towards the mid-palpebral point. Compared with *Hillyardina semicylindrica* from Laurentia, *H. tubularis* from Australia differs in having a shorter preglabellar field, a tubular anterior cranidial border, a more strongly arched palpebral lobe, a coarser and more sparsely tuberculated cranidial exoskeleton, and a weaker pygidial fulcral ridge. Like comparison of *H. tubularis* and *H. semicylindrica*, *C. tasmanacarinatus* from Australia also differs from *Carinahystricurus* species from Laurentia, in many aspects (see *C. tasmanacarinatus*). It is conceivable that *C. tasmanacarinatus* and *H. tubularis* adapted to the environments of Australia, so that they develop the same features in the palpebral lobe and palpebral furrow.

Configuration of Thoracic Segments. The articulated specimen of *Hillyardina tubularis* (Pl. III-48, Figs. 4, 5, 7) has 11 thoracic segments and a pygidium which has at least three axial rings. The fulcral ridge continues from the pygidium into the third or fourth thoracic segment from the posterior. The anterior segments have a smoothly curved pleura with a rather pointed distal end. This arrangement of thoracic pleurae is similar to that of *Parahillyardina sulcata* (Pl. III-56, Figs. 13, 16, 17) which however has the posterior seven segments with the fulcral ridge, and the fifth anterior segment possessing a long axial spine. The same pattern as *P. sulcata* is observed in *Spinohystricurus robustus* (Pl. III-16, Figs. 4-6) and *Spinohystricurus terescurvus* (Pl. III-16, Figs. 1-3) which, however, have only three or four anterior segments possessing a spinose distal pleural end and the three or four middle segments possessing the long axial spine.

The thoracic pleural bands of the partially articulated specimen of *Hillyardina tubularis* are ornamented with a row of small tubercles which diminish towards the posterior and finally disappear on at least the posterior most thoracic segment and pygidium. This suggests that the presence or absence of tuberculation cannot be used as a criterion for associationg pygidium with cranidium. The same pattern is observed in the articulated specimen of *Glabellosulcatus koreanicus* (Pl. III-79, Fig. 5) and *Spinohystricurus robustus* (Pl. III-16, Figs. 4-6). The articulated thoracopygidium of *Parahillyardina sulcata* (Pl. III-56 , Figs. 13, 16, 17) lacks the tubercles altogether in its pleural bands.

Genus **PACHYCRANIUM** Ross, 1951

Type Species. *Pachycranium faciclunis* Ross, 1951; *Rossaspis superciliosa* Zone;

243

Garden City Formation, southern Idaho.

Included Species. *P. profundus* n. sp.

Diagnosis. Glabella large and convex dorsally. Anterior border and preglabellar field relatively narrow (sag.). Anterior cranidial margin rounded. Posterior fixigenal area triangular and relatively long (exsag.). Palpebral lobe relatively small. Palpebral furrow straight to slightly curved inwards. Anterior facial suture convex laterally. Preglabellar median furrow weakly developed.

Comparison with "Hystricurids". *Pachycranium* is similar to *Hillyardina* in terms of the overall cranidial architecture including a semi-circular palpebral lobe and a laterally convex anterior facial suture. It is readily differentiated by a short preglabellar field and anterior cranidial border, a large glabella, a smooth exoskeletal surface, and a rounded anterior cranidial margin. Apart from *Hillyardina*, the overall cranidial architecture of *Pachycranium* is similar to that of *Parahystricurus oculirotundus* (Ross, 1951, pl. 12, figs. 36, 44, 46). In particular, the smaller cranidia (Pl. III-57, Fig. 2; Ross, 1951, pl. 12, figs. 33, 39) share a greater resemblance, suggesting a close relationship of both genera. *Pachycranium* is discernible by a divergent anterior facial suture, a smaller palpebral lobe, and a smooth exoskeletal surface.

Taxonomic Conclusion. *Pachycranium* is placed in the Hystricuridae, based on similarities with *Hillyardina* and *Parahystricurus*.

Pachycranium faciclunis Ross, 1951
Pl. III-57, Figs. 14-20

1951 *Pachycranium faciclunis* Ross, [part], p. 72-73, pl. 16, figs. 12, 13, 17-21, 23, 24, 29 [only, not figs. 22, 28].

Holotype. Y.P.M. 18038, cranidium; Ross, 1951, pl. 16, figs. 23, 24, 29; *Rossaspis superciliosa* Zone; Garden City Formation, southern Idaho.

Lectotype. Y.P.M. 18039, cranidium; Ross, 1951, pl. 16, figs. 18, 20, 21. the holotype cranidium is broken into pieces so that it cannot be used as the type.

Diagnosis. Anterior cranidial border furrow narrow. Palpebral lobe located anterior to mid-glabellar length.

Remarks. A free cheek associated with this species by Ross (1951, pl. 16, figs. 22, 28) has a larger eye and a less steep posterior facial suture, compared to the cranidia. It is most likely that this species has a free cheek whose lateral and posterior border furrows merge at postero-lateral corner like *Pachycranium profundus* (Boyce, 1989, pl. 5, figs. 1-5). The lateral and posterior librigenal border furrows of the free cheek specimen are not confluent and much shallower. They are similar to free cheeks of *Tasmanaspis* (e.g., see Pl. III-82, Figs. 6, 13).

Pachycranium profundus n. sp.

1989 *Hillyardina minuspustulata* Boyce [part], p. 35, pl. 4, figs. 4-8, pl. 5, figs. 1-5 [only].

Etymology. "profundus" indicates that anterior cranidial and librigenal lateral border furrows are deep and wide.

Holotype. NFM F-128, cranidium; Boyce, 1989, pl. 4, figs. 4-6; *Randaynia saundersi* Zone of Canadian Series; Boat Harbour Formation, western Newfoundland.

Diagnosis. Anterior cranidial and librigenal lateral border furrows deep and wide.

244

Palpebral lobe located at mid-glabellar length.

Remarks. Of cranidia assigned to *Hillyardina minuspustulata* by Boyce (1989), the cranidia of *Pachycranium profundus* are easily differentiated by having a large and less strongly forward-tapering glabella and lacking two pairs of glabellar furrows.

Genus PARAHILLYARDINA n. gen.

Etymology. "Parahillyardina" depicts the similarity to *Hillyardina*.

Type Species. *Parahillyardina sulcata* n. sp.; *Paraplethopeltis* or *Leiostegium-Kainella* Zone; Garden City Formation, southern Idaho and northern Utah.

Included Species. *P. minuspustulata* (Boyce, 1989), *P. newfoundlandia* n. sp.

Diagnosis. S1 glabellar furrows long, discrete, slit-like, and located posterior to palpebral lobe. Palpebral lobe arched laterally and of moderate-size. Palpebral furrow nearly straight or slight convex outwards in mid-palpebral point. Anterior facial suture divergent. Posterior facial suture ventrally cuts doublure well adaxial to dorsal distal end of posterior fixigenal area (in ventral view of free cheek, the doublure adaxially extends beyond dorsal distal end of posterior facial suture.) Preglabellar median furrow weakly impressed. Anterior border broad (sag. and exsag.) and flat. Exoskeletal surface sparsely ornamented with small granules or smooth. Pygidium semi-elliptical in outline, with rapidly tapering narrow axis and strong ridge dividing inner and outer pleural field.

Comparison with "Hystricurids". Undoubtedly, *Parahillyardina* is closely related to *Hillyardina*. Both share a divergent anterior facial suture, weak preglabellar median furrow, glabellar furrows, and a moderately long (sag.) frontal area. *Parahillyardina* is distinguished by long and discrete S1 glabellar furrows, a convex posterior glabella, a larger palpebral lobe, a shorter genal spine, and a moderately tubular lateral librigenal border.

Comparison with Proetides. Boyce (1989) suggested a close evolutionary relationship between *Hillyardina* and the Aulacopleuridae. The cranidia of *Parahillyardina* resemble those of such aulacopleurids as *Songkania* (see Adrain and Chatterton, 1995a, fig. 5). With some variations, all these taxa share a long preglabellar field, a divergent anterior facial suture, a relatively smaller palpebral lobe with straight palpebral furrow, and a narrow posterior fixigenal area. In particular, *Parahillyardina* shows a condition of S1 glabellar furrows which appears to be an intermediate between *Hillyardina* (the S1 is an small indentation from the axial furrows or expressed as non-pustulose patches) and *Songkania* (the S1 is long and meets with the occipital furrow, which is typical of the Aulacopleuridae, see Adrain and Chatterton, 1995a, fig. 5). Apart from the S1 glabellar furrows typical of the Aulacopleuridae, *Songkania* is distinguished from *Parahillyardina* and *Hillyardina* by its strongly convex forward anterior border, deepest anterior border furrow, relatively truncated glabellar front, the possession of one long thoracic axial spine on the fifth thoracic segment from the anterior, and tubular anterior cranidial and librigenal lateral borders, and its pygidium lacking the ridge along distal edge of inner pleural field which is present in *Parahillyardina* and *Hillyardina*.

Taxonomic Conclusion. The cranidial features of *Parahillyardina* lead to place it in the Hystricuridae along with *Hillyardina*. The pygidial features of *Parahillyardina* are very similar to those of several other definite hystricurids such as *Carinahystricurus* and *Spinohystricurus*. In particular, the presence of a fulcral ridge on pygidium lends additional support to its placement in the Hystricuridae.

245

Hypotheses of Evolutionary Relationships. These morphologic similarities are considered sufficient to evolutionarily connect these taxa. No definite records of *Hillyardina* and its allied genera have been documented in the Middle Ordovician afterwards. The earliest definite record of the Aulacopleuridae is from the Llandovery of the Silurian. There are a few aulacopleurid species which were reported from the Ordovician, but their stratigraphic occurrence and taxonomic affinities are ambiguous. Of interest is that there are few known intermediate taxa found between the Early Ordovician hystricurids and Siluro-Devonian aulacopleurids; the questionable status of the age of *Aulacopleura szechuanica* which was reportedly from the Tremadoc of China, is discussed in Adrain and Chatterton (1995a).

<div align="center">

Parahillyardina sulcata n. gen. n. sp.

Pl. III-56, Figs. 1-23

</div>

1951 unassigned thoracopygidium, Ross, pl. 19, fig. 37.
1951 unassigned pygidium, Ross, pl. 19, figs. 33, 36.
1953 undetermined pygidium, Hintze, pl. 8, fig. 13.
1973 unassigned pygidia, Terrell, pl. 6, figs. 4, 7, 8, 10, 11.

Etymology. "sulcata" denotes that this species has very discrete S1 glabellar furrows
Holotype. UA 12453, cranidium; Pl. III-56, Figs. 2, 6, 9, 12; *Paraplethopeltis* or *Leiostegium-Kainella* Zone; Garden City Formation; northeastern Utah.
Diagnosis. S2 and S3 weakly impressed compared to S1 which is deeply impressed;S2 located opposite mid-palpebral point, and S3 opposite anterior end of palpebral lobe. Posterior facial suture runs gently transversely and then rapidly turns backwards at its distal end, forming rounded distal end. Anterior border furrow shallow. Occipital furrow strongly convex posteriorly; posterior glabella convex dorsally and posteriorly. Thorax with at least 10 segments; long axial spine on fifth thoracic segment from posterior.
Association of Pygidium. Ross (1951) illustrated, but did not taxonomically assess, an articulated thoraco-pygidial specimen (pl. 19, fig. 37; see also Pl. III-56, Figs. 13, 16, 17). This specimen bears a long axial spine in its fifth thoracic segment from the posterior, like the specimen of *Parahillyardina newfoundlandia* (see Boyce, 1989, pl. 6, fig. 6). The cranidial similarities of this species with *P. newfoundlandia*, amongst others, the development of slit-like S1 glabellar furrows, support the assignment of the thoracopygidium to this species.

A large pygidium (Pl. III-56, Figs. 20, 21, 23) was recovered from R5-87.7. It has a semi-elliptical outline and a fulcral ridge. Although no cranidial materials of this species were recovered from that horizon, this pygidium is associated with this species since the cranidial materials are secured from R5-76.4 which belongs to the same biozone as R5-87.7. It is possible that this pygidium is associated with *Parahillyardina minuspustulata*. Terrell (1973) illustrated unassigned several pygidia of which some (pl. 6, figs. 4, 7, 8, 10, 11) are indistinguishable from the pygidium from R5-87.7.

<div align="center">

Parahillyardina minuspustulata (Boyce, 1989)

Pl. III-57, Figs. 1-13.

</div>

1989 *Hillyardina minuspustulata* Boyce, [part], p. 35, pl. 4, figs. 1-3, 9, pl. 5, figs. 6-9, [only].
· 1989 *Hillyardina levis* Boyce, [part], p. 35-38, pl. 6, figs. 4, 5, pl. 7, figs. 6-10, [only].

<div align="center">

246

</div>

1989 *Parahystricurus smithiae* Boyce, [part], p. 41-43, pl. 16, figs. 7-10, [only].

Holotype. NFM F-127, cranidium; Boyce, 1989, pl. 4, figs. 1-3; *Randaynia saundersi* Zone of Canadian Series; Boat Harbour Formation, western Newfoundland.

Diagnosis. S1 and S2 slit-like and of equal depth. Anterior cranidial border furrow deep. Posterior facial suture steeply sloping.

Association of Pygidium. The smaller pygidia co-occurring with cranidia of this species from R6-38 exhibit features of those assigned to *Parahillyardina sulcata*. A pygidium associated with *Pseudohystricurus smithiae* (Boyce, 1989, pl. 16, figs. 7-10) is similar to those of this species (see pl. 7, figs. 6-10) in developing a fulcral ridge along the distal edge of the inner pleural field. The pygidia of *Pseudohystricurus* develop short or long spines along the distal edge of the inner pleural field (see Pl. III-77, Figs. 8-11).

Remarks. Three free cheeks were associated with this species by Boyce (1989, pl. 5, figs. 1-5). They have a deep and wide lateral border furrow which is half-pipe like in cross-section. This does not agree with the anterior cranidial border furrow of this species, but with that of co-occurring *Pachycranium profundus*.

<center>

Parahillyardina newfoundlandia n. gen. n. sp.
Pl. III-21, Fig. 9

</center>

1989, *Hillyardina levis* Boyce, [part], p. 35-38, pl. 6, fig. 6, [only].

Etymology. "newfoundlandia" denotes its geographic occurrence.

Holotype. NFM F-131, articulated specimen; Boyce, 1989, pl. 6, fig. 6 (re-illustrated in Pl. III-21, Fig. 9); *Randaynia saundersi* Zone of Canadian Series; Boat Harbour Formation, western Newfoundland.

Diagnosis. Anterior facial suture not strongly divergent. Palpebral lobe small. Palpebral furrow moderately curved inwards. Nine thoracic segments; long axial spine on fifth segment from anterior.

Remarks. A partially articulated specimen from Newfoundland (Boyce, 1989, pl. 6, fig. 6) was assigned to *Hillyardina levis*. This specimen occurs in the Brig Bay area, whereas all the other specimens of *H. levis* occur in Boat Harbour. Compared with two cranidia assigned to *H. levis* by Boyce (1989, pl. 6, figs. 4, 5, which are re-assigned to *Hillyardina minuspustulata* herein), the cranidium of the articulated specimen bears a long, distinct, slit-like S1 glabellar furrow, a posterior glabella convex posteriorly as if the glabellar base overhangs the occipital ring, and a posterior facial suture that is nearly transverse and then rapidly turns posteriorly at the distal end. The cranidial features are more similar to *Parahillyardina* than to *Hillyardina* (see Pl. III-47, Fig. 2). From *Parahillyardina sulcata* from the Garden City Formation, this species differs in having a less divergent anterior facial suture, a smaller palpebral lobe, and nine thoracic segments (at least 10 in *P. sulcata*, see Pl. III-56, Figs. 13, 16, 17).

This articulated specimen allowed Boyce (1989) to associate several pygidia with his two *Hillyardina* species (*H. minuspustulata* and *H. levis*). All the pygidia are assigned to *Parahillyardina minuspustulata* in this study, mainly because their co-occurrence. This association leads me to associate pygidia with *Hillyardina*. The cranidial similarities of *Hillyardina* and *Parahillyardina* suggest that their pygidial morphologies are equally similar to each other. All the pygidia assigned to *Parahillyardina* species are semi-elliptical in outline and bear a fulcral ridge and a pair of knobs on the terminal piece. The pygidia associated with *Hillyardina semicylindrica* (Pl. III-56, Figs. 16-25) bear these

<center>247</center>

features, but differ in having fewer axial rings on a wider axis, and a stronger fulcral ridge.

Genus PARAHYSTRICURUS Ross, 1951

Type Species. *Parahystricurus fraudator* Ross, 1951; *Rossaspis superciliosa* Zone; Garden City Formation, southern Idaho.

Included Species. *P. oculirotundus* Ross, 1951, *P. pustulosus* Ross, 1951, *P. bispicatus* Hintze, 1953

Diagnosis. Palpebral lobe semi-circular in outline, located at mid-cranidial length, and ornamented with small tubercles. Palpebral furrow weakly developed and straight or curved inwards.

Comparison with "Hystricurids". Ross (1951, p. 57) distinguished *Parahystricurus* from *Hystricurus* in having a more inflated glabella, a small palpebral lobe, and a triangular posterior fixgena, and lacking an eye socle. Of these, the palpebral lobe which is semi-circular in outline and delineated by a nearly straight palpebral furrow is the most useful diagnostic feature. Many "hystricurid" genera such as *Pachycranium* (see Pl. III-57, Fig. 14), *Amblycranium* (see Pl. III-28, Fig. 1) and *Pseudoetheridgaspis* (see Pl. III-75, Fig. 1) have a straight palpebral furrow, but their palpebral lobe is not as strongly arched laterally, nor ornamented with small tubercles, as is the case for the palpebral lobe of *Parahystricurus*. The triangular posterior fixigena, and mostly forward-convergent anterior facial suture are reminiscent of *Glabellosulcatus* (see Pl. III-79, Fig. 2). However, *Glabellosulcatus* is easily differentiated by a very short preglabellar field, a weakly arched, relatively slender palpebral lobe, and deeply impressed glabellar furrows. The overall cranidial architecture of *Parahystricurus* is similar to that of *Amblycranium*, but is distinguished by a smaller glabella, and a shorter and narrower frontal area.

The small cranidia of *Parahystricurus* (Pl. III-63, Figs. 15, 16) are greatly similar to those of *Hillyardina* (Pl. III-47, Fig. 8) and *Pachycranium* (Pl. III-57, Figs. 18-20).

Comparison with Proetides. The semi-circular palpebral lobe defined by a straight or slightly incurved palpebral furrow, the most diagnostic feature of *Parahystricurus*, is found in several aulacopleurids (see *Harpidella*, Adrain and Chatterton, 1995b, fig. 6.2; *Cyphaspis*, Adrain and Chatterton, 1996, fig. 5.1). The aulacopleurid palpebral lobe, however, is smaller and more posteriorly located. The aulacopleurid is easily differentiated by its conspicuous S1 glabellar furrows. The glabellar spines (G1-3, Adrain and Chatterton, 1994, fig. 1) of the aulacopleurid are found in the smaller cranidia of *Parahystricurus* (see Pl. III-63, Figs. 15, 16).

The overall cranidial outline of *Parahystricurus* is comparable to that of *Dimeropygiella* (e.g., see Pl. III-51, Figs. 2, 3, 6). *Parahystricurus* is differentiated by having a longer preglabellar field, a wider anterior cranidial border, and most conspicuously, a semi-circular palpebral lobe. Free cheeks of two genera are also similar to each other. In particular, those of *Parahystricurus pustulosus* (see Ross, 1951, pl. 12, figs. 28, 31) are indistinguishable from free cheeks of *Dimeropygiella* (see Pl. III-51, Figs. 10, 11), if their anterior sagittal portion is not preserved; *Dimeropygiella* has a deep depression on the rostral plate that is strongly protruded ventrally.

Comparison with Ptychopariides. The cranidia of *Holmdalia punctata* (a questionable marjumiid, Robison, 1988, figs. 27.1-27.5) are comparable to those of *Parahystricurus oculilunatus* in having a similar relative ratio of the width of the frontal area and posterior

248

fixigena, a forward-convex anterior margin and a triangular posterior fixigena. However, the palpebral lobe of *H. punctata* is not comparable to that of *P. fraudator*. The pygidium of *H. punctata* is not of a typical ptychoparid-type (see also Pratt, 1992, p. 61), since it has a steeply downsloping outer pleural field and a flat inner pleural field, which is much more comparable to the pygidia of many hystricurids. Although no definite pygidium is known to *Parahystricurus*, the pygidium which is questionably associated with *Parahystricurus pustulosus taperus* (Pl. III-63, Figs. 13, 14) is similar to that of *H. puncata*, except for the development of the strong pygidial fulcral ridge.

Taxonomic Conclusion. The similarities of early cranidia with *Hillyardina* and *Pachycranium* indicate that *Parahystricurus* is a member of the Hystricuridae that is characterized by the semi-circular palpebral lobe.

<center>

Parahystricurus fraudator Ross, 1951

</center>

1951 *Parahystricurus fraudator* Ross, p. 58-59, pl. 12, figs. 1-16.
1973 unassigned librigena, Young, pl. 7, fig. 8.
1973 *Parahystricurus* sp., Terrell, pl. 5, fig. 4

Holotype. Y.P.M. 17988, cranidium; Ross, 1951, pl. 12, figs. 11, 15, 16; *Rossaspis superciliosa* Zone; Garden City Formation, southern Idaho.

Diagnosis. Palpebral furrow straight. Genal spine with longitudinal median furrow continuous from posterior librigenal border furrow.

Remarks. The cranidium and free cheek from the Fillmore Formation (Terrell, 1973, pl. 5, fig. 4; Young, 1973, pl. 7, fig. 8) each are not distinguishable from the specimens figured by Ross (1951).

<center>

Parahystricurus oculirotundus Ross, 1951
Pl. III-64, Figs. 1-10

</center>

1951 *Parahystricurus oculirotundus* Ross, p. 59-60, pl. 12, figs. 33-49.
1982 *Pseudohystricurus* sp. aff. *P. rotundus* Ross, Fortey in Fortey *et al.*, [part], p. 113, pl. 3, figs. 12, 15, [only].

Holotype. Y.P.M. 18003, cranidium; Ross, 1951, pl. 12, figs. 44, 48, 49; *Rossaspis superciliosa* Zone; Garden City Formation, southern Idaho.

Diagnosis. Palpebral furrow curved inwards. Genal spine with longitudinal median furrow continuous from posterior librigenal border furrow.

Remarks. A cranidium from western Newfoundland was questionably referred to *Pseudohystricurus rotundus* (=*Hystricurus rotundus* herein) by Fortey *et al.* (1982, pl. 3, figs. 12, 15). Its highly convex glabella was a main attribute for this assessment. *P. rotundus* is characterized by a slender and weakly arched palpebral lobe, and a transversly elongated narrow posterior fixigena. Although incompletely preserved, the palpebral lobe of the Newfoundlandian cranidium appears to be strongly arched laterally and defined by a slightly incurved palpebral furrow (see the left palpebral lobe). This condition of palpebral lobe is diagnostic to *Parahystricurus*, preferrably to *P. oculirotundus*; *Pseudohystricurus* has a crescentic palpebral lobe. *P. oculirotundus* has a glabella that is equally convex as *Hystricurus rotundus* (Pl. III-4, Figs. 8-10).

<center>

Parahystricurus sp. nov. A
Pl. III-64, Figs. 11-15

</center>

<center>

249

</center>

1953 *Parahystricurus* aff. *P. fraudator*, Hintze, p. 195, pl. 8, fig. 1.
Remarks. This cranidium differs from other *Parahystricurus* species in having a pointed anterior cranidial margin, a parallel-sided anterior facial suture, and a sharply terminated distal end of the posterior fixigena.

Parahystricurus pustulosus Ross, 1951
Diagnosis. Frontal area relatively narrow (tr.).

Parahystricurus pustulosus pustulosus Ross, 1951
Pl. III-63, Figs. 1-8
1951 *Parahystricurus pustulosus* Ross, [part], p. 60, pl. 12, figs. 17-32, [only].
1973 *Parahystricurus pustulosus*, Terrell, [part], p. 82, pl. 2, fig. 11 [only].
? 1973 *Parahystricurus pustulosus* (?), Terrell, pl. 4, fig. 10.
Holotype. Y.P.M. 17995, cranidium; Ross, 1951, pl. 14, figs. 23, 24, 26; *Rossaspis superciliosa* Zone; Garden City Formation, southern Idaho.
Diagnosis. Anterior facial suture convergent. Posterior fixigena widest.
Remarks. A free cheek (Terrell, 1973, pl. 4, fig. 10) is questionably associated with this subspecies because its anterior portion is broken. The anterior portion is crucial in separating free cheeks of *Parahystricurus* from those of *Dimeropygiella* which has a deep sagittal depression (see Pl. III-51, Figs. 1, 7).

Parahystricurus pustulosus rectangulofrontalis n. subsp.
Pl. III-63, Figs 9-11
1951 *Parahystricurus pustulosus* Ross, [part], p. 60, pl. 14, figs. 23, 24, 26, [only].
Etymology. "rectangulofrontalis " describes the rectangle-shaped frontal area.
Holotype. UA 12530, cranidium; Pl. III-63, Figs. 9-11; *Rossaspis superciliosa* Zone; Garden City Formation, southern Idaho.
Diagnosis. Anterior facial suture parallel-sided. Posterior cranidial margin strongly wavy in outline. Glabella least forward-tapering.

Parahystricurus pustulosus taperus n. subsp.
Pl. III-63, Figs. 12-16
Etymology. "taperus" depicts its strongly tapering glabella.
Holotype. UA 12531, cranidium; Pl. III-63, Fig. 12; *Hintzeia celsaora* to *Protopliomerella contracta* Zone; Garden City Formation, southern Idaho.
Diagnosis. Glabella very strongly forward-tapering. Anterior facial suture convergent. Posterior cranidial margin distally curves forwards.
Remarks. A pygidium (Pl. III-63, Figs. 13, 14) is questionably associated with this species. It is similar to *Spinohystricurus robustus*, but differs in having a triangular outline and distinctively disconnected fulcral ridge by interpleural and pleural furrows. It may belong to a *Hystricurus* species.

Parahystricurus bispicatus Hintze, 1953
1953 *Parahystricurus bispicatus* Hintze, p. 195-196, pl. 8, figs. 3a-4c.
1973 *Parahystricurus* cf. *bispicatus*, Terrell, p. 80, pl. 5, fig. 5.
Holotype. 26189, cranidium; Hintze, 1953, pl. 18, figs. 4a-4c; *Rossaspis superciliosa*

250

Zone; Fillmore Formation, Utah.

Diagnosis. Pair of long spines on occipital ring.

Genus **PARAMBLYCRANIUM** n. gen.

Etymology. "Paramblycranium" refers to the history that the species assigned to this genus were previously assigned to *Amblycranium*.

Type Species. *Amblycranium cornutum* Ross, 1951; *Rossaspis superciliosa* Zone; Garden City Formation, southern Idaho.

Included Species. *P. populum* (Ross, 1951), *P. taperum* n. sp.

Diagnosis. Doublure corresponding to genal spine base strongly raised as ridge. Genal spine more than twice as long as librigenal field, with stout base. Longitudinal median furrow, continuous from posterior librigenal border furrow, developed along genal spine. Inner margin of genal spine ornamented with very short spines. Posterior fixigena long (tr.), being three times longer than transverse width of frontal area. Palpebral furrow moderately arched laterally.

Comparison with Other "Hystricurids". With respect to cranidial features, species of *Paramblycranium* resembles *Amblycranium* or *Carinahystricurus*. *Paramblycranium cornutum* bears *Amblycranium*-like features such as a curved posterior cranidial margin and two or three short spines at distal end of posterior cranidial border. *Paramblycranium populum* bears *Carinahystricurus*-like features such as a subtriangular glabella and parallel-sided anterior facial suture. From these two genera, *Paramblycranium* is easily differentiated by, amongst others, the librigenal features. The free cheek bears a doublure ventral to genal spine base forming a ridge, a very long genal spine with wider base and a posterior border furrow running into genal spine as a longitudinal medial furrow. The longitudinal median furrow occurs in such *Hystricurus* species as *H.* (*Triangulocaudatus*) *convexomarginalis* (see Pl. III-13, Fig. 1), *Flectihystricurus* (see Pl. III-49, Fig. 1) and *Psalikilus* (see Pl. III-70, Figs. 3, 5).

If the association of pygidium with *Paramblycranium* (see below) is correct, the development of ridge along the distal edge of the inner pleural field is comparable to many hystricurids, in particular, *Carinahystricurus* (see Pl. III-35, Figs. 17, 22)

Taxonomic Conclusion. The cranidial and pygidial similarities with *Carinahystricurus* suggest inclusion of *Paramblycranium* in the Hystricuridae.

Paramblycranium cornutum (Ross, 1951)
Pl. III-61, Figs. 1-26
1951 *Amblycranium cornutum* Ross, 1951, p. 67, pl. 13, figs. 1-9
? 1951 unassigned pygidium, Ross, pl. 19, figs. 32, 35.

Holotype. Y.P.M. 18014, cranidium; Ross, 1951, pl. 13, figs. 3-5; *Rossaspis superciliosa* Zone; Garden City Formation, southern Idaho.

Diagnosis. Genal spine directed transversely and then smoothly curves posteriorly. Posterior cranidial margin distally curves forwards and bears two or three short spines at distal end. Posterior facial suture gently curves posteriorly. Glabella short (sag.) and parabolic in outline. Palpebral lobe small and located posterior to mid-cranidial length. Anterior facial suture parallel-sided. Anterior cranidial margin straight. Anterior cranidial border furrow slightly incurved sagittally. Cranidial exoskeleton relatively flat.

Association of Pygidium. A thoracic specimen recovered from R6E3 (Pl. III-61, Figs.

251

23, 24) consists of eight thoracic segments. The anterior six segments have a spinose distal pleural end and the seventh segment from the anterior has a long axial spine. The posterior two segments develop a long spine from their posterior pleural band as well as the spinose distal end like the anterior segments. The presence of the thoracic axial spine and spinose distal end of pleurae resembles the architecture of thoracic segments of *Amblycranium variabile* (Pl. III-27, Figs. 1-4). The thoracic specimen differs in having a sharper distal end and long spine extended from the posterior pleural band.

From R6-114 where no cranidial materials of *Paramblycranium cornutum* were recovered, two pygidial specimens (Pl. III-61, Figs. 25, 26) were recovered that should be assigned to the same taxon. The smaller specimen (Fig. 26) develops a spinose distal pleural end. This spinose end conforms to that of the thoracic specimen recovered from R6E3. It is conceivable that all the segments possessing a spinose distal end would have been released as thoracic segments, leaving no spinose margin on the pygidium seen in the larger specimen (Fig. 25). This ontogenetic development differs from that of *Amblycranium* which retains the spines as pygidial marginal spines. The larger pygidiuim (Fig. 25) is indistinguishable from the pygidia (Pl. III-61, Figs. 18-22) occurring in R6E2, R6E3, and R6-114 (97) where cranidial materials of *P. cornutum* were recovered. It only differs in developing tubercles on pleural bands. These morphologic comparisons suggest that all these specimens belong to the same taxon. These pygidia are characterized by a flat exoskeleton, an elongated subtriangular outline, a very narrow (tr.) axis, a deeply depressed outer pleural field which is interrupted by a postaxial ridge, and a continous fulcral ridge along the distal margin of a wide inner pleural field. It is the flat exoskeleton of the pygidia conforming to that of the cranidia of *P. cornutum* that strongly suggests their association with *P. cornutum*.

However, another possibility such as an association with *Parahystricurus* which co-occurs with *Paramblycranium cornutum*, cannot be ruled out until more reliable information becomes available.

These pygidia are similar to those of *Ptychaspis* (see Westrop, 1986, pl. 8, fig. 13) and *Bowmania* (see Westrop, 1995, pl. 14, fig. 7). They share a semi-circular outline, a continuous fulcral ridge, pleural and interpleural furrows reaching the ridge, and a wide pleural field. The presence of the fulcral ridge separating inner and outer pleural fields in these two taxa is not directly observed, because all the illustrations available are in dorsal view. However, the presence of the ridge appears to be most apparent in the two figures cited above.

Paramblycranium populum (Ross, 1951)
Pl. III-62, Figs. 1-16

1951 *Amblycranium*? *populum* Ross, p. 67-68, pl. 13, figs. 19-22.
1973 unassigned cranidium, Terrell, pl. 2, fig. 3.
1991a *Hystricurus* sp. cf. *H. eurycephalus* Shergold, [part], p. 33-34, pl. 6, figs. 16, 17, [only].

Holotype. Y.P.M. 18043, cranidium; Ross, 1951, pl. 13, figs. 20-22; *Tesselacauda* Zone; Garden City Formation, southern Idaho.

Diagnosis. Genal spine slightly curved. Longitudinal median furrow on genal spine well impressed ventrally as well as dorsally. Glabella subtriangular in outline. Distal end of occipital furrow deepens as pit. Posterior facial suture diagonal and smoothly curved

252

posteriorly. Posterior margin of posterior cranidial border relatively straight. Swelling moderately developed lateral to glabellar base.

Remarks. Two free cheeks of *Hystricurus* sp. cf. *H. eurycephalus* from Australia (Shergold, 1991a, pl. 6, figs. 16, 17) are remarkably similar to those of this species. In particular, their posterior border furrow continues into the long genal spine, which is diagnostic of this species.

<center>

Paramblycranium taperum n. gen. n. sp.
Pl. III-62, Figs. 17-23

</center>

Etymology. "taperus" denotes that cranidial outline most strongly tapers forwards.
Holotype. UA 12515, cranidium; Pl. III-62, Figs. 17-20; *Tesselacauda* Zone; Garden City Formation, southern Idaho.
Diagnosis. Anterior cranidial border and border furrow moderately convex forwards. Swelling present adjacent to glabellar base. Glabella most strongly tapering forwards. Cranidium convex dorsally.
Remarks. A great resemblance with *Paramblycranium populum* is found in the smaller cranidia. The differences in the larger cranidia include a forward-convex anterior cranidial margin and a convex cranidium and glabella.

<center>

Genus **POLITOHYSTRICURUS** n. gen.

</center>

Etymology. "*Politohystricurus*" is from the species name of the type species *Hystricurus politus*.
Type Species. *Hystricurus politus* Ross, 1951; *Symphysurina* Zone; Garden City Formation, southern Idaho.
Included Species. *P. brevispinosus* n. sp., *P. concavofrontalis* n. sp., *P. pseudopsalikilus* n. sp.
Diagnosis. Occipital spine present. Palpebral lobe of medium-size and located posterior to mid-cranidial length. Cranidium trapezoidal in outline. Posterior fixigena transversely elongated and narrow exsagittally. Anterior cranidial border strongly arched dorsally. Free cheek with long genal spine and relatively wide ocular platform. Lateral and posterior librigenal border furrows shallow out towards postero-lateral corner of ocular platform. Pygidium with distinct separation of inner and outer pleural fields by abrupt change of slope; prominent tubercle present along distal edge of inner pleural field.
Comparison with "Hystricurids". This new genus, *Politohystricurus*, is characterized by the presence of the occipital spine, trapezoidal cranidial outline, and posteriorly-located palpebral lobe. Two questionable *Hystricurus* species such as *H.?* armatus and *H.?* sulcatus (see Pl. III-2, Figs. 2, 11) have the occipital spine. However, the spine is much stouter than that of *Politohystricurus*. Other cranidial differences of *Politohystricurus* include a less divergent anterior facial suture, a transversely wider glabella, a much more posteriorly-located palpebral lobe, and a much more finely and sparsely granulated, if any, exoskeletal surface. The posteriorly-located palpebral lobe is seen in *Psalikilus* (see Pl. III-69, Figs. 1, 8, 15). However, *Psalikilus* is readily distinguished by deep glabellar furrows, a discrete eye ridge, and a strongly tuberculated cranidial exoskeletal surface.

The associated pygidia (see "Association of Pygidium with *Hystricurus* (*Aequituberculatus*) *genalatus*, *Hystricurus* (*Triangulocaudatus*) *paragenalatus* and

<center>253</center>

Politohystricurus and Their Allied Species") differ from the pygidia of *Hystricurus*
(*Aequituberculatus*) (see Pl. III-8, Fig. 13) and *Hystricurus* (*Triangulocaudatus*) (see Pl.
III-13, Fig. 10) in having a transversely shorter outline, a taller lateral profile, a wider
axis, a narrower inner pleural field, and wider outer pleural field. Nonetheless, there are
some morphologic intermediates into *Hystricurus* (*Aequituberculatus*). These differences
lend additional support to the status of this new genus.

Taxonomic Conclusion. Except for the presence of the occipital spine, the cranidial
features of *Politohystricurus* are well accommodated within the concept of the
Hystricuridae. The pygidia, with some intermediate forms with those of *Hystricurus*
(*Aequituberculatus*), further lend support to this taxonomic conclusion.

<center>

Politohystricurus politus (Ross, 1951)

</center>

Diagnosis. Occipital spine slender and long. Glabella longer than wide. Anterior cranidial
border straight to convex forwards. Preglabellar field long.

Remarks. Four subspecies are recognized on the basis of the curvature of the anterior
cranidial margin and the anterior facial suture. These cranidial variations are seen in the
specimens of *Hystricurus politus* figured by Ross (1951) and Hintze (1953). The
association of pygidia for each subspecies is mainly based on their co-occurrence.

<center>

Politohystricurus politus politus (Ross, 1951)
Pl. III-22, Figs. 1-23

</center>

1951 *Hystricurus politus* Ross, [part], p. 45-47, pl. 9, figs. 23, 24, 28, pl. 15, figs. 1-6,
    [only].
1951 indefinitely assigned pygidium, Ross, pl. 9, figs. 13, 19.
1953 *Hystricurus politus*, Hintze, [part], p. 165-166, pl. 6, fig. 8, [only].
Holotype. Y.P.M. 17955, cranidium; Ross, 1951, pl. 15, figs. 3, 4, 6; *Symphysurina*
Zone; Garden City Formation, southern Idaho.
Diagnosis. Anterior cranidial border long (tr.) and straight. Anterior facial suture slightly
divergent to parallel-sided. Posterior pygidial margin arched dorsomedially.

<center>

Politohystricurus politus convexofrontalis n. gen. *et.* n. subsp.
Pl. III-23, Figs. 1-13

</center>

1951 *Hystricurus*? sp. F, Ross, p. 55, pl. 15, figs. 7-9.
1951 *Hystricurus politus*, Hintze, [part], p. 165-166, pl. 6, figs. 7a, 7b, [only].
Etymology. "convexofrontalis" describes its forward-convex anterior cranidial border.
Holotype. UA 12196, cranidium; Pl. III-23, Figs. 1, 2, 6; *Symphysurina* Zone; Fillmore
Formation, Utah.
Diagnosis. Anterior border short (tr.) and convex forwards, and most strongly arched
dorsally. Preglabellar field moderately convex dorsally. Anterior facial suture parallel-
sided and turn inwards before anterior cranidial border furrow. Posterior pygidial margin
straight. Three or four short spines on axial rings.

<center>

Politohystricurus politus convergia n. gen. *et.* n. subsp.
Pl. III-24, Figs. 1-13

</center>

1953 *Hystricurus politus*, Hintze, [part] p. 165-166, pl. 6, figs. 9-11, [only].
Etymology. "convergia" depicts the convergent anterior facial suture.

<center>254</center>

Holotype. UA 12202, cranidium; Pl. III-24, Figs. 1, 2, 4; *Symphysurina* Zone; Fillmore Formation, Utah.

Diagnosis. Anterior facial suture parallel-sided and then strongly convergent before anterior cranidial border furrow. Anterior border short and straight (tr.). Pygidium with fine granules on outer pleural field. Posterior pygidial margin strongly arched dorsomedially. Genal spine three times longer than ocular platform. Glabellar front rounded.

Politohystricurus sp. aff. *P. politus convergia*
Pl. III-15, Figs. 7-9

Remarks. This pygidium differs from those of *Politohystricurus politus convergia* (see Pl. III-24, Figs. 9, 10, 11, 13) in having a series of tubercles along the distal edge of the inner pleural field and a straight (not arched medially) posterior margin.

Politohystricurus politus longifrontalis n. gen. *et.* n. subsp.
Pl. III-25, Figs. 1-7

1951 *Hystricurus politus* Ross, [part], p. 45-47, pl. 9, figs. 27, 32, 33, [only].

Etymology. "longifrontalis" describes its transversely long anterior cranidial border.

Holotype. UA 12209, cranidium; Pl. III-25, Fig. 1; *Symphysurina* Zone; Garden City Formation, southern Idaho.

Diagnosis. Anterior cranidial border long (tr.) and short (sag.), and not arched dorsally. Anterior facial suture slightly divergent before anterior border furrow. Palpebral lobe very small and little arched laterally. Pygidium with narrow axis and pair of prominent spines on anteromost axial rings.

Politohystricurus brevispinosus n. gen. n. sp.
Pl. III-25, Figs. 8-15

1953 *Hystricurus lepidus* Hintze, [part], p. 166-167, pl. 7, figs. 10, 11, [only].

Etymology. "brevispinosus" describes its very short occipital spine.

Holotype. UA 12213, cranidium; Pl. III-25, Figs. 8, 11, 12; *Symphysurina* Zone; Fillmore Formation, Utah.

Diagnosis. Occipital spine very short and stout. Glabella strongly arched anteriorly. Pygidium with relatively gently down-sloping outer pleural field.

Remarks. Two free cheeks from Fillmore Formation were assigned to *Hystricurus lepidus* (Hintze, 1953, pl. 7, figs. 10, 11). They have a genal spine which is about three times longer than librigenal field and meets posterior librigenal border at nearly a right angle. These two features agree with the free cheeks of *Politohystricurus* species.

Two free cheeks referred to *Hystricurus truncatus* by Park (1993, pl. 4, figs. 5, 8) have a semi-circular librigenal field, a long genal spine based at posterior one-third of the lateral margin of the platform, and a swelling at the genal spine base that separates the lateral and posterior librigenal border furrows. These features are found in the free cheeks of *Politohystricurus brevispinosus* (Pl. III-25, Figs. 9, 10, 13).

Politohystricurus concavofrontalis n. gen. n. sp.
Pl. III-26, Figs. 1-8

Etymology. "concavofrontalis" describes its anterior cranidial border which is curved

255

backwards sagittally.

Holotype. UA 12217, cranidium; Pl. III-26, Figs. 1-3; *Symphysurina* Zone; Fillmore Formation, Utah.

Diagnosis. Anterior cranidial border moderately curved backwards and strongly arched dorsally; anterior cranidial border furrow curved backwards sagittally, resulting in short (sag.) preglabellar field. Posterior pygidial margin very strongly arched dorsomedially. Anterior facial suture divergent and then rapidly turns inwards before anterior cranidial border furrow. Glabellar front relatively pointed.

Politohystricurus pseudopsalikilus n. gen. n. sp.
Pl. III-26, Figs. 9-15

Holotype. UA 12221, cranidium; Pl. III-26, Figs. 11, 14, 15; *Symphysurina* Zone; Fillmore Formation, Utah.

Etymology. "pseudopsalikilus" indicates that this species shares some resemblance with the genus *Psalikilus*.

Diagnosis. Posterior fixigena terminated with sharply blunted end with short spine. Palpebral lobe located far posteriorly, overhanging posterior fixigena. Anterior cranidial border furrow sagittally curved backwards, resulting in short (sag.) preglabellar field. Inner margin of genal spine and posterior librigenal border ornamented with short spines. Pygidium with straight (not arched) posterior margin in posterior view. Small granules on pleural fields and smaller granules on marginal border.

Remarks. The architecture of the frontal area of this species greatly resembles that of *Psalikilus* with respect to the parallel-sided anterior facial suture and posteriorly incurved anterior border (compare with Pl. III-69, Fig. 1). The position of the palpebral lobe and the presence of short spines along the inner margin of the genal spine and posterior librigenal border are the other shared features. Although several other features including the tuberculation, glabellar furrows, and eye ridge, and pleural field ridge on the pygidium easily distinguish *Psalikilus*, these shared cranidial features may be indicative of their taxonomic affinity.

Genus PSEUDOPLETHOPELTIS n. gen.

Etymology. "Pseudoplethopeltis" denotes the taxonomic history that the genus is assigned to the same family with *Plethopeltis*.

Type Species. *Paraplethopeltis*? *genacurvus* Hintze, 1953; *Paraplethopeltis* Zone; Fillmore Formation, Utah.

Included Species. *P. minuta* (Heller, 1954)

Diagnosis. Posterior facial suture runs transversely and curves smoothly backwards. Glabella smoothly forward-tapering. Occipital ring convex backwards. Palpebral lobe of medium size and well defined by palpebral furrow. Preglabellar field relatively long. Anterior facial suture slightly divergent. Free cheeks with strongly curved long genal spine. Pygidium with distinct pleural and interpleural furrows and slender but distinct border. Outer pleural field gently down-sloping and separated from flat inner pleural field only by change of slope.

Comparison with "Hystricurids". The oval-shaped glabella, slightly divergent anterior facial suture, relatively long preglabellar field, and medium-sized moderately arched palpebral lobe of the *Pseudoplethopeltis* cranidia, each is seen in many different

256

Hystricurus species. *Pseudoplethopeltis* is characterized by the posterior facial suture that runs transversely and then smoothly curves posteriorly, resulting in a very rounded distal end. Such *Spinohystricurus* species as *S. terescurvus* has a comparable configuration, but the course is steeper than in *Pseudoplethopeltis*. The pygidia of *Pseudoplethopeltis* are most similar to those of *Hystricurus* (*Butuberculatus*) *scrofulosus* from Greenland (Pl. III-3, Figs. 1, 2, 4), except for the smooth surface.

Comparison with Ptychopariides. From *Paraplethopeltis*, *Pseudoplethopeltis* differs in having a relatively shorter and more strongly tapering glabella, longer preglabellar field, narrower (exsag.) posterior fixigena with a rounded distal end, and distinct pygidial interpleural furrows.

Taxonomic Conclusion. Cranidial and pygidial similarities with some *Hystricurus* species lead to place *Pseudoplethopeltis* in the Hystricuridae.

Pseudoplethopeltis genacurvus (Hintze, 1953)

1951 *Pachycranium* ? sp. Ross, [part], p. 73, pl. 17, figs. 4, 5, 9-11, 15, [only].
1953 *Paraplethopeltis* ? *genacurvus* Hintze, p. 202-204, pl. 7, figs. 1-5.
1959 *Hystricurus* ? sp. aff. *H.* ? *genacurvus* Berg and Ross, [part], p. 112, pl. 21, fig. 21, [only].
1983 *Paraplethopeltis genacurva*, Stitt, p. 22, pl. 2, fig. 10.

Holotype. 26173, free cheek; Hintze, 1953, pl. 7, figs. 2a-2c; *Paraplethopeltis* Zone; Fillmore Formation, Utah.

Diagnosis. Preglabellar field short. Anterior facial suture parallel-sided or slightly divergent.

Remarks. Two cranidial specimens of *Pachycranium*? sp. from the Garden City Formation (Ross, 1951, pl. 17, figs. 4, 5, 9-11, 15) are transferred into this species. These cranidia are different from *Pachycranium* (see Pl. III-57, Figs. 14-17) in having a more posteriorly located palpebral lobe, less discrete palpebral furrows, and a less steep posterior facial suture, and lacking a preglabellar median furrow.

Pseudoplethopeltis minuta (Heller, 1954)

? 1948 *Hystricurus binodosus* Weber, [part], p. 7-9, pl. 1, figs. 9, 10, [only].
1951 *Hystricurus* ? sp. E Ross, p. 54-55, pl. 15, figs. 10, 11, 13, 14.
1953 *Paraplethopeltis* ? *generectus* Hintze, [part], p. 204, pl. 7, figs. 9a, 9b, [only].
1959 *Hystricurus* ? sp. aff. *H.* ? *genacurvus* Berg and Ross, [part], p. 112, pl. 21, fig. 23, [only].
1954 *Paraplethopeltis minuta* Heller, p. 45-46, pl. 18, figs. 13-15.

Holotype. U. Mo. No. 10335, cranidium; Heller, 1951, pl. 18, figs. 14, 15; Demingian Stage; Roubidoux Formation, Missouri.

Diagnosis. Preglabellar field long. Palpebral lobe posteriorly located. Anterior facial suture divergent. Pygidial outline long sagittally.

Remarks. Two poorly-preserved cranidia of *Hystricurus binodosus* from Siberia (Weber, 1948, pl. 1, figs. 9, 10) exhibit an architecture similar to the holotype cranidium. Their poor preservation prevents me from confidently assigning them to this species.

A cranidium of *Hystricurus*? sp. E from the Garden City Formation (Ross, 1951, pl. 15, figs. 10, 11, 14) is greatly similar to the holotype cranidium (Heller, 1954, pl. 18, figs. 14, 15). Only difference is a distinct anterior cranidial border furrow which is not well

257

preserved in the holotype cranidium.

The cranidium and free cheeks of *Paraplethopeltis? generectus* (Hintze, 1953, pl. 7, figs. 6-8) are assigned to *Onchopeltis* (compare with Rasetti, 1944). The pygidium (Hintze, 1953, pl. 7, figs. 9a, 9b) is similar to the pygidium of *Pseudoplethopeltis genacurvus* (Hintze, 1953, pl. 7, figs. 4, 5), but differs in having a relatively longer outline. The pygidium is assigned to this new species.

Genus SPINOHYSTRICURUS n. gen.

Etymology. "Spino-" depicts the presence of three or four thoracic axial spines.

Type Species. *Hystricurus robustus* Ross, 1951; *Tesselacauda* Zone; Garden City Formation, southern Idaho.

Included Species. *S. robustus* (Ross, 1951), *S. terescurvus* n. sp., *S. antiquus* (Lisogor, 1961).

Diagnosis. Three or four thoracic axial spines. Pygidium with tall outer pleural field and flat inner pleural field. Pygidial fulcral ridge strongly developed and interrupted by interpleural furrows.

Remarks. *Spinohystricurus* is similar to *Carinahystricurus* in many aspects. It is, amongst others, the size and curvature of the palpebral lobe that differentiate each genus. *Spinohystricurus* has a much larger palpebral lobe which is much more strongly convex laterally and a palpebral furrow that is strongly curved laterally following the outline of the palpebral lobe (see Pl. III-18, Fig. 1). In contrast, *Carinahystricurus* has a smaller palpebral lobe and a straight palpebral furrow (see Pl. III-33, Fig. 2).

Spinohystricurus robustus (Ross, 1951)
Pl. III-16, Figs. 4-6, Pl. III-17, Figs. 8, 9, Pl. III-19, Figs. 1-8

1951 *Hystricurus robustus* Ross, [part], p. 51-53, pl. 10, figs. 13, 16, 20, [only].

1951 unassigned pygidium, Ross, pl. 19, figs. 6, 11, 15.

1951 unassigned hypostome, Ross, pl. 19, figs. 21, 23.

1997a *Parahystricurus carinatus* Ross, Lee and Chatterton, [part], p. 866-869, figs. 5.2, 5.7, 5.12, [part].

Holotype. Y.P.M. 17964, cranidium; Ross, 1951, pl. 10, figs. 13, 16, 20; *Tesselacauda* Zone; Garden City Formation, southern Idaho.

Diagnosis. First two thoracic axial rings with two pairs of small tubercles; four axial rings posterior to those with relatively long axial spine. Posterior thoracic segment(s) with strongly developed fulcral ridge which is continuous with the ridge between inner and outer pygidial pleural fields.

Anterior cranidial border furrow incurved sagittally. Anterior border carinated and ornamented with terrace lines. Palpebral lobe of medium size, strongly arched laterally, thick (but both ends rapidly taper), well defined by palpebral furrow which has the same curvature as palpebral lobe, and located at mid-cranidial length. Posterior facial suture distally turns rapidly inwards at acute angle.

Lateral librigenal border carinated as ridge and ornamented with terrace lines. Genal spine shorter than librigenal field. Eye socle present.

Pygidium with four axial rings and terminal piece; the posteriormost ring not completely separated from terminal piece. Border tubular and ornamented with fine granules.

258

Hypostome with entire posterior and lateral margins and tubular border.

Remarks. A pygidium figured by Ross (1951, pl. 19, figs. 6, 11, 15) is remarkably similar to those assigned to *Spinohystricurus terescurvus* in this study (see Pl. III-20, Figs. 1-12). However, it differs in having a more discrete marginal border furrow. Considering the cranidial similarities with *S. terescurvus*, this pygidium is assigned to this species. The assignment of the hypostomes and the articulated specimens to this species are discussed below.

Comparison with Other "Hystricurids". *Carinahystricurus* (see Pl. III-35, Figs. 2, 17) shares cranidial and pygidial resemblances with *Spinohystricurus robustus*. This species differs in having a larger, thicker, laterally arched palpebral lobe defined by a well impressed palpebral furrow, tuberculated cranidial surface, an eye socle, a shallower and posteriorly incurved anterior cranidial border furrow, and a ridge between the inner and outer pygidial pleural fields interrupted by interpleural furrows.

Spinohystricurus sp. aff. *S. robustus*
Pl. III-18, Figs. 20-23

Remarks. The cranidium from R5-76.4 (Pl. III-18, Figs. 20-23) is similar to similar-sized cranidia of *Spinohystricurus robustus*. Ontogenetic transformations from a small cranidium of *Spinohystricurus terescurvus* (Pl. III-18, Fig. 14) into this cranidium and other larger cranidia of *Spinohystricurus robustus* (e.g., Pl. III-19, Fig. 4) appear to be reasonable. However, this cranidium has a shorter (tr.) posterior fixigena and more strongly incurved anterior cranidial border furrow. This cranidium also resembles cranidia of *Glabellosulcatus*? *crassilimbatus* (Pl. III-78, Figs. 1-17), and differs in having a more strongly arched palpebral lobe and transverse posterior facial suture.

Spinohystricurus terescurvus n. gen. n. sp.
Pl. III-16, Figs. 1-3, 7-12, Pl. III-17, Figs. 1-7, 10-12, Pl. III-18, Figs. 1-19, Pl. III-20, Figs. 1-18

1951 *Hystricurus robustus* Ross, [part], p. 51-53, pl. 10, figs. 11, 14, 15, pl. 14, fig. 27, [only]

1951 unassigned hypostomes, Ross, pl. 19, figs. 23-26.

1953 *Hystricurus robustus*, Hintze, p. 166, pl. 8, figs. 2a-2c.

1997 *Hystricurus* ? sp. A, Lee and Chatterton, p. 864, figs. 3.2, 5.8, 5.13.

1997a *Parahystricurus carinatus* Ross, Lee and Chatterton, [part], p. 866-869, figs. 5.1, 5.5-5.7, 5.9-5.11, [part].

Etymology. "terescurvus" is composed of "teres" (smooth) and "curvus" (curved), depicting that posterior facial suture distally curves smoothly.

Holotype. Y.P.M. 17965, cranidium; Ross, 1951, pl. 10, figs. 11, 14, 15; *Tesselacauda* Zone; Garden City Formation, southern Idaho.

Diagnosis. Posterior facial suture distally turns smoothly backwards (an sometimes inwards). First three thoracic axial rings with two pairs of small tubercles; three axial rings posterior to these with relatively long axial spine.

Differentiation from *Spinohystricurus robustus*. Ross (1951) figured two cranidia and assigned both to *Hystricurus rubustus* (=*Spinohystricurus robustus* herein). The smaller one (pl. 10, figs. 11, 14, 15) differs from the larger one (pl. 10, figs. 13, 16, 20) in having a rounded distal end of the posterior fixigena. Although this difference could be

ontogenetic, other evidence below indicates these cranidia belong to two different species.

Discovery of two completely articulated meraspid specimens indicates the existence of two different species which share very similar cranidial and pygidial morphologies. Lee and Chatterton (1997a) assigned the two specimens (Pl. III-16, Figs. 1-3 and Figs. 4-6) to *Parahystricurus carinatus* which is transferred to *Carinahystricurus carinatus* in this study. A smaller cranidium of *C. carinatus* (Ross, 1951, pl. 13, fig. 25) has a small palpebral lobe located posterior to mid-cranidial length, a straight palpebral furrow, a slightly divergent anterior facial suture, and a smoothly curved posterior facial suture. In contrast, cranidia of similar size were discovered (see Pl. III-16, Figs. 9, 11) that show a curved palpebral lobe located at mid-cranidial length, a slightly convergent anterior facial suture, and a rapidly posteriorly curved posterior facial suture. These cranidia are considered to transform into a large cranidium (Pl. III-18, Fig. 1) which is similar to *Spinohystricurus robustus*. This large cranidium differs from the holotype of *C. carinatus* (Ross, 1951, pl. 13, fig. 27) with respect to all the above-mentioned features. Morphologies of smaller cranidia (see Pl. III-18, Figs. 13, 15, 18) are similar to cranidia of the two articulated specimens (Pl. III-16, Figs. 1-6). Morphologies of these cranidia are more reasonably transformed into the larger cranidia similar to *Spinohystricurus robustus*. As a result, the two meraspid articulated specimens do not belong to *C. carinatus*, but to *S. robustus* or a similar species.

The two articulated specimens differ from each other with respect to the development of thoracic axial spines. In the larger specimen (Pl. III-16, Figs. 1-3), the anterior three thoracic segments lack the axial spine and the fourth to sixth segments possess long axial spines (thus, it has three thoracic axial spines). In contrast, the smaller specimen (Pl. III-16, Figs. 4-6) has the anterior two segments lacking a spine, and the third to sixth segments possessing spines (thus, it has four thoracic axial spines). This difference is considered taxonomic, unless a thoracic segment lacking the spine is ontogenetically budded into two segments lacking the spine or the the thoracic segment with an axial spine is ontogenetically modified into the segment with paired node.

Three partially articulated specimens, showing the same configuration of spine development as the larger articulated specimen, were discovered (Pl. III-16, Figs. 7, 8, Pl. III-17, Figs. 1-4, 6, 7). One thoracopygidial specimen (Pl. III-17, Figs. 8, 9) has four axial spines (two on released segments and the remaining two on the anterior two segments of the transitory pygidium). This accords with the configuration of the smaller articulated specimen mentioned above.

In terms of relative abundance of discovered materials, the larger cranidia with a rounded distal end of the posterior fixigena (e.g., Pl. III-18, Figs. 1, 2, 5, 6, 9, 12) are much more abundant than those with a blunted distal end (e.g., Pl. III-19, Figs. 2, 4). The articulated specimens with three thoracic axial spines and anterior three thoracic segments lacking a spine are associated with cranidia with a rounded distal end of the posterior fixigena, simply because of their relative abundances. The specimens with four axial spines and anterior two segments lacking the spine are associated with the cranidia with a blunted end. These latter forms are assigned to *Spinohystricurus robustus* whose holotype cranidium has a blunted end of the posterior fixigena (see Ross, 1951, pl. 10, fig. 20). The former specimens are assigned to a new species, *Spinohystricurus terescurvus*.

260

Another difference between *Spinohystricurus robustus* and *Spinohystricurus terescurvus* is the presence or absence of a hypostomal marginal spine pair. The articulated specimen of *S. robustus* (see Lee and Chatterton, 1997a, fig. 5-12) has a pair of short spines at the postero-lateral corner of the hypostome, whereas the specimen of *S. terescurvus* (see Pl. III-17, Fig. 12) lacks this spine pair. Of unassigned hypostomes (Ross, 1951, pl. 19, figs. 21-29), those with the spine pair (figs. 21, 22) are assigned to *S. robustus*, and those lacking the spine pair (figs. 23-26) are assigned to *S. terescurvus*. **Association of Protaspides.** In a degree 2 meraspis (Pl. III-16, Figs. 9, 10), the axial spine lacks on two released thoracic segments and the most anterior segment of the transitory pygidium, but the spine is present on the second to fourth anterior segments of the transitory pygidium. This specimen is assigned to *Spinohystricurus terescurvus*. Cranidial morphologies are considered to reasonably transform from those of a protaspis (Pl. III-16, Fig. 12) which is very similar to the protaspis figured by Lee and Chatterton (1997, fig. 5.1). Both protaspides are assigned to *S. terescurvus*. Two protaspid specimens of *Hystricurus* ? sp. A (Lee anc Chatterton, 1997a, figs. 5.8, 5.13) are also transferred to *S. terescurvus*.

Lee and Chatterton (1997a) argued that protaspides of *Parahystricurus* differ from those of *Hystricurus* in having an inner series tubercles on the protopygidium. However, since the protaspis of *Parahystricurus carinatus* is assigned to *Spinohystricurus terescurvus* and *P. carinatus* is transferred to *Carinahystricurus*, this difference is not meaningful.

Association of Pygidium. All the articulated specimens of *Spinohystricurus terescurvus* possessing a pygidium appear to represent early ontogenetic stages. Cranidial similarities of *S. terescurvus* with *Carinahystricurus* and *Parahillyardina* lead me to assume that pygidia of *S. terescurvus* are similar to those of the two genera. From the sampling horizons where the cranidial materials of *S. terescurvus* occur, several pygidia were discovered (Pl. III-20, Figs. 1-18) that are similar to those of *Carinahystricurus* and *Parahillyardina*. These pygidia are assigned to *S. terescurvus*. Since they cannot be separated into two morphotypes, all of them are assigned to *S. terescurvus* whose cranidial materials are most abundant; it seems possible that *Spinohystricurus robustus* has a similar or even same-type of pygidium.

The smaller pygidia (e.g., Pl. III-20, Figs. 13, 15, 16, 18) could represent earlier stages of *Carinahystricurus* or *Parahillyardina*. The development of the fulcral ridge and the configuation of the inner and outer pleural fields are identical in these taxa.

Spinohystricurus antiquus (Lisogor, 1961)
Pl. III-19, Figs. 9-17

1961 *Hystricurus antiquus*, Lisogor, [part], p. 67-68, pl. 1, fig. 15, [only].
? 1961 *Hystricurus antiquus*, Lisogor, [part], p. 67-68, pl. 1, figs. 16, 17, [only].
Holotype. no specimen number designated, cranidium; Lisogor, 1961, pl. 1, fig. 15; late Tremadocian; Kazakhstan.
NEOTYPE. UA 12162, cranidium; Pl. III-19, 9, 10, 12, 16; *Tesselacauda* Zone; Garden City Formation, southern Idaho.
Diagnosis. Posterior fixigena obliquely directed posteriorly and ends with a rounded tip. Glabella weakly tapered forwards. Palpebral furrow weakly curved laterally. Anterior cranidial border furrow straight (tr.). Preglabellar median furrow present.

261

Remarks. Lisogor (1961) described three poorly preserved cranidia of *Hystricurus antiquus* (pl. 1, figs. 15-17) from Kazakhstan. The larger one (pl. 1, fig. 15), although only its frontal area is preserved, is indistinguishable from a cranidium from the Garden City Formation (Pl. III-19, Fig. 10). The other two smaller cranidia from Kazakhstan are too poorly preserved to be accurately assessed.

Association of Pygidium. The pygidium indistinguishable from that of *Spinohystricurus robustus* is found in R6-55 which is the only sampling horizon where cranidial materials of this species were collected.

Remarks. Cranidial morphologies of this species are very similar to those of *Spinohystricurus robustus*, so that it is transferred into *Spinohystricurus*.

<div align="center">

***Spinohystricurus* sp. nov.**

Pl. III-19, Figs. 18-21

</div>

Remarks. A few cranidia are found that have a triangular glabella, a convergent anterior facial suture, and a long (tr.) posterior cranidial margin. They certainly have similarities to the *Spinohystricurus* species. The paucity of materials prevents from formally erecting a new species.

<div align="center">

Genus TANYBREGMA Jell and Stait, 1985b

</div>

Type Species. *Tanybregma tasmaniensis* Jell and Stait, 1985b; La1.5 Zone of Lancefieldian Series; Florentine Valley Formation, Tasmania, Australia.

Included Species. *T. timsheansis* n. sp., *T. paratimsheansis* n. sp.

Diagnosis. Palpebral lobe large (about two-thirds of glabellar length), strongly arched laterally, slender, and its posterior ends located far posteriorly (resulting in very narrow posterior fixigena). Palpebral furrow follows outline of palpebral lobe. Lateral and posterior librigenal border furrows continue into genal spine, with developing longitudinal median ridge in between.

Comparison. Jell and Stait (1985b) erected a monotypic genus, *Tanybregma*, with the type species, *T. tasmaniensis*. Boyce (1989) synonymized *Tanybregma* with *Hillyardina*. However, *T. tasmaniensis* differs from *Hillyardina* (Pl. III-47, Fig. 2) in having a large palpebral lobe with curved palpebral furrow (a small lobe with straight palpebral furrow in *Hillyardina*), truncated anterior margin of glabella (rounded or pointed in *Hillyardina*), very narrow (or absent) posterior fixigenal area (relatively broad and triangular in *Hillyardina*), eye socle (absent in *Hillyardina*), denticles on adaxial side of genal spine (absent in *Hillyardina*), deep S1 furrow (shallow or non-pustulose patches in *Hillyardina*), and very narrow (sag.) anterior border (relatively broad and flat in *Hillyardina*). These differences are of generic value, so that *Tanybregma* is resurrected as a valid genus.

Jell and Stait (1985b) mentioned a possibility that *Tanybregma tasmaniensis* would have been derived from a form like their *Hystricurus penchiensis* from Tasmania. These Tasmanian materials are transferred into two new species of *Tanybregma*, *T. timsheansis* and *T. paratimsheansis*; see below for the complicated taxonomy of these two new species. Cranidia of these two species (Pl. III-85, Figs. 8-16) share with the type species, amongst others, a slender and highly arcuated palpebral lobe located far posteriorly and posterior and lateral librigenal border furrow that continue into genal spine with developing a longitudinal median ridge. These features are unique to these three species

<div align="center">

262

</div>

of the "hystricurids" and thus, considered to be diagnostic to the genus *Tanybregma*. Similar architecture of palpebral lobe of *Tanybregma* is found in such definite *Hystricurus* species as *oculilunatus* and *crotalifrons* and *Paratersella* (e.g., see Pl. III-65, Fig. 1). However, the palpebral lobe of *Tanybregma* is larger and more strongly arched laterally. The librigenal feature is unique to *Tanybregma*. It is common to "hystricurids" that posterior and lateral librigenal border furrows both continue into the genal spine; for example, *Hyperbolochilus* (Pl. III-53, Fig. 1). However, each furrow in *Tanybregma* continues into the genal spine without merging each other.

Cranidial architecture of the two new *Tanybregma* species is comparable to *Hystricurus penchiensis* (see Pl. III-4, Fig. 6). Such differences as glabellar length and size of palpebral lobe would fit in evolutionary transformation of the Hystricuridae.

An articulated specimen of *Tanybregma timsheansis* was figured by Jell and Stait (see Pl. III-85, Fig. 11). Morphologies of the pygidium and the illustrated disarticulated pygidia (see Pl. III-85, Figs. 14-16) differ from those of other "hystricurids" (e.g., see Pl. III-35, Figs. 17-22) in lacking the pygidial fulcral ridge and having strongly posteriorly directed pleural and interpleural furrows. From pygidia of such definite *Hystricurus* species as *oculilunatus* and *crotalifrons* (see Ross, 1951, pl. 17, figs. 23, 28, 29), they are similar in having a bilobed terminal piece, postaxial ridge, and node on axial rings, but differ in lacking the fusion of bands of adjacent pleurae. No pygidia are associated for the other two *Tanybregma* species.

Taxonomic Conclusion. The two diagnostic features of *Tanybregma* and pygidial features of *Tanybregma timsheansis* are regarded as variations within the Hystricuridae, which have been tranformed from or into features of other "hystricurids" including *Hystricurus*. Thus, *Tanybregma* is retained in the Hystricuridae.

Tanybregma tasmaniensis Jell and Stait, 1985b
Pl. III-85, Figs. 1-4

1985b *Tanybregma tasmaniensis* Jell and Stait [part], p. 9, pl. 3, figs. 1-7 [only]
Holotype. UTGD 95983, cranidium; Jell and Stait, 1985b, pl. 3, fig. 3 (re-illustrated in Pl. III-85, Figs. 1-3); La1.5 Zone of Lancefieldian Series; Florentine Valley Formation, Tasmania, Australia.
Diagnosis. Cephalic doublure wide (sag. and exsag.). Preglabellar field very long (nearly half of glabellar length). Anterior cranidial margin straight (tr.). Anterior border narrow (sag. and exsag.); no distinct separation between preglabellar field and anterior border furrow. Anterior facial suture strongly divergent. S1 glabellar furrows long and isolated from axial furrows. Glabella with straight lateral margin and relatively truncated anterior margin. Tubercles discernibly developed only on glabella, occipital ring, and palpebral fixigena. Free cheeks with eye socle and row of short spines along inner margin of genal spine. Pygidium unknown.
Remarks. This species is easily differentiated from other two species by its long and wide frontal area. The long preglabellar field is seen in *Metabowmania*, (see Dean, 1989, pl. 17, figs. 1, 4), deep S1 furrows isolated from axial furrows in some *Graciella* species (see Peng, 1990b, pl. 8, figs. 6, 8b), and row of spines along adaxial margin of free cheeks in *Psalikilus*, (see Pl. III-70, Fig. 5). The cephalic doublure is broadest among taxa that have been assigned to the Hystricuridae, which characterizes this species. The strongly divergent anterior facial suture of this species is similar to *Metabowmania*,

263

Graciella (see Pl. III-84, Figs. 1, 4) and *Hyperbolochilus* (see Pl. III-52, Fig. 2).

The divergent anterior facial suture, strongly arched palpebral lobe, narrow posterior fixigena, and narrow anterior cranidial border are observed in such bathyurids as *Punka* (see Fortey, 1979, pl. 33, figs. 3, 9). However, *Punka* is differentiated by its subrectangular glabella with steeply down-sloping glabellar front, and fingerprint-like ornaments.

Tanybregma timsheansis n. sp.
Pl. III-85, Figs. 11-16

1985b *Hystricurus penchiensis*, Jell and Stait [part], p. 4-5, pl. 1, figs. 1, 4, 5, 6, 7, 8 (only pygidial specimen; UTGD 122508), 9, 10, 11, 13, 15 (only two librigenal specimens; UTGD 122517, UTGD 122518) [only].

? 1985b *Hystricurus* sp. cf. *H. robustus* Jell and Stait [part], p. 8, pl. 3, fig. 14, [only].

1985b *Tanybregma tasmaniensis* Jell and Stait, [part], p. 9, pl. 8, fig. 7 (left cranidial specimen only), [only].

Etymology. "timsheansis" is adapted from the name of sample locality, Timshea area, Tasmania

Holotype. UTGD 95867, articulated specimen; Jell and Stait, 1985b, pl. 1, fig. 4 (re-illustrated in Pl. III-85, Fig. 11); La1.5 of Lancefieldian Series; Florentine Valley Formation, Tasmania, Australia.

Diagnosis. Palpebral lobe long. Anterior border furrow wide and shallow. Glabella with rounded anterior margin. Anterior facial suture straight and slightly divergent. Tubercles developed on surface except for anterior border and border furrow. Pygidium suboval in outline. Pleural field smoothly down-sloping. Four axial rings and bilobed terminal piece; node on anterior most axial ring. Pleural furrows deeper and longer than interpleural furrows, and reach marginal border; both furrows smoothly curved posteriorly in their distal ends. Posterior margin slightly indented forwards and arched dorsally. Marginal border tubular and ornamented with terrace lines. Small tubercles on pleural bands. Post-axial ridge relatively distinct. Bimodal-sized tubercles developed proximal half of ocular platform. Fine genal cecae present distal half of ocular platform. Lateral border ornamented with terrace lines. Thorax with nine segments. Posterior pleural bands with row of fine tubercles. Small node on axial rings.

Remarks. Jell and Stait (1985b) illustrated several disarticulated specimens and a partially articulated specimen from Tasmania, and assigned all of them to *Hystricurus penchiensis* Lu *in* Lu *et al.* 1976 in the text. However, in the figure caption, all the specimens were assigned to *Hystricurus timsheansis* which was not described in the text.

The cranidial specimens from Tasmania can be grouped into two morphotypes. The first is characterized by a narrow anterior border that is gently arched forwards and defined by a wide and shallow border furrow, and a glabella with a rounded anterior margin and straight-sided lateral margin (see Pl. III-85, Figs. 11, 13). The second morphotype exhibits a wider anterior border, an anterior border furrow that is slightly posteriorly curved sagittally, and a glabella with a relatively truncated anterior margin and slightly laterally convex lateral margin (see Pl. III-85, Fig. 8). The pygidial specimens can also be grouped into two forms. The first is characterized by a suboval outline, tubular marginal border, and a smoothly down-sloping pleural field (see Pl. III-85, Figs. 14-16). The second morphotype shows a more transversely elongated outline,

264

distinct separation of inner and outer pleural fields, and a narrow and flat marginal border (see Pl. III-85, Figs. 5-7). The first cranidial and pygidial morphotype is assigned to *timsheansis* and the second to *paratimsheansis*.

A pygidium of *Hystricurus* sp. cf. *H. robustus* (Jell and Stait, 1985b, pl. 3, fig. 14) resembles this species in its overall outline and in lacking distinct separation of inner and outer pleural fields. However, it is covered with densely-distributed small tubercles and lacks a distinct marginal border. A cranidium was assigned to *Tanybregma tasmaniensis* by Jell and Stait (1985b, pl. 8, fig. 7). However, it has a wider anterior cranidial border and narrower preglabellar field, which better accord with *Tanybregma timsheansis*.

<div align="center">

Tanybregma paratimsheansis n. sp.
Pl. III-85, Figs. 5-10

</div>

? 1954 *Hystricurus* sp. A Heller, p. 44, pl. 18, figs. 4, 5.
1976 *Hystricurus penchiensis* Lu *in* Lu *et al.*, [part], p. 54, pl. 7, fig. 11, [only].
1985b *Hystricurus penchiensis*, Jell and Stait [part], p. 4-5, pl. 1, figs. 2, 3 , 8 (only cranidial specimen; UTGD 122509), 12, 15 (only pygidial specimen; UTGD 122516), [only].
? 1985b *Hystricurus penchiensis*, Jell and Stait [part], p. 4-5, pl. 1, fig. 15 (only pygidial specimen; UTGD 122516), [only].
? 1985b *Hystricurus lewisi* (Kobayashi, 1940), Jell and Stait, [part], p. 5-8, pl. 2, fig. 12, [only]
? 1985b *Hystricurus penchiensis*, Jell and Stait [part], p. 4-5, pl. 1, fig. 14, [only].

Etymology. "paratimsheansis" depicts morphologic similarities to *Hystricurus timsheansis*.

Holotype. UTGD 122503, cranidium; Jell and Stait, 1985b, pl. 1, fig. 3 (re-illustrated in Pl. III-85, Figs. 8-10); La1.5 of Lancefieldian Series; Florentine Valley Formation, Tasmania, Australia.

Diagnosis. Glabella subrectangular in outline, with moderately truncated anterior margin and slightly convex lateral margin. Anterior border gently widens sagittally. Anterior cranidial border furrow slightly curved backwards sagittally.

Association of Pygidium. A pygidium figured by Jell and Stait (1985b, pl. 1, fig. 15, see also Pl. III-85, Figs. 5-7) is more similar to those *Hystricurus* (*Hystricurus*) *oculilunatus* (see Boyce, 1989, pl. 10, figs. 7-10) than to those of *Tanybregma timsheansis*. Straight pleural and interpleural furrows and narrow but steeply down-sloping outer pleural field are shared with *H.* (*H.*) *oculilunatus*, not shown in *T. timsheansis*. The poorly-preserved other pygidium (Jell and Stait, 1985b, pl. 1, fig. 14) is similar to the first one. Cranidial similarities with *T. timsheansis* suggest that this species would have a pygidium similar to *T. timsheansis*. Thus, these pygidia are questionably referred to this species.

Remarks. Heller (1954) illustrated an incomplete cranidium (pl. 18, figs. 4, 5). Although its subrectangular glabella agrees with that of *Tanybregma timsheansis*, the deeply-impressed anterior border furrow and relatively narrow anterior border do not agree with the concept of *T. timsheansis*. The specimen is tentatively assigned to this species. A cranidium of *penchiensis* (Lu *et al.*, 1976, pl. 7, fig. 11) exhibits all the diagnostic features of this new species. A pygidium figured by Jell and Stait (1985b, pl. 1, fig. 14) exhibits a nearly parallel-sided axis and lacks a bilobed terminal piece, which does not allow me to confidently associate it with this species. A poorly preserved free cheek (Jell

<div align="center">

265

</div>

and Stait, 1985b, pl. 2, fig. 12) is similar to those of *Tanybregma timsheansis* with respect to the size and curvature of the eye and eye socle. However, the inside of the genal spine is covered with matrix, so that it cannot be determined whether the two librigenal border furrows continue into the genal spine.

<div align="center">

?Family **HYSTRICURIDAE** Hupé, 1953
?Genus **HYSTRICURUS** Raymond, 1913b

</div>

Remarks. Species listed below share features with the Upper Cambrian ptychopariides such as aphelaspidines and elviniids, and with the species that are definitely included within *Hystricurus* in this study. These species appear to be evolutionarily intermediate between *Hystricurus* and the ptychopariides. They are placed questionably in *Hystricurus*.

Hystricurus? *millardensis* and *Hystricurus*? *paramillardensis* are closely related, and *Hystricurus*? *armatus*, *Hystricurus*? *sulcatus*, and *Hystricurus*? *longicephalus*, are related to each other. *Hystricurus*? *parascrofulosus*, *Hystricurus*? *paucituberculatus*, and *Hystricurus*? *clavus*, each are a distinct taxon among the species described below.

<div align="center">

Hystricurus? *millardensis* Hintze, 1953

</div>

1953 *Hystricurus millardensis* Hintze, [part], p. 168, pl. 6, figs. 17a-c, 20, 21, [only].
? 1953 *Hystricurus millardensis* Hintze, [part], p. 168, pl. 6, figs. 18, 19, [only].
1971 *Hystricurus millardensis*, Stitt, [part], p. 46, pl. 8, fig. 18, [only].
? 1988 *Hystricurus millardensis*, Orndoff *et al.*, pl. 1, fig. 13.

Holotype. 26161 housed at Columbia University (no prefix), cranidium; Hintze, 1953, pl. 6, fig. 17; *Symphysurina* Zone; Fillmore Formation, Utah.

Diagnosis. Pair of distinct fossulae at antero-lateral corners of glabella. Preglabellar field moderately swollen. Three pairs of glabellar furrows; S1 long and obliquely directed posteriorly; S2 and S3 short and obliquely directed anteriorly. Eye ridge weakly developed. Anterior cranidial border wide (sag. and exsag.) and moderately convex forwards. Posterior fixigena transverse and ends with rounded distal end. Posterior facial suture transverse and turns smoothly backwards. Glabella with truncated anterior margin and straight lateral margin. Palpebral lobe medium-sized and relatively weakly arched laterally.

Pygidium with semi-circular outline. Axis highly convex with four axial rings. Border furrow weakly impressed. Anterior two pleural and interpleural furrows well-impressed; posterior ones nearly imperceptible.

Remarks. Two free cheeks figured by Hintze (1953, pl. 6, figs. 18, 19) have a very shallow lateral border furrow, which does not correspond to the deep anterior border furrow of the cranidium (Hintze, 1953, pl. 6, fig. 17c). The free cheeks are retained in this species with question.

Specimens referred to *Hystricurus millardensis* after Hintze (1953) exhibit some morphologic deviations from the holotype cranidium from Utah (Hintze, 1953, pl. 6, figs. 17-21). A cranidium from Oklahoma (Stitt, 1971, pl. 8, fig. 17) has a proportionately larger glabella, a narrower (sag.) anterior border and preglabellar field, a much more densely tuberculated fixigenal area, and glabellar furrows as non-pustulose patches rather than furrows per se. Cranidia from New York (Taylor and Halley, 1974, pl. 3, figs. 11-16) have more densely-spaced smaller tubercles on the surface, non-pustulose patches

<div align="center">

266

</div>

representing glabellar furrows, a transverse posterior border, and a more steeply angled posterior facial suture. A cranidium from Newfoundland (Fortey *et al.*, 1982, pl. 3, fig. 10) is similar to the New York cranidium and differs in having glabellar furrows—not as pustulose patches—and a distinct eye ridge running across axial furrows. Of two cranidia from Oklahoma (Stitt, 1983, pl. 4, figs. 1, 2), the larger one (fig. 2) is very similar to the New York and Newfoundland cranidia, but differs in having more slit-like glabellar furrows. All these differences are considered interspecific and all the cranidial materials are assigned to *Hystricurus? paramillardensis* (see below).

The smaller cranidium from Oklahoma (Stitt, 1983, pl. 4, fig. 1), which is smaller (4.6 mm in sagittal length) than the holotype cranidium of *Hystricurus? millardensis*, has a relatively shorter (sag.) and wider (tr.) glabella, an anterior border furrow that shallows sagittally, and a wider anterior border. Orndoff *et al.* (1998, pl. 1, fig. 13) reported the occurrence of *H.? millardensis* from Virginia. The incomplete cranidium has a wider than longer outline, which seems to be due to a sagittal deformation; if it is not deformed, it is more similar to the eulomid (e.g., see Peng, 1992, fig. 18D). These two cranidia are questionably referred to this species. Of interest is that all specimens of *Hystricurus? paramillardensis* occur south of the Transcontinental Arch, indicating that the arch would have played a role as a geographic barrier that separate these two species.

Three pygidia have been referred to this species. Those from Utah (Hintze, 1953, pl. 6, figs. 20, 21) and Oklahoma (Stitt, 1971, pl. 8, fig. 18) are similar to each other. The pygidium from New York (Taylor and Halley, 1974, pl. 3, fig. 10), which is smaller than the Oklahoma specimen and larger than the Utah specimen, mainly differs in having well-developed pleural and interpleural furrows—the other two have weakly-developed furrows, except for the anteriormost one. The New York pygidium is associated with *Hystricurus? paramillardensis*.

Hystricurus? paramillardensis n. sp.

1971 *Hystricurus millardensis*, Stitt, [part], p. 46, pl. 8, fig. 17, [only].
1974 *Hystricurus millardensis*, Taylor and Halley, p. 31-32, pl. 3, figs. 10-16.
1982 *Hystricurus millardensis*, Fortey *et al.*, p. 108, pl. 3, fig. 10.
1983 *Hystricurus millardensis*, Stitt, [part], p. 25-26, pl. 4, fig. 2, [only].

Etymology. "paramillardensis" indicates the morphologic similarities with *Hystricurus? millardensis*.

Holotype. UT 14076, cranidium; Stitt, 1971, pl. 8, fig. 17; *Symphysurina* Zone; McKenzie Hill Limestone, Oklahoma.

Differential Diagnosis. Anterior cranidial border narrow (tr.) and long. Frontal area wider (tr.). Cranidial surface covered with densely-distributed small tubercles. Posterior facial suture diagonal. Palpebral lobe more strongly arched laterally and located more anteriorly (at mid-cranidial length). Pygidium with distinct post-axial ridge. Free cheeks with deep lateral border furrow. Lateral border covered with fine terrace lines. Other features similar to *Hystricurus? millardensis*.

Comparison and Taxonomy of *Hystricurus? millardensis* and *Hystricurus? paramillardensis*. Cranidia of *Hystricurus? millardensis* and *Hystricurus? paramillardensis* are similar to those of the Upper Cambrian aphelaspidines such as *Aphelaspis*. The cranidia of *H.? millardensis* have a pair of fossulae, a slender ocular ridge, slit-like glabellar furrows, truncated anterior and straight-sided lateral glabellar

267

margins, and a swollen preglabellar field. These features are evident in many *Aphelaspis* species (see Palmer, 1965, pl. 8, fig. 14), but not in *Hystricurus* species. The cranidia of *Aphelaspis* mainly differ in having a sharply terminated distal end of the posterior fixigena, a pointed anterior cranidial margin, and in lacking tubercles on the cranidial surface. Pygidia of *H.? millardensis* and *Aphelaspis* (e.g., see Palmer, 1965, pl. 8, figs. 20) are remarkably similar to each other. Their pygidia have a relatively flat pleural field and only one or two anterior pleural furrow(s) that are discernibly impressed. The similarities of *H.? millardensis* to *Aphelaspis* are easily applicable to *H.? paramillardensis*. These two species are questionably retained in *Hystricurus*.

It appears to be protaspid morphologies of *Hystricurus? millardensis* and *Hystricurus? paramillardensis* that will ultimately resolve their taxonomic status. Protaspides of *Aphelaspis* strikingly differ from those of *Hystricurus* (compare Pl. II-44, Figs. 3-6 with Lee and Chatterton, 1997a, figs. 2.1-2.4), which denies any close relationship between the aphelaspidines and *Hystricurus*.

<div align="center">

Hystricurus? armatus (Poulsen, 1937)
Pl. III-2, Figs. 1-6

</div>

1937 *Hystricurus armatus* Poulsen, p. 31, pl. 2, figs. 3-9.
? 1993 *Hystricurus* cf. *H. oculilunatus*, Westrop *et al.*, p. 1631-1632, pl. 3, figs. 10-12.
Holotype. MGUH 3641, cranidium; Poulsen, 1937, pl. 2, figs. 4, 5; possibly *Symphysurina* Zone; Antiklinalbugt Formation, east Greenland.
Diagnosis. Occipital spine with stout base. Anterior cranidial border wide (sag.) and strongly arched dorsally. Anterior cranidial margin strongly convex forwards. Preglabellar field moderately swollen. Glabella with straight lateral margin and rounded anterior margin. Genal caeca weakly developed on anterior fixigena and preglabellar field. Ocular ridge slender, weakly developed, and runs across axial furrows. Three pairs of glabellar furrows weakly impressed.

Pygidium semi-circular in outline. Post-axial ridge weakly developed. Inner pleural field flat and narrow and outer pleural field gently down-sloping; transition between two pleural fields relatively smooth. Border narrow and tubular, and confluent with post-axial ridge. Posterior margin narrowly arched dorsally. Interpleural furrows reach border. Exoskeletal surface smooth.

Free cheek with short genal spine. Genal caeca weakly developed on librigenal field. Posterior facial suture runs outward, resulting in short posterior librigenal border furrow. Lateral and posterior librigenal border furrows merged at postero-lateral corner of librigenal field.

Remarks. A cranidium of *Hystricurus* cf. *H. oculilunatus* from New York (Westrop *et al.*, pl. 3, figs. 10, 12) is remarkably similar to the holotype from East Greenland, except for the presence of terrace lines on the anterior cranidial border and the absence of genal caeca on the frontal area. The pygidium from Greenland lacks tubercles, whereas the one from New York (Westrop *et al.*, pl. 3, fig. 11) bears them. These differences in the ornamentation could be ontogenetic or due to preservation.

<div align="center">

Hystricurus? sulcatus (Poulsen, 1937)
Pl. III-2, Figs. 10-12

</div>

1937 *Hystricurus sulcatus* Poulsen, p. 33-34, pl. 2, figs 1-2.

<div align="center">

268

</div>

? 1983 *Hystricurus millardensis*, Stitt, [part], p. 25-26, pl. 4, fig.1, [only].

Holotype. MGUH 3638, cranidium; Poulsen, 1937, pl. 2, fig. 1; possibly *Symphysurina* Zone; Antiklinalbugt Formation, East Greenland.

Differential Diagnosis. Three pairs of glabellar furrows; S1 obliquely directed posteriorly; S2 and S3 transverse or slightly obliquely directed anteriorly. Glabella wide (tr.) with truncated anterior margin. Anterior cranidial border and border furrow straight transversely. Other cranidial features similar to *Hystricurus*? *armatus*. No other skeletal parts known.

Remarks. An incomplete cranidium from Oklahoma (Stitt, 1983, pl. 4, fig. 1) was identified as *Hystricurus millardensis* (=*Hystricurus*? *millardensis* herein). However, from other specimens of *H.*? *millardensis*, the cranidium differs in having a straight anterior border furrow and posteriorly-curved occipital furrow. These features more agree with the holotype of *Hystricurus*? *sulcatus*. In addition, both have three pairs of slit-like glabellar furrows. However, the Oklahoma cranidium develops a pair of deep fossulae and does not develop the occipital spine. The smaller size of the Oklahoma cranidium suggests that these differences could be ontogenetic. This cranidiium is tentatively assigned to this species.

Comparison and Taxonomy of *Hystricurus*? *armatus* and *Hystricurus*? *sulcatus*. In many aspects, cranidial and pygidial morphologies of *Hystricurus*? *armatus* and *Hystricurus*? *sulcatus* are comparable to those of the Upper Cambrian aphelaspidines (e.g., *Aphelaspis*, see Rasetti, 1965) and elviniids (e.g., *Dunderbergia*, see Rasetti, 1965, pl. 15, figs. 1-11). The aphelaspidines have a smooth exoskeletal surface (tuberculated in *H.*? *armatus* and *H.*? *sulcatus*) and a transverse posterior fixigena with a sharply terminated distal end (forwardly-curved and rounded distal end in *H.*? *armatus* and *H.*? *sulcatus*). Although the presence of the occipital spine is not common to aphelaspidines, such *Aphelaspis* species as *A. arses* bear the spine (see Rasetti, 1965, pl. 13, figs. 16-18). The associated pygidium of *H.*? *armatus* (Pl. III-2, Figs. 3, 4, 6) differs from the aphelaspidine pygidia (e.g., see Rasetti, 1965, pl. 18, fig. 6) by having a wider (tr.) and more convex axis, a taller profile with an abrupt slope change between the flat inner pleural field and the down-sloping outer pleural field, and a wider border and narrower border furrow. The pygidium differs from definite *Hystricurus* species such as H. (*Hystricurus*) *oculilunatus* and H. (*Hystricurus*) *crotalifrons* in that the bands of adjacent pleurae are not fused distally, the terminal piece does not protrude posteriorly, and the postaxial ridge is weakly developed. It seems reasonable that these morphologic differences are morphologic variations within an evolutionary lineage.

Hystricurus? *longicephalus* (Poulsen, 1927)
Pl. III-2, Figs. 7-9

1927 *Hystricurus longicephalus* Poulsen, p. 284-285, pl. 18, fig. 11.

1927 *Hystricurus ravni* Poulsen [part], p. 283-284, pl. 18, figs. 7, 10 [only; include an undescribed pygidium in the bottom of fig. 7; re-illustrated in Pl. III-2, Figs. 7, 8].

? 1927 *Hystricurus quadratus* Poulsen, p. 290, pl. 18, figs. 18, 19.

? 1948 *Hystricurus* aff. *H. missouriensis*, [part], Cloud and Barnes, pl. 38, fig. 19, [only].

1967 *Hystricurus millardensis*, Winston and Nicholls, [part], p. 76, pl. 12, fig. 14, [only].

269

Holotype. MGUH 2344a, cranidium; Poulsen, 1927, pl. 18, fig. 11; possibly *Symphysurina* Zone; Cass Fjord Formation, northwest Greenland.

Differential Diagnosis. Glabella forward-tapering with straight sided lateral margins and truncated anterior margin. Fossulae weakly developed. Preglabellar field slightly swollen. Anterior cranidial border furrow straight. Anterior facial suture laterally convex before anterior cranidial border furrow. Posterior cranidial border furrow straight and obliquely directed forwards. Anterior cranidial border wide (sag.).

Pygidium with transversely elongated outline. Pleural field moderately convex dorsally; separation between inner and outer pleural fields imperceptible. Other features similar to *Hystricurus*? *armatus*.

Remarks. A cranidium of *Hystricurus* (*Triangulocaudatus*) *ravni* (Poulsen, 1927, pl. 18, fig. 7; see also, Pl. III-2, Fig. 9) differs from the holotype of *H.* (*T.*) *ravni* (Pl. III-21, Fig. 8) in having a less strongly forward-tapering glabella with a straight anterior and lateral margin, and a much less divergent anterior facial suture. These cranidial features well accord with the holotype of *Hystricurus*? *longicephalus* (Poulsen, 1927, pl. 18, fig. 11).

A pygidium in the same sample with the holotype cranidium (Poulsen, 1927, pl. 18, fig. 7) and a pygidium assigned to *Hystricurus* (*Triangulocaudatus*) *ravni* are indistinguishable from each other. They differ from the pygidium of the articulated specimen of *H.* (*T.*) *ravni* in having a more transversely elongated outline, a transversely narrower axis, and a shorter terminal piece. The pygidium illustrated together with the holotype cranidium is assigned to *Hystricurus*? *longicephalus*, and the other pygidium assigned to *H.* (*T.*) *ravni* is also transferred into *H.*? *longicephalus*.

Two poorly-preserved cranidia with a rectangular glabella were assigned to *Hystricurus quadratus* (Poulsen, 1927, pl. 18, figs. 18, 19). One of them (fig. 18) bears a strongly convex small palpebral lobe on its right side, which is reminiscent of this species. The rectangular glabella could be due to the deformation.

A pygidium of *Hystricurus* aff. *H. missouriensis* from central Texas (Cloud and Barnes, 1948, pl. 38, fig. 19) is greatly similar to that of *Hystricurus*? *longicephalus*. It differs in having deeper interpleural furrows.

A cranidium of *Hystricurus millardensis* from Texas (Whinston and Nicholls, 1967, pl. 12, fig. 14) is greatly similar to the holotype cranidium of *Hystricurus*? *longicephalus* from northwest Greenland (see Pl. III-2, Fig. 9). The Texas cranidium does not develop three pairs of glabellar furrows which is diagnostic to *Hystricurus*? *millardensis*.

Comparison and Taxonomy. Like the above species, aphelaspidine and elviniid morphologies are evident in cranidia and pygidia of *Hystricurus*? *longicephalus*.

Hystricurus? *parascrofulosus* n. sp.
Pl. III-3, Figs. 9-14

1989 *Hystricurus* (*Paraplethopeltis*) sp. nov. A, Fortey and Peel, p. 12-13, figs. 7A-7G.

Etymology. "parascrofulosus" depicts the similarities with *Hystricurus scrofulosus*.

Holotype. MGUH 18.998, cranidium; Fortey and Peel, 1989, fig. 7A (re-illustrated in Pl. III-3, Figs. 9-11); possibly *Tesselacauda* Zone; Christian Elv Formation, North Greenland.

Diagnosis. Posterior fixigena sharply terminated distally. Posterior facial suture diagonal. Glabella parabolic in outline. Preglabellar field relatively long. Anterior cranidial margin convex forwards. Anterior cranidial border narrow and weakly arched dorsally. Anterior

270

facial suture slightly divergent. Palpebral lobe crescentic and located at mid-cranidial length.

Pygidium semi-circular in outline. Axis wide (tr.); four axial rings and weakly bilobed terminal piece. Outer pleural field gently down-sloping and slightly concave; inner pleural field flat; two fields separated by slope change. Interpleural furrows more weakly impressed and shorter than pleural furrows. Border very narrow and border furrow imperceptible.

Free cheeks with long and slender genal spine. Cranidial surface covered with fine tubercles. Pygidial and librigenal surface smooth.

Remarks. An aphelaspidine affinity is suggested by such pygidial features as a concave outer pleural field, and interpleural furrows that are shallower than pleural furrows, but reach the border; only one pygidial specimen is associated. The presence of bilobation of the terminal piece indicates an affinity with *Hystricurus*. However, the cranidial architecture, in particular the diagonal posterior facial suture and the sharply terminated distal end of the posterior fixigena, approximate aphelaspidine morphologies. This new species is questionably referred to *Hystricurus*. As a result, the subgeneric status of *Hystricurus* (*Paraplethopeltis*) proposed by Fortey and Peel (1989) is denied herein; *Paraplethopeltis* is considered as a separate genus from *Hystricurus*, and placed in the Plethopeltidae (see below).

Hystricurus? *paucituberculatus* Fortey, 1983

1982 *Hystricurus* sp. nov. Fortey *in* Fortey *et al.*, p. 108, pl. 3, figs. 14, 17
1982 *Hystricurus* sp., Kindle, pl. 1.5, fig. 22.
1983 *Hystricurus paucituberculatus* Fortey, p. 185-186, pl. 23, figs. 1-7.

Holotype. ROM 42292, cranidium; Fortey, 1983, pl. 23, figs. 1, 3, 4; *Symphysurina* Zone; Cow Head Group, western Newfoundland.

Diagnosis. Cranidium triangular in outline; anterior cranidial margin strongly forward convex. Anterior cranidial border wide (sag.) and covered with terrace lines and sparsely-distributed tubercles. Anterior cranidial border furrow deep but shallows out towards sagittal line. Preglabellar field slightly swollen and sagittally encroaches anterior cranidial border furrow. Anterior facial suture slightly convergent before anterior cranidial border furrow. Glabella short (sag.). Palpebral lobe of medium-size, weakly arched laterally and located at mid-cranidial length. Posterior facial suture diagonal. Cranidial surface covered with sparsely-distributed tubercles.

Free cheeks with distinct eye socle and short genal spine. Lateral and posterior border furrows merge at postero-lateral corner of librigenal field. Row of tubercles on librigenal field and small and sparsely-distributed tubercles and fine terrace lines on lateral border and genal spine.

Comparison and Taxonomy. From definite *Hystricurus* species, *Hystricurus*? *paucituberculatus* differs in having a shorter (sag.) and wider (tr.) glabella, a straight palpebral furrow, a preglabellar field encroaching the anterior cranidial border furrow— resulting in the furrow shallowing out towards the sagittal line—and a wider (sag.) anterior cranidial border. A similar cranidial architecture is observed in some Upper and Middle Cambrian ptychopariides. *Taenicephalina* from the Upper Cambrian of Newfoundland (see Ludvigsen *et al.*, 1989, pl. 14, fig. 4) only differs in having a relatively smaller glabella and palpebral lobe. *Marjumia* and *Modocia* from the Middle

271

Cambrian of Utah (see Robison, 1964, pl. 87, figs. 2, 10) only differ in having a narrower glabella and a transverse posterior fixigena. The cranidia of these Cambrian ptychopariides lack tubercles, whereas those of *H.? paucituberculatus* bear sparsely-distributed small tubercles.

Since only single small pygidium is associated with *Hystricurus? paucituberculatus* (Fortey, 1983, pl. 23, fig. 5), it is certain that the more information is required to incorporate pygidial formation into the taxonomic assessment. The pygidium differs from those of *Modocia* (see Robison, 1964, pl. 87, fig. 5) in having a pointed posterior margin, a more rapidly tapering axis, and small tubercles on the border, but they share a distinct post-axial ridge and a convex axis. The pygidium of *H.? paucituberculatus* differs from those of Hystricurus in having small tubercles on the border and a pointed posterior margin. The free cheeks of these Middle Cambrian species and *H.? paucituberculatus* are similar to one another, and only differ in the latter having tubercles on their surface. The free cheek of *H.? paucituberculatus* develops a distinct eye socle as those of some Hystricurus species (e.g., see Pl. III-5, Figs. 9, 10). The similarities with the ptychopariides lead to exclude this species from *Hystricurus* and retain it with question.

As for the case of the above species, the protaspid information of *Hystricurus? paucituberculatus* will provide crucial information for the taxonomic status of this species. Protaspides of *Modocia* (see Pl. II-47, Figs. 1-10) greatly differ from those of *Hystricurus* (Lee and Chatterton, 1997a).

<center>

***Hystricurus*? *clavus* Kobayashi, 1960**
Pl. III-4, Figs. 1-5, 7

</center>

1960 *Hystricurus clavus* Kobayashi, p. 236, pl. 14, fig. 5, 6.
1976 *Hystricurus penchiensis* Lu *in* Lu *et al.*, [part], p. 54, pl. 7, fig. 13, [only].
? 1978 *Hystricurus* (*Guizhouhystricurus*) *yinjiangensis* Yin *in* Yin and Lee, p. 486, pl. 164, fig. 8.
1982 *Hystricurus penchiensis*, Kuo *et al.*, pl. 1, fig. 8.
1986 *Hystricurus penchiensis*, Zhou and Fortey, p. 172-173, pl. 1, figs. 5, 8, 12.
1989 *Hystricurus oculilunatus* Ross, Dean [part], p. 23, pl. 14, fig. 2 [only].
1989 *Hystricurus* sp. Dean [part], p. 23, pl. 14, fig. 13 [only].
1996 *Hystricurus* (?*Guizhouhystricurus*) sp. indet., Laurie and Shergold, [part], p. 89, pl. 5, fig. 15, [only; not figs. 13, 14, 16-23].

Holotype. No holotype was designated by Kobayashi (1960).
Neotype. NI 80386, cranidium; Zhou and Fortey, 1986, pl. 1, fig. 5 (re-illustrated in Pl. III-4, Figs. 1, 4, 5); *Callograptus taizehoensis* Zone (equivalent to *Protopliomerops* Zone); Upper Yehli Formation, Northeast China.
Diagnosis. Ocular ridge distinct, runs across axial furrows and apparently confluent with glabellar front. S1 glabellar furrows long, slit-like, obliquely directed posteriorly; S2 short, obliquely directely posterioly, and located behind ocular ridge. Palpebral lobe strongly arcuate. Palpebral furrow deeply impressed. Glabella arch-shaped. Anterior cranidial border straight.

Pygidium with five axial rings and terminal piece. Axis rapidly tapering. Pleural field flat. Pleural and interpleural furrows of nearly equal depth and length. Border narrow and well delimited.
Remarks. Kobayashi (1960) erected *Hystricurus clavus* upon the basis of a poorly-

<center>272</center>

preserved cranidium and free cheek from South Korea (pl. 14, figs. 5, 6). The frontal area of the cranidium is indistinguishable from that of two cranidia of *Hystricurus penchiensis* (=*Hystricurus*? *penchiensis* herein) from northeast China described by Zhou and Fortey (1986, pl. 1, figs. 5, 8). All of them have a nearly parallel-sided anterior facial suture, an arch-shaped glabella, a straight anterior cranidial border furrow, and a preglabellar median furrow. The Chinese cranidia are characterized by having a shorter glabella, a distinct eye ridge running across the axial furrows, and a strongly curved slender palpebral lobe. However, Kobayashi (1960, p. 236) described that it has no glabellar furrows and no eye ridge. Based on the information available to the author, the absence of these structures cannot be justified. It is the architecture of the glabella and the frontal area that leads to assign the Chinese specimens to *H. clavus*. The discovery of a better-preserved cranidium from South Korea (Pl. III-4, Fig. 7) lends additional support to this taxonomic assessment.

As mentioned above, Zhou and Fortey (1986) assigned two cranidia and one pygidium (pl. 1, figs. 5, 8, 12) to *Hystricurus*? *penchiensis*. However, the cranidia differ from the holotype of *H.*? *penchiensis* (Lu *et al.*, 1976, pl. 7, fig. 10) in having a strongly tapering glabella, a distinct eye ridge running across the axial furrows, a preglabellar median furrow, and a deep and long S1 glabellar furrow. These differences are not intraspecific or ontogenetic. These cranidia figured by Zhou and Fortey are re-assigned to *Hystricurus*? *clavus*.

A cranidium from Alberta, which was assigned to *Hystricurus* (*Hystricurus*) *oculilunatus* by Dean (1989, pl. 14, fig. 2) displays amongst others, the ocular ridge reaching the glabellar front. Another small cranidium from Alberta (Dean, 1989, pl. 14, fig. 13) only lacks the preglabellar median furrow and exhibits the cranidial architecture of *Hystricurus*? *clavus*. This small cranidium is considered to represent an earlier ontogenetic stage of *H.*? *clavus*. A cranidium assigned to *H.*? *penchiensis* by Kuo *et al.* (1982, pl. 1, fig. 8) is indistinguishable from the Albertan cranidia.

Yin (*in* Yin and Lee, 1978) erected a subgenus of *Hystricurus*, *Guizhouhystricurus* based on a single cranidium (pl. 164, fig. 8). The cranidium has a distinct ocular ridge and a glabella similar to *Hystricurus*? *clavus*. However, it has a longer (tr.), narrower, and more forward-convex anterior border. Since it is smaller than other specimens, these differences could be ontogenetic or they may be intraspecific. There is little evidence to support *Guizhouhystricurus* as a subgenus of *Hystricurus*. The validity of *Guizhouhystricurus* requires more materials.

Laurie and Shergold (1996) figured two cranidia and several pygidia and questionably identified them as *Hystricurus* (?*Guizhouhystricurus*) sp. indet. One of the cranidia (pl. 5, fig. 15) exhibits all the features of *Hystricurus*? *clavus*. The other cranidium could be referred to a bathyurid such as *Bathyurellus*. The associated pygidia can be referred to a telephinid, since they are very similar to co-occurring telephinids such as *Ompheter* (e.g., see Laurie and Shergold, 1996, pl. 2, figs. 10, 13, 16).

Association of Pygidium. Zhou and Fortey (1986) associated a pygidium (Pl. III-4, Figs. 2, 3) with the two cranidia that are assigned to *Hystricurus*? *clavus* in this study. This pygidium is indistinguishable from a pygidium figured by Lu *et al.* (1976, pl. 7, fig. 13). Both were assigned to *Hystricurus*? *penchiensis*. Since *H.*? *penchiensis* and *Hystricurus*? *clavus* appear to geographically and stratigraphically co-occur—Lu *et* al. (1976) documented the two species in the same sampling horizon—the association of these

273

pygidia to one of these species needs other evidence.

The cranidia of *Hystricurus*? *penchiensis* are more comparable to those of *Tanybregma timsheansis* from Australia, with respect to the glabellar shape, palpebral lobe and the absence of ocular ridge. Thus, *H.*? *penchiensis* is assumed to have a pygidium similar to that of *T. timsheansis*. From the pygidia figured by Zhou and Fortey (1986) and Lu *et al.* (1976), the pygidia of *T. timsheansis* (Pl. III-85, Figs. 11, 14-16) differ in having a subcircular outline, a short spine on the anteriormost axial ring, and a bilobed terminal piece. As a result, the pygidia illustrated by Zhou and Fortey (1986) and Lu *et al.* (1976) are assigned to *Hystricurus*? *clavus*.

Taxonomic conclusion. The presence of a distinct ocular ridge that runs across the axial furrows is a diagnostic feature of *Hystricurus*? *clavus*. A similar condition is evident in some cranidia of *Hystricurus*? *paramillardensis* (e.g., see Stitt, 1971, pl. 8, fig. 17; Fortey *et al.*, 1982, pl. 3, fig. 10) and many Upper Cambrian *Aphelaspis* species (e.g., see Rasetti, 1965, pl. 18, fig. 15). In these taxa, however, the ocular ridge does not cross the axial furrows as conspicuously as it doesin *H.*? *clavus*. In addition, *H.*? *clavus* is easily differentiated by having a larger and highly arched palpebral lobe, a straight anterior cranidial border furrow, a shorter glabella, S1 glabellar furrows that are long and slit-like, and a preglabellar median furrow. The pygidium of *H.*? *clavus* from the Sino-Korean platform is greatly similar to those of *Flectihystricurus*? *wilsoni* (Gobbett, 1960, pl. 15, figs. 10-13); no cranidium of *F.*? *wilsoni* has been reported from outside of Greenland. Compared to the pygidia of other questionable *Hystricurus* species described above, the pygidia of *H.*? *clavus* have a much flattened pleural field and a narrower axis. *H.*? *clavus* appears to be the most morphologically distinct species, among the species that are assigned to *Hystricurus* with question. This species could belong to a family other than the Hystricuridae.

Hystricurus? sp. aff. *H.*? *clavus*

1989 *Hystricurus* sp. Dean [part], pl. 15, figs. 4, 5, 7 [only]

Remarks. A single cranidium of *Hystricurus* sp. from Alberta (Dean, 1989, pl. 15, figs. 4, 5, 7) bears a cranidial architecture similar to *Hystricurus*? *clavus* with respect to the glabellar shape, frontal area, and presence of a preglabellar median furrow. However, it lacks the distinct ocular ridge and has a deep anterior border furrow, two pairs of glabellar furrows, and a strongly forward-convex anterior border.

HYSTRICURUS SPECIES WHOSE TAXONOMIC STATUS CANNOT BE DETERMINED DUE TO POOR PRESERVATION AND/OR ILLUSTRATION

?**Bathyuridae** sp.

1948 *Hystricurus* (?) *antonovi* Weber, p. 9, pl. 1, figs. 19-20.

Remarks. Two incomplete pygidia are assigned to this species. The shape of their axis and their outline are reminiscent of a bathyurid.

Hystricurus? sp.

1948 *Hystricurus binodosus* Weber, [part], p. 7-9, pl. 1, figs. 13, 14, [only].

Remarks. Two incomplete free cheeks from Siberia are assigned to *Hystricurus*

binodosus (Weber, 1948, pl. 1, figs. 13, 14). They have genal caeca which are found in many *Hystricurus* species such as *globosus* and *hillyardensis* (Stitt, 1983, pl. 4, fig. 5, pl. 5, figs. 3, 4). However, their librigenal field is much wider and their lateral border is much narrower.

?**Hystricuridae** sp.

1948 *Hystricurus binodosus* Weber, [part], p. 7-9, pl. 1, figs. 15, 16, [only].

1948 *Hystricurus* (?) sp. cf. *H. quadratus*, Weber, p. 9, pl. 1, fig. 21.

Remarks. Two incomplete free cheeks from Siberia are assigned to *Hystricurus binodosus* (Weber, 1948, pl. 1, figs. 15, 16). They lack a genal spine, which is never observed in *Hystricurus* nor even in the Hystricuridae.

One of the co-occurring cranidia (Weber, 1948, pl. 1, fig. 21), which lacks most of the features except for the glabella, cannot be accurately evaluated. From *Hystricurus*? *quadratus* (Poulsen, 1927, pl. 18, figs. 18, 19) whose generic position is considered questionable in this study, the Siberian cranidium differs in having a much more rounded glabellar margin.

Leiostegium? sp.

1965 (?) *Hystricurus* (?) *kaipingensis* Chang, Lu *et al.*, [part], p. 197, pl. 34, fig. 9, [only].

Remarks. Although poorly preserved and illustrated, the cranidium apparently has no preglabellar field, which indicates that it may belong to *Leiostegium*.

?**Pliomeridae** sp.

1965 *Hystricurus* (?) *kaipingensis* Chang, Lu *et al.*, [part], p. 197, pl. 34, fig. 10, [only].

Remarks. Although poorly preserved and illustrated, the pygidium (Lu *et al.*, pl. 34, fig. 10) appears to have long marginal spines, which indicate it could belong to the Pliomeridae.

?Family HYSTRICURIDAE Hupé, 1953
Genus ROLLIA Cullison, 1944

Type Species. *Rollia goodwini* Cullison, 1944; Jeffersonian Stage; Rich Fountain Formation of Jefferson Group, Missouri.

Included Species. *R. mirabilis* (Ogienko, 1972).

Diagnosis. Palpebral lobe slender, of medium size, and strongly arched laterally. Glabella subquadrate with weakly rounded anterior margin and covered by sparsely distributed tubercles. Three pairs of glabellar furrows; S1 obliquely directed posteriorly and long: S2 obliquely anteriorly or posteriorly and located at mid-glabellar length; S3 being almost imperceptible. Preglabellar field relatively long. Anterior facial suture moderately convex laterally. Palpebral fixigena moderately convex dorsally and covered with sparsely-distributed tubercles.

Comparison with "Hystricurids". Cullison (1944, p. 81) distinguished *Rollia* from *Hystricurus* in having "a relatively shorter, less prominent glabellar furrows, a wider and flatter frontal limb, and larger pustulose palpebral lobes." It is the strongly arched slender

275

palpebral lobes that allows me to readily distinguish *Rollia* from other "hystricurids." *Tanybregma* (see Pl. 85, Figs. 1, 3, 8, 13) and *Hystricurus* (*Hystricurus*) *crotalifrons* (Boyce, 1989, pl. 10, fig. 1) have a palpebral lobe with a curvature similar to that of *Rollia*, but their palpebral lobe is larger and thicker (see Jell and Stait, 1985b, pl. 1, fig. 3, Boyce, 1989, pl. 8, fig. 5). Several *Hystricurus* species, for example, *H.* (*Aequituberculatus*) *globosus* (Stitt, 1983, pl. 5, fig. 1) and *H.* (*Hystricurus*) *exilis* (Ross, 1951, pl. 10, fig. 12) have a slender palpebral lobe comparable to that of *Rollia*. However, the palpebral lobes of the *Hystricurus* species are much more weakly arched laterally. The palpebral lobe of *Flectihystricurus* (see Pl. III-49, Figs. 3) and *Tanybregma* (see Pl. III-85, Figs. 1, 3) is similar to that of *Rollia*, but the lobe of *Flectihystricurus* is more tightly arched and that of *Tanybregma* is much larger. Compared to the palpebral lobe of *Tersella* (see Burskyi, 1970, pl. 2, fig. 1) and *Paratersella* (see Pl. III-65, Fig. 1), that of *Rollia* is much smaller and more slender. With respect to the nature of the palpebral lobes and furrows, *Psalikilopsis* displays the closest condition (Pl. III-73, Figs. 3-5). With *Psalikilopsis*, *Rollia* additionally shares a triangular posterior fixigena and a laterally convex anterior facial suture. However, *Psalikilopsis* is readily differentiated by the posteriorly curved anterior cranidial border. The subquadrate glabella of *Rollia* is similar to that of *Tanybregma timsheansis* (Pl. III-85, Figs. 11-13). The orientation of S1 and S2 glabellar furrows is similar to that of *Hystricurus*? *millardensis* (see Hintze, 1953, pl. 6, fig. 17c). The long preglabellar field of *Rollia*, in particular *R. goodwini*, invites comparsion with *Hyperbolochilus* (see Pl. III-52, Fig. 2) or *Metabowmania* (see Dean, 1989, pl. 17, figs. 1, 4, 11). However, the two latter taxa have a forward-tapering glabella and a small palpebral lobe defined by a straight palpebral furrow.

Ogienko (1984) associated a pygidium (pl. 12, fig. 4) from Siberia with *Hystricurus secundus* (=*Patomaspis*? *secundus* herein). Without any explanation, the same pygidium was associated with *Hystricurus mirabilis* (Ogienko, 1992, pl. 5, fig. 7) which is transferred into *Rollia* in this study. The pygidium bears a strong resemblance to those from Alberta figured by Dean (1989, pl. 14, figs. 5, 6). They share fused adjacent pleural bands separated by deeply and widely impressed pleural furrows, shallow interpleural furrows and tubercles on both pleural bands. A similar pygidial condition is observed in *Hystricurus* (*Hystricurus*) *crotalifrons* (see Boyce, 1989, pl. 10, fig. 7). These pygidia from Siberia and Alberta lack the bilobed terminal piece and have a much wider marginal border furrow and finer tubercles. Although they are considered to represent the pygidium of *Rollia*, more materials are needed for using pygidial information to assess the taxonommic status of *Rollia*.

Comparison with Proetides. The proportional size and curvature of palpebral lobe and depth of palpebral furrow of *Rollia* are close to conditions seen in bathyurids such as *Jeffersonia* (see Cullison, 1944, pl. 34, fig. 17), *Peltabellia* (see Ross, 1951, pl. 17, fig. 12), and *Goniotelina* (see Ross, 1951, pl. 14, fig. 21); see Whittington (1953a) for detailed account for taxonomy of *Peltabellia* and *Goniotelina*. The cranidia of *Peltabellia* bear more similarities with those of *Rollia* with respect to the frontal area and anterior border; these features are more similar to *Rollia mirabilis* than to *Rollia goodwini*.

The pygidium of *Rollia mirabilis* is similar to the bathyurid pygidia in having a concave marginal border and pleural furrows deeper than interpleural furrows (see Whittington, 1953a, pl. 65, fig. 7). Since these two features are not unique to these two taxa (see Boyce, 1989, pl. 10, fig. 7 for *Hystricurus* (*Hystricurus*)), however, these

276

features are not considered to be of taxonomic significance. The pygidia from Alberta appear to be intermediate between the bathyurids and *Hystricurus*.

Taxonomic Conclusion. The similarities to some bathyurids and cranidial similarities to the taxa that are not considered to belong to the Hystricuridae *sensu* herein (e.g., *Psalikilopsis*, *Hyperbolochilus*, etc.) render me to questionably place *Rollia* in the Hystricuridae. More information on the pygidia is needed for more accurate taxonomic assessment.

<center>

Rollia goodwini Cullison, 1944

Pl. III-84, Figs. 11-13

</center>

   1944 *Rollia goodwini* Cullison, p. 81, pl. 34, figs. 33-35.
Holotype. USNM (no specimen number designated); Cullison, 1944, pl. 34, fig. 35 (re-illustrated in Pl. III-84, Figs. 11-13); Jeffersonian Stage; Rich Fountain Formation of Jefferson Group, Missouri.
Diagnosis. S2 glabellar furrow obliquely directed anteriorly. Preglabellar field longer. Glabella short. Tubercles on exoskeletal surface fine and not densely distributed.

<center>

Rollia mirabilis (Ogienko, 1972)

</center>

   1972 *Hystricurus mirabilis* Ogienko, p. 237, pl. 55, figs. 6-8.
   1984 *Hystricurus mirabilis*, Ogienko, [part], p. 64-65, pl. 12, figs. 1, 2, [only].
   1984 *Hystricurus secundus* Ogienko, [part], p. 65, pl. 12, fig. 4, [only].
   ? 1989 *Hystricurus oculilunatus*?, Dean [part], p. 23, pl. 14, figs. 5, 6 [only].
   1992 *Hystricurus mirabilis* Ogienko, p. 93, pl. 5, figs. 5-7.
Holotype. No. 725B/55, cranidium (stored in IgiG museum); Ogienko, 1984, pl. 12, fig. 4; *Pseudomera-Biolgina* Zone; Kimayskiy Horizon, South Siberia.
Diagnosis. S2 glabellar furrows obliquely directed posteriorly. Preglabellar field short. Glabella long. Tubercles on exoskeletal surface coars and densely distributed.
Association of Pygidium. As mentioned above, a pygidium of this species was inadvertently assigned to *Hystricurus secundus* (=*Patomaspis*? *secundus* herein) by Ogienko (1984, pl. 12, fig. 4); no written description of pygidium is found for *P.*? *secundus* (Ogienko, 1984, p. 65). The Alokistocaridae to which *Patomaspis* belongs has a more-generalized ptychopariid-type pygidium (see *Elrathia*, Moore, 1959, fig. 179.1). Two pygidia from Alberta (Dean, 1989, pl. 14, figs. 5, 6) are questionably associated with this species; they could be assigned to another *Rollia* species. They show some similarities to to those of *Paratersella mediasulcata* in having a concave outer pleural field, convex axis, and narrow marginal border furrow, but they differ in lacking tubercles along the distal edge of inner pleural field.

<center>

Genus AMBLYCRANIUM Ross, 1951

</center>

Type Species. *Amblycranium variabile* Ross, 1951; *Tesselacauda* Zone; Garden City Formation, southern Idaho.
Included Species. *A. convergia* n. sp., *A. inflatus* n. sp., *A. transversus* n. sp., *A. hystricuriensis* n. sp., *A.*? *dubium* Lu, 1975.
Diagnosis. Pygidium triangular in outline, with two, three or five marginal spines and tuberculated surface; marginal spines directed partially ventrally. Two or three short

<center>277</center>

spines at distal tip of posterior cranidial border. Anterior cranidial border and lateral librigenal border ornamented with short spines or small tubercles. Lateral and posterior librigenal border furrows shallow out to be absent before postero-lateral corner of librigenal field. Posterior librigenal border short (tr.). Eye socle absent. Posterior facial suture sharply cuts doublure of posterior cranidial border and librigena at acute angle relative to transverse line; doublure of corresponding librigenal region forms triangular projection in dorsal view. Thoracic segments with wide pointed distal end; corresponding ventral doublure of distal end is of equal width. Anterior four segments lacking axial spine, middle segments (at least three) with long axial spine, and posterior segments lacking axial spine.

Comparison with "Hystricurids". Protaspid morphologies of *Amblycranium variabile* (Pl. III-27, Figs. 11-13), in particular, the tuberculation pattern, imply that *Amblycranium* is a member of the Hystricuridae (compare with protaspides of *Hystricurus*, Lee and Chatterton, 1997a, figs. 2.1-2.4). *Paramblycranium*, in particular *P. populum* (see Pl. III-62, Figs. 5, 16), which was formerly identified as *Amblycranium*? *populum* by Ross (1951), shows the closest cranidial morphologies. *Amblycranium* differs in having a less strongly forward-tapering glabella, a straight or slightly curved palpebral furrow, a shorter and more slender genal spine lacking a long median furrow, and short spines along the lateral margin of the librigenal field and genal spine. Some *Parahystricurus* species such as *P. fraudator* and *P. oculirotundus* (Pl. III-64, Figs. 7, 13, Pl. III-63, Figs. 2, 12; see also Ross, 1951) are comparable to *Amblycranium* in lacking tubercles on most of posterior fixigena, and showing a parabolic glabellar outline and parallel to slightly convergent anterior facial suture, but differ in terms of their highly elevated semi-circular palpebral lobe and much wider (exsag.) posterior fixigena. *Flectihystricurus flectimembrus* (see P. III-49, Fig. 3) shares with *Amblycranium* a forward-curving posterior cranidial border, spines at distal tip of posterior border, and a preglabellar field of similar length, but the species differs in having a strongly arched palpebral lobe and furrow, an eye socle, two pairs of glabellar furrows, a genal spine with a median furrow, and a more pointed anterior margin.

In contrast to these cranidial similarities to the "hystricurids," pygidia of *Amblycranium* species radically differ from those associated with any "hystricurid" taxon. They are characterized by having two, three or five pairs of marginal spines.

Comparison with Ptychopariides. Pygidia of *Amblycranium* are similar to those of some olenids such as *Peltura*. However, the former has a sawtooth-shaped outline and tuberculated exoskeleton. Other features of olenids, such as a fused connective suture, are not present in *Amblycranium*.

Comparison with Proetides. A great pygidial similarity is found between *Amblycranium* and *Stenoblepharum*. The Upper Ordovician tropidocoryphid from Argentina has pygidia with three pairs of marginal spines (see Edgecombe *et al.*, 1997, figs. 6.15, 6.16, 6.17) as those of *Amblycranium* species. The pygidia of *Stenoblepharum* differ in having a much wider (tr.) and less strongly tapering axis and lacking regularly-distributed tubercles on the surface. In contrast, the cranidial morphologies differ much from each other (compare Edgecombe *et al.*, 1997, fig. 4. 19 with Pl. III-28, Fig. 1).

Taxonomic Conclusion. Protaspid and cranidial features of *Amblycranium* suggest its placement in the Hystricuridae. In contrast, pygidial features of *Amblycranium* lend no support to this taxonomic assessment. For the present, *Amblycranium* is questionably left

278

in the Hystricuridae.

<center>*Amblycranium variabile* Ross, 1951</center>

Diagnosis. Glabella parabolic in outline and longer than wide, with lateral margin being parallel-sided or slightly convex laterally. Anterior facial suture parallel-sided to slightly convergent. Palpebral lobe located at mid-cranidial length. Posterior facial suture wavy in outline. Pygidium with three pairs of marginal spines and rapidly tapering axis with three axial rings and terminal piece.

Separation of *Amblycranium* Species Based on Cranidial Morphologies. Ross (1951) claimed that there is a great variation on the course of the anterior facial suture in his collections of *Amblycranium variabile*. Two extremes are illustrated; one with a parallel-sided suture (pl. 13, fig. 14) and the other with a convergent suture (pl. 13, fig. 11). However, materials collected in this study reveal that there are other variations such as the glabellar shape and size, and the nature of the posterior cranidial border, which are regarded as of specific value. *Amblycranium convergia* is differentiated from *A. variabile* in having a convergent anterior facial suture (thus resulting in a transversely narrower frontal area), a rounded anterior cranidial margin and a relatively shorter and wider glabella. *Amblycranium inflatus* is readily distinguished by a forward-expanding large glabella and a relatively shorter preglabellar field, *Amblycranium transversus* by a transversely straight and very narrow (exsag.) posterior fixigena, and *Amblycranium hystricuriensis* by a strongly forward-tapering glabella with lateral margins being straight-sided. These differences appear to be manifest in the fairly large cranidia, whereas smaller cranidia are much more similar. The smaller cranidia are assigned to whichever species of *Amblycranium* is represented by the larger co-occurring cranidia.

Association of Pygidium. A partially articulated specimen (UA 12224) from R5-86 consists of five thoracic segments and a complete pygidium (Pl. III-27, Figs. 3, 4). All the thoracic pleurae have a distal tip that is flat, wide, and curved backwards, and the anterior three segments have a long axial spine and the posterior two lack the spine. Doublure corresponding with these distal tips is broad (tr.), being of equal dimension to the dorsal counterpart. The pygidium has three marginal spines that are curved in the same fashion as the distal thoracic pleural tips (see ventral view, Pl. III-27, Fig. 4). Another partially articulated specimen (UA 12223) of *Amblycranium variabile* from R5-76.4 consists of a complete cranidium, free cheeks, and four thoracic segments (Pl. III-27, Figs. 1, 2). The anterior two thoracic segments have a spinose flat distal pleural end and the posterior two have a wider, backwardly-curved distal end. A conspicuous tubercle is present on the posterior thoracic pleural band at the mid-pleural length. The shape of the distal end of the posterior segments and the presence of the tubercle are indistinguishable from the articulated thoracopygidium from R5-86 (UA 12224). This leads to assign the thoracopygidial specimen to *A. variabile*.

A pygidium indistinguishable from the pygidium of UA 12224 is illustrated by Ross (1951, pl. 19, figs. 5, 7). Pygidia showing indistinguishable morphologies are found in R6-55, R6-35, R6-38, R5-76.4, R5-86, R5-87.7, and SE-152, all of which belong to the *Tesselacauda* Zone; cranidial materials of many *Amblycranium* species occur in the same sampling horizons. Ross (1951) suggested that the pygidium would be possibly associated with *Protopeltura* or *Paenebeltella* of the Olenidae. Ross (1951) assigned a pygidium (pl. 19, fig. 10) to *Paenebeltella vultulata* with some confidence. Many

<center>279</center>

pygidial materials of *P. vultulata* co-occur in several sampling horizons with the cranidial materials (Pl. III-58, Figs. 12, 16-25), supporting the association of the pygidium. No cranidial materials referrable to *Protopeltura* have been found either in the Garden City Formation or Fillmore Formation.

Many olenids indeed have a pygidium with marginal spines and conforming spinose thoracic pleural tips (Henningsmoen, 1957; Moore, 1959). However, it is rare that the olenids develop a long thoracic axial spine on only some thoracic segments. Some olenids such as *Parabolina* have a small node or short spine on "all" thoracic segments (Moore, 1959, fig. 195.3), and others such as *Eurycare* have a long axial spine on only "one" thoracic segment (Moore, 1959, fig. 195.8). *Protopletura* (Henningsmoen, 1957, pl. 2, fig. 2, pl. 24, fig. 1) does have a pygidium with three pairs of marginal spines, but it lacks thoracic axial spine(s). *Peltura* (Henningsmoen, 1957, pl. 2, fig. 1, pl. 25, figs. 9, 11, 14, 15, 17) has a pygidium possessing three pairs of spines which is most similar to the pygidium of UA 12224, but the spines are much longer and are connected by a very smoothly indented margin, not a sawtooth-shaped margin as observed in UA 12224. The olenid pygidia do not develop tubercles on their surface, whereas the pygidium of UA 12224 and other disarticulated pygidia collected in this study have distinct tubercles on their surface. It is concluded that the partially articulated thoracopygidial specimen, UA 12224 cannot be associated with the olenids.

The association of a pygidium with other *Amblycranium* species is made upon the basis of co-occurrence data and degree of cranidial similarities with *Amblycranium variabile*. In terms of the number of marginal spines, there are three variations, two, three, and five; those with three, assigned to *Amblycranium variabile*, are most abundant in several sampling horizons. A pygidium with two pairs of marginal spines was recovered from a single sampling horizon, R5-76.4 (97) (Pl. III-30, Fig. 2). Since it is of similar size to many other pygidial specimens with three pairs of spines, it is considered to be a fully-grown specimen. Due to its rarity, the pygidium is associated with a rare co-occurring subspecies, *Amblycranium convergia convergia*.

From R6-35, R6-38, and R11-48.7, two pygidial morphotypes (one with three marginal spines and the second with five spines) occur. From the same sampling horizons, cranidial materials of two *Amblycranium* species, *A. transversus* and *A. hystricuriensis* occur. The pygidia with three marginal spines differ from those of *Amblycranium variabile* in being more dorsally convex, and having a more convex axis and a dorsally arched posterior margin. The cranidia of *A. variabile* are more similar to those of *A. hystricuriensis* than to those of *A. transversus*, which is characterized by a transversely elongated posterior fixigena. Thus, the pygidia with three marginal spines are assigned to *A. hystricuriensis* and those with five marginal spines to *A. transversus*. **Different Configurations of Thoracic Axial Spine(s).** Besides the possession of the pygidial marginal spines, it is also possible to separate *Amblycranium* from other "hystricurids" with respect to which thoracic segment from the anterior begins to develop the axial spine. A degree three meraspid specimen of *Amblycranium variabile* (Pl. III-27, Figs. 14, 15) demonstrates that at least three thoracic segments have the long axial spine and the most anterior one is located in the fifth thoracic segment from the anterior. In comparison, the meraspid specimens of *Spinohystricurus* (Pl. III-16, Figs. 1, 4) demonstrate that the axial spine develops in the third or fourth segment from the anterior. Both taxa develop more than three axial spines in consecutive middle segments.

280

Parahillyardina newfoundlandia (Boyce, 1989, pl. 6, fig. 6; see also Pl. III-21, Fig. 9) and *Songkania smithi* (an aulacopleurine, Adrain and Chatterton, 1995a, fig. 5.1) each develops only one thoracic axial spine on their fifth thoracic segment from the anterior, and *Otarion diffractum* (an otarionine, Adrain and Chatterton, 1994, fig. 12.1, 12.5) develops only one in its sixth segment: the latter configuration is common among other aulacopleurids.

Paenebeltella vultulata develops a long axial spine on at least two thoracic segments. Unlike the proetid species mentioned above, there is a thoracic segment lacking the axial spine between the two thoracic segments (Pl. 58, Figs. 9, 10).

Four Subspecies of *Amblycranium variabile*. In this study, four subspecies of *Amblycranium variabile* are recognized on the basis of the cranidial features. *A. variabile profusum* is characterized by a parallel-sided anterior facial suture and a parallel-sided lateral glabellar margin. *A. variabile flexum* is distinguished by a posteriorly strongly curved posterior cranidial border and a strongly convergent anterior facial suture. *A. variabile rectum* is discriminated by a pointed distal end of the posterior fixigena and a straight posterior facial suture. *A. variabile parallelum* is separated from other subspecies in having a large and short (sag.) glabella with a convex lateral margin. There appear to be intermediate forms (in particular, smaller-sized cranidia) between these subspecies.

Amblycranium variabile profusum **n. subsp.**
Pl. III-27, Figs. 1-15, Pl. III-28, Figs. 1-15

1951 *Amblycranium variabile* Ross, [part], p. 64-66, pl. 13, figs. 10, 12-14, 17, 18, [only].

1973 *Amblycranium variabile*, Terrell, p. 71, pl. 4, figs. 5, 6.

? 1975 *Amblycranium* (?) *dubium* Lu, [part], p. 286-287, pl. 2, fig. 13, [only].

1997a *Amblycranium variabile*, Lee and Chatterton, [part], p. 869, figs. 3.5, 7.1-7.3, 7.9, [only].

Etymology. "profusum" denotes that it is most abundant subspecies of *Amblycranium* found in this study.

Holotype. Y.P.M. 18020, cranidium; Ross, 1951, pl. 13, figs. 14, 17, 18; *Tesselacauda* Zone; Garden City Formation, southern Idaho.

Diagnosis. Anterior facial suture parallel-sided and turns inwards before anterior border furrow. Glabella with parallel-sided lateral margin. Short spines develop along lateral librigenal border and outer and inner margins of genal spine.

Remarks. Three protaspid specimens (Lee and Chatterton, 1997a, figs. 7.1-7.3) are assigned to this subspecies. A poorly-preserved cranidium from China (Lu, 1975, pl. 2, fig. 13) has a parabolic glabella with a straight lateral margin. Because other features are not preserved, the specimen is questionably assigned to this subspecies.

Amblycranium variabile flexum **n. subsp.**
Pl. III-28, Figs. 16-23

1951 *Amblycranium variabile* Ross, [part], p. 64-66, pl. 13, figs. 11, 15, 16, [only].

Etymology. "flexum" denotes that the posterior cranidial border strongly turns forwards at distal end.

Holotype. Y.P.M. 18019, cranidium; Ross, 1951, pl. 13, figs. 11, 15, 16; *Tesselacauda* Zone; Garden City Formation, southern Idaho.

281

Diagnosis. Posterior cranidial border strongly turns forwards at distal end. Anterior facial suture strongly convergent.

Remarks. A pygidium (Pl. III-28, Fig. 22), which is almost indistinguishable from pygidia of *Amblycranium variabile profusum*, is assigned to this species simply because of the co-occurrence with cranidial materials in SE-152.

Amblycranium variabile rectum n. subsp.
Pl. III-29, Figs. 1-6

Etymology. "rectum" describes the straight posterior facial suture.

Holotype. UA 12246, cranidium; Pl. III-29, Fig. 1; *Tesselacauda* Zone; Garden City Formation, southern Idaho.

Diagnosis. Posterior fixigena with pointed distal end and posterior facial suture fairly straight. Pygidium with shorter axis and rounded terminal piece. Pygidial axis ends well short of posterior margin.

Amblycranium variabile parallelum n. subsp.
Pl. III-29, Figs. 7-14

1997a *Amblycranium variabile*, Lee and Chatterton, [part], p. 869, figs. 7.6, 7.7 [only].

Etymology. "parallelum" describes the parallel-sided anterior facial suture.

Holotype. UA 12250, cranidium; Pl. III-29, Figs. 7-10; *Tesselacauda* Zone; Garden City Formation, southern Idaho.

Diagnosis. Anterior facial suture straight and parallel-sided. Glabella large and shorter (sag.), with lateral margin being convex laterally. Librigenal lateral border ornamented with very small tubercles.

Amblycranium convergium n. sp.

Etymology. "convergium" describes the anterior facial sutures that are gently convergent forwards.

Diagnosis. Anterior facial suture strongly convergent. Anterior border convex forwards and short (tr.). Preglabellar field long (sag.). Glabella short with lateral margin being slightly convex laterally.

Amblycranium convergium convergium n. subsp.
Pl. III-30, Figs. 1-3

Holotype. UA 12254, cranidium; Pl. III-30, Fig. 1; *Tesselacauda* Zone; Garden City Formation, southern Idaho.

Diagnosis. Pygidium with two pairs of marginal spines. Glabella short and parabolic in outline, with lateral margin being straight.

Amblycranium convergium paraconvergium n. subsp.
Pl. III-30, Figs. 4-12

1997a *Amblycranium variabile*, Lee and Chatterton, [part], p. 869, figs. 7.4, 7.5 [only].

Etymology. "paraconvergium" describes the cranidial similarities with *Amblycranium convergium convergium*.

Holotype. UA 12258, cranidium; Pl. III-30, Figs. 5-7; *Tesselacauda* Zone; Garden City Formation, southern Idaho.

Diagnosis. Frontal area long (sag.) and narrow (tr.). Glabella large with lateral margin being convex laterally and frontal margin being rather pointed. Exoskeletal surface covered with finer tubercles.

Remarks. Three pygidia from R5-87.7, R5-87.7A, and R5-86, are tentatively associated with this species. They co-occur with cranidial materials of this species.

<center>

Amblycranium inflatum n. sp.

Pl. III-30, Figs. 13-17

</center>

Etymology. "inflatum" describes the inflated forward-expanding glabella.

Holotype. UA 12265, cranidium; Pl. III-30, Figs. 14-17; *Tesselacauda* Zone; Garden City Formation, southern Idaho.

Diagnosis. Glabella large, strongly convex, and expanding forwards up to mid-palpebral point and then rapidly tapering forwards. Palpebral lobe located anterior to mid-cranidial length. Anterior cranidial border very narrow (sag. and exsag.). Anterior facial suture relatively straight and convergent. Posterior fixigena wide (exsag. and tr.)

<center>

Amblycranium transversum n. sp.

Pl. III-31, Figs. 1-19

</center>

Etymology. "transversum" depicts that the posterior fixigena is transversely straight and narrow.

Holotype. UA 12266, cranidium; Pl. III-31, Figs. 1-4; *Paraplethopeltis* or *Leiostegium-Kainella* Zone; Garden City Formation, southern Idaho.

Diagnosis. Posterior fixigena very narrow (exsag.) and straight transversely. Palpebral lobe located posterior to mid-cranidial length. Base of genal spine attached to librigenal field without very little change of curvature of lateral margin of free cheek. Pygidium with five marginal spines and coarse tubercles.

<center>

Amblycranium hystricurusum n. sp.

Pl. III-32, Figs. 1-17

</center>

? 1951 *Amblycranium*? sp. Ross, pl. 16, figs. 11, 15, 16.

Etymology. "hystricurusum" denotes its cranidial morphologic similarities with *Hystricurus*.

Holotype. UA 12284, cranidium; Pl. III-32, Figs. 8-10; *Paraplethopeltis* or *Leiostegium-Kainella* Zone; Garden City Formation, southern Idaho.

Diagnosis. Glabella forward-tapering with lateral margin being straight. Frontal area wide (tr.). Pygidium with wide convex axis, and dorsally uparched posterior margin.

Remarks. The forward-tapering glabella of this species is similar to that of such species as *Hystricurus*? *missouriensis* and *Spinohystricurus terescurvus* (see Pl. III-18, Fig. 1), but not similar to those of *Amblycranium* species that are mostly parabolic in outline. However, it has a slightly curved palpebral furrow and three short spines at distal end of posterior cranidial border which are diagnostic of *Amblycranium. Hystricurus*? aff. *H.*? *missouriensis* (Pl. III-21, Figs. 1-7) is similar to this species in having a forward-tapering glabella with straight-sided lateral margin and slightly convergent anterior facial suture.

A cranidium (Ross, 1951, pl. 16, figs. 11, 15, 16) is questionably assigned to this species because it has a forward-tapering glabella, a pointed posterior fixigena and a moderately forward-curved posterior border, but the specimen shows an inflated

<center>

283

</center>

palpebral lobe and a slightly divergent anterior facial suture.

Amblycranium? *dubium* Lu, 1975

1975 *Amblycranium* (?) *dubium* Lu, [part], p. 286-287, pl. 2, figs. 11, 12, 15, [only; not fig. 14].

Diagnosis. Glabellar forward-expanding, with pair of glabellar furrows which is isolated from axial furrows. Anterior cranidial margin long (tr.) and straight; frontal area wide (tr.). Anterior facial suture parallel-sided and abruptly turns at anterior border furrow. Palpebral furrow shallow and wide, and moderately curved outwards. Genal spine base located much anterior to posterior margin. Exoskeletal surface ornamented by coarse tubercles.

Remarks. The presence of the distinct glabellar furrow pair and wider (tr.) frontal area suggest a questionable assignment of this species to *Amblycranium*. With regard to the long anterior cranidial margin, this species is similar to *Amblycranium hystricurusum*. The cranidium illustrated in plate 2, figure 14 (Lu, 1975) cannot be taxonomically determined, because it is illustrated at an oblique angle. The forward-expanding glabella and its proportional size are reminiscent of *Heterocaryon* (e.g., see Ludvigsen, 1982, figs. 55A-D). But the latter taxon has a very small palpebral lobe, a steep posterior facial suture, and a convergent anterior facial suture.

Genus TERSELLA Petrunina, 1973

Type Species. *Tersella strobilata* Petrunina, 1973; Tremadocian; west Siberian.

Included Species. *T. novozemelica* (Burskyi, 1970), *T. sulcata* Ogienko 1984, *T. paichoica* (Burskyi, 1970), *T. magnaocula* Burskyi, 1970, *T. truncata* (Park, 1993), *T.? altaica* Petrunina, 1973.

Diagnosis. Palpebral lobe large (equal to glabellar length to one-third of cranidial length) and crescentic in outline. Glabella slightly forward-tapering and elongated, with truncated anterior margin and straight lateral margin. Preglabellar field convex dorsally; furrow present in some species to laterally define swelling. Anterior fixigenal area narrow (tr.). Palpebral area of fixigenae moderately convex. Posterior facial suture straight and diagonal; posterior fixigena sharply terminated. Pygidium semi-circular in outline, with four axial rings including terminal piece. Outer pleural field slightly concave.

Comparison with "Hystricurids". Although it was Burskyi (1970) who firstly illustrated specimens of *Tersella*—four specimens of *Tersella* (?) *magnaoculus* and one pygidial specimen of *Tersella* sp.—he provided no written accounts for the genus. Later, Petrunina (1973) officially erected *Tersella* as a new genus and placed it in the Hystricuridae. Petrunina (1973) noted that *Tersella* resembles *Nyaya* which was erected as a new genus by Rozova (1963) and later assigned to the Hystricuridae by Rozova (1968), without providing any detailed account of the similarities. The similarities, if any, seem to be general which are shared by many other taxa. Petrunina (1973) differentiated *Tersella* from *Nyaya* based on that the former has a larger palpebral lobe, a less divergent anterior facial suture, and a swelling on the preglabellar field. In addition, the curvature of the palpebral lobe in *Tersella* is much greater than that of *Nyaya* and the palpebral furrow is much deeper in *Tersella*. The anterior cranidial border furrow of *Nyaya* shallows out sagittally like some *Tersella* species such as *T. novozemelica* (see Petrunina, 1973, pl. 1, fig. 4). Pygidia of *Nyaya* (see, Rozova, 1963, pl. 2, fig. 12) have interpleural

284

furrows that are of equal depth and width as the pleural furrows, whereas those of *Tersella* (see Burskyi, 1970, pl. 3, fig. 4) do not have any recognizable interpleural furrows. These similarities and dissimilarities are applicable to many Upper Cambrian taxa from Siberia such as *Nganasanella* and *Amorphella* (see Rozova, 1963, pl. 1, fig. 2, pl. 2, fig. 1)

It is the large palpebral lobe that characterizes *Tersella*. Such "hystricurid" taxa as *Tanybregma* and *Paratersella* have a similar-sized palpebral lobe. The palpebral lobe of *Tanybregma* is more slender and more strongly arched and that of *Paratersella* is defined by a less deeply impressed palpebral furrow. Other cranidial features, for instance, the long preglabellar field of *Tanybregma* and the preglabellar median furrow of *Paratersella* allow for easily differentiating *Tersella* from these other genera possessing a large palpebral lobe. Pygidia of *Paratersella* (see Pl. III-66, Figs. 1-4) are similar to those of *Tersella* in sharing a semi-circular outline and a concave outer pleural field. However, the pygidia of *Paratersella* have a tubercle along the distal edge of the inner pleural field (most conspicuous on the anteriormost pleural segment), whereas those of *Tersella* lack this feature, thus lacking any distinct separation of inner and outer pleural fields.

Comparison with Ptychopariides. A similarity is observed in cranidia of *Tersella* and some *Changshania* species such as *C. equalis* from China (a changshaniid, see Lu *et al.*, 1965, pl. 92, figs. 7, 8; Qian, 1994, pl. 17, fig. 8); Shergold and Webers (1992) placed the Changshaniidae in the superfamily Damesellacea. The cranidia of *C. equalis* have an elongated forward-tapering glabella with a truncated anterior margin, a glabellar front slightly expanding anterior to the palpebral lobe, and a palpebral furrow curving towards the center of palpebral fixigena at its anterior and posterior end. The presence of the preglabellar swelling is not observed in *Changshania* species. Pygidia of some other *Changshania* species (e.g., see Qian, 1994, pl. 17, fig. 4) are comparable to those of *Tersella*, in particular, to *T. paichoica* and *T. magnaocula* (see Burskyi, 1970, pl. 2, fig. 6, pl. 3, figs. 4, 7), and differ only in having a discrete marginal border and a narrower (tr.) axis.

Cranidia of *Prosaukia* from the Laurentian continent (e.g., see Westrop, 1986, pl. 4, figs. 8-13) resemble those of *Tersella*. The cranidia share an anterior border furrow which shallows out sagittally and a palpebral furrow which displays the same curvature. Such *Tersella* species as *T. paichoica* have two pairs of glabellar furrows like most *Prosaukia* species do. However, the cranidia and glabella are much wider than those of *Tersella*, as if the latter would have been laterally compressed. However, the saukiid pygidia greatly differ from those of *Tersella* in having a broad concave outer pleural field (often referred to as a marginal border, but the pleural field is considered to be an area which the pleural and/or interpleural furrows reach), a narrower axis with more axial rings, and a slender postaxial ridge. The cranidial architecture of *Tersella* is comparable to that of *Crepicephalina* (a crepicephalid, Zhang and Jell, 1987, pl. 37, figs. 12, 13), but the pygidia of *Crepicephalina* are much different from those of *Tersella* in developing a pair of long marginal spines (see Zhang and Jell, 1987, pl. 38, fig. 4).

Comparison with Proetides. The large arched palpebral lobe of *Tersella* is comparable to that of some bathyurids such as *Omuliovia* (Chugaeva, 1973, pl. 6, figs. 1-6). However, the bathyurids have a glabella with a pointed anterior margin reaching the anterior border furrow. The relatively wide and slightly concave pygidial marginal border of *Tersella* is also comparable to many bathyurids including *Omuliovia* (Chugaeva, 1973,

285

pl. 5, figs. 1-3).

Taxonomic Conclusion. Cranidial similarities with the Lower Ordovician *Nyaya* and other Upper Cambrian taxa from Siberia make it possible to place *Tersella* in the same group that includes all these Siberian taxa. The similarities with *Paratersella*, which is questionably placed in the Hystricuridae, suggest the assignment of *Tersella* to the family with question.

<div align="center">

Tersella strobilata Petrunina, 1973
</div>

? 1946 *Hystricurus affinis* Poulsen, p. 331-332, pl. 23, figs. 12, 13.

1973 *Tersella strobilata* Petrunina, p. 61-62, pl. 1, figs. 12, 13, 15.

Holotype. No. 1324/13, cranidium; Petrunina, 1973, pl. 1, fig, 12; late Tremadocian to early Arenigian; west Siberia.

Diagnosis. Palpebral lobe large (about half of cranidial length) and slender, with inwardly strongly curved anterior and posterior ends. Swelling on preglabellar field inverted trapezoidal in outline and defined laterally by moderately broad furrows. Anterior cranidial border furrow distinctly impressed anterior to preglabellar swelling. Anterior cranidial border slender. Pygidium with strongly convex axis and post-axial ridge.

Association of Pygidium. Pygidia were associated for five species of *Tersella*. The pygidia of *T. strobilata* (Petrunina, 1973, pl. 1, fig. 15; Timokhin, 1989, pl. 7, figs. 8, 9) have a highly convex and gently tapering axis, a moderately convex pleural field, and a post-axial ridge, whereas that of *T. concinna* (=*T. novozemelica* herein) has a less convex subtriangular axis and a rather flat pleural field (Petrunina, 1973, pl. 1, fig. 14). The pygidia of *T. truncata* (e.g., Pl. III-46, Figs. 8, 9) are similar to those of the former species. Pygidia of *T. paichoica* and *T. magnaocula* (Burskyi, 1970, pl. 2, fig. 6, pl. 3, fig. 4) differ from those of *T. strobilata* in having a less convex axis and a more transversely elongated outline. Of these pygidia, the pygidium of *T. novozemelica* appears to be flattened; if it is not deformed, it resembles pygidia of olenid-like species (see Pl. III-15, Figs. 5, 6).

Cranidial similarities with *Paratersella*, in particular, the large palpebral lobe, allow for assuming that pygidia of *Tersella* are similar to those of *Paratersella*. The pygidia of both genera are similar to each other in having fused adjacent pleural bands; those of *Paratersella* differ in developing tubercles at the end of the fused pleural bands (Pl. III-66, Figs. 1-10).

Remarks. A poorly preserved cranidium identified as *Hystricurus affinis* from Ellesmere Land (Poulsen, 1946, p. 23, figs.12, 13) has a swelling on the preglabellar field, a truncated anterior margin of the glabella, and a tuberculated cranidial surface. These features are indistinguishable from *Tersella strobilata* (Petrurina, 1973, pl. 1, figs. 12, 13). However, the glabellar lateral margin is more strongly convergent and the anterior cranidial border furrow is deeper. The cranidium from Ellesmere Land is questionably assigned to this species.

<div align="center">

Tersella novozemelica (Burskyi, 1970)
</div>

1970 *Nyaya novozemelica*, Burskyi, pl. 2, figs. 1, 3

1970 *Tersella* (?) *magnaoculus*, Burskyi, pl. 3, fig. 3

1973 *Tersella concinna* Petrunina, p. 62, pl. 1, figs. 4, 14.

<div align="center">

286
</div>

Holotype. no specimen number designated; cranidium, Burskyi, 1970, pl. 2, fig. 1; Early Ordovician; Sokolysky Horizon, nothern Pai-Khoya, Russia

Diagnosis. Cranidial exoskeleton smooth. Anterior cranidial border thick. Anterior cranidial border furrow curved backwards sagittally. Pygidium with wide axis and straight pleural furrows.

Remarks. Cranidial morphologies of *Nyaya novozemelica* (Burskyi, 1970, pl. 2, figs. 1, 3) cannot be accommodated within the concept of *Nyaya*. In particular, the large palpebral lobe and preglabellar swelling allow for readily removing the species from *Nyaya*. These features are diagnostic of *Tersella*, and the cranidia differ from *Tersella strobilata* in having a smooth exoskeleton and a thicker anterior border.

Cranidia of *Tersella concinna* (Petrunina, 1973, pl. 1, figs. 4, 14) and *Tersella*? *magnaocula* (Burskyi, 1970, pl. 3, fig. 3) are indistinguishable from those of *T. novozemelica*.

Tersella sulcata Ogienko, 1984

1984 *Tersella sulcata* Ogienko, p. 64, pl. 7, figs. 15, 16.
1989 *Tersella sulcata*, Timokhin, p. 87, pl. 7, fig. 5.
1989 *Tersella lenaica* Timokhin, [part], p. 87-89, pl. 7, figs. 6, 7, 8, 9.
1992 *Tersella sulcata*, Ogienko, [part], p. 91-93, pl. 5, figs. 1, 2, 4, 7 [only].
? 1994 Gen *et*. sp. indet. 2, Qian, pl. 34, fig. 1.

Holotype. No. 727B/45, cranidium; Ogienko, 1984, pl. 7, fig. 15; *Ijacephalus-Nyaya* Zone; Loparski horizon, south Siberia.

Diagnosis. Palpebral lobe of medium size (one-third of cranidial length) with curved anterior and posterior ends. S1 glabellar furrows straight, distinctively-impressed, and obliquely directed posteriorly. S2 weakly impressed and obliquely directed posteriorly. Cranidial surface ornamented with small tubercles.

Remarks. *Tersella lenaica* erected by Timokhin (1989) is synonymized under this species. Their cranidial morphologies are not distinguishable from each other.

Qian (1994) illustrated a cranidium from the Upper Cambrian Changshan Stage in China. Only the frontal half of this cranidium is preserved (pl. 34, fig. 1) and it is very similar to this species.

Tersella paichoica (Burskyi, 1970)

1948 *Hystricurus*(?) *oculeus*, Weber, p. 9-10, pl. 11, fig. 28.
1970 *Nyaya paichoica*, Burskyi, pl. 2, figs. 4, 6
1970 *Nyaya*? sp., Burskyi, pl. 2, fig. 2
1970 *Nyaya sokoliensis*, Burskyi, pl. 3, fig. 5
1970 *Tersella* sp., Burskyi, pl. 3, fig. 7

Holotype. no specimen number designated; cranidium, Burskyi, 1970, pl. 2, fig. 4; Early Ordovician; Sokolysky Horizon, nothern Pai-Khoya, Russia.

Diagnosis. S1 and S2 glabellar furrows weakly-developed and obliquely directed backwards. Anterior cranidial border furrow anterior to preglabellar swelling weakly impressed. Glabella short (sag.).

Remarks. A pygidium (Burskyi, 1970, pl. 2, fig. 6) is associated with this species. Cranidial similarities with *Paratersella mediasulcata* support this association. A pygidium of *Tersella* sp. (Burskyi, pl. 3, fig. 7) is assigned to this species because it bears

287

a great resemblance and occurs in the same biozone as *Tersella paichoica*.

Tersella magnaocula Burskyi, 1970

1970 *Tersella* (?) *magnaoculus*, Burskyi, pl. 3, figs. 1, 2, 4

Holotype. no specimen number designated; cranidium; Burskyi, 1970, pl. 3, fig. 2; Early Ordovician; Sokolysky Horizon, nothern Pai-Khoya, Russia.

Diagnosis. Palpebral lobe very large (tr. and exsag.) and frontal area very short (sag.). Glabellar lateral margin parallel-sided in posterior half and convegent in anterior half.

Tersella truncata (Park, 1993)
Pl. III-46, Figs. 6-12

? 1960 *Hystricurus* cfr. *megalops* Kobayashi, p. 236, pl. 13, fig. 21.

1993 *Hystricurus truncatus* Park, [part], p. 90-93, pl. 4, figs. 1-4, 6, 7, 9, 10 [only].

1994 *Hystricurus* sp. cf. *H. megalops* Choi *et al.*, p. 217-218, fig. 2H, I.

1997 *Hystricurus megalops*, Kim and Choi, fig. 3O, P.

Holotype. SNUP 338, cranidium; see Pl. III-46, Figs. 6, 7, 10; *Protopliomerops* Zone; Mungok Formation, South Korea.

Diagnosis. Cranidium short (sag.). Anterior border moderately arched dorsally. Preglabellar field moderately convex. Palpebral furrow deep and wide. Free cheek with semi-circular ocular platform.

Remarks. The slender (sag.and exsag.) anterior border and divergent anterior facial suture are very similar to those of *Tersella strobilata*. Except for having three axial rings including a terminal piece, the pygidium greatly resembles the pygidium of *Tersella lenaica* (see Timokhin, 1989, pl. 7, figs. 8, 9) and that of *Tersella novozemelica* (see Petrurina, 1973, pl. 1, fig. 14) in having a distinct postaxial ridge, a convex axis and a relatively distinct marginal border furrow.

A poorly preserved pygidium of *Hystricurus* cfr. *megalops* by Kobayashi (1960, pl. 13, fig. 21) is questionably assigned to this species. It appears to have three axial rings and a distinctive postaxial ridge.

Tersella? *altaica* Petrunina, 1973

? 1955 *Hystricurus* sp., Maximova, p. 118, pl. 7, fig. 3.

? 1962 *Hystricurus* sp., Maximova, p. 21, pl. 1, fig. 12.

1973 *Tersella altaica* Petrunina, p. 62, pl. 1, figs. 9, 11.

Holotype. No. 1324/11, cranidium; Petrunina, 1973, pl. 1, fig, 9; Arenigian; west Siberia.

Diagnosis. Axial furrows strongly curved outwards opposite palpebral lobe. Anterior facial suture strongly divergent.

Remarks. Two poorly-preserved cranidia appear to have the anterior limit of the palpebral lobe reaching the axial furrows (in particular see Petrunina, 1973, pl. 1, fig. 9), which is characteristic of remopleuridaceans such as *Kainella*, not dikelocephalaceans such as *Prosaukia* (see Fortey and Chatterton, 1988, text-fig. 19). Further, they appear to have a much more divergent anterior facial suture which also differentiates remopleuridacians from dikelocephalaceans. These remopleuridacean similarities make it impossible to assign this species to *Tersella* with confidence. The course of the axial furrows of this species appears to be intermediate between that of *Tersella magnaocula* and a remopleuridacian. A cranidium illustrated by Maximova (1955, pl. 7, fig. 3; 1962,

pl. 1 , fig. 12) differs in having a smaller palpebral lobe.

Genus PARATERSELLA n. gen.

Type Species. *Paratersella mediasulcata* n. sp.; *Tesselacauda* Zone; Survey Peak Formation, Alberta, Garden City Formation, southern Idaho, Fillmore Formation, Utah.
Included Species. *P. eos* (Kobayashi, 1955), *P. flexa* n. sp., *P. acutula* n. sp., *P.? acuta* n. sp., *P.? obscura* n. sp.
Diagnosis. Palpebral lobe large (about half of cranidial length), slightly convex dorsally, crescentic in outline with smooth curvature, and posterior end located far posteriorly (resulting in very narrow (exsag.) posterior fixigena). Pygidium with pleural furrows that are deeper and longer than interpleural furrows, slightly concave, relatively narrow outer pleural field, tubercles along distal end of posterior pleural band of inner pleural field (anteriormost one most prominent), and moderately distinct pair of nodes on terminal piece.
Comparison with "Hystricurids". Such *Hystricurus* (*Hystricurus*) species as *H.* (*H.*) *crotalifrons*, and *H.* (*H.*) *oculilunatus* have a palpebral lobe with the same curvature as does *Paratersella*. However, their palpebral lobe is exsagittally shorter than that of *Paratersella* (compare Pl. III-1, Fig. 8 with Pl. III-65, Fig. 1). The palpebral furrow of *Paratersella* is shallower than that of these *Hystricurus* species. The cranidial surface of *Paratersella* is ornamented with sparsely-distributed fine tubercles, whereas that of the *Hystricurus* species is coaserly and densely tuberculated (see Boyce, 1989, pl. 10, fig. 1).

Pygidia of the *Hystricurus* (*Hystricurus*) species (see Boyce, 1989, pl. 10, figs. 7-10) differ from those of *Paratersella* in having much more prominent tubercles on the pleural bands of the inner pleural field, deeper pleural furrows, a distinct postaxial ridge, tubercles on sides of the axial rings, and a more prominent pair of nodes on the terminal piece. Characteristically, the pygidia of these *Hystricurus* species and *Paratersella* share pleural furrows that are relatively more deeply impressed and reach the border, interpleural furrows that are relatively shallower and end with tubercles without even reaching the distal edge of the inner pleural field, and fused bands of adjacent pleurae.

Smaller cranidia of *Paratersella mediasulcata* greatly resemble those of *Flectihystricurus flectimembrus* of similar size (see *F. flectimembrus*). Both species have a prominent tubercle on the posterior band of the anteriormost pygidial pleura. The pygidia of *F. flectimembrus* (Pl. III-50, Figs. 19, 20, 23, 26) are distinguished by having a row of smaller tubercles on the pleural bands and axial rings, a more discrete marginal border furrow, and axial ring furrows that deepen as pits at their abaxial ends, and lack the distinct separation of inner and outer pleural fields.

Among other "hystricurids," *Tersella* bears a great resemblance to *Paratersella*; in particular, both taxa possess a palpebral lobe with the same curvature, convexity, and size. From *Tersella* (see Burskyi, 1970, pl. 2, figs. 1-4), *Paratersella* differs in having a more strongly forward-tapering glabella with a rounded anterior margin, a forward-convex anterior border furrow of the consistent depth, a posterior fixigena with a rounded distal end, and a preglabellar median furrow, and in lacking a preglabellar swelling. The pygidia of *Tersella* (see Burskyi, 1970, pl. 3, fig. 4) and *Paratersella* are similar to each other in having a slightly concave outer pleural field, and deeper and longer pleural furrows, but differ in the latter having prominent tubercles on the distal end of the posterior pleural band.

289

Protaspides of *Paratersella mediasulcata* (see Pl. III-65, Figs. 5, 6) greatly differ from those of other typical hystricurids (see Pl. III-16, Fig. 12) in lacking regularly-distributed tubercles, and having a discrete ocular ridge and transverse glabellar furrows. *Paratersella*? *obscurus* have similar protaspides (see Pl. III-68, Figs. 16-21) which however have a posterior fixigenal spine pair and a spindle-shaped axis with a sagittal furrow.

Comparison with Ptychopariides. The large arcuate palpebral lobe and elongated posterior fixigena of *Paratersella* are seen in some changshaniid species from China which is of Middle to Upper Cambrian age. The cranidia of *Changshania conica* (see Qian, 1994, pl. 17, figs. 1, 2) resemble those of *Paratersella mediasulcata* of similar size (see Terrell, 1973, pl. 2, figs. 12, 14, 15). The cranidia of *C. conica* differ in having a much narrower glabella and a more transversely elongated posterior fixigena with a relatively sharp distal end. From the pygidia of the Changshaniidae (see Qian, 1994, pl. 16, fig. 5, pl. 17, figs. 3-5), *Paratersella* differs in developing a prominent tubercle along the distal edge of the inner pleural field and a relatively more distinct separation between the inner and outer pleural fields. The changshaniid pygidia are more similar to those of *Tersella*. Other *Changshania* species distinctively have a short marginal spine extended from the merged anterior band of the anteromost pleura and marginal border (see Qian, 1994, pl. 16, fig. 5).

Coosia (Palmer, 1962b, pl. 3, figs. 17, 24) also displays a similar cranidial architecture, but is differentiated by a down-sloping palpebral lobe and a straight posterior facial suture.

Comparison with Proetides. The large palpebral lobe and transversely elongated narrow posterior fixigena of *Paratersella* are similar to many bathyurids (see Fortey, 1979, fig. 12). However, the bathyurids have a large subrectangular glabella and a much shorter preglabellar field. The pygidia of *Paratersella* are reminiscent of some bathyurids (e.g., *Bathyurus*, Whittington, 1953, pl. 65, figs. 1-3) in having a concave outer pleural field, a slender border, and pleural furrows that are more deeply-impressed than interpleural furrows. They are differentiated from the bathyurids in having fewer axial rings and a prominent tubercle developed along the distal edge of the posterior pleural band of the inner pleural field.

Taxonomic Conclusion. The strong holaspid cranidial similarities with such *Hystricurus* species as *H.* (*Hystricurus*) *crotalifrons* suggest the placement of *Paratersella* within the Hystricuridae. However, the protaspides of *Paratersella* certainly contradict this assessment. For the present, *Paratersella* is questionably assigned to the Hystricuridae. It is necessary to analyze both protaspid and holaspid characters to further assess the taxonomic status of *Paratersella*.

Hypotheses of Evolutionary Relationships. Similarities with Ordovician *Tersella* and the Cambrian changshaniids with *Paratersella* need to be explored to determine the relationships of these taxa.

Paratersella mediasulcata n. gen. n. sp.
Pl. III-65, Figs. 1-19, Pl. III-66, Figs. 1-10
1951 *Hystricurus* sp. B Ross [part], p. 53-54, pl. 10, figs. 18, 19, 23 [only].
? 1955 *Hystricurus* sp. Maximova [part], p. 118, pl. 7, fig. 4 [only].
? 1965 *Hystricurus* sp. undet. Lochman, p. 477, pl. 63, fig. 8.

290

? 1973 *Hystricurus* sp. J, Terrell, p. 78, pl. 2, figs. 12, 14, 15.

1973 *Hystricurus oculilunatus*, Terrell, [part], p. 73, pl. 1, figs. 15, 16, [only].

1989 *Hystricurus* cf. *H.* sp. B, Dean, pl. 14, figs. 9, 12, 15.

1997a '*Paraplethopeltis*' n. sp. A, Lee and Chatterton, p. 871-872, figs. 3.6, 3.7, 8.1-8.4, 8.6, 8.10, 8.11.

Etymology. "media" means middle and "sulcata" means furrow, depicting the presence of the preglabellar median furrow.

Holotype. GSC 62235, cranidium; Dean, 1989, pl. 14, figs. 9, 12, 15; *Tesselacauda* Zone; middle member of Survey Peak Formation, Alberta, Canada

Diagnosis. Palpebral lobe broadens at mid-palpebral point and then relatively rapidly tapers anteriorly and posteriorly. Anterior facial suture moderately convex laterally. Preglabellar median furrow well-impressed.

Association of Pygidium. The association of pygidia with *Paratersella mediasulcata* is based on its cranidial similarities with such *Hystricurus* (*Hystricurus*) species as *H.* (*H.*) *oculilunatus* and *H.* (*H.*) *crotalifrons* and *Tersella*. With *H.* (*H.*) *oculilunatus* (Pl. III-1, Fig. 8), *Paratersella* shares a laterally convex anterior facial suture, a transversely elongated posterior fixigena, and a slightly incurved lateral glabellar margin. Palpebral lobe of *H.* (*H.*) *oculilunatus* exhibits the same curvature as that of *Paratersella*, but the former (one-third of cranidial length) is smaller than the latter (half of cranidial length).

Pygidial specimens (Pl. III-66, Figs. 1-10) similar to those of *Hystricurus* (*Hystricurus*) species (see Ross, 1951, pl. 17, figs. 23, 28, 29) are found in the same sampling horizons where cranidia of *Paratersella mediasulcata* occur. These pygidia share a semi-circular outline, wider and deeper pleural furrows which are restricted to a flat and wide inner pleural field, a moderately concave outer pleural field, and a gently tapering axis. The pygidia of *Hystricurus* (*Hystricurus*) species are characterized by having much more prominent tubercles along the distal edge of the inner pleural field and a distinct post-axial ridge.

Upon the basis of the cranidial similarities of *Paratersella* and *Hystricurus* (*Hystricurus*) species, the pygidial specimens found (Pl. III-66, Figs. 1-10) are associated with *Paratersella*. They are associated with *Paratersella mediasulcata* because there appears to be no variation found in the collected specimens which can be regarded as interspecific. It cannot be ruled out that some of them could be associated with *Paratersella acutula* which co-occurs with *P. mediasulcata*.

Remarks. A Siberian specimen of *Hystricurus* sp. (Maximova, 1955, pl. 7, fig. 4) is similar to the cranidia of *Paratersella mediasulcata*. However, it shows a relatively truncated anterior margin of the glabella and a moderately pointed anterior cranidial margin, which more agrees with *Hystricurus* (*Hystricurus*) *oculilunatus*, than with *P. mediasulcata*. This morphologically intermediate specimen is tentatively assigned to *P. mediasulcata*.

A pygidium from Montana (Lochman, 1965, pl. 63, fig. 8), although only the right half is preserved, displays an overall morphology similar to those of *Paratersella mediasulcata*. Since the pygidium has one more pleural rib and no distinct tubercle on the anterior pleurae, it is only tentatively assigned to *P. mediasulcata*, even though it is much larger than the specimens described in this study.

Two poorly-preserved cranidia of *Hystricurus* sp. were described by Terrell (1973, pl. 2, figs. 12, 14, 15). Like *Paratersella mediasulcata*, their glabella has a lateral margin

291

slightly curved inwards at an anterior one-third of glabellar length. The palpebral lobe of both cranidia, although incompletely preserved, shows a weaker curvature than the specimens of *P. mediasulcata*. Since the two cranidia are three times larger than the specimens in this study, the difference in the palpebral lobe may be ontogenetic. Their features, such as a parallel-sided anterior facial suture, a less strongly curved palpebral lobe, and a steeply down-sloping palpebral fixigena, are reminiscent of *Changshania conica* (see Qian, 1994, pl. 17, figs. 1, 2).

Due to lack of larger specimens, Lee and Chatterton (1997a) assigned several specimens including protaspides to '*Paraplethopeltis*.' However, the large cranidia (figs. 8.6, 8.10) available for that study apparently represent early stages of *Paratersella mediasulcata*.

Paratersella eos (Kobayashi, 1955)

1955 *Dimeropygiella eos* Kobayashi, p. 457, pl. 6, fig. 10.
1989 *Hystricurus* cf. *H.* sp. B, Dean, p. 23, pl. 14, figs. 9, 12, 15.
1989 *Hystricurus oculilunatus*, Dean [part], p. 23, pl. 14, fig. 4, pl. 15, fig. 12 [only].
1989 *Ischyrotoma eos* (Kobayashi, 1955), Dean, pl. 15, figs. 3, 6.
1989 *Ischyrotoma* cf. *I. eos* (Kobayashi, 1955), Dean, p. 37, pl. 28, figs. 1-3, 5, 6.

Holotype. GSC 12712, pygidium; Kobayashi, 1955, pl. 6, fig. 10 (re-illustrated by Dean, 1989, pl. 15, figs. 3, 6); *Kainella-Evanaspis* fauna; McKay Group, British Columbia.
Diagnosis. Palpebral lobe moderately arched laterally. Posterior facial suture nearly straight and sharply terminated distally. Glabella elongated. Outer pygidial pleural field and post-axial region relatively steeply down-sloping.
Remarks. Several pygidia from British Columbia and Alberta were assigned to *Ischyrotoma* by Kobayashi (1955, pl. 6, fig. 10) and Dean (1989). These are greatly similar to those of *Paratersella mediasulcata*, but differ in lacking a distinct pair of nodes on the axial rings and having a more slender border with a smooth surface. The pygidia of *Ischyrotoma* (transferred into *Dimeropygiella* in this study) are characterized by a steep and long outer pleural field, distinct interpleural and pleural furrows reaching a tubular border, ridge-shaped pleural bands, and a pair of nodes on the terminal piece (Pl. III-51, Figs. 4, 5, 8, 9, 15, 16).

Paratersella flexa n. gen. n. sp.
Pl. III-66, Figs. 11-15

Etymology. "flexa" denotes that the anterior border is bent dorsally.
Holotype. UA 12554, cranidium; Pl. III-66, Figs. 11, 13-15; *Tesselacauda* Zone; Fillmore Formation, Utah.
Diagnosis. Anterior border wide and arched dorsally. Anterior cranidial border furrow curves backwards sagittally, resulting in very short preglabellar field. Glabella slightly tapers forwards. Preglabellar field shortest (sag.). Free cheek with short genal spine.
Remarks. This new species, although no pygidial specimens are available, differs from other *Paratersella* species in having a dorsally arched anterior border, a subrectangular glabella, a shorter preglabellar field, and a less strongly curved and longer palpebral lobe. Except for the first feature, all the other features of this species are comparable to *Tersella magnaocula* (see Burskyi, 1970, pl. 3, fig. 2). *T. magnaocula* differs in having a more strongly arched palpebral lobe and laterally convex axial furrows in the palpebral

292

area of the fixigena. Nonetheless, the similarities support a strong taxonomic affinity between *Tersella* from Siberia and *Paratersella* from Laurentia.

Paratersella acutula n. gen. n. sp.
Pl. III-67, Figs. 1-14

1973 *Hystricurus* sp. B. (?), Terrell, p. 76-78, pl. 2, fig. 10.
Etymology. "acutula" describes that the anterior cranidial margin is relatively pointed.
Holotype. UA 12556, cranidium; Pl. III-67, Fig. 1; *Tesselacauda* Zone; Garden City Formation, southern Idaho.
Diagnosis. Anterior cranidial border relatively pointed sagittally. Frontal area wide. Anterior facial suture straight and divergent. Posterior cranidial border transversely elongated. Genal spine more strongly curved inwards.
Remarks. This species differs from *Paratersella mediasulcata* in having a transversely elongated posterior fixigena, a wider (tr.) frontal area, a pointed anterior cranidial margin, and a more strongly curved genal spine. The smaller cranidia of this species are greatly similar to those of *P. mediasulcata* (compare Pl. III-67, Figs. 4, 5. 6 with Pl. III-65, Figs. 9, 10, 17).

A cranidium from R6E2 and free cheek from R6-55 (Pl. III-67, Figs. 12-14) are tentatively assigned to this species, although the differences such as a wider posterior fixigena and relatively shorter preglabellar field could be ontogenetic.

Paratersella? *acuta* n. sp.
Pl. III-67, Figs. 15-22

Etymology. "acuta" describes that the anterior cranidial border is triangular in outline
Holotype. UA 12565, cranidium; Pl. III-67, Figs. 16, 18, 21, 22; *Paraplethopeltis* or *Leiostegium-Kainella* Zone; Garden City Formation, southern Idaho.
Diagnosis. Palpebral lobe of medium size and less strongly curved laterally. Anterior cranidial border elongated triangular in shape. Posterior cranidial border widens and curves backwards distally. Glabella very narrow (tr.). Genal spine short and stout.
Remarks. This species apparently has an affinity with *Paratersella* because its cranidial outline is similar to the smaller cranidia of *Paratersella acutula* (Pl. III-67, Figs. 4, 5). However, it has a less strongly curved and medium-sized palpebral lobe, which prevents me from confidently assigning this species to *Paratersella*. The triangular anterior border is reminiscent of *Flectihystricurus acumennasus* (Ross, 1951, pl. 11, figs. 11, 15).

Paratersella? *obscura* n. sp.
Pl. III-68, Figs. 1-11, 16-21

1997b Proetide A, Lee and Chatterton, p. 434-438, figs. 2.1-2.14, 3.1.
Etymology. "obscura" describes that all the furrows in cranidium are weakly developed.
Holotype. UA 12568, cranidium; Pl. III-68, Figs. 1-4; *Tesselacauda* Zone; Garden City Formation, southern Idaho.
Diagnosis. Axial furrows, preoccipital furrow, and anterior cranidial border furrow weakly impressed. Palpebral lobe relatively weakly curved laterally. Glabella small (tr.) and strongly tapered forwards, with lateral margin being straight-sided. Anterior facial suture moderately convex laterally. Posterior fixigena relatively short (tr.).
Remarks. Due to lack of larger cranidial materials, Lee and Chatterton (1997b) described

293

this species in open nomenclature. This species differs from definite *Paratersella* species in having weakly impressed dorsal furrows in the cranidia and a much narrower (tr.) glabella.

Protaspides assigned to this species (Lee and Chatterton, 1997b, figs. 2.1-2.11, 2.14) are different from those of *Paratersella mediasulcata* (Lee and Chatterton, 1997a, figs. 8.1-8.4) in many respects. They have a pair of posterior fixigenal spines, a flat lateral border, and a convex axis with a discrete sagittal furrow. If these differences of earlier ontogenetic stages are considered taxonomically important, following von Baer's laws, this species should be placed outside the Hystricuridae. This contradicts the affinity with *Paratersella* suggested by their cranidial similarities of the later ontogenetic stages with other *Paratersella* species.

<center>

***Paratersella?* sp. aff. *P.?* obscura**
Pl. III-68, Figs. 12-15.

</center>

1970 *Hystricurus* cf. *H. oculilunatus* Ross, p. 72, pl. 10, fig. 35. Pogonip Group Limestone, Nevada

Remarks. The cranidia of this possible new species differ from *Paratersella?* obscura in having a convergent anterior facial suture and a dorsally convex cranidium. The nature of the palpebral lobe and glabella is similar to that of *Paratersella flexa*. Since all the materials are poorly preserved, they are questionaly referred to *P.?* obscura.

<center>

Genus **FLECTIHYSTRICURUS** n. gen.

</center>

Etymology. "flecti" is adopted from "flectimembrus", the species name of the type species.

Type Species. *Hystricurus flectimembrus* Ross, 1951; *Rossaspis superciliosa* Zone; Garden City Formation, Idaho.

Included Species. *F. acumennasus* (Ross, 1951), *F.?* *wilsoni* Gobbett, 1960

Diagnosis. Seventh thoracic segment (from anterior) with long macropleural spine. Palpebral lobe strongly arched laterally, of medium size, slender, and ornamented with small tubercles. Distal end of posterior facial suture sharply turns at about right angle. Posterior librigenal border furrow continues into genal spine as a longitudinal median furrow. Row of small tubercles on pleural bands of inner pleural field and axial rings. Prominent large tubercle on posterior band of anterior most pleura along distal edge of inner pleural field. Pleural field gently convex; no discernible separation between inner and outer pleural fields. Pygidial border flat and ornamented with terrace lines. Pygidial axial ring furrows deepen at distal ends.

Comparison with "Hystricurids". With respect to the size and curvature of the palpebral lobe, the shape of the frontal area, and the nature of the posterior fixigena, smaller cranidia of *Paratersella mediasulcata* are nearly indistinguishable from those of *Flectihystricurus flectimembrus* of similar size (compare Pl. III-65, Fig. 17 with Pl. III-50, Fig. 2). The latter has a less strongly tapering and shorter glabella, and a less rounded distal end of the posterior fixigena. Like *Paratersella*, the pygidia of *F. flectimembrus* have a prominent tubercle on the posterior band of the most anterior pleura, but they develop a row of smaller tubercles on both pleural bands and axial rings, a relatively wider border defined by a narrow but discrete marginal border furrow, and axial ring furrows that deepen as pits at the abaxial ends.

<center>

294

</center>

Flectihystricurus differ from *Hystricurus* in having a strongly arched slender palpebral lobe, a transversely elongated posterior fixigena with short spines at its distal end, a narrower frontal area, a macropleural spine on a thoracic segment, and nearly imperceptible separation of inner and outer pygidial pleural fields. These differences are considered to be of generic value.

The cranidia and free cheeks of *Flectihystricurus* are similar to those of *Amblycranium*. The cranidia of *Flectihystricurus* differ in having a pointed anterior margin, a curved palpebral furrow, a much less steep posterior facial suture, and an occipital spine. The free cheeks of *Flectihystricurus* differ in lacking short spines on the border and genal spine, and in having an eye socle.

Comparison with Ptychopariides. The development of a macropleural spine on a thoracic segment is common to the ptychopariides. For example, the Upper Cambrian *Housia* develops a macropleural spine on the most posterior thoracic segment (see Pl. II-18, Figs. 11, 14; see also Walcott, 1916b, pl. 65, fig. 1). In effect, the smallest transitory pygidium (Pl. III-50, Fig. 18) is greatly similar to that of *Housia* (see Pl. II-18, Fig. 13). However, the macropleural spine of most ptychopariides is an extension of the entire thoracic segment, whereas the spine of *Flectihystricurus* is based only on the posterior pleural band (see Pl. III-50, Fig. 24).

Taxonomic Conclusion. Similarities of pygidia and smaller cranidia with *Paratersella* and differences from *Hystricurus* lead to questionably assign this new genus *Flectihystricurus* to the Hystricuridae.

Hypotheses of Evolutionary Relationships. The morphologic comparison suggests that the following taxa seem to be evolutionarily related; such *Hystricurus* species as *H. (Hystricurus) exilis, H. (Hystricurus) crotalifrons*, and *H. (Hystricurus) oculilunatus, Flectihystricurus*, and *Paratersella* from the Lower Ordovician of the Lauretian continent; *Tersella* from the Lower Ordovician of the Siberian and Sino-Korean Platform; the Changshaniidae from the Middle to Upper Cambrian of the Sino-Korean Platform (see each taxon for detailed comparison). The similarities appear to diminish from Gondwana to Laurentia and from Cambrian to Ordovician, implying a possible migration of these taxa in such direction.

Flectihystricurus flectimembrus (Ross, 1951)
Pl. III-49, Figs. 1-10, Pl. III-50, Figs. 1-27.

? 1884 *Bathyurus*? *tuberculatus* Walcott, p. 91-92, pl. 12, fig. 9.

1951 *Hystricurus acumennasus* Ross, [part], p. 50-51, pl. 11, figs. 17, 18, [only].

1951 *Hystricurus flectimembrus* Ross, p. 48-50, pl. 10, figs. 25, 26, 29-33, pl. 11, figs. 16, 21-33.

1970 *Hystricurus* aff. *H. genalatus* Ross [part], p. 72, pl. 10, figs. 26-28 [only].

1973 *Hystricurus flectimembrus*, Terrell, p. 73, pl. 1, figs. 2, 3, 7.

1973 *Hystricurus acumenis* [= *acumennasus*] Ross, Terrell [part], p. 73, pl. 1, fig. 1, 4-6, 7 [only].

1973 *Hystricurus* (?) sp. Terrell, p. 79, pl. 4, fig. 8.

1989 *Hystricurus* sp. Dean, [part], p. 23, pl. 14, fig. 11, pl. 15, figs. 10, 11 [only].

1989 *Hystricurus* sp. Dean [part], p. 23, pl. 15, figs. 9, 10, 11, 14 [only].

Holotype. Y.P.M. 17972, cranidium; Ross, 1951, pl. 10, figs. 29-31; *Rossaspis superciliosa* Zone; Garden City Formation, Idaho.

Diagnosis. Anterior cranidial border transversely elongated triangular in outline and covered with thin terrace ridges. Preglabellar field long. Anterior facial suture parallel-sided. Occipital spine present. Short spine developed on distal end of posterior cranidial border.

Association of Pygidium. Ross (1951) tentatively associated three pygidia with his *Hystricurus flectimembrus* and *Hystricurus acumennasus* (pl. 11, figs. 16-18, 24) which are transferred into a new genus *Flectihystricurus* in this study. This association is confirmed by evidence from comparative analyses of related taxa and ontogenies. As mentioned above, the smaller cranidia of *Flectihystricurus flectimembrus* are similar to those of *Paratersella mediasulcata*. The cranidial similarities make it plausible to assume that their pygidia are similar to each other. The pygidia associated with *Flectihystricurus* by Ross (1951) share with the pygidia of *Paratersella* (Pl. III-66, Figs. 1-10) a semi-circular outline and tubercles on the posterior pleural band (the anteriormost one is most prominent). However, the pygidia of *Flectihystricurus* are differentiated in developing a row of smaller tubercles on the pleural bands and axial rings, a wider flat border defined by a narrow but distinctly-impressed border furrow, axial ring furrows abaxially deepening as pits, a more flattened profile, and an indented and upturned posterior margin. The same type of large pygidia (Pl. III-50, Figs. 4, 19-23, 25-27) occur in R6-114(97), R6E2, and R6E3 where the cranidial materials of *F. flectimembrus* occur.

Ross (1951) illustrated an incomplete articulated specimen consisting of a partially preserved cranidium and left free cheek, and ten thoracic segments (pl. 11, fig. 33). The curvature of the palpebral lobe and spine development on the occipital ring confirms that the specimen belongs to *Flectihystricurus flectimembrus*. The seventh thoracic segment from the anterior develops a long macropleural spine which extends from the posterior pleural band. Many smaller pygidia with a macropleural spine extending from the posterior pleural band of the anteriormost segment (Pl. III-50, Figs. 13, 14, 16-18) occur in the same sampling horizons (R6-114(97), R6E2, and R6E3) where the above-mentioned large pygidia occur. The isolated disarticulated thoracic segment (Pl. III-50, Fig. 24) and the pygidium tentatively associated with *Flectihystricurus acumennasus* by Ross (1951, pl. 11, figs. 17, 18) also display the same position of the macropleural spine.

Two smaller transitory pygidia (Pl. III-50, Figs. 13, 18) each have a spine on the second segment from the anterior and the fourth segment from the anterior, respectively. This indicates that there are several thoracic segments lacking a macropleural spine anterior to the segment possessing the macropleural spine. This configuration well corresponds with that of the incomplete articulated specimen (Ross, 1951, pl. 11, fig. 33). The morphologic transformations from the smaller transitory pygidia (Pl. III-50, Figs. 13, 18) into the larger pygidia (e.g., Pl. III-50, Figs. 4, 5) are within such a continuous range that the smaller pygidia are certain to represent earlier ontogenetic stages of the larger pygidia. All the evidence confirms the association of the pygidia by Ross (1951) with *Flectihystricurus flectimembrus*.

Newly found pygidia (Pl. III-49, Figs. 11-13) are questionably associated with *Flectihystricurus acumennasus*. These pygidia share with those of *Flectihystricurus flectimembrus* a prominent tubercle on the posterior band of the most anterior pleural segment, an indented posterior margin, axial furrows connected with the posterior marginal border furrow, and abaxially deeply impressed axial ring furrows. However, they are differentiated by the presence of only two axial rings and a much wider (tr.) axis.

296

Such cranidial peculiarities of *F. acumennasus* as a protruded anterior border appear to make the association of these pygidia with this species plausible.

Remarks. Walcott (1884) illustrated a line-drawing of an incomplete cranidium of *Bathyurus*? *tuberculatus*. The drawing shows a moderate-sized forward-tapering glabella, a long (tr.) posterior fixigenal area, and an occipital spine. From *Flectihystricurus flectimembrus*, it differs in having a more diagonal course of the posterior facial suture. *B*.? *tuberculatus* is questionably assigned to *F. flectimembrus*. Three free cheek specimens of *Hystricurus* sp. illustrated by Dean (1989, pl. 15, figs. 9-11) have their posterior border furrow continue into the genal spine, without being merged with the lateral librigenal border furrow, which is observed in free cheeks of *Flectihystricurus*.

<div style="text-align:center">

Flectihystricurus acumennasus (Ross, 1951)
Pl. III-49, Figs. 11-13.

</div>

1951 *Hystricurus acumennasus* Ross, [part], p. 50-51, pl. 11, figs. 6, 7, 10, 11, 12, 15, [only].
? 1951 unassigned pygidium, Ross, pl. 30, fig. 9.

Holotype. Y.P.M. 17980, cranidium; Ross, 1951, pl. 11, figs. 6, 7, 11; *Rossaspis superciliosa* Zone; Garden City Formation, Idaho.

Diagnosis. Forwardly-protruded triangular anterior cranidial border. Glabella larger and parabolic in outline. Anterior facial suture convergent.

Remarks. A pygidium from *Rossaspis superciliosa* Zone figured by Ross (1951, pl. 30, fig. 9) is indistinguishable from pygidia tentatively associated with this species in this study (Pl. III-49, Figs. 11-13).

The protruded anterior cranidial border, short spine, and swollen pleural fields on the pygidium indicate that this species is very specialized. Apart from these unique features, this species differs from *Flectihystricurus flectimembrus* in having a larger glabella and a more strongly convergent anterior facial suture. Pygidia with specialized features such as an axial ring that is apparently merged into the pleural field, and the presence of only two countable axial rings (see Pl. III-49, Figs. 11-13) are tentatively assigned to this species, following the assumption that the specialization most probably takes place in both the cranidium and pygidium.

The pygidia are similar to that of *Hystricurus* (*Aequituberculatus*) aff. *H.* (*A.*) *occipitospinosus* (Pl. III-15, Figs. 10, 11) in having a spine development and a strongly forward-indented posterior margin.

<div style="text-align:center">

***Flectihystricurus*?** *wilsoni* Gobbett, 1960

</div>

1958 *Hystricurus* aff. *flectimembrus* Ross, Hallam, p. 72.
1960 *Hystricurus wilsoni* Gobbett, p. 457-459, text-fig. 6, pl. 15, figs. 1-14.

Holotype. A50804, cranidium; Gobbett, 1960, pl. 15, fig. 1; Lower Ordovician; Lower Oslobreen Limestone, Spitsbergen.

Diagnosis. Anterior cranidial margin straight. Glabella short (sag.) and wide (tr.). Palpebral lobe moderately arched; its anterior and posterior ends curved adaxially. Three short spines on occipital ring and one short spine at distal end of posterior cranidial border. Pygidium with four axial rings and terminal piece; axial furrows shallow out posteriorly; surface finely granulated. Marginal border relatively narrow. Axial ring furrows with consistent depth. Pleural and interpleural furrows equally deep; pleural

<div style="text-align:center">297</div>

furrows longer than interpleural furrows. Thoracic segment with long macropleural spine at its distal end and axial spine. Macropleural spine with median furrow. Thoracic pleural segments covered with row of small tubercles.

Remarks. The cranidial features of this species differ from *Flectihystricurus flectimembrus* (see Pl. III-49, Figs. 3, 6) in having a larger glabella with a higher ratio of width to length, a moderately arched palpebral lobe, a shorter preglabellar field, a straight anterior border of equal sagittal width, and lacking in glabellar furrows. The pygidia of this species differ in having a rather straight posterior margin and a less prominent marginal border, and lacking prominent tubercles on the distal edge of the inner pleural field. The most distinguishing feature is the presence of a thoracic axial spine (Gobbett, 1960, text-fig. 6, pl. 15, fig. 14; compare with Pl. III-50, Fig. 24). These differences prevent me from definitely assigning this species to *Flectihystricurus*.

<div align="center">Subfamily HYPOBOLOCHILINAE n. subfam.</div>

Etymology. "Hyperbolochilinae" is adopted from the name of the type genus *Hyperbolochilus*.

Type Genus. *Hyperbolochilus* Ross, 1951.

Diagnosis. Frontal area long (sag.). Posterior fixigena directed posteriorly and its distal tip pointed. Palpebral lobe small and located about mid-cranidial length. Palpebral furrow weakly developed, and straight or slightly convex adaxially.

Remarks. Unlike many other "hystricurids" such as *Hillyardina*, earlier meraspid cranidia of *Hyperbolochilus* lack tubercles on their cranidial surface (see Pl. III-53, Figs. 7, 9, 10). Protaspides of *Hyperbolochilus platysus* (Lee and Chatterton, 1997a, figs. 7.10-7.13) lack any of the kinds of regularly-distributed tubercles that are seen in *Hystricurus* protaspides (see Lee and Chatterton, 1997a, figs. 2.2, 2.3, see also Pl. III-16, Fig. 12). Such differences in earlier ontogenetic stages is considered of significant taxonomic value, to exclude *Hyperbolochilus* from the Hystricuridae. A new subfamily is erected to accommodate such taxa, with divergent anterior facial suture and a long frontal area as *Hyperbolochilus*, and *Metabowmania*. Information on pygidial morphologies is needed to further assess the taxonomic status of this new subfamily.

<div align="center">Genus HYPERBOLOCHILUS Ross, 1951</div>

Type Species. *Hyperbolochilus marginauctus* Ross, 1951; *Rossaspis superciliosa* Zone; Garden City Formation, southern Idaho.

Included Species. *H. platysus* n. sp., *H. convexus* n. sp., *H. expansus* Kobayashi, 1955, *H.? cristus* n. sp.

Diagnosis. Doublure of anterior cranidial border tightly infolded, half of anterior border in width, and transversely half of frontal area, and ornamented with terrace lines. Lateral and posterior librigenal border furrows meet at postero-lateral corner of librigenal field and continue into genal spine as median furrow; posterior librigenal border continues into genal spine as ridge. Lateral librigenal border flat and wide; its doublure tightly infolded and ornamented with terrace lines. Frontal area including anterior cranidial border long (more than one third of cranidial length).

Comparison with "Hystricurids". Ross (1951) differentiated *Hyperbolochilus* from *Hillyardina* by that the latter genus has a swelling on the postero-lateral corner of the librigenal field. Hintze (1953) described a species, *Hillyardina* sp. A with a

<div align="center">298</div>

Hyperbolochilus-like cranidium and a *Hillyardina*-like free cheek (pl. 8, figs. 5, 6), and suggested a possible synonymy of the two genera (see also Terell, 1973). It was Boyce (1989) who officially synoymized *Hyperbolochilus* with *Hillyardina*, noting that the convexity of the swelling varies from species to species.

New species described from this study provide morphologic information that allows for retaining *Hyperbolochilus* as a valid genus separated from *Hillyardina*. Both taxa share two important features of the free cheek that the lateral and posterior librigenal border furrows meet at the postero-lateral corner of the librigenal field and continue into the genal spine, and the posterior border continue into the inner half of the genal spine as a ridge. The free cheek of *Hillyardina semicylindrica* has a much narrower lateral border and doublure (compare Pl. III-47, Figs. 1, 3 with Pl. III-53, Figs. 1, 3). The surface of the librigenal field of *H. semicylindrica* is tuberculated, which is more obvious in ventral illustration (Pl. III-47, Fig. 1), whereas that of *Hyperbolochilus* is smooth. The genal spine of *H. semicylindrica* is much longer and more slender than that of *Hyperbolochilus*. In the cranidium, the doublure of the anterior border of *Hyperbolochilus* is half of the anterior border in width, and tightly infolded (see Pl. III-52, Figs. 4, 10, Pl. III-53, Figs. 12, 19), whereas that of *Hillyardina* is much narrower and more loosely infolded (see Pl. III-47, Figs. 10). The axial furrows of *Hillyardina* shallow out to disappear at the glabellar base (see Pl. III-47, Figs. 2, 7, 11), whereas those of *Hyperbolochilus* weakly shallow out or are consistent in depth (e.g., see Pl. III-52, Figs. 2). In *Hillyardina*, two pairs of glabellar furrows are present as non-pustulose patches or small adaxial indentations from the axial furrows. These are absent in *Hyperbolochilus*. Other cranidial features such as the palpebral lobe and the anterior facial suture are similar in both genera.

Lee and Chatterton (1997a) described protaspides (figs. 7.8, 7.10-7.13) which were assigned to *Hyperbolochilus* cf. *marginauctum*, which is assigned to *Hyperbolochilus platysus* in this study. They do not bear tuberculation pattern seen in such hystricurid genera as *Hystricurus* and *Amblycranium* (Lee and Chatterton, 1997a, fig. 3). Smaller cranidia of *H. platysus* also do not develop the tubercles (Pl. III-53, Figs. 7, 9, 10), supporting the absence of tubercles throughout the life cycle of this form. In contrast, those of *Hillyardina* (e.g., see Pl. III-47, Fig. 8) do develop the same tuberculation as protaspides of *Hystricurus* (see Lee and Chatterton, 1997a, figs. 2.2, 5.3, 5.4; Pl. III-16, Fig. 12) and smaller cranidia of *Pachycranium* (see Pl. III-57, Figs. 18-20).

Comparison with Proetides. The remarkable resemblance of cephalic morphologies of *Hyperbolochilus*? n. sp. C is found with *Aulacopleura*? *ranfordi* from Silurian strata of northwestern Canada (see below for details). The similarities are easily extended into other definite *Hyperbolochilus* species and allied genera such as *Hillyardina* and *Pachycranium*, and most aulacopleurids. In particular, their palpebral lobe is strongly arched laterally and well defined by a straight or slightly incurved palpebral furrow, and their posterior facial suture is steeply inclined and sharply terminated distally. However, most aulacopleurids, including *A.*? *ranfordi*, have a tubular narrow cephalic border (e.g., Adrain and Chatterton, 1995a, figs. 3.19, 6.1), whereas *Hyperbolochilus* has a flat and ventrally tightly infolded cephalic border. In most aulacopleurids, the lateral and posterior librigenal border furrows meet at the postero-lateral corner of the librigenal field, as in *Hyperbolochilus* and *Hillyardina*. However, the confluent furrows do not extend into the genal spine as a median furrow as in *Hyperbolochilus* and *Hillyardina*;

299

some aulacopleurid taxa have the median furrow (e.g., see Adrain and Chatterton, 1995a, figs. 5.12), which however extends only in a short distance. The S1 glabellar furrows of the aulacopleurids, that are connected with the axial furrows and occipital furrow, are the most significant difference from the "hystricurids," including *Hyperbolochilus*.

Peng (1990b) described a new scharyiine genus, *Proscharyia* from Tremadocian strata of South China (pl. 19, figs. 7-15) and considered it as a root of the Scharyinae. *Proscharyia* is similar to such *Hyperbolochilus* species as *H. marginauctus* in terms of the divergent anterior facial suture, sharply terminated posterior fixigena, and forward-tapering glabella, but *Proscharyia* has a more strongly divergent anterior facial suture, a more strongly tapering glabella, a pointed anterior cranidial margin, and two pairs of glabellar furrows. Peng (1990b) included *Hyperbolochilus*? sp. nov. from Newfoundland (Fortey, 1983, pl. 25, figs. 10, 11) within his new genus. The nature of the glabellar shape, anterior facial suture and posterior fixigena of the Newfoundland specimen is indistinguishable from *Proscharyia*, but the Newfoundland specimen has a much longer preglabellar field and a less pointed anterior cranidial margin, and no glabellar furrows. This specimen appears to be a morphologic intermediate between *Hyperbolochilus* and *Proscharyia*. Information on the pygidium of *Hyperbolochilus* and the Newfoundland specimen is needed to further assess the taxonomic relationships of these three taxa. Peng (1990b) noted a possible affinity of *Proscharyia* with the aulacopleurids, which is implied by the similarities with the Lower Ordovician *Hyperbolochilus*? n. sp. C and the Silurian *Aulacopleura*? *ranfordi*.

Comparison with Ptychopariides. Fortey (1983) noted cranidial similarities of his *Hyperbolochilus*? sp. nov. from Newfoundland with Middle Cambrian Chinese asaphiscid, *Liaoyangaspis* (Lu *et al.* 1965, pl. 57). The location of the palpebral lobe was regarded as a difference. Compared with other *Hyperbolochilus* species, *Liaoyangaspis* differs in having a posterior facial suture that runs transversely for quite a distance, a slender palpebral lobe, and two pairs of glabellar furrows. The pygidia of *Liaoyangaspis* are not comparable with those of any hystricurids, in lacking pleural and interpleural furrows and having a broad and concave marginal border.

Fortey (1983) also noted that the Newfoundland specimen is comparable with the Upper Cambrian *Coosia*. *Coosia* has a moderately arched, slender palpebral lobe, a less sharply terminated posterior fixigena, and a much shallower anterior border furrow (e.g., see Palmer, 1954b, pl. 78, fig. 6).

Taxonomic Conclusion. Cranidial similarities suggest that *Hyperbolochilus* is a member of the Hystricuridae along with *Hillyardina*. The most critical information to evaluate the taxonomic position of *Hyperbolochilus* is its pygidial morphology. Cranidial similarities with *Hillyardina* suggest that *Hyperbolochilus* would have a pygidium with a fulcral ridge that separates a flat inner pleural field and a steeply down-sloping outer pleural field. This will confirm its placement in the Hystricuridae. However, earlier ontogenetic stages, such as protaspides and smaller cranidia of *Hyperbolochilus* are different from those of *Hillyardina* in lacking regularly-distributed tubercles, contradicting a close relationship. *Hyperbolochilus* is only tentatively placed in the Hystricuridae.

Hyperbolochilus marginauctus Ross, 1951

Diagnosis. Preglabellar field more than twice sagittally longer than anterior border (in lateral view). Swelling present at postero-lateral corner of librigenal field. Palpebral lobe

300

strongly arched laterally, defined by inwardly curved palpebral furrow, and located posterior to mid-cranidial length. Posterior facial suture straight and diagonal, and ventrally cuts posterior border doublure at same angle as it does dorsally. Posterior cranidial border sharply terminated distally.

Four Subspecies. Four subspecies of *Hyperbolochilus marginauctus* are recognized with respect to the width and depth of the cephalic border furrow and the shape of the glabellar front. *H. marginauctus marginauctus* is characterized by a narrowly impressed cephalic border furrow and a slightly pointed glabellar front. *H. marginauctus angustolimbus* is distinguished by a very narrowly impressed lateral librigenal border furrow and a most distinct pair of swellings at the postero-lateral corner of the librigenal field. *H. marginauctums concavosulcatus* is characterized by wide and concave cephalic border furrows. *H. marginauctus convexofrontalis* is distinguished by a strongly convex anterior cranidial margin and a rounded glabellar front.

<div align="center">

Hyperbolochilus marginauctus marginauctus Ross, 1951

Pl. III-52, Figs. 1-12

</div>

1951 *Hyperbolochilus marginauctum* Ross, [part] p. 77-78, figs. 26, 27, 30-31, 34-35 [only].

1951 *Hillyardina semicylindrica* Ross, [part], p. 71-72, pl. 16, figs. 2, 8 [only] (re-illustrated in Pl. III-52, Figs. 3, 7).

Holotype. Y.P.M. 18057, cranidium; Ross, 1951, pl. 17, figs. 27, 34, 35 (re-illustrated in Pl. III-52, Figs. 1, 2, 4, 5); *Rossaspis superciliosa* Zone; Garden City Formation, southern Idaho.

Diagnosis. Cephalic border furrows very narrowly impressed. Glabellar front slightly pointed.

Remarks. Ross (1951) assigned a free cheek to *Hillyardina semicylindrica* (pl. 16, figs. 2, 8; see Pl. III-52, Figs. 3, 7). It lacks the tubercles developed on the cranidial surface of *H. semicylindrica*. Compared with a free cheek of *H. semicylindrica* collected in this study (Pl. III-47, Figs. 1, 3, 6), it has a wider lateral border which better corresponds with the anterior cranidial border of *Hyperbolochilus marginauctus marginauctus*.

<div align="center">

Hyperbolochilus marginauctus angustolimbus n. subsp.

</div>

1953 *Hillyardina* sp. A, Hintze, [part], p. 162-163, pl. 8, figs. 5, 6.

1973 *Hillyardina* sp. A, Terrell, [part], p. 71-72, pl. 3, figs. 1, 4, [only].

? 1973 *Hillyardina* sp. A, Terrell, [part], p. 71-72, pl. 3, fig. 3, [only].

Etymology. "angustolimbus" is a composite word of "angusto" from Latin meaning "narrow" and "limbus" from Latin meaning " border", depicting the narrow anterior cranidial border.

Holotype. 26186, cranidium; Hintze, 1953, pl. 8, fig. 6; *Rossaspis superciliosa* Zone; Fillmore Formation, Utah.

Differential Diagnosis. Lateral librigenal border relatively tubular. Cephalic border furrow narrowest and deepest. Swelling at postero-lateral corner of librigenal field most distinct. Glabellar front slightly pointed.

Remarks. Four free cheeks assigned to *Hillyardina* sp. A by Hintze (1953, pl. 8, fig. 5) and Terrell (1973, pl. 3, figs. 1, 3, 4) cannot be referred to *Hillyardina* because of their strongly divergent anterior facial suture. They are assigned to this new subspecies. A free

<div align="center">

301

</div>

cheek assigned to *Hillyardina* sp. A by Terrell (pl. 3, fig. 3) has a long and strongly curved genal spine, so that it is questionably assigned to this subspecies.

Hyperbolochilus marginauctus concavosulcatus n. subsp.

1989 *Hillyardina levis* Boyce, [part], p. 35-38, pl. 6, figs. 1-3, 7-10, pl. 7, figs. 1-5, [only].

1989 *Hyperbolochilus* cf. *H. expansus* Kobayashi, [part], Dean, p. 24, pl. 17, fig. 7 [only].

1989 *Hillyardina* sp., Dean, p. 25, pl. 16, figs. 3, 8.

Etymology. "concavosulcatus" describes its wide and concave anterior cranidial and lateral librigenal border furrow.

Holotype. NFM F-93, cranidium; Boyce, 1989, pl. 6, figs. 1-3; *Randaynia saundersi* Zone; Boat Harbour Formation, western Newfoundland.

Diagnosis. Anterior cranidial and lateral librigenal border furrow wide and concave. Glabellar front slightly pointed.

Remarks. Several free cheeks from western Newfoundland were assigned to *Hillyardina levis* by Boyce (1989). Of cranidia assigned to *H. levis* by Boyce, two (pl. 6, figs. 4, 5) are assigned to *Parahillyardina minuspustulata* and one articulated specimen (pl. 6, fig. 6) to *Parahillyardina newfoundlandia* (see "*Parahillyardina*"). The cranidium (pl. 6, fig. 1) has an anterior cranidial border furrow that is wide and distinctively concave, which distinguishes it from the cranidia of *Hyperbolochilus marginauctus marginauctus*. This condition of the furrow well corresponds with the lateral border furrow of the free cheeks assigned to *H. levis* by Boyce. An identical condition of the anterior cranidial and lateral librigenal border furrow is observed in a cranidium and two free cheeks from Alberta (Dean, 1989, pl. 17, fig. 7, pl. 16, figs. 3, 8).

Hyperbolochilus marginauctus convexofrontalis n. subsp.

1989 *Hyperbolochilus*? sp., Dean, p. 24, pl. 17, figs. 2, 5, 8.

Etymology. "convexofrontalis" depicts that the anterior cranidial margin is strongly convex forwards.

Holotype. GSC 62252, cranidium; Dean, 1989, pl. 17, figs. 2, 5, 8; *Rossaspis superciliosa* Zone; upper massive member of Survey Peak Formation, Alberta.

Diagnosis. Anterior cranidial margin strongly convex forwards. Glabellar front rounded.

Remarks. This subspecies is comparable to *Hyperbolochilus expansus* in having a relatively rounded anterior cranidial margin and a parabolic glabellar outline. However, *H. expansus* has a much larger glabella with a sagittal keel, an occipital furrow that shallows out at half of the transverse length, and a less strongly convex anterior cranidial margin.

Hyperbolochilus platysus n. sp.
Pl. III-53, Figs. 1-12

1951 *Hyperbolochilus marginauctum* Ross, [part], p. 77-78, figs. 24-25, [only].

1997a *Hyperbolochilus* cf. *marginauctum*, Lee and Chatterton, p. 872, figs. 7.8, 7.10-7.13.

Etymology. "platysus" denotes its flat exoskeleton.

Holotype. UA 12417, cranidium; Pl. III-53, Fig. 2; *Rossaspis superciliosa* Zone; Garden

302

City Formation, southern Idaho.

Diagnosis. Cranidial exoskeleton flat. Posterior cranidial doublure protrudes beyond posterior cranidial border, forming a small triangle projection; posterior facial suture ventrally inwardly cuts posterior border doublure. Inner margin of genal spine rather straight. Palpebral lobe small and palpebral furrow weakly impressed. Anterior facial suture strongly divergent.

Remarks. A free cheek was assigned to *Hyperbolochilus marginauctus* by Ross (1951, pl. 16, figs. 24, 25). The specimen shows a wider lateral border and shallow border furrows which are consistent with cranidia of this new species, not with *H. marginauctus*. Furthermore, the posterior facial suture ventrally cuts the posterior border doublure at a steep angle, which is best seen in ventral view of free cheek (Pl. III-53, Fig. 3). This corresponds with a posterior cranidial border doublure which protrudes abaxially as a triangular projection (see Pl. III-53, Figs. 2, 11).

Five protaspides from R5-50.3 were assigned to *Hyperbolochilus* cf. *marginauctum* by Lee and Chatterton (1997a, figs. 7.8, 7.10-7.13). They are transferred into this species because those share with its meraspid cranidia (Pl. III-53, Figs. 7, 9, 10) a lack of regularly-distributed tubercles.

<center>

Hyperbolochilus convexus n. sp.

Pl. III-53, Figs. 13-19

</center>

Etymology. "convexus" because the posterior facial suture is convex antero-laterally, not straight as in any other *Hyperbolochilus* species.

Holotype. UA 12423, cranidium; Pl. III-53, Figs. 13-15, 19; *Hintzeia celsaora* to *Protopliomerella contracta* Zone, Garden City Formation, southern Idaho.

Diagnosis. Posterior facial suture convex antero-laterally in middle portion. Anterior facial suture laterally convex. Posterior cranidial border doublure strongly protrudes beyond posterior cranidial border, forming a triangular projection. Palpebral lobe small and located at mid-cranidial length.

Remarks. The nature of the doublure ventral to the distal end of the posterior cranidial border of this species is the same as seen in *Hyperbolochilus platypus*. The course of the facial suture, anterior one being laterally convex and posterior one being antero-laterally convex, distinguishes this species from other *Hyperbolochilus* species. Two pygidia (Pl. III-53, Figs. 15-18) are tentatively associated to this species. They co-occur with the cranidium in R6-114. From the sampling horizon, pygidia of *Hillyardina* (see Pl. III-47, Figs. 16, 17), *Parahystricurus* (see Pl. III-63, Figs. 13, 14), *Paramblycranium* (see Pl. III-61, Figs. 25, 26), and *Psalikilus* (see Pl. III-69, Figs. 3, 4, 12-14) co-occur. Since the assignment of some sclerites to *Parahystricurus* and *Paramblycranium* is provisional, these pygidia from R6-114 (Pl. III-53, Figs. 15-18) could belong to the other taxon. They are similar to those that are provisionally associated with *Paramblycranium* in having an inwardly depressed narrow outer pleural field and flat and a broad inner pleural field.

<center>

Hyperbolochilus expansus Kobayashi, 1955

</center>

1955 *Hyperbolochilus expansus* Kobayashi, p. 422-424, pl. 3, fig. 1.

1989 *Hyperbolochilus expansus*, Dean, pl. 17, figs. 9, 10, 12.

Holotype. GSC 12636, cranidium; Kobayashi, pl. 3, fig. 1 (re-illustrated by Dean, 1989, pl. 17, figs. 9, 10, 12; *Evanaspis-Kainella* fauna; McKay Group, British Columbia.

<center>303</center>

Diagnosis. Glabella large with keeled crest. Occipital furrow shallows to disappear at distal one-third. Posterior facial suture curved. Anterior facial suture strongly divergent.

Hyperbolochilus? sp. aff. *H. expansus*
Pl. III-54, Figs. 10-13

? 1989 *Hyperbolochilus* cf. *H. expansus* Kobayashi, [part], Dean, p. 24, pl. 16, figs. 7, 9, 10 [only].

Remarks. This species differs from other definite *Hyperbolochilus* species in having a large glabella and a distal tip of the posterior fixigenal area that is not directed posteriorly. The closest species is *Hyperbolochilus expansus*. The larger and parabolic glabella is similar to a cranidium of *Hyperbolochilus* cf. *H. expansus* (Dean, 1989, pl. 16, figs. 7, 9, 10). Since the glabella of this species is longer, which could be an ontogenetic difference, the latter form is questionably assigned to this species.

Hyperbolochilus? *cristus* n. sp.
Pl. III-55, Figs. 1-14

Etymology. "cristus" describes the ridge-like anterior cranidial and lateral librigenal borders.

Holotype. UA 12427, cranidium; Pl. III-55, Figs. 2, 4, 6; *Tesselacauda* Zone; Fillmore Formation, Utah.

Diagnosis. Anterior cranidial and lateral librigenal borders carinated. Anterior cranidial and lateral librigenal border furrows wide and concave. Anterior facial suture parallel-sided. Panderian notch present at librigenal doublure corresponding to postero-lateral corner of librigenal field. Cranidial surface covered with sparsely distributed small tubercles.

Remarks. The wide and concave anterior cranidial and lateral librigenal border furrow of this species is the same as seen in *Hyperbolochilus marginauctus concavosulcatus*. The parallel-sided anterior facial suture easily distinguishes this species from other *Hyperbolochilus* species. The condition of the anterior cranidial and lateral librigenal border furrow is similar to that of *Carinahystricurus minuocularis* (Pl. III-35, Figs. 1-3). However, *C. minuocularis* has a posterior facial suture which turns rapidly at its distal end and lacks a long median furrow on the genal spine and a panderian notch. The posterior fixigena of this species is reminiscent of *Amblycranium* (e.g., see Pl. III-28, Fig. 1) in that the posterior cranidial border is tube-like and slightly curved forwards distally. This species differs in having a straight anterior margin, a parallel-sided anterior facial suture, shallower axial furrows, and deeper and confluent librigenal border furrows, and lacks spines along the librigenal margin.

Hyperbolochilus? n. sp. A

1983 *Hyperbolochilus*? sp. nov. Fortey, p. 193-194, pl. 25, figs. 10, 11.

Remarks. Many of the diagnostic features listed by Fortey (1983) agree with other *Hyperbolochilus* species. Differences from *Hyperbolochilus* mentioned by Fortey are seen in materials from this study: the more strongly tapering glabella is seen in smaller cranidia of *Hyperbolochilus platypus* (Pl. III-53, Figs. 7, 9, 10); and the less steeply downsloping preglabellar field is seen in the larger cranidia of *H. platypus* (Pl. III-53, Fig. 4). The larger palpebral lobe whose anterior end is opposite the glabellar front

304

appears to be a noticeable difference from *Hyperbolochilus* which usually has the palpebral lobe posterior to the glabellar front. Peng (1990) assigned this Newfoundland specimen to *Proscharyia*. It differs from the Chinese *Proscharyia* in having a less pointed anterior cranidial margin, a longer preglabellar field and a larger and more anteriorly-located palpebral lobe, and lacking glabellar furrows; except for the condition of the palpebral lobe, all the other features are seen in *Hyperbolochilus*. With *Proscharyia*, it shares a strongly tapering glabella and a strongly divergent anterior facial suture; conditions of these features in *Hyperbolochilus* are a less strongly tapering glabella and a less divergent anterior facial suture. The small glabella is also reminiscent of *Metabowmania* (see Dean, 1989, pl. 17, fig. 6).

It is a new species, but its generic assessment is questionable. Temporarily it is questionably assigned to *Hyperbolochilus*. Information on pygidial morphologies will be required for a further taxonomic assessment.

Hyperbolochilus? n. sp. B

1966 Hystricurids, genus & species indet., Lochman, p. 533, p. 65, fig. 35.
? 1992 *Tersella sulcata* Ogienko, [part], p. 91-92, pl. 5, fig. 3 [only].
Remarks. The strongly divergent anterior facial suture and long preglabellar field of the cranidium from the Williston Basin strongly indicate an affinity with *Hyperbolochilus*. However, the oval-shaped glabella and incurved anterior cranidial border resemble those of *Psalikilopsis* (Pl. III-73, Figs. 3-5). A poorly-preserved cranidium of *Tersella sulcata* (Ogienko, 1992, pl. 5, fig. 3) from Siberia has a backwardly-curved anterior border and border furrow, and a similar anterior facial suture. All the specimens referred to *Tersella* have a straight or forward-convex anterior border; the largest specimen of *Tersella* species (Burskyi, 1970, pl. 3, fig. 2) which is of similar size to the cranidium also has a forward-convex anterior border.

Hyperbolochilus? n. sp. C
Pl. III-54, Figs. 1-9

Remarks. Compared with cranidia of *Aulacopleura*? *ranfordi* (Adrain and Chatterton, 1995a, figs. 3.1, 3.8, 3.10, 3.15, 4.1-4.5), this new species only differs in having sparsely-distributed small tubercles developed on the cranidial surface, a more steeply inclined frontal area, and less discretely impressed S1 glabellar furrows, and lacking S2 glabellar furrows. These differences are far overwhelmed by their strong similarities, suggesting that this species could be closely related to or represent an ancestor of the aulacopleurids; the earliest confirmed stratigraphic record of the aulacopleurids is the Late Ordovician. There is a long stratigraphic gap between this *Hyperbolochilus* species and the Silurian aulacopleurid.

Due to the development of tubercles alongside the glabella in earlier meraspid stages (see Pl. III-54, Figs. 4, 6), this species is questionably assigned to *Hyperbolochilus*.

Genus METABOWMANIA Kobayashi, 1955
Type Species. *Metabowmania latilimbata* Kobayashi, 1955; McKay Group, British Columbia.
Diagnosis. Preglabellar field extremely long. Anterior border very narrow. Anterior facial suture strongly divergent. Posterior facial suture straight and diagonal. Glabella

small and strongly forward-tapering.

Comparison with "Hystricurids". *Metabowmania* (see Dean, 1989, pl. 17, figs. 1, 4, 11) is similar to *Tanybregma tasmaniensis* (Pl. III-85, Figs. 1-4), both sharing a long preglabellar field, a narrow anterior border, and a strongly divergent anterior facial suture. However, *Metabowmania* has a much smaller palpebral lobe and a much wider (exsag.) posterior fixigenal area, and lacks slit-like S1 glabellar furrows. Morphologic resemblance is also found to *Hyperbolochilus* (see Pl. III-52, Figs. 2, 4, 5) which has a divergent anterior facial suture, a long preglabellar field, and a relatively wide posterior fixigenal area. However, *Hyperbolochilus* bears a larger, less strongly tapering glabella, a wider (sag.) anterior cranidial border, a shorter preglabellar field, and a less divergent anterior facial suture. An Albertan cranidium of *Metabowmania latilimbata* (Dean, 1989, pl. 17, figs. 3, 6) and *Hyperbolochilus* n. sp. B from Newfoundland (Fortey, 1983, pl. 25, figs. 10, 11) display intermediate cranidial morphologies between the two genera.

Comparison with Ptychopariides. Kobayashi (1955)'s line-drawing (p. 9, fig. 7) of *Metabowmania latilimbata* is misleading to incorrectly demonstrate the similarties with *Bowmania*, an entomaspidid. In the drawing, the palpebral lobe is too far away from the glabella, the anterior facial suture is less strongly divergent, and the posterior fixigenal area is too short transversely, compared with Dean (1989)'s re-illustration of the holotype cranidium (pl. 17, figs. 1, 4, 11). From entomaspidids, *Metabowmania* differs in lacking discrete glabellar furrows and an eye ridge, and having a forward-tapering elongated glabella, and a more adaxially located palpebral lobe.

Taxonomic Conclusion. *Metabowmania* is placed in the same subfamily Hyperbolochilinae together with *Hyperbolochilus*.

Metabowmania latilimbata Kobayashi, 1955

1955 *Metabowmania latilimbata* Kobayashi, p. 458-459, pl. 6, fig. 13, pl. 8, fig. 9.
1955 *Amechilus tuberculatus* Kobayashi, p. 459-460, pl. 6, fig. 11
1989 *Metabowmania latilimbata*, Dean, p. 24, pl. 17, figs. 1, 3, 4, 6, 11.

Diagnosis. see generic diagnosis.
Remarks. Dean (1989) provided detailed accounts for the synonymy of this species.

Metabowmania sp.

1989 *Metabowmania* sp. Dean, p. 24-25, pl. 16, figs. 1, 2, 4-6.

Subfamily PSALIKILINAE n. subfam.

Etymology. "Psalikilinae" is adopted from the type genus *Psalikilus*.
Type Genus. *Psalikilus* Ross, 1951.
Diagnosis. Ocular ridge distinct and connected with axial furrows. Palpebral lobe located far posteriorly. Cranidium subtrapezoidal (wider than long). Axial furrows deep and wide. S1 very distinctively impressed. Occipital furrow (S0) deeply depressed as pit at its distal ends. Free cheek with long genal spine. Pygidium with continuous fulcral ridge separating inner and outer pleural fields.
Remarks. A new subfamily, the Psalikilinae, is erected to accommodate *Psalikilus* and *Natmus*. Cranidial features of both genera such as a distinct ocular ridge and a posteriorly located palpebral lobe are distinct from those of "hystricurids." (see below *Psalikilus* and *Natmus* for details). The cranidial morphologies are more similar to those of some

306

menomoniids and nepeiids. However, the pygidia of the Psalikilinae have a fulcral ridge separating inner and outer pleural fields, that is observed in many "hystricurid" taxa. Librigenal morphologies are also comparable to some "hystricurid" taxa. It is concluded that this new subfamily is questionably placed in the Hystricuridae.

Hypotheses of Evolutionary Relationships. The Psalikilinae appears to have been derived either from some menomoniids of Laurentia or from some nepeids of Gondwana. It will be interesting to cladistically investigate where is the ancestral area for the Psalikilinae, which would reveal whether a menomoniid or nepeid is more likely to be ancestral to the subfamily. The Psalikilinae seems to have gone extinct during the early Arenigian, leaving no descendants.

Genus **PSALIKILUS** Ross, 1951

Type Species. *Psalikilus typicum* Ross, 1951; *Hintzeia celsaora* to *Protopliomerella contracta* Zone; Garden City Formation, southern Idaho.

Included Species. *P. pikum* Hintze, 1953, *P. spinosum* Hintze, 1953, *P. paraspinosum* Hintze, 1953

Diagnosis. Cranidium trapezoidal in outline. Palpebral lobe strongly arched laterally and strongly convex, and located far posteriorly; its posterior end overhangs posterior fixigena. Ocular ridge well-developed and ornamented with small tubercles; its adaxial end immediately anterior to S2 glabellar furrows. Two pairs of glabellar furrows short, deeply impressed and connected with axial furrows; S1 obliquely directed posteriorly, and S2 obliquely directed anteriorly. Axial furrows deepen and broaden opposite palpebral fixigena. Preglabellar furrows shallow. Posterior fixigena extremely narrow exsagittally and sharply terminated distally. Anterior cranidial border relatively short (tr.), incurved sagittally.

Free cheek with long genal spine (three times longer than librigenal field). Posterior librigenal border furrow continues into genal spine as longitudinal median furrow. Lateral librigenal border furrow shallows out anterior to postero-lateral corner of librigenal field.

Pygidium subtriangular in outline. Pygidial axis rapidly tapers posteriorly. Fulcral ridge between inner and outer pleural fields slender and protruded posteromedially together with terminal piece. Marginal border furrow weakly impressed and delimits tubular marginal border that is ornamented with coarser tubercles than those on outer pleural field.

Comparison with "Hystricurids". Lochman (*in* Moore, 1959) assigned *Psalikilus* to the Hystricuridae. Among the features listed in the diagnosis of the Hystricuridae, the forward-tapering glabella and tuberculated exoskeletal surface appear to apply to *Psalikilus*, but these two features are apparently of little taxonomic significance at this taxonomic level because they even apply for some taxa outside the old concept of the Hystricuridae.

The cranidial features of *Psalikilus* strongly deviate from those of *Hystricurus*. *Psalikilus* is distinguished by having two pairs of deeply impressed glabellar furrows, a strongly arched, convex, inflated palpebral lobe with a distinct ocular ridge, and deep and wide axial furrows. Some "hystricurids" have two pairs of glabellar furrows which are not as deep as in *Psalikilus* (e.g., *Flectihystricurus*, see Ross, 1951, pl. 10, fig. 26) and/or expressed only as non-pustulose patches (e.g., *Hillyardina*, see Ross, 1951, pl. 16, fig. 1). The palpebral lobe of *Psalikilus* is located far posteriorly, overhanging the very narrow

307

posterior fixigenal area. The same position of the palpebral lobe is seen in *Tanybregma* (Jell and Stait, 1985b, pl. 3, figs. 2, 3; Pl. III-85, Fig. 1), which however has a much slender and larger palpebral lobe. The newly described *Politohystricurus pseudopsalikilus* (Pl. III-26, Figs. 11, 14) has a palpebral lobe which is displaced posteriorly, as seen in *Psalikilus*. This *Politohystricurus* species shows a posteriorly incurved anterior border furrow, a slightly convergent short anterior facial suture, and an occipital spine, all of which are visible in *Psalikilus paraspinosus*. However, the *Politohystricurus* species differs in having a sharply truncated distal end of the posterior fixigena and a much larger glabella with a parabolic outline.

Natmus from Australia is the morphologically closest taxon that has been placed in the Hystricuridae (Jell, 1985). A cranidial specimen of *Natmus victus* (Jell, 1985, pl. 21, fig. 15; Pl. III-59, Figs. 10, 11) is remarkably similar to the cranidium of *Psalikilus pikum* (Hintze, 1953, pl. 9, fig. 1) and only differs in having a longer anterior border. *Natmus tuberculatus* (Pl. III-60, Figs. 3-8) from the Garden City Formation appears to be a morphologic intermediate between Australian *Natmus* and Laurentian *Psalikilus*.

Several smaller cranidia (Pl. III-70, Figs. 8-14) are obtained from the same sampling horizon (R6-114) together with the larger cranidia of *Psalikilus typicus*. The presence of the distinct ocular ridge confirms that they represent earlier ontogenetic stages of *Psalikilus*. These smaller cranidia have a row of tubercles alongside the glabella; two in the palpebral fixigena and the third on the proximal end of the ocular ridge. A protaspid specimen recovered from the same sampling horizon (Pl. III-70, Figs. 15-17) displays the same tuberculation pattern as these smaller cranidia. These regularly-distributed tubercles become difficult to be recognized with growth due to the addition of tubercles in a random fashion. A very similar tuberculation pattern in the protaspis and smaller cranidia is observed in *Hystricurus* protaspides (see Lee and Chatterton, 1997a, fig. 3). In addition, the overall cranidial outlines of the smaller cranidia are comparable to those of the "hystricurids" (see Lee and Chatterton, 1997a). However, the presence of a distinct ocular ridge throughout the cranidial development is unique to *Psalikilus*, and is not seen in any "hystricurids" for which information on similar ontogenetic stages is known.

The pygidia of *Psalikilus* have a fulcral ridge separating the inner and outer pleural fields that is visible in many hystricurids such as *Spinohystricurus*, *Carinahystricurus* and *Hillyardina*. Unlike these hystricurids (e.g., see Pl. III-20, fig. 3), *Psalikilus* has a wider (exsag.) outer pleural field and a much narrower inner field, and has a ridge that is continuous, without being interrupted by interpleural furrows—accordingly all interpleural and pleural furrows do not extend beyond the ridge. The fulcral ridge of these hystricurids is ontogenetically preceded by small tubercles or spines that are fused into the ridge in later ontogeny (e.g., *Spinohystricurus*, Pl. III-20). Of interest is that the transitory pygidia of *Psalikilus* of similar size still have a continuous ridge that is not interrupted by interpleural furrows (Pl. III-69, Figs. 18-21). These different ontogenetic pathways would indicate that the ridge of *Psalikilus* would be of independent origin from that of the hystricurids. It is the development of a postero-median protrusion that additionally distinguishes *Psalikilus*; the protrusion is continuous into the ridge. In terms of the width of the inner and outer pleural field, the *Psalikilus* pygidia are similar to those of *Eurylimbatus* (see Pl. III-40, Fig. 4). However, the pygidia of *Eurylimbatus* lack a distinct fulcral ridge and develop a stout spine at the distal edge of the inner pleural field.

No pygidium is known for *Natmus* which has the greatest cranidial resemblance to

308

Psalikilus. Judging from the curvature of an articulated thoracic specimen and the architecture of the posterior thoracic pleurae (Pl. III-59, Fig. 5), the pygidium of *Natmus* does not appear to have a steeply down-sloping outer pleural field and a narrow and flat inner pleural field, as seen in *Psalikilus* (see *Natmus* for details)

Free cheeks of *Psalikilus* are characterized by having an extremely long genal spine (more than three times longer than librigenal field), and a median furrow on the genal spine continued from a librigenal posterior border furrow that is not merged with the lateral librigenal border furrow. The latter feature is seen in such "hystricurids" as *Parahystricurus* (see Ross, 1951, pl. 12, fig. 43), *Paramblycranium* (see Pl. III-62, Fig. 4) and *Flectihystricurus* (Ross, 1951, pl. 10, fig. 32). The posterior librigenal border furrow of *Natmus* from the Garden City Formation (Pl. III-60, Fig. 1) is merged with the lateral librigenal border furrow and this merged furrow then continues into the long genal spine. The length of the genal spine of *Psalikilus* is comparable to that of *Politohystricurus* species (see Pl. III-24, Fig. 6). The free cheeks of *Politohystricurus* have much shallower border furrows, and lack the median furrow on the genal spine.

Comparison with Ptychopariides. The cranidial features of *Psalikilus* are comparable to those of the Middle Cambrian menomoniid genus *Bolaspidella* (see Robison, 1964, pl. 88, figs. 8, 10, 17, pl. 89, figs. 1) and Upper Cambrian genera like *Calymenidius* (Ludvigsen *et al.*, 1989) and *Phylacterus* and *Westonaspis* (the Phylacteridae, Ludvigsen *et al.*, 1989). With *Bolaspidella*, *Psalikilus* shares a relatively small glabella with two pairs of distinct glabellar furrows, fairly deep axial furrows, a fairly convex palpebral lobe with an ocular ridge, and a slightly convergent or parallel-sided anterior facial suture. Like many *Psalikilus* species, many menomoniids (e.g., *Menomonia*, Pratt, 1992, pl. 29, figs. 1-6) have a transversely short anterior border that is also curved backwards sagittally. These cranidial similarities are extended into the Upper Cambrian *Aulacodigma* from Australia (Öpik, 1967, pl. 40, figs. 8, 9, pl. 41, figs. 1-10). The smaller cranidia of *Bolaspidella* (Pl. II-42, figs. 1-13) and *Aulacodigma* (Öpik, 1967, pl. 41, fig. 10) both retain an ocular ridge from comparatively early ontogenetic stages.

Calymenidius is an Upper Cambrian genus whose familial assignment is yet to be determined. The holotype cranidium of the type species, *C. tuberculatus* (see Ludvigsen *et al.*, 1989, pl. 50, fig. 27) shares with *Psalikilus* the following features; deep broad axial furrows, a distinct ocular ridge, two pairs of deep glabellar furrows which are confluent with the axial furrows, a backwardly-curved anterior border furrow, and a tuberculated exoskeletal surface. The major difference is that *Psalikilus* has a larger and more inflated palpebral lobe which is located further posteriorly, and *Calymenidius* has a deeper anterior border furrow. The other *Calymenidius* species, *C. acutus* (Ludvigsen *et al.*, 1989) is less similar to *Psalikilus*. With the phylacterids (Ludvigsen *et al.*, 1989, pl. 13, pl. 14, figs. 1-14), *Psalikilus* shares most features that it shares with *Calymenidius*, except for the backwardly-curved anterior border furrow. In addition, *Psalikilus* shares with the phylacterids (especially, *Westonaspis*) a preglabellar furrow which shallows out sagittally.

Harrington and Leanze (1957) described *Colpocoryphoides trapezoidalis* from Tremadocian strata of Argentina (figs. 123.1-123.6). The genus *Colpocoryphoides* was synonymized under *Pharostomina* by Peng (1984). This assessment was based on cranidia from South China (e.g., Peng, 1990, pl. 22, figs. 9a, b). Since the Chinese materials are transferred into a new hystricurid genus *Glabellosulcatus* in this study, the

309

assessment by Peng (1984) does not seem to be valid. Compared with the typical *Pharostomina* from Bohemia (see Sduzy, 1955, pl. 6, figs. 62-64), the Chinese cranidia lack S2 glabellar furrows and have a much more strongly forward-tapering glabella; *Pharostomina* is characterized by its possession of both S1 and S2 and a subrectangular glabella (see Sdzuy, 1955, pl. 6, figs. 62, 63). The features of the typical *Pharostomina* are more similar to those of *Calymenidius*. The calymenid-like Argentine *Colpocoryphoides* species bears a great resemblance with *Psalikilus*, except for the wide posterior fixigena, small palpebral lobe, and possession of S3. If *Calymenidius* and *Colpocoryphoides* are true members of the Calymenidae, their cranidial similarities with *Psalikilus* would give a new insight to the origin of the Phacopida.

Some Lower Ordovician eulomids such as *Euloma* (Tjernvik, 1956, pl. 11, fig. 4) bear deep axial furrows, a shallow preglabellar furrow, two pairs of glabellar furrows which are deeply indented from axial furrows, and a palpebral lobe that is strongly arched laterally and connected to axial furrows through a discrete ocular ridge; all these features are definitely visible in *Psalikilus*. The eulomid however has a fossula at the antero-lateral glabellar corner, S2 glabellar furrows that are obliquely directed backwards, a much wider frontal area, pits developed along the anterior cranidial border furrow, and an occipital furrow with a consistent depth.

In contrast to these cranidial similarities, the pygidia of *Psalikilus* greatly differ from those of the above-mentioned Cambrian and Lower Ordovician ptychopariides. It is the development of the fulcral ridge between the inner and outer pleural fields in *Psalikilus* that differentiates *Psalikilus* from these taxa. The pygidia of *Bolaspidella* are of generalized ptychopariide-type (see Robison, 1964, pl. 88, fig. 15), The phylacterid pygidia (e.g., see Ludvigsen *et al.*, 1989, pl. 44, figs. 4, 13, 14) are characterized by having much more pleural and axial segments, interpleural and pleural furrows reaching the pygidial margin, and no distinct border; these features do not accord with the *Psalikilus* pygidia. No pygidium has been described for *Calymenidius*. The pygidium associated with *Colpocoryphoides* (Harrington and Leanza, 1957, fig. 123.2) is more similar to those of phylacterids, and not similar to those of *Psalikilus*. The pygidia of many eulomids including *Euloma* (see Apollonov and Chugaeva, 1983, pl. 7, figs. 10-12) are easily differentiated from those of *Psalikilus* in having a distinct tubular marginal border, gently sloping pleural fields—thus, no distinct separation between the inner and outer pleural fields—and a parallel-sided axis whose posterior end is well delineated. A pygidium of *Holmdalia* (a marjumiid, Robison, 1988, figs. 27.5a, 27.5b) is similar to those of *Psalikilus* in having a wide and steeply down-sloping outer pleural field and narrow inner pleural field, but differs in lacking a distinct fulcral ridge and in having only one axial ring.

A remarkable pygidial similarity is found with *Euptychaspis* (see, Westrop, 1995, pl. 7, fig. 21; Ludvigsen, 1982, figs. 58S-U). The pygidia of *Euptychaspis* share with those of *Psalikilus* the continuous fulcral ridge that protrudes posteriorly and sagittally, a triangular inner pleural field, and a wide outer pleural field. The former differs in having a much less steeply inclining outer pleural field ornamented with the terrace lines, and a less strongly tapering axis. However, the cranidia of *Euptychaspis* are easily differentiated from those of *Psalikilus*; for example, *Euptychaspis* has a bulb-like glabella whereas *Psalikilus* has a forward-tapering glabella.

Free cheeks of these ptychopariid taxa differ from those of *Psalikilus* as much as their

310

pygidia do. In particular, the presence of a median furrow on the long genal spine easily differentiates *Psalikilus* from the ptychopariides.

Taxonomic Conclusion. Different parts of *Psalikilus* suggest affinities with different taxa. The cranidial architecture cannot be accommodated within the Hystricuridae. In particular, ontogenetic retainment of the ocular ridge in *Psalikilus* is not assignable to the Hystricuridae *sensu* herein. The cranidial features suggest affinities with the Menomoniidae and Phylacteridae. The definite affinity with *Natmus*, which appears to be related to the Nepeidae (see below), also lends no support to confidently placing *Psalikilus* in the Hystricuridae.

In contrast, the smaller cranidia of *Psalikilus* possessing tubercles alongside the glabella strongly suggest its affinity with the Hystricuridae. Pygidial and librigenal features further suggest the hystricurid affinity and strongly deny the affinities with any ptychopariides. *Psalikilus*, along with *Natmus* is placed in a new subfamily, the Psalikilinae, which is temporarily placed in the Hystricuridae.

Hypotheses of Evolutionary Relationships. It seems possible that *Psalikilus* attained novel pygidial and librigenal morphologies comparable to the hystricurids, while retaining cranidial features similar to those of Cambrian ptychopariides. Alternatively, the cranidial features could be convergent with the ptychopariides, and the pygidial and librigenal features could unite *Psalikilus* with the hystricurids.

Stratigraphic Range. Previously, species of *Psalikilus* have been reported from the *Hintzeia celsaora* to *Trigonocerca typica* Zone. However, the discovery of a cranidium of *P. paraspinosus* from R5-34.1, which belongs to the *Symphysurina* Zone, extends the stratigraphic range down into the *Symphysurina* Zone. The pygidia of *Psalikilus* sp. A and those provisionally associated with *Psalikilus pikus* are from the *Tesselacauda* Zone, which fills the stratigraphic gap between the *Symphysurina* Zone and the *Trigonocerca typica* Zone, even though no cranidial materials referrable to *Psalikilus* were recovered from the *Tesselacauda* Zone. *Psalikilus* appears to have the longest stratigraphic range of the "hystricurids."

Psalikilus typicus Ross, 1951
Pl. III-69, Figs. 1-21, Pl. III-70, Figs. 1-17
1951 *Psalikilus typicum* Ross, p. 62-63, pl. 11, 1-5, 8, 9, 13, 14.
1951 unassigned pygidium, Ross, 19, pl. 30, figs. 11, 15.
1953 *Psalikilus typicum*, Hintze, p. 213, pl. 9, fig. 2, pl. 20, fig. 15

Holotype. Y.P.M. 17985, cranidium; Ross, 1951, pl. 11, figs. 2-5; *Hintzeia celsaora* to *Protopliomerella contracta* Zone; Garden City Formation, southern Idaho.

Differential Diagnosis. Cranidial surface most densely and coarsely tuberculated. Occipital ring most strongly convex posteriorly. Exsagittal length of palpebral lobe one third of cranidial length. Pleural and interpleural furrows of anteriormost pygidial segments weakly impressed on inner pleural field.

Association of Pygidium. Hintze (1953, p. 213) was convinced that the pygidium which was questionably associated with cranidial materials by Ross (1951, pl. 30, figs. 11, 15) is associated with *Psalikilus typicus*. In this study, the same pygidial and cranidial morphotypes are found together from the two sampling horizons, R6-114 and R6-100. This co-occurrence supports the association by Hintze.

Association of Protaspides. The smaller cranidia from R6-114 (Pl. III-70, Figs. 8-14)

311

develop three tubercles alongside the glabella. The posterior two are developed on the palpebral fixigena and the anteriormost one on the proximal end of the ocular ridge which is homologous with Fx4 of the otarionine meraspides (Adrain and Chatterton, 1994, fig. 1). A protaspis discovered together with these cranidia (Pl. III-70, Figs. 15-17) shows the same configuration of tubercles. Numerous small cranidia and pygidia were obtained from R6-114. Several smaller protaspides that have a spindle-shaped axis with a sagittal furrow and a pair of short posterior marginal spines, and lack anterior pits, were also obtained from this sampling horizon (Pl. III-69, Figs. 22-26). The marginal spine pair is common to the protaspides of the proetides (see Chatterton *et al.*, 1999, fig. 1) and many ptychopariides. The spindle-shaped axis with the sagittal furrow and without the anterior pits is not common to the proetide protaspides (see Chatterton *et al.*, 1999, fig. 1). The spindle-shaped axis is similar to protaspides of the plethopeltids (see Pl. 24, Fig. 24), norwoodiids (see Pl. 25, Figs. 14, 17), and *Arapahoia* (see Hu, 1986, pl. 16, fig. 1). However, these ptychopariide protaspides do not develop a sagittal furrow and have a distinct pair of anterior pits. It is open to question whether these anaprotaspides from R6-114 are an earlier protaspid stage of *Psalikilus* or belong to other co-occurring "hystricurids" such as *Hyperbolochilus* and *Parahystricurus*.

<center>

Psalikilus pikus Hintze, 1953
Pl. III-71, Figs. 1-17

</center>

1953 *Psalikilus pikum* Hintze, p. 214, pl. 9, fig. 1

Holotype. 26198, cranidium; Hintze, 1953, pl. 9, figs. 1a-1c; *Trigonocerca typica* Zone; Fillmore Formation, Utah.

Diagnosis. Anterior cranidial border short (tr.). Exsagittal length of palpebral lobe half of cranidial length. Palpebral fixigena ornamented with most-sparsely distributed tubercles. Preglabellar field steeply down-sloping. Glabella small.

Association of Pygidium. The pygidia provisionally associated with this species (Pl. III-71, Figs. 6-17) occur in R5-86 and R5-76.4, that belong to the *Tesselacauda* Zone. From these horizons, no *Psalikilus*-like cranidium was recovered. Since the cranidial materials of *Psalikilus* species occur in the *Symphysurina* Zone (see *P. paraspinosum*) to the *Trigonocerca typica* Zone (this species), the stratigraphic occurrence of these pygidia does not contradict their association with a species of *Psalikilus*. The pygidia are of definite *Psalikilus*-type in having a distinct fulcral ridge between narrow inner and broad outer pleural fields and an inverted triangular axis. They are characterized by the possession of three axial rings, whereas the pygidia of *P. typicus* and *P. paraspinosus* have four axial rings. For these two *Psalikilus* species, the pygidia have been found together with their cranidia. The association of the pygidia from the *Tesselacauda* Zone with *P. spinosus* is considered less certain, because the cranidia of *P. spinosum* are much more similar to those of *P. paraspinosus*, indicating that *P. spinosus* would have a pygidium similar to *P. paraspinosus* and thus have four axial rings. Consequently, the pygidia with three axial rings from the *Tesselacauda* Zone are tentatively associated with *P. pikus*, even though no cranidia of *P. pikus* were recovered from the *Tesselacauda* Zone.

<center>

Psalikilus spinosus Hintze, 1953

</center>

1953 *Psalikilus spinosum* Hintze, [part], p. 212-213, pl. 9, figs. 3, 6, [only].

<center>312</center>

Holotype. 26200, cranidium; Hintze, 1953, pl. 9, figs. 3a-3c; *Hintzeia celsaora* Zone; Fillmore Formation, Utah.

Diagnosis. Anterior border little arched dorsally. Occipital spine relatively slender.

Remarks. The pygidium identified as this species (Hintze, 1953, pl. 9, fig. 7) is transferred to a new *Psalikilopsis* species, because it lacks a distinct border which is present in all *Psalikilus* pygidia, but absent in the *Psalikilopsis* pygidia.

Psalikilus paraspinosus Hintze, 1953
Pl. III-72, Figs. 1-12

1953 *Psalikilus paraspinosum* Hintze, p. 213-214, pl. 9, figs. 4, 5.
1966 *Psalikilus paraspinosum*, Lochman, [part], p. 545-546, pl. 62, fig. 15, [only, not
    figs. 13, 14, 16].
? 1966 *Psalikilus* sp. undet., Lochman, p. 546, pl. 62, fig. 18.

Holotype. 26202, cranidium; Hintze, 1953, pl. 9, fig. 5; *Protopliomerella contracta* Zone; Fillmore Formation, Utah.

Diagnosis. Occipital spine stout. Anterior cranidial border most strongly incurved sagittally and strongly arched dorsally. Exsagittal length of palpebral lobe one third of cranidial length. Axial furrows deepen and widen at mid-glabellar point. Posterior pygidial margin strongly arched dorsally. Pleural and interpleural furrows of anterior two pygidial segments relatively deeply impressed on inner pleural field.

Remarks. Lochman (1966) described a poorly preserved cranidium and three pygidia from the Arenigian strata of the Williston Basin (pl. 62, figs. 13-16). The cranidium has two deeply impressed glabellar furrows, deep axial furrows, a posteriorly incurved anterior border furrow, and an occipital spine; the last two features well agree with the cranidia from the Fillmore Formation (Hintze, 1953, pl. 9, figs. 4, 5). The three pygidia develop no sign of a distinct separation of the inner and outer pleural fields by a fulcral ridge which is diagnostic to *Psalikilus*. They bear some resemblance to pygidia of *Hystricurus* species (see Pl. III-8, Fig. 13, Pl. III-13, Fig. 7), but differ in having a terminal piece whose posterior end is distinctively delimited by a deep furrow, and have deeply impressed axial furrows and pleural furrows. The pygidia from the Williston Basin are more similar to pygidia of such telephinids as *Ompheter* and *Opipeuter* (see Laurie and Shergold, 1996, pl. 2, figs. 10, 23) in having a convex axis, a subcircular outline, and axial furrows which are deep all the way to the posterior end of the terminal piece. The pygidia most likely belong to a telephinid species that is close to *Carolinites*, which is the most abundant telephinid in Laurentia.

Psalikilus sp. A

1973 unassigned pygidium, Terrell, pl. 5, fig. 14.

Remarks. In considering that this species has two wide axial rings, the pygidium is similar to *Psalikilus*? sp. B. However, it shows a postero-medial protrusion extended from the ridge dividing the inner and outer pleural fields, which is diagnostic to *Psalikilus*. It is differentiated from the pygidia of other *Psalikilus* species by the presence of a post-axial ridge.

Psalikilus? sp. A
Pl. III-72, Figs. 13-15.

313

1951 unassigned pygidia, Ross, pl. 19, figs. 8, 9.

Remarks. Ross (1953) mentioned that this specimen could belong to a new *Psalikilopsis* species. Unlike *Psalikilopsis*, the pygidium has a postero-median protrusion which is fused with the axis, and a distinct border. From the pygidia of definite *Psalikilus* species, it differs in having a much less convex axis, a much wider inner pleural field, and a narrower and moderately depressed outer pleural field. The overall triangular outline leads to its questionable assignment to *Psalikilus*. The species represented by this pygidium could be a morphologic intermediate between *Psalikilus* and *Psalikilopsis*.

A smaller pygidium (Pl. III-72, Figs. 13-15) is questionably assigned to this species. It has a depressed outer pleural field and a fulcral ridge protruded posteriorly in its entire transverse width. However, it has a wider and more convex axis which could be ontogenetic difference. Furthermore, it occurs in the *Hintzeia celsaora* to *Protopliomerella contracta* Zone, whereas the pygidium figured by Ross occurs in the *Tesselacauda* Zone.

Psalikilus? sp. B
Pl. III-71, Figs. 18-24
1951 unassigned pygidia, Ross, pl. 19, figs. 12, 16.
1973 unassigned pygidium, Terrell, pl. 5, fig. 10.

Remarks. These pygidia have a tubular-shaped fulcral ridge and smaller tubercles on the outer pleural field, indicating an affinity with *Psalikilus*. However, they have a very wide axis with only two axial rings and an extremely narrow (tr.) inner pleural field. They are questionably referred to *Psalikilus*. A pygidium figured by Terrell (1973, pl. 5, fig. 10) differs in having a less distinct postero-median part of the ridge. Since it is the largest specimen, the difference is considered ontogenetic.

A remarkable similarity to these pygidia is found in *Diceratocephalus armatus* from the Upper Cambrian of North China (Lu, 1954, pl. 1, figs. 8, 9, 11). The presence of two axial rings and continuous tubular fulcral ridge is shared by these two taxa. The pygidia of *D. armatus* only differ in having terrace lines on the outer pleural field parallel to the pygidial margin.

Genus NATMUS Jell, 1985
Type Species. *Natmus victus* Jell, 1985; La1 Zone of the Lancefieldian Series; Digger Island Formation, Victoria, Australia.

Included Species. *N. tuberus* Jell, 1985, *N. tuberculatus* n. sp.

Diagnosis. Ocular ridge slender and directed at about 45 degree angle to exsagittal line. Palpebral lobe relatively small and strongly arched. Occipital spine present. Glabella with parallel-sided lateral margin and rounded anterior margin. Frontal area wide (tr.). Anterior facial sutures parallel-sided or slightly divergent, and sagittally meet at acute angle in anterior view. Distal end of posterior cranidial border ornamented with short spine.

Comparison with "Hystricurids". Jell (1985) assigned *Natmus* to the Hystricuridae with a suspicion that the genus may belong to a separate lineage from other hystricurids. As he mentioned, it is *Psalikilus* that most shares cranidial similarities with *Natmus*. *Psalikilus* is characterized by having a larger and more convex palpebral lobe, a forward-tapering glabella, and a convergent anterior facial suture (see Pl. III-69, Fig. 1). *Natmus* is

314

characterized by having an ocular ridge directed diagonal at about 45 degrees to exsagittal line and a glabella with parallel-sided lateral margins (see Pl. III-59, Fig. 11). However, both genera share many features, including deep and wide axial furrows, deeply impressed glabellar furrows and distal ends of occipital furrow, an ocular ridge, a short (tr.) anterior cranidial border, and a palpebral lobe displaced far posteriorly; for example, compare *Psalikilus pikum* (Hintze, 1953, pl. 9, fig. 1b) and *Natmus victus* (Jell, 1985, pl. 21, fig. 15, see also Pl. III-59, Fig. 11). Although each one of these features may be seen in some "hystricurids", combinations of all these features are rare among "hystricurids."

No pygidium is known for *Natmus*. Jell (1985) figured two partially articulated specimens (pl. 21, figs. 10, 11). One of them (Pl. III-59, Fig. 5) has 17 thoracic segments of which, in particular, the posterior ones are gently sloping ventrally, without displaying any discernible separation between inner and outer pleural fields along a fulcral ridge. Judging from the outline of the thorax, the specimen is most likely to have had no more thoracic segments, or if any, no more than two additional segments. It is probable that the pygidium of *Natmus* is extremely small and does not develop any distinct separation between the inner and outer pleural fields, which conforms to the architecture of the posterior thoracic segments. As a result, the pygidium of *Natmus* is not considered to be as similar to that of *Psalikilus* as might be expected from their strong cranidial similarities.

A free cheek of Australian *Natmus* species (Pl. III-59, Fig. 8; see also Jell, 1985, pl. 21, fig. 12) differs from that of *Psalikilus* in lacking a long median furrow on the genal spine which is continuous from the posterior librigenal border furrow in *Psalikilus*. However, the free cheeks associated with the Laurentian *Natmus* species (Pl. III-60, Figs. 1, 2) are similar to those of *Psalikilus* in having the long median furrow, but differ in having the lateral librigenal border furrow merged with the posterior librigenal border furrow.

Comparison with Ptychopariides. *Natmus tuberus* (Pl. III-59, Figs. 1-4) characteristically develops a preglabellar swelling and genal caeca. Another Australian species, *Natmus victus* develops genal caeca, but it develops preglabellar swelling only when preglabellar field is present (compare Jell, 1985, pl. 21, figs. 1, 5 with fig. 2). The Laurentian species, *Natmus tuberculatus* possesses neither of these two features.

These two specialized features are reminiscent of Upper Cambrian *Amzasskiella* (a nepeid, Peng, 1990b, pl. 7, fig. 1) from China and Kazahstan. In addition to these two features, *Natmus tuberus* shares with *Amzasskiella sanduensis* glabellar furrows which are deeply indented from the axial furrows, a slender ocular ridge, a short spine at the distal end of the posterior fixigena, and pits along the anterior border furrow. *Amzasskiella* is distinguished by an ocular ridge that runs transversely, a much wider (tr.) fixigena, and a smaller glabella. The development of pits along the anterior cranidial border furrow, deep axial furrows, and two pairs of glabellar furrows, seen in the Australian *Natmus* species, is reminiscent of such eulomids as *Euloma* (Tjernvik, 1956, pl. 11, fig. 4).

As mentioned above, no pygidium is known to *Natmus*. Judging from the curvature and change of the slope of the posterior thoracic segments of the articulated segment (Pl. III-59, Fig. 5), *Natmus* is most likely to have a pygidium similar to that of *Amzasskiella* (Peng, 1990b, pl. 7, fig. 4).

315

Taxonomic Conclusion. *Amzasskiella* is a member of the family Nepeidae which was abundant during the Upper Cambrian in Australia and China. The two Australian *Natmus* species undoubtedly have closer relationships with the Nepeidae. The Nepeidae has been known to have a taxonomic affinity with the Menomoniidae (Öpik, 1967, 1970) which includes *Bolaspidella* which in turn is herein considered to be related to *Psalikilus* upon the basis of their cranidial similarities. This further supports close relationship between *Natmus* and *Psalikilus*; and both genera would have had the same Cambrian root. *Natmus* is placed in the Psalikilinae together with *Psalikilus*.

Hypothesis of Evolutionary Relationships. It should be tested whether *Natmus*, in particular, the Australian species, are Tremadoc representatives of the Nepeidae.

<center>

Natmus victus Jell, 1985
Pl. III-59, Figs. 5-11

</center>

1985 *Natmus victus* Jell, p. 61-63, pl. 21, figs. 1-15, pl. 29, fig. 12

Holotype. NMVP 74352, cranidium; Jell, 1985, pl. 21, figs. 3A, 3B (re-illustrated in Pl. III-59, Figs. 6, 7, 9); La1 Zone of the Lancefieldian Series; Digger Island Formation, Victoria, Australia.

Diagnosis. Glabella large and subrectangular. Preglabellar field very narrow (sag.) or absent. Pits developed along anterior cranidial border furrow. Anterior cranidial border very long (tr.). Genal caeca developed on anterior fixigena and librigenal field. Three pairs of glabellar furrows; S1 obliquely directed posteriorly, S2 and S3 shorter and obliquely directed anteriorly. Anterior and lateral librigenal border furrows shallow out towards postero-lateral corner of librigenal field. Eye socle present.

Discussion. See Jell (1985, p. 61-63)

<center>

Natmus tuberus Jell, 1985
Pl. III-59, Figs. 1-4

</center>

1985 *Natmus tuberus* Jell, p. 63, pl. 20, figs. 9-12.

Holotype. NMVP 74349, cranidium; Jell, 1985, pl. 20, figs. 12A, 12B (re-illustrated in Pl. III-59, Figs. 1-4); La1 Zone of the Lancefieldian Series; Digger Island Formation, Victoria, Australia.

Diagnosis. Swelling present on preglabellar field and laterally defined by distinct furrows. Genal caeca present on anterior fixigena. Pits developed along anterior cranidial border furrow. Three pairs of glabellar furrows.

Discussion. See Jell (1985, p. 63)

<center>

Natmus tuberculatus n. sp.
Pl. III-60, Figs. 1-8

</center>

Etymology. "Tuberculatus" depicts that the cranidial surface is ornamented by tubercles, instead of genal ceca.

Holotype. UA 12481, cranidium; Pl. III-60, Figs. 3, 4; *Hintzeia celsaora* to *Protopliomerella contracta* Zone; Garden City Formation, southern Idaho.

Diagnosis. Tubercles on cranidial and librigenal field surface. Anterior border furrow curves backwards sagittally. Occipital spine slender. Lateral and posterior librigenal border furrow merge at postero-lateral corner of librigenal field and continue into long genal spine. Glabella very convex and perpendicularly down-sloping. S1 deeply

<center>316</center>

impressed and connected with furrow defining ocular ridge posteriorly.

Remarks. This new species differs from the Australian species in mainly having tubercles on cranidial surface, instead of genal ceca.

<div align="center">

Natmus sp. aff. *N. tuberculatus*

Pl. III-60, Figs. 9-13

</div>

Remarks. Compared with *Natmus tuberculatus*, these cranidia have a less steeply down-sloping glabella profile, a sagittally shorter cranidial length, and more deeply impressed S1 glabellar furrows that are connected with furrow defining eye ridge posteriorly.

<div align="center">

?Subfamily PSALIKILINAE n. subfam.

Genus PSALIKILOPSIS Ross, 1953

</div>

Type Species. *Psalikilopsis cuspidicauda* Ross, 1953; *Protopliomerella contracta* Zone; Garden City Formation, southern Idaho.

Included Species. *P. brachyspinosus* n. sp.

Diagnosis. Palpebral lobe slender in width, strongly arched, located at mid-cranidial length, and well defined by palpebral furrow. Sagittal portion of anterior cranidial border and furrow strongly curved posteriorly. Posterior fixigenal area triangular. Preglabellar furrow deep. Glabella oval and strongly convex. Anterior facial suture moderately convex laterally. Pygidium with a postero-median spine that extends from fulcral ridge dividing inner and outer pleural fields. Fulcral ridge ornamented with three or four short denticles. Inner pleural field wide and flat. Outer pleural field steeply (more than the right angle towards the inside) downsloping and covered with terrace lines. No distinct pygidial marginal border. Posterior margin strongly indented dorsally. Lateral and posterior librigenal border furrow separated by a swelling developed at postero-lateral corner of ocular platform. Lateral librigenal border and genal spine covered with terrace lines.

Comparison with "Hystricurids". *Psalikilopsis* was thought of as a relative to *Psalikilus* by Ross (1953) and included in the Hystricuridae along with *Psalikilus* (Lochman *in* Moore, 1959). However, the cranidia of *Psalikilopsis* are easily differentiated from those of *Psalikilus* in lacking glabellar furrows and an ocular ridge, and in having a slender strongly arcuate palpebral lobe located at mid-cranidial length, a triangular posterior fixigena, an oval-shaped strongly convex glabella, a much deeper preglabellar furrow, an anterior border furrow that deepens sagittally, and a laterally convex anterior facial suture. The cranidial architecture of *Psalikilopsis* does not seem to accord with that of *Psalikilus* as previously suggested. The elongated oval-shaped glabella is similar to that of *Hystricurus* (*Aequituberculatus*) *ellipticus* (Westrop *et al.*, 1993, pl. 3, fig. 1). The glabellar shape and the nature of the palpebral lobe are similar to *Rollia goodwini* (see Pl. III-84, Figs. 11-13). However, *Rollia* has a rather long preglabellar field and three short pairs of glabellar furrows.

The pygidia of *Psalikilopsis* have an architecture similar to those of *Psalikilus*. The *Psalikilopsis* pygidia have a row of short denticles on the fulcral ridge that are progressively shorter posteriorly, whereas the *Psalikilus* pygidia have a smooth ridge. These short denticles topographically correspond to tubercle(s) developed on the distal edge of the inner pleural field in such *Hystricurus* (*Hystricurus*) species as *H.* (*H.*)

<div align="center">

317

</div>

crotalifrons (see Boyce, 1989, pl. 11, fig. 3), and in *Eurylimbatus* (see Pl. III-40, Figs. 3, 4, 15) and *Paratersella* (see Pl. III-66, Figs. 1, 3). These latter taxa, however, do not develop a fulcral ridge. *Eurylimbatus* and *Psalikilopsis* have their pygidial interpleural and pleural furrows confined to the inner pleural field. *Psalikilopsis* lacks a distinct pygidial border and has the outer pleural field covered with terrace lines, whereas *Psalikilus* has the distinct border and the outer pleural field covered with small tubercles. The development of a long postero-median spine, steeply sloping outer pleural field, and deeply indented posterior margin are unique to *Psalikilopsis*. However, some *Psalikilus* pygidia have a short protrusion of the fulcral ridge (see Pl. III-71, Figs. 8, 9) and show a moderate indentation of the posterior margin (see Pl. III-69, Figs. 3, 4).

Free cheeks of *Psalikilopsis* are comparable to those of *Flectihystricurus* (see Pl. III-49, Fig. 1) and *Paraplethopeltis* (see Hintze, 1953, pl. 7, fig. 2). They are different from the free cheeks of *Psalikilus* in having a shorter genal spine and in lacking a long median furrow on the genal spine.

Comparison with Proetides. The condition of the palpebral lobe and palpebral furrow is reminiscent of such bathyurids as *Jeffersonia* (see Cullison, 1944, pl. 34, fig. 17), *Peltabellia* (see Ross, 1951, pl. 17, fig. 12), and *Goniotelina* (see Ross, 1951, pl. 14, fig. 21); see Whittington (1953a) for detailed account for taxonomy of *Peltabellia* and *Goniotelina*. The narrow preglabellar field of *Psalikilopsis* is comparable to many bathyurids in terms of the width. However, the narrow width appears to be due to the backward encroachment of the anterior border in *Psalikilopsis*, whereas it appears to be due to the forward encroachment of the glabella in the bathyurids. Other cranidial features, and all the pygidial features, are not comparable with the bathyurids.

Taxonomic Conclusion. The pygidial architecture of *Psalikilopsis* is most comparable to that of *Psalikilus*, and such specialized features as the postero-median spine and short denticles on pleural field ridge can be considered to be evolutionary specializations from *Psalikilus*. However, the cranidial architecture of *Psalikilopsis* does not support a close taxonomic affinity to *Psalikilus*. *Psalikilopsis* is questionably placed in the subfamily Psalikilinae, to which *Psalikilus* and *Natmus* belong.

<div align="center">

Psalikilopsis cuspidicauda Ross, 1953

Pl. III-73, Figs. 1-6

</div>

1953 *Psalikilopsis cuspidicauda* Ross, p. 639-640, pl. 63, figs. 2-9, 12.

? 1986 *Omuliovia* sp. Zhou and Fortey, [part], p. 199, pl. 11, fig. 10, [only].

Holotype. Y.P.M. 18774, cranidium; Ross, 1953, pl. 63, figs. 4, 5, 9; *Protopliomerella contracta* Zone; Garden City Formation, southern Idaho.

Diagnosis. Postero-median pygidial spine slender and long (half of axial length). Anterior pygidial margin transverse.

Association of Pygidium. Ross (1953) associated a pygidium with this species (pl. 63, figs. 2, 6, 7). Pygidia showing similar morphologies (Pl. III-73, Figs. 7-11) were recovered from SR6U, where cranidia of this species were also discovered. These pygidia differ from that described by Ross in having a stout postero-median spine. This difference is considered to be of specific value.

The pygidia associated with *Psalikilopsis* species differ from those of *Psalikilus* in having a long postero-median spine that extends from the fulcral ridge, a very steeply inclined outer pleural field lacking a distinct border and covered with terrace lines, a

<div align="center">

318

</div>

wider inner pleural field, and three or four short denticles on a fulcral ridge. The pygidia of *Psalikilus* have a short protrusion of the postero-median portion of the fulcral ridge which appears to topographically correspond with the long postero-median spine of *Psalikilopsis*. The pygidia of ?*Psalikilus* sp. A (see Ross, 1951, pl. 19, figs. 8, 9, Pl. III-72, Figs. 13-15) appear to be intermediate between pygidia of both genera. The overall pygidial architecture of both genera is similar.

The association of pygidia with *Psalikilopsis* by Ross (1953) was mainly based on his assumption that the pygidia are similar to those of *Psalikilus* whose cranidial morphologies were considered to be most similar to those of *Psalikilopsis*, and that the materials co-occur in the same locality. However, the cranidial features of *Psalikilopsis* are not as similar to those of *Psalikilus* as previously suggested (see above). The assumption that cranidial similarities are extrapolated into pygidial similarities does not always seem to be useful. It is only the co-occurrence of the pygidia with the cranidia from SR6U that only supports the association of pygidia with *Psalikilopsis*.

Since the cranidia of *Psalikilopsis cuspidicauda* and pygidia of *Psalikilopsis brachyspinosus* were obtained from the same sampling horizon (SR6U) collected by this author, it is possible that the associations of pygidium with each species may be crossed.
Remarks. Zhou and Fortey (1986) figured a cranidium of *Omuliovia* sp. The cranidium from northeast China shows an anterior border that is curved backwards sagittally, and an elongated oval-shaped glabella. These two features are evident in the cranidia of *Psalikilopsis cuspidicauda*. The Chinese cranidium differs in having a straight anterior facial suture—but it is divergent as in *P. cuspidicauda*—and more strongly arcuate palpebral lobe.

Psalikilopsis brachyspinosus n. sp.
Pl. III-73, Figs. 7-11

1951 *Psalikilus* ? sp. Ross, p. 63, pl. 13, figs. 28, 29, 33, 34, pl. 30, figs. 1-3.
Etymology. "brachyspinosus" comes from Latin "brachys" meaning "short" and "spinosus" meaning "spine".
Holotype. UA 12634, pygidium; Pl. III-73, Figs. 8-11; *Hintzeia celsaora* to *Protopliomerella contracta* Zone; Garden City Formation, southern Idaho.
Diagnosis. Postero-median pygidial spine stout and short (less than one-third of axial length). Anterior pygidial margin strongly directed backwards. Anterior facial suture more divergent. Glabella more convex laterally.
Remarks. A cranidium and free cheek (Ross, 1951, pl. 13, 28, 29, 33, 34) were questionably assigned to *Psalikilus*. However, they are characterized by having a divergent anterior facial suture, a strongly incurved anterior cranidial border, and an oval-shaped glabella, and lacking a long median furrow in the genal spine. These features well accord with the concept of *Psalikilopsis*. This species differs from other *Psalikilopsis* species in having short and stout postero-median pygidial spine.

Psalikilopsis sp. nov.
1953 *Psalikilus spinosum* Hintze, p. 212-213, pl. 9, figs. 7a-7c.
? 1953 *Jeffersonia*? sp. B, Hintze, [part] p. 175-176, pl. 9, fig. 11 [only].
Diagnosis. Postero-median spine protruded as tongue-like extension in pygidium.
Remarks. Hintze (1953) assigned this pygidium to *Psalikilus spinosum*. The pygidia of

319

Psalikilopsis lack a border, whereas those of *Psalikilus* have a distinct border. The pygidium is re-assigned to a new *Psalikilopsis* species, because it develops no distinct border and has a steeply inclined outer pleural field. The nature of the postero-median extension of the fulcral ridge is similar to that of *?Psalikilus* sp. A (Ross, 1951, pl. 19, figs. 8, 9). Ross (1953) mentioned a possbility that the cranidium that was questionably identified as *Jeffersonia* by Hintze (1953) would belong to *Psalikilopsis*. However, the crucial frontal area including the anterior border and the preglabellar field, is not preserved in that specimen.

Family **DIMEROPYGIDAE** Hupé, 1953
Genus **DIMEROPYGIELLA** Ross, 1951

Type Species. *Dimeropygiella caudanodosa* Ross, 1951; *Pseudocybele nasuta* to *Hesperonomiella minor* Zone; Garden City Formation, northern Utah.
Remarks: *Dimeropygiella* was recently resurrected as a valid genus separated from *Ischyrotoma* by Adrain *et al.* (2001). Detailed accounts for its diagnosis are found in their article.

Dimeropygiella ovata Hintze, 1953
Pl. III-51, Figs. 1-16.
1953 *Dimeropygiella ovata* Hintze, p. 155, pl. 19, figs. 1-4
1973 *Ischyrotoma blanda*, Young, [part], p. 102, pl. 2, fig. 1, [only].
1973 *Ischyrotoma* (?), Young, p. 102, pl. 7, figs. 10, 11.
2001 *Dimeropygiella ovata*, Adrain *et al.*, figs. 10, 11.1-11.8, 11.10-11.12.
Holotype: 26347, cranidium; Hintze, 1953, pl. 19, figs. 1a-1c; *Trigonocerca typica* Zone; Fillmore Formation, Utah.
Diagnosis: see Adrain *et al.* (2001)
Remarks. see Adrain et al. (2001, p. 965).

?Family **DIMEROPYGIDAE** Hupé, 1953
Genus **PSEUDOHYSTRICURUS** Ross, 1951

Type Species. *Pseudohystricurus obesus* Ross, 1951; *Rossaspis superciliosa* Zone; Garden City Formation, southern Idaho.
Included Species. *P. bathysulcatus* n. sp., *P.? parvus* n. sp., *P.? orbus* Ross, 1953.
Diagnosis. Pygidium with relatively wide axis and steeply down-sloping outer pleural field and spines along distal edge of inner pleural field. Glabella oval-shaped. Palpebral lobe slender and small, and palpebral furrow straight.
Comparison with "Hystricurids". The oval-shaped glabella of *Pseudohystricurus* is similar to that of such *Hystricurus* species as *H.* (*Aequituberculatus*) *globosus* and *H.* (*Butuberculatus*) *hillyardensis* (Stitt, 1983, pl. 4, figs. 3, 4, pl. 5, figs. 1, 2). However, these *Hystricurus* species are easily differentiated by lacking a row of spines along the distal edge of the inner pygidial pleural field. Like *Pseudohystricurus*, most *Parahystricurus* species have a triangular posterior fixigena and a convergent anterior facial suture. However, *Parahystricurus* is differentiated by a semi-circular palpebal lobe. The pygidia of *Pseudohystricurus* are characterized by developing a row of spines between the flat inner pleural field and steeply down-sloping outer pleural field. Interestingly, the hystricurids such as *Spinohystricurus* (Pl. III-20, Figs. 1, 2, 5) and

320

Hillyardina (Pl. III-47, Figs. 14-25) develop a fulcral ridge that appears to correspond topographically to the row of spines of *Pseudohystricurus*.

Comparison with Ptychopariides. *Onchonotellus abnormis* from the Upper Cambrian strata of Kazakhstan (Ivshin, 1956, pl. 9, figs. 9-16; 1962, pl. 7, fig. 12) and South China (Peng, 1992, fig. 39J) has an oval-shaped glabella, a transversely short anterior border, an anterior border furrow and preglabellar furrow that sagittally meet each other, forming a "X"-shaped cross in anterior view, a steeply directed posterior facial suture, a strongly convergent anterior facial suture, and a relatively small palpebral lobe. All these features are evident in *Pseudohystricurus obesus*. *O. abnormis* differs in that all the cranidial furrows are much more deeply impressed, the posterior cranidial border furrow curves forwards distally, and the palpebral fixigena is broader transversely. Other *Onchonotellus* species from China and Kazakhstan (e.g., see Peng, 1992, figs. 39B-39I), if the assessment to the genus by Peng (1992) is accepted, have a transversely much wider fixigena and a subrectangular glabella. These features are different from the conditions seen in *Pseudohystricurus*. Shergold (1980) placed *Onchonotellus* in the Catillicephalidae, which has been accepted by Peng (1992) and Pratt (1992).

Based on information available to the author, the pygidium of *Onchonotellus* (Ivshin, 1956, p. 30, pl. 9, fig. 11) does not have a separation of the inner and outer pleural fields by developing a fulcral ridge or row of spines. It is presumed that *Onchonotellus* has a generalized ptychopariide-type pygidium like most catillicephalids. Like many "hystricurids," *Pseudohystricurus* has a pygidium with a separation of the two pleural fields by developing a row of spines.

The overall cranidial architecture of *Pseudohystricurus bathysulcatus* is similar to that of *Onchonotopsis* (Robison, 1988, figs. 24.6-24.12). The parallel-sided anterior facial suture and convex-forward anterior cranidial margin are shared by *P. bathysulcatus* and *Onchonotopsis*; *Onchonotopsis* has a much larger and more convex glabella and does not develop tubercles on the cranidial surface. These similarities and dissimilarities are applicable for *Onchonotus* (Onchonotidae, Ludvigsen *et al.*, 1989, pls. 40, 41).

The development of a row of spines along the distal edge of the inner pleural field in *Pseudohystricurus* is evident in *Heterocaryon*, an Upper Cambrian entomaspidid (see Ludvigsen, 1982, figs. 55I-K, M, N). The spines of *Heterocaryon* are bifurcated, whereas those of *Pseudohystricurus* are non-bifurcated.

Comparison with Proetides. The overall cranidial architecture of *Pseudohystricurus* is strongly similar to that of *Dimeropygiella*, a dimeropygid. *Pseudohystricurus*? *orbus* (Ross, 1953, pl. 63, figs. 10, 15, 16) shows cranidial features that appear to be intermediate between the two genera. The pygidia of *Pseudohystricurus* do not develop discrete ridges on the outer pleural field extended from pleural ribs of the inner pleural field and a tubular border ornamented with terrace lines, which characterize *Dimeropygiella* (see Pl. III-51, Figs. 4, 5, 8, 9, 15, 16). However, the pygidia of *Dimeropygiella* develop a row of shorter spines which topographically corresponds to that of *Pseudohystricurus*; the transitory pygidium of *Dimeropygiella* (Pl. III-51, Figs. 15, 16) displays a more similar configuration of the row of spines to *Pseudohystricurus*. The *Pseudohystricurus* pygidia are strongly similar to those of *Dimeropyge* (Chatterton, 1994, figs. 7.15, 7.16, 7.19, 7.20) in having a tall outer pleural field and flat inner pleural field, and spines that are located along the distal edge of the inner pleural field and extended from the posterior pleural bands. The pygidia of *Heckethornia* (Pl. III-80, Figs.

8-12) are comparable to those of *Pseudohystricurus* (Pl. III-77, Figs. 8-11) with respect to the development of spines along the distal edge of the inner pleural field and in having a tall outer pleural field. These features are evidently visible in *Dimeropygiella*.

Adrain et al. (2001) placed *Pseudohystricurus* in the Dimeropygidae, mainly on the basis of *Pseudohystricurus orbus*, whose cranidial morphologies are considered herein to be intermediate between *Pseudohystricurus* and *Dimeropygiella*. They suggested *P. orbus* may belong to *Dimeropygiella*. The extension of the similarities into the Cambrian taxa was not in their scope of the study.

Taxonomic Conclusion. The cranidial features of *Pseudohystricurus* undoubtedly indicate that the genus is closely related to *Onchonotellus*, a catillicephalid. In contrast, the pygidium of *Pseudohystricurus* strongly suggests that the genus should be placed in the Dimeropygidae, along with *Heckethornia*. Cranidial similarities with *Parahystricurus* and *Spinohystricurus robustus* conradict this assignment. Due to this complicated similarites, *Pseudohystricurus* is excluded from the Hystricuridae, and tentatively assigned to the Dimeropygidae.

Hypotheses of Evolutionary Relationships. It is certain that such Upper Cambrian taxa as *Onchonotellus* are related to the Lower Ordovician *Pseudohystricurus*, which in turn is related to *Dimeropygiella*. Their relationshihps need to be tested to determine the taxonomic status of each of these taxa.

The topographic correspondence between the row of spines of *Pseudohystricurus* and the fulcral ridge of *Spinohystricurus* needs to be tested to determine whether these pygidial features are homologous. This will enlighten how *Pseudohystricurus* is related to the Hystricuridae.

<div align="center">

***Pseudohystricurus obesus* Ross, 1951**
Pl. III-77, Figs. 1-11
</div>

1951 *Pseudohystricurus obesus* Ross, p. 74, pl. 16, figs. 25, 30, 34.
1951 indefinitely assigned pygidium, Ross, pl. 9, figs, 25, 29, 30.
1973 *Pseudohystricurus obesus*, Terrell, p. 88-89, pl. 5, fig. 1.
1973 *Pseudohystricurus obesus*, Demeter, p. 64-65, pl. 6, figs. 13, 14.

Holotype. Y.P.M. 18049, cranidium; Ross, 1951, pl. 16, figs. 25, 30, 34; *Rossaspis superciliosa* Zone; Garden City Formation, southern Idaho.

Diagnosis. Glabella large and oval-shaped. Posterior facial suture diagonal. Anterior facial suture convergent. Anterior cranidial border furrow moderately incurved sagittally. Preglabellar field very short (sag.). Row of short spines along distal edge of inner pleural field. Outer pleural field steeply down-sloping and slightly concave.

Association of Pygidium. Demeter (1973) illustrated an articulated meraspid specimen (pl. 6, figs. 13a-13c) and described its pygidium as "Distinctly segmented pleurae end in short marginal spines." (p. 65). These spines do not appear to develop along the pygidial margin, but they develop along the distal edge of the inner pleural field. A majority of cranidial specimens of *P. obesus* occur in a single sampling horizon, SE-90T. From the same horizon pygidia occur that have a row of short spines along the distal edge of the inner pleural field (see Pl. III-77, Figs. 8-11).

<div align="center">

***Pseudohystricurus bathysulcatus* n. sp.**
Pl. III-77, Figs. 12-19
</div>

<div align="center">322</div>

1951 *Parahystricurus*? sp. A, Ross, p. 61, pl. 14, figs. 5, 8, 12.

1951 *Parahystricurus*? sp. B Ross, p. 61-62, pl. 14, figs. 4, 6, 7.

Etymology. "bathysulcatus" is composed of "bathy" (deep) and "sulcatus" (furrow) depicting the distinctively-impressed anterior cranidial border furrow.

Holotype. UA 12689, cranidium; Pl. III-77, Fig. 15; *Symphysurina* Zone; Fillmore Formation, Utah.

Diagnosis. Preglabellar field relatively long. Anterior cranidial border and border furrow gently convex forwards. Anterior cranidial border furrow distinctly impressed. Anterior facial suture parallel-sided. Glabella relatively small.

Remarks. Two cranidia described by Ross (1951, pl. 14, figs. 4-8, 12) are larger than those described in this study. These cranidia differ in having a straight posterior facial suture, which is considered ontogenetic.

Pseudohystricurus? *parvus* n. sp.
Pl. III-77, Figs. 20-30

Etymology. "parvus" depicts the small glabella

Holotype. UA 12693, cranidium; Pl. III-77, Figs. 20, 22, 25, 26; *Paraplethopeltis* or *Leiostegium-Kainella* Zone; Garden City Formation, southern Idaho.

Diagnosis. Glabella elongated, proportionately small, and forward-tapering. Distal end of posterior fixigena rounded. Outer pleural field narrower and inner pleural field broader. Genal spine short.

Association of Pygidium. From the same sampling horizon, R6-38, pygidia possessing row of short spines along the distal edge of inner pleural field are found. These pygidia (see Pl. III-77, Figs. 28-30) are associated with this species. This association lends support the affinity of this species to *Pseudohystricurus*.

Remarks. This species resemble *Hystricurus*? aff. *H.*? *missouriensis* and *Spinohystricurus* sp. nov. With *S.* sp. nov. (Pl. III-19, Figs. 18-21) , this species shares a trapezoidal cranidial outline and a long (tr.) posterior fixigena with a rounded distal end, but it differs in having a straight palpebral furrow. With *H.*? aff. *H.*? *missouriensis* (Pl. III-21, Figs. 1-7), it shares the form of the glabella and the posterior fixigena, but it differs in having a more strongly convergent anterior facial suture. The similarities to these taxa make the assignment of this species to *Pseudohystricurus* less definite.

Pseudohystricurus? sp. A
Pl. III-51, Figs. 17-21

1951 *Parahystricurus* ? sp. C, Ross, p. 62, pl. 28, figs. 17, 18, 21, 22.

? 1951 undetermined genus and species B, Ross, p. 121-122, pl. 28, figs. 16, 20, 25-28.

? 1973 unassigned cranidium, Terrell, pl. 3, fig. 8.

Remarks. The cranidium figured by Ross (1951, pl. 28, figs. 17, 18, 21) has the palpebral lobe incompletely preserved. New materials from this study (Pl. III-51, Figs. 17-21) show that this species has a weakly arched palpebral lobe that does not accord with the concept of *Parahystricurus*. This species has a forward-tapering glabella, a weakly arched palpebral lobe and a triangular, although relatively short, posterior fixigena. These features indicate an affinity with *Pseudohystricurus*. However, the parallel-sided anterior facial suture, relatively long preglabellar field, wide frontal area, and terrace lines on the anterior border suggest that this species shwould be included in

323

Pseudohystricurus with question. The two distinct rows of tubercles on the glabella of this species are seen in both *Pseudohystricurus* as well as *Parahystricurus*.

The overall cranidial outline of undetermined genus and species B (Ross, 1951, pl. 28, figs. 16, 20, 25-28) and an unassigned cranidium (Terrell, 1973, pl. 3, fig. 8) is very similar to that of this species. They differ in lacking paired tubercles on the glabella and in having much shallower axial furrows. As noted by Ross (1951), they resemble the cranidia of *Platycolpus*? sp. (see Ross, 1951, pl. 29, fig. 27) which is assigned to *Benthamaspis* in this study. However, the cranidia differ from *Benthamaspis* in having a less strongly arched palpebral lobe, a sagittally longer anterior border, and a much deeper anterior border furrow.

Pseudohystricurus? *orbus* Ross, 1953

1953 *Pseudohystricurus orbus* Ross, [part], p. 640-642, pl. 63, figs. 10, 11, 15-23, [only, not figs. 13, 14].

Holotype. YPM 18779, cranidium; Ross, 1953, pl. 63, figs. 10, 15, 16; *Hintzeia celsaora* Zone; Garden City Formation, southern Idaho.

Diagnosis. Anterior cranidial margin pointed forwards and ventrally. Palpebral lobe relatively long and well delimited by palpebral furrow that is moderately curved laterally.

Remarks. The generic assignment of this species appears to be suspicious because of its cranidial similarities with *Dimeropygiella*. In particular, the triangular anterior border that is relatively acutely pointed ventrally (*Pseudohystricurus* has a dorsally upturned anterior cranidial border) is strongly reminiscent of *Dimeropygiella* (see Pl. III-51, Figs. 2, 3, 6). The sagittal portion of the free cheek is ventrally protruded, which is also seen in *Dimeropygiella* (see Pl. III-51, Figs. 7, 14). It is certain that this species is a morphologic intermediate between *Pseudohystricurus* and *Dimeropygiella*. The pygidial morphology is needed to further assess its taxonomic placement. The two pygidia figured by Ross (1953, pl. 63, figs. 13, 14) must belong to *Goniotelina* or *Eleutheroncentrus*, the bathyurids that are characterized by the possession of a long spine extended from pygidial axis.

Genus HECKETHORNIA Adrain *et al.*, 2001

Type Species. *Heckethornia borderinnensis* Adrain *et al.*, 2001; *Hintzeia celsaora* to *Protopliomerella contracta* Zone; Garden City Formation, southern Idaho.

Included Species. *H. alticapitis* (Young, 1973), *H.*? *linearus* (Young, 1973)

Diagnosis. Cranidium covered long spines. Row of long spines along the distal edge of flat and narrow inner pleural field.

Remarks. *Heckethornia* is undoubtedly closely related to *Pseudohystricurus*. The obvious morphologic difference is that *Heckethornia* develops much longer spines on the cranidia and pygidia.

The smaller cranidia of many aulacopleurids have a long occipital spine and a very short fixigenal spine, Fx1 (see *Otarion*, Adrain and Chatterton, 1994, figs. 5.23, 5.25; *Cyphaspis*, Adrain and Chatterton, 1996, figs. 1.47, 2.1). *Heckethornia alticapitis* has the same configuration of spine development. Apart from the slender palpebral lobe of *Heckethornia* and the conspicuous S1 glabellar furrows of the aulacopleurids, the overall cranidial architectures of both taxa are remarkably similar. However, the aulacopleurid pygidium is of generalized ptychopariide type, whereas the *Heckethornia* pygidia are

324

much closer to those of many "hystricurids," in having, amongst others, a distinct separation of outer and inner pleural fields. The spine development along the margin of the transitory pygidia of the aulacopleurids (see Adrain and Chatterton, 1996, fig. 2.6; Adrain and Chatterton, 1994, fig. 7.7) is comparable to the spinose pygidia of *Heckethornia*.

The overall cranidial architecture of *Heckethornia alticapitis* is similar to that of *Onchonotopsis* (Robison, 1988, figs. 24.6-24.12). The strongly convex oval-shaped glabella is shared by *H. alticapitis* and *Onchonotopsis*. *H. alticapitis* develops tubercles on the glabella and spines on the occipital ring and posterior cranidial border surface whereas *Onchonotopsis* has a smooth cranidial surface.

From *Dimeropygiella*, *Heckethornia* differs in having spines on the exoskeletal surface, and in lacking a sagittal ventral librigenal protrusion and ridges on the outer pygidial pleural field. The oval-shaped glabella, course of facial sutures, tall outer pygidial pleural fields, and narrow inner pygidial pleural fields are shared by both taxa.

The similarities of smaller aulacopleurid cranidia and pygidia with *Heckethornia* indicate their close evolutionary relationships. It seems plausible that the aulacopleurids evolved from *Heckethornia* through *Parahystricurus* by attaining a semi-circular palpebral lobe from *Parahystricurus*. The ptychopariid-type pygidium of the aulacopleurids could be a re-curring morphotype that adapted to an environment similar to that was occupied by the ptychopariids (a homeomorphy, Hughes and Chapman, 1995), whereas the *Heckethornia* pygidium could be a feature adaptive to the environments inhabited by many other "hystricurids."

Taxonomic Conclusion. *Heckethornia* is placed in the Dimeropygidae with question like *Pseudohystricurus*. The development of a distinct separation of the inner and outer pygidial pleural fields suggest an affinity with the "hystricurids."

<div align="center">

Heckethornia borderinnensis Adrain *et al.*, 2001
Pl. III-80, Figs. 1-14

</div>

1973 unassigned pygidium, Terrell, pl. 6, fig. 9.
2001 *Heckethornia borderinnensis*, pl. 1, figs. 1-44.

Holotype. UA 12708, cranidium; *Hintzeia celsaora* to *Protopliomerella contracta* Zone; Garden City Formation, southern Idaho.

Diagnosis. Cranidium ornamented with long spines. Pair of long occipital spines. Glabella forward-tapering. Anterior cranidial border relatively straight transversely. Pygidial fulcral ridge ornamented with long spines. Inner pleural field flat and narrow. Outer pleural field steeply down-sloping.

Association of Pygidium. From the same sampling horizon where cranidial materials of this species were secured, a pygidium was found that develops four pairs of long spines along the distal edge of the inner pleural field. The spine development makes it fairly reasonable to associate this pygidium with this species, whose cranidia develop long spines on the exoskeletal surface. The most anterior pleural segment of the pygidium is thoracic (see the posterior view illustration, Pl. III-80, Fig. 12). Like many other "hystricurids," the pygidium has a steeply-downsloping outer pleural field and narrow and flat inner pleural field.

The pygidia from the Fillmore Formation referred to *Dimeropygiella* (Hintze, 1953, pl. 19, fig. 9; Terrell, 1973, pl. 6, fig. 9; Young, 1973, pl. 6, fig. 1) are assigned to this

<div align="center">325</div>

species. It is possible that *Dimeropygiella* develops long spines and loses them later in ontogeny. Since no protaspid materials have been reported for *Dimeropygiella*, this assessment is still open to question.

Heckethornia alticapitis (Young, 1973)
Pl. III-81, Figs. 1-19

1951 undertermined species, Hintze, pl. 19, figs. 11-13.
1953 *Dimeropygiella* ?, Hintze, pl. 19, fig. 9.
1973 *Psalikilopsis* (?) *alticapitis* Young, p. 106-108, pl. 4, figs. 1-8.
1973 *Ischyrotoma* (?), Young, pl. 6, fig. 1.
1973 unassigned librigena 4, Young, pl. 7, fig. 8.
2001 *Heckethornia alticapitis* (Young, 1973), pl. 2, figs. 1-32.

Holotype. BYU 2102, cranidium; Young, pl. 4, figs. 1-3; *Trigonocerca typica* Zone; Fillmore Formation, Utah.

Diagnosis. Long spine on occipital ring and posterior fixigena; rest of cranidial exoskeletal surface ornamented with tubercles. Glabella oval-shaped and highly convex dorsally; axial furrows impressed sagittally. Anterior cranidial border upturned dorsally. Anterior cranidial margin straight.

Association of Pygidium. SH-1, a locality where all the cranidial materials of this species were found, also produces pygidia that are similar to those of *Heckethornia borderinnensis* (Pl. III-80, Figs. 8, 9, 12). A pygidium (Pl. III-81, Figs. 18, 19) with a similar size to that of *H. borderinnensis* bears a much longer pair of spines on its terminal piece, and all the spines appear to be of equal length. This resemblance and difference allow the assignment of these pygidia to this species.

Remarks. *Psalikilopsis* has a slender, strongly arched palpebral lobe, a laterally convex anterior facial suture, and a sagittally incurved anterior border and border furrow (see Pl. III-73, Figs. 3-5). The cranidia of this species show none of these features. This species differs from *Heckethornia borderinnensis* in having only one occipital spine, and an oval-shaped glabella.

Heckethornia n. sp.
Pl. III-80, Figs. 15-21

Diagnosis. Exoskeletal surface covered with many irregularly-distributed long spines. Posterior fixigena sharply terminated distally. Glabella strongly forward-tapering (triangular in outline).

Remarks. The posterior fixigena of this species is similar to that of *Glabellosulcatus koreanicus* (see Pl. III-79, Fig. 5) in that it is transversely long and sharply terminated distally. The anterior facial suture is similar to *Glabellosulcatus crassilimbatus* (see Pl. III-78, Fig. 2)

Heckethornia? *lineara* (Young, 1973)
Pl. III-78, Fig. 18-20

1973 *Amblycranium* (?) *linearus* Young, p. 96-97, pl. 4, figs. 9-15.
1973 *Amblycranium* (?) sp. 2, Young, p. 97, pl. 4, figs. 16-20.
Holotype. BYU 2105, cranidium; Young, 1973, pl. 4, figs. 9, 13; *Trigonocerca typica*

326

Zone; Fillmore Formation, Utah.

Diagnosis. Palpebral lobe large, slender, and defined by strongly curved palpebral furrow. Glabella oval-shaped, with maximum width being at level of palpebral lobe, and ornamented by two rows of spines or tubercles at its crest. Occipital ring with pair of spines. Posterior fixigena transverse and narrow (exsag.). Anterior border pointed anteriorly. Posterior facial suture laterally deeply cut librigena, resulting in no posterior librigenal border.

Remarks. Young (1973) assigned a cranidium and free cheek to *Amblycranium* (?) sp. 2 (pl. 4, figs. 16-20) because the cranidum bears two rows of tubercles—not spines as in his *Amblycranium* (?) *linearus*—and lacks tubercles on the occipital ring, and the free cheek is ornamented with finer tubercles. Since these two specimens are larger than those of *Amblycranium* (?) *linearus*, the variations are considered to be ontogenetic and thus they are assigned to this species.

With *Psalikilopsis* (Pl. III-73, Figs. 3-5), this species shares an oval shaped-glabella, slender palpebral lobe, and laterally convex anterior facial suture, but it differs in having two rows of spines on the glabella and occipital ring, transverse posterior fixigena, and pointed anterior margin.

The possible affinity of this species to *Heckethornia* and *Pseudohystricurus* is supported by the spine development on the glabella and occipital ring (observed in *Heckethornia borderinnensis*), and the oval-shaped glabella (observed in *Pseudohystricurus obesus*). However, this species bears a crescentic palpebral lobe, a transverse posterior fixigena, and a slightly divergent anterior facial suture. These features cannot be accommodated within the concept of *Pseudohystricurus* or *Heckethornia*. The questionable assignment of this species to *Heckethornia* is due to the development of the spines on glabella.

<center>?Family TOERNQUISTIIDAE Hupé, 1953
Genus EURYLIMBATUS n. gen.</center>

Etymology. "Eurylimbatus" denotes that this genus has a broad anterior cranidial border and posterior fixigena.

Type Species. *Eurylimbatus amplissimus* n. sp.; *Tesselacauda* Zone. Fillmore Formation, Utah.

Included Species. *E. sphaerus* n. sp., *E. acutus* n. sp.

Diagnosis. Posterior fixigena broad (exsag.). Glabella large and subtriangular in outline. Palpebral lobe of medium-size, slender, and weakly arched laterally. Posterior cranidial border furrow broad and shallow. Anterior cranidial and lateral librigenal border wide and tubular. Anterior cranidial border slightly arched dorsally. Occipital furrow deepens distally as pit and broadens sagittally. Palpebral fixigena moderately convex dorsally.

Free cheek with eye socle which narrows towards mid-ocular point, and small node or short spine at postero-lateral corner as genal spine, and lacking posterior border furrow. Panderian notch present on doublure ventral to postero-lateral corner of librigenal field.

Pygidium semi-elliptical in outline. Pygidial axis wide (tr.) and defined by weakly impressed axial furrows, with three segments including terminal piece. Axial ring furrows shallow sagittally. Inner pleural field narrow and flat, and outer pleural field steeply inclined and wide. Pleural and interpleural furrows very weakly impressed. Short stout spine present where posterior band of anteriormost pleura and distal edge of inner

<center>327</center>

pleural field meet. No discrete border. Doublure of border ornamented with terrace lines. Pygidial surface ornamented with fine granules.

Comparison with "Hystricurids". The cranidia of *Eurylimbatus* are characterized by a subtriangular glabella, an exsagittally wide posterior fixigena, an anterior border that is thick, tubular and moderately arched dorsally, and a relatively large palpebral lobe. The overall cranidial outline and glabellar shape of *Eurylimbatus* are comparable to those of *Spinohystricurus robustus* (Pl. III-18, Fig. 1). *S. robustus* is readily differentiated by having a strongly arched palpebral lobe, a narrower posterior fixigena, a posteriorly curved sagittal portion of the anterior border, and a more strongly tuberculated surface. *Carinahystricurus* displays a similar cranidial architecture to *Eurylimbatus* (see Pl. III-33, Figs. 2, 6). The glabella and palpebral lobe of *Carinahystricurus* are much smaller, the posterior fixigena is longer transversely, and most characteristically the anterior border of *Carinahystricurus* is carinated. The presence of a panderian notch and the absence of a genal spine in the free cheek of *Eurylimbatus* readily distinguish the genus from *Carinahystricurus* (compare Pl. III-35, Figs. 1, 3 with Pl. III-40, Figs. 12, 13). Like many "hystricurids," the pygidia of *Eurylimbatus* have the tall and steeply down-sloping outer pleural field and the flat and narrow inner pleural field, resulting in a relatively distinct separation of the two pleural fields. However, instead of developing the fulcral ridge seen in many hystricurids including *Carinahystricurus* (see Pl. III-35, Figs. 17-22) and *Spinohystricurus* (see Pl. III-20, Figs. 1, 3), the *Eurylimbatus* pygidia develop a pair of stout spines where the hystricurid pygidia develop a fulcral ridge (see Pl. III-40, Figs. 3, 4). A pair of short spines present in the *Politohystricurus* pygidia (see Pl. III-24, Figs. 7-13) topographically corresponds to the pair of *Eurylimbatus*. The pygidia of *Politohystricurus* are further similar to those of *Eurylimbatus* in lacking a distinct fulcral ridge and in having a comparable proportion of inner and outer pleural fields, but differ in having a distinct tubular border and discretely impressed pleural and interpleural furrows.

Lee and Chatterton (1997a) illustrated three protaspid specimens and six meraspid specimens of *Hystricurus* n. sp. A that is assigned to *Eurylimbatus sphaerus* in this study (see below). The protaspid specimens (figs. 2.9, 2.12, 2.13) develop three pairs of smaller tubercles alongside the glabella, which is considered to be characteristic of *Hystricurus* protaspides (see Lee and Chatterton, 1997a, figs. 2.2, 2.3).

Comparison with Ptychopariides. Several taxa of the Marjumiidae have a cranidial architecture similar to that of *Eurylimbatus*. The concept of the Marjumiidae, which is beyond the scope of this study, appears to be confined to the species from the Marjuman Stage and is yet to be segregated morphologically from that of other families such as the Crepicephalidae. The marjumiid cranidia are characterized by a strongly forward-tapering (nearly triangular) glabella, a sagittally wider but transversely shorter, thick anterior border, and a weakly arched palpebral lobe (see *Syspacheilus*, Pl. II-15, Figs. 21-23; *Talbotina*, Lochman and Duncan, 1944, pl. 12, figs. 6, 8; *Modocia*, Pratt, 1992, pl. 20, fig. 13). From these marjumiid taxa, the *Eurylimbatus* cranidia are differentiated by having a truncated distal end of the posterior fixigena and a transverse posterior facial suture. The pygidia of these Laurentian marjumiid taxa have a relatively flat pleural field, thus lacking any distinctive separation of the inner and outer pleural fields. *Holmdalia*, a questionable marjumiid (Pratt, 1992), has a pygidium possessing the separation, but lacks the pair of the short stout spines of *Eurylimbatus* (see Robison, 1988, figs. 27.5a, b). The cranidia of *Holmdalia* (figs. 27.1-27.4) are much more similar to those of

328

Parahystricurus oculirotundus (Pl. III-64, Figs. 2, 7).

A cranidium of *Elegantaspis* from Kazakhstan (Ivshin, 1962, pl. 5, fig. 7) displays the closest configuration of the posterior fixigena, palpebral lobe and glabellar furrows to *Eurylimbatus*. These similarities can be extended into *Lorrettina*, a dokimocephalid from Australia (see Shergold, 1971, pl. 17, figs. 1-4) and China (see Peng, 1992, figs. 22D-22F). However, the dokimocephalids usually have a divergent anterior facial suture, whereas *Eurylimbatus* has a parallel-sided or convergent suture. Two *Eurylimbatus* species in open nomenclature, *E.* sp. nov. A and B, have a divergent facial suture and exhibit a cranidial architecture similar to these dokimocephalids.

Comparison with Proetides. The smaller cranidia of *Eurylimbatus* are comparable to the cranidia of the Middle to Upper Ordovician toernquistiids. The cranidia of *Lasarchopyge* from Argentina (Chatterton *et al.*, 1998, figs. 12.3, 12.10, 12.19) display the closest architecture. The smaller cranidia of *Eurylimbatus* (see Pl. III-42, Figs. 7, 10, 11, Pl. III-44, Figs. 12, 15) develop a prominent depression immediately in front of the glabellar front. This feature is considered to be diagnostic to the Toernquistiidae (Chatterton *et al.*, 1998) and observed in the adults of many toernquistiids (see Chatterton *et al.*, 1998, figs. 7.2, 8.20, 14.21).

The pygidia of *Paratoernquistia* from Argentina are greatly similar to those of *Eurylimbatus* in having a narrow inner pleural field and steeply down-sloping outer pleural field, and lacking the fulcral ridge (see Chatterton *et al.*, 1998, figs. 7.10, 7.12, 7.13, 7.15). The *Paratoernquistia* pygidia lack the pair of the prominent short spines on the posterior band of the anterior most pleura, which is evident in *Eurylimbatus*.

The free cheeks of these Middle Ordovician toernquistiids have a relatively long genal spine—*Eurylimbatus* lacks it—,and a narrower librigenal field, and lack the panderian notch (see Chatterton *et al.*, 1998, figs. 12.13). In addition, many toernquistiids have a long thoracic axial spine (see Chatterton *et al.*, 1998, figs. 7.14, 7.16, 7.21-24), whereas *Eurylimbatus* has no thoracic axial spine (see Pl. III-41, Fig. 2).

Chatterton *et al.* (1998) noted the taxonomic significance of two toernquistiid features, the absence of connective sutures in cephalic doublure of adults and presence of a sagittal furrow towards the back of the distinct preglabellar field. Judging from the transverse length of the anterior genal doublure (see Pl. III-40, Figs. 2, 12, 13, Pl. III-41, Figs. 3, 8, Pl. III-43, Figs. 13, 15), *Eurylimbatus* is likely to have a rostral plate. Unlike most toernquistiids, *Eurylimbatus* has a preglabellar median furrow which shows an equal depth throughout its entire length. However, the presence of the prominent depression in front of the glabella in the smaller cranidia of *Eurylimbatus* is comparable to the toernquistiids. The protaspides of *Paratoernquistia* are similar to those of *Hystricurus* and *Eurylimbatus*, all belonging to the Type C metaprotaspides of Chatterton *et al.* (1999)

The large glabella, subtriangular or subrectangular, is seen in many species of the Proetidae (see Owens, 1973; Šnajdr, 1980). Some proetid species have a configuration of frontal area similar to *Eurylimbatus*. The distinguishing differences of *Eurylimbatus* are the wider (tr.) posterior fixigena, posterior facial suture that runs transversely and then turns posteriorly—proetids usually have a straight posterior facial suture, and the presence of prominent tubercles on the posterior pygidial pleural bands.

A *Cyphaspis* species from the Devonian of Morocco shares a pygidial resemblance with *Eurylimbatus*. The abrupt change of the slope between the inner and outer pleural

329

fields (Pl. III-44, Fig. 16) is very similar to that of *Eurylimbatus*, but the *Cyphaspis* species lacks the tubercles.

Taxonomic Conclusion. *Eurylimbatus* displays the closest cranidial and pygidial architecture to those of the toernquistiids, suggesting that the Lower Ordovician *Eurylimbatus* could be a root stock for the toernquistiids of Middle to Upper Ordovician age. However, the presence of the pair of the prominent spines on the posterior band of the anteriormost pleura, and a panderian notch on the postero-lateral corner of the genal doublure, and the absence of the thoracic axial spine do not support this assessment. *Eurylimbatus* is questionably referred to the Toernquistiidae. The protaspides of *Eurylimbatus* are similar to those of *Hystricurus* as well as *Paratoernquistia*, suggesting that they belong to a higher taxonomic group.

Hypotheses of Evolutionary Relationshiops. The hypothesis that cranidial features of *Eurylimbatus* are carried over from those the Upper Cambrian marjumiids and dokimocephaliids into Middle to Upper Ordovician toernquistiids need to be cladistically tested to improve the current understanding of relationships between *Eurylimbatus* and these taxa. The pygidial similarities to *Politohystricurus* would a convergent feature that was acquired during the Early Ordovician and continued into the Middle Ordovician toernquistiids and the Devonian aulacopleurids.

We also need to test whether or not the ridge developed in hystricurid pygidia (e.g., *Carinahystricurus*) is homologous with the abrupt change of slope between the inner and outer pleural fields and the pair of prominent spines observed in *Eurylimbatus*.

Eurylimbatus amplissimus n. gen. n. sp.
Pl. III-40, Figs. 1-16, Pl. III-42, Figs. 1-6

Etymology. "amplissimus" from Latin, meaning 'largest', denotes that this species has the largest glabella.

Holotype. UA 12331, cranidium; Pl. III-40, Figs. 1, 5-7; *Tesselacauda* Zone. Fillmore Formation, Utah.

Differential Diagnosis From Generic Diagnosis. Glabella very large and triangular. Axial furrows rapidly turns inwards at glabellar base. Posterior facial suture runs diagonally and then abruptly turns posteriorly. Anterior facial suture slightly convergent. Two pairs of glabellar furrows; S1 located opposite posterior end of palpebral lobe and S2 opposite anterior end of palpebral lobe.

At least 11 thoracic segments present. Thoracic axial rings ornamented with two different sized tubercles. Thoracic pleurae run horizontally and ventrally down-sloping at proximal one-third of the length, without discrete fulcral ridge. Distal end of thoracic pleura triangular in outline.

Remarks: This species differs from other *Eurylimbatus* species in having nearly triangular glabella and slightly convergent anterior facial suture and in lacking a genal spine.

Eurylimbatus sphaerus n. gen. n. sp.
Pl. III-41, Figs. 1-8, Pl. III-42, Figs. 7-12.

1997a *Hystricurus* n. sp. A, Lee and Chatterton, p. 863-864, figs. 2.9-2.17.
Etymology. "sphaerus" from Latin denotes the enrolled specimen of this species.
Holotype. UA 12338, cranidium; Pl. III-41, Figs. 1-8; *Tesselacauda* Zone. Fillmore

330

Formation, Utah.

Differential Diagnosis from Generic Diagnosis. Glabella elongated and less strongly tapering fowards. 11 thoracic segments present. Pygidim with most conspicuous spine developed where posterior band of anteromost pleura and distal end of inner pleural field meet. S1 and S2 weakly impressed.

Remarks. This species is differentiated from other *Eurylimbatus* species by having an elongated glabella and most conspicuous stout spine on the distal edge of the inner pygidial pleural field. Smaller cranidial specimens and protaspides assigned to *Hystricurus* n. sp. A by Lee and Chatterton (1997a) all are transferred into this species.

<center>

***Eurylimbatus acutus* n. gen. n. sp.**

Pl. III-43, Figs. 1-15, Pl. III-44, Figs. 1-15.

</center>

? 1957 *Hystricurus* sp., Ross, [part], p. 488, pl. 43, fig. 22.

Etymology. "acutus" from Latin describes the rather pointed glabellar front.

Holotype. UA 12348, cranidium; Pl. III-43, Figs. 1, 2, 6, 8; *Tesselacauda* Zone; Garden City Formation, southern Idaho.

Diagnosis. Glabella relatively large, with rather pointed front. Anterior facial suture parallel-sided. Cranidial surface ornamented with small tubercles. Free cheek with short genal spine. Eye socle weakly developed.

Remarks. A poorly preserved cranidium from the Deadwood Formation (Ross, 1957, pl. 43, fig. 22) has a laterally convex anterior facial suture and a medium-sized palpebral lobe that is moderately arched laterally. It is very similar to the cranidia of this species from the Garden City Formation (see Pl. III-43, Fig. 14), except for the relatively large glabella with a rounded anterior glabellar margin.

This species is discriminated from other *Eurylimbatus* species by having a parallel-sided anterior facial suture and short stout genal spine.

<center>

***Eurylimbatus* sp. nov. A**

Pl. III-45, Figs. 1-4

</center>

1951 *Hystricurus?* sp. C Ross, p. 54, pl. 10, figs. 17, 21, 22.

Remarks. This apparently new species is characterized by a parabolic outline of the axial furrows, a laterally convex anterior facial suture, and a posterior facial suture that strongly turns posteriorly at its distal end. A cranidium assigned to *Hystricurus* ? sp. C by Ross (1951) is assigned to this species. Compared with other cranidia referred to as *Hystricurus?* sp. C which are reassigned to *Eurylimbatus* sp. nov. B in this study, this specimen has a palpebral furrow which is absent in *E*. sp. nov. B. The other features of cranidial architecture of these specimens is similar to those of this species.

<center>

***Eurylimbatus* sp. nov. B**

Pl. III-45, Figs. 5-8

</center>

1953 *Hystricurus* sp. C, Hintze [part], p. 166, pl. 6, figs. 15 [only, not fig. 16].
1973 *Hystricurus* sp. A Terrell, p. 76, pl. 1, figs. 9, 10, 13.

Remarks. This species is most simliar to *Eurylimbatus* sp. nov. A in terms of the divergent anterior facial suture and the large glabella, but mainly differs in lacking a palpebral furrow and in having a subrectangular glabella and a wide doublure. Hintze

<center>331</center>

(1953) associated a free cheek (pl. 6, fig. 16) with this species upon the basis of which he assigned this species to *Hystricurus*. However, the free cheek lacks broad border furrows as an extension of the cranidial border furrows of the associated cranidium, indicating that the association is likely to be incorrect.

A pagodiine, *Ptychopleurites* (see Ludvigsen *et al.*, 1989, pl. 21, figs. 17, 22), has a similiar cranidial architecture, including a subrectangular glabella and distally broadening posterior border. However, this Upper Cambrian taxon has a much deeper anterior border furrow, a short (or absent) preglabellar field and a distinctly impressed palpebral furrow.

Eurylimbatus sp. nov. C
Pl.III-45, Figs. 9-12

Remarks. This species is characterized by the most discretely impressed palpebral furrow. A cranidium from R5-76.4 (Pl. III-44, Fig. 14), which is tenatively assigned to *Eurylimbatus acutus*, may belong to this species. However, the glabella tapers more strongly forwards and the posterior facial suture turns less acutely posteriorly.

Family TELEPHINIDAE Marek, 1952
Genus PYRAUSTOCRANIUM Ross, 1951

Type Species. *Pyraustocranium orbatum* Ross, 1951; *Rossaspis superciliosa* Zone; Garden City Formation, southern Idaho.

Diagnosis. Eye large and librigenal field very narrow. Ocular ridge slender and obliquely directed antero-laterally. Occipital spine slender and long. Cranidium trapezoidal in outline. Anterior facial suture convergent and posterior facial suture divergent. Posterior cranidial border strongly bent forwards distally.

Remarks. Ross (1951) noted similarities of *Pyraustocranium* with olenid genera such as *Parabolina*, *Leptoplastus*, and *Ctenopyge*, but distinguishes the genus from the olenid genera in lacking glabellar furrows and having larger eyes. However, there are olenid species that lack glabellar furrows due to effacement (e.g., *Svalbardites*, Fortey, 1975) and eyes of comparable size (e.g., *Psilocara comma*, Fortey, 1975). *Pyraustocranium* is characterized by having an ocular ridge which is obliquely oriented backwards and a long occipital spine. These features are not common in the olenids. The orientation of S1 glabellar furrows is not comparable to that of the olenids that have less obliquely directed S1 furrows. Although some olenids (e.g., *Protopeltura*, see Henningsmoen, 1957, fig. 3) have a similiar orientation of the ocular ridge, *Pyraustocranium* has the ocular ridge that is oriented at the steepest angle to the sagittal line. An occipital spine and smoothly anteriorly curved posterior border are rare among the olenids. The convergent anterior facial suture is seen in some pelturines. Henningsmeon (1957) considered the affinity of *Pyraustocranium* with the Olenidae to be doubtful.

The large eye, the most conspicuous feature of this genus, is reminiscent of a co-occuring telephinid such as *Goniophrys prima*. In effect, the smaller meraspid cranidia of *Pyraustocranium* are indistinguishable from those of *G. prima* (Pl. III-74, Figs. 12-19; Lee and Chatterton, 1997b, figs. 4.5, 4.7). Since *Goniophrys* and *Pyraustocranium* both are known to occur in the *Rossaspis superciliosa* Zone, the smaller meraspid cranidia could be earlier stages of *Goniophrys*. However, the sampling horizons from which *Pyraustocranium* materials were secured does not yield any large *Goniophrys* materials. The cranidia of *Pyraustocranium* differ from those of *Goniophrys* of similar size in

332

having a wider (tr.) frontal area and less distinct axial furrows and smaller glabella, but most importantly, in begining to develop an occipital spine (see Pl. III-74, Figs. 15, 16; compare with Lee and Chatterton, 1997b, figs. 4.5, 4.7). With growth, the cranidia of *Pyraustocranium* morphologically deviate from those of *Goniophrys* by lengthening the occipital spine, retaining the distinctness of the ocular ridge, retaining the preglabellar field, and broadening (exsag.) the posterior fixigenal area. Under the assumption that the more similar the earlier stages of two taxa are, the closer are their phylogenetic relationships (von Baer's biogenetic law), *Pyraustocranium* is considered to belong to the Telephinidae, although its pygidium has not been found.

Taxonomic Conclusion. The similarities of small cranidia of *Pyraustocranium* with those of *Goniophrys* lead me to assign this genus to the Telephinidae, denying the possible affinity of *Pyraustocranium* to the "hystricurids" (personal communication, Adrain, 2000).

<center>

***Pyraustocranium orbatum* Ross, 1951**
Pl. III-74, Figs. 1-7, 12-19

</center>

1951 *Pyraustocranium orbatum* Ross, p. 80-81, pl. 18, figs. 3, 4, 7, 8, 10-14, 16.
Holotype. Y.P.M. 18072, cranidium; Ross, 1951, pl. 18, figs. 3, 4, 7, 8; *Rossaspis superciliosa* Zone; Garden City Formation, southern Idaho.
Diagnosis. same as generic diagnosis above

<center>

Genus GONIOPHRYS Ross, 1951

</center>

Type Species. *Goniophrys prima* Ross, 1951; *Rossaspis superciliosa* Zone; Garden City Formation, southern Idaho.

<center>

***Goniophrys prima* Ross, 1951**
Pl. III-74, Figs. 8-11

</center>

1951 *Goniophrys prima* Ross, p. 81, pl. 18, figs. 9, 15, 17-20, 22, 27.
1953 *Goniophrys prima*, Hintze, p. 156-157, pl. 20, fig. 1.
1997b *Goniophrys prima*, Lee and Chatterton, p. 438-439, figs. 4.1-4.9.
Holotype. Y.P.M. 18075, cranidium; Ross, 1951, pl. 18, figs. 9, 15, 17; *Rossaspis superciliosa* Zone; Garden City Formation, southern Idaho.
Diagnosis. see Ross (1951, p. 81-82)

<center>

Family BATHYURIDAE Walcott, 1886
Genus TASMANASPIS Kobayashi, 1940

</center>

Type Species. *Tasmanaspis lewisi*; La1.5 Zone of Lancefieldian Series; Florentine Valley Formation, Tasmania, Australia.
Diagnosis. Anterior cranidial border wide and flat, and covered with fine terrace lines. Preglabellar field long. Palpebral lobe of moderate size, crescentic in outline, and located posterior to mid-cranidial length. Palpebral furrow very shallow. Posterior fixigena very narrow (exsag.) and elongated transversely. Glabella large and parabolic in outline; surface covered with fingerprint-like ornament. Occipital furrow deeply impressed and strongly curved posteriorly. Free cheek with long genal spine covered with terrace lines in herringbone pattern. Lateral librigenal border furrow weakly impressed and shallows out well short of postero-lateral corner of ocular platform. Posterior librigenal border

<center>333</center>

furrow confluent with inside margin of genal spine.

Comparison with "Hystricurids". Jell and Stait (1985b) synonymized *Tasmanaspis* under *Hystricurus*. They regarded the diagnostic features of *Tasmanaspis* such as the long frontal area, posteriorly located palpebral lobe, and very narrow transverse posterior fixigena observed in the holotype cranidium (Kobayashi, 1940, pl. 11, fig. 3; see also Jell and Stait, 1985b, pl. 2, fig. 2) as deformed conditions of *Hystricurus lewisi*. Specimens of *H. lewisi* collected by Jell and Stait (1985b) are transferred to *Carinahystricurus* and *Hillyardina*, in this study (see *Carinahystricurus* for detailed taxonomic account of these specimens). The Tasmanian specimens appear to be deformed, but the deformation is not considered to be sufficient to mislead the taxonomic assessment. Silicified materials from the Garden City Formation and Fillmore Formation (see Pl. III-82, Figs. 1-15, 18-23) preserve all the above-mentioned diagnostic features in an undeformed condition. As a result, *Tasmanaspis* is resurrected as a separate genus from *Hystricurus* and *Carinahystricurus*.

Tasmanaspis differs from *Carinahystricurus* in having a flat and wide anterior border (carinated border in *Carinahystricurus*), a much narrower and shallower anterior border furrow, a narrower posterior fixigena, a longer frontal area, and shallower axial furrows, and a very weakly impressed palpebral furrow. The parabolic glabella and strongly posteriorly convex occipital ring of *Tasmanaspis* are reminiscent of those of *Paraplethopeltis* (Hintze, 1953, pl. 7, figs. 1, 3, 8), but *Tasmanaspis* has a strongly divergent anterior facial suture, a strongly arched palpebral lobe, a much narrower posterior fixigena, and a very weakly impressed palpebral furrow. The strongly divergent anterior facial suture and long frontal area of *Tasmanaspis* resemble those of *Hyperbolochilus* (e.g., see Pl. III-52, Fig. 2, Pl. III-53, Fig. 2). However, *Tasmanaspis* does not have a triangular posterior fixigena and the infolded sagittally long doublure of the anterior cranidial border of *Hyperbolochilus*, and has a much larger, crescentic palpebral lobe. The free cheek of *Tasmanaspis* differs from that of *Hyperbolochilus* in having a long tubular genal spine with a narrow base and in lacking a median furrow on the genal spine.

Comparison with Ptychopariides. Kobayashi (1940) compared *Tasmanaspis* with *Blountia*, a member of the Asaphiscidae. However, that Upper Cambrian ptychopariid taxon has a much shorter frontal area, a far less divergent anterior facial suture and a much wider (exsag.) posterior fixigena. The morphologically closest is *Blountia ovata* (Lochman and Duncan, 1944, pl. 11, figs. 1, 2), showing a similar proportion of the frontal area relative to the preglabellar field and anterior border to that of *Tasmanaspis*. The species however has a much wider posterior fixigena.

Comparison with Proetides. It is *Licnocephala* of the Bathyuridae that displays the strongest morphologic resemblance with *Tasmanaspis*. The cranidia of *Licnocephala ovata* (Ross, 1953, pl. 64, figs. 1-3) and *Licnocephala bicornuta* (see Pl. III-83, Figs. 5-11) possess an anterior facial suture, a frontal area, and a palpebral lobe that are similar to those of *Tasmanaspis lewisi*. However, *Tasmanaspis* is easily differentiated from *Licnocephala* by having a larger forward-tapering glabella, a long tubular genal spine, a deep preoccipital furrow, and a strongly posteriorly convex occipital ring.

The cranidial features of *Tasmanaspis* are also found in many bathyurids. For example, Young (1973) described a small cranidium of *Bathyurellus* (?) *teretus* (pl. 2, fig. 10) that is comparable to that of *Tasmanaspis*, but has a larger palpebral lobe, an

334

oval-shaped glabella, and a pointed anterior cranidial margin. *Bathyurellus* (e.g., see Fortey, 1979, pl. 32) in general differs from *Tasmanaspis* in having an elongated subrectangular glabella, a wide genal spine and librigenal field, and a preglabellar furrow that shallows out sagittally.

Taxonomic Conclusion. The stronger cranidial similarities with such bathyurids as *Licnocephala* than with any "hystricurids" lead to the placement of *Tasmanaspis* in the Bathyuridae.

<div align="center">

Tasmanaspis lewisi Kobayashi, 1940

Pl. III-82, Figs. 1-15

</div>

1940 *Tasmanaspis lewisi* Kobayashi, [part], p. 65-66, pl. 11, fig. 3 [only].

1940 *Tasmanaspis longus* Kobayashi, p. 66, pl. 11, fig. 5.

? 1953 undetermined pygidium, Hintze, pl. 20, fig. 16.

1954 *Jeffersonia bridgei* Heller, [part], p. 46, pl. 18, fig. 16, [only; not fig. 17].

? 1973 *Hillyardina* sp. A, Terrell, [part], p. 71-73, pl. 3, fig. 5, [only].

1985b *Hystricurus lewisi*, Jell and Stait, [part], p. 5-8, pl. 2, figs. 1-4, [only].

Holotype. Z 151, cranidium; Kobayashi, 1940, pl. 11, fig. 3 (re-illustrated by Jell and Stait, 1985b, pl. 2, fig. 2); La1.5 Zone of Lancefieldian Series; Florentine Valley Formation, Tasmania

Diagnosis. Frontal area wider transversely. Preglabellar field and anterior cranidial border of equal sagittal length. Anterior facial suture strongly divergent. Occipital ring moderately convex backwards.

Remarks. Heller (1954) described two cranidia of *Jeffersonia bridgei* from Missouri (pl. 18, figs. 16, 17). The Missouri specimens cannot be assigned to *Jeffersonia* because they lack, amongst others, the slender palpebral lobe defined by a strongly arched palpebral furrow that is diagnostic to *Jeffersonia* (see Ross, 1951, pl. 17, fig. 12). The larger one (fig. 16) possesses an overall architecture that is indistinguishable from that of *Tasmanaspis lewisi* from the Garden City Formation. The Missouri cranidium differs in having an anterior border with a relatively consistent width (anterior border of the Garden City Formation specimens narrows distally) and a slightly more anteriorly located palpebral lobe. In considering that it is about 6 mm long, which is twice long as the largest specimen from the Garden City Formation, the difference is considered to be ontogenetic. The smaller cranidium from Missouri (Heller, 1954, pl. 18, fig. 17) has a glabella with a truncated anterior margin. Since all the smaller cranidia from the Garden City Formation have a rounded anterior margin, the truncated margin of the Missouri cranidium is not an ontogenetic change that can be accommodated within the concept of this species. Due to poor preservation, the specimen cannot be taxonomically further assessed.

Terrell (1973) described a cranidium of *Hillyardina* sp. A from the Fillmore Formation (pl. 3, fig. 5). The specimen does not agree with the concept of *Hillyardina* because it has a posterior fixigena with a rounded distal end, a larger glabella, and a less strongly curved palpebral lobe. The anterior facial suture and glabella of the cranidium is well accomodated within the concept of *Tasmanaspis*. However, the cranidium shows a wider (exsag.) posterior fixigena and a less convex smaller palpebral lobe; in effect, the palpebral lobe does not appear to be completely preserved. Because of these two differences, this specimen is questionably assigned to *Tasmanaspis lewisi*.

<div align="center">

335

</div>

Tasmanaspis n. sp.

Pl. III-82, Figs. 18-23

Remarks. Only two cranidia are illustrated. From *Tasmanaspis lewisi*, this species differs in having a narrower fronta area and more strongly arched occipital ring.

Tasmanaspis? sp.

Pl. III-83, Figs. 1-4

Remarks. The S1 glabellar furrows, pointed anterior glabellar margin and shallower anterior cranidial border furrow of this species suggest that it cannot be confidently placed in *Tasmanaspis*.

Genus LICNOCEPHALA Ross, 1951

Type Species. *Licnocephala bicornuta* Ross, 1951; *Protopliomerella contracta* Zone; Garden City Formation, southern Idaho.

Licnocephala bicornuta Ross, 1951

Pl. III-83, Figs. 5-11

1951 *Licnocephala bicornuta* Ross, p. 110-111, pl. 28, figs. 12-14.

Holotype. Y.P.M. 18180, cranidium; Ross, 1951, pl. 28, figs. 13, 14; *Hintzeia celsaora* Zone; Garden City Formation, southern Idaho.

Diagnosis. see Ross (1951, p. 110-111)

Remarks. *Licnocephala bicornuta* is similar to *Tasmanaspis lewisi* with respect to the nature of the anterior facial suture, palpebal lobe, and posterior fixigena. *L. bicornuta* differs in having a much smaller glabella, a much longer preglabellar field ornamented with genal caeca, and a more forward convex anterior border.

Licnocephala bicornuta has widely-distributed genal caeca on the frontal area. This feature is observed in *Hungaia* (a questionable dikelocephalacean, see Ludvigsen *et al.*, 1989, pl. 17, figs. 2, 8). With *Hungaia*, this species shares a strongly divergent anterior facial suture, a strongly arched palpebral lobe, and a very narrow posterior fixigena. The dikelocephalacean is differentiated from *Licnocephala bicornuta* by a large glabella, a palpebral lobe that is very close to the axial furrows, a narrower anterior border, and the presence of bacculae.

The pygidia of some olenaceans are similar to those of *Licnocephala*; compare *Saratogia serapio* (an Idahoiidae, Ludvigsen and Westrop, 1983, pl. 9, fig. 3) and *Licnocephala cavigladius* (Ross, 1953, pl. 64, fig. 25). The pygidia share a semi-circular outline, a sagittally short axis, a wide doublure, and pleural and interpleural furrows that do not reach the margin.

Bathyuridae sp.

Pl. III-82, Figs. 16, 17

Remarks. This pygidium from SE-152 co-occurs with cranidia of *Tasmanaspis lewisi*. It is characterized by a postero-median spine extended from the axis and fingerprint-like ornament on the exoskeletal surface. The pygidia of *Goniotelus* (see Hintze, 1953, pl. 26, figs. 8, 10) and *Eleutherocentrus* (=*Goniotelina*) (see Ross, 1951, pl. 14, figs. 16, 17; see Whittington, 1953a for taxonomy of *Eleutherocentrus*) have the same postero-median

336

axial spine. However, the spine of *Goniotelus* is extended from the pygidial margin as well as the axis, and is very long and covered with tubercles, not fingerprint-like ornament seen in this pygidium. The fingerprint-like ornament is observed on the cranidial surface of *T. lewisi* (see Pl. III-82, Fig. 7).

Genus BENTHAMASPIS Poulsen, 1946

Type Species. *Benthamaspis problematica* Poulsen, 1946; possibly *Trigonocerca typica* Zone; Nunatami Formation, Ellesmere Island.

Remarks. Fortey (1979) tentatively placed *Benthamaspis* in the Lecanopygidae. It is the pygidium lacking pleural furrows that led him to this taxonomic assessment. The cranidial similarities of *Benthamaspis* species described herein with *Benthamaspis abdita* indicate a bathyurid affinity for *Benthamaspis*, as suggested by Lochman (1966) and Fortey and Owen (1975). Boyce (1989) placed *Benthamaspis* in the Bathyuridae upon the basis of the cranidial similarities with *Bathyurellus* and *Punka*. Fortey's rejection (1979) of the bathyurid affinity was based on the facts that *Benthamaspis* has a truncated glabellar front and a pygidium lacking pleural furrows. The first feature is found in *B. abdita* (see Ross, 1951, pl. 29, figs. 31, 32) and the second is comparable to those of *Bolbocephalus* (see Fortey, 1979, pl. 26, figs. 7, 8; see also Whittington, 1953a, pl. 69, figs. 23-25). Thus, *Benthamaspis* is placed in the Bathyuridae, supporting the assessment of Boyce (1989). Compared to the Lecanopygidae (see Ludvigsen *et al.*, 1989, pl. 23, figs. 4, 8), *Benthamaspis* has a larger palpebral lobe, a transversely wider palpebral fixigena, a narrower (exsag.) posterior fixigena, and a longer preglabellar field. The lecanopygid pygidia are very similar to those of *Licnocephala* (compare with Ludvigsen *et al.*, 1989, pl. 23, fig. 5) and *Benthamaspis* (compare with Westrop, 1986, pl. 35, fig. 12). It seems probable that the Lecanopygidae and such Bathyuridae as *Benthamaspis* are related.

Benthamaspis obreptus (Lochman, 1966)
Pl. III-83, Figs. 12-15

1951 undetermined genus and species C, Ross, p. 120-121, pl. 29, figs. 20, 21, 24.
1953 undetermined gen. and sp. B, Hintze, [part], p. 242, pl. 13, figs. 14, 17, [only].
1966 ?*Oculomagnus obreptus* Lochman, p. 541-542, pl. 62, figs. 3, 5, 6, 7

Holotype. YPM 18201, cranidium; *Hintzeia celsaora* Zone; Garden City Formation, southern Idaho.

Diagnosis. see Lochman (1966, p. 541)

Remarks. Hintze (1953) assigned two different morphotypes to his undetermined species; compare pl. 13, figs. 14, 17 and pl. 13, fig. 15. The former which is assigned here to this species has a parallel-sided glabellar lateral margin, whereas the latter has a laterally convex glabella.

The remaining specimens of ?*Oculomagnus obreptus* are assigned to *Benthamaspis conica* (Fortey, 1979).

Benthamaspis abdita (Ross, *in* Whittington, 1953a)
1951 *Platycolpus*? sp., Ross, p. 121, pl. 29, figs. 22, 23, 25-34.
1953a *Strigigenalis abdita* Ross *in* Whittington, p. 671-673, pl. 67, figs. 11, 12, 16-18, 21-23, 26, 27.

337

1953 undetermined gen. and sp. C, Hintze, [part], p. 243, pl. 9, fig. 14, [only].

? 1974 *Hystricurus* sp. Corbett and Bank, pl. 1, fig. 20.

Holotype. YPM 18735, cranidium; Whittington, 1953a, pl. 67, figs. 11, 12, 17; *Hintzeia celsaora* Zone; Garden City Formation, southern Idaho.

Diagnosis. see Whittington (1953a, p. 672-673)

Remarks. Ross (*in* Whittington, 1953a) erected a new genus *Strigigenalis* under the family Leiostegiidae to accommodate all specimens that were earlier identified as *Platycolpus*? sp. by Ross (1951, pl. 29, figs. 22, 23, 25-34). Ross (*in* Whittington, 1953a) illustrated additional two cranidia, two librigenae, one pygidium, and a fragmentary thoracic segment (pl. 67, figs. 11, 12, 16-18, 21-23, 26, 27). In the Treatise (Moore, 1959), *Strigigenalis* was placed in the Lecanopygidae. Later Fortey (1979) placed *Strigigenalis* in the Bathyuridae and excluded this species from *Strigigenalis* because it lacks a genal spine, and has the non-spinose pygidium.

The cranidium of *Strigigenalis cassinensis* (Whittington, 1953a, pl. 67, figs. 6-8), the type species of *Strigigenalis*, differs from those of later described species in having a relatively rounded anterior glabellar margin and a longer preglabellar field. A typical condition of these features of the Bathyuridae is a relatively pointed glabellar front and a shorter preglabellar field, which is seen in many later described species (see Fortey, 1979, pl. 30, fig. 2, Boyce, 1985, pl. 29, fig. 8). All the cranidial specimens assigned to this species by Ross (*in* Whittington, 1953a) have a rounded anterior glabellar margin and a relatively long preglabellar field. This supports the exclusion of this species from *Strigigenalis*, and suggests that the concept of *Strigigenalis* needs to be re-investigated. Since the glabellar shape, nature of the frontal area, absence of a genal spine, and pygidial shape are comparable to *Benthamaspis*, this species is transferred to *Benthamaspis*.

A cranidium of *Hystricurus* sp. by Corbett and Bank (1974) shows the palpebral lobe and frontal area which are very similar to this species in terms of their proportion and location. The cranidium appears to have the S1 furrows of the same condition as this species. However, the specimen appears to have a relatively straight lateral glabellar margin and a discrete palpebral furrow.

Benthamaspis? sp.
Pl. III-83, Figs. 16-18

1953 undetermined gen. and sp. C, Hintze, [part], p. 243, pl. 9, figs. 13, 15, [only].

1953 undetermined gen. and sp. B, Hintze, [part], p. 242, pl. 13, figs. 13, 15, 16, [only].

Remarks. This species differs from *Benthamaspis obreptus* in having a smaller palpebral lobe, and a larger glabella with a laterally convex lateral margin. The cranidia of this species are similar to those of *Holubaspis perneri* (see Mergl, 1994, pl. 4, fig. 3-6), but differ in lacking a palpebral furrow and in developing a short preglabellar field.

Genus OMULIOVIA Chugaeva, 1962
Omuliovia? sp.

1944 *Hystricurus abruptus* Cullison [part], p. 80, pl. 34, figs. 45, 46, [only].

Remarks. The glabella of these two poorly-preserved cranidial specimens from Missouri is elongated, parallel-sided, and covered with fine tubercles. It suggests that these cranidial specimens may belong to *Omuliovia*.

338

Order **PTYCHOPARIIDA** Swinnerton, 1915
Suborder **PTYCHOPARIINA** Ritcher, 1932
Superfamily **OLENACEA** Burmeister, 1843
?Family **OLENIDAE** Burmeister, 1843
?Subfamily **PELTURINAE** Corda, 1847
Genus **PAENEBELTELLA** Ross, 1951

Type Species. *Paenebeltella vultulata* Ross, 1951; *Tesselacauda* Zone; Garden City Formation, southern Idaho.

Remarks. Henningsmoen (1957) questionably assigned *Paenebeltella* to the Pelturinae. The pygidia associated for *Paenebeltella* in this study (Pl. III-58, Figs. 16-25) make that assignment more questionable, because they are more similar to those of aphelaspidines (e.g., see Rasetti, 1965, pl. 13, fig. 7, pl. 16, fig. 12). The configuration of thoracic segments possessing long axial spine seen in *Paenebeltella* is rare among the Olenidae. Between the two thoracic segments possessing the long axial spine, there is a thoracic segment that lacks the axial spine (see Pl. III-58, Figs. 9-11, 24, 25). This configuration of the thoracic segments appears to make *Paenebeltella* more distantly related to the olenids.

The presence of the long thoracic axial spine is observed in many proetides including several "hystricurids" such as *Amblycranium* (Pl. III-27, Figs. 3, 4) and *Spinohystricurus* (Pl. III-16, Figs. 1-8). The thoracic segments of *Paenebeltella* are differentiated from those of the "hystricurids" by having non-spinose distal ends and a thoracic segment lacking an axial spine between the segments possessing the spine. In addition, the very small palpebral lobe and steep posterior facial suture of *Paenebeltella*—these features are olenid-like—are not visible in the "hystricurids."

Taxonomic Conclusion. The above-mentioned cranidial and pygidial features deny the affinity of *Paenebeltella* with the "hystricurids," which was previously suggested (personal communication, Adrain, 2000). *Paenebeltella* is questionably retained in the Olenidae.

Paenebeltella vultulata Ross, 1951
Pl. III-58, Figs. 1-25

1951 *Paenebeltella vultulata* Ross, p. 79, pl. 18, figs. 1, 2, 5, 6, pl. 19, fig. 10.
1957 *Paenebeltella vultulata*, Henningsmoen, p. 271, pl. 2, fig. 3.
? 1970 unidentified pygidium, Ross, p. 72, pl. 10, figs. 20, 21.
1973 *Paenebeltella vultulata*, Terrell, p. 78-79, pl. 5, figs. 2, 3.

Holotype. Y.P.M. 18063, cephalon lacking left free cheek; Ross, 1951, pl. 18, figs. 1, 2, 5; *Tesselacauda* Zone; Garden City Formation, southern Idaho.

Diagnosis. Cranidium trapezoidal in outline. Pygidium elongated triangular in outline. Pygidial axis very narrow (tr.) with three axial rings. At least two thoracic segments with long axial spine, interrupted by thoracic segment lacking axial spine.

Remarks. A pygidium from the Goodwin Limestone of Nevada (Ross, 1970, pl. 10, figs. 20, 21) differs from the specimens from the Garden City Formation in having much shallow posterior ends of the axial furrows and a more deeply impressed border furrow. These differences could be ontogenetic.

339

Olenidae sp.
Pl. III-15, Figs. 12-14

Remarks. These pygidia are very similar to those of olenids (e.g., see Henningsmoen, 1957, pl. 16, fig. 2) in having a very convex axis reaching marginal border furrow, flat pleural field, and tubular marginal border.

Superfamily UNCERTAIN
?Family ALOKISTOCARIDAE Resser 1939
Genus PATOMASPIS Ogienko, 1974
Patomaspis? *secundus* Ogienko, 1972

1972 *Hystricurus secundus* Ogienko, p. 238, pl. 55, figs. 9-11.
1984 *Hystricurus secundus* Ogienko, [part], p. 65, pl. 12, figs. 3, 5, 6, [only].
1992 *Hystricurus secundus* Ogienko, p. 93-94, pl. 5, figs. 8-10.

Holotype. No. 727B/55 (confusingly the specimen is designated No. 4/1777 in Ogienko, 1972), cranidium; Ogienko, 1992, pl. 5, fig. 8; *Pseudomera-Biolgina* Zone; Kimayskiy Horizon, South Siberia.

Diagnosis. Two pairs of glabellar furrows slit-like and isolated from axial furrows; S1 and S2 opposite palpebral fixigena. Glabella barrel-shaped with rather pointed anterior margin. Palpebral lobe slender, strongly arcuate and well defined by palpebral furrow.

Comparison. This species is similar to *Hystricurus*? sp. G (Ross, 1951, pl. 14, figs. 1-3) in possessing a barrel-shaped glabella, two pairs of glabellar furrows which are well inside the glabella, and a large palpebral lobe. It differs in having a palpebral furrow and a keel-shaped glabella. Although the shorter and pointed glabella, and long preglabellar field rule out its assignment to *Omuliovia* suggested by Zhou and Fortey (1986), the strongly arched palpebral lobe suggests an affinity with *Omuliovia*. Cranidia of this species are similar to *Glaphurus* (see Ogienko, 1992, pl. 10, figs. 1-6), but differ in having a crescentic slender palpebral lobe. The co-occurring Upper Cambrian *Patomaspis* (Ogienko, 1992, pl. 3, fig. 9) shares the greatest cranidial similarities with this species. This species differs in having a more strongly tapering glabella and less divergent anterior facial suture.

?Family EULOMIDAE Kobayashi, 1955

Remarks. *Etheridgaspis* and *Pseudoetheridgaspis* display cranidial morphologies which suggest that both genera belong to the same higher taxon, but not in the Hystricuridae. The comparative analyses (see below) demonstrate that the cranidial morphologies suggest a closer affinity with some eulomids, but cannot be definitely placed in the Eulomidae. The pygidia of both genera are not of definite eulomid-type; the similarities again seem to be indicative of their being placed in the same higher taxonomic rank. The pygidia of *Etheridgaspis* are of more generalized ptychopariid-type, and not comparable with those of any "hystricurids." In contrast, the pygidia of *Pseudoetheridgaspis* are similar to those of some "hystricurids" in displaying the separation of inner and outer pleural fields and developing small tubercles along the distal edge of the inner pleural field. No definite taxonomic assessment of both genera seems possible, including an option of erecting a new family to accommodate both genera. Upon the basis of cranidial similarities to the eulomids, *Etheridgaspis* and *Pseudoetheridgaspis* are tentatively placed in the Eulomidae.

340

Genus **ETHERIDGASPIS** Kobayashi, 1940

Type Species. *Ptychoparia*? *carolinensis* Etheridge, 1919; early Bendigonian Stage; Caroline Creek Sandstone, Tasmania, Australia.

Diagnosis. Two pairs of glabellar furrows. S1 triangular depression and isolated from axial furrows; S2 short, shallow, and connected with axial furrows. Palpebral lobe large, crescentic, and inflated dorsally. Palpebral furrow moderately deep and shallows towards mid-palpebral point. Glabella with parallel-sided lateral margin and pointed anterior margin. Glabellar front steeply down-sloping. Preglabellar field short. Pygidium with relatively flat pleural field, axis with a strong independent convexity and reaches border, and shallow axial furrows. Border convex and thick. Free cheek with deep lateral border furrow and deep furrow underneath ocular surface.

Comparison with "Hystricurids". When assigning *Etheridgaspis* to the Hystricuridae, Jell and Stait (1985a) mentioned a possibility that the genus is not a hystricurid member mainly because of the condition of the glabellar furrows. Jell and Stait (1985a, p. 37-38) stated, "Structure of the anterior of cranidium, size, shape and position of palpebral lobe, shape of posterior cephalic limb, impression of pleural and interpleural furrows on pygidium and structure of pygidial border all suggest relationship with the Hystricuridae." These cranidial features are too general to support its hystricurid affinity.

The inflated large palpebral lobe and S1 glabellar furrows isolated from axial furrows are diagnostic to *Etheridgaspis*. *Hystricurus*? *megalops* (Pl. III-37, Figs. 13-15) has a palpebral lobe of similar size and convexity, but the species is easily differentiated from *Etheridgaspis* by a strongly forward-tapering shorter glabella, a much longer preglabellar field, a shorter anterior border and the absence of glabellar furrows. The longitudinal sagittal keel on the glabella of *Etheridgaspis* is seen in such genera as *Nyaya* (see Rozova, 1968, pl. 16, fig. 15), but is not common to the "hystricurids." The deep furrow underneath the eye is unique to *Etheridgaspis* among "hystricurids."

The pygidia of *Etheridgaspis* are distinguished from those of other "hystricurids" by the flat pleural field without being differentiated into inner and outer fields, and the thick tubular border.

Comparison with Proetides. *Etheridgaspis* has two glabellar furrows, with S1 being a triangular depression isolated from axial furrows and S2 being slit-like and connected with the axial furrows. This condition of the glabellar furrows readily distinguishes *Etheridgaspis* from the "hystricurids." Some proetides, such as *Glaphurus divisus* (a Glaphuridae, Whittington, 1963) and *Ischyrophyma marnorea* (a Dimeropygidae, Dean, 1970) have S1 furrows isolated from the axial furrows and S2 connected with the axial furrows. However, S1 furrows of these Ordovician proetides are much longer and slit-like, and no other cranidial features of the glaphurid and dimerpygid further support their affinity with *Etheridgaspis*; these proetides are easily differentiated by having amongst others, a larger glabella and a much smaller palpebral lobe.

In addition to the glabellar furrows, *Etheridgaspis* displays a combination of cranidial features that are found in groups outside of the "hystricurids." Several elongated specimens of *Etheridgaspis* show a long glabella with a pointed anterior margin which closely approaches the anterior border furrow, resulting in a very short preglabellar field. This condition of frontal area is seen in many bathyurids (see Fortey, 1979, pl. 30, figs. 2, 7, 8, pl. 31, figs. 1, 3, pl. 33, figs. 2, 3). The Bathyuridae has a palpebral lobe and a

341

posterior fixigena which are of the same proportional size as *Etheridgaspis* (Fortey, 1979, fig. 12). The palpebral furrow of the bathyurids is very weakly developed, or run along the margin of the palpebral lobe, resulting in a slender palpebral lobe, whereas that of *Etheridgaspis* shallows out towards the middle and rather straight, resulting a crescentic palpebral lobe.

Comparison with Ptychopariides. The palpebral furrow of *Etheridgaspis* is broad and deep, and shallows towards the mid-palpebral point. In addition to this palpebral furrow, the above-mentioned condition of glabellar furrows is seen in an eulomid from the Tremadocian strata of west Siberia, *Bilacunaspis obliterata* (Petrunina, 1973, pl. 1, fig. 8). The condition of the palpebral furrow is common to the eulomids (e.g., *Ketyna*, Peng, 1992, fig. 18D), but most eulomids have the palpebral furrow that is more strongly curved laterally. Further, most eulomids have deeply impressed two pairs of glabellar furrows both of which are well connected with axial furrows. The sagittally compressed smaller cranidial specimens of *Etheridgaspis* (see Jell and Stait, 1985a, pl. 14, fig. 11) shows a closer cranidial architecture to *B. obliterata* and most eulomids, in having a relatively straight anterior border and border furrow and a laterally convex anterior facial suture. However, the eulomids have a smaller glabella, a much wider (tr.) palpebral fixigena, a laterally less convex and narrower palpebral lobe. Like most eulomids, the pygidia of *Etheridgaspis* have a distinct border and a convex and wide axis. However, the pygidia of *Etheridgaspis* have their axis reaching the border, whereas the pygidial axis of most eulomids falls short of the border (e.g., Peng, 1992, fig. 18J).

An Upper Cambrian atratebiine, *Aktugaiella* (Peng, 1992, figs. 27.M-O) has the same configuration of S1 and S2 as *Etheridgaspis*. The palpebral lobe of *Aktugaiella* is well defined by a palpebral furrow that has the same curvature as the palpebral lobe, whereas that of *Etheridgaspis* is defined by a nearly straight palpebral furrow that shallows out towards the middle. Other differences are that *Aktugaiella* has a longer preglabellar field and a posterior fixigena that gently curves forwards distally. The pygidium of *Aktugaiella* (Ergaliev, 1980, pl. 19, fig. 9), typical of the Atratebiinae, has a concave and broad border furrow and a narrow ridge-shaped pleural segment reaching the margin. In contrast, the pygidia of *Etheridgaspis* have a tubular border and broad pleural furrows. A Middle Cambrian catillicephalid, *Agelagma* (Robison, 1988) has two pairs of glabellar furrows in a similar condition to *Etheridgaspis*; however, S1 and S2 both are separated from the axial furrows. The catillicephalid cranidial morphologies are much more similar to those of the glaphurids.

A similar cranidial architecture is found in a Tremadocian dikelocephalinid, *Dactylocephalus* from South China (Peng, 1990a, pl. 10, figs. 2, 5). In particular, its conditions of the palpebral lobe and glabellar furrows are strongly similar to those of *Etheridgaspis*; the palpebral lobe of *Dactylocephalus* is more strongly arched. However, *Dactylocephalus* has a longer preglabellar field and a slender and transverse posterior fixigena, and a pygidium typical of the dikelocephalinids that greatly differs from that of *Etheridgaspis*.

A poorly known Argentine Tremadocian genus, *Bodenbenderia* (Harrington and Leanza, 1957, fig. 124.2) is similar to *Etheridgaspis*, but it has no distinct preglabellar field and has a very deep anterior cranidial border furrow and a more elongated rectangular glabella.

342

Etheridgaspis carolinensis (Etheridge, 1919)
Pl. III-37, Figs. 1-12

1883 *Conocephalites stephensi* Etheridge [part], pl. 1, figs. 2, 3 [only]
1883 (?)*Conocephalites* sp. Etheridge, p. 156, 162, pl. 1, figs. 8, 9, 11 (re-illustrated by Jell, 1985, figs. 2A, B)
1883 (?)*Conocephalites* sp. Etheridge, p. 157, 162, pl. 1, fig. 10 (re-illustrated by Jell, 1985, fig. 2C)
1888 *Conocephalites* sp. indet. Johnston, p. 37, pl. 1, figs. 7, 10, 11, 16.
1888 *Conocephalites stephensi* Etheridge, Johnston [part], pl. 1, fig. 14 [only].
1919 *Ptychoparia* (?) *carolinensis* Etheridge, p. 391.
1919 *Ptychoparia* (?) *johnstoni* Etheridge, p. 392.
1940 *Etheridgaspis carolinensis* (Etheridge); Kobayashi, p. 71, pl. 12, figs. 10, 11.
1940 *Etheridgaspis johnstoni* (Etheridge); Kobayashi, p. 72, pl. 12, figs. 12-14 (see also, Jell, 1985, figs. 2E-G).
1974 *Hystricurus*, Corbett and Bank, pl. 1, figs. 26.
? 1974 *Hystricurus*, Corbett and Bank, pl. 1, figs. 25, 27.
1985b *Hystricurus lewisi*, Jell and Stait, [part], p. 5-8, pl. 2, fig. 10 [only].
1985a *Etheridgaspis carolinensis*, Jell and Stait, p. 38-40, fig. 2, pl. 14, figs. 1-15, pl. 18, fig. 15.

Lectotype. Z 1385, cranidium; Jell and Stait, 1985a, figs. 2A, B; early Bendigonian Stage; Caroline Creek Sandstone, Tasmania.

Diagnosis. same as generic diagnosis.

Remarks. Jell and Stait (1985a) considered variations such as the preglabellar field length and glabellar width shown in the materials available for them to be due to post-depositional deformation, and amalgamated the two species described by Kobayashi (1940) and Etheridge (1883). Corbett and Banks (1974) figured a free cheek and two cranidia of *Hystricurus* from the Florentine Valley Formation, Tasmania, which is stratigraphically older than the Caroline Creek Sandstone. Although poorly-illustrated, the free cheek appears to have a deep furrow underneath the ocular surface and a deep lateral border furrow, and lacks a posterior border furrow. The two cranidia have S1 glabellar furrows in the same condition as *Etheridgaspis*, but they have a more strongly tapering glabella, narrower anterior border, and a smaller palpebral lobe. The materials from the Florentine Valley Formation could be the second species. The free cheek from the Florentine Valley Formation is assigned to this species and the two cranidia are assigned to this species with question.

Genus PSEUDOETHERIDGASPIS n. gen.

Etymology. "*Pseudoetheridgaspis*" denotes morphologic similarities with *Etheridgaspis* from Tasmania, Australia.

Type Species. *Pseudoetheridgaspis typica* n. sp.; *Paraplethopeltis* to *Leiostegium-Kainella* Zone; Garden City Formation, northern Utah.

Included Species. *P. cylindricus* n. sp.

Diagnosis. Palpebral lobe semi-circular in shape, dorsally inflated and relatively highly elevated, and defined by palpebral furrow that is slightly curved outwards medially or straight. Doublure ventral to anterior cranidial border half of width of anterior border and relatively tightly infolded. Preglabellar median furrow distinct. Posterior fixigena

343

transverse. Anterior facial suture moderately divergent. Librigenal border furrow relatively shallow. Pygidium with indented and uparched posterior margin. Axis strongly convex. Outer pleural field gently downsloping and slightly convave. Border tubular and distinctively defined by border furrow. Prominent tubercles on posterior pleural bands and along the distal edge of inner pleural field. Postaxial ridge weakly defined by axial furrows; axial furrows confluent with border furrow.

Comparison with "Hystricurids". The semi-circular inflated palpebral lobe and distinct palpebral furrow of *Pseudoetheridgaspis* greatly resemble those of *Etheridgaspis* (Pl. III-37, Figs. 1, 3). The relatively pointed glabellar front of *Pseudoetheridgaspis typica* is seen in some laterally compressed cranidial specimens of *Etheridgaspis* (see Pl. III-37, Fig. 1). The palpebral lobe of *Pseudoetheridgaspis* is smaller and the palpebral furrow does not shallow towards the middle. In addition, *Pseudoetheridgaspis* lacks glabellar furrows and has a distinct preglabellar median furrow. The cranidia of *Etheridgaspis* are characterized by S1 furrows that are short and isolated from the axial furrows. The pygidia of *Pseudoetheridgaspis*, like those of *Etheridgaspis* (see Pl. III-37, Figs. 8-11) have a tubular border and a convex axis reaching border (see "Association of Pygidium" below). However, the pygidia of *Pseudoetheridgaspis* have a post-axial ridge and a distinct separation of inner and outer pleural fields and a row of pleural field tubercles along the distal edge of the inner pleural field. These features are visible in many *Hystricurus* species and other "hystricurids."

It is *Amblycranium transversus*, of other hystricurids besides *Etheridgaspis*, that appears to have similar cranidial morphologies; in particular, more similarities are found in the smaller cranidia (compare Pl. III-75, Fig. 15 with Pl. III-31, Fig. 18). However, the subcylindrical glabella, more anteriorly located palpebral lobe and divergent anterior facial suture distinguish *Pseudoetheridgaspis* from *A. transversus*. The pygidia of *Amblycranium* have marginal spines, which is unique to *Amblycranium* among the "hystricurids."

Comparison with Ptychopariides. The cranidia of *Pseudoetheridgaspis cylindricus* resemble those of *Bilacunaspis obliterata*, a Tremadocian eulomid from Siberia (Petrunina, 1973, pl. 1, figs. 2, 8). Both species share a trapezoidal cranidial outline, a cylindrical glabella, a deep anterior border furrow, and an inflated palpebral lobe. *P. cylindricus* differs from the eulomids including *B. obliterata* in having a more elongated glabella, a smaller palpebral lobe, a narrower and less convex palpebral fixigena, and a shallower and narrower palpebral furrow with a consistent depth, and lacks glabellar furrows. *B. obliterata* is more similar to *P. cylindricus* than to *Etheridgaspis* (see above).

The cranidia of *Pseudoetheridgaspis typica* resemble those of the Upper Cambrian *Aktugaiella* (Peng, 1992, figs. 27.M-O) which are in turn comparable to those of *Etheridgaspis* (see above). The proportional sagittal length of the preglabellar field and anterior border and transversely elongated posterior fixigena of *Pseudoetheridgaspis typica* are closer to those of *Aktugaiella* than those of *Etheridgaspis*.

Comparison with Proetides. A bathyurid affinity can be extended from *Etheridgaspis* into *Pseudoetheridgaspis*. The elongated glabella, arched palpebral lobe and narrow posterior fixigena of *Pseudoetheridgaspis typica* are indicative of some bathyurid affinity.

Taxonomic Conclusion. It is *Etheridgaspis* which has the closest affinity with *Pseudoetheridgaspis*. Although *Etheridgaspis* has a complicated affinity with bathyurids

344

and other Upper Cambrian taxa such as *Aktugaiella*, the eulomid affinity appears to be most plausible. The eulomid affinity of *Pseudoetheridgaspis* is suggested by the shared similarities between *Pseudoetheridgaspis cylindricus* and *Bilacunaspis*. The pygidia of *Pseudoetheridgaspis* suggest its affinity with the hystricurids. It seems to be the best conclusion for the present that together with *Etheridgaspis*, *Pseudoetheridgaspis* is excluded from the Hystricuridae and is questionably placed in the Eulomidae.

<center>

Pseudoetheridgaspis typica n. gen. n. sp.
Pl. III-75, Figs. 1-19, Pl. III-76, Figs. 16-24.
</center>

Etymology. "typica" denotes that this species shows a typical architecture of *Pseudoetheridgaspis*.

Holotype. UA 12649, cranidium; Pl. III-75, Figs. 1-3, 5; *Paraplethopeltis* or *Leiostegium-Kainella* Zone; Garden City Formation, northern Utah.

Diagnosis. Cranidium longer (sag.). Posterior fixigena narrower and transversely longer. Glabella more rapidly forward-tapering.

Association of Pygidium. The cranidial materials of both *Pseudoetheridgaspis* species occur in three sampling horizons, R6-38, R6-35, and R11-48.7; the majority of them occur in R11-48.7. From R11-48.7, several pygidia with a convex axis and an indented and uparched posterior margin are found. The pygidial axis has a relative width and dorsal convexity comparable to the pygidia of *Etheridgaspis* from Tasmania (Jell and Stait, 1985a, figs. 2.F, 2.G, pl. 14, figs. 13-15; see also Pl. III-37, Figs. 6, 8-11). All illustrated pygidial specimens of *Etheridgaspis* are much larger (more than four times) than the specimens from R11-48.7. The smallest one (pl. 14, fig. 13) from Tasmania has a slightly indented posterior margin; the margin in *Pseudoetheridgaspis* is more strongly indented. In addition to co-occurrence, the resemblance with the pygidia of *Etheridgaspis* allows for the association of the pygidia from R11-48.7 with *Pseudoetheridgaspis* which has a strong cranidial resemblance with *Etheridgaspis*. All the pygidial specimens are temporarily assigned to *Pseudoetheridgaspis typica* for the present, because there is no separable morphologic variations among the collected specimens.

<center>

Pseudoetheridgaspis cylindricus n. gen. n. sp.
Pl. III-76, Figs. 1-15
</center>

Etymology. "cylindricus" describes the cylindrical glabella

Holotype. UA 12663, cranidium; Pl. III-76, Figs. 2, 3, 5, 6; *Paraplethopeltis* or *Leiostegium-Kainella* Zone; Garden City Formation, northern Utah.

Differential Diagnosis. Cranidium shorter (sag.). Glabella cylindrical (less forward-tapering). Posterior fixigena shorter transversely. Anterior border furrow deeply impressed. Posterior facial suture rapidly turns backwards at distal end. Lateral librigenal border more deeply impressed. Librigenal field narrower (tr.).

Remarks. This species certainly shares the overall cranidial architecture with *Pseudoetheridgaspis typica* such as the highly-elevated palpebral lobe and slightly curved palpebral furrow. However, the more convex cranidium, deep anterior border furrow, and tightly infolded wide cranidial doublure readily differentiate this species from *P. typica*.

<center>

?Family **LONCHOCEPHALIDAE** Hupé, 1955
Genus **PSEUDOTALBOTINA** Benedetto, 1977
</center>

<center>345</center>

Type Species. *Pseudotalbotina ovalis*; Tremadocian; Santa Rosita Formation, Sierra de Cajas, Jujuy Province, Argentina.

Diagnosis. Glabella large, convex, and ovoid. Three pairs of glabellar furrows. Ocular ridge faintly developed. Anterior facial suture parallel-sided. Preglabellar field narrow (sag.)

Remarks. This poorly known monotypic genus, based on five fragmentary cranidias from Argentina was questionably assigned to the Lonchocephalidae by Benedetto (1977, pl. 1, figs. 1-5). He differentiated *Pseudotalbotina* by having an oval-shaped convex glabella with three pairs of lateral furrows, a moderate-sized palpebral lobe located at mid-glabellar length, and a relatively narrow (tr.) palpebral area. Of species that have been assigned to the Hystricuridae, *Hystricurus rotundus*—it was previously placed in *Pseudohystricurus*—shows the greatest similarity (see Pl. III-4, Figs. 8-10). *H. rotundus* mainly differs in having a tuberculated surface and a narrower (exsag.) posterior fixigenal area. The oval-shaped convex glabella and three pairs of glabellar furrows of *Pseudotalbotina* are not uncommon to the species of *Hystricurus*; for example, see *H. (Aequituberculatus) ellipticus* and *H. (Butuberculatus) hillyardensis* (see Stitt, 1983, pl. 5, figs. 1, 2) for the oval-shaped glabella and *H.?* *millardensis* and *H.?* *sulcatus* (see Pl. III-2, Figs. 10-12) for the three pairs of glabellar furrows. The size and location of the palpebral lobe and the transverse width of the palpebral area of *Pseudotalbotina* are not only common to the Hystricuridae but also to many ptychopariids including the lonchocephalids or catillicephalids. The relatively narrow (exsag.) posterior fixigenal area with the more transverse posterior facial suture, and the parallel-sided anterior facial suture of *Pseudotalbotina* are of *Hystricurus*-type, rather than the lonchocephalid- or catillicephalid-type.

Beneditto (1977) mentioned cranidial similarities of *Pseudotalbotina* with *Sphaerocare* from Argentina (Harrington and Leanza, 1957, figs. 124.4a, b) in terms of the glabellar form and convexity and the nature of the anterior cranidial border. *Talbotina* (Lochman, 1938, pl. 56, figs. 12, 13, 16, 17), a lonchocephalid or marjumiid apparently resembles *Pseudotalbotina*, but differs in having a less convex glabella and in lacking the third pair of glabellar furrows, as mentioned by Benedetto (1977). The cranidial features of *Pseudotalbotina* are not much different from those of the Lonchocephalidae or Catillicephalidae; and these two families should be united (see Pratt, 1992).

Taxonomic Conclusion. The possible affinity of *Pseudotalbotina* with the Hystricuridae was suggested (personal communication, Adrain, 2000), which appears to be supported by the above-mentioned similarities with some *Hystricurus* species. Nonetheless, much more information (e.g., discovery of pygidia and better preserved cranidia) is required to improve our understanding of this genus. For the present, *Pseudotalbotina* is retained in the Lonchocephalidae with question.

Pseudotalbotina ovalis Benedetto, 1977

1977 *Pseudotalbotina ovalis* Benedetto, p. 191, pl.1, figs. 1-5.

Holotype. UMSA-PI 01003, cranidium; Benedetto, 1977, pl. 1, fig. 1; Tremadocian; Santa Rosita Formation, Sierra de Cajas, Jujuy Province, Argentina.

Diagnosis. Same as generic diagnosis.

Family **DOKIMOCEPHALIDAE** Kobayashi, 1935
Genus **APACHIA** Frederickson, 1949

Type Species. *Apachia trigonis* Frederickson, 1949

Remarks. *Apachia* was questionably placed in the Hystricuridae in the Treatise (Moore, 1959). Palmer (1965) referred the genus *Apachia* to the Dokimocephalidae, which is accepted herein. Other *Apachia* species have a deeper anterior border furrow, a more strongly forward-convex anterior border, and more distinct glabellar furrows than the type species, *Apachia trigonis* (Frederickton, 1949, pl. 70, figs. 14-17). Of *Hystricurus* species, it is *H. (Aequituberculatus) ellipticus* (Westrop *et al.*, 1993, pl. 3, figs. 1-7) that shows the closest cranidial morphologies. *A. trigonis* differs in having a larger glabella with a relatively truncated front, a diagonal posterior facial suture, and a smooth cranidial surface.

Dokimocephalidae n. gen. and n. sp.
Pl. III-84, Figs. 14-18

1985 Hystricuridae gen *et* sp. nov. Jell, p. 60-61, pl. 20, figs. 4-8.

Remarks. Jell (1985) noted cranidial similarities of these specimens with *Onchonotus*, *Onchopeltis*, and *Onchonotina* (=*Onchonotellus*), and *Pseudotalbotina*. Since no definite affinities could be made with any of these taxa, Jell placed them in the Hystricuridae. This species is mostly similar to *Apachia trigonis* in lacking distinct glabellar furrows and having a convex glabella and a relatively straight anterior border furrow, but it differs in having discrete fossulae, a convergent anterior facial suture, a larger palpebral lobe and an imperceptible palpebral furrow. Of dokimocephalids, *Whittingtonella* from Newfoundland (Ludvigsen *et al.*, 1989, pl. 16, figs. 1-9) shows the closest cranidial morphologies which include a triangular anterior border, fossulae, a slender ocular ridge, and a slightly incurved anterior border furrow. This dokimocephalid from Australia appears to be more similar to Laurentian dokimocephalids than Gondwanan dokimocephalids such as *Lorrettina* (see Shergold, 1975, pl. 14, figs. 1-10).

?Family **ELVINIIDAE** Kobayashi, 1935
Genus **ONCHOPELTIS** Rasetti, 1944

Type Species. *Onchopeltis spectabilis* Rasetti, 1944; Tremadocian; Levi Conglomerate, Quebec.

Diagnosis. see Rasetti (1944, p. 249)

Remarks. Rasetti (1944) erected *Onchopeltis* based on materials from the Tremadocian Levis Conglomerate, Quebec. Shergold and Webers (1992) discussed the status of *Onchopeltis* in detail, and assigned it to the Elviniidae. They described a new species, *Onchopeltis variabilis* from west Antarctica. However, the Antarctica species (Shergold and Webers, 1992, pl. 4, figs. 1-10) differs from the type species in having a much longer glabella with a truncated anterior margin, a transversely shorter anterior border, a more anteriorly located palpebral lobe, and a less stout genal spine base. These features are considered to deviate from the type species too much to be included in the same genus. Rasetti (1961, p. 108) argued that *Onchopeltis* is a closer relative to *Dunderbergia* which however has a truncated anterior glabellar margin, a longer preglabellar field, a narrower (sag. and exsag.) anterior border. It is concluded that *Onchopeltis* is restricted to the type species and the species described below, and questionably placed in the Elviniidae.

347

Onchopeltis generectus (Hintze, 1953)

1953 *Paraplethopeltis?* *generectus* Hintze, [part], p. 204, pl. 7, figs. 6-8, [only].
Holotype. 26178 (no acronym provided but the specimen was said to be stored in Columbia University, New York), free cheek; Hintze, 1953, pl. 7, figs. 6, 7; *Paraplethopeltis* Zone; Fillmore Formation, Utah.
Diagnosis. Posterior fixigena triangular, with rounded distal end. No glabellar furrows. Anterior border narrow and forward-convex. Smooth surface.
Remarks. From *Paraplethopeltis?* *generectus* which is transferred into *Pseudoplethopeltis* in this study, this species differs in having a divergent anterior facial suture that turns relatively acutely at the anterior border furrow, a diagonal posterior facial suture, and a stout and uncurved genal spine. These features accord well with *Onchopeltis*, not with *Paraplethopeltis* nor with *Pseudoplethopeltis*. This species differs from the type species in having a narrower anterior cranidial border and lacking tubercles on the cranidial and librigenal surfaces.

Onchopeltis? n. sp.

1951 *Hystricurus* ? sp. I Ross, p. 56, pl. 17, figs. 1-3.
Holotype. Y.P.M. 18306, cranidium; Ross, 1951, pl. 17, figs. 1-3; *Paraplethopeltis* Zone; Garden City Formation, southern Idaho.
Diagnosis. Glabella large and oval-shaped. No glabellar furrows. Anterior border narrow and forward-convex.
Remarks. Compared to *Hystricurus*, this species has a much larger oval-shaped glabella, a more strongly convex forward anterior cranidial margin, and a diagonal posterior facial suture. This species differs from *Onchopeltis* in having an oval-shaped glabella. This species is questionably referred to *Onchopeltis*.

Family **PLETHOPELTIDAE** Raymond, 1925
Genus **PARAPLETHOPELTIS** Bridge and Cloud, 1947

Type Species. *Paraplethopeltis obesa* Bridge and Cloud, 1947; Lower Ordovician; Ellenburger Formation, central Texas.
Included Species. *P. depressa*, Bridge and Cloud, 1947, *P. cordai*, (Billings, 1859), *P. seelyi*, (Whitfield, 1889), *P. nudus*, (Poulsen, 1937), *P. carinifera*, Flower, 1969.
Diagnosis. Glabella large and longer than wide, with lateral margin being moderately convergent to parallel-sided. Anterior facial suture slightly divergent to parallel-sided. Palpebral lobe of medium-size and located at mid-cranidial length. Posterior fixigena wide (exsag.) and posterior facial suture convex antero-laterally. Pygidium with very narrow but deeply impressed axial ring furrows and pleural furrows; interpleural furrows imperceptible. Marginal border very narrow.
Comparison with "Hystricurids". Other species from New York and Newfoundland differ from the type species, *Paraplethopeltis obesa* from central Texas (Bridge and Cloud, 1947, pl. 2, figs. 1-7, 12-14) in having a distinct anterior cranidial border furrow, forward-tapering glabella, larger and weakly-arched palpebral lobe, and divergent anterior facial suture. These features are comparable to such "hystricurids" as *Paratersella*, and *Hystricurus* (*Hystricurus*) *crotalifrons* and *Hystricurus* (*Hystricurus*) *oculilunatus* (see Boyce, 1989, pl. 8, fig. 5, pl. 12, fig. 4). *Paratersella* has a much

348

narrower (exsag.) posterior fixigena, a more elongated glabella, a long preglabellar field with a median furrow, and a larger and more strongly arched palpebral lobe. The *Hystricurus* species differ in having an exoskeletal surface covered with large tubercles, a broader anterior border furrow, a more strongly arched palpebral lobe, and a longer (tr.) and straight posterior facial suture.

Unlike pygidia of "hystricurids" and *Hystricurus*, the pygidia of *Paraplethopeltis* (see Boyce, 1989, pl. 19, figs. 3-8) have very narrow but deeply impressed pleural furrows reaching the border, and a weakly tapering wide axis, and lack any discernible structure such as tubercles or fulcral ridges separating inner and outer pleural fields; *Pseudoplethopeltis* shows a relatively gentle change of the slope between the two fields.

Comparison with Ptychopariides. From other plethopeltids such as *Plethopeltis*, *Stenopilus*, and *Leiocoryphe* (see Ludvigsen *et al.*, 1989 for detailed accounts of the Plethopeltidae), *Paraplethopeltis* differs in having a larger palpebral lobe, a much less steep posterior facial suture, a much steeper outer pygidial pleural field, and shallowly-impressed pygidial interpleural furrows. Cranidial features of the type species, *Paraplethopeltis obesa*, are much more similar to those of *Plethopeltis* than the later-described species.

Comparison with Proetides. From the bathyurids, *Paraplethopeltis* differs in having a longer preglabellar field, a wider (exsag.) posterior fixigena, a wider pygidial axis with deep ring furrows, and a more steeply down-sloping outer pygidial pleural field

Taxonomic Conclusion. *Paraplethopeltis* has been placed in the Plethopeltidae (Bridge and Cloud, 1947; Stitt, 1983) or the Hystricuridae (Boyce, 1989), or was considered to be a subgenus of *Hystricurus* (Berg and Ross, 1959; Fortey and Peel, 1989). The hystricurid affinity has been established through the two Utah species, *Paraplethopeltis*? *genacurvus* and *Paraplethopeltis*? *generectus*. Since the former is assigned to the new genus *Pseudoplethopeltis* and the latter to *Onchopeltis* (see below), the hystricurid affinity of *Paraplethopeltis* is denied in this study. It is the pygidial features that more strongly contradict the hystricurid affinity of *Paraplethopeltis*. The cranidia of the type species, *Paraplethopeltis obesa*, demonstrate a definite affinity with *Plethopeltis* as argued by Bridge and Cloud (1947).

Lee and Chatterton (1997a) restricted the concept of *Paraplethopeltis* to the type species. A detailed comparative analysis of, in particular, the pygidial features, indicates that *Paraplethopeltis* should accommodate other species from Newfoundland and New York.

Hypotheses of Evolutionary Relationships. It is plausible that morphological transformations from highly effaced *Leiocoryphe* to *Paraplethopeltis* species of Newfoundland and New York through *Paraplethopeltis* species of Texas and *Plethopeltis* can be accommodated within an evolutionary lineage. In this case, the cranidial similarities of those species from Newfoundland and New York with some "hystricurids" could be due to convergence.

Paraplethopeltis obesa Bridge and Cloud, 1947

1947 *Paraplethopeltis obesa* Bridge and Cloud, p. 557-558, pl. 2, figs. 1-7, 12-14.
1948 *Paraplethopeltis obesa*, Cloud and Barnes, pl. 38, figs. 4-9, 11-13.
1948 *Hystricurus* aff. *H. missouriensis* Ulrich *in* Bridge, Cloud and Barnes, [part], pl. 38, fig. 17, [only].

349

1983 *Paraplethopeltis obesa*, Stitt, p. 22-23, pl. 2, fig. 9.

Lectotype. cranidium; Bridge and Cloud, 1947, pl. 2, fig. 7. Bridge and Cloud (1947) designated two cranidia as the holotype. The cranidium illustrated in pl. 2 and fig. 7 is selected herein as the lectotype.

Diagnosis. Anterior border furrow imperceptibly impressed. Anterior facial suture parallel-sided. Posterior fixigena widest (exsag.).

Remarks. A pygidium of *Hystricurus* aff. *H. missouriensis* (Cloud and Barnes, 1948, pl. 38, fig. 17) lacks pleural furrows and tubercles on pleural bands, which distinguishes *Paraplethopeltis* from such *Hystricurus* species as *H. (Butuberculatus) scrofulosus* with a similar pygidium. This species differs from other *Paraplethopeltis* species in having parallel-sided anterior facial suture and wide (exsag.) posterior fixigenal area.

Paraplethopeltis depressa Bridge and Cloud, 1947

1947 *Paraplethopeltis depressa* Bridge and Cloud, p. 558, pl. 2, figs. 8-11.
? 1948 *Paraplethopeltis?*, Cloud and Barnes, pl. 38, fig. 14.

Lectotype. cranidium; Bridge and Cloud, 1947, pl. 2, fig. 11; Lower Ordovician; Ellenburger Formation, central Texas. Bridge and Cloud (1947) designated two cranidia as the holotype. The cranidium illustrated in pl. 2 and fig. 11 is selected herein as the lectotype.

Diagnosis. Anterior border furrow imperceptibly impressed. Posterior fixigena narrowest (exsag.). Glabella with relatively truncated anterior margin.

Remarks. A poorly-preserved free cheek (Cloud and Barnes, 1948, pl. 38, fig. 14) is tentatively assigned to this species because the posterior facial suture of this species runs more transversely than co-occurring *Paraplethopeltis obesa*. This species is differentiated from other *Paraplethopeltis* species by a very narrow posterior fixigenal area and a truncated glabellar front.

Paraplethopeltis cordai (Billings, 1859)

1859 *Bathyurus cordai* Billings; Billings, p. 321, fig. 26
1989 *Paraplethopeltis cordai*, Boyce, pl. 17, figs. 1-4.
? 1989 *Hystricurus* sp., Dean, [part], p. 23, pl. 14, fig. 3, [only].

Lectotype. GSC 836c, cranidium; Billings, 1859, fig. 26 (re-illustrated by Boyce, 1989, pl. 17, figs. 1-4); Tremadocian; Levis Formation, Quebec.

Diagnosis. Anterior border furrow deeply impressed. Glabella forward-tapering. Anterior facial suture slightly divergent. Palpebral lobe moderately arched laterally.

Remarks. The overall cranidial architecture of a cranidium from Alberta (Dean, 1989, pl. 14, fig. 3) is comparable to the *Paraplethopeltis* species from Newfoundland and New York. It has a conical glabella, a relatively wide (exsag.) posterior fixigena, and a moderately-arched palpebral lobe, which are more similar to *Paraplethopeltis cordai*. However, the cranidium from Alberta has a relatively straight anterior margin and a proportionately wider (sag.) occipital ring. Since it is smaller than the lectotype of *P. cordai*, these differences could be ontogenetic.

Paraplethopeltis seelyi (Whitfield, 1889)

1889 *Bathyurus seelyi* Whitfield, p. 62-63, pl. 13, figs. 8-14.
? 1948 *Hystricurus binodosus* Weber, [part], p. 7-9, pl. 1, figs. 17, 18, [only].

350

1913b *Hystricurus cordai* (Billings), Raymond, p. 61.

1983 *Paraplethopeltis seelyi*, Boyce *in* Stouge and Boyce, pl. 15, figs. 6-8.

1983 *Paraplethopeltis seelyi*, Boyce, p. 126-131, p. 10, figs. 2-7, pl. 11, figs. 1, 2.

1989 *Paraplethopeltis seelyi*, Boyce, p. 43-45, pl. 17, figs. 5-8, pl.18, figs. 1-8, pl. 19, figs. 1-8, pl. 20, figs. 1-5.

Lectotype. AMNH 35504, cranidium; Whitfield, 1889, pl. 13, figs. 11-12 (re-illustrated by Boyce, 1989, pl. 17, fig. 8, pl. 18, figs. 4-6); *Randaynia saundersi* Zone of Canadian Series; Fort Ann Formation, New York.

Diagnosis. Anterior border furrow deeply impressed. Glabellar forward-tapering. Palpebral lobe large. Preglabellar field long. Anterior facial suture slightly divergent. Pygidium with four axial rings.

Remarks. Two poorly-preserved pygidial specimens of *Hystricurus binodosus* from Siberia (Weber, 1948, pl. 1, figs. 17, 18) have deeply and narrowly impressed pleural furrows and appear to show no development of the interpleural furrows. These features are observed in the pygidia of this species. The Siberian pygidia are questionably referred to this species. The detailed accounts on the other synonyms are found in Boyce (1989).

Paraplethopeltis nudus (Poulsen, 1937)

1937 *Hystricurus nudus* Poulsen, p. 34-35, pl. 2, fig. 10.

Holotype. cranidium; Poulsen, 1937, pl. 2, fig. 10; Lower Ordovician; Cass Fjord Formation, East Greenland.

Diagnosis. Glabella shortest with weakly impressed three pairs of glabellar furrows. Ocular ridge distinct.

Remarks. Boyce (1989) transferred this species into *Paraplethopeltis*, which is accepted herein. This species is only known from one cranidial specimen and differs from other *Paraplethopeltis* species in having a distinct ocular ridge.

Paraplethopeltis carinifera Flower, 1969

1969 *Paraplethopeltis carinifera* Flower, p. 27, pl. 6, figs. 1-4, 19, 34.

Holotype. no. 1169, cranidium; Flower, 1969, pl. 6, fig. 1; Lower Ordovician; Smith Basin Limestone, New York.

Diagnosis. Glabella small.

Remarks. Although the poor illustration prevents any further taxonomic assessment, the conical glabella and pygidium with a wide axis suggest a definite affinity of this species to *Paraplethopeltis*.

Family UNCERTAIN

Genus HOLUBASPIS Přibyl, 1950

Type Species. *Holubaspis perneri* (Ružička, 1926); early Tremadocian; Trenice Formation in western part of the Prague Basin, Czech Republic.

Diagnosis. Large trapezoidal glabella with straight anterior margin. No preglabellar field. Anterior border straight to slightly curved backwards. Large palpebral lobe with well-impressed palpebral furrow. Occipital furrow curved forwards sagittally. Small pygidium with two axial rings and terminal piece, very strong postaxial ridge, very wide (tr.) axis, and tubular border. No pleural furrows but anteriormost one. Pleural field relatively flat. Axial furrows impressed inwards, resulting in that the lateral portion of axis overhangs.

351

Comparison with "Hystricurids". When initially erected, *Holubaspis* was regarded as an olenid, but later Vaněk(1965) assigned it to the Hystricuridae. Of the cranidial features of *Holubaspis*, the transversely elongated posterior fixigenal area, and medium-sized well-defined palpebral lobe located at mid-cranidial length are also visible in many "hystricurids," in particular, in *Eurylimbatus*. The subrectangular large glabella of *Holubaspis* is not comparable to any "hystricurids." Many *Hystricurus* and other "hystricurids" lack a preglabellar field like *Holubaspis*. However, *Holubaspis* lacks this feature throughout the entire glabellar front, whereas the other taxa lack it only at sagittal point of the glabellar front due to an anterior border and border furrow that are sagittally curved backwards.

The diagnostic pygidial features of *Holubaspis* are comparable to *Tersella truncatus* from Korea (Pl. III-46, Figs. 8, 9). The latter however has a much longer and narrower axis and a relatively convex pleural field with three pleural segments. Such *Hystricurus* (*Hystricurus*) species as *H.* (*H.*) *crotalifrons* has a post-axial ridge and/or tubular border. However, the convexity of the post-axial ridge is not comparable to that of *Holubaspis*. The pygidia of most "hystricurids" have more than one countable segments on their pleural field, whereas those of Holubaspis have only one visible segment. A Kazakhstan pygidium, which was referred to *Hystricurus conicus* (Balashova, 1961, pl. 1, fig. 14), has a wider axis and only one distinct pleural furrow which is comparable to the pygidia of *Holubaspis*. However, the Kazakhstan pygidium lacks the post-axial ridge, and the specimen is most likely to be associated with an olenid such as *Peltura* (see Henningsmoen, 1957, pl. 26, fig. 6).

Free cheeks of *Holubaspis* (see Mergl, 1994, pl. 4, figs. 7, 8) are similar to those of *Eurylimbatus* with respect to the width of lateral border and the absence of the genal spine.

Comparison with Ptychopariides. The subrectangular glabella of *Holubaspis* with a similar proportional size is found in various ptychopariides; *Corbinia* (an eurekiid, see Westrop and Ludvigsen, 1986, fig. 2), *Jujuyaspis borealis* (an olenid, see Dean, 1989, pl. 7, figs. 1, 6), *Probilacunaspis* (an eulomid, see Peng, 1992, figs. 33I, 33N), *Lorrettina* (a dokimocephalid, see Shergold, 1980, pl. 14, figs. 1-7), and *Modocia* (a marjumid, see Pratt, 1992, pl. 20, fig. 21). *Corbinia* and *J. borealis* lack the preglabellar field and have a forwardly-curved preoccipital furrow and wide axial furrows, like *Holubaspis*. *J. borealis* and *Corbinia* have a much wider (exsag.) posterior fixigena, and *Corbinia* has two pairs of glabellar furrows and a longer glabella, which distinguishes *Holubaspis* from these two taxa. Their pygidia (see Westrop, 1986, pl. 5, fig. 12; Dean, 1989, pl. 7, fig. 7) are not comparable to that of *Holubaspis*, which is the most compelling evidence to contradict the affinity of *Holubaspis* with these taxa. Except for having a preglabellar field and glabellar furrows, the cranidial architecture of *Holubaspis* is most similar to that of *Lorrettina*. However, the pygidia of *Lorrettina* (see Shergold, 1980, pl. 14, figs. 9, 10) lack the post-axial ridge and have a wider pleural field with more than one countable pleural segments.

The pygidium of *Holubaspis* is indistinguishable from that of *Skreiaspis* (an Agraulidae) from the Middle Cambrian Bohemia (see Šnajdr, 1990, p. 109). Except for the wide axis and strong post-axial ridge, some eulomid pygidia (see Peng, 1990, pl. 2, fig. 12) are comparable to those of *Holubaspis*. The cranidia of *Skreiaspis* (see Šnajdr, 1958, pl. 37, fig. 28) and the eulomids (see Peng, 1990, pl. 2, fig. 7) are not comparable

352

to those of *Holubaspis*.

Comparison with Proetides. With respect to the glabellar size and absence of preglabellar field, such proetides as *Gerastos* (see Šnajdr, 1980, pl. 5, fig. 15) are comparable to *Holubaspis*. The cranidia of some *Benthamaspis* species (a bathyurid, e.g., see Hintze, 1953, pl. 13, fig. 15) are similar to those of *Holubaspis perneri*. They differ in having a distinct palpebral furrow and lacking a preglabellar field. The pygidia of *Benthamaspis* (see Fortey, 1979, pl. 34, figs. 8, 9) are greatly different from those of *Holubaspis*. The genal spine is absent in *Benthamaspis* and *Holubaspis* (see Fortey, 1979, pl. 35, fig. 2; Mergl, 1994, pl. 4, figs. 7-9).

Comparison with Other Taxa. Such a leiostegiacean as *Shengia* (Peng, 1992, fig. 40-F) has a cranidium that looks as if it has a *Holubaspis*-like cranidium that is stretched longitudinally. Both have no preglabellar field, a transversely elongated posterior fixigenal area and a forwardly-curved occipital furrow. *Shengia* has a divergent anterior facial suture, and more posteriorly located palpebral lobe, and its leiostegiacean-type pygidia are not comparable to those of *Holubaspis*.

Taxonomic Conclusion. Cranidial and pygidial features of *Holubaspis* are much more similar to taxa other than "hystricurids," so that the genus is removed from the Hystricuridae. Since the cranidia and pygidia are similar to various different ptychopariides, *Holubaspis* cannot definitely be placed in any family at this time.

<div align="center">

Holubaspis perneri (Ružička, 1926)
</div>

1994 *Holubaspis perneri* (Ružička, 1926), Mergl [part], p. 16-17, pl. 4, figs. 3-6 [only].
Lectotype. NML 18889, cranidium; Ružička, 1926, pl. 2, fig. 1 (re-illustrated by Mergl, 1994, pl. 4, fig. 5).
Diagnosis. Lateral glabellar margin laterally convex. Anterior border furrow backwardly curved. Palpebral lobe large. Anterior facial suture slightly divergent.
Remarks. A remarkable cranidial similarity is found with *Benthamaspis* sp. A (see Pl. III-83, Figs. 16-18; see also, Hintze, 1953, pl. 13, fig. 15). The cranidia of *B*. sp. A are large and have a laterally convex glabellar margin. The only noticeable difference is that the cranidia of *Holubaspis perneri* have a distinct palpebral furrow, a slightly divergent anterior facial suture, and a truncated anterior margin. The pygidia of *Holubaspis* (Pl. III-46, Figs. 3-5) differ greatly from those of *Benthamaspis* (see Fortey, 1979, pl. 34, figs. 8, 9).

<div align="center">

Holubaspis paraperneri n. sp.
Pl. III-46, Figs. 1-5
</div>

? 1965 *Holubaspis perneri* (Ružička, 1926), Vaněk[part], p. 268-271, pl. 23, fig. 12 [only]
1965 *Holubaspis perneri* (Ružička, 1926), Vaněk[part], p. 268-271, pl. 23, fig. 13-17, pl. 26, figs. 41-46 [only] (see synonym list to date).
1965 *Eulomina mitrata* (Ružička, 1926), Vaněk[part], p. 285-286, pl. 25, figs. 36, 37.
1984 *Holubaspis perneri* (Ružička, 1926), Mergl, p. 35-37, pl. 4, figs. 1-9, text-fig. 8 (see synonym list to date)
1994 *Holubaspis perneri* (Ružička, 1926), Mergl [part], p. 16-17, pl. 4 figs. 1, 2, 7-11 [only].
Holotype. MM 190, cranidium; Mergl, 1984, pl. 4, fig. 1; Tremadocian; Trenice

<div align="center">353</div>

Formation, Central Bohemia.

Diagnosis. Lateral glabellar margin straight. Anterior cranidial border furrow straight. Palpebral lobe smaller.

Remarks. Two pygidia were assigned to *Eulomina* by Vaněk(1965, pl. 25, figs. 36, 37). Their wide axis and strong post-axial ridge are not distinguishable from the pygidia of this species. A cranidium identified as this species by Vaněk(1965, pl. 23, fig. 12) is questionably assigned to this species because its glabella is much longer than wide. The pygidia with a strong post-axial ridge are also tentatively assigned to this species.

Genus NYAYA Rozova, 1963

Type Species. *Nyaya nyaensis* Rozova, 1963; Nya Horizon (Lower Ordovician); Siberia.
Included Species. *N. orientalis*, Ogienko, 1974.
Diagnosis. Anterior border furrow shallow and shallows sagittally. Glabella forward-tapering and subtrapezoidal with straight-sided lateral margin and relatively truncated anterior margin. Two or three pairs of weakly-developed glabellar furrows isolated from axial furrows. Preglabellar field slightly convex dorsally. Palpebral lobe moderately arched. Palpebral furrow moderately deep. Anterior facial suture moderately divergent. Pygidium semi-circular. Border furrow wide and moderately deep and concave. Exoskeletal surface smooth.

COMPARISON. Many features of *Nyaya* are visible in taxa which have been assigned to the Hystricuridae. For example, the subtrapezoidal glabella is seen in *Hystricurus? longicephalus* (Pl. III-2, Fig. 9); the sagittally shallowing anterior border furrow is seen in *Tersella* (Burskyi, 1970, pl. 2, figs. 1, 3). However, the cranidial architecture of *Nyaya* is much more similar to that of several Upper Cambrian genera erected by Rozova (1963, 1968) from Siberian Platform such as *Amorphella, Nganasanella, Tamaranella, Monosulcatina*, and *Nordia*. These taxa have a subtrapezoidal glabella, a preglabellar furrow deepening towards the antero-lateral glabellar corner, a slender and weakly developed ocular ridge, a moderate-sized palpebral lobe located at mid-cranidial length, and two or three pairs of weakly-developed glabellar furrows which are isolated from the axial furrows, and some species of these taxa have a slightly swollen preglabellar field (e.g., *Amorphella*, Rozova, 1963, pl. 2, Figs. 1, 2). The same features are comparable to those of mainly Laurentian aphelaspidines (e.g., *Aphelaspis*, Rasetti, 1965, pl. 19), and the Siberian forms only differ in having an anterior cranidial border furrow that shallows sagittally. The Tremadocian *Nyaya* obviously displays cranidial features which were evolutionarily carried over from these Upper Cambrian genera.

Of these Upper Cambrian genera, a pygidium is only known to *Amorphella* (Rozova, 1968, pl. 7, fig. 14); only a single specimen is illustrated. It shows a wide, a concave border furrow, a narrow border, and less distinct pleural and interpleural furrows, which are found in many aphelaspidines. The pygidium of *Nyaya* (Rozova, 1968, pl. 16, figs. 11, 12) differs from the *Amorphella* pygidium in having deeper pleural and interpleural furrows and a more convex pleural field. The *Nyaya* pygidium is most similar to that of *Tersella* (see Burskyi, 1970, pl. 3, fig. 4), but differs in having distinct interpleural furrows. The pygidium is also similar to those of the Sibrian eulomids such as *Ketyna* and *Euloma* (see Apollonov and Chugaeva, 1983, pl. 7, figs. 10-12, pl. 8, figs. 7-9).

Of *Hystricurus* species, a very similar pygidial architecture is found in *H.? millardensis* (Taylor and Halley, 1974, pl. 3, fig. 10); the pygidium of *H.? millardensis*

354

differs from those of other *Hystricurus* species in having a less distinct border that is only defined by a change of slope in the pleural field. The pygidium of *Nyaya* only differs in having a smooth exoskeletal surface. The cranidium of *H.*? *millardensis* is characterized by possessing a preglabellar furrow deepening at the antero-lateral corner of the glabella as a fossula (Stitt, 1971, pl. 8, fig. 17) which is present in *Nyaya* and the Upper Cambrian Russian genera and many aphelaspidines from Laurentia.

Taxonomic Conclusion. It seems most probable that *Nyaya* was derived from one of the above-mentioned Upper Cambrian genera and thus *Nyaya* is best placed in the same group to which the Upper Cambrian genera are assigned, not in the Hystricuridae.

Hypotheses of Evolutionary Relationships. The phylogenetic relationship of the Hystricuridae with the Aphelaspidinae (and Elviniidae) which most probably turns out to include the above-mentioned Siberian Upper Cambrian genera is yet to be established. The relationships between the Eulomidae and Aphelaspidinae needs to be investigated.

Nyaya nyaensis Rozova, 1963

1963 *Nyaya nyaensis* Rozova, p. 18-19, pl. 2, figs. 12-13
1968 *Nyaya nyaensis* Rozova, p. 205-209, pl. 16, figs. 1-12, text-fig. 54.
1968 *Nyaya* aff. *nyaensis* Rozova, p. 209-211, pl. 16, figs. 13-15, text-fig. 55
1968 *Nyaya grata* Rozova, p. 211-213, pl. 16, figs. 16-22, text-fig. 56

Holotype. No. 113/1999, cranidium; Rozova, 1963, pl. 2, fig. 13; Lower Ordovician, Nya Horizon, Siberia

Diagnosis. Preglabellar furrow deepens at antero-lateral corner of glabella. Glabella with longitudinal keel.

Remarks. Rozova (1968) distinguished *Nyaya grata* (Rozova, 1968, pl. 16, figs. 16-22) from *Nyaya nyaensis* by a granulated surface and a strongly arched anterior cranidial border. However, these differences are not discernible in the cranidia illustrated for these two species, so that *N. grata* is considered here as a junior synonym of *N. nyaensis*.

The possession of three pairs of glabellar furrows led Rozova (1968) to discern *Nyaya* aff. *nyaensis*. Since most cranidial specimens of *N. nyaensis* have faintly developed S3 glabellar furrows, *N.* aff. *nyaensis* is also assigned to this species.

Nyaya orientalis Ogienko, 1974

1968 *Nyaya* sp. Rozova, p. 213-214, pl. 17, figs. 1-3, text-fig. 57
1974 *Nyaya orientalis* Ogienko, pl. 12, figs. 1-4.
1984 *Nyaya orientalis* Ogienko, pl. 7, figs. 11, 12.
1992 *Nyaya orientalis* Ogienko, p. 91, pl. 4, figs. 15-17.

Holotype. No. 727B/42, cranidium; *Ijacephalus-Nyaya* horizon; Siberia.

Diagnosis. Glabella less convex. Anterior cranidial border shallow. Preglabellar furrow consistently deep throught entire stretch.

Remarks. A shallower anterior cranidial border furrow and less convex glabella lead me to assign *Nyaya* sp. to this species.

Genus TAOYUANIA Liu *in* Zhou *et al.*, 1977

1983 *Batyraspis* Apollonov and Chugaeva, p. 88.

Type Species. *Taoyuania xenisma*, Liu *in* Zhou *et al.*, 1977; Panjiazui Formation; Lower Tremadocian; Taoyuan, South China.

355

Included Species. *T. affinis* Liu *in* Zhou *et al.*, 1977, *T. nobilis* Peng, 1984

Diagnosis. Anterior cranidial margin long (tr.). Anterior cranidial border wide (sag. and exsag.), being wider than preglabellar field. Anterior facial suture divergent. Glabella elongated with truncated anterior margin. Occipital spine present. Palpebral lobe of moderate size, moderately arched and well defined by palpebral furrows. Posterior fixigenal area transversely long.

Remarks. Peng (1990b) synonymized *Batyraspis* Apollonov and Chugaeva, 1983 from Kazakhstan with *Taoyuania* from South China, which is accepted herein.

Comparison with "Hystricurids". The frontal area of *Taoyuania* that is delimited by a transversely long anterior cranidial margin and divergent anterior facial suture is similar to that of *Tanybregma tasmaniensis* from Australia (see Pl. III-85, Figs. 1-4) and *Hystricurus ravni* from Greenland (see Pl. III-21, Fig. 8). The two latter taxa have a much narrower anterior border and *Tanybregma* is characterized by an extremely long preglabellar field and a slender and large palpebral lobe. The divergent anterior facial suture of *Taoyuania* is comparable to *Metabowmania* and *Hyperbolochilus*. The latter two genera are easily differentiated by having a long preglabellar field, and a relatively smaller and forward-tapering glabella with a rounded anterior margin. *Hillyardina tubularis* from Australia (Pl. III-48, Figs. 1-3) bears a frontal area, although transversely narrower, similar to the *Taoyuania* species from South China, a very short preglabellar field, and a backwardly-curved anterior border furrow. However, *H. tubularis* differs in having a narrower anterior border, a parabolic glabella, and a straight palpebral furrow. The size and curvature of the palpebral lobe of *Taoyuania* are comparable to many *Hystricurus* species such as *H. (Aequituberculatus) genalatus*. The posterior fixigena of the *Taoyuania* species from China that is sharply terminated distally and transversely elongated is evident in *Carinahystricurus tasmanacarinatus* (Pl. III-36, Fig. 1).

Peng (1984) assigned a poorly-preserved pygidium (Pl. III-84, Figs. 5-7) to *Taoyuania nobilis*. It is characterized by having a parallel-sided axis, a slightly concave marginal border ornamented with fine terrace lines, and a weakly-developed post-axial ridge, and in lacking a distinct border furrow. *Tersella* (see Burskyi, 1970, pl. 3, fig. 4) and *Nyaya* (see Rozova, 1968, pl. 16, fig. 11) from Siberia have a pygidium that is most comparable to that of *Taoyuania*, if the pygidium is correctly associated with *T. nobilis*. Based on the information available, they share a similar elongated outline and a broad concave border lacking a distinct border furrow. The pygidia of many hystricurids have a tube-like pygidial border which is well defined by the border furrow.

Comparison with Ptychopariides. The cranidial architecture of *Taoyuania* is greatly similar to that of *Graciella*, a monotypic genus from northwestern Siberia (see Rozova, 1963, pl. 2, fig. 5). Both share a divergent anterior facial suture, a transversely long anterior margin, a glabella with a truncated anterior margin, a palpebral lobe of similar size and curvature, a well impressed palpebral furrow, and an occipital spine. From most cranidial specimens of *Taoyuania*, *Graciella* is differentiated by having a gently forward-convex anterior cranidial border furrow—resulting in a longer preglabellar field, and a straight lateral glabellar margin. However, these features appear to be evident in some specimens of *Taoyuania* species (see Peng, 1984, pl. 9, fig. 3, Peng, 1990b, pl. 8, fig. 8a). This suggests that *Graciella* and *Taoyuania* are very closely related to each other. *Graciella graciensis* from Siberia, the type species of *Graciella*, differs from the *Taoyuania* species from Kazakhstan and South China in lacking tubercles on the

356

exoskeletal surface and in having a gently convex forward anterior margin and a relatively shorter (tr.) posterior fixigena.

The similarities of *Taoyuania* with *Graciella* are easily extended into several Upper Cambrian and Lower Ordovician taxa from Siberia such as *Amorphella*, *Nganasanella*, and *Nyaya* (see Rozova, 1963). In effect, it would not be an easy task to differentiate morphologically these taxa. The pygidium assigned to *Taoyuania nobilis* from South China is of ptychopariide type. Most "hystricurids" have a border defined by a distinct border furrow, whereas the pygidium of *T. nobilis* has a concave wide border without any distinct border furrow. The pygidium of *T. nobilis* is greatly similar to those of *Lophosaukia* sp. cf. *L. jiangnanensis* (Peng, 1992, figs. 24D, 24E) from a lower sampling horizon of the same section from which the pygidium of *T. nobilis* is collected. They share fine terrace lines on the border, a row of small tubercles on the anterior and posterior pleural bands, and a post-axial ridge. Although the pygidium of *T. nobilis* only differs in having a parallel-sided axis, the smaller specimen of *Lophosaukia* (Peng, 1992, fig. 24D) appears to have a parallel-sided axis. It seems possible that the pygidium of *T. nobilis* belongs to a younger *Lophosaukia* species. The overall cranidial outline of *Tatulaspis* from Kazakhstan (Ivshin 1956, pl. 9, figs. 1-4) resemble those of *Taoyuania*. The former differs in having a more forward-convex anterior cranidial border and a less divergent anterior facial suture.

When erecting *Batyraspis*, which is a junior synonym of *Taoyuania*, Apollonov and Chugaeva (1983) noted similarities with such leiostegiids as *Lloydia* and *Iranochuangia* and assigned it to the Leiostegiidae. The rectangular glabella encroaching the anterior border and the medium-sized palpebral lobe with a distinct palpebral furrow of some leiostegiids (see *Chosenia*, Peng, 1990b) do not deviate from the cranidial morphologies of *Taoyuania*. However, the leiostegiid pygidia are characterized by a semi-circular outline, as many as eight axial rings and at least four pleural furrows, a flat marginal border with a uniform thickness, and a pair of marginal spines in many species.

Comparison with Proetides. The pygidial morphologies of *Taoyuania*, if the pygidium of *T. nobilis* is correctly associated, are similar to those of bathyurids (see Whittington, 1953a) in having a concave wide border lacking distinct border furrow.

Taxonomic Conclusion. The strong similarities of *Taoyuania* with Upper Cambrian *Graciella* from Siberia and other Upper Cambrian and Lower Ordovician Siberian taxa lead to exclude *Taoyuania* from the Hystricuridae. If our understanding of these Siberian trilobites is improved, *Taoyuania* may be a junior synonym of *Graciella*. In such case, *Taoyuania* will be placed in the same higher taxon that includes those Siberian taxa and Lower Ordovician *Nyaya*. The similarities with some "hystricurids" appear to be convergent or valid at a higher taxonomic rank. It seems possible that *Graciella* from Siberia belongs to the same group with the Upper Cambrian Siberian taxa, and *Taoyuania* from Kazakhstan and South China are placed in a different group which is stemmed from Siberian *Graciella*. Undoubtedly, more information on the Siberian taxa is required to make a more detailed taxonomic assessment.

Hypotheses of Evolutionary Relationships. It seems a plausible evolutionary scenario that *Taoyuania* was originated from a Siberian Upper Cambrian taxon such as *Graciella* and migrated into South China through Kazakhstan. The *Taoyuania* species from South China develop tubercles on the exoskeletal surface and a backwardly-curved anterior border furrow. It seems crucial to examine the Siberian Upper Cambrian taxa in greater

357

detail, and analyze them with *Taoyuania*, *Nyaya*, and *Tersella* which were considered to belong to the Hystricuridae. Rozova (1968) placed several of these taxa in the family Talbotinidae which appears to contain members of the eulomids (e.g., *Amorphella modesta*) and aphelaspids (e.g., *Olentella shidertensis*).

<p align="center">***Taoyuania xenisma*** Liu *in* Zhou *et al.*, 1977</p>
<p align="center">Pl. III-84, Figs. 1-4</p>

1977 *Taoyuania xenisma* Liu *in* Zhou *et al.*, p. 161, pl. 49, figs. 1-3.

1982 *Taoyuania xenisma*, Liu, p. 311, pl. 218, figs. 13-15.

1983 *Batyraspis inceptoris* Apollonov and Chugaeva, p. 88-89, pl. 10, figs. 5, 6, text-fig. 24

1990b *Taoyuania xenisma*, Peng, p. 86-87, pl. 8, figs. 1-5.

Holotype. IV 13031, cranidium; Liu *in* Zhou *et al.*, 1977, pl. 49, fig. 1; Taoyuan, South China.

Diagnosis. Anterior cranidial border weakly curved backwards sagittally. Palpebral lobe narrows anteriorly and connected with more slender ocular ridge which is obliquely directed at about 45 degrees. Tubercles on exoskeletal surface but absent on anterior border.

Remarks. Cranidia of *Batyraspis inceptoris* from Kazakhstan show a medial backward protrusion of the anterior border and an incurved lateral glabellar margin, and lack tubercles on the anterior cranidial border. *B. inceptoris* is considered to be a junior synonym of this species.

<p align="center">***Taoyuania affinis*** Liu *in* Zhou *et al.*, 1977</p>

1977 *Taoyuania*? *affinis* Liu *in* Zhou *et al.*, p. 161, pl. 49, fig. 4

1982 *Taoyuania*? *affinis*, Liu, p. 311, pl. 219, fig. 1

1984 *Taoyuania* sp. Peng, p. 338-339, pl. 9, fig. 7, 8

1990 *Taoyuania affinis*, Peng, p. 87-88, pl. 8, figs. 6-9

Holotype. IV 13035, cranidium; Liu *in* Zhou *et al.*, pl. 49, fig. 4; Taoyuan, South China.

Diagnosis. Tubercles on anterior border. Ocular ridge absent.

<p align="center">***Taoyuania nobilis*** Peng, 1984</p>
<p align="center">Pl. III-84, Figs. 5-10</p>

1955 *Hystricurus* sp., Maximova [part], p. 118, pl. 7, fig. 3 [only]

1962 *Hystricurus* sp., Maximova, p. 21, pl. 1, fig. 12.

1983 *Taoyuania nobilis* Peng, pl. 3, fig. 9

1984 *Taoyuania nobilis* Peng, [part], p. 337-338, pl.9, figs. 1-4, 6, [only].

? 1984 *Taoyuania nobilis* Peng, [part], p. 337-338, pl.9, fig. 5, [only].

Holotype. No. 83110, cranidium; Peng, 1983, pl. 3, fig. 9; *Onychopyge-Hysterolenus* Assemblage Zone (correlated with *Pseudokainella* Zone) Panjiazui Formation, South China.

Diagnosis. Glabella subrectangular with incurved lateral margin.

Remarks. The cranidium of *Hystricurus* sp. from the Siberian Platform has a waisted glabella which accords well with the diagnosis of this species. The strong similarities of the pygidium assigned to this species by Peng (1984; see Pl. III-84, Fgis. 5-7) with pygidia of a *Lophosaukia* species (Peng, 1992, figs. 24D-24F) suggest that the pygidium

<p align="center">358</p>

may not belong to this species (see above for details).

Genus CHATTERTONELLA n. gen.

Etymology. For Brian Chatterton of University of Alberta.

Type Species. *Hystricurus abruptus* Cullison, 1994; Jeffersonian Stage; Rich Fountain Formation, Missouri.

Diagnosis. Glabella forward-tapering with parallel-sided or slightly convex lateral margin. Anterior facial suture moderately divergent and straight, and then rapidly turns inwards. Anterior cranidial margin weakly pointed. Anterior cranidial border flat and wide, being of equal sagittal length to preglabellar field. Palpebral lobe of moderate-size, moderately arched laterally, and located posterior to mid-cranidial length. Palpebral furrow weakly impressed. Posterior fixigena narrow (exsag.) and transversely short.

Pygidium subelliptical in outline. Axis with four axial rings. Pleural field flat proximally and steeply down-sloping distally. Pleural furrows more discretely impressed than interpleural furrows. Interpleural furrows become more discrete towards pygidal margin and reach pygidial margin. Posterior pleural band reaches pygidial margin as weak ridge.

Comparison with "Hystricurids". The morphologically closest taxon to this new genus is *Hystricurus secundus* (*=Patomaspis*? *secundus* herein) (see Ogienko, 1984, pl. 12, figs. 3, 5, 6). However, *P.*? *secundus* bears two pairs of glabellar furrows, a discretely impressed palpebral furrow, and a narrow and rounded anterior cranidial border, and a more strongly convex palpebral lobe. The pygidia of *Chattertonella* are distinctive from those of "hystricurids" in having ridge-shaped posterior bands reaching the pygidial margin and a well demarcated posterior end of the pygidial axis, and in lacking a fulcral ridge.

Comparison with Ptychopariides. Cranidially, no particular ptychopariid taxa bear resemblance with this new genus. The pointed anterior cranidial border and slightly divergent anterior facial suture suggest affinity to some elviniids (e.g., *Dytremacephalus*, Palmer, 1965, pl. 18, figs. 10, 14) or aphelaspids (e.g., *Aphelaspis*, Palmer, pl. 8, fig. 14). However, the cranidia of these Upper Cambrian taxa have a discrete palpebral furrow, a smaller palpebral lobe, a truncated glabellar front, a deeper anterior cranidial border furrow, a narrower (sag. and exsag.) anterior cranidial border, and a diagonal posterior facial suture.

The pygidia of *Chattertonella* are similar to those of *Glaphyraspis parva*, a lonchocephalid (e.g., see Pratt, 1992, pl. 26, fig. 19) in developing ridge-shaped posterior pleural bands reaching the margin. However, the lonchocephalid pygidia have a much less strongly tapering axis.

Comparison with Proetides. The pygidia of *Proscharyia sinensis*, a Tremadocian scharyiine from South China (Peng, 1990, pl. 19, figs. 9, 11, 13-15), although compressed, resemble those of *Chattertonella*. In particular, the ridge-shaped posterior pleural bands of both taxa reach the pygidial margin. Many species belonging to the Proetidae have their posterior pleural bands extended into the margin (see Owens, 1973; Šnajdr, 1980). In contrast, the cranidia of *P. sinensis* (Peng, 1990, pl. 19, figs. 7, 8, 10, 12) differ from those of *Chattertonella* in having a more pointed anterior margin, a much more strongly forward-tapering glabella, a much more strongly divergent anterior facial suture, two pairs of glabellar furrows, and a sharply terminated posterior fixigena.

359

Taxonomic Conclusion. No particular taxa have a strong enough resemblance with *Chattertonella* to indicate the definite taxonomic affinity of *Chattertonella*.

Chattertonella abrupta (Cullison, 1944)
Pl. III-38, Figs. 1-12, Pl. III-39, Figs. 1-11.

1944 *Hystricurus abruptus* Cullison [part], p. 80, pl. 34, figs. 48, 49 [only].
1951 *Hystricurus*? sp. G Ross, p. 55, pl. 14, figs. 1-3.
1951 *Clelandia utahensis* Ross, [part], p. 117, pl. 29, figs. 4, 6, 7.
1953 *Clelandia utahensis*, Hintze, [part], p. 147, pl. 4, figs. 15a, 15b.

Holotype. USNM (no number was designated), pygidium; Cullison, 1944, pl. 34, figs. 48, 49; Jeffersonian Stage; Rich Fountain Formation, Missouri.

Neotype. UA 12320, cranidium; Pl. III-38, Figs. 2, 5, 6; *Symphysurina* Zone; Fillmore Formation, Utah.

Diagnosis. Same as generic diagnosis.

Association of Pygidium. It is the stratigraphic co-occurrence that allows for associating the pygidia with this species. From the sampling horizons, R5-34.1, SE-82, SE-87.5, and E-4 (Figs. I-5, I-8) where cranidial materials of this species were recovered, the pygidia co-occur with the cranidial materials. These pygidia were assigned to *Clelandia utahensis* (Ross, 1951, pl. 29, figs. 4, 6, 7; Hintze, 1953, pl. 4, figs. 15). However, the discovery of an articulated meraspid specimen (Pl. III-38, Figs. 13, 14, Pl. III-39, Figs. 13-17) reveals that *Clelandia* has a pygidium with short and stout marginal spines that are directed inwards.

?Family **KINGSTONIDAE** Kobayashi, 1935
Genus **CLELANDIA** Cossman, 1902

Type Species. *Harrisia parabola* Cleland, 1900; Tribes Hill Formation, New York.

Clelandia albertensis Norford, 1969
Pl. III-39, Figs. 17-19

1969 *Clelandia albertensis* Norford, p. 8-10, pl. 1, figs. 15-18, 22-40

Holotype. GSC 23617, cranidium; *Symphysurina-Euloma* Zone; Survey Peak Formation, Alberta.

Remarks. Pygidium of this species is nearly indistinguishable from that of *Clelandia* sp. aff. *Clelandia utahensis* (Pl. III-39, Fig. 12) from Zone B of Garden City Formation.

Clelandia sp. aff. *Clelandia utahensis* Ross, 1951
Pl. III-38, Figs. 13, 14, Pl. III-39, Figs. 12-17

Remarks. An articulated meraspid specimen from SL6F has six thoracic segments. The pygidium has marginal spines that are short and directed inwards. Although occurring from a stratigraphically much lower horizon, a pygidium (Pl. III-39, Fig. 12) from R5-34.1 of the *Symphysurina* Zone where many cranidia of *Clelandia utahensis* (Ross, 1951; Hintze, 1953; Norford, 1969) occur is morphologically indistinguishable from that of the meraspis. The cranidium of the meraspis differs from those figured by Ross (1951, pl. 29, figs. 1-3) and Hintze (1953, pl. 4, fig. 17) in having a stouter occipital spine. Although this difference can be readily considered to be ontogenetic, the existing stratigraphic gap

360

makes the assignment of these specimens to *C. utahensis* less definite.

Order **AGNOSTIDA** Salter, 1864
Family **PTYCHAGNOSTIDAE** Kobayashi, 1939
Genus **PTYCHAGNOSTUS** Jaekel, 1909
Ptychagnostus aculeatus (Rusconi, 1951)
1951 *Hystricurus? corralensis* Rusconi, p. 17, fig. 27.
Remarks. Tortello and Bordonaro (1997) re-examined the specimen that was identified as cranidium of *Hystricurus? corralensis* from Argentina by Rusconi (1951). They concluded that the specimen is a pygidium of the agnostid *Ptychagnostus aculeatus*.

Order **CORYNEXOCHIDA** Kobayashi, 1935
Family **LEIOSTEGIIDAE** Bradley, 1925
Genus **ANNAMITELLA** Mansuy, 1920
Annamitella rectangularia (Endo, 1935)
1935 *Hystricurus granosus* Endo [part], p. 218, pl. 13, figs. 16-20, [only].
Remarks. Zhou and Fortey (1986) transferred the specimens of *Hystricurus granosus* to *Annamitella*, which is accepted herein.

Genus **LEIOSTEGIUM** Raymond, 1913b
***Leiostegium convexium*** (Endo, 1935)
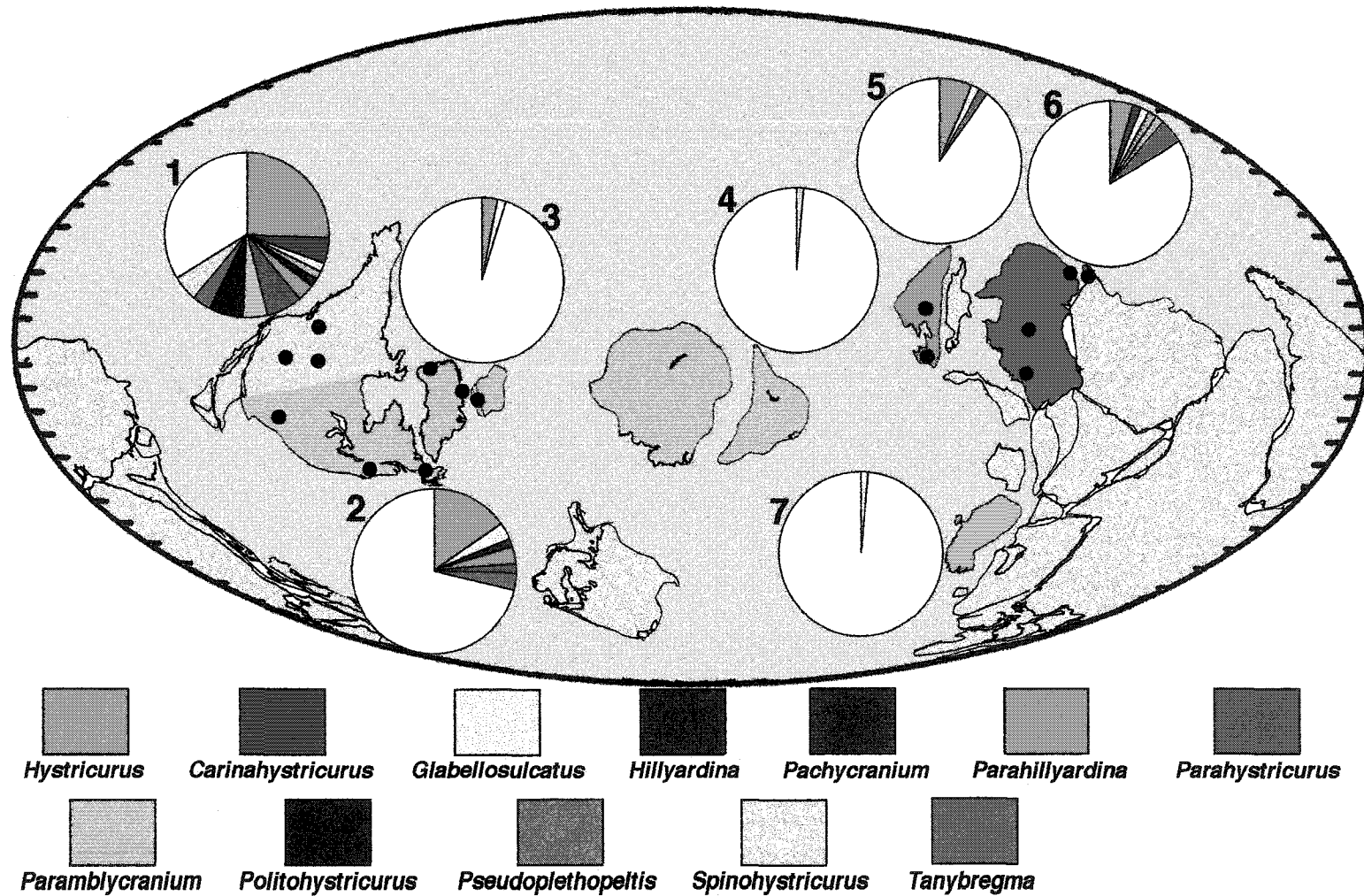1935 *Hystricurus convexus* Endo, p. 217-218, pl. 15, figs. 6-8.
Remarks. The cranidium re-illustrated in Lu *et al.* (1965, pl. 34, fig. 7) shows no preglabellar field and a truncated glabellar front and a straight-sided glabella which is well in agreement with the features of *Leiostegium* cranidia (e.g., see Berg and Ross, 1959, pl. 21, figs. 1, 6, 10).

361
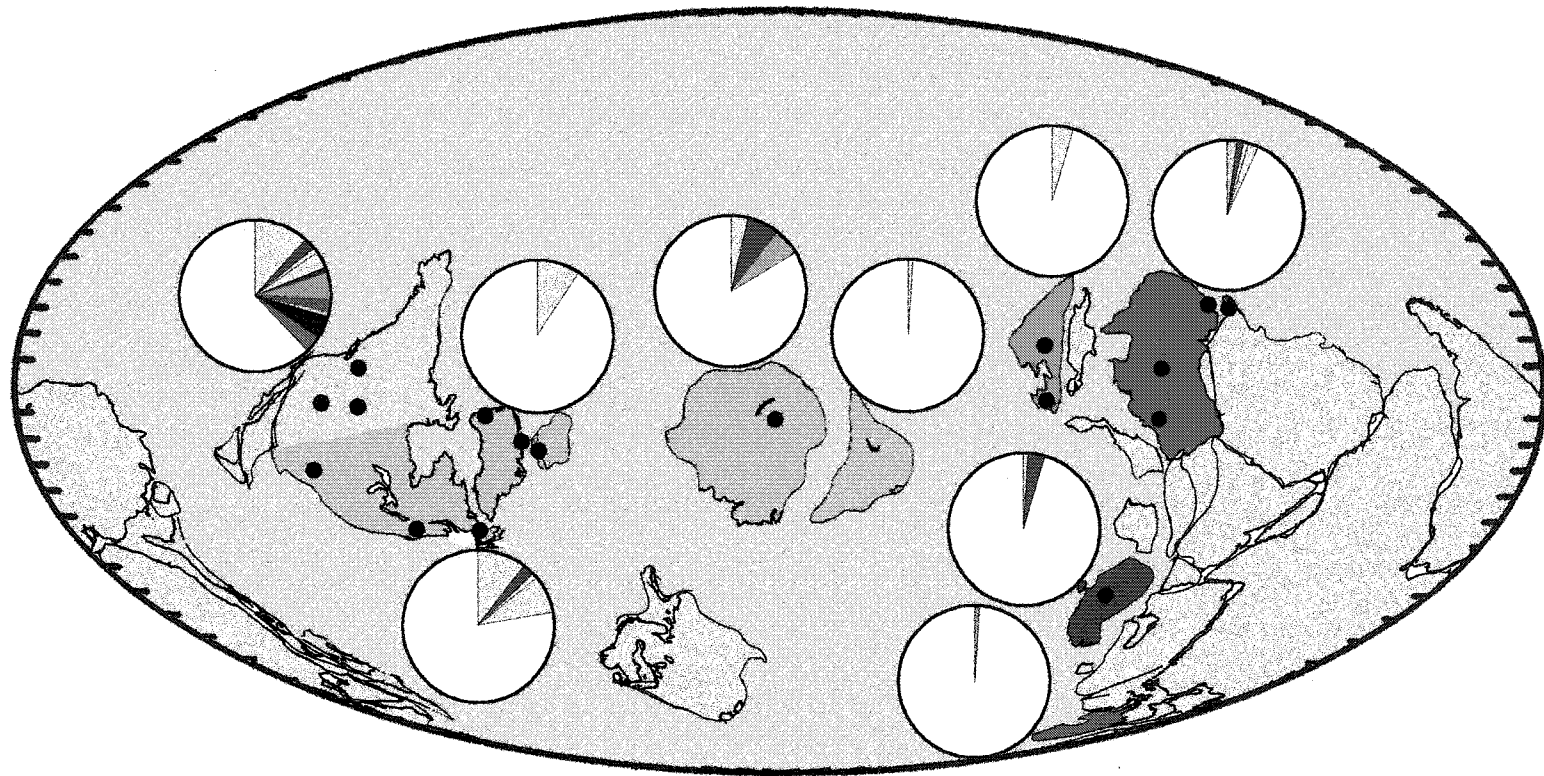
TEXT-FIGURE III-1. Paleogeographic distribution of 89 formally named species of 18 genera that have been referred to the Hystricuridae before this taxonomic revision. 35 species were referred to *Hystricurus* and 35 species had their pygidia associated. Different tones in each pie diagram represent different genera. Each dot indicates the major locality from which the "hystricurid" species were documented. See Text-fig. III-2 for detailed information on the localities in the Laurentia.
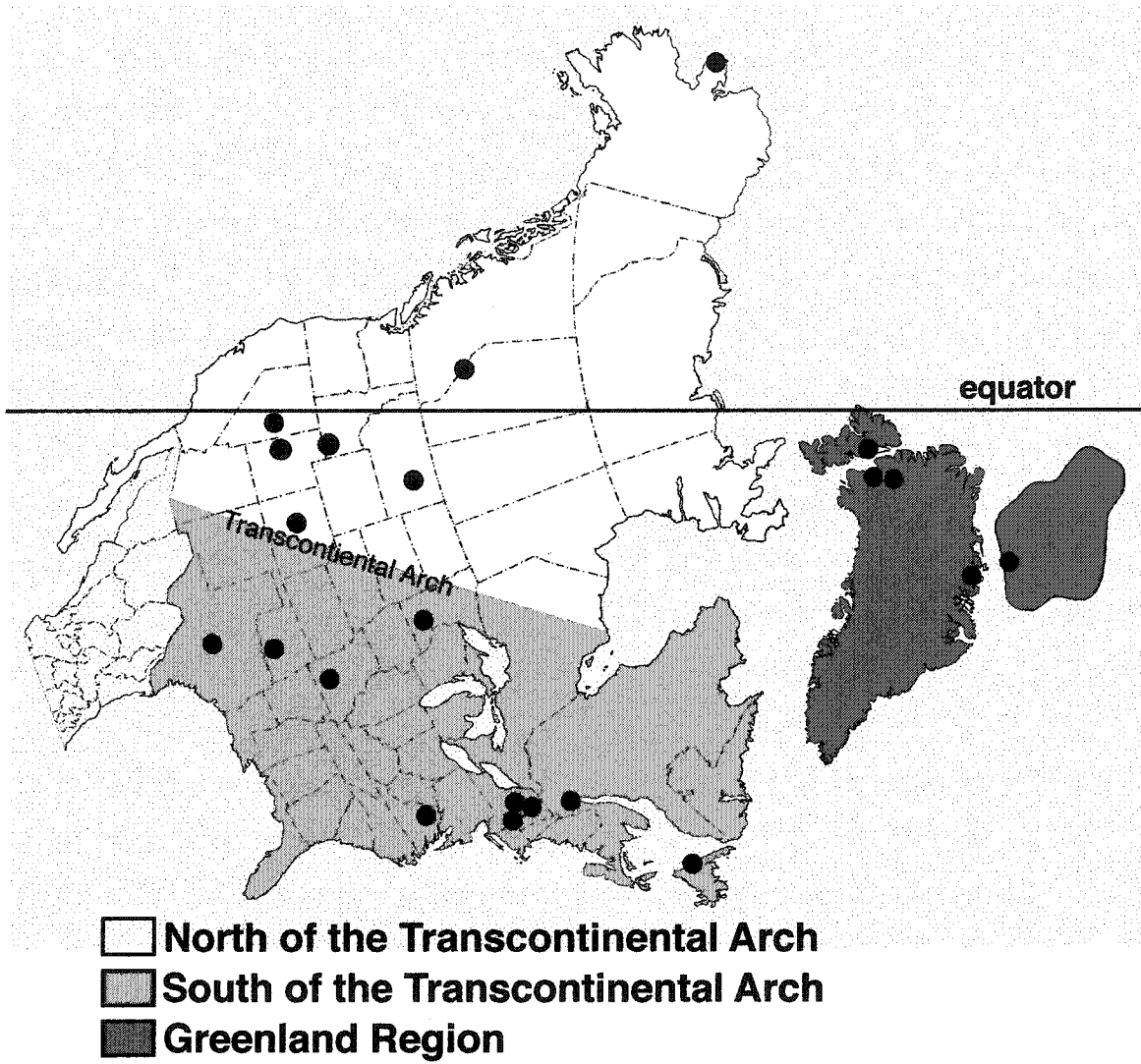
TEXT-FIGURE III-2. Paleogeographic distribution of localities (represented by dot) where the "hystricurids" were documented in Laurentia.

363

Hystricurus   Carinahystricurus   Glabellosulcatus   Hillyardina   Pachycranium   Parahillyardina   Parahystricurus

Paramblycranium   Politohystricurus   Pseudoplethopeltis   Spinohystricurus   Tanybregma

TEXT-FIGURE III-3. Paleogeographic distribution of 59 formally named species of 12 genera of the Hystricuridae. 44 species are endemic and 31 species have their pygidia associated. Paleo-continent configuration is adapted from Scotese and McKerrow (1991, fig. 2). 1. North of Transcontinental Arch, 2. South of Transcontinental Arch, 3. Greenland region, 4. Kazakhstan, 5. Sino-Korean Platform, 6. Australia, 7. South China.
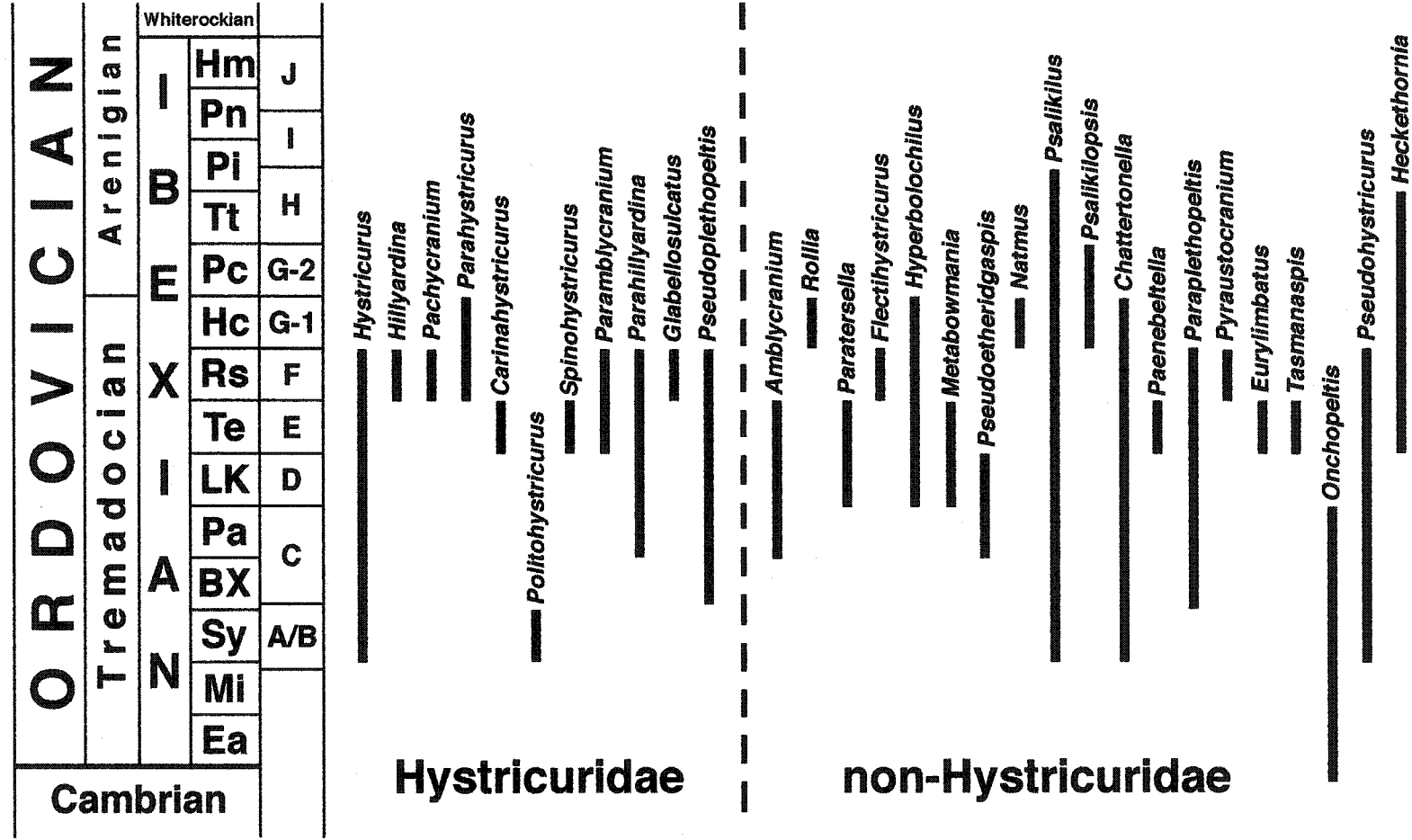
TEXT-FIGURE III-4. Compiled stratigraphic range of the Laurentian genera that are included in the Hystricuridae and those that are excluded from the Hystricuridae. Trilobite zonation of the Ibexian Series follows Ross *et al.* (1997, fig. 10). Acrony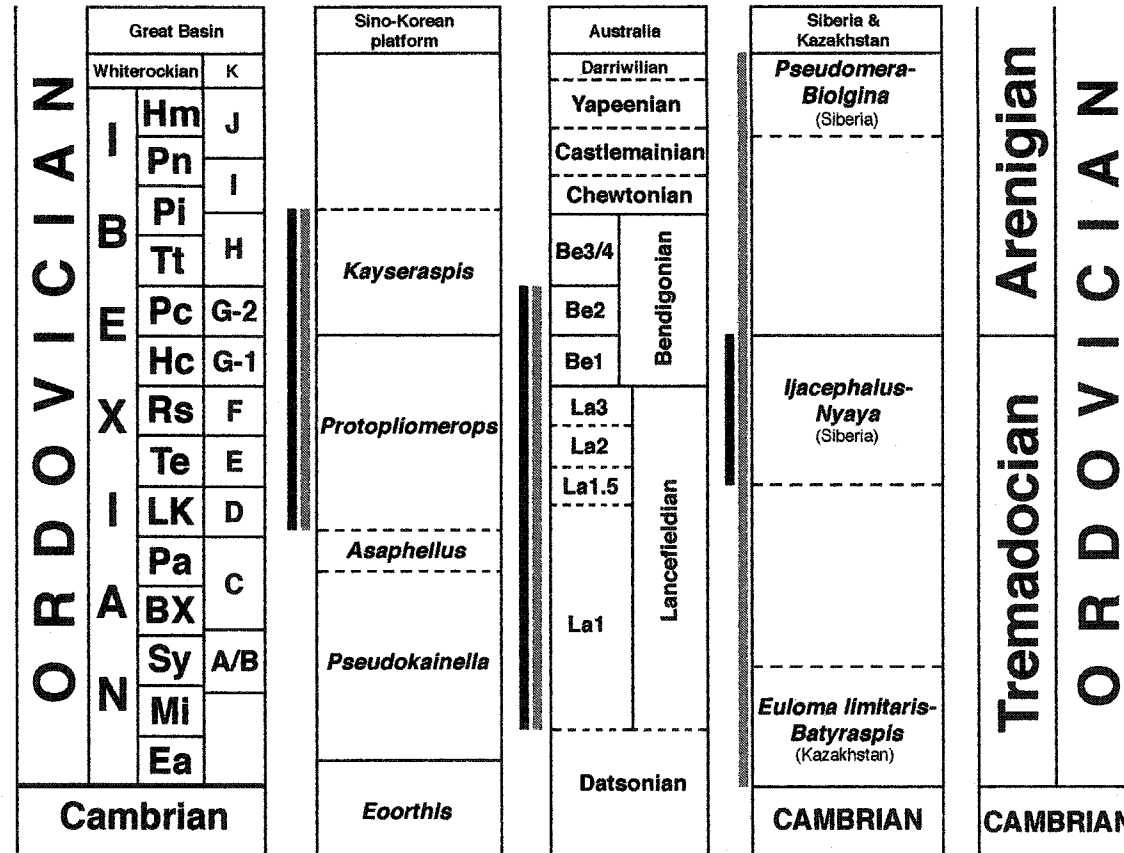ms of the zones are Ea (*Eurekia apopsis*), Mi (*Missisquoia*), Sy (*Symphysurina*) BX (*Bellefontia-Xenostegium*), Pa (*Paraplethopeltis*), LK (*Leiostegium-Kainella*), Te (*Tesselacauda*), Rs (*Rossaspis superciliosa*), Hc (*Hintzeia celsaora*), Pc (*Protopliomerella contracta*), Tt (*Trigonocerca typica*), Pi (*Prebynileus ibexensis*), Pn (*Pseudocybele nasuta*), and Hm (*Hesperonomiella minor*).

ORDOVICIAN		Great Basin		'Canadian' Series	western Newfoundland	Missouri		Northwest Greenland	Ellesmere Island	East Greenland
		Whiterockian	K							Narwhale Sound
	I B E X I A N	Hm	J	Cassinian		Powell		Cape Webster	Bay Fjord	
		Pn	I							
		Pi			Benthamaspis gibberula					
		Tt	H			Cotter				
		Pc	G-2	Jeffersonian	Striglgenalis caudata			Nunatami	Eleanor River	Cape Weber
		Hc	G-1		Striglgenalis brevicaudata	Theodosia	Jefferson City	Canyon Elv		
					hiatus	Rich Fountain		Nygaard Bay		
		Rs	F		Randaynia saudersi			Poulsen Cliff	Baumann Fjord	
		Te	E	Demingian	Leiostegium proprium	Roubidoux				
					Hystricurus ocullunatue					
		LK	D		hiatus			Christian Elv		
		Pa	C		Parahystricurus sp. I			Cape Clay	Copes Bay	
		BX			Hystricurus ellipticus	Gasconade				Antiklinbugt
		Sy	A/B	Gasconadian	Hystricurus millardensis			Cass Fjord		
		Mi			Missisquoia typicalis					Dolomite point
		Ea						Telt Bugt	Parrish Glacier	Hyolithus Creek
	Cambrian									

TEXT-FIGURE III-5. Biostratigraphic and lithostratigraphic correlation of Great Basin, western Newfoundland, Missouri, and Greenland region. Trilobite biostratigraphic scheme of western Newfoundland and its correlation is adapted from Boyce (1997) and Boyce and Stouge (1997, fig. 4). Lithostratigraphic scheme of Missouri and its correlation is based on Heller (1954, pl. 2) and Boyce (1989, fig. 8). Lithostratigraphic schemes of Greenland region and their correlation are based on Frykman (1979), Peel and Christie (1982), and Fortey and Peel (1989). Black vertical bar represents stratigraphic range of the Hystricuridae and grey vertical bar represents that of the "hystricurids." Dotted horizontal lines indicate that correlation of the boundary between biozones and formations into the Ibexian zonation is tentative.

Great Basin — Whiterockian | K

O R D O V I C I A N	I B E X I A N		
	Hm	J
	Pn	I
	Pi	
	Tt	H
	Pc	G-2
	Hc	G-1
	Rs	F
	Te	E
	LK	D
	Pa	C
	BX	
	Sy	A/B
	Mi	
	Ea	

Cambrian

Sino-Korean platform

Kayseraspis

Protopliomerops

Asaphellus

Pseudokainella

Eoorthis

Australia

Darriwilian
Yapeenian
Castlemainian
Chewtonian

Be3/4 — Bendigonian
Be2
Be1
La3 — Lancefieldian
La2
La1.5
La1

Datsonian

Siberia & Kazakhstan

Pseudomera-Biolgina (Siberia)

Ijacephalus-Nyaya (Siberia)

Euloma limitaris-Batyraspis (Kazakhstan)

CAMBRIAN

Arenigian

Tremadocian

O R D O V I C I A N

CAMBRIAN

TEXT-FIGURE III-6. Biostratigraphic and lithostratigraphic correlation of Great Basin, Australia, Sino-Korean Platform, Siberia and Kazakhstan. Biostratigraphic scheme of Australia and its correlation is compiled from Shergold (1991, fig. 4), Webby *et al.* (1991, table 1, 2), and Laurie and Shergold (1996, text-fig. 6). Trilobite biostratigraphic scheme of Sino-Korean Platform and its correlation is adapted from Kim and Choi (1997, fig. 4). Trilobite biostratigraphic scheme of Siberia and Kazakhstan is compiled from Apollonov *et al.* (1988, fig. 2) and Ogienko (1992, fig. 2). Black vertical bar represents stratigraphic range of the Hystricuridae and grey vertical bar represents that of the "hystricurids." Dotted horizontal lines indicate that correlation of the boundary between biozones and formations into the Ibexian zonation is tentative.
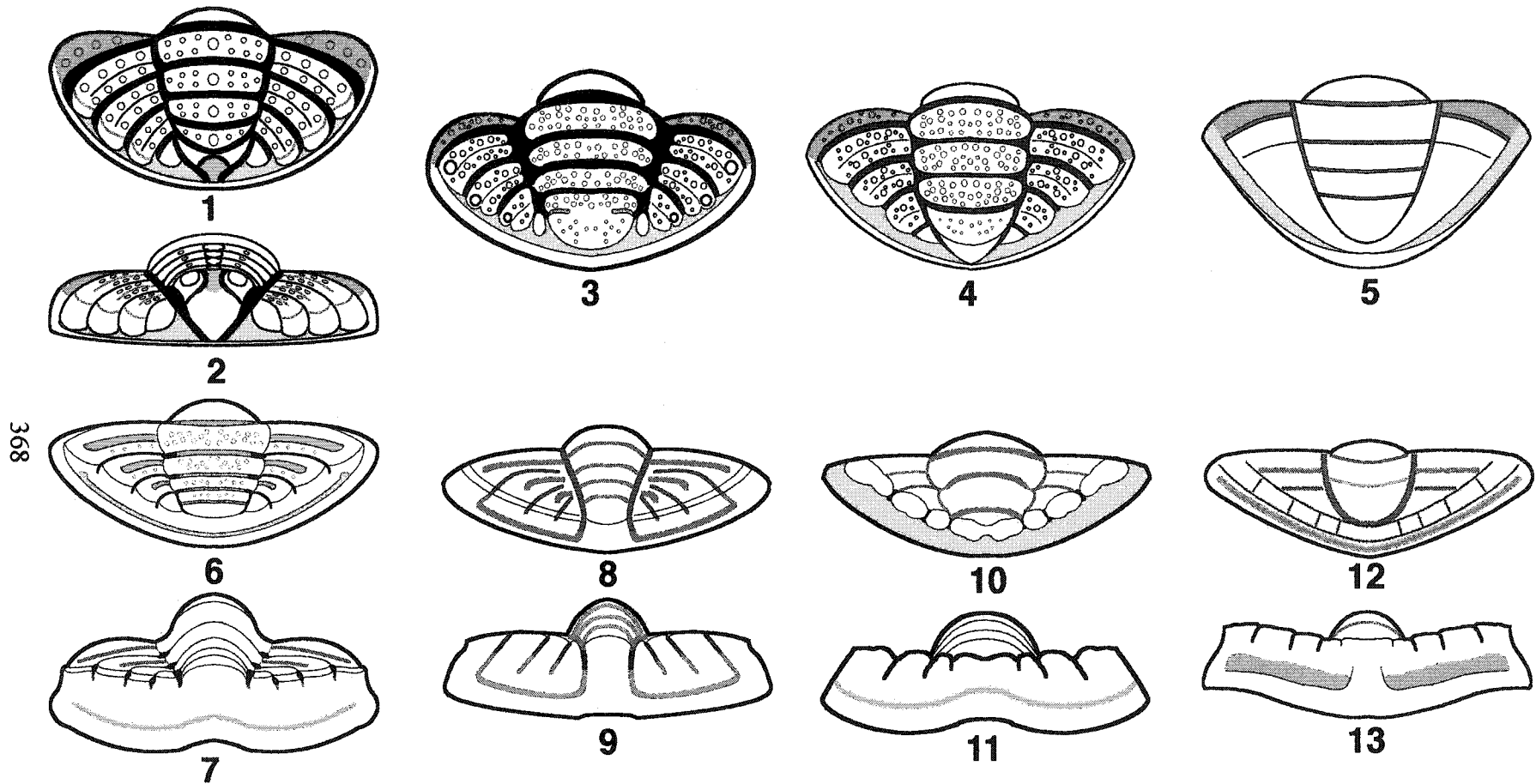
TEXT-FIGURE III-07. Pygidial morphologies of the Hystricuridae. 1, 2. *Hystricurus* (*Hystricurus*), 1. Dorsal view, 2. Posterior view. 3. Dorsal view of *Hystricurus* (*Butuberculatus*). 4. Dorsal view of *Hystricurus* (*Aequituberculatus*). 5. Dorsal view of *Hystricurus* (*Triangulocaudatus*). 6, 7. *Spinohystricurus*, 6. Dorsal view, 7. Posterior view. 8, 9. *Parahillyardina*, 8. Dorsal view, 9. Posterior view. 10, 11. *Hillyardina*, 10. Dorsal view, 11. Posterior view. 12, 13. *Carinahystricurus*, 12. Dorsal view, 13. Posterior view.

PLATE III-1. *Hystricurus (Hystricurus) conicus* (Billings, 1859), *Hystricurus?* n. sp. aff. *H. (H.) conicus* and *Hystricurus (Hystricurus) oculilunatus* Ross, 1951.

1-4. *Hystricurus (Hystricurus) conicus* (Billings, 1859)
   1-4. GSC 516, holotype, cranidium, from Beekmantwon Group (Lower Ordovician), near Beauharnois, Quebec, x 5; 1. Dorsal view, 2. Left lateral view, 3. Right lateral view, 4. Anterior view. All figures are taken with light photography.

5-7. *Hystricurus?* n. sp. aff. *H. (H.) conicus*
   5-7. UCGM 41558, cranidium, from Deadwood Formation (Lower Ordovician), Wyoming, x 5; 5. Dorsal view (light photography), 6. Left lateral view, 7. Anterior view.

8-11. *Hystricurus (Hystricurus) oculilunatus* Ross, 1951
   8-11. YPM 17960, cranidium, from *Rossaspis superciliosa* Zone, Garden City Formation, southern Idaho, x 10; 8. Dorsal view (right posterior fixigena was inadvertently broken), 9. Anterior view, 10. Ventral view, 11. Left lateral view.
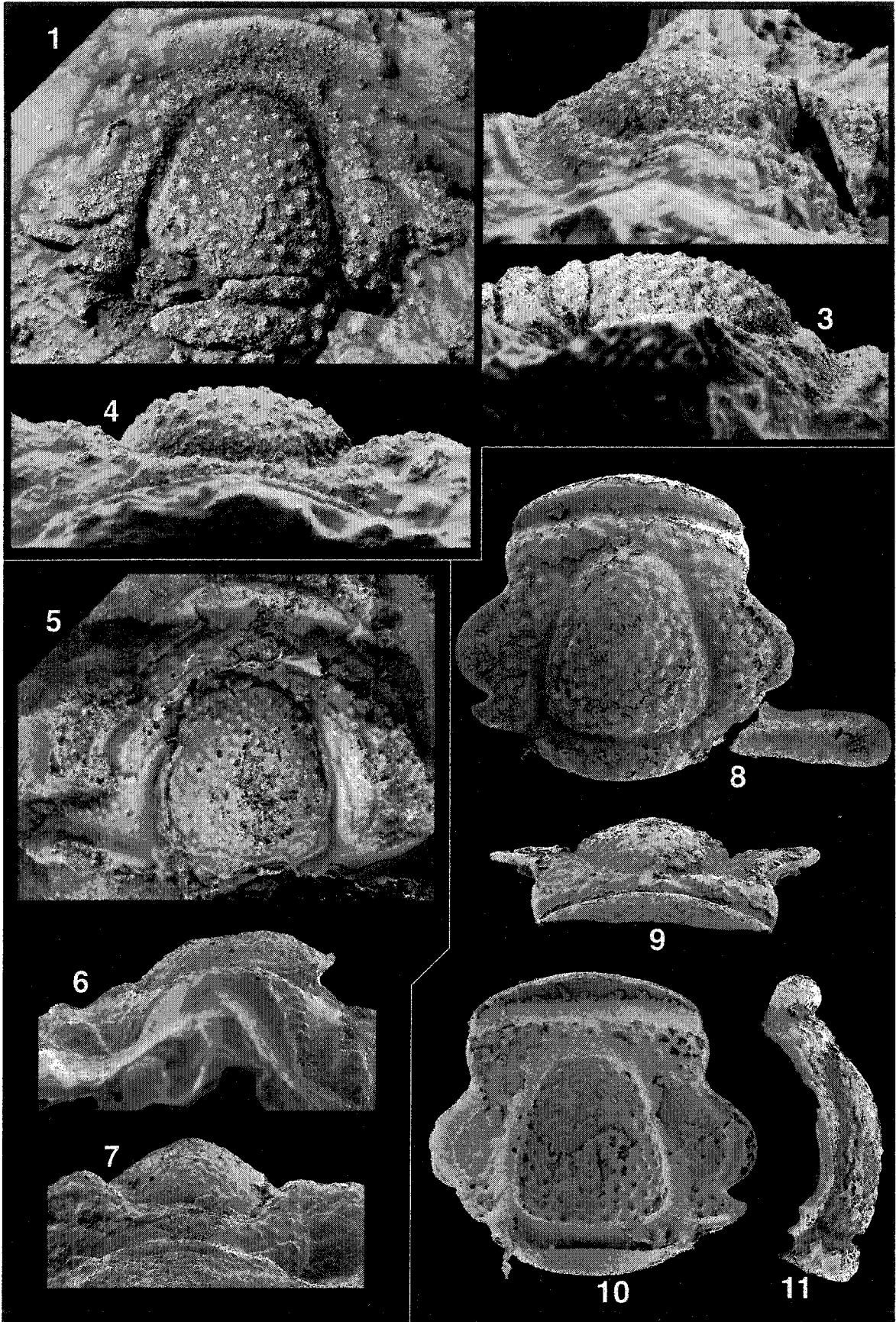
370

PLATE III-2. *Hystricurus? armatus* (Poulsen 1937), *Hystricurus? longicephalus* (Poulsen 1927) and *Hystricurus? sulcatus* (Poulsen 1927).

1-6. *Hystricurus? armatus* (Poulsen 1937). All specimens are from probably *Symphysurina* Zone of Antiklinalbugt Formation, East Greenland.
   1, 2, 5. MGUH 3641, holotype, cast of cranidium, x 7; 1. Dorsal view, 2. Left lateral view, 5. Anterior view.
   3, 4, 6. MGUH 3645, cast of pygidium, x 7; 3. Left lateral view, 4. Posterior view, 6. Dorsal view.
7-9. *Hystricurus? longicephalus* (Poulsen 1927). All specimens are from possibly *Symphysurina* Zone of Cass Fjord Formation, Northwest Greenland.
   7, 8. MGUH 2344a, cast of pygidium, x 5; 7. Left lateral view, 8. Dorsal view.
   9. MGUH 2344b, holotype, cast of cranidium, dorsal view, x 4.
10-12. *Hystricurus? sulcatus* (Poulsen 1927). All specimens are from probably *Symphysurina* Zone of Antiklinalbugt Formation, East Greenland.
   10-12. MGUH 3638, holotype, cast of cranidium, x 7; 10. Dorsal view, 11. Right lateral view, 12. Anterior view.

372
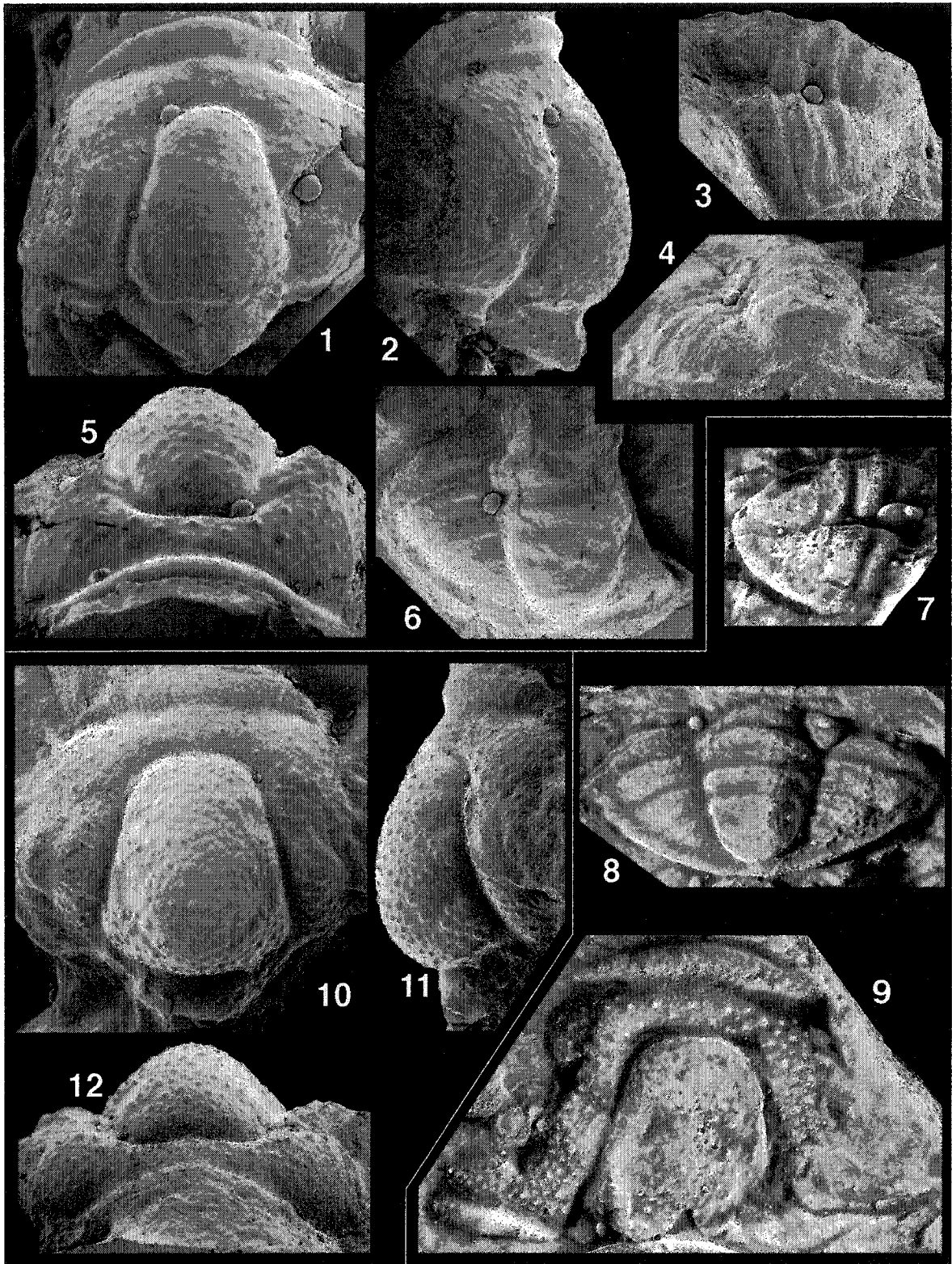
PLATE III-3. *Hystricurus (Butuberculatus) scrofulosus* Fortey and Peel, 1989, *Hystricurus? parascrofulosus* n. sp. and *Hystricurus (Aequituberculatus) ellipticus* (Cleland, 1900).

1-8. *Hystricurus (Butuberculatus) scrofulosus* Fortey and Peel, 1989. All specimens are from possibly *Tesselacauda* Zone of Christian Elv Formation, western North Greenland.

    1, 2, 4. MGUH 18.993, holotype, cast of pygidium, x 10; 1. Dorsal view, 2. Right lateral view, 3. Posterior view.

    3, 8. MGUH 18.989, cast of free cheek, x 10; 3. Dorsal view, 8. Anterior view.

    5-7. MGUH 18.990, cast of cranidium, x 5; 5. Anterior view, 6. Dorsal view, 7. Left lateral view.

9-14. *Hystricurus? parascrofulosus* n. sp. All specimens are from possibly *Tesselacauda* Zone of Christian Elv Formation, western North Greenland.

    9-11. MGUH 18.998, holotype, cast of cranidium, x 5; 9. Dorsal view, 10. Right lateral view, 11. Anterior view.

    12-14. MGUH 19.001, cast of pygidium, x 7; 12. Dorsal view, 13. Posterior view, 14. Right lateral view.

15-17. *Hystricurus (Aequituberculatus) ellipticus* (Cleland, 1900). The specimen is from *Symphysurina* Zone of Tribes Hill Formation, New York State.

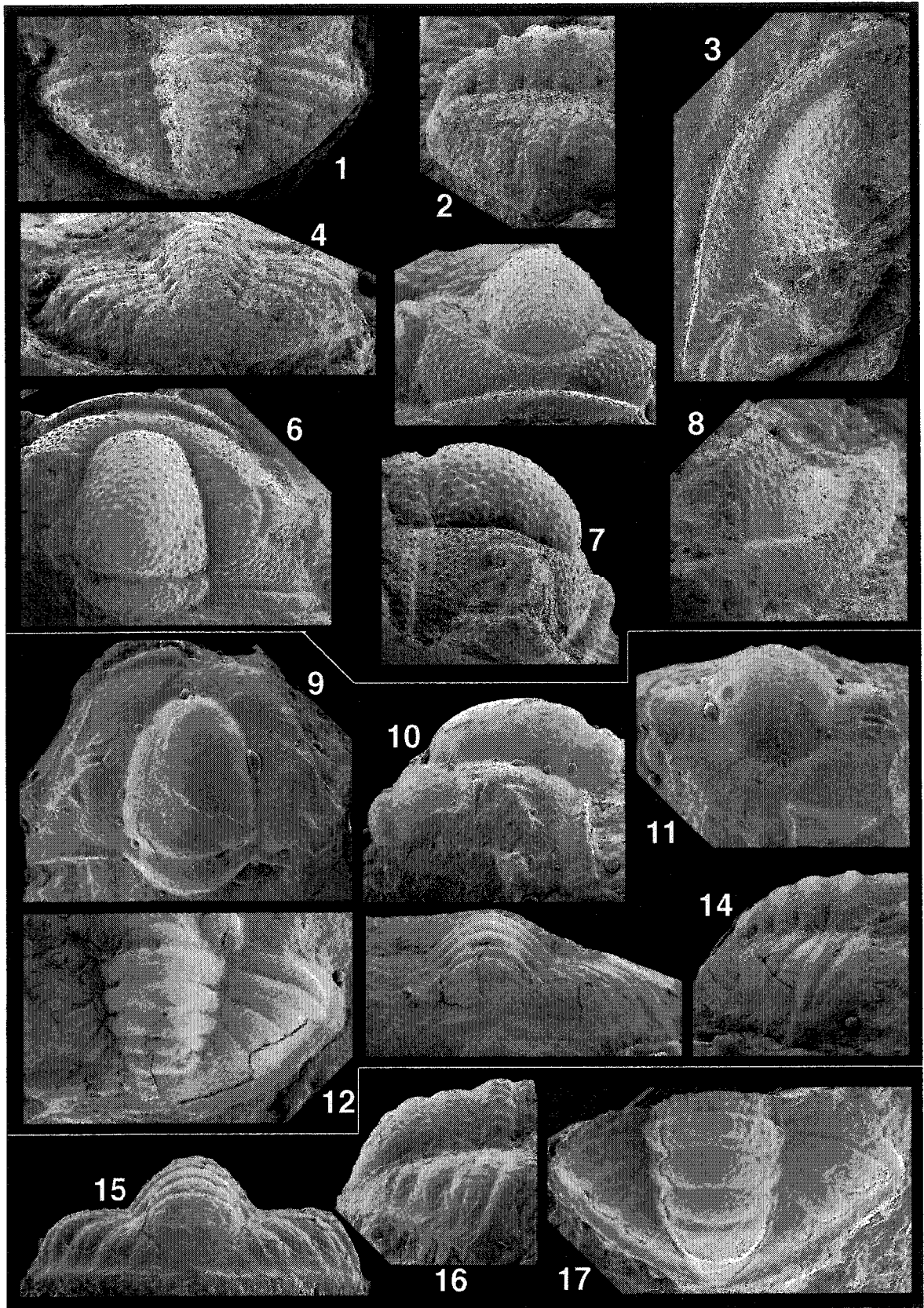   15-17. NYSM 15228, cast of pygidium, x 7; 15. Posterior view, 16. Right lateral view, 17. Dorsal view.

374

PLATE III-4. *Hystricurus*? *clavus* Kobayashi, 1960, *Hystricurus*? *penchiensis* Lu, *in* Lu *et al.*, 1976 and *Hystricurus rotundus* (Ross, 1951).

1-5, 7. *Hystricurus*? *clavus* Kobayashi, 1960. Specimens, NI 80386 and NI 80388, are from *Protopliomerops* Zone of Upper Yehli Formation, northeast China.

    1, 4, 5. NI 80386, holotype, cast of cranidium, x 5; 1. Dorsal view (light photography), 4. Anterior view, 5. Right lateral view.

    2, 3. NI 80388, cast of pygidium, x 10; 2. Dorsal view (light photography), 3. Posterior view.

    7. BK56-5, cranidium, from Sambangsan Formation, South Korea, dorsal view, x 10.

6. *Hystricurus*? *penchiensis* Lu, *in* Lu *et al.*, 1976

    6. BK 55-3, cranidium, from *Protopliomerops* Zone of Sambangsan Formation, South Korea, dorsal view, x 8.

8-10. *Hystricurus rotundus* (Ross, 1951)

    8-10. Y.P.M. 18305, holotype, cast of cranidium from *Symphysurina* Zone of Garden City Formation, southern Idaho, x 20; 8. Dorsal view, 9. Left lateral view, 10. Anterior view.
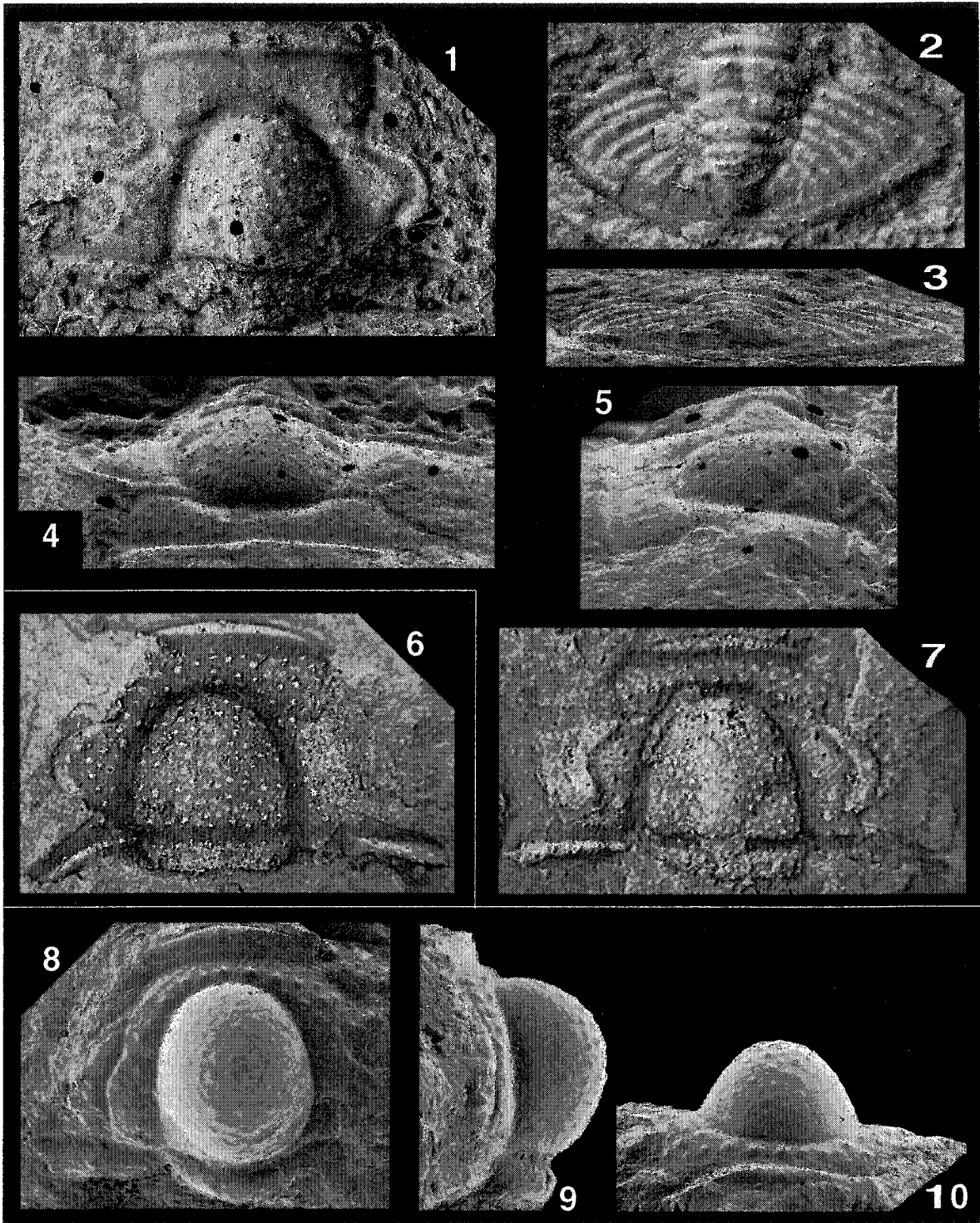
376

PLATE III-5. *Hystricurus (Aequituberculatus) genalatus* Ross, 1951.

1-13. *Hystricurus (Aequituberculatus) genalatus* Ross, 1951.
    1, 2, 4, 6. UA 11838, cranidium, from R5-34.1, x 20; 1. Dorsal view, 2. Left lateral
        view, 4. Anterior view, 6. Ventral view.
    3. UA 11840, cranidium, from R6-15, dorsal view, x 20.
    5. UA 11841, cranidium, from R6-15, dorsal view, x 20.
    7. UA 11844, cranidium, from R5-34.1, dorsal view, x 10.
    8. UA 11845, cranidium, from R5-34.1, dorsal view, x 20.
    9, 10, 12. UA 11846, free cheek, from R5-34.1, x 20; 9. Dorsal view, 10. Oblique
        dorsal view, 12. Right lateral view.
    11. UA 11855, cranidium, from R5-34.1, dorsal view, x 10.
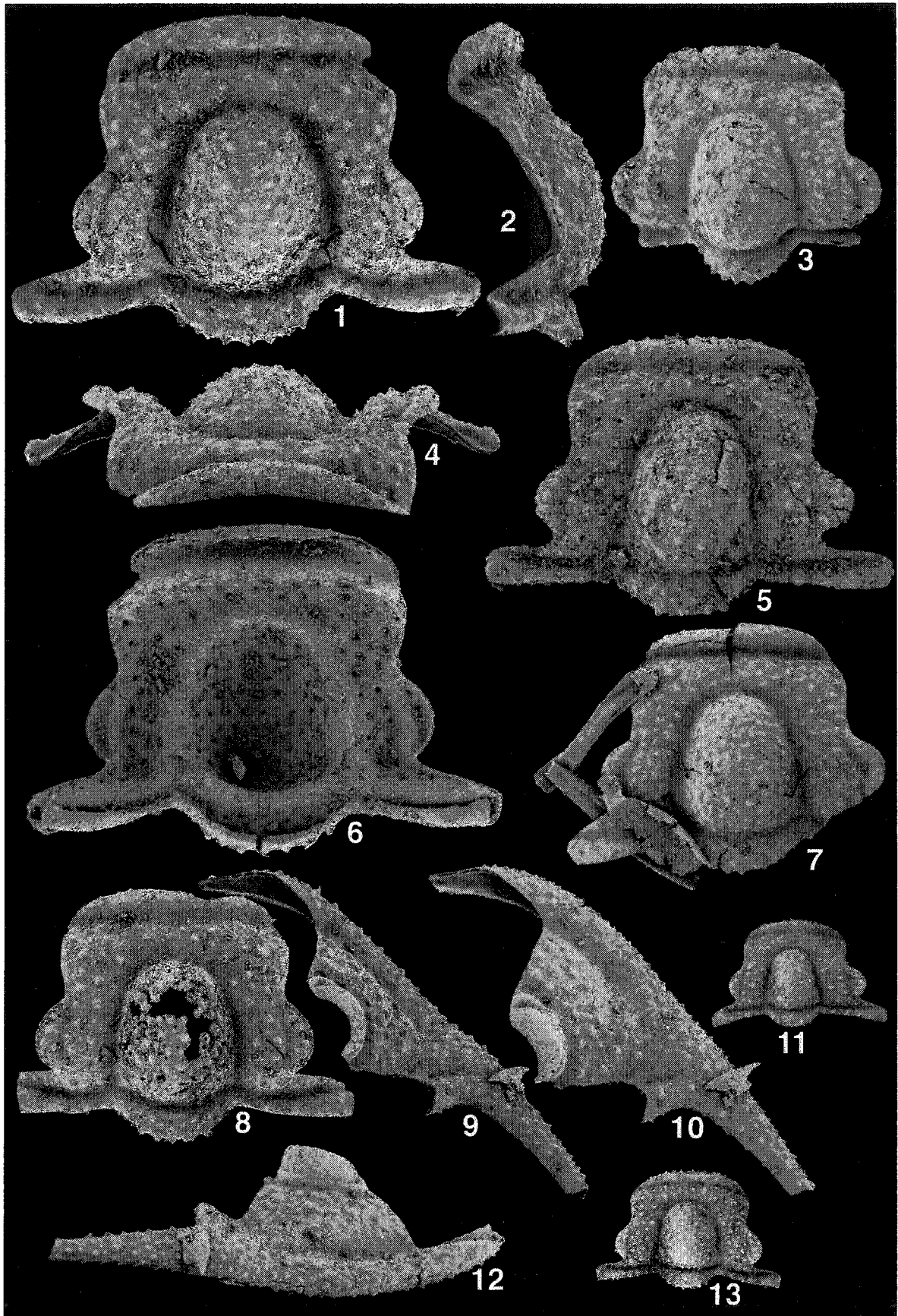   13. UA 11842, cranidium, from R5-34.1, dorsal view, x 10.

378

PLATE III-6. *Hystricurus* (*Aequituberculatus*) *genalatus* Ross, 1951 and *Hystricurus* (*Aequituberculatus*) *minutuberculatus* n. sp.

1-9. *Hystricurus* (*Aequituberculatus*) *genalatus* Ross, 1951.

    1, 2, 4. UA 11839, pygidium, from R5-34.1, x 20; 1. Dorsal view, 2. Left lateral view, 4. Posterior view.

    3, 5, 7. UA 11858, pygidium, from R5-34.1, x 20; 3. Dorsal view, 5. Ventral view, 7. Posterior view.

    6. UA 11859, pygidium, from R5-34.1, dorsal view, x 20.

    8, 9. UA 11843, pygidium, from R5-34.1, x 20; 8. Dorsal view, 9. Posterior view.

10-20. *Hystricurus* (*Aequituberculatus*) *minutuberculatus* n. sp.

    10, 11, 14, 18. UA 11863, holotype, cranidium, from E-4, x 10; 10. Dorsal view, 11. Right lateral view, 14. Ventral view, 18. Anterior view.

    12, 13, 15. UA 11869, cranidium, from E-4, x 10; 12. Dorsal view, 13. Left lateral view, 15. Anterior view.

    16. UA 11870, cranidium, from E-2, dorsal view, x 10.

    17, 20. UA 11871, cranidium, from E-4, x 10; 17. Ventral view, 20. Dorsal view.

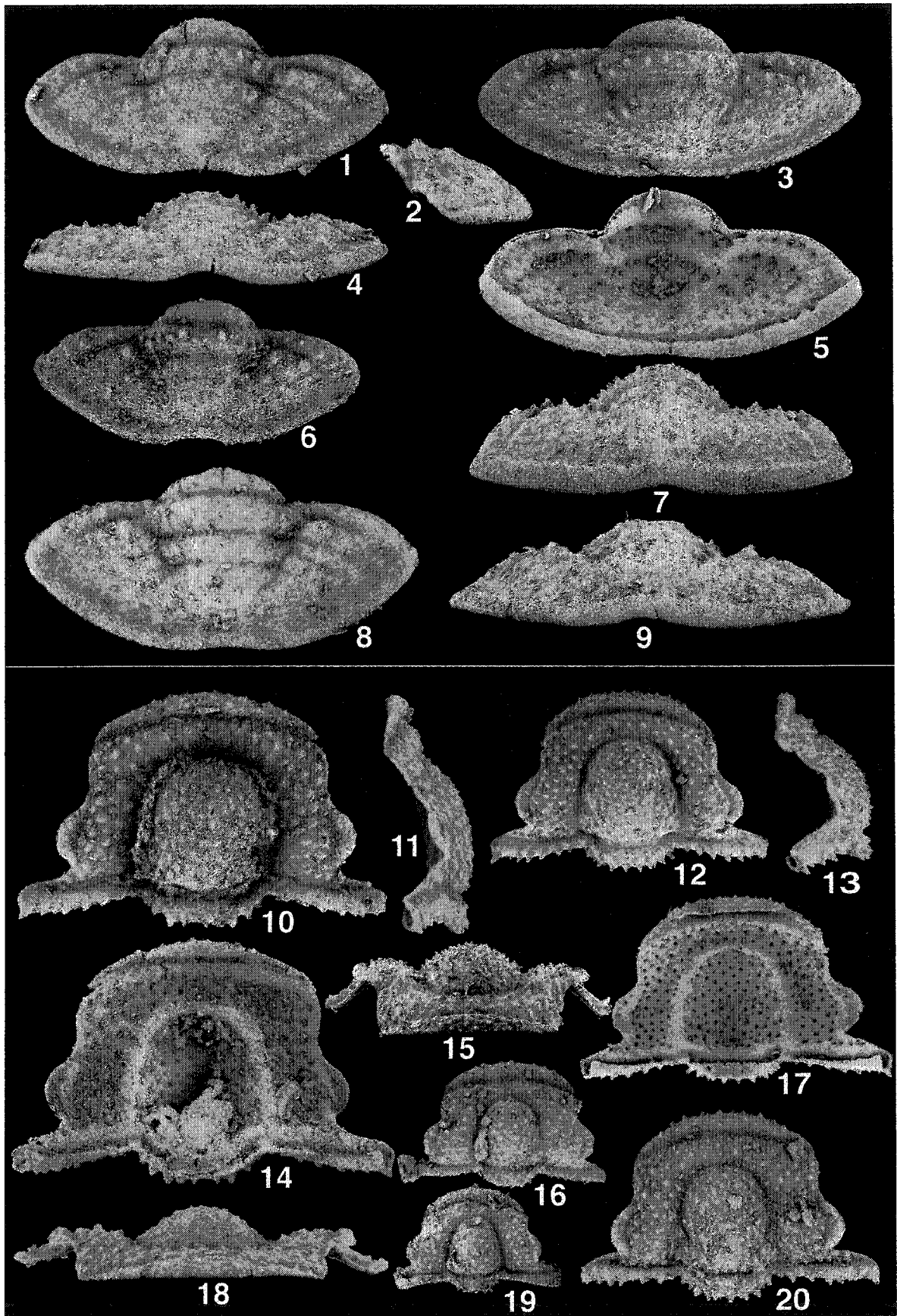   19. UA 11872, cranidium, from E-2, dorsal view, x 10.

380

PLATE III-7. *Hystricurus (Aequituberculatus) minutuberculatus* n. sp., *Hystricurus (Aequituberculatus)* n. sp. A aff. *H. (A.) minutuberculatus* and *Hystricurus (Aequituberculatus)* n. sp. B aff. *H. (A.) minutuberculatus.*

1, 2, 7, 10-21. *Hystricurus (Aequituberculatus) minutuberculatus* n. sp.
  1. UA 11877, cranidium, from E-3, dorsal view, x 10.
  2. UA 11880, free cheek, from E-3, dorsal view, x 10.
  7. UA 11881, cranidium, from E-2, dorsal view, x 10.
  10, 11. UA 11882, cranidium, from SE-82T, x 10; 10. Dorsal view, 11. Anterior view.
  12. UA 11884, pygidium, from E-4, dorsal view, x 10.
  13, 14. UA 11885, pygidium, from E-2, x 15; 13. Dorsal view, 14. Posterior view.
  15-18. UA 11886, pygidium, from E-2, x 15; 15. Dorsal view, 16. Left lateral view, 17. Posterior view, 18. Ventral view.
  19. UA 11887, pygidium, from SE-82T, dorsal view, x 15.
  20. UA 11888, pygidium, from E-3, dorsal view, x 15.
  21. UA 11889, pygidium, from E-4, dorsal view, x 15.
3-6. *Hystricurus (Aequituberculatus)* n. sp. A aff. *H. (A.) minutuberculatus*
  3. UA 11890, free cheek, from E-2, dorsal view, x 10.
  4-6. UA 11891, cranidium, from E-2, x 10; 4. Dorsal view, 5. Left lateral view, 6. Anterior view.
8, 9. *Hystricurus (Aequituberculatus)* n. sp. B aff. *H. (A.) minutuberculatus*
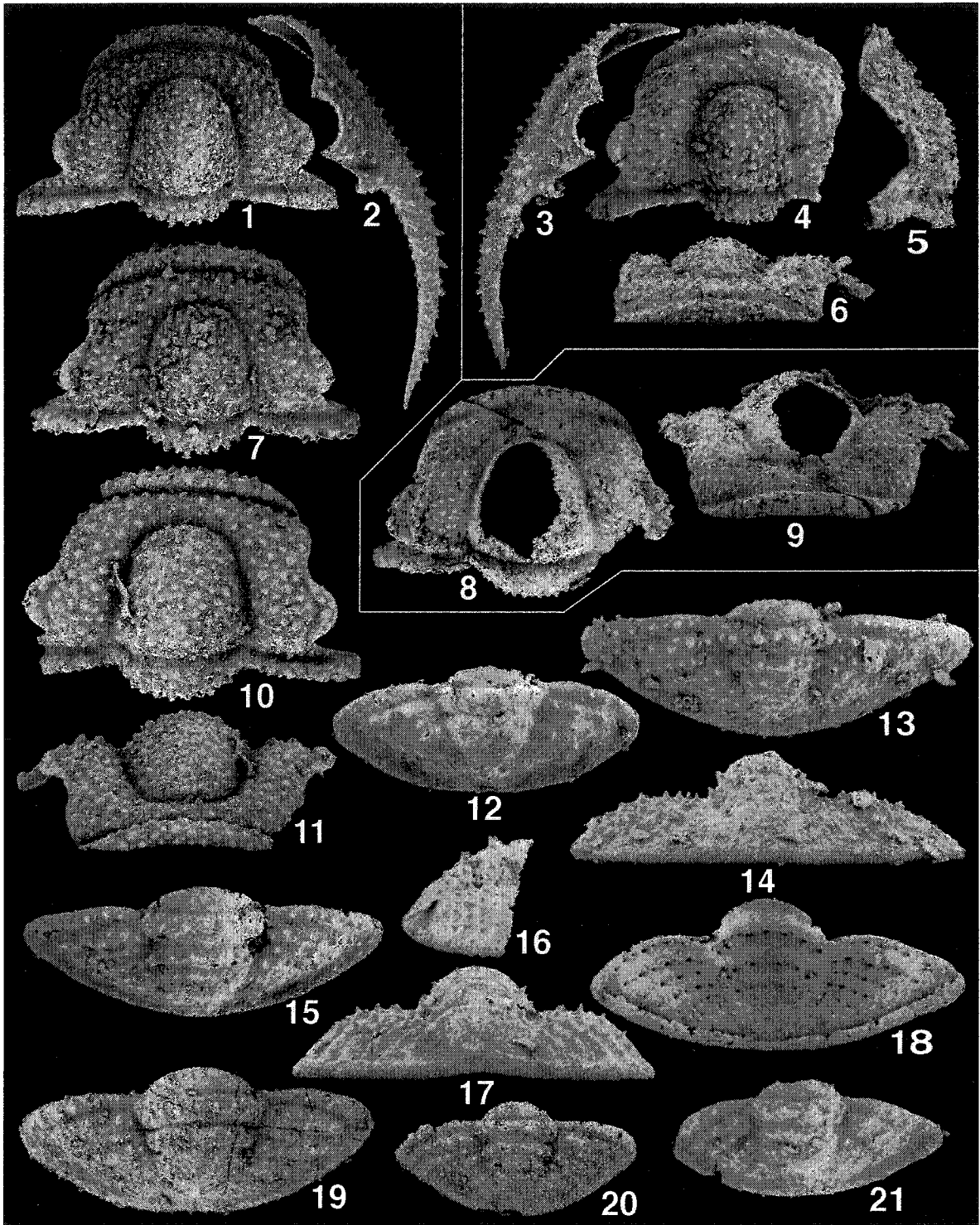 8, 9. UA 11892, cranidium, from E-5, x 10; 8. Dorsal view, 9. Anterior view.

PLATE III-8. *Hystricurus (Aequituberculatus) lepidus* Hintze, 1953.

1-19. *Hystricurus (Aequituberculatus) lepidus* Hintze, 1953.
    1, 3, 5. UA 11893, free cheek, from SE-87.5, x 10; 1. Dorsal view, 3. Ventral view, 5.
      Left lateral view.
    2, 4, 6, 7. UA 11894, cranidium, from SE-87.5, x 10; 2. Dorsal view, 4. Left lateral
      view, 6. Anterior view, 7. Ventral view.
    8. UA 11895, cranidium, from SE-87.5, dorsal view, x 10.
    9. UA 11897, cranidium, from SE-87.5, dorsal view, x 10.
    10. UA 11898, cranidium, from SE-90T, dorsal view, x 5.
    11. UA 11899, cranidium, from SE-87.5, dorsal view, x 10.
    12. UA 11900, cranidium, from SE-87.5, dorsal view, x 10.
    13, 15. UA 11901, pygidium, from SE-87.5, x 15; 13. Dorsal view, 15. Posterior view.
    14. UA 11902, pygidium, from SE-87.5, dorsal view, x 15.
    16. UA 11903, pygidium, from SE-87.5, dorsal view, x 15.
    17. UA 11904, pygidium, from SE-87.5, dorsal view, x 15.
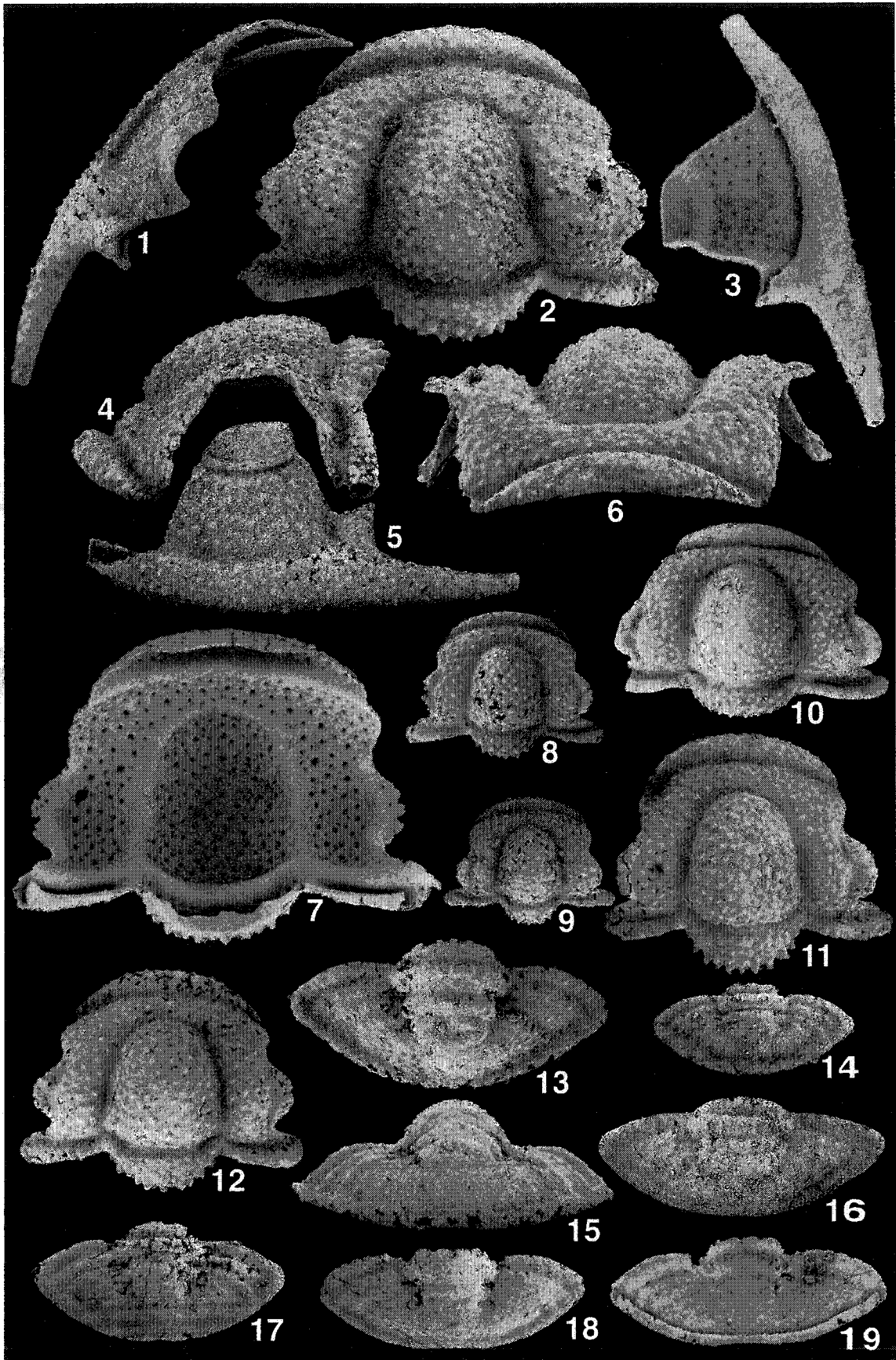   18, 19. UA 11905, pygidium, from SE-87.5, x 15; 18. Dorsal view, 19. Ventral view.

384

PLATE III-9. *Hystricurus (Aequituberculatus) lepidus* Hintze, 1953.

1-13. *Hystricurus (Aequituberculatus) lepidus* Hintze, 1953.

    1, 2, 4, 11. UA 11906, cephalon, from R6-20, x 20; 1. Dorsal view, 2. Left lateral view, 4. Ventral view, 11. Anterior view.

    3. UA 11907, cranidium, from R6-20, dorsal view, x 10.

    5, 6, 10. UA 11908, cranidium, from R5-34.1, x 10; 5. Dorsal view, 6. Left lateral view, 10. Anterior view.

    7, 8. UA 11909, pygidium, from R6-20, x 20; 7. Dorsal view, 8. Posterior view.

    9. UA 11913, pygidium, from R5-34.1, dorsal view, x 15.

    12, 13. UA 11916, pygidium, from R5-34.1, x 15; 12. Dorsal view, 13. Posterior view.

    14. UA 11917, pygidium, from SE-82T, dorsal view, x 10.

    15. UA 11921, pygidium, from SE-80T, dorsal view, x 10.

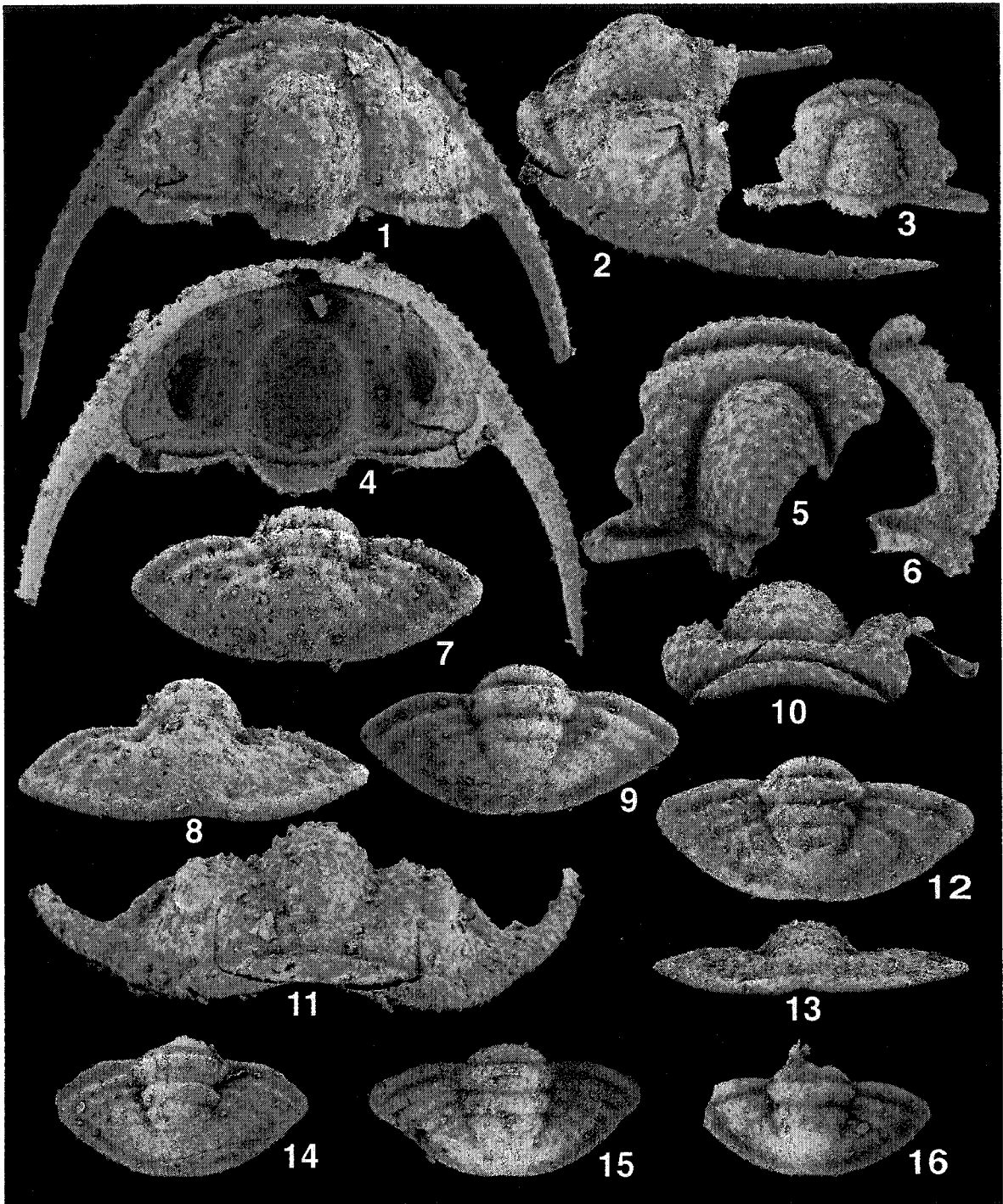   16. UA 11922, pygidium, from SE-90T, dorsal view, x 10.

386

PLATE III-10. *Hystricurus (Aequituberculatus) occipitospinosus* n. sp.

1-15. *Hystricurus (Aequituberculatus) occipitospinosus* n. sp.
  1, 3, 6, 9. UA 11923, free cheek, from SE-80T, x 10; 1. Ventral view, 3. Dorsal view, 6.
    Right lateral view, 9. Oblique dorsal view.
  2, 4, 5, 8. UA 11925, holotype, cranidium, from SE-80T, x 10; 2. Dorsal view, 4.
    Anterior view, 5. Right lateral view, 8. Ventral view.
  7. UA 11927, cranidium, from SE-80T, dorsal view, x 10.
  10. UA 11928, cranidium, from SE-80T, dorsal view, x 10.
  11, 13, 14. UA 11932, pygidium, from SE-80T, x 10; 11. Dorsal view, 13. Ventral
    view, 14. Posterior view.
  12, 15. UA 12757, pygidium, from SE-80T, x 20; 12. Dorsal view, 15. Posterior view.
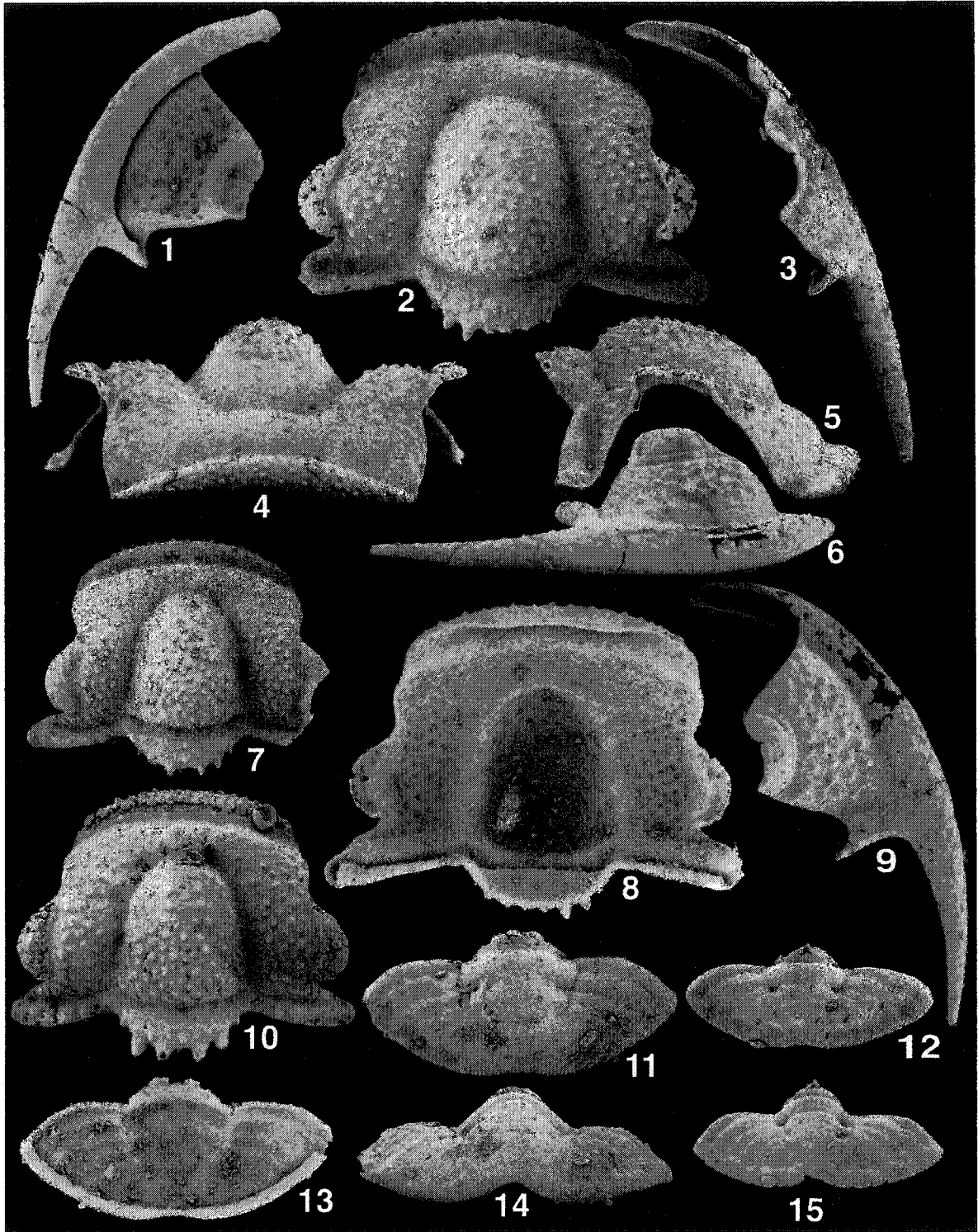
388

PLATE III-11. *Hystricurus (Triangulocaudatus) paragenalatus* Ross, 1951.

1-13. *Hystricurus (Triangulocaudatus) paragenalatus* Ross, 1951.
    1. UA 11934, free cheek, from SE-82T, dorsal view, x 15.
    2, 3, 5. UA 11935, cranidium, from SE-82T, x 15; 2. Dorsal view, 3. Left lateral view,
       5. Anterior view.
    4. UA 11936, cranidium, from SE-82T, dorsal view, x 15.
    6. UA 11937, cranidium, from SE-80T, dorsal view, x 15.
    7. UA 11938, cranidium, from E-3, dorsal view, x 15.
    8. UA 11939, cranidium, from SE-82T, dorsal view, x 15.
    9. UA 11940, pygidium, from SE-82T, dorsal view, x 10.
    10, 13. UA 12094, pygidium, from SE-82T, x 10; 10. Dorsal view, 13. Ventral view.
    11. UA 12095, pygidium with one thoracic segment whose right pleura is only released,
       from SE-82T, dorsal view, x 10.
    12. UA 12096, pygidium, from SE-80T, dorsal view, x 15.
    14. UA 12097, free cheek, from R5-34.1, dorsal view, x 15.
    15, 17. UA 12098, cranidium, from R5-34.1, x 15; 15. Dorsal view, 17. Ventral view.
    16. UA 12099, cranidium, from R5-34.1, dorsal view, x 15.
    18. UA 11848, pygidium, from R5-34.1, dorsal view, x 15.
    19. UA 11849, pygidium, from R5-34.1, dorsal view, x 15.
    20-22. UA 12100, pygidium, from R5-34.1, x 15; 20. Right lateral view, 21. Posterior
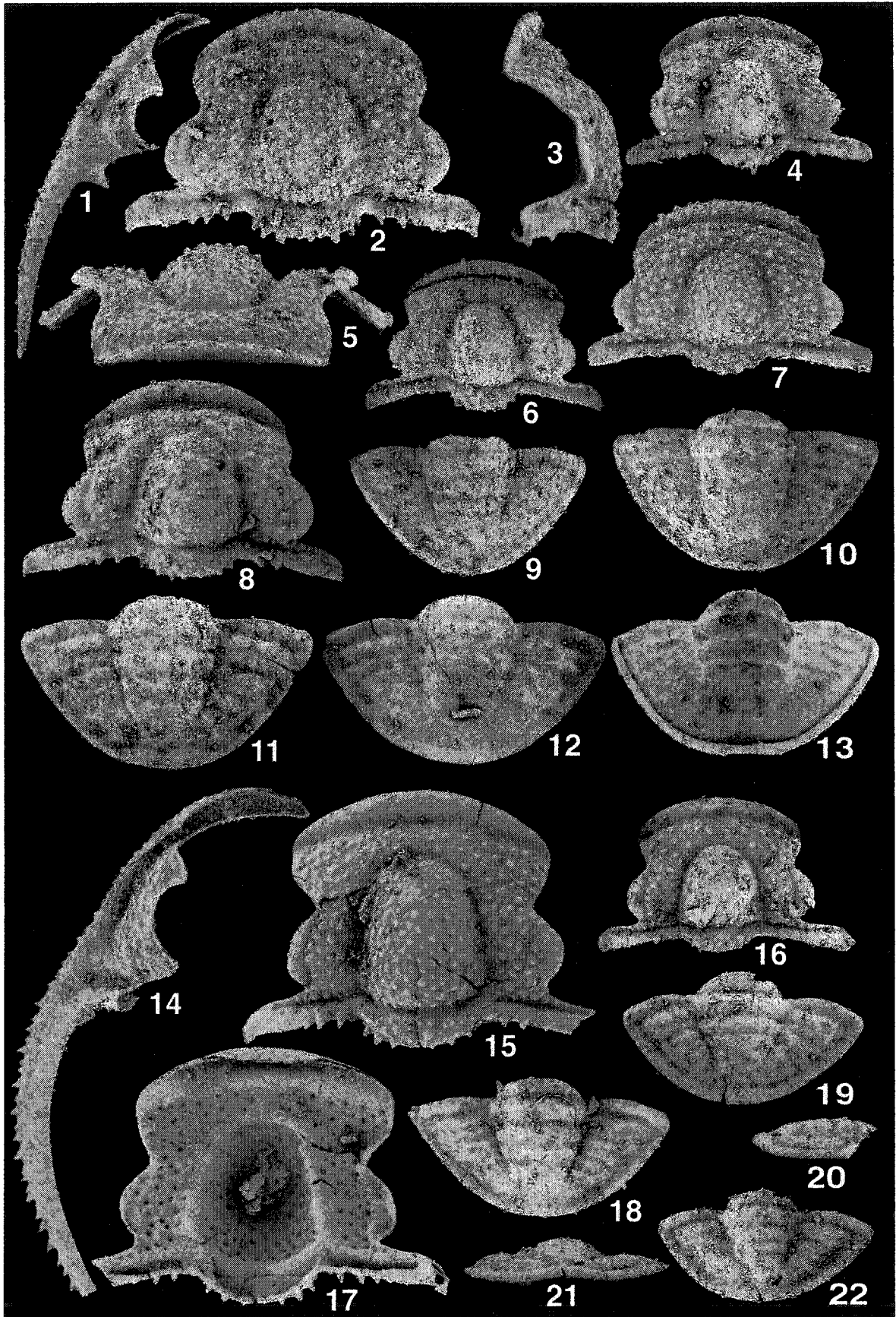   view, 22. Dorsal view.

390

PLATE III-12. *Hystricurus (Triangulocaudatus) paragenalatus* Ross, 1951.

1-15. *Hystricurus (Triangulocaudatus) paragenalatus* Ross, 1951.
  1. UA 12101, free cheek, from E-5, dorsal view, x 15.
  2, 3. UA 12102, cranidium, from E-5, x 15; 2. Dorsal view, 3. Ventral view.
  4. UA 12103, cranidium, from SE-80T, dorsal view, x 15.
  5. UA 12104, cranidium, from SE-82T, dorsal view, x 15.
  6, 7, 10. UA 12105, cranidium, from R5-34.1, x 15; 6. Right lateral view, 7. Dorsal
      view, 10. Anterior view.
  8. UA 12106, cranidium, from E-4, dorsal view, x 15.
  9. UA 12107, pygidium, from SE-82T, dorsal view, x 15.
  11, 12, 14, 15. UA 12108, pygidium, from E-5, x 15; 11. Left lateral view, 12. Dorsal
      view, 14. Ventral view, 15. Posterior view.
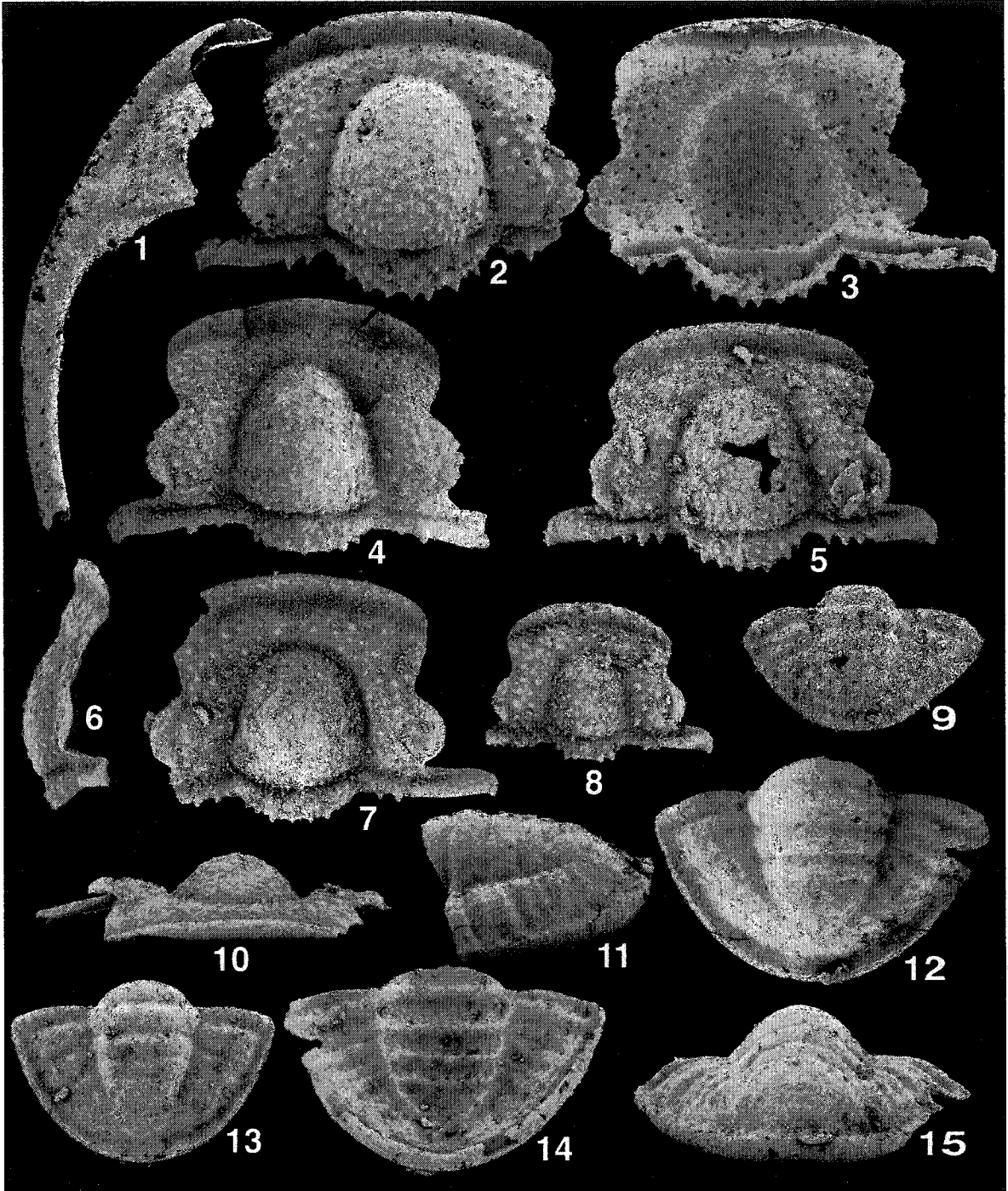 13. UA 12109, pygidium, from E-5, dorsal view, x 15.

392

PLATE III-13. *Hystricurus (Triangulocaudatus) convexomarginalis* n. sp.

1-11. *Hystricurus (Triangulocaudatus) convexomarginalis* n. sp.
   1. UA 12110, free cheek, from SE-82T, dorsal view, x 15.
   2, 6. UA 12111, holotype, cranidium, from SE-82T; 2. Dorsal view, x 15, 6. Ventral
      view, x 10.
   3. UA 12112, cranidium, from R6-15, dorsal view, x 15.
   4, 5. 7. UA 12113, pygidium, from SE-82T, x 15; 4. Posterior view, 5. Left lateral
      view, 7. Dorsal view.
   8. UA 12114, cranidium, from SE-80T, dorsal view, x 15.
   9. UA 12115, free cheek, from SE-80T, dorsal view, x 10.
   10, 11. UA 12116, pygidium, from SE-82T, x 15; 10. Dorsal view, 11. Ventral view.

394

PLATE III-14. *Hystricurus (Triangulocaudatus) convexomarginalis* n. sp.

1-16. *Hystricurus (Triangulocaudatus) convexomarginalis* n. sp.
    1, 2, 5. UA 12117, cranidium, from SE-87.5, x 15; 1. Dorsal view, 2. Left lateral view,
       5. Anterior view.
    3. UA 12118, cranidium, from SE-80T, dorsal view, x 15.
    4. UA 12119, cranidium, from E-4, dorsal view, x 15.
    6. UA 12120, cranidium, from SE-87.5, dorsal view, x 15.
    7, 9. UA 12755, free cheek, from SE-87.5, x 10; 7. Ventral view, 9. Dorsal view.
    8. UA 12121, cranidium, from SE-87.5, dorsal view, x 15.
    10. UA 12122, cranidium, from SE-87.5, dorsal view, x 15.
    11. UA 12123, cranidium, from SE-80T, dorsal view, x 10.
    12, 13. UA 12124, pygidium with one thoracic segment, from SE-87.5, x 10; 12. Dorsal
       view, 13. Left lateral view.
    14, 16. UA 12125, pygidium, from SE-87.5, x 10; 14. Dorsal view, 16. Posterior view.
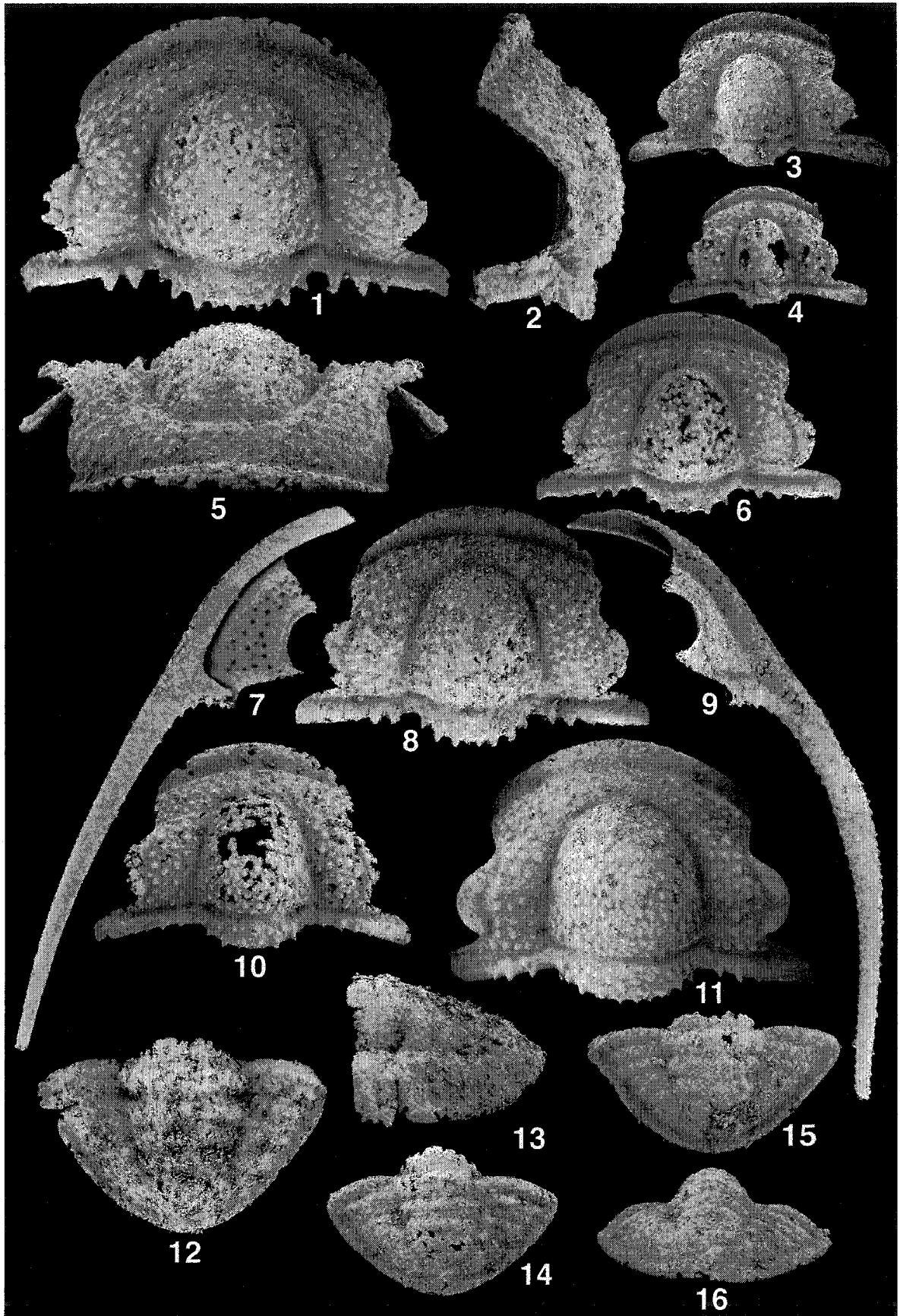   15. UA 12126, pygidium, from SE-87.5, dorsal view, x 15.

396

PLATE III-15. *Hystricurus (Aequituberculatus)* sp. A aff. *H. (A.) minutuberculatus*, *Hystricurus (Triangulocaudatus)* sp. B aff. *H. (T.) paragenalatus*, *Hystricurus (Triangulocaudatus)* sp. aff. *H. (T.) convexomarginalis*, *Hystricurus (Triangulocaudatus)* sp. C aff. *H. (T.) paragenalatus*, *Politohystricurus* sp. aff. *P. politus convergia*, *Hystricurus (Aequituberculatus)* sp. aff. *H. (A.) occipitospinosus*, Olenidae sp., *Hystricurus (Triangulocaudatus)* sp. D aff. *H. (T.) paragenalatus* and *Hystricurus (Triangulocaudatus)* sp. A aff. *H. (T.) paragenalatus*.

1. *Hystricurus (Aequituberculatus)* sp. A aff. *H. (A.) minutuberculatus.*
   1. UA 12127, cranidium, from R6-20, dorsal view, x 15.
2. *Hystricurus (Triangulocaudatus)* sp. B aff. *H. (T.) paragenalatus.*
   2. UA 12128, cranidium, from E-4, dorsal view, x 15.
3, 4. *Hystricurus (Triangulocaudatus)* sp. aff. *H. (T.) convexomarginalis.*
   3, 4. UA 12129, cranidium, from E-4, x 10; 3. Dorsal view, 4. Ventral view.
5, 6. *Hystricurus (Triangulocaudatus)* sp. C aff. *H. (T.) paragenalatus.*
   5, 6. UA 12130, pygidium, from R5-34.1, x 15; 5. Dorsal view, 6. Ventral view.
7-9. *Politohystricurus* sp. aff. *P. politus convergia.*
   7-9. UA 12131, pygidium, from SE-82T, x 10; 7. Dorsal view, 8. Posterior view, 9. Ventral view.
10, 11. *Hystricurus (Aequituberculatus)* sp. aff. *H. (A.) occipitospinosus.*
   10, 11. UA 12132, pygidium, from E-5, x 15; 13. Dorsal view, 14. Posterior view.
12-14. **Olenidae** sp.
   12, 13. UA 12133, pygidium, from R6-20, x 15; 17. Posterior view, 18. Dorsal view.
   14. UA 12134, pygidium, from R6-20, dorsal view, x 15.
15. *Hystricurus (Triangulocaudatus)* sp. D aff. *H. (T.) paragenalatus.*
   15. UA 12135, cranidium, from E-5, dorsal view, x 15.
16. *Hystricurus (Triangulocaudatus)* sp. A aff. *H. (T.) paragenalatus.*
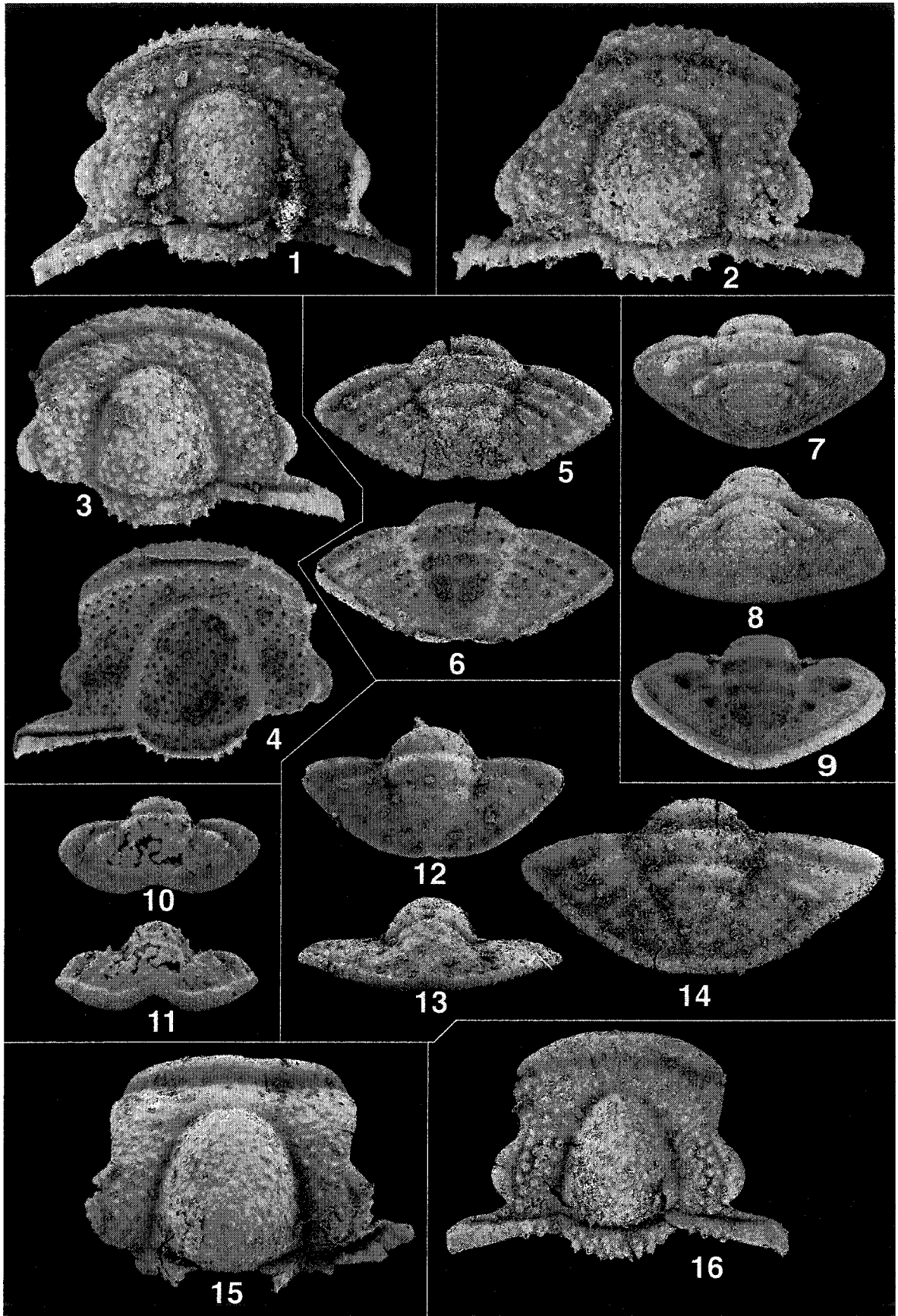   12. UA 12136, cranidium, from R5-34.1, dorsal view, x 15.

398

PLATE III-16. *Spinohystricurus terescurvus* n. gen. *et.* n. sp. and *Spinohystricurus robustus* (Ross, 1951).

1-3, 7-12. *Spinohystricurus terescurvus* n. gen. *et.* n. sp.
    1-3. UA 11015 articulated specimen with 7 thoracic segments, from R5-76.4, x 40; 1. Dorsal view of cranidium and ventral view of thoracopygidium, 2. Lateral view, 3. Dorsal view of thoracopygidium.
    7, 8. UA 12137, articulated specimen with 7 thoracic segments, from R5-76.4(98) x 40; 7. Dorsal view of cranidium, 8. Lateral view.
    9, 10. UA 11878, meraspis with four thoracic segments, from R5-76.4, x 40; 9. Dorsal view, 10. Right lateral view.
    11. UA 11876, meraspid cranidium, from R5-76.4, dorsal view, x 40.
    12. UA 12138, protaspis, from R5-76.4, dorsal view, x 100.
4-6. *Spinohystricurus robustus* (Ross, 1951).
    4-6. UA 11022, meraspis with five thoracic segments, from R5-86, x 40; 4. Dorsal view, 5. Posterior view, 6. Right lateral view.
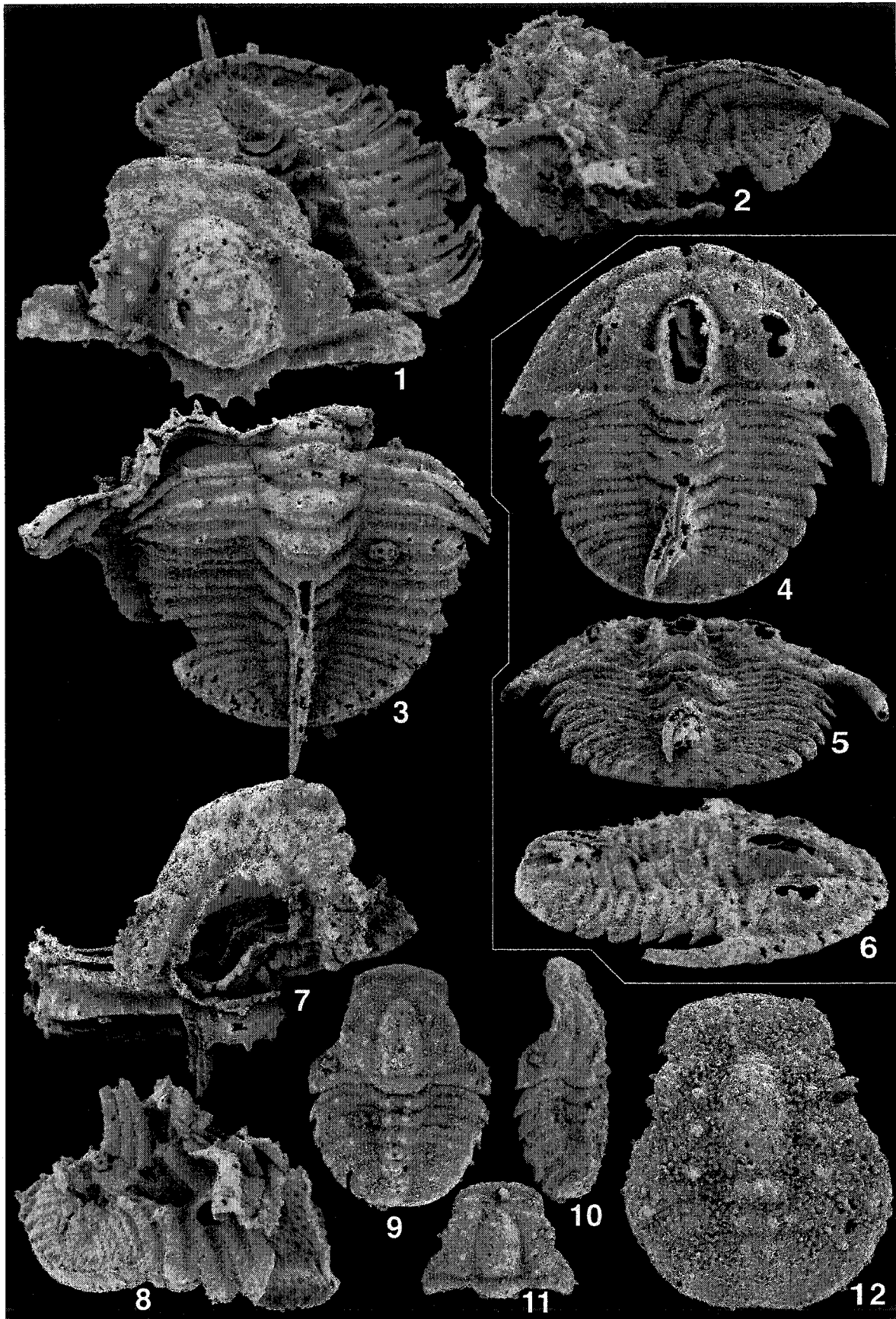
400

PLATE III-17. *Spinohystricurus terescurvus* n. gen. and n. sp. and *Spinohystricurus robustus* (Ross, 1951).

1-7, 10-12. *Spinohystricurus terescurvus* n. gen. and n. sp.

    1-4. UA 12139, partially articulated specimen with four thoracic segments, from R5-87.7, x 10; 1. Dorsal view, 2. Right lateral view, 3. Ventral view, 4. Left lateral view.

    5. UA 12140, partially articulated thoracopygidium, from SE-152, dorsal view, x 10.

    6, 7, 12. UA 12141, partially articulated specimen with six thoracic segments, from R5-76.4(98); 6. Ventral view, x 40, 7. Left lateral view, x 40, 12. Magnified view of hypostome, x 100.

    10. UA 12142, four thoracic segments, from R5-76.4(97), dorsal view, x 10.

    11. UA 12143, partially articulated thoracopygidium with four thoracic segments, from R5-86, dorsal view, x 10.

8, 9. *Spinohystricurus robustus* (Ross, 1951).

    8, 9. UA 12144, partially articulated thoracopygidium and free cheeks, from R5-86, x 40; 8. Dorsal view, 9. Ventral view.
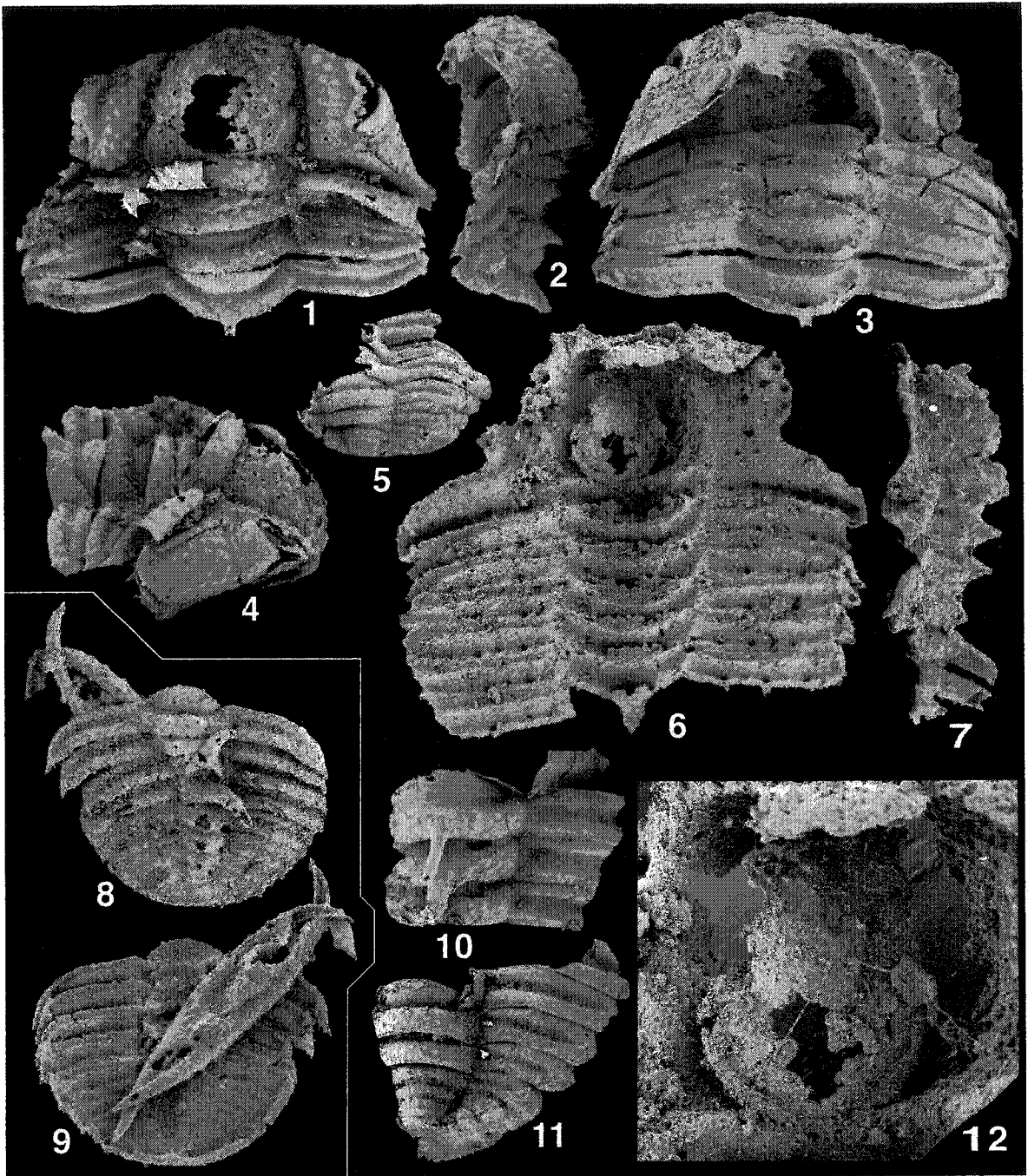
402

PLATE III-18. *Spinohystricurus terescurvus* n. gen. and n. sp. and *Spinohystricurus* sp. aff. *S. robustus*.

1-19. *Spinohystricurus terescurvus* n. gen. and n. sp.
  1. UA 11856, cranidium, from R5-76.4, dorsal view, x 10.
  2, 4, 7. UA 12145, cranidium, from SE-152, x 10; 2. Dorsal view, 4. Anterior view, 7. Right lateral view.
  3, 8, 10. UA 12146, right free cheek, from SE-152, x 10; 3. Dorsal view, 8. Right lateral view, 10. Ventral view.
  5. UA 12147, cranidium, from R5-86, dorsal view, x 10.
  6. UA 11929, cranidium, from R5-87.7, dorsal view, x 10.
  9. UA 12148, cranidium, from SE-152, dorsal view, x 10.
  11. UA 12149, left free cheek, from R5-87.7, dorsal view, x 10.
  12, 16. UA 12150, cranidium, from R5-87.7, x 10; 12. Dorsal view, 16. Ventral view.
  13. UA 12151, small cranidium, from R6-55, dorsal view, x 40.
  14. UA 12152, small cranidium, from R6-55, dorsal view, x 20.
  15. UA 12153, small cranidium, from R6-55, dorsal view, x 40.
  17. UA 11857, cranidium, from R5-76.4, dorsal view, x 10.
  18. UA 12154, small cranidium, from R6-55, dorsal view, x 40.
  19. UA 12155, small cranidium, from R5-76.4, dorsal view, x 30.
20-23. *Spinohystricurus* sp. aff. *S. robustus*.
  20-23. UA 11875, cranidium, from R5-76.4, x 20; 14. Dorsal view, 15. Left lateral view, 16. Anterior view, 17. Ventral view.
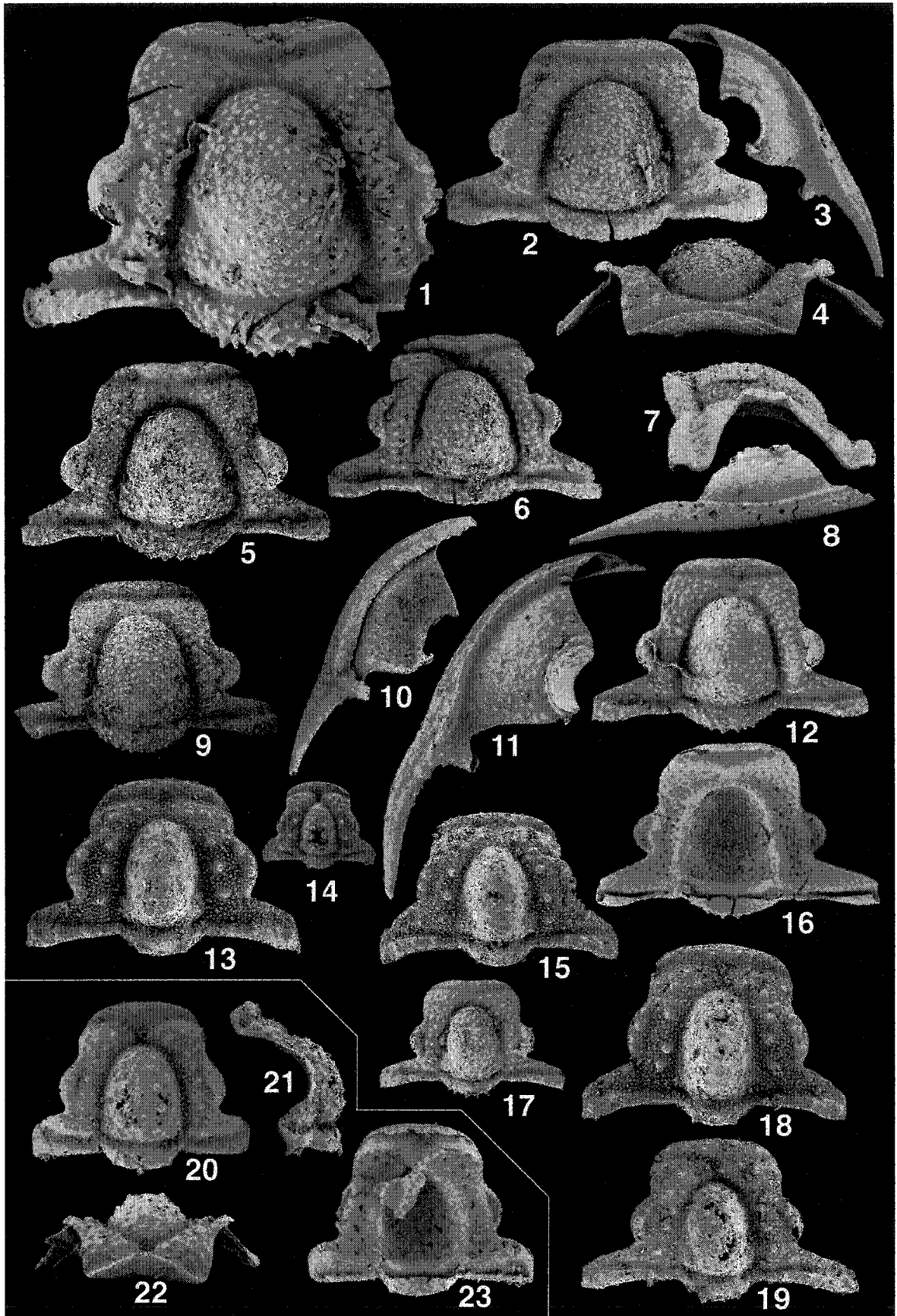
404

PLATE III-19. *Spinohystricurus robustus* (Ross, 1951), *Spinohystricurus antiquus* (Lisogor, 1961) and *Spinohystricurus* n. sp.

1-8. *Spinohystricurus robustus* (Ross, 1951).
  1, 2, 6. UA 12156, cranidium, from R5-76.4(97), x 20; 1. Left lateral view, 2. Dorsal view, 6. Anterior view.
  3. UA 12157, free cheek, from R5-76.4(97), dorsal view, x 20.
  4. UA 12158, cranidium, from R5-76.4, dorsal view, x 20.
  5. UA 12159, smaller cranidium, from R6-55, dorsal view, x 20.
  7. UA 12160, free cheek, from R5-76.4(98), dorsal view, x 20.
  8. UA 12161, cranidium, from R5-76.4(98), dorsal view, x 20.
9-18. *Spinohystricurus antiquus* (Lisogor, 1961).
  9, 10, 12, 16. UA 12162, neotype, cranidium, from R6-55, x 20; 9. Right lateral view, 10. Dorsal view, 12. Anterior view, 13. Ventral view.
  11. UA 12163, free cheek, from R6-55, dorsal view, x 20.
  13. UA 12164, cranidium, from R6-55, dorsal view, x 20.
  14, 15. UA 12165, pygidium, from R6-55, x 20; 14. Dorsal view, 15. Posterior view.
  17. UA 12166, protaspis, from R6-55, dorsal view, x 75.
18-21. *Spinohystricurus* n. sp.
  18, 20. UA 12167, cranidium, from SE-152, x 7; 18. Anterior view, 20. Dorsal view.
  19. UA 12168, free cheek, from SE-152, dorsal view, x 15.
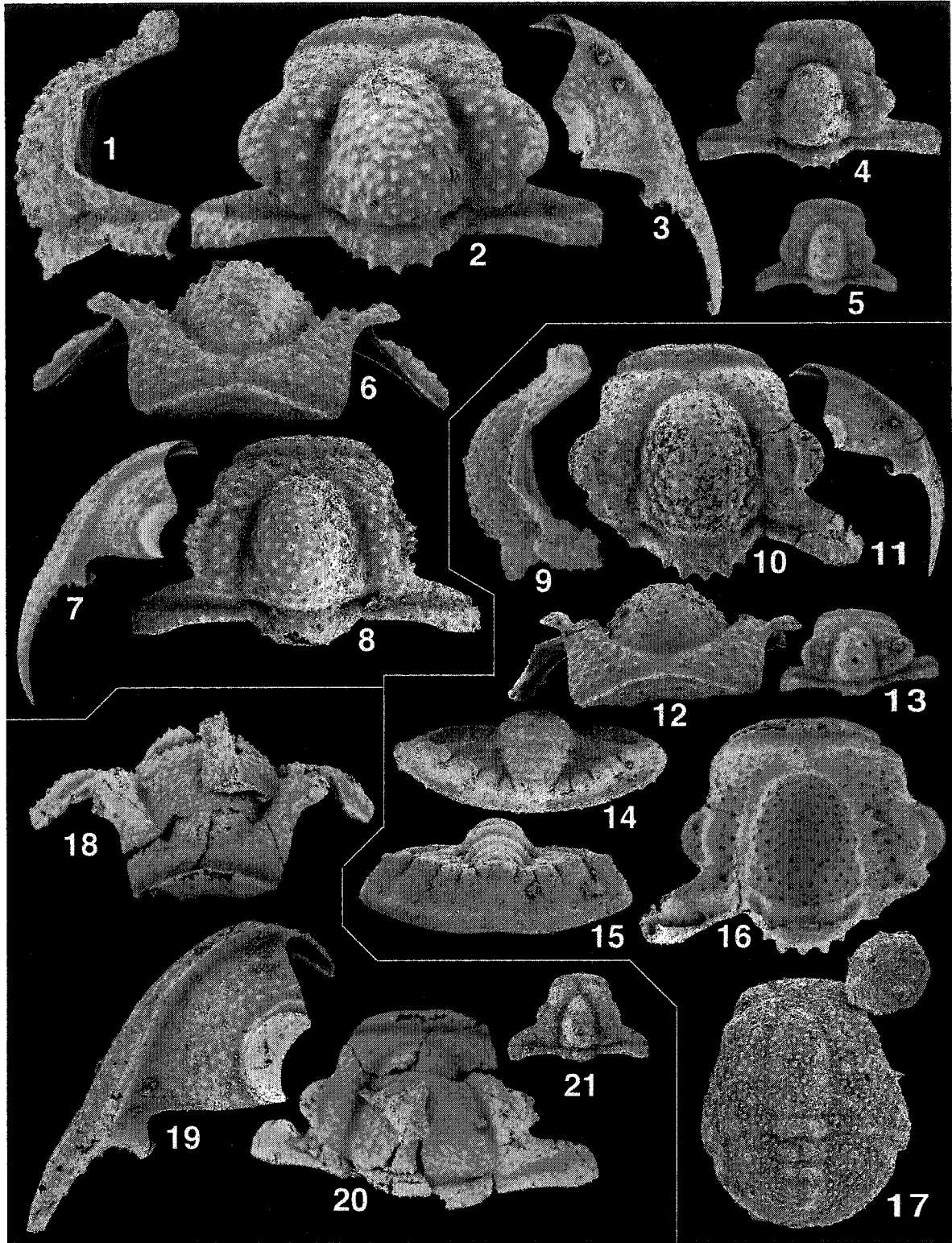 21. UA 12169, cranidium, from R6-55, dorsal view, x 20.

PLATE III-20. *Spinohystricurus terescurvus* n. gen. and n. sp.

1-18. *Spinohystricurus terescurvus* n. gen. and n. sp.
   1, 3. UA 11862, pygidium, from R5-76.4, x 20; 1. Dorsal view, 3. Posterior view.
   2, 5. UA 11861, pygidium with one thoracic segment, from R5-76.4, x 20; 2. Dorsal
      view, 5. Right lateral view.
   4. UA 12170, pygidium, from R5-76.4(97), dorsal view, x 20.
   6. UA 12171, pygidium, from R5-76.4, dorsal view, x 20.
   7. UA 12172, pygidium, from R5-76.4(97), dorsal view, x 20.
   8. UA 12173, pygidium, from SE-152, dorsal view, x 10.
   9, 12. UA 12174, pygidium, from SE-152, x 20; 9. Dorsal view, 11. Ventral view.
   10. UA 12175, pygidium, from R5-87.7(97), dorsal view, x 10.
   11. UA 12176, pygidium, from R5-86, dorsal view, x 20.
   13. UA 12177, transitory pygidium, from R5-76.4, dorsal view, x 30.
   14. UA 12178, transitory pygidium, from R5-76.4A, dorsal view, x 30.
   15. UA 11860, transitory pygidium, from R5-76.4, dorsal view, x 30.
   16. UA 12179, transitory pygidium, from R5-76.4, dorsal view, x 30.
   17. UA 12180, pygidium, from R5-87.7, dorsal view, x 20.
   18. UA 12181, transitory pygidium, from R5-86, dorsal view, x 30.
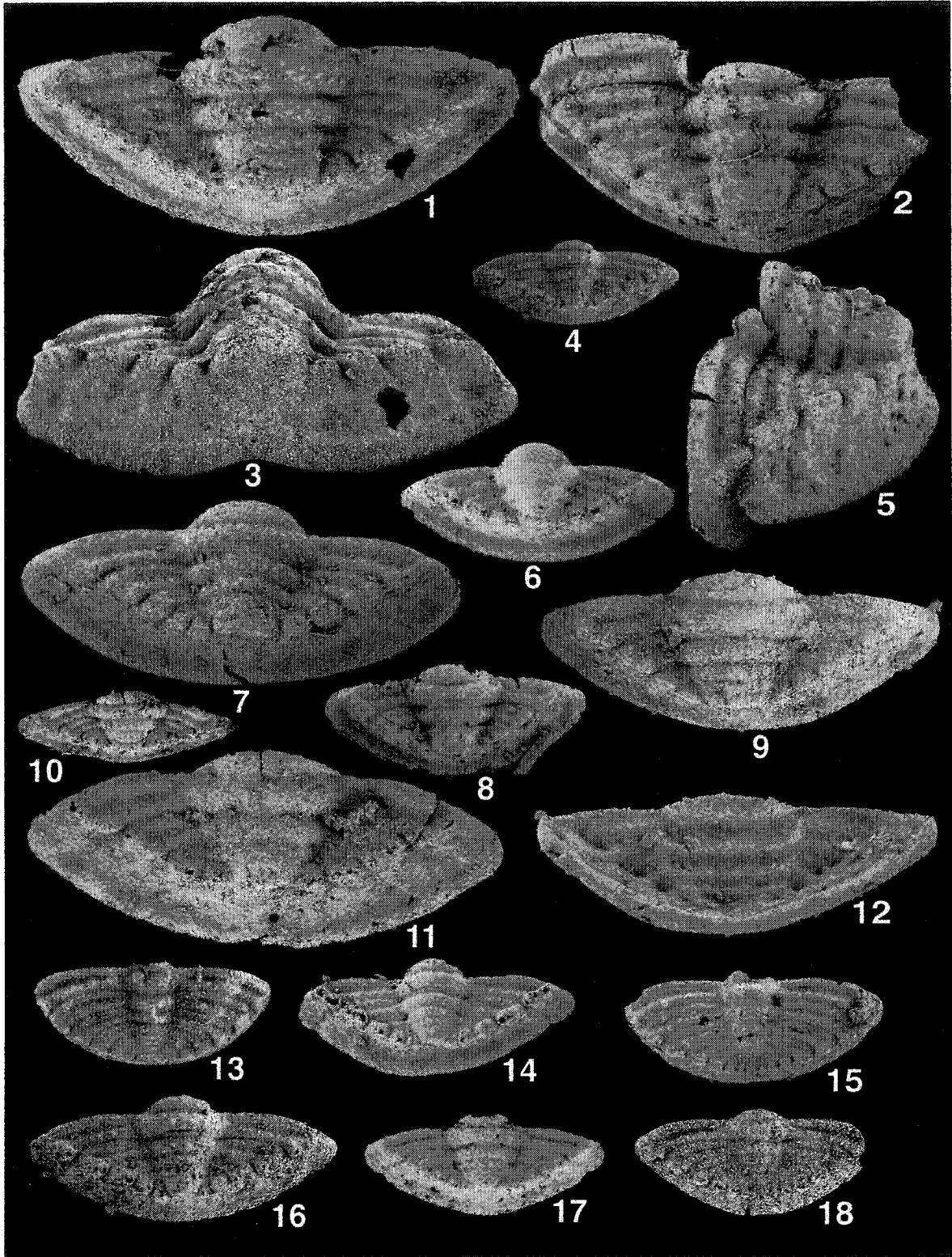
408

PLATE III-21. *Hystricurus*? aff. *H.*? *missouriensis*, *Hystricurus* (*Triangulocaudatus*) *ravni* Poulsen, 1927 and *Parahillyardina newfoundlandia* n. gen. and n. sp.

1-7. *Hystricurus*? aff. *H.*? *missouriensis*.
  1, 2. UTGD 122521, cranidium, from La3 Zone (Lancefieldian Series) of Florentine Valley Formation, Tasmania, Australia, x 10; 1. Dorsal view, 2. Right lateral view.
  3. UA 12182, cranidium, from E-4, dorsal view, x 15.
  4-7. UA 12183, cranidium, from R11-48.7, x 15; 4. Anterior view, 5. Ventral view, 6. Right lateral view, 7. Dorsal view.
8. *Hystricurus* (*Triangulocaudatus*) *ravni* Poulsen, 1927.
  8. MGUH 2342, holotype, cast of articulated specimen, from probably *Symphysurina* Zone of Cass Fjord Formation, Northwest Greenland, dorsal view, x 2.5: the white arrow points the boundary between thorax and pygidium.
9. *Parahillyardina newfoundlandia* n. gen. and n. sp.
  9. NFM F-131, holotype, cast of partially articulated specimen, from *Randaynia saundersi* Zone of Boat Harbour Formation, western Newfoundland, dorsal view, x 7.5: the white arrow points the boundary between thorax and pygidium.

410
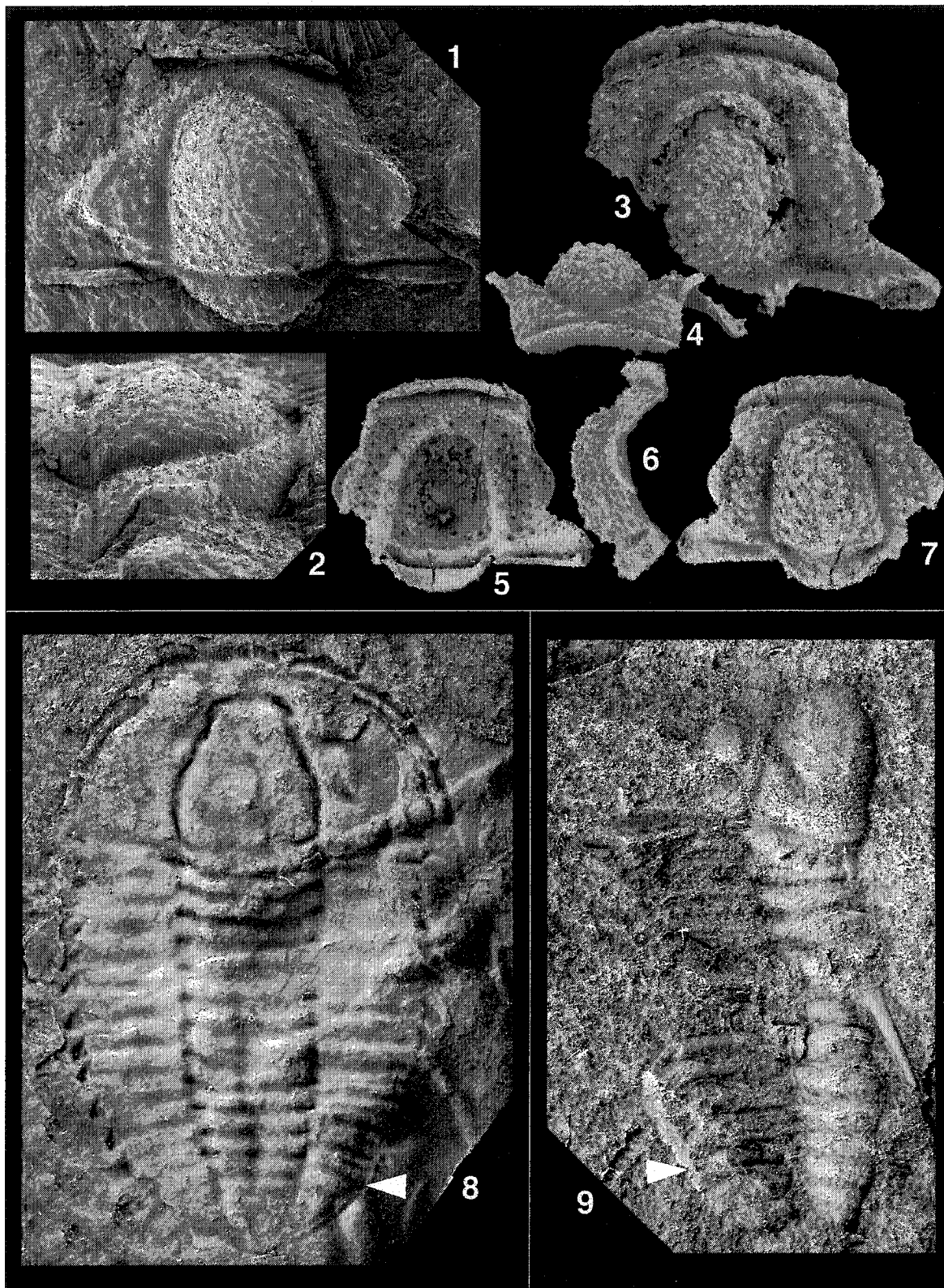
PLATE III-22. *Politohystricurus politus politus* Ross, 1951.

1-23. *Politohystricurus politus politus* ross, 1951.

1, 2, 4. UA 12184, cranidium, from SE-80T, x 10; 1. Left lateral view, 2. Dorsal view, 4. Anterior view.

3. UA 12185, cranidium, from SE-82T, dorsal view, x 10.

5, 6. UA 12186, cranidium, from SE-80T, x 10; 5. Dorsal view, 6. Ventral view.

7. UA 11847, cranidium, from R5-34.1, dorsal view, x 10.

8. UA 12187, cranidium, from SE-82T, dorsal view, x 10.

9, 10. UA 12188, free cheek, from SE-80T, x 10; 9. Oblique dorsal view, 10. Dorsal view.

11. UA 12189, cranidium, from SE-82T, dorsal view, x 10.

12. UA 12190, cranidium, from R6-20, dorsal view, x 10.

13. UA 12191, cranidium, from E-4, dorsal view, x 5.

14, 15. UA 12192, free cheek, from SE-80T, x 10; 14. Dorsal view, 15. Ventral view.

16, 19, 21, 22. UA 12193, pygidium, from SE-80T, x 15; 16. Left lateral view, 19. Ventral view, 21. Dorsal view, 22. Posterior view.

17, 18. UA 12194, pygidium, from SE-80T, x 15; 17. Posterior view, 18. Dorsal view.

20, 23. UA 12195, pygidium, from R6-20, x 10; 20. Dorsal view, 23. Posterior view.

412

PLATE III-23. *Politohystricurus politus convexofrontalis* n. gen. *et*. n. subsp.

1-13. *Politohystricurus politus convexofrontalis* n. gen. *et*. n. subsp.
    1, 2, 6. UA 12196, holotype, cranidium, from SE-80T, x 10; 1. Dorsal view, 2. Right
        lateral view, 6. Anterior view.
    3. UA 12197, cranidium, from SE-87.5, dorsal view, x 10.
    4. UA 12198, cranidium, from E-2, dorsal view, x 10.
    5, 8, 9, 13. UA 12199, cranidium, from E-3, x 10; 5. Dorsal view, 8. Ventral view, 9.
        Anterior view, 13. Right lateral view.
    7, 10. UA 12200, free cheek, from E-2, x 10; 7. Dorsal view, 10. Oblique dorsal view.
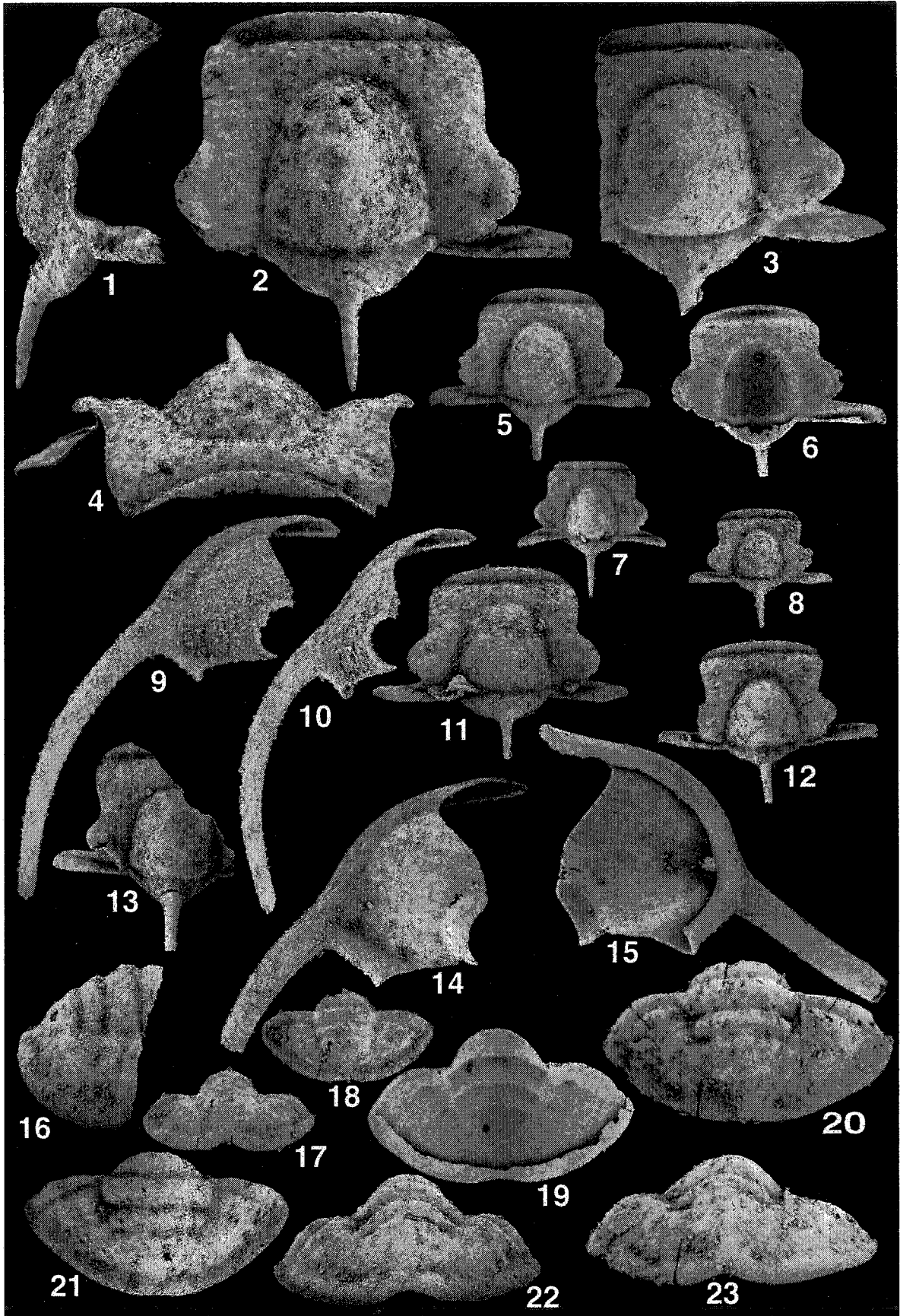   11, 12. UA 12201, pygidium, from E-2, x 10; 11. Posterior view, 12. Dorsal view.

414
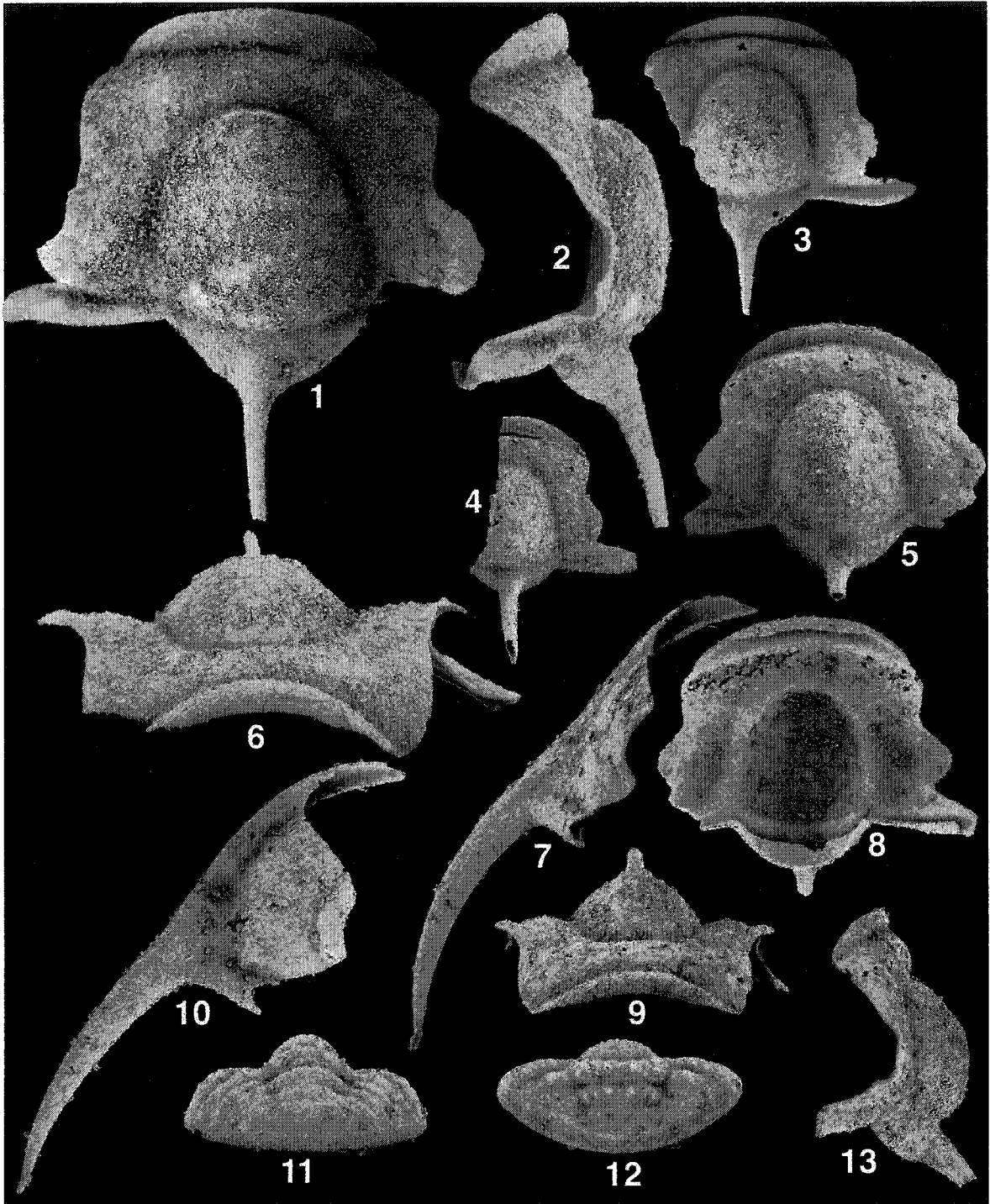
PLATE III-24. *Politohystricurus politus convergia* n. gen. *et.* n. subsp.

1-13. *Politohystricurus politus convergia* n. gen. *et.* n. subsp.

    1, 2, 4. UA 12202, holotype, cranidium, from SE-87.5, x 10; 1. Dorsal view, 2. Anterior view, 4. Ventral view.

    3. UA 12203, cranidium, from SE-87.5, dorsal view, x 10.

    5. UA 12204, cranidium, from SE-87.5, dorsal view, x 10.

    6. UA 12205, free cheek, from SE-87.5, dorsal view, x 10.

    7, 8. UA 12206, pygidium, from SE-87.5, x 10; 7. Dorsal view, 8. Posterior view.

    9-11, 13. UA 12207, pygidium, from SE-87.5, x 10; 9. Dorsal view, 10. Left lateral view, 11. Ventral view, 13. Posterior view.

    12. UA 12208, cranidium, from SE-87.5, dorsal view, x 10.

416
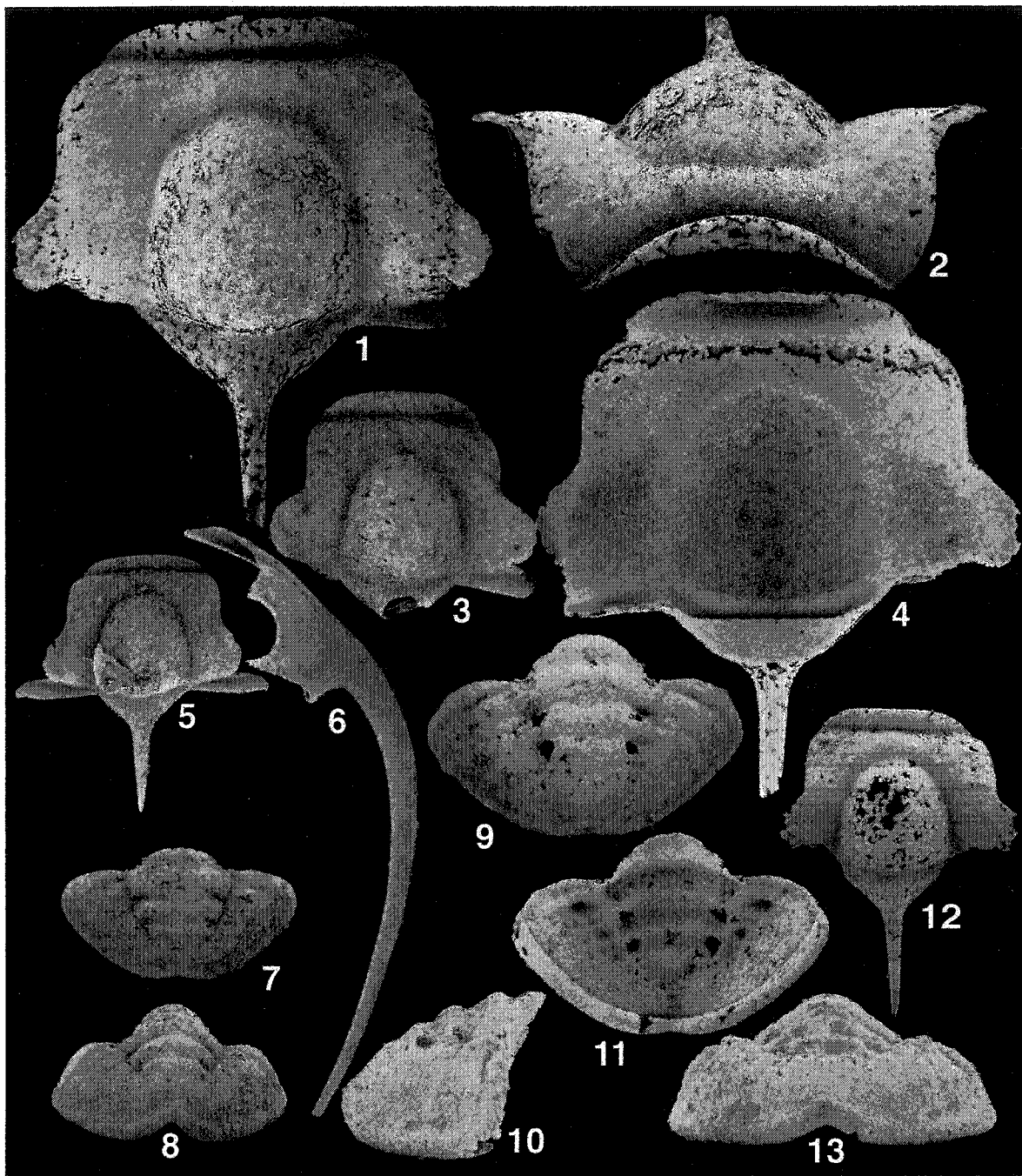
PLATE III-25. *Politohystricurus politus longifrontalis* n. gen. *et.* n. subsp. and
   Politohystricurus brevispinosus n. gen. and n. sp.

1-7. *Politohystricurus politus longifrontalis* n. gen. *et.* n. subsp.
  1. UA 12209, holotype, cranidium, from R6-15, dorsal view, x 10.
  2, 7. UA 12210, cranidium, from R6-15, x 10; 2. Dorsal view, 7. Anterior view.
  3. UA 12211, free cheek, from R6-15, dorsal view, x 10.
  4-6. UA 12212, pygidium, from R6-15, x 20; 4. Dorsal view, 5. Left lateral view, 6.
    Posterior view.
8-15. *Politohystricurus brevispinosus* n. gen. and n. sp.
  8, 11, 12. UA 12213, holotype, cranidium, from E-5, x 10; 8. Dorsal view, 11. Ventral
    view, 12. Anterior view.
  9, 10. UA 12214, free cheek, from E-5, x 10; 9. Dorsal view, 10. Oblique dorsal view.
  13. UA 12215, free cheek, from E-5, dorsal view, x 10.
  14, 15. UA 12216, pygidium, from E-5, x 20; 14. Dorsal view, 15. Posterior view.
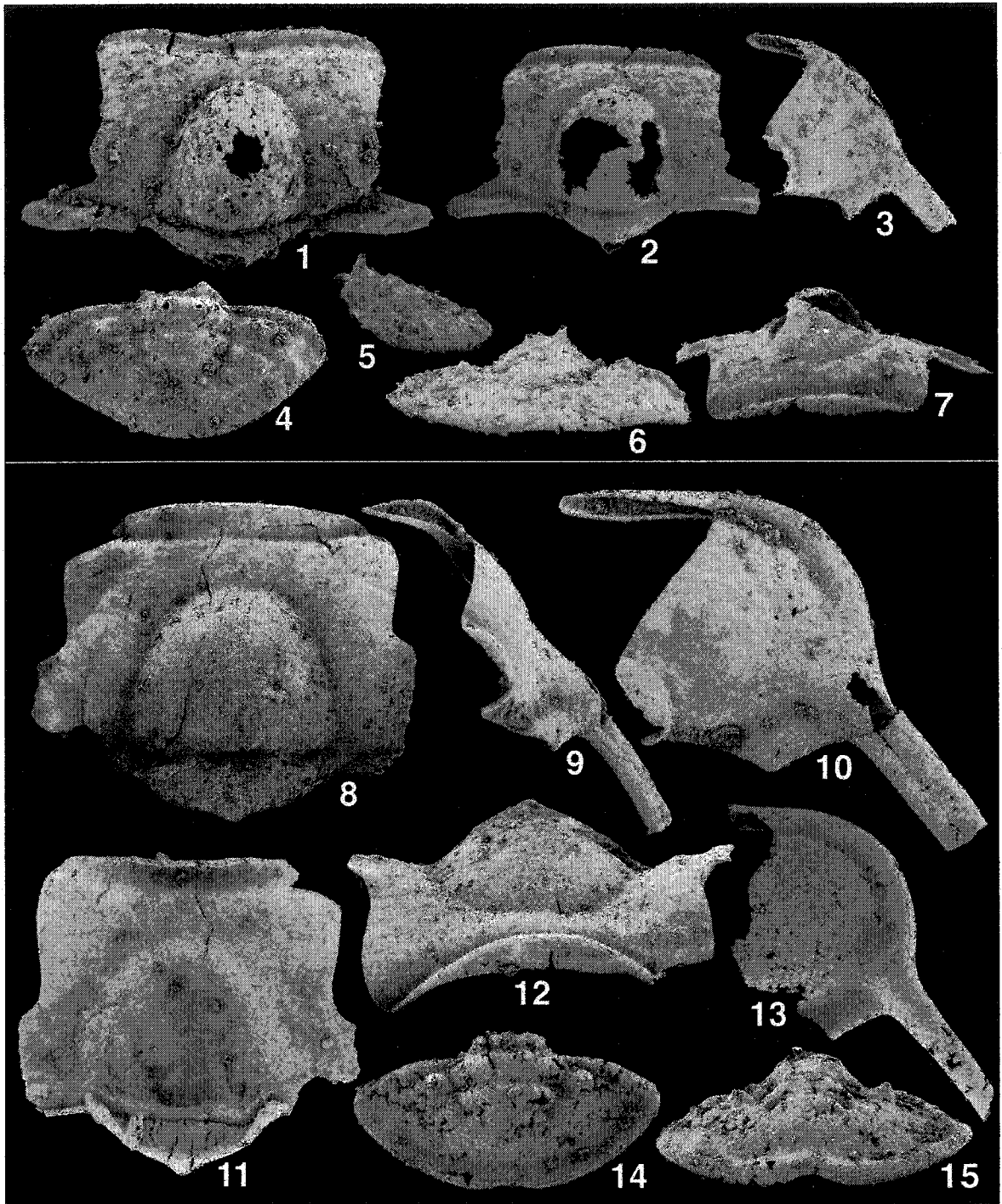
PLATE III-26. *Politohystricurus concavofrontalis* n. gen. and n. sp. and
Politohystricurus pseudopsalikilus n. gen. and n. sp.

1-8. *Politohystricurus concavofrontalis* n. gen. and n. sp.
   1-3. UA 12217, holotype, cranidium, from SE-90T, x 10; 1. Dorsal view, 2. Anterior
      view, 3. Ventral view.
   4-6. UA 12218, pygidium, from SE-90T, x 10; 4. Dorsal view, 5. Posterior view, 6.
      Ventral view.
   7, 8. UA 12219, free cheek, from SE-90T, x 10; 7. Ventral view, 8. Dorsal view.
9-15. *Politohystricurus pseudopsalikilus* n. gen. and n. sp.
   9, 10. UA 12220, free cheek, from SE-80T, x 20; 9. Dorsal view, 10. Oblique dorsal
      view.
   11, 14, 15. UA 12221, holotype, cranidium, from SE-80T, x 10; 11. Dorsal view, 14.
      Anterior view, 15. Ventral view.
   12, 13. UA 12222, pygidium, from SE-80T, x 20; 12. Dorsal view, 13. Posterior view.

420
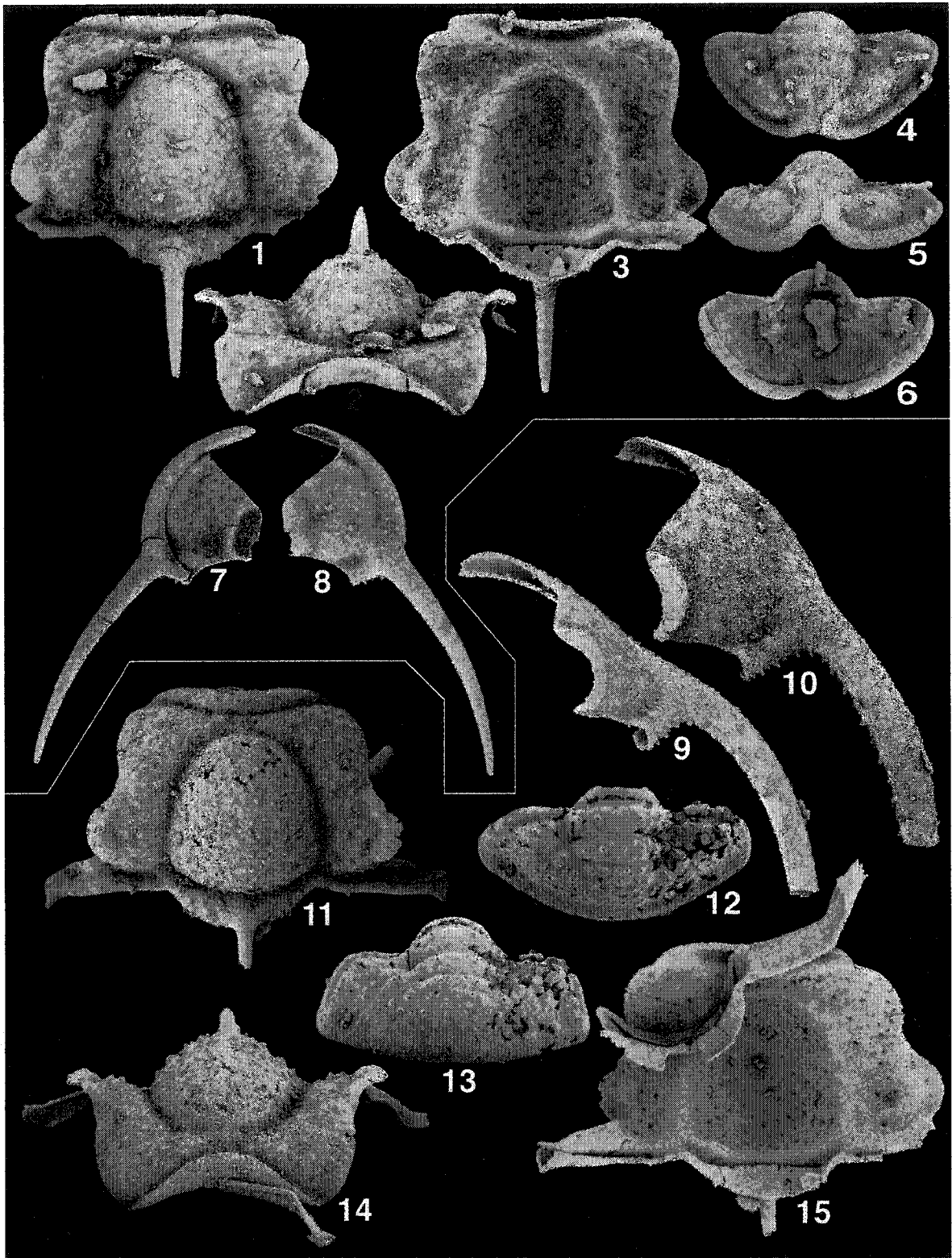
PLATE III-27. *Amblycranium variabile profusus* n. subsp.

1-15. *Amblycranium variabile profusus* n. subsp.

    1, 2. UA 12223, partially articulated specimen consisting of cranidium, free cheeks, and four thoracic segments, from R5-76.4, x 15; 1. Dorsal view, 2. Ventral view.

    3, 4. UA 12224, partially articulated specimen consisting of pygidium and five thoracic segments (anterior three possessing a long axial spine and posterior two lacking it), from R5-86, x 15; 3. Dorsal view, 4. Ventral view.

    5, UA 12225, partially articulated specimen consisting of cranidium, free cheeks and one thoracic segment, from SE-152, dorsal view, x 15.

    6-9. UA 12226, cephalon from R5-76.4A, x 15; 6. Dorsal view, 7. Left lateral view, 8. Ventral view, 9. Anterior view.

    10. UA 11026, meraspid cranidium, from R5-86, dorsal view, x 50.

    11, 12. UA 11023, protaspis, from R5-76.4, x 100; 11. right lateral view, 12. Dorsal view.

    13. UA 12227, protaspis, from R6-55, dorsal view, x 100: this specimen may be proven to belong to *Amblycranium variabile rectus*.

    14, 15. UA 12228, degree 3 meraspis without free cheeks, from R5-76.4, x 50; 14. Right lateral view, 15. Dorsal view.

422

PLATE III-28. *Amblycranium variabile profusus* n. subsp. and *Amblycranium variabile flexus* n. subsp.

1-15. *Amblycranium variabile profusus* n. subsp.
    1-4 UA 12229, cranidium, from R5-76.4 (97), x 15; 1. Dorsal view, 2. Left lateral view, 3. Ventral view, 4. Anterior view.
    5. UA 12230, cranidium, from R5-76.4 (98), dorsal view, x 20.
    6. UA 11027, cranidium, from R5-76.4, dorsal view, x 20.
    7. UA 12231, free cheek, from R5-76.4 (98), dorsal view, x 20.
    8. UA 12232, cranidium, from R5-76.4 (98), dorsal view, x 20.
    9. UA 12233, cranidium, from R6-55, dorsal view, x 20.
    10. UA 12234, free cheek, from R6-55, dorsal view, x 20.
    11. UA 12235, pygidium, from R5-76.4A, dorsal view, x 20.
    12. UA 12236, pygidium, from R5-76.4A, dorsal view, x 20.
    13. UA 12237, pygidium, from R5-76.4 (98), dorsal view, x 20.
    14. UA 12238, pygidium, from R5-76.4, dorsal view, x 20.
    15. UA 12239, transitory pygidium with one unreleased thoracic segment possessing an axial spine, from R5-76.4, dorsal view, x 20.
16-23. *Amblycranium variabile flexus* n. subsp.
    16-18. UA 12240, holotype, cranidium, from SE-152, x 10; 16. Dorsal view, 17. Left lateral view, 18. Anterior view.
    19. UA 12241, cranidium, from R6-55, dorsal view, x 10.
    20. UA 12242, cranidium, from SE-152, dorsal view, x 15.
    21. UA 12243, cranidium, from SE-152, dorsal view, x 10.
    22. UA 12244, transitory pygidium possessing one unreleased thoracic segment lacking axial spine, from SE-152, dorsal view, x 15.
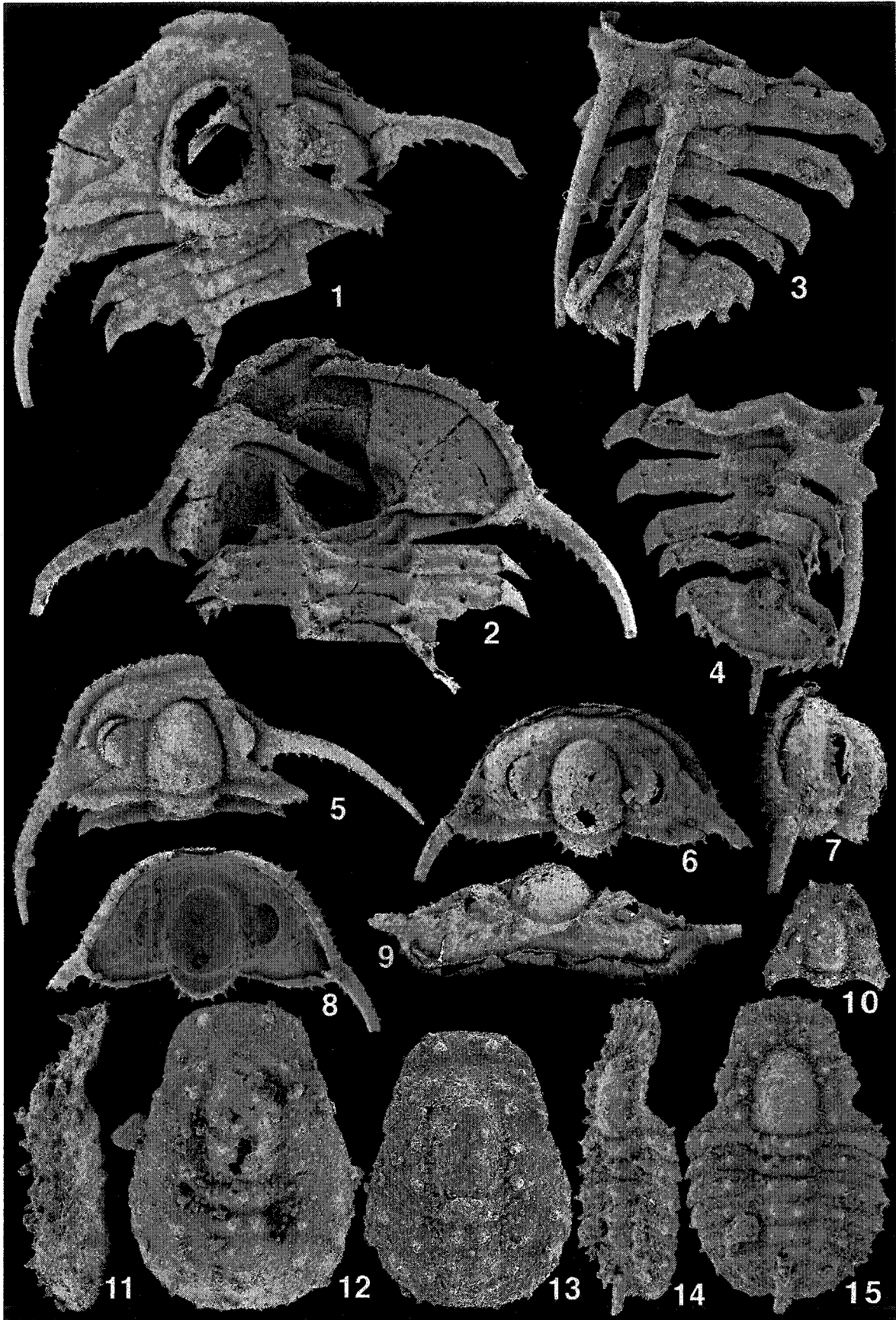   23. UA 12245, cranidium, from R5-76.4A, dorsal view, x 10.

424
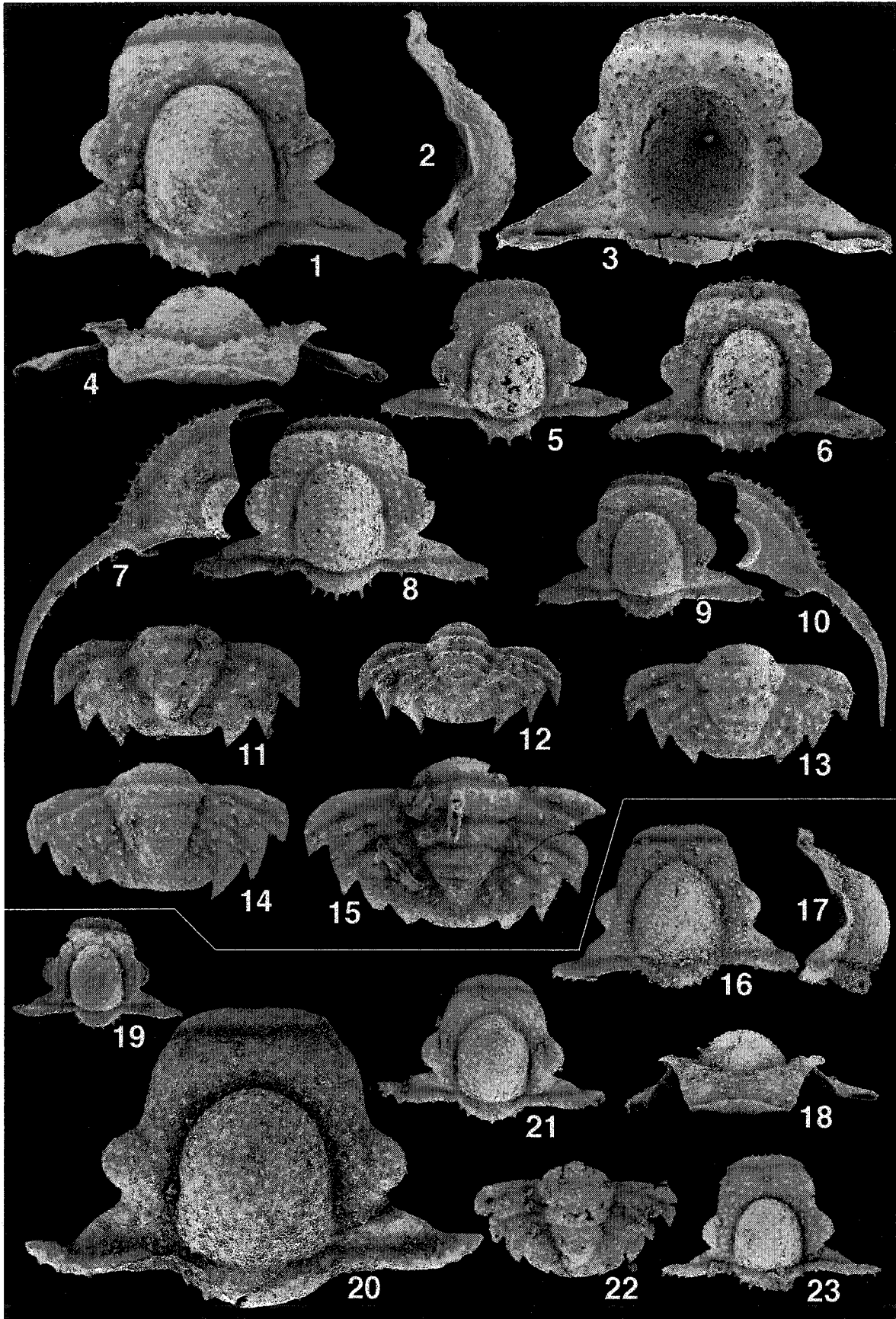
PLATE III-29. *Amblycranium variabile rectus* n. subsp. and *Amblycranium variabile parallelus* n. subsp.

1-6. *Amblycranium variabile rectus* n. subsp.
  1. UA 12246, holotype, cranidium, from R6-55, dorsal view, x 15.
  2. UA 12247, cranidium, from R6-55, dorsal view, x 20.
  3-5. UA 12248, pygidium, from R6-55, x 20; 3. Left lateral view, 4. Dorsal view, 5. Posterior view.
  6. UA 12249, small cranidium from R6-55, dorsal view, x 40.
7-14. *Amblycranium variabile parallelus* n. subsp.
  7-10. UA 12250, holotype, cranidium, from R5-87.7, x 20; 7. Ventral view, 8. Right lateral view, 9. Dorsal view, 10. Anterior view.
  11. UA 12251, cranidium, from R5-87.7, dorsal view, x 20.
  12. UA 12252, free cheek, from R5-87.7, dorsal view, x 20.
  13. UA 11031, cranidium, from R5-86, dorsal view, x 20. (note: Lee and Chatterton (1997) inadvertently noted that the specimen occurs in R6-76.4)
  14. UA 12253, cranidium, from R5-87.7, dorsal view, x 20.

426
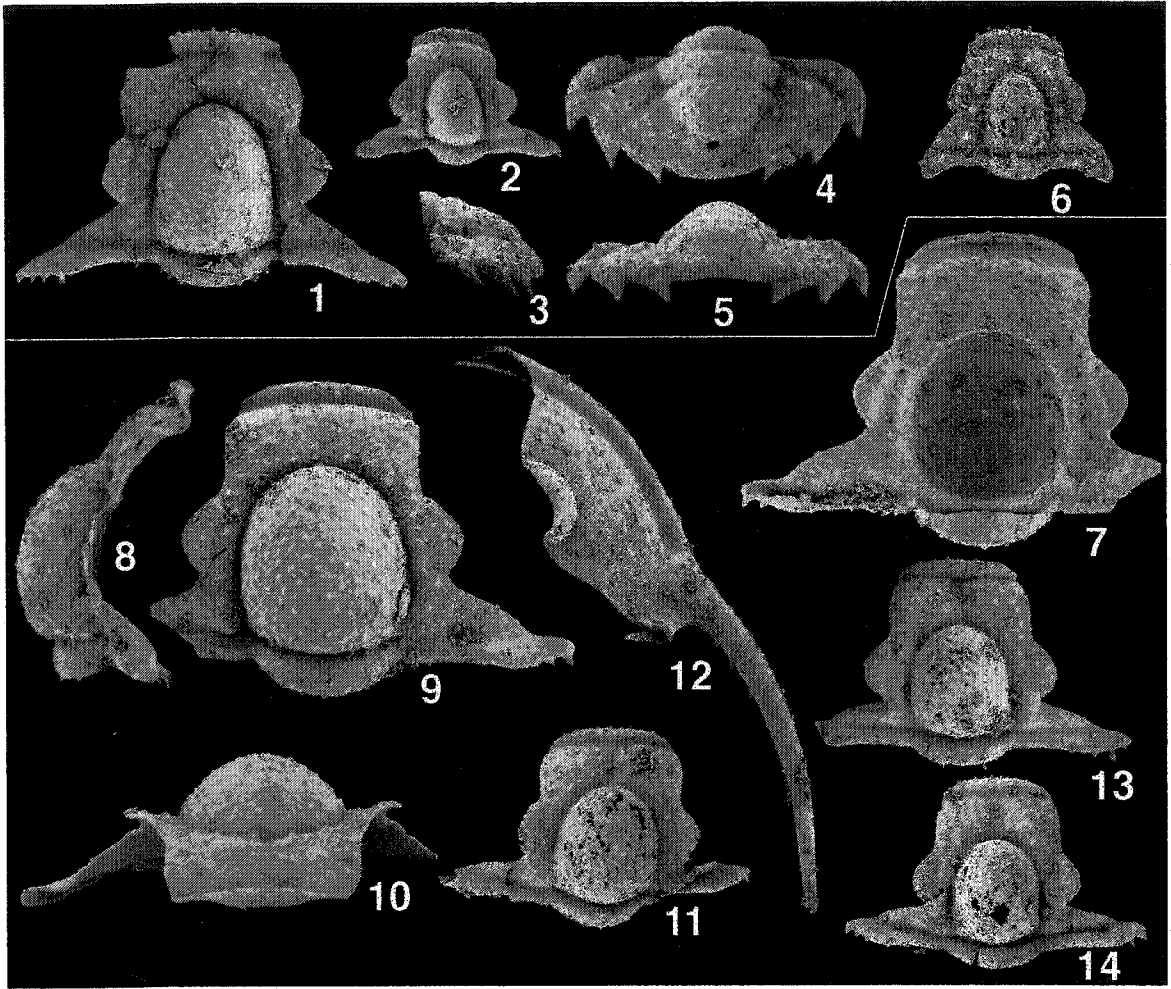
PLATE III-30. *Amblycranium convergia convergia* n. subsp., *Amblycranium convergia paraconvergia* n. subsp. and *Amblycranium inflatus* n. sp.

1-3. *Amblycranium convergia convergia* n. subsp.
   1. UA 12254, holotype, cranidium, from R5-76.4 (97), dorsal view, x 20.
   2. UA 12255, pygidium,from R5-76.4 (97), dorsal view, x 20.
   3. UA 12256, cranidium, from R5-76.4A, dorsal view, x 20.
4-12. *Amblycranium convergia paraconvergia* n. subsp.
   4. UA 12257, free cheek, from R5-87.7(97), dorsal view, x 20.
   5-7. UA 12258, holotype, cranidium, from R5-87.7(97), x 20; 5. Dorsal view, 6. Left lateral view, 7. Anterior view.
   8. UA 12259, pygidium, from R5-87.7(97), dorsal view, x 20.
   9. UA 12260, pygidium, from R5-86, dorsal view, x 20.
   10. UA 12261, cranidium, from R5-86, dorsal view, x 20.
   11. UA 12262, small cranidium, from R5-86, dorsal view, x 30.
   12. UA 12263, pygidium, from R5-86, dorsal view, x 20.
13-17. *Amblycranium inflatus* n. sp.
   13. UA 12264, cranidium, from R5-86, dorsal view, x 15.
   14-17 UA 12265, holotype, cranidium, from R5-87.7, x 20; 14. Dorsal view, 15. Anterior view, 16. Left lateral view, 17. Ventral view.
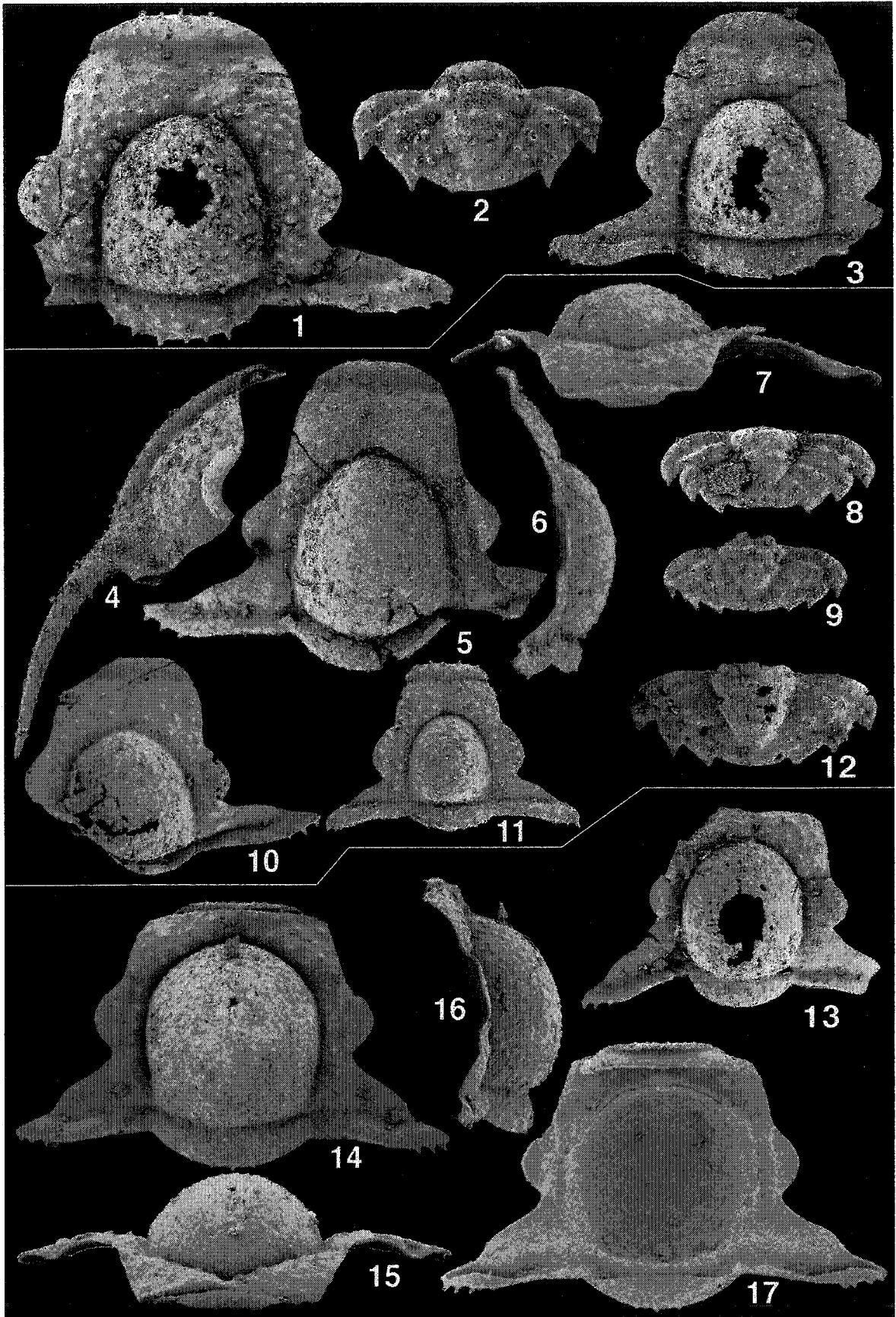
PLATE III-31. *Amblycranium transversus* n. sp.

1-19. *Amblycranium transversus* n. sp.
    1-4. UA 12266, holotype, cranidium, from R6-35, x 20; 1. Right lateral view, 2. Dorsal view, 3. Ventral view, 4. Anterior view.
    5. UA 12267, free cheek, from R6-38, dorsal view, x 20.
    6. UA 12268, cranidium, from R6-35, dorsal view, x 20.
    7, 15. UA 12269, free cheek, from R6-35, x 20; 7. Ventral view, 15. Dorsal view.
    8. UA 12270, pygidium, from R6-35, dorsal view, x 15.
    9. UA 12271, pygidium, from R6-35, dorsal view, x 15.
    10. UA 12272, pygidium, from R6-38, dorsal view, x 15.
    11. UA 12273, cranidium, from R6-38, dorsal view, x 20.
    12-14. UA 12274, pygidium, from R6-35, x 15; 12. Dorsal view, 13. Posterior view, 14. Ventral view.
    16. UA 12275, cranidium, from R6-38, dorsal view, x 20.
    17. UA 12276, pygidium, from R6-38, dorsal view, x 20.
    18. UA 12277, cranidium, from R6-35, dorsal view, x 20.
    19. UA 12278, pygidium, from R6-35, dorsal view, x 15.
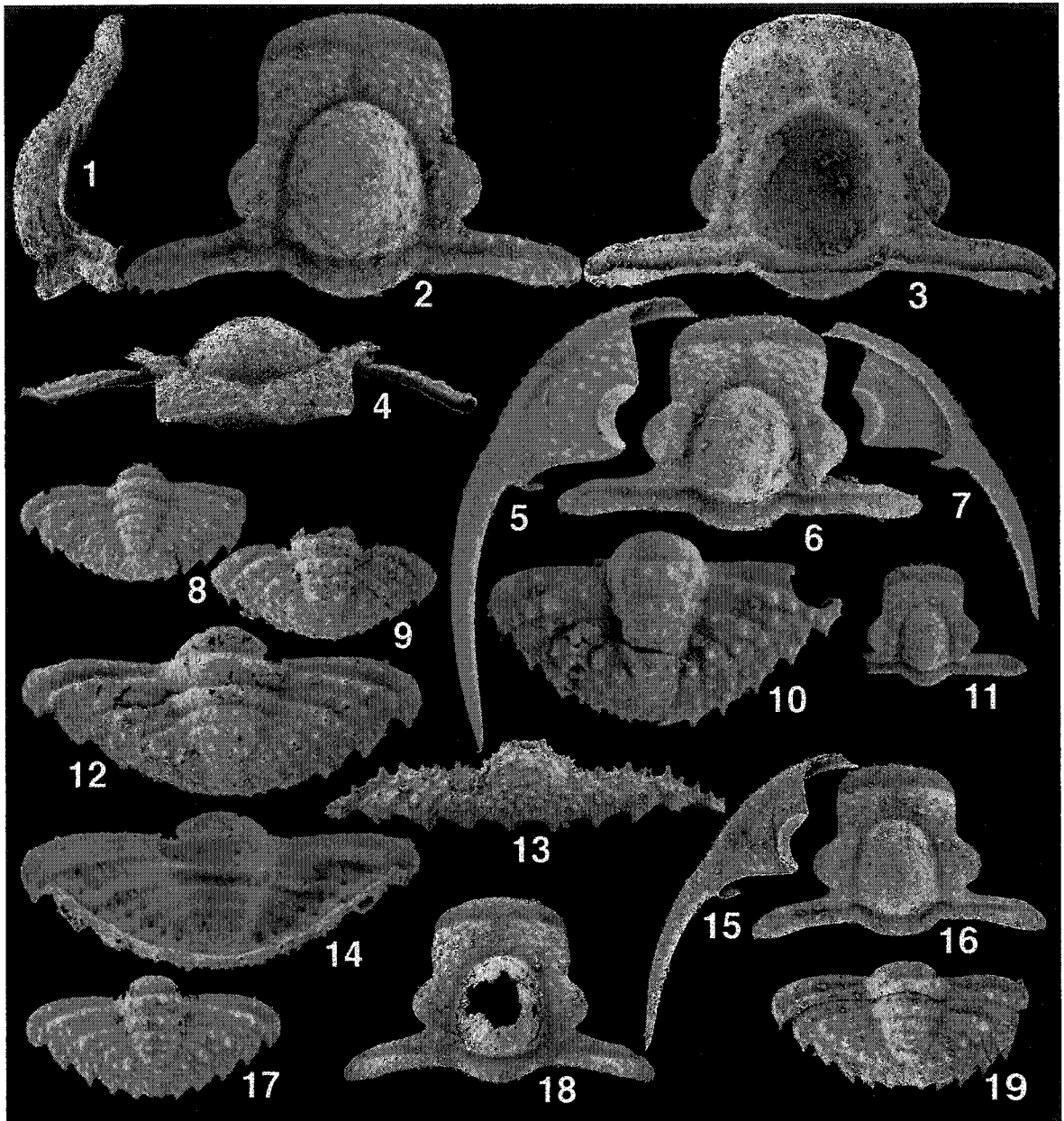
PLATE III-32. *Amblycranium hystricuriensis* n. sp.

1-17. *Amblycranium hystricuriensis* n. sp.
1. UA 12279, cranidium, from R6-35, dorsal view, x 20.
2. UA 12280, cranidium, from R6-38, dorsal view, x 20.
3. UA 12281, cranidium, from R6-35, dorsal view, x 20.
4. UA 12282, pygidium, from R6-38, dorsal view, x 20.
5-7. UA 12283, pygidium, from R6-38, x 20; 5. Ventral view, 6. Dorsal view, 7. Posterior view.
8-10. UA 12284, holotype, cranidium, from R6-35, x 20; 8. Dorsal view, 9. Left lateral view, 10. Anterior view.
11. UA 12285, free cheek, from R6-38, dorsal view, x 20.
12. UA 12286, free cheek, from R6-35, dorsal view, x 20.
13. UA 12287, pygidium, from R6-38, dorsal view, x 20.
14. UA 12288, pygidium, from R6-35, dorsal view, x 40.
15. UA 12289, cranidium, from R6-35, dorsal view, x 20.
16. UA 12290, cranidium, from R5-93.5, dorsal view, x 20.
17. UA 12291, cranidium, from R6-38, dorsal view, x 20.

432
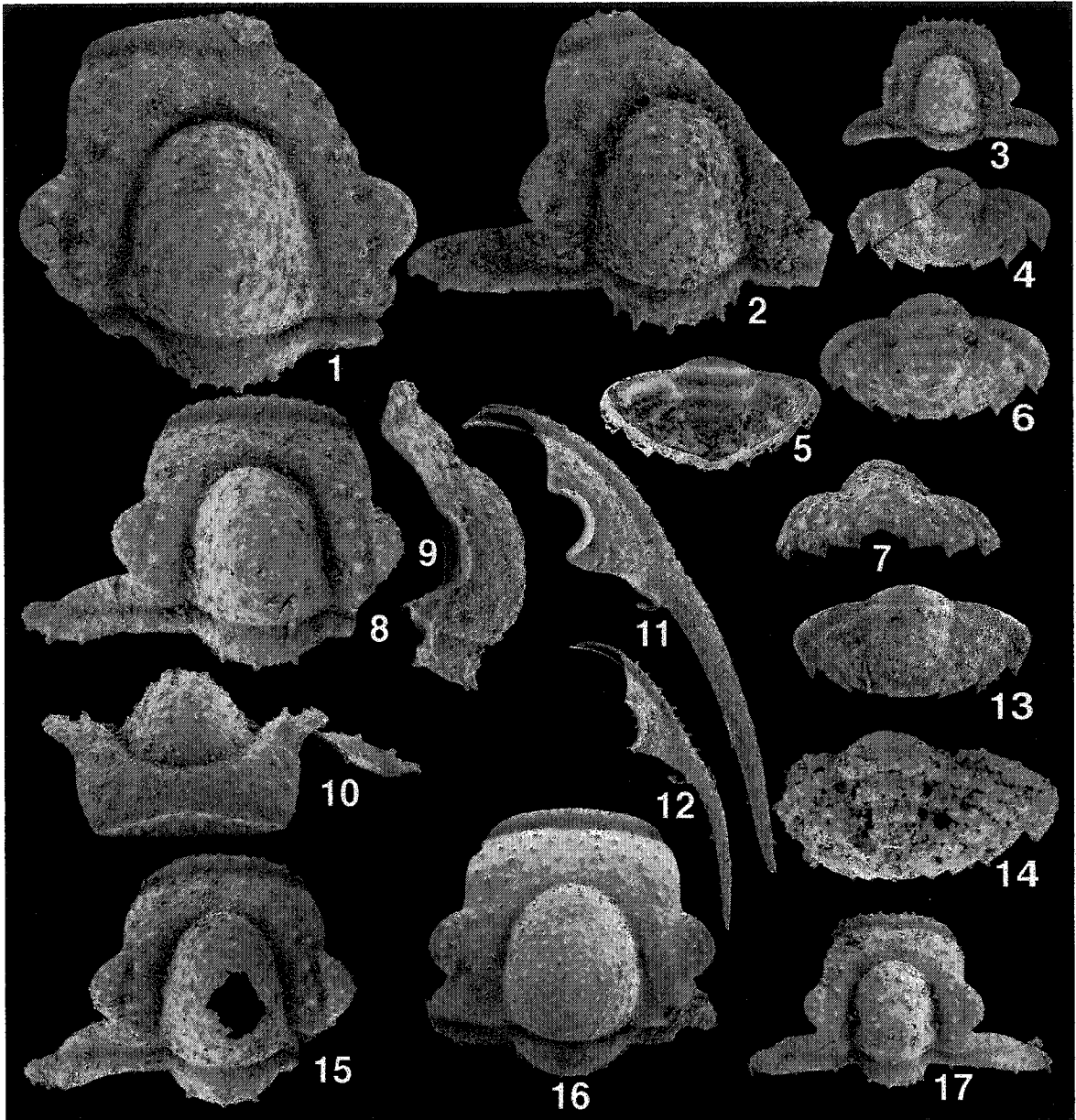
PLATE III-33. *Carinahystricurus triangularus* n. gen. and n. sp. and
Carinahystricurus carinatus (Ross, 1951).

1-18. *Carinahystricurus triangularus* n. gen. and n. sp.
  1-3. UA 12292, holotype, partially articulated specimen consisting of cranidium and three thoracic segments, from R5-76.4, x 20; 1. Oblique right lateral view, 2. Dorsal view, 3. Anterior view.
  4. UA 12293, cranidium, from R5-76.4A, dorsal view, x 10.
  5, 6. UA 12294, cranidium, from R5-76.4, x 10; 5. Right lateral view, 6. Dorsal view.
  7. UA 12295, cranidium ,from R5-76.4, dorsal view, x 10.
  8. UA 12296, cranidium, from R5-76.4A, dorsal view, x 10.
  9, 10. UA 12297, cranidium, from R5-76.4, x 10; 9. Dorsal view, 10. Ventral view.
  11. UA 12298, cranidium, from R5-76.4, dorsal view, x 15.
  12. UA 12299, cranidium, from R5-76.4, dorsal view, x 10.
  13. UA 12300, cranidium, from R5-76.4A, dorsal view, x 10.
  14-16. UA 12301, partially articulated specimen consisting of cranidium, left free cheek and two thoracic segments, from R5-76.4, x 20; 14. Dorsal view, 15. Anterior view, 16. Left lateral view.
  17. UA 12302, thoracopygidium with two thoracic segments, from R5-76.4 (98), dorsal view, x 20.
  18. UA 12303, thoracopygidium with two thoracic segments, from R5-76.4, dorsal view, x 20.
19. *Carinahystricurus carinatus* (Ross, 1951).
  19. UA 12304, cranidium, from R5-76.4A, dorsal view, x 20.

434
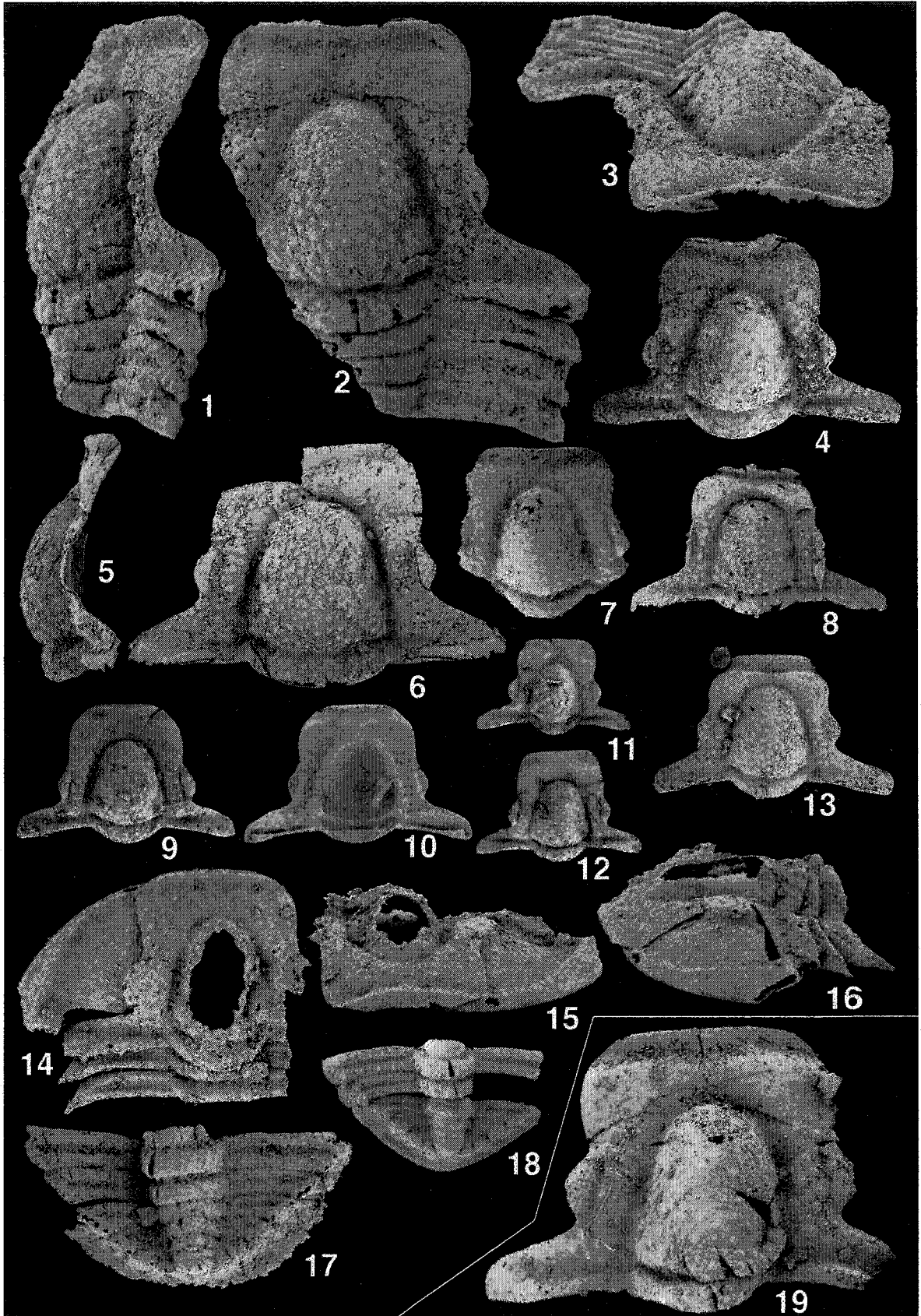
PLATE III-34. *Carinahystricurus triangularus* n. gen. and n. sp.

1-9. *Carinahystricurus triangularus* n. gen. and n. sp.

    1, 2, 4-6. UA 12305, partially articulated specimen consisting of cranidium, left free cheek, and nine thoracic segments, from R5-87.7; 1. Dorsal view, x 15, 2. Posterior view, x 10, 4. Oblique right lateral view, x 10, 5. Oblique left lateral view showing free cheek, x 10, 6. Oblique ventral view, x 15.

    3. UA 12306, pygidium, from R5-87.7, dorsal view, x 20.

    7-9. UA 12307, pygidium, from R5-87.7, x 10; 7. Dorsal view, 8. Posterior view, 9. Right lateral view.

436
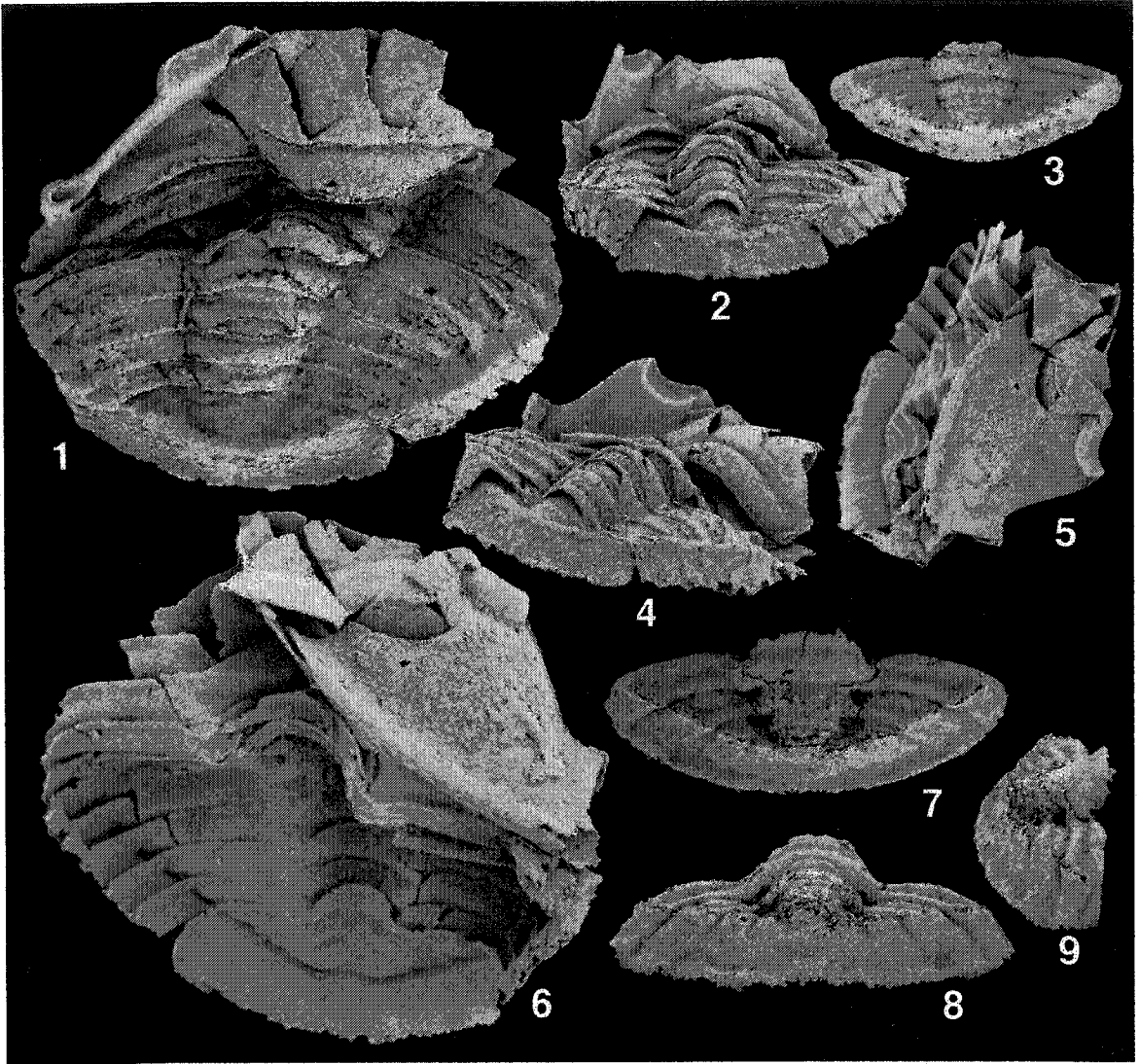
PLATE III-35. *Carinahystricurus minuocularis* n. gen. and n. sp.

1-22. *Carinahystricurus minuocularis* n. gen. and n. sp.

  1, 3, 8. UA 12308, free cheek, from SE-152; 1. Dorsal view, x 10, 3. Ventral view, x 10, 8. Oblique right lateral view, x 5.

  2. UA 12309, holotype, cranidium, from SE-152, dorsal view, x 10.

  4-7. UA 12310, cranidium, from SE-152, x 10; 4. Dorsal view, 5. Anterior view, 6. Ventral view, 7. Left lateral view.

  9. UA 12311, cranidium, from SE-152, dorsal view, x 10.

  10. UA 12312, cranidium, from R6-55, dorsal view, x 15.

  11. UA 12313, free cheek, from R6-55, dorsal view, x 20.

  12, 13, 16. UA 12314, free cheek, from SE-152, x 10; 12. Oblique dorsal view representing the life position, 13. Dorsal view, 16. Left lateral view.

  14. UA 12315, cranidium, from SE-152, dorsal view, x 10.

  15. UA 12316, cranidium, from R6-55, dorsal view, x 10.

  17-20. UA 12317, pygidium, from SE-152, x 20; 17. Dorsal view, 18. Posterior view, 19. Oblique left lateral view, 20. Ventral view.

  21, 22. UA 12318, pygidium, from SE-152, x 20; 21. Right lateral view, 22. Drosal view.

438
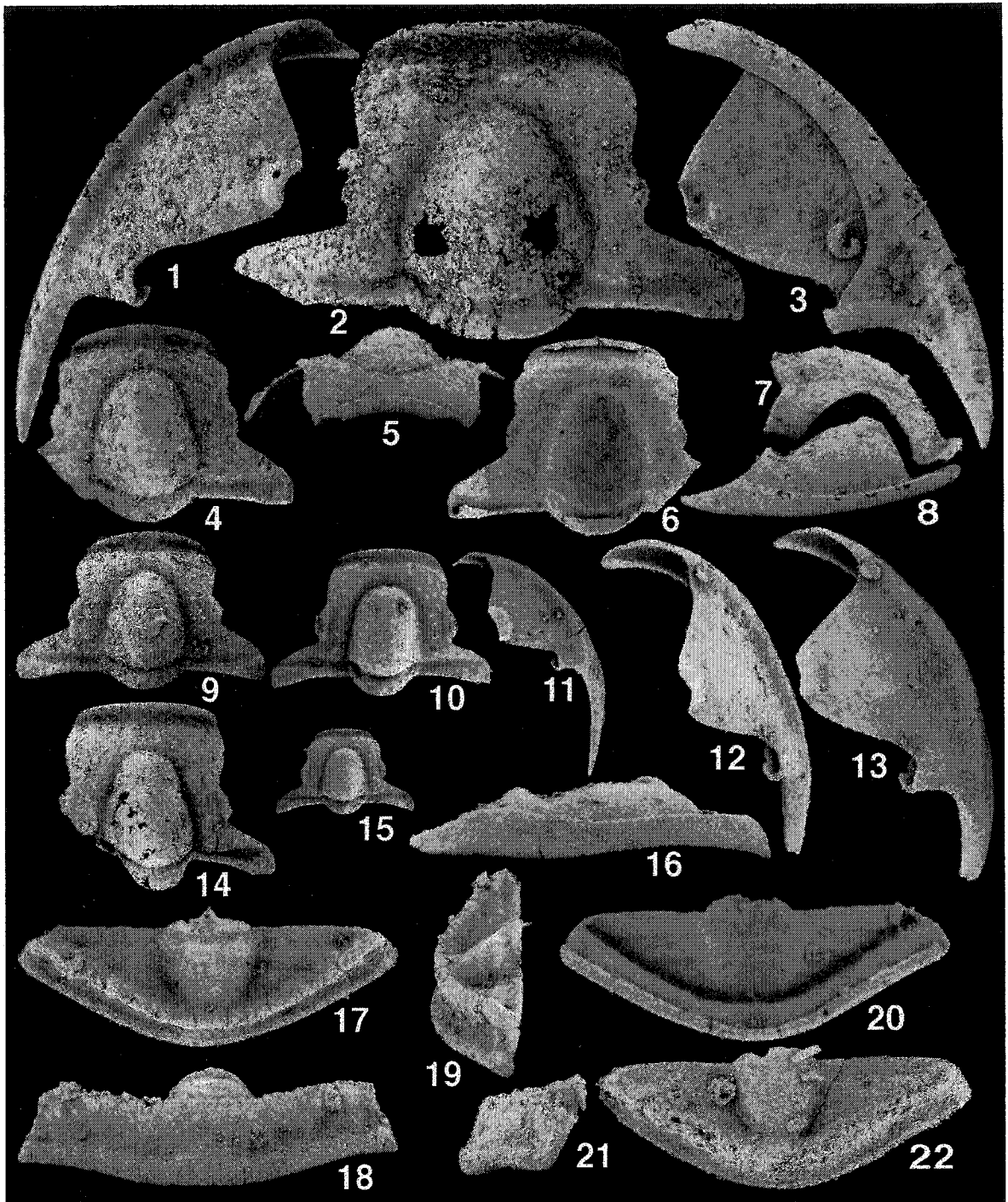
PLATE III-36. *Carinahystricurus tasmanacarinatus* n. gen. and n. sp.

1-9. *Carinahystricurus tasmanacarinatus* n. gen. and n. sp. All specimens are from La1.5 Zone (Lancefieldian Series) of Florentine Valley Formation, Tasmania, Australia.
  1-3. UTGD 81049, cast of cranidium, x 7.5; 1. Dorsal view, 2, Right lateral view, 3. Anterior view.
  4, 6, 7. UTGD 98080, cast of pygidium, x 7.5; 4. Oblique right lateral view, 6. Dorsal view, 7. Posterior view.
  5, 8, 9. UTGD 98084, cast of free cheek; 5. Dorsal view, 6. Left lateral view, 9. Oblique anterior view.
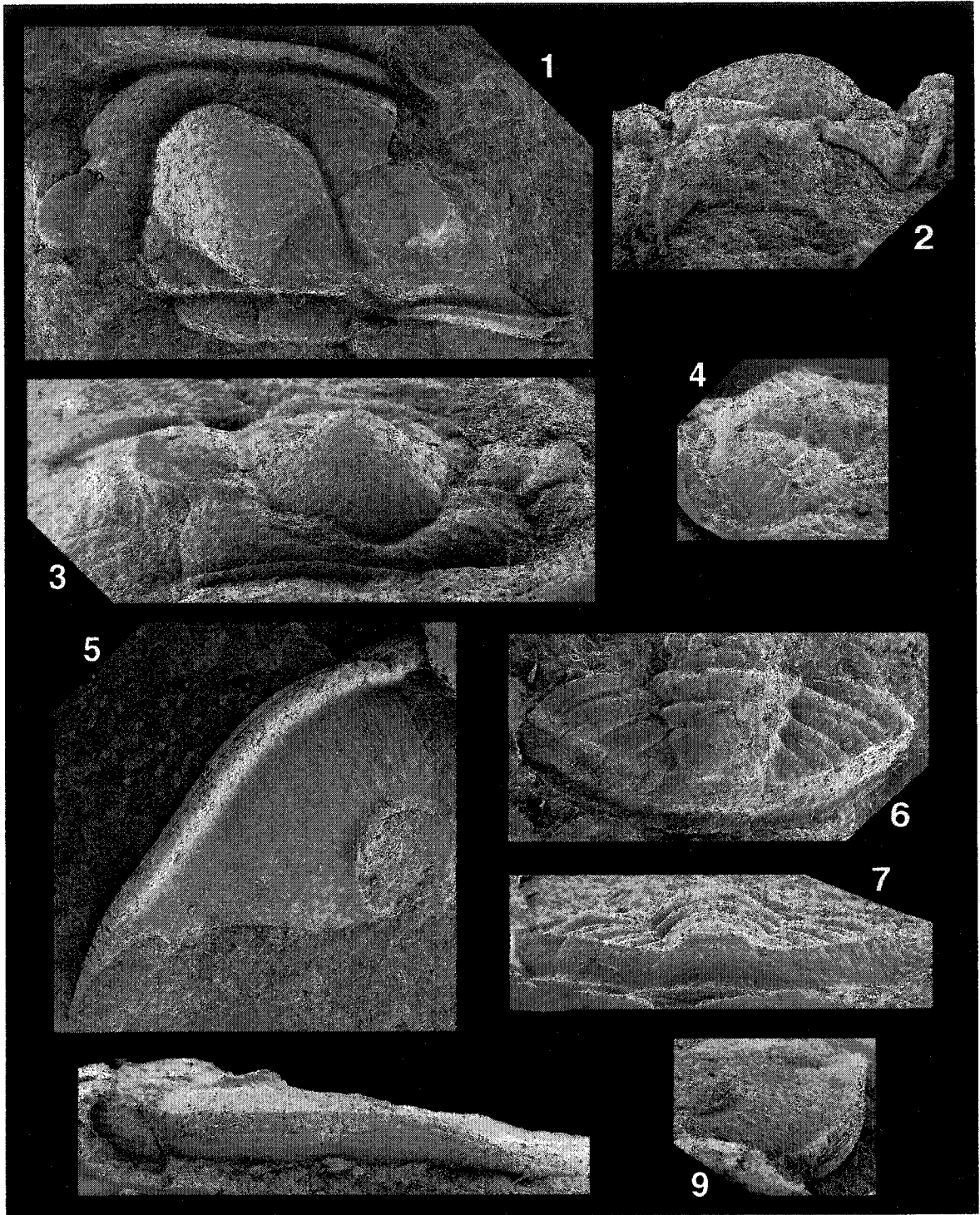
PLATE III-37. *Etheridgaspis carolinensis* (Etheridgaspis, 1919) and *Hystricurus?*
megalops Kobayashi, 1934.

1-12. *Etheridgaspis carolinensis* (Etheridgaspis, 1919). All specimens are from early
Bendigonian strata of Caroline Creek Sandstone,Tasmania, Australia.
  1, 2, 4. NMVP 74262, cranidium, x 5; 1. Dorsal view, 2. Oblique right lateral view, 4.
    Oblique anterior view.
  3, 5, 6. NMVP 74267, cranidium, x 5; 3. Dorsal view, 5. Left lateral view, 6. Anterior
    view.
  7-9. NMVP 74273, pygidium, x 5; 7. Dorsal view, 8. Left lateral view, 9. Posterior
    view.
  10, 11. NMVP 74272, pygidium, x 5; 10. Dorsal view, 11. Posterior view.
  12. NMVP 74263, free cheek, dorsal view, x 5.
13-15. *Hystricurus? megalops* Kobayashi, 1934. The cranidium is from La3 Zone
  (Lancefieldian Series) of Florentine Valley Formation, Tasmania, Australia.
  13-15. UTGD 122519, neotype, cranidium, x 7.5; 13. Dorsal view, 14. Oblique left
    lateral view, 15. Anterior view.

442
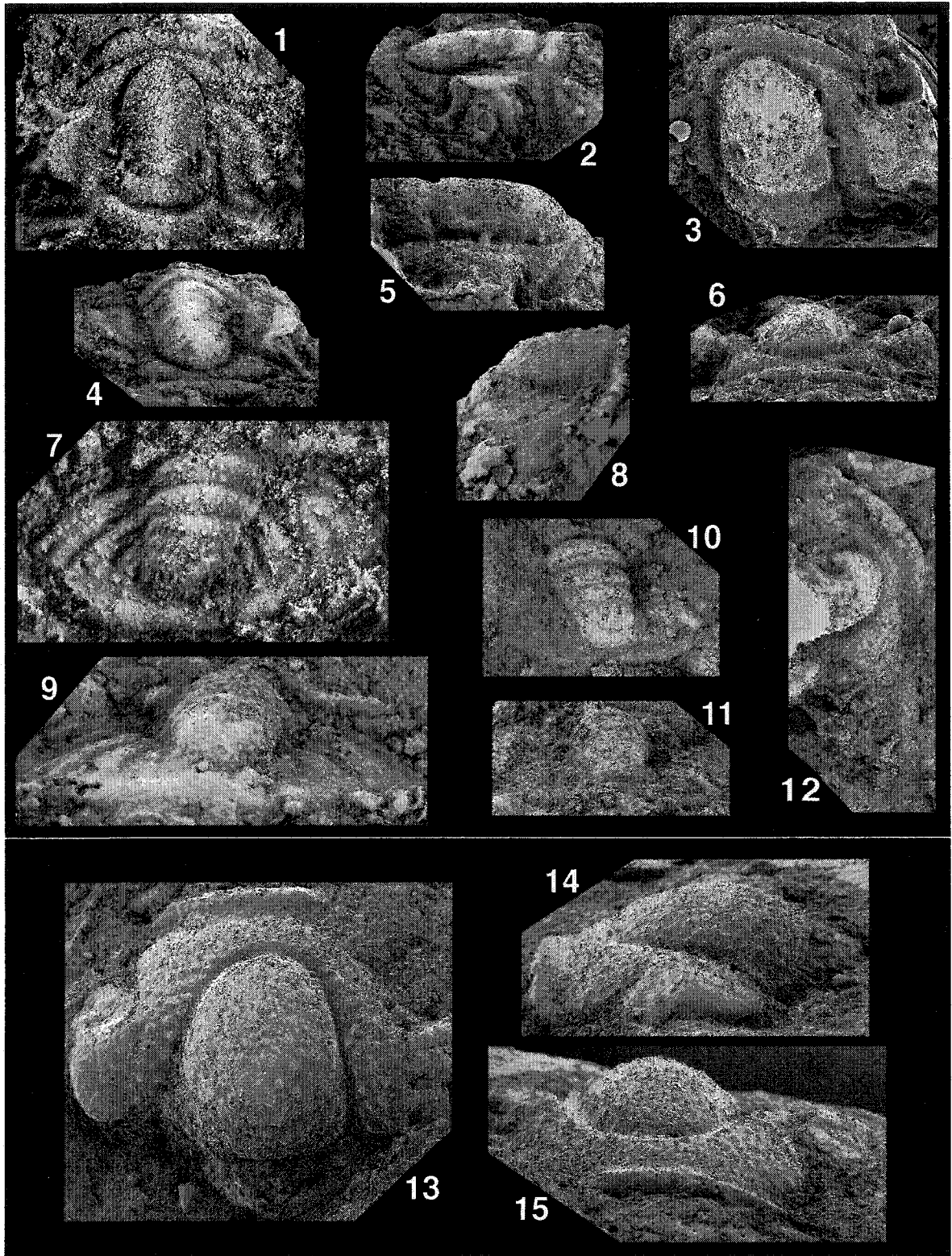
PLATE III-38. *Chattertonella abrupta* (Cullison, 1944) and *Clelandia* sp. aff. *Clelandia utahensis* Ross, 1951.

1-12. *Chattertonella abrupta* (Cullison, 1944).
    1. UA 12319, free cheek, from E-4, dorsal view, x 10.
    2, 5, 6. UA 12320, from SE-87.5, x 20; 2. Dorsal view, 5. Anterior view, 6. Left lateral view.
    3. UA 11850, cranidium, from R5-34.1, dorsal view, x 20.
    4. UA 11851, cranidium, from R5-34.1, dorsal view, x 20.
    7. UA 12321, cranidium, from SE-82T, dorsal view, x 20.
    8. UA 12322, cranidium, from SE-90T, dorsal view, x 20.
    9. UA 11852, cranidium, from R5-34.1, dorsal view, x 20.
    10-12. UA 12323, cranidium, from E-4, x 20; 10. Dorsal view, 11. Left lateral view, 12. Anterior view.
13, 14. *Clelandia* sp. aff. *Clelandia utahensis* Ross, 1951.
    13, 14. UA 12833, complete meraspis, from SL6F, x 40; 13. Left lateral view, 14. Right lateral view.

444
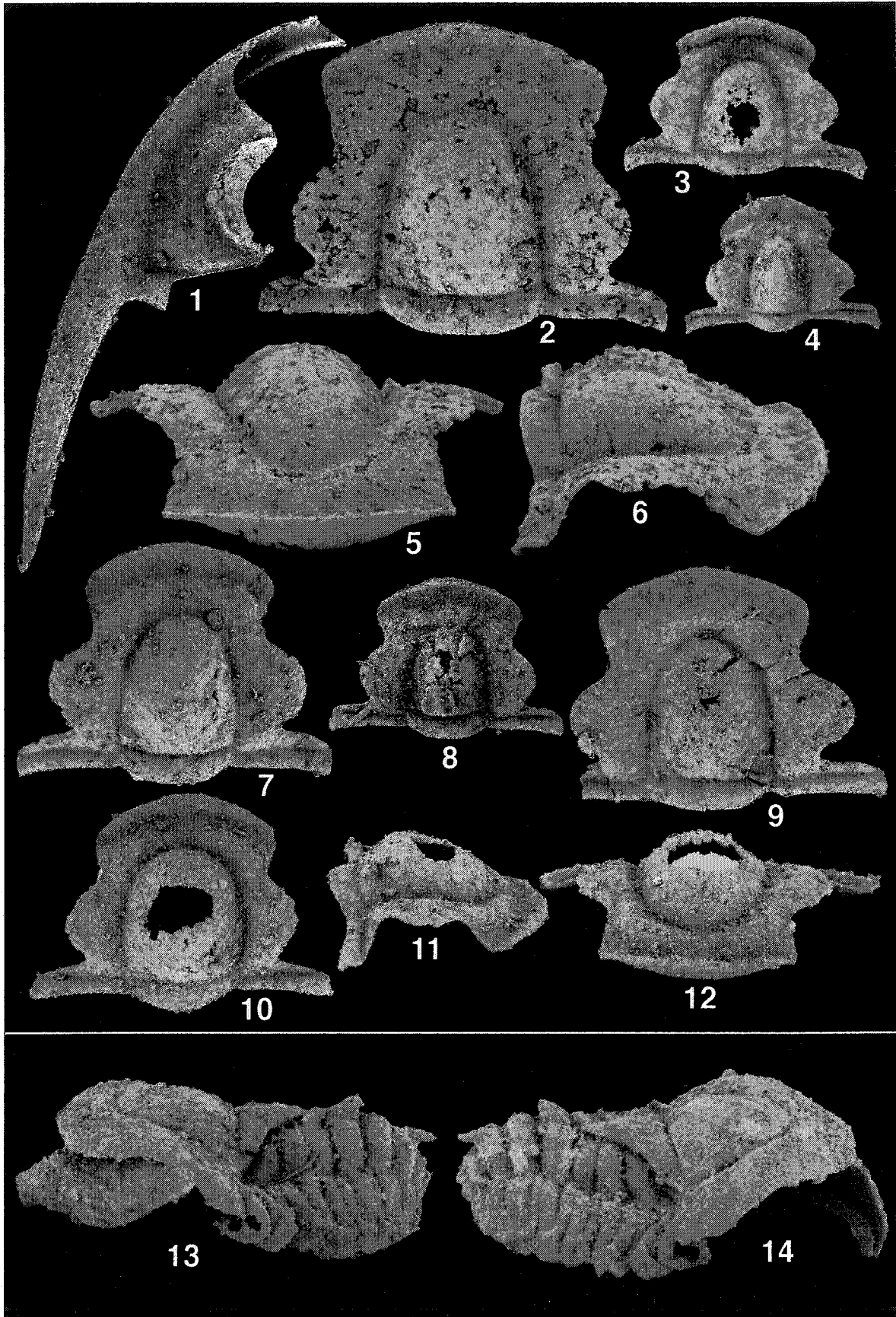
PLATE III-39. *Chattertonella abrupta* (Cullison, 1944), *Clelandia* sp. aff. *Clelandia utahensis* Ross, 1951 and *Clelandia albertensis* Norford, 1969.

1-12. *Chattertonella abrupta* (Cullison, 1944).
  1. UA 11853, pygidium, from R5-34.1, dorsal view, x 20.
  2. UA 12324, pygidium, from SE-82T, dorsal view, x 20.
  3, 5. UA 12325, pygidium, from SE-82T, x 20; 3. Left lateral view, 5. Dorsal view.
  4, 6. UA 12326, pygidium, from SE-87.5, x 20; 4. Dorsal view, 6. Posterior view.
  7. UA 12327, small pygidium, from R5-34.1, dorsal view, x 20.
  8. UA 12328, small pygidium, from R5-34.1, dorsal view, x 20.
  9. UA 12329, small pygidium, from E-4, dorsal view, x 20.
  10. UA 11854, pygidium, from R5-34.1, dorsal view, x 20.
  11. UA 12330, pygidium, from E-4, dorsal view, x 20.
12-17. *Clelandia* sp. aff. *Clelandia utahensis* Ross, 1951.
  12. UA 12834, pygidium, from R5-34.1, x 44, dorsal view.
  13-16. UA 12833, complete meraspis, from SL6F, x 40; 13. Oblique posterior view, 14. Dorsal view (right half of yoked free cheek was inadvertently broken), 15. Ventral view, 16. Posterior view.
17-19. *Clelandia albertensis* Norford, 1969 from *Symphysurina* Zone of Survey Peak Formation, Alberta.
  17. GSC 23618, cranidium, x 20, dorsal view.
  18, 19. GSC 23619, pygidium, x 40; 18. Dorsal view, 19. Posterior view.

446
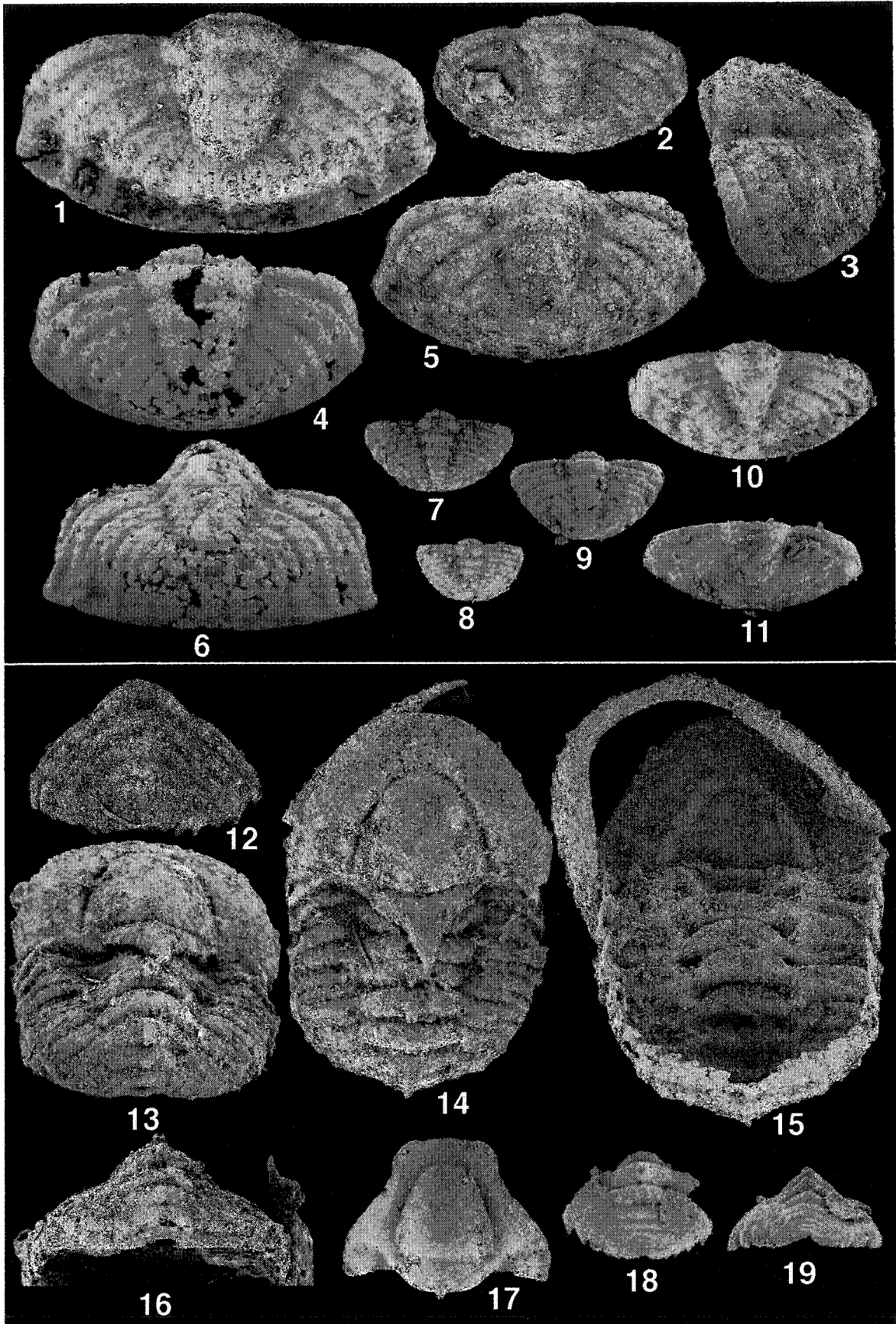
PLATE III-40. *Eurylimbatus amplissimus* n. gen. and n. sp.

1-16. *Eurylimbatus amplissimus* n. gen. and n. sp.
  1, 5-7. UA 12331, holotype, cranidium, from SE-152, x 20; 1. Dorsal view, 5. Anterior view, 6. Left lateral view, 7. Ventral view.
  2, 9, 12, 13. UA 12332, free cheek, from SE-152, x 20; 2. Dorsal view, 9. Right lateral view, 12. Ventral view (note panderian notch), 13. Dorsal view (conventional).
  3, 4, 8. UA 12333, pygidium, from SE-152, x 20; 3. Dorsal view, 4. Posterior view, 8. Left lateral view.
  10. UA 12334, cranidium, from R5-76.4(97), dorsal view, x 20.
  11. UA 12335, cranidium, from SE-152, dorsal view, x 10.
  14. UA 12336, cranidium, from SE-152, dorsal view, x 10.
  15, 16. UA 12337, cranidium, from SE-152, x 20; 15. Dorsal view, 16. Ventral view.

448
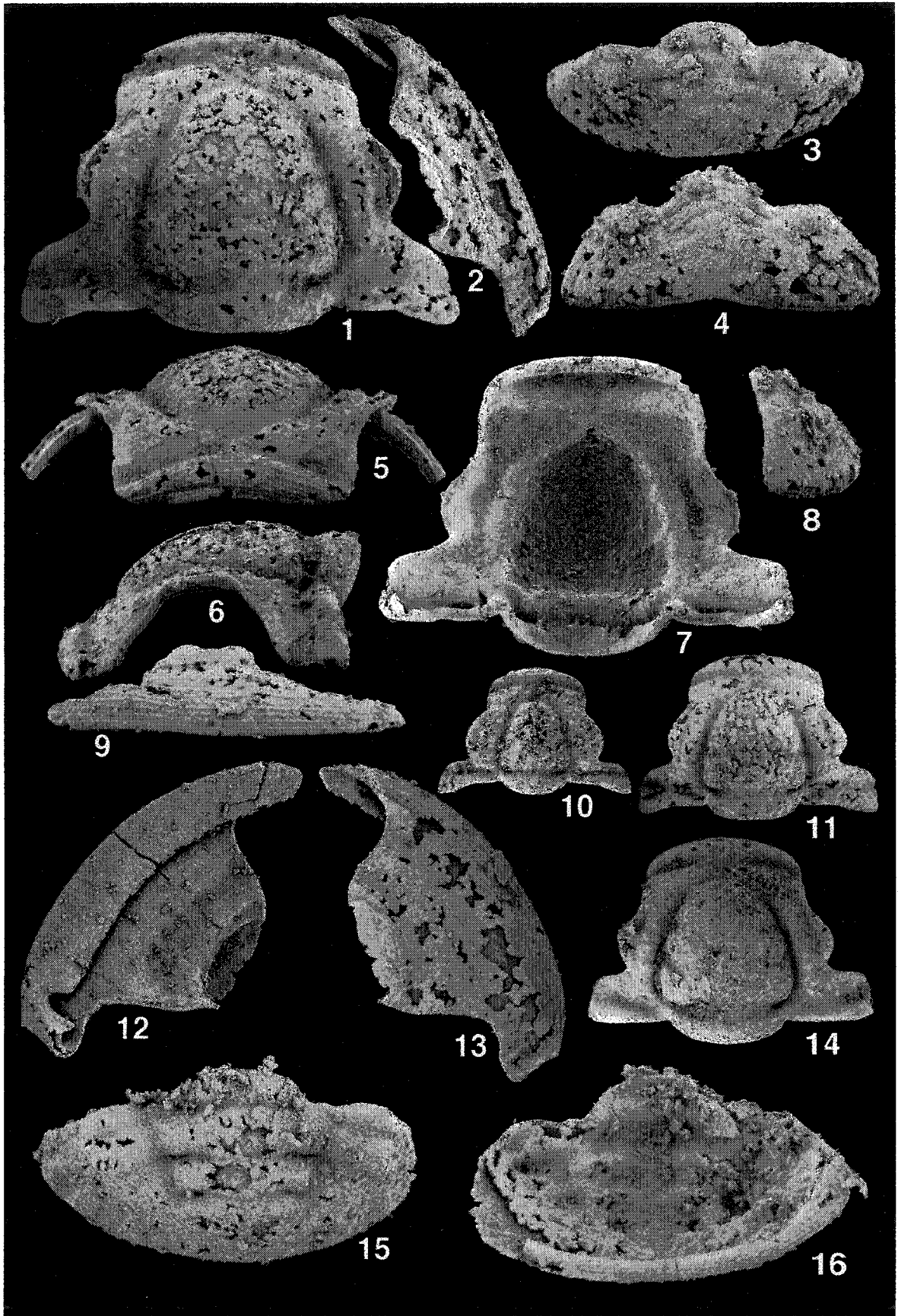
PLATE III-41. *Eurylimbatus sphaerus* n. gen. and n. sp.

1-8. *Eurylimbatus sphaerus* n. gen. and n. sp.
    1-8. UA 12338, holotype, enrolled specimen consisting of 11 thoracic segments, from
        SE-152; 1. Dorsal view, x 20, 2. Right lateral view, x 20, 3. Anterior view, x 20, 4.
        Left lateral view, x 20, 5. Internal view showing overlapping of thoracic segments,
        x 40, 6. Ventral view, x 15, 7. Internal view showing ventral features of pygidium, x
        20, 8. Oblique anterior view, x 20.

450
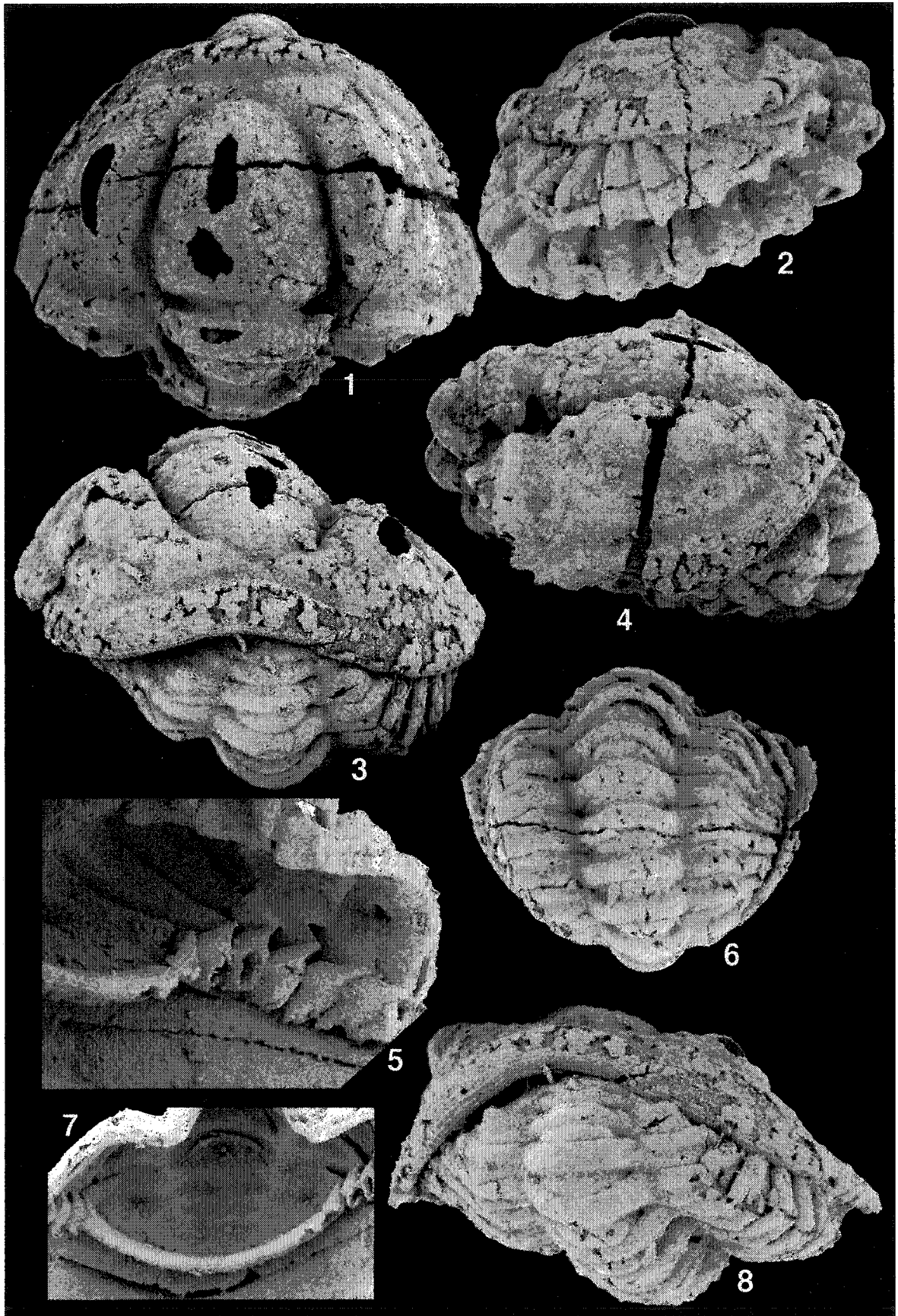
PLATE III-42. *Eurylimbatus amplissimus* n. gen. and n. sp. and *Eurylimbatus sphaerus* n. gen. and n. sp.

1-6. *Eurylimbatus amplissimus* n. gen. and n. sp.
  1. UA 12339, incomplete cranidium with three thoracic segments, from SE-152, dorsal view, x 15.
  2, 3, 5. UA 12340, thoracopygidium consisting of severn thoracic segments and pygidium, from SE-152, x 15; 2. Dorsal view, 3. Posterior view showing posterior features of pygidium, 5. Right lateral view.
  4. UA 12341, thorax consisting of 11 segments, from SE-152, dorsal view, x 10.
  6. UA 12342, partial thorax consisting of 6 thoracic segments, from SE-152, dorsal view, x 10.
7-12. *Eurylimbatus sphaerus* n. gen. and n. sp.
  7. UA 11865, small cranidium, from R5-76.4, dorsal view, x 20.
  8. UA 12343, small cranidium, from R5-87.7, dorsal view, x 20.
  9. UA 12344, cranidium, from R5-87.7, dorsal view, x 20.
  10. UA 11006, small cranidium, from R5-76.4, dorsal view, x 20.
  11. UA 12346, small cranidium, from R5-76.4 (98), dorsal view, x 20.
  12. UA 12347, cranidium, from R5-86, dorsal view, x 20.

452
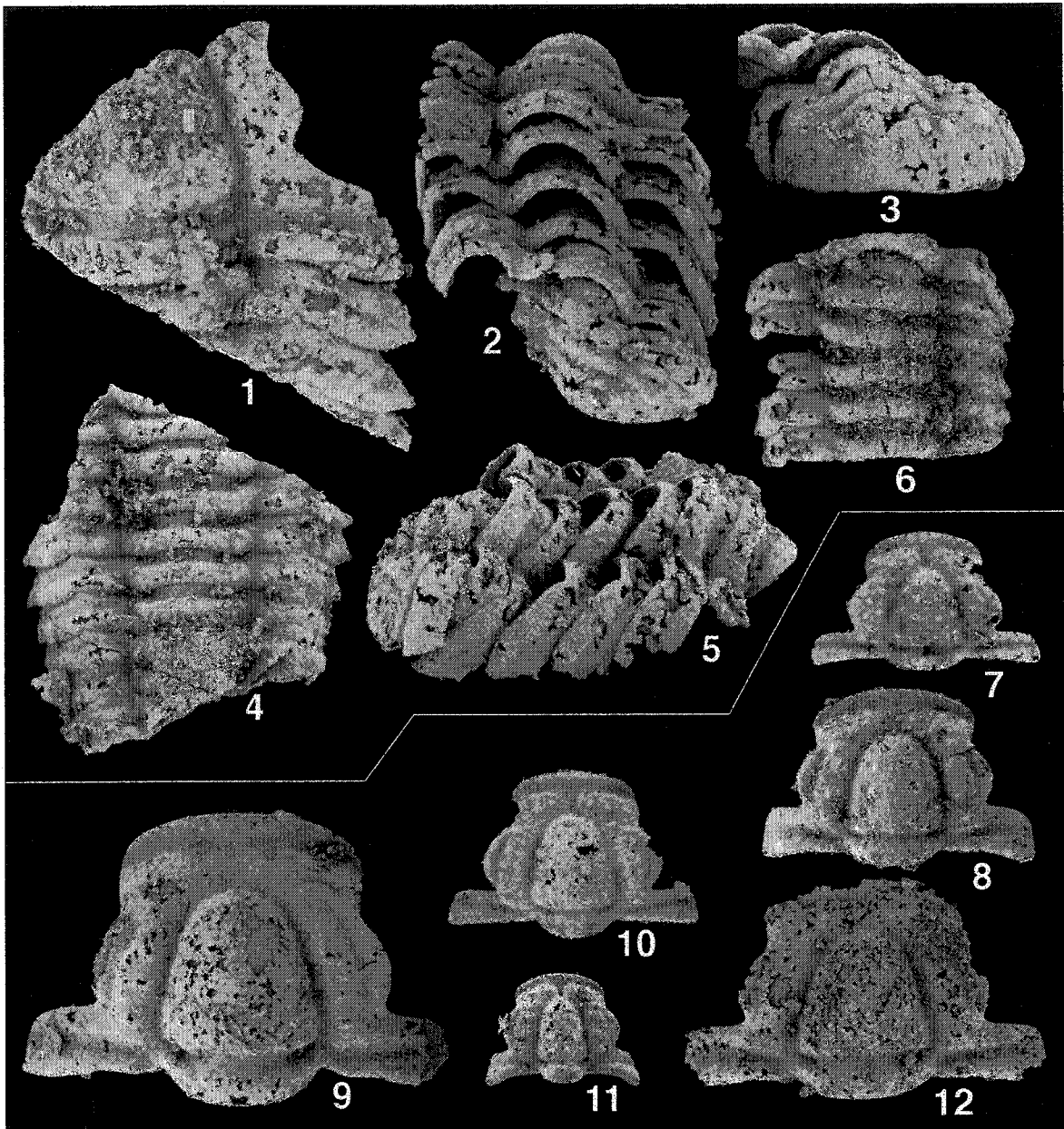
PLATE III-43. *Eurylimbatus acutus* n. gen. and n. sp.

1-15. *Eurylimbatus acutus* n. gen. and n. sp.

    1, 2, 6, 8. UA 12348, holotype, cranidium, from R5-86, x 20; 1. Dorsal view, 2. Left lateral view, 6. Anterior view, 8. Ventral view.

    3, 4. UA 12349, pygidium from R5-87.7, x20; 3. Dorsal view, 4. Posterior view.

    5. UA 12350, pygidium, from R5-87.7, dorsal view, x 20.

    7. UA 12351, pygidium, from R5-76.4 (98), dorsal view, x20.

    9, 11. UA 11874, pygidium, from R5-76.4, x 20; 9. Dorsal view, 10. Posterior view.

    10. UA 12352, pygidium, from R5-87.7(97), dorsal view, x 20.

    12. UA 12353, pygidium, from R5-76.4(97), dorsal view, x 20.

    13, 15. UA 12354, free cheek, from R5-76.4(98), x 20; 12. Dorsal view, 14. Ventral view (note the presence of panderian notch)

    14. UA 12355, cranidium, from R5-76.4(98), dorsal view, x 20.

    16. UA 12356, thoracopygidium consisting of four thoracic segments and pygidium, from R5-76.4(97), x 15.

454
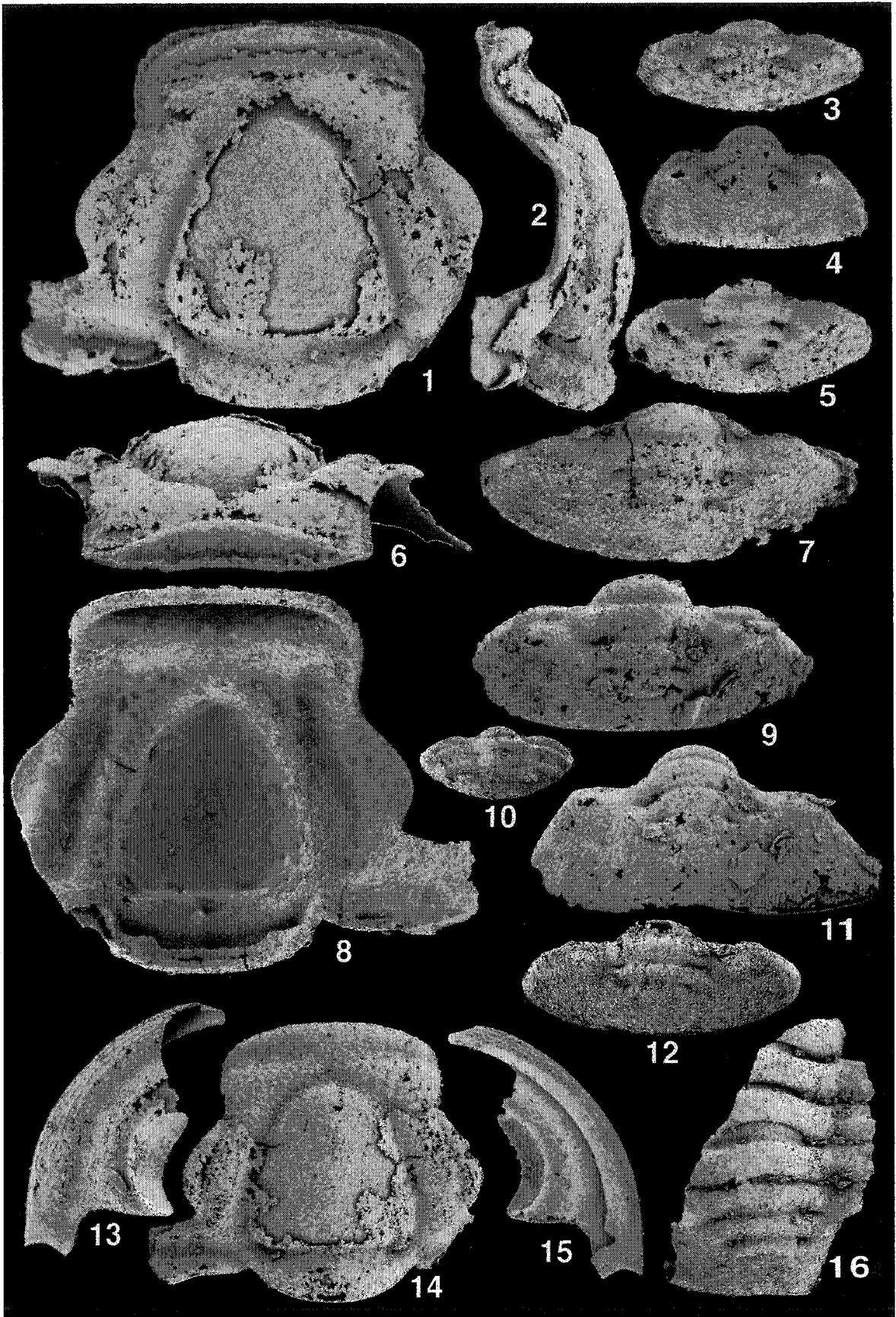
PLATE III-44. *Eurylimbatus acutus* n. gen. and n. sp. and *Cyphaspis* sp.

1-15. *Eurylimbatus acutus* n. gen. and n. sp.
    1-4. UA 12357, cephalon, from R5-86, x 15; 1. Dorsal view, 2. Anterior view, 3.
        Ventral view, 4. Right lateral view.
    5. UA 12358, small cranidium, from R5-86, dorsal view, x 20.
    6. UA 12359, cranidium, from R5-86, dorsal view, x 20.
    7. UA 12360, small cranidium, from R5-86, dorsal view, x 20.
    8. UA 12361, cranidium, from R5-76.4 (97), dorsal view, x 20.
    9. UA 11930, cranidium, from R5-87.7, dorsal view, x 20.
    10. UA 11879, cranidium, from R5-86, dorsal view, x 20.
    11. UA 12362, small cranidium, from R5-86, dorsal view, x 20.
    12. UA 11866, small cranidium, from R5-76.4, dorsal view, x 20.
    13. UA 11864, cranidium, from R5-76.4, dorsal view, x 20: it is provisionally assigned
        to this species and could be assigned to *Eurylimbatus* sp. nov. C.
    14. UA 12363, cranidium, from R5-87.7, dorsal view, x 20.
    15. UA 12364, small cranidium, from R5-76.4, dorsal view, x 40.
16. *Cyphaspis* sp.
    16. UA 12365, pygidium, from Devonian of Morroco, posterior view, x 20.

456
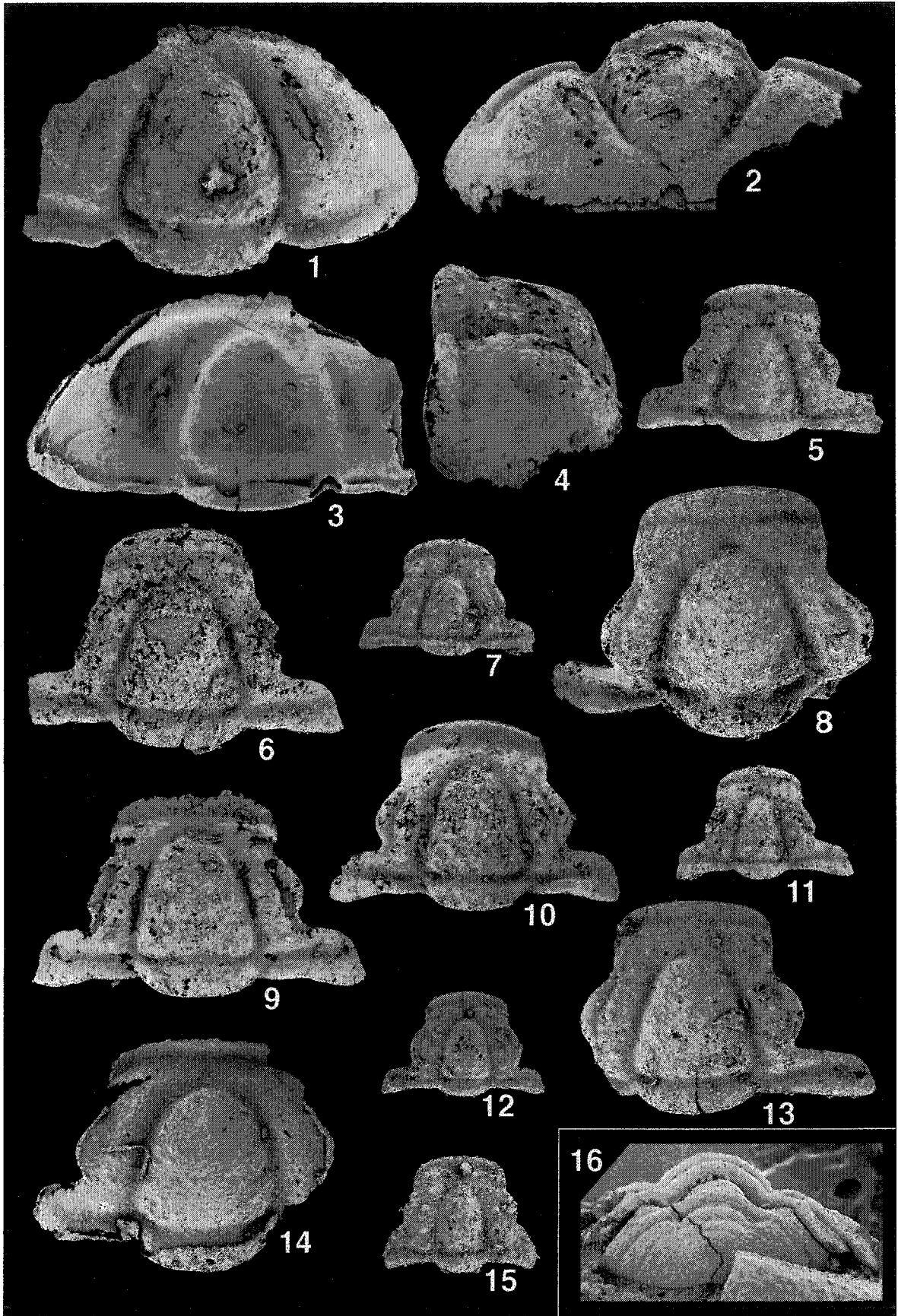
PLATE III-45. *Eurylimbatus* sp. nov. A, *Eurylimbatus* sp. nov. B and *Eurylimbatus* sp. nov. C.

1-4. *Eurylimbatus* sp. nov. A.
  1-4. UA 12366, cranidium, from R5-86, x 30; 1. Anterior view, 2. Ventral view, 3. Dorsal view, 4. Left lateral view.
5-8. *Eurylimbatus* sp. nov. B.
  5-8. UA 11896, cranidium, from R5-93.5, x 30; 5. Dorsal view, 6. Left lateral view, 7. Anterior view, 8. Ventral view.
9-12. *Eurylimbatus* sp. nov. C.
  9-12. UA 12367, cranidium, from R6-55, x 20; 9. Right lateral view, 10. Dorsal view, 11. Anterior view, 12. Ventral view.

458

PLATE III-46. *Holubaspis paraperneri* n. sp. and *Tersella truncatus* (Park, 1993).

1-5. *Holubaspis paraperneri* n. sp. All specimens are from early Tremadocian of Trenice Formation, Central Bohemia.
    1, 2. UA 12368, cranidium, x 3; 1. Dorsal view, 2. Anterior view: both are taken with light photography.
    3-5. UA 12369, pygidium, x 6; 3. Dorsal view, 4. Posterior view, 5. Right lateral view.
6-12. *Tersella truncatus* (Park, 1993). All specimens are from *Protopliomerops* Zone of Mungok Formation, South Korea.
    6, 7, 10. SNUP 338, cranidium, x 10; 6. Dorsal view, 7. Anterior view. 10. Left lateral view.
    8, 9. SNUP 347, pygidium, x 10; 8. Dorsal view, 9. Anterior view.
    11, 12. SNUP ???, cranidium. x 10; 11. Dorsal view, 12. Anterior view.
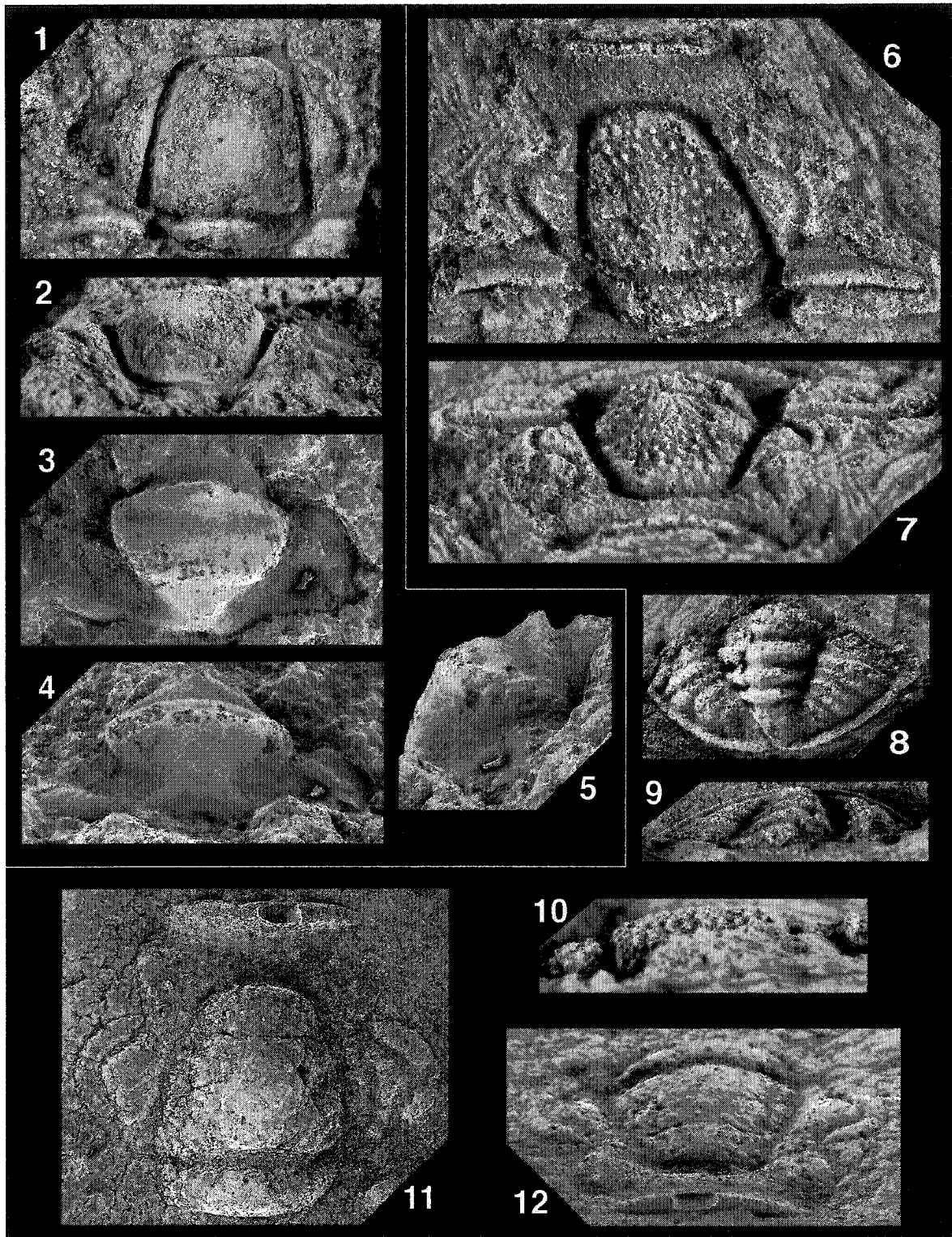
PLATE III-47. *Hillyardina semicylindrica* Ross, 1951.

1-25. *Hillyardina semicylindrica* Ross, 1951.

    1, 3, 6, 12. UA 12370, free cheek, from R6-114 (97); 1. Ventral view, x 15, 3. Dorsal view, x 15. 6. Right lateral view, x 15, 12. Dorsal (conventional) view, x 10.

    2, 4, 5, 10. UA 12371, cranidium, from R6E2, x 15; 2. Dorsal view, 4. Anterior view, 5. Left lateral view, 10. Ventral view.

    7. UA 12372, cranidium, from R5-76.4, x 20.

    8. UA 12373, small cranidium, from R6E2, x 40.

    9. UA 12374, cranidium, from R6E3, x 20.

    11. UA 12375, cranidium, from R6-114 (97), x 10.

    13. UA 12376, cranidium, from R6-114 (97), x 20.

    14, 15. UA 12377, pygidium, from R6-114 (97), x 20; 14. Dorsal view, 15. Posterior view.

    16-18. UA 12378, pygidium, from R6-114 (97), x 20; 16. Oblique dorsal view, 17. Dorsal view, 18. Ventral view.

    19. UA 12379, pygidium, from R6E3, x 10.

    20, 21. UA 11924, pygidium, from R6E2, x 20; 20. Posterior view, 21. Dorsal view.

    22, 23. UA 12380, transitory pygidium with three released thoracic segments, from R6-114 (97), x 20; 22. Dorsal view; 23. Posterior view.

    24, 25. UA 12381, transitory pygidium with two released thoracic segments, from R6-114 (97), x 20; 24. Dorsal view, 25. Posterior view; note the spinose distal end of thoracic pleurae.

462
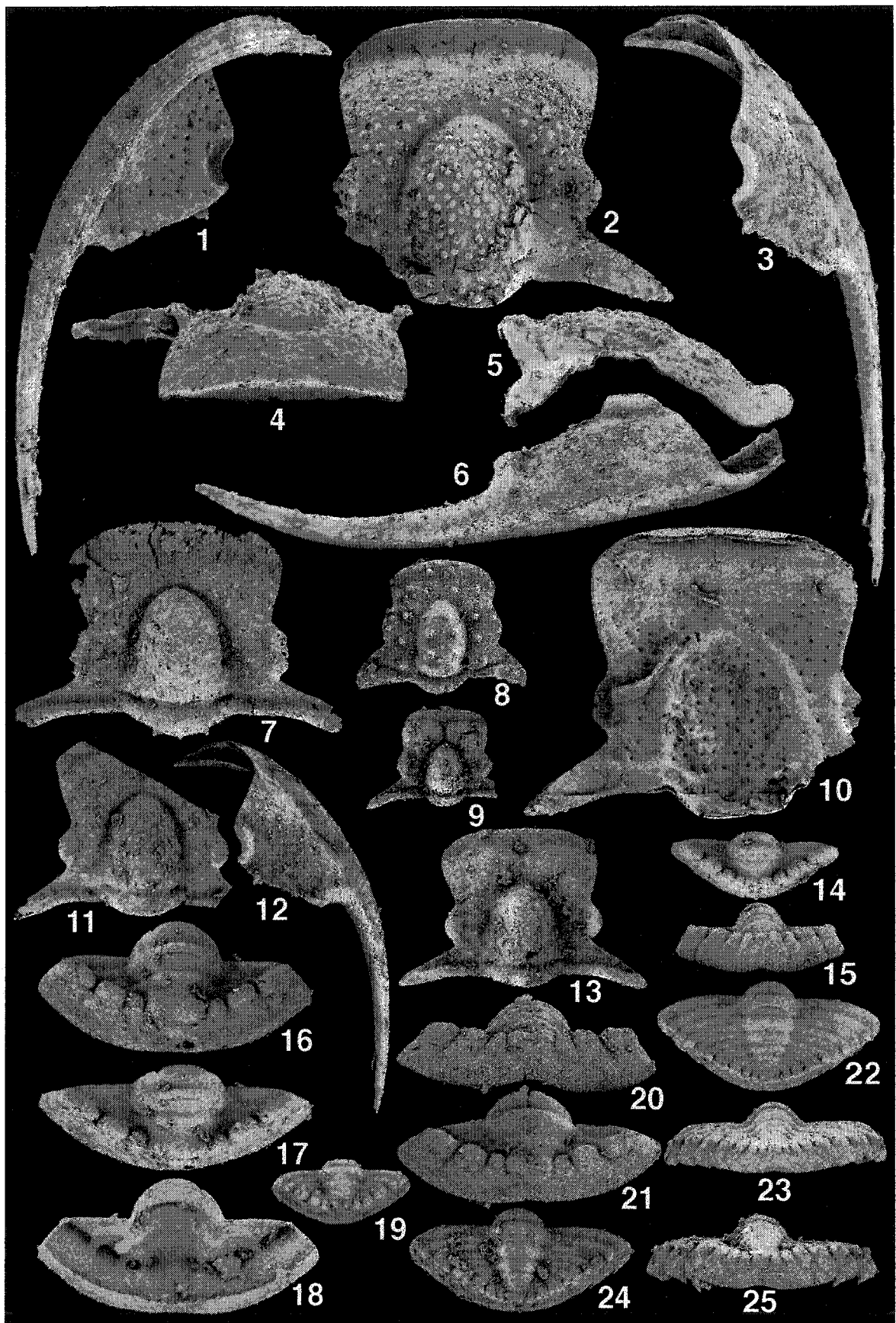
PLATE III-48. *Hillyardina tubularis* n. sp.

1-10. *Hillyardina tubularis* n. sp. All specimens are from La3 Zone (Lancefieldian
   Series) of Florentine Valley Formation, Tasmania, Australia.
   1-3. UTGD 96708, holotype, cast of cranidium, x 5; 1. Dorsal view, 2. Oblique right
      lateral view, 3. Anterior view.
   4, 5, 7. UTGD 96040, partially articularted specimen consisting of incomplete
      cranidium, 11 thoracic segments, and incomplete pygidium; 4. Dorsal view, x 5, 5.
      Magnified view of right lateral view of posterior portion, x 12, 7. Right lateral view,
      x 5. Note: the black arrow points the boundary between thorax and pygidium.
   6. UTGD 96049, pygidiium, dorsal view, x 5.
   8-10. UTGD 96603, cranidium, x 3; 8. Anterior view, 9. Right lateral view, 10. Dorsal
      view.
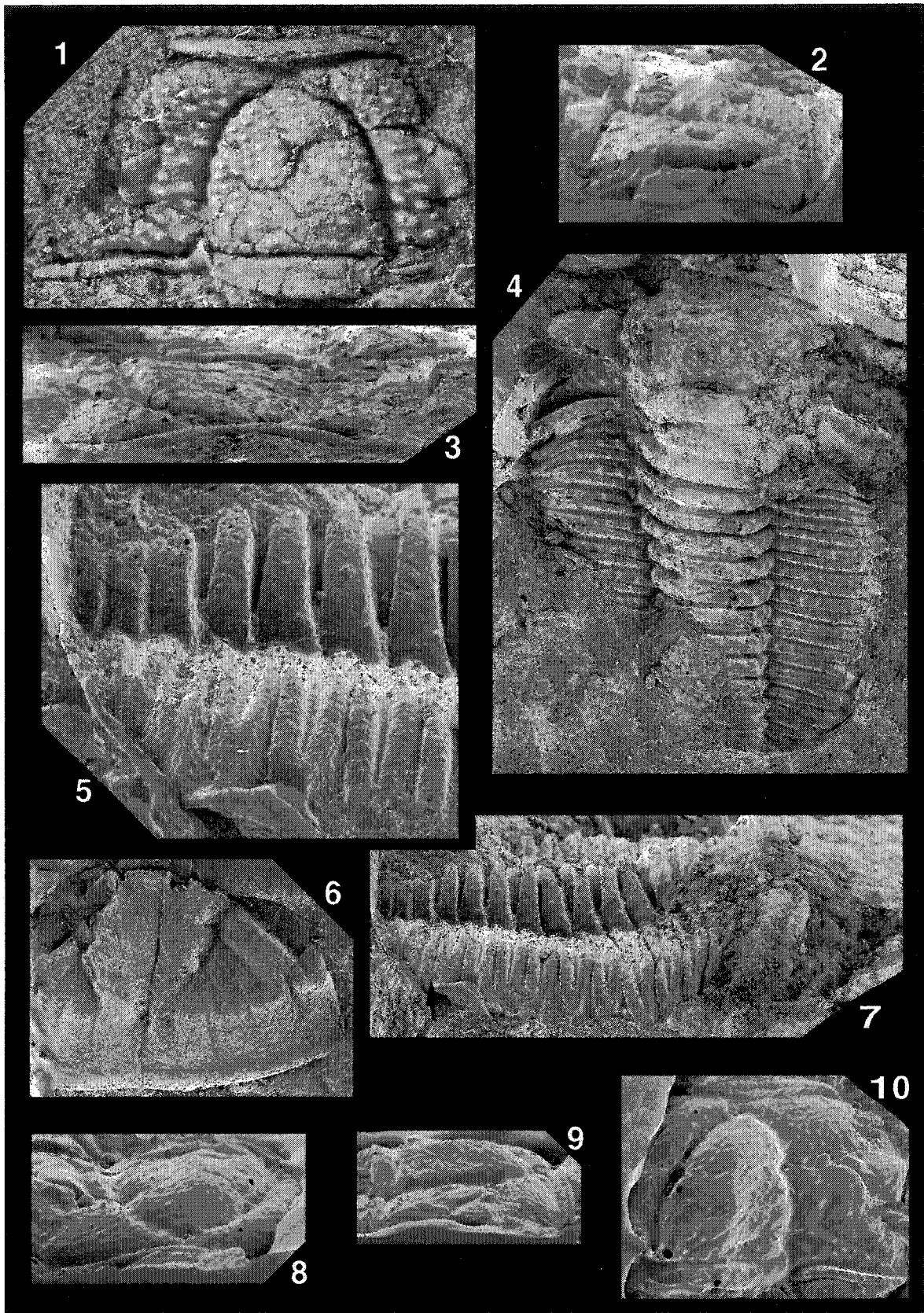
PLATE III-49. *Flectihystricurus flectimembrus* (Ross, 1951) and *Flectihystricurus acumennasus* (Ross, 1951).

1-10. *Flectihystricurus flectimembrus* (Ross, 1951).
　　1, 4. UA 12382, free cheek, from R6E3, x 10; 1. Dorsal view, 4. Left lateral view.
　　2, 5, 6, 9. UA 12383, cranidium, from R6E2, x 15; 2. Anterior view, 5. Right lateral view, 6. Dorsal view, 9. Ventral view.
　　3. UA 11915, cranidium, from R6E2, dorsal view, x 15.
　　7. UA 12384, cranidium, from R6-114 (97), dorsal view, x 20.
　　8. UA 12385, free cheek, from R6E2, dorsal view, x 10.
　　10. UA 12386, cranidium, from R6-114 (97), dorsal view, x 20.
11-13. *Flectihystricurus acumennasus* (Ross, 1951). These pygidia are tentatively assigned to this species.
　　11. UA 12387, pygidium, from R6-114 (97), dorsal view, x 20.
　　12, 13. UA 11911, pygidium, from R6E2, x 20; 12. Posterior view, 13. Dorsal view.

466
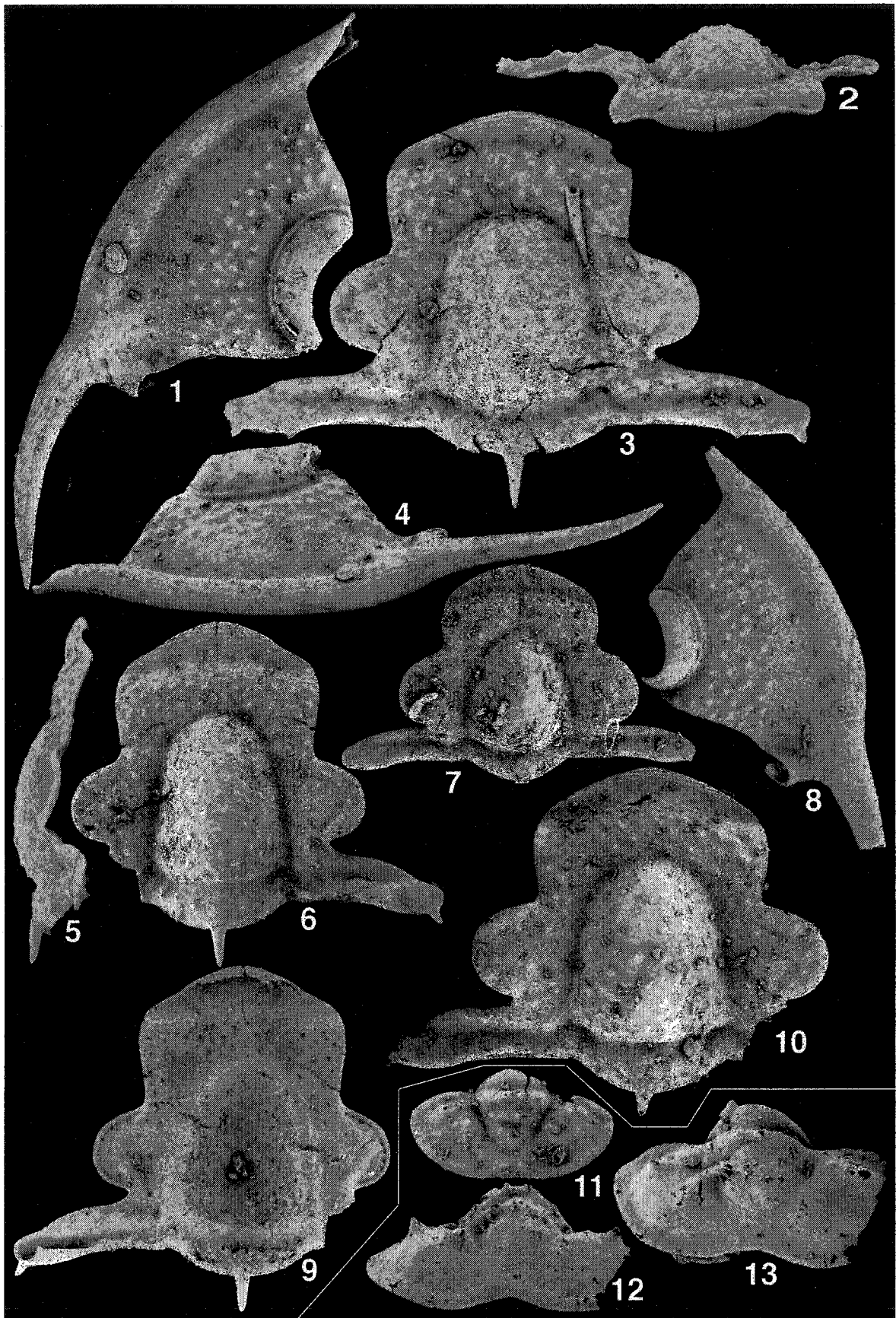
PLATE III-50. *Flectihystricurus flectimembrus* (Ross, 1951).

1-27. *Flectihystricurus flectimembrus* (Ross, 1951).
  1, 3. UA 12388, free cheek, from R6E3, x 20; 1. Dorsal view, 3. Ventral view.
  2. UA 12389, cranidium, from R6E2, dorsal view, x 20.
  4. UA 12390, pygidium, from R6-114 (97), dorsal view, x 20.
  5. UA 12391, pygidium, from R6-114 (97), dorsal view, x 20.
  6, 7. UA 12392, pygidium, from R6-114 (97), x 20; 6. Dorsal view, 7. Posterior view.
  8. UA 12393, free cheek, from R6-114 (97), dorsal view, x 20.
  9. UA 12394, cranidium, from R6E3, dorsal view, x 20.
  10. UA 12395, small cranidium, from R6-114 (97), dorsal view, x 20.
  11. UA 12396, cranidium, from R6-114 (97), dorsal view, x 20.
  12. UA 12397, cranidium, from R6-114 (97), dorsal view, x 20.
  13. UA 11914, pygidium, from R6E2, dorsal view, x 20.
  14. UA 11918, pygidium, from R6E2, dorsal view, x 20.
  15. UA 12398, pygidium, from R6E2, dorsal view, x 20.
  16, 17. UA 12399, pygidium, from R6E2, x 20; 16. Dorsal view, 17. Posterior view.
  18. UA 11920, small pygidium, from R6E2, dorsal view, x 20.
  19, 20, 23, 26. UA 12400, pygidium, from R6-114 (97), x 20; 19. Dorsal view, 20. Left
      lateral view, 23. Posterior view, 26. Ventral view.
  21, 22. UA 11926, pygidium, from R6E2, x 5; 21. Dorsal view, 22. Posterior view.
  24. UA 11919, thoracic segment, from R6E2, dorsal view, x 20.
  25. UA 12401, pygidium, from R6E3, dorsal view, x 20.
  27. UA 12402, pygidium, from R6E2, dorsal view, x 20.

468
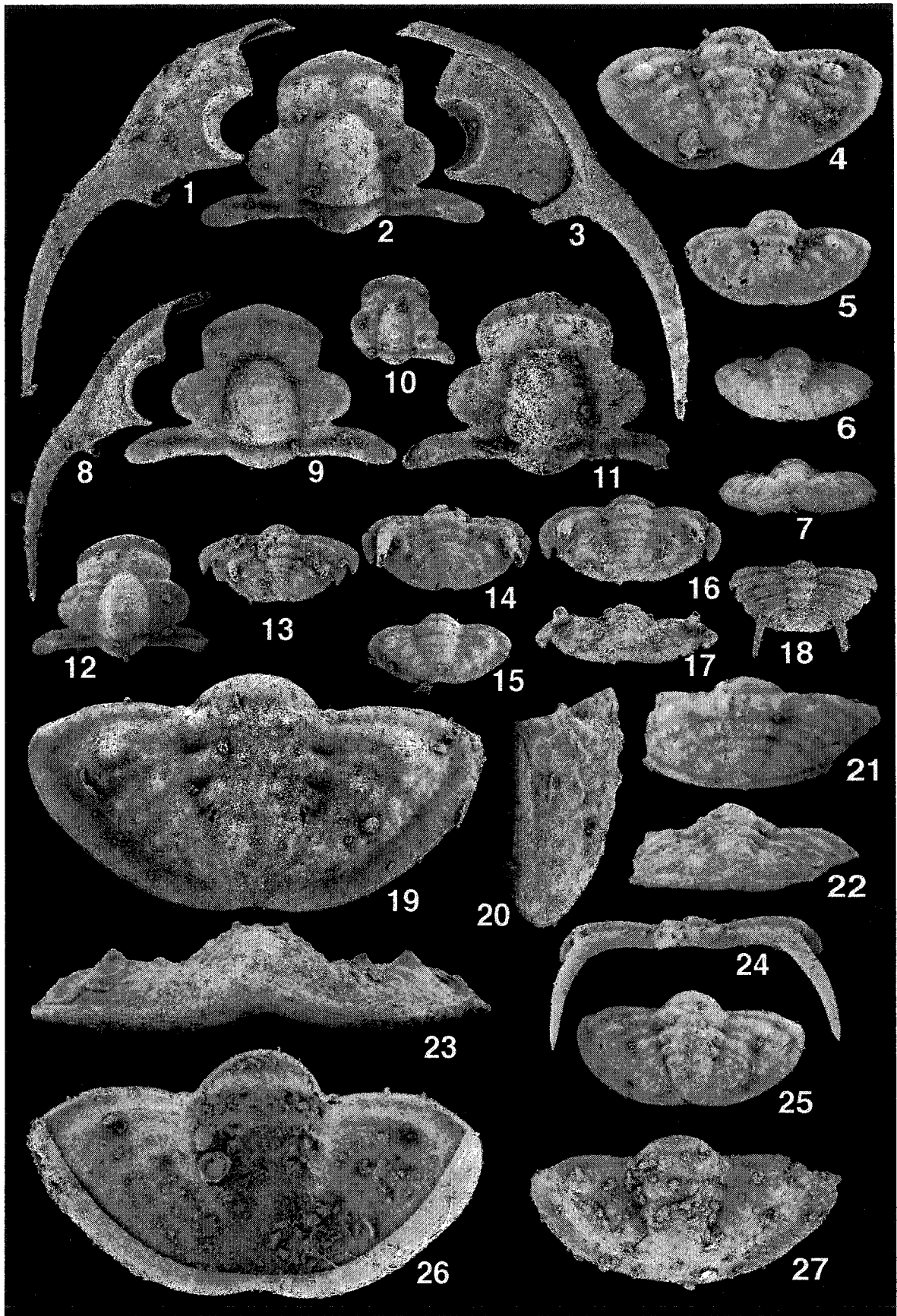
PLATE III-51. *Dimeropygiella ovata* (Hintze, 1953) and *Pseudohystricurus*? sp. A.

1-16. *Dimeropygiella ovata* (Hintze, 1953).

1, 7. UA 12403, fused free cheeks, from SH-1, x 30; 1. Dorsal view, 7. Anterior view.

2, 3, 6. UA 12404, cranidium, from SH-1, x 15; 1. Dorsal view, 3. Right lateral view, 6. Anterior view.

4, 5, 9. UA 12405, pygidium, from SH-1, x 30; 4. Dorsal view, 5. Posterior view, 9. Right lateral view.

8. UA 12406, pygidium with one thoracic segment, from SH-1, ventral view, x 30.

10, 11. UA 12407, free cheek, from SH-1, x 15; 10. Oblique dorsal view, 11. Dorsal view.

12. UA 12408, fused free cheek, from SH-1, dorsal view, x 30.

13. UA 12409, small cranidium, from SH-1, dorsal view, x 30.

14. UA 12410, isolated free cheek, from SH-1, dorsal view, x 30.

15, 16. UA 12411, transitory pygidium, from SH-1, x 30; 15. Dorsal view, 16. Posterior view.

17-21. *Pseudohystricurus*? sp. A.

17-19, 21. UA 12412, cranidium, from R6E2, x 30; 17. Right lateral view, 18. Dorsal view, 19. Ventral view, 21. Anterior view.

20. UA 12413, cranidium, from R6-114(97), dorsal view, x 30.

470
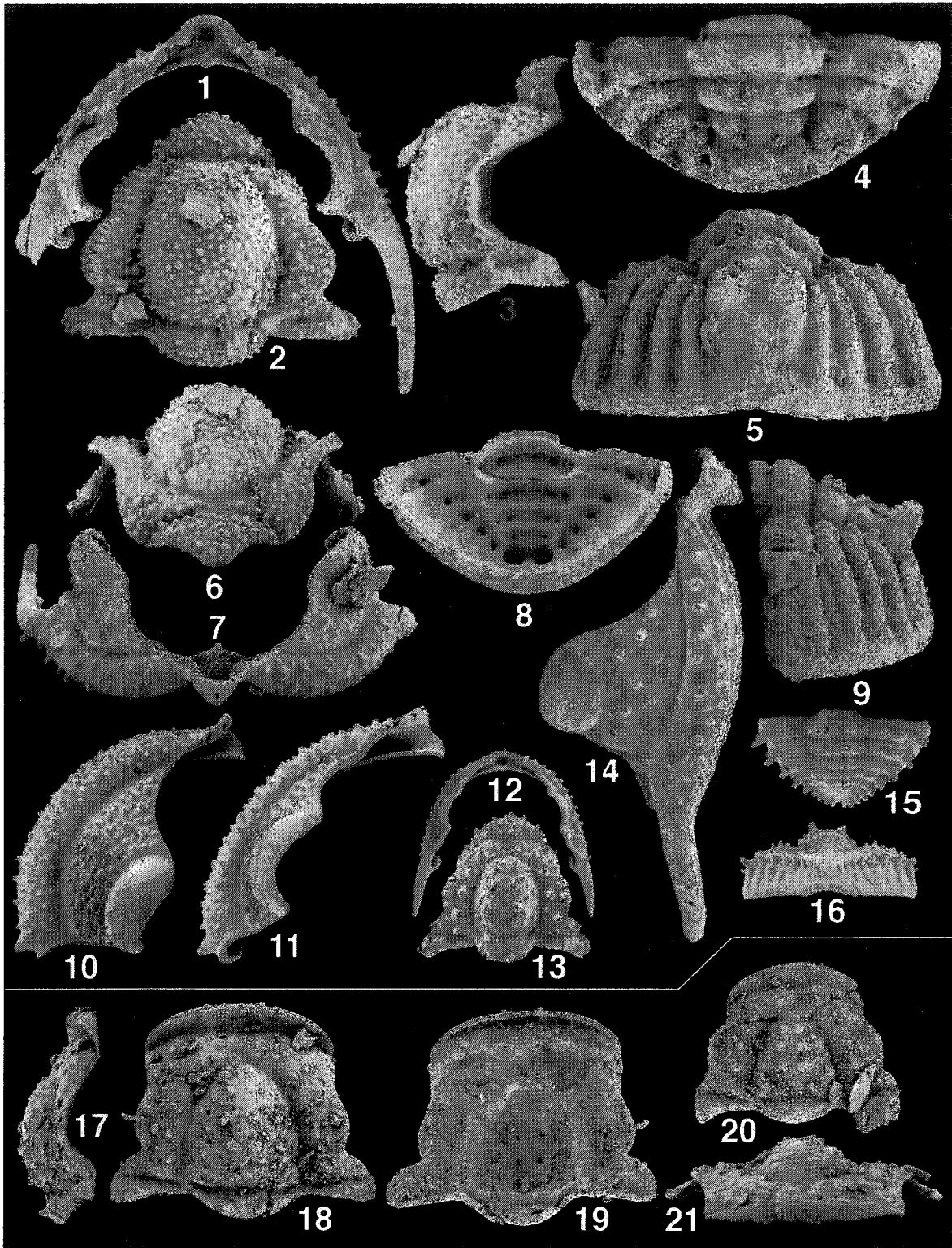
PLATE III-52. *Hyperbolochilus marginauctus marginauctus* Ross, 1951.

1-12. *Hyperbolochilus marginauctus marginauctus* Ross, 1951.

    1, 2, 4, 5. Y.P.M. 18057, holotype, cranidium, from Zone F, locality 6, x 10; 1. Left lateral view, 2. Dorsal view, 4. Ventral view, 5. Anterior view.

    3, 7. Y.P.M. 18037, free cheek, from Zone F, locality 6; 3. Dorsal view, x 20, 7. Right lateral view, x 15 (note: the illustration is flipped over horizontally to place it in accord with Fig. 6)

    6, 8. UA 12414, cranidium, from R5-87.7 (97), x 20; 6. Left lateral view, 8. Dorsal view.

    9-12. UA 12415, cranidium, from R6-114 (97), x 20; 9. Dorsal view, 10. Ventral view, 11. Anterior view, 12. Left lateral view (note: the left posterior fixigena is inadvertenly broken)

472
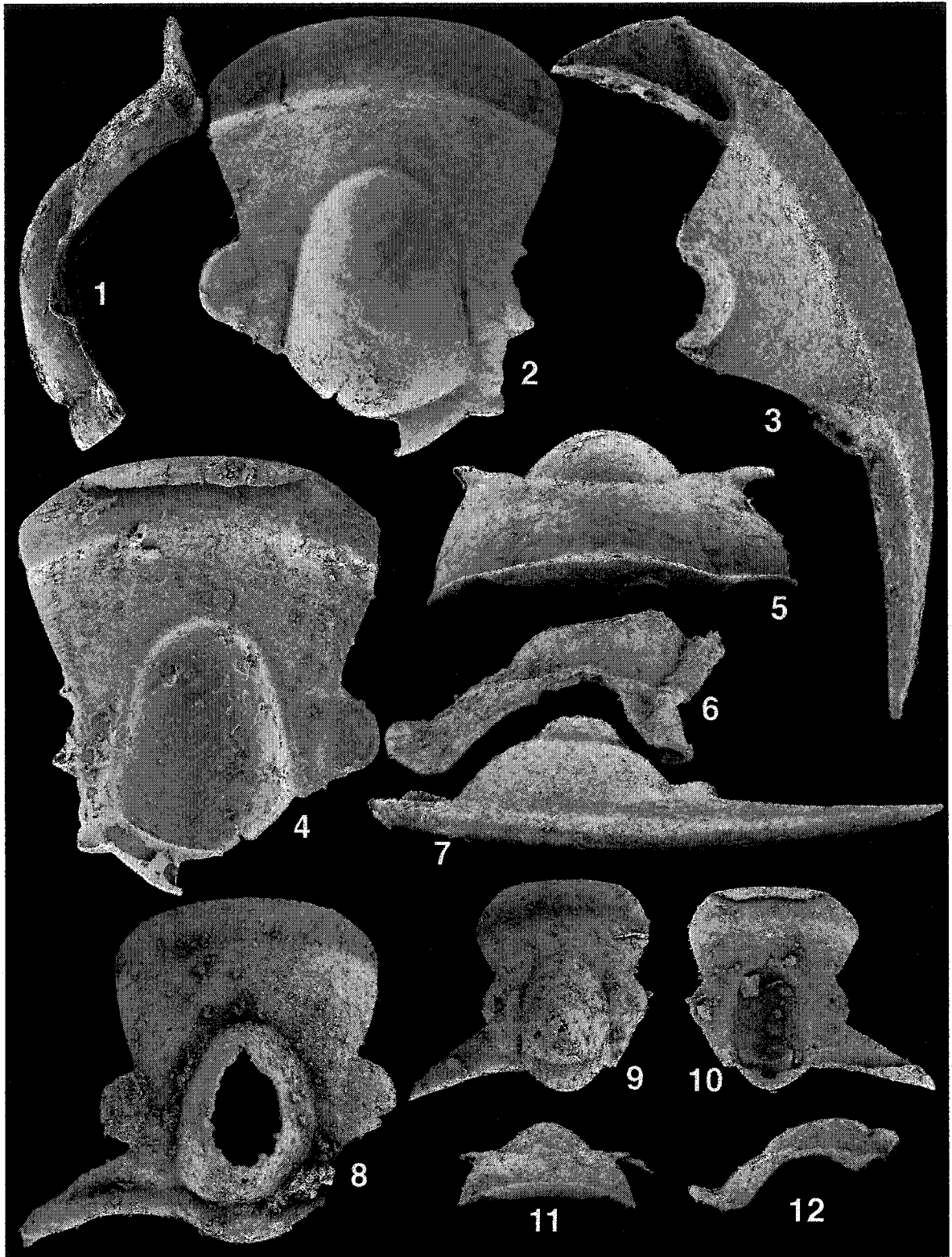
PLATE III-53. *Hyperbolochilus platysus* n. sp. and *Hyperbolochilus convexus* n. sp.

1-12. *Hyperbolochilus platysus* n. sp.
    1, 3, 5. UA 12416, free cheek, from R6E3, x 20; 1. Dorsal view, 3. Ventral view, 5.
       Left lateral view.
    2. UA 12417, holotype, cranidium, from R6E2, dorsal view, x 10.
    4, 6, 8. UA 12418, cranidium, from R6E2, x 20; 4. Left lateral view, 6. Anterior view,
       8. Dorsal view.
    7. UA 12419, small cranidium, from R6E2, dorsal view, x 20
    9. UA 12420, small cranidium, from R6E2, dorsal view, x 20
    10. UA 12421, small cranidium, from R6E3, dorsal view, x 20.
    11, 12. UA 12422, cranidium, from R6E3, x 5; 11. Dorsal view, 12. Ventral view.
13-19. *Hyperbolochilus convexus* n. sp. The association of pygidia (Figs. 16-18) is
    tenative.
    13-15, 19. UA 12423, holotype, cranidium, from R6-114, x 20; 13. Right lateral view,
       14. Dorsal view, 15. Anterior view, 19. Ventral view.
    16. UA 12424, pygidium, from R6-114, dorsal view, x 20
   17, 18. UA 12425, pygidium, from R6-114, x 20; 17. Posterior view, 18. Dorsal view.
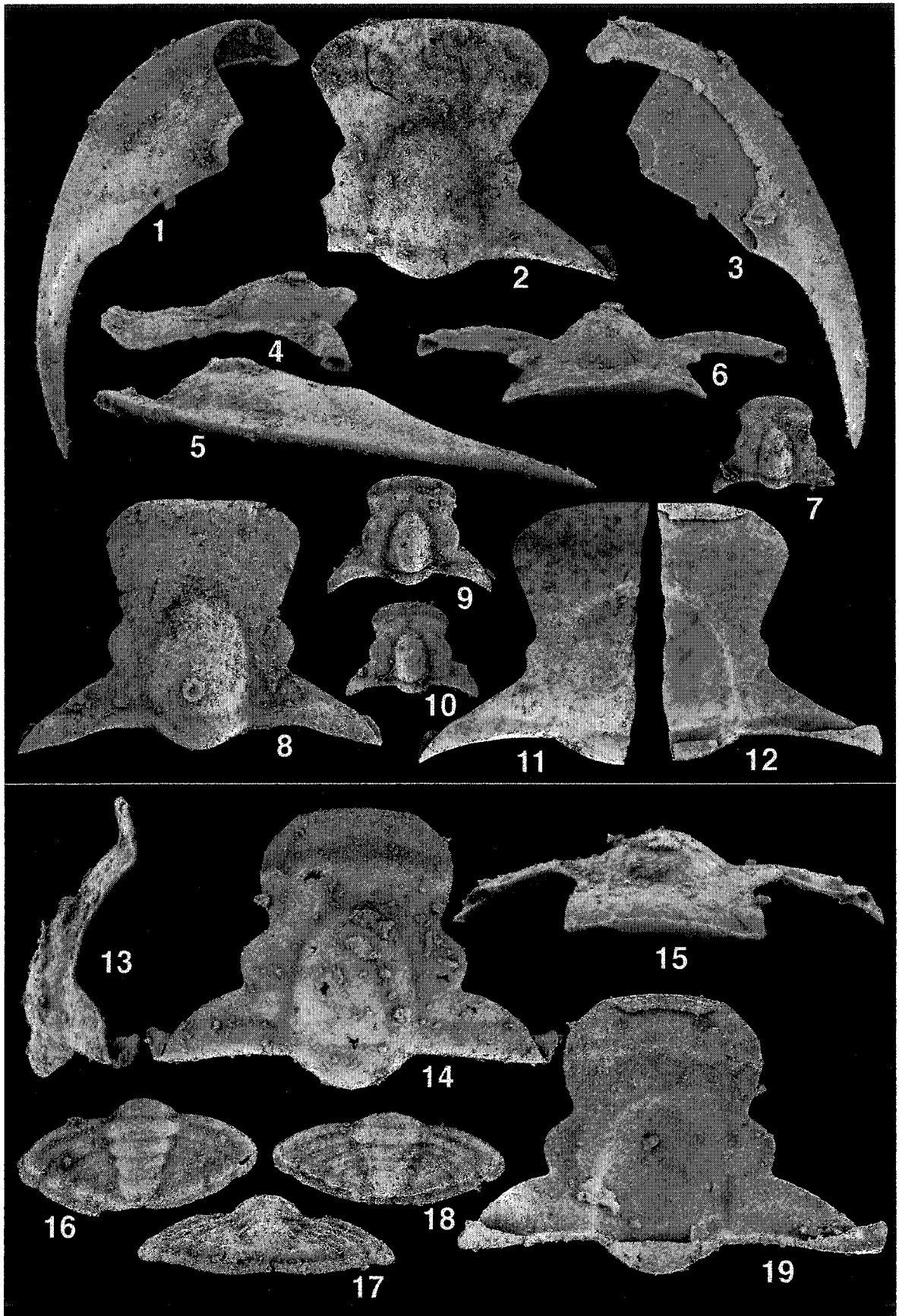
PLATE III-54. *Hyperbolochilus*? *pseudoranfordi* n. sp. and *Hyperbolochilus*? *paraexpansus* n. sp.

1-9. *Hyperbolochilus*? *pseudoranfordi* n. sp.
    1-3, 5. UA 12432, holotype, cranidiium, from R6E2, x 30; 1. Dorsal view, 2. Anterior view, 3. Ventral view, 5. Oblique right lateral view.
    4. UA 12433, small cranidium, from R5-86, dorsal view, x 30.
    6. UA 12434, cranidium, from R6E2, dorsal view, x 30.
    7. UA 12435, cranidium, from R6E2, dorsal view, x 30.
    8. UA 12436, small cranidium, from R5-86, dorsal view, x 30.
    9. UA 12437, cranidium, from R5-86, dorsal view, x 30.
10-13. *Hyperbolochilus*? *paraexpansus* n. sp.
    10-13. UA 12438, holotype, cranidium, from R5-76.4, x 10; 10. Dorsal view, 11. Left lateral view, 12. Anterior view, 13. Ventral view.

476

PLATE III-55. *Hyperbolochilus? cristus* n. sp.

1-12. *Hyperbolochilus? cristus* n. sp. The small cranidium (Fig. 10) is tentatively assigned.

    1, 3, 5. UA 12426, free cheek, from SE 152, x 10; 1. Ventral view, 3. Dorsal view, 5. Right lateral view.

    2, 4, 6. UA 12427, holotype, cranidium, from SE-152, x 10; 2. Dorsal view, 4, Left lateral view, 6. Ventral view.

    7. UA 12428, free cheek, from SE-152, dorsal view, x 10.

    8, 9, 12, 13. UA 12429, cranidium, from SE-152, x 20; 8. Dorsal view, 9. Right lateral view, 12. Ventral view, 13. Anterior view.

    10. UA 12430, cranidium, from SE-152, dorsal view, x 20

    11, 14. UA 12431, free cheek, from SE-152, x 20; 11. Ventral view, 14. Dorsal view.

478
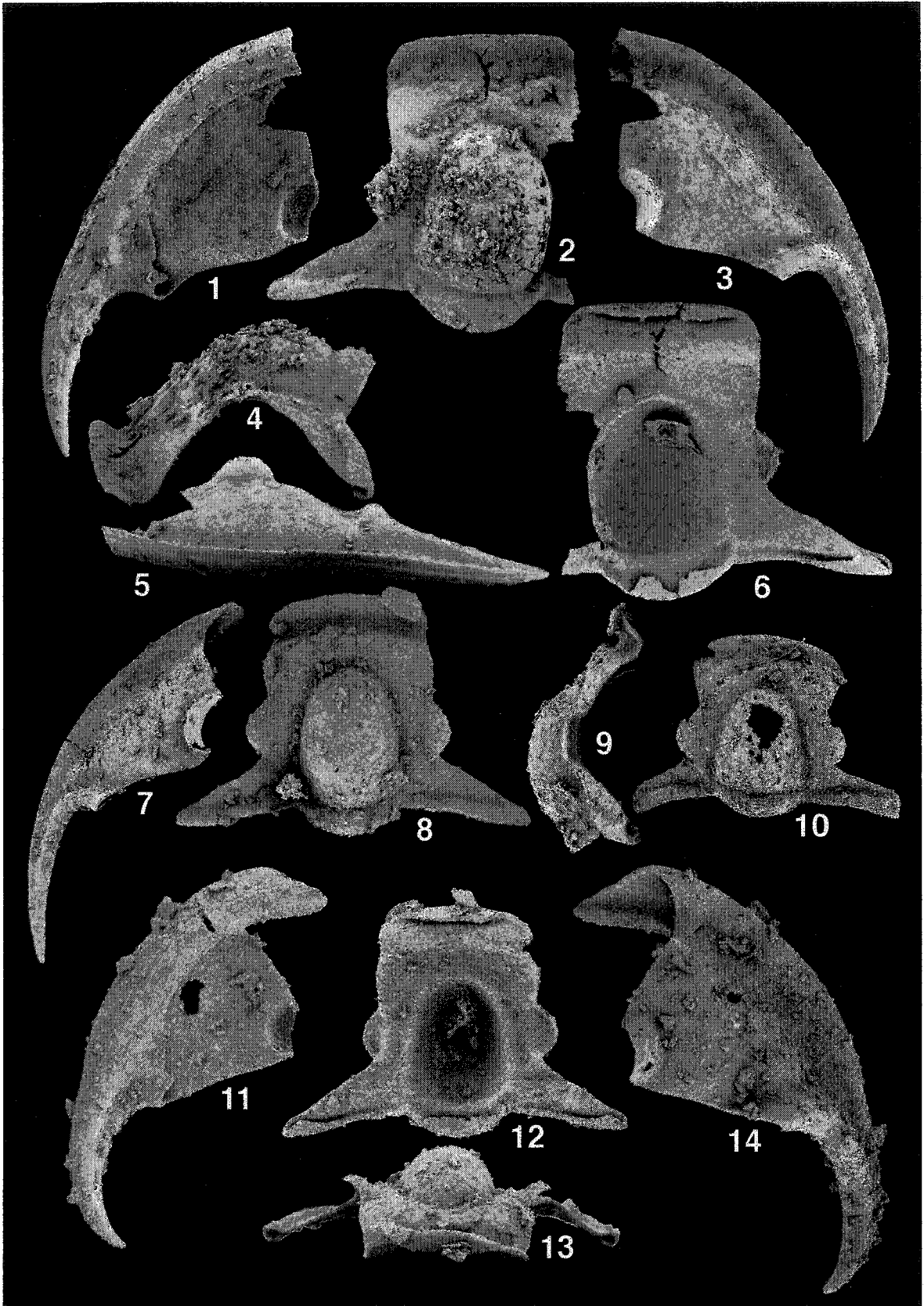
PLATE III-56. *Parahillyardina sulcata* n. gen. and n. sp.

1-23. *Parahillyardina sulcata* n. gen. and n. sp.
  1, 3. UA 12452, free cheek, from R11-48.7, x 20; 1. Dorsal view, 3. Ventral view.
  2, 6, 9, 12. UA 12453, holotype, cranidium, from R11-48.7, x 20; 2. Dorsal view, 6. Right lateral view, 9. Anterior view, 12. Ventral view.
  4. UA 12454, cranidium, from R6-38, dorsal view, x 20.
  5. UA 12455, pygidium, from R11-48.7, dorsal view, x 20.
  7, 11. UA 12456, free cheek, from R11-48.7, x 20; 7. Right lateral view, 11. Dorsal view.
  8. UA 12457, cranidium, from R5-76.4, dorsal view, x 20.
  10. UA 12458, cranidium, from R6-38, dorsal view, x 20.
  13, 16, 17. Y.P.M. 18221, thoracopygidium consisting of ten thoracic segments (the fifth segment from the anterior with long axial spine) and pygidium, from Zone F, x 20; 13. Right lateral view, 16. Ventral view, 17. Dorsal view.
  14. UA 12459, cranidium, from R6-38, dorsal view, x 20.
  15. UA 12460, pygidium, from R11-48.7, dorsal view, x 20.
  18. UA 12461, cranidium, from R11-48.7, dorsal view, x 20.
  19. UA 12462, pygidium, from R11-48.7, dorsal view, x 20.
  20-23. UA 11910, pygidium, from R5-87.7, x 10; 20. Dorsal view, 21. Posterior view, 23. Oblique right lateral view.

480
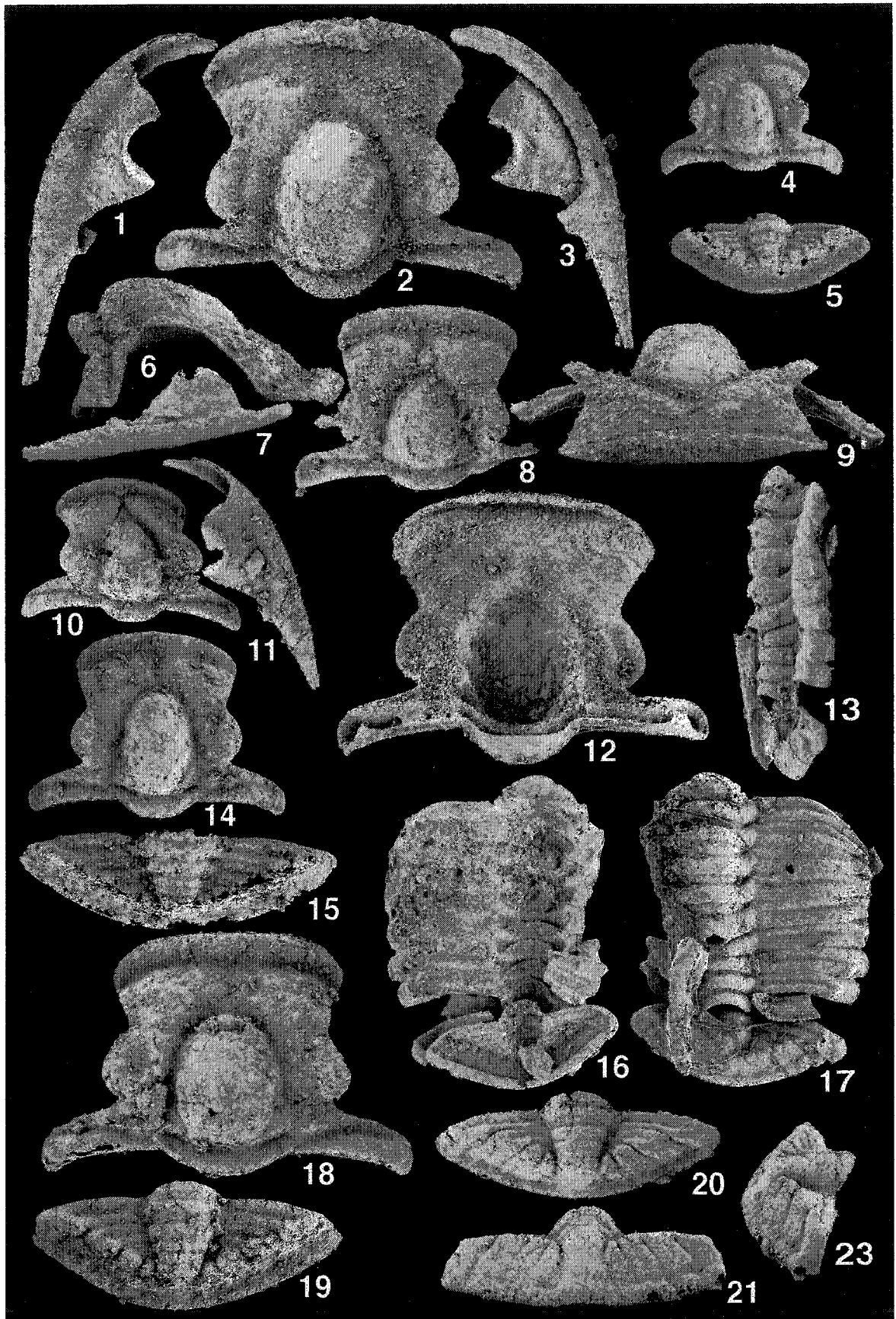
PLATE III-57. *Parahillyardina minuspustulata* (Boyce, 1989) and *Pachycranium faciclunis* Ross, 1951.

1-13. *Parahillyardina minuspustulata* (Boyce, 1989).
   1, 2. UA 12439, cranidium, from R6-35, x 20; 1. Dorsal view, 2. Ventral view.
   3-5. UA 12440, cranidium, from R6-38, x 20; 3. Left lateral view, 4. Dorsal view, 5. Anterior view.
   6. UA 12441, cranidium, from R6-35, dorsal view, x 20.
   7. UA 12442, cranidium, from R6-35, dorsal view, x 20.
   8,9. UA 12443, pygidium, from R6-38, x 20; 8. Posterior view, 9. Dorsal view.
   10. UA 12444, pygidium, from R6-38, dorsal view, x 20.
   11. UA 12445, cranidium, from R6-35, dorsal view, x 20.
   12. UA 12446, free cheek, from R6-35, dorsal view, x 20.
   13. UA 12447, pygidium, from R6-38, dorsal view, x 20.
14-20. *Pachycranium faciclunis* Ross, 1951.
   14-17. UA 12448, cranidium, from R6-114 (97), x 30; 14. Dorsal view, 15. Anterior view, 16. Ventral view, 17. Oblique left lateral view.
   18. UA 12449, small cranidium, from R6-114 (97), dorsal view, x 30.
   19. UA 12450, small cranidium, from R6-114 (97), dorsal view, x 30.
   20. UA 12451, small cranidium, from R6-114 (97), dorsal view, x 30. The association with *Pachycranium faciclunis* is provisional, because it bears some similarities with *Parahystricurus oculilunatus* (Pl. III-64, Fig. 2)

482
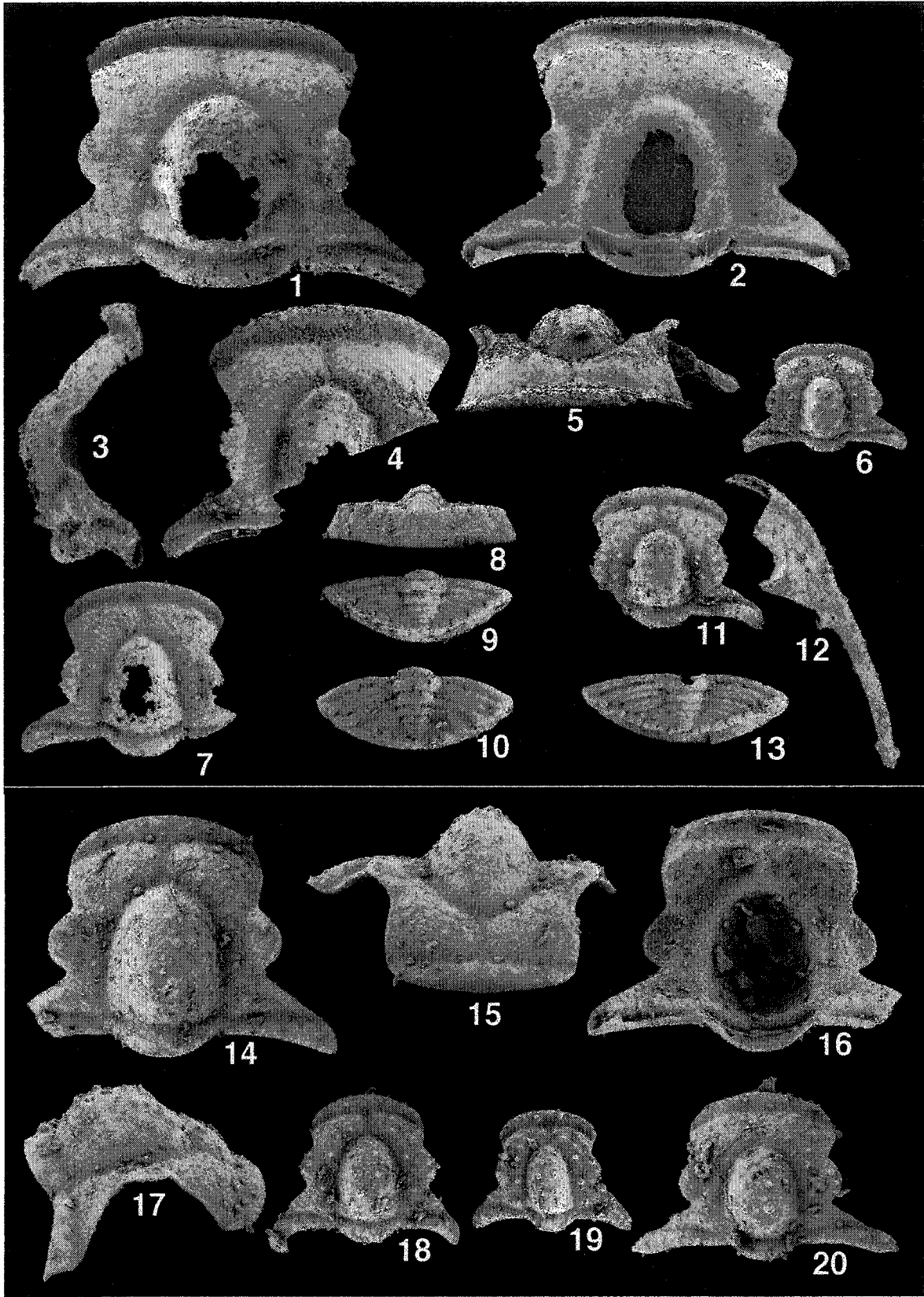
PLATE III-58. *Paenebeltella vultulata* Ross, 1951.

1-25. *Paenebeltella vultulata* Ross, 1951.
    1-3. UA 12463, cranidium from R5-76.4 (97), x 20; 1. Right lateral view, 2. Dorsal view, 3. Anterior view.
    4. UA 12464, cranidium from R5-76.4A, dorsal view, x 10.
    5. UA 12465, cranidium from R5-76.4 (98), dorsal view, x 20.
    6. UA 12466, cranidium from R5-76.4A, dorsal view, x 10.
    7. UA 12467, cranidium from R5-87.7, dorsal view, x 20.
    8. UA 12468, cranidium from R5-87.7(97), dorsal view, x 20.
    9-11. UA 12469, partially articulated specimen five thoracic segments and pygidium from R5-76.4 (97), x 20; 9. Right lateral view, 10. Dorsal view, 11. Ventral view. Note that there is a thoracic segment between the two thoracic segments possessing a long axial spine.
    12. UA 12470, pygidium from R5-87.7(97), dorsal view, x 20.
    13. UA 12471, cranidium from R6-38, dorsal view, x 20.
    14. UA 12472, free cheek from R5-76.4 (97), dorsal view, x 20.
    15. UA 12473, cranidium from R5-86, dorsal view, x 20.
    16. UA 12474, pygidium from R5-76.4 (97), dorsal view, x 10.
    17. UA 12475, pygidium from R5-86, dorsal view, x 20.
    18. UA 12476, pygidium from R5-76.4A, dorsal view, x 10.
    19, 20. UA 11933, pygidium from R5-87.7, x 20; 19. Dorsal view, 20. Posterior view.
    21, 22. UA 12477, pygidium from SE-152, x 20; 21. Dorsal view, 22. Ventral view.
    23. UA 12478, pygidium from R6-55, dorsal view, x 10.
    24, 25. UA 12479, transitory pygidium from R6-55, x 20; 24. Dorsal view, 25. Ventral view. Note that the arrangement of the thoracic segments possessing axial spine and those lacking it is identical to the larger specimen (Figs. 9-11).

484
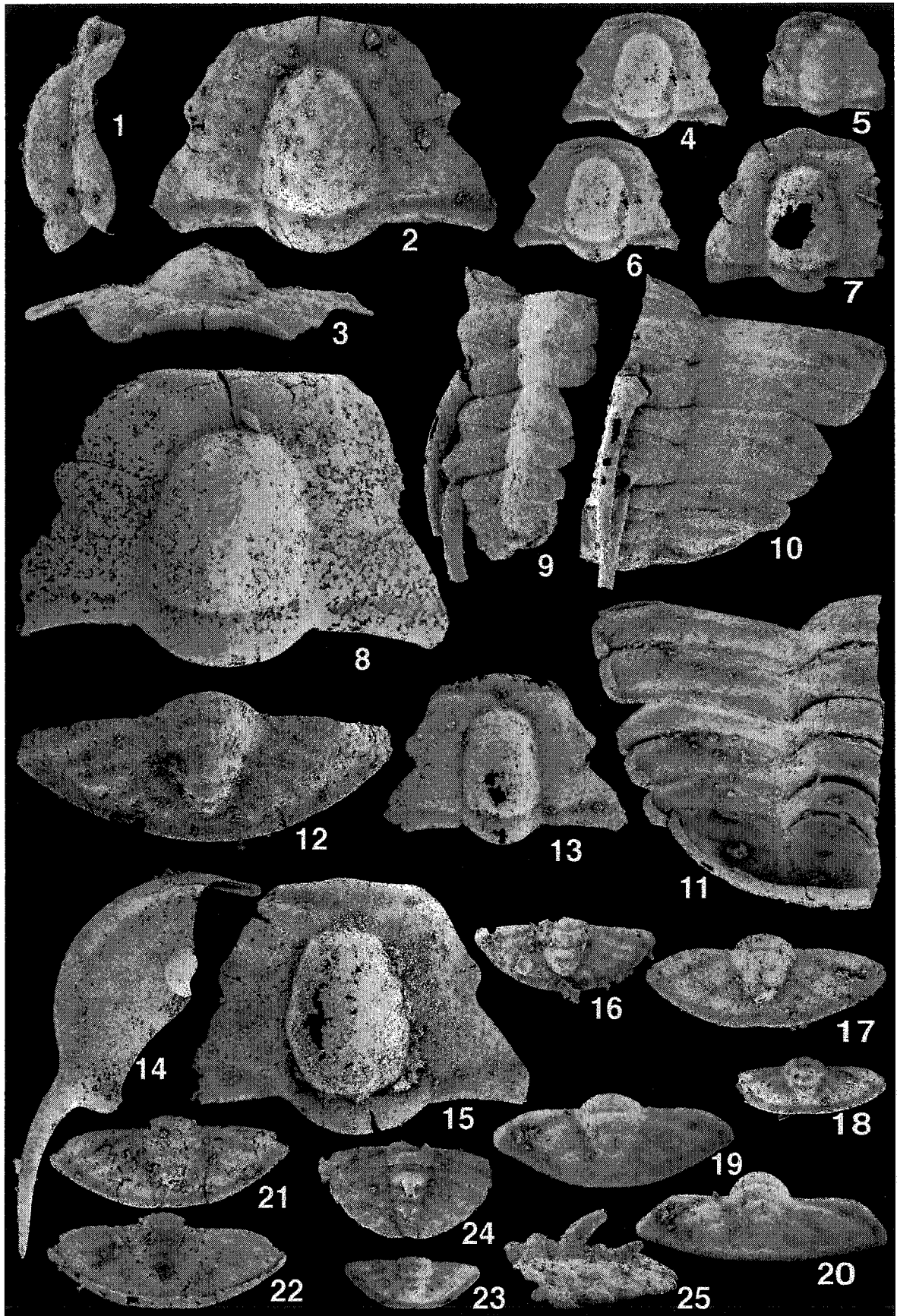
PLATE III-59. *Natmus tuberus* Jell, 1985 and *Natmus victus* Jell, 1985.

1-4. *Natmus tuberus* Jell, 1985. All specimens are from La1 Zone (Lancefieldian Series) of Digger Island Formation, Victoria, Australia.
    1-4. NMVP 74349, holotype, cast of internal mold, cranidium, x 10; 1. Right lateral view, 2. Dorsal view, 3. Anterior view, 4. Oblique right lateral view.
5-11. *Natmus victus* Jell, 1985. All specimens are from La1 Zone (Lancefieldian Series) of Digger Island Formation, Victoria, Australia.
    5. NMVP 74359, cast of external mold, incomplete articulated specimen consisting of at least 17 thoracic segments, dorsal view, x 10.
    6, 7, 9. NMVP 74352, holotype, cast of external mold, cranidium, x 10; 6. Dorsal view, 7. Left lateral view, 9. Anterior view.
    8. NMVP 74361, cast of external mold, free cheek, dorsal view, x 10.
    10, 11. NMVP 74364, cast of internal mold, cranidium, x 5; 10. Right lateral view, 11. Dorsal view (light photography).
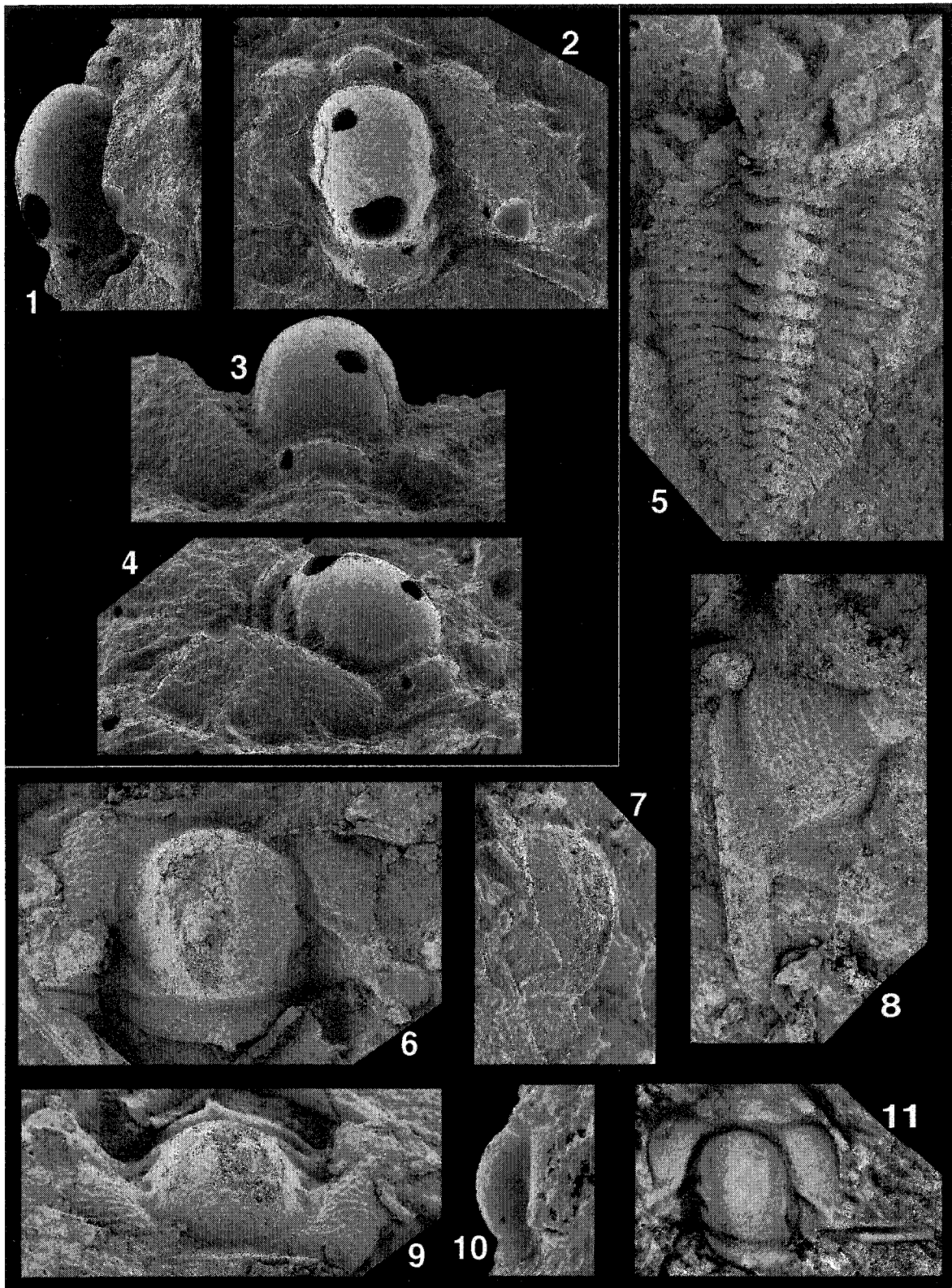
PLATE III-60. *Natmus tuberculatus* n. sp. and *Natmus* sp. aff. *N. tuberculatus*.

1-8. *Natmus tuberculatus* n. sp.
    1, 2. UA 12480, free cheek, from R6-114, x 20; 1. Dorsal (conventional) view, 2. Dorsal view.
    3, 4. UA 12481, holotype, cranidium, from R6-114, x 20; 3. Anterior view, 4. Dorsal view.
    5, 6. UA 12482, cranidium, from R6-114 (97), x 20; 5. Ventral view, 6. Dorsal view.
    7, 8. UA 12483, cranidium, from R6-114, x 20; 7. Dorsal view, 8. Oblique anterior view.
9-13. *Natmus* sp. aff. *N. tuberculatus*.
    9, 11-13. UA 12484, cranidium, from R6-100, x 20; 9. Anterior view, 11. Dorsal view, 12. Left lateral view, 13. Ventral view.
    10. UA 12485, cranidium, from R6-100, dorsal view, x 20.
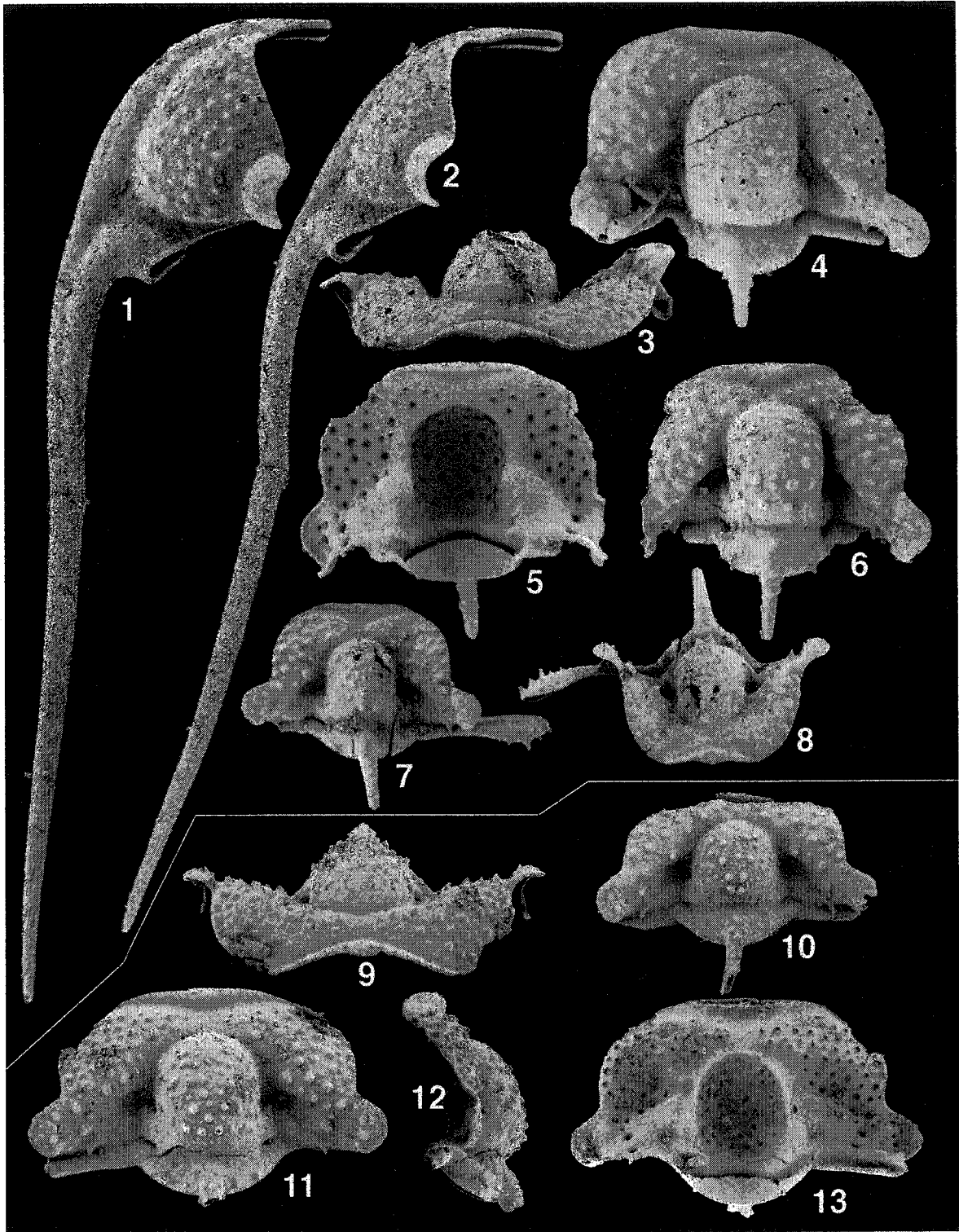
PLATE III-61. *Paramblycranium cornutum* (Ross, 1951).

1-26. *Paramblycranium cornutum* (Ross, 1951). Note that the pygidia (Figs. 18-22, 25, 26) and thorax (Figs. 23, 24) are provisionally associated with this species. They may be proven to be associated with some *Parahystricurus* species.
1. UA 12486, cranidium, from R6E2, dorsal view, x 15.
2. UA 12487, cranidium, from R6E2, dorsal view, x 20.
3. UA 12488, cranidium, from R6E2, dorsal view, x 20.
4. UA 12489, cranidium, from R6-114 (97), dorsal view, x 15.
5-8. UA 12490, cranidium, from R6E2, x 15; 5. Righ lateral view, 6. Dorsal view, 7. Ventral view, 8. Anterior view.
9. UA 12491, cranidium, from R6E2, dorsal view, x 20.
10. UA 12492, cranidium, from R6E2, dorsal view, x 20.
11. UA 12493, free cheek, from R6E3, dorsal view, x 15.
12. UA 12494, cranidium, from R6E3, dorsal view, x 15.
13-15, 17. UA 12495, free cheek, from R6-114 (97), x 15; 13. Lateral view, 14. Dorsal view, 15. Anterior ventral view, 17. Ventral view.
16. UA 12496, cranidium, from R6-114 (97), dorsal view, x 15.
18, 19. UA 12497, pygidium, from R6E2, x 10; 18. Dorsal view, 19. Posterior view.
20. UA 12498, pygidium, from R6E2, dorsal view, x 10.
21. UA 12499, pygidium, from R6E3, dorsal view, x 5.
22. UA 12500, pygidium, from R6E2, dorsal view, x 20.
23, 24. UA 12501, thorax with eight segments from R6E3, x 5; 23. Dorsal view, 24. Left lateral view.
25. UA 12502, pygidium, from R6-114, dorsal view, x 10.
26. UA 12503, pygidium, from R6-114, dorsal view, x 20. Note: Anterior two segments have a spinose distal end.

490
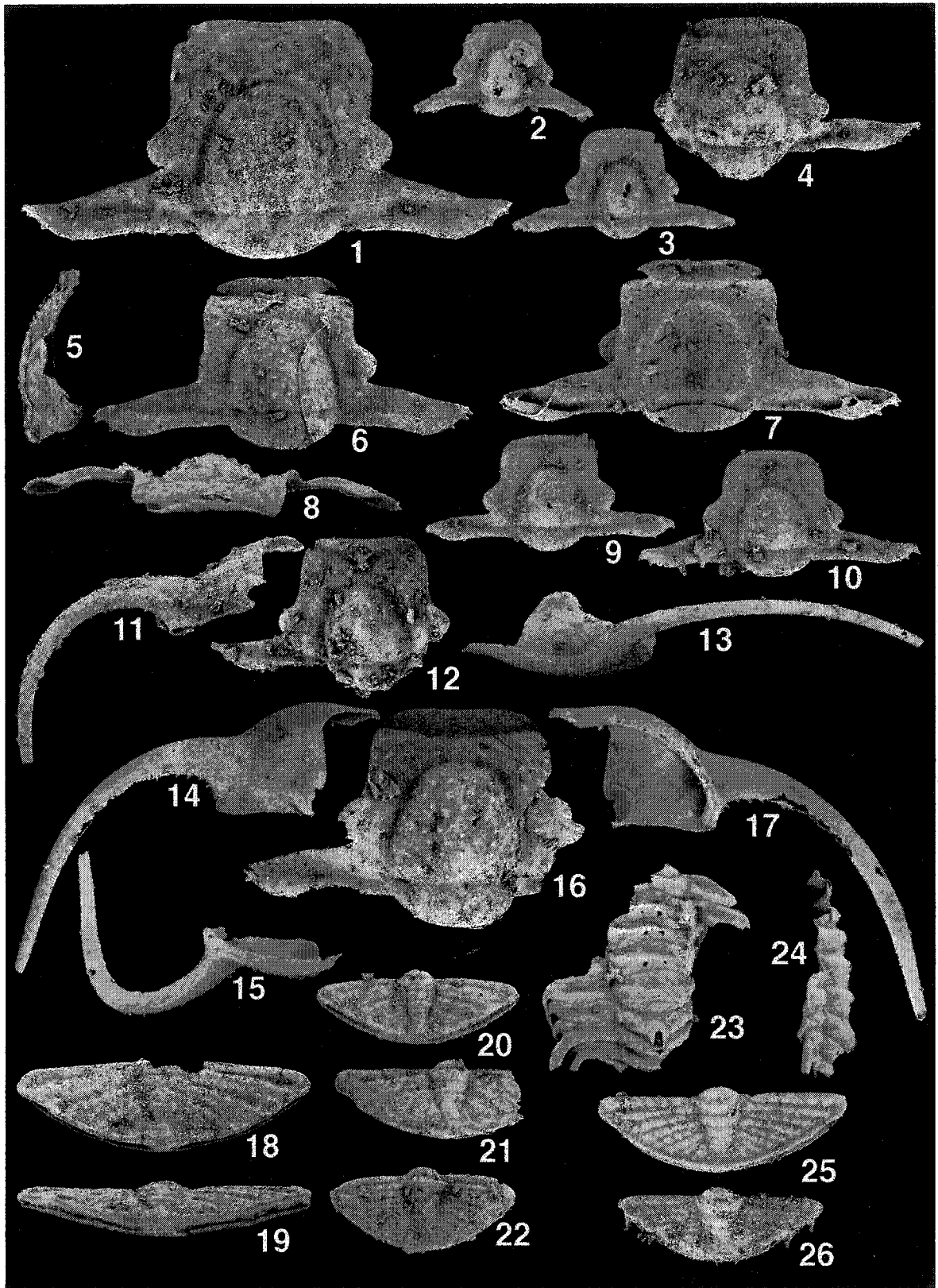
PLATE III-62. *Paramblycranium populum* (Ross, 1951) and *Paramblycranium tapera* n. gen. and n. sp.

1-16. *Paramblycranium populum* (Ross, 1951).
  1. UA 12504, cranidium, from R5-76.4A, dorsal view, x 10.
  2. UA 12505, cranidium, from R6-55, dorsal view, x 20.
  3. UA 12506, cranidium, from R5-76.4, dorsal view, x 20.
  4, 9. UA 12507, free cheek, from R5-76.4, x 15; 4. Dorsal view, 9. Ventral view.
  5-7. UA 12508, cranidium, from R5-76.4, x 15; 5. Dorsal view, 6. Left lateral view, 7. Anterior view.
  8, 12. UA 12509, cranidium, from R5-76.4, x 15; 8. Dorsal view, 12. Ventral view.
  10. UA 12510, cranidium, from R5-76.4A, dorsal view, x 15.
  11. UA 12511, free cheek, from R5-76.4A, dorsal view, x 20.
  13, 15. UA 12512, free cheek, from R6-55, x 15; 13. Lateral view, 15. Dorsal view.
  14. UA 12513, cranidium, from R6-55, dorsal view, x 20.
  16. UA 12514, cranidium, from R5-76.4A, dorsal view, x 15.
17-23. *Paramblycranium tapera* n. gen. and n. sp.
  17-20. UA 12515, holotype, cranidium, from R5-76.4, x 20; 17. Ventral view, 18. Dorsal view, 19. Left lateral view, 20. Anterior view.
  21. UA 12516, cranidium, from R5-76.4, dorsal view, x 20.
  22. UA 12517, cranidium, from R5-76.4 (97), dorsal view, x 20.
  23. UA 12518, cranidium, from R5-76.4A, dorsal view, x 20.

492
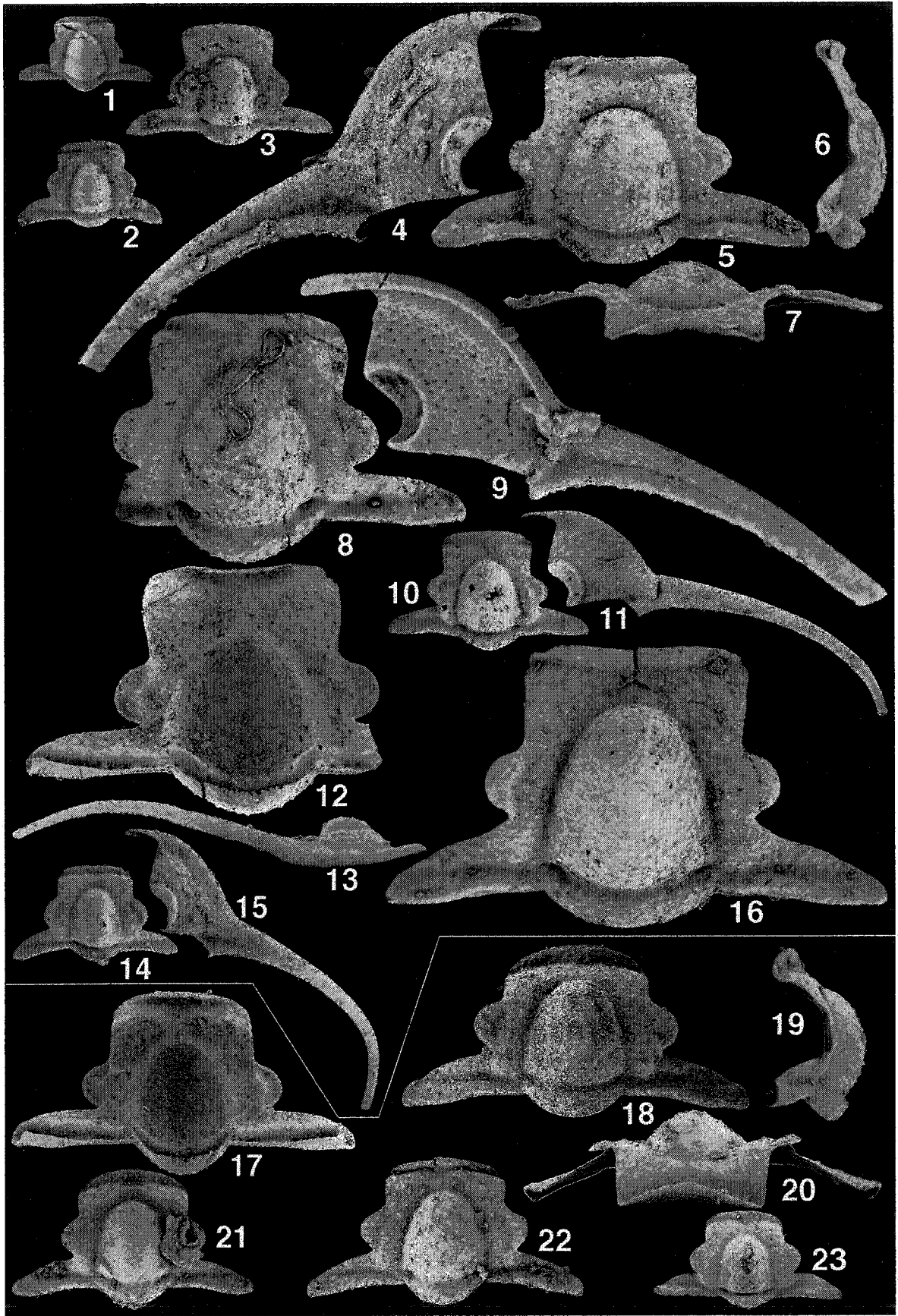
PLATE III-63. *Parahystricurus pustulosus pustulosus* Ross, 1951, *Parahystricurus pustulosus rectangulofrontalis* n. subsp. and *Parahystricurus pustulosus taperus* n. subsp.

1-8. *Parahystricurus pustulosus pustulosus* Ross, 1951.
    1, 2, 5, 7. UA 12525, cranidium, from R6E2, x 15; 1. Right lateral view, 2. Dorsal view, 5. Anterior view, 7. Ventral view.
    3. UA 12526, small cranidium, from R6E2, dorsal view, x 20.
    4. UA 12527, small cranidium, from R6E2, dorsal view, x 20.
    6. UA 12528, cranidium, from R6E2, dorsal view, x 10.
    8. UA 12529, cranidium, from R6E2, dorsal view, x 15.
9-11. *Parahystricurus pustulosus rectangulofrontalis* n. subsp.
    9-11. UA 12530, holotype, cranidium, from R6E2, x 10; 9. Dorsal view, 10. Anterior view, 11. Left lateral view.
12-16. *Parahystricurus pustulosus taperus* n. subsp. Note that the association of pygidium (Figs. 13, 14) is provisional.
    12. UA 12531, holotype, cranidium, from R6-114, dorsal view, x 20.
    13, 14. UA 12532, pygidium, from R6-114, x 20; 13. Dorsal view, 14. Posterior view.
    15, 16. UA 12533, small cranidium, from R6-114(97), x 40; 15. Dorsal view, 16. Oblique anterior view.

494
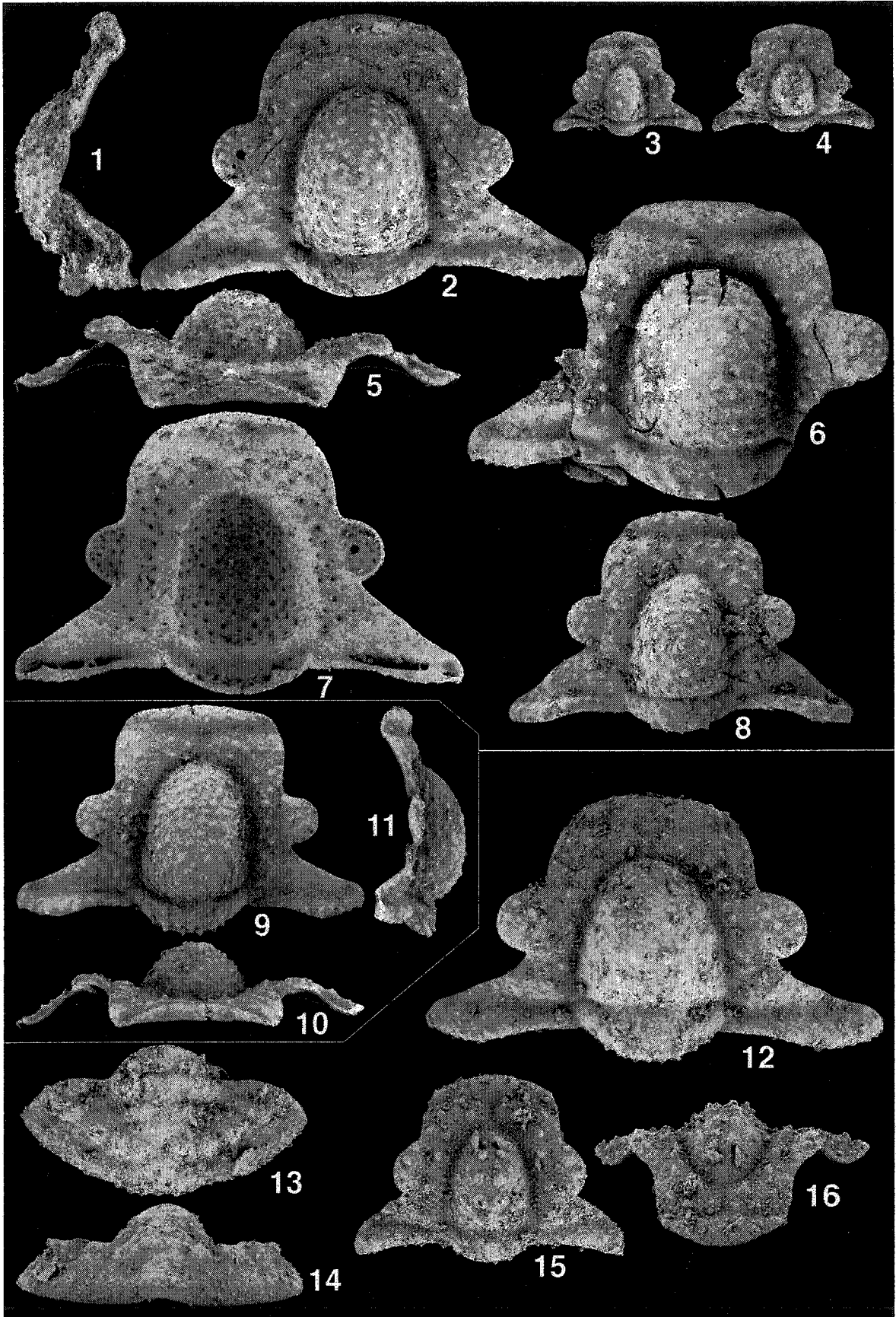
PLATE III-64. *Parahystricurus oculirotundus* Ross, 1951 and *Parahystricurus* sp. nov. A.

1-10. *Parahystricurus oculirotundus* Ross, 1951.

    1, 5, 6. UA 12519, free cheek, from R6-114 (97), x 20; 1. Oblique dorsal view, 5. Right lateral view, 6. Dorsal (conventional) view.

    2. UA 12520, cranidium, from R6-114 (97), dorsal view, x 20.

    3, 7, 9, 10. UA 12521, cranidium, from R6-114 (97), x 20; 3. Right lateral view, 7. Dorsal view, 9. Anterior view, 10. Ventral view.

    4, 8. UA 12522, free cheek, from R6-114 (97), x 10; 4. Right lateral view, 11. Dorsal view.

11-15. *Parahystricurus* sp. nov. A.

    11. UA 12523, cranidium, from R6-114, dorsal view, x 20.

    12-15. UA 12524, cranidium, from R6-114, x 20; 12. Anterior view, 13. Dorsal view, 14. Left lateral view, 15. Ventral view.

496
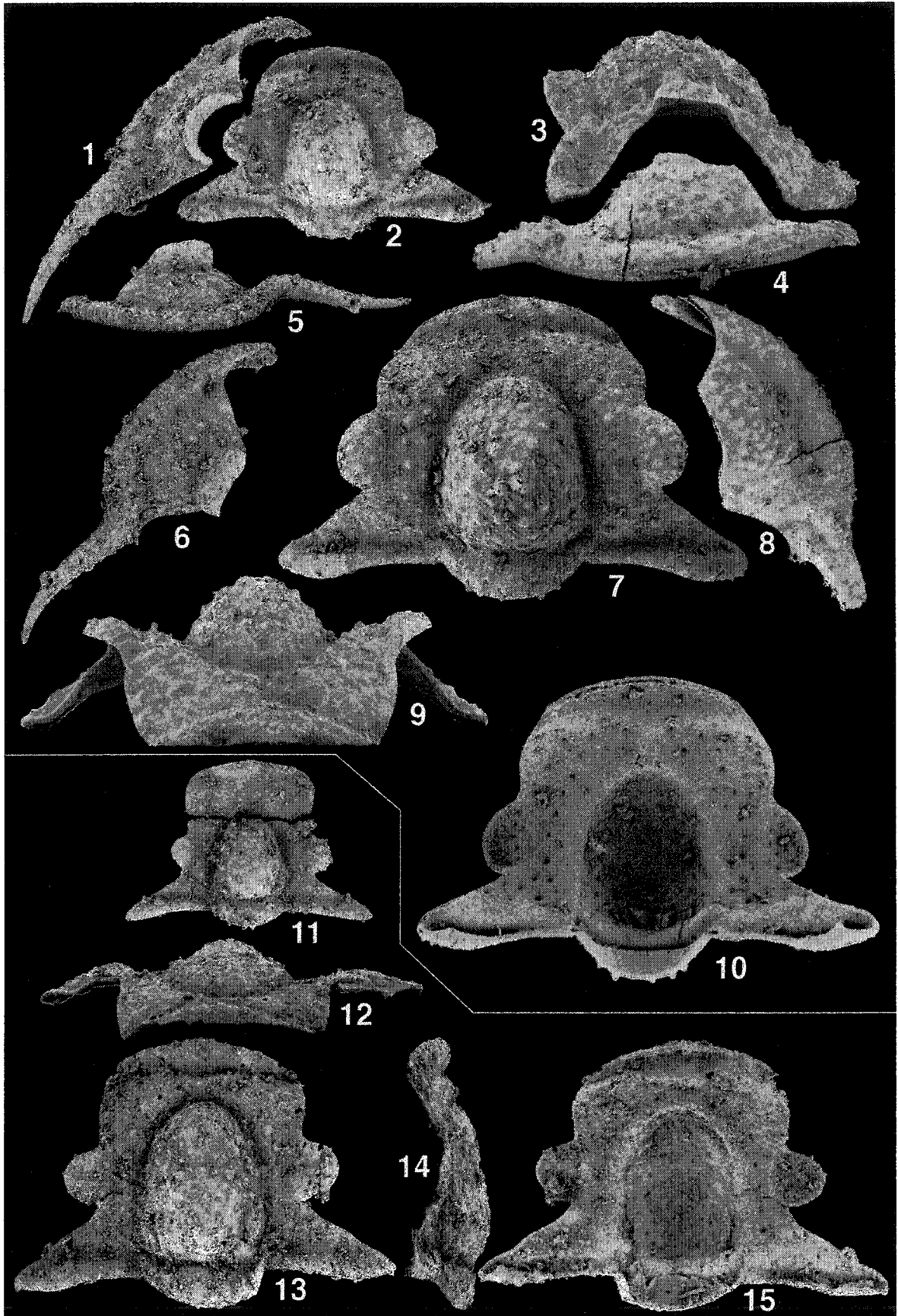
PLATE III-65. *Paratersella mediasulcata* n. gen. and n. sp.

1-19. *Paratersella mediasulcata* n. gen. and n. sp.
    1-4. UA 12534, cranidium, from SE-152, x 20; 1. Dorsal view, 2. Oblique left lateral
        view, 3. Oblique anterior view, 4. Ventral view.
    5. UA 12535, protaspis, from R5-76.4, dorsal view, x 50.
    6. UA 12536, protaspis, from R5-87.7(97), dorsal view, x 50.
    7, 9. UA 12537, free cheek, from R5-76.4A, x 20; 6. Ventral view, 8. Dorsal view.
    8. UA 12538, cranidium, from R5-76.4 (97), dorsal view, x 20.
    10. UA 12539, cranidium, from R5-76.4, dorsal view, x 20.
    11. UA 12540, cranidium, from R6-55, dorsal view, x 20.
    12. UA 12541, cranidium, from R5-86, dorsal view, x 20.
    13. UA 12542, free cheek, from R5-86, dorsal view, x 20.
    14. UA 12543, free cheek, from R5-87.7, dorsal view, x 20.
    15. UA 12544, cranidium, from R5-87.7 (97), dorsal view, x 20.
    16. UA 12545, cranidium, from R5-76.4, dorsal view, x 20.
    17. UA 12546, cranidium, from R5-76.4 (98), dorsal view, x 20.
    18. UA 12547, cranidium, from R5-76.4A, dorsal view, x 20.
    19. UA 12548, cranidium, from R5-86, dorsal view, x 10.

498
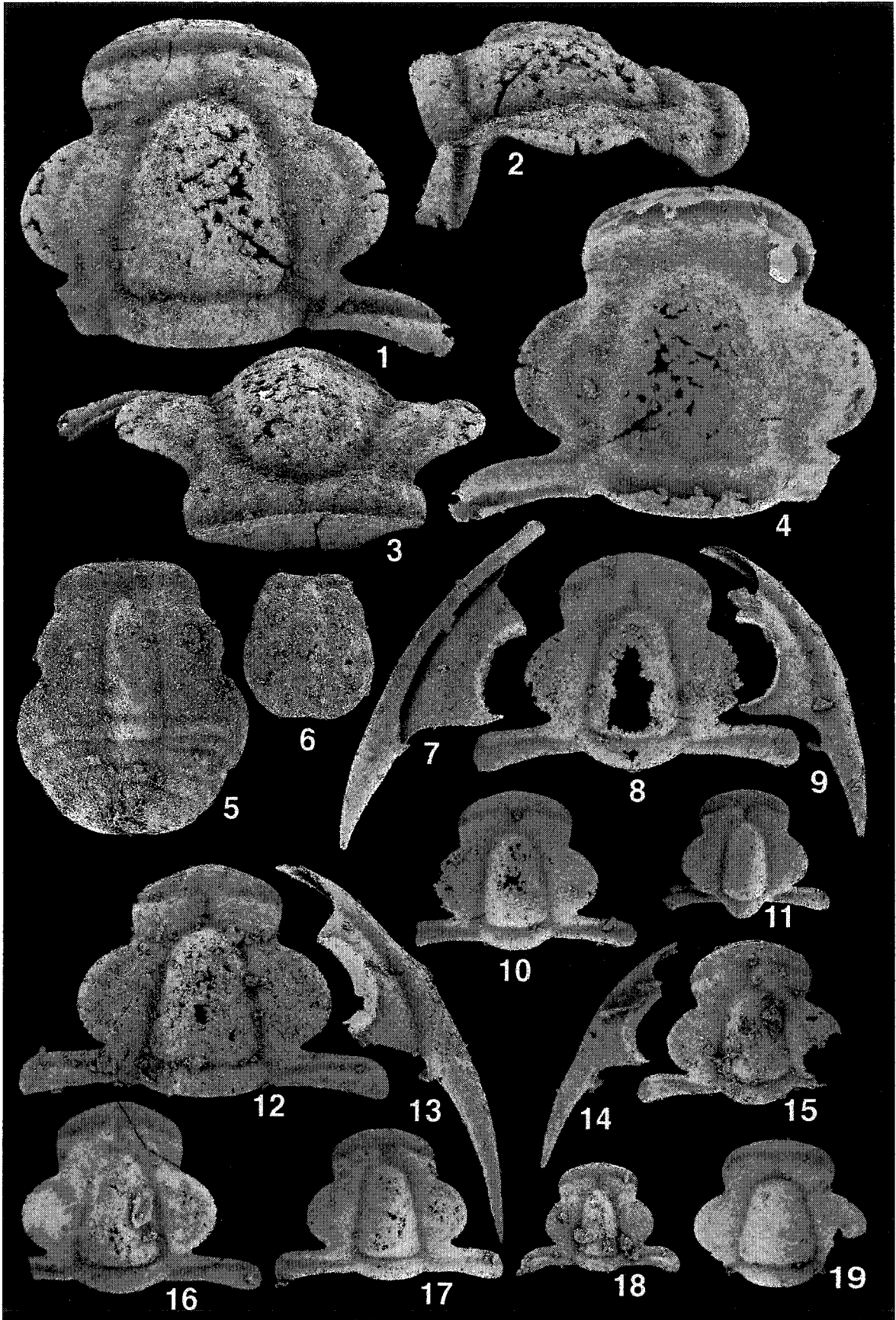
PLATE III-66. *Paratersella mediasulcata* n. gen. and n. sp. and *Paratersella flexa* n. gen. and n. sp.

1-10. *Paratersella mediasulcatua* n. gen. and n. sp.
    1-4. UA 12549, pygidium, from SE-152, x 20; 1. Dorsal view, 2. Ventral view, 3. Posterior view (the right anterior portion of the specimen is inadvertently broken), 4. Right lateral view.
    5, 8. UA 12550, pygidium, from R5-86, x 20; 5. Dorsal view, 8. Left lateral view.
    6. UA 12551, pygidium, from R5-76.4 (98), dorsal view, x 20.
    7. UA 12552, pygidium, from R5-86, dorsal view, x 20.
    9. UA 11931, pygidium, from R5-87.7, dorsal view, x 15.
    10. UA 12553, pygidium, from SE-152, dorsal view, x 10.
11-15. *Paratersella flexa* n. gen. and n. sp.
    11, 13-15. UA 12554, holotype, cranidium, from SE-152, x 15; 11. Dorsal view, 13. Ventral view, 14. Anterior view, 15. Right lateral view.
    12. UA 12555, free cheek, from SE-152, dorsal view, x 20.

500
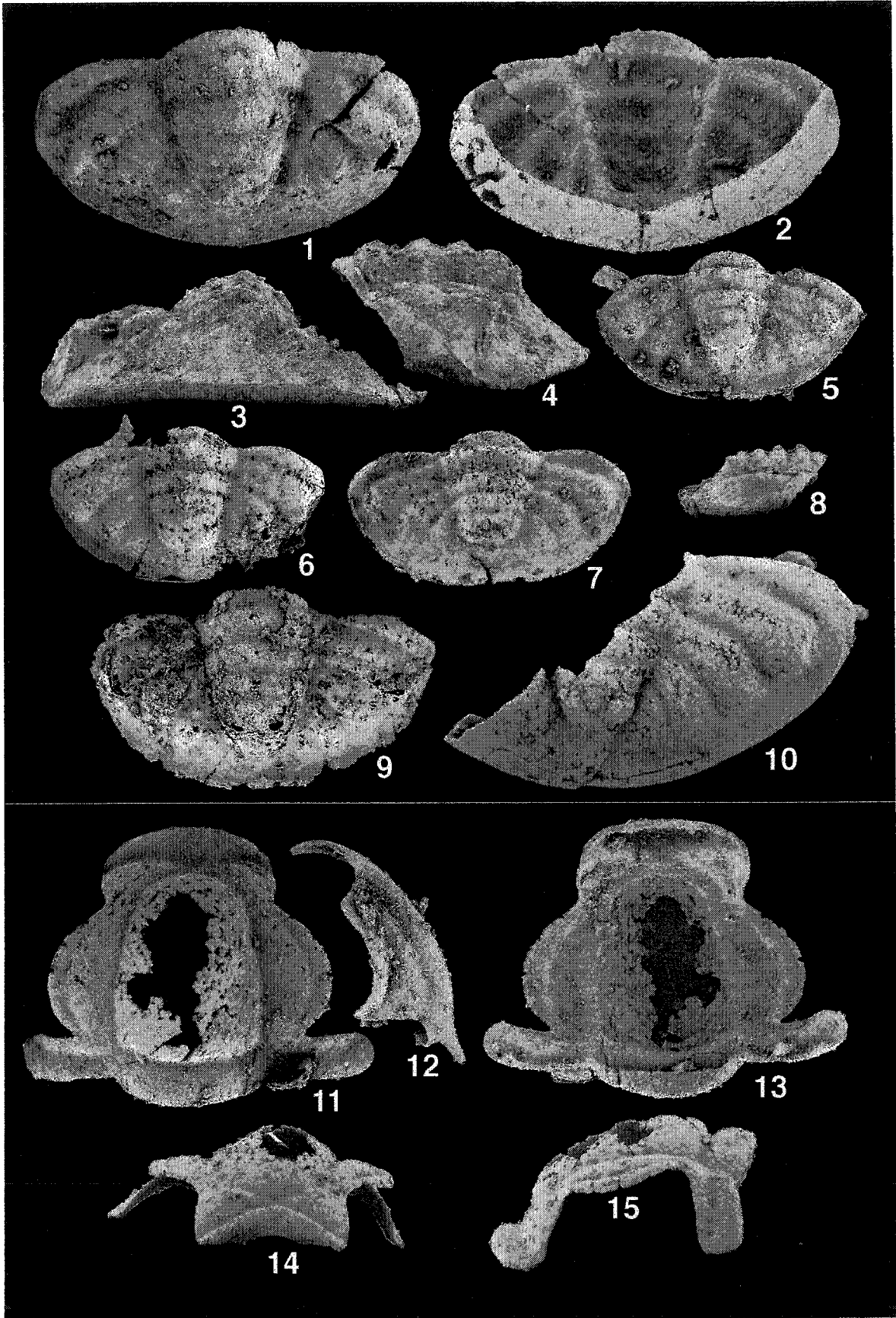
PLATE III-67. *Paratersella aculata* n. gen. and n. sp. and *Paratersella?* *acuta* n. sp.

1-14. *Paratersella aculata* n. gen. and n. sp. Note that the assignment of free cheek (Figs. 12, 14) and cranidium (Fig. 13) is tentative.

    1. UA 12556, holotype, cranidium, from R5-87.7, dorsal view, x 20.

    2, 9. UA 12557, free cheek, from R5-87.7, x 20; 2. Dorsal view, 9. Right lateral view.

    3. UA 12558, cranidium, from R5-76.4, dorsal view, x 20.

    4. UA 12559, small cranidium, from R5-87.7, dorsal view, x 20.

    5. UA 12560, small cranidium, from R5-86, dorsal view, x 20.

    6-8, 10. UA 12561, cranidium, from R6-55, x 20; 6. Dorsal view, 7. Anterior view, 8. Oblique right lateral view, 10. Ventral view.

    11. UA 12756, free cheek, from R5-87.7, dorsal view, x 20. Note: The image was flipped over vertically.

    12, 14. UA 12562, free cheek, from R6-55, x 20; 12. Ventral view, 14. Dorsal view.

    13. UA 12563, cranidium, from R6E2, dorsal view, x 20.

15-22. *Paratersella?* *acuta* n. sp.

    15, 17. UA 12564, free cheek, from R11-48.7, x 20; 15. Ventral view, 17. Dorsal view.

    16, 18, 21, 22. UA 12565, holotype, cranidium, from R11-48.7, x 20; 16. Dorsal view, 18. Anterior view, 21. Left lateral view, 22. Ventral view.

    19. UA 12566, cranidium, from R11-48.7, dorsal view, x 20.

    20. UA 12567, cranidium, from R6-38, dorsal view, x 20.

502
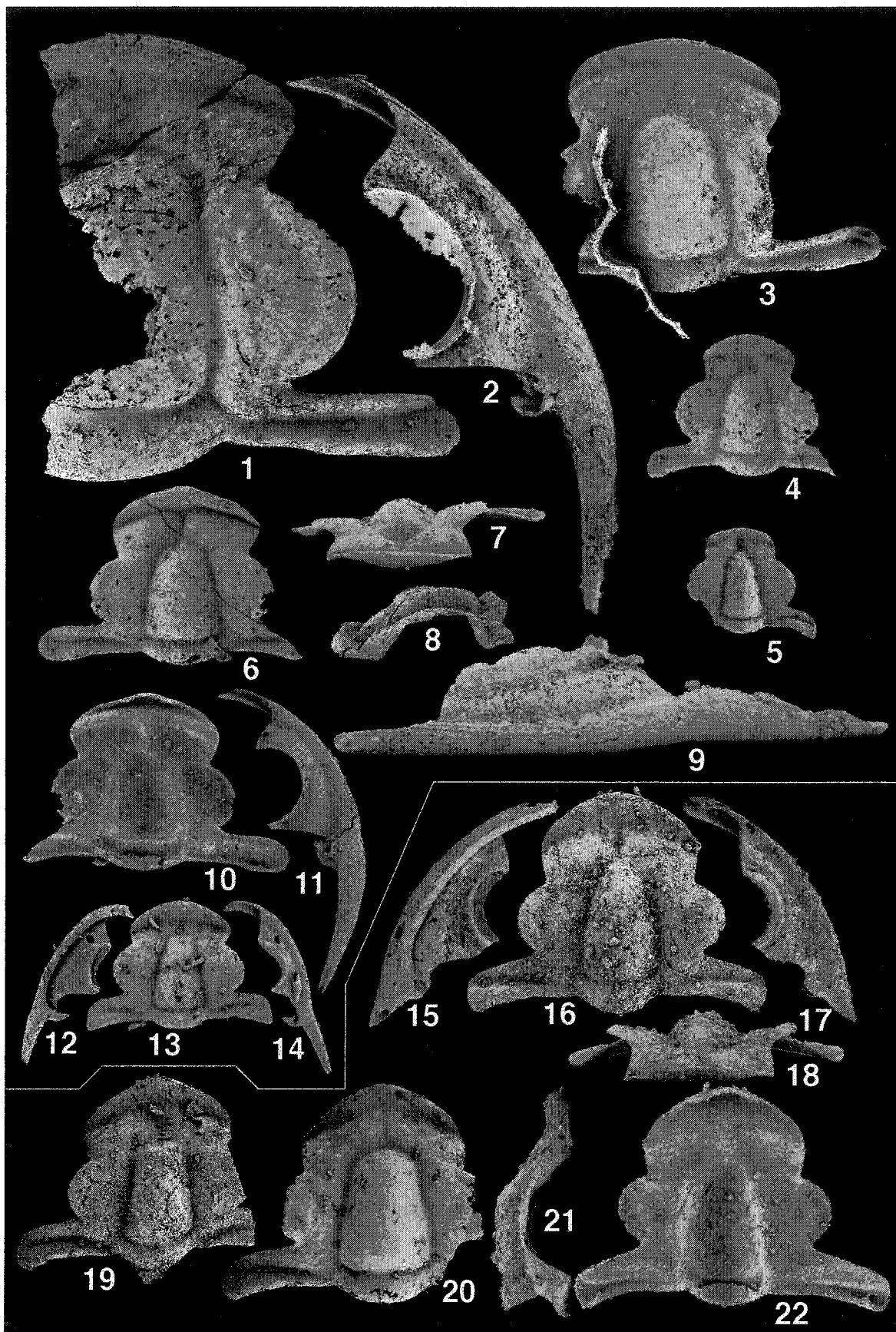
PLATE III-68. *Paratersella? obscurua* n. sp. and *Paratersella?* sp. aff. *P.? obscura.*

1-11, 16-21. *Paratersella? obscurua* n. sp.
  1-4. UA 12568, holotype, cranidium, from R5-86, x 30; 1. Right lateral view, 2. Dorsal
      view, 3. Ventral view, 4. Anterior view.
  5. UA 12569, cranidium, from R5-86, dorsal view, x 20.
  6. UA 12570, cranidium, from R5-76.4, dorsal view, x 20.
 7. UA 12571, cranidium, from R5-76.4, dorsal view, x 20.
  8. UA 12572, small cranidium, from R5-87.7, dorsal view, x 20.
  9. UA 12573, small cranidium, from R5-76.4, dorsal view, x 20.
  10. UA 12574, small cranidium, from R5-76.4, dorsal view, x 20.
  11. UA 12575, cranidium, from R5-86, dorsal view, x 20.
  16. UA 12576, protaspis, from R5-76.4, dorsal view, x 50.
  17. UA 12577, protaspis, from R5-76.4, dorsal view, x 50.
  18. UA 12578, protaspis, from R5-76.4, dorsal view, x 50.
  19. UA 12579, protaspis, from R5-76.4, dorsal view, x 50.
  20. UA 12580, protaspis, from R5-87.7(97), dorsal view, x 40.
  21. UA 12581, protaspis, from R5-76.4, dorsal view, x 30.
12-15. *Paratersella?* sp. aff. *P.? obscura.*
  12, 13. UA 12582, cranidium, from SE-152, x 20; 12. Dorsal view, 13. Oblique right
      lateral view.
  14, 15. UA 12583, cranidium, from SE-152, x 10; 14. Oblique left lateral view, 15.
      Dorsal view.

504
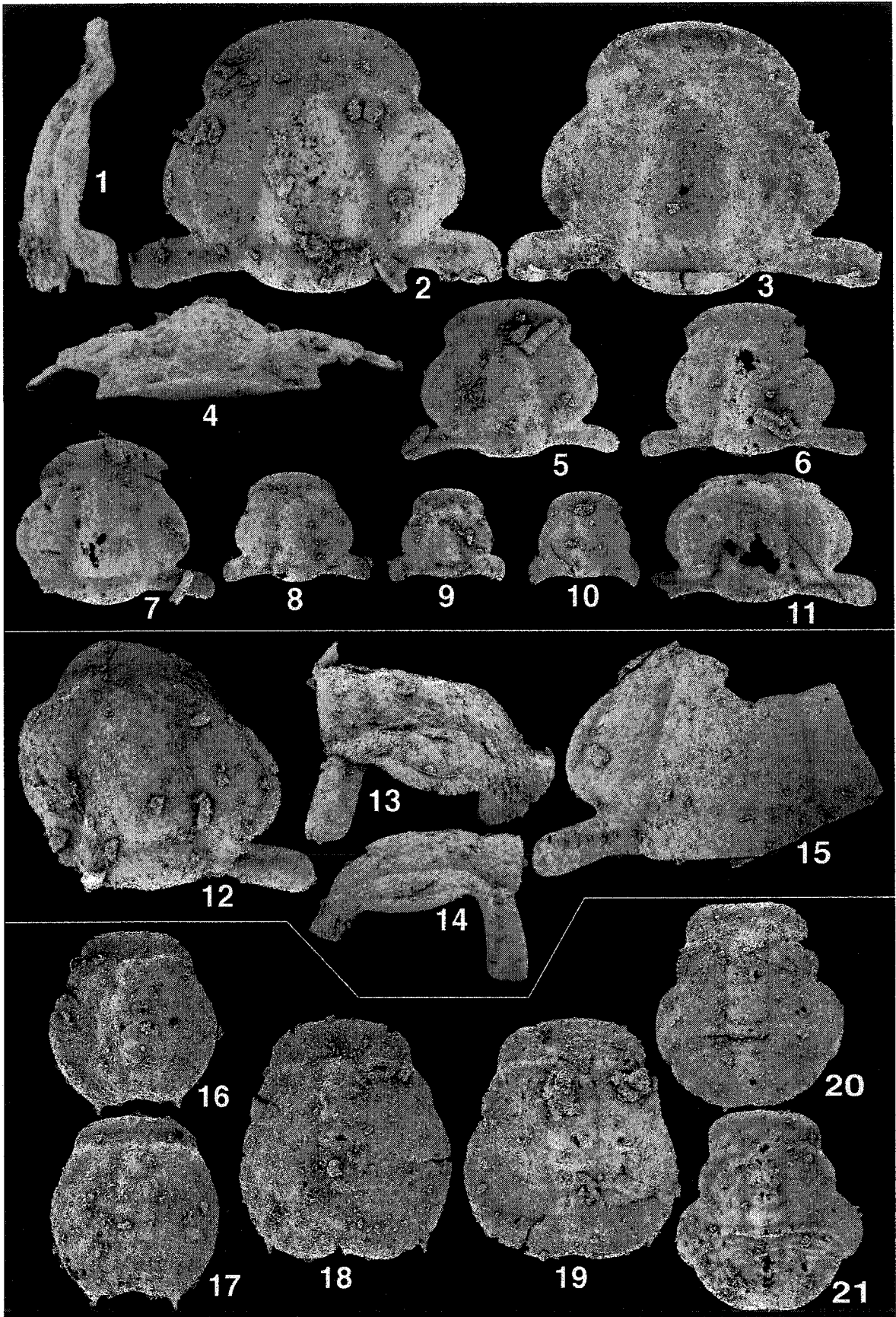
PLATE III-69. *Psalikilus typicus* Ross, 1951.

1-21. *Psalikilus typicus* Ross, 1951.

    1, 2, 5, 7. UA 12584, cranidium, from R6-100, x 20; 1. Dorsal view, 2. Right lateral view, 5. Anterior view, 7. Ventral view.

    3, 4. UA 12585, pygidium, from R6-114, x 20; 3. Dorsal view, 4. Posterior view.

    6. UA 12586, pygidium, from R6-100, dorsal view, x 20.

    8, 10, 16. UA 12587, cranidium, from R6-114, x 10; 8. Dorsal view, 10. Anterior view, 16. Right lateral view.

    9, 17. UA 12588, free cheek, from R6-100, x 20; 9. Dorsal view, 17. Left lateral view.

    11, 12, 14. UA 12589, pygidium, from R6-114, x 20; 11. Oblique left lateral view, 12. Dorsal view, 14. Ventral view.

    13. UA 12590, pygidium, from R6-114, dorsal view, x 20.

    15. UA 12591, cranidium, from R6-114, dorsal view, x 20.

    18, 19. UA 12592, transitory pygidium with two unreleased thoracic segments, from R6-114, x 20; 18. Posterior view, 19. Dorsal view.

    20, 21. UA 12593, transitory pygidium with one unreleased thoracic segment, from R6-114, x 20; 20. Dorsal view, 21. Posterior view.

22-26. Unassigned protaspides which could be associated with *Psalikilus*.

    22-24. UA 12594, protaspis, from R6-114, x 75; 22. Ventral view, 23. Dorsal view, 24. Oblique anterior view.

    25, 26. UA 12595, protaspis, from R6-114, x 75; 25. Right lateral view, 26. Dorsal view.

506
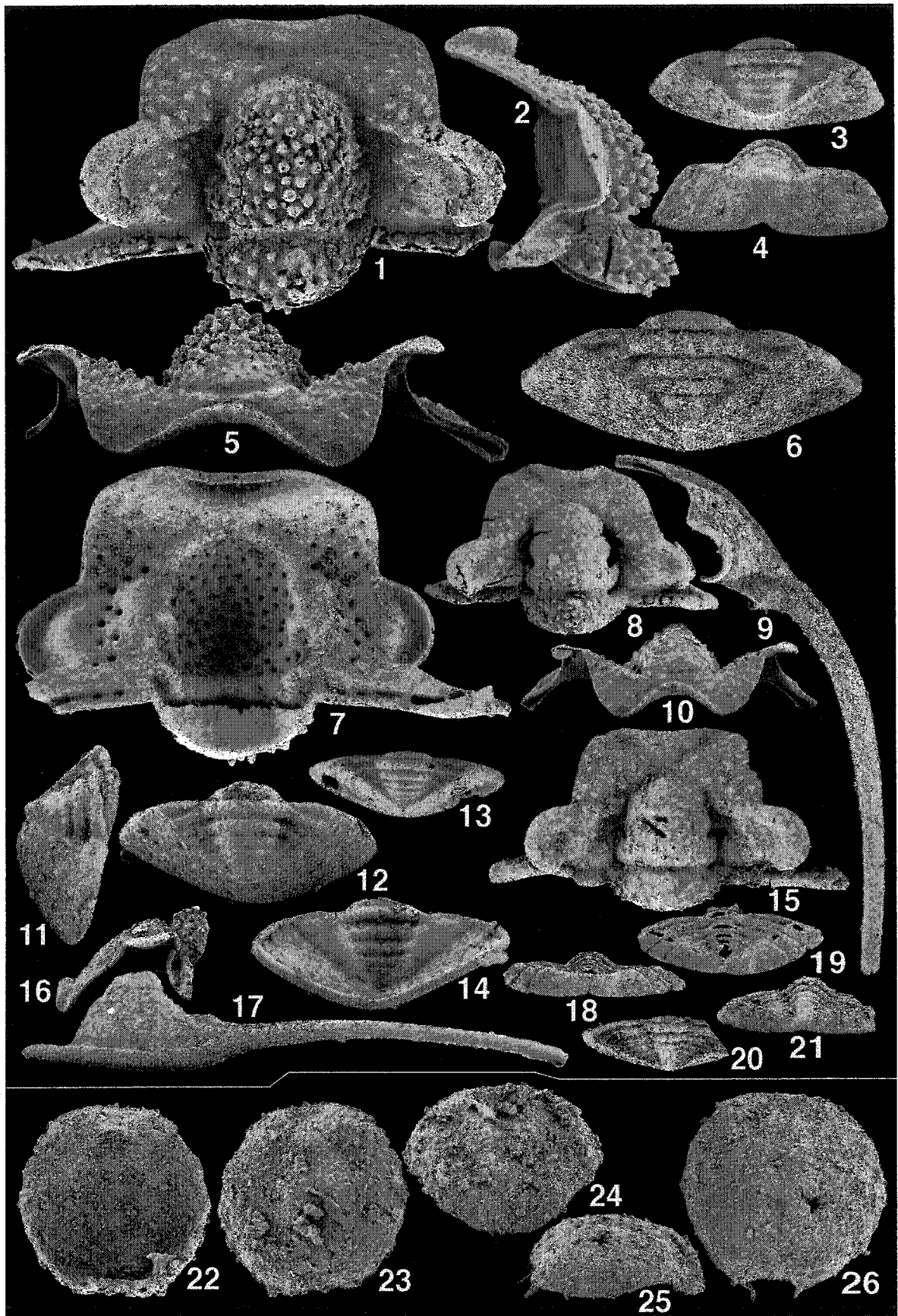
PLATE III-70. *Psalikilus typicus* Ross, 1951.

1-17. *Psalikilus typicus* Ross, 1951.

    1. UA 12596, cranidium, from R6-114, dorsal view, x 20.

    2, 3. UA 12597, free cheek, from R6-114, x 20; 2. Dorsal view, 3. Dorsal (conventional) view.

    4. UA 12598, cranidium, from SR6U, dorsal view, x 20.

    5. UA 12599, free cheek, from R6-114, dorsal view, x 20.

    6, 7. UA 12600, free cheek, from R6-114, x 20; 6. Dorsal view, 7. Ventral view.

    8. UA 12601, partially articulated specimen consisting of small cranidium and three thoracic segments, from R6-114, dorsal view, x 40.

    9. UA 12602, small cranidium, from R6-114, dorsal view, x 40.

    10. UA 12603, small cranidium, from R6-114, dorsal view, x 40.

    11. UA 12604, small cranidium, from R6-114, dorsal view, x 40

    12. UA 12605, small cranidium, from R6-114, dorsal view, x 40

    13. UA 12606, small cranidium, from R6-114, dorsal view, x 100.

    14. UA 12607, small cranidium, from R6-114, dorsal view, x 100.

    15-17. UA 12608, protaspis, from R6-114, x 75; 15. Dorsal view, 16. Oblique anterior view, 17. Oblique right lateral view.

508
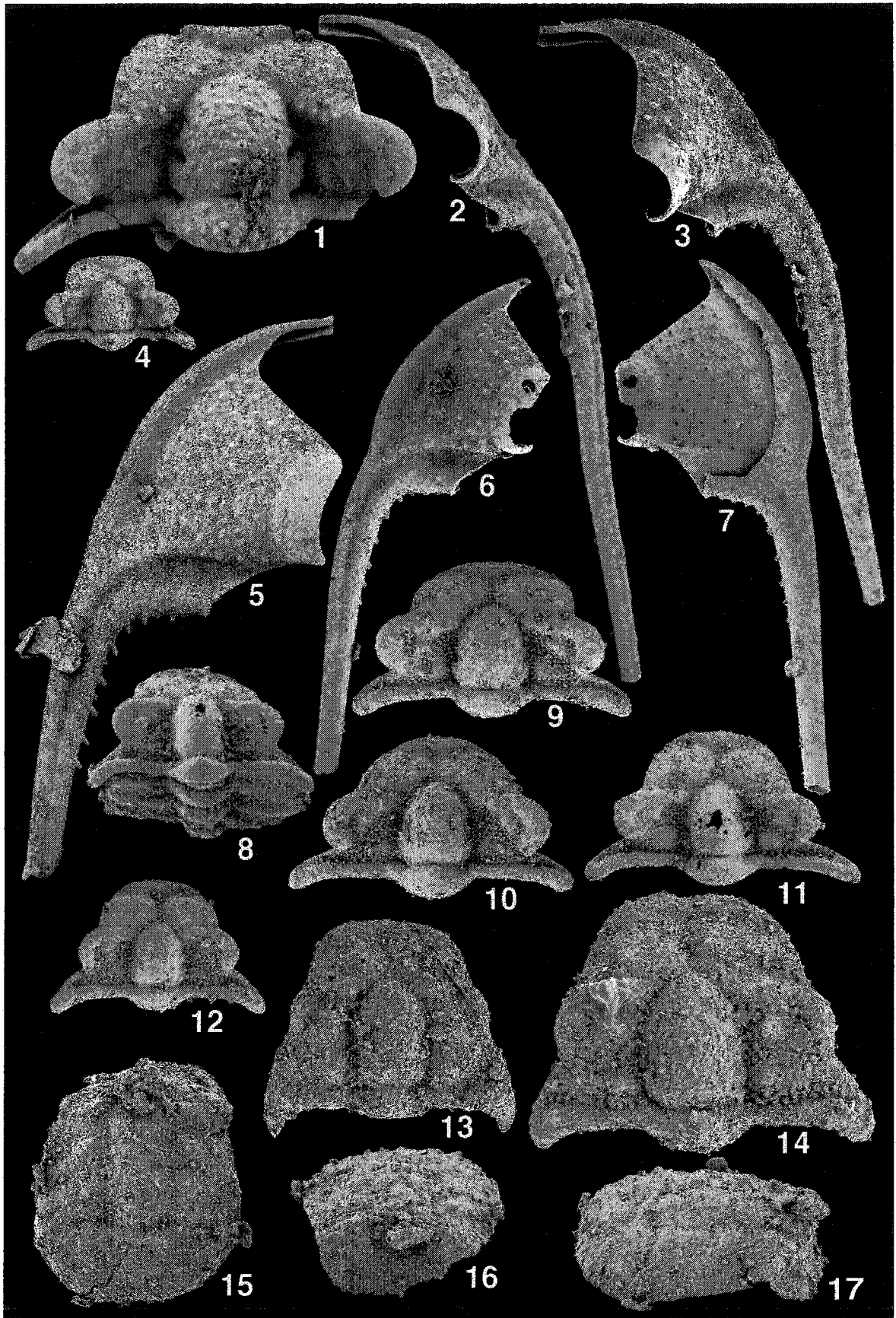
PLATE III-71. *Psalikilus pikus* Hintze, 1953 and *Psalikilus*? sp. B.

1-17. *Psalikilus pikus* Hintze, 1953. Assignment of pygidia (Figs. 6-17) is provisional.
    1, 2, 4, 5. UA 12609, cranidium, from R6-100, x 20; 1. Dorsal view, 2. Left lateral view, 4, Ventral view, 5. Anterior view.
    3. UA 12610, cranidium, from R6-114, dorsal view, x 20.
    6, 10. UA 12611, pygidium, from R5-76.4, x 20; 6. Dorsal view, 10. Ventral view.
    7. UA 12612, transitory pygidium, from R5-76.4 (97), dorsal view, x 20.
    8, 9. UA 12613, pygidium, from R5-86, x 20; 8. Dorsal view, 9. Right lateral view.
    11. UA 12614, transitory pygidium, from R5-76.4, dorsal view, x 20.
    12, 13. UA 11868, pygidium, from R5-76.4, x 20; 12. Dorsal view, 13. Posterior view.
    14, 15. UA 11867, transitory pygidium, from R5-76.4, x 20; 14. Dorsal view, 15. Oblique posterior view.
    16. UA 12615, transitory pygidium, from R5-76.4, dorsal view, x 20.
    17. UA 12616, transitory pygidium, from R5-76.4, dorsal view, x 20.
18-24. *Psalikilus*? sp. B.
    18, 19. UA 11873, pygidium, from R5-76.4, x 20; 18. Dorsal view, 19. Posterior view.
    20, 21. UA 12617, pygidium, from R5-76.4, x 20; 20. Dorsal view, 21. Ventral view.
    22. UA 12618, pygidium, from R5-76.4, dorsal view, x 20.
    23. UA 12619, pygidium, from R5-76.4A, dorsal view, x 20.
    24. UA 12620, pygidium, from R5-76.4A, dorsal view, x 20.

510
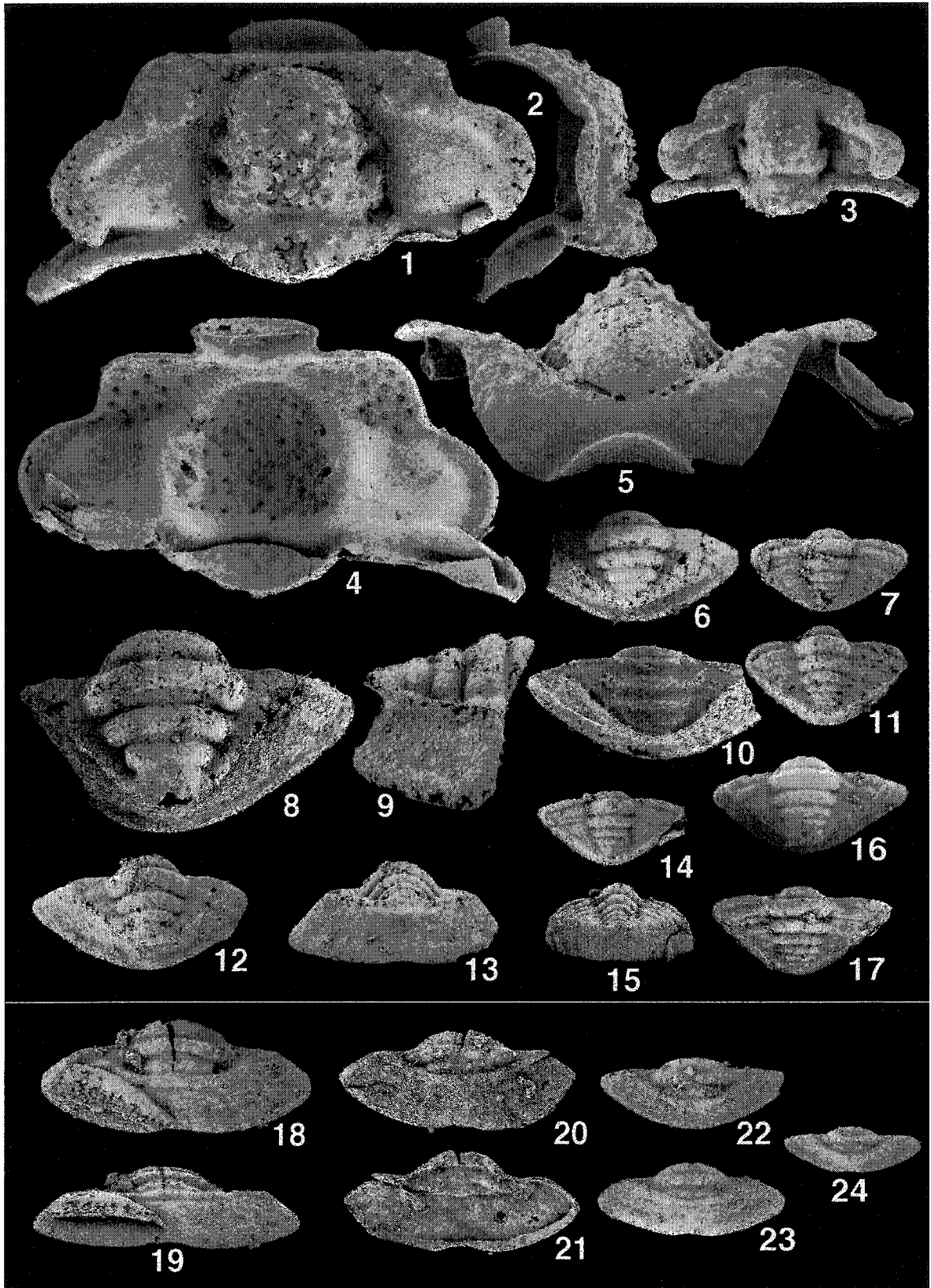
PLATE III-72. *Psalikilus paraspinosum* Hintze, 1953 and *Psalikilus?* sp. A.

1-12. *Psalikilus paraspinosus* Hintze, 1953.
    1, 4, 5. UA 12621, cranidium, from R5-34.1, x 20; 1. Dorsal view, 4. Anterior view, 5. Left lateral view.
    2. UA 12622, free cheek, from SR6U, dorsal view, x 20.
    3. UA 12623, free cheek, from SR6U, dorsal view, x 20.
    6. UA 12624, small cranidium, from R6-114, dorsal view, x 40.
    7, 10. UA 12625, pygidium, from SR6U, x 20; 7. Dorsal view, 10. Posterior view.
    8. UA 12626, pygidium, from SR6U, dorsal view, x 20.
    9. UA 12627, cranidium, from SR6U, dorsal view, x 20.
    11, 12. UA 12628, pygidium, from SR6U, x 20; 11. Right lateral view, 12. Dorsal view.
13-15. *Psalikilus?* sp. A.
    13-15. UA 12629, pygidium, from SR6U, x 30; 13. Dorsal view, 14. Posterior view, 15. Left lateral view.

512
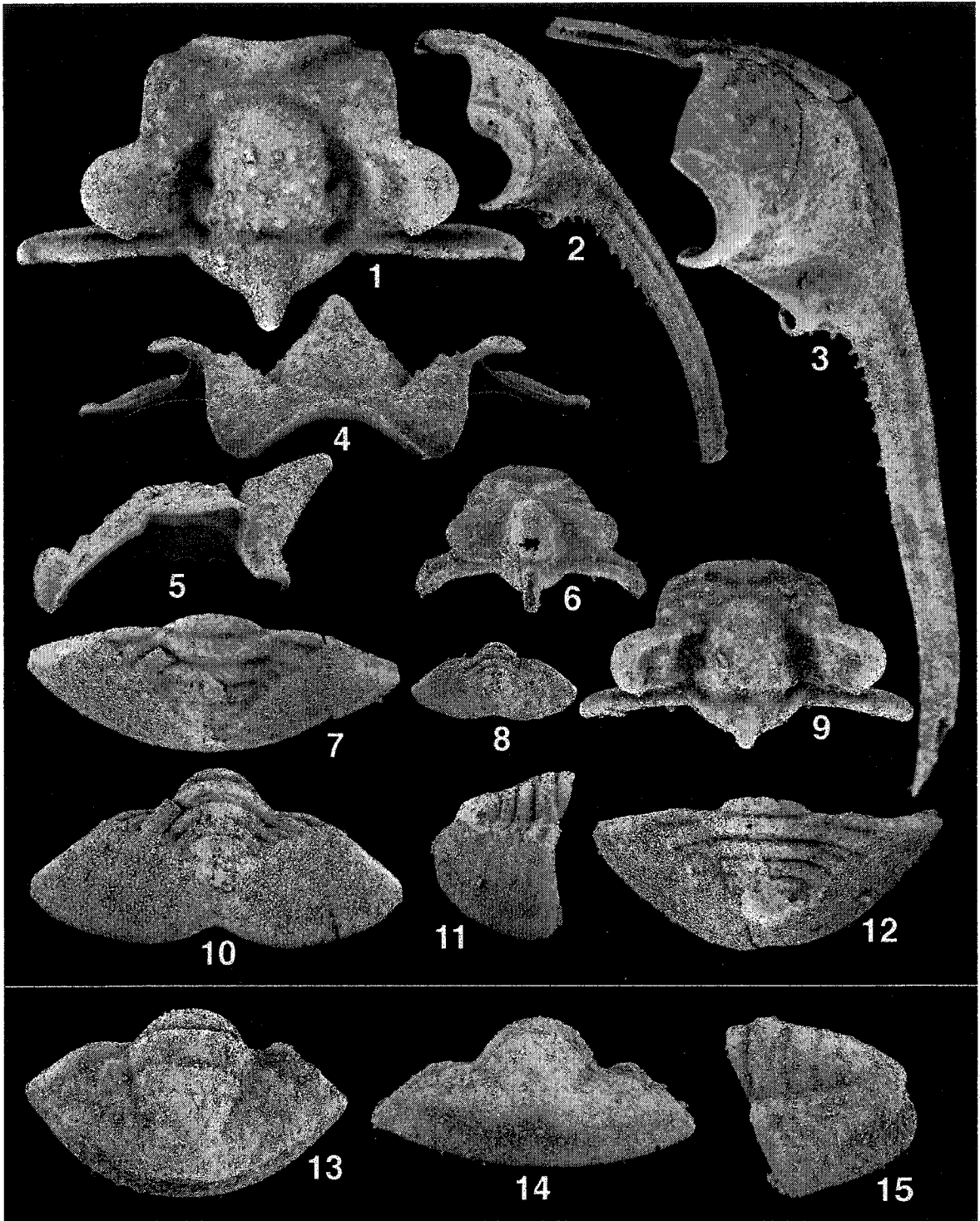
PLATE III-73. *Psalikilopsis cuspidicauda* Ross, 1953 and *Psalikilopsis brachyspinosus* n. sp.

1-6. *Psalikilopsis cuspidicauda* Ross, 1953.
    1, 2. UA 12630, free cheek, from SR6U, x 15; 1. Dorsal (conventional) view, 2. Dorsal view.
    3-5. UA 12631, cranidium, from SR6U, x 10; 3. Dorsal view, 4. Anterior view, 5. Right lateral view.
    6. UA 12632, free cheek, from SR6U, dorsal view, x 15.
7-11. *Psalikilopsis brachyspinosus* n. sp.
    7. UA 12633, pygidium, from SR6U, dorsal view, x 20.
    8-11. UA 12634, holotype, pygidium, from SR6U, x 20; 8. Dorsal view, 9. Posterior view, 10. Left lateral view, 11. Ventral view.

514

PLATE III-74. *Pyraustocranium orbatum* Ross, 1951 and *Goniophrys prima* Ross, 1951.

1-7, 12-19. *Pyraustocranium orbatum* Ross, 1951.
    1, 2, 6. UA 12635, cranidium, from R6-114(97), x 10; 1. Dorsal view, 2. Oblique right lateral view, 6. Anterior view.
    3. UA 12636, cranidium, from R6E2, dorsal view, x 10.
    4. UA 12637, free cheek, from R6-114(97), dorsal view, x 10.
    5, 7. UA 12638, cranidium, from R6E3, x 10; 5. Dorsal view, 7. Ventral view.
    12. UA 12639, small cranidium, from R6E3, dorsal view, x 20.
    13. UA 12640, small cranidium, from R6-114(97), dorsal view, x 20.
    14. UA 12641, small cranidium, from R6-114(97), dorsal view, x 20.
    15. UA 12642, small cranidium, from R6-114(97), dorsal view, x 20.
    16. UA 12643, small cranidium, from R6-114(97), dorsal view, x 20.
    17. UA 12644, cranidium, from R6-114(97), dorsal view, x 20.
    18. UA 12645, cranidium, from R6-114(97), dorsal view, x 20.
    19. UA 12646, cranidium, from R6-114(97), dorsal view, x 20.
8-11. *Goniophrys prima* Ross, 1951.
    8-10. UA 12647, cranidium, from R6-114, x 20; 8. Right lateral view, 9. Dorsal view, 10. Anterior view.
    11. UA 12648, free cheek, from R6-114, dorsal view, x 20.

516
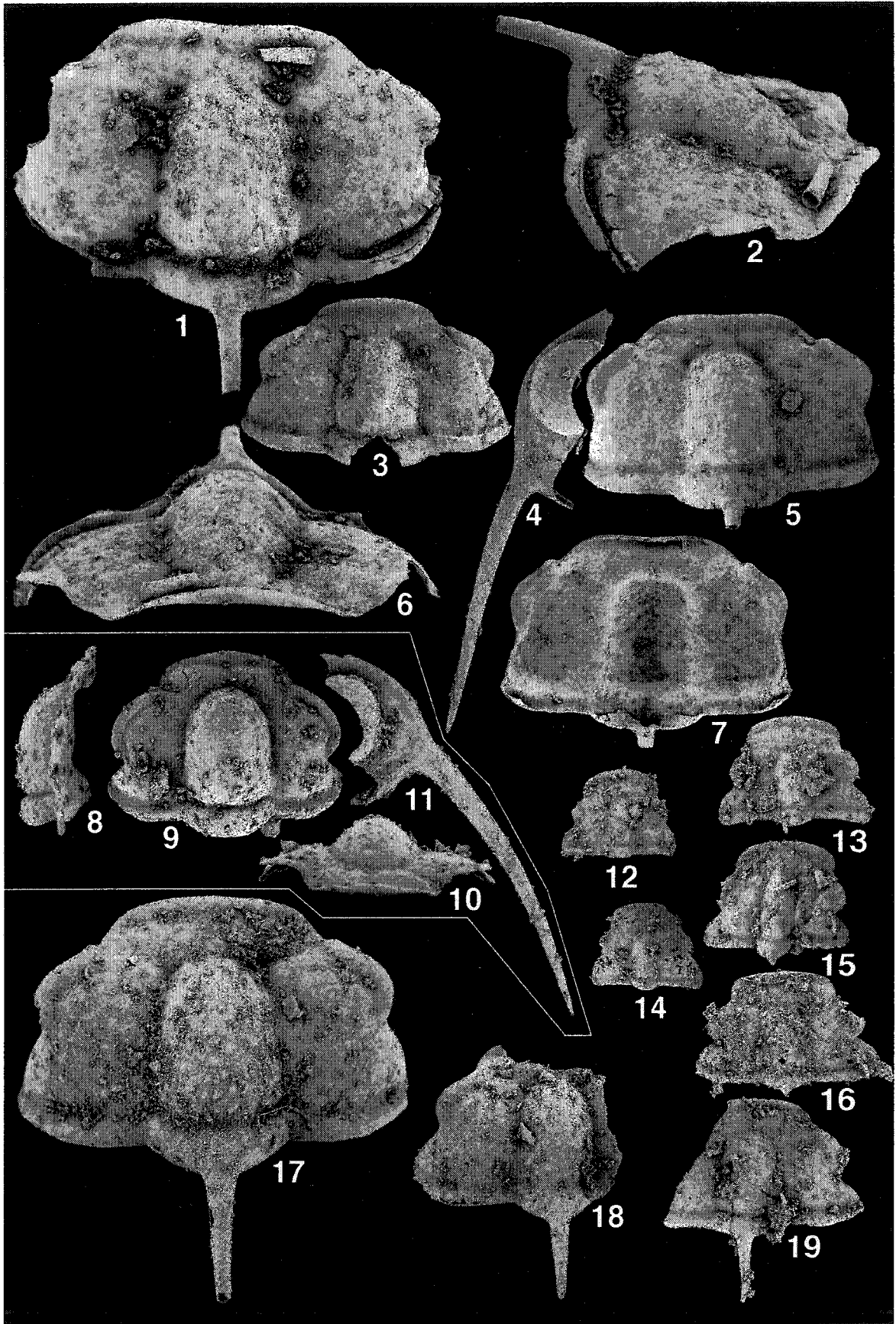
PLATE III-75. *Pseudoetheridgaspis typica* n. gen. and n. sp.

1-19. *Pseudoetheridgaspis typica* n. gen. and n. sp. Note that the cranidium (Fig. 15) could be assigned to *Amblycranium transversus*.

1-3, 5. UA 12649, holotype, cranidium, from R11-48.7, x 20; 1. Dorsal view, 2. Left lateral view, 3. Ventral view, 5. Anterior view.

4, 8. UA 12650, free cheek, from R11-48.7, x 20; 4. Ventral view, 8. Dorsal view.

6. UA 12651, cranidium, from R6-35, dorsal view, x 20.

7. UA 12652, cranidium, from R11-48.7, dorsal view, x 20.

9. UA 12653, cranidium, from R11-48.7, dorsal view, x 20.

10. UA 12654, free cheek, from R11-48.7, dorsal view, x 20.

11. UA 12655, cranidium, from R11-48.7, dorsal view, x 20.

12. UA 12656, cranidium, from R11-48.7, dorsal view, x 20.

13. UA 12657, cranidium, from R11-48.7, dorsal view, x 20.

14. UA 12658, cranidium, from R6-35, dorsal view, x 20.

15. UA 12659, cranidium, from R6-38, dorsal view, x 20.

16-18. UA 12660, cranidium, from R11-48.7, x 20; 16. Dorsal view, 17. Left lateral view, 18. Anterior view.

19. UA 12661, cranidium, from R6-35, dorsal view, x 20.
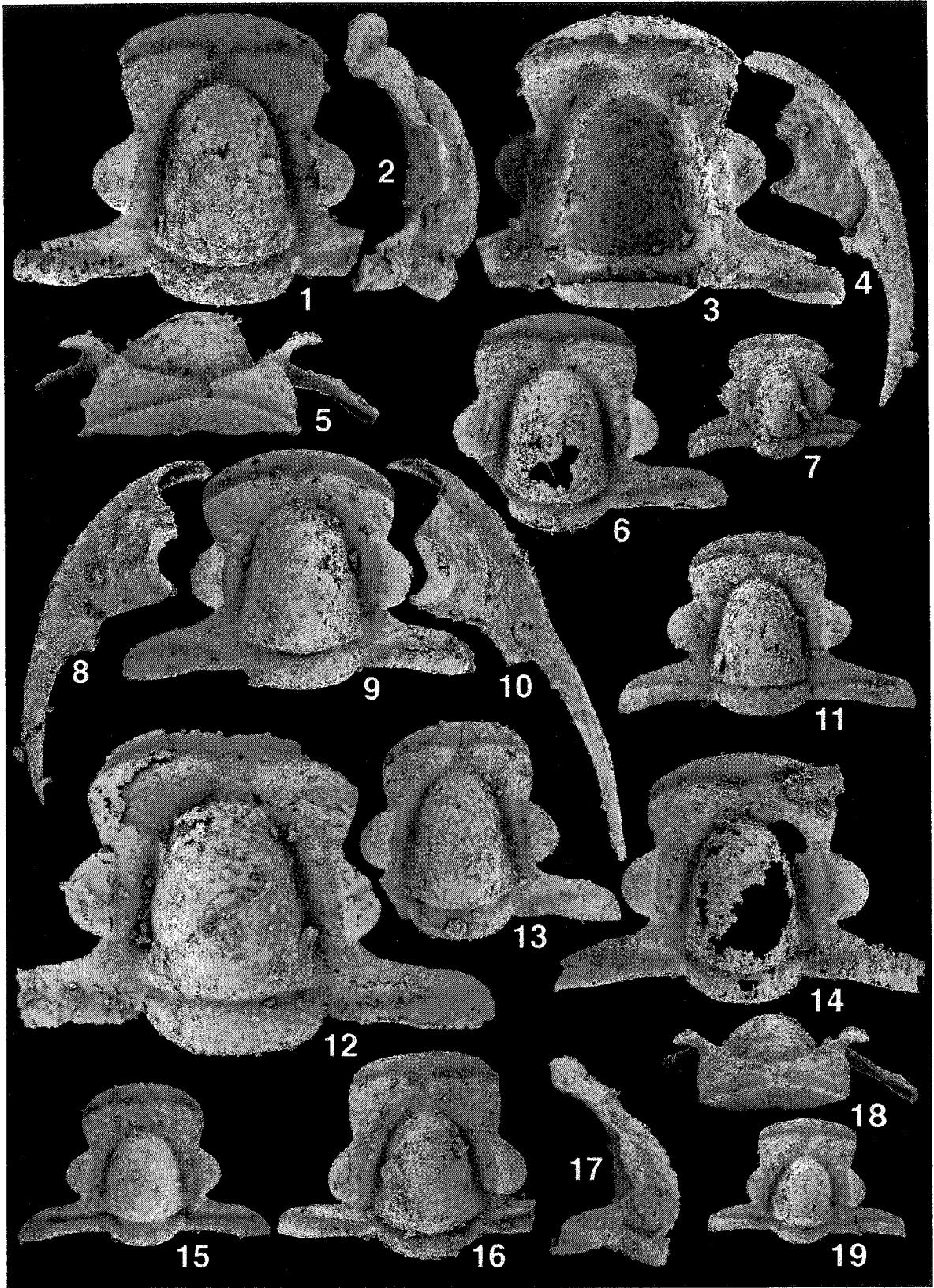
PLATE III-76. *Pseudoetheridgaspis cylindricus* n. gen. and n. sp. and
  Pseudoetheridgaspis typica n. gen. and n. sp.

1-15. *Pseudoetheridgaspis cylindricus* n. gen. and n. sp.
   1. UA 12662, free cheek, from R11-48.7, dorsal view, x 20.
   2, 3, 5, 9. UA 12663, holotype, cranidium, from R11-48.7, x 20; 2. Dorsal view, 3. Left
     lateral view, 5. Anterior view, 9. Ventral view.
   4. UA 12664, cranidium, from R11-48.7, dorsal view, x 20.
   6. UA 12665, cranidium, from R6-38, dorsal view, x 20.
   7. UA 12666, cranidium, from R11-48.7, dorsal view, x 20.
   8. UA 12667, free cheek, from R11-48.7, dorsal view, x 20.
   10. UA 12668, cranidium, from R6-38, dorsal view, x 20.
   11. UA 12669, cranidium, from R11-48.7, dorsal view, x 20.
   12. UA 12670, cranidium, from R6-38, dorsal view, x 20.
   13. UA 12671, cranidium, from R11-48.7, dorsal view, x 20.
   14. UA 12672, cranidium, from R11-48.7, dorsal view, x 20.
   15. UA 12673, cranidium, from R11-48.7, dorsal view, x 20.
16-24. *Pseudoetheridgaspis typica* n. gen. and n. sp.
   16, 23, 24. UA 12674, pygidium, from R11-48.7, x 20; 17. Dorsal view, 24. Ventral
     view, 25. Posterior view.
   17, 18. UA 12675, transitory pygidium, from R11-48.7, x 20; 18. Dorsal view, 19.
     Posterior view.
   19. UA 12676, transitory pygidium, from R11-48.7, dorsal view, x 20.
   20. UA 12677, transitory pygidium, from R11-48.7, dorsal view, x 20.
   21. UA 12678, transitory pygidium, from R11-48.7, dorsal view, x 20.
   22. UA 12679, transitory pygidium, from R11-48.7, dorsal view, x 20.

520
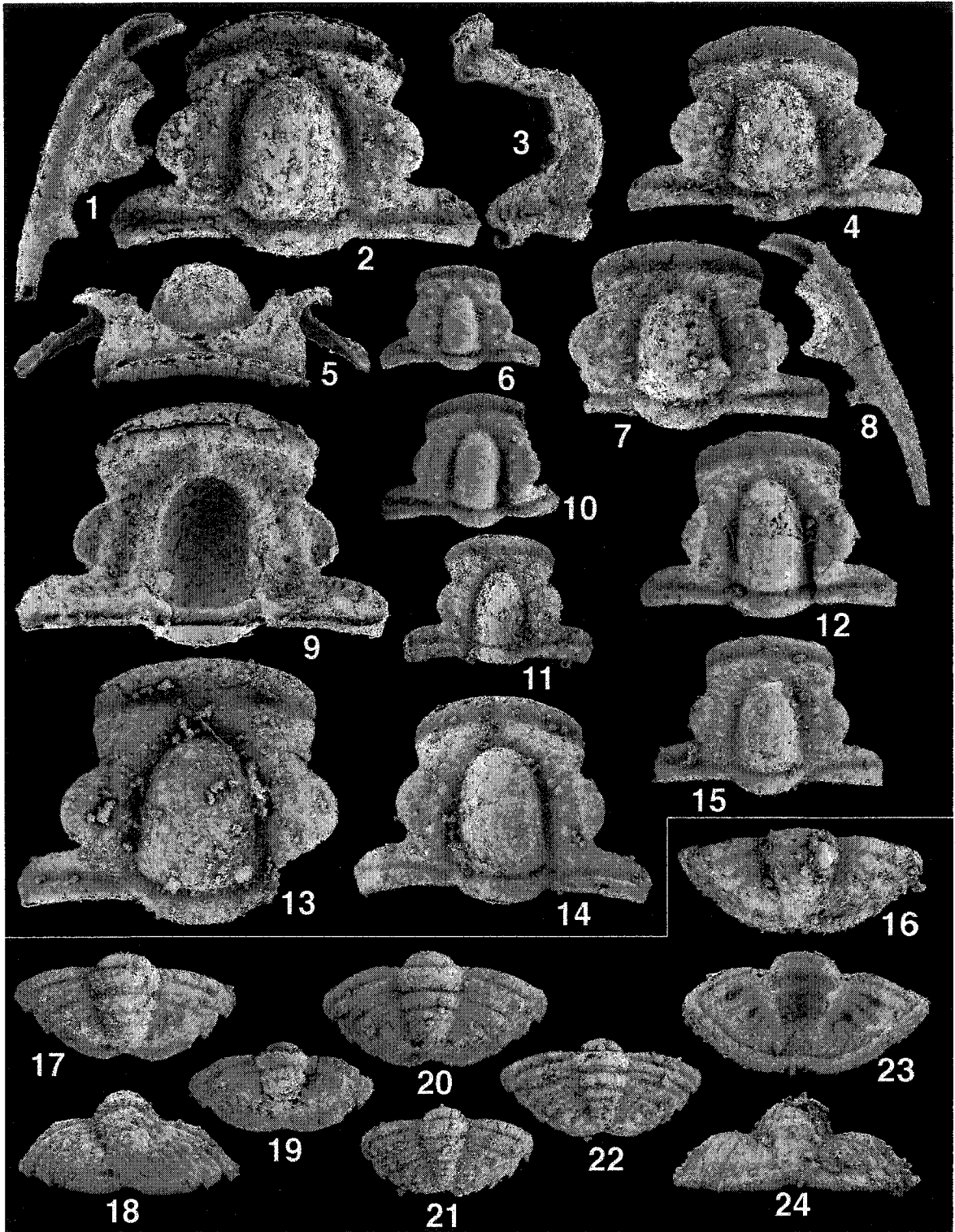
PLATE III-77. *Pseudohystricurus obesus* Ross, 1951, *Pseudohystricurus*
   bathysulcatus n. sp. and *Pseudohystricurus*? *parvus* n. sp.

1-11. *Pseudohystricurus obesus* Ross, 1951.
   1, 5. UA 12680, cranidium, from SE-90T, x 20; 1. Dorsal view, 5. Left lateral view.
   2. UA 12681, cranidium, from R6-114(97), dorsal view, x 20.
   3. UA 12682, cranidium, from R6-114(97), dorsal view, x 20.
   4. UA 12683, cranidium, from R6-114(97), dorsal view, x 40.
   6, 7. UA 12684, cranidium, from R6-114(97), x 40; 6. Dorsal view, 7. Anterior view.
   8, 9. UA 12685, pygidium, from SE-90T, x 20; 8. Dorsal view, 9. Posterior view.
   10, 11. UA 12686, pygidium, from SE-90T, x 20; 8. Dorsal view, 9. Oblique right
      lateral view.
12-19. *Pseudohystricurus bathysulcatus* n. sp.
   12, 13, 16. UA 12687, cranidium, from SE-90T, x 20; 12. Dorsal view, 13. Oblique
      right lateral view, 16. Anterior view.
   14. UA 12688, cranidium, from SE-90T, dorsal view, x 20.
   15. UA 12689, holotype, cranidium, from SE-80T, dorsal view, x 20.
   17. UA 12690, cranidium, from E-2, dorsal view, x 20.
   18. UA 12691, cranidium, from R5-34.1, dorsal view, x 20.
   19. UA 12692, cranidium, from R5-34.1, dorsal view, x 20.
20-30. *Pseudohystricurus*? *parvus* n. sp.
   20, 22, 25, 26. UA 12693, holotype, cranidium, from R6-38, x 20; 20. Dorsal view, 22.
      Ventral view, 25. Anterior view, 26. Right lateral view.
   21. UA 12694, free cheek, from R6-38, dorsal view, x 20.
   23, 24. UA 12695, fragmentary cranidium with two thoracic segments, from R6-38, x
      20; 23. Dorsal view, 24. Right lateral view.
   27. UA 12696, cranidium, from R11-48.7, dorsal view, x 20.
   28-30. UA 12697, pygidium, from R6-38, x 20; 28. Left lateral view, 29. Dorsal view,
      30. Posterior view.

522
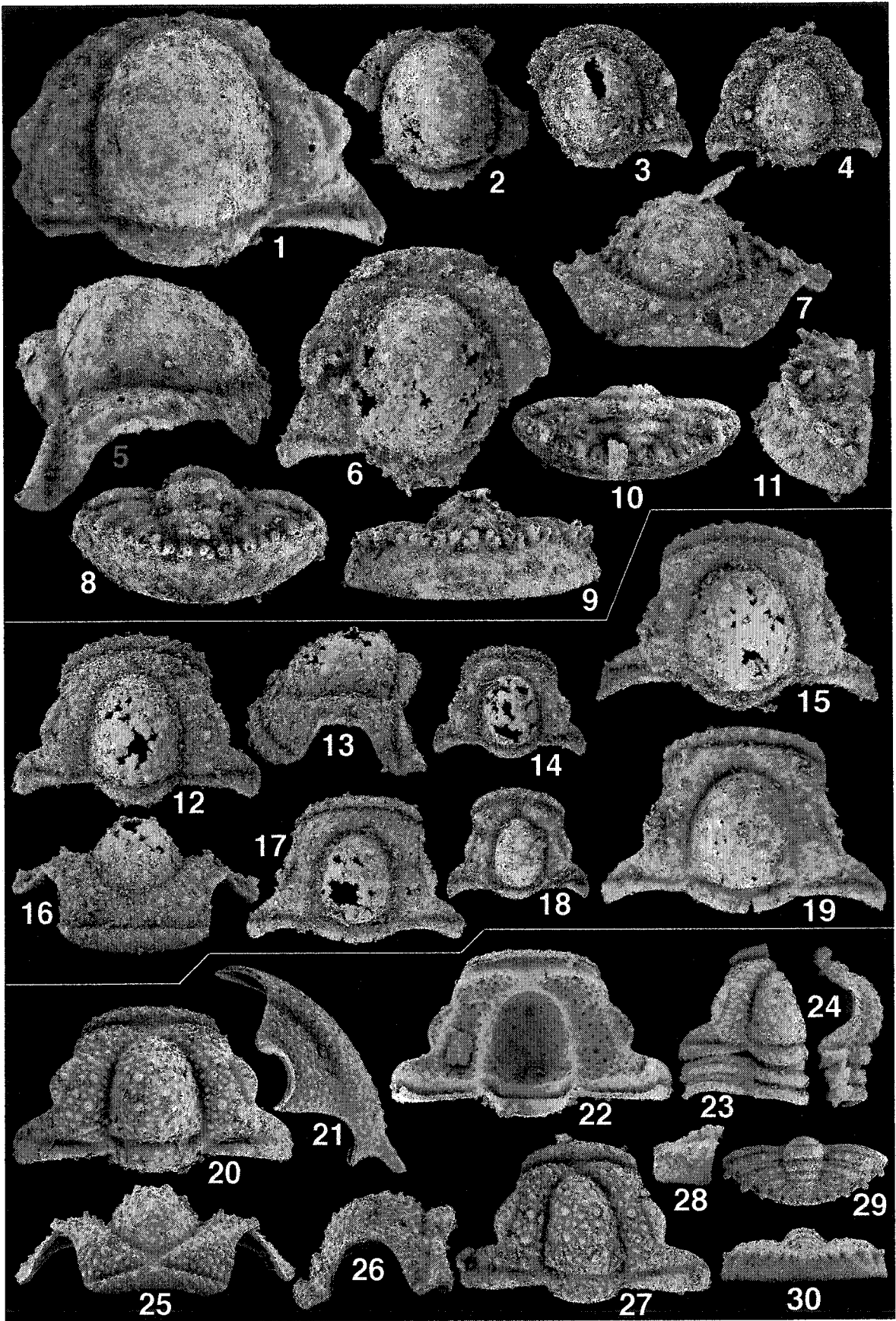
PLATE III-78. *Glabellosulcatus? crassilimbatus* (Poulsen, 1937) and *Heckethornia? linearus* (Young, 1973)

1-17. *Glabellosulcatus? crassilimbatus* (Poulsen, 1937).
    1-3, 5. UA 12698, cranidium, from R5-86, x 20; 1. Right lateral view, 2. Dorsal view, 3. Oblique dorsal view, 5. Anterior view.
    4. UA 12699, cranidium, from R5-86, dorsal view, x 20.
    6, 7, 9. UA 12700, fragmentary cranidium, from R5-76.4, x 10; 6. Anterior view, 7. Ventral view, 9. Dorsal view.
    8. UA 12701, cranidium, from R5-87.7, dorsal view, x 20.
    10. UA 12702, cranidium, from R5-76.4, dorsal view, x 20.
    11. UA 12703, cranidium, from R5-86, dorsal view, x 20.
    12-14. MGUH 3685, holotype, cranidium, from Cape Weber Formation (Lower Ordovician), East Greenland, x 10; 12. Dorsal view, 13. Anterior view. 14. Left lateral view.
    15. UA 12704, cranidium, from R5-76.4, dorsal view, x 20.
    16. UA 12705, cranidium, from R5-86, dorsal view, x 20.
    17. UA 12706, cranidium, from R5-86, dorsal view, x 20.
18-20. *Heckethornia? linearus* (Young, 1973).
    18-20. UA 12707, cranidium, from SH-5T, x 20; 18. Right lateral view, 19. Dorsal view, 20. Anterior view.
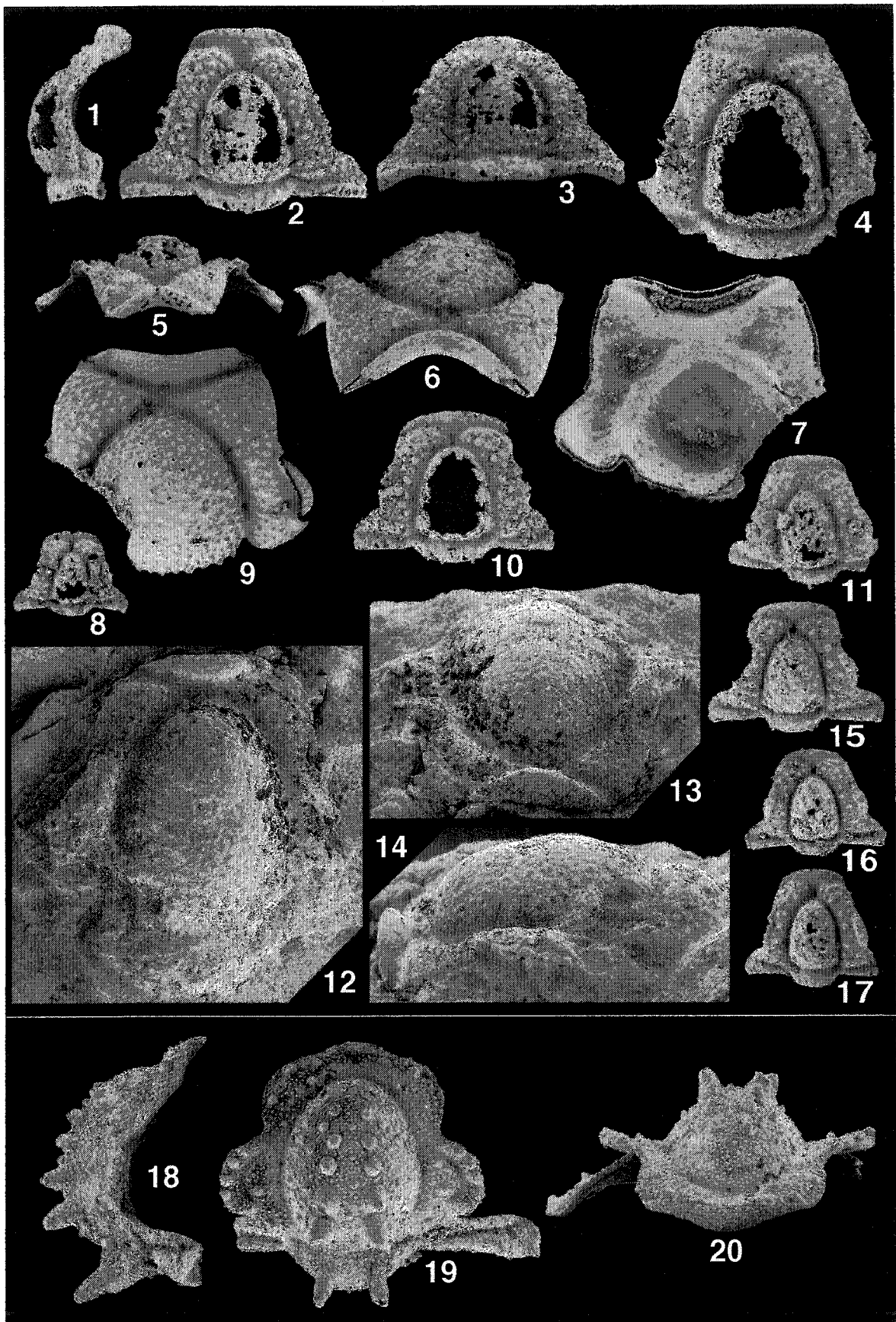
PLATE III-79. *Glabellosculcatus sanduensis* (Zhou, 1981) and *Glabellosculcatus koreanicus* n. gen. and n. sp.

1-4. *Glabellosculcatus sanduensis* (Zhou, 1981). Both specimens are from La1 Zone (Lancefieldian Series) of Digger Island Formation, Victoria, Australia.
   1, 3. NMVP 74338, cranidium, x 10; 1. Dorsal view, 3. Right lateral view.
   2, 4. NMVP 74339, cranidium, x 10; 2. Dorsal view, 4. Anterior view.
5-9. *Glabellosculcatus koreanicus* n. gen. and n. sp. The specimens is from *Protopliomerops* Zone of Mungok Formation, South Korea. Figs. 5 and 6 are photographed by light photographic technique.
   5-9. SNUP 573, holotype, articulated specimen; 5. Dorsal view, x 10, 6. Oblique anterior view, x 10, 7. Magnified right lateral view of posterior portion of cast, x 20, 8. Magnified posterior view of posterior portion of cast, x 20, 9. Magnified left lateral view of posterior portion of cast, x 20.
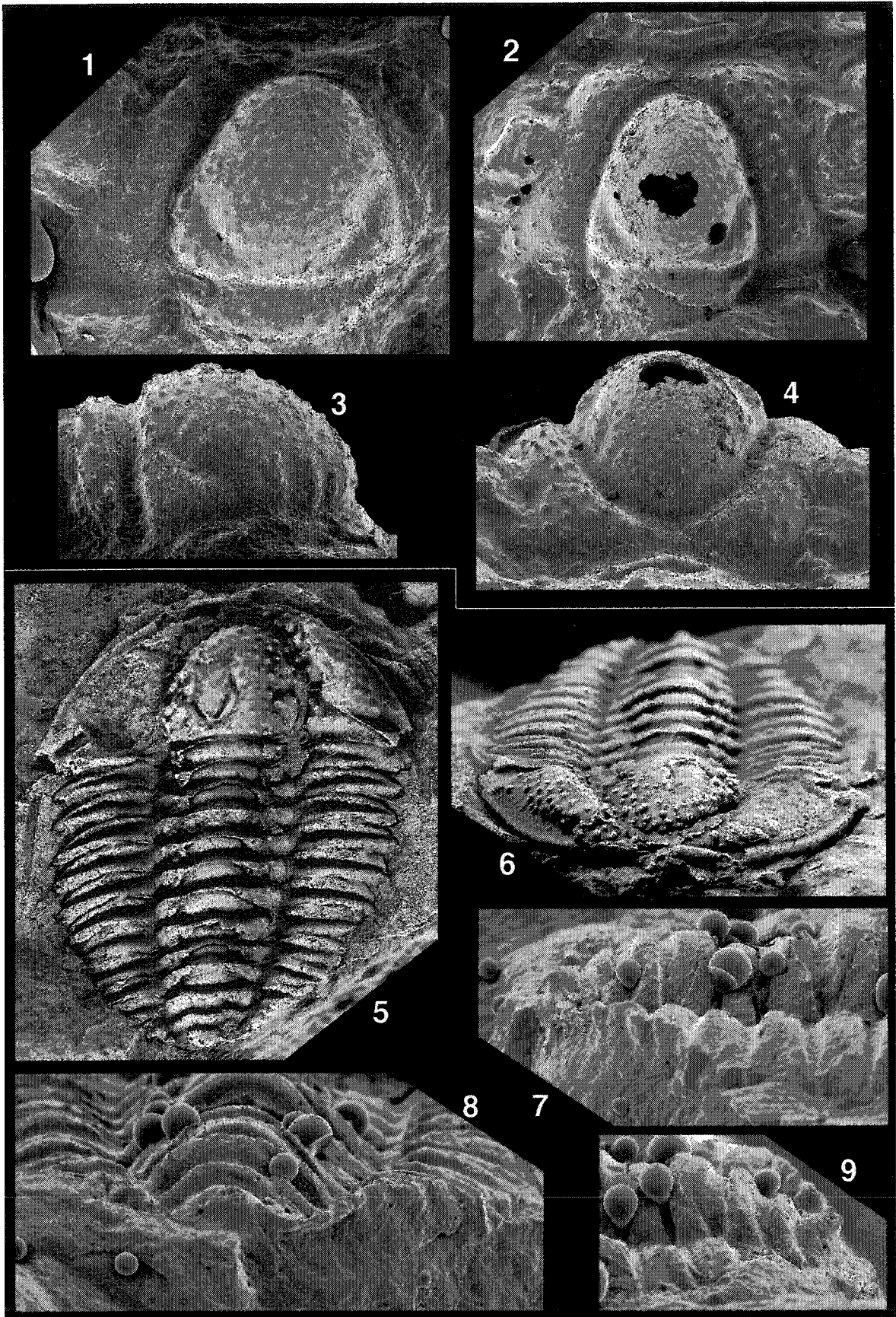
PLATE III-80. *Heckethornia borderinnensis* n. gen. and n. sp. and *Heckethornia* n. sp.

1-14. *Heckethornia borderinnensis* n. gen. and n. sp.
    1, 2, 5. UA 12708, holotype, cranidium, from R6-114, x 40; 1. Dorsal view, 2. Left lateral view, 5. Anterior view.
    3, 4. UA 12709, cranidium, from R6-114, x 20; 3. Dorsal view, 4. Anterior view.
    6. UA 12710, cranidium, from R6-114(97), dorsal view, x 40.
    7, 13. UA 12711, free cheek, from R6-114, x 40; 7. Dorsal view, 13. Right lateral view.
    8, 9, 12. UA 12712, pygidium, from R6-114, x 40; 8. Dorsal view, 9. Oblique left lateral view, 12. Posterior view.
    10. UA 12713, cranidium, from R6-35, dorsal view, x 40.
    11. UA 12714, cranidium, from R6-55, dorsal view, x 40.
    14. UA 12715, pygidium, from R6-114, dorsal view, x 40.
15-21. *Heckethornia* n. sp.
    15. UA 12716, cranidium, from R5-87.7(97), dorsal view, x 15; the specimen is inadvertently broken.
    16. UA 12717, cranidium, from R5-86, dorsal view, x 40.
    17. UA 12718, cranidium, from R5-86, dorsal view, x 20.
    18. UA 12719, cranidium, from R5-86, dorsal view, x 20.
    19. UA 12720, free cheek, from R5-86, dorsal view, x 40.
    20. UA 12721, cranidium, from R5-87.7, dorsal view, x 40.
    21. UA 12722, pygidium, from R5-87.7(97), dorsal view, x 40.

528
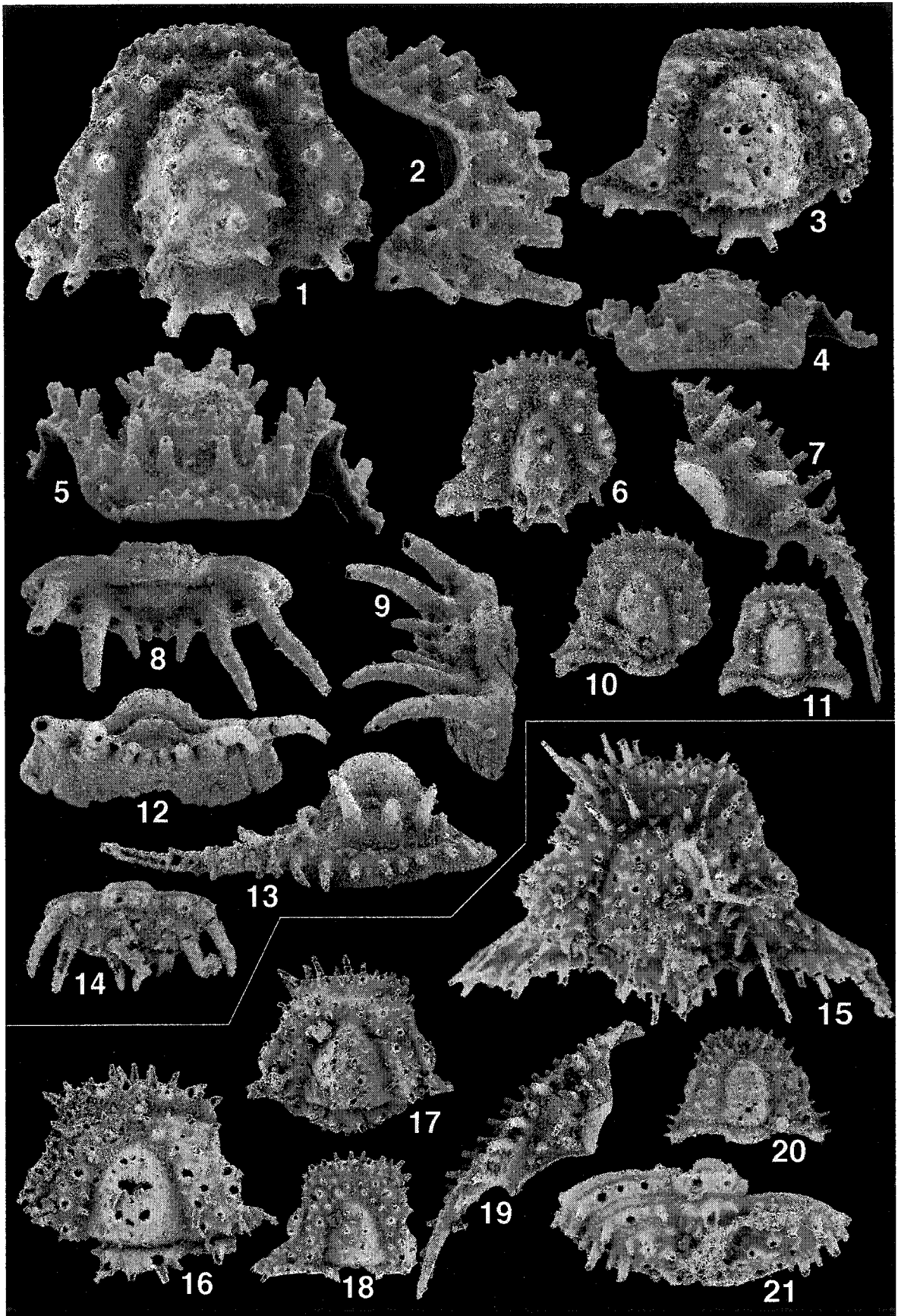
PLATE III-81. *Heckethornia alticapitis* (Young, 1973).

1-19. *Heckethornia alticapitis* (Young, 1973).
1. UA 12723, free cheek, from SH-1, dorsal view, x 30.
2-4. UA 12724, cranidium, from SH-1, x 15; 2. Dorsal view, 3. Right lateral view, 4. Anterior view.
5. UA 12725, cranidium, from SH-1, ventral view, x 15.
6. UA 12726, cranidium, from SH-1, dorsal view, x 15.
7, 8. UA 12727, cranidium, from SH-1, x 15; 7. Left lateral view, 8. Dorsal view.
9. UA 12728, cranidium, from SH-1, dorsal view, x 30.
10, 11. UA 12729, free cheek, from SH-1, x 30; 10. Oblique dorsal view, 11. Dorsal view.
12. UA 12730, cranidium, from SH-1, dorsal view, x 30.
13. UA 12731, free cheek, from SH-1, ventral view, x 30.
14. UA 12732, pygidium, from SH-1, dorsal view, x 30.
15-17. UA 12733, pygidium, from SH-1, x 30; 15. Posterior view, 16. Right lateral view, 17. Oblique dorsal view.
18, 19. UA 12734, pygidium, from SH-1, x 30; 18. Dorsal view, 19. Posterior view.
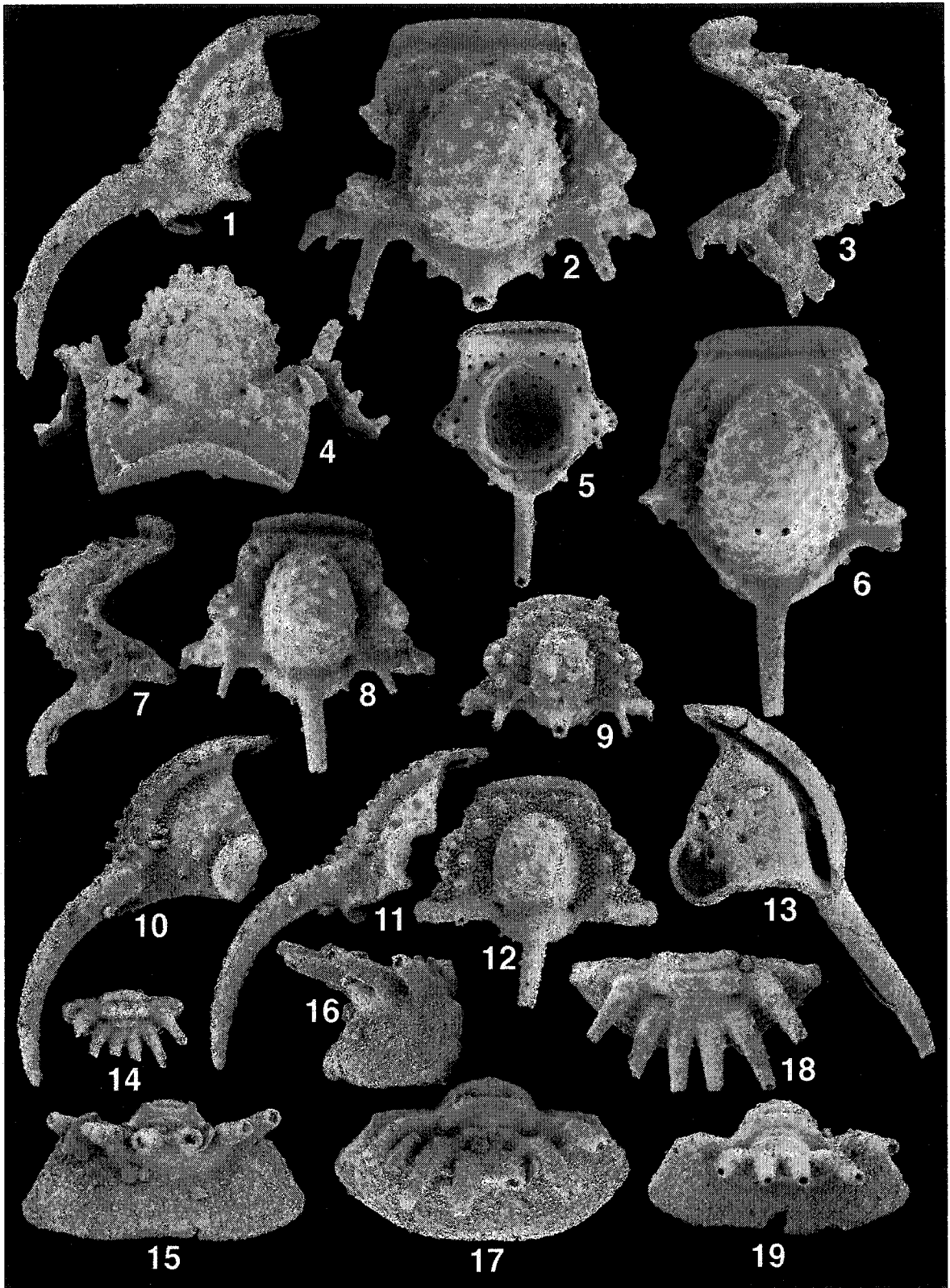
PLATE III-82. *Tasmanaspis lewisi* Kobayashi, 1940, **Bathyuridae** sp. and
   Tasmanaspis latuscompressus n. sp.

1-15. *Tasmanaspis lewisi* Kobayashi, 1940.
   1, 2. UA 12735, cranidium, from SE-152, x 15; 1. Dorsal view, 2. Anterior view.
   3, 5. UA 12736, cranidium, from R5-86, x 20; 3. Dorsal view, 5. Ventral view.
   4, 7. UA 11883, cranidium, from R5-86, x 15; 4. Oblique right lateral view, 7. Dorsal
      view.
   6, 8. UA 12737, free cheek, from SE-152, x 10; 6. Dorsal view, 8. Ventral view.
   9. UA 12738, cranidium, from R5-76.4, dorsal view, x 20.
   10. UA 12739, cranidium, from R5-86, dorsal view, x 20.
   11. UA 12740, cranidium, from R5-76.4, dorsal view, x 20.
   12. UA 12741, cranidium, from R5-87.7, dorsal view, x 20.
   13. UA 12742, free cheek, from SE-152, dorsal view, x 15.
   14. UA 12743, cranidium, from R5-87.7, dorsal view, x 20.
   15. UA 12744, cranidium, from R5-76.4(98), dorsal view, x 20.
16, 17. **Bathyuridae** sp.
   16, 17. UA 12745, pygidium, SE-152, x 20; 16. Dorsal view, 17. Oblique right lateral
      view.
18-23. *Tasmanaspis* n. sp.
   18. UA 12746, cranidium, from R5-76.4, dorsal view, x 20.
   19. UA 12747, cranidium, from R5-86, dorsal view, x 20.
   20-23. UA 12748, cranidium, from SE-152, x 15; 20. Ventral view, 21. Left lateral
      view, 22. Dorsal view, 23. Anterior view.

532
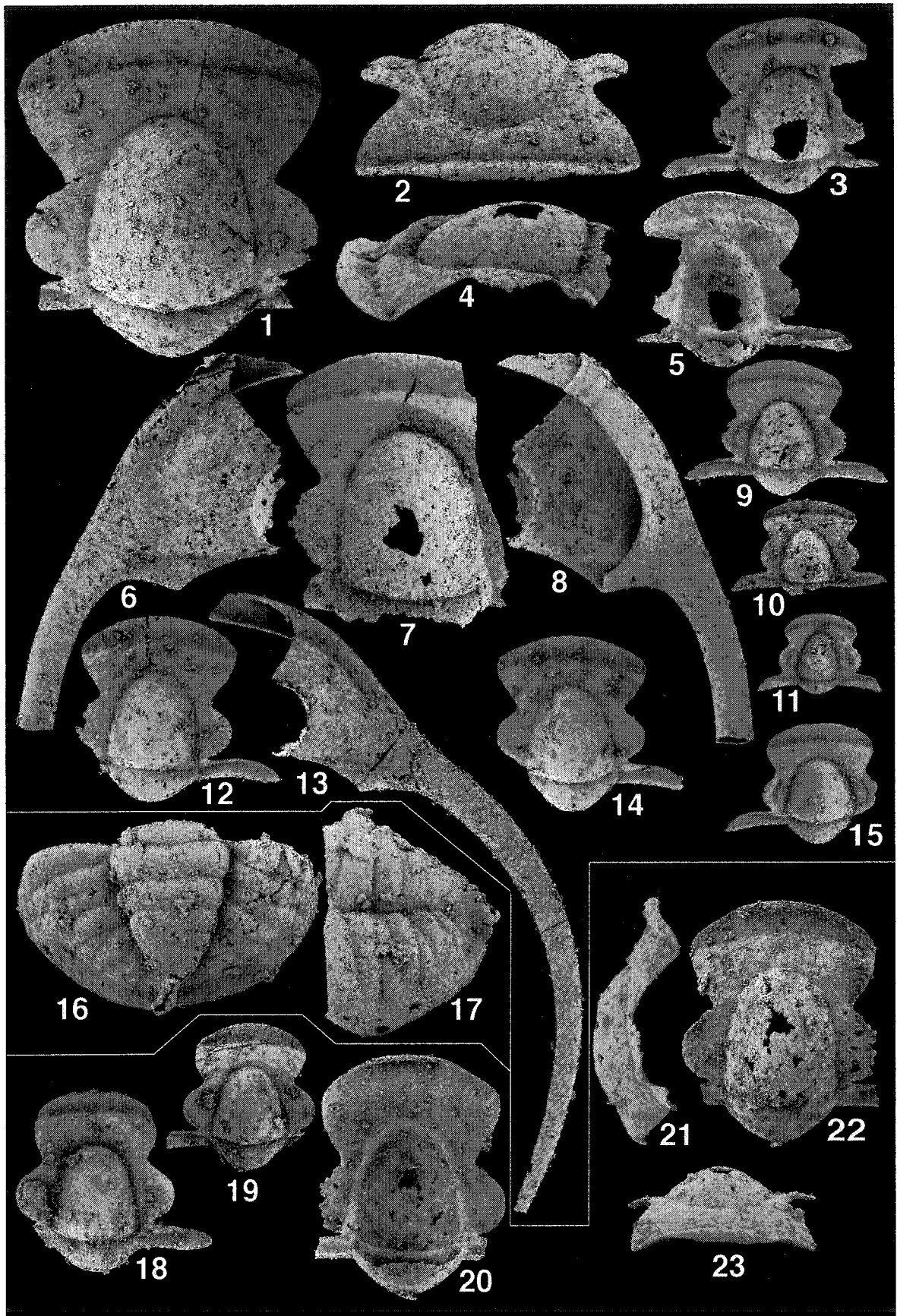
PLATE III-83. *Tasmanaspis*? sp., *Licnocephala bicornuta* Ross, 1951, *Benthamaspis obreptus* (Lochman, 1966) and *Benthamaspis*? sp.

1-4. *Tasmanaspis*? sp.
   1-3. UA 12749, cranidium, from SR6U, x 20; 1. Dorsal view, 2. Anterior view, 3. Oblique left lateral view.
   4. UA 12750, cranidium, from SR6U, dorsal view, x 20.
5-11. *Licnocephala bicornuta* Ross, 1951.
   5-8. UA 12751, cranidium, from R6-100, x 15; 5. Left lateral view, 6. Dorsal view, 7. Ventral view, 8. Anterior view.
   9-11. UA 12752, cranidium, from R6-114, x 10; 9. Oblique anterior view, 10. Left lateral view, 11. Dorsal view.
12-15. *Benthamaspis obreptus* (Lochman, 1966).
   12-15. UA 12753, cranidium, from R6-100, x 10; 12. Dorsal view, 13. Left lateral view, 14. Ventral view, 15. Anterior view.
16-18. *Benthamaspis*? sp.
   16-18.. UA 12754, cranidium, from R6-100, x 10; 16. Anterior view, 17. Right lateral view, 18. Dorsal view.

534
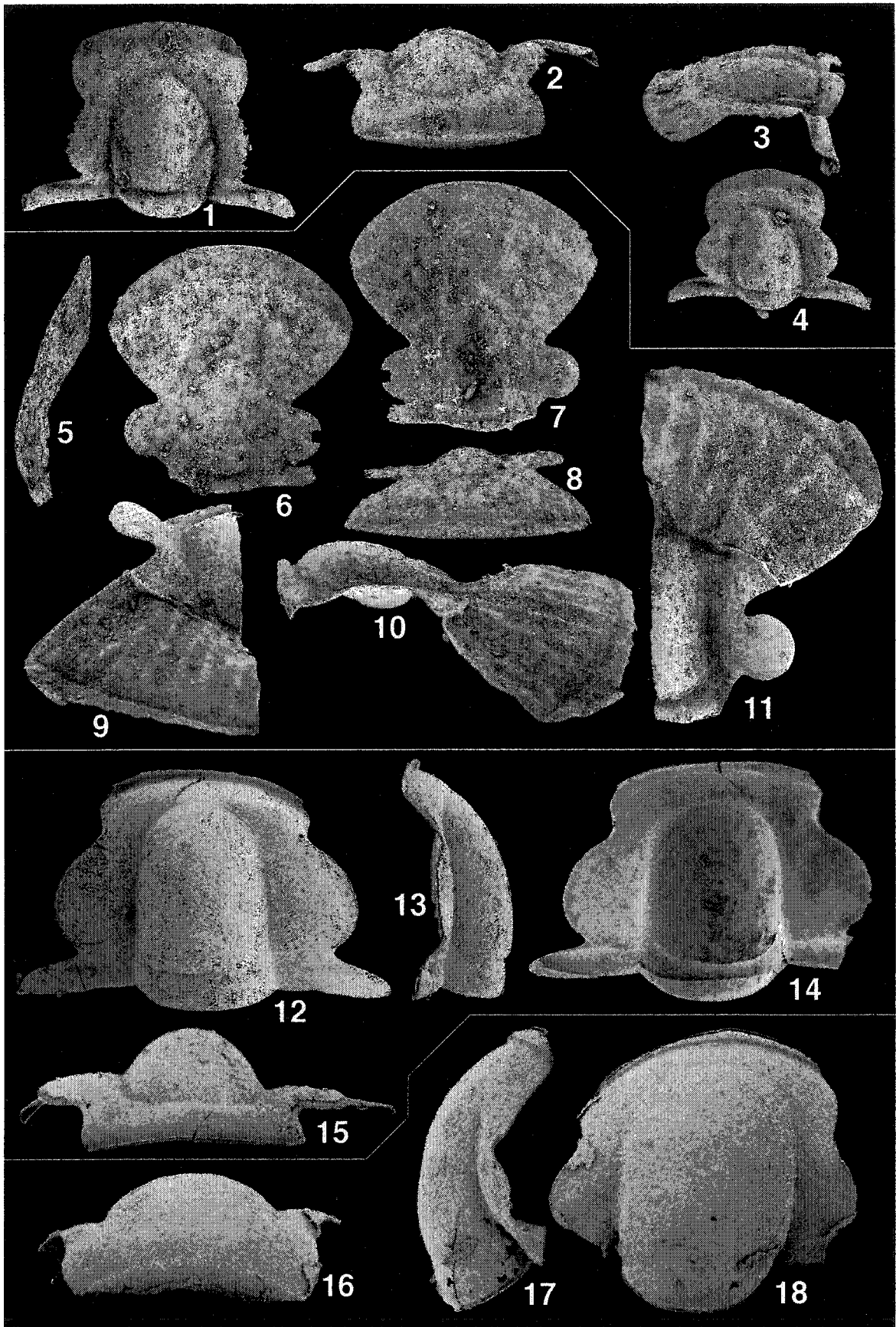
PLATE III-84. *Taoyuania xenisma* Liu *in* Zhou *et al.*, 1977, *Taoyuania Nobilis* Peng, 1984, *Rollia goodwini* Cullison, 1944 and **Dokimocephalidae** n. gen. and n. sp.

1-4. *Taoyuania xenisma* Liu *in* Zhou *et al.*, 1977. The specimens are from *Onychopyge-Hysterolenus* Assemblage Zone (early Tremadocian) of Panjiazui Formation, Hunan, South China.

   1-3. NIGP 108105, cast of cranidium, x 5; 1. Dorsal view, 2. Right lateral view, 3. Anterior view.

   4. NIGP 108106, cast of cranidium, dorsal view, x 1.5.

5-10. *Taoyuania Nobilis* Peng, 1984. The specimen is from *Onychopyge-Hysterolenus* Assemblage Zone (early Tremadocian) of Panjiazui Formation, Hunan, South China. The pygidium could belong to the other genus such as *Lophosaukia*.

   5-7. NI 83110, holotype, cast of cranidium, x 2; 5. Dorsal view, 6. Left lateral view, 7. Anterior view.

   8-10. NI 83111, cast of pygidium, x 5; 8. Dorsal view, 9. Left lateral view, 10. Posterior view.

11-13. *Rollia goodwini* Cullison, 1944. The specimen is from possibly *Hintzeia celsaora* Zone of Rich Fountain Formation, Missouri.

   11-13. YPM 17175, paratype, cast of cranidium, x 10; 11. Anterior view, 12. Dorsal view, 13. Right lateral view.

14-18. **Dokimocephalidae** n. gen. and n. sp. The specimens are from La1 Zone (Lancefieldian Series) of Digger Island Formation, Victoria, Australia.

   14, 16, 17. NMVP 74341, cast of cranidium, x 10; 14. Dorsal view, 16. Right lateral view, 17. Anterior view.

   15, 18. NMVP 74344, cast of cranidium, x 10; 15. Anterior view, 18. Dorsal view.

536
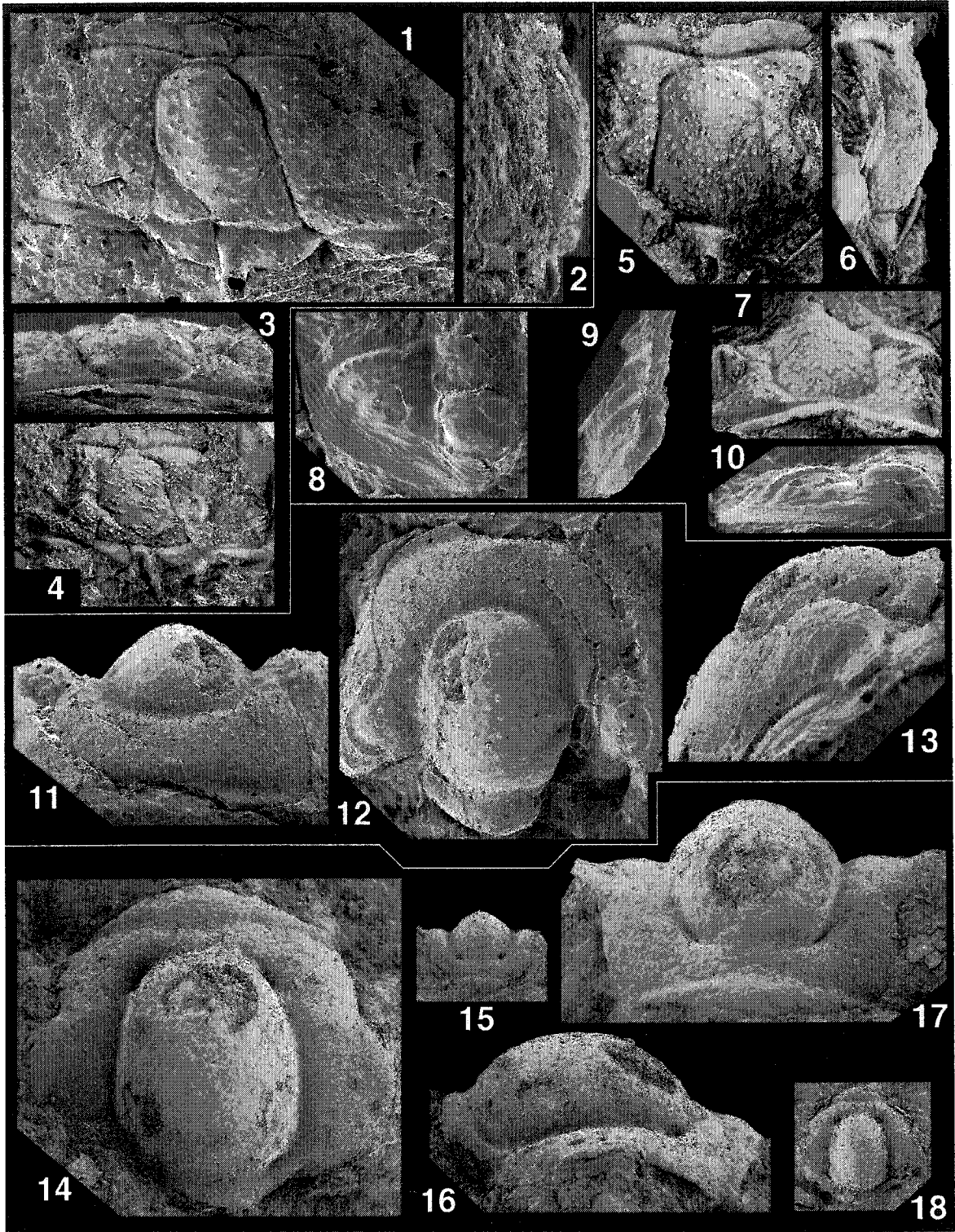
PLATE III-85. *Tanybregma tasmaniensis* Jell and Stait, 1985b, *Tanybregma paratimsheansis* n. sp. and *Tanybregma timsheansis* n. sp.

1-4. *Tanybregma tasmaniensis* Jell and Stait, 1985b. All specimens are from La1.5 Zone (Lancefieldian Series) of Florentine Valley Formation, Tasmania, Australia.
   1, 2, 4. UTGD 95983, holotype, cast of cranidium, x 5; 1. Dorsal view (light photography), 2. Left lateral view, 4. Anterior view.
   3. UTGD 96674, cast of cranidium, dorsal view, x 5 (light photography).
5-10. *Tanybregma paratimsheansis* n. sp. All specimens are from La1.5 Zone (Lancefieldian Series) of Florentine Valley Formation,Tasmania, Australia.
   5-7. UTGD 122516, cast of pygidium, x 4; 5. Dorsal view, 6. Right lateral view, 7. Posterior view: the association of this pygidium is tentative (see text for the details)
   8-10. UTGD 122503, holotype, cast of cranidium, x 5; 8. Dorsal view (light photography), 9. Left lateral view, 10. Anterior view.
11-16. *Tanybregma timsheansis* n. sp. All specimens are from La1.5 Zone (Lancefieldian Series) of Florentine Valley Formation, Tasmania, Australia.
   11. UTGD 95867, holotype, cast of articulated specimen, dorsal view, x 1.4.
   12-13. UTGD 122504, cast of cranidium, x 5; 12. Left lateral view, 13. Dorsal view (light photography).
   14-16. UTGD 122510, cast of pygidium, x 5; 14. Right lateral view, 15. Dorsal view, 16. Posterior view.

538
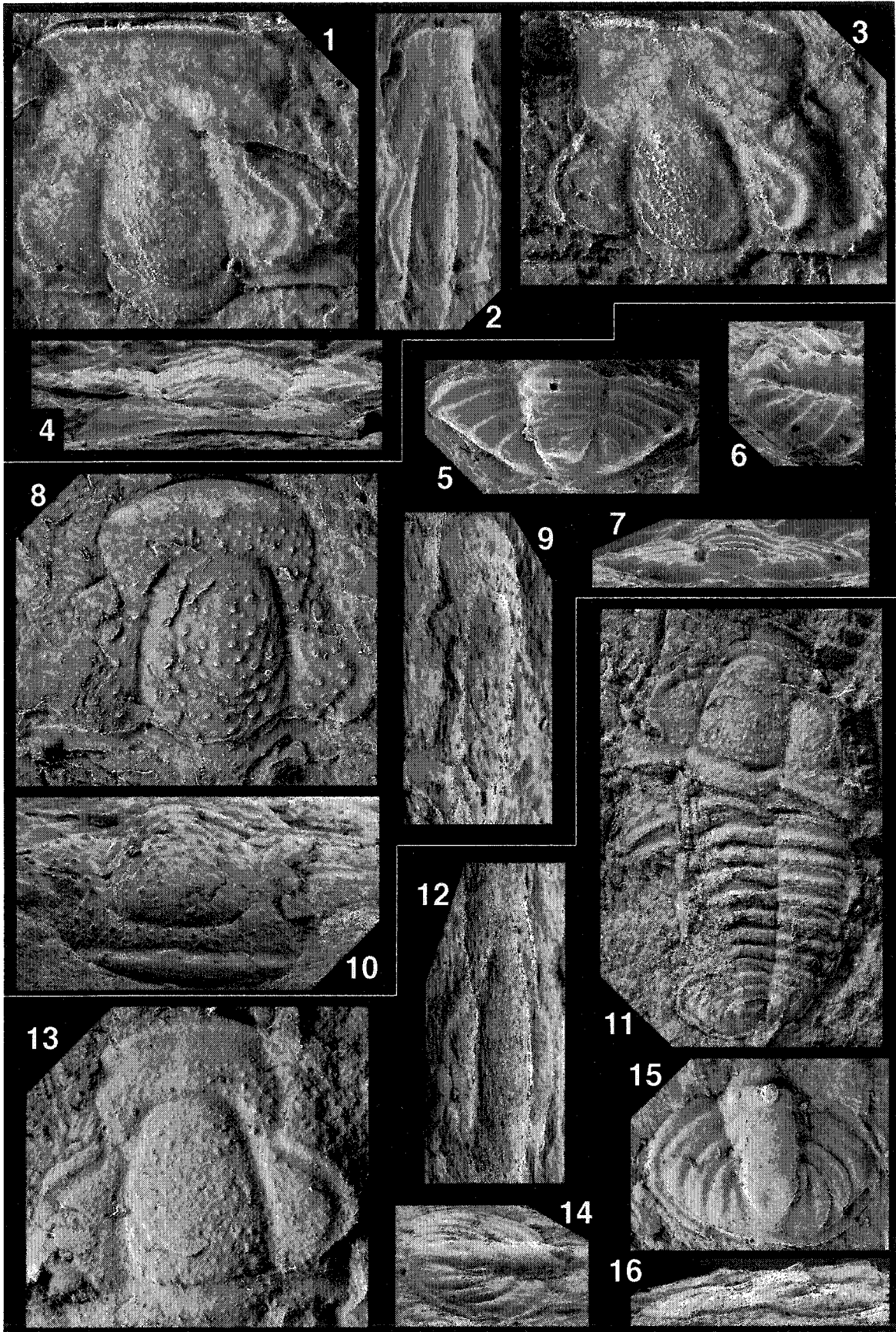
CHAPTER IV

PROBLEMS OF ESTABLISHING RELATIONSHIPS ON THE BASIS OF ONTOGENETIC DATA

INTRODUCTION

The taxonomy practiced in Chapter II utilizes both protaspid and holaspid features. The groups are reconstructed using perceived similarities and differences among taxa, and by assuming that the similarities are indicative of the membership of a group. When there is a conflict between the groupings based on protaspid and holaspid features, the protaspid features are considered more informative. The similarities shared by the taxa are considered homologous, in other words, derived from a common ancestor. This conjecture of homology will be tested by a pending cladistic analysis.

Many groupings proposed in Chapter II (Appendix II-1) are new to trilobite higher-level classification, in particular, at the superfamily level. Two categories of groupings are recognized. The first category is those in conflict with previous taxonomic schemes reconstructed upon the basis of only holaspid features. For example, the Pterocephalidae was considered to consist of three subfamilies, the Pterocephalinae, Housiinae, and Aphelaspidinae. Palmer (1965b) presented an anagenetic lineage among these subfamilies through Upper Cambrian stratigraphic sequences in the Great Basin, and defined the taxa based on their stratigraphic occurrences. This suggested a close taxonomic affinity between the three subfamilies. However, the protaspides of the Aphelaspidinae are of morphotype E, whereas those of the Housiinae of morphotype C. As a result, the protaspid features suggest that the Housiinae and Aphelaspidinae each may belong to different taxa of higher rank.

Secondly, some groupings are newly discovered only through protaspid similarities. For instance, *Komaspidella laevis* of the Kingstoniidae, *Glaphyraspis parva* of the Lonchocephalidae and *Bolaspidella housensis* of the Menomoniidae share protaspid morphotype A, suggesting that the three families may belong to the same superfamily. Their holaspid features are so different from one another (compare Pl. II-8, Figs. 11, 14 with Pl. II-9, Figs. 20, 24) that their taxonomic affinities have never been even speculated. Another example is a putative superfamily consisting of the Housiinae, Norwoodidae and Phylacteridae characterized by protaspid morphotype C. The taxonomy of the Hystricuridae revised in Chapter III (Appendix III-2, 3), entails the same problem. For example, *Paratersella*, has holaspid morphologies similar to many members of the Hystricuridae, but has protaspid morphologies much different from those of *Hystricurus*. *Psalikilus* has holaspid morphologies much different from the hystricurids, but has earlier meraspid cranidia similar to those of the hystricurids.

Which ontogenetic stage should be considered more informative when the groupings based on different ontogenetic stages are in conflict? Is this relative informativeness of a particular ontogenetic stage a legitimate assumption for systematics? If so, how can we incorporate the relative informativeness into systematic analyses? Are the protaspid features informative in grouping the taxa in the case where holaspid features are not informative? These questions need to be answered to justify the groupings proposed in the Chapter II. These questions are discussed below as are relevant issues from the

539

perspective of ontogeny being a character-provider. In addition, available methods by which both protaspid and holaspid features can be integrated into a pending cladistic analysis are also discussed from the same perspective.

HISTORICAL ACCOUNTS.
Little attention has been paid by systematists or taxonomists to the perspective of viewing ontogeny as a morphologic character-provider. Every ontogenetic stage provides different characters and different states of the characters, because ontogeny is dynamic. Observations of ontogeny have been utilized for interpreting heterochronic patterns within established lineages (e.g., Gould, 1977), and for discovering causal relationships of development to evolution by mapping developmental features onto phylogenetic hypotheses generated by adult features in the field of evolutionary developmental biology (e.g., Wray, 1992). In the field of systematics, ontogeny has been used for conjecturing the homology of the features (e.g., Roth, 1984), and for determining the polarity, derived versus primitive, of character states coded for terminal taxa in cladistic analyses (e.g., Nelson, 1978). In both cases, the characters to be homologized and polarized are of adult stages. The ontogenetic approach for polaritiy determination has been most extensively investigated in comparison with the other approach for polarity determination, such as outgroup comparison method. The ontogenetic method has been advocated by 'pattern cladists' who claim that evolution is superfluous for revealing the phylogenetic relationships of organisms. The ontogenetic approach appears to be outpowered by the outgroup method favored by 'phylogenetic systematists' who integrate, into their systematic practices, evolution as an axiom on which the phylogenetic relationships must be based.

The role of ontogeny as a character-provider in systematics or taxonomy has been recognized by some authors. For example, Kluge (1985) stated, "Obervations of ontogeny ... serve as an *extra* source of observations with which to judge historical relationships" [*italics* by the author]. Nonetheless, most practices in seeking for the classification schemes of organisms—see Christoffersen (1995) for definition of different schools of taxonomy—have been overwhelmingly swamped by adult features which are only a part of the whole ontogeny. By comparison, a lesser amount of input into systematics has been made by the features of ontogenetic stages preceding the adults. Due to technological advances in research fields such as embryology and developmental biology, more information on the earlier ontogenetic stages has been compiled. Accordingly, more systematic studies began to employ the features from earlier ontogenetic stages. Notable examples in the trilobite literature are Chatterton *et al.* (1990) and Edgecombe (1992). The former cladistically tested the previously-suggested hypotheses of the relationships of calymenine trilobites with the protaspid data set, and the latter analyzed the protaspid and holaspid data sets of the Phacopida together and found that the two phylogenies are congruent. As Hickman (1999, p. 52) stated, however, "The use of invertebrate larval data in cladistic analysis is in its infancy." The characters from the earlier ontogenetic stages are still at most supplementary to the adult features in reconstructing classifications and phylogenetic relationships.

Traditionally, diagnosis of a taxon is based on the adult features. However, as seen in some ptychopariides in Chapter II, the species of the families possessing the protaspid morphotype A and C have a similar protaspid form, but their holaspid morphologies are

540

so different that little has been known of their taxonomic affinity. It is conceivable that a taxon can be only defined by features of a particular ontogenetic stage. Hennig (1966) claimed that it may not be at issue to find diagnostic features for all ontogenetic stages because synapomorphies, not morphologic similarities, may not be found through the entire ontogeny. Morphologies of members of a taxon possessing a similar larval form may progressively deviate from one another to the extent that their holaspid features are not recognized to be similar to one another. Their holaspid similarities, if any, are plesiomorphous which are of taxonomic value at hierarchical levels more inclusive than the one estalished by the larval features. Chatterton and Speyer (*in* Whittington *et al.*, 1997) state, "Some synapomorphies visible only in larval stages may be used to recognize and define large groups of trilobites." The statement suggests that a higher taxon can be defined only by the protaspid features.

ONTOGENY AS CHARACTER-PROVIDER.

To view ontogeny as a character-provider raises theoretical and methodological issues about how to use characters from earlier ontogenetic stages in the systematics, while simultaneously considering the adult features which have been regarded as the standardized point of comparison. This new perspective necessitates a review of the relationships between ontogeny and phylogeny—or development and evolution in more process-oriented terms—from different standpoints. The integration of phylogeny and ontogeny, each based on two different fields of biology, evolutionary biology and developmental biology, was initiated by nineteen century embryologists, Ernst Haeckel and Karl Ernst von Baer (see Gould, 1977 for historical summary).

Haeckel proposed a biogenetic law that ontogenies of descendants not only repeat ancestral ontogeny but they also add additional features to the end of the ancestral ontogeny, which is representatively summarized as the phrase, 'ontogeny recapitulates phylogeny.' As mentioned above, the law has provided some grounds on which the extensive studies on the heterochrony are based. von Baer formulated four laws of development. The first two laws state, "1. The general features of a large group of animals appear earlier in the embryo than the special features," and "2. Less general characters are developed from the most general, and so forth, until finally the most specialized appear" (translation from Gould, 1977). These laws have been invoked for many theoretical and empirical arguments about character polarity determination. The latter two laws state, "3. Each embryo of a given species, instead of passing through the stages of other animals, departs more and more from them" and "4. Fundamentally therefore, the embryo of a higher animal is never like a lower animal, but only like its embryo." (translation from Gould, 1977). These two laws can be rephrased as increase of morphologic dissimilarities through ontogenies among members of a taxon. These laws were formulated by observing development of members of taxa that had already been established by the adult features; the development of these taxa entails no metamorphosis. It has been rarely empirically or theoretically tested whether and how these formulations can be reciprocally applied to reconstruct groups of taxa (see below).

The perspective of ontogeny as a character-provider follows the 'total evidence principle' (Kluge, 1989), so that characters from any particular ontogenetic stage should not be ignored. Since every single moment of a life cycle of an individual organism is subject to selection, features of all the stages should be examined and incorporated into

541

systematic studies (Danser, 1950; Kluge, 1988). Thus, for instance, the protaspides and holaspides of trilobites must be equally regarded as character-providers.

Ontogeny proceeds from 'simple' to 'complex,' or from 'absent' to 'present' in many cases of the morphologic realm. Ontogeny of all individual animals starts with a single-celled spherical zygote and ends with a great disparity of forms. Morphologic changes from the fertilized egg to embryo entail cleavage, blastulation and gastrulation. In the morphological context, these changes are only meaningful at much higher taxonomic ranks—for example, the recognition of Protostomes and Deuterostomes. The variations would lie in the size of the egg, and the different patterns of blastulation and gastrulation. The morphologic context of these characters does not seem to display variations sufficient for separate character state coding, in particular, at the lower taxonomic levels. The reasonable starting point for comparative approaches of morphologic changes through ontogeny is the stage when the *bauplan* or *ünterbauplan* of the taxon is laid out and thus the morphologies are observable and variable to the extent that they can be separately described for each terminal taxon. This stage is called 'phylotypic stage' which Slack *et al.* (1993) defined as "the stage at which all members of the phylum show the maximum degree of similarity." For example, vertebrate animals pass through pharyngular stage possessing gill pouches, limb buds, tail, notochord, dorsal nerve tube, and paired body muscle bands (Text-fig. IV-1). The pharyngular stage is a phylotypic stage of the Vertebrata. Many insects pass through a germ-band stage, and then morphologically diverge into a great disparity of forms. Below, unless otherwise noted, the earlier ontogenetic stages refer to those at or immediately after the phylotypic stage.

SYSTEMATIC IMPLICATIONS OF ONTOGENETIC PATTERNS REPRESENTED BY HAECKEL'S AND VON BAER'S LAWS.

von Baer's laws and Haeckel's biogenetic laws both assert that more morphological modifications occur in later ontogenetic stages by terminal addition or deviation, and more similarities are expected at earlier ontogenetic stages in members of a taxon. The similarities at the earlier ontogenetic stages have been considered informative, and perhaps more informative than those at the later stages, in reconstructing taxonomy of organisms. Darwin (1859, p. 449) stated, "... the structure of the embryo is even more important for classification than that of the adult. ... Community in embryonic structure reveals community of descent." Gould (1977, p. 71) supported this notion by stating, "It [von Baer's laws] is a statement prescribing a course of action for the recognition of homology: look for similarity in embryos since evidence of common ancestry is so often obscured by highly particular adult modifications." The informativeness of a feature from a particular ontogenetic stage refers to that the shared possession of the feature allows one to conjecture that it is the evidence of common ancestry. Darwin's favorite group, the barnacles, well illustrates this implication. The barnacles had been classified under the Mollusca until it was discovered that their larva is of nauplius-type, which is one of the most diagnostic features of the Crustacea. The barnacles are assigned to the Crustacea. As an example of trilobites, the possession of a bulbous, asaphoid protaspis is regarded as a synapomorphy of the Asaphida (Fortey and Chatterton, 1988).

Focusing on von Baer's laws, Rieppel (1988, 1990) provided a different interpretation of systematic implications of the laws in the context of hierarchy. The features appearing in earlier ontogenetic stages are claimed to define a more inclusive level of phylogenetic

542

hierarchy. For example (Text-fig. IV-1), the pharyngular stage defines the Vertebrata including fish, chick, calf, and human. Tetrapod features appearing later in ontogenies of chick, calf and human define the Tetrapoda that includes chick, calf, and human. Mammalian features appear even later in the ontogenies of calf and human and group both animals into the Mammalia. As a result, the shared features from different ontogenetic stages are considered to be equally informative for systematics, simply at different levels of the phylogenetic hierarchy.

Text-figure IV-2 and IV-3 compare the different interpretations of systematic implications of von Baer's and Haeckel's laws. For six taxa, ontogenetic transformations of six features or forms are depicted that follow von Baer's laws (subterminal insertion or deviation; see Text-fig. IV-2-1), and Haeckel's biogenetic law (terminal addition; see Text-fig. IV-3-1). Ontogenies of the six taxa are segmented into six stages that are considered comparable to one another. Ontogenetic sequences of Text-figure IV-2-1 follow von Baer's laws because 1) more general features, for example a_1, appear earlier in ontogeny and the more general features develop into less general features, and 2) once a feature is subterminally inserted, the feature is retained to the end of the ontogenies and no ontogenetic reversals are assumed to take place. Text-figure IV-3-1 depicts ontogenies following Haeckel's law because once a feature is added into the end of the pre-existing ontogeny, the feature is assumed to be pushed into the next earlier stage in the subsequent ontogeny, maintaining the same length of ontogeny for all the six taxa. These ontogenetic patterns are based on the assumption of ontogeny proceeding from 'simple' to 'complex'; in other words, taxon A is ancestral and taxon F is the latest descendant. If the reverse is the case, the ontogenetic patterns represent a case of paedomorphosis where ancestral juvenile features become adult features of descendants. These assumptions of pre-conceived phylogenetic relationships, however, are irrelevant to investigating systematic implications of the laws. It is because whatever pre-conceived relationships we assume, the data matrix of Text-figures IV-2-1 and IV-3-1 remains unchanged, which only relates to the investigation of systematic implications of the patterns. Both patterns show that morphologic similarities decrease towards the final ontogenetic stage.

The systematic implications of the laws mentioned above, the relative informativeness of the earlier ontogenetic stages, and Rieppel's equal informativeness at different hierarchical levels are made on the basis of the perceived similarities and differences; more than two taxa are clustered into a group if they share the same feature. When comparing the final ontogenetic stage with one of the preceding stages, the final stage in both matrices provides no grouping information, whereas each stage preceding the final one reveals a subgroup of the six taxa (Text-figs. IV-2-2 and IV-3-2), demonstrating the informativeness of the earlier ontogenetic stages for reconstructing groups. The groupings based on the perceived similarities allow one to make a proposition of primary homology. For example, at the fourth ontogenetic stages, a_1 is shared by taxon A, B, and C in the data matrix of Haeckel's law, and d_1 is shared by taxon D, E, and F in the matrix of von Baer's laws. The feature a_1 is assumed to be homologous in taxon A, B, and C and so is the feature d_1 in taxon D, E, and F. This homology conjecture must be tested by such a cladistic methodology as character congruence (de Pinna, 1991).

The groupings in Text-figures IV-2-2 and IV-3-2 demonstrate that the features from earlier ontogenetic stages cluster *more* taxa into a group; in the matrix of von Baer's

laws, b_1 diagnoses a group of [BCDEF] whereas e_1 diagnoses a group of [EF]. Is b_1 still more informative than e_1, simply because b_1 appears earlier than e_1? Since both features cluster taxa into a group, the relative informativeness cannot be claimed. The argument of the relative informativeness is certain to be based on only a few segments of the whole ontogeny. If ontogenies are accompanied with a radical metamorphosis, the features available for analysis will be fewer than those shown in Text-figures IV-2-1 and IV-3-1; the same type of larvae may metamorphose into morphologically drastically different juveniles or adults. Furthermore, currently available ontogenetic data are far from complete; it is not common for systematists to have a complete ontogenetic information for all the taxa under their systematic studies. This reality appears to force systematists to choose and compare fewer comparable ontogenetic segments (see below). As a result, the first interpretation of the relative informativeness is considered to be a special case of Rieppel's interpretation that compare relatively complete ontogenetic patterns. Of another significant difference is whether the hierarchical ranks of the group is taken into consideration. The first interpretation does not incorporate hierarchical ranks into determining the relative informativeness. When ontogenies are continuous and all the ontogenetic transformations are observed, Rieppel's interpretation into which to incorporate phylogenetic hierarchy will be a more reasonable assessment (see below for detailed discussion).

It seems apparent from both interpretations that no differences in systematic implications of Haeckel's and von Baer's laws are expected to exist. However, the detailed analyses below reveal that each law makes different systematic implications. All ontogenetic stages preceding the final stage generate groups that can be arranged into an inclusive hierarchy; [A[B[C[D[EF]]]]] for the matrix of von Baer's laws (Text-figs. IV-2-2) and [[[[[AB]C]D]E]F] for the matrix of Haeckel's law (Text-figs. IV-3-2). Rieppel (1988) claimed that Haeckel's law specifies a linear exclusive hierarchy whereas von Baer's laws specify a subordinated inclusive hierarchy. Rieppel further argued that the linear exclusive hierarchy is translated into a subordinated inclusive hierarchy and the former is a special case of the latter. However, as shown in Text-figure IV-2-2 and IV-3-2, Haeckel's and von Baer's laws both specify an inclusive hierarchy. Ontogenetic transformations of character states of Haeckel's and von Baer's laws can be arranged into a hierarchical fashion (Text-fig. IV-2-4 and IV-3-4, respectively). Each hierarchy of transformation series accords with the inclusive hierarchy into which the groups are arranged (compare with Text-fig. IV-2-2 and 2-4, and IV-3-2 and 3-4). This further supports that both laws conform to the subordinated inclusive hierarchy.

Haeckel's law has been considered to support and lend an explanatory power to the 'Great Chain of Being' which was the prevailing idea on how organisms must be classified during the 18th century. For example (see Rieppel, 1988, fig. 5; see also Text-fig. IV-4), plant is diagnosed by the vegetative soul, animal by the sensitive soul, and man by the rational soul. Each state of soul for each group is added into the end of ontogeny of the lower-graded group. Each group is exclusive and does not include any other groups (Text-fig. IV-4-1b). Rieppel argued that this exclusive hierarchy is translated into an inclusive hierarchy where plant, animal and man belong to 'living thing' diagnosed by vegetative soul, and animal and man belong to 'animalia' diagnosed by sensitive soul (Text-fig. IV-4-1c). As a result, the linear exclusive hierarchy simply

does not acknowledge the existence of the inclusive group such as 'living thing', and 'animalia.'

When examining systematic implicatons of Haeckel's and von Baer's laws in a systematic context, however, Rieppel did not take into consideration the fact that plant retains the vegetative soul at the ontogenetic stages when animal acquires the sensitive soul and man does the sensitive and rational soul. In other words, ontogenetic data employed are not complete; only single ontogenetic stage is counted for plant and two stages for animal. As a result, the data matrix that Rieppel considered is missing three character states (Text-fig. IV-4-1a), in comparison to the complete data matrices shown in Text-figure IV-8-2a and 3a. Unless expanded as shown in the latter two matrices, Rieppel's matrix cannot be analyzed for systematics where comparable ontogenetic stages (or semaphoronts) must be subjects for analysis (Wiley, 1981). In the matrix of Text-figure IV-4-1a, the vegetative soul of plant cannot be compared with that of animal and man, because it is not specified whether the stage when plant displays the vegetative soul is a comparable semaphoront with the stage when animal and man display the feature. Furthermore, the data matrix does not specify whether animal acquires the sensitive soul by terminal addition or subterminal insertion. In effect, the animal can obtain the sensitive soul by terminal addition (Text-fig. IV-4-2a) or subterminal insertion (Text-fig. IV-4-3a), which solely depends on our detailed ontogenetic observation.

Although both laws specify an inclusive hierarchy, the grouping information displayed by the hierarchy differs. For example, at the fourth ontogenetic stage, Haeckel's law forms a group of [ABC], whereas von Baer's laws a group of [DEF] (compare Text-fig. IV-2-2 with Text-fig. IV-3-2, and Text-fig. IV-4-2b and 3b). This indicates that each law allows one to make a different conjecture of primary homology.

Another difference lies in the feature that diagnoses each group in the inclusive hierarchy. Each group from von Baer's laws is diagnosed by a feature that is subterminally inserted into the ontogenies. For example, a group of animal and man is diagnosed by the sensitive soul (Text-fig. IV-4-3a) and a group of [CDEF] is diagnosed by c_1 which is inserted at the third ontogenetic stage (Text-fig. IV-2-2). In contrast, all groups from Haeckel's law are diagnosed by the same feature, a_1, appearing at the earliest ontogenetic stage (Text-fig. IV-3-2) and the 'living thing' and 'animalia' each are diagnosed by the vegetative soul (Text-fig. IV-4-2b). The hierarchical pattern of the groups from von Baer's laws and the diagnostic features at each group accord with Rieppel's interpretation that features from earlier ontogenetic stages define a more inclusive group. In contrast, the hierarchical pattern from Haeckel's law does not comply with any previous interpretations mentioned above. Haeckel's law makes a different systematic implication from von Baer's laws, at this level of systematic exercise based on the perceived similarities and differences.

Cladistic analyses of the data matrix of Text-fig. IV-2-1 and IV-3-1, and IV-4-2a and 3a further contrast differences in the systematic implications of Haeckel's and von Baer's laws. The ontogenetic sequence data is translated into the data matrix as seen in IV-2-3 and IV-3-3 by regarding each ontogenetic stage as a character. One assumption needs to be made for the analysis that the ontogenetic sequence, $a_1 \to b_1 \to c_1 \to d_1 \to e_1 \to f_1$, and vegetative $\to$ sensitive $\to$ rational soul, and parts of these sequences are irreversible; no character state reversals are assumed to be observed in any of the terminal taxa.

Accordingly, the states of each character are ordered and polarized based on these ontogenetic transformation series of the character states. This assumption parallels the ontogenetic criterion of polarity determination based on generality (Nelson, 1978); a_1 is most primitive because it is the most general, common, and widely distributed character state.

Under this assumption, each data matrix, representing ontogenetic pattern due to either terminal addition or subterminal insertion, generates a topographically identical tree (compare Text-fig. IV-2-5 and IV-3-5, and IV-4-2c and 3c). However, the synapomorphy distributions are different. Each node of the tree from von Baer's laws (Text-fig. IV-2-5 and 2-5) is supported by the same character state. For example, a clade of [BCDEF] is defined by character states $2_{(1)}$, $3_{(1)}$, $4_{(1)}$, $5_{(1)}$, and $6_{(1)}$, each of which represents the same character state, b_1. Towards the terminal twigs of the tree, the synapomorphies at each node are the features inserted into the ontogenies. The topology and character distribution of the tree parallel the inclusive hierarchy of the groups based on the perceived similarities and differences shown in Text-figures IV-2-2 and IV-4-3b. Another perfect parallelism is found with the hierarchical arrangement of ontogenetic transformation series shown in Text-figure IV-2-4. At each node representing each ontogenetic stage, the developmental program of each terminal taxon determines the pathways of the character state transformation. For example, taxon B, C, D, E, and F acquire b_1 at the second ontogenetic stage, and at the third stage, taxon C, D, E, and F acquire c_1 while taxon B retains b_1. These developmental sequences perfectly correspond to the synapomorphy distributions in the tree of Text-figure IV-2-6.

Of interest is that the increase of character support towards the root of the tree; five b_1s support the clade of [BCDEF] and two e_1s support the clade of [EF]. This indicates that in order to collapse the clade of [BCDEF], evolutionary steps entailing five b_1s need to be disturbed, whereas evolutionary steps of only two e_1s need to be perturbed to destroy the clade of [EF]. This may support that the more inclusive taxa defined by earlier ontogenetic features are more stable than the less inclusive ones (Rieppel, 1990; see below for further discussion).

The tree generated from Haeckel's law, although topographically identical with that generated from von Baer's laws, shows a different character distribution (Text-figs. IV-3-5 and 3-6). Towards the terminal twigs of the tree, the clades are defined by all the states subsequently added into the ontogenies and thus by a greater number of synapomorphies. The topology and character distribution of the tree do not parallel the inclusive hierarchy of the groups based on the perceived similarities shown in Text-figures IV-3-2 and IV-4-2b. The tree does not accord, in terms of the topology, with the hierarchical arrangement of ontogenetic transformation series shown in Text-figure IV-3-4. However, the developmental sequences read from the transformation series (Text-fig. IV-3-4) parallel the synapomorphy distributions of the tree. At the third ontogenetic stage, for example, taxon F develops c_1 as a new feature and taxon E does b_1, whereas remaining taxa retain a_1. The developmental pathways are sequentially duplicated along the axis of the cladogram where, for example, b_1 and c_1 define the third node from the root of the tree.

In summary, von Baer's laws specify an inclusive phylogenetic hierarchy which is compatible with the groupings based on the perceived similarities and differences, ontogenetic transformation series, and cladogram. By contrast, Haeckel's laws specifiy

546

inclusive hierarchies of different patterns, depending on different perspectives employed. Rieppel's interpretation that features appearing earlier in ontogeny define more inclusive levels of hierarchy is fully supported by von Baer's laws, but not by Haeckel's law. For six taxa whose ontogenies follow von Baer's laws, their ontogenies reflect how they should be classified, as claimed by Rieppel (1990). It should be emphasized that how morphologic divergence through ontogenies is achieved, whether by subterminal insertion or terminal addition, makes different implications on how taxa are clustered and which feature supports each group. This indicates the significance of intermediate ontogenetic stages, contrasting Alberch (1985)'s arguments.

PROPERTIES OF ONTOGENY THAT NEED TO BE CONSIDERED.

The two patterns investigated above are theoretical and take into consideration transformation of only one feature. In reality, many ontogenetic patterns do not exactly follow as shown in Text-figures IV-2-1 and IV-3-1. Other properties of ontogeny or development need to be considered when incorporating morphologic data from ontogenies into systematics.

Hierarchical nature of ontogeny. Ontogeny itself is considered to be hierarchical (e.g., Arthur, 1988; Rieppel, 1990). Adjacent ontogenetic stages are causally linked with each other, so that features of the preceding stages are pre-requisite to those of the succeeding ones (Alberch, 1985). The causally linked features can be arranged in a hierarchical fashion ('morphogenetic tree' by Arthur, 1988). A feature at the earlier ontogenetic stages differentiates into more than one feature in a subsequent stage (see Text-fig. IV-2-4 and IV-3-4). Unlike the authors (e.g., Arthur, 1988) who depicted the hierarchy from the zygote, the hierarchy of ontogeny herein is depicted from the phylotypic stage. It is because the development before the phylotypic stage is found to be not strongly constrained or less constrained than the development after the phylotypic stage. This developmental phenomenon is called the 'developmental hourglass,' at the neck of which lies the phylotypic stage (Raff, 1996, fig. 6.7). Furthermore, the stages before the phylotypic stage reveal little information in the context of morphology, as mentioned above.

However, not all features are considered to be connected in a hierarchical fashion. Some features are simply connected in a linear fashion. For example, the shape of glabella in many ptychopariide trilobites simply changes from forward-expanding to forward-tapering. Thus, a more realistic representation of morphologic changes during ontogeny is to include linear components in the hierarchy.

The causal links between features at each hierarchical level will be broken when a radical metamorphosis occurs. For example, indirectly-developing sea urchins set aside a group of cells at their larval stage and use them to generate a juvenile body (Wray, 1997). Across the boundary, most larval morphologic features are simply abandoned and cannot be causally linked with the features of juveniles. Arthur (1988, fig. 1.4) proposed the use of two morphogenetic trees, one for larval stages and the other for the post-larval stages. In trilobites, the Asaphidae experienced a radical, although not as severe as in the sea urchins, metamorphosis after the protaspid period. Many protaspid features such as three long marginal spines and hypostomal spines are lost (see Tripp and Evitt, 1986).

In Chapter II, ontogenies of the ptychopariides are considered not to entail a metamorphosis due to the paucity of the co-occurrence information. In assuming no

547

metamorphosis, morphological changes in trilobite development can be portrayed in a hierarchical fashion (Text-fig. IV-5). A trilobite protaspid body consists of three broad longitudinal regions, axial and two pleural regions. Each of the three regions is subdivided into two transverse regions as the separation of cephalon and protopygidium appears, resulting in six broad body regions. As the trilobite releases thoracic segments, these six regions differentiate into subdivided regions in increments of three. It is certain that changes occurring in any of the three broad regions of the protaspis will affect the six regions of the meraspis. It is also clear that fewer describable morphologic characters are present in earlier stages. Three other relatively small regions are present during the ontogeny of the trilobites. The hypostome and free cheeks are considered to be present from the protaspid period, from which however no new segment or regions are differentiated. The proliferative zone, which is considered to be present at the posteriormost axial region (designated as 'Lp' by Lee and Chatterton, 1996), disappears when the trilobite completed releasing thoracic segments. This zone possesses the potential of budding off all the thoracic and pygidial segments.

This hierarchical nature of ontogeny indicates that fewer features are describable as morphologic characters in earlier ontogenetic stages. However, although fewer in number, those earlier features may contain the same amount of phylogenetic signals as the later features differentiated from those earlier features. This argument cannot be envisioned in the morphologic context. If each region of a protaspid body is considered equal to a 'morphogenetic field,' where the appearance of all subsequent features is controlled and regulated in a genetic context, however, the value of the earlier features cannot be ignored.

Stability of Larvae. Ever since Haeckel and von Baer formulated their biogenetic laws, it has been increasingly documented that members of a higher animal taxon have a typical larval form. For example, the nauplius larva characterizes the Crustacea; see Nielsen (1995) for larval forms diagnosing higher animal taxa. This has been taken as evidence to indicate that larval form is evolutionarily stable. Paleontological evidence lends support to this evolutionary stability of larvae. Müller and Walossek (1986) discovered the nauplius larval form from Upper Cambrian strata of Sweden, indicating that the larval form has been retained for a very long time. By contrast, adult crustacean forms have been highly modified throughout geologic time. The echinoderm pluteus larval form has been conserved for about 250 million years (Wray, 1992).

The most compelling empirical evidence for evolutionary stability of early ontogenetic stages such as larvae come from developmental genetics and experimental embryology—or 'evolutionary developmental biology' in a contemporary term—not from comparative approaches of ontogenetic changes in morphology. These studies provide evidence that developments of many animal species are strongly constrained during early developmental stages, in particular, at the phylotypic stage; see Raff (1996) for summary of theoretical and empirical arguments of evolutionary developmental biology. The vertebrates have the pharyngula as their phylotypic stage, and insects have the germ-band stage. Passing through a particular phylotypic stage during ontogeny indicates that the animal belongs to the group with that stage. These experimental approaches of evolutionary developmental biology lend support to the evolutionary stability of the earlier ontogenetic stages.

548

The above notion that ontogeny is hierarchical also lends support to the stability of the ealier ontogenetic stage. To view ontogeny as hierarchically arranged causal links of features indicates that the changes occurring in the preceding ontogenetic stages have an extensive effect on the succeeding stages. For example of the trilobite development (Text-fig. IV-5), any changes in the pleural regions in the protaspid period will affect cephalic, thoracic and pygidial pleural regions in the meraspid period onwards. If any lower points of the hierarchy are affected by a radical evolutionary process such as mutation, the whole structure above them should be extensively affected which would lead to a macroevolutionary jump to create a new body plan. Otherwise, the whole hierarchical structure will collapse which leads to a mutant that cannot survive. As a result, it is very difficult, if not impossible, to make substantial modifications in the earlier developmental stages (Rieppel, 1990; Raff, 1996). This indicates that the earlier ontogenetic stages appear to resist to evolutionary changes. Such stability of the earlier ontogenetic stages must be incorporated into systematic practices.

Ontogenetic increase of morphologic similarities. The comparative stability of larvae is contradicted by the arguments that larvae are so susceptible to ambient environments that they would adapt themselves to the environments and thus their morphologies are not evolutionarily stable. For example in the trilobite literature, Bergström (1977) cautioned that, "The larvae referred to share a common 'generalized' appearance, and the value for phylogenetic discussion should not be exaggerated." (see Lane and Thomas (1983) and Thomas and Holloway (1988) for similar arguments). Regardless of the evolutionary mechanisms responsible, these caenogenetic arguments suggest the existence of ontogenetic pattern that dissimilar larvae may develop into a similar adult form. This violates the general assertion of Haeckel's and von Baer's laws that morphologic similarities decrease towards the final ontogenetic stage.

The ontogenetic increase of morphologic dissimilarities among the members of a group has been found to be applied for many animal groups. However, the reverse case of ontogenetic increase of morphologic similarities have long been noticed and recently increasingly documented. Darwin (1860, p. 599) stated, "... but dissimiliarity in embryonic development does not prove discommunity of descent, for in one of two groups the [*earlier or embryonic*] developmental stages may have been suppressed, or may have been so greatly modified through adaption to new habits of life, as to be no longer recognisable" [*italics* added by author]. Of members belonging to the same group of sea urchins, species of pencil urchins with a similar adult form are developed from different types of pluteus larvae (see Raff, 1996, fig. 7.3). Williamson (1992, fig. 4.1) illustrated that two similar adult decapods are developed from very dissimilar larvae. Williamson (1992) has gone so far to claim that some groups have 'hybrid life-histories' with a larval type acquired from another group by lateral gene transfer. This idea was rejected empirically (see Smith, 1997), but the existence of the case of dissimilar decapod larvae becoming a similar adult form is accepted. This reverse case has also been observed at the level of characters, particularly in relation to von Baer's laws; in other words, less general characters develop into more general ones. For example, teleost fishes develop the dorsal nerve cord as a solid rod which hollows out later in ontogeny. However, many chordates develop a hollow dorsal nerve cord by folding a plate of ectodermal tissue. The more general feature (the hollow cord) is developed from the less general feature (the solid rod) in teleosts' ontogeny. The amnion develops prior to

tetrapod features, although the Amniota is less inclusive than the Tetrapoda (Patterson, 1983).

The reverse cases have been reported in the trilobites. Chatterton and Speyer (*in* Whittington *et al.*, 1997) noted, "Some genera include species that have protaspides that are very similar to one another ...; others show a great disparity in larval form ..." It is evident that ontogenies following and violating von Baer's laws co-existed in the trilobites. For example, the protaspides of the species belonging to *Telephina* exhibit more morphologic differences from one another than the holaspides that have been served as a stable diagnosis for the genus (Chatterton *et al.*, 1999, compare fig. 1.16 of *Telephina argentina* with fig. 9.1 of *Telephina problematica*). Chatterton and Speyer (*in* Whittington *et al.*, 1997) cited *Ceraurinella* as an example.

It is true that the protaspides have been described for an extremely small number of species out of those named based on the holaspid features in the trilobite literatures. The paucity of publications where earlier developmental stages are described is also true for living animal species. It is because discovery and description of earlier developmental stages requires "effort in the time-consuming but rewarding detailed examination" (Hickman, 1999, p. 52), and at the turn of the century, most embryologists shifted their focus onto the experimental (not comparative morphological) aspects of ontogeny. In the case of trilobites, the discovery of protaspides requires exceptional or different mode of preservation and different techniques such as SEM (Scanning Electron Micrography) to reveal detailed morphologic features. Such a bias in the quantity of information accumulated could have been translated into our contention of the ontogenetic decrease of morphologic similarities. In other words, the fewer data of earlier developmental stages could have misled us to believe that earlier stages are more similar. The increasing discoveries of reverse cases appear to support this.

The ontogenetic increase of morphologic similarities in Text-figure IV-6-1 can be achieved by two different patterns, depending on the assumption of pre-conceived phylogenetic relationships. Under the assumption of the more 'complex' ontogeny being ancestral, the earliest ontogenetic stage is suppressed or deleted and replaced by the next earliest ontogenetic stage. If we assume that the 'simpler' ontogeny is ancestral, a new feature is inserted at the earliest ontogenetic stage, and retained until it is reversed into the ontogenetic sequence of the previous ontogeny. The data set is the reverse case of von Baer's laws shown in Text-figure IV-6-1; ontogenetic patterns for ontogenetic increase of morphologic similarities have not been investigated as much as those for ontogenetic decrease of morphologic similarities (e.g., Kluge and Strauss, 1985).

As expected, the perceived similarities and differences generate groups (Text-fig. IV-6-2) that can be arranged into a hierarchical pattern. The determination of polarity is still based on the assumption that ontogenetic sequences are irreversable. Unlike the cases of ontogenetic increase of morphologic dissimilarities (Text-figs. IV-2 and 3), this assumption contradicts the ontogenetic criterion of polarity determination based on generality. Although f_1 is most general, common and widely distributed, and a_1 is least general, common and widely distributed, f_1 is forced to be the most derived and a_1 the most primitive. This phenomenon is considered as a falsifier of ontogenetic criterion of polaritiy determination by Nelson (1978). Nonetheless, the character matrix still generates a tree where earlier ontogenetic characters support more inclusive levels of hierarchy; the character support, however, increases towards the twigs of the tree. The

tree cannot be comparable with the ontogenetic transformation series (Text-fig. IV-6-4) because the transformation is not hierarchical: the two features, for example, c_1 and d_1 merge into d_1.

Responsible evolutionary mechanisms and hierarchies. As discussed above, the stability of the earlier ontogenetic stages is considered to be caused by mechanisms inherent to organisms, of which developmental constraints are most important. In contrast, the similarities of the earlier ontogenetic stages are alternatively interpreted as being due to adaptation. Rieppel (1990) contrasted these two mechanisms in the context of phylogenetic and ontogenetic hierarchy. It is claimed that as long as von Baer's laws hold, developmental constraints increase towards the earlier ontogenetic stages of the higher hierarchical ranks and adaptive plasticities increase towards the later ontogenetic stages of the lower hierarchical ranks (Text-fig. IV-7-2). Although not clearly evidenced, the ontogenetic increase of morphologic similarities (Text-fig. IV-6-1) can be explained by the reverse operation of each mechanism; in other words, developmental constraints decrease towards the earlier ontogenetic stages of the higher ranks, whereas adaptive plasticities decrease towards the later stages of the lower ranks (Text-fig. IV-7-4). It has to be examined whether the two mechanisms operate in equal intensity and equal amount of variation of their intensities along the hierarchical ranks, or the intensity and its variation change according to the hierarchical ranks (Text-fig. IV-7-3).

As shown in Text-figure IV-7-1, the two mechanisms are considered to operate in a continuous fashion without any break of any hierarchical rank. Chatterton and Speyer (*in* Whittington *et al.*, 1997, p. 211) stated, " Work to date supports the contention that monophyletic groups of trilobites from the family at least to the subordinal level have similar larvae, ... others [*other genera*] show a greater disparity in larval form" [*italics* added by author]. It suggests that at least in the trilobites, ontogenies following von Baer's laws occur at hierarchical levels higher than genus and those violating von Baer's laws at ranks lower than family (Text-fig. IV-7-4). In effect, all the examples cited above for ontogenies violating von Baer's laws appear to occur at relatively lower taxonomic ranks. Therefore, there seems to be a critical hierarchical rank that draws the boundary between two cases of ontogenies in a group. It needs to be investigated whether the co-existence of the two ontogenies in a group can be generalized as a feature of all the animal groups, and whether the two mechanisms operate in the opposite way across the taxonomic boundary.

PROBLEMS IN DEALING WITH ONTOGENETIC DATA AT OPERATIONAL LEVEL OF SYSTEMATICS.

If all the information on ontogeny of the taxa as discussed above, was available for systematists, all that systematists would need to do is transform the information into a character matrix and calculate phylogenetic trees. However, the information currently available for systematists is far from complete, and does not fully incorporate the implications of Haeckel and von Baer's laws and the properties of ontogeny discussed above. Below will be discussed realistic problems that systematists cope with and recommended solutions at the level of operation, for dealing with morphologic data from ontogenies.

Multiple data sets. Ontogenetic records that are available for systematists are not usually complete. In many cases, ontogenies of taxa that systematists attempt to classify are not

551

known for all the members of the taxon. Biologists, including systematists, tend to segment ontogeny into several stages that are regarded as comparable. For example, trilobite ontogeny is divided into three periods with reference to significant developmental events (Text-fig. IV-5). Differentiation of the protopygidium separates the protaspid period from the meraspid period, and completion of release of thoracic segments is the boundary between meraspid and holaspid periods. The arbitrariness of segmenting ontogeny is reduced when the boundaries between the ontogenetic segments are accompanied by a radical metamorphic event. For example, sea urchin larvae discard nearly all their membranes and then metamorphose into a juvenile from the small group of set-aside larval cells; all the larval morphologic features cannot be traced into the juvenile stage. To divide ontogeny with reference to this boundary appears not to be arbitrary. Other ontogenies that display continuous morphologic changes cannot be segmented without arbitrariness. To view ontogeny as a hierarchy also necessitates segmenting because a hierarchy consists of elements (e.g., morphologic features) at the same level (e.g., comparable ontogenetic stage).

It is customary to build separate character sets from each ontogenetic segment; as an example of trilobite studies, see Edgecombe (1992, table 5.2 and 5.4). It is not uncommon to find their phylogenies or groupings generated from these different ontogenetic data set are not congruent. For example, the classification of the Housiinae and Aphelaspidinae proposed in Chapter II (see Appendix II-1) is in conflict with the previous taxonomic scheme. This disagreement must be brought into congruence by appropriate methods, because there is only a single phylogeny of a particular taxon that should be represented by a corresponding classification scheme (Hennig, 1966).

Kluge (1985)'s figure 1 well demonstrates the problems at the operational level that occur when systematists deal with ontogenetic morphologic data (Text-fig. IV-8-1). Three comparable ontogenetic stages, larva, juvenile and adult, are recognized for four taxa. Two characters, x and y, are described, each of which has three character states, x_1, x_2, x_3 and y_1, y_2, y_3. Character y demonstrates the reverse case of decrease of morphologic similarities through ontogeny, since all the three character states are coded for the larval stage of three taxa whereas only one state for the adult stage. Character x demonstrates ontogenetic pathway corresponding to the case of decrease of morphologic similarities through ontogeny.

Each ontogenetic stage groups three taxa differently as shown in Text-figure IV-8-2. How can systematists bring these different groupings into congruence? It can be accomplished by analyzing different data sets separately and then obtaining a consensus ('taxonomic congruence approach'; Swofford, 1991), by combining all available data sets into a single set and analyzing it ('character congruence approach'; Kluge and Wolf, 1993), or by regarding ontogenetic transformation of character states as a character ('ontogenetic transformation character approach'; de Queiroz, 1985). The 'character congruence approach' offers two options; all the characters are equally weighted, or characters from a particular ontogenetic stage are given more weight by assuming that the stage is considered evolutionarily more important. The latter option will be discussed below separately.

Miyamoto and Fitch (1995) contrasted the taxonomic congruence and character congruence approaches, and summarizes the assumptions behind each approach (table 1). The advocates of the taxonomic congruence approach believe that each data set is

552

independent in terms of evolutionary rules (Bull *et al.*, 1993). More independence would be seen for characters from different data sets than for characters from the same sets. For example, some trilobite protaspides radically metamorphose into a very different meraspid form in accompanying with the change of life mode (Chatterton and Speyer *in* Whittington *et al.*, 1997). Each stage would have been governed by different evolutionary rules or mechanisms. To combine the protaspid and meraspid data sets in this case will reduce or mask important phylogenetic signals from each ontogenetic stage. Therefore, each data set must be analyzed separately and a consensus will be sought from the trees generated by each data set (Text-fig. IV-8-2).

The character congruence approach is fundamentally based on the belief that it is not natural to recognize separate data sets, whether they are molecular versus morphological or larval versus adult. To separate characters into different types is believed to be a mere artifact. Furthermore, the advocates argue against the taxonomic congruence approach because there are so many different ways of obtaining a consensus tree with the taxonomic congruence approach and each generates different consensus trees. Therefore the phylogeny must be obtained by directly resolving character conflicts within a single data set following the total evidence principle (Text-fig. IV-8-3). Because these two methods place equal weights on characters, none of them are burdened by *a priori* assumptions relevant to the causal explanations between development and evolution, for example, von Baer's laws, discussed above. Each method does not require any *a priori* assumptions on relative significance of particular ontogenetic stage in the overall context of the phylogenetic reconstruction or on equal significance at different phylogenetic hierarchical levels.

The ontogenetic transformation character approach assumes the existence of polarity at two different levels, one at the character level ('character adjacency' in Wheeler, 1990) existing, for example, among x_1, x_2 and x_3, and the other at the phylogeny existing, for example, between x and y (Text-fig. IV-8-4). It is made possible to separate the two different polarities, by describing ontogenetic transformation as a character; for example $x_1 \rightarrow x_2 \rightarrow x_1$ and $y_2 \rightarrow y_3 \rightarrow y_3$ each is a different character. This approach certainly removes the logical dependence existing between features of the larvae and adults in the combined data set; different states of the same feature of the two ontogenetic stages are causally related to, and logically dependent on, each other in the context of development. This method also increases the information content. For instance, the meraspid period of the trilobites has largely been ignored in reconstructing the phylogenies. It is partly because the meraspid characters usually change their character states—thus, cannot be described as instantaneous morphology—during the period and partly because the information is not available. If the former is the reason for not incorporating the meraspid data, describing ontogenetic transformation as a character solves the problem. With this concept of character, ontogenetic criterion of polarity determination is of no use because all the ontogenetic transformation is incorporated into a character. The issue of homology also enters into a totally new perspective. Roth (1984) and others argue that the two features are homologous if they share an identical ontogenetic pathway. With the ontogenetic transformation character concept, the ontogenetic pathway, itself, will be a unit of comparison for the homology conjecture.

It needs to be investigated whether one approach has the precedence over the others and whether each approach needs to be applied for different character sets (e.g.,

molecular versus morphological and larval versus adult). The problem can be approached by applying all three methods for ontogenetic data sets of a particular group of organisms and compare the reliabillity of the resultant trees with reference to such tree comparing statistics as bootstrapping. The resultant trees will also be compared with the trees generated by data sets that are believed to be independent of those used. For example, the trees from ontogenetic data sets can be contrasted by those from molecular data sets. **Problem of weightings**. The morphologic stability of the earlier ontogenetic stages and the hierarchy of ontogeny discussed above can be taken to indicate that their characters are more systematically significant. Darwin (1859, p. 449) stated, "… the structure of the embryo is even more important for classification than that of the adult." Chatterton and Speyer (*in* Whittington *et al.*, 1997, p. 211), claim, "As a rule, monophyletic groups based on characteristics of adult growth stages have similar larvae and life-history strategies so that larval morphology appears to be a useful indicator of relationship." These statements, as they stand, imply that earlier ontogenetic stages are informative, and more informative, for systematics.

The contrary standpoint has been proposed by the adaptationists as discussed above. They claim that the similarities of earlier ontogenetic stages are due to the adaptation and thus, the features of earlier stages are generally considered of little systematic value because of the suspected rampant homoplasy (Smith, 1997 for example of echinoid larvae), in particular, at the lower taxonomic ranks. On one hand this argument directly opposes Rieppel's arguments that later ontogenetic stages are more adaptive and earlier stages are more resistant to changes. On the other hand, to claim the prevalence of homoplasy at the lower taxonomic ranks appear to comply with Rieppel's argument that at lower ranks, adaptive plasticity would play a greater role.

Regardless of which stage must be considered to be reliable, the problem of weighting occurs when the assumption of the relative systematic importance of the particular ontogenetic stage is incorporated into the cladistic analysis. Cladistic analysis does not *a priori* assume the existence of homoplasy—the features that we assume to be less evolutionarily significant—following Hennig's 'auxiliary principle' (Wiley *et al.*, 1991). If we assume the existence of homoplasy before obtaining phylogenetic hypothesis, "phylogenetic systematics would lose all the ground on which it stands." (Hennig, 1966, p. 121; see also Wiley *et al.*, 1991). Ultimately, the homoplasies, if any, will be read from the phylogeny reconstructed using the parsimony principle. Thus, to weigh down the characters due to the a possibility of their homoplasy is not justified by the operational level.

However, more developmentally oriented researches provide the data that a certain ontogenetic stage is more stable than the others (see above). It seems that these results are needed to be incorporated into the cladistic analysis as a form of weighting. It cannot be easily determined how features of the larvae or adults are relatively weighed to incorporate their relative significance over the other. One way to give more weight to characters from a particular ontogenetic stage is to arrange all the features into a hierarchical fashion (e.g., Text-fig. IV-2-4) and count how many steps are required to differentiate a certain feature and use this numerical count as a relative weight. In the example shown in Text-figure IV-2-4, all features require 5 steps of differentiation. Or if the intensity of the two evolutionary mechanisms (Text-fig. IV-7-3) would be quantified, this can be used as a guide to weigh characters from different ontogenetic stages.

process

pattern

fish   chick   calf   human

adaptive plasticities decrease
developmental constraints increase

level of inclusiveness increases
morphologic similarities increase
morphologically describable features decrease

mammalian stage

tetrapod stage

vertebrate stage
(pharyngular stage)
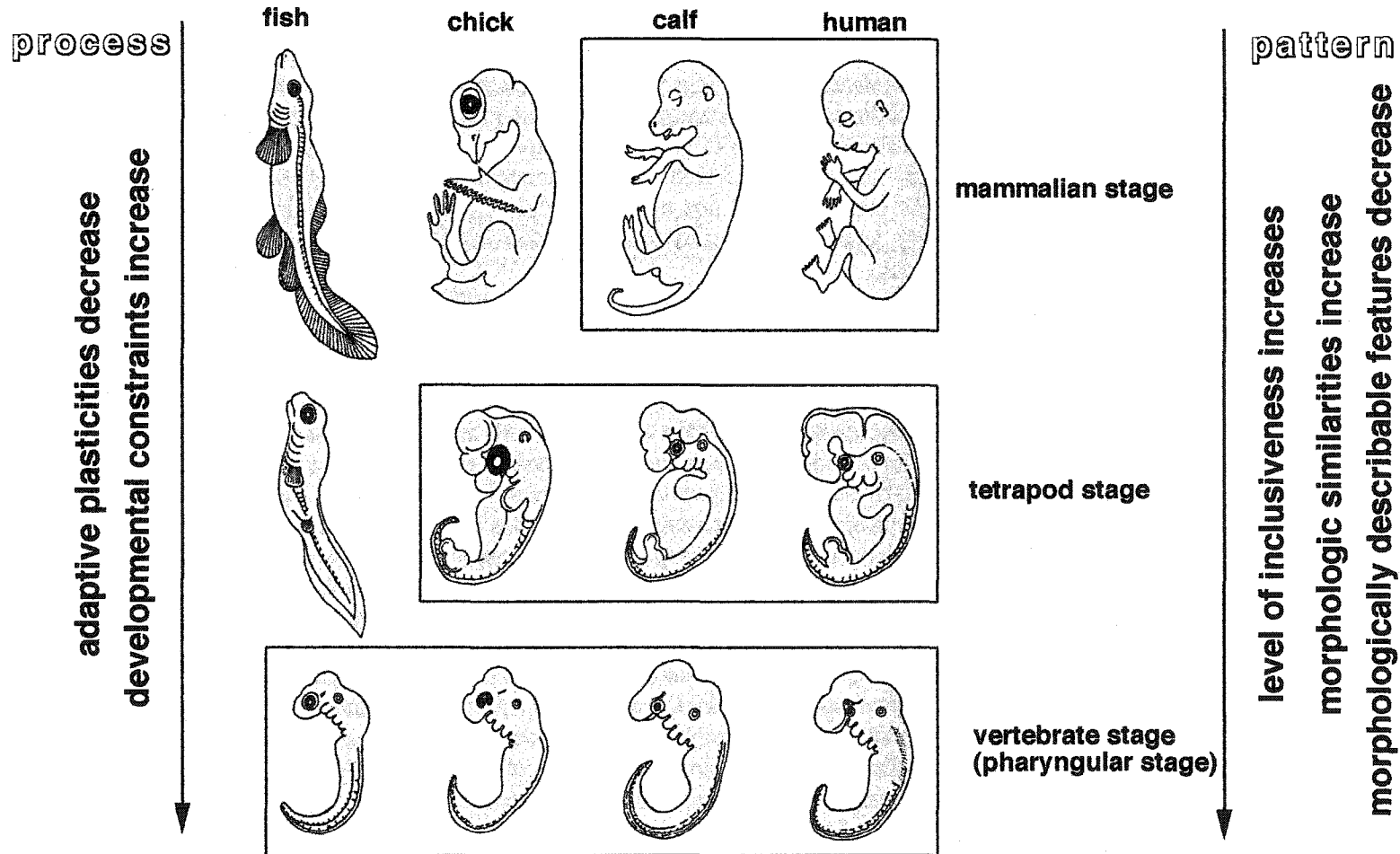
TEXT-FIGURE IV-1. A part of Haeckel's diagram of progressive stages of development of representative vertebrates. The earliest stages shown are at the bottom of the diagram, and progressively later stages towards the top. (modified from Raff, 1996, fig. 6.4). The animals in a rectangle share features defining a particular hierachical rank such as the Vertebrata, Tetrapoda, and Mammalia.
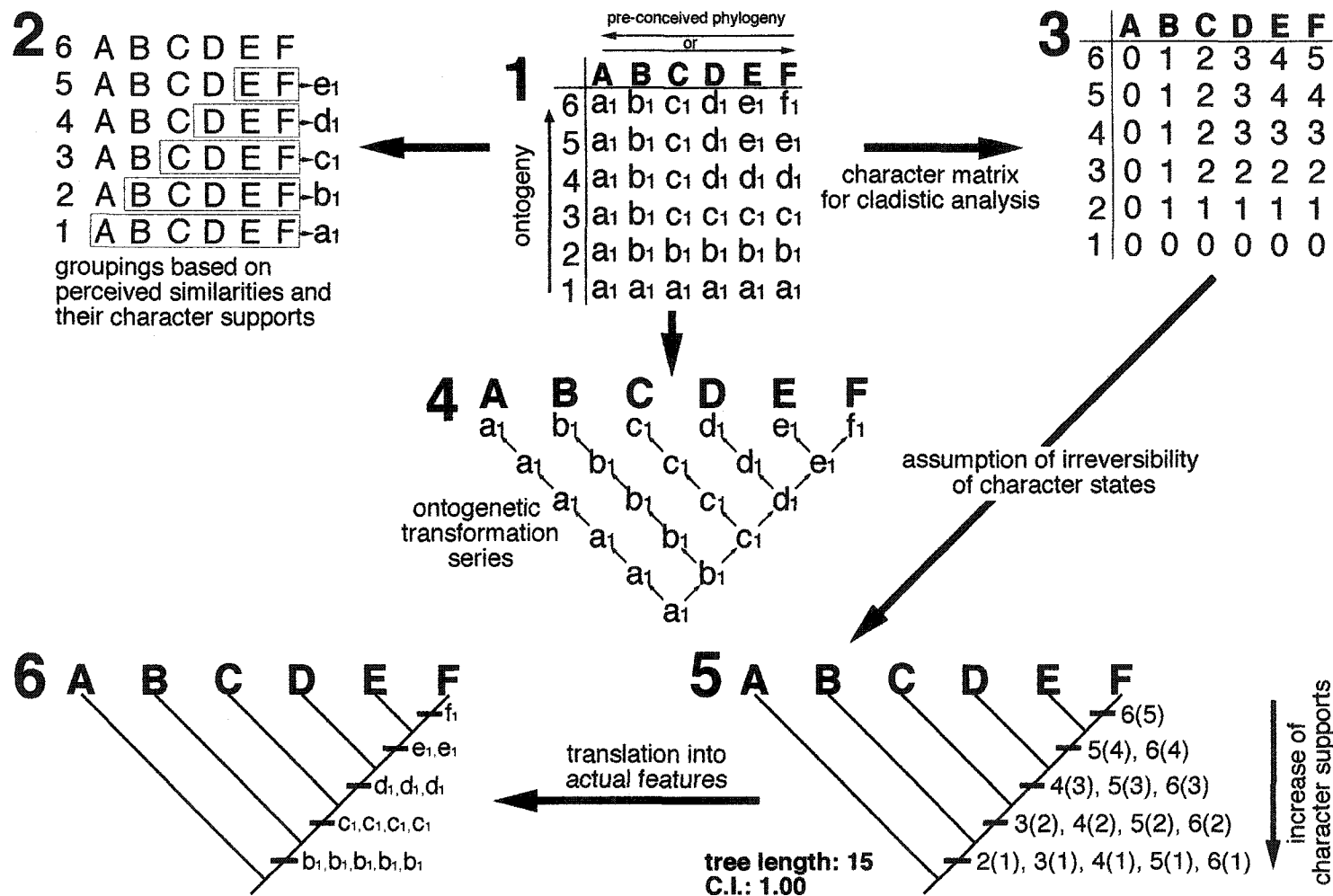
TEXT-FIGURE IV-2. Systematic analysis of ontogenies of a group that follow von Baer's laws. 1. Ontogenetic sequence data of six taxa. 2. Groupings based on perceived similarities and their character supports. 3. Character matrix for cladistic analysis. 4. Ontogenetic transformation series. 5. Cladogram with synapomorphies. 6. Cladogram with translation of synapomorphies into actual character states.

2

6	A	B	C	D	E	F

$a_1 - 5$ A B C D E F

$a_1 - 4$ A B C D E F

$a_1 - 3$ A B C D E F

$a_1 - 2$ A B C D E F

$a_1 - 1$ A B C D E F

groupings based on
perceived similarities and
their character supports

1

pre-conceived phylogeny

or

ontogeny

	A	B	C	D	E	F
6	a_1	b_1	c_1	d_1	e_1	f_1
5	a_1	a_1	b_1	c_1	d_1	e_1
4	a_1	a_1	a_1	b_1	c_1	d_1
3	a_1	a_1	a_1	a_1	b_1	c_1
2	a_1	a_1	a_1	a_1	a_1	b_1
1	a_1	a_1	a_1	a_1	a_1	a_1

character matrix
for cladistic analysis

3

	A	B	C	D	E	F
6	0	1	2	3	4	5
5	0	0	1	2	3	4
4	0	0	0	1	2	3
3	0	0	0	0	1	2
2	0	0	0	0	0	1
1	0	0	0	0	0	0

4 A   B   C   D   E   F

a_1 b_1 c_1 d_1 e_1 f_1

a_1 b_1 c_1 d_1 e_1

a_1 b_1 c_1 d_1

a_1 b_1 c_1

a_1 b_1

a_1

ontogenetic
transformation
series

assumption of irreversibility
of character states

6 A   B   C   D   E   F

b_1, c_1, d_1, e_1, f_1

b_1, c_1, d_1, e_1

b_1, c_1, d_1

b_1, c_1

b_1

translation into
actual features

5 A   B   C   D   E   F

2(1), 3(2), 4(3), 5(4), 6(5)

3(1), 4(2), 5(3), 6(4)

4(1), 5(2), 6(3)

5(1), 6(2)

6(1)

tree length: 15
C.I.: 1.00

increase of
character supports

TEXT-FIGURE IV-3. Systematic analysis of ontogenies of a group that follow Haeckel's law. 1. Ontogenetic sequence data of six taxa. 2. Groupings based on perceived similarities and their character supports. 3. Character matrix for cladistic analysis. 4. Ontogenetic transformation series. 5. Cladogram with synapomorphies. 6. Cladogram with translation of synapomorphies into actual character states.

557

1a

	plant	animal	man
	V	S	r
		V	S
			V

1b

plant	animal	man
ᴅS	ᴅr	

or

plant	animal	man
+S	+S	+r

linear exclusive hierarchy

1c

plant	animal	man
V	S	r

subordinated inclusive hierarchy

2a

	plant	animal	man
3	V	S	r
2	V	V	S
1	V	V	V

2b

plant animal	man
V₂	V₁

perceived similarities

2c

cladistic paradigm

3a

	plant	animal	man
3	V	S	r
2	V	S	S
1	V	V	V

3b

plant	animal man
V₁	S₂

perceived similarities

3c

cladistic paradigm

V: vegetative soul   S: sensitive soul   r: rational soul
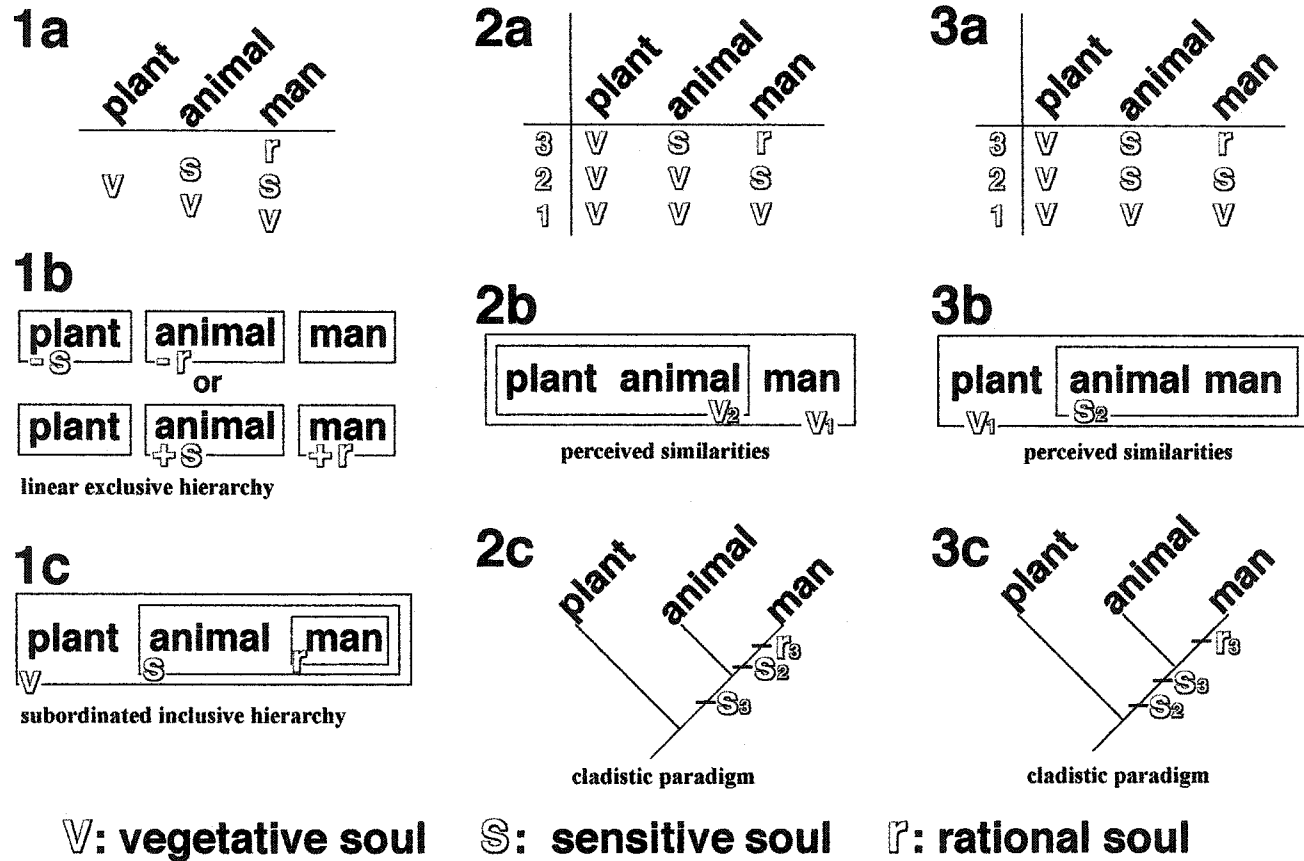
TEXT-FIGURE IV-4. Systematic analysis of ontogenetic changes of the character 'soul' of plants, animals and human, in the hierarchical context. 1. Rieppel (1988)'s interpretation. a. Data set implied by Rieppel (1988). b. Linear exclusive hierarchy implied by the data set. c. Translation of the linear hierarchy into a subordinated inclusive hierarchy. 2. Interpretation based on that ontogenetic changes are caused by terminal addition. a. Complete data set. b. Groupings based on the perceived similarities. c. Cladogram generated from the character matrix of 2a. 3. Interpretation based on that ontogenetic changes are caused by subterminal insertion. a. Complete data set. b. Groupings based on the perceived similarities. c. Cladogram generated from the character matrix of 3a.
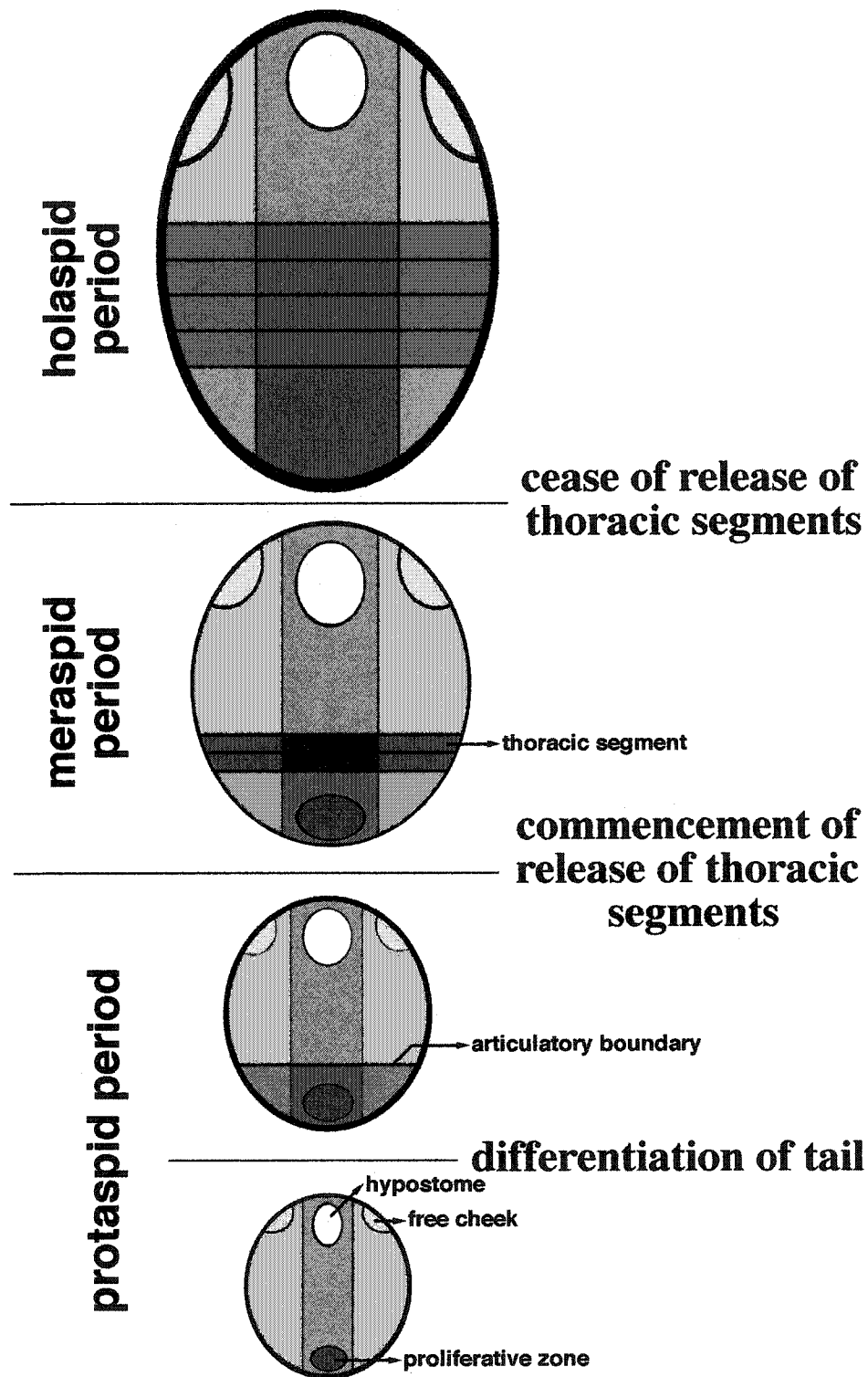
TEXT-FIGURE IV-5. Hierarchical arrangement of ontogenetic changes of the trilobites. Different tones of darkness indicate a morphologic region which is differentiated from a region of preceding ontogenetic stage or differentiated into a region of succeeding stage.

559
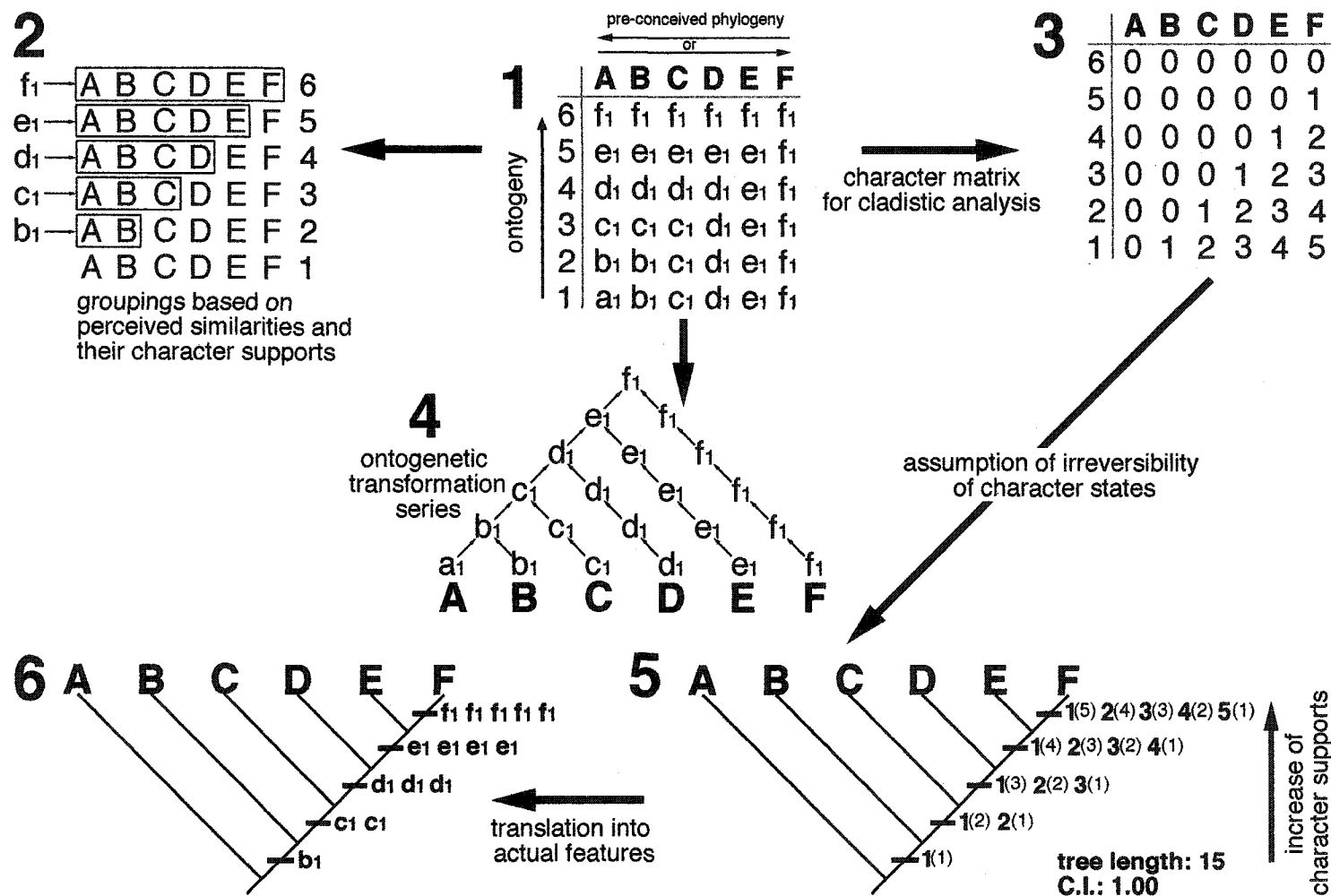
TEXT-FIGURE IV-6. Systematic analysis of ontogenies of a group showing increase of morphologic similarities with growth. 1. Ontogenetic sequence data of six taxa. 2. Groupings based on perceived similarities and their character supports. 3. Character matrix for cladistic analysis. 4. Ontogenetic transformation series. 5. Cladogram with synapomorphies. 6. Cladogram with translation of synapomorphies into actual character states.
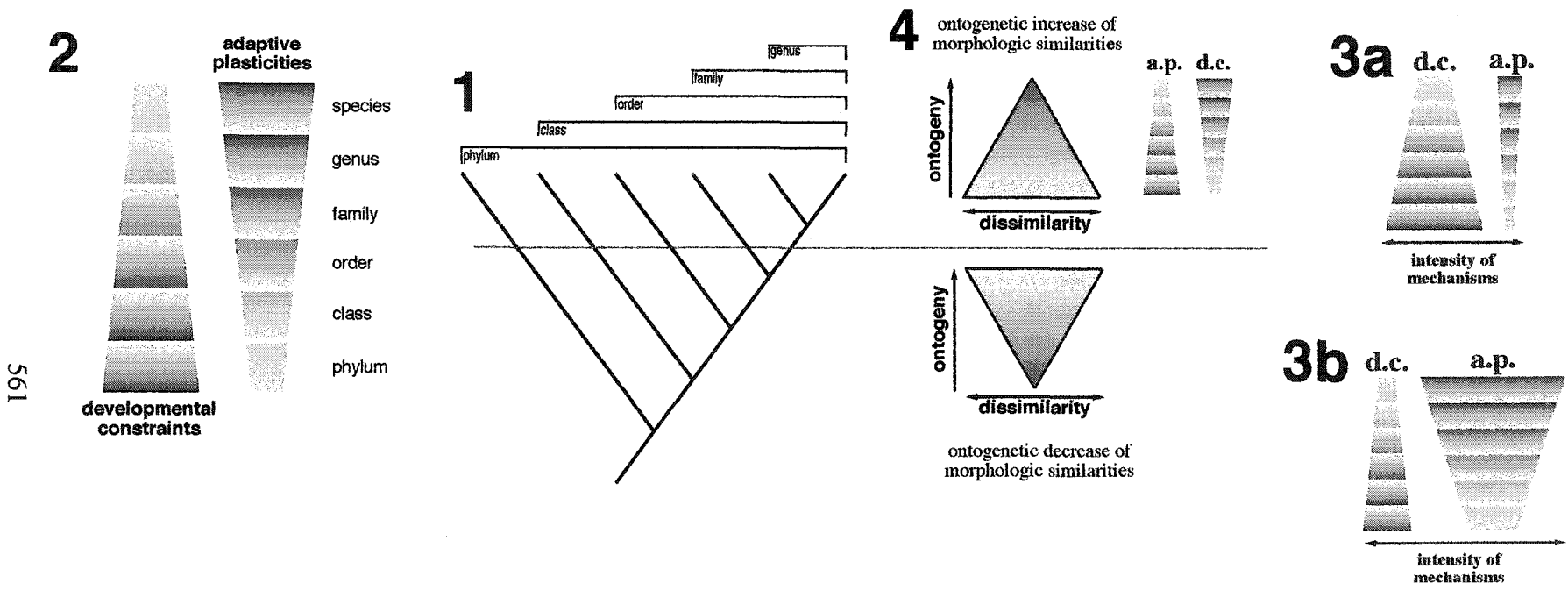
TEXT-FIGURE IV-7. 1. Cladogram of six taxa, each node being ranked according to Linnean hierarchy. 2. Two evolutionary mechanisms, developmental constraints (d.c.) and adaptive plasticities (a.p.) responsible for ontogenetic increase of morphologic dissimilarities. The width and tone represent the intensity of each mechanism; the wider and darker indicate that the mechanism operate more intensively. Each segment represents the gradual change in the intensity of each mechanism at each taxonomic rank. 3. Possible interrelated variations of intensity of each mechanism; only two examples are shown. a. The stronger developmental constraints and weaker adaptive plasticities. b. The stronger adaptive plasticities and weaker developmental constraints. 4. Cases of trilobites where ontogenetic increase of morphologic dissimilarities occur in higher taxonomic ranks and ontogenetic decrease of morphologic dissimilarities. The latter case may be due to the ontogenetic increase of the intensity of developmental constraints and the ontogenetic decrease of the intensity of adaptive plasticities.

1

		A	B	C	D
		0	1	2	3
y-adult	**6**	y_3	y_3	y_3	y_3
y-juvenile	**5**	y_2	y_2	y_3	y_3
y-larva	**4**	y_1	y_2	y_2	y_3
		0	1	2	2
x-adult	**3**	x_1	x_2	x_3	x_3
x-juvenile	**2**	x_2	x_2	x_3	x_3
x-larva	**1**	x_1	x_3	x_3	x_3

2

larva

juvenile

adult

strict consensus

4

	A	B	C	D
y-otc	0	1	2	3
x-otc	0	1	2	2

3

		A	B	C	D
y-adult	**6**	3	3	3	3
y-juvenile	**5**	2	2	3	3
y-larva	**4**	1	2	2	3
x-adult	**3**	1	2	3	3
x-juvenile	**2**	2	2	3	3
x-larva	**1**	1	3	3	3
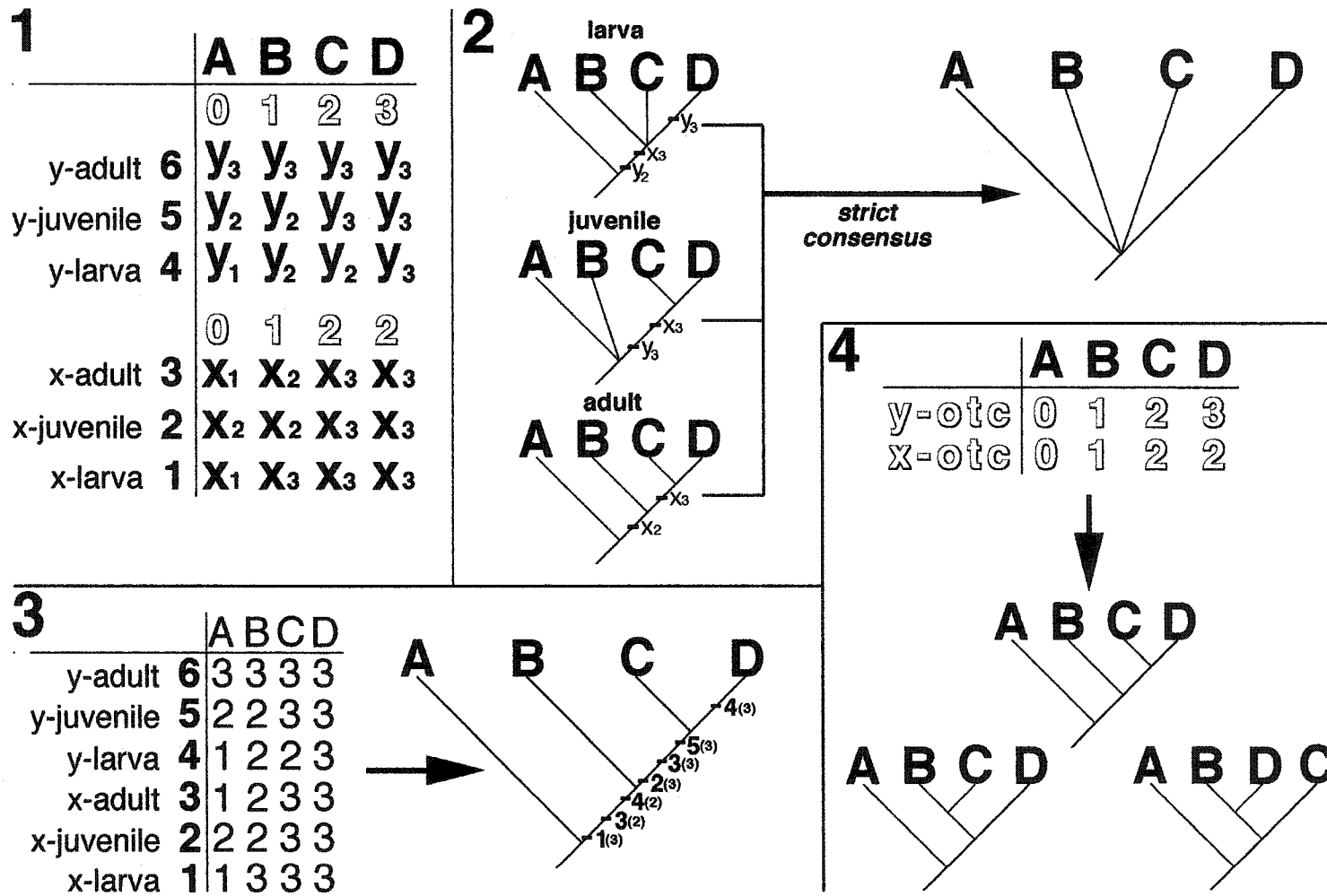
TEXT-FIGURE IV-8. Realistic example of data sets from ontogeny. 1. Two characters, x and y and their character states for four taxa (modified from Kluge, 1985, fig. 1). 2. Taxonomic congruence approach. 3. Character congruence approach. 4. Ontogenetic transformation character (OTC) approach.

562

CHAPTER V

CONCLUSIONS AND DISCUSSIONS

Taxonomy of two trilobite groups, Ptychopariida and Hystricuridae, has been re-examined. Protaspides of 34 species of the Ptychopariida that were described by Hu are re-illustrated and re-examined in Chapter II. The comparative analysis of the protaspid morphologies aimed to reveal a new classification scheme within the order Ptychopariida. More than 150 species that have been referred to the family Hystricuridae are re-examined. New materials were collected from the Great Basin in western United States where more than half of the species of the family has been documented. The taxonomic revision of the family in Chapter III is mainly based on post-protaspid specimens. The taxonomic studies of these two groups aims at giving an insight to the origin of the Proetida, that is believed to lie within the Hystricuridae and ultimately within the Ptychopariida, which constitutes an integral part of the apparently intractable "ptychopariid problem."

For the present, a meaningful cladistic analysis to incorporate all of these taxa cannot be implemeted because compared to the number of describable and cladistically informative characters, the number of taxa to be included is too large to calculate reasonably resolved cladograms. The cladistic analysis for each group is pending that needs to be carefully framed with respect to the selection of taxa.

MORPHOLOGIES OF PTYCHOPARIID PROTASPID MORPHOTYPES

Protaspides of 34 ptychopariide species re-described in Chapter II are grouped into nine morphotypes (Appendix II-1). Morphotype A is characterized by a subrectangular to subcircular and relatively flattened shield, a forward-expanding axis with slightly more strongly forward-expanding glabellar front or L4, and a small and transversely elongated protopygidium (Text-fig. V-2-1 to 2-4). Morphotype B is characterized by an oval to subrectangular and relatively convex shield, a forward-expanding glabellar front, a narrow anterior border, a pair of relatively shallow anterior pits, and a relatively large protopygidium (Text-fig. V-2-5 to 2-11). Morphotype C is characterized by the anaprotaspides having a very convex, circular to oval shield, and the metaprotaspides having a suboval shield, a laterally convex glabella with a parallel-sided or slightly forward-expanding glabellar front or L4, axial furrows that shallow out anteriorly, and a relatively large protopygidium (Text-fig. V-3-1 to 3-8). Morphotype D is characterized by a circular to subquadrate shield, a narrow and parallel-sided axis, relatively deep anterior pits, and a very small protopygidium (Text-fig. V-4-1 and 4-2). Protaspid morphotype E is characterized by a subrectangular to subquadrate to elliptical shield, a slightly forward-expanding axis with a more strongly expanding L4, distinct transglabellar furrows, anterior pits that are not distinguishable from the axial furrows, and a protopygidium that is strongly directed ventrally (Text-fig. V-4-4, 4-5, 4-7, 4-8). Protaspid morphotype F is characterized by a circular shield, a spindle-shaped axis with a L4 that is waisted at its mid-length, a distinct eye ridge, and a long post-axial region (Text-fig. V-4-6).

Each morphotype is considered to represent a higher taxonomic rank such as a

563

superfamily or family that has never been designated. Some are entirely new to trilobite systematics (e.g., groups represented by morphotype A and C) and others are in partial agreement with previous suggestions on their evolutionary relationships (e.g., group represented by morphotype B). Each grouping was not officially named, because 1) it seems precarious to name a taxon upon the basis of larval features of only those few taxa for which the protaspides are known, 2) the classification scheme will certainly be improved by incorporating all other available information, such as morphologies from other growth stages and geographic distributions, and 3) methodologically, classification scheme that entails a large number of taxa should be tested by other means, such as computational analysis to find and resolve any errors.

The other morphotypes are considered to represent those of the previously-named groups. Protaspides of the superfamily Dikelocephalacea are distinguished by a circular shield, a narrow parallel-sided axis, a wide eye ridge, and fingerprint-like ornaments on the shield surface (Text-fig. V-4-3). Protaspides of the Solenopleuracea are characterized by a circular shield, a forward-expanding L4, spindle-shaped L3/L2/L1, and distinct anterior pits that are located well inside the shield margin. Protaspides of the family Olenidae are characterized by a circular to oval shield, a forward-expanding to forward-tapering axis, relatively distinct anterior pits, a slender eye ridge, a long posterior marginal spine pair, and a long protopygidial marginal spine pair (Text-fig. V-4-9 to 4-11); the last two features are observed in the metaprotaspides where the protopygidium is differentiated from the rest of the shield.

Features common to all the ptychopariide protaspides include (1) a shield that is of relatively low convexity, which may be indicative of a benthic life mode; (2) a shield lacking any conspicuous ornament, other than posterior marginal spines in the anaprotaspid stages, such as spines or tubercles or pits—exceptions are found in some species of morphotype E; (2) a forward-expanding axis—a noticeable exception is morphotype C; (3) an anterior cranidial border that is not differentiated, and a glabellar front that touches the anterior shield margin—an exception is the metaprotaspides of *Ptychaspis*, *Syspacheilus* and *Crepicephalus*; (4) the presence of anterior pits—but morphotype C has no anterior pits that are distinguishable from the axial furrows; (5) a palpebro-ocular ridge that extends from the posterior of the anterior pits and is well elongated posteriorly—but morphotype C lacks the ridge; the presence of the palpebro-ocular ridge appears to correspond consistently with the presence of anterior pits.

High-Level Classifications of Ptychopariida Implied By Protaspid Morphotypes

The possession of each protaspid morphotype listed above by ptychopariid taxa suggests that they may belong to an identifiable superfamily (Appendix II-1). The discussion below assumes that the developmental pattern of ptychopariide taxa follow von Baer's laws at all hierarchical levels, thus the sharing of similar protaspid forms is taken to indicate that the taxa belong to the same taxon (see Chapter IV). Taxa with similar earlier growth stages are taken to indicate that they should be clustered into the same higher taxa.

The two suborders of the Ptychopariida, the Ptychopariina and Olenina, are accepted as Fortey (*in* Whittington *et al.*, 1997; but see Westrop, 1995). The suborder Ptychopariina is subdivided into five groups upon the basis of distinctive protaspid

564

morphotypes; two of them were officially named. The protaspid morphotype A is shared by *Komaspidella*, *Glaphyraspis*, and *Bolaspidella*. Each genus is assigned in this work to the Family Kingstoniidae, Lonchocephalidae, and Menomoniidae, respectively. It has never been speculated that these three families should be classified in the same superfamily. The holaspid morphologies seem too different to cluster these three families into a higher taxon. However, ontogenies of these three species evidently indicate that they share morphologic similarities until early meraspid stages. As discussed in Chapter IV, a monophyletic group is not necessarily defined by shared derived features from every single ontogenetic stage; some clades may be defined only by larval features and others only by adult features. *Welleraspis* of the Catillicephalidae is provisionally placed in this group, because of the recurring opinion that the Catillicephalidae and Lonchocephalidae may be united. However, protaspides of *Welleraspis* are characterized by a strongly forward-expanding, wide axis, and a bilobed L3/L2, which are features not shared by the above three taxa; *Welleraspis* protaspides were not re-examined by the author.

The protaspid morphotype B is shared by *Cedarina* of the Cedariidae, *Apomodocia* of the questionable Cedariidae, *Glyphaspis* of the Anomocaridae, *Crepicephalus* of the Crepicephalidae, *Syspacheilus* and *Modocia* of the Marjumidae and *Nixonella* of the Llanoaspididae. Many previous workers, on the basis of holaspid morphologies, have suggested that the Cedariidae, Llanoaspididae, Crepicephalidae and Marjumidae are closely related to one another. Thus, it is not surprising that these families share a similar protaspid form. Of interest is the possession of the same morphotype by the Middle Cambrian anomocarid, *Glyphaspis*. Fortey and Chatterton (1988, text-figs. 2-4) concluded that the Anomocaridae is an immediate sistergroup to the two major superfamilies of the order Asaphida, the Cyclopygacea and Asaphacea. The protaspides of *Glyphaspis* are not of an "asaphoid" type that is characterized by a spherical to ovoid exoskeleton and three pairs of submarginal spines. The morphologic information supplied by the protaspides clearly contradicts that taxonomic assessment of the Anomocaridae based on the holaspid morphologies. The holaspid synapomorphies uniting the Anomocaridae with the two asaphid groups in Fortey and Chatterton (1988)'s cladograms must be tested by the protaspid characters using methods outlined in Chapter IV.

The protaspid morphotype C is present in *Housia* of the Housiinae, *Pulchricapitus* of the Pterocephaliinae, *Drabia*, *Aphelotoxon*, *Ponumia*, and *Paranumia* of the Phylacteridae, *Arapahoia* of the Plethopeltidae, and *Norwoodella* of the Norwoodiidae. All these families have never been clustered into a higher taxonomic group, because their holaspid morphologies are not similar, and most similarities found among these families are symplesiomorphies regarded as the concept of 'ptychopariid morphology,' in other words, a much higher level of classification. The similarities shared by the housiines and phylacterids until early meraspid stages are remarkable, suggesting that these two taxa are very closely related.

Two superfamilies, Dikelocephalacea and Solenopleuracea, each are represented by one species in this study, *Ptychaspis bullasa* and *Solenopleura acadia*. Each species has a distinctive protaspid form that is separated from all the other protaspid morphotypes, supporting their natural status. More information on protaspides of other members of the superfamilies is required to assess further the status of each superfamily.

The suborder Olenina of the Ptychopariida is subdivided into four groups upon the

565

basis of the protaspid morphotypes. It is one of the most remarkable discoveries made in this study that the Olenidae is not represented by a single protaspid form that is uniform throughout its members as expected from the strongly accepted monophyly of the group. The protaspid morphologies of the Olenidae lead the author to suggest that the Olenidae may be paraphyletic or even polyphyletic; for example, the protaspides of *Olenus* are strongly similar to those of *Aphelaspis* and their similarities are extended well into the meraspid stages, and *Apolanias* protaspides are similar to the parabolinoidid protaspides. The appropriate methodologies discussed in Chapter IV need to be employed to reveal the true nature of the Olenidae.

The Parabolinoididae is considered to constitute its own higher-taxonomic rank. The protaspid morphotype D shared by *Taenicephalus* and *Orygmaspis* is clearly differentiated from the olenid protaspid morphologies, contradicting the prevailing opinion that the Parabolinoididae belongs to the Olenacea along with the Olenidae. This does not lend support to Fortey and Chatterton (1988) who placed the family in the Anomocaroidea of the Asaphida; the parabolinoidids have a median suture that was considered to be diagnostic of the Asaphida by Fortey and Chatterton (1988), but they do not have the "asaphoid"-type protaspis.

The protaspid morphotype E is shared by taxa that are considered to belong to the Aphelaspidinae. It is of most interest that *Aphelaspis* has larvae of morphotype E but *Housia* has larvae of morphotype C, because these two taxa have long been considered to belong to the family Pterocephaliidae. Their protaspid morphologies suggest that both taxa cannot be placed in the same family, contradicting the prevailing taxonomic convention based on holaspid morphologies. Chatterton and Speyer (*in* Whittington *et al.*, 1997) included *Aphelaspis* in the Anomocaracea of the Asaphida, while Fortey and Chatterton (1988) implied the exclusion of *Aphelaspis* from the Pterocephaliidae.

The morphotype F is present in two taxa, *Elvinia* and *Irvingella*. It displays different morphologies from the olenids and any other above-mentioned taxa of the Olenina. This contradicts the currently-accepted taxonomic scheme where the Elviniidae including *Elvinia* and *Irvingella* is placed in the Olenacea. More protaspid materials are required to assess the position of *Irvingella* for which only two protaspid specimens are described.

Each protaspid morphotype within the Olenina is represented by taxa that are assigned to one subfamily or family. Contrary to the classification scheme depicted in the Appendix II-1, it seems possible that each family or subfamily is a member of the Olenacea; in this case, the concept of the Olenina proposed by Fortey (1990) is superfluous. In order to assess the concept of the Olenacea or Olenina, it is important to have protaspid information for other families or superfamilies that have been assigned to the Olenacea or Olenina. Fortey (1990) restricted the concept of the Olenina to the Olenidae and transferred many families that were considered to belong to the Olenina into the Asaphida, as defined by Fortey and Chatterton (1988). The Parabolinoididae, Aphelaspidinae, and Elviniidae, for which the protaspides are described in this study, have been united with the Olenidae into the Olenina or the Olenacea by various workers (e.g., Ludvigsen *et al.*, 1989, Westrop, 1986). The similarities of different olenid protaspides to one of these taxa strongly suggest that the Olenidae could be paraphyletic.

CONCEPT OF HYSTRICURIDAE

Below in the text, the term Hystricuridae indicates the concept that is defined as in

566

Chapter III; however, the term "hystricurid(s)" indicates that the taxa can be accommodated within the old concept of the Hystricuridae.

Taxonomic revision of 89 named species of 18 "hystricurid" genera results in the conclusion that the Hystricuridae consists of 52 species of the following 12 genera, including seven new genera; *Hystricurus sensu lato*, *Carinahystricurus* n. gen., *Glabellolsulcatus* n. gen., *Hillyardina*, *Pachycranium*, *Parahillyardina* n. gen., *Parahystricurus*, *Paramblycranium* n. gen., *Politohystricurus* n. gen., *Pseudoplethopeltis* n. gen., *Spinohystricurus* n. gen., and *Tanybregma* (see Appendices III-1 and III-2). The concept of *Hystricurus* is still *sensu lato* because the species belonging to *Hystricurus* (*Butuberculatus*) and *Hystricurus* (*Aequituberculatus*) show cranidial and pygidial morphologies similar to those of some ptychopariides, indicating that these species may be as closely related to some ptychopariids as to other hystricurids (see below).

The morphologic comparison with non-hystricurid proetides and ptychopariides leads to the exclusion of 13 genera that have been referred to the Hystricuridae (Appendices III-1, III-3, and III-4). Many of these genera are retained in the Hystricuridae with question. Six genera are newly established on the basis of materials from the Great Basin; two of these are retained in the Hystricuridae with question. The questionable retention is because their features from different ontogenetic stages suggest different taxonomic affinities. For instance, holaspid morphologies of *Paratersella* are similar to those of many members of the Hystricuridae indicating its affinity to the Hystricuridae, whereas its protaspid morphologies are quite different from those of the hystricurid protaspides, suggesting a remote affinity to the Hystricuridae. The genus *Psalikilus* has holaspid morphologies that are quite different from the hystricurids, but has earlier meraspid cranidia that are similar to those of the hystricurids. Other genera are assigned to proetide or ptychopariide families with confidence or question. Four genera, *Holubaspis*, *Nyaya*, *Taoyuania*, and *Chattertonella*, cannot be placed in any known family with certainty (Appendices III-3 and III-4).

EVOLUTIONARY RELATIONSHIPS OF PROETIDA TO HYSTRICURIDAE AND PTYCHOPARIIDA

Systematics of the order Proetida cannot be fully understood without understanding its relationships with the Hystricuridae and Ptychopariida (see Text-fig. I-1). While erecting the order Proetida, Fortey and Owens (1975) claimed that the families of the Proetida have their origin in various species of the Hystricuridae. For example, *Pseudohystricurus* was considered to lie very close to the origin of the Dimeropygidae. This indicates that different "hystricurid" members gave rise to different non-"hystricurid" proetides—the "hystricurids" are paraphyletic. Fortey (1983) noticed the great cranidial similarities between *Onchopeltis spectabilis* (Rasetti, 1944, pl. 39, fig. 1) from Upper Cambrian strata in Quebec and some *Hystricurus* species such as *H.?* *paucituberculatus* (Fortey, 1983, pl. 23, fig. 1). He claimed that *Hystricurus* re-evolved from the Upper Cambrian off-shelf trilobites that invaded the craton at the Cambrian-Ordovician boundary.

Fortey (1990) maintained the monophyletic status of the Proetida by claiming that the protaspides develop a preglabellar field, representing the presence of the natant hypostomal condition (e.g., see Pl. III-16, Fig. 12), which is considered to have been derived from the ptychopariide protaspides that do not differentiate a preglabellar field;

567

see Text-figs. V-1 to V-4 for the ptychopariide protaspides. Fortey (1990) recognized that the Hystricuridae might not be the ancestral stock to some other younger proetide families such as the Proetidae and Aulacopleuridae. The ancestry of the Proetida was considered to be older than the Hystricuridae and Fortey (1990) suggested that it may lie in the Middle Cambrian Solenopleuridae whose morphologies are indistinguishable from those of *Hystricurus*. This suggestion agrees with Edgecombe (1992) who suggested, upon the basis of the cladistic analysis, that the ancestry of the Proetida was pre-late Middle Cambrian in age.

Bergström (1977) denied the monophyletic status of the Proetida based on the existence of two different protaspid morphotypes in the Proetida. One of them, evident in such taxa as some *Hystricurus* species (Lee and Chatterton, 1997a) and *Dimeropyge* (Chatterton, 1994), is characterized by having regularly-distributed tubercles. The second is characterized by having smooth exoskeleton which is observed in such taxa as *Bathyurus* (Chatterton, 1980). This suggests the existence of two lineages of the Proetida, each of which has a separate evolutionary origin.

Several families have been assigned to the Proetida since Fortey and Owen (1975). Fortey (*in* Whittington *et al.*, 1997), in the most recent classification, included 12 families in that order. Of them, the Proetidae, Aulacopleuridae, Bathyuridae, Dimeropygidae, Telephinidae, Toernquistiidae which is separated from the Dimeropygidae (see Chatterton *et al.*, 1998), and Tropidocoryphidae that seems to be assigned to the Proetidae by Fortey (*in* Whittington *et al.*, 1997), have morphologies that are comparable to those of the hystricurids. This scheme excluded the Hystricuridae and did not clearly state to which taxon the family belongs. Recently, Adrain and Westrop (2001) proposed a new order Aulacopleurida which includes the family Aulacopleuridae, reducing the scope of the Proetida.

Below are discussed the systematics of the Proetida by considering morphologies of different exoskeletal parts and different ontogenetic stages.

Pygidial features. In Chapter III, much new information on pygidial morphologies of the Hystricuridae is presented. Comparison of pygidial morphologies of the hystricurids, non-hystricurid proetides, and ptychopariides is expected to shed new light on the systematic status of the Proetida.

Pygidial similarities are noticed between *Hystricurus* (*Aequituberculatus*) and Upper Cambrian ptychopariides such as aphelaspidines; the similarities are easily extended into Middle Cambrian ptychopariides such as *Elrathia* (see Robison, 1988, fig. 26.6). The relatively lower-profiled, smooth ptychopariide pygidia would have been transformed into the taller, finely tuberculated pygidia of *H.* (*Aequituberculatus*) (see Text-fig. V-5). The pygidia of *Hystricurus*? *longicephalus* (Pl. III-2, Figs. 7-8) and *Hystricurus*? *armatus* (Pl. III-2, Figs. 3, 4, 6) appear to be intermediate. The pygidia of *H.* (*Aequituberculatus*) would then have been transformed into those of *Hystricurus* (*Butuberculatus*) by acquiring a tubercle on the distal edge of the inner pleural field and only on the posterior pleural bands. As the final evolutionary step in *Hystricurus*, *Hystricurus* (*Hystricurus*) species added a large tubercle on the crest of the pygidial axial rings, a strongly bilobed terminal piece, and a post-axial ridge. Of non-*Hystricurus* genera, *Politohystricurus* and *Pseudoplethopeltis* have pygidia comparable to those of *Hystricurus* (*Aequituberculatus*), and *Tanybregma* has a pygidium similar to those of *Hystricurus* (*Hystricurus*). These non-*Hystricurus* genera of each group show a similar stratigraphic occurrence to each

568

Hystricurus subgenus.

Of non-hystricurid proetides, the aulacopleurids have remarkably similar pygidia to those of *Hystricurus* (*Aequituberculatus*) (Text-fig. V-5). The aulacopleurid pygidia are considered to be a recurring ptychopariide-type (Hughes and Chapman, 1995), which is also applicable to those of *Hystricurus* (*Aequituberculatus*). It is presumed that the aulacopleurids retained the pygidial morphotype of *Hystricurus* (*Aequituberculatus*) (Text-fig. V-5) which is considered to have been carried over from the ptychopariides such as the aphelaspidines. There is a relatively large stratigraphic gap between *Hystricurus* and aulacopleurids; *Hystricurus* appeared shortly after the Cambrian-Ordovician boundary, whereas the earliest aulacopleurid is Late Ordovician in age.

The smooth subtriangular pygidia of *Hystricurus* (*Triangulocaudatus*) are similar to those of some *Hystricurus* (*Aequituberculatus*) species (compare Pl. III-11, Fig. 22 and Pl. III-9, Fig. 16). The variations found among these pygidial morphotypes are the number of segments, ratio of sagittal length and transverse width, and relative axial width. All these variations can be accommodated within an evolutionary lineage. The pygidia of *Hystricurus* (*Aequituberculatus*) and *Hystricurus* (*Triangulocaudatus*) are of the ptychopariide-type and represent the most primitive condition of pygidial evolution of *Hystricurus*. It is the olenids that have pygidia similar to those of these two *Hystricurus* subgenera; see the pygidia of *Acerocare* (Pl. 31, Fig. 25) and *Apoplanias* (Pl. 30, Fig. 22).

Pygidia of many stratigraphically younger non-*Hystricurus* genera (mainly Zone E upwards) are characterized by a pygidial fulcral ridge along the distal edge of the inner pleural field that is interruped by interpleural furrows (Text-fig. V-6); *Carinahystricurus*, *Glabellosulcatus*, *Hillyardina*, *Parahillyardina*, and *Spinohystricurus* possess this structure. The fulcral ridge separates the tall, steeply down-sloping outer pleural field from the flat inner pleural field. The smaller pygidia of *Spinohystricurus* develop a row of short spines along the distal edge of the inner pleural field but only on the posterior pleural bands (Text-fig. V-5). This row of spines is the ontogenetic precursor of the pygidial fulcral ridge. These short spines are considered to be homologous with the prominent tubercles developed at the same position in the pygidia of *Hystricurus* (*Butuberculatus*) (see Stitt, 1983, pl. 4, fig. 6). This suggests that the condition shown in *Hystricurus* (*Butuberculatus*) is the ontogenetic and phylogenetic precursor of the pygidial fulcral ridge (Text-fig. V-5). The fulcral ridge is regarded as an evolutionary innovation acquired by these non-*Hystricurus* genera. This interrupted fulcral ridge is not common in the ptychopariide and proetide trilobites.

Another evolutionary innovation attained by these non-*Hystricurus* genera from *Hystricurus* is a different configuration of pleural and interpleural furrows. In *Hystricurus*, the pleural furrows are very deeply impressed and the interpleural furrows are shallow. The deeply-impressed pleural furrows are confluent with one another to define the pleural ribs (see Text-fig. V-6). The modified condition is found in many ptychopariides (e.g., *Aphelaspis*, see Text-fig. V-5) and some proetides (e.g., *Proetus*, Owen, 1973, pl. 5, fig. 4a). In these trilobites, either only the anterior-most pleural furrow is recognizable or the subsequent pleural furrows are not confluent with one another. However, their pleural furrows are much more deeply incised and, in many cases, longer compared with the interpleural furrows, thus indicating the presence of the pleural ribs. By contrast, *Spinohystricurus* has pleural furrows that fall short of the fulcral ridge and interpleural furrows that extend beyond the ridge (Text-fig. V-6). This condition is likely

569

to be derived from *Hystricurus* and thus, from the ptychopariides. The same configuration of pleural and interpleural furrows occurs in a few proetide trilobites such as dimeropygids (e.g., *Dimeropyge*, Chatterton, 1994, fig. 6.22) and telephinids (e.g., *Carolinites*, McCormick and Fortey, 1999, fig. 3.24).

At the same topographic location where these non-*Hystricurus* genera develop the interrupted fulcral ridge, the taxa that are excluded from the Hystricuridae develop a row of slender spines (e.g., *Pseudohystricurus*, Pl. III-77, Fig. 8), an uninterrupted continuous ridge (e.g., *Psalikilus*, Pl. III-69, Fig. 6), or show a rapid change of slope from the inner to the outer pleural field (e.g., *Eurylimbatus*, Pl. III-40, Fig. 3). It is yet to be determined whether these structures are homologous with the pygidial fulcral ridge of the non-*Hystricurus* genera. For example, the smaller pygidia of *Psalikilus* have the same uninterrupted fulcral ridge as the larger pygidia (Pl. III-69, Fig. 19), indicating that the uninterrupted condition would have been retained throughout its ontogeny. Each of these structures is found in a few ptychopariide trilobites. For example, the row of spines along the edge are seen in *Heterocaryon* (an entomaspidid, Ludvigsen, 1982, figs. 55I-K, M, N), the uninterrupted continuous ridge in *Euptychaspis* (a ptychaspidine, Westrop, 1995, pl. 7, fig. 21; Ludvigsen, 1982, figs. 58S-U), and the rapid change of slope from inner to outer pleural field in *Holmdalia* (a marjumiid, Robison, 1988, figs. 27.5a, 27.5b). They are also observed in some proetide trilobites. The row of short spines is seen in *Dimeropygiella* (Pl. III-51, Fig. 4), the uninterrupted ridge in *Chomatopyge* (Whittington, 1953b, pl. 5, fig. 7), and the rapid change of slope in *Paratoernquistia* (Chatterton *et al.*, 1998, figs. 7.10, 7.12, 7.13, 7.15). This implies that each non-hystricurid taxon could have attained each of these features from a different Cambrian ptychopariide taxon and carried over into a different proetide taxon, indicating the evolutionary heterogeneity of the non-hystricurids.

Pygidial morphologies suggest that 1) the Hystricuridae would be monophyletic since the variations observed in the pygidial features are traced down into *Hystricurus* (*Aequituberculatus*), 2) *Hystricurus* is paraphyletic and *Hystricurus* (*Aequituberculatus*) and *Hystricurus* (*Butuberculatus*) are also paraphyletic; the concept of the genus *Hystricurus* may be restricted to *Hystricurus* (*Hystricurus*), 3) non-*Hystricurus* genera possessing the fulcral ridge and the pleural ribe represent an evolutionary dead end that is separated from non-*Hystricurus* genera possessing pygidia similar to *Hystricurus*, suggesting the existence of more than one lineage of non-*Hystricurus* genera, 4) the Proetida is heterogeneous, containing at least two lineages; one contains most of the proetide families that show the presence of pleural ribs, and the other contains a few proetide families such as the Dimeropygidae, and does not have pleural ribs, and 5) many taxa that are excluded from the Hystricuridae have different ptychopariide origins and gave rise to different proetide taxa, further supporting the evolutionary heterogeneity (paraphyly and polyphyly) of the Proetida.

Protaspid features. Chatterton *et al.* (1999) classified the proetide protaspides into three morphotypes; Type A and B are anaprotaspides, a protaspid stage before the differentiation of protopygidium, and Type C is a metaprotaspis that develops a furrow delineating the protopygidium from the cranidium. The protaspides known for the "hystricurids" belong to the Type C. *Hystricurus, Spinohystricurus, Amblycranium*, and *Paratersella* are the genera for which the protaspides are known; earlier protaspides of *Paratersella* (Pl. III-65, Fig. 6) belong to the Type B. No Type A and B protaspides are

570

known for the other genera. These protaspides clearly develop the preglabellar field which is interpreted as a distinctive synapomorphy of the Proetida by Fortey (1990).

Most of the ptychopariid protaspides described in Chapter II do not have the preglabellar field (see Text-fig. V-1 to V-4). However, its absence is ambiguous in some species of the superfamily B. For example, in the metaprotaspis of *Crepicephalus deadwoodiensis* (Pl. II-14, Fig. 22), the area in front of glabella, although much shorter (sag.) than in the Type C protaspides, bears no furrow or border-like structure. Thus, it cannot be claimed whether the metaprotaspis has a preglabellar field or not. Of the species of the superfamily B to which *C. deadwoodiensis* is assigned, the metaprotaspides of *Syspacheilus dunoirensis* (Pl. II-15, Figs. 9, 11) and *Nixonella montanensis* (Pl. II-16, Figs. 4, 6) have an anterior border that meets the glabellar front without any preglabellar field.

The presence of a preglabellar field is ambiguous even in the proetide anaprotaspides (Chatterton et al., 1999, figs. 1.1-1.11) which do not develop any feature in front of anterior pits. Anaprotaspides of some ptychopariide species exhibit the same condition in which the anterior pits are the only discernible feature (see, Pl. II-14, Fig. 6, Pl. II-16, Fig. 1). Most of the hystricurids and ptychopariides develop the preglabellar field during their ontogenies. Therefore, the difference only lies in the timing of its development; the proetides develop in the protaspid period and the ptychopariides do so later in ontogeny.

Another protaspid synapomorphy of the Proetida listed by Fortey (1990) was the forward-tapering glabella under the assumption that most ptychopariide protaspides have a forward-expanding glabella. A re-examination in Chapter II reveals that many ptychopariide protaspides have the forward-tapering glabella. The most noticeable are those classified under the superfamily C (see Text-fig. V-3). The glabellar front of many of these ptychopariides is not delineated by axial furrows, whereas that of proetide protaspides is well delimited by axial furrows. The closest condition is found in the metaprotaspides of *Crepicephalus deadwoodiensis* (Text-fig. V-2). Remarkably, these protaspides develop three pairs of tubercles alongside the glabella and paired tubercles along the glabellar crest, which are observed in the protaspides of *Hystricurus* and many other Type C metaprotaspides. This indicates that the forward-tapering glabella may not be an evolutionary novelty of the Proetida, since it is found in many ptychopariide protaspides.

Of Type C metaprotaspides which have been considered to diagnose the Proetida (Fortey, 1990), those of *Stenoblepharum astinii* (Edgecombe et al., 1997, figs. 4.1-4.4) are similar to those of *Syspacheilus* (Pl. II-15, Figs. 9, 13) and *Nixonella* (Pl. II-16, Figs. 4, 8, 11) representing the protaspid morphotype B. They share a smooth shield, a parallel-sided L3/L2/L1, the presence of a protopygidial marginal border, a relatively large protopygidium, and the presence of an anterior border. The metaprotaspides of a group characterized by morphotype B differ in having a narrow (sag.) anterior border and protopygidial marginal border, no preglabellar field, and a slightly forward-expanding glabella. The similarities can be extended into many proetide genera such as *Scharyia* (a scharyiid, Chatterton and Speyer, 1997, fig. 180.10), *Licnocephala* (a bathyurid, Lee and Chatterton, 1997b, fig. 6.2), and *Songkania* (an aulacopleurid, Adrain and Chatterton, 1995, figs. 7.11, 7.12). The anaprotaspides of morphotype B such as those of *Crepicephalus deadwoodiensis* (Pl. II-14, Fig. 6) and *Nixonella montanensis* (Pl. II-16, Fig. 1) are also similar to those of Type A proetide protaspides, in having a subovoid

571

shield without any discernible features other than anterior pits.

Two different subordinated protaspid morphotypes are recognized in the morphotype B; a tuberculated one represented by *Crepicephalus* and a non-tuberculated one by *Syspacheilus*. (Text-fig. V-7). These two morphotypes appear to have continued in the "hystricurids" and are carried over into Type C metaprotaspides. The protaspides of *Hystricurus* and *Spinohystricurus* are very similar to those of dimeropygids, telephinids, toernquistiids, and aulacopleurids (Chatterton *et al.*, 1999, figs. 1.25, 9.2), in sharing the three large tubercles alongside the glabella. A remarkable similarity is also found with the protaspides of *Amblycranium* which is excluded from the Hystricuridae because of its spinose pygidium. The protaspides of *Paratersella* are similar to those of the bathyurids, tropidodcoryphids, and scharyiids, in lacking tuberculation. This implies the existence of more than one lineage within the Proetida, as suggested by Bergström (1977).

Since *Crepicephalus* and *Syspacheilus* of the morphotype B occur in the *Crepicephalus* or *Cedaria* Zone of the Marjuman Stage, the lowermost stage of the Upper Cambrian, the ancestry of the Proetida must predate the early Upper Cambrian, which supports Edgecombe's (1992) suggestion. Of the species possessing the protaspid morphotype B, *Glyphaspis paucisulcata* is Middle Cambrian in age. Its metaprotaspides (Pl. II-13, Figs. 4, 8) only differ from those of the Upper Cambrian species in having no anterior border and a more strongly forward-expanding L4. It seems that this species has metaprotaspid morphologies from which those of *Syspacheilus dunoirensis* (Pl. II-15, Fig. 9) were derived. The morphologic transformations include the appearance of an anterior border and transverse narrowing of L4. Subsequently, the metaprotaspid morphologies of *S. dunoirensis* appear to be transformed into those of *Crepicephalus deadwoodiensis* (Plate II-14, Figure 22), in association with the development of tubercles alongside the glabella and possibly a preglabellar field, and a forward-tapering of L4. Therefore, it can be presumed that non-tuberculated proetide protaspides such as *Paratersella* and *Stenoblepharum* would have been derived from those of *S. dunoirensis* and the tuberculated ones such as *Hystricurus* from those of *Crepicephalus deadwoodiensis* (Text-fig. V-7). As implied by Lee and Chatterton (1997a), non-tuberculated ones appear to have preceded tuberculated protaspides.

If this scenario is the case, the ancestries of the Proetida and Asaphida would lie in the same taxon, the family Anomocaridae to which *Glyphaspis* is assigned (see Fortey and Chatterton, 1988, text-fig. 27). However, Fortey and Chatterton (1988) noted that the classification of the Anomocaracea is artificial (see text-fig. 27), implying that the further detailed analysis will segregate the group into smaller groups which might be ancestral to other taxa. The hypothesis that *Glyphaspis* is ancestral to the Proetida supports that the Anomocaracea, and even Anomocaridae is an unnatural group. The hypothesis of the ancestry of the Proetida also suggests that the group represented by protaspid morphotype B is paraphyletic, since it does not include all the descendants.

Cranidial and other features. Many authors who have proposed the taxonomic status of the "hystricurids" have noticed the cranidia of the "hystricurids" are similar to those of some ptychopariides. Several authors noticed the cranidial similarities of *Hystricurus* with solenopleuracean genera such as *Solenopleura* and *Onchopeltis*. In this study, it is acknowledged that species questionably assigned to *Hystricurus* such as *Hystricurus*? *millardensis* and *Hystricurus*? *armatus* have cranidia that are remarkably similar to the Upper Cambrian aphelaspidines and elviniids. The cranidial morphologies of these

572

species could be intermediate between Cambrian taxa and *Hystricurus*. It is true that cranidial morphologies of the hystricurids are within the range of variation of the general 'ptychopariid morphology.' Thus, it is not difficult to find a ptychopariid species which can be evolutionarily connected with the hystricurids on the basis of cranidial morphology. Of the non-hystricurid proetides, the aulacopleurids approximate hystricurid cranidial morphologies, except for the S1 that is long and confluent with axial furrows and occipital furrow.

A few articulated specimens of *Spinohystricurus* and *Glabellosulcatus* are found with the hypostome attached. These hypostomes are no different from those showing the natant condition (see Fortey, 1990, text-fig. 11). The hypostomal features of the Hystricuridae are considered to be of little value for understanding its systematic relationships to the Proetida and Ptychopariida.

There are conflicts among evolutionary suggestions on the basis of different exoskeletal parts and different ontogenetic stages. The suggestions made above will serve as a guide as to which taxa and characters will be selected for future analyses.

TEXT-FIGURE V-1. Reconstructions of protaspides described in the Chapter II that are considered to be related to the Corynexochida. All reconstructions are x 100.

1. Anaprotaspis of *Ptarmigania aurita* Resser, 1939.
2. Metaprotaspis of *Ptarmigania aurita* Resser, 1939.
3. Anaprotaspis of *Leiostegium formosa* Hintze, 1953.
4. Metaprotaspis of *Leiostegium formosa* Hintze, 1953.
5. Anaprotaspis of *Blountia bristolensis* Resser, 1938a.
6. Metaprotaspis of *Blountia bristolensis* Resser, 1938a.
7. Metaprotaspis of *Missisquoia cyclochila* Hu, 1971.

575
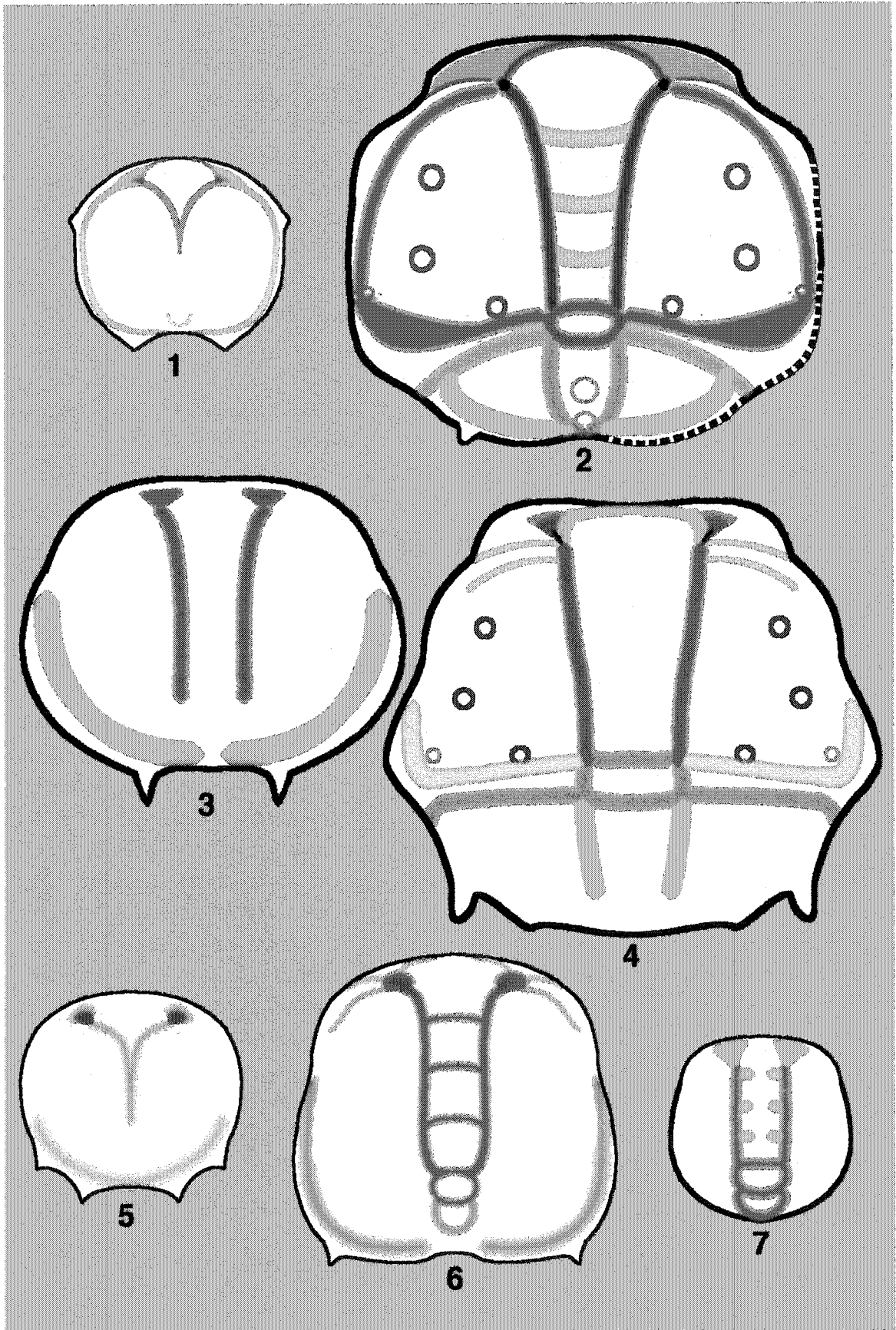
TEXT-FIGURE V-2. Reconstructions of protaspides of morphotype "A" and "B" described in the Chapter II. All reconstructions are x 100.

1. Metaprotaspis of **Catillicephalidae** sp. A. (A)
2. Metaprotaspis of *Komaspidella laevis* Rasetti, 1961 (A)
3. Metaprotaspis of *Glaphyraspis parva* (Walcott, 1899) (A)
4. Metaprotaspis of *Bolaspidella housensis* (Walcott, 1886) (B)
5. Metaprotaspis of *Cedarina cordillerae* (Howell and Duncan, 1939) (B)
6. Metaprotaspis of *Apomodocia conica* Hu, 1971 (B)
7. Metaprotaspis of *Nixonella montanensis* Lochman *in* Lochman and Duncan, 1944 (B)
8. Metaprotaspis of *Syspacheilus dunoirensis* (Miller, 1936) (B)
9. Metaprotaspis of *Glyphaspis paucisulcata* Deiss, 1939 (B)
10. Metaprotaspis of *Crepicephalus deadwoodiensis* Hu, 1971 (B)
11. Metaprotaspis of *Modocia laevinucha* Robison, 1964 (B)

577
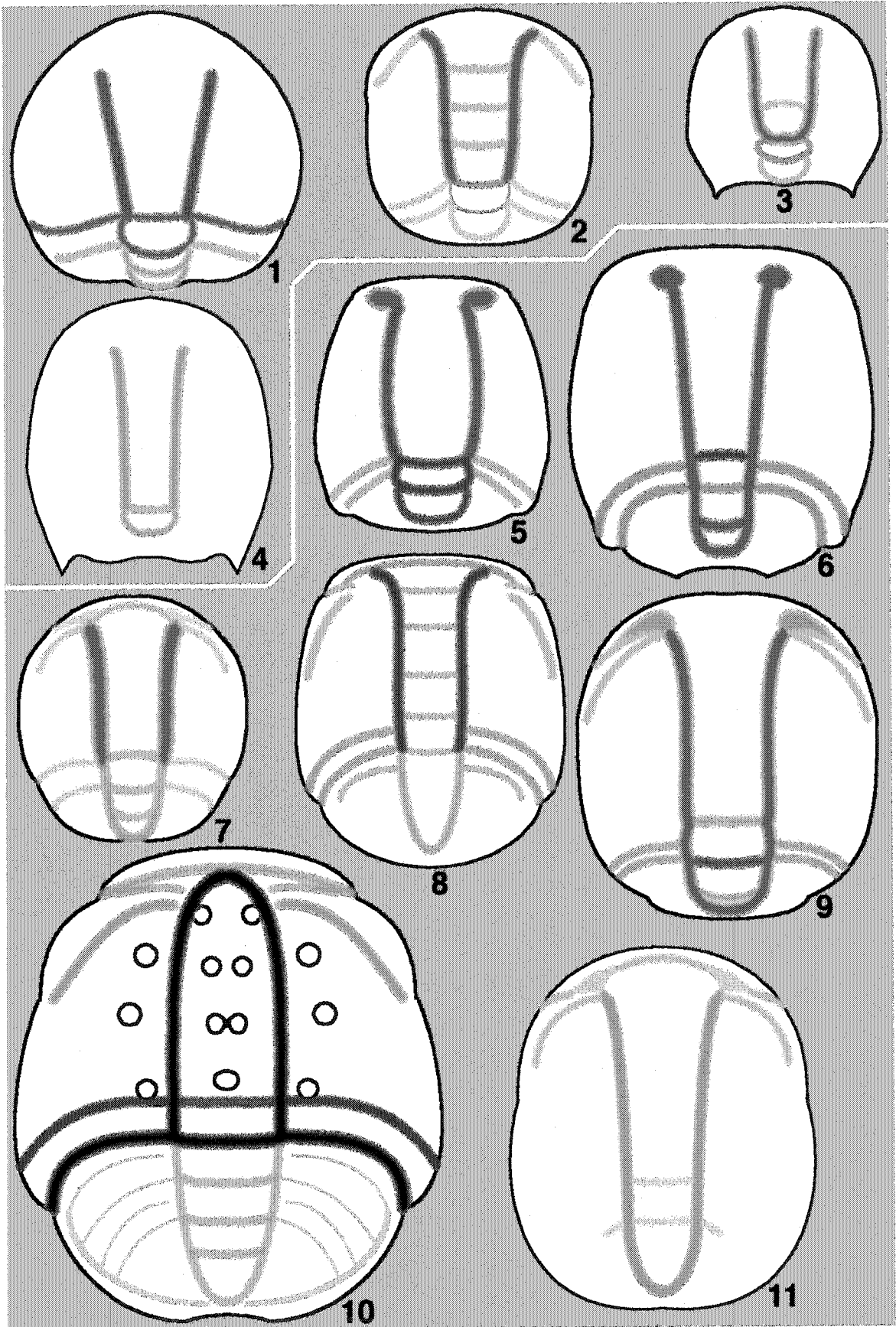
TEXT-FIGURE V-3. Reconstructions of protaspides of morphotype "C" described in the Chapter II. All reconstructions are x 100.

1. Metaprotaspis of *Aphelotoxon triangulata* Hu, 1980
2. Metaprotaspis of *Arapahoia arbucklensis* (Stitt, 1971)
3. Metaprotaspis of *Drabia typica* (Hu, 1979)
4. Metaprotaspis of *Paranumia triangularia* Hu, 1973
5. Metaprotaspis of *Pulchricapitus davisi* Kurtz, 1975
6. Metaprotaspis of *Ponumia obscura* (Lochman, 1964)
7. Metaprotaspis of *Norwoodella halli* Resser, 1938a
8. Metaprotaspis of *Housia ovata* Palmer, 1965

579
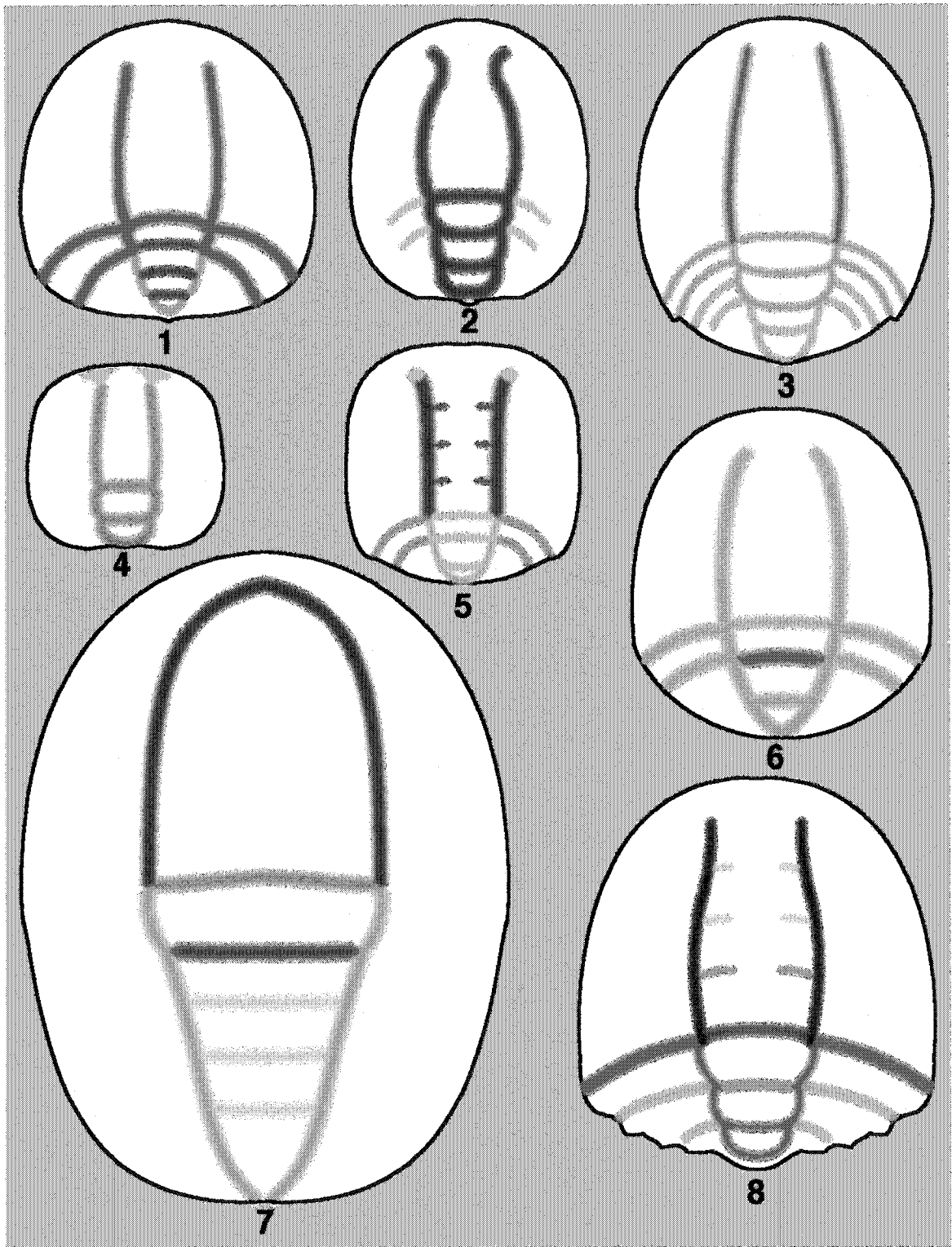
TEXT-FIGURE V-4. Reconstructions of protaspides of Dikelocephalacea, Olenacea, and morphotype "D," "E," and "F" described in the Chapter II. All reconstructions are x 100.

1. Metaprotaspis of *Orygmaspis* (*Parabolinoides*) *contractus* (Frederickson, 1949) (D)
2. Metaprotaspis of *Taenicephalus shumardi* (Hall, 1863) (D)
3. Metaprotaspis of *Ptychaspis bullasa* Lochman and Hu, 1959 (Dikelocephalacea)
4. Metaprotaspis of *Aphelaspis*? *anyta* (Hall and Whitfield, 1877) (E)
5. Metaprotaspis of *Aphelaspis haguei* (Hall and Whitfield, 1877) (E)
6. Metaprotaspis of *Elvinia roemeri* (Shumard, 1861) (F)
7. Metaprotaspis of *Aphelaspis brachyphasis* Palmer, 1962 (E)
8. Metaprotaspis of *Dytremacephalus granulosus* Palmer, 1954b (E)
9. Metaprotaspis of *Acerocare ecorne* Angelin, 1878 (Olenacea)
10. Metaprotaspis of *Apoplanias rejectus* Lochman, 1964 (Olenacea)
11. Metaprotaspis of *Olenus gibbosus* (Wahlenberg, 1821) (Olenacea)

581

non-"hystricurid" proetide
(e.g., aulacopleurids)

Stratigraphically younger
non-*Hystricurus* genera
(e.g., *Spinohystricurus*)

Hystricurus
(*Hystricurus*)

Hystricurus
(*Triangulocaudatus*)

Hystricurus
(*Aequituberculatus*)

Hystricurus
(*Butuberculatus*)
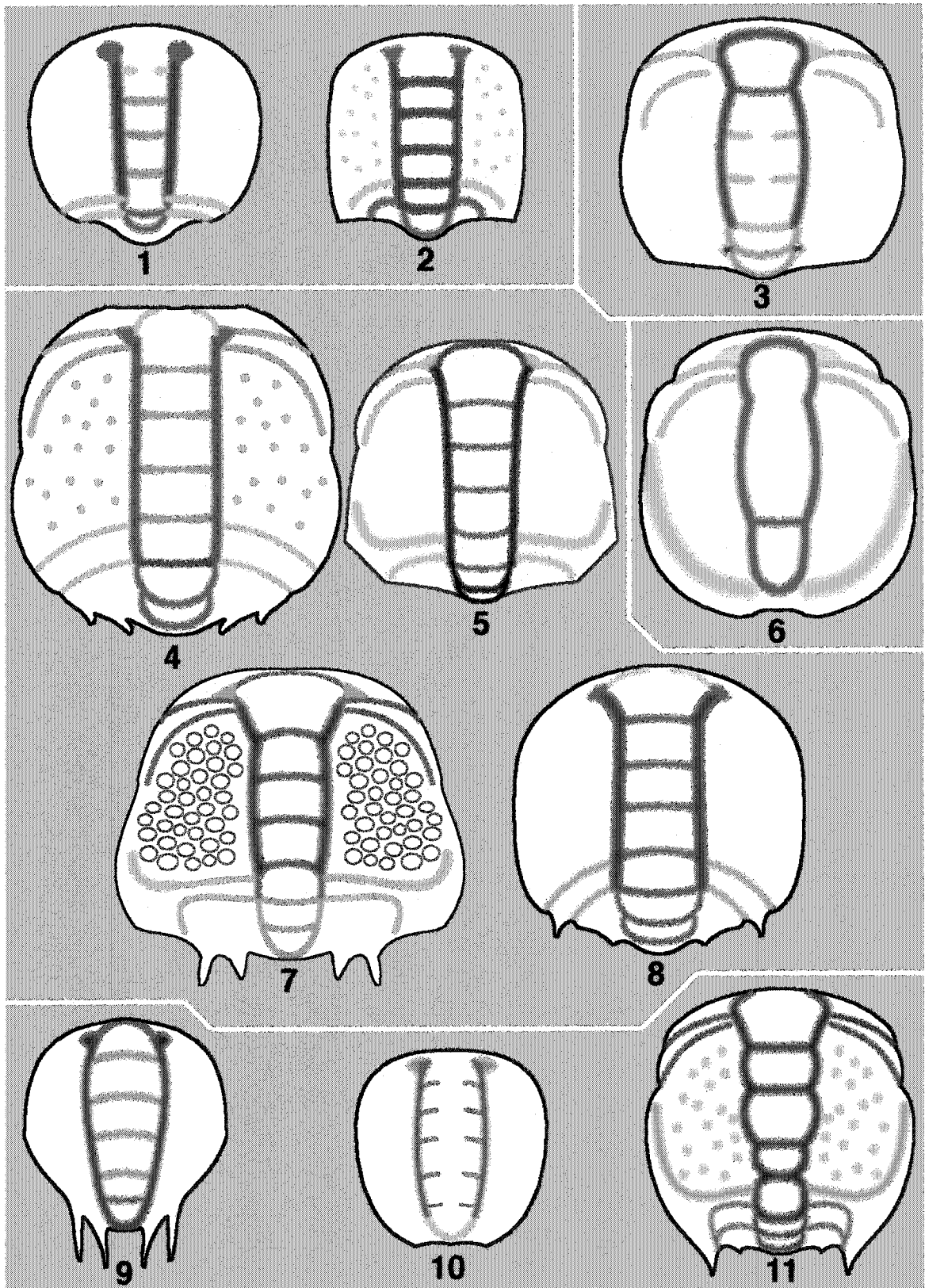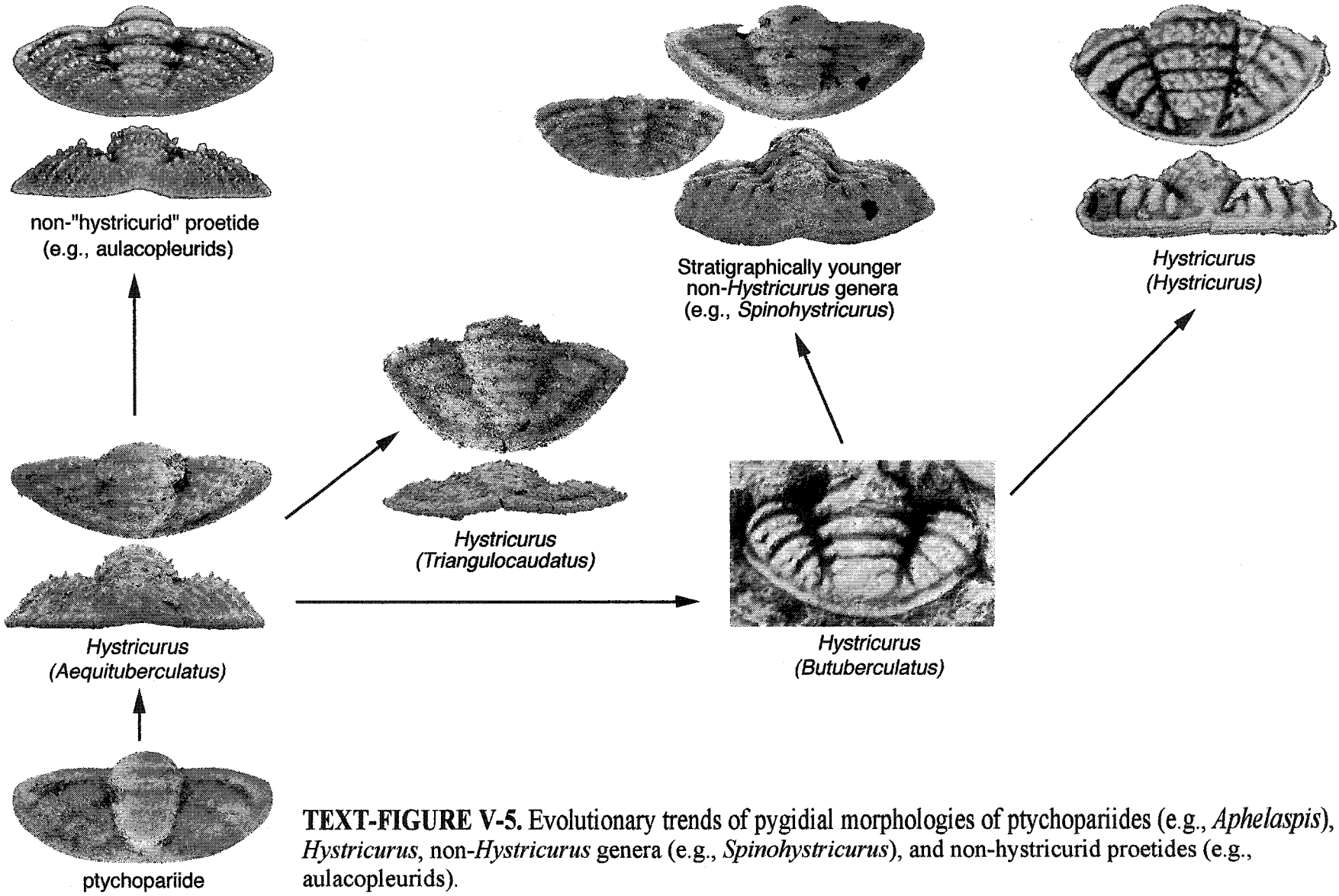
ptychopariide

TEXT-FIGURE V-5. Evolutionary trends of pygidial morphologies of ptychopariides (e.g., *Aphelaspis*), *Hystricurus*, non-*Hystricurus* genera (e.g., *Spinohystricurus*), and non-hystricurid proetides (e.g., aulacopleurids).
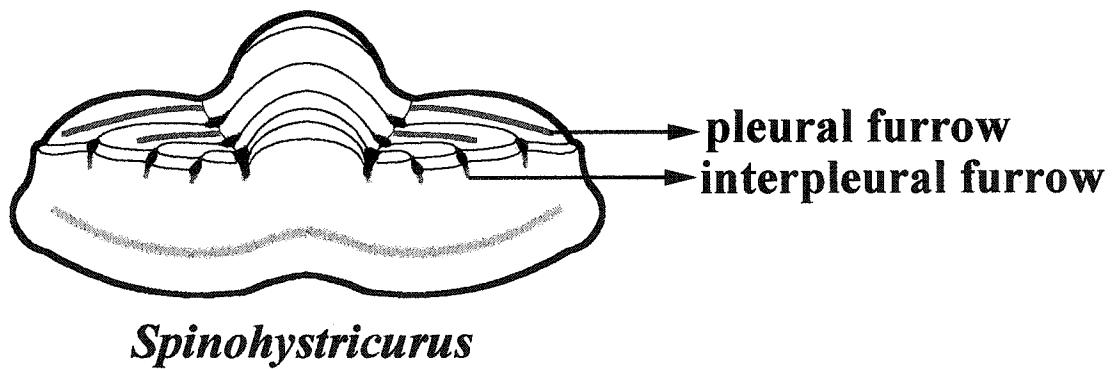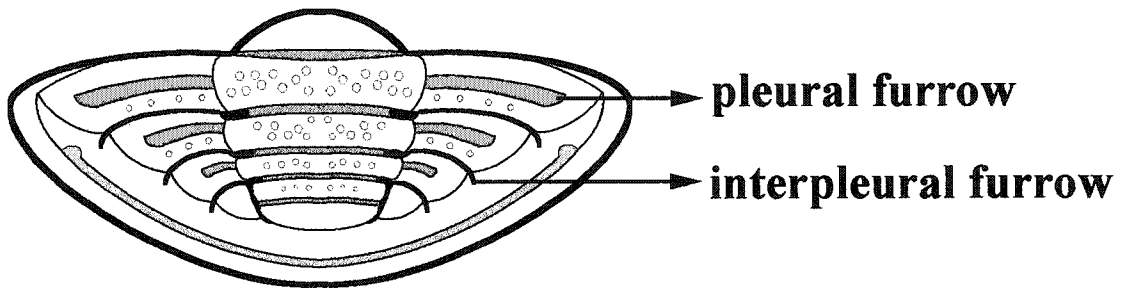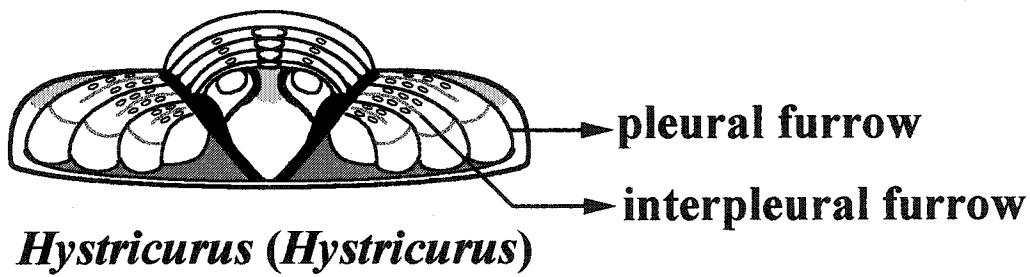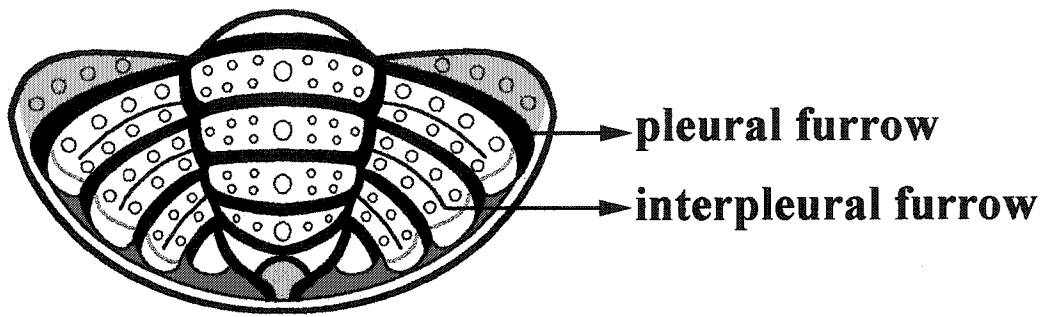
TEXT-FIGURE V-6. Different configuration of pleural and interpleural furrows between *Hystricurus* (e.g., *Hystricurus* (*Hystricurus*)) and non-*Hystricurus* genera (e.g., *Spinohystricurus*).

583
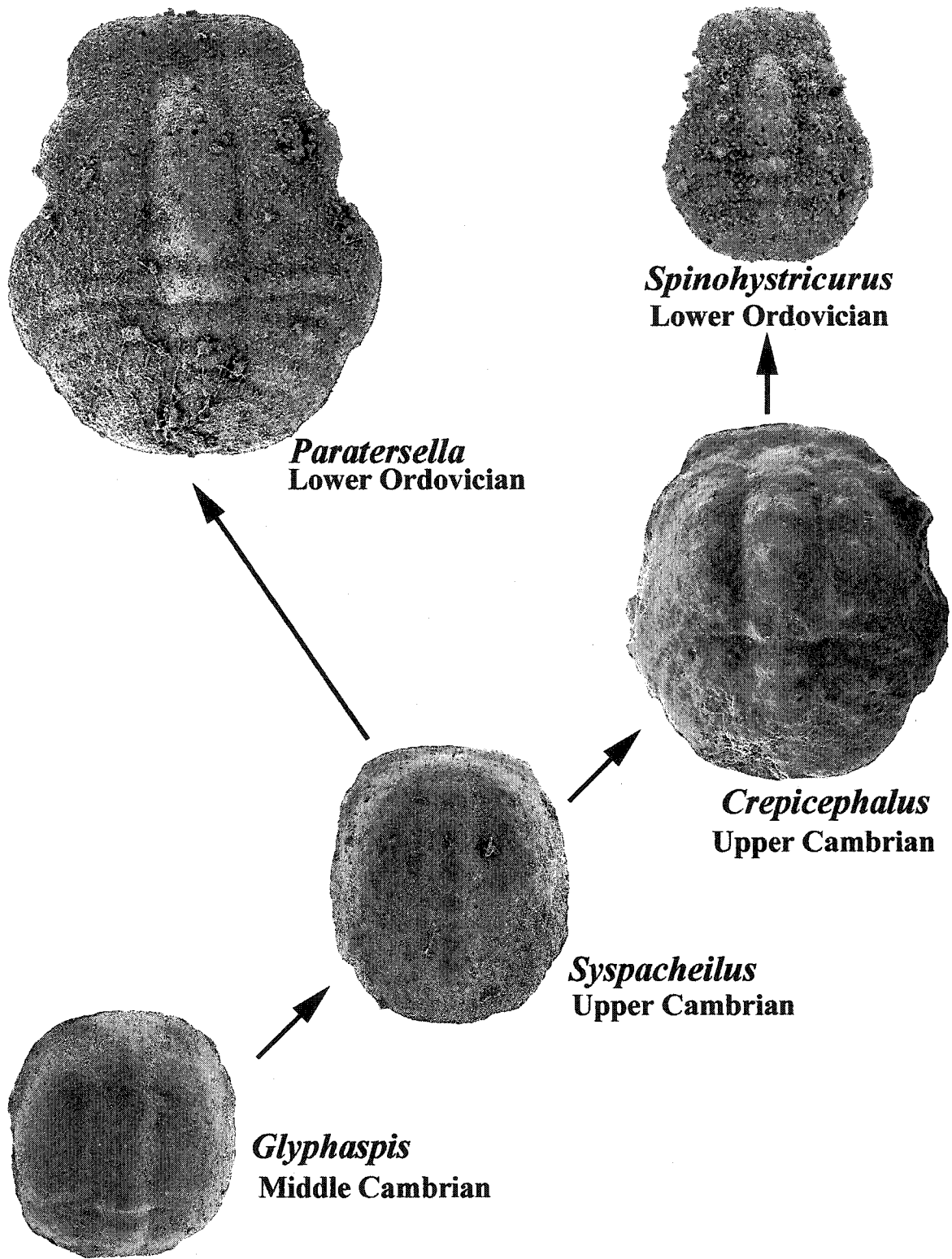
TEXT-FIGURE V-7. A hypothesis of evolutionary relationships of the Lower Ordovician "hystricurids" and the ptychopariide superfamily B on the basis of protaspid morphologies.

584

CHAPTER VI

BIBLIOGRAPHY

Adrain, J. M. and Chatterton, B. D. E. 1994. The aulacopleurid trilobite *Otarion*, with new species from the Silurian of northwestern Canada. Journal of Paleontology, v. 68(2), P. 305-323.

Adrain, J. M. and Chatterton, B. D. E. 1995a. Aulacopleurine trilobites from the Llandovery of northwestern Canada. Journal of Paleontology, v. 69(2), p. 326-340.

Adrain, J. M. and Chatterton, B. D. E. 1995b. The otarionine trilobites *Harpidella* and *Maurotarion*, with species from northwestern Canada, the United States, and Australia. Journal of Paleontology, v. 69(2), p. 307-326.

Adrain, J. M. and Chatterton, B. D. E. 1996. The otarionine trilobite *Cyphaspis*, with new species from the Silurian of northwestern Canada. Journal of Paleontology, v. 70(1), p. 100-110.

Adrain, J. M, Fortey, R. A., and Westrop, S. R. 1998. Post-Cambrian trilobite diversity and evolutionary faunas. Science, v. 280, p. 1922-1925.

Adrain, J. M., Westrop, S. R., Landing E., and Fortey, R. A. 2001. Systematics of the Ordovician trilobites Ischyrotoma and Dimeropygiella, with species from the type Ibexian area, western U.S.A. Journal of Paleontology, v. 75, p. 947-971.

Alberch, P. 1985. Problems with the interpretation of developmental sequences. Systematic Zoology, v. 34(1), p. 46-58.

Angelin, N. P. 1854. Palaeontologia Scandinavica. Pars 1. Crustacea Formationis Transitionis, p. 21-92.

Angelin, N. P. 1878. Palaeontologia Scandinavica. Pars 1. Crustacea Formationis Transitionis, Norstedt and Söner. Stockholm, 96 p.

585

Apollonov, M. K. and Chugaeva, M. N. 1983. Some trilobites from the Cambrian and Ordovician boudnary deposits of Batyrbai Valley in Malyi Karatau. p. 66-90. *in* Apollonov, M. K., Bandaletov, C. M., and Ivshin, H. K. (eds.). The Lower Palaeozoic Stratigraphy and Palaeontology of Kazakhstan. Alma-Ata (Nauka Kazakh SSR Publishing House) [In Russian].

Apollonov, M. K., Chugaeva, M. N., Dubinina, S. V., Zhemchuzhnikov, V. G. 1988. Batyrbay section, south Kazakhstan, U.S.S.R.—potential stratotype for the Cambrian-Ordovician boundary. Geological Magazine, v.125(4), p. 445-449 [In Russian].

Arthur, W. 1988. A Theory of the Evolution of Development. John Wiley and Sons, Chichester and New York. 94 p.

Babcock, L. E. 1994. Systematics and phylogenetics of polymerid trilobites from the Henson Gletscher and Kap Stanton formations (Middle Cambrian), North Greenland. Bulletin of Grønlands Geologiske Undersøgelse, v. 169, p. 79-127.

Balashova, E. A. 1961. Some Tremadocian trilobites Aktyubinsk district. Trudy Geologicheskii Institut Akademia nauk SSSR, no. 18, p. 102-145. [In Russian].

Banks, M. R. and Burrett C. F. 1980. A preliminary Ordovician biostratigraphy of Tasmania. Journal of the Geological Society of Australia, v. 26, p. 363-376.

Beecher, C. E. 1893. A larval form of *Triarthrus*. American Journal of Science (series 3), v. 46, p. 361-362.

Beecher, C. E. 1895. The larval stages of trilobites. The American Geologist, v. 16, p. 166-197.

Bell, W. C. and Ellinwood, H. L. 1962. Upper Franconian and Lower Trempealeauan Cambrian trilobites and brachiopods, Wilberns Formation, Central Texas. Journal of Paleontology, v. 36(3), p. 385-423.

Bell, W. C., Feniak, O. W., and Kurtz, V. E. 1952. Trilobites of the Franconia Formation, southeast Minnesota. Journal of Paleontology, v. 26(1), p. 175-198.

586

Benedetto, J. L. 1977. Una nueva fauna de trilobites Tremadocianos de la Provincia de Jujuy (Sierra de Cajas), Argentina. Ameghiniana, Revista de la Asociación Paleontológica Argentina, v. 14(1), p. 186-214. [In Spanish].

Berg, R. T. 1953. Franconian trilobites from Minnesota and Wisconsin. Journal of Paleontology, v. 27(4), p. 553-568.

Berg, R. R. and Ross, R. J. Jr. 1959. Trilobites from the Peerless and Manitou Formations, Colorado. Journal of Paleontology, v. 33(1), p. 106-119.

Bergström, J. 1977. Proetida—a disorderly order of trilobites. Lethaia, v. 10, p. 95-105.

Billings, E. 1859. Fossils of the Calciferous sandrock, including those of a white limestone at Mingan supposed to belong to the formation. Canadian Naturalist and Zoologist, v. 4, p. 345-367.

Billings, E. 1860. On some new species of fossils from the limestone near Point Levis opposite Quebec. Canadian Naturalist, v. 5, p. 301-324.

Blaker, M. R. and Peel, J. S. 1997. Lower Cambrian trilobites from North Greenland. Meddelelser om Grønland, Geoscience, no. 35, 145 p.

Boyce, W. D. 1983. Early Ordovician trilobite faunas of the Boat Harbour and Catoche Formations (St. George Group) in the Boat Harbour-Cape Norman area, western Newfoundland. Unpublished M.Sc. thesis, Memorial University of Newfoundland, 272 p.

Boyce, W. D. 1989. Early Ordovician trilobite faunas of the Boat harbour and Catoche Formations (St. George Group) in the Boat Harbour-Cape Norman area, Great Northern Peninsula, western Newfoundland. Geological Survey Branch, Department of Mines and Energy, Government of Newfoundland and Labrador, Report 89-2, 168 p.

Boyce, W. D. 1997. Early to middle Ordovician trilobite-based biostratigrapic zonation of the autochthon and parautochthon, western Newfoundland. Second International Trilobite Conference Abstracts with program, p. 10.

Boyce, W. D. and Stouge, S. 1997. Trilobite and conodont biostratigraphy of the St. George Group, Eddies Cove West Area, western Newfoundland. Current Research, Newfoundland Department of Mines and Energy, Geological Survey Report, v. 97-1, p. 183-200.

Bradley, J. H. 1925. Trilobites of the Beekmantown in the Philipsburg region of Quebec. Canadian Field Naturalists, v. 39, p. 5-9.

Bridge, J. 1930. Geology of the Eminence and Cardareva quadrangles. Missouri Bureau of Geology and Mines, 2nd series, v. 24, 228 p.

Bridge, J. and Cloud, P. E. Jr. 1947. New gastropods and trilobites critical in the correlation of Lower Ordovician rocks. American Journal of Science, v. 245, p. 545-559.

Brögger, W. C. 1886. Ueber die Ausbildung des Hypostomes bei einigen skandinavischen Asaphiden . Geologiska Föreningens i Stockholm Förhandlingar, v. 8, p. 212.

Brusca, R. C. and Brusca, G. J. 1990. Invertebrates. Sinauer Associates, Sunderland, Massachusetts. 922 p.

Bull, J. J., Huelsenbeck, J. P., Cunningham, C. W., Swofford, D. L., and Waddell, P. J. 1993. Partitioning and combining data in phylogenetic analysis. Systematic Biology, v. 42(3), p. 384-397.

Burmeister, H. 1843. Die Organization der Trilobiten aus ihren lebenden Verwandten entwickelt; nebst einer systematischen Uebersicht aller ziether beschriebenen Arten. Berlin, 148 p.

Burskyi, A. Z. 1970. Early Ordovician trilobites of Northern Pak-Khoya, *in* Bondarev, V. I. (ed.). Key sections of Ordovician deposits in Pai-Khoya Mountains, Vaigach Island, and S. Novaya Zemlya Island. Scientific Research Institute of Arctic Geology, USSR Ministry of Geology, p. 96-138. [In Russian].

Chatterton, B. D. E. 1980. Ontogenetic studies of Middle Ordovician trilobites from the Esbataottine Formation, Mackenzie Mountains, Canada. Palaeontographica Abteilung A, no. 171, 74 p.

Chatterton, B. D. E. 1994 Ordovician proetide trilobite *Dimeropyge*, with a new species from northwestern Canada. Journal of Paleontology, v. 68(3), p. 541-556.

Chatterton, B. D. E., Edgecombe, G. D., Vaccari, N. E., and Waisfeld, B. G. 1999. Ontogenies of some Ordovician Telephinidae from Argentina, and larval patterns in the Proetida (Trilobita). Journal of Paleontology, v. 73(2), p. 219-239.

Chatterton, B. D. E., Edgecombe, G. D., Waisfeld, B. G., and Vaccari, N. E. 1998. Ontogeny and systematics of Toernquistiidae (Trilobita, Proetida) from the Ordovician of the Argentine Precordillera. Journal of Paleontology, v. 72(2), p. 273-303.

Chatterton, B. D. E., Siveter, D. J., Edgecombe, G. D., and Hunt, A. S. 1990. Larvae and relationships of the Calymenina (Trilobita). Journal of Paleontology, v. 64(2), p. 255-277.

Choi, D. K., Park, G.-H., and Kim, D. H. 1994. Tremadocian trilobites from the Mungog Formation, Yeongweol area, Korea. Journal of the Paleontological Society of Korea, v. 10(2), p. 209-226.

Christoffersen, M. L. 1995. Cladistic taxonomy, phylogenetic systematics, and evolutionary ranking. Systematic Biology, v. 44(3), p. 440-454.

Chugaeva, M. N. 1973. Trilobites, ostracods, brachiopods, and conodonts from the lower part of the Ordovician, Elgenchakskikh Mountains. p. 43-222. *in* Chugaeva, M. N., Ivanova, V. A., Oradovskaya, M. M., and Yakovlev, V. N. (compl.), Biostratigraphy of the lower part of the Ordovician in the north-east of the USSR and biogeography of the uppermost Lower Ordovician. Publishing Office, Nauka, Moscow. [In Russian].

Clark, T. H. 1924. The paleontology of the Beekmantown Series at Lévis, Quebec. Bulletins of American Paleontology, v. 10 (41), 134 p.

589

Clarkson, E. N. K. and Taylor, C. M. 1995. Ontogeny of the trilobite *Olenus wahlenbergi* Westergård, 1922 from the Upper Cambrian Alum Shales of Andrarum, Skåne, Sweden. Transactions of the Royal Society of Edinburgh, Earth Sciences, v. 86, p. 13-34.

Clarkson, E. N. K., Taylor, C. M., and Ahlberg, P. 1997. Ontogeny of the trilobite *Parabolina spinulosa* (Wahlenberg, 1818) from the Upper Cambrian Alum Shales of Sweden. Transactions of the Royal Society of Edinburgh: Earth Science, v. 88, p. 69-89.

Cleland, H. F. 1900. The Calciferous of the Mohawk Valley. Bulletin of American Paleontology, v. 3, p. 1-26.

Cloud, P. E. Jr. and Barnes, V. E. 1948. The Ellenburger Group of central Texas. The University of Texas Publication, no. 4621, 460 p.

Cooper, G. A., Arellano, A. R. V., Johnson, J. H., Okulitch, V. J., Stoyanow, A., and Lochman, C. 1952. Cambrian stratigraphy and paleontology near Caborca, northwestern Sonora, Mexico. Smithsonian Miscellaneous Collections, v. 119, no. 1, 184 p.

Corbett, K. D. and Banks, M. R. 1974. Ordovician stratigraphy of the Florentine synclinorium, southwest Tasmania. Papers and Proceedings of the Royal Society of Tasmania, v. 107, p. 207-238.

Corda, A. J. C. 1847. *in* Hawle, I. and Corda, A. J. C. 1847. Prodrom einer Monographie der böhmischen Trilobiten. Abhandlungen der königlichen böhmischen Gesellschaft der Wissenschaften, Abhandlungen, no. 5, 176 p.

Cossman, M. 1902. Rectifications de nomenclature. Revue Critique de Paléozoologie, v. 6, p. 52.

Cullison, J. S. 1944. The stratigraphy of some Lower Ordovician formations of the Ozark Uplift. University of Missouri, School of Mines and Metallurgy, Technical Series Bulletin, v. 15(2), 112 p.

Dalman, J. W. 1827. Om Palaeaderna eller de så kallade Trilobiterna. Kungliga Svenska Vetenskapsakademiens Handlingar (1826), p. 113-152, 226-294.

Danser, B. H. 1950. A theory of systematics. Bibliotheca Biotheoretica, v. 4, p. 117-180.

Darwin, C. 1859. The origin of species, John Murray, London, 490 p.

Darwin, C. 1860. The origin of species, (2nd edition), John Murray, London, 666 p.

Dean, W. T. 1970. Lower Ordovician trilobites from the vicinity of South Catcher Pond, northeastern Newfoundland. Geological Survey of Canada, Paper, 70-44. 15 p.

Dean, W. T. 1977. The early Ordovician trilobite genus Missisquoia Shaw 1951 in the southern Canadian Rocky Mountains of Alberta and British Columbia. Geological Survey of Canada Paper, no. 76-33, 7 p.

Dean, W. T. 1982. Middle Cambrian trilobites from the Sosink Formation, Derik-Mardin district, south-eastern Turkey. Bulletin of British Museum of Natural History (Geology), v. 36(1), p. 1-41.

Dean, W. T. 1989. Trilobites from the Survey Peak, Outram and Skoki Formations (Upper Cambrian - Lower Ordovician) at Wilcox Pass, Jasper National Park, Alberta. Geological Survey of Canada, Bulletin, no. 389, 141 p.

Deiss, C. 1939. Cambrian stratigraphy and trilobites of northwestern Montana. Geological Society of America Special Paper, no. 18, 135 p.

Deland, C. R. and Shaw, A. B. 1956. Upper Cambrian trilobites from western Wyoming. Journal of Paleontology, v. 30(3), p. 542-562.

Demeter, E. J. 1973. Lower Ordovician pliomerid trilobites from western Utah. Brigham Young Univerisity Geology Studies, v. 20(4), p. 37-65.

de Pinna, M. C. C. 1991. Concepts and tests of homology in the cladistic paradigm. Cladistics, v. 7, p. 367-394.

de Queiroz, K. 1985. The ontogenetic method for determining character polarity and its relevance to phylogenetic systematics. Systematic Zoology, v. 34, p. 280-299.

Desbiens, S., Bolton, T. E., McCracken, A. D. 1996. Fauna of the lower Beauharnois Formation (Beekmantown Group, Lower Ordovician), Grande-île, Quebec. Canadian Journal of Earth Sciences, v. 33, p. 1132-1153.

Dwight, W. B. 1884. Recent explorations in the Wappinger Valley limestone of Duchess County, New York. American Journal of Science, series 3, v. 27, p. 156-167.

Edgecombe, G. D. Trilobite phylogeny and the Cambrian-Ordovician "event": cladistic reappraisal. p. 144-177. in Novacek M. J. and Wheeler Q. D. (eds.) Extinction and Phylogeny. Columbia University Press, New York.

Edgecombe, G. D., Chatterton, B. D. E., Vaccari, N. E., and Waisfeld, B. G. 1997. Ontogeny of the proetoid trilobite *Stenoblepharum*, and relationships of a new species from the Upper Ordovician of Argentina. Journal of Paleontology, v. 71(3), p. 419-433.

Endo, R. 1932. The Canadian and Ordovician formations and fossils of South Manchuria. United States National Museum Bulletin, no. 164.

Endo, R. 1935. Additional fossils from the Canadian and Ordovician rocks of the southern part of Manchoukuo. Scientific Report of Tohoku Imperial University, Geology, v. 16(4), p. 191-223.

Endo, R. 1937. Description of fossils. Bulletin of the Central National Museum of Manchoukuo, no. 1, p. 308-369.

Ergaliev, G. Kh. 1980. Middle and Upper Cambrian trilobites of the Malyi Karatau Range. Academy of Sciences of Kazakhstan SSR. K. I. Nauka Publicing House, Alma-Ata. 211p. [In Russian].

592

Etheridge, R. Jr. 1883. A description of the remains of trilobites from the Lower Silurian rocks of the Mersey River district, Tasmania. Papers and Proceedings of the Royal Society of Tasmania, v. 1882, p. 150-162.

Etheridge, R. Jr. 1919. The Cambrian trilobites of Australia and Tasmania. Transactions of the Royal Society of South Australia, v. 43, p. 373-393.

Evitt, W. R. 1961. Early ontogeny in the trilobite family Asaphidae. Journal of Paleontology, v. 35, p. 986-995.

Fisher, D. W. 1954. Lower Ordovician (Canadian) stratigraphy of the Mohawk Valley, New York. Bulletin of the Geological Society of America, v. 65, p. 71-96.

Flower, R. H. 1964. The nautiloid order Ellesmeroceratida (Cephalopoda). New Mexico Bureau of Mines and Mineral Resources, Memoir, n. 12, 234 p.

Flower, R. H. 1969. Fossils from the Fort Ann Formation. New Mexico Bureau of Mines and Mineral Resources, Memoir, no. 22, p. 29-34.

Flower, R. H. 1978. St. George and Table Head cephalopod zonation in western Newfoundland. Current Research, Part A, Geological Survey of Canada Paper 78-1A, p. 217-224.

Fortey, R. A. 1974. The Ordovician trilobites of Spitsbergen I. Olenidae. Norsk Polarinstitutt Skrifter, n. 160, 128 p.

Fortey, R. A. 1975. The Ordovician trilobites of Spitsbergen II. Asaphidae, Nileidae, Raphiophoridae and Telephinidae of the Valhallfonna Formation. Norsk Polarinstitutt Skrifter, n. 162, 125 p.

Fortey, R. A. 1979. Early Ordovician trilobites from the Catoche Formation (St. George Group), western Newfoundland. Geological Survey of Canada Bulletin, v. 321, p. 61-114.

Fortey, R. A. 1983. Cambrian-Ordovician trilobites from the boundary beds in western Newfoundland and their phylogenetic significance. Special Papers in Palaeontology, no. 30, p. 179-211.

Fortey, R. A. 1986. Early Ordovician trilobites from the Wandel Valley Formation, eastern North Greenland. Rapport of Grønlands Geologiske Undersøgelse, v. 132, p. 15-25.

Fortey, R. A. 1989. There are extinctions and extinctions: examples from the Lower Paleozoic. Philosophical Transactions of the Royal Society of London, Series B, v. 325, p. 327-355.

Fortey, R. A. 1990. Ontogeny, Hypostome attachment and trilobite classification. Palaeontology, v. 33(3), p. 529-576.

Fortey, R. A. and Bruton, D. L. 1973. Cambrian-Ordovician rocks adjacent to Hinlopenstretet, North Ny Friesland, Spitsbergen. Geological Society of Amercia Bulletin, v. 84, p. 2227-2242.

Fortey, R. A. and Chatterton, B. D. E. 1988. Classification of the trilobite suborder Asaphina. Palaeontology, v. 31(1), p. 165-222.

Fortey, R. A., Landing, E., and Skevington, D. 1982. Cambrian-Ordovician boundary sections in the Cow Head Group, western Newfoundland. p. 95-129. *in* Bassett, M. G. and Dean, W. T. (eds.) The Cambrian-Ordovician Boundary: sections, fossil distributions, and correlations. National Museum of Wales, Geological Series, no. 3.

Fortey, R. A. and Owens, R. M. 1975. Proetida—a new order of trilobites. Fossils and Strata, v. 4, p. 227-239.

Fortey, R. A. and Owens, R. M. 1990. Trilobites. p. 121-142. *in* McNamara, K. J. (ed.), Evolutionary Trends. Belhaven Press, London.

Fortey, R. A. and Peel, J. S. 1982. Fossils from the Poulsen Cliff Formation, Washington Land, western north Greenland. Rapport of Grønlands Geologiske Undersøgelse, v. 108, p. 24.

594

Fortey, R. A. and Peel, J. S. 1989. Stratigraphy and hystricurid trilobites of the Christian Elv Formation (Lower Ordovician) of western North Greenland. Rapport of Grønlands Geologiske Undersøgelse, v. 144, p. 5-15.

Fortey, R. A. and Shergold, J. H. 1984. Early Ordovician trilobites, Nora Formation, central Australia. Palaeontology, v. 27, p. 315-366.

Frederickson, E. A. 1949. Trilobite fauna of the Upper Cambrian Honey Creek formation. Journal of Paleontology, v. 23(4), p. 341-363.

Frykman, P. 1979. Cambro-Ordovician rocks of C. H. Ostenfeld Nunatak, northern East Greenland. Rapport of Grønlands Geologiske Undersøgelse, v. 91, p. 125-132.

Geyer, G. 1998. Intercontinental, trilobite-based correlation of the Moroccan early Middle Cambrian. Canadian Journal of Earth Sciences, v. 35, p. 374-401.

Gobbett, D. J. 1960. A new species of trilobite from the lower Oslobreen Limestone. Geological Magazine, v. 97(6), p. 457-460.

Gould, S. J. 1977. Ontogeny and Phylogeny. Harvard University Press, Cambridge and London, 501 p.

Grant, R. E. 1965. Faunas and stratigraphy of the Snowy Range Formation (Upper Cambrian) in southwestern Montana and northeastern Wyoming. Geological Society of America Memoir, no. 96, 171 p.

Hall, J. 1861. Supplementary note to the thirteenth report of the Regents of the State Cabinet. in 15th Annual Report of the New York State Cabinet for Natural History. Albany, New York, p. 113-119.

Hall, J. 1863. Preliminary notice of the fauna of the Potsdam Sandstone. Albany, 16th Annual Report of the Regents of the University of the State of New York on the condition of the State Cabinet of Natural History, p. 119-222.

595

Hall, J. and Whitfield, R. P. 1877. Paleontology (Part II. Fossils of the Potsdam Group). *In* King C. (ed.), Report of the United States geological exploration, Fortieth Parallel, v. 4. United States Army Engineer Department Professional Paper, no. 18, p. 199-231.

Hallam, A. 1958. A Cambro-Ordovician fauna from the Hecla Hock succession of Ny Friesland, Spitsbergen. Geological Magazine, v. 95(1), p. 71-76.

Hart, W. D., Stitt, J. H., Hohensee, S. R., and Ethington, R. L. 1987. Geological implications of Late Cambrian trilobites from the Collier Shale, Jessieville area, Arkansas. Geology, v. 15, p. 447-450.

Harrington, H. J. and Leanza, A. F. 1957. Ordovician trilobites of Argentina. Department of Geology, University of Kansas, Special Publication, no. 1, 276 p.

Hawle, I. and Corda, A. J. C. 1847. Prodrom einer Monographie der böhmischen Trilobiten. Abhandlungen der königlichen böhmischen Gesellschaft der Wissenschaften, Abhandlungen, no. 5, 176 p.

Heller, R. L. 1954. Stratigraphy and paleontology of the Roubidoux Formation of Missouri. Bulletin of Missouri Geological Survey, v. 35, p. 1-118.

Hennig, W. 1966. Phylogenetic Systematics. University of Illinois Press, Urbana and Chicago, 263 p.

Henningsmoen, G. 1957. The trilobite family Olenidae. Norske Videnskaps-Akademi i Oslo, Matematisk-naturvidenskapelig klasse Skrifter, no. 1, 303 p.

Hickman, C. S. 1999. Larvae in invertebrate development and evolution. p. 21-59. *in* Hall, B. K. and Wake, M. H. (eds.) The Origin and Evolution of Larval Forms. Academic Press, New York.

Hintze, L. F. 1953. Lower Ordovician trilobites from western Utah and eastern Nevada. Utah Geological and Mineralogical Survey Bulletin, no. 48, 249 p.

596

Hohensee, S. R. and Stitt, J. H. 1989 Redeposited *Elvinia* Zone (Upper Cambrian) trilobites from the Collier Shale, Ouachita Mountains, west-central Arkansas. Journal of Paleontology, v. 63(6), p. 857-879.

Howell, B. F. and Duncan, D. 1939. Middle-Upper Cambrian transition faunas of North America. Bulletin of the Wagner Free Institute of Science, v. 14, p. 1-11.

Hu, C.-H, 1963. The dimorphism and ontogeny of *Norwoodella halli* Resser. Transactions and Proceedings of Palaeontological Society of Japan, New Series, no. 52, p. 129-132.

Hu, C.-H. 1964. The ontogeny and dimorphism of *Welleraspis lata* Howell (Trilobita). Journal of Paleontology, v. 38(1), p. 95-97.

Hu, C.-H. 1968. Notes on the ontogeny and sexual dimorphism of Upper Cambrian trilobites of the Welleraspis faunule from Pennsylvania. The Journal of Nanyang University, v. 2, p. 321-357.

Hu, C.-H. 1969. Ontogeny and sexual dimorphism of three Upper Cambrian trilobites. The Nanyang University Journal, v. 3, p. 438-462.

Hu, C.-H. 1970a. Ontogenies and sexual dimorphisms of two Upper Cambrian trilobites. Proceedings of the Geological Society of China, no. 13, p. 143-155.

Hu, C.-H. 1970b. The ontogenies of *Ponumia obscura* (Lochman), n. g., and *Housia canadensis* (Walcott) (Trilobita) from the Upper Cambrian of the Big Horn Mountains, Wyoming. Transactions and Proceedings of Palaeontological Society of Japan, New Series, no. 77, p. 253-264.

Hu, C.-H. 1971. Ontogeny and sexual dimorphism of Lower Paleozoic Trilobita. Palaeontographica Americana, v. 7, no. 44, 155p.

Hu, C.-H. 1972. Ontogeny of three *Cedaria* Zone trilobites from Upper Cambrian, Montana. Transactions and Proceedings of Palaeontological Society of Japan, New Series, no. 85, p. 245-259.

597

Hu, C.-H. 1973. Description of basal Ordovician trilobites from the Deadwood Formation, northern Black Hills, South Dakota. Proceedings of Geological Society of China, no. 16, p. 85-95.

Hu, C.-H. 1975. Ontogenies of three Late Cambrian trilobites from the Deadwood Formation, northern Black Hills, South Dakota. Bulletins of American Paleontology, v. 67(287), p. 251-273.

Hu, C.-H. 1979. Ontogenetic studies of a few Upper Cambrian trilobites from the Deadwood Formation, South Dakota. Transactions and Proceedings of Palaeontological Society of Japan, New Series, no. 114, p. 49-63.

Hu, C.-H. 1980. Ontogenies of a few Upper Cambrian trilobites from the Deadwood Formation, South Dakota. Transactions and Proceedings of Palaeontological Society of Japan, New Series, no. 119, p. 371-387.

Hu, C.-H. 1981. Studies on the ontogenic and phylogenic development of two Upper Cambrian trilobites from South Dakota. Transactions and Proceedings of Palaeontological Society of Japan, New Series, no. 123, p. 159-167.

Hu, C.-H. 1983. Ontogenic and phylogenic development of two Upper Cambrian trilobites from the Nolichuky Formation, Tennessee. Transactions and Proceedings of Palaeontological Society of Japan, New Series, no. 129, p. 26-34.

Hu, C.-H. 1986. Ontogenetic development of Cambrian trilobites from British Columbia and Alberta, Canada (Part II). Journal of Taiwan Museum, v. 39(1), p. 1-44.

Hu, C.-H. and Li, I-L. 1971 Ontogenies of four proparian trilobites from Upper Cambrian, Montana, U. S. A. (with a description of *Vernaculina lushini*, n. sp.). Proceedings of Geological Society of China, no. 14, p. 165-184.

Hu, C.-H. and Tan, L.-L. 1971 Ontogenies of two Upper Cambrian trilobites from Northern Black Hills, South Dakota. Transactions and Proceedings of Palaeontological Society of Japan, New Series, no. 82, p. 61-72.

Hughes, N. C. and Chapman, R. E. 1995. Growth and variation in the Silurian proetide trilobite *Aulacopleura konincki* and its implications for trilobite palaeobiology. Lethaia, v. 28, p. 333-353.

Hupé, P. 1953. Classification des trilobites. Annales de Paléontologie, v. 39, p. 61-168. [In French].

Hupé, P. 1955. Classification des trilobites. Annales de Paléontologie, v. 41, p. 91-325. [In French].

Ivshin, N. K. 1956. Upper Cambrian trilobites of Kazakhstan, 1. Kazakhstan SSR Academy of Sciences, Transactions of the Institute of Geological Sciences, 119 p. [In Russian].

Ivshin, N. K. 1962. Upper Cambrian trilobites of Kazakhstan, 2. Kazakhstan SSR Academy of Sciences, Transactions of the Institute of Geological Sciences, 412 p. [In Russian].

Jaekel, O. 1909. Über die Agnostiden. Zeitschrift der Deutschen Geologischen Gesellschaft, v. 61, p. 380-400.

Jell, P. A. 1985. Tremadoc trilobites of the Digger Island Formation, Waratah Bay, Victoria. Memoirs of the Victoria Museum, v. 46, p. 53-88.

Jell, P. A. and Stait, B. 1985a. Revision of an early Arenig trilobite faunule from the Caroline Creek Sandston, near Latrobe, Tasmania. Memoirs of the Victoria Museum, v. 46, p. 35-51.

Jell, P. A. and Stait, B. 1985b. Tremadoc trilobites from the Florentine Valley Formation, Tim Shea Area, Tasmania. Memoirs of the National Museum of Victoria, no. 46, p. 1-34.

Johnston, R. M., 1888. Systematic account of the geology of Tasmania. Government Printer, Hobart.

Kim, D. H. and Choi, D. K. 1997. Tremadoc trilobites from the Mungog Formation, Yeongweol, Korea. Proceedings of 30th International Geologist Congress, v. 11, p. 75-84.

Kindle, C. H. 1982. The C. H. Kindle collection: Middle Cambrian to Lower Ordovician trilobites from the Cow Head Group, western Newfoundland. in Current Research, Part C, Geological Survey of Canada Paper 82-1C, p. 1-17.

Kluge, A. G. 1985. Ontogeny and phylogenetic systematics. Cladists, v. 1(1), p. 13-27.

Kluge, A. G. 1988. The characterization of ontogeny. p. 57-81. in Humphries, C. J. (ed.) Ontogeny and Systematics, Columbia University Press, New York.

Kluge, A. G. 1989. A concern for evidence and a phylogenetic hypothesis of relationships among *Epicrates* (Boidae, Serpentes). Systematic Zoology, v. 38, p. 7-25.

Kluge, A. G. and Strauss, R. E. 1985. Ontogeny and systematics. Annual Review of Ecology and Systematics, v. 16, p. 247-268.

Kluge, A. G. and Wolf, A. J. 1989. Cladistics: What's in a word? Cladistics, v. 9, p. 183-199.

Kobayashi, T. 1934. The Cambro-Ordovician formations and faunas of south Chosen. Palaeontology, Part 2, Lower Ordovician faunas. Journal of the Faculty of Science, Imperial University of Tokyo, section 2, v. 3, p. 521-585.

Kobayashi, T. 1935. The Cambro-Ordovician formations and faunas of South Chosen. Palaeontology. Part 3. Cambrian faunas of South Chosen with a special study on the Cambrian trilobite genera and families. Journal of the Faculty of Science, Imperial University of Tokyo, section II, v. 4, p. 49-344.

Kobayashi, T. 1938 Upper Cambrian fossils from British Columbia with a discussion on the isolated occurrence of the so-called "*Olenus*" beds of Mt. Jubilee. Japanese Journal of Geology and Geography, v. 15, p. 149-192.

Kobayashi, T. 1939. On the agnostids (Part I). Journal of the Faculty of Science, Imperial University of Tokyo, section II, v. 6, p. 271-334.

Kobayashi, T. 1940. Lower Ordovician fossils from Junee, Tasmania. Papers and Proceedings of the Royal Society of Tasmania, 1939, p. 61-66.

Kobayashi, T. 1943. Brief notes on the eodiscids, Parts 1 and 2. Proceedings of Imperial Academy of Japan, v. 19, p. 37-47.

Kobayashi, T. 1944. On the eodiscids. Journal of the Faculty of Science, Imperial University of Tokyo, section II, v. 7, p. 1-74.

Kobayashi, T. 1955. The Ordovician fossils from the McKay Group in British Columbia, western Canada, with a note on the Early Ordovician palaeogeography. Journal of the Faculty of Science, University of Tokyo, section 2, v. 9, part 3, p. 355-487.

Kobayashi, T. 1960. The Cambro-Ordovician formations and faunas of South Korea, Part 6, Paleontology 5. Journal of the Faculty of Science, Tokyo University, series 2, v. 12, p. 217-275.

Kopaska-Merkel, D. C. 1981 Ontogeny of *Ehmaniella*—implications for trilobite ecology. United States Geological Survey, Open-file Report, no. 81-743, p. 111-114.

Kuo, H.-C., Duan, J.-Y., and An, S.-I. 1982. Cambrian-Ordovician boundary in the North China platform with descriptions of trilobites. Paper for the Fourth International Symposium on the Ordovician System. Department of Geology, Changchun College of Geology, Changchun, China. 31 p.

Kurtz, V. E. 1975. Franconian (Upper Cambrian) trilobite faunas from the Elvins Group of southwest Missouri. Journal of Paleontology, v. 49(6), p. 1009-1043.

Kurtz, V. E. and Miller, J. F. 1981. Early Ordovician conodont faunas from central East Greenland. Abstracts with programs, Geological Society of America, v. 13, p. 285.

Landing, E. and Barnes, C. R. 1981. Conodonts from the Cape Clay Formation (Lower Ordovician), southern Devon island, Arctic Archipelago. Canadian Journal of Earth Sciences, v. 18, p. 1609-1628.

Lane, P. D. and Thomas, A. T. 1983. A review of the trilobite suborder Scutelluina. Special Papers in Palaeontology, no. 30, p. 141-160.

Laurie, J. R. and Shergold, J. H. 1996. Early Ordovician trilobite taxonomy and biostratigraphy of the Emanuel Formation, Canning Basin, Western Australia. Palaeontographica Abteilung A. no. 240, p. 65-144.

Lee, D.-C. and Chatterton, B. D. E. 1996. Terminology of glabellar lobes in trilobite larvae based on homology. Journal of Paleontology, v. 70, p. 439-442.

Lee, D.-C. and Chatterton, B. D. E. 1997a. Hystricurid trilobite larvae from the Garden City Formation (Lower Ordovician) of Idaho and their phylogenetic implications. Journal of Paleontology, v. 71(5), p. 862-877.

Lee, D.-C. and Chatterton, B. D. E. 1997b. Three new proetide trilobite larvae from the Lower Ordovician Garden City Formation in southern Idaho. Journal of Paleontology, v. 71(3), p. 434-441.

Lee, D.-C. and Chatterton, B. D. E. 1999. Paleogeography and biostratigraphy of the Hystricuridae (Trilobita): a preliminary study on their evolutionary implicatioins. Acta Universitatis Carolinae, Geologica, v. 43, p. 365-368.

Lee, D.-C. and Chatterton, B. D. E. 2001. Protaspides of Cambrian ptychopariid trilobites, Abstracts of Oral Presentations and Posters, Third International Conference on Trilobites and Their Relatives, p. 39.

Leggs, D. P. 1976. Ordovician trilobites and graptolites from the Canning Basin, Western Australia. Geologica et Palaeontologica, v. 10, p. 1-58.

Lisogor, K. A. 1961. Trilobita of the Tremadoc and adjacent strata of Kendyktas. Trudy Geologicheskii Institut Akademia nauk SSSR, no. 18, p. 55-92. [In Russian].

Liu, Y. 1982. Trilobites. p. 290-347. *in* Palaeontological Atlas of Hunan. Geological Memoir, v. 2(1).

Lochman, C. 1936. New trilobite genera from the Bonneterre Dolomite (Upper Cambrian) of Missouri. Journal of Paleontology, v. 10(1), p. 35-43.

Lochman, C. 1938. Upper Cambrian faunas of the Cap Mountain Formation of Texas. Journal of Paleontology, v. 12, p. 72-85.

Lochman, C. 1940. Fauna of the basal Bonneterre Dolomite (Upper Cambrian) of southeastern Missouri. Journal of Paleontology, v. 14, p. 1-53.

Lochman, C. 1950. Upper Cambrian faunas of the Little Rocky Mountains, Montana. Journal of Paleontology, v. 24(3), p. 322-349.

Lochman, C. 1956. The evolution of some Upper Cambrian and Lower Ordovician trilobite families. Journal of Paleontology, v. 30, p. 445-462.

Lochman, C. 1964. Upper Cambrian faunas from the subsurface Deadwood Formation, Williston Basin, Montana. Journal of Paleontology, v. 38(1), p. 33-60.

Lochman, C. 1965. Lower Ordovician (Zone D) faunules from the Williston Basin, Montana. Journal of Paleontology, v. 39(3), p. 466-486.

Lochman, C. 1966. Lower Ordovician (Arenigian) faunas from the Williston Basin of Montana and North Dakota. Journal of Paleontology, v. 40, p. 512-548.

Lochman, C. 1968. *Crepicephalus* faunule from the Bonneterre Dolomite (Upper Cambrian) of Missouri. Journal of Paleontology, v. 42(5), P. 1153-1162.

Lochman, C. and Duncan, D. 1944. Early Upper Cambrian faunas of central Montana. Geological Society of America Special Papers, no. 54, 181 p.

Lochman, C. and Hu, C.-H. 1959. A *Ptychaspis* faunule from the Bear River Range, southeastern Idaho. Journal of Paleontology, v. 33(3), p. 404-427.

Lochman, C. and Hu, C.-H. 1960. Upper Cambrian faunas from the northwest Wind River Mountains, Wyoming. Part I. Journal of Paleontology, v. 34(5), p. 793-834.

Lochman, C. and Hu, C.-H. 1961. Upper Cambrian faunas from the northwest Wind River Mountains, Wyoming. Part II. Journal of Paleontology, v. 35(1), p. 125-146.

Lochman, C. and Hu, C.-H. 1962. Upper Cambrian faunas from the northwest Wind River Mountains, Wyoming. Part III. Journal of Paleontology, v. 36(1), p. 1-28.

Longacre, S. A. 1970. Trilobites of the Upper Cambrian ptychaspid biomere, Wilberns Formation, Central Texas. The Paleontological Society Memoir 4, 70p.

Lu, Y.-H. 1954. Two new trilobite genera of the Kushan Formation. Acta Palaeontologica Sinica, v. 1(1), p. 409-438.

Lu, Y.-H. 1975. Ordovician trilobite faunas of central and southwestern China. Paleontologica Sinica, Whole number 152, New Series B, no. 11, 465 p.

Lu, Y.-H., Chang, W.-T., Chu, C.-L., Chien, Y.-Y., and Hsiang, L.-W. 1965. Chinese Fossils of All Groups: Trilobites of China. Science Press, 766 p. [In Chinese].

Lu, Y.-H, Chu, C.-L., Chien, Y.-Y., Zhou, Z.-Y., Chen, J.-Y., Liu, G.-W., Yu, W., Chen, X., and Xu, H.-K. 1976. Ordovician biostratigraphy and palaeozoogeography of China. Nanjing Institute of Geology and Palaeontology, Academia Sinica, Memoir, no.7, 83 p.

Ludvigsen, R. 1982. Upper Cambrian and Lower Ordovician trilobite biostratigraphy of the Rabbitkettle Formation, Western District of Mackenzie. Life Sciences Contribution, Royal Ontario Museum, no. 134, 188 p.

Ludvigsen, R. 1986. Revision of Acheilus and Theodenisia (Late Cambrian, Trilobita). Journal of Paleontology, v. 60(1), p. 61-67.

Ludvigsen, R. and Westrop, S. R. 1983. Franconian trilobites of New York State. New York State Museum Memoir, no. 23, 82 p.

604

Ludvigsen, R., Westrop, S. R., and Kindle C. H. 1989. Sunwaptan (Upper Cambrian) trilobites of the Cow Head Group, western Newfoundland, Canada. Palaeontographica Canadiana, no. 6, 175 p.

McCormick, T. and Fortey, R. A. 1999. The most widely distributed trilobite species: Ordovician *Carolinites genacinaca*. Journal of Paleontology, v. 73, no. 2, p. 202-218.

Månsson, K. 1998 Middle Ordovician olenid trilobites (*Triarthrus* Green and *Porterfieldia* Cooper) from Jämtland, central Sweden. Transactions of the Royal Society of Edinburgh, Earth Sciences, v. 89, p. 47-62.

Mansuy, H. 1920. Nouvelle Contibution à l'Étude des Faunes Paléozoiques et Mesozoiques de l'Annam septentrional, Région de ThanhHoa. Memoir of the Geological Services of Indochina, no. 7, 64 p.

Marek, L. 1952. Contribution to the stratigraphy and fauna of the uppermost part of Králu v Dvu r Shales (Ashgillian). Sborník U středního Ú stavu Geologisckeho, v. 19, p. 429-455.

Matthew, M. A. 1885. Illustrations of the Fauna of the St. John Group continued. No. III-Descriptions of new genera and speices, (including a description of a new species of *Solenopleura* by J. F. Whiteaves). Proceedings and Transactions of the Royal Society of Canada, Section IV, p. 29-84.

Matthew, M. A. 1887. Illustrations of the Fauna of the St. John Group. No. 4, Part 1. Description of a new species of *Paradoxides* (*Paradoxides regina*). Part II. The smaller trilobites with eye (Ptychoparidae and Ellipsocephalidae). Proceedings and Transactions of the Royal Society of Canada, Section IV, p. 115-166.

Maximova, Z. 1955. Trilobita. p. 117-134. *in* Nikiforova, O. I. (ed.) Field Atlas of the Ordovician and Silurian faunas of the Siberian Platform. [In Russian]

Maximova, Z. 1962. Ordovician and Silurian trilobites of the Siberian Platform. Geological Institution, no. 76, 215 p. [In Russian]

Mergl, M. 1984. Fauna of the Upper Tremadocian of Central Bohemia. Sbor. geol. ved. Paleontologie, v. 26, p. 9-46.

Mergl, M. 1994. Trilobite fauna from the Trenice Formation (Tremadoc) in Central Bohemia. Folia Musei Rerum Naturalium Bohemiae Occidentalis Ser. Geologica no. 39, 31 p.

Miller, B. M. 1936. Cambrian trilobites from northwestern Wyoming. Journal of Paleontology, v. 10(1), p. 23-34.

Miller, S. A. 1889. North American geology and palaeontology. Western Methodist Book Concern, Cincinnati, 664 p.\

Miyamoto, M. M. and Fitch, W. M. 1995. Testing species phylogenies and phylogenetic methods with congruence. Systematic Biology, v. 44(1), p. 64-76.

Moberg, J. C. and Möller, H. 1898. Om Acerocarezonen. Geologiska Föreningens i Stockholm Förhandlingar., v. 20(5), p. 197-290.

Moore, R. C. (ed.) 1959. Treatise on Invertebrate Paleontology, Part O, Arthropoda 1. Geological Society of America and University of Kansas Press, 560 p.

Müller, G. B. and Walossek, D. 1986. Arthropod larvae from the Upper Cambrian of Sweden. Transactions of the Royal Society of Edinburgh: Earth Sciences, v. 77, p. 157-179.

Nelson, G. 1978. Ontogeny, phylogeny, paleontology, and the biogenic law. Systematic Zoology, v. 27, p. 324-345.

Nielsen, C. 1994. Larval and adult characters in animal phylogeny. American Zoologists, v. 34, p. 492-501.

Nielsen, C. 1995. Animal Evolution: Interrelationships of the Living Phyla. Oxford University Press, Oxford, 467 p.

Norford, B. S. 1969. The early Canadian (Tremadocian) trilobites *Clelandia* and *Jujuyaspis* from the southern Rocky Mountains of Canada. Geological Survey of Canada Bulletin, no. 182, p. 1-15.

Ogienko, L. V. 1972. New Lower and Middle Ordovician trilobites from Siberia, Publishing Office, Nauka, Moscow, p. 237-242. [In Russian].

Ogienko, L. V. 1974. Lower Ordovician trilobites. p. 109-130. [In Russian].

Ogienko, L. V. 1984. Lower Ordovician trilobites from southern Siberian Platform. p. 57-72. *in* Kanygin, A. V., Oboot, A. M., and Volkova, K. N. (eds.), Ordovician of Siberian Platform. Paleontological Atlas. Academy of Sciences of the USSR, Siberian Branch, Tranactions of Institution of Geology and Geophysics, no. 590. [In Russian].

Ogienko, L. V. 1992. Trilobites and biostratigraphy of Lower Ordovician strata in the south Siberian platform. East Siberian Scientific Institute of Geology, Geophysics, and Mineral Resources. 145 p. [In Russian].

Öpik, A. A. 1963. Early Upper Cambrian fossils from Queensland. Bureau of Mineral Resources, Geology and Geophysics, Bulletin, no. 64, 124 p.

Öpik, A. A. 1967. The Mindyallan Fauna of north-western Queensland. Bureau of Mineral Resources, Geology and Geophysics, Bulletin, no. 74, 404 p.

Öpik, A. A. 1970. Nepeid trilobites of the Middle Cambrian of Northern Australia. Bureau of Mineral Resources, Geology and Geophysics Bulletin, no. 113, 48 p.

Orndoff, R. C., Taylor, J. F., and Traut, R. W. 1988. Uppermost Cambrian and Lowest Ordovician conodont and trilobite biostratigraphy in northwestern Virginia. Virginia Minerals, v. 34(2), p. 13-20.

Owen, D. D. 1852. Report of a geological survey of Wisconsin, Iowa, and Minnesota, and incidentally a portion of Nebraska Territory. Lippincott, Grambo and Co., Philadelphia, 638 p.

Owens, R. M. 1973. British Ordovician and Silurian Proetidae (Trilobita). Monographs of Palaeontolographical Society, v. 127, no. 535, 98 p.

Packard, J. and Mayr, U. 1982. Cambrian and Ordovician stratigraphy of southern Ellesmere Island, District of Franklin. Current Research, Part A, Geological Survey of Canada, Paper 82-1A, p. 67-74.

Palmer, A. R. 1954a. An appraisal of the Great Basin Middle Cambrian trilobites described before 1900. United States Geological Survey, Professional Paper, 264-D, p. 55-86.

Palmer, A. R. 1954b. The faunas of the Riley Formation in Central Texas. Journal of Paleontology, v. 28(6), p. 709-786.

Palmer, A. R. 1958. Morphology and ontogeny of a Lower Cambrian ptychoparioid trilobite from Nevada. Journal of Paleontology, v. 32(1), p. 154-170.

Palmer, A. R. 1960. Trilobites of the Upper Cambrian Dunderberg Shale, Eureka District, Nevada. United States Geological Survey, Professional Paper, no. 334-C, p. 53-109.

Palmer, A. R. 1962a. Comparative ontogeny of some opisthoparian, gonatoparian and proparian Upper Cambrian trilobites. Journal of Paleontology, v. 36(1), p. 87-96.

Palmer, A. R. 1962b. *Glyptagnostus* and associated trilobites in the United States. U. G. Geological Survey, Professional Paper, no. 374-F, 49 p.

Palmer, A. R. 1965a. Biomere—a new kind of biostratigraphic unit. Journal of Paleontology, v. 39, p. 149-153.

Palmer, A. R. 1965b. Trilobites of the Late Cambrian pterocephaliid biomere in the Great Basin, United States. United States Geological Survey Professional Papers, no. 493, 105 p.

Palmer, A. R. 1982. Fossils of Dresbachian and Franconian (Cambrian) age from the subsurface of west-central Indiana. Department of Natural Resources, Geological Survey Special Report, no. 29, 12 p.

608

Palmer, A. R. 1984. The biomere: evolution of an idea. Journal of Paleontology, v. 58, p. 599-611.

Palmer, A. R. and Peel, J. S. 1981. Dresbachian trilobites and stratigraphy of the Cass Fjord Formation, western North Greenland. Grønlands Geologiske Undersøgelse Bulletin, no. 141, 46 p.

Park, G.-H. 1993. Trilobite fauna from the Mungog Formation (Lower Ordovician) in the northern part of Yeongweol area, Korea. Unpublished M.Sc. thesis, Seoul National University, 182 p.

Patterson, C. 1983. How does phylogeny differ from ontogeny? p. 1-31. in Goodwin, B. C., Holder, N. and Wylie, C. C. (eds.), Development and Evolution. University Press, Cambridge.

Peel, J. S. and Christie, R. L. 1982. Cambrian-Ordovician platform stratigraphy: correlations around Kane Basin. Meddelelser om Grønland, Geoscience, v. 8, p. 117-135.

Peel, J. S. and Cowie, J. W. 1979. New names for Ordovician formations in Greenland. Rapport of Grønlands Geologiske Undersøgelse, v. 91, p. 117-124.

Peng, S. 1983. Cambrian-Ordovician boundary at Huanghuachang of Yichang, Hubei. p. 44-52. in Papers for the Symposium on the Cambrian-Ordovician and Ordovician-Silurian Boundaries, Nanjing, China, 1983. Nanjing Institute of Geology and Palaeontology, Academia Sinica.

Peng, S. 1984. Cambrian-Ordovician boundary in the Cili-Taoyuan border area, north-western Hunan with descriptions of relative trilobites. p. 285-405. in Stratigraphy and Palaeontology of Systemic Boundaries in China, Cambrian-Ordovician Boundary, Anhui Science and Technology Publishing House.

Peng, S. 1990a Tremadoc stratigraphy and trilobite faunas of northwestern Hunan, 1. Trilobites from the Nantsinkwan Formation of the Yangtze Platform. Beringeria, v. 2, p. 3-53.

Peng, S. 1990b Tremadoc stratigraphy and trilobite faunas of northwestern Hunan 2. Trilobites from the Panjiazui Formation and the Madaoyu Formation in the Jiangnan Slope Belt. Beringeria, v. 2, p. 55-171.

Peng, S. 1992. Upper Cambrian biostratigraphy and trilobite faunas of the Cili-Taoyuan area, northwestern Hunan, China. Association of Australian Palaeontologists Memoir, no. 13, 119 p.

Petrunina, Z. E. New Tremadocian trilobite genus and species from west Siberia. in New data on Geology and useful fossils from west Siberia, West Siberian Geoological Branch, issue 8, p. 59-68. [In Russian].

Poulsen, C. 1927. The Cambrian, Ozarkian and Canadian faunas of northwest Greenland. Meddelelser om Grønlands, v. 70, p. 233-343.

Poulsen, C. 1937. On the Lower Ordovician faunas of east Greenland. Meddelelser om Grønlands, v. 119(3), p. 1-72.

Poulsen, C. 1946. Notes on Cambro-Ordovician fossils collected by the Oxford University Ellesmere Land expedition, 1934-5. Quarterly Journal of the Geological Society of London, v. 102, p. 299-337.

Poulsen, C. 1954. Attempt at a classification of the trilobite Family Solenopleuridae. Meddelelser fra Dansk Gologisk Forening København, v. 12, p. 443-447.

Powell, L. H. 1935. A study of the Ozarkian faunas of southeastern Minnesota. The Science Museum of the Saint Paul Institute, Science Bulletin, no. 1, 80 p.

Pratt, B. R. 1992. Trilobites of the Marjuman and Steptoean stages (Upper Cambrian), Rabbitkettle Formation, southern Mackenzie Mountains, northwest Canada. Palaeontographica Canadiana, no. 19, 179 p.

Přibyl, A. 1950. Nová pojmenování pro několik homonymických jmen českysch i cizích trilobitových rodů. Sbor. stát. geol. Ůst. ČSR. Republ., Odd. paleont., v. 17, p. 193-200. o[In Czech].

Qian, Y. 1994. Trilobites from middle Upper Cambrian (Changshan Stage) of north and northeast China. Palaeontologica Sinica, Whole Number 183, New Series B, no. 30, 177 p.

Raff, R. A. 1996. The Shape of Life: genes, development, and the evolution of animal form. The University of Chicago Press, 520 p.

Rasetti, F. 1943. New Lower Ordovician trilobites from Lévis, Quebec. Journal of Paleontology, v. 17, p. 101-104.

Rasetti, F. 1944. Upper Cambrian trilobites from the Lévis Conglomerate. Journal of Paleontology, v. 18(3), p. 229-258.

Rasetti, F. 1945. New Upper Cambrian trilobites from the Lévis Conglomerate. Journal of Paleontology, v. 19(5), p. 462-478.

Rasetti, F. 1951. Middle Cambrian stratigraphy and faunas of the Canadian Rocky Mountains. Smithsonian Miscellaneous Collections, v. 116, no. 5, 270 p.

Rasetti, F. 1954. Phylogeny of the Cambrian trilobite family Catillicephalidae and the ontogeny of *Welleraspis*. Journal of Paleontology, v. 28(5), v. 599-612.

Rasetti, F. 1956. Revision of the trilobite genus *Maryvillia* Walcott. Journal of Paleontology, v. 30, p. 1266-1269.

Rasetti, F. 1961. Dresbachian and Franconian trilobites of the Conococheague and Frederick Limestones of the Central Appalachians. Journal of Paleontology, v. 35(1), p. 104-124.

Rasetti, F. 1965. Upper Cambrian trilobite faunas of northeastern Tennessee. Smithsonian Miscellaneous Collections, v. 148, no. 3, 127 p.

Rasetti, F. 1966. Revision of the North American species of the Cambrian trilobite genus *Pagetia*. Journal of Paleontology, v. 40(3), p. 502-511.

Raw, F. 1925. The development of *Leptoplastus salteri* (Callaway), and of other trilobites (Olenidae, Ptychoparidae, Conocoryphidae, Paradoxidae, Phacopidae, and Mesonacidae). Quarterly Journal of the Geological Society of London, v. 81, p. 223-324.

Raw, F. 1927. The ontogenies of trilobites and their significance. American Journal of Science (series 5), v. 14, p. 7-35, 131-149.

Raymond, P. E. 1913a. Some changes in the names of genera of trilobites. The Ottawa Naturalist, v. 26, p. 137-142.

Raymond, P. E. 1913b. Revision of the species which have been referred to the genus *Bathyurus*. Victoria Memorial Museum, Bulletin, no. 1, p. 51-80.

Raymond, P. E. 1924. New Upper Cambrian and Lower ordovician trilobites from Vermont. Proceedings of the Boston Society for Natural History, v. 37, p. 389-466.

Raymond, P. E. 1925. Some trilobites of the lower Middle Ordovician of eastern North America. Bulletin of the Museum of Comparative Zoology at Harvard College, v. 67(1), 180 p.

Raymond, P. E. 1928. Two new Cambrian trilobites. American Journal of Science (series 5), v. 15(88), p. 309-313.

Raymond, P. E. 1937. Upper Cambrian and Lower Ordovician Trilobita and Ostracoda from Vermont. Geological Society of America Bulletin, no. 48, p. 1079-1146.

Raymond, P. E. 1938. Nomenclature note. Geological Society of America Bulletin, no. 48 (suppl.), p. 15.

Resser, C. E. 1935. Nomenclature of some Cambrian trilobites. Smithsonian Miscellaneous Collections, v. 93, no. 5, 46 p.

Resser, C. E. 1937. Third contribution to nomenclature of Cambrian trilobites. Smithsonian Miscellaneous Collections, v. 95, no. 22, 29 p.

Resser, C. E. 1938a Cambrian System (restricted) of the southern Appalachians. Geological Society of America, Special Paper, no. 15, 140 p.

Resser, C. E. 1939. The Ptarmigania strata of the northern Wasatch Mountains. Smithsonian Miscellaneous Collections, v. 98, no. 24, 72 p.

Resser, C. E. 1942 New Upper Cambrian trilobites. Smithsonian Miscellaneous Collections, v. 103, no. 5, 136 p.

Richter, R. 1932. Crustacea (Paläontologie). *in* Dittler, R., Joos, G., Korschelt, E., Linek, G., Oltmanns, F., and Schaum, K. (eds.) Handwörterbuch der Naturwissenschaften, 2nd ed. Gustav Fisher. Jena. p. 840-864.

Rieppel, O. 1990. Ontogeny—a way forward for systematics, a way backward for phylogeny. Biological Journal of the Linnean Society, v. 39, p. 177-191.

Robison, R. A. 1964. Late Middle Cambrian faunas from western Utah. Journal of Paleontology, v. 38(3), p. 79-92.

Robison, R. A. 1967. Ontogeny of *Bathyuriscus fimbriatus* and its bearing on the affinities of the corynexochid trilobites. Journal of Paleontology, v. 41, p. 213-221.

Robison, R. A. 1987 Superclass Trilobitomorpha. *in* Boardman, R. S., Cheetham, A. H., and Rowell, A. J. (eds.). Fossil Invertebrates. Blackwell, Palo Alto, p. 221-241.

Robison, R. A. 1988 Trilobites of the Holm Dal Formation (late Middle Cambrian), central North Greenland. Meddelelser om Grønlands, Geoscience, v. 20, p. 23-103.

Roemer, F. 1849. Texas, mit besondered Rucksicht auf deutsche Auswanderung und die physischen Verhaltnisse des Landes. Bonn, 464 p.

Ross, R. J. Jr. 1951. Stratigraphy of the Garden City Formation in northeastern Utah, and its trilobite fauna. Yale University, Peabody Museum of Natural History Bulletin, no. 6, 155 p.

Ross, R. J. Jr. 1953. Additional Garden City (Early Ordovician) trilobites. Journal of Paleontology, v. 27(5), p. 633-646.

Ross, R. J. Jr. 1957. Ordovician fossils from wells in the Williston Basin, eastern Montana. United States Geological Survey Bulletin, no. 1021-M, p. 439-510.

Ross, R. J. Jr. 1965. Early Ordovician trilobites from the Seward Peninsula, Alaska. Journal of Paleontology, v. 39(1), p. 17-20.

Ross, R. J. Jr. 1970. Ordovician brachiopods, trilobites, and stratigraphy in eastern and central Nevada. United States Geological Survey Professional Papers, no. 639, 103 p.

Ross, R. J. Jr., Hintze, L. F., Ethington, R. L., Miller, J. F., Taylor, M. E., and Repetski, J. E. 1997. The Ibexian, Lowermost Series in the North American Ordovician. Unites States Geological Survey Professional Paper, v. 1579, p.1-50.

Roth, V. L. 1984. On homology. Biological Journal of the Linnean Society, v. 22, p. 13-29.

Rozova, A. V. 1963. Biostratigraphic scheme for subdividing Upper and upper part of Middle Cambrian of northwestern Siberian platform and new Upper Cambrian trilobites of the River Kulyumbe area. Academy of Sciences of the USSR, Siberian Branch, Geology and Geophysics, no. 9. p. 3-19. [In Russian].

Rozova, A. V. 1968. Biostratigraphic zoning and trilobites of the Upper Cambrian and Lower Ordovician of the northwestern Siberian platform. Trudy Instituta Geologii I Geofiziki, no. 36, 243 p. [In Russian].

Rusconi, C. 1951. Más Trilobitas cámbricos de San Isidro, Cerro Pelado y Canota. Revista del Museo Historia Natural de Mendoza, v. 5, p. 3-30. [In Spanish].

Ružička, R. 1926. Fauna vrstev Eulomových rudního ložiska u Holoubkova (v Ouzkém). Část I. Trilobiti. Rozpravy II. TřŇídy České Akademie. v. 35(39), p. 1-26. [In Czech].

Salter, J. W. 1864. A monograph of the British trilobites from the Cambrian, Silurian, and Devonian formations. Palaeontolographical Society (London) Monographs, 80 p.

Scotese, C. R. and McKerrow, W. S. 1991 Ordovician plate tectonic reconstructions. p. 271-282. *in* Barnes, C. R. and Williams, S. H. (eds.) Advances in Ordovician Geology, Geological Survey of Canada, Paper, no. 90-9.

Sdzuy, K. 1955. Die Fauna der Leimitz-Schiefer (Tremadoc). Abhandlungen der Senckenbergischen Naturforschenden Gesellschaft, v. 492, p. 1-74. [In German].

Shaw, A. B. 1951. The paleontology of northwestern Vermont. I. new Late Cambrian trilobites. Journal of Paleontology, v. 25(1), p. 97-114.

Shaw, A. B. 1956. A Cambrian *Aphelaspis* fauna from Steele Butte, near Boulder, Wyoming. Journal of Paleontology, v. 30(1), p. 48-52.

Shaw, A. B. 1966. Paleontology of northwestern Vermont X. Fossils from the (Cambrian) Skeels Corners Formation. Journal of Paleontology, v. 40, p. 269-295.

Shergold, J. H. 1971. Late Upper Cambrian trilobites from the Gola beds, western Queensland. Bureau of Mineral Resources, Geology and Geophysics, Bulletin, no. 112, 127 p.

Shergold, J. H. 1975. Late Cambrian and Early Ordovician trilobites from the Burke River Structural Belt, Western Queensland, Australia. Bureau of Mineral Resources, Geology and Geophysics, Bulletin, no. 153, 251 p.

Shergold, J. H. 1980. Late Cambrian trilobites from the Chatsworth Limestone, western Queensland. Bureau of Mineral Resources, Geology and Geophysics, Bulletin, no. 186, 111 p.

Shergold, J. H. 1991a. Late Cambrian and Early Ordovician trilobite faunas of the Pacoota Sandstone, Amadeus Basin, central Australia. Bureau of Mineral Resources, Geology and Geophysics, Bulletin, no. 237, p. 15-75.

Shergold, J. H. 1991b. Protaspid and early meraspid growth stages of the eodiscoid trilobite *Pagetia ocellata* Jell, and their implications for classification. Alcheringa, v. 15, p. 65-86.

Shergold, J. H. and Cooper, R. A. 1985. Late Cambrian trilobites from the Mariner Group, northern Victoria Land, Antarctica. Journal of Australian Geology and Geophysics, v. 9, p. 91-106.

Shergold, J. H., Gorter, J. D., Nicoll, R. S., and Haines, P. W. 1991 Stratigraphy of the Pacoota Sandston (Cambrian-Ordovician), Amadeus Basin, N. T. Bureau of Mineral Resources, Geology and Geophysics Bulletin, no. 237, p. 2-14.

Shergold, J. H. and Szudy, K. 1984. Cambrian and early Tremadocian trilobites from Sultan Dag, central Turkey. Senckenbergiana lethaea, v. 65(1), p. 51-135.

Shergold, J. H. and Webers, G. F. 1992. Late Dresbachian (Idamean) and other trilobite faunas from the Heritage Range, Ellsworth Mountains, West Antarctica. p. 125-165. *in* Webers, G. F., Craddock, C., Splettstoesser, J. F. (eds.) Geology and Paleontology of the Ellsworth Mountains, West Antarctica. Geological Society of America Memoir, no. 170.

Shimer, H. W. and Shrock, R. R. 1944. Index Fossils of North America. Wiley, New York, 837 p.

Shumard, B. F. 1861. The primodial zone of Texas with descriptions of new fossils. American Journal of Science (series 2), v. 32, p. 213-221.

Slack, J. M. W., Holland, P. W. H., and Graham, C. F. 1993. The zootype and the phylotypic stage. Nature, v. 361, p. 490-492.

Smith, A. B. 1994. Systematics and the Fossil Record: Documenting Evolutionary Patterns. Blackwell Science, Oxford, 223 p.

Smith, A. B. 1997. Echinoderm larvae and phylogeny. Annual Reviews of Ecology and Systematics, v. 28, p. 219-241.

Smith, M. P. 1991. Early Ordovician conodonts of East and North Greenland. Meddelelser om Grønlands, Geoscience, v. 26, p. 1-81.

Šnajdr, M. 1958. Trilobiti Českěho středního Kambria. Rozpravy Ústředniho ústavu Geologisckěho, no. 24, 280 p. [In Czech].

Šnajdr, M. 1980. Bohemian Silurian and Devonian Proetidae (Trilobita). Rozpravy Ústředniho ústavu Geologisckěho, no. 45, 324 p.

Šnajdr, M. 1990. Bohemian Trilobites. Geological Survey, Prague, 265 p.

Stitt, J. H. 1971. Cambrian-Ordovician trilobites from western Arbuckle Mountains. Oklahoma Geological Survey Bulletin, no. 110, 83 p.

Stitt, J. H. 1975. Adaptive radiation, trilobite paleoecology, and extinction, Ptychaspidid Biomere, Late Cambrian of Oklahoma. Fossils and Strata, v. 4, p. 381-390.

Stitt, J. H. 1977. Late Cambrian and earliest Ordovician trilobites Wichita Mountains Area, Oklahoma. Oklahoma Geological Survey Bulletin, no. 124, 79 p.

Stitt, J. H. 1983. Trilobites, biostratigraphy, and lithostratigraphy of the McKenzie Hill Limestone (Lower Ordovician), Wichita and Arbuckle Mountains, Oklahoma. Oklahoma Geological Survey Bulletin, no. 134, 54 p.

Stitt, J. H. 1998. Trilobites from the *Cedarina dakotaensis* Zone, lowermost part of the Deadwood Formation (Marjuman Stage, Upper Cambrian), Black Hills, South Dakota. Journal of Paleontology, v. 72(6), p. 1030-1046.

Stitt, J. H. and Straatmann, W. M. 1997. Trilobites from the upper part of the Deadwood Formation (Upper Franconian and Trempealeauan stages, Upper Cambrian), Black Hills, South Dakota. Journal of Paleontology, v. 71(1), p. 86-102.

Størmer, L. 1942. Studies on trilobite morphology Part II. The larval development, the segmentation and the sutures, and their bearing on trilobite classification. Norsk Geologisk Tidsskrift, v. 21, p. 50-163.

Stouge, S. and Boyce, W. D. 1983. Fossils of northwestern Newfoundland and southeastern Labrador: conodonts and trilobites. Newfoundland Department of Mines and Energy, Mineral Development Division, Report 83-3, 55 p.

617

Strand, T. 1927. The ontogeny of *Olenus gibbosus*. Norsk Geologisk Tidsskrift, v. 9, p. 320-329.

Swinnerton, H. H. 1915. Suggestions for a revised classification of trilobites. Geological Magazine (new series 2) p. 487-496, 538-545.

Swofford, D. L. 1991. When are phylogeny estimates from molecular and morphological data in congruent? p. 295-333. *in* Miyamoto, M. M. and Cracraft, J. (eds.) Phylogenetic Analysis of DNA Sequences. Oxford University Press, New York.

Taylor, M. E. and Halley, R. B. 1974. Systematics, environment, and biogeography of some Late Cambrian and Early Ordovician trilobites from eastern New York State. United States Geological Survey, Professional Paper, no. 834, 38 p.

Terrell, F. M. 1973. Silicified trilobite zonation in the lower Fillmore Formation in western Utah. Brigham Young University, Geology Studies, v. 20(4), p. 67-90.

Thomas, A. T. and Holloway, D. J. 1988. Classification and phylogeny of the trilobite order Lichida. Philosophical Transaction of the Royal Society of London, Series B, Biological Science, v. 321, p. 179-262.

Timokhin, A. V. 1989. Lower Ordovician trilobites. p. 82-91. *in* Kanygin, A. V., Moskalenko, T. A., Yadrenkina, A. G., Abaimova, G. P., Semenova, O. V., Sychev, O. V., and Timokhin, A. V. (eds.). Ordovician of Siberian Platform. Academy of Sciences of the USSR. Siberian Branch, Transactions of Institution of Geology and Geophysics, no. 751. [In Russian].

Tjernvik, T. E. 1956. On the Early Ordovician of Sweden. Geology Institution of University of Uppsala Bulletin, v. 36(9), p. 107-284.

Tortello, M. F. and Bordonaro, O. L. 1997. Cambrian agnostid trilobites from Mendoza, Argentina: a systematic revision and biostratigraphic implications. Journal of Paleontology, v. 71(1), p. 74-86.

Tripp, R. P. and Evitt, W. R. 1986. Silicified trilobites of the family Asaphidae from the Middle Ordovician of Virginia. Palaeontology, v. 29, p. 705-724.

618

Vaněk, J. 1965. Die trilobiten des mittelböhmischen Tremadoc. Senckenbergiana lethaea, v. 46, p. 263-308. [In German].

Wahlenberg, G. 1821. Petrificata Telluris Svecana. Nova Acta Soc. Regiae Sci., v. 8, p. 1-16.

Walcott, C. D. 1884. Paleontology of the Eureka District. Monographs of the United States Geological Survey, v. 8, 298 p.

Walcott, C. D. 1886. Second contribution to the studies on the Cambrian faunas of North America. United States Geological Survey Bulletin, no. 30, 369 p.

Walcott, C. D. 1890. The fauna of the Lower Cambrian or *Olenellus* zone. *in* 10th Annual Report of the Director, 1888-1889, United States Geological Survey, p. 509-774.

Walcott, C. D. 1899. Cambrian fossils of the Yellowstone National Park. United States Geological Survey Monograph, no. 32, p. 440-478.

Walcott, C. D. 1913. Cambrian geology and paleontology II, no. 11—New Lower Cambrian subfauna. Smithsonian Miscellaneous Collections v. 57, no. 11, p. 309-326.

Walcott, C. D. 1916a. Cambrian geology and paleontology III, no. 3—Cambrian trilobites. Smithsonian Miscellaneous Collections v. 64, no. 3, p. 157-256.

Walcott, C. D. 1916b. Cambrian geology and paleontology III, no. 5—Cambrian trilobites. Smithsonian Miscellaneous Collections v. 64, no. 5, p. 303-410.

Walcott, C. D. 1917. Cambrian geology and paleontology IV, no. 3—Fauna of the Mount Whyte Formation. Smithsonian Miscellaneous Collections v. 67, no. 5, p. 61-114.

Walcott, C. D. 1924. Cambrian geology and paleontology V, no. 2—Cambrian and Ozarkian trilobites. Smithsonian Miscellaneous Collections v. 75, no. 2, p. 53-60.

Walcott, C. D. 1925 Cambrian geology and paleontology V, no. 3—Cambrian and Ozarkian trilobites. Smithsonian Miscellaneous Collections v. 75, no. 3, p. 61-145.

Webby, B. D., VandenBerg, A. H. M., Cooper, R. A., Stewart, I., Shergold, J. H., Nicoll, R. S., Burrett, C. F., Stait, B., Cooper, B. J., Laurie, J., and Sherwin, L. 1991 Subdivision of the Ordovician System in Australia. p. 47-57. *in* Barnes, C. R. and Williams, S. H. (eds.) Advances in Ordovician Geology, Geological Survey of Canada, Paper, no. 90-9.

Weber, V. N. 1948. Trilobites of the Silurian beds No.1. Lower Silurian trilobites. Monografii po Paleontologii SSSR, no. 69, 113 p. [In Russian].

Welby, C. W. 1962. Paleontology of the Champlain Basin in Vermont. Vermont Geological Survey, Special Publication, no. 1, 87 p.

Westrop, S. R. 1986. Trilobites of the Upper Cambrian Sunwaptan Stage, southern Canadian Rocky Mountains, Alberta. Palaeontographica Canadiana, no. 3, 179 p.

Westrop, S. R. 1989. Trilobite mass extinction near the Cambrian-Ordovician boundary in North America. p. 89-103. *in* Donovan, S. K. (ed.) Mass Extinctions: Processes and Evidences. Columbia University Press, New York.

Westrop, S. R. 1992. Upper Cambrian (Marjuman-Steptoean) trilobites from the Port Au Port Group, western Newfoundland. Journal of Paleontology, v. 66(2), p. 228-255.

Westrop, S. R. 1995. Sunwaptan and Ibexian (Upper Cambrian-Lower Ordovician) trilobites of the Rabbitkettle Formation, Mountain River region, northern Mackenzie Mountains, northwest Canada. Palaeontographica Canadiana, no. 12, 74 p.

Westrop, S. R. and Ludvigsen, R. 1986. Type species of the Ibexian trilobite *Corbinia* Walcott, 1924. Journal of Paleontology, v. 60, p. 68-75.

Westrop, S. R., Knox, L. A., and Landing E. 1993. Lower Ordovician (Ibexian) trilobites from the Tribes Hill Formation, central Mohawk Valley, New York State. Canadian Journal of Earth Sciences, v. 30, p. 1618-1633.

Whitfield, R. P. 1889. Observations on some imperfectly known fossils from the Calciferous sandrock of Lake Champlain and descriptions of several new forms. American Museum of Natural History Bulletin, v. 2, p. 41-63.

Whittington, H. B. 1953a. North American Bathyuridae and Leiostegiidae (Trilobita). Journal of Paleontology, v. 27(5), p. 647-678.

Whittington, H. B. 1953b. Silicified Middle Ordovician trilobites. Geological Society of America Memoir, no. 59, 137 p.

Whittington, H. B. 1957. Ontogeny of *Elliptocephala*, *Paradoxides*, *Sao*, *Blainia* and *Triarthrus* (Trilobita). Journal of Paleontology, v. 31, p. 934-946.

Whittington, H. B. 1958. Ontogeny of the trilobite *Peltura scarabaeoides* from Upper Cambrian, Denmark. Palaeontology, v. 1(3), p. 200-206.

Whittington, H. B. 1963. Middle Ordovician trilobites from Lower Head, western Newfoundland. Bulletin of the Museum of Comparative Zoology at Harvard College, v. 129(1), 118 p.

Whittington, H. B. 1981. Paedomorphosis and cryptogenesis in trilobites. Geological Magazine, v. 118(6), p. 591-602.

Whittington, H. B., Chatterton, B. D. E., Speyer, S. E., Fortey, R. A., Owens, R. M., Chang, W. T., Dean, W. T., Jell, P. A., Laurie, J. R., Palmer, A. R., Repina, J. N., Rushton, A. W. A., Shergold, J. H., Clarkson, E. N. K., Wilmot, N. V., and Kelly, S. R. A. 1997. Treatise on Invertebrate Paleontology, Part O, Arthropoda 1, Trilobita Revised, v. 1: Introduction, Order Agnostida, Order Redlichiida. Geological Society of America and University of Kansas, 530 p.

Whitworth, P. H. 1970. Ontogeny of the Upper Cambrian trilobite *Leptoplastus crassicornis* (Westergård) from Sweden. Palaeontology, v. 13(1), p. 100-111.

Wiley, E. O. 1981. Phylogenetics. The Theory and Practice of Phylogenetic Systematics. John Wiley & Sons, New York. 439 p.

Wiley, E. O., Siegel-Causey D., Brooks, D. R., and Funk, V. A. 1991. The Compleat Cladist: A Primer of Phylogenetic Procedures. The University of Kansas and Museum of Natural History, Special Publication, no. 19, 158 p.

Williamson, D. I. 1992. Larvae and Evolution: towards a new zoology. Chapman and Hall, 223 p.

Wilson, J. L. 1951. Franconian trilobites of the Central Appalachians. Journal of Paleontology, v. 25(5), p. 617-654.

Winston, D. and Nicholls, H. 1967. Late Cambrian and Early Ordovician faunas from the Wilberns Formation of central Texas. Journal of Paleontology, v. 41(1), p. 66-96.

Wray, G. A. 1992. The evolution of larval morphology during the post-Paleozoic radiation of echinoids. Paleobiology, v. 18(3), p. 258-287.

Wray, G. A. 1997. Chapter 16 Echinoderms. p. 309-330. *in* Gilbert, S. F. and Raunio, A. M. (eds.) Embryology: Constructing the Organism. Sinauer Associates, Sunderland.

Yin, C. and Lee, S. 1978. Trilobita. in Guizhou Stratigraphy/Palaeontology Working Team (ed.), Atlas of Palaeontology of southwest China, Guizhou Province, v. 1, Cambrian to Devonian. p. 385-595. [In Chinese].

Young, G. E. 1973. An Ordovidian (Arenigian) trilobite faunule of great diversity from the Ibex area, western Utah. Brigham Young University Geology Studies, v.20(4), p. 91-115.

Zhang, W. and Jell, P. A. 1987. Cambrian trilobites of north China—Chinese Cambrian trilobites housed in the Smithsonian Institution. Science Press, Beijing, 459 p.

Zhang, X.-G. 1989. Ontogeny of an Early Cambrian eodiscoid trilobite from Henan, China. Lethaia, v. 22, p. 13-29.

Zhang, X.-G. and Clarkson, E. N. K. 1993. Ontogeny of the eodiscid trilobite Shizhudiscus longquanensis from the Lower Cambrian of China. Palaeontology, v. 36(4), p. 785-806.

622

Zhang, X.-G. and Pratt, B. R. 1999. Early Cambrian trilobite larvae and ontogeny of *Ichangia ichangensis* Chang, 1957 (Protolenidae) from Henan, China. Journal of Paleontology, v. 73(1), p. 117-128.

Zhou, T.-R. 1981. New materials of early Tremadocian trilobites from Sandu and Pu'an, Guizhou. Acta Palaeontologica Sinica, v. 20(3), p. 241-246.

Zhou, T., Liu, Y., Meng, X., and Sun, Z. 1977. Class Trilobita, in Palaeontological Atlas of central and south China. I. Early Paleozoic. Geological Publishing House, Beijing, p. 104-266.

Zhou, Z. and Fortey, R. A. 1986. Ordovician trilobites from north and northeast China. Palaeontographica Abteilung A. no. 192, p. 157-210.

APPENDIX II-1. Hierarchical arrangement of the ptychopariide species described in the Chapter II.

Order	Suborder	Possible superfamilial grouping	Family	Subfamily	Genus	Species
Ptychopariida	Ptychopariina	A	Kingstoniidae		*Komaspidella*	*laevis*
			Lonchocephalidae		*Glaphyraspis*	*parva*
			Menomoniidae		*Bolaspidella*	*housensis*
		B	Cedariidae		*Cedarina*	*cordillerae*
			?Cedariidae		*Apomodocia*	*conica*
			Anomocaridae		*Glyphaspis*	*paucisulcata*
			Crepicephalidae		*Crepicephalus*	*deadwoodiensis*
			Marjumiidae		*Syspacheilus*	*dunoirensis*
					Modocia	*laevinucha*
			Llanoaspididae		*Nixonella*	*montanensis*
		C	Pterocephaliidae	Housiinae	*Housia*	*ovata*
						vacuna
				?Pterocephaliinae	*Pulchricapitus*	*davisi*
			Phylacteridae		*Drabia*	*typica*
					Aphelotoxon	*triangulata*
					Ponumia	*obscura*
			?Phylacteridae		*Paranumia*	*triangularia*
			Plethopeltidae		*Arapahoia*	*arbucklensis*
			Norwoodiidae		*Norwoodella*	*halli*
		Dikelocephalacea	Ptychaspididae	Ptychaspidinae	*Ptychaspis*	*bullasa*
		Solenopleuracea	Solenopleuridae	Solenopleurinae	*Solenopleura*	*acadica*

APPENDIX II-1. continued.

Order	Suborder	Possible superfamilial grouping	Family	Subfamily	Genus	Species
Ptychopariida	Olenina	Olenacea	Olenidae	Oleninae	*Olenus*	*gibbosus*
					Apoplanias	*rejectus*
				Pelturinae	*Acerocare*	*ecorne*
		D	Parabolinoididae		*Orygmaspis*	*contractus*
					Taenicephalus	*shumardi*
		E	uncertain	Aphelaspidinae	*Aphelaspis*	*subditus*
						haguei
						tarda
						brachyphasis
					? Aphelaspis	*anyta*
				?Aphelaspidinae	*Dytremacephalus*	*granulosus*
		F	Elviniidae	Elviniinae	*Elvinia*	*roemeri*
			?Elviniidae		*Irvingella*	*major*

APPENDIX III-1. 18 genera that have been referred to the Hystricuridae before this study. Number behind each genus indicates the number of species that were assigned to the genus.

GENUS	STATUS AFTER REVISION	REMARKS
Hystricurus (35)	Partially retained	Some species transferred into *Politohystricurus* n. gen., *Spinohystricurus* n. gen., and *Tanybregma* n. gen. of the Hystricuridae. Other species are transferred into taxa such as *Flectihystricurus* n. gen. that are excluded from the Hystricuridae
Hillyardina (6)	Partially retained	Some species transferred into *Parahillyardina* n. gen., and *Tanybregma* of the Hystricuridae. Other species are transferred into *Hyperbolochilus* which is excluded from the Hystricuridae.
Glabretina (1)	Synonymized into *Hystricurus*	
Pachycranium (2)	Retained	
Parahystricurus (6)	Retained	
Rollia (1)	Excluded	
Etheridgaspis (1)	Excluded	
Holubaspis (1)	Excluded	
Metabowmania (1)	Excluded	
Natmus (2)	Excluded	
Nyaya (6)	Excluded	
Psalikilopsis (1)	Excluded	
Psalikilus (4)	Excluded	
Pseudohystricurus (3)	Excluded	
Taoyuania (3)	Excluded	
Tersella (5)	Excluded	
Amblycranium (2)	Excluded	Some species transferred into *Paramblycranium* n. gen.
Parapelthopeltis (9)	Excluded	Some species transferred into *Pseudoplethopeltis* n. gen.

626

APPENDIX III-2. Species that are assigned to the Hystricuridae. 52 species are formally named and 7 species are in open namenclature. * indicates species for which pygidium is not known.

Genus	Subgenus	Species	Subspecies
Hystricurus	*Hystricurus*	*conicus**	
		oculilunatus	
		exilis	
		crotalifrons	
	Hystricurus?	*sainsburyi*	
	Aequituberculatus	*genalatus*	
		lepidus	
		occipitospinosus	
		minutuberculata	
		ellipticus	
	Triangulocaudatus	*paragenalatus*	
		convexomarginalis	
		ravni	
	Butuberculatus	*globosus*	
		hillyardensis	
		scrofulosus	
		andrewsi	
		*elevatus**	
		*rotundus**	
Hystricurus?		*megalops**	
		*eurycephalus**	
		*granosus**	
		*missouriensis**	
		*penchiensis**	
		amadeusus	
Carinahystricurus n. gen.		*carinatus*	
		triangularia	
		minuocularis	
		tasmanacarinatus	
Glabellosulcatus n. gen.		*koreanicus*	
		*sanduensis**	
		*smithiae**	
Glabellosulcatus?		*crassilimbatus**	
Hillyardina		*semicylindrica*	
		tubularis	
Pachycranium		*faciclunis**	
		*profundus**	
Parahillyardina n. gen.		*sulcata*	
		minuspustulata	
		newfoundlandia	

627

Genus	Subgenus	Species	Subspecies
Parahystricurus		*fraudator**	
		*oculirotundus**	
		pustulosus	*pustulosus**
			*parallelia**
			*taperus**
		*bispicatus**	
Paramblycranium n. gen.		*cornutum*	
		*populum**	
		*taperum**	
Politohystricurus n. gen.		*politus*	*politus*
			convexofrontalis
			convergia
			*longifrontalis**
		*brevispinosus**	
		concavofrontalis	
		pseudopsalikilus	
Pseudoplethopeltis n. gen.		*genacurvus*	
		minuta	
Spinohystricurus n. gen.		*robustus*	
		terescurvus	
		*antiquus**	
Tanybregma		*tasmaniensis**	
		timsheansis	
		paratimsheansis	

APPENDIX III-3. Taxa that are excluded from the Hystricuridae, but still within the concept of the Proetida. * indicates the species for which no pygidium is known.

Family	Subfamily	Genus	Species	Subspecies
?Hystricuridae		Hystricurus?	millardensis	
			paramillardensis	
			armatus	
			sulcatus*	
			longicephalus	
			parascrofulosus	
			paucituberculatus	
			clavus	
?Hystricuridae		Rollia	goodwini*	
			mirabilis	
?Hystricuridae		Amblycranium	variabile	profusum
				flexum*
				rectum*
				parallum*
			convergium	convergium
				paraconvergium*
			inflatum*	
			transversum	
			hystricurusum	
		Amblycranium?	dubium*	

629

APPENDIX III-3. continued.

Family	Subfamily	Genus	Species	Subspecies
?Hystricuridae		*Tersella*	*strobilata*	
			novozemelica	
			sulcata	
			paichoica	
			magnaocula	
			truncata	
		Tersella?	*altaica**	
?Hystricuridae		*Paratersella* n. gen.	*mediasulcata*	
			eos	
			flexa*	
			acutula*	
		Paratersella?	*acuta**	
			obscura*	
?Hystricuridae		*Flectihystricurus* n. gen.	*felctimembrus*	
			acumennasus	
		Flectihystricurus?	*wilsoni*	
?Hystricuridae	Hyperbolochilinae n. subfam.	*Hyperbolochilus*	*marginauctus*	*marginauctus**
				angustolimbus*
				concavosulcatus*
				convexofrontalus*
			platysus*	
			convexus*	
			expansus*	
		Hyperbolochilus?	*cristus**	
		Metabowmania	*latilimbata**	

630

APPENDIX III-3. continued.

Family	Subfamily	Genus	Species	Subspecies
?Hystricuridae	Psalikilinae n. subfam.	*Psalikilus*	*typicus*	
			pikus	
			spinosus*	
			paraspinosus	
	?Psalikilinae	*Natmus*	*victus**	
			tuberus*	
			tuberculatus*	
		Psalikilopsis	*cuspidicauda*	
			brachyspinosus	
?Dimeropygidae		*Pseudohystricurus*	*obesus*	
			bathysulcatus*	
		Pseudohystricurus?	*parvus*	
			orbus*	
		Heckethornia n. gen.	*borderinnensis*	
			alticapitus	
		Heckethornia?	*linearus*	
?Toernquistiidae		*Eurylimbatus* n. gen.	*amplissimus*	
			sphaera	
			acutus*	
Telephinidae		*Pyraustocranium*	*orbatum**	
Bathyuridae		*Tasmanaspis*	*lewisi**	

631

APPENDIX III-4. Taxa that were previously referred to the Hystricuridae, but are revised to be included within the Ptychopariida.

Superfamily	Family	Subfamily	Genus	Species
Olenacea	?Olenidae	?Pelturinae	*Paenebeltella*	*vultulata*
Uncertain	?Alokistocaridae		*Patomaspis?*	*secundus**
	?Eulomidae		*Etheridgaspis*	*carolinensis**
			Pseudoetheridgaspis	*typica*
				*cylindricus**
	?Lonchocephalidae		*Pseudotalbotina*	*ovalis**
	Elviniidae		*Onchocephalus*	*generectus**
	Plethopeltidae		*Paraplethopeltis*	*obesa*
				*depressa**
				seelyi
				*nudus**
				*carinifera**
				*cordai**
	Uncertain		*Holubaspis*	*perneri**
				paraperneri
			Nyaya	*nyaensis*
				*orientalis**
			Taoyuania	*xenisma**
				*affinis**
				*nobilis**
			Chattertonella	*abruptus*

632

APPENDIX III-5. Number of species of each genus of the Hystricuridaein accorinding to their paleogeographic distribution. NTA: North of Transcontinental Arch, STA: South of Transcontinental Arch. "?" indicates number of species that are described in open nomenclature.

GENUS	NTA	STA	Greenland	Kazakhstan	Sino-Korean	Australia	South China
Hystricurus	15 (?2)	9 (?1)	2		4 (?4)	3 (?2)	
Carinahystricurus	3					1	
Glabellosulcatus	1 (?1)	2 (?1)	1 (?1)		1	1	1
Hillyardina	1					1	
Pachycranium	1	1					
Parahillyardina	2	2					
Parahystricurus	4	1					
Paramblycranium	3					1	
Politohystricurus	4						
Pseudoplethopeltis	2	2					
Spinohystricurus	3			1			
Tanybregma					1	3	
Total	39	17	3	1	6	10	1

633

APPENDIX III-6. List of all species described in Chapter III that have been referred to the Hystricuridae before the taxonomic revision and their new names after the taxonomic revision. The species are listed by alphabetical order of the authors.

Reference	Species	Illustrations	Revised name	Remarks	Locality	Age
Apollonov and Chugaeva (1983)	*Batyraspis inceptoris*	pl. 10, figs. 5, 6, text-fig. 24	*Taoyuania xenisma*		Kazakhstan	early Tremadocian
Balashova (1961)	*Hystricurus conicus*	pl. 1, figs. 12, 13 [only]	*Hystricurus (Hystricurus?) sainsburyi*	questionable	Kazakhstan	Ordovician
Benedetto (1977)	*Pseudotalbotina ovalis*	pl. 1, figs. 1-5	*Pseudotalbotina ovalis*		Santa Rosita Formation, Aregentina	Tremadocian
Berg and Ross (1959)	*Hystricurus oculilunatus*	pl. 21, fig. 2	*Hystricurus (Hystricurus) crotalifrons*		Manitou Formation, Colorado	Zone E or F
	Hystricurus ? sp. aff. H. ? genacurvus	pl. 21, fig. 21 [only]	*Pseudoplethopeltis genacurvus*			
		pl. 21, fig. 23 [only]	*Pseudoplethopeltis minuta*			
Billings (1859)	*Bathyurus conicus*	fig. 12c	*Hystricurus (Hystricurus) conicus*		Beekmantown Group, Quebec	Early Ordovician
	Bathyurus cordai	fig. 26	*Paraplethopeltis cordai*	re-illustrated by Boyce, (1989, pl. 17, figs. 1-4)	Levi Formation, Quebec	Tremadocian
Boyce (1983a)	*Hystricurus* sp. nov.	pl. 12, figs. 7, 8	*Hystricurus (Hystricurus) oculilunatus*			
Boyce (1983b)	*Hystricurus pseudoculilunatus*	pl. 8, figs. 4-8	*Hystricurus (Hystricurus) oculilunatus*		Boat harbour Formation, western Newfoundland	*Randaynia saundersi* Zone (=Zone F)
	Hystricurus oculilunatus	pl. 6, figs. 7, 8, pl. 7, figs. 1-8, pl. 8, figs. 1-3	*Hystricurus (Hystricurus) crotalifrons*			
	Paraplethopeltis seelyi	pl. 10, figs. 2-7, pl. 11, figs. 1, 2	*Paraplethopeltis seelyi*			

634

APPENDIX III-6. continued.

Reference	Species	Illustrations	Revised name	Remarks	Locality	Age
Boyce (1989)	*Hillyardina levis*	pl. 6, figs. 4, 5, pl. 7, figs. 6-10 [only]	*Parahillyardina minuspustulata*		Boat harbour Formation, western Newfoundland	*Randaynia saundersi* Zone (=Zone F)
		pl. 6, fig. 6 [only]	*Parahillyardina newfoundlandia*			
		pl. 6, figs. 1-3, 7-10, pl. 7, figs. 1-5 [only]	*Hyperbolochilus marginauctus concavosulcatus*			
	Hillyardina minuspustulata	pl. 4, figs. 1-3, 9, pl. 5, figs. 6-9 [only]	*Parahillyardina minuspustulata*			
		pl. 4, figs. 4-8, pl. 5, figs. 1-5 [only]	*Pachycranium profundus*			
	Hystricurus deflectus	pl. 12, figs. 1-10, pl. 13, figs. 1-10.	*Hystricurus (Hystricurus) oculilunatus*			
	Hystricurus oculilunatus	pl. 8, figs. 1-4 [only]	*Hystricurus (Hystricurus) exilis*			
		pl. 8, figs. 5-8, pl. 9, figs. 7-10, pl. 10, figs. 1-10, pl. 11, figs. 1-11 [only]	*Hystricurus (Hystricurus) crotalifrons*	pl. 9, figs. 1-6 originally illustrated by Whitfield (1889)		
	Parahystricurus smithiae	pl. 16, figs. 7-10 [only]	*Parahillyardina minuspustulata*			
		pl. 14, figs. 1-8, pl. 15, figs. 1-8, pl. 16, figs. 1-6 [only]	*Glabellosulcatus smithiae*			
	Paraplethopeltis seelyi	pl. 17, figs. 5-7, pl.18, figs. 1-3, 7, 8, pl. 19, figs. 1-4, pl. 20, figs. 1, 2	*Paraplethopeltis seelyi*			

APPENDIX III-6. continued.

Reference	Species	Illustrations	Revised name	Remarks	Locality	Age
Bridge and Cloud (1947)	*Paraplethopeltis obesa*	pl. 2, figs. 1-7, 12-14	*Paraplethopeltis obesa*		Ellenburger Formation, central Texas	early Ordovidian
	Paraplethopeltis depressa	pl. 2, figs. 8-11	*Paraplethopeltis depressa*		Ellenburger Formation, central Texas	early Ordovidian
Burskyi (1970)	*Nyaya novozemelica*	pl. 2, figs. 1, 3	*Tersella novozemelica*		Sokolysky horizon, Russia	early Ordovician
	Nyaya paichoica	pl. 2, figs. 4, 6	*Tersella paichoica*			
	Nyaya sokoliensis	pl. 3, fig. 5	*Tersella paichoica*			
	Nyaya? sp.	pl. 2, fig. 2	*Tersella paichoica*			
	Tersella (?) *magnaoculus*	pl. 3, figs. 1, 2, 4	*Tersella magnaocula*			
	Tersella (?) *novozemelica*	pl. 3, fig. 3	*Tersella novozemelica*			
	Tersella sp.	pl. 3, fig. 7	*Tersella paichoica*			
Choi *et al.* (1994)	*Hystricurus* sp. cf. *H. megalops*	fig. 2h [only]	*Tersella truncata*		Mungok Formation, South Korea	*Protopliomerops* Zone (late Tremadocian)
		fig. 2I [only]	*Tersella truncata*	questionable	Mungok Formation, South Korea	*Protopliomerops* Zone (late Tremadocian)
Cleland (1900)	*Bathyurus ellipticus*	pl. 16, figs. 5, 6	*Hystricurus (Aequituberculatus) ellipticus*		Calciferous Rocks, New York	?
Cloud and Barnes (1948)	*Hystricurus* aff. *H. missouriensis*	pl. 38, fig. 19 [only]	*Hystricurus*? *longicephalus*	questionable	Ellenburger Group, central Texas	higher than Sy Zone
		pl. 38, fig. 20 [only]	*Hystricurus (Butuberculatus) scrofulosus*	questionable		
		pl. 38, fig. 17 [only]	*Paraplethopeltis obesa*			
	Hystricurus sp.	pl. 38, fig. 15	*Hystricurus*? *missouriensis*	questionable		
	Paraplethopeltis obesa	pl. 38, figs. 4-9, 11-13	*Paraplethopeltis obesa*			
	Paraplethopeltis?	pl. 38, fig. 14	*Paraplethopeltis depressa*			

636

APPENDIX III-6. continued.

Reference	Species	Illustrations	Revised name	Remarks	Locality	Age
Corbett and Bank (1974)	*Hystricurus* sp.	pl. 1, fig. 21 [only]	*Carinahystricurus tasmanacarinatus*		Florentine Valley Formation, Tasmania, Australia	Lancefieldian (late Tremadocian to early Arenigian)
		pl. 1, fig. 20 [only]	*Benthamaspis abdita*	questionable		
	Hystricurus	pl. 1, fig. 26 [only]	*Etheridgaspis carolinensis*			
		pl. 1, fig. 25, 27 [only]	*Etheridgaspis carolinensis*	questionable		
Cullison (1944)	*Hystricurus abruptus*	pl. 34, figs. 45, 46 [only]	*Omuliovia?* sp.		Rich Fountain Formation, Missouri	Jeffersonian (?Hc Zone)
		pl. 34, figs. 48, 49 [only]	*Chattertonella abruptus*			
	Rollia goodwini	pl. 34, figs. 33-35	*Rollia goodwini*			
Dean (1989)	*Hillyardina* sp.	pl. 16, figs. 3, 8	*Hyperbolochilus marginauctus concavosulcatus*		Survey Peak Formation, Alberta	Zone E
	Hyperbolochilus cf. *H. expansus*	pl. 17, fig. 7 [only]	*Hyperbolochilus marginauctus concavosulcatus*			
		pl. 16, figs. 7, 9, 10 [only]	*Hyperbolochilus? paraexpansus*	questionable		
	Hyperbolochilus? sp.	pl. 17, figs. 2, 5, 8	*Hyperbolochilus marginauctus convexofrontalis*			Zone F
	Hystricurus oculilunatus	pl. 15, figs. 1, 2 [only]	*Hystricurus (Hystricurus) exilis*	originally illustrated by Kobayashi (1955, pl. 6, fig. 4)	McKay Group, British Columbia	*Kainella-Evanaspis* fauna (Zone D – E)
		pl. 14, fig. 2 [only]	*Hystricurus? clavus*		Survey Peak Formation, Alberta	Zone E
		pl. 14, figs. 5, 6 [only]	*Paratersella mediasulcata*	questionable		
		pl. 14, fig. 4, pl. 15, fig. 12 [only]	*Paratersella eos*			

APPENDIX III-6. continued.

Reference	Species	Illustrations	Revised name	Remarks	Locality	Age
Dean (1989)	*Hystricurus oculilunatus*?	pl. 14, figs. 5, 6 [only]	*Rollia mirabilis*	questionable	Survey Peak Formation, Alberta	Zone E
	Hystricurus cf. *H.* sp. A	pl. 14, fig. 10 [only]	*Hystricurus (Hystricurus) conicus*	questionable		
		pl. 14, fig. 14 [only]	*Hystricurus (Hystricurus) crotalifrons*	questionable		
	Hystricurus cf. *H.* sp. B	pl. 14, figs. 9, 12, 15	*Paratersella mediasulcata*			
	Hystricurus sp.	pl. 14, fig. 13 [only]	*Hystricurus*? *clavus*			Zone E
		pl. 14, fig. 11, pl. 15, figs. 10, 11 [only]	*Flectihystricurus flectimembrus*			Zone E to F
		pl. 15, figs. 9, 10, 11, 14 [only]	*Flectihystricurus flectimembrus*			Zone E
		pl. 14, fig. 3 [only]	*Paraplethopeltis cordai*	questionable		
	Ischyrotoma cf. *I. eos*	pl. 28, figs. 1-3, 5, 6	*Paratersella eos*			
	Metabowmania latilimbata	pl. 17, figs. 1, 4, 11	*Metabowmania latilimbata*			
	Metabowmania sp.	pl. 16, figs. 1, 2, 4-6	*Metabowmania* sp.			
Demeter (1973)	*Pseudohystricurus obesus*	pl. 6, figs. 13, 14	*Pseudohystricurus obesus*		Fillmore Formation, Utah	Zone F
Desbiens *et al.* (1996)	*Hystricurus conicus*	pl. 3, figs. 8, 12 [only]	*Hystricurus (Hystricurus) conicus*	questionable	Beauharnois Formation, Quebec	late Jeffersonian to early Cassinian (Zone G2 – H)
		pl. 3, figs. 4, 10, 15 [only]	*Hystricurus (Hystricurus) crotalifrons*	questionable		
		pl. 2, fig. 15, pl. 3, figs. 1-3, 5-7, 11 [only]	*Hystricurus (Hystricurus) crotalifrons*			

638

APPENDIX III-6. continued.

Reference	Species	Illustrations	Revised name	Remarks	Locality	Age
Dwight (1884)	*Bathyurus? crotalifrons*	figs. 4-6	*Hystricurus (Hystricurus) crotalifrons*		Calciferous Rocks, New York	
Endo (1932)	*Bathyurus* sp. (?) indetermined	pl. 26, fig. 1	*Hystricurus? granosus*		Wuting Formation, Manchoukuo, northeast China	
Endo (1935)	*Hystricurus convexus*	pl. 15, figs. 6-8	*Leiostegium convexium*		Wuting Formation, Manchoukuo, northeast China	*Adelograptus-Clonograptus* Zone and *Callograptus taitzehoensis* Zone
	Hystricurus granosus	pl. 13, figs. 10, 11	*Hystricurus? granosus*	re-illustrated by Lu *et al.* (1965, pl. 34, fig. 8)		
		pl. 13, figs. 16-20 [only]	*Annamitella rectangularia*			
Fisher (1954)	*Hystricurus ellipticus*	pl. 4, figs. 12, 13	*Hystricurus (Aequituberculatus) ellipticus*		Tribes Hill Formation, New York	Zone B
Flower (1969)	*Hystricurus* cf. *conicus*	pl. 7, fig. 4	*Hystricurus elevatus*	questionable	Fort Ann Formation, New York	Demingian (Zone D-F)
	Hystricurus sp.	pl. 2, fig. 5	*Hystricurus elevatus*			
	Paraplethopeltis carinefera	pl. 6, figs. 1-4, 19, 34	*Paraplethopeltis carinefera*		Smith Basin Limestone, New York	Early Ordovician
Fortey (1983)	*Hyperbolochilus?* sp. nov.	pl. 25, figs. 10, 11	*Hyperbolochilus ?* n. sp. A		*Symphysurina* Conglomerate, Cow head Group, western Newfoundland	Sy Zone
	Hystricurus paucituberculatus	pl. 23, figs. 1-7	*Hystricurus? paucituberculatus*			
Fortey and Peel (1989)	*Hystricurus (Hystricurus) scrofulosus*	fig. 6A-6M	*Hystricurus (Butuberculatus) scrofulosus*		Christian Elv Formation, western North Greenland	*Rossodus manitouensis* Zone (BX to LK Zone)
	Hystricurus (Paraplethopeltis) sp. nov. A	figs. 7A-7G	*Hystricurus? parascrofulosus*			

APPENDIX III-6. continued.

Reference	Species	Illustrations	Revised name	Remarks	Locality	Age
Fortey *et al.* (1982)	*Hystricurus millardensis*	pl. 3, fig. 10	*Hystricurus? paramillardensis*		*Symphysurina* Conglomerate, Cow head Group, western Newfoundland	Sy Zone
	Hystricurus sp. nov.	pl. 3, figs. 14, 17	*Hystricurus? paucituberculatus*			
	Pseudohystricurus sp. aff. *P. rotundus*	pl. 2, figs. 17, 24 [only]	*Hystricurus (Hystricurus) oculilunatus*			
		pl. 3, figs. 12, 15 [only]	*Parahystricurus oculirotundus*			
Gobbett (1960)	*Hystricurus wilsoni*	text-fig. 6, pl. 15, figs. 1-14	*Flectihystricurus? wilsoni*		Lower Oslobreen Limestone, Spitsbergen	Sy to LK Zone (?)
Heller (1954)	*Hystricurus deflectus*	pl. 18, fig. 6	*Hystricurus (Hystricurus) oculilunatus*		Roubidoux Formation, Missouri	Demingian (Zone D – F)
	Hystricurus elevatus	pl. 18, figs. 1-3, 10-12	*Hystricurus elevatus*			
	Hystricurus sp.	pl. 18, figs. 7, 8 [only]	*Hystricurus (Hystricurus) oculilunatus*			
		pl. 18, fig. 9 [only]	*Hystricurus elevatus*			
		pl. 18, fig. 18 [only]	*Hystricurus (Hystricurus) crotalifrons*			
		pl. 18, figs. 4, 5 [only]	*Hystricurus paratimsheansis*	questionable		
	Jeffersonia bridgei	pl. 18, fig. 16 [only]	*Tasmanaspis lewisi*			
	Paraplethopeltis minuta	pl. 18, figs. 13-15	*Pseudoplethopeltis minuta*			

APPENDIX III-6. continued.

Reference	Species	Illustrations	Revised name	Remarks	Locality	Age
Hintze (1953)	*Clelandia utahensis*	pl. 4, figs. 15a, 15b [only]	*Chattertonella abruptus*		Fillmore Formation, Utah	Zone B
	Dimeropygiella?	pl. 19, fig. 9	*Hheckethornia alticapitis*			Zone H
	Hillyardina sp. A	pl. 8, figs. 5, 6	*Hyperbolochilus marginauctus angustolimbus*			Zone F
	Hystricurus genalatus	pl. 6, figs. 1-4, 6 [only]	*Hystricurus (Aequituberculatus) lepidus*			Zone B
		pl. 6, fig. 5 [only]	*Hystricurus (Aequituberculatus) occipitospinosus*			
	Hystricurus lepidus	pl. 7, figs. 12a-12c [only]	*Hystricurus (Aequituberculatus) lepidus*			
		pl. 7, figs. 10, 11 [only]	*Politohystricurus brevispinosus*			
	Hystricurus millardensis	pl. 6, figs. 17-21	*Hystricurus? millardensis*			
	Hystricurus paragenalatus	pl. 6, figs. 12-14	*Hystricurus (Triangulocaudatus) paragenalatus*			
	Hystricurus politus	pl. 6, fig. 8 [only]	*Politohystricurus politus politus*			
		pl. 6, figs. 7a, 7b [only]	*Politohystricurus politus convexofrontalis*			
		pl. 6, figs. 9-11 [only]	*Politohystricurus politus convergia*			
	Hystricurus robustus	pl. 8, figs. 2a-2c	*Spinohystricurus terescurvus*			Zone E
	Hystricurus sp.	pl. 6, figs. 25, 26	*Hystricurus (Aequituberculatus) lepidus*			Zone B

APPENDIX III-6. continued.

Reference	Species	Illustrations	Revised name	Remarks	Locality	Age
Hintze (1953)	*Hystricurus* sp. C	pl. 6, figs. 15 [only]	*Eurylimbatus* sp. nov. B		Fillmore Formation, Utah	Zone E
	Jeffersonia? sp. B	pl. 9, fig. 11 [only]	*Psalikilopsis* sp. nov. A			Zone G1
	Parahystricurus bispicatus	pl. 8, figs. 3a-4c	*Parahystricurus bispicatus*			Zone F
	Parahystricurus aff. *P. fraudator*	pl. 8, fig. 1	*Parahystricurus* sp. nov. A			Zone B
	Paraplethopeltis? genacurvus	pl. 7, figs. 1-5	*Pseudoplethopeltis genacurvus*			Zone C
	Paraplethopeltis ? generectus	pl. 7, figs. 9a, 9b [only]	*Pseudoplethopeltis minuta*			
		pl. 7, figs. 6-8, [only]	*Onchopeltis generectus*			
	Psalikilus paraspinosum	pl. 9, figs. 4, 5	*Psalikilus paraspinosus*			Zone G2
	Psalikilus pikum	pl. 9, fig. 1	*Psalikilus pikus*			Zone H
	Psalikilus spinosum	pl. 9, figs. 3, 6 [only]	*Psalikilus spinosus*			Zone G1
		pl. 9, figs. 7a-7c [only]	*Psalikilopsis* sp. nov. A			Zone G1
	Psalikilus typicum	pl. 9, fig. 2, pl. 20, fig. 15	*Psalikilus typicus*			Zone G2
	undetermined gen. and sp. B	pl. 13, figs. 14, 17 [only]	*Benthamaspis obreptus*			
		pl. 13, figs. 13, 15, 16 [only]	*Benthamaspis?* sp.			
	undetermined gen. and sp. C	pl. 9, fig. 14 [only]	*Benthamaspis abdita*			
		pl. 9, figs. 13, 15 [only]	*Benthamaspis?* sp.			
		pl. 19, figs. 11-13	*Heckethornia alticapitis*			Zone G2 to h

642

APPENDIX III-6. continued.

Reference	Species	Illustrations	Revised name	Remarks	Locality	Age
Hintze (1953)	unassigned pygidium	pl. 8, fig. 13	*Parahillyardina sulcata*		Fillmore Formation, Utah	Zone E
	unassigned pygidium	pl. 20, fig. 16	*Tasmanaspis lewisi*	questionable		Zone G1
Jell (1985)	*Parahystricurus* sp. cf. *P. fraudator*	pl. 20, figs. 1-3B	*Glabellosculcatus sanduensis*		Digger Island Formation, Victoria, Australia	Lancefieldian (early Tremadocian)
	Natmus victus	pl. 21, figs. 1-15.	*Natmus victus*			
	Natmus tuberus	pl. 20, figs. 9-12	*Natmus tuberus*			
Jell and Stait (1985a)	*Etheridgaspis carolinensis*	fig. 2, pl. 14, figs. 1-15, pl. 18, fig. 15	*Etheridgaspis carolinensis*	see Jell and Stait (1985a) for synonymy to date	Caroline Creek Sandstone, Tasmania. Australia	early Bendigonian (early Arenigian)
Jell and Stait (1985b)	*Hystricurus lewisi*	pl. 2, figs. 5A, 5B [only]	*Hystricurus? megalops*		Florentine Valley Formation, Tasmania, Australia	Lancefieldian (late Tremadocian to early Arenigian)
		pl. 2, figs. 6, 7, 10 [only]	*Hystricurus?* sp. aff. *H.? missouriensis*			
		pl. 2, fig. 8 [only]	*Hillyardina tubularis*			
		pl. 2, fig. 12, [only]	*Tanybregma paratimsheansis*	questionable		
		pl. 2, figs. 11, 13-15, pl. 3, figs. 9, 10, 13, [only]	*Carinahystricurus tasmanacarinatus*			
		pl. 2, figs. 10A, B [only]	*Etheridgaspis carolinensis*			
		pl. 2, figs. 1-4 [only]	*Tasmanaspis lewisi*			

643

APPENDIX III-6. continued.

Reference	Species	Illustrations	Revised name	Remarks	Locality	Age
Jell and Stait (1985b)	*Hystricurus penchiensis*	pl. 1, figs. 1, 4, 5, 6, 7, 8 (only pygidial specimen; UTGD 122508), 9, 10, 11, 13, 15 (only two librigenal specimens; UTGD 122517, UTGD 122518) [only]	*Tanybregma timsheansis*		Florentine Valley Formation, Tasmania, Australia	Lancefieldian (late Tremadocian to early Arenigian)
		pl. 1, figs. 2, 3, 8 (only cranidial specimen; UTGD 122509), 12, 15 (only pygidial specimen; UTGD 122516) [only]	*Tanybregma paratimsheansis*			
		pl. 1, fig. 15 (only pygidial specimen; UTGD 122516) [only]	*Tanybregma paratimsheansis*	questionable		
		pl. 1, fig. 14, [only]	*Tanybregma paratimsheansis*	questionable		
	Hystricurus sp. cf. *H. robustus*	pl. 3, figs. 8, 11, 12, pl. 4, figs. 1, 3, 4, 6 [only]	*Hillyardina tubularis*			
		pl. 4, figs. 2, 5, 7[only]	*Hillyardina tubularis*	questionable		
		pl. 3, fig. 14, [only]	*Tanybregma tasmaniensis*	questionable		

644

APPENDIX III-6. continued.

Reference	Species	Illustrations	Revised name	Remarks	Locality	Age
Jell and Stait (1985)	*Tanybregma tasmaniensis*	pl. 3, figs. 1-7 [only]	*Tanybregma tasmaniensis*		Florentine Valley Formation, Tasmania, Australia	Lancefieldian (late Tremadocian to early Arenigian)
		pl. 8, fig. 7 (left cranidial specimen only) [only]	*Tanybregma timsheansis*			
Kim and Choid (1997)	*Hystricurus megalops*	fig. 3O [only]	*Tersella truncata*		Mungok Formation, South Korea	*Protopliomerops* Zone (late Tremadocian)
		fig. 3P [only]	*Tersella truncata*	questionable		
Kindle (1982)	*Hystricurus* sp.	pl. 1.5, fig. 22	*Hystricurus? paucituberculatus*		Cow head Group, western Newfoundland	Sy Zone
Kobayashi (1934)	*Hystricurus eurycephalus*	pl. 6, fig. 10	*Hystricurus? eurycephalus*	re-illustrated by Shergold (1991, pl. 6, fig. 22)	Mungok Formation, South Korea	*Kayseraspis* Zone (?Pc Zone)
	Hystricurus megalops	pl. 6, figs. 8, 9	*Hystricurus? megalops*			
Kobayashi (1940)	*Tasmanaspis lewisi*	pl. 11, fig. 3 [only]	*Tasmanaspis lewisi*	re-illustrated by Jell and Stait (1985, pl. 2, fig. 2)	Florentine Valley Formation, Tasmania, Australia	Lancefieldian (late Tremadocian to early Arenigian)
	Tasmanaspis longus	pl. 11, fig. 5	*Tasmanaspis lewisi*			
Kobayashi (1955)	*Amechilus tuberculatus*	pl. 6, fig. 11	*Metabowmania latilimbata*	re-illustrated by Dean (1989, pl. 17, figs. 3, 6)	McKay Group, British Columbia	*Kainella-Evanaspis* fauna (Zone D – E)
	Dimeropygiella eos	pl. 6, fig. 10	*Paratersella eos*	re-illustrated by Dean (1989, pl. 15, figs. 3, 6)		
	Hyperbolochilus expansus	pl. 3, fig. 1	*Hyperbolochilus expansus*	re-illustrated by Dean (1989, pl. 17, figs. 9, 10, 12)		
	Metabowmania latilimbata	pl. 6, fig. 13, pl. 8, fig. 9.	*Metabowmania latilimbata*			
	Vermilionites bisulcatus	pl. 6, fig. 4, pl. 9, fig. 2	*Hystricurus (Hystricurus) exilis*			

645

APPENDIX III-6. continued.

Reference	Species	Illustrations	Revised name	Remarks	Locality	Age
Kobayashi (1960)	*Hystricurus clavus*	pl. 14, fig. 5, 6	*Hystricurus? clavus*		Mungok Formation, South Korea	*Protopliomerops* Zone (?Rs Zone)
	Hystricurus megalops	pl. 13, fig. 20	*Hystricurus? megalops*	questionable		
	Hystricurus cfr. *megalops*	pl. 13, fig. 21	*Tersella truncata*	questionable		
Kuo *et al.* (1982)	*Hystricurus penchiensis*	pl. 1, fig. 8	*Hystricurus? clavus*		Yehli Formation, northeast China	*Koraipsis-Hystricurus* zone (?Rs Zone)
Laurie and Shergold (1996)	*Hystricurus* (*?Guizhouhystricurus*) sp. *indet*	pl. 5, fig. 15 [only]	*Hystricurus? clavus*		Emanuel Formation, western Australia	Be2 of Bendigonian (Pc Zone)
	Hystricurus (*Hystricurus*) sp. cf. *H.* (*H.*) *lewisi*	pl. 5, figs. 9-12	*Hystricurus eurycephalus*			Be1 of Bendigonian (Hc Zone)
Lee and Chatterton (1997a)	*Amblycranium variabile*	figs. 3.5, 7.1-7.3, 7.9 [only]	*Amblycranium variabile profusum*		Garden City Formation, Idaho	Zone E
		figs. 7.4, 7.5 [only]	*Amblycranium convergium paraconvergium*			
		figs. 7.6, 7.7 [only]	*Amblycranium variabile parallelum*			
	Hyperbolochilus cf. *marginauctum*	figs. 7.8, 7.10-7.13	*Hyperbolochilus platysus*			
	Hystricurus? sp. A	figs. 3.2, 5.8, 5.13	*Spinohystricurus terescurvus*			
	Parahystricurus carinatus	figs. 5.2, 5.7, 5.12 [only]	*Spinohystricurus robustus*			
		figs. figs. 5.1, 5.5-5.7, 5.9-5.11 [only]	*Spinohystricurus terescurvus*			
	'*Paraplethopeltis*' n. sp. A	figs. 3.6, 3.7, 8.1-8.4, 8.6, 8.10, 8.11	*Paratersella mediasulcata*			
	Proetide A	figs. 2.1-2.14, 3.1	*Paratersella? obscura*			
Leggs (1976)	*Hystricurus* sp.	pl. 1, fig. 1 [only]	*Hystricurus? megalops*		Emanuel Formation, western Australia	Be2 of Bendigonian (Pc Zone)
		pl. 1, fig. 2 [only]	*Hystricurus? eurycephalus*	questionable		

APPENDIX III-6. continued.

Reference	Species	Illustrations	Revised name	Remarks	Locality	Age
Lisogor (1961)	*Hystricurus antiquus*	pl. 1, fig. 15 [only]	*Spinohystricurus antiquus*		Kazakhstan	late Tremadocian
		pl. 1, fig. 16, 17 [only]	*Spinohystricurus antiquus*	questionable		
Liu (*in* Zhou *et al.*, 1977)	*Taoyuania xenisma*	pl. 49, figs. 1-3	*Taoyuania xenisma*		Panjiazui Formation, South China	early Tremadocian
	Taoyuania? affinis	pl. 49, fig. 4	*Taoyuania affinis*			late Tremadocian
Liu (1982)	*Taoyuania xenisma*	pl. 218, figs. 13-15	*Taoyuania xenisma*		Panjiazui Formation, South China	early Tremadocian
	Taoyuania? affinis	pl. 219, fig. 1	*Taoyuania affinis*			late Tremadocian
Lochman (1965)	*Glabretina andrewsi*	pl. 62, figs. 1-8, 10-18 [only]	*Hystricurus (Butuberculatus) andrewsi*		Deadwood Formation, Montana	Zone D
	Hystricurus sp. undet.	pl. 63, fig. 8	*Paratersella mediasulcatus*	questionable		
Lochman (1966)	*Glabretina* sp.	pl. 62, fig. 33	*Hystricurus (Butuberculatus) andrewsi*	questionable	Deadwood Formation, Montana	Zone G
	Hystricurus crassilimbatus	pl. 65, fig. 41	*Glabellosculcatus? crassilimbatus*	questionable		Zone E
	cf. *Hystricurus*	p. 65, fig. 35	*Hyperbolochilus* ? n. sp. B			Zone E to F
	cf. *Parahystricurus* sp.	pl. 65, fig. 34	*Glabellosculcatus? crassilimbatus*			Zone G
	?*Oculomagnus obreptus*	pl. 62, figs. 3, 5, 6, 7	*Benthamaspis obreptus*			Zone G1
	Psalikilus paraspinosum	pl. 62, fig. 15 [only]	*Psalikilus paraspinosus*			Zone G2
	Psalikilus sp. undet.	pl. 62, fig. 18	*Psalikilus paraspinosus*	questionable		Zone G
Lu (1975)	*Amblycranium* (?) *dubium*	pl. 2, fig. 11, 12, 15 [only]	*Amblycranium? dubium*		Dawan Formation, Central and Southwestern China	late Arenigian
		pl. 2, fig. 13 [only]	*Amblycranium variabile profusum*	questionable		
Lu *et al.* (1965)	(?) *Hystricurus* (?) *kaipingensis*	pl. 34, fig. 9	?*Leiosteigum* sp.		China	Ordovician
		pl. 34, fig. 9	Pliomeridae sp.			

APPENDIX III-6. continued.

Reference	Species	Illustrations	Revised name	Remarks	Locality	Age
Lu et al. (1976)	Hystricurus penchiensis	pl. 7, figs. 10, 12 [only]	Hystricurus? penchiensis		Upper Yehi Formation, northeast China	Callograptus? taitzehoensis zone (?Rs Zone)
		pl. 7, fig. 13 [only]	Hystricurus? clavus			
		pl. 7, fig. 11 [only]	Hystricurus paratimsheansis			
Maximova (1955)	Hystricurus sp	pl. 7, fig. 3 [only]	Taoyuania nobilis	questionable	Siberia	Ordovician
		pl. 7, fig. 4 [only]	Paratersella mediasulcata	questionable		
Maximova (1962)	Hystricurus sp	pl. 1, fig. 12	Taoyuania nobilis	questionable	Siberia	Ordovician
Mergl (1984)	Holubaspis perneri	pl. 4, figs. 1-9, text-fig. 8	Holubaspis paraperneri	see Mergl (1984) for synonymy to date	Trenice Formation, Czech Republic	early Tremadocian
Mergl (1994)	Holubaspis perneri	pl. 4, figs. 3-6 [only]	Holubaspis perneri		Trenice Formation, Czech Republic	early Tremadocian
		pl. 4 figs. 1, 2, 7-11 [only]	Holubaspis paraperneri			
Ogienko (in Abdullaev et al., 1972)	Hystricurus mirabilis	pl. 55, figs. 6-8	Rollia mirabilis		Siberia	Lower Ordovician
		pl. 12, figs. 1, 2 [only]	Rollia mirabilis			
	Hystricurus secundus	pl. 55, figs. 9-11	Patomaspis? secundus			
		pl. 12, fig. 4 [only]	Rollia mirabilis			
Ogienko (1984)	Tersella sulcata	pl. 7, figs. 15, 16	Tersella sulcata		Loparski horizon, south Siberia	Ijacephalus-Nyaya Zone (Tremadocian)
Ogienko (1992)	Hystricurus mirabilis	pl. 5, figs. 5-7	Rollia mirabilis		Kimayskiy horizon, Siberia	Pseudomera-Biolgina Zone (late Arenigian)
	Hystricurus secundus	pl. 5, figs. 8-10	Patomaspis? secundus	questionable		
	Nyaya orientalis	pl. 4, figs. 15-17	Nyaya orientalis		Nyayskiy horizon, Siberia	Ijacephalus-Nyaya Zone (late Tremadocian)
	Tersella sulcata	pl. 5, figs. 1, 2, 4, 7 [only]	Tersella sulcata		Kimayskiy horizon, Siberia	Pseudomera-Biolgina Zone (late Arenigian)
		pl. 5, fig. 3 [only]	Hyperbolochilus ? n. sp. B			

APPENDIX III-6. continued.

Reference	Species	Illustrations	Revised name	Remarks	Locality	Age
Orndoff *et al.* (1988)	*Hystricurus millardensis*	pl. 1, fig. 13	*Hystricurus? millardensis*	questionable	Stonehenge Formation, Virginia	Sy Zone
Park (1993)	*Hystricurus truncatus*	pl. 4, figs. 5, 8 [only]	*Politohystricurus brevispinosus*	questionable	Mungok Formation, South Korea	*Protopliomerops* Zone (late Tremadocian)
		pl. 4, figs. 1-4, 6, 7 [only]	*Tersella truncata*			
		pl. 4, figs. 9, 10 [only]	*Tersella truncata*	questionable		
	Hystricurus sp.	pl. 4, fig. 11	*Hystricurus? megalops*			
Peng (1983)	*Taoyuania nobilis*	pl. 3, fig. 9	*Taoyuania nobilis*		Panjiazui and Shenjiawan Formation, South China	*Leiosteigum* (*Leiostegium*) *constrictum* (Upper Cambrian) to *Onychopyge-Hysterolenus* (early Tremadocian) Assemblage Zone
Peng (1984)	*Pharostomina* cf. *sanduensis*	pl. 9, figs. 9a, b	*Glabellosulcatus sanduensis*	questionable	Panjiazui Formation, hunan, South China	*Onchopyge-Hysterolenus* Assemblage Zone (early Tremadocian)
	Taoyuania nobilis	pl. 9, figs. 1-4, 6 [only]	*Taoyuania nobilis*		Panjiazui and Shenjiawan Formation, South China	*Leiosteigum* (*Leiostegium*) *constrictum* (Upper Cambrian) to *Onychopyge-Hysterolenus* (early Tremadocian) Assemblage Zone
		pl. 9, fig. 5 [only]	*Taoyuania nobilis*	questionable	Panjiazui Formation, South China	*Onychopyge-Hysterolenus* (early Tremadocian) Assemblage Zone

APPENDIX III-6. continued.

Reference	Species	Illustrations	Revised name	Remarks	Locality	Age
Peng (1984)	*Taoyuania* sp.	pl. 9, fig. 7, 8	*Taoyuania affinis*		Panjiazui Formation, hunan, South China	*Apatokephalus-latilimbatus-Taoyuania affinis* Assemblage zone (late Tremadocian)
Peng (1990)	*Pharostomina panjiazuiensis*	pl. 22, figs. 9a, 9b	*Glabellosulcatus sanduensis*	questionable	Panjiazui Formation, Hunan, South Chin	*Onchopyge-Hysterolenus* Assemblage Zone (early Tremadocian)
	Taoyuania affinis	pl. 8, figs. 6-9	*Taoyuania affinis*			*Apatokephalus-latilimbatus-Taoyuania affinis* Assemblage zone (late Tremadocian)
	Taoyuania xenisma	pl. 8, figs. 1-5	*Taoyuania xenisma*			*Onchopyge-Hysterolenus* Assemblage Zone (early Tremadocian)
Petrunina (1973)	*Tersella altaica*	pl. 1, figs. 9, 11	*Tersella? altaica*		west Siberia	Late Tremadoc to Arenig
	Tersella concinna	pl. 1, figs. 4, 14	*Tersella novozemelica*			
	Tersella strobilata	pl. 1, figs. 12, 13, 15	*Tersella strobilata*			
Poulsen (1927)	*Hystricurus longicephalus*	pl. 18, fig. 11	*Hystricurus? longicephalus*		Cass Fjord Formation, northwest Greenland	Zone A or B (Mi to Sy Zone)
	Hystricurus quadratus	pl. 18, figs. 18, 19	*Hystricurus? longicephalus*	questionable	Cape Clay Formation, northwest Greenland	BX to Pa Zone
	Hystricurus ravni	pl. 18, figs. 5, 9 [only]	*Hystricurus (Triangulocaudatus) ravni*		Cass Fjord Formation, northwest Greenland	Zone A or B (Mi to Sy Zone)
		pl. 18, figs. 7, 10 [only]	*Hystricurus? longicephalus*			
		pl. 18, fig. 8 [only]	*Hystricurus (Butuberculatus) scrofulosus*			

650

APPENDIX III-6. continued.

Reference	Species	Illustrations	Revised name	Remarks	Locality	Age
Poulsen (1937)	*Hystricurus armatus*	pl. 2, figs. 3-9	*Hystricurus? armatus*		Antiklinalbugt Formation, East Greenland	Sy to BX Zone
	Hystricurus crassilimbatus	pl. 5, figs. 6-8 [only]	*Glabellosulcatus? crassilimbatus*		Cape Weber Formation, East Greenland	?Zone F to G
	Hystricurus nudus	pl. 2, fig. 10	*Paraplethopeltis nudus*		Antiklinalbugt Formation, East Greenland	Sy to BX Zone
	Hystricurus sulcatus	pl. 2, figs. 1-2	*Hystricurus? sulcatus*		Antiklinalbugt Formation, East Greenland	Sy to BX Zone
Poulsen (1946)	*Hystricurus affinis*	pl. 23, figs. 12, 13	*Tersella strobilata*	questionable	Eleanor River Formation, southern Ellesmere Island	?early Arenigian
	Hystricurus crassilimbatus	pl. 22, fig. 18	*Glabellosulcatus? crassilimbatus*			
Poulsen (*in* Moore, 1959)	*Hystricurus conicus*	figs. 204-4a, b	*Hystricurus (Hystricurus) crotalifrons*		Calciferous Rocks, New York	
Powell (1935)	*Hystricurus oneotensis*	pl. 13, figs. 6-8.	*Hystricurus elevatus*	questionable	Oneota Dolomite, Minnesota	Lower Ordovician
Quian (1994)	Gen. et. sp. *indet.* 2	pl. 34, fig. 1	*Tersella sulcata*	questionable	Changshan Formation, northeast China	Upper Cambrian
Raymond (1913)	*Hystricurus conicus*	pl. 7, fig. 9	*Hystricurus (Hystricurus) conicus*		Beekmantown Group, Quebec	

651

APPENDIX III-6. continued.

Reference	Species	Illustrations	Revised name	Remarks	Locality	Age
Ross (1951)	*Amblycranium cornutum*	pl. 13, figs. 3-5	*Paramblycranium cornutum*		Garden City Formation, Idaho	Zone F
	Amblycranium variabile	pl. 13, figs. 10, 12-14, 17, 18 [only]	*Amblycranium variabile profusum*			Zone E
		pl. 13, figs. 11, 15, 16 [only]	*Amblycranium variabile flexum*			
	Amblycranium? populus	pl. 13, figs. 19-22	*Paramblycranium populum*			
	Amblycranium? sp.	pl. 16, figs. 11, 15, 16	*Amblycranium hystricurusum*			
	Clelandia utahensis	pl. 29, figs. 4, 6, 7 [only]	*Chattertonella abrupta*			Zone B
	Hillyardina semicylindrica	pl. 16, figs. 1, 3-7, 9 [only]	*Hillyardina semicylindrica*			Zone F
		pl. 16, figs. 2, 8 [only]	*Hyperbolochilus marginauctus marginauctus*			
	Hyperbolochilus marginauctum	pl. 17, figs. 26, 27, 30-31, 34-35 [only]	*Hyperbolochilus marginauctus marginauctus*			
		pl. 17, figs. 24-25 [only]	*Hyperbolochilus platysus*			
	Hystricurus acumennasus	pl. 11, figs. 17, 18 [only]	*Flectihystricurus flectimembrus*			
		pl. 11, figs. 6, 7, 10, 11, 12, 15 [only]	*Flectihystricurus acumennasus*			
	Hystricurus contractus	pl. 10, figs. 4, 6, 7, 10	*Hystricurus? missouriensis*			
	Hystricurus flectimembrus	pl. 10, figs. 25, 26, 29-33, pl. 11, figs. 16, 21-33	*Flectihystricurus flectimembrus*			

APPENDIX III-6. continued.

Reference	Species	Illustrations	Revised name	Remarks	Locality	Age
Ross (1951)	*Hystricurus genalatus*	pl. 8, figs. 1-6 [only]	*Hystricurus (Aequituberculatus) genalatus*		Garden City Formation, Idaho	Zone B
		pl. 8, figs. 7-10, 12, 13 [only]	*Hystricurus (Aequituberculatus) lepidus*			
		pl. 8, fig. 11 [only]	*Hystricurus (Aequituberculatus) minutuberculata*			
	Hystricurus oculilunatus	pl. 10, figs. 1-3, 5 [only]	*Hystricurus (Hystricurus) oculilunatus*			Zone F
		pl. 10, figs. 8, 9, 12 [only]	*Hystricurus (Hystricurus) exilis*			
	Hystricurus paragenalatus	pl. 8, figs. 14-26	*Hystricurus (Triangulocaudatus) paragenalatus*			Zone B
	Hystricurus politus	pl. 9, figs. 23, 24, 28, pl. 15, figs. 1-6 [only]	*Politohystricurus politus politus*			
		pl. 9, figs. 27, 32, 33 [only]	*Politohystricurus politus longifrontalis*			
	Hystricurus robustus	pl. 10, figs. 13, 16, 20 [only]	*Spinohystricurus robustus*			Zone E
		pl. 10, figs. 11, 14, 15, pl. 14, fig. 27 [only]	*Spinohystricurus terescurvus*			
	Hystricurus sp. A	pl. 9, figs. 31, 34, 37	*Hystricurus (Hystricurus) conicus*	questionable		
	Hystricurus sp. B	pl. 10, figs. 18, 19, 23 [only]	*Paratersella mediasulcata*			
	Hystricurus? sp. C	pl. 10, figs. 17, 21, 22	*Eurylimbatus* sp. nov. A			
	Hystricurus sp. D	pl. 9, figs. 35, 36, 38-41	*Hystricurus (Butuberculatus) hillyardensis*			Zone A

APPENDIX III-6. continued.

Reference	Species	Illustrations	Revised name	Remarks	Locality	Age
Ross (1951)	Hystricurus? sp. E	pl. 15, figs. 10, 11, 13, 14	Pseudoplethopeltis minuta		Garden City Formation, Idaho	Zone unknown
	Hystricurus? sp. F	pl. 15, figs. 7-9	Politohystricurus politus convexofrontalis			Zone B
	Hystricurus? sp. G	pl. 14, figs. 1-3	Chattertonella abruptus			
	Hystricurus? sp. H	pl. 14, figs. 11, 14, 15 [only]	Hystricurus (Triangulocaudatus) paragenalatus	questionable		
		pl. 14, figs. 9, 10, 13 [only]	Hystricurus (Butuberculatus) hillyardensis	questionable		
	Hystricurus? sp. I	pl. 17, figs. 1-3	Onchopeltis? n. sp.			Zone C
	Pachycranium faciclunis	pl. 16, figs. 12, 13, 17-21, 23, 24, 29 [only]	Pachycranium faciclunis			Zone F
	Pachycranium? sp.	pl. 17, figs. 6, 14 [only]	Carinahystricurus carinatus			Zone C
		pl. 17, figs. 4, 5, 9-11, 15 [only]	Pseudoplethopeltis genacurvus			
	Paenebeltella vultulata	pl. 18, figs. 1, 2, 5, 6, pl. 19, fig. 10	Paenebeltella vultulata	line-drawing of holotype figured by henningsmoen (1957, pl. 2, fig. 3)		Zone E
	Parahystricurus carinatus	pl. 13, 23-26, 27, 30-32, 35-37	Carinahystricurus carinatus			
	Parahystricurus fraudator	pl. 12, figs. 1-16	Parahystricurus fraudator			Zone F
	Parahystricurus oculirotundus	pl. 12, figs 33-49	Parahystricurus oculirotundus			
	Parahystricurus pustulosus	pl. 12, figs. 17-32 [only]	Parahystricurus pustulosus pustulosus			Zone F
		pl. 14, figs. 23, 24, 26 [only]	Parahystricurus pustulosus parallelia			

APPENDIX III-6. continued.

Reference	Species	Illustrations	Revised name	Remarks	Locality	Age
Ross (1951)	*Parahystricurus*? sp. A	pl. 14, figs. 5, 8, 12	*Pseudohystricurus parallelia*		Garden City Formation, Idaho	Zone B
	Parahystricurus? sp. B	pl. 14, figs. 4, 6, 7	*Hystricurus (Triangulocaudatus) paragenalatus*	questionable		
	Parahystricurus? sp. C	pl. 28, figs. 17, 18, 21, 22	*Pseudohystricurus* ? sp. A			Zone F
	Platycolpus? sp.	pl. 29, figs. 22, 23, 25-34	*Benthamaspis abdita*			Zone G2
	Pseudohystricurus rotundus	pl. 16, figs. 32, 33, 35-37	*Hystricurus rotundus*			Zone A
	Pseudohystricurus sp.	pl. 16, figs. 26, 27, 31	*Glabellosulcatus*? *crassilimbatus*			Zone E
	Psalikilus typicum	pl. 11, 1-5, 8, 9, 13, 14	*Psalikilus typicus*			Zone G
	Psalikilus? sp.	pl. 13, figs. 28, 29, 33, 34, pl. 30, figs. 1-3	*Psalikilopsis brachyspinosus*			Zone G2
	Pseudohystricurus obesus	pl. 16, figs. 25, 30, 34	*Pseudohystricurus obesus*			Zone F
	Pyraustocranium orbatum	pl. 18, figs. 3, 4, 7, 8, 10-14, 16	*Pyraustocranium orbatum*			
	undetermined genus and species B	pl. 28, figs. 16, 20, 25-28	*Pseudohystricurus* ? sp. A	questionable		
	undetermined genus and species C	pl. 29, figs. 20, 21, 24	*Benthamaspis obreptus*			Zone G1
	unassigned hypostome	pl. 19, figs. 21, 22	*Spinohystricurus robustus*			Zone F
	unassigned hypostome	pl. 19, figs. 23-26	*Spinohystricurus terescurvus*			
	unassigned pygidium	pl. 17, figs. 23, 28, 29, pl. 19, figs. 13, 14, 17	*Hystricurus (Hystricurus) exilis*			Zone F

655

APPENDIX III-6. continued.

Reference	Species	Illustrations	Revised name	Remarks	Locality	Age
Ross (1951)	unassigned pygidium	pl. 9, fig. 1	*Hystricurus (Triangulocaudatus) paragenalatus*		Garden City Formation, Idaho	Zone B
	unassigned pygidium	pl. 9, figs. 2-5, 7-10, 12, 18	*Hystricurus (Aequituberculatus) lepidus*			
	unassigned pygidium	pl. 9, figs. 6, 11, 17	*Hystricurus (Aequituberculatus) minutuberculata*			
	unassigned pygidium	p. 19, figs. 34, 38	*Hillyardina semicylindrica*			Zone F
	unassigned pygidium	pl. 9, figs. 13, 19	*Politohystricurus politus politus*			Zone B
	unassigned pygidium	pl. 19, figs. 6, 11, 15	*Spinohystricurus robustus*			Zone E
	unassigned pygidium	pl. 19, figs. 32, 35	*Paramblycranium cornutum*	questionable		Zone F
	unassigned pygidium	pl. 19, figs. 33, 36	*Para*Hillyardina *sulcata*			
	unassigned pygidium	pl. 30, fig. 9	*Flectihystricurus acumennasus*	questionable		
	unassigned pygidium	pl. 30, figs. 11, 15	*Psalikilus typicus*			Zone G2
	unassigned pygidium	pl. 19, figs. 8, 9	*Psalikilus?* sp. A			Zone E
	unassigned pygidium	pl. 19, figs. 12, 16	*Psalikilus?* sp. B			Zone E
	unassigned pygidium	pl. 9, figs. 25, 29, 30	*Pseudohystricurus obesus*			Zone B
	unassigned thoracopygidium	pl. 19, fig. 37	*Parahillyardina sulcata*			Zone F
Ross (1953)	*Psalikilopsis cuspidicauda*	pl. 63, figs. 2-9, 12	*Psalikilopsis cuspidicauda*		Garden City Formation, Idaho	Zone G2
	Pseudohystricurus orbus	pl. 63, figs. 10, 11, 15-23 [only]	*Pseudohystricurus? orbus*			Zone G1

APPENDIX III-6. continued.

Reference	Species	Illustrations	Revised name	Remarks	Locality	Age
Ross (*in* Whittington, 1953)	*Strigigenalis abdita*	pl. 67, figs. 11, 12, 16-18, 21-23, 26, 27	*Benthamaspis abdita*		Garden City Formation, Idaho	Zone G1
Ross (1957)	*Hystricurus* sp.	pl. 43, fig. 21	*Hystricurus (Butuberculatus) andrewsi*		Deadwood Formation, Montana	early Early Ordovician
		pl. 43, figs. 25, 26	*Glabellosulcatus? crassilimbatus*	questionable		
		pl. 43, fig. 22	*Eurylimbatus acutus*	questionable		
Ross (1965)	*Hystricurus? sainsburyi*	pl. 8, figs. 1-3, 5-7. 10, 11	*Hystricurus (Hystricurus?) sainsburyi*		Alaska	Lower Ordovician
Ross (1970)	*Hystricurus* aff. *H. genalatus*	pl. 10, figs. 22-25 [only]	*Hystricurus (Hystricurus) oculilunatus*	questionable	Goodwin Limestone, Nevada	Zone G1(?)
		pl. 10, figs. 26-28 [only]	*Flectihystricurus flectimembrus*			
	Hystricurus cf. *H. oculilunatus*	pl. 10, fig. 35	*Paratersella?* sp. aff. *P.? obscura*			
	Pseudohystricurus sp.	pl. 10, figs. 29-31	*Hystricurus rotundus*			
	unassigned pygidium	pl. 10, figs. 20, 21	*Paenebeltella vultulata*		Pogonip Group, Nevada	unknown
Rozova (1963)	*Nyaya nyaensis*	pl. 2, figs. 12, 13	*Nyaya nyaensis*		Nya (Nyaiskii) horizon, Siberia	Early Ordovician
Rozova (1968)	*Nyaya grata*	pl. 16, figs. 16-22, text-fig. 56	*Nyaya nyaensis*		Nya (Nyaiskii) horizon, Siberia	Early Ordovician
	Nyaya nyaensis	pl. 16, figs. 1-12, text-fig. 54	*Nyaya nyaensis*			
	Nyaya aff. *nyaensis*	pl. 16, figs. 13-15, text-fig. 55	*Nyaya nyaensis*			
	Nyaya sp.	pl. 17, figs. 1-3, text-fig. 57	*Nyaya orientalis*			
Rusconi (1951)	*Hystricurus? corralensis*	fig. 27	*Ptychagnostus aculeatus*		Argentina	Upper Cambrian

APPENDIX III-6. continued.

Reference	Species	Illustrations	Revised name	Remarks	Locality	Age
Shergold (1991)	*Hystricurus* sp. cf. *H. eurycephalus*	pl. 6, figs. 10-15, 18 [only]	*Hystricurus amadeus*		Pacoota Sandstone, Northern Territory, Australia	Warendian (late Tremadocian; ?Rs Zone)
		pl. 6, figs. 16, 17 [only]	*Paramblycranium populum*			
Stitt (1971)	*Hystricurus millardensis*	pl. 8, fig. 18 [only]	*Hystricurus? millardensis*		McKenzie Hill Limestone, Oklahoma	Sy Zone
		pl. 8, fig. 17 [only]	*Hystricurus? paramillardensis*			
Stitt (1983)	*Hystricurus globosus*	pl. 5, figs. 1, 5, 6 [only]	*Hystricurus (Butuberculatus) globosus*		McKenzie Hill Limestone, Oklahoma	BX Zone
		pl. 5, fig. 3 [only]	*Hystricurus (Butuberculatus) globosus*	questionable		
		pl. 5, fig. 4 [only]	*Hystricurus (Butuberculatus) hillyardensis*			
		pl. 5, fig. 2 [only]	*Hystricurus (Aequituberculatus) ellipticus*			
	Hystricurus hillyardensis	pl. 4, figs. 3-6	*Hystricurus (Butuberculatus) hillyardensis*			Sy to BX Zone
	Hystricurus millardensis	pl. 4, fig. 1 [only]	*Hystricurus? sulcatus*	questionable		Sy Zone
		pl. 4, fig. 2 [only]	*Hystricurus? paramillardensis*			
	Hystricurus missouriensis	pl. 5, fig. 7 [only]	*Hystricurus (Aequituberculatus) ellipticus*			BX to Pa Zone
		pl. 5, fig. 8 [only]	*Hystricurus (Aequituberculatus) ellipticus*	questionable		
	Paraplethopeltis genacurva	pl. 2, fig. 10	*Pseudoplethopeltis genacurvus*			

APPENDIX III-6. continued.

Reference	Species	Illustrations	Revised name	Remarks	Locality	Age
Stitt (1983)	*Paraplethopeltis obesa*	pl. 2, fig. 9	*Paraplethopeltis obesa*		McKenzie Hill Limestone, Oklahoma	Pa Zone
Stouge and Boyce (1983)	*Hystricurus oculilunatus*	pl. 12, figs. 5, 6.	*Hystricurus (Hystricurus) crotalifrons*		Newfoundland	Lower Ordovician
	Hystricurus sp. nov.	pl. 13, figs. 5, 6	*Glabellosulcatus smithiae*			
	Paraplethopeltis seelyi	pl. 15, figs. 6-8	*Paraplethopeltis seelyi*			
Taylor and halley (1974)	*Hystricurus millardensis*	pl. 3, figs. 10-16	*Hystricurus? paramillardensis*		Whitefall Formation, New York	Mi Zone
Terrell (1973)	*Amblycranium variabile*	pl. 4, figs. 5, 6	*Amblycranium variabile profusum*		Fillmore Formation, Utah	Zone E
	Hillyardina sp. A	pl. 3, fig. 2 [only]	*Hillyardina semicylindrica*			
		pl. 3, figs. 1, 4 [only]	*Hyperbolochilus marginauctus angustolimbus*			
		pl. 3, fig. 3 [only]	*Hyperbolochilus marginauctus angustolimbus*	questionable		
		pl. 3, fig. 5 [only]	*Tasmanaspis lewisi*	questionable		
	Hystricurus acumenis [= acumennasus]	pl. 1, fig. 1, 4-6, 7 [only]	*Flectihystricurus flectimembrus*			
		pl. 1, fig. 8 [only]	*Hystricurus (Hystricurus) oculilunatus*	questionable		
	Hystricurus flectimembrus	pl. 1, figs. 2, 3, 7	*Flectihystricurus flectimembrus*			
	Hystricurus oculilunatus	pl. 1, figs. 12, 14 [only]	*Hystricurus (Hystricurus) oculilunatus*			
		pl. 1, figs. 15, 16 [only]	*Paratersella mediasulcata*			

APPENDIX III-6. continued.

Reference	Species	Illustrations	Revised name	Remarks	Locality	Age
Terrell (1973)	*Hystricurus* sp. A	pl. 1, figs. 9, 10, 13	*Eurylimbatus* sp. nov. B		Fillmore Formation, Utah	Zone E
	Hystricurus sp. B (?)	pl. 2, fig. 10	*Paratersella triangularia*			
	Hystricurus sp. J	pl. 2, figs. 12, 14, 15	*Paratersella mediasulcata*	questionable		
	Hystricurus (?) sp.	pl. 4, fig. 8	*Flectihystricurus flectimembrus*			
	Paenebeltella vultulata	pl. 5, figs. 2, 3	*Paenebeltella vultulata*			
	Parahystricurus carinatus	pl. 4, figs. 11, 14	*Carinahystricurus carinatus*			
	Parahystricurus pustulosus	pl. 2, fig. 11 [only]	*Parahystricurus pustulosus pustulosus*			
	Parahystricurus sp.	pl. 5, fig. 4	*Parahystricurus fraudator*			
	Parahystricurus pustulosus (?)	pl. 4, fig. 10	*Parahystricurus pustulosus pustulosus*	questionable		
	Parahystricurus cf. *bispicatus*	pl. 5, fig. 5	*Parahystricurus bispicatus*			
	Parahystricurus sp.	pl. 2, figs. 2, 4	*Glabellosulcatus? crassilimbatus*			
	Pseudohystricurus obesus	pl. 5, fig. 1	*Pseudohystricurus obesus*			
	unassigned cranidium	pl. 2, fig. 3	*Paramblycranium populus*			
	unassigned cranidium	pl. 3, fig. 8	*Pseudohystricurus* ? sp. A			
	unassigned pygidium	pl. 5, figs. 12, 13, pl. 6, fig. 5	*Carinahystricurus carinatus*			
	unassigned pygidium	pl. 6, figs. 4, 7, 8, 10, 11	*Parahillyardina sulcata*			
	unassigned pygidium	pl. 5, fig. 14	*Psalikilus* sp. A			
	unassigned pygidium	pl. 6, fig. 9	*Heckethornia borderinnensis*			
	unassigned pygidium	pl. 5, fig. 10	*Psalikilus?* sp. B			

660

APPENDIX III-6. continued.

Reference	Species	Illustrations	Revised name	Remarks	Locality	Age
Timokhin (1989)	*Tersella lenaica*	pl. 7, figs. 6, 7, 8, 9 [only]	*Tersella sulcata*		Nyayskiy horizon, Siberia	Ordovician
	Tersella sulcata	pl. 7, fig. 5	*Tersella sulcata*			
Ulrich (*in* Bridge, 1930)	*Hystricurus missouriensis*	pl. 21, figs. 1, 2	*Hystricurus? missouriensis*		Gasconade Dolomite, Missouri	Gasconidian (Zone B to C)
Vaněk (1965)	*Eulomina mitrata*	pl. 25, figs. 36, 37	*Holubaspis paraperneri*		Trenice Formation, Czech Republic	early Tremadocian
	Holubaspis perneri	23, fig. 12 [only]	*Holubaspis paraperneri*	questionable		
		23, fig. 13-17, pl. 26, figs. 41-46 [only]	*Holubaspis paraperneri*	see Vanek (1965) for synonymy to date.		
Walcott (1884)	*Bathyurus? tuberculatus*	pl. 12, fig. 9	*Flectihystricurus flectimembrus*	questionable	Pogonip Group, Nevada	Lower Ordovician
Weber (1948)	*Hystricurus binodosus*	pl. 1, figs. 11, 12 [only]	*Hystricurus (Hystricurus) exillis*	questionable	Siberia	Lower Ordovician
		pl. 1, figs. 13, 14 [only]	*Hystricurus?* sp.			
		pl. 1, figs. 15, 16 [only]	?Hystricuridae sp.			
		pl. 1, figs. 9, 10 [only]	*Pseudoplethopeltis minuta*	questionable		
		pl. 1, figs. 17, 18 [only]	*Paraplethopeltis seelyi*	questionable		
	Hystricurus (?) antonovi	pl. 1, figs. 19-20	Bathyuridae sp.			
	Hystricurus (?) oculeus	pl. 11, fig. 28	*Tersella paichoica*			
	Hystricurus (?) sp. cf. *H. quadratus*	pl. 1, fig. 21	?Hystricuridae sp.			
Welby (1962)	*Hystricurus conicus*	pl. 13, fig. 10	*Hystricurus (Hystricurus) crotalifrons*		Cassin Limestone, Vermont	
Westrop *et al.* (1993)	*Hystricurus ellipticus*	pl. 3, figs. 1-9	*Hystricurus (Aequituberculatus) ellipticus*		Tribes Hill Formation, New York	Zone B
	Hystricurus cf. *H. oculilunatus*	pl. 3, figs. 10-12	*Hystricurus? armatus*	questionable		

661

APPENDIX III-6. continued.

Reference	Species	Illustrations	Revised name	Remarks	Locality	Age
Whitfield (1889)	*Bathyurus conicus*	pl. 13, figs. 15-21	*Hystricurus (Hystricurus) crotalifrons*		Calciferous Rocks, New York	Lower Ordovician
	Bathyurus seelyi	pl. 13, figs. 8-14	*Paraplethopeltis seelyi*	partially re-illustrated by Boyce (1989, pl. 17, fig. 8, pl. 18, figs. 4-6, pl. 19, figs. 5-8, pl. 20, figs. 3-5)	Fort Ann Formation, New York	
Winston and Nicholls (1967)	*Hystricurus millardensis*	pl. 12, fig. 18 [only]	*Hystricurus (Hystricurus) oculilunatus*		Wilberns Formation, central Texas	Mi to Sy Zone
		pl. 12, fig. 14 [only]	*Hystricurus? longicephalus*			
	Hystricurus cf. *H.* sp. D	pl. 12, figs. 12, 22, 25	*Hystricurus (Butuberculatus) hillyardensis*	questionable		
Yin and Lee (1978)	*Hystricurus (Guizhouhystricurus) yinjiangensis*	pl. 164, fig. 8	*Hystricurus? clavus*	questionable	southwest China	Tremadocian
Young (1973)	*Amblycranium* (?) *linearus*	pl. 4, figs. 9-15	*Heckethornia? linearus*		Fillmore Formation, Utah	Zone H
	Amblycranium (?) sp. 2	pl. 4, figs. 16-20	*Heckethornia? linearus*			
	Psalikilopsis (?) *alticapitis*	pl. 4, figs. 1-8	*Heckethornia alticapitis*			
	Ischyrotoma (?)	pl. 4, figs. 1-8	*Heckethornia alticapitis*			
	unassigned librigena	pl. 7, fig. 8	*Parahystricurus fraudator*			
Zhou (1981)	*Pharostomina sanduensis*	pl. 1, figs. 10, 11	*Glabellosculcatus sanduensis*		Guotang Formation, Southeast China	early Tremadocian

APPENDIX III-6. continued.

Reference	Species	Illustrations	Revised name	Remarks	Locality	Age
Zhou and Fortey (1986)	*Hystricurus penchiensis*	pl. 1, figs. 5, 8, 12	*Hystricurus? clavus*		Upper Yehli Formation, northeast China	*Callograptus taitzehoensis* Zone
	Omuliovia sp.	pl. 11, fig. 10	*Psalikilopsis cuspicauda*	questionable	Upper Yehli Formation, northeast China	*Callograptus taitzehoensis* Zone